ARL-SR-0392 ● FEB 2018

US Army Research Laboratory

Proceedings of the Second Workshop on Numerical Analysis of Human and Surrogate Response to Accelerative Loading

by Michael Kleinberger

NOTICES

Disclaimers

ARL-SR-0392 ● FEB 2018

US Army Research Laboratory

Proceedings of the Second Workshop on Numerical Analysis of Human and Surrogate Response to Accelerative Loading

by Michael Kleinberger
Weapons and Materials Research Directorate, ARL

<table>
<tr><td colspan="4">REPORT DOCUMENTATION PAGE</td><td colspan="2">Form Approved
OMB No. 0704-0188</td></tr>
<tr><td colspan="6">Public reporting burden for this collection of information is estimated to average 1 hour per response, including the time for reviewing instructions, searching existing data sources, gathering and maintaining the data needed, and completing and reviewing the collection information. Send comments regarding this burden estimate or any other aspect of this collection of information, including suggestions for reducing the burden, to Department of Defense, Washington Headquarters Services, Directorate for Information Operations and Reports (0704-0188), 1215 Jefferson Davis Highway, Suite 1204, Arlington, VA 22202-4302. Respondents should be aware that notwithstanding any other provision of law, no person shall be subject to any penalty for failing to comply with a collection of information if it does not display a currently valid OMB control number.
PLEASE DO NOT RETURN YOUR FORM TO THE ABOVE ADDRESS.</td></tr>
<tr><td colspan="2">1. REPORT DATE (DD-MM-YYYY)
February 2018</td><td colspan="2">2. REPORT TYPE
Special Report</td><td colspan="2">3. DATES COVERED (From - To)
12 January 2016–14 January 2016</td></tr>
<tr><td colspan="4" rowspan="3">4. TITLE AND SUBTITLE
Proceedings of the Second Workshop on Numerical Analysis of Human and Surrogate Response to Accelerative Loading</td><td colspan="2">5a. CONTRACT NUMBER</td></tr>
<tr><td colspan="2">5b. GRANT NUMBER</td></tr>
<tr><td colspan="2">5c. PROGRAM ELEMENT NUMBER</td></tr>
<tr><td colspan="4" rowspan="3">6. AUTHOR(S)
Michael Kleinberger</td><td colspan="2">5d. PROJECT NUMBER</td></tr>
<tr><td colspan="2">5e. TASK NUMBER</td></tr>
<tr><td colspan="2">5f. WORK UNIT NUMBER</td></tr>
<tr><td colspan="4">7. PERFORMING ORGANIZATION NAME(S) AND ADDRESS(ES)
US Army Research Laboratory
ATTN: RDRL-WMP-B
Aberdeen Proving Ground, MD 21005-5069</td><td colspan="2">8. PERFORMING ORGANIZATION REPORT NUMBER
ARL-SR-0392</td></tr>
<tr><td colspan="4" rowspan="2">9. SPONSORING/MONITORING AGENCY NAME(S) AND ADDRESS(ES)</td><td colspan="2">10. SPONSOR/MONITOR'S ACRONYM(S)</td></tr>
<tr><td colspan="2">11. SPONSOR/MONITOR'S REPORT NUMBER(S)</td></tr>
<tr><td colspan="6">12. DISTRIBUTION/AVAILABILITY STATEMENT
Approved for public release; distribution is unlimited.</td></tr>
<tr><td colspan="6">13. SUPPLEMENTARY NOTES</td></tr>
<tr><td colspan="6">14. ABSTRACT
The Army Research Laboratory hosted a Workshop on Numerical Analysis of Human and Surrogate Response to Accelerative Loading on January 12–14, 2016, at the Aberdeen Proving Ground, Maryland. This 3-day workshop included 36 technical presentations organized into six technical sessions on (I) Under Body Blast Events; (II) ATD Model Development; (III) Human Biofidelic Response Corridors for Model Validation; (IV) Development of Human Body Models; (V) Topics Related to Prediction of TBI; and (VI) Validation, Scaling, and Material Properties. Focused discussions addressed the assessment of existing injury criteria, methods for quantifying model validation, scaling techniques for modeling the broad anthropometric spectrum of the Soldier population, and novel imaging techniques for documenting injury. Discussions also helped to identify gaps in the current research, and to set short-term goals for continued model development, validation, and application.</td></tr>
<tr><td colspan="6">15. SUBJECT TERMS
biomechanics, finite element modeling, anthropomorphic test devices, injury criteria, under body blast</td></tr>
<tr><td colspan="3">16. SECURITY CLASSIFICATION OF:</td><td rowspan="2">17. LIMITATION OF ABSTRACT
UU</td><td rowspan="2">18. NUMBER OF PAGES
962</td><td>19a. NAME OF RESPONSIBLE PERSON
Michael Kleinberger</td></tr>
<tr><td>a. REPORT
Unclassified</td><td>b. ABSTRACT
Unclassified</td><td>c. THIS PAGE
Unclassified</td><td>19b. TELEPHONE NUMBER (Include area code)
410-278-7979</td></tr>
</table>

Standard Form 298 (Rev. 8/98)
Prescribed by ANSI Std. Z39.18

Acknowledgements

As Chair of the Workshop, I would like to acknowledge the critical contributions of the many people who helped make this event a success both on stage and behind the scenes. First, I would like to thank all of the session chairs for helping to organize and coordinate the technical sessions, helping to lead the technical discussions, and for preparing and presenting the summaries from their sessions. I would also like to thank all of the presenters for sharing their latest research and providing their perspectives on the current state of the art. My appreciation also extends to the many attendees from all over the world who participated in the technical discussions and helped identify existing gaps in our current knowledge, and offered opinions on future research needs and priorities for the biomechanics and soldier protection communities moving forward. Finally, I would like to thank everyone in ARL's Protection Division that helped behind the scenes with registration, refreshments, transportation, and other tasks that came up before and during the Workshop.

I would like to thank and acknowledge the co-sponsors of the Workshop, namely the Warrior Injury Assessment Manikin (WIAMan) Engineering Office and the Blast Protection for Platforms and Personnel Institute (BP3I). In particular, I would like to thank Ken Tarcza (WIAMan) and Scott Kukuck (BP3I) for their support, and for helping to spread the word and encourage participation from their respective organizations. I would like to specifically thank Chris Hoppel for his extended efforts in obtaining approval to hold the Workshop, and for his continued advice and assistance in many of the administrative and organizational matters. I would also like to especially thank Jackie Czarnecki and Kim Sappington for their help in coordinating meals and refreshments, and for processing the numerous visit requests and transportation required by the international attendees.

Second Workshop on Numerical Analysis of Human and Surrogate Response to Accelerative Loading

Proceedings

Table of Contents

Executive Summary

The Army Research Laboratory hosted a Workshop on Numerical Analysis of Human and Surrogate Response to Accelerative Loading on January 12-14, 2016 at the Aberdeen Proving Ground. Co-sponsored by the Warrior Injury Assessment Manikin (WIAMan) Engineering Office and the Blast Protection for Platforms and Personnel Institute (BP3I), this workshop addressed the numerical analysis tools and methods available to simulate and investigate the response of vehicle occupants to accelerative loading induced from blast events, with an emphasis on under-body blast. The objectives of the workshop were to explore the scope of current research activities, highlight recent advances in models and techniques, document the capabilities of existing numerical analysis tools, extract knowledge and insights gained from using these tools, and identify technical gaps and numerical tools for critical future needs. The workshop provided a venue for the presentation of science and engineering that reflected the latest innovations in state-of-the-art technologies for characterizing and simulating the human response to typical accelerative loading conditions seen in the field.

This 3-day workshop was held in the Mallette Auditorium, and was attended by approximately 170 attendees representing 9 countries, 14 universities, 13 industrial partners, and numerous organizations throughout the DoD and other government agencies. A total of 36 technical presentations highlighted current capabilities in computational modeling of the human body. These presentations were organized into six technical sessions on (I) Under Body Blast Events; (II) ATD Model Development; (III) Human Biofidelic Response Corridors for Model Validation; (IV) Development of Human Body Models; (V) Topics Related to Prediction of TBI; and (VI) Validation, Scaling, and Material Properties. Focused discussions addressed the assessment of existing injury criteria, methods for quantifying model validation, scaling techniques for modeling the broad anthropometric spectrum of the Soldier population, and novel imaging techniques for documenting injury. Discussions also helped to identify gaps in the current research, and to set short-term goals for continued model development, validation, and application.

Second Workshop on Numerical Analysis of Human and Surrogate Response to Accelerative Loading

Aberdeen Proving Ground, Bldg. 6008, Mallette Auditorium

Tuesday, 12 January 2016

08:00 **Registration**

08:30 **Opening Comments:**

Michael Kleinberger	ARL, WMRD Protection Division, Soldier Protection Sciences Branch
Ken Tarcza	Warfighter Injury Assessment Manikin (WIAMan) Program Engineering Office
Scott Kukuck	Blast Protection for Platforms and Personnel Institute (BP3I)

Session I: Under Body Blast Events

Co-Chairs: Julie Klima (TARDEC), Andrew Merkle (JHU/APL)

09:00	Robert Kargus	Lab Simulation of Seated Occupant Response to a UBB Event	ARL
09:15	Craig Foster	Generic Hull III: Structural Vertical Accel. and ATD Responses	TARDEC
09:40	Dan Pope	The Phenomenology and Analysis of Vehicle Mine Loading	DSTL, UK
10:05	**BREAK**		
10:20	Piet Jan Leerdam	Validation for UBB Numerical Vehicle Models	TNO, NL
10:45	Warren Hardy	Comparison of ATD to PMHS Response in UBB Environment	Virginia Tech
11:10	Daniel Possley	Clinical Perspective on Underbody Blast Injuries	Fort Hood
11:35	**DISCUSSION**		
12:05	**LUNCH BREAK**		

Session II: ATD Model Development

Co-Chairs: Mostafiz Chowdhury (ARL), Ravi Thyagarajan (TARDEC)

13:15	Jai Ramalingam	Assess. of Automotive Hybrid ATD Models for Prediction of Lower Ext. and Lumbar Spine Injuries under Mine Blast Loadings	TARDEC
13:40	King Yang	Hybrid III Crash-Dummy Lower Ext. under High Speed Vertical Loading: A Combined Experimental and Computational Study	Wayne State
14:05	Scott Gayzik	Modeling and Sensitivity Analysis of the WIAMan ATD Head and Neck: A Finite Element Study	Wake Forest
14:30	Cameron Bell	WIAMan Pelvis FE Model Application and Testing	Corvid
14:55	**BREAK**		
15:10	Connor Pyles	M&S of Lumbar Surrogate Response for UBB Loading	JHU/APL
15:35	Costin Untaroiu	Preliminary Development of an FEM of WIAMan Lower Extremity: Sensitivity Analysis to Impact Loading Conditions	VA Tech
15:50	Michael Boyle	WIAMan Lower Leg Strength of Design and Soft Materials Sensitivity Study Using DOE	JHU/APL
16:05	Cameron Bell	WIAMan FE Model Development and Application	Corvid
16:30	**DISCUSSION**		
17:00	**ADJOURN**		

Wednesday, 13 January 2016

08:00 **Opening Comments:**
Michael Kleinberger ARL, WMRD Protection Division, Soldier Protection Sciences Branch

Session III: Human Biofidelic Response Corridors for Model Validation
Co-Chairs: Dan Nicolella (SWRI), Scott Gayzik (Wake Forest)

08:15	Liming Voo	Response Corridors of Cadaveric Human Head-Neck in Nominal Posture under Accelerative Loading	JHU/APL
08:40	JiangYue Zhang	Effects of Lordosis on Lumbar Spine Biomechanical Responses under Vertical Accelerative Loading	JHU/APL
09:05	JiangYue Zhang	Effects of Flesh on Pelvis Biomechanical Responses under Vertical Accelerative Loading	JHU/APL
09:30	Liming Voo	Response Corridors of Cadaveric Human Leg-Foot under Accelerative Loading: Effect of Posture and Input Rise Time	JHU/APL
09:55	**DISCUSSION**		
10:25	**BREAK**		

Session IV: Development of Human Body Models
Co-Chairs: Dan Pope (DSTL), Adam Sokolow (ARL)

10:40	Joe Cordell	Use of Numerical Techniques to Identify Key Factors Associated with In-Vehicle, Lower Leg Response to UBB Loading	DSTL, UK
11:05	Carolyn Hampton	Effect of Boots on Leg Injury Mitigation in UBB Events	ORISE / ARL
11:30	**LUNCH BREAK**		
12:50	Dale Robinson	Development of a Computational Method to Predict Pelvic Fractures in Military Vehicles	U. Melbourne, AU
13:15	Caitlin Weaver	Pelvic Injury Analysis of a Total Human Body FEM during Simulated UBB Impacts using Cross-Sectional Force	WF / ARL
13:40	Connor Pyles	Validation of 50th Percentile Lumbar FEM for Vertical Loading	JHU/APL
14:05	**DISCUSSION**		
14:35	**BREAK**		

Session V: Topics Related to Prediction of TBI
Co-Chairs: Sikhanda Satapathy (ARL), King Yang (Wayne State)

14:50	Kim Thompson	A numerical study of impact induced load transfer to porcine and human head	ARL
15:15	Keegan Yates	Identifying TBI Thresholds using Animal and Human FEM Based on In-Vivo Impact Test Data	VA Tech
15:40	Nitin Daphalapurkar	A Multiscale Virtual Human Head Model Validated using 3D Dynamic Deformations in the Live Human Brain	Johns Hopkins Univ.
16:05	Joseph Orgel	Detection of Load-Induced Structural Changes to Neurons and the Brain using X-ray Diffraction	Illinois Inst. Technology
16:30	**DISCUSSION**		
17:00	**ADJOURN**		

Thursday, 14 January 2016

08:00 **Opening Comments:**

Michael Kleinberger — ARL, WMRD Protection Division, Soldier Protection Sciences Branch

Session VI: Validation, Scaling, and Material Properties

Co-Chairs: Mat Philippens (TNO), Barry Shender (NavAir)

08:15	Jeff Somers	Overview of Occupant Protection Research at NASA	Wyle / NASA
08:40	Dan Nicolella	Quantitative Validation of High Fidelity Human Injury FE Models using a Quantitative Probabilistic Error Metric	SWRI
09:05	Tim Westerhof	DRI vs. L1-L5 Human Body Model as Tool for Scaling Lumbar Spine Tolerance for 5th & 95th Percentile Occupants	TNO, NL
09:30	Matthew Davis	An Objective Evaluation of Mass Scaling Techniques Utilizing Computational Human Body Models	Wake Forest
09:55	Adam Sokolow	Scaling and Posture Trends in FEM Simulations of Pendulum Impacts on Lower Leg	ARL
10:20	**BREAK**		
10:35	Rob Fryer	Study to Determine the Variation of Vulnerable Thoracic-Abdominal Structures using Computed Tomography	DSTL, UK
11:00	Nathan Drenkow	Computational Pipeline Enabling the Generation of Multi-Organ Statistical Atlases for Improved Human Model Development	JHU/APL
11:25	Tusit Weerasooriya	Mechanical Response of Human and Animal Bones: Overview of ARL Experimental Research	ARL
11:50	Wayne Chen	Experimental Challenges in Determining Dynamic Response of Soft Tissues	Purdue
12:15	**DISCUSSION**		
12:45	**LUNCH BREAK**		

Session VII: Summary and Next Steps

Co-Chairs: Mike Kleinberger (ARL), Neil Gniazdowski (ARL)

14:00 **SESSION SUMMARIES**

15 minute summaries from session chairs

15:30 **BREAK**

15:45 **OPEN DISCUSSION – NEXT STEPS**

17:00 **ADJOURN**

1. Introduction

This proceedings provides a brief summary of the material presented in each of the six technical sessions. These sessions included the following topics: (I) Under Body Blast Events; (II) ATD Model Development; (III) Human Biofidelic Response Corridors for Model Validation; (IV) Development of Human Body Models; (V) Topics Related to Prediction of TBI; and (VI) Validation, Scaling, and Material Properties. For further details on the technical sessions, the reader is referred to Appendix A for the session overview slides created by the session chairs, and to Appendix B for the complete set of slides presented by each speaker during the workshop.

Presentations lasted for approximately 15 minutes followed by a 10-minute period for questions. Each session included a 30-minute period for open discussion and/or any additional questions for the presenters moderated by the session chairs. An extended period of open discussion was included at the end of the workshop to discuss overall research gaps, research priorities for the biomechanics and military communities, and next steps. An overview of the discussions, both during the sessions and at the conclusion of the workshop, is provided in the Section 3. A list of near-term research priorities is provided in Section 4.

2. Brief Summary of Technical Sessions

Session I: Under Body Blast Events

This session was chaired by Julie Klima (TARDEC) and Andrew Merkle (JHU/APL), and included six technical presentations that provided the audience with some insight on the real-world under body blast environment. Presentations offered various perspectives on the complex sequence of events beginning with detonation and continuing through soil acceleration, vehicle loading, local effects on occupant, longer term motion and return to earth impact. It is important to understand all phases of this event, and to realize that the occupants may be subjected to non-vertical forces. Injuries sustained from under body blast can vary based on specific exposure and environment. Recent studies suggest that orthopedic injuries from accelerative loading can be as lethal as those sustained from ballistic events. In addition, damage to the soft tissues can have a large impact on treatment and ultimate outcome for the soldiers.

Session II: ATD Model Development

This session was chaired by Mostafiz Chowdhury (ARL) and Ravi Thyagarajan (TARDEC), and included eight technical presentations on the development of computational models of anthropomorphic test devices, or ATDs. The first two presentations focused on the behavior of the currently available Hybrid III ATD models, and the remaining six presentations focused on creating models of the WIAMan ATD Tech Demonstrator (TD) and validating them at the component level. These models were used to identify potential design limitations and critical design risks to inform the development of the TD/Gen 1 design.

Session III: Human Biofidelic Response Corridors for Model Validation

This session was chaired by Dan Nicolella (SwRI) and Scott Gayzik (Wake Forest U.), and included four technical presentations on the biomechanical testing of post-mortem human subjects and the development of human biofidelic response corridors (BRCs). Presentations were broken down by anatomic region, and included the head/neck, lumbar spine, pelvis, and lower limb. Analysis of the head/neck response included two separate phases of the experiments, considering both before and after roof contact. Analysis of lumbar spine tests considered the effect of lordosis on the measured response. Pelvis experiments were run both with and without flesh. Lower limb experiments considered the effect of initial orientation on the resulting response. In general, the experiments were designed with consideration for model validation and were well controlled and documented. BRCs were developed using a consistent data processing methodology.

Session IV: Development of Human Body Models

This session was chaired by Dan Pope (DSTL) and Adam Sokolow (ARL), and included five technical presentations on the application of computational models to assess the predicted response and injury risk to soldiers following military relevant exposures. Models of the pelvis, lumbar spine, and lower

extremities were presented and validated against available laboratory experiments simulating under body blast events. A comparison of the response of the lower extremity to vertical loading both with and without boots was presented. Presentations generally included validation results and examples of model sensitivity to material properties and initial orientation. Leg/foot models showed sensitivity to heel pad soft tissue properties, while pelvic models showed sensitivity to flexion at the sacroiliac joint. Accounting for the effects of muscle activation and appropriately defining properties for biological soft tissues continue to be major challenges for the development of human body models.

Session V: Topics Related to Prediction of Traumatic Brain Injury

This session was chaired by Sikhanda Satapathy (ARL) and King Yang (Wayne State), and included four technical presentations related to the prediction or detection of traumatic brain injury. Two talks presented porcine models subjected to low velocity impacts to help develop a transfer function for predicting human injury. One presentation used tagged MRI data from low rate rotations of human volunteers to develop a human head model using the material point method. One presentation discussed the use of X-ray diffraction methods to study the thresholds of brain tissue.

Session VI: Validation, Scaling, and Material Properties

This session was chaired by Mat Philippens (TNO) and Barry Shender (NavAir), and included nine technical presentations related to determining material properties, scaling across the soldier population, and addressing the issue of variability. One presentation provided a general overview of occupant protection research at NASA, which incorporates a probabilistic approach to modeling to account for the effects of a large number of uncontrolled variables. Another presentation focused on defining the quality of a model and quantifying the uncertainty in reference data, the environment, and the model. Several presentations discussed the importance of anatomic variability and being able to simulate the biomechanical response and predict injuries across the broad soldier population.

3. Summary of Open Discussion

The final session of the Workshop was an open discussion moderated by Michael Kleinberger (ARL) and Neil Gniazdowski (ARL). The following discussion summarizes the main points addressed during this final session, along with some of the key discussion topics from the individual technical sessions.

Appropriate Model Fidelity

A considerable amount of time was spent discussing the appropriate level of fidelity, or detail, for computational models. It is important to consider the intended use of a model before setting out to develop and validate the model. Is the model being used to discover new mechanisms of injury deep within the brain or to determine whether a new seat design will prevent a soldier's head from striking the roof of a vehicle during an under body blast event? Understanding the intended purpose can help determine the required level of detail. It is also important to understand the quality of the data that will be used to validate the model. If the available validation data is limited to response corridors based on a small number of experiments with relatively large confidence bands, it may not be warranted to use a high fidelity model with complex material models and microstructural details. Model fidelity does not equal accuracy.

Another factor that should be considered in determining the appropriate level of model fidelity is the time step and overall run time for the planned simulations. If the intended application will require simulations with a full vehicle and multiple full body human occupants subjected to a long duration acceleration pulse, run times may become the limiting factor in the simulation plan. This may preclude the use of microstructural details that would require a large number of relatively small elements. Weighing the importance of specific computational factors (e.g. - mesh size, material models, contact definitions, analysis code) needs to be considered at the start of the model development effort.

Model Validation

Another topic of discussion, which may be related to model fidelity, is the definition of model validation. When comparing simulation results with experimental data, how good does the comparison need to be? Also, what is the best method for quantifying model validity? Several presentations used CORA (CORrelation and Analysis) to quantify how well a candidate response matched a target corridor. CORA combines two independent methods to adjust for time shifts in the data and to quantify how well a response curve fits within a given time history corridor. CORA scores range from 0 to 1, where a value of 1 indicates a perfect match. CORA values around 0.8 were used to justify that a model was valid for a particular loading scenario and for prediction of a specific response variable. The challenge remains, however, to determine which variables are most critical and how to weigh the relative CORA scores from multiple response traces. If the predicted acceleration of a body region falls within the target corridor but the forces or strains do not match experimental data, should that be considered a validated model? The answer is most likely not, but it may depend on the intended application.

It is also important to clearly document under what conditions a model has been validated. Validation of a model under multiple loading scenarios over a range of displacements and rates gives more confidence in the model's response, especially when simulating conditions within those ranges. Use of the model to

predict responses outside of the validated ranges is often required, but results need to be carefully reviewed and interpreted cautiously.

Determining What is Good Enough

Closely related to model fidelity and validation is the question of when is a model good enough. This topic was raised during several of the discussion periods, and continues to promote considerable debate. It represents the fundamental conflict between model development and application. On one side of this debate, modelers always strive to develop and validate high fidelity models with sufficient details to capture the multi-directional, higher order responses of the subject structure. For human body models, this might require the inclusion of anatomic microstructural elements (e.g. - neural tracts, trabeculae, muscle fibers) and complex material models, such as hyperelastic viscoelastic solid. These more complex structures and material definitions will require additional experimental data for validation, which will extend the overall time needed for model development. One argument that is commonly made in support of this approach is that this level of detail is needed to properly predict the mechanisms and thresholds of injury, which typically occurs at the microstructural (or possibly even cellular) level.

In contrast to the desire for modelers to develop these detailed high fidelity models, designers and developers of protection systems often face short timelines for producing and fielding equipment that could enhance soldier protection and reduce the number of injuries or fatalities. These people commonly search for the “70 percent solution”, which can be applied immediately to the engineering design process. For them, a 70 percent solution today is much more valuable than a 95 percent solution in 3 years. Perhaps the best compromise for this debate is for modelers to continue to strive to develop validated high fidelity models but to release lower fidelity versions of their models for immediate application. Users of these lower fidelity models will clearly need to interpret their results cautiously given the limitations of the models. In addition, the user community should consult with the model developers whenever possible to avoid any unintentional misuse of the models. These collaborations can also provide the modelers with important feedback that can help improve the models and focus on the most critical parameters.

Thoughts on Injury Prediction

Numerous discussions were held on the subject of how to prioritize the prediction of injury. Many of the presenters during this Workshop have worked extensively in the area of automotive safety, and have based their injury prediction on the likelihood of sustaining serious injuries as defined by the Abbreviated Injury Scale, or AIS. This injury scale is focused on injuries sustained during typical automotive collisions, and attempts to quantify the risk of a fatality. Several attempts have been made to define a military equivalent to the AIS injury scale but no consensus has been reached to date. The AIS scale has been criticized for being solely focused on fatalities rather than on functional incapacity or debilitation. For example, bilateral eye enucleation (loss of both eyes) would be scored as a minor (AIS 1) injury because it is unlikely to result in a fatality despite the fact that it would be extremely debilitating. In a military environment, blindness could preclude a soldier from exiting a vehicle and finding his way out of hostile territory, which could ultimately result in a fatality. Assessment of injury risk should consider not only the immediate physical injuries sustained but the associated loss of functionality and potential risk to mission success.

A recommendation was made to consider developing a military version of the Functional Capacity Index, which has received limited use within the automotive community. The idea is that it is more important to quantify a person's ability to perform their duty, or continue their mission, than to simply predict a fatal injury. This injury scale would take into consideration a soldier's ability to exit a vehicle, communicate with their unit, continue to fight, and other operational requirements. NASA uses a similar operational rating system to determine an astronaut's flight status.

One of the presentations that led to a considerable amount of discussion, both during and following the Workshop, was given by MAJ Daniel Possley from the Orthopaedic Surgery Department at Fort Hood. In his talk, he emphasized the importance of maintaining stable soft tissue with minimal contamination. He pointed out the fact that bony fractures are relatively simple to repair as compared to soft tissue disruption with infection, which can often result in the loss of a limb. This has important implications for existing injury scaling systems, which typically give low weight to soft tissue injuries and generally disregard the risk of infection. The prioritization of injury prevention or reduction should consider the clinical aspects of acute treatment and expected long-term outcome.

Biomechanical Response and Injury Scaling

Presentations in Session 3 (Human Biofidelic Response Corridors for Model Validation) provided a summary of experimental testing performed on different anatomic regions of the human body under the WIAMan (Warrior Injury Assessment Manikin) project. Measured response corridors were presented as a means for defining target responses for manikin development, and for validating computational models currently under development. Experimental performers attempted to select post-mortem human surrogates that were anthropometrically within 1.5 standard deviations of a 50^{th}-percentile male Soldier in an attempt to reduce the effects of anatomic variability. All subjects tested were male. The age of the subjects, however, varied over a large range and were clearly older than the target Soldier population.

Understanding the effects of anthropometry, mass distribution, age, and gender was an area that received a significant amount of discussion but no overall consensus on the best methods for scaling available data. Most recent studies have applied mass scaling, assuming similar geometries and material properties, which have not produced reliable results. It was noted during the presentations that anthropometric variation is not equal along different axes, and that proper scaling should employ a 3-dimensional technique based on available measurements. Researchers should consider using "worst case" scenarios (e.g. - long legs with short torso) to design systems that will provide sufficient protection to the overall Soldier population.

Injury prediction based on general scaling principles is a huge challenge since actual injuries will occur at points of local stress concentration or pre-existing defects. Computational models typically do not include this level of detail, especially since these anatomic points of weakness may change over time for any given subject based on activity and loading history and a dynamic healing process. Probabilistic modeling techniques may be able to account for some of these unknowns, along with the ability to predict response and injury across a broad population with varying anthropometry, age, and gender.

It was also pointed out during the discussion that most computational models do not explicitly model the fracture of bones and rupture of soft tissues, and are therefore not valid beyond the initial point of injury. These models are suitable for predicting the occurrence of injury but may not be capable of accurately

predicting the extent and severity of the resulting trauma. Additional experimental data beyond the point of initial failure would help to further validate injury models and provide a statistical basis for the development of injury criteria and the prediction of injury severity. A multi-scale modeling approach may also help to predict micro level injuries resulting from a macro level loading phenomenon.

Collaboration and Coordination of Modeling Efforts

An interesting discussion stemmed from an observation that there appears to be multiple organizations developing similar models, and that there should be better collaboration and coordination between these organizations. It was suggested that the Army is in an excellent position to take a leading role in coordinating model development and setting priorities for which capabilities are most critically needed. Similar modeling efforts within different organizations should be coordinated and leveraged to help shorten the development timeline. Experimental data being collected for the purpose of model validation should be shared across all stakeholders.

Several people suggested that some level of redundancy in both computational and experimental studies is desired. It not only provides some level of quality control, but might also help to account for anatomic variability. Additional experimental tests should improve the statistical power of the collected data, and computational predictions are not all derived from a single model representing a single individual.

Some Final Thoughts

Simulations presented during the Workshop were run using a variety of different analysis programs, which might complicate collaboration between different organizations. Although mesh geometries can typically be converted from one program to another, there may not be sufficient consistency between the material models and contact definitions available in the different codes. Efforts should continue to identify the most appropriate material models for the highest priority applications, and to further develop compatible definitions across the various codes. Similar efforts related to contact definitions and energy control should also be undertaken.

Development and improvement of models for existing PPE needs to continue, and should be included in the analyses. Simulations need to capture operationally relevant exposure conditions, which would include standard issued protective systems. Experiments should be conducted both with and without PPE to provide suitable test data for the validation of the PPE and human body models.

If possible, models should be shared between different organizations as part of an overall collaboration effort. A suggestion was made to establish a repository for models and data to help support the continued development and archiving of models for the biomechanics and soldier protection communities. Further discussion on this subject is needed to determine what models are currently available or under development within the various organizations. Additionally, it will need to be determined whether certain models could be safely shared with the general scientific community.

Another question that was discussed and debated dealt with the general philosophy of how to account for biological variability between test subjects used to generate validation data. The question that was posed during the discussion was whether it would be better to use a smaller sample of test subjects that better match the target population (e.g. - anthropometry, age, bone density). This would reduce the

effects of subject variability, which is desirable, but at the expense of sample size. Given the already difficult challenge of acquiring suitable PMHS test subjects, it is not clear whether the biomechanics community would have the luxury of being more selective in specimen selection. As discussed previously, alternate approaches may be used to evaluate worst-case scenarios or to account for biological variability using probabilistic modeling methods.

Aside from developing models to account for anatomic variability to represent the overall Soldier population, it is also important to be able to position these models in various initial postures to support development of protective systems intended for different environments. Most models are generated from medical image data that is most commonly collected in a supine position, which is not the position that soldiers are in during a blast or ballistic event of interest. Being able to manipulate the models into various initial postures, such as sitting or kneeling, is an important capability that needs to be addressed.

Finally, there is a huge challenge in trying to predict specific injuries that initiate within the microstructural anatomy using macrostructural models. It would be computationally impossible to model the entire body with a finite element mesh that captures the microscopic details of the bony architecture, soft tissue fiber orientation, or neural connectivity. The community needs to continue to explore methods for incorporating multiscale system and subsystem models into the process of simulating the biomechanical response and prediction of injuries under operationally relevant loading conditions.

4. Near-Term Research Priorities

Based on the presentations and discussions held during this 3-day Workshop, the following list of research topics was identified as areas of high importance to the biomechanics and soldier protection communities. Focused work in these areas is needed to further develop the capabilities necessary to study the mechanisms and thresholds of injury, and to assess the efficacy of existing and future protective systems.

1. Modelers must clearly identify the steps taken to validate their models, and also to define the range of conditions under which the model's response is valid. This information needs to be clearly relayed to all potential users of the model.
2. Develop a military injury scale that can be used to evaluate the overall risk of injury, including the potential loss of mission capabilities. This injury scale should consider the immediate loss of functional capacity and operational readiness, as well as the longer-term clinical outcomes that may be associated with soft tissue damage and potential infection.
3. Develop computational methods to account for anatomic variability across the general Soldier population. These methods should account for the effects of varying anthropometry, age, gender, and bone quality.
4. Use probabilistic modeling techniques to evaluate the response and injury potential associated with operationally relevant exposure conditions. These techniques should be able to account for variabilities associated with soldier anatomy, threat levels, available protective systems, and other uncontrollable variables.
5. Seek out opportunities for collaboration and coordination of modeling efforts. This could include the creation of a model repository to support potential collaboration efforts.
6. Identify the most critical material models needed by the biomechanics and soldier protection communities and incorporate equivalent formulations into the various analysis codes being used.
7. Develop and improve models for PPE and other protective systems.
8. Develop methods to modify the initial posture of human body models to support the development and assessment of various protective systems in a wide range of environments.
9. Develop multiscale modeling techniques to enable the prediction of microscopic injury occurrence using macrostructural models.

5. APPENDIX A

SESSION OVERVIEWS

U.S. ARMY RDECOM

ARL

Summary: Session 1
Under Body Blast Events

Julie Klima (TARDEC), Andrew Merkle (JHU/APL)
Session Chairs

Second Workshop on Numerical Analysis of Human and Surrogate Response to Accelerative Loading
12-14 January 2016

Session 1: Underbody Blast Events

Co-Chairs:
Julie Klima (TARDEC), Andrew Merkle (JHU/APL)

09:00	Robert Kargus ARL	Lab Simulation of Seated Occupant Response to a UBB Event
09:15	Craig Foster TARDEC	Generic Hull III: Structural Vertical Accel. and ATD Responses
09:40	Dan Pope DSTL, UK	The Phenomenology and Analysis of Vehicle Mine Loading
10:05	BREAK	
10:20	Piet Jan Leerdam TNO, NL	Validation for UBB Numerical Vehicle Models
10:45	Warren Hardy Virginia Tech	Comparison of ATD to PMHS Response in UBB Environment
11:10	Daniel Possley Fort Hood	Clinical Perspective on Underbody Blast Injuries
11:35	DISCUSSION	30 Minute Open Discussion

Session 1 - Summary

- The Event
  - Important to understand all phases
  - Complex sequence of events beginning with detonation, soil acceleration, vehicle loading, local effects on occupant, longer term motion and return to earth impact.
- Accelerative Loading / Laboratory Test Methods
  - Should properly capture loading phase
    - This may ultimately include non-vertical forces on the occupant
- Validation of models is critical
- Sustained injuries can vary based on the exposure and environment
  - Soft tissue damage drives consideration for outcomes
  - Recent studies suggest that orthopedic injuries from blunt can be as lethal as those sustained from ballistic (pelvis)

Session 1 – Critical Challenges/Gaps

- The Event
  - If models are going to simulate the actual event, they must either replicate the physical elements (blast, sand, moisture, etc.) quite closely or use the subsequent loading as the initiation of their model
  - Does the longer term response need to be modeled? Most models currently focus on the short duration response (local effects).
  - Do models need to examine occupant sensitivity to threat placement ?
- Accelerative Loading / Laboratory Test Methods
  - Do these test systems adequately replicate the live-fire event?
  - What level of detail is needed when modeling these systems (eg, lateral wall flexure or floor pullback)?
- Validation
  - Need an accepted method for validating that the model matches the experiment
- Injury
  - Correlation of mounted soldier loading to bony and/or soft tissue relationship.

U.S. ARMY RDECOM

Session 1 – Future Priorities

ARL

- The Event
  - Fully characterize (consider different vehicles, seats, etc.) and determine what aspects are critical for occupant loading.
  - Use modeling results (of an occupant in the simulated vehicle) to determine the impact on the occupant.
  - Confirm through modeling or prior testing the contribution of the 3 phases of vehicle response to the timing of occupant loading/injury.
- Accelerative Loading / Laboratory Test Methods
  - Determine if the critical aspects found above can be replicated by current test systems. If not, the systems should be modified to capture this impactful loading condition.
- Injury
  - Use existing injury data to further specify incidence of injury type in a vehicle
  - Human injury prediction response

U.S. ARMY RDECOM

Session 1 – Existing Capabilities

ARL

- Live-Fire data for vehicle response characterization
  - Further classify vehicle response and determine what effects should be captured in an experimental or computational model based on their contribution to occupant loading
- Test Systems: Determine how well they mimic live-fire beyond the metrics of Velocity and Time To Peak
  - WIAMan Laboratory and Blast driven systems have been developed
  - Various blast ranges used to evaluate generic vehicle analogs
- Soil models have been developed. Can be used to understand loading profile on structure.
- Injury
  - JTAPIC data reviewed for theater data trends
  - WIAMan and other activities used to determine dose-injury response relationships

Summary: Session 2
ATD Model Development

Mostafiz Chowdhury (ARL), Ravi Thyagarajan (TARDEC)
Session Chairs

Second Workshop on Numerical Analysis of Human and Surrogate Response to Accelerative Loading
12-14 January 2016

Session 2: ATD Model Development

Session Co-Chairs:
Ravi Thyagarajan (TARDEC), Mostafiz Chowdhury (ARL)

13:15	Jai Ramalingam TARDEC	Assessment of Automotive Hybrid ATD Models for Prediction of Lower Ext. and Lumbar Spine Injuries under Mine Blast Loadings
13:40	King Yang Wayne State	Hybrid III Crash-Dummy Lower Ext. under High Speed Vertical Loading: A Combined Experimental and Computational Study
14:05	Scott Gayzik Wake Forest	Modeling and Sensitivity Analysis of the WIAMan ATD Head and Neck: A Finite Element Study
14:30	Cameron Bell Corvid	WIAMan Pelvis FE Model Application and Testing
14:55	BREAK	
15:10	Connor Pyles JHU/APL	M&S of Lumbar Surrogate Response for UBB Loading
15:35	Costin Untaroiu Virginia Tech	Preliminary Development of an FEM of WIAMan Lower Extremity: Sensitivity Analysis to Impact Loading Conditions
15:50	Michael Boyle JHU/APL	WIAMan Lower Leg Strength of Design and Soft Materials Sensitivity Study Using DOE
16:05	Cameron Bell Corvid	WIAMan FE Model Development and Application
16:30	DISCUSSION	30 Minute Open Discussion

Session 2 - Overview

- Summary of presentations given in session
  - The first two papers focused on the behavior of the currently available H-III ATD models.
    - The first one dealt with comparing ATD responses from M&S to that of the actual physical ATD, as well as the PMHS results from the same testing scenarios. While the dataset is limited to a small number of tests, the results are somewhat surprisingly close for the injuries considered by the authors.
    - The second paper considered re-modeling the materials in the LSTC version of the H-III ATD for the heel pad foam, foot skin and lower leg flesh. The authors showed better correlations with tests for the lower leg injuries with these improved models. Their goal was not to develop a better bio-fidelic model, rather make the M&S model match the physical ATD better. In the Army, this improvements have already been implemented in the GEN2 Humanetics H-III model for over 5 years.
    - Both papers indicated the need for an improved ATD model for vertical accelerative environment
  - The next 6 papers in the session were focused on building Tech Demonstrator (TD) models of the WIAMAN TDP ATD, and validating them at the component level. To the extent of this limited scope, namely on the ATD rather than the human/PMHS behavior, the papers adequately described the manner in which the models were co-developed in 2 codes.
    - Predictive modeling capability of WAIMan Tech Demonstrator components (Pelvis, Lumbar Spine, and Cervical Spine) FE models is demonstrated for component level test simulations.
    - Demonstrated material selection sensitivity within the Lumbar Spine and suggested an optimal material
    - Identified potential design limitations and critical design risks to inform the TD/Gen 1 design development

Session 2:
Critical challenges facing the modeling community

- Designing an ATD with the right strength and durability has become the current primary focus of the WIAMAN program. The challenge to make it more biofidelic and human-like in injury corridor behavior is still a major one.
- Because it is still a Tech Demonstrator stage, and the focus has been as described above, quantitative comparisons of the models to PMHS tests are few and need much more improvement. This is a natural step in the development process, but nevertheless a major challenge.
- The Army is in a position where some decisions about whether to spend resources on continuing to improve the H-III ATD for blast modeling need to be made, depending on when the WIAMAN ATDs will be rolled in to LFTEs and the model quality/ability to replicate the physical ATDs.
- Some of the computational challenges include:
  - Computational stability of softer materials within the WIAMan (e.g. Pelvis Flesh, Foot Flesh) under server loading
  - Incorporation of potential material changes from Tech Demonstrator (TD) to Gen-1
  - Nonlinear, viscoelastic and isotropic materials pose challenges at high rates
  - With any strength of design work, failure prediction is a function of the mesh and caution should be exercised
  - Modeling w/ PPE presents unique challenges (friction between PPE and dummy, uncertainty of PPE model)
  - Uncertainty in material characteristics data when come from different sources (same material but different vendors) is a challenge to the modeling community
  - Tradeoff between the ability to match the BRC and strength of design simultaneously

U.S. ARMY RDECOM ARL

Session 2: Limitations and/or Opportunities

- Adequately accounting for uncertainty in experimental setups must be done as small deviations can induce errors in the model when compared to experimental results, sensitivity studies can be used to combat this. More detail on experimental setups for ATD and PMHS tests will improve correlations.
- Models are very good at exploring design space and determine factors that influence performance. Less concern should be spent moving a CORA score from 0.85 to 0.90 as uncertainty in experiment may account for this. Instead the opportunity is to reach a reasonable level of validation and then begin using the model to explore design alternatives (geometrical, material), optimization of load cell location, strength of design, etc.
- Long-term opportunity to create a tool to complement live-fire testing by varying extrinsic parameters: threat conditions, vehicle protection system, & PPE, as well as varying intrinsic surrogate parameters: size (scaling), posture, etc.

UNCLASSIFIED

U.S. ARMY RDECOM ARL

Session 2: Critical gaps not currently being addressed

- One question was raised in the end discussion. Are we building these ATDs only with current vehicles in mind, will they be robust enough for next-gen ground vehicles, which may have different blast pulse signatures (different rise times, pull-backs etc?). Vehicles fielded in Europe have different characteristic response than currently being used in the WIAMan program.
- What are the characteristics of "good" or "acceptable" biofidelity? Are these published? These are not only for quantitative metrics but also qualitative metrics such as whether do the legs kick up or not, for a certain scenario. This also came up in the Discussion. Otherwise we will be making subjective statements like "this ATD is more biofidelic than that one…" without consideration of the right criteria.Also, the risk of not having well-defined criteria could result in construction of a new ATD and model that can measure a lot more data, but is no better than current ATDs as far as biofidelity and closeness to human behavior go.
- Failure testing of the WIAMan ATD for verification of the WIAMan FE model subject to extreme loading
- Evaluating scaled surrogate response representing 5% to 95% Male/Female occupants
- A fast running model from users' perspective
- Balancing model run time (6 days for 300 ms run including settling time) vs. model fidelity

Session 2: Recommended priorities for future efforts

- PPE Validation: Comment from one attendee that accurate representation of inertias and geometry may not be enough, and material properties are also critical. This needs to be evaluated.
- Model Size: Modeling everything except the kitchen sink…. Concern that models are too fine with too small a time step. At full vehicle level, inclusion of multiple ATD models may make simulation run times too large. Models of different sizes need to be built?
- Continue improving ATD FE models (Components and Whole body) confidence by validating simulated results against more test data
- Optimize ATD performance (meet BRC and SoD criteria simultaneously)

UNCLASSIFIED

Session 2: Existing capabilities/resources that can be leveraged

- There have been multiple papers on lessons learned from modeling of the current H-III ATDs. Were these considered during the construction of the current Tech Demonstrator WIAMAN ATD? Several attendees raised why some known working features of the H-III were not in the baseline design, since the authors acknowledged that those may "well be in the next generation" models
- GHMBC and THUMS models should be leveraged as much as possible.
- Independent verification of the validated models by DOD Users' community
- Exploring options to balance model run vs. model fidelity
- Continue exploring material models (parameter estimations) for better prediction of the unloading phase of the simulated response
- Leverage materials models for increased confidence in the model prediction

Summary: Session 3
Human Biofidelic Response Corridors for Model Validation

Dan Nicolella (SwRI), Scott Gayzik (Wake Forest)
Session Chairs

Second Workshop on Numerical Analysis of Human and Surrogate Response to Accelerative Loading
12-14 January 2016

Session 3: Human Biofidelic Response Corridors for Model Validation

Co-Chairs:
Dan Nicolella (SWRI), Scott Gayzik (Wake Forest)

08:15	Liming Voo JHU/APL	Response Corridors of Cadaveric Human Head-Neck in Nominal Posture under Accelerative Loading
08:40	JiangYue Zhang JHU/APL	Effects of Lordosis on Lumbar Spine Biomechanical Responses under Vertical Accelerative Loading
09:05	JiangYue Zhang JHU/APL	Effects of Flesh on Pelvis Biomechanical Responses under Vertical Accelerative Loading
09:30	Liming Voo JHU/APL	Response Corridors of Cadaveric Human Leg-Foot under Accelerative Loading: Effect of Posture and Input Rise Time
09:55	DISCUSSION	30 Minute Open Discussion

Session 3 - Overview

- **Summary of presentations given in session**

- Series of experiments performed to support the WIAMan Blast ATD development and computational modeling validation – BRC's
- Sub-components of the whole body
  - Head and neck – before and after roof contact
  - Lumbar Spine – effect of lordosis
  - Pelvis – flesh vs no flesh
  - Lower Limb – limb orientation
- Characteristics of each specimen reasonably controlled
- Each series of experiments consisted of repeat experiments
  - Initial level of variability quantified
- Combinations of increasing impact velocities and subsystem configurations
- Experimental configuration was well controlled and documented
- BRC's developed using a consistent data processing pipeline
- Experiments designed with consideration for model validation

UNCLASSIFIED

Session 3 - Overview

Critical challenges facing the modeling community

- Small sample sizes
- Data scaling from cadaver to human, old to young
- Criteria for inclusion or exclusion of specimens/results
- ATD to PMHS conversion of response data
- Two separate phenomenon occur in a single test (e.g. vertical acceleration and then roof contact).
- Are component tests indicative of what would occur in whole body?
- Development of a clear validation plan to help define validation hierarchy
  - Clearly define what the model will be used for
  - Top level definition of model use
- Clear definition of response quantities of interest
  - Support ultimate purpose of model
  - Kinematic response
  - Tissue level response for injury prediction

- Close collaboration between modelers and experimentalists to design validation experiments

- Define experiments for model validation
  - Typically not how experiments are designed

Session 3 - Overview

Critical gaps not currently being addressed

- Clearly define intended use of the model
- Define appropriate response variables – kinematics vs. injury
- ATD to PMHS anatomical correspondence of data collection location
- Data transforms meticulously recorded? Pre-test faro data?
- BRC usage in practice not discussed, you get this data and then what?
- Tissue level experimental response to define failure (injury)
    - Tissue level
    - How will this be experimentally characterized at the component level and higher?
    - How will failure/injury be accounted for in the model?
- Effect of age of specimens used in validation experiments
    - Extremely difficult to obtain young PMHS
    - Effect of aging on tissue level responses is not well characterized, particularly at high loading rates
- Small sample sizes

UNCLASSIFIED

Session 3 - Overview

Recommended priorities for future efforts

- Focus on intended use of the model
    - Develop a Validation Plan and Hierarchy
- Begin with end in mind, what is the key body response, key posture, begin with BRC and even model sensitivity in those regions and determine if more resources are needed
- Prioritize by most critical body region, loading rates given finite resources
- Think about decoupling multipurpose experiments
    - Validation experiments often do not generate new knowledge
    - Experiments developed to generate new knowledge are often poor validation experiments
    - Constrained by available resources

Existing capabilities/resources that can be leveraged

- BRC methodology and code
- University partner testing labs are set up to conduct follow on testing
- Use Probabilistic methods – sensitivity analysis
    - Can help allocate resources for focus validation experiments

- Think about National Repository
    - Validation data
    - Validated models
    - Building off of previous efforts will allow for much more rapid advances
    - Programmatic requirement

U.S. ARMY RDECOM

ARL

Summary: Session 4
Development of Human Body Models

Dan Pope (DSTL), Adam Sokolow (ARL)
Session Chairs

Second Workshop on Numerical Analysis of Human and Surrogate Response to Accelerative Loading
12-14 January 2016

Session 4: Human Body Models

Co-Chairs:
Dan Pope (DSTL), Adam Sokolow (ARL)

10:40	Joe Cordell DSTL, UK	Use of Numerical Techniques to Identify Key Factors Associated with In-Vehicle, Lower Leg Response to UBB Loading
11:05	Carolyn Hampton ORISE / ARL	Effect of Boots on Leg Injury Mitigation in UBB Events
11:30	LUNCH BREAK	
12:50	Dale Robinson U. Melbourne, AU	Development of a Computational Method to Predict Pelvic Fractures in Military Vehicles
13:15	Caitlin Weaver ARL / Wake Forest	Pelvic Injury Analysis of a Total Human Body FEM during Simulated UBB Impacts using Cross-Sectional Force
13:40	Connor Pyles JHU/APL	Validation of 50th Percentile Lumbar FEM for Vertical Loading
14:05	DISCUSSION	30 Minute Open Discussion

Session 4 - Overview

- Summary of presentations given in session.
  - Biofidelic FEM
    - lower extremities
    - lumbar spine and pelvis
    - Effects of Boot vs Unbooted response
  - Biofidelic OpenSim/Anybody Models
    - Only attempt to account for muscle forces/activation
    - Attempt at bridging scales between lower order model with FEM
  - Examples given in each case for sensitivity and validation
    - Pendulum impact tests
      - generally good with individual experiment and corridors
      - Identified sensitivities to soft tissue properties of heelpad
    - Isolated Pelvic Impact/Compression Test
      - Identified sensitives to flexion at SI joint

Session 4 - Overview

- Critical challenges facing the modeling community
  - Validation
  - Appropriate model resolution/Tailoring this to the question/problem?
  - Adequate material models
  - Appropriate process for engineering solution/tuning of material properties
  - Contact
  - Stability of numerical simulation
  - Geometric representation, biodiversity
  - Cartilage, bone interfaces, soft tissues

U.S. ARMY RDECOM ARL

Session 4 - Overview

- Critical gaps not currently being addressed
  - Material models - Inadequate high-rate and failure models for all tissues (hard and soft)
  - Including statistics into material modeling
  - Multiaxial test cases for "validation" – confidence outside of training datasets
  - One model predicting all cases

UNCLASSIFIED

U.S. ARMY RDECOM ARL

Session 4 - Overview

- Recommended priorities for future efforts
  - Develop/strengthen international modeling community
    - Prevent duplication of work/efforts
  - Establish model test standards/benchmarks
  - Establish standards for comparison across codes and across models
  - more discussion about nuances and niceties
  - Contribute back to experiments
    - what can we learn from the simulations to help design of experimental, not just take data

- Existing capabilities/resources that can be leveraged:
  - Community
    - UK for general peer review and material model development
    - U Melbourne for multiscale approaches, muscle loading/pre-stress effects
    - MCW/others for DOE

U.S. ARMY RDECOM

ARL

Summary: Session 5
Topics Related to Prediction of TBI

Sikhanda Satapathy (ARL), King Yang (Wayne State)
Session Chairs

Second Workshop on Numerical Analysis of Human and Surrogate Response to Accelerative Loading
12-14 January 2016

U.S. ARMY RDECOM

Session 5: Prediction of TBI

ARL

Co-Chairs:
Sikhanda Satapathy (ARL), King Yang (Wayne State)

14:50	Kim Thompson ARL	A numerical study of impact induced load transfer to porcine and human head
15:15	Keegan Yates Virginia Tech	Identifying TBI Thresholds using Animal and Human FEM Based on In-Vivo Impact Test Data
15:40	Nitin Daphalapurkar Johns Hopkins Univ.	A Multiscale Virtual Human Head Model Validated using 3D Dynamic Deformations in the Live Human Brain
16:05	Joseph Orgel Illinois Inst. Tech.	Detection of Load-Induced Structural Changes to Neurons and the the Brain using X-ray Diffraction
16:30	DISCUSSION	30 Minute Open Discussion

Session 5 - Overview

- **Summary of presentations given in session.**
  - Thompson and Yates presented porcine models subjected to low velocity impacts related to developing a transfer function for humans
  - Daphalapurkar used tagged MRI data from low rate rotations to develop a human head model using the material point method
  - Orgel talked about using X-ray diffraction to study the thresholds of brain tissue

- **Critical challenges facing the modeling community**
  - Injury correlates for computed parameters
  - Computational fidelity and resolution
    - o Need convergence studies
      - Difficult with contact problems and non-linear material models
  - Transfer function
    - o Is it reasonable to assume that tissue properties and injury thresholds are the same between human and surrogate models?
  - Extend short time model predictions to time dependent injury effects
    - o Damage recovery

Session 5 - Overview

- **Critical gaps**
  - Material response
    - o Rate dependent properties of soft tissues
    - o Injury criteria and thesholds
  - Biovariability

- **Recommended priorities for future efforts**
  - Biofidelic geometries and mesh (what is appropriate level of detail)
  - Accurate material models (deformation response and failure thresholds)
  - Comparison of animal and human tissue material response

- **Existing capabilities/resources that can be leveraged**
  - Add more instrumentation to experimental tests when possible
    - o e.g., add strain gages to force-displacement tests
  - Extend material point method to biomechanical modeling
  - XRD data presented by Orgel may help to better understand injury thresholds

Summary: Session 6
Validation, Scaling, and Material Properties

Mat Philippens (TNO), Barry Shender (Navy/Pax River)
Session Chairs

Second Workshop on Numerical Analysis of Human and Surrogate Response to Accelerative Loading
12-14 January 2016

Session 6: Validation, Scaling, and Material Properties

Co-Chairs:

Mat Philippens (TNO), Barry Shender (Navy/Pax River)

08:15	Jeff Somers Wyle / NASA	Overview of Occupant Protection Research at NASA
08:40	Dan Nicolella SWRI	Quantitative Validation of High Fidelity Human Injury FE Models using a Quantitative Probabilistic Error Metric
09:05	Tim Westerhof TNO, NL	DRI vs. L1-L5 Human Body Model as Tool for Scaling Lumbar Spine Tolerance for 5th & 95th Percentile Occupants
09:30	Matthew Davis Wake Forest	An Objective Evaluation of Mass Scaling Techniques Utilizing Computational Human Body Models
09:55	Adam Sokolow ARL	Scaling and Posture Trends in FEM Simulations of Pendulum Impacts on Lower Leg
10:20	BREAK	
10:35	Rob Fryer DSTL, UK	Study to Determine the Variation of Vulnerable Thoracic-Abdominal Structures using Computed Tomography
11:00	Nathan Drenkow JHU/APL	Computational Pipeline Enabling the Generation of Multi-Organ Statistical Atlases for Improved Human Model Development
11:25	Tusit Weerasooriya ARL	Mechanical Response of Human and Animal Bones: Overview of ARL Experimental Research
11:50	Wayne Chen Purdue	Experimental Challenges in Determining Dynamic Response of Soft Tissues
12:15	DISCUSSION	30 Minute Open Discussion

Summaries

- **Jeff Somers (Wyle / NASA) Overview of Occupant Protection Research at NASA**
  - Probabilistic approach; unique vehicle and PPE issues, deconditioning
- **Dan Nicolella (SWRI) Quantitative Validation of High Fidelity Human Injury FE Models using a Quantitative Probabilistic Error Metric**
  - Fidelity is not validation; quality of model / predictions determined by utility and what user requires; literature data may not be relevant; quantify uncertainty in reference data, environment, and model
- **Tim Westerhof (TNO, NL) Spine injury risk assessment model for the 5th & 95th Percentile Occupant**
  - DRI based, linked to STANAG, tool to evaluate vehicles for non 50th percentile occupants; Challenge is size and accurate sex scaling; Need successor for DRI
- **Matthew Davis (Wake Forest) An Objective Evaluation of Mass Scaling Techniques Utilizing Computational Human Body Models**
  - Investigated scaling issues when scale 50th GHBMC model to small and large occupants; recommended using each factor of ISO/TS 18571 score (phase, magnitude, slope) to really determine the effect of scaling
- **Adam Sokolow (ARL) Framework for FEM Scaling and Posture**
  - Evaluated different scaling techniques; consequences on validity of numerical model; not all scaling techniques valid for all conditions

UNCLASSIFIED

Summaries

- **Rob Fryer (DSTL, UK) Study to Determine the Variation of Vulnerable Thoracic-Abdominal Structures using Computed Tomography**
  - CT scans of thorax organs – most important were heart, aorta, spleen; cannot just scale for stature; use of anthropometric hard points
- **Nathan Drenkow (JHU/APL) Computational Pipeline Enabling the Generation of Multi-Organ Statistical Atlases for Improved Human Model Development**
  - Methodology to Predict internal anatomy from external factors; develop an automated technique to generate shapes; generate organ atlas; issues included availability of actual anthropometry, supine vs. upright position, respiration phase
- **Tusit Weerasooriya (ARL) Mechanical response of human and animal bones: Overview of ARL experimental research**
  - Described methodologies for determining long bone fracture properties and mini-pig skull bone structure – issues of porosity, anisotropy per layer, differences in location
- **Wayne Chen (Purdue) Experimental Challenges in Determining Dynamic Response of Soft Tissues**
  - Fixture and measurement considerations for characterizing soft tissues using Kolsky Compression Bar; provided several recommendations for specimen preparation, pulse shaping, bar material, holding specimen in fixture

Session 6 - Overview

- **Critical challenges facing the modeling community**
  - Clear definition from customer of requirements for how the tool will be used, specific injury, and what the tool will be used for
  - Injury vs. functional outcome
  - Lack of synergy /coordination between model needs and experimentalists
  - Lack of standardization / agreement on scaling techniques
  - Lack of standardization / agreement on validation techniques
  - Relevant soft tissue material models
  - What are the most important injuries to focus on – soft vs. hard tissue from an outcome/ / morbidity perspective

- **Critical gaps not currently being addressed**
  - We're developing component models with constrained boundaries, but the goal is whole body response – how to combine these?
  - Lack of information on how injury impacts mission functionality – consequence if one soldier is injured
  - How to apply modeling predictions to engineering design recommendations for industry

UNCLASSIFIED

Session 6 - Overview

- **Recommended priorities for future efforts**
  - Take lesson from NASA to view soldier and vehicle as a system for determining risk assessments
  - Validated human or ATD models need similar models of vehicles, body-borne equipment, seating, and understanding of typical behavior
  - Overcoming challenges in determining soft tissue properties
  - Tradeoff between protection, risk, and functional capabilities before and after injury

- **Existing capabilities/resources that can be leveraged**
  - Libraries of vehicle, equipment models available?

UNCLASSIFIED / Distribution A The Nation's Premier Laboratory for Land Forces

6. APPENDIX B

PRESENTATIONS

U.S. Army Research, Development and Engineering Command

Laboratory Simulation of Seated Occupant Response to an Under-Body Blast Event

TECHNOLOGY DRIVEN. WARFIGHTER FOCUSED.

Presenter: Robert Kargus
Weapons & Materiel Research Directorate
Blast Protection Branch
Robert.g.Kargus.civ@mail.mil
(301) 394-5738

2nd Workshop on Numerical Analysis of Human and Surrogate Response to Accelerative Loading

January 12-14, 2016

Introduction

- Laboratory simulation of seated occupant response allows for efficient development of protection technologies and the study of injury mechanisms
- Strive for realism while ensuring robustness and repeatability of the apparatus
- Elements of UBB engagement that are important to capture
    - Event timing
    - Translation and rotation of components
    - Potential for injury or damage

Event timing

- The time window of interest for *assessed injuries* in UBB scenarios is early (well below 100 ms)
- Details will depend on specifics of threat and vehicle
- The concept of a fully unconstrained blast simulation rig was deemed unneccessary in light of the following
  - Total translation and rotation are quite small in the early time of the event, so relevant motion could be captured with special fixtures
  - An unconstrained platform was likely to be heavier, and therefore more difficult to reach higher velocities

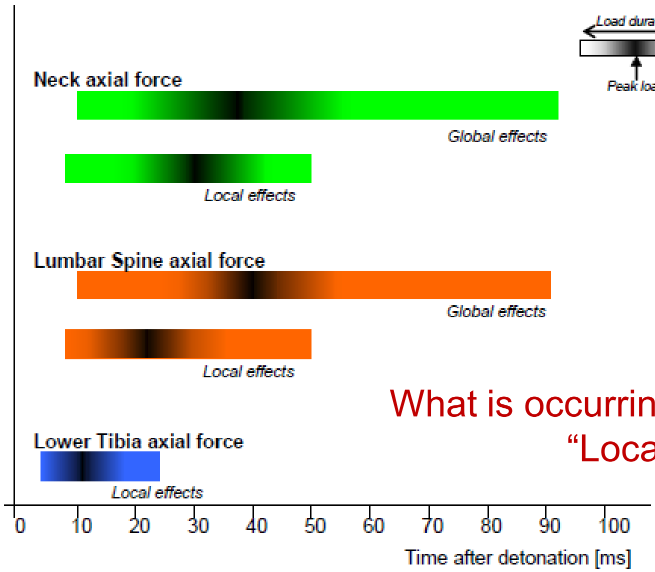

Figure 2.5: Loading Process in Human Body Due to Mine Detonation. Based on test data [Leerdam, 2002].

What is occurring in this timeframe?
"Local Effects"

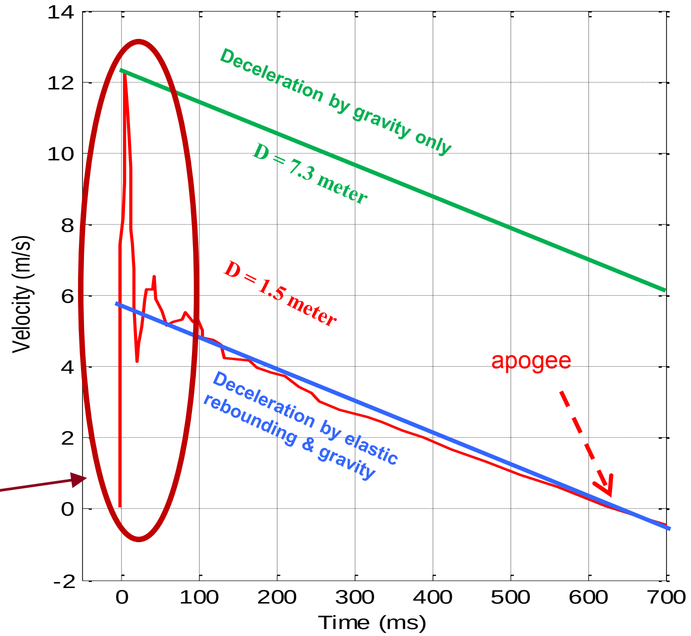

DISTRIBUTION STATEMENT A. Approved for public release; distribution is unlimited.

Simulation of local effects using coupled rigid bodies

- Colliding a **bullet mass into** the **test platform mass** and then into **arresting mass** simulates the elastic recovery of the vehicle floor
- This 'knee' profile can be varied in proportion by tuning the body velocities and arrestor mass

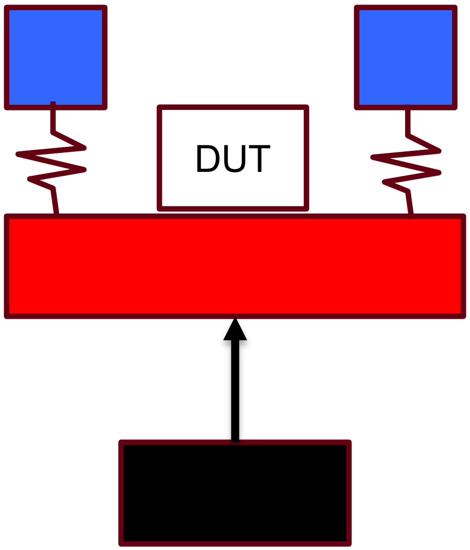

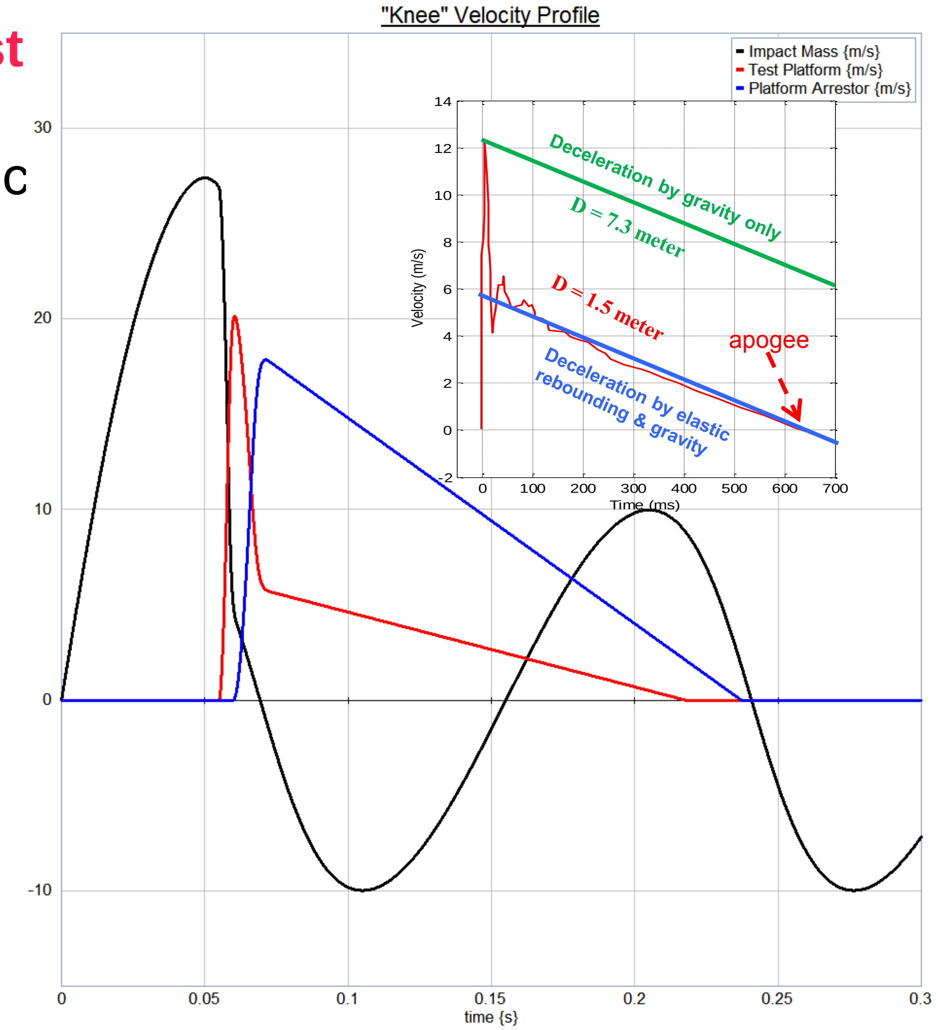

DISTRIBUTION STATEMENT A. Approved for public release; distribution is unlimited.

What about non-vertical local effects?

- Local effects are not strictly vertical
  - Shock wave transmits through the structure
- May have injury potential, and may have consequences for protection systems like wall-mounted seats
- Case for a generic ‘blast box’ is shown below

LOFFI Triaxial Locations (red dots)

Displacements calculated by double integration of time histories

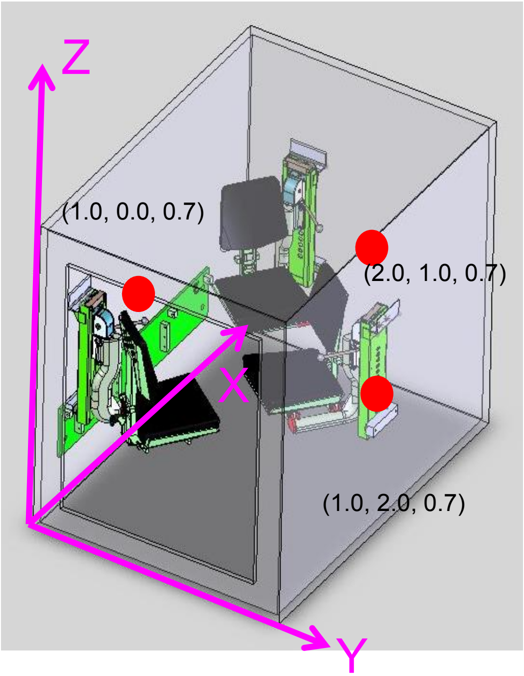

3D plot of displacements (0-50 ms)

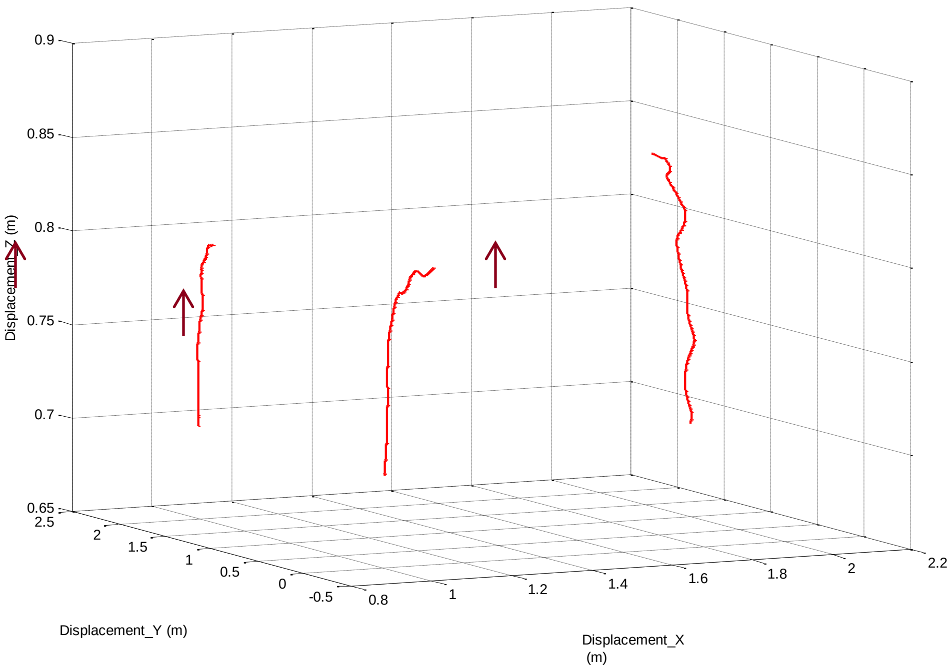

2D Wall Motion of UBB/Blast Box

Viewed from the front of the box (looking in), outward/inward deflection of wall plates is typical of box section loaded from below

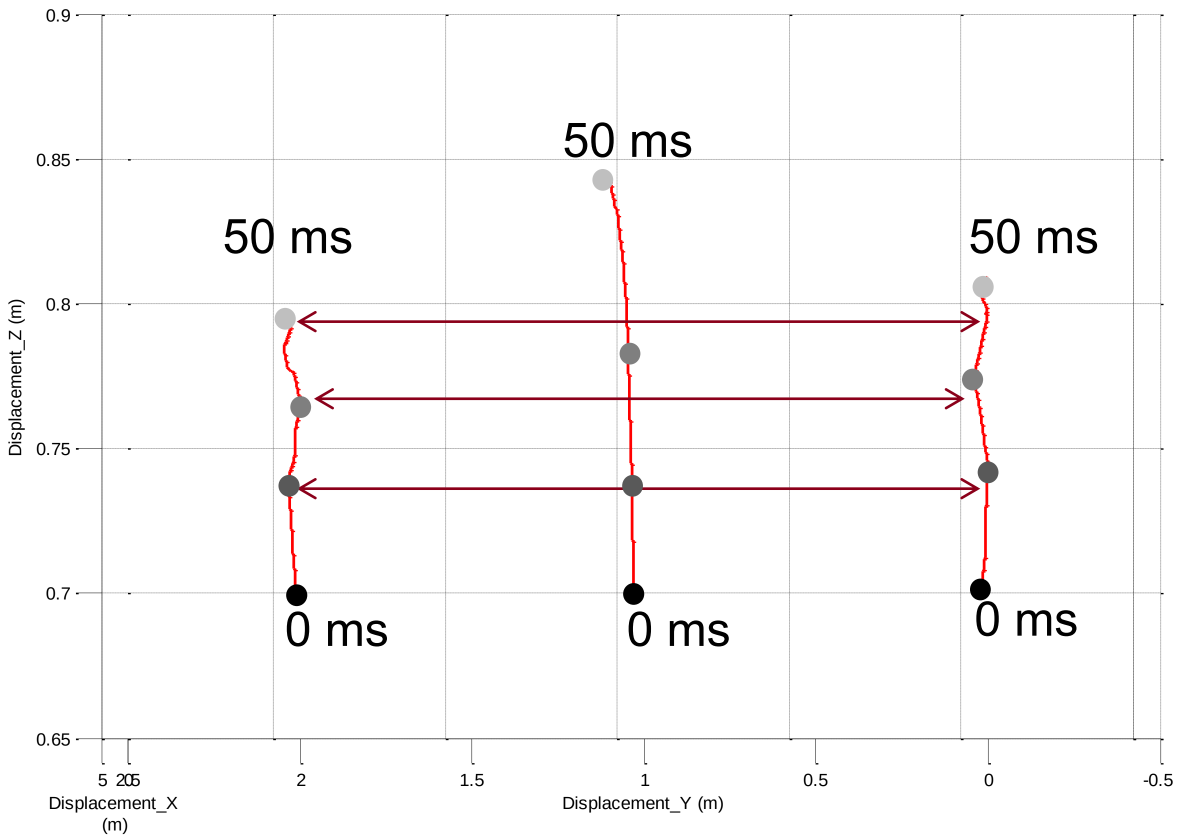

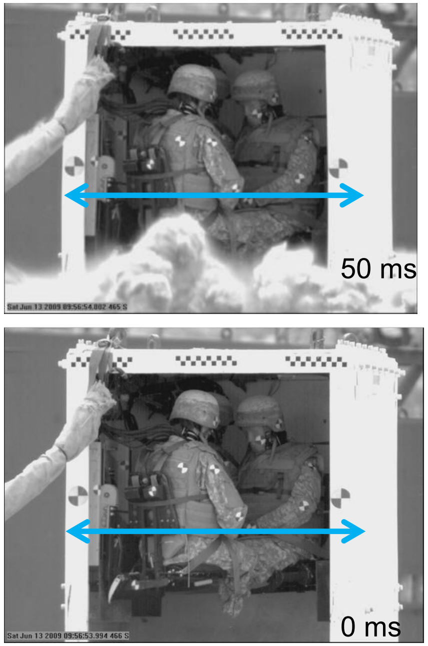

DISTRIBUTION STATEMENT A. Approved for public release; distribution is unlimited.

Simulated motion of UBB/Box Section

- Non-vertical wall effects can be simulated using a fixture that resembles a half box section

Generalized Wall Motion of Box Section
(produced on drop tower)

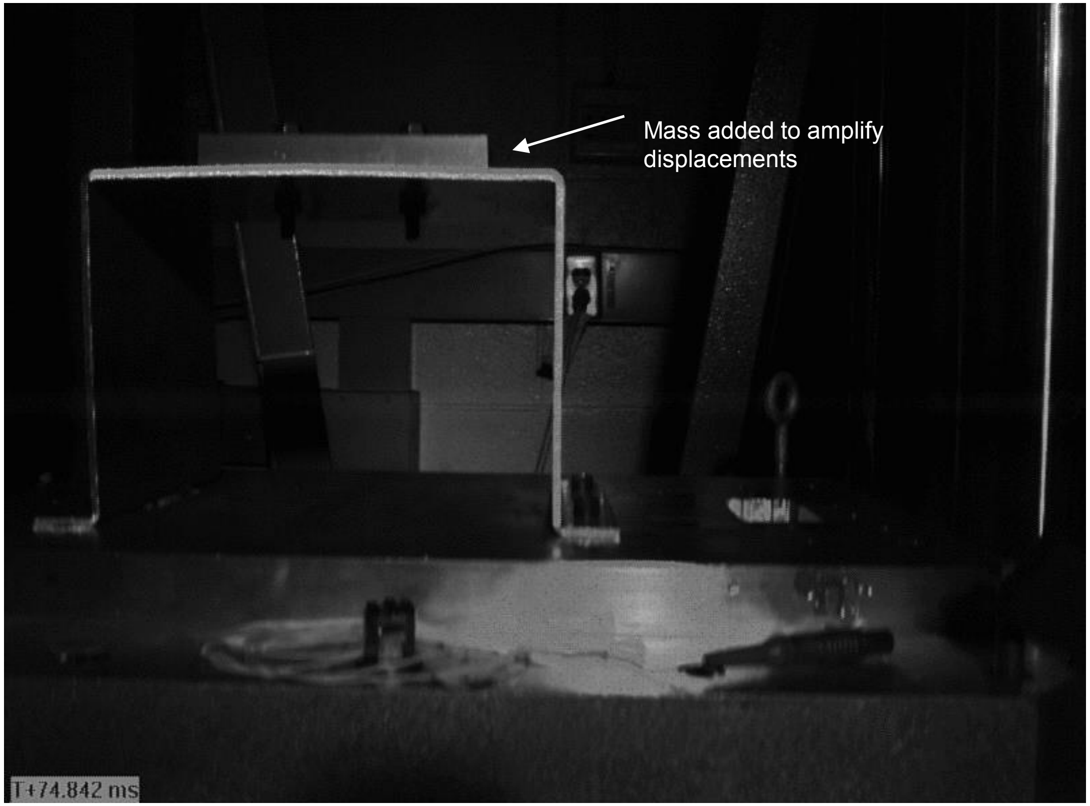

Acknowledgment of Support

- This work has been supported by the Office of Naval Research (Jeff Bradel, Rodney Peterson, Maureen Foley, Howie Draisen)
- Anne Purtell and the USMC survivability community
- Ami Frydman and Dean Li (Retired) inspired and began this area of research and were key to fostering the ARL/ONR relationship
- Neil Gniazdowski for his ongoing support of the mechanical shock lab
- Branch colleagues for their intensive support of this project
  - Neil Gniazdowski, ARL/WMRD
  - Daniel Malone, Survice Engineering
  - Jeffrey Nesta, ARL/WMRD
  - Rene Ramirez, Bowhead

RDECOM

GHIII: Structural Vertical Accelerations and ATD Responses

TARDEC

TECHNOLOGY DRIVEN. WARFIGHTER FOCUSED.

Craig D. Foster
Engineer

Modeling and Simulation Symposium
11 JAN 2016, Aberdeen Proving Grounds, Maryland

Introduction

- Generic Hull, Military Surrogate Vehicle
- Conducted February 2015 at ATC
- Six HIII 50^{th} ATDs
- Assess Seat Protective Capability
- Head Impact Protection Material
- Injury Potential Determined via IARVs
- Mainly Lower Limbs

Introduction

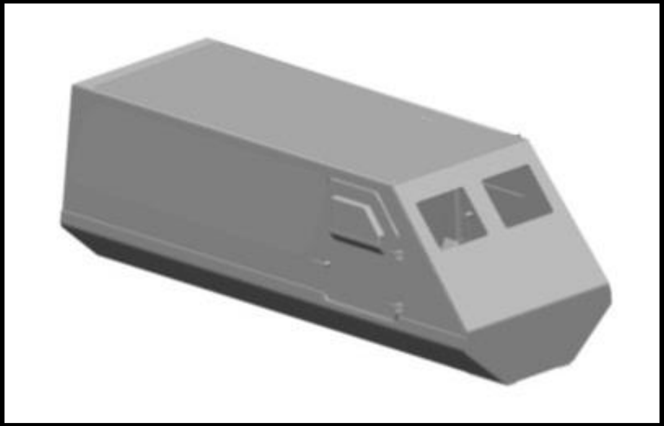

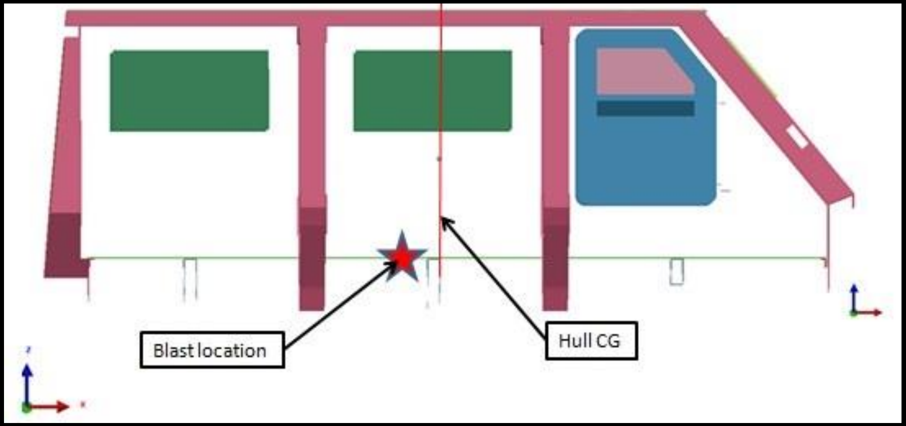

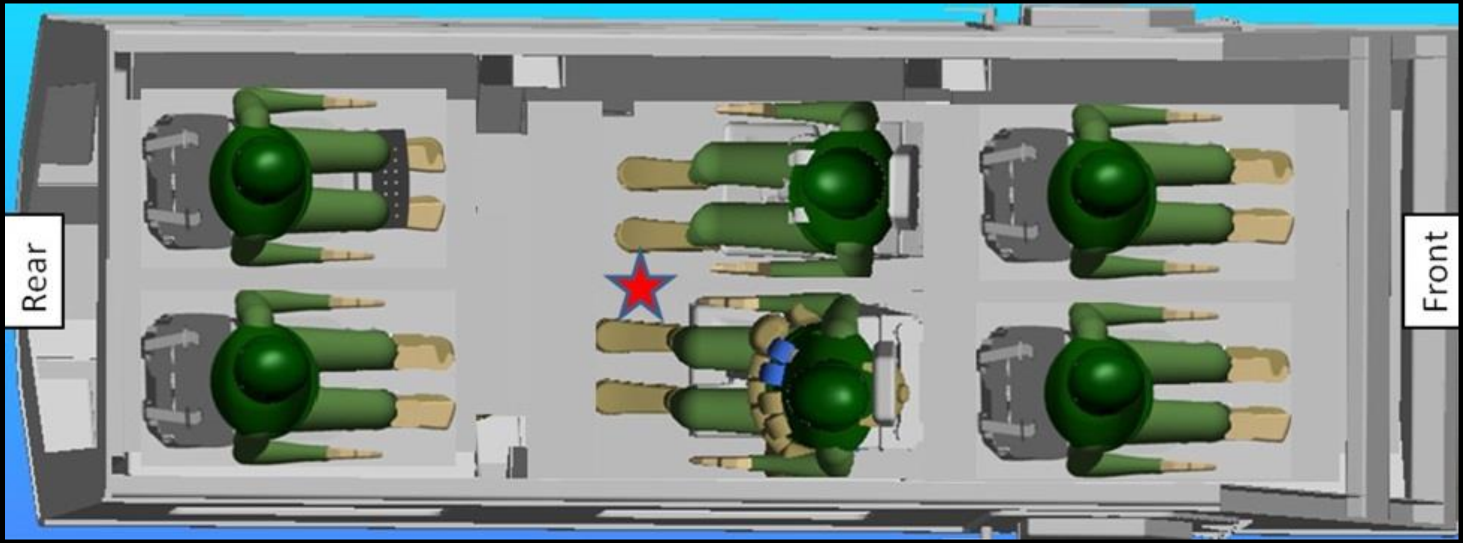

Instrumentation

- Head Accelerations CG
- Upper Neck Forces and Moments
- Chest Accelerations
- Lumbar Spine Forces and Moments
- Pelvis Accelerations
- Femur Forces and Moments
- Upper and Lower Tibia Forces and Moments

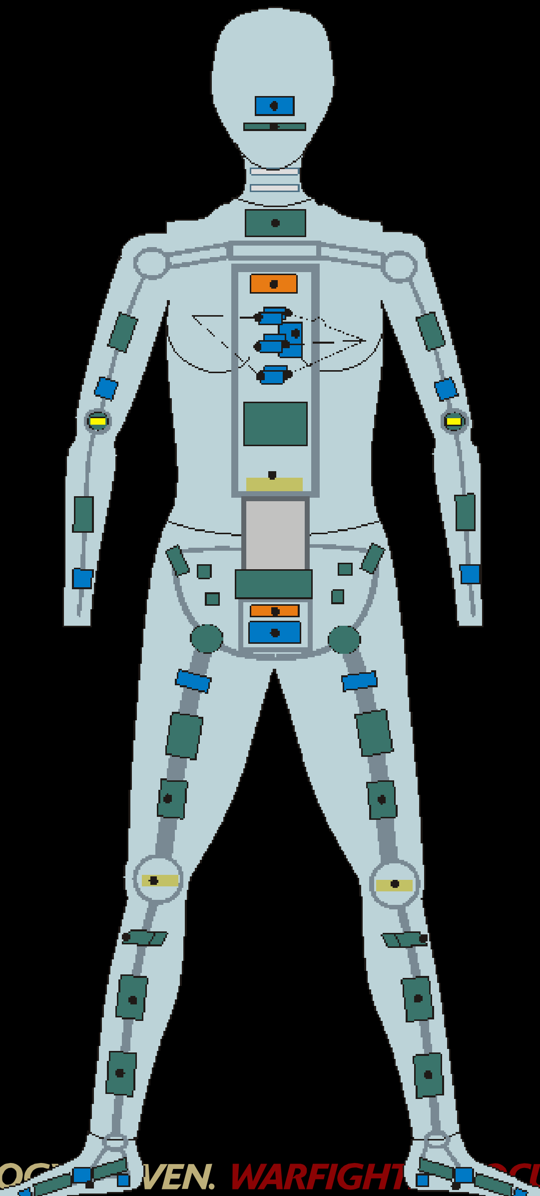

- DTS Inc., 1720 Apollo Court Seal Beach, CA 90740 USA

Instrumentation

- SAE J211

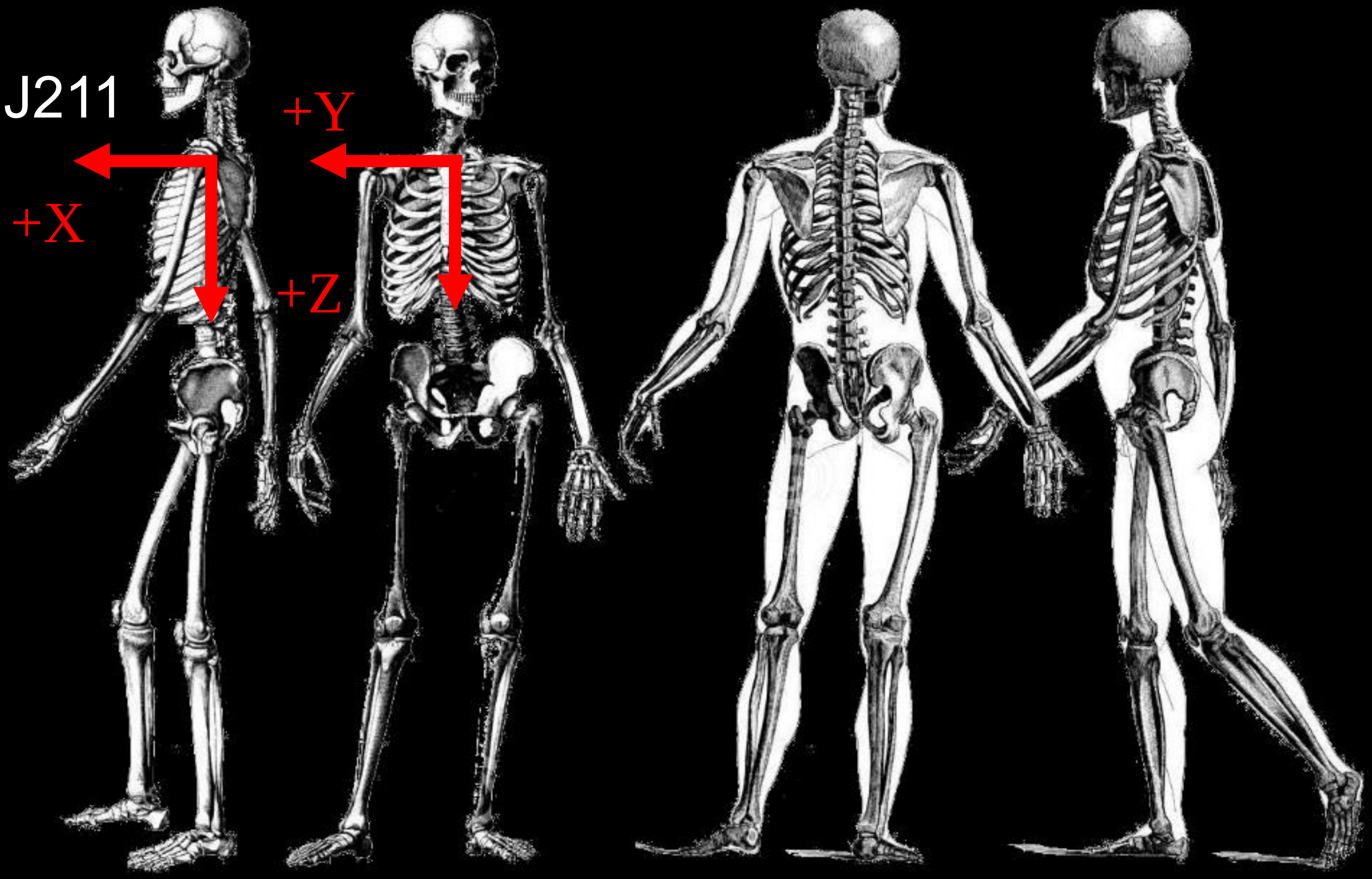

- http://thumbs.dreamstime.com/z/human-skeleton-15389374.jpg

Instrumentation

- Vehicle Structural Accelerations
- 2264-2k LOFFI (40 kHz)
- 7270A-20k BOBKAT (40kHz)
- Seat frame Input and Seat Pan Accelerations
- 7270A-20k LOFFI and BOBKAT
- 7270A-20k Rigid Mount

IARV

- Injury Assessment Reference Values
- Mertz and Irwin, 1984
- Thresholds
- If not Exceeded in Prescribed Test
- Risk of Associated Injury Unlikely
- Set at Lower Bounds of Injury

RDECOM

Results Percent of IARV

TARDEC

IARV		Driver	Commander	Crew 3	Crew 5	Crew 4	Crew 6
Lumbar Spine Fz		-	-	-	110	-	-
Femur	My(R)	-	-	109	-	-	-
Femur	My(L)	-	-	115	-	-	-
Tibia Upper	Fz(R)	-	-	129	114	-	-
Tibia Upper	Fz(L)	-	-	138	101	-	-
Tibia Lower	Fz(R)	-	-	174	146	-	148
Tibia Lower	Fz(L)	-	-	175	135	-	153
Tibia Lower	My(R)	-	-	126	116	-	-
Tibia Lower	My(L)	117	101	118	-	-	-

Results

IARV	(%)
Tibia Axial Load Fz Right Lower	174
Tibia Axial Load Fz Left Lower	175

Crew 3 Comparisons

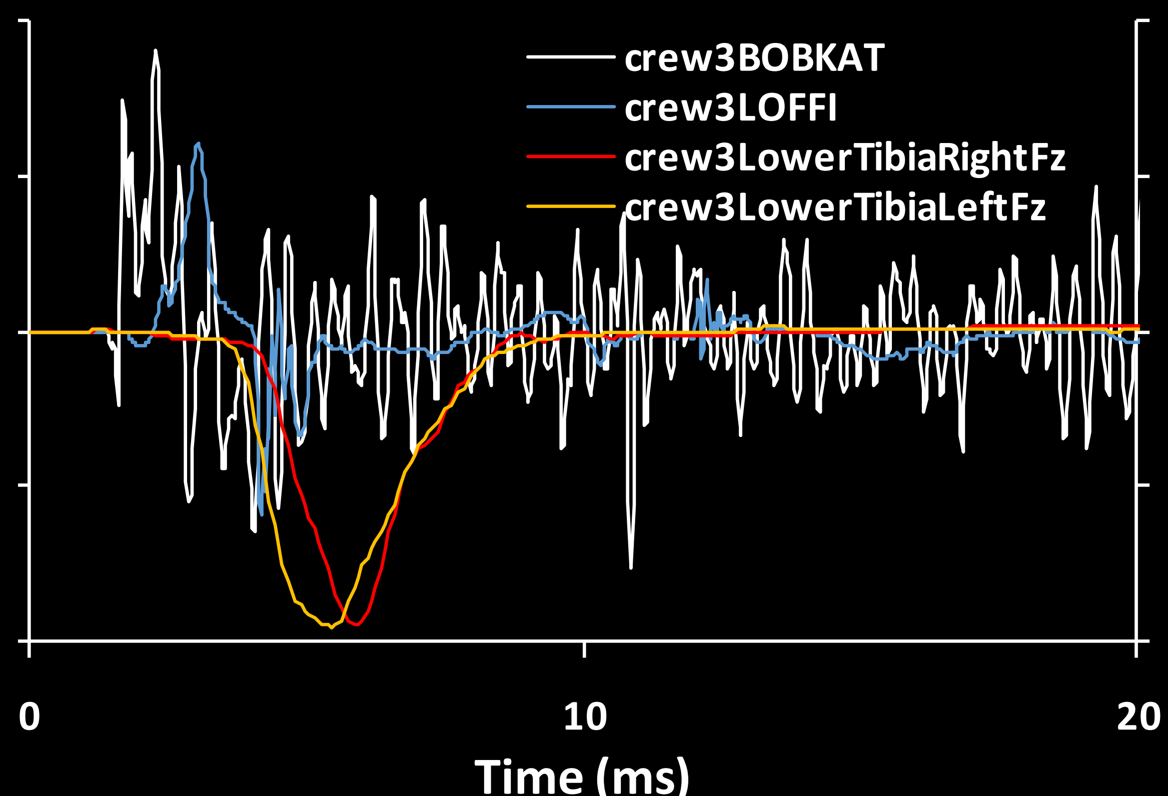

Results

IARV		(%)
Tibia Axial Load Fz	Right Lower	146
Tibia Axial Load Fz	Left Lower	135

Crew 5 Comparisons

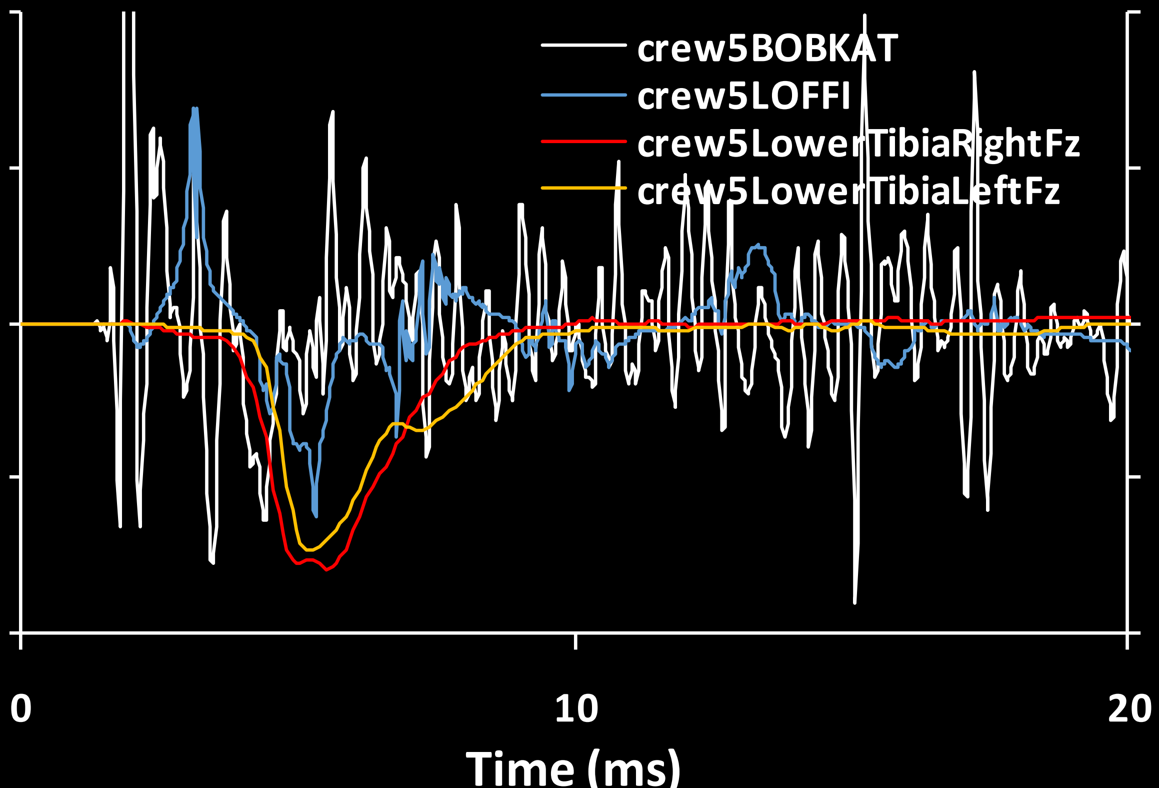

Floor versus Tibia Loads

- FITA System Simulates Cadaver Tests
- WSU Generated Compound Tibia Fractures

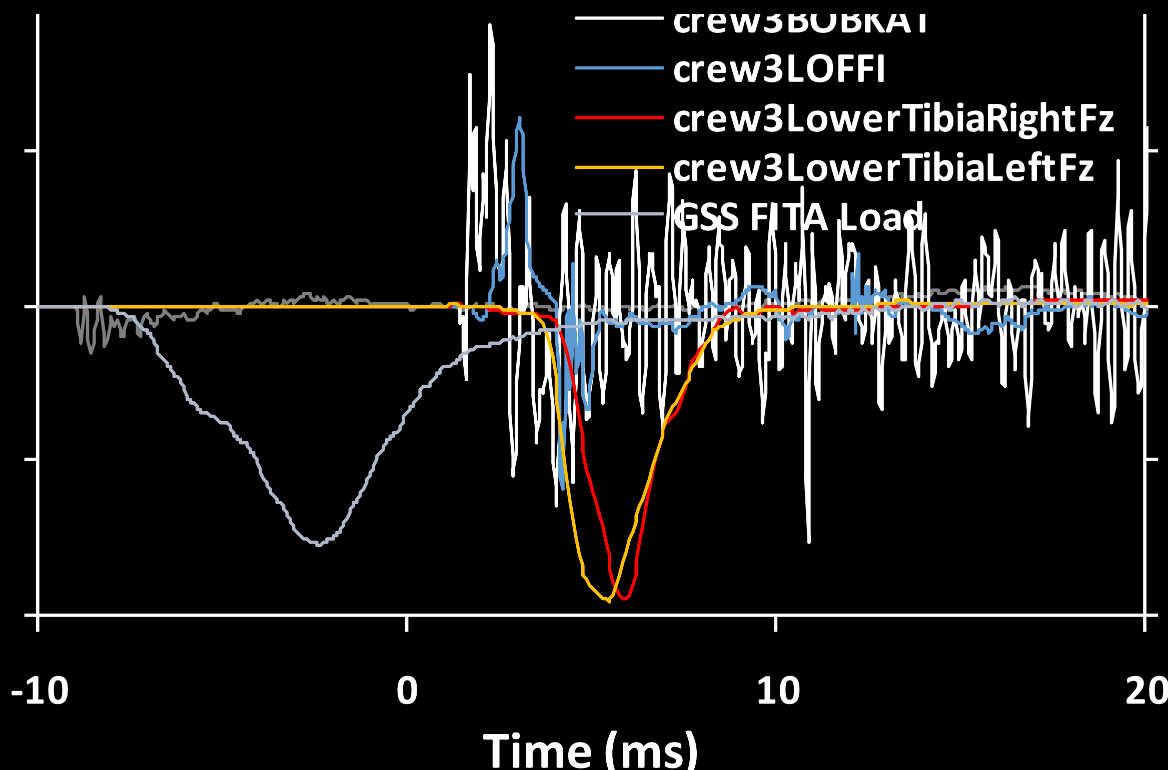

Discussion

- Comparable WIAMan Data
- Danielson et. Al. STAPP 2015
- Comprehensive Blast Loading Study
- Whole Body PMHS Paired with ATDs
- ATD Tibia Axial Loads Similar
- PMHS Fractures to Calcaneus/Talus
- Tibia Index Values >1.0

Discussion

- Tibia IARV
- Cadaver Knee Joint Bias Study
- Hirsch and Sullivan (1965)
- Tibial Plateau Fractures (Medial/Lateral)
- Mertz used the GM Impact Sled
- Efficacy of IARV Demonstrated w/HIII 50th
- Tibia Index Combines Axial Load and Moment
- Moment was Prime Injury Mechanism

Discussion

- Restrained at Ends
- Mid-Tibia Impacts
- 35 kg Impactor
- Impact Speed 3.8 m/s
- Loading Duration ~ 7.5 ms
- Failure Loads 280 Nm to 320 Nm

Tibia Bending: Strength and Response

Nyquist, G.W., Cheng, R., El-Bohy, A.A.R., King, A.I.

30th Stapp Car Crash Conference SAE 851728

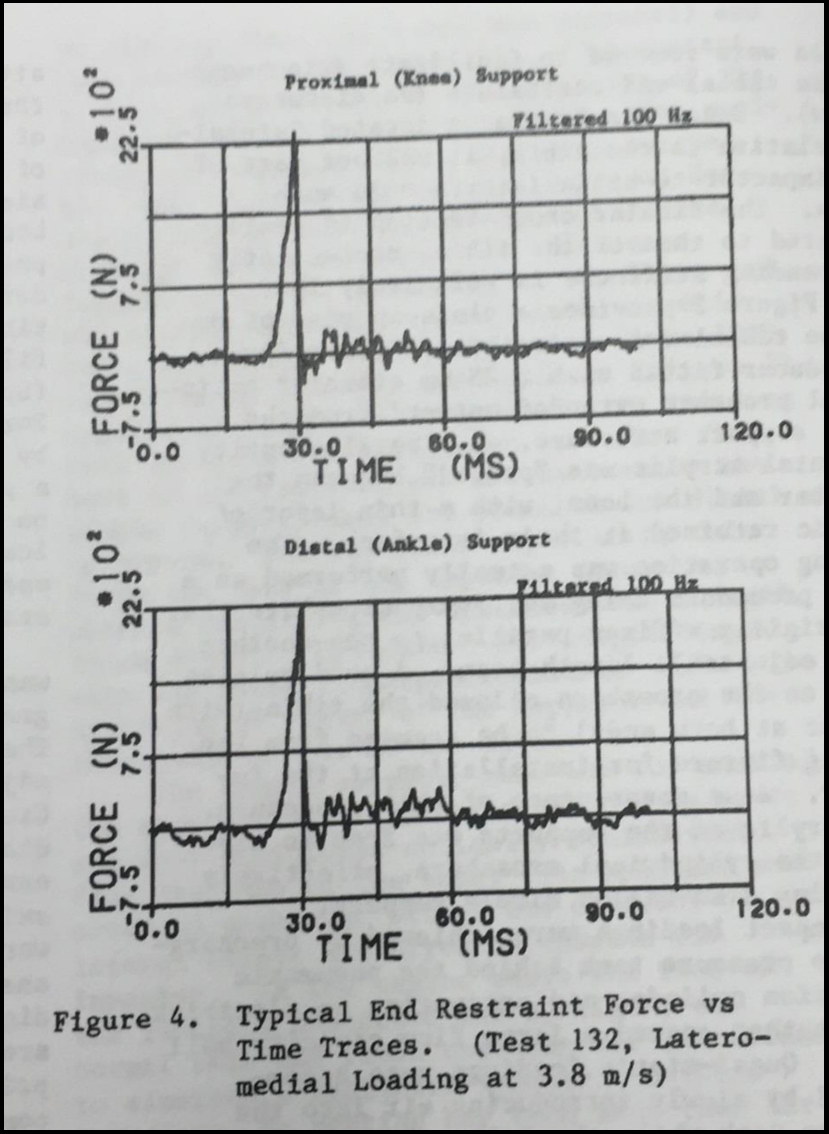

Discussion

IARV		Crew 3	Crew 5
Right Upper Tibia Axial Load	Fz (N)	129	114
Left Upper Tibia Axial Load	Fz (N)	138	101
Right Lower Tibia Axial Load	Fz (N)	174	146
Left Lower Tibia Axial Load	Fz (N)	175	135
Right Lower Tibia Moment	My (Nm)	126	116
Left Lower Tibia Moment	My (Nm)	118	98

- Axial Load Limit 8.0 kN
- 4.0 kN is Tibial Plateau Tolerance

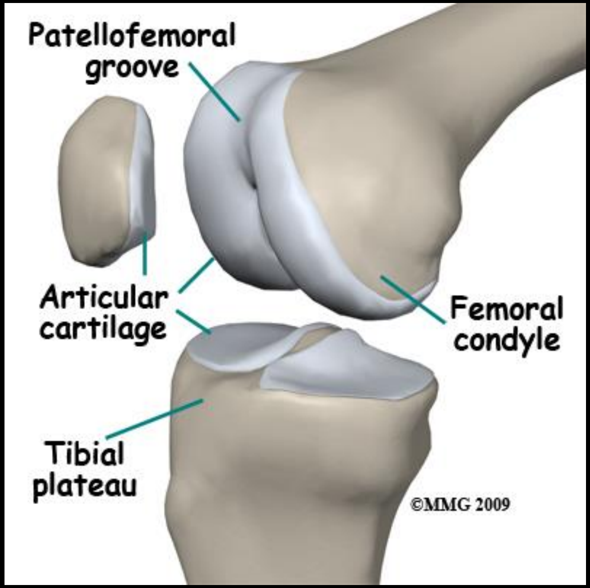

Discussion

- 50% Risk at 317 Nm
- GH3 Peak Values Under 50% Risk

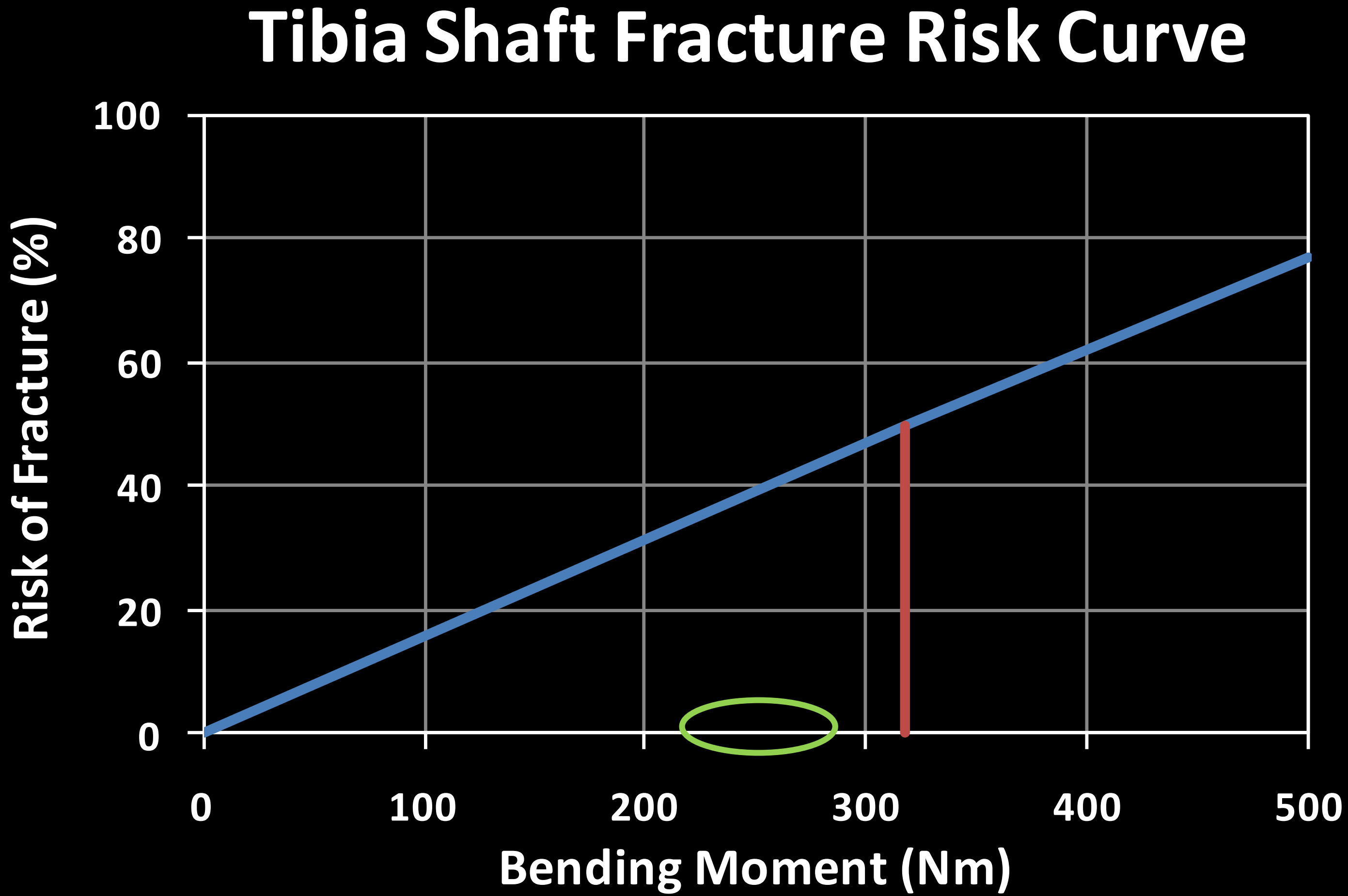

RDECOM

Discussion

TARDEC

- Injury Tolerance is Duration Dependent

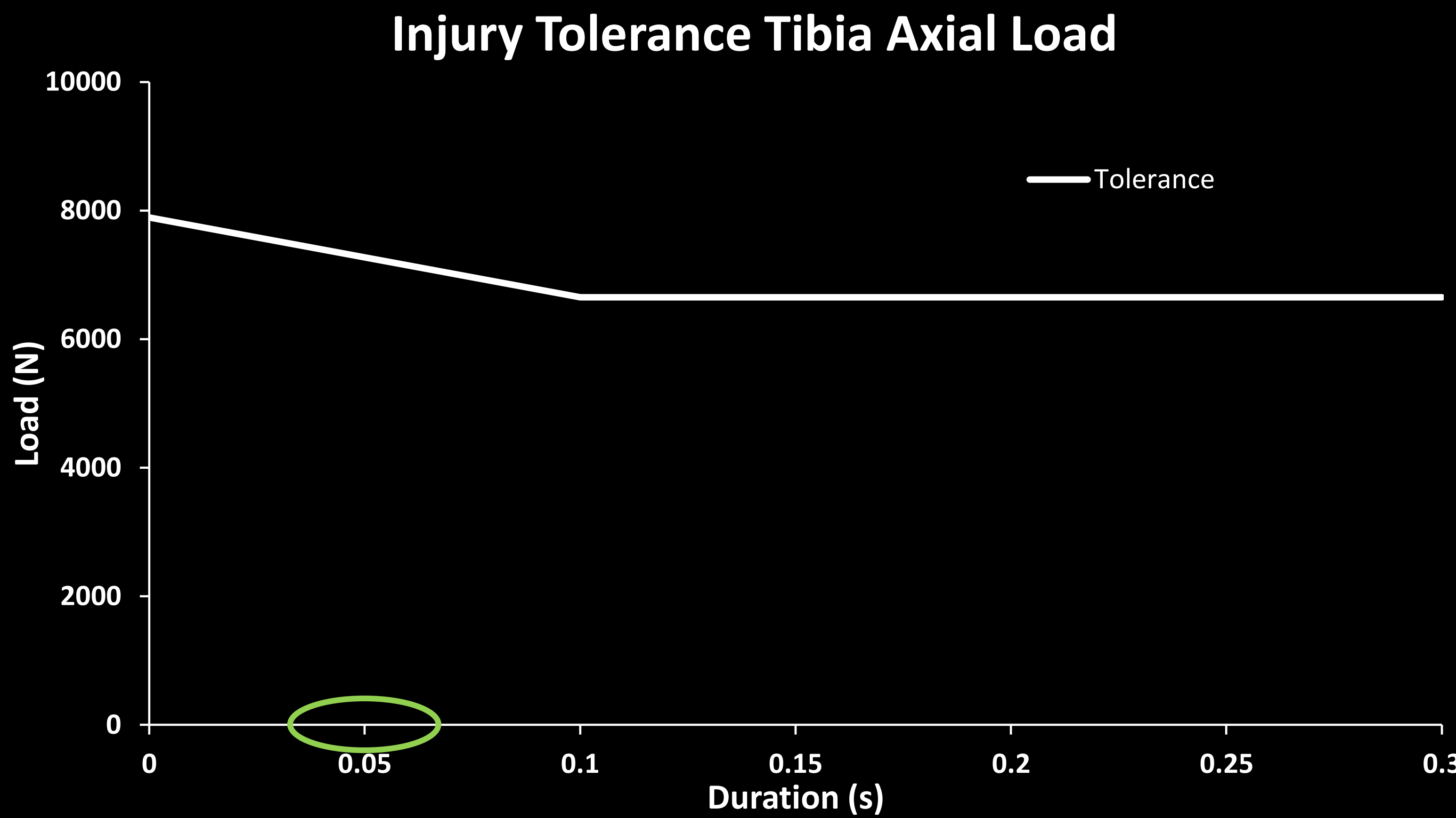

- 50th Percentile Male

TECHNOLOGY DRIVEN. WARFIGHTER FOCUSED.

Future Efforts

- Accelerometer Mounting
- Determine Appropriate Filters
- Clearer Side-by-Side Comparators
- Further Examine Response versus Inputs

RDECOM

Conclusion

TARDEC

- Data Compared to WIAMan Live Fire PMHS
- WSU Cadaver Data and OPL Laboratory Data
- IARVs Exceeded
- Applied Loads ~ 5 ms
- Highest Loads were in Lower Torso Region
- Loads Correlated with Vertical Floor Accelerations
- ATD Applicability
- Lack of Video Hampers Analysis

Thank You

21 January 2016

Ministry of Defence

The Phenomenology and Analysis of Vehicle Mine Loading

The Accelerative Loading Conference, January 2016 (ARL)

Prof Dan J Pope[1], Joe Cordell[1], Chris Taggart[4], Dr Sam Rigby[3], Dr Sam Clarke[3], Prof Andy Tyas[3], Ian Elgy[2], Matt Gant[2]

1: Dstl-Structural Dynamics

2. Dstl-Mounted Protection

3: University of Sheffield- Dept. of Civil Engineering

4: AWE-Engineering Analysis Group

Page
Intentionally
Left
Blank

VALIDATION FOR UBB NUMERICAL VEHICLE MODELS

The physical phenomena of mine/IED explosions | Piet-Jan Leerdam

UNCLASSIFIED

INTRODUCTION

- Piet-Jan Leerdam,
  - Aerospace Engineering, MSc (1987-1993)
  - Military duty: 42 BLJ, cdr YPR-765 PRI (1993-1994)
  - TNO employee since 1996
- Program manager “Protection & Survivability of land based vehicles”
- Expert in mine and IED protection evaluation
- Chairman HFM task groups on Injury Criteria for Vehicle Occupants (STANAG 4569)

INTRODUCTION

Military user with requirements

Threat

Vehicle and its protection design

Test and Qualification Procedure or Standards

OUTLINE

- Accelerative human body loads from Under Belly Blast explosions
- The local and global response effects
- The way to model the effects
- The way to validate the models
- The need for improvements on the injury assessment

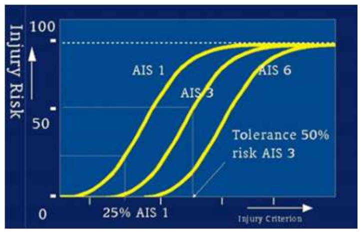

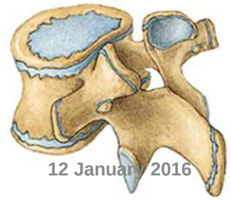

UBB LOCAL AND GLOBAL EFFECTS

Detonation

Local effects:
wheel rupture
plate deformation
shock

Global effects:
vehicle motion
crash accident

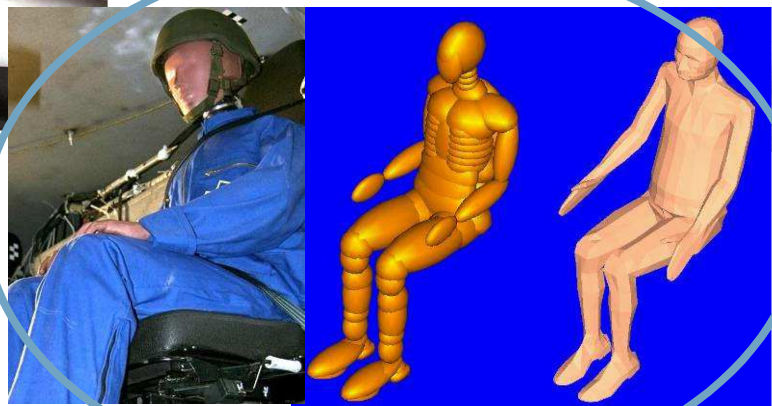

Crew

UBB LOCAL AND GLOBAL EFFECTS

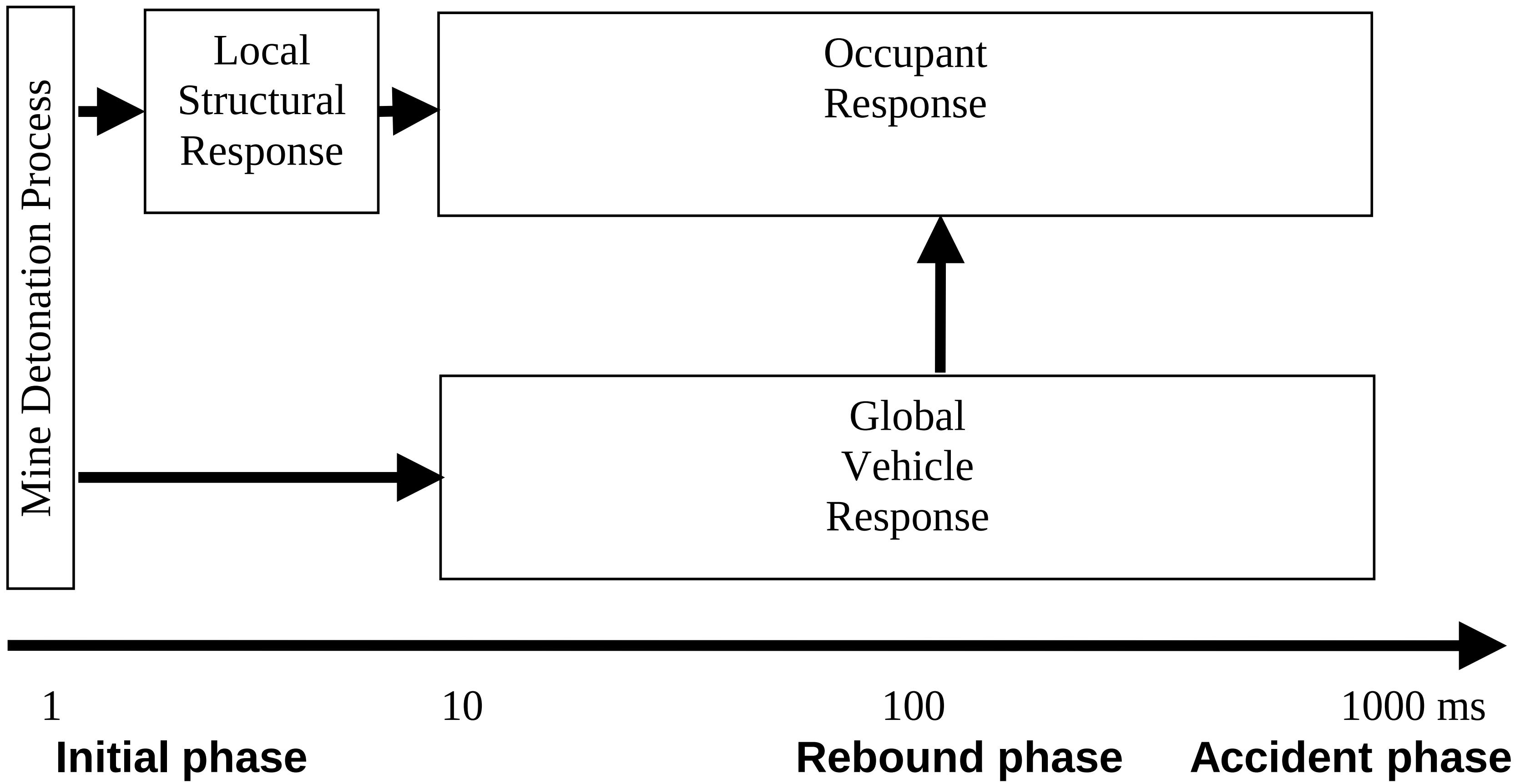

OCCUPANT RESPONSE FOR LOCAL EFFECT

Inside

- Strong local effects
- Risk of leg injury based on tibia compression criterion

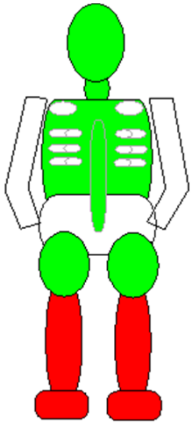

OCCUPANT RESPONSE FOR GLOBAL EFFECT

- Severe global motion
- Risk of spine injury based on Dynamic Response Index

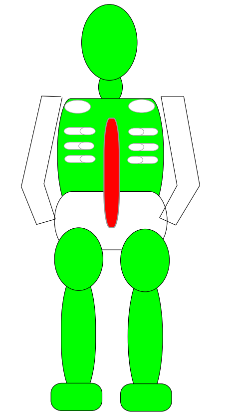

OUT-OF-CENTRE GLOBAL EFFECT

- Severe global motion resulting into flip-over of the vehicle
- High risk of spine injury based on Dynamic Response Index

SIMULATION OF UBB EFFECTS

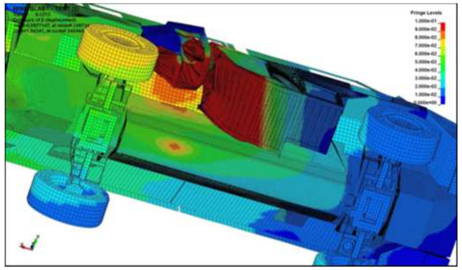

- Local response
  - Finite Element Method
- Global response
  - Analytical method
  - Multi-body method
  - Finite Element Method
- Human body response
  - Analytical method(s)
  - Multi-body method
  - Finite Element Method

Relevant simulation parameters:

- Explosive charge specifications
- Soil specifications
- Material specifications
- Vehicle structure
- Seat structure
- Spring/damper parameters
- Contact definitions
- Charge location

VALIDATION IS A MUST

KEEP IT SIMPLE

BOTTOM PLATE RESPONSE SIMULATION

- Blast model in LS Dyna:
  - Full ALE method
  - Westine model
  - TNO model

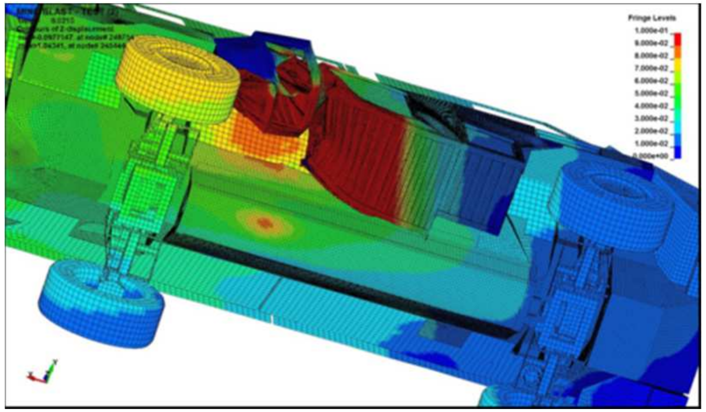

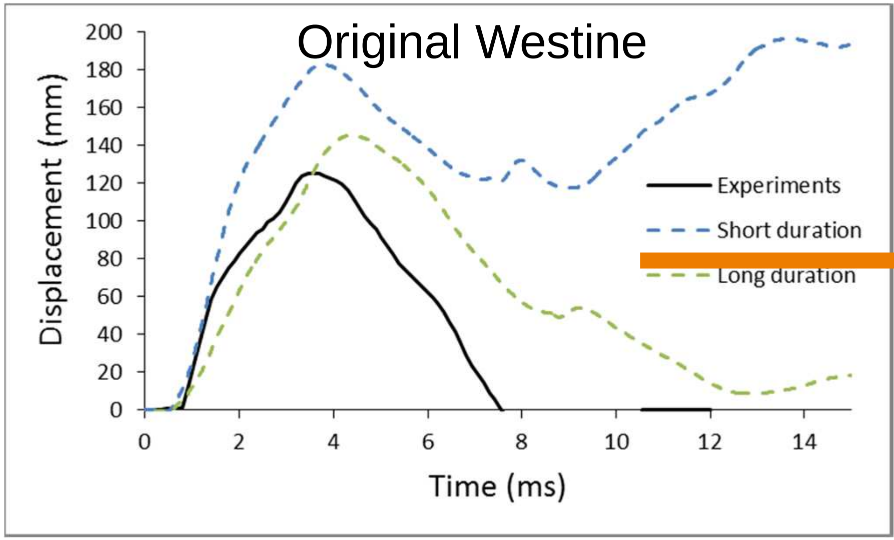

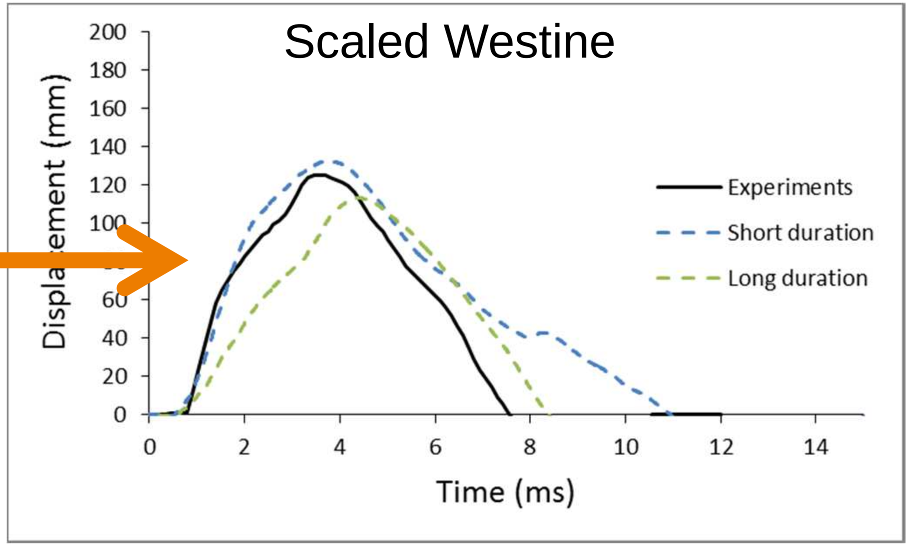

BOTTOM PLATE RESPONSE SIMULATION

- Simplified blast model
- Validation input from test rig tests
- Data base with load scenarios

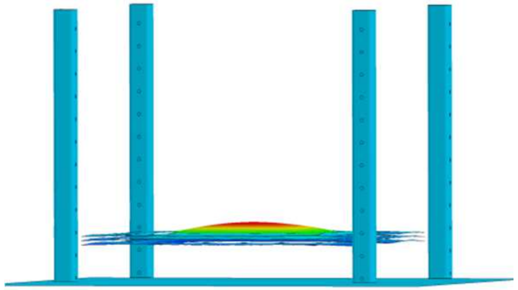

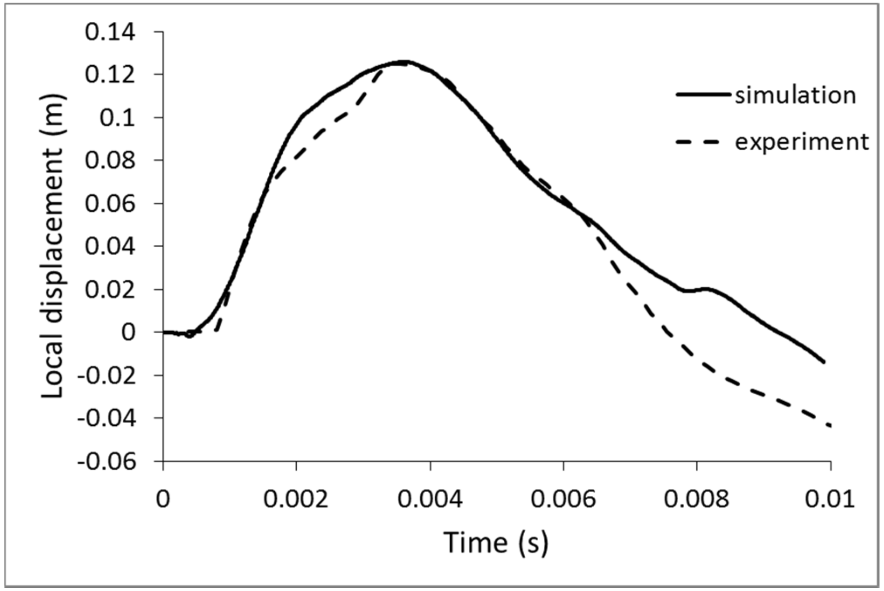

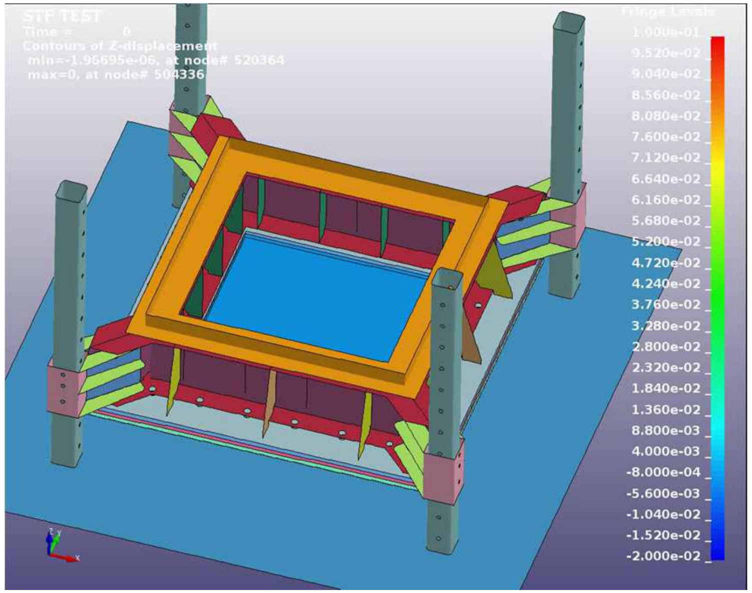

VEHICLE GLOBAL MOTION MODEL

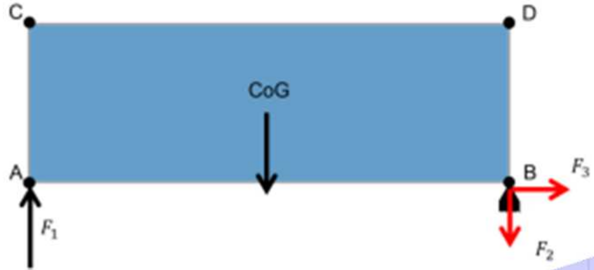

- Analytical model based on:
  - Vehicle dimensions and mass
  - Centre of Gravity and Moments of Inertia
  - Equations of Motion (3D)

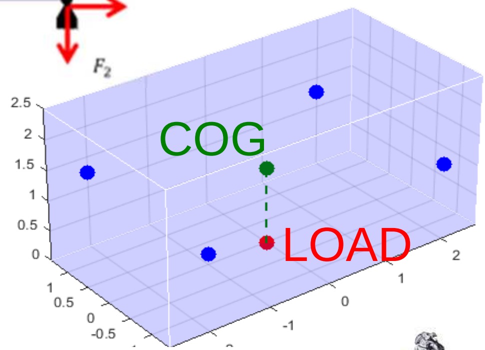

- Input:
  - Force-time for impulse value
  - At any location

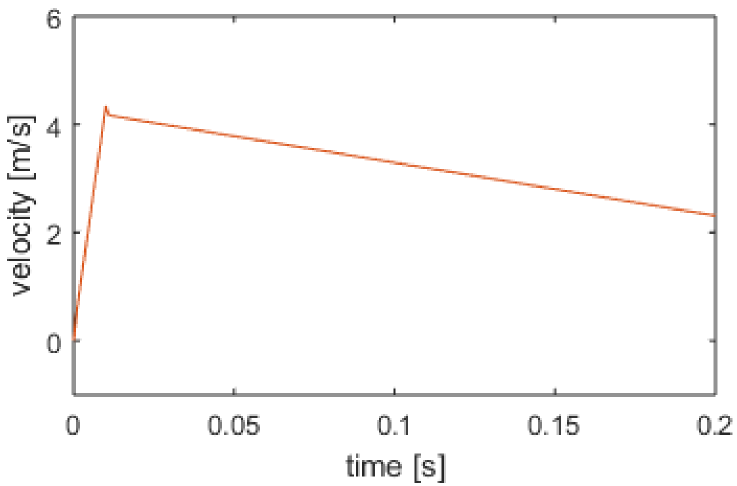

- Output:
  - Global motion/velocity
  - DRI

VALIDATION WITH TEST RIG DATA

- Test rig (TNO and Dutch MoD):
  - Simulation of a ‘vehicle’ in 10 tons range
  - Bottom plate area of 1.8x1.8 m

- Effects to be measured:
  - Local: Bottom plate deformation by 3D HS video and Digital Imaging Correlation
  - Global: Jump height by 2D HS and NS video

VALIDATION WITH TEST RIG DATA

- Different threat scenarios tested
- Normal speed and high-speed video to analyse jump height
- Impulse calculation based on jump height and total mass

VALIDATION WITH TEST RIG DATA

- 3D high-speed video
- 3D Digital Imaging Correlation
- Local response parameters, including strain information

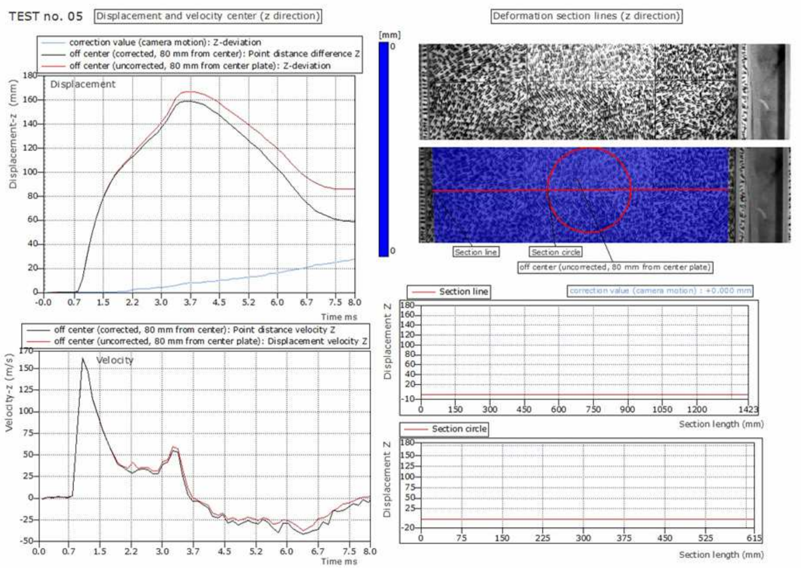

Floor plate strain

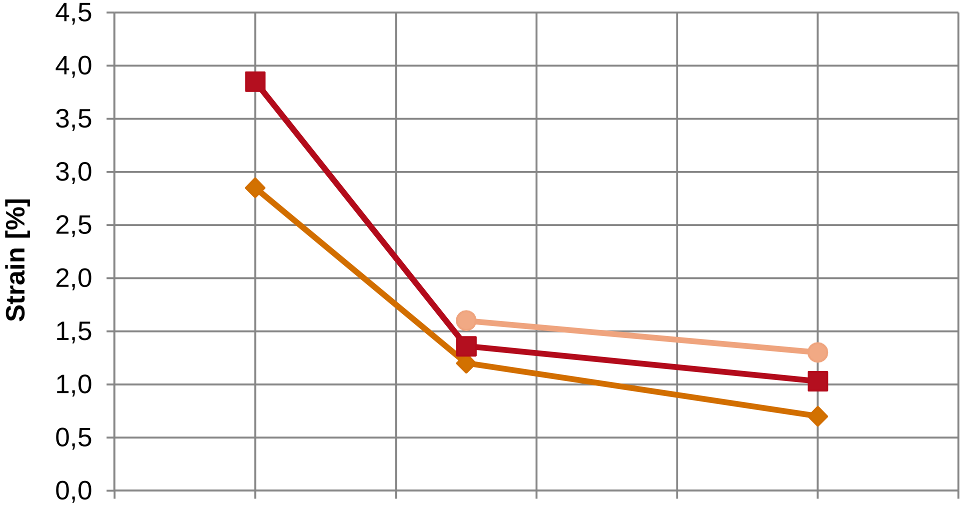

MODELS NEEDED FOR IMPROVEMENTS

Military user with requirements

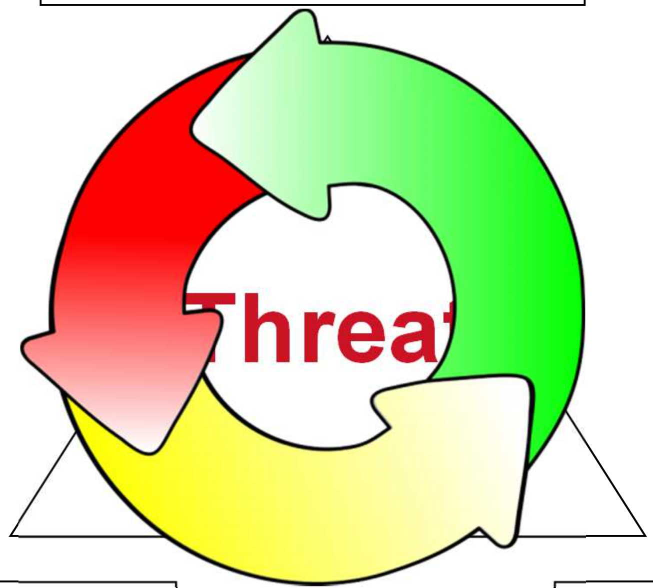

Vehicle and its protection design

Test and Qualification Procedure or Standards

- Current standard has resulted in well protected vehicles….!
- Changing threats, lighter vehicles, range in population and new (active) technologies ask for improved injury criteria and assessment methods

IMPROVEMENTS IN INJURY CRITERIA

- STANAG 4569 development:
  - HFM-090 criteria (UBB mine)
  - HFM-148 criteria (IED: both UBB and RS)
  - HFM-198: no update, only information

Body region/criterion	10% risk on AIS2 injuries
Lower leg: •Lower tibia axial force	5.4 kN
Spine: •DRIz	17.7
Neck: •Axial compression force •Bending moment	4 kN @ 0 ms 1.1 kN @ 30+ ms 190 Nm flexion 57 Nm extension
Gas filled organs: •Chest Wall Velocity Predictor	3.6 m/s

- New HFM-working group: HFM-271
  - 2016-2018
  - Improvement of current criteria
  - Improvement of current tools (ATD)

Body region	IARV	Pass/fail level (10% AIS2+)
Head	HIC_{15}	250
Neck (upper load cell)	Fz- Fz+ Fx+- and Fy+- My+ My-	4.0 kN @ 0 ms / 1.1 kN > 30 ms 3.3 kN @ 0 ms / 2.8 kN @ 35 ms / 1.1 kN > 60 ms 3.1 kN @ 0 ms / 1.5kN @ 25-35 ms / 1.1 kN > 45 ms 190 Nm 96 Nm
Thorax	$TCC_{frontal}$ $VC_{frontal}$	30 mm 0.70 m/s
Spine	DRI_z	17.7
Upper legs	Fz-	6.9 kN
Lower legs	Fz-	2.6 kN (Mil-Lx leg upper load cell) *5.4 kN (Denton leg lower load cell)*

IMPROVEMENTS IN INJURY CRITERIA

Body region (Hybrid III)	IARV	Pass/fail level (10% AIS2+)
Head	HIC_{15}	250
Neck (upper load cell)	Fz- Fz+ Fx+- and Fy+- My+ My-	4.0 kN @ 0 ms / 1.1 kN > 30 ms 3.3 kN @ 0 ms / 2.8 kN @ 35 ms / 1.1 kN > 60 ms 3.1 kN @ 0 ms / 1.5kN @ 25-35 ms / 1.1 kN > 45 ms 190 Nm 96 Nm
Thorax	$TCC_{frontal}$ $VC_{frontal}$	30 mm 0.70 m/s
Spine	DRI_z	17.7
Upper legs	Fz-	6.9 kN
Lower legs	Fz-	2.6 kN (Mil-Lx leg upper load cell) *5.4 kN (Denton leg lower load cell)*

IMPROVEMENTS IN INJURY CRITERIA

Body region (ES-2re ATD)	**IARV**	**Pass/fail level (10% AIS2+)**
Head	HIC_{15}	250
Neck (upper load cell)	Fz +	1.8 kN
Shoulder	Fy	1.4 kN
Thorax	$RDC_{lateral}$ $VC_{lateral}$	28 mm 0.58 m/s
Abdomen	F_{total}	1.8 kN
Spine	DRI_z	17.7
Pelvis	Fy	2.6 kN
Lower legs	Fz	2.6 kN (Mil-Lx upper load cell) *5.4 kN (Denton leg lower load cell)*

IMPROVEMENTS IN INJURY CRITERIA

- Criteria and assessment methods for:
  - Different body postures
  - Occupant sizes: 5/50/95%
  - Occupants with/without Personal Protective Equipment (PPE)

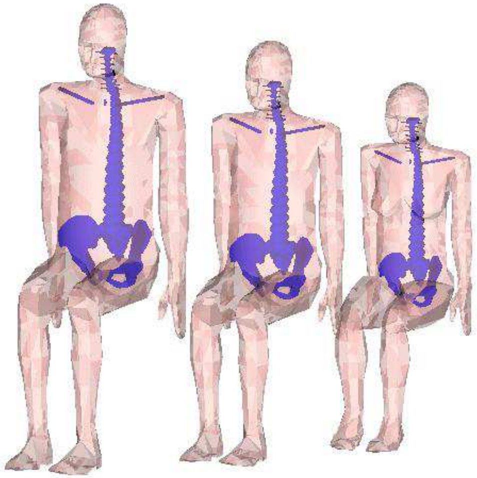

- Assessment methods applied to:
  - New seat types
  - Active seat damper systems
  - Airbag solutions
  - Lift-off, drop-down, accidental phase

FINAL REMARKS

- Current protection technologies and qualification standards have resulted in well protected vehicles against both the mine and IED threat;
- For future steps, new and/or improved injury assessments methods are needed;
- Analytical and numerical models for prediction of acceleration effects needed to improve injury assessment methods;
- Models only useable after correct validation based on experimental research with appropriate test rigs.

THANK YOU FOR YOUR ATTENTION

Piet-Jan Leerdam
TNO Defence
PO Box 45, 2280 AA Rijswijk
The Netherlands
Piet-jan.leerdam@tno.nl
+31 88 86 61290

UNCLASSIFIED

Comparison of ATD to PMHS Response in the Under-Body Blast Environment

Kerry A. Danelson, Andrew R. Kemper, Matthew J. Mason, Michael Tegtmeyer, Sean A. Swiatkowski (USN), John H. Bolte IV, and Warren N. Hardy

2nd Workshop on Numerical Analysis of Human and Surrogate Response to Accelerative Loading
12 JAN 2016
Aberdeen Proving Ground

Wake Forest School of Medicine
ARL
The Ohio State University
VirginiaTech

Introduction

- Over 2 million service members deployed to OIF, OEF
- Limited military injury epidemiology
  - 80% of WIA injuries were to lower extremities (Owens 2008)
- Underbody blast (UBB)
  - Skeletal and ligamentous (Alvarez 2011, Ramasamy 2011)

T+: +3.365 ms

Introduction

- Previous Vertical Loading
  - Eiband (1959): ejection seat tolerance
  - Stapp (1964): human volunteers and bears in caudal to cranial loading
  - King (1975): damage to the spine resulting from caudocephalad acceleration
  - Myklebust et al. (1983): tolerance of the PMHS spine to axial compression
  - Paskoff (2004), Bass (2006): helicopter crash loading

Stapp 1964, "Trauma caused by impact and blast"

APPROVED FOR PUBLIC RELEASE // DISTRIBUTION UNLIMITED

Objectives

Explore and identify focus areas of human response and mechanisms of injury in an under-body blast environment.

Conduct paired-comparison tests of whole-body cadavers and ATDs in an explosive-driven, vertical environment relevant to military testing.

Provide foundational information to the WIAMan medical research effort.

APPROVED FOR PUBLIC RELEASE // DISTRIBUTION UNLIMITED

Methods

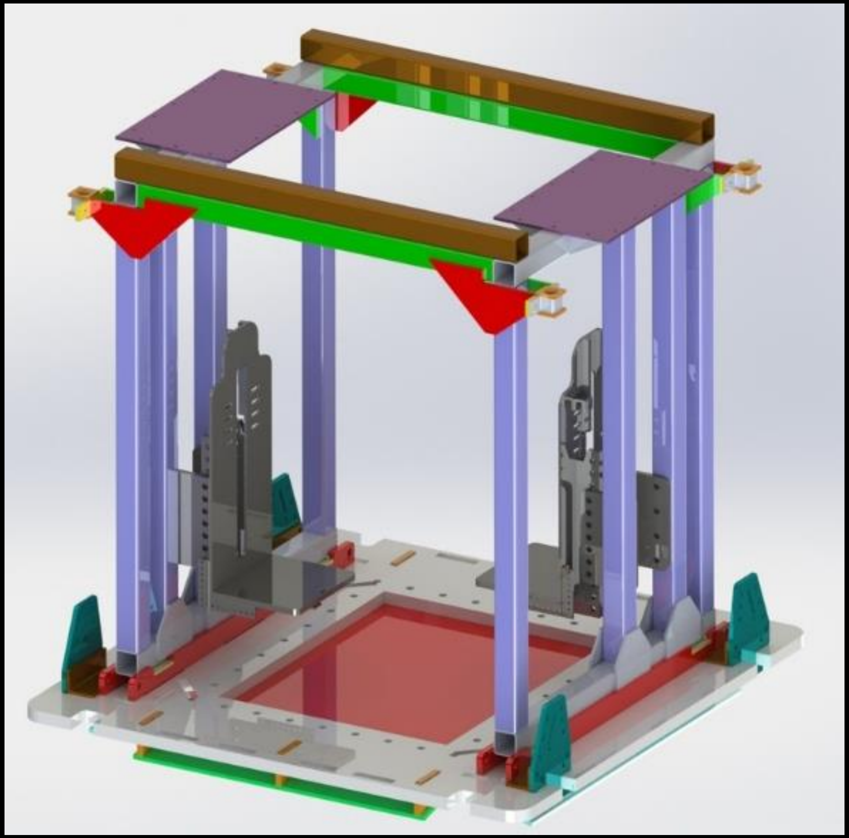

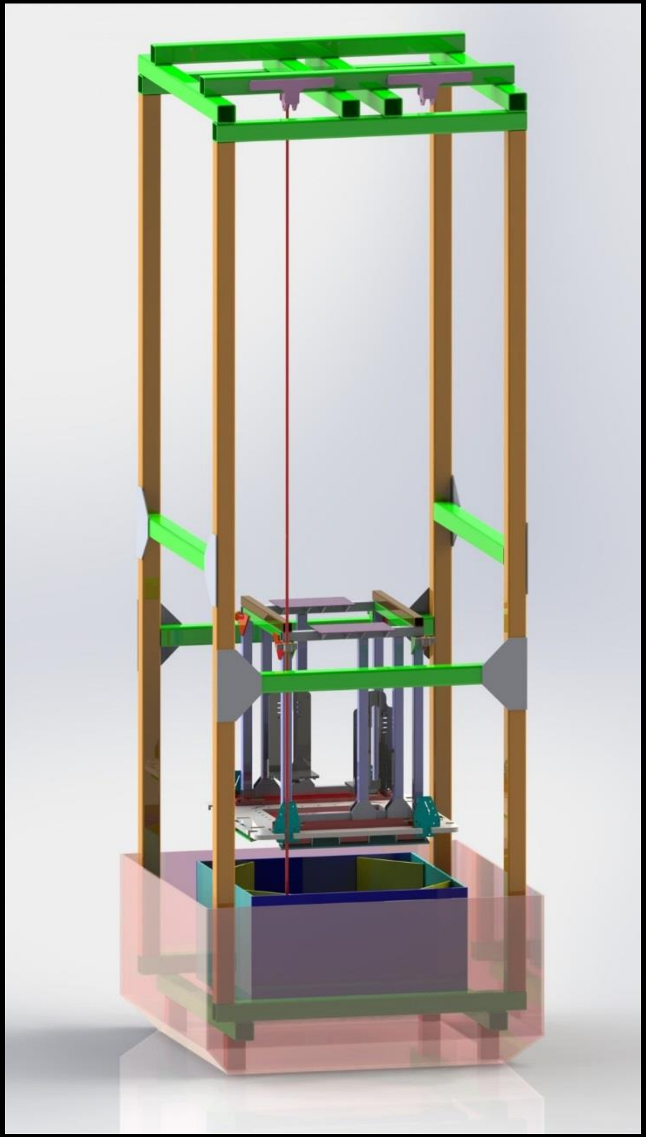

APPROVED FOR PUBLIC RELEASE // DISTRIBUTION UNLIMITED

Test Matrix

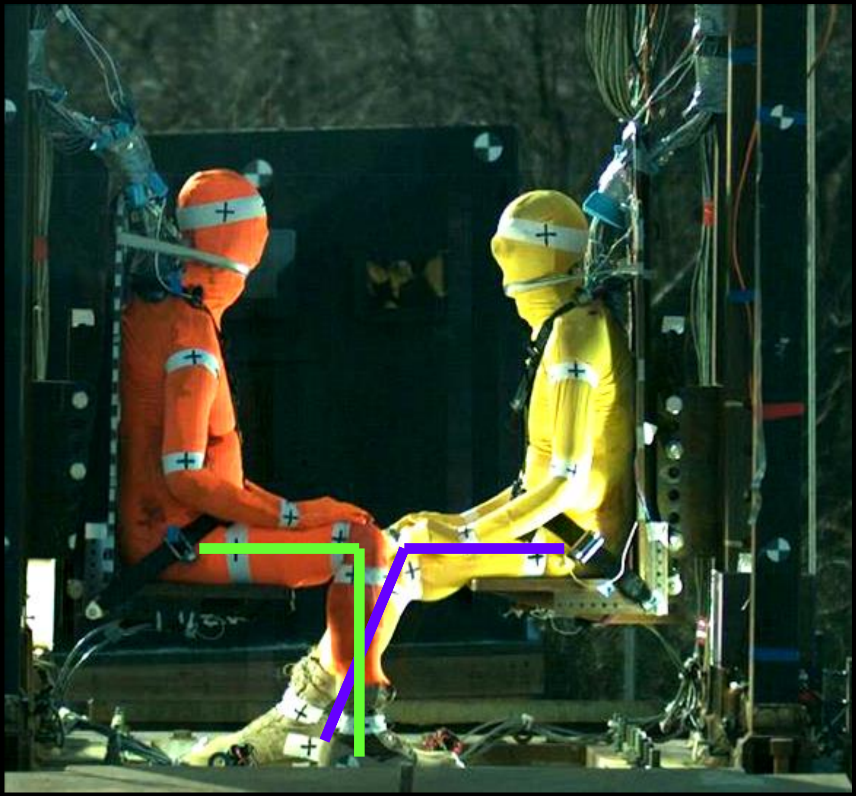

Posture

PPE

Test Matrix

Matrix Shot #	Crew #	Crew Type: PMHS	Crew Type: ATD	Posture: Nom	Posture: Obt	PPE: Y	PPE: N	Level
1	1	X		X			X	Enh
	2		X	X			X	
2	1	X			X		X	Enh
	2		X		X		X	
3	1		X	X		X		Enh
	2		X	X			X	
4	1	X		X			X	Enh
	2	X			X		X	
5	1	X		X		X		Enh
	2	X		X			X	
6	1	X			X	X		Enh
	2	X			X		X	
7	1	X		X		X		Enh
	2	X			X	X		

Test Matrix

Matrix Shot #	Crew #	Crew Type PMHS	Crew Type ATD	Posture Nom	Posture Obt	PPE Y	PPE N	Level
8	1		X	X			X	Mild
	2		X		X		X	
9	1		X	X		X		Mild
	2		X	X			X	
10	1		X		X	X		Mild
	2		X		X		X	
11	1	X		X			X	Mild
	2	X			X		X	
12	1		X	X		X		Mild
	2		X		X	X		
13	1		X	X		X		Enh
	2		X		X	X		
14	1	X		X			X	Mild
	2	X			X	X		

APPROVED FOR PUBLIC RELEASE // DISTRIBUTION UNLIMITED

Instrumentation

- DAS:
  - TDAS Pro, 64 channels, 20,000 sps with 4,300-Hz cutoff, 8th order Butterworth profile, low pass filters
  - DTS G5, 32 channels, 100,000 sps with 30-kHz cutoff, 8th order Butterworth profile, low-pass filters

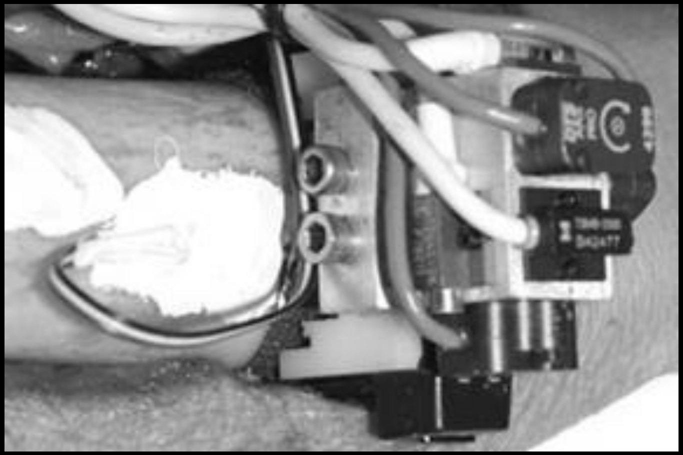

Distal Femur Motion Block

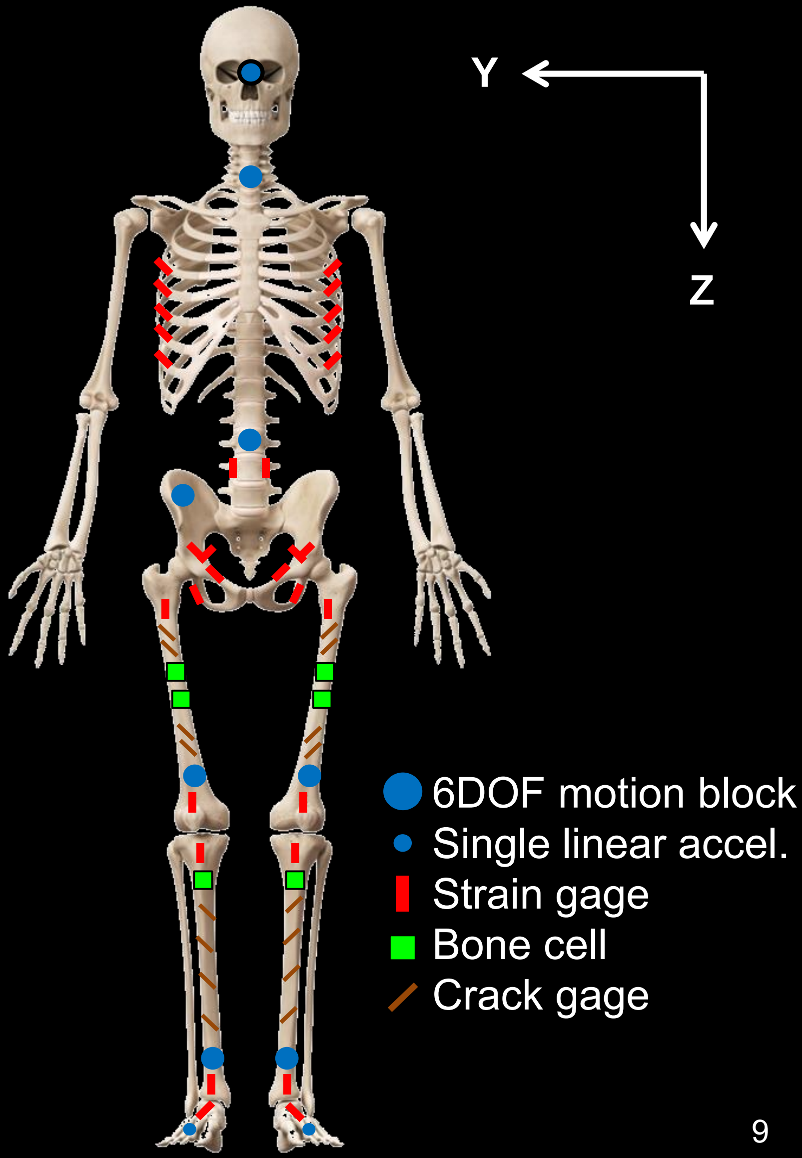

APPROVED FOR PUBLIC RELEASE // DISTRIBUTION UNLIMITED

Data Processing

- Over 1300 PMHS data channels and 750 ATD and structural channels were collected
  – Filtering: SAE J211 CFC 1000
  – Large spikes were removed (due to cable pulls, etc.)
  – Short-duration, low amplitude spikes were left
  – Transformation aligned the signals with the anatomical coordinate system

APPROVED FOR PUBLIC RELEASE // DISTRIBUTION UNLIMITED

Data Analysis

- Resultants and velocities were calculated for acceleration signals
- Time to Peak (TTP) point clouds
  - Start time was the onset of foot motion
- CORA Analysis (Gehre 2011)
  - CORA release 3.6
  - Outer corridor 0.25 (Thunert, 2012)
  - PMHS - reference curve
  - Crew and rig comparisons

APPROVED FOR PUBLIC RELEASE // DISTRIBUTION UNLIMITED

Results Outline

- Overall blast buck performance
- PMHS damage
- PMHS body region timing
- ATD to PMHS comparison
  – Qualitative kinematic comparison
  – CORA similarity analysis

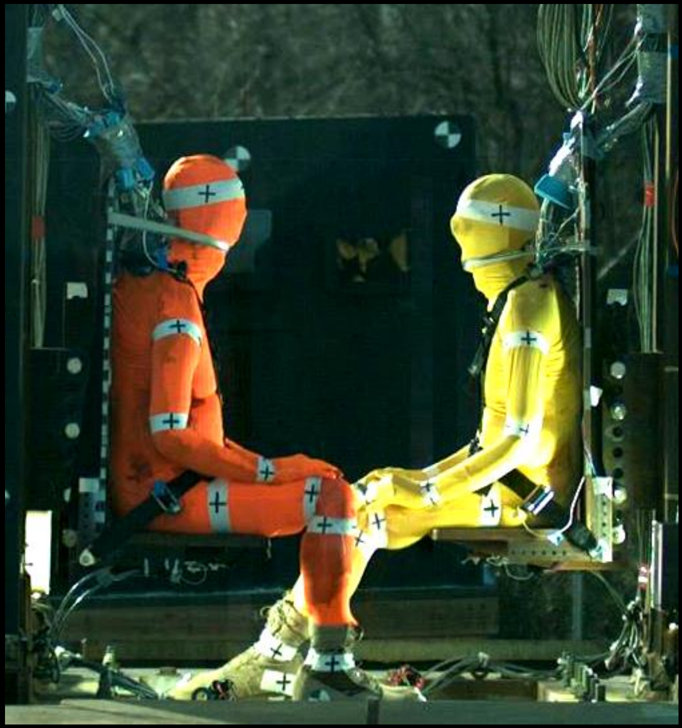

APPROVED FOR PUBLIC RELEASE // DISTRIBUTION UNLIMITED

Results

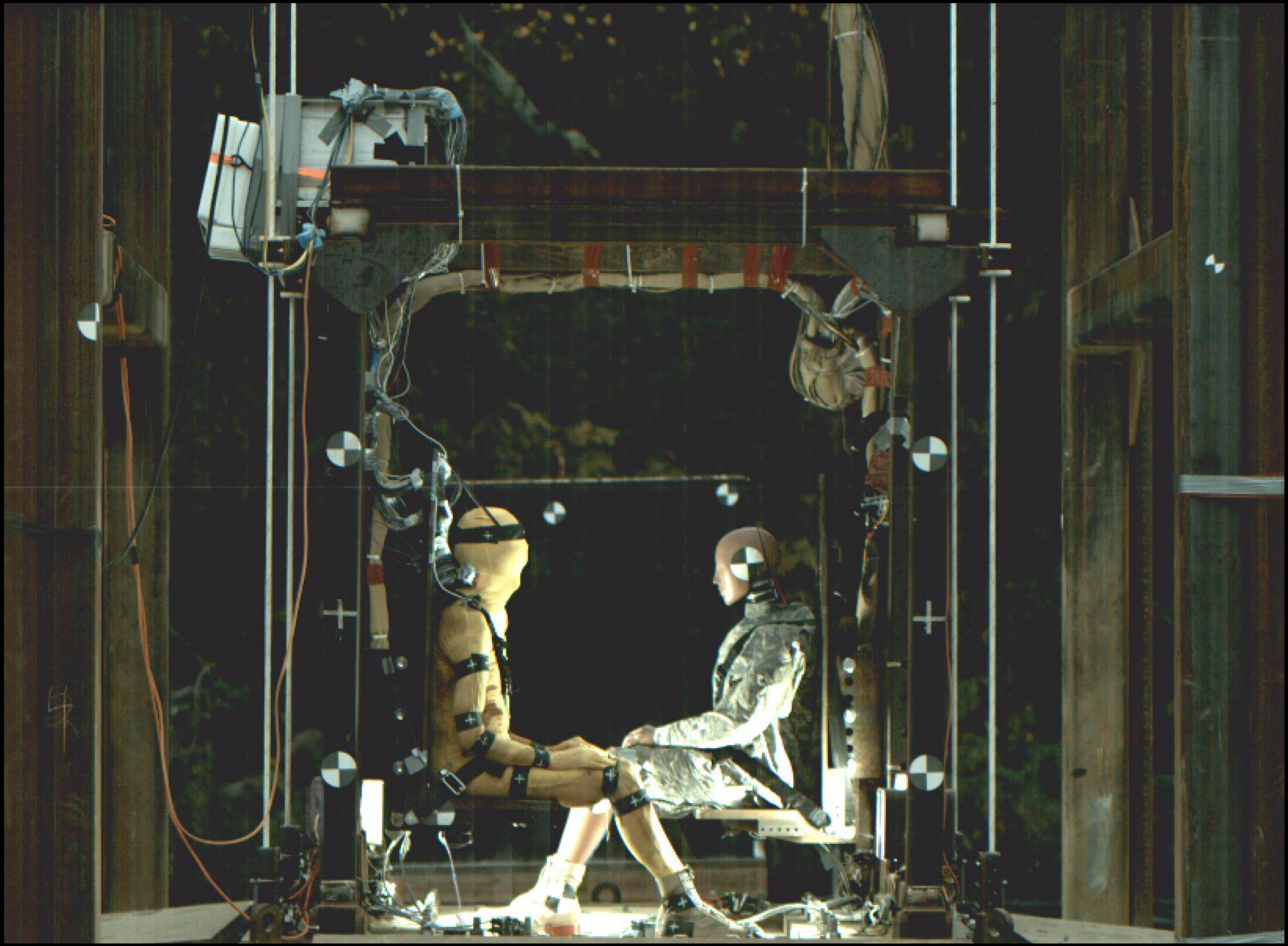

APPROVED FOR PUBLIC RELEASE // DISTRIBUTION UNLIMITED

PMHS Damage

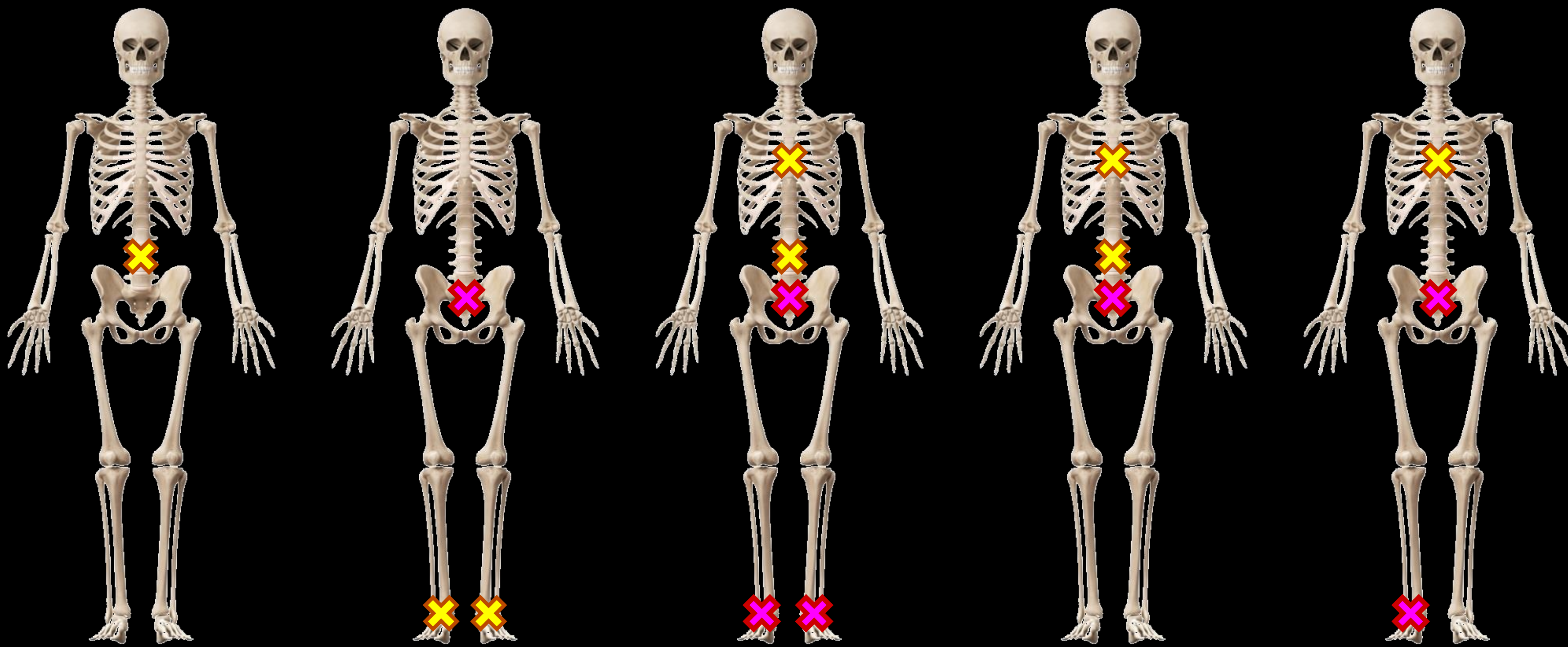

MS 1, C1 | MS 2, C1 | MS 4, C1 | MS 4, C2 | MS 5, C1

Minor Damage (not operationally relevant, i.e. transverse process fx)

Major Damage

PMHS Damage

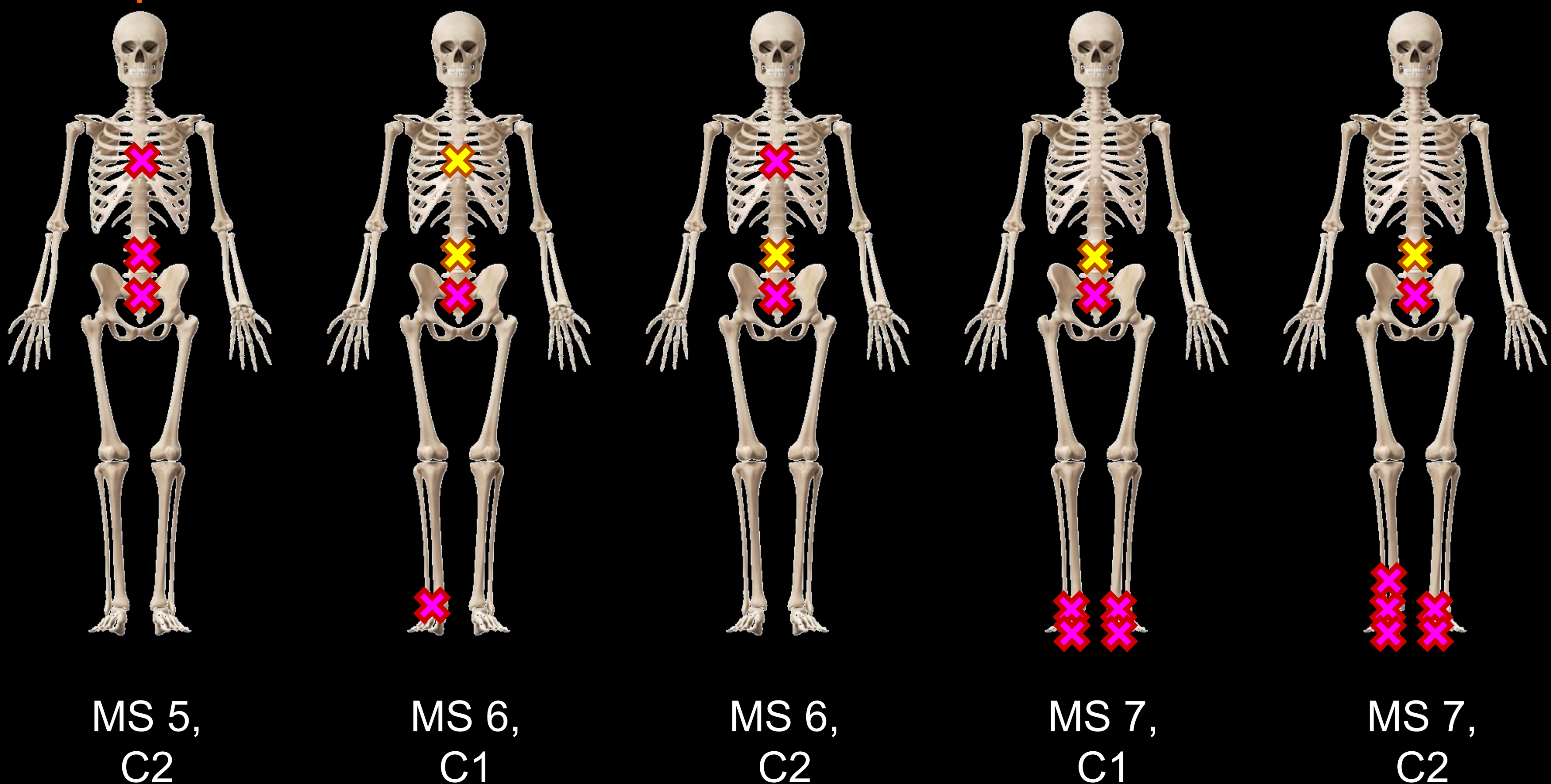

Minor Damage (not operationally relevant, i.e. transverse process fx)

Major Damage

APPROVED FOR PUBLIC RELEASE // DISTRIBUTION UNLIMITED

Pelvis Damage

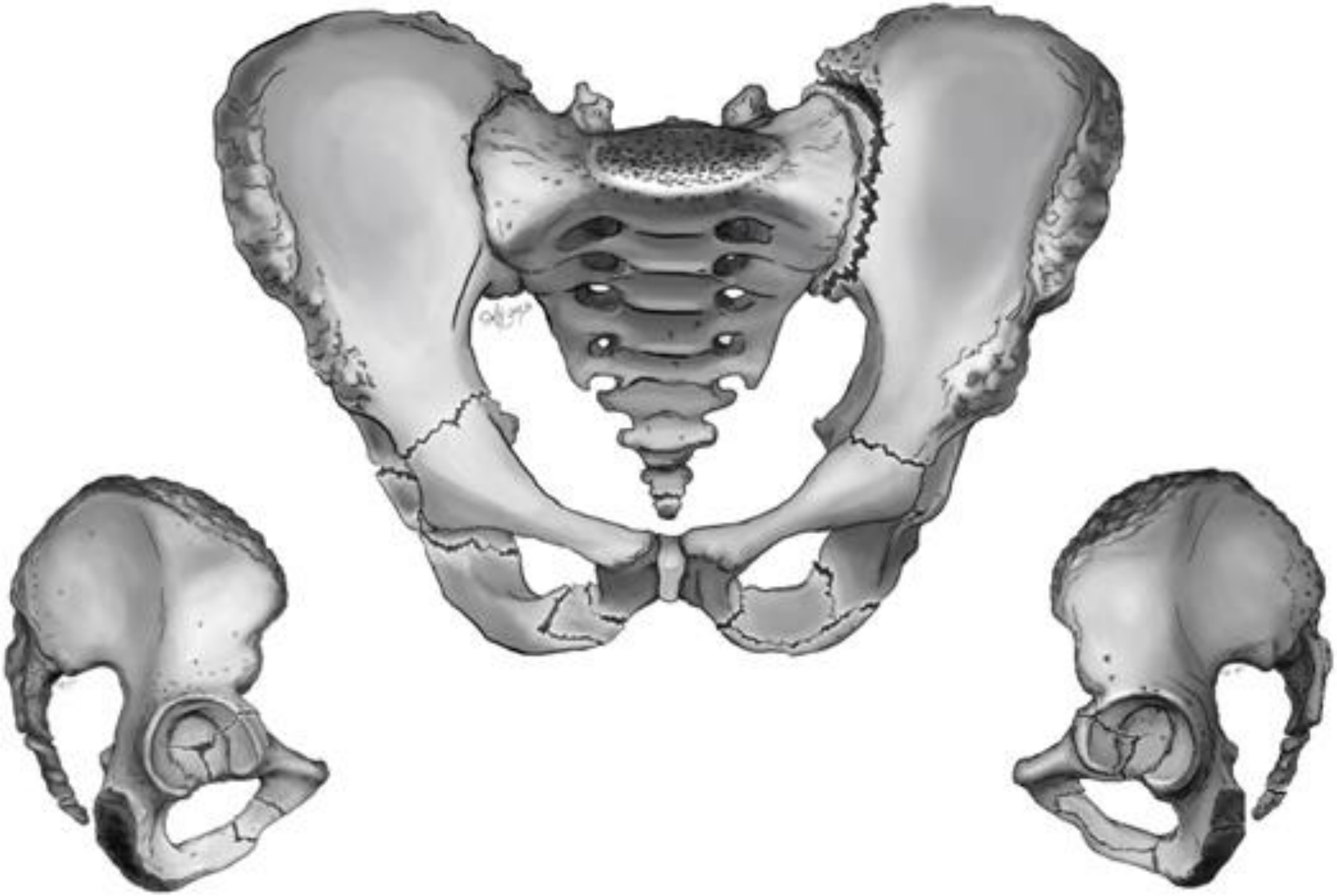

APPROVED FOR PUBLIC RELEASE // DISTRIBUTION UNLIMITED

AFME Injury Description

- Damage is indicative of horizontal Input
- Pelvis fractures in the absence of lumbar spine injury
  - In the real-world experience the L-spine fractures before the pelvis
- Acetabulum and femoral neck damage patterns
  - In testing and the real world: acetabulum fx with no damage to the femoral head and neck
  - In the real world: femoral neck fx with out acetabulum fx
  - In the real world: femur fx from axial or lateral femur loading

Tibia, Talus Damage

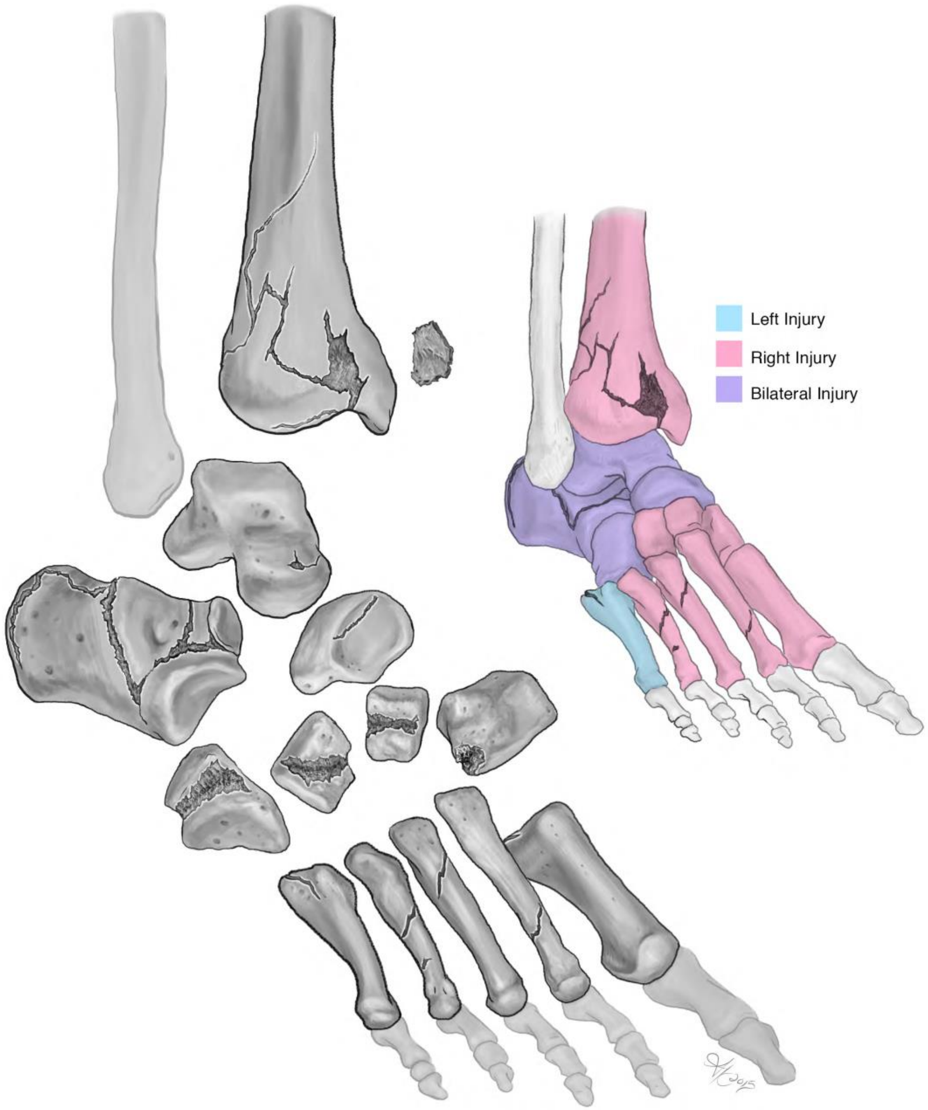

AFME Injury Description

- Tibia
  - One fracture, obtuse condition
  - Tibia injury is seen in real world cases
  - Influence of foot rotation, or the importance of contact duration vs. initial posture
- Talus
  - Chips (MS 7) and one neck fracture (MS 11)
  - High levels of intrusion associated with overmatch condition
  - Neck fracture in a mild test – influence of contact duration and loading rate?

PMHS Damage, Rig Revised

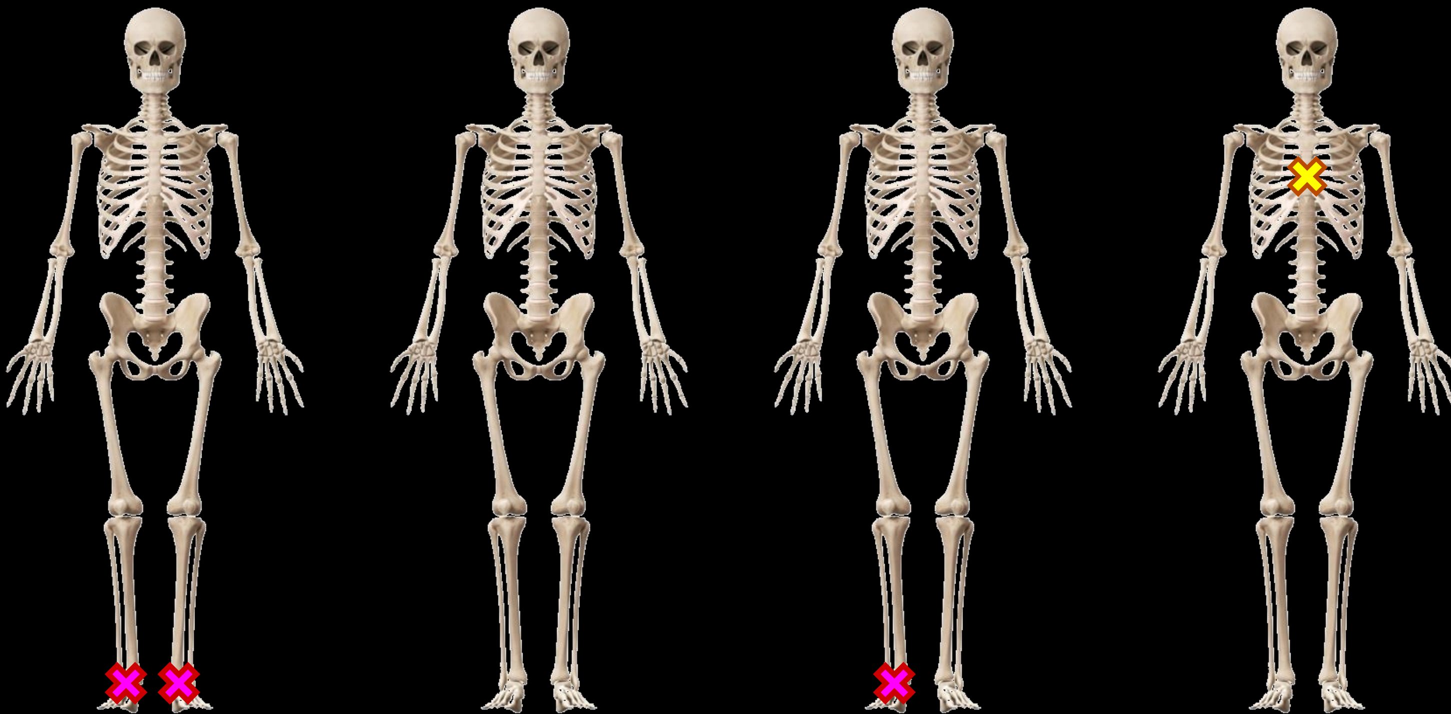

MS 11, C 1 | MS 11, C 2 | MS 14, C 1 | MS 14, C2

Minor Damage (not operationally relevant, i.e. transverse process fx)

Major Damage

APPROVED FOR PUBLIC RELEASE // DISTRIBUTION UNLIMITED

Calcaneus Damage

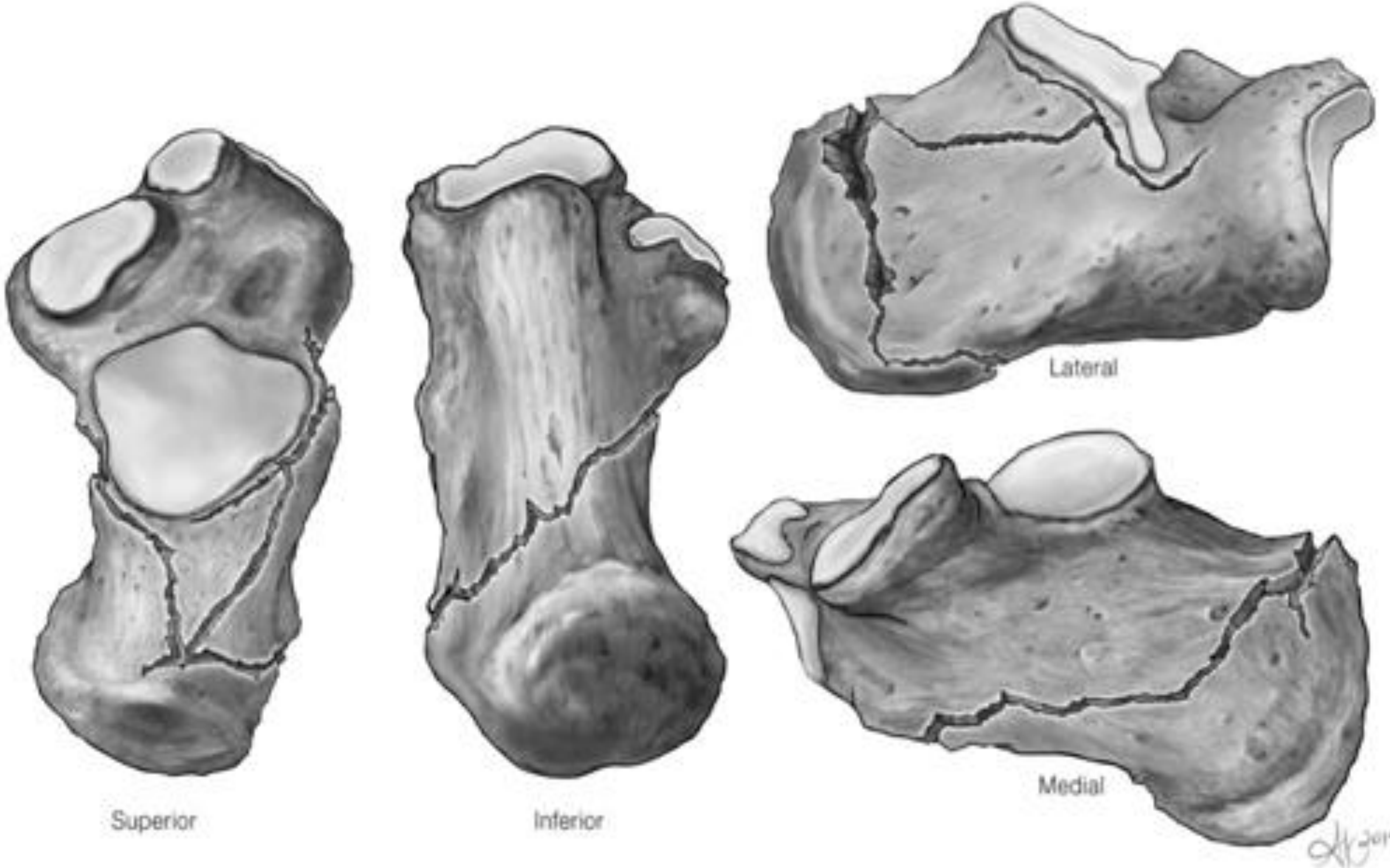

AFME Injury Description

- Calcaneus
  - Damaged approximately ¼ of the time
  - Outboard extremity most frequently damaged
  - Large floor deformation = bilateral
  - Non-displaced fx in testing
  - Mimics the real world experience

APPROVED FOR PUBLIC RELEASE // DISTRIBUTION UNLIMITED

Whole-Body Velocities (MS11)

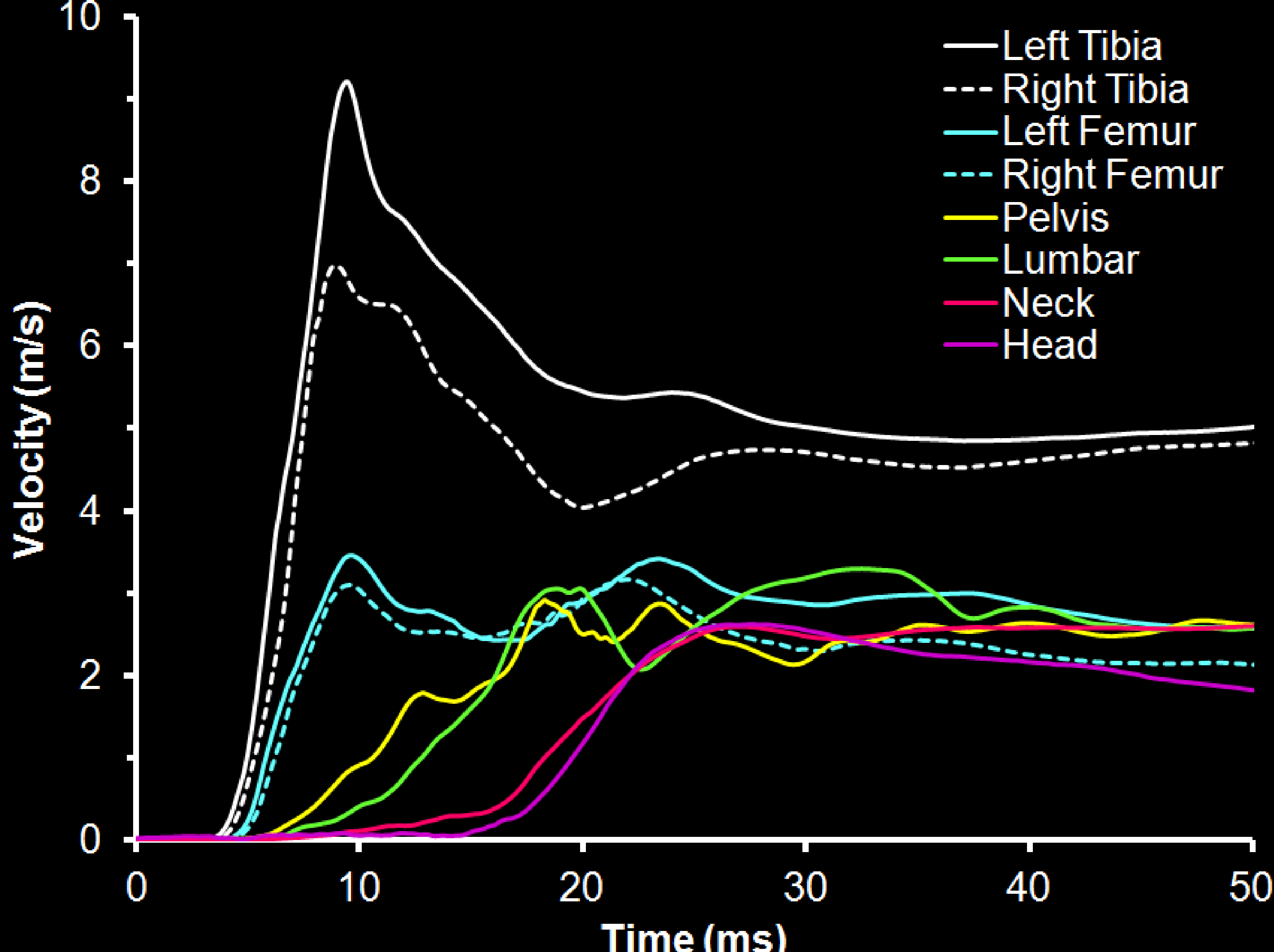

APPROVED FOR PUBLIC RELEASE // DISTRIBUTION UNLIMITED

Whole-Body Accel. (MS11)

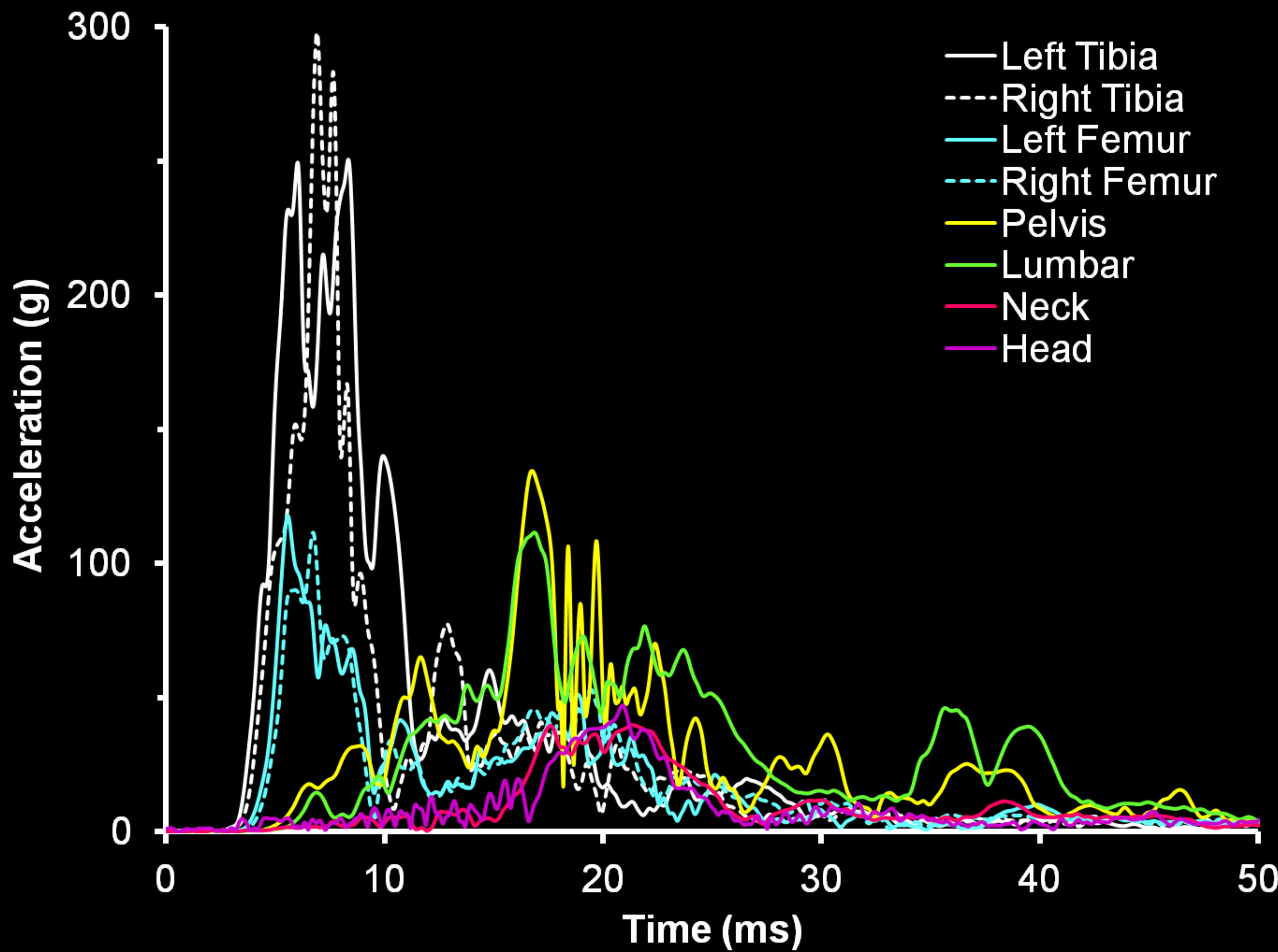

Signal Start Times

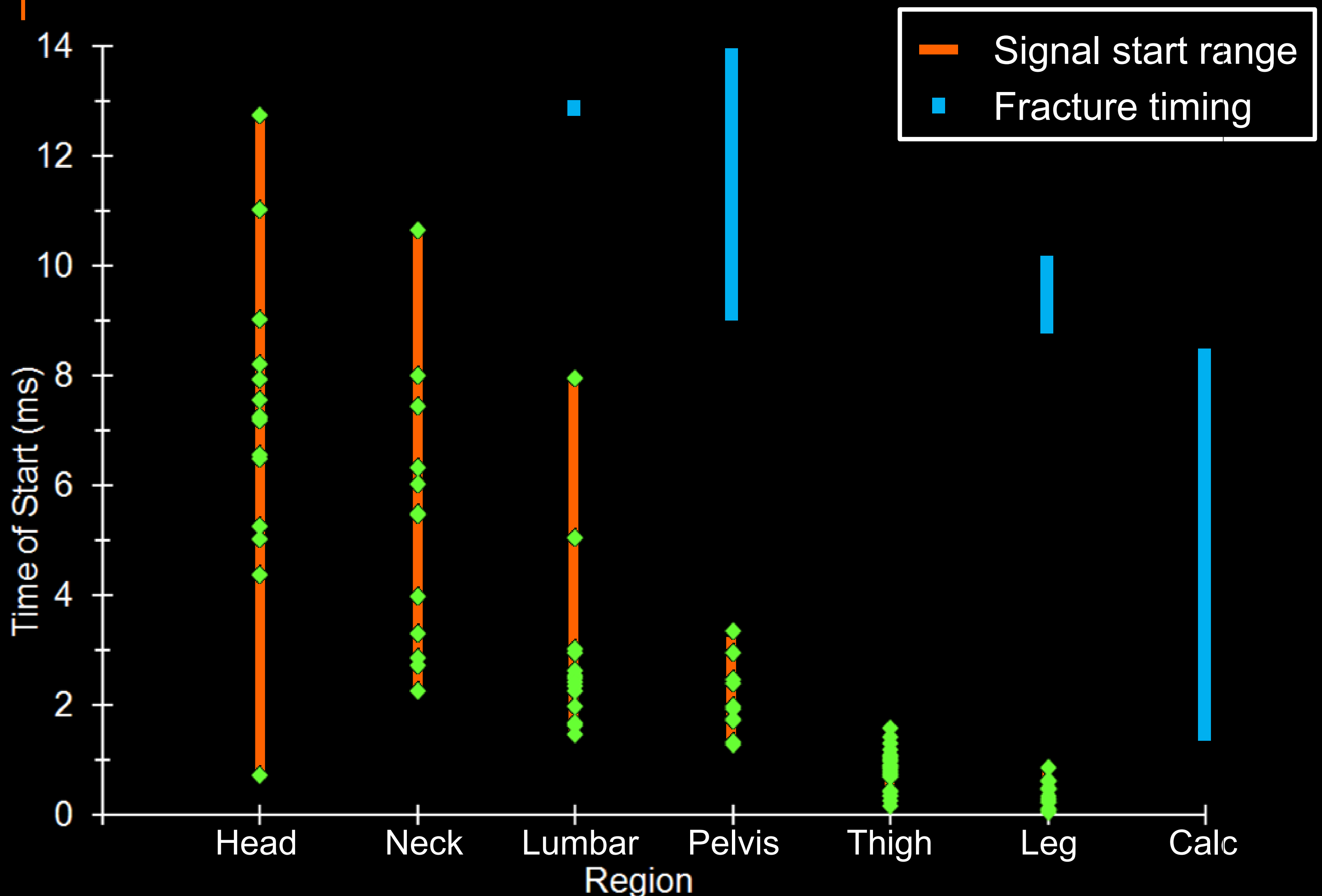

Comparison Matrix

MS Pairs	Reference Occupant (PMHS)			Comparison Occupant (ATD)			Comparison
	Position	Posture	PPE	Position	Posture	PPE	
-	Crew1	Nominal	No	Crew2	Nominal	No	1
-	Crew1	Obtuse	No	Crew2	Obtuse	No	2
4-13	Crew1	Nominal	No	Crew1	Nominal	Yes	3
	Crew2	Obtuse	No	Crew2	Obtuse	Yes	4
5-3	Crew1	Nominal	Yes	Crew1	Nominal	Yes	5
	Crew2	Nominal	No	Crew2	Nominal	No	6
6-10	Crew1	Obtuse	Yes	Crew1	Obtuse	Yes	7
	Crew2	Obtuse	No	Crew2	Obtuse	No	8
7-13	Crew1	Nominal	Yes	Crew1	Nominal	Yes	9
	Crew2	Obtuse	Yes	Crew2	Obtuse	Yes	10
11-8	Crew1	Nominal	No	Crew1	Nominal	No	11
	Crew2	Obtuse	No	Crew2	Obtuse	No	12
14-12	Crew1	Nominal	No	Crew1	Nominal	Yes	13
	Crew2	Obtuse	Yes	Crew2	Obtuse	Yes	14

APPROVED FOR PUBLIC RELEASE // DISTRIBUTION UNLIMITED

Event Sequence- Floor

Maximum foot and boot compression

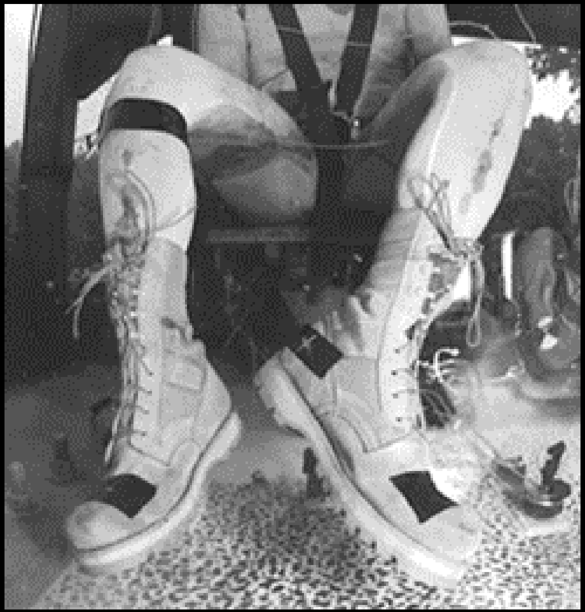

PMHS foot motion off the floor

ATD foot motion off the floor

LX Motion

Nominal Initial Condition

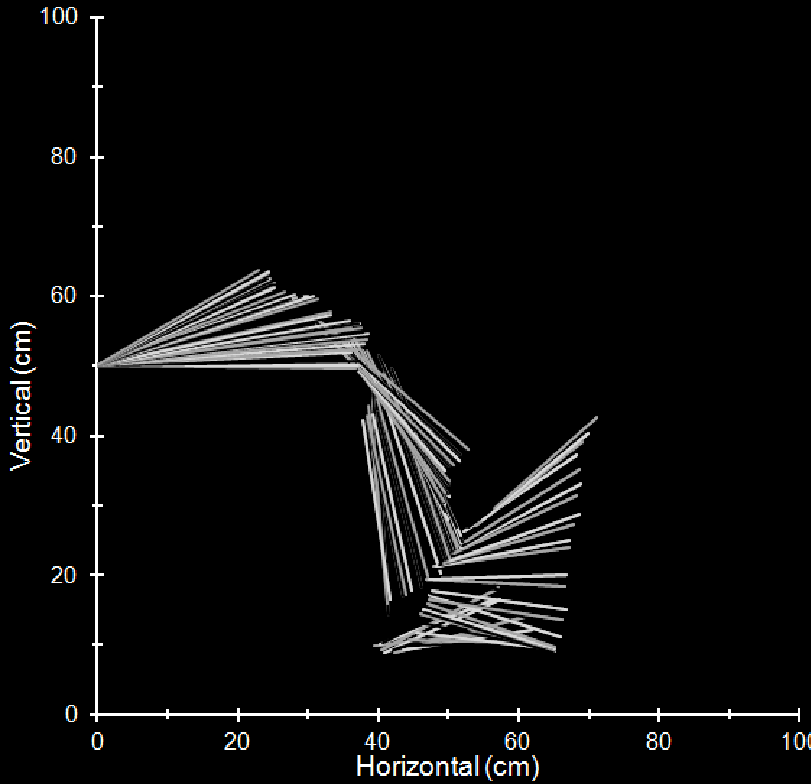

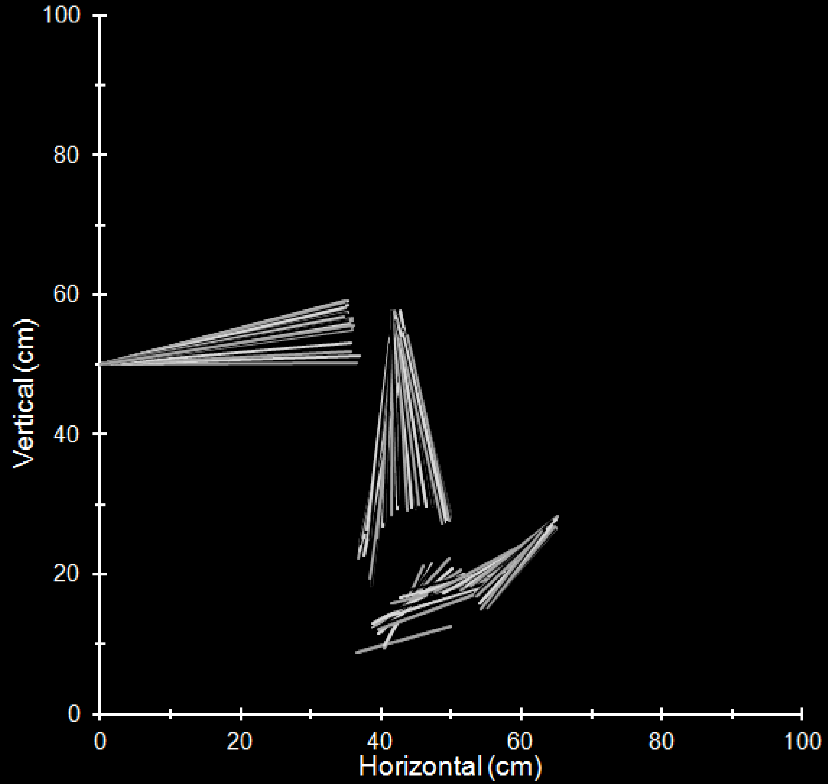

PMHS- Sweeping motion with rotation about the knee, limited ankle rotation

ATD- Less knee rotation but more ankle rotation

APPROVED FOR PUBLIC RELEASE // DISTRIBUTION UNLIMITED

LX Motion

Obtuse Initial Condition

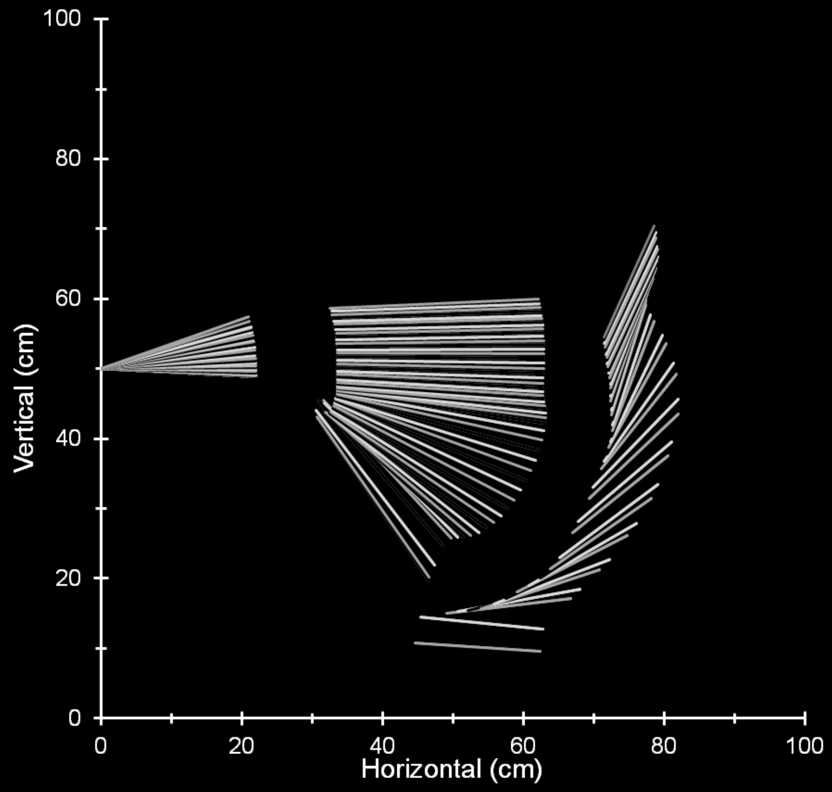

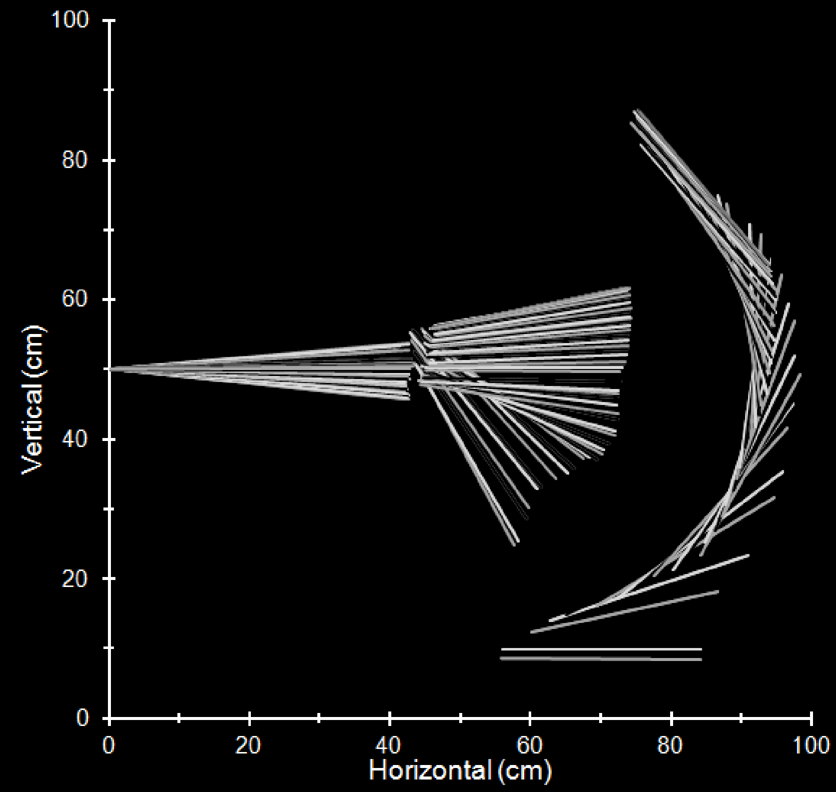

PMHS- limited knee rotation, ankle rotation

ATD- More knee and ankle rotation

Event Sequence

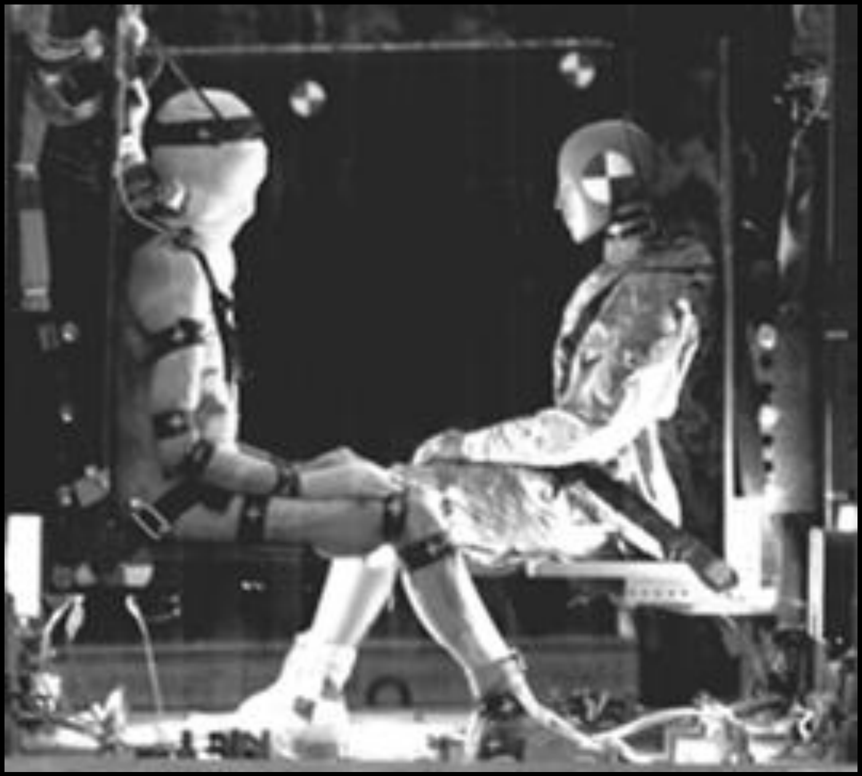

Start of floor motion

Maximal reduction of PMHS torso height.

APPROVED FOR PUBLIC RELEASE // DISTRIBUTION UNLIMITED

Event Sequence

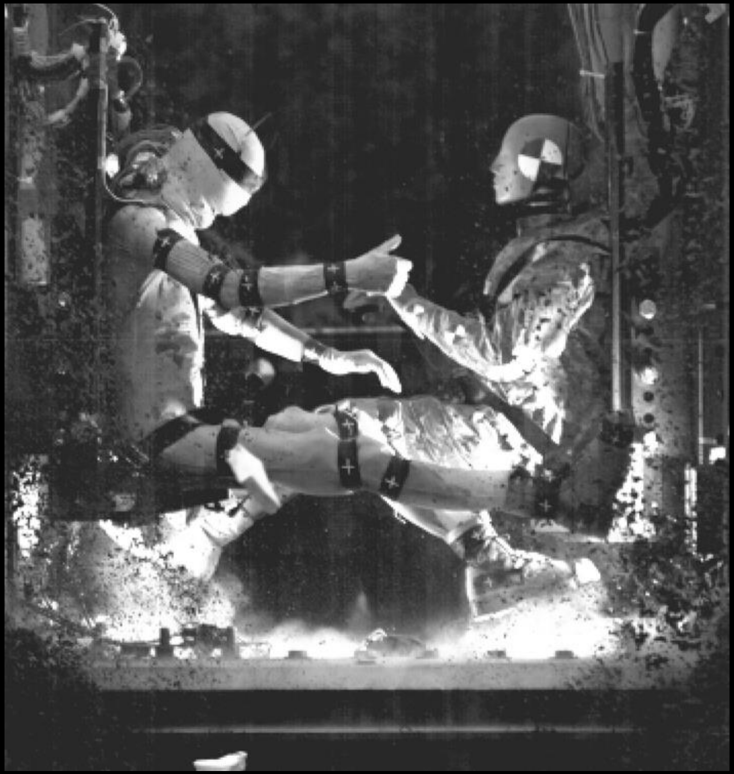

Comparison of peak ATD neck flexion at approximately 70 ms after Tzero (Left), and peak PMHS neck flexion at approximately 170 ms after Tzero (Right).

Scatter Plot - PMHS LX

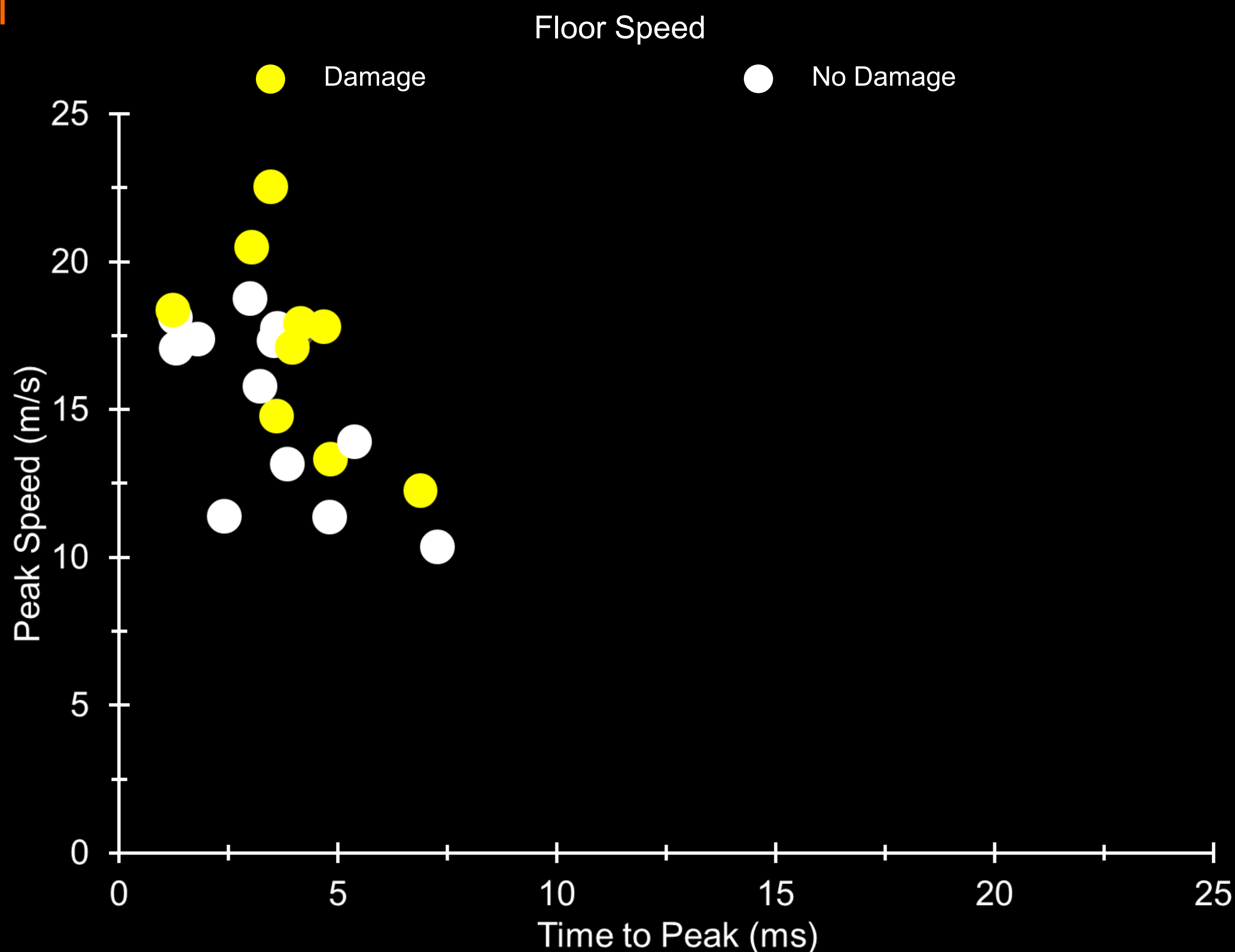

APPROVED FOR PUBLIC RELEASE // DISTRIBUTION UNLIMITED

Scatter Plots – ATD LX

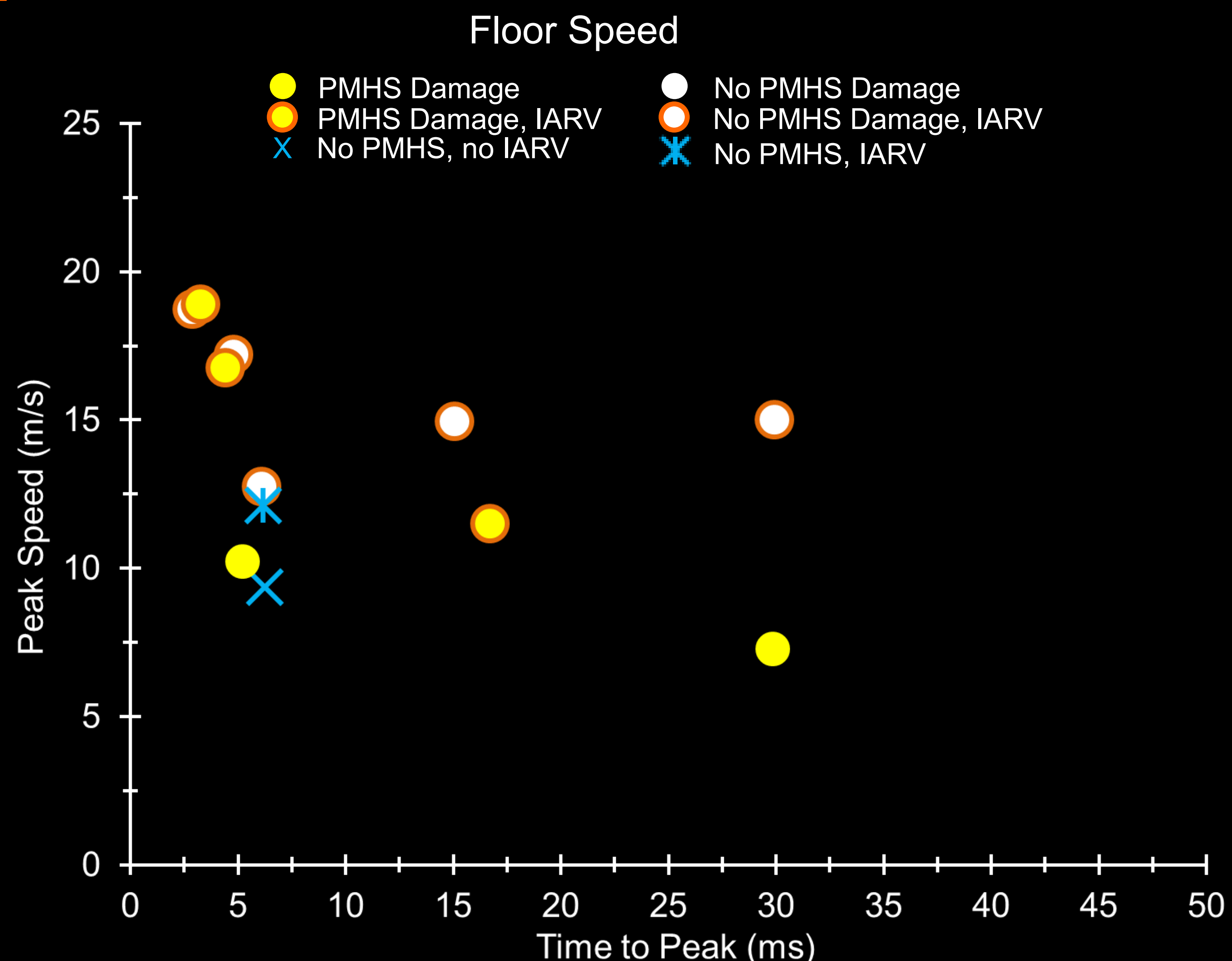

ATD: No clear trend in possible injury prediction

Summary of Scatter Plots

- Lower extremity: Larger floor accelerations in short time frame, higher floor speed
- Pelvis: High accelerations over a short time or lower accelerations over a longer time frame
- PPE supported the trunk, increased pelvis damage incidence, lowered pelvis and L-spine speed responses
- ATD predictions correct: 24%

APPROVED FOR PUBLIC RELEASE // DISTRIBUTION UNLIMITED

CORA Comparison Plot

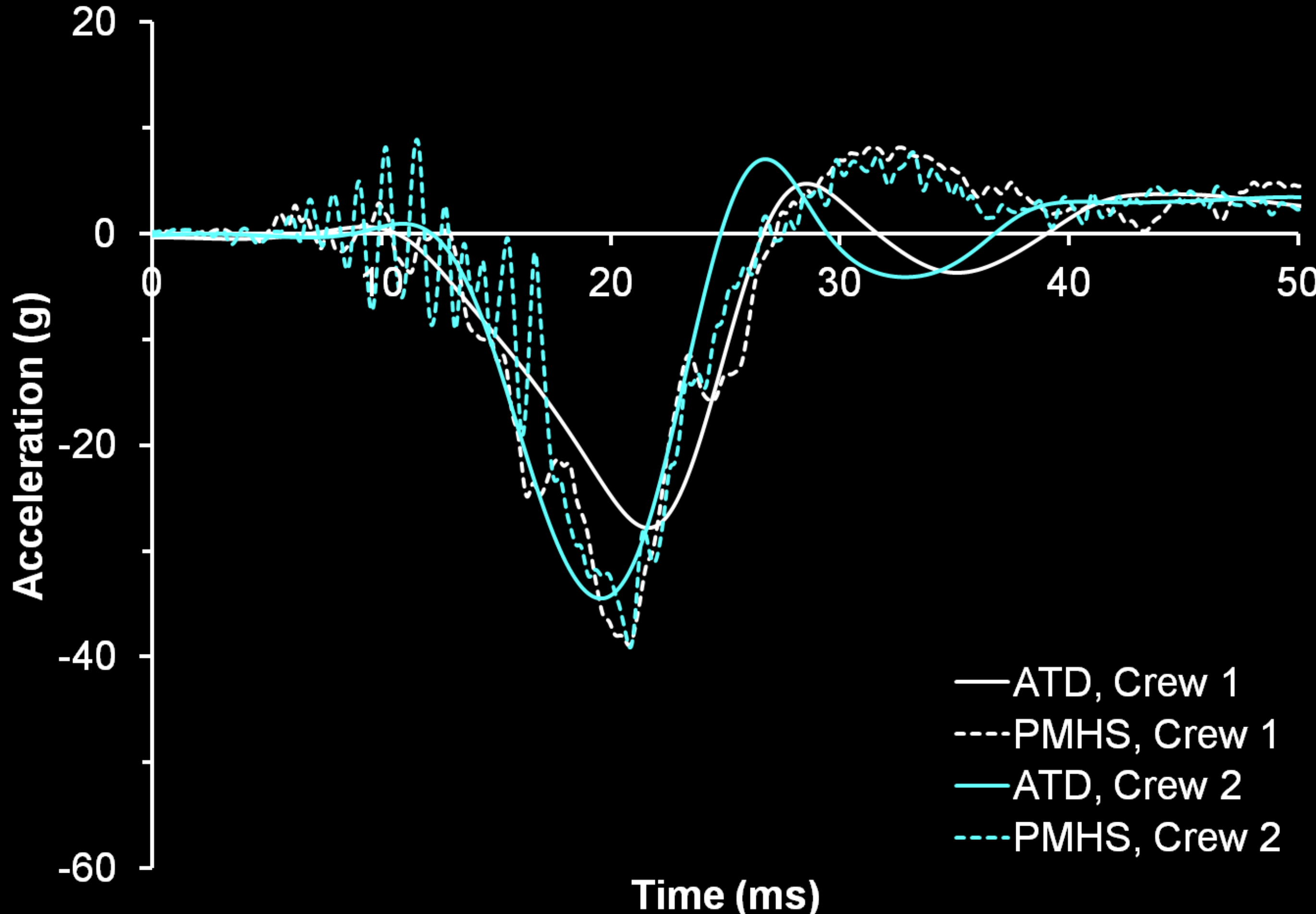

Head Z-acceleration from comparison 12, CORA: 0.78

APPROVED FOR PUBLIC RELEASE // DISTRIBUTION UNLIMITED

CORA Comparison Plot

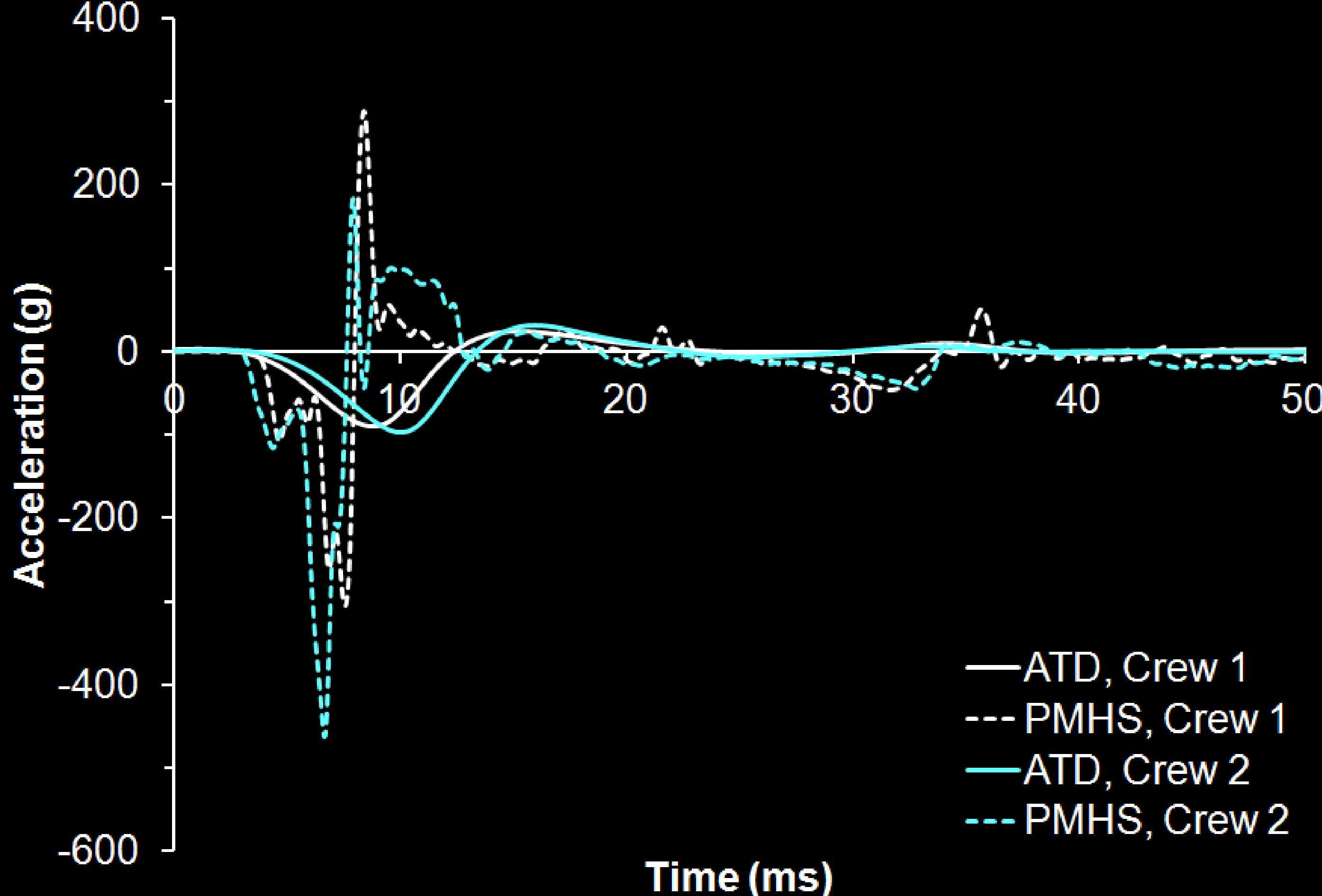

Right tibia Z-acceleration from comparison 8, CORA: 0.10

APPROVED FOR PUBLIC RELEASE // DISTRIBUTION UNLIMITED

Summary of CORA Findings

- CORA rating ≥ 0.5
  - Head Z-acceleration: 43%
  - Pelvis Z-acceleration, Left Tibia Z-acceleration: 8%
  - Pelvis X-acceleration, Right Tibia Z-acceleration: 0%
- Highest: 0.78, comparison 13, Head Az
- Lowest: 0.10, comparison 8, Right Tibia Az

Limitations

- Few repeat conditions were tested
- Hybrid III ATD was designed for automotive use
  - Standard spine instead of straight spine was used
- Deformation of the buck cage resulted in horizontal inputs

APPROVED FOR PUBLIC RELEASE // DISTRIBUTION UNLIMITED

Summary and Conclusions

- The ALF provides an appropriate environment for the study of under-body blast
  - PMHS damage is commensurate with injuries experienced in theater
- PMHS Damage
  - Load is transmitted caudal-to-cranial
  - Damage within 20 ms of foot motion
  - Pelvis and ankle most frequent
  - Lower extremity damage - higher acceleration and floor speed
  - Pelvis - higher acceleration (seat and pelvis) with a short duration, and lower acceleration over a longer duration

APPROVED FOR PUBLIC RELEASE // DISTRIBUTION UNLIMITED

Summary and Conclusions

- HIII response differs from the PMHS
  - Stiffer response compared to the PMHS
  - ATD cannot assume the same posture as the PMHS
  - Different lower extremity kinematic response
- The HIII ATD does not have the capability to predict the potential for injury in the high-rate, vertical loading environment
- A new ATD dedicated to the UBB environment is needed to assist in the effort to mitigate injuries sustained by the mounted soldier

Thank You

- ACKNOWLEDGMENTS: This work was funded by the USAMRMC under Award Number W81XWH-10-2-0165.

- Other contributors: Craig D. Foster, John N. Owen, Paul J. Benedetto, Dr. Yun Seok Kang, Rakshit Ramachandra, Dr. Kyle Icke, Dr. David Porta, Thomas Jeffries, Dawn E. Gietzen, Dr. Shean E. Phelps, Ms. Autumn R. Kulaga, and participants from the University of Michigan, Wayne State University, the Georgia Institute of Technology, the University of Virginia, the Medical College of Wisconsin, and Design Research Engineering.

- This work reflects the opinions of the authors only, and not the opinions of the funding agency, nor of any of the organizations with which the authors are affiliated.

APPROVED FOR PUBLIC RELEASE // DISTRIBUTION UNLIMITED

Clinical Perspective on Underbody Blast Injuries

Daniel R. Possley DO, MS
MAJ, MC, USA
12JAN16
Daniel.r.possley.mil@mail.mil

Disclosures

- No personal disclosures

The opinions or assertions contained herein are the private views of the author and are not to be construed as official or as reflecting the views of the United States Department of the Army or the United States Department of Defense.

Objectives

- What we do
- What we see
- What we are doing

America at War

- OEF/OIF
  - >50,000 casualties
  - >4,600 hostile deaths
- Overall injuries and extremity injuries have been well reported
- Increasing incidence of unconventional warfare

Owens BD, Kragh JF Jr, Wenke JC, et al. Combat Wounds in Operation Iraqi Freedom and Operation Enduring Freedom. J Trauma 2008;64:295-299.

Belmont PJ Jr, McCriskin BJ, Sieg RN, et al. Combat wounds in Iraq and Afghanistan from 2005 to 2009. J Trauma Acute Care Surg. 2012;73(1):3-12.

Owens BD, Kragh JF Jr, Macaitis J, Svoboda SJ, Wenke JC. Characterization of extremity wounds in Operation Iraqi Freedom and Operating Enduring Freedom. *J Orthop Trauma*. 2007;21:254-257.

Context: Soft tissues

Context: Soft tissues

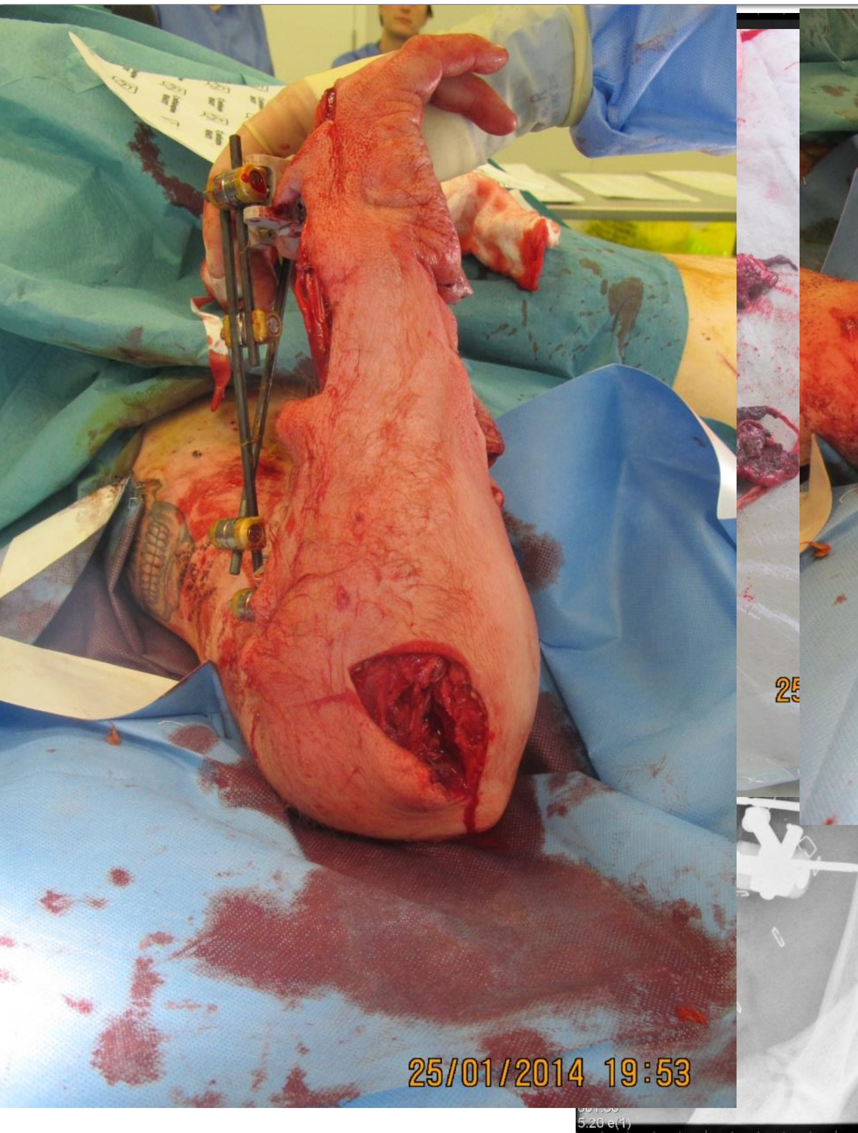

Context: Negative Pressure Wound Vacuum

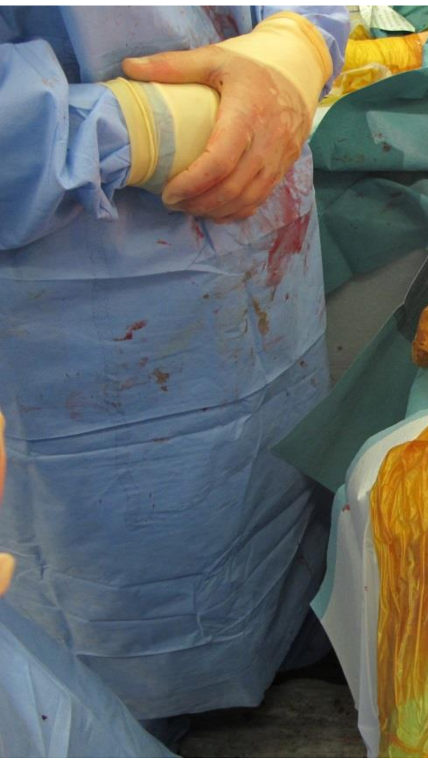

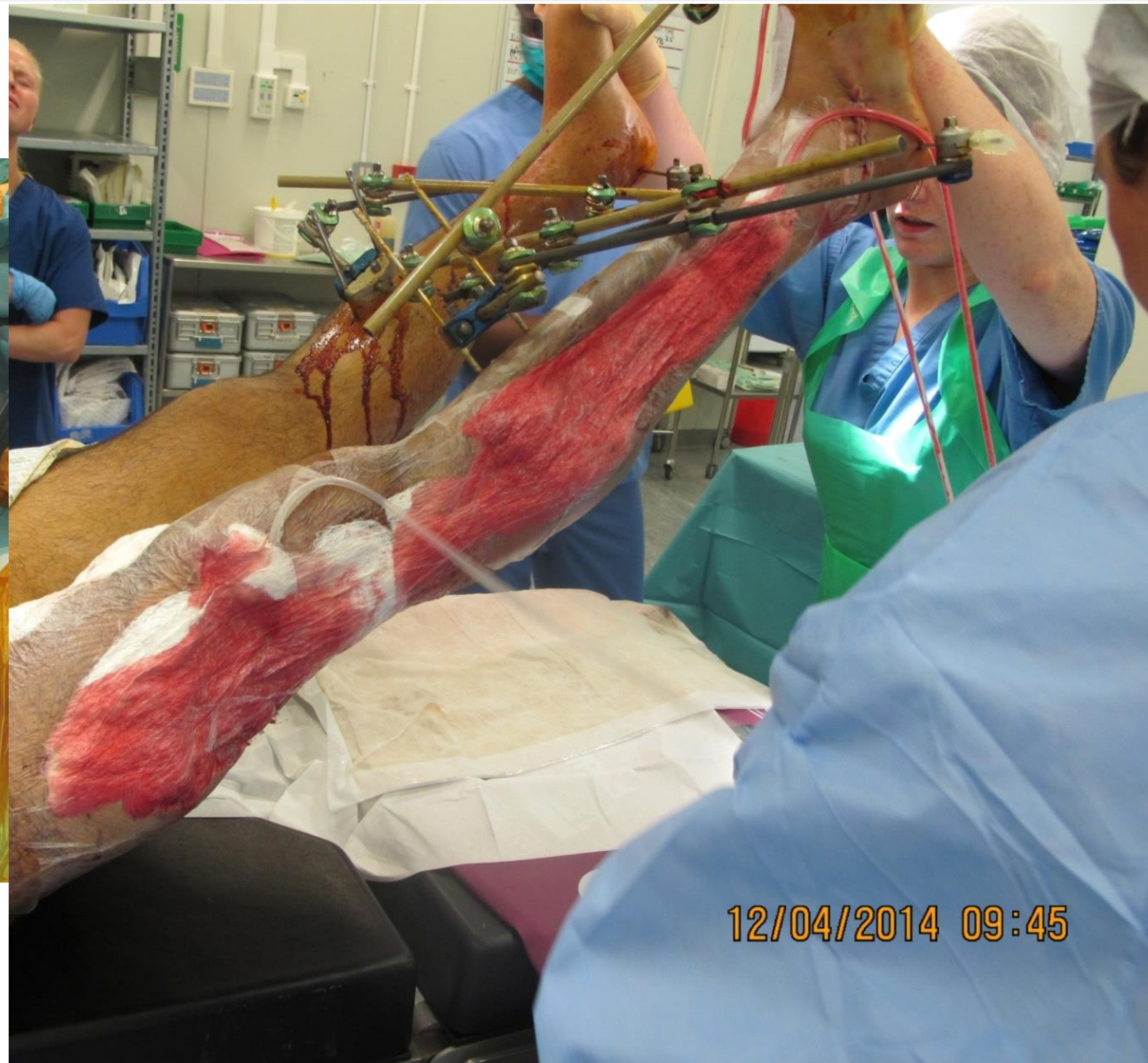

Context: Soft tissue coverage

Context: Infection

USS Cole: OCT 2000

Damage Control Orthopaedics

Flooding: **Hemorrhage**
Shoring of bulkheads, decks, frames to prevent structural collapse: **Fracture Fixation**
Fire Suppression: **Inflammation/Infection**
Prevent sinking: **Death**

USS Cole: Damage Control

Damage Control Orthopaedics

Damage Control Orthopaedics

- What are my resources
- Availability of next echelon of care
- Time to evacuation

"Enhance the immediate survival of the patient with the least stress to the patient's physiologic condition"

Damage Control Orthopaedics

1. "Cut off the pipe"
2. "Stabilize the bone"
3. "Cut out the dead"

Lt Col Alistair Mountain, Consultant Trauma and Orthopaedic Surgeon

Biography pending.

Secretary: 0121 371 2807

Extension: 12807

Fax: 0121 371 4947

UHB

CARE AND CONCERN

Continuous En Route Care

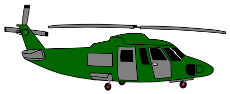

Point of Injury to Definitive Care

CASEVAC
1 Hour

BAS
Level 1

Forward Surgical
Teams
Level 2

Intratheater
EVAC
24 Hours

CSH, EMF,
Theater Hospital
Level 3

Intertheater
EVAC
48-72 Hours

CONUS/OCONUS MTF
Level 4/5

Surgical Capability

EWS CH4, pg 4.2 4.3 *Evacuation as an issue*

Advances in Combat Casualty Care

- Two procedures prior to arrival to U.S.

Lin DL, Kirk KL, Murphy KP, et al. Evaluation of Orthopaedic Injuries in Operation Enduring Freedom. *J Orthop Trauma*. 2004;18:S48-S53.

Advances in Combat Casualty Care

- Improved body armor
- Field combat casualty
  - Tourniquet

Kragh JF Jr, Walters TJ, Baer DG, et al. Survival wit
Emergency Tourniquet use to Stop Bleeding in Majo
Trauma. *Ann Surg* 2009;249(1):1-7.

Damage control orthopa

- Early debridement and irriga
- External fixation
- Fasciotomies
- Revascularization

Gajewski D, Granville R. The United States
Armed Forces Amputee Patient Care Program.
Am Acad Orthop Surg 2006;14:S183-S187.

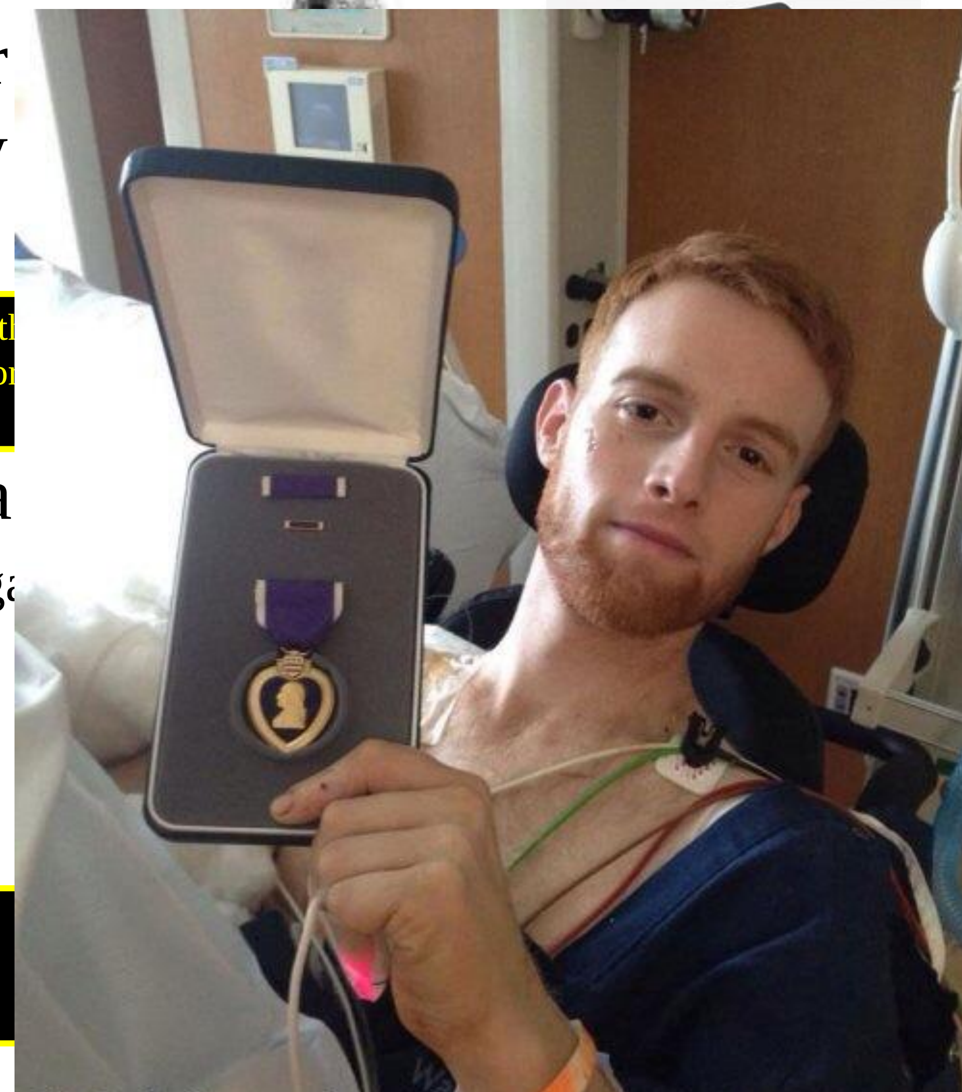

Why So Many Extremity Injuries?

Body Armor = Increased Survival

American Soldier Shot to Ceramic Chest Plate

Greer, M.A.M.-E., M.E. et al. A review of 41 upper extremity war injuries and the protective gear worn during OEF and OIF. *Mil Med* 2006;**171**(7):595-7.

Kosashvili, Y.H., J. et al. Influence of personal armor on distribution of entry wounds: lessons learned from urban warfare fatalities. *J Trauma* 2005;**58**(6):1236-40.

Mabry, R.L.H., J.B. et al. United States Army Rangers in Somalia: an analysis of combat casualties on an urban battlefield. *J Trauma* 2000;**49**(3):515-28.

McNeil, J.D.et al. Combat Casualty care in an air force theater hospital: perspectives of recently deployed cardiothoracic surgeons. *SemThorCardioSur* 2008;**20**(1):p.78-84.

Paquette, E.L.,Genitourinary trauma at a combat support hospital during Operation Iraqi Freedom: the impact of body armor. *J Urology* 2007;**177**(6):2196-9.

Peleg, K.R., A. et al. Does body armor protect from firearm injuries? *J Am Coll Surgeons* 2006;**202**(4):643-8.

OEF/OIF Mechanisms of Injury

56%

78%

82%

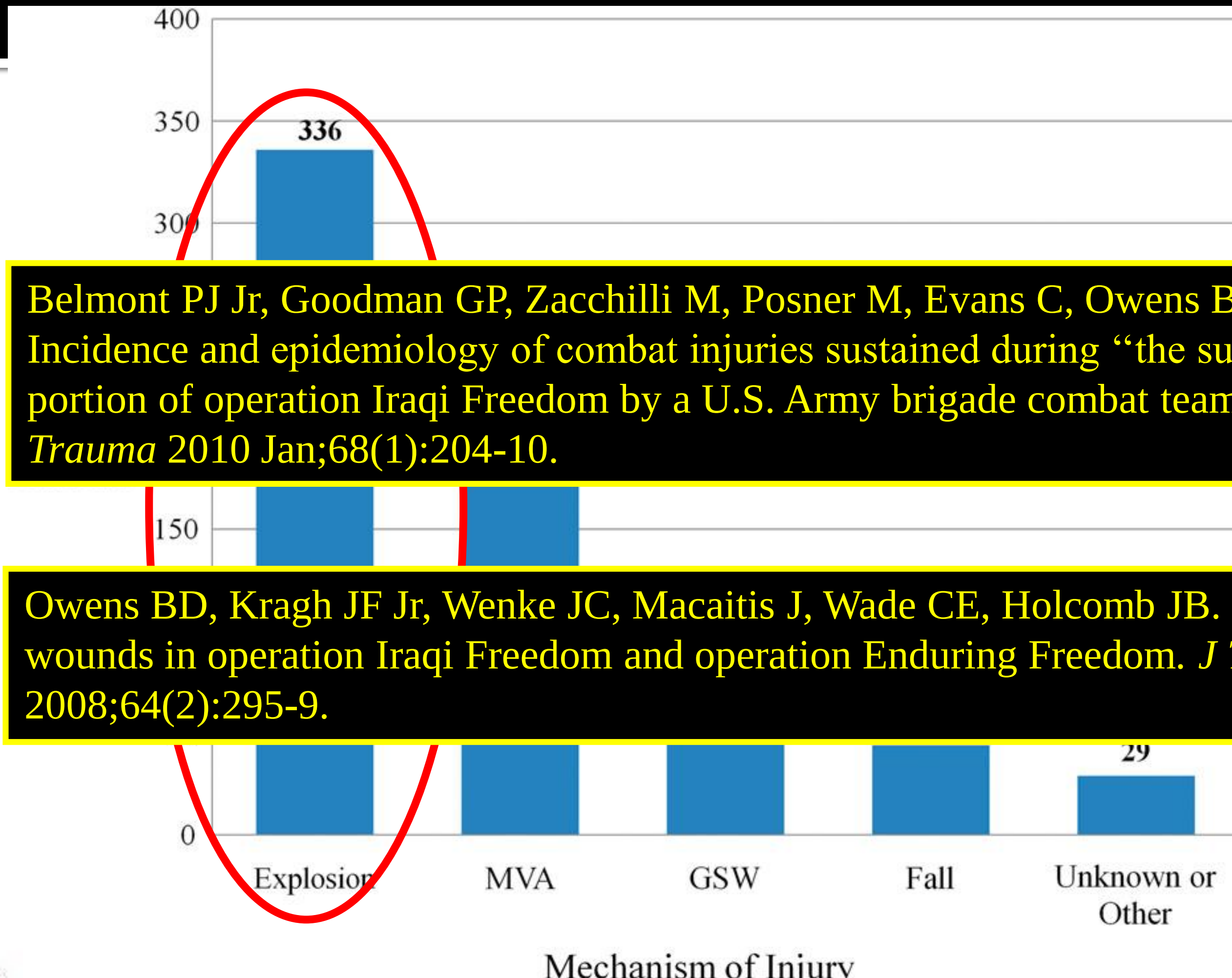

Belmont PJ Jr, Goodman GP, Zacchilli M, Posner M, Evans C, Owens BD. Incidence and epidemiology of combat injuries sustained during "the surge" portion of operation Iraqi Freedom by a U.S. Army brigade combat team. *J Trauma* 2010 Jan;68(1):204-10.

Owens BD, Kragh JF Jr, Wenke JC, Macaitis J, Wade CE, Holcomb JB. Combat wounds in operation Iraqi Freedom and operation Enduring Freedom. *J Trauma* 2008;64(2):295-9.

Blair JA, et al. Spinal Column Injuries Among Americans in the Global War on Terroism. *J Bone Joint Surg Am* 2012;94:e135(1-9).

Characterization

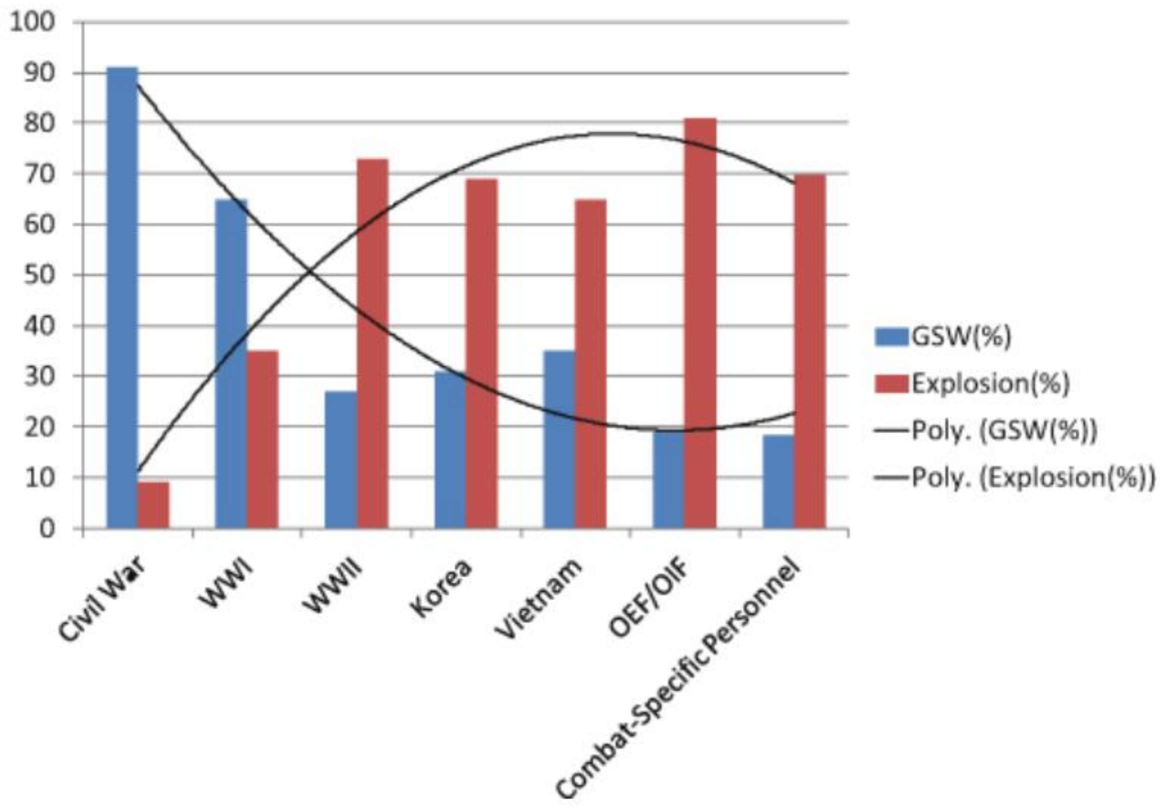

Cameron K, Owens B. Musculoskeletal Injuries in the Military. Springer 2015.

Characterization

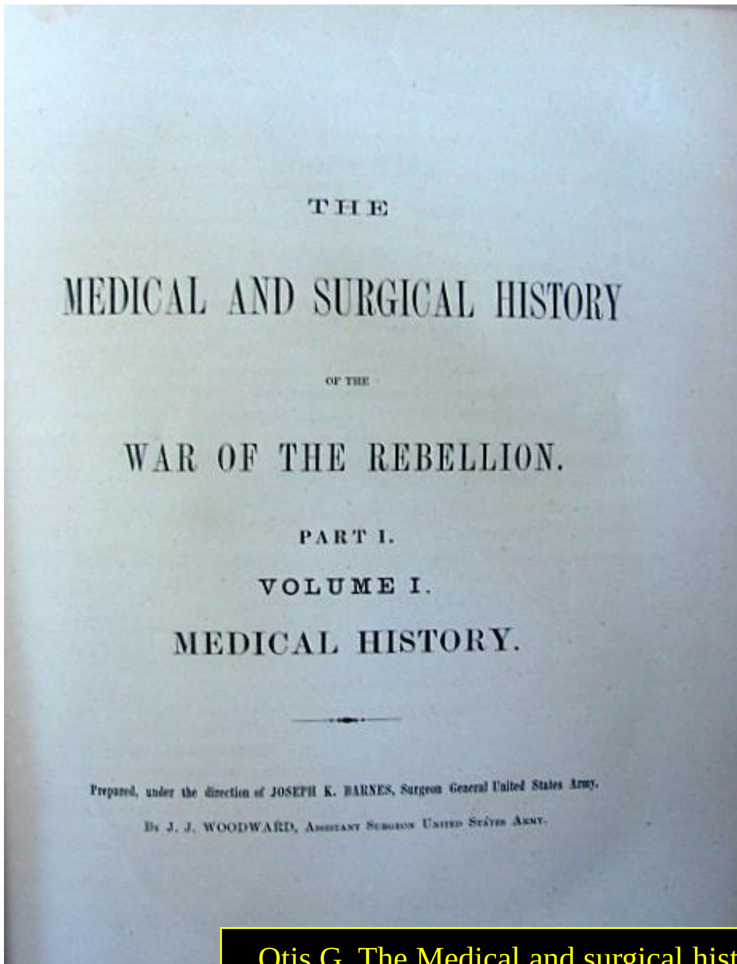

THE

MEDICAL AND SURGICAL HISTORY

OF THE

WAR OF THE REBELLION.

PART I.

VOLUME I.

MEDICAL HISTORY.

Prepared, under the direction of JOSEPH K. BARNES, Surgeon General United States Army.

By J. J. WOODWARD, Assistant Surgeon United States Army.

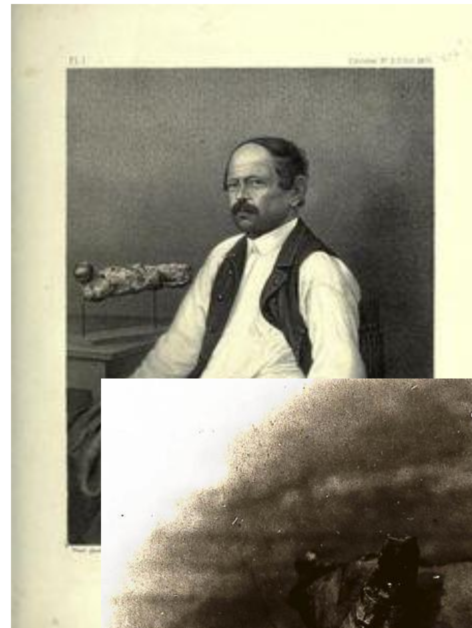

Otis G. The Medical and surgical history of the war of the rebellion, 1861-1865. Surgical History. Vol II. Washington, DC. Government Printing Office; 1870.

Characterization

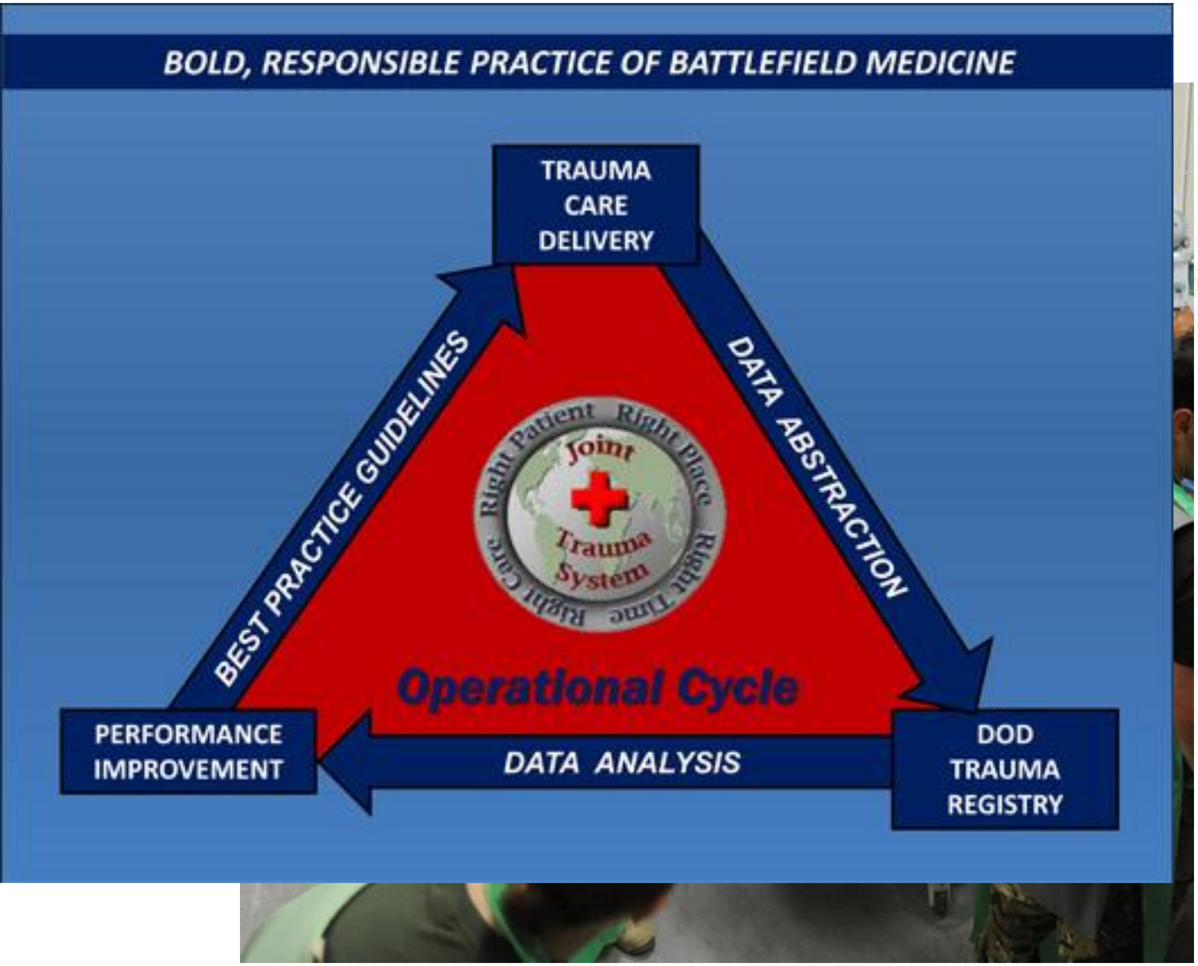

Characterization

Characterization of Extremity Wounds in Operation Iraqi Freedom and Operation Enduring Freedom

Brett D. Owens, MD, John F. Kragh, Jr, MD, Joseph Macaitis, BS, Steven J. Svoboda, MD, and Joseph C. Wenke, PhD

(*J Orthop Trauma* 2007;21:254–257)

- 1,566 soldiers sustained 6,609 combat wounds
  - 4.2 wounds per soldier
- 3,575 extremity wounds (82% of soldiers with at least one extremity wound)

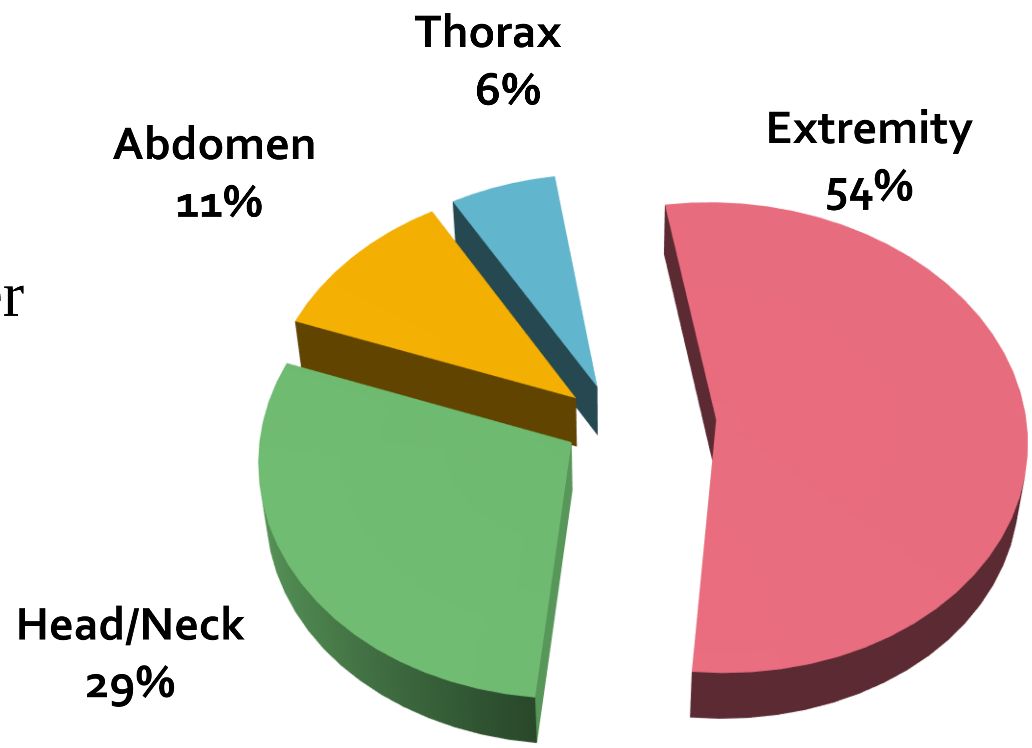

Characterization

Battlefield injuries

- 82% of casualties sustain extremity injuries

Owens B D, et al.: Combat Wounds in Operation Iraqi Freedom and Operation Enduring Freedom. *Journal of Trauma* 2008; 64(2):295-299.

Traumatic Amputations

- 2.3 % of all battle injuries
- 7.4% of major limb injuries
- Consistent with prior conflicts

Stansbury LG, et al.: Amputations in U.S. Military Personnel in the Current Conflicts in Afghanistan and Iraq. *J Orthop Trauma* 2008; 22(1):43-46.

Characterization

Major Amputation Rates as a Percentage of All Battle Injuries A... ...d Current US Military Conflicts

	Raw Percentage	Percentage With Multiple Limb Amputations
American Civil War[3]	12%	Unknown
World War I[4]	1.7%	2%
World War II[5]	1.2%	7%
Korean War[6]	1.4%	8%
Vietnam conflict[7]	3.4%	20%
Global war on terrorism (OEF/OIF)*	2.3%	16%

* Data as of December 31, 2005. (US Army Amputee Patient Care Program

OEF = Operation Enduring Freedom, OIF = Operation Iraqi Freedom

1.7%
1.2%
1.4%
3.4%
2.3%

Potter B, et al. Amputation is not Isolated: An Overview of the US Army Patient Care Amputee Program and Associated Amputee Injuries. *JAAOS* 2006;14:s188.

Cha

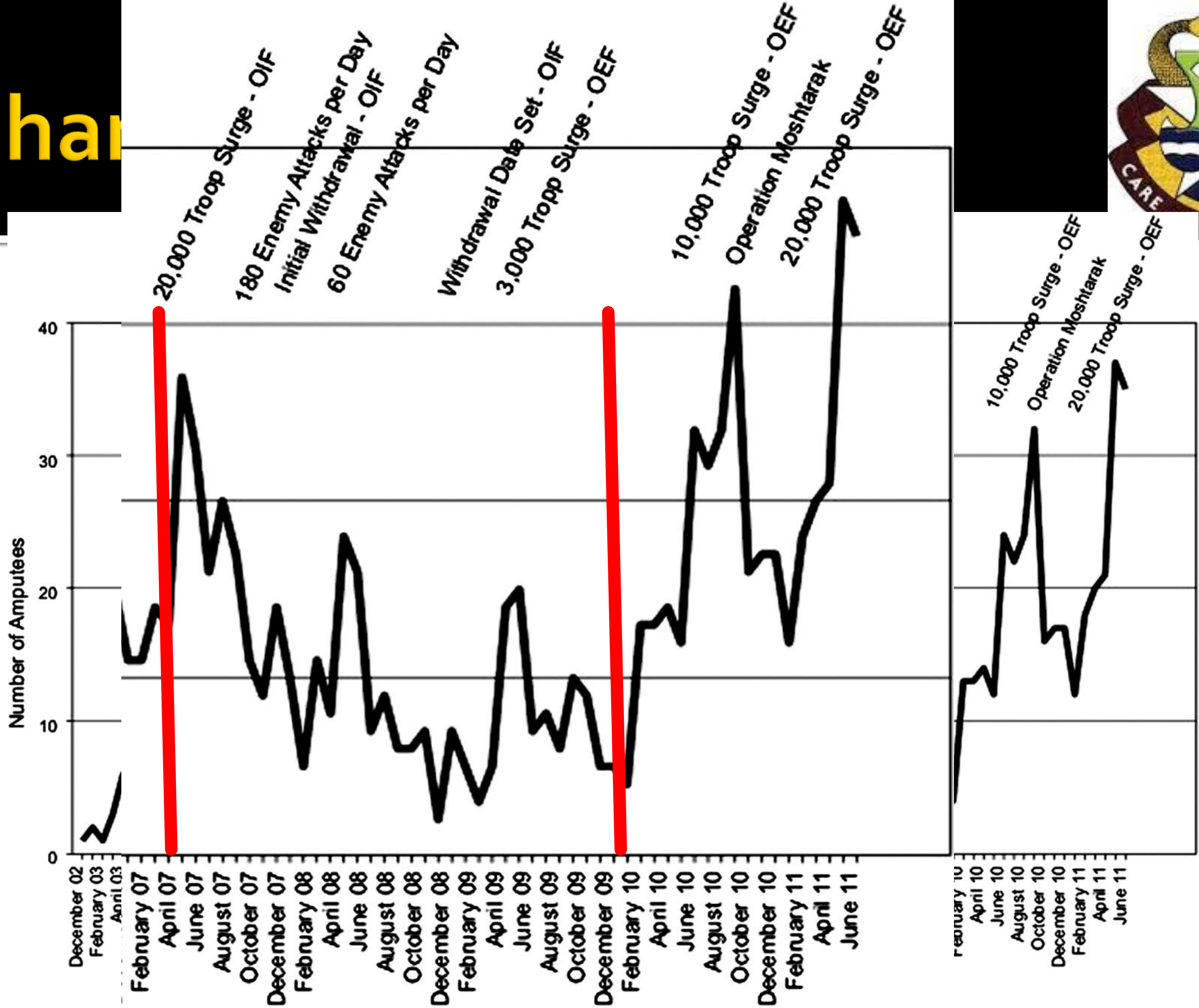

Krueger C, Wenke J, Ficke J. Ten years at war: Comprehensive analysis of amputation trends. J Trauma Acute Care Surg 2012:73(6);S438-444.

Characterization

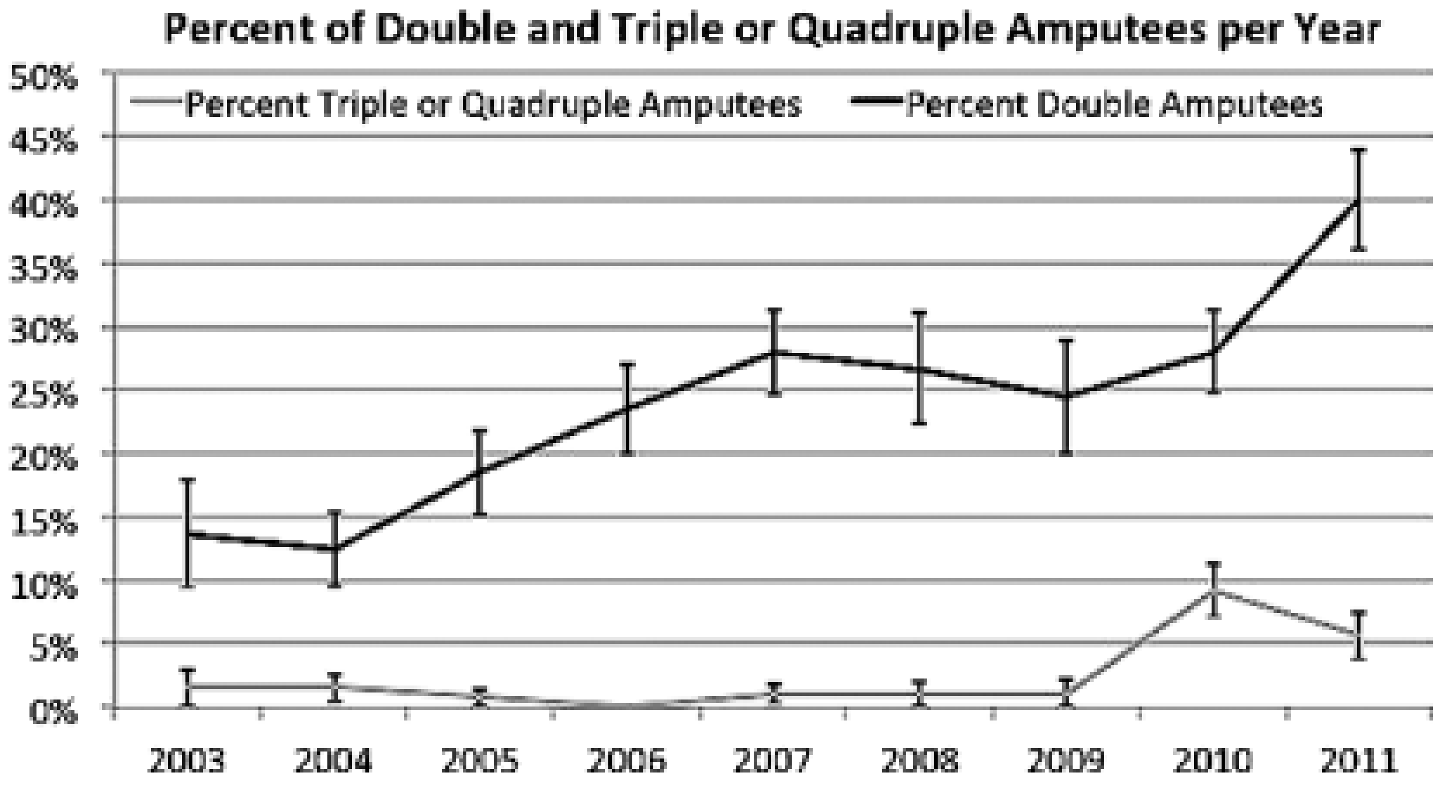

Krueger C, Wenke J, Ficke J. Ten years at war: Comprehensive analysis of amputation trends. J Trauma Acute Care Surg 2012:73(6);S438-444.

Characterization

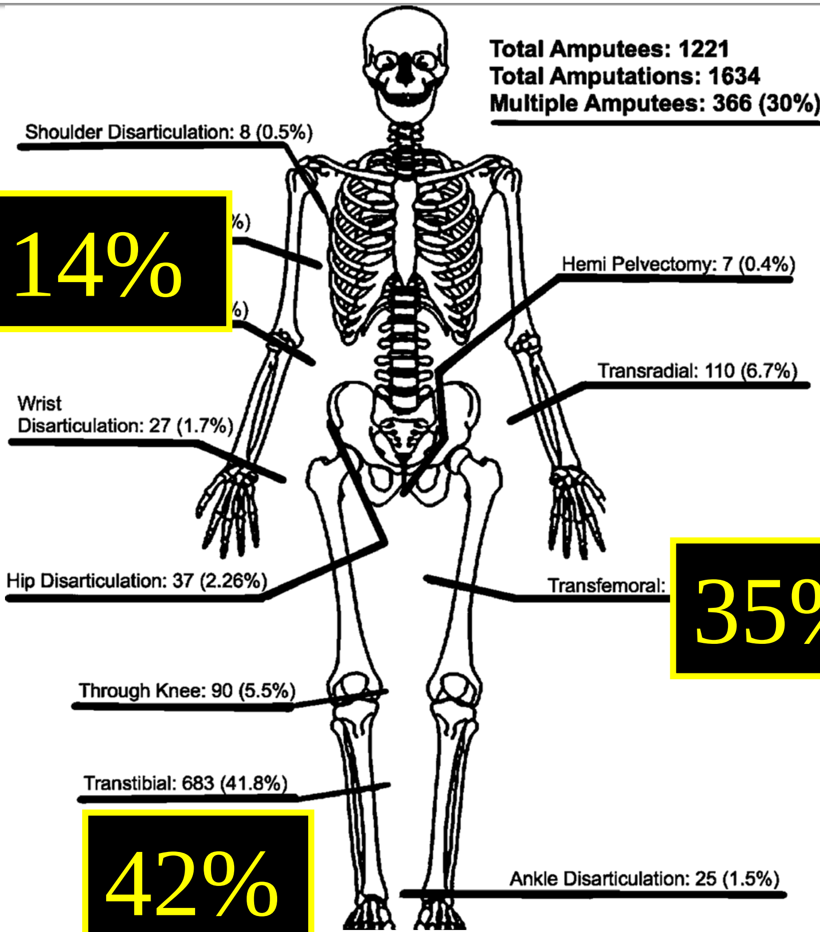

14%

35%

42%

93% due to explosion

76% penetrating wound

Krueger C, Wenke J, Ficke J. Ten years at war: Comprehensive analysis of amputation trends. J Trauma Acute Care Surg 2012:73(6);S438-444.

Characterization

Patient Demographics and Mechanism of Injury in Combat-related Pelvic Fracture

Mortality Rate and Associated Injuries in Stable and Unstable Combat-related Pelvic Fracture[a]

Fracture Type	Large Vessel Injury	Anatomic Brain Injury	Unstable Fractures	No. of Survivors	No. of Nonsurvivors	Mortality (%)	*P* Value
Unstable[b]	N	N	Y	2	11	84.62	<0.05
Stable[c]	N	N	N	8	6	42.86	<0.05

N = no, Y = yes
[a] Controlling for extrapelvic injuries with 100% mortality
[b] Tile types B and C, and unable to classify
[c] Tile type A

Other	2	1

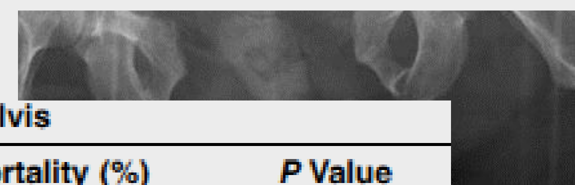

Combined Results by Mechanism of Injury to the Individual Person and to the Pelvis

MOI Person (Pelvis)	Survivors (group 1)	Nonsurvivors (group 2)	Mortality (%)	*P* Value
Blast (blunt)	2	27	93.10	<0.05
Conventional (blunt)	3	4	57.14	<0.05
Penetrating	5	60	92.31	<0.05

MOI = mechanism of injury

Characterization

5.5%

Spinal Column Injuries Among Americans in the Global War on Terrorism

James A. Blair, MD, Jeanne C. Patzkowski, MD, Andrew J. Schoenfeld, MD, Jessica D. Cross Rivera, MD, Eric S. Grenier, MD, Ronald A. Lehman Jr., MD, Joseph R. Hsu, MD, and the Skeletal Trauma Research Consortium (STReC)

10,979 servicemembers

598 injuries

1929 fractures

92%

Blair JA, et al. Spinal Column Injuries Among Americans in the Global War on Terrorism. *JBJSAM*. 2012;94:31351-1359.

Characterization

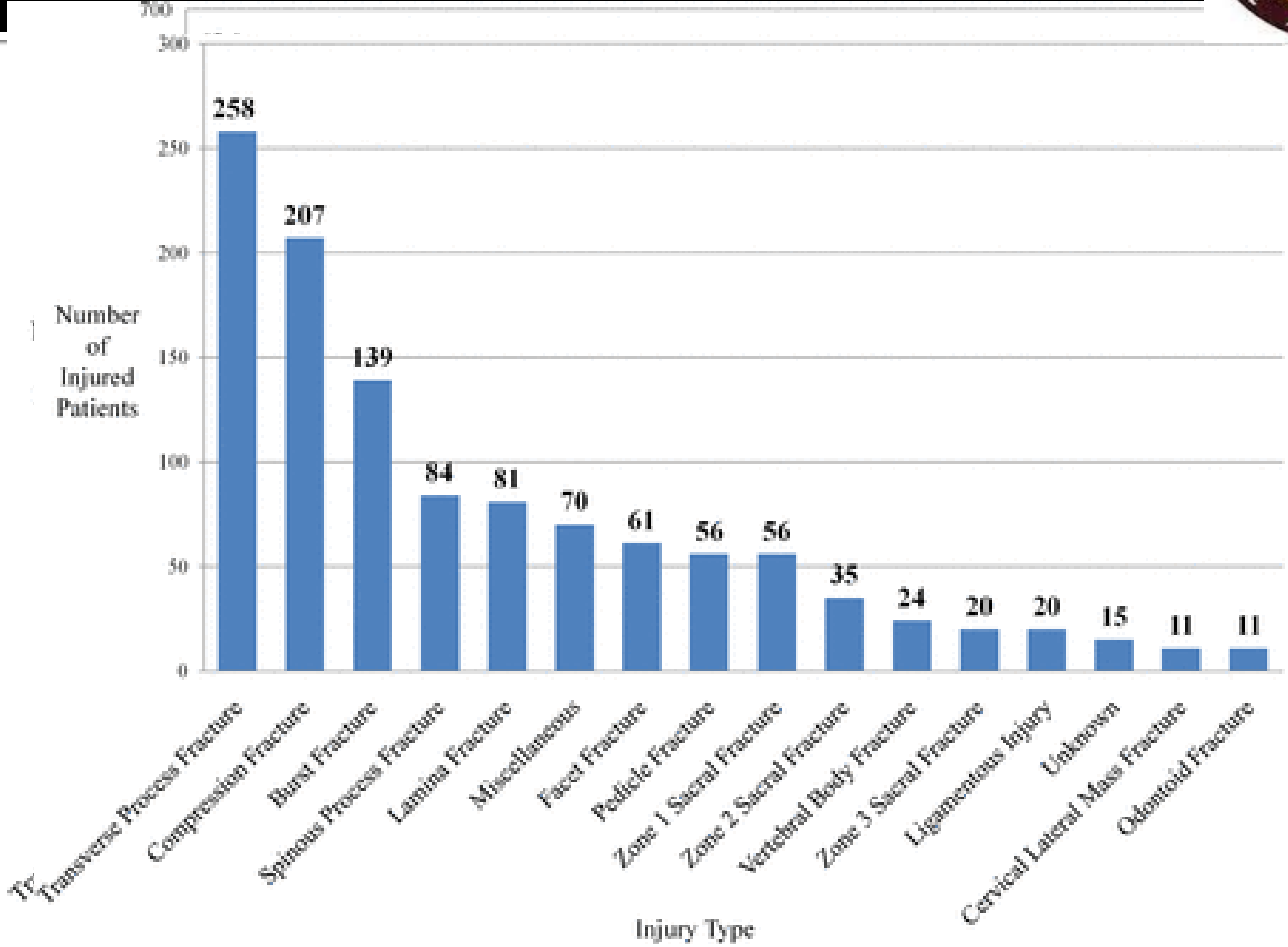

Characterization

Combat Musculoskeletal Wounds in a US Army Brigade Combat Team During Operation Iraqi Freedom

Philip J. Belmont, Jr., MD, Dimitri Thomas, MD, Gens P. Goodman, DO, Andrew J. Schoenfeld, MD, Michael Zacchilli, MD, Rob Burks, PhD, and Brett D. Owens, MD

7.4%

Schoenfeld AJ, et al. Characterization of combat related spinal injuries sustained by a US brigade combat team during Operation Iraqi Freedom. Spine J. 2012;12:771-776.

Characterization

C ... ed by American
s ... nistan: A study
... uma

Andrew ... Andrew W. Cleveland, III, MD,

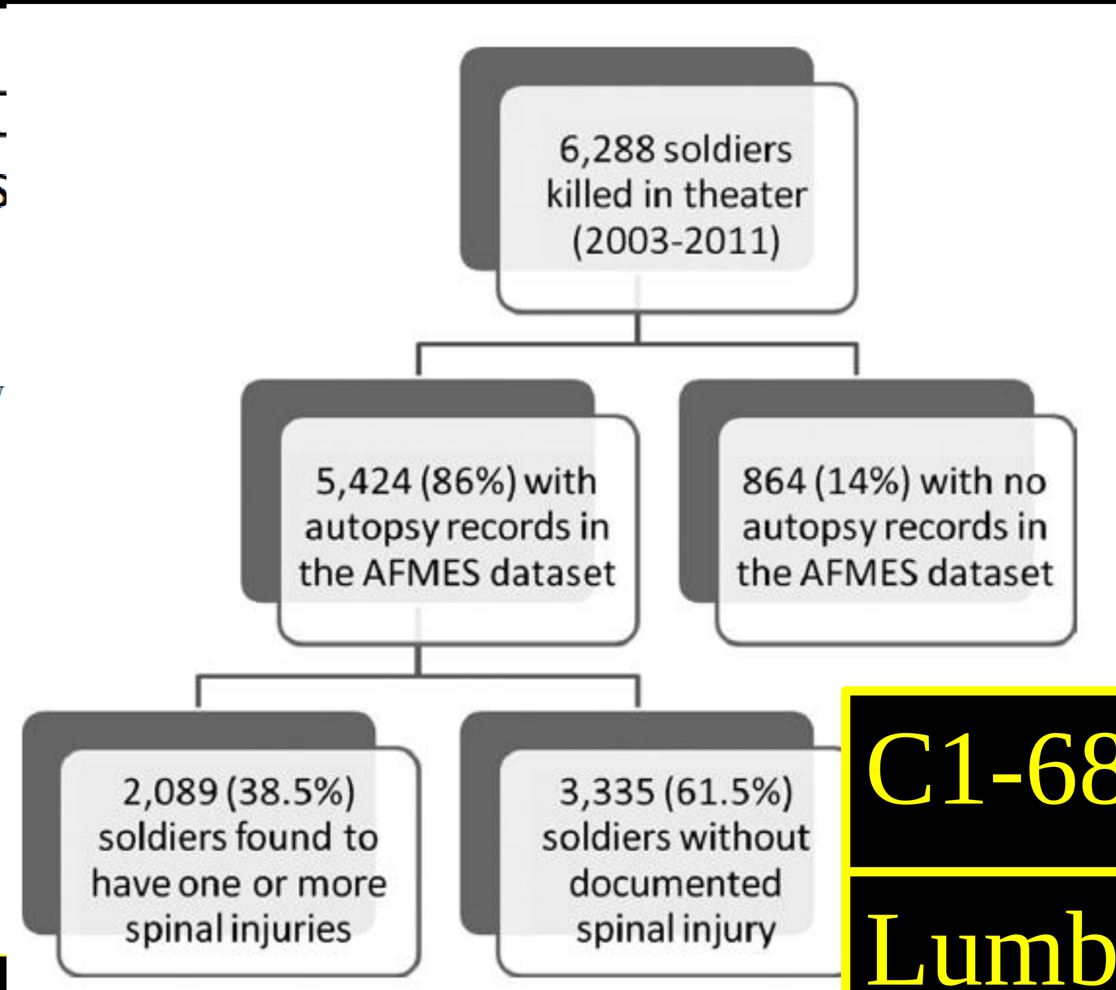

38.5%

C1-686

Lumbar-638

Afghanistan: A study of 2,089 instances of spine trauma. *J T*

Characterization

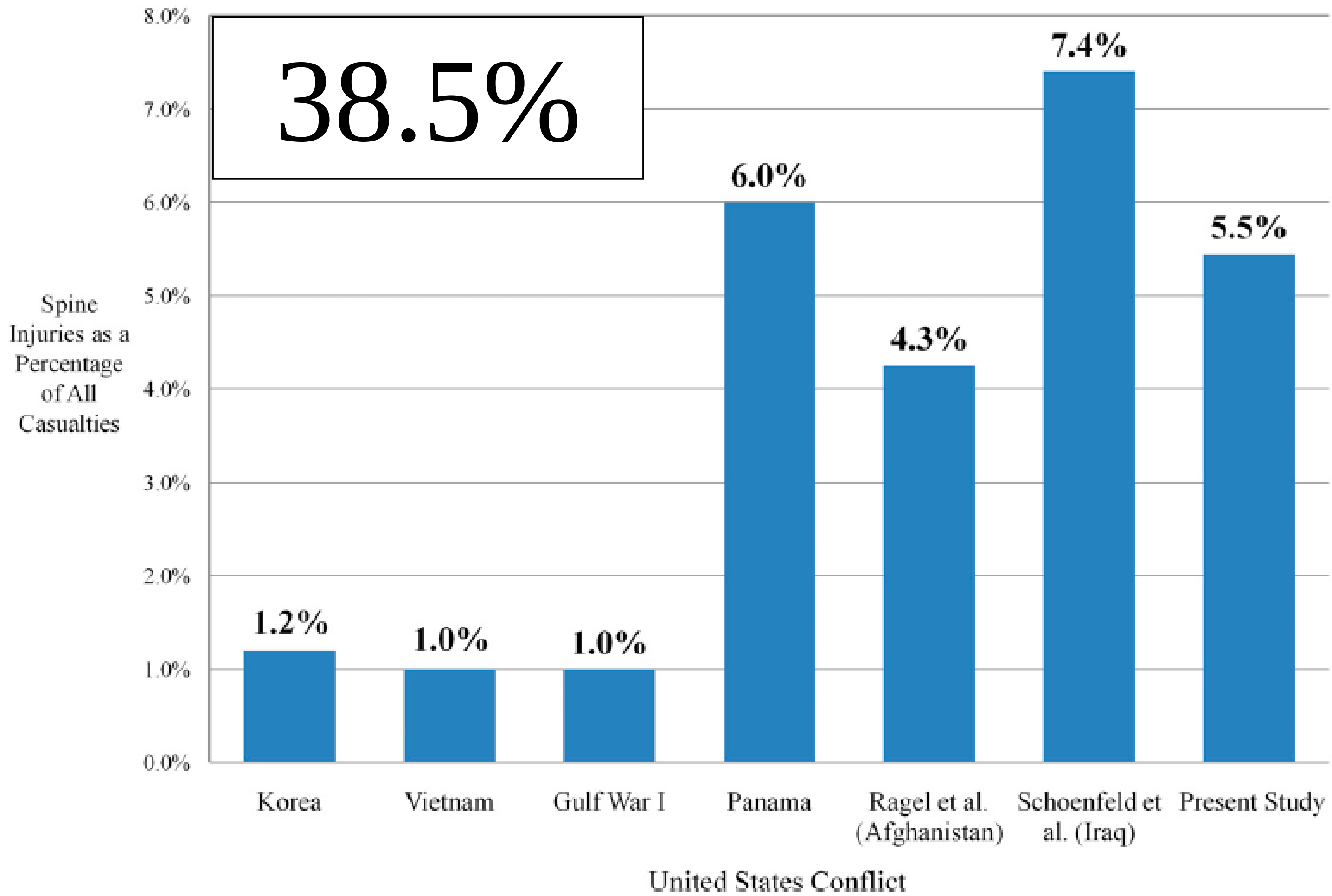

Blair JA, et al. Spinal Column Injuries Among Americans in the Global War on Terrorism. *JBJSAM*. 2012;94:31351-1359.

Characterization

ELSEVIER

The Spine Journal 12 (2012) 762–768

THE SPINE JOURNAL

Clinical Study

Military penetrating spine injuries compared with blunt

James A. Blair, MD[a,*], Daniel R. Possley, DO, MS[a], Joseph L. Petfield, MD[a], Andrew J. Schoenfeld, MD[b], Ronald A. Lehman, MD[c], Joseph R. Hsu, MD[d], Skeletal Trauma Research Consortium (STReC)[d]

CARE AND CONCERN

Characterization

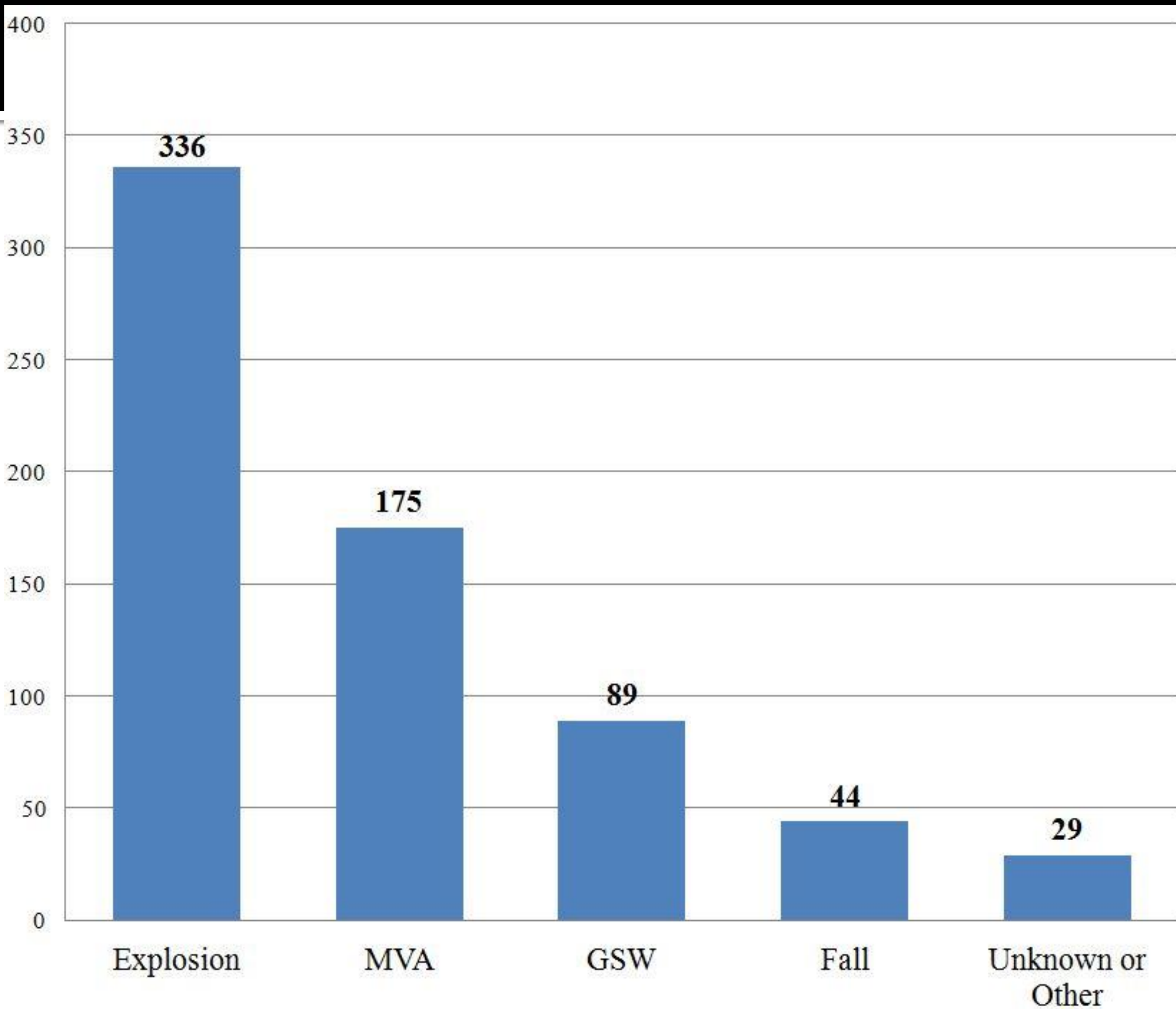

- Blunt: 71%
- Penetrating: 33%

Blair JA, Possley DR, Petfield JL, Schoenfeld AJ, Lehman RA, Hsu JR, STReC. Military penetrating spine injuries compared to blunt. *Spine J.* 2011 Nov 17. [Epub ahead of print].

Characterization

- October 2001 to December 2009
  - **10,979 casualties** registered in the JTTR
  - **598** servicemembers with spine injuries
    - **396** servicemembers with isolated BLUNT spine injuries (66%)
    - **165** servicemembers with isolated PENETRATING spine injuries (28%)
    - **30** servicemembers with COMBINED spine injuries (5%)

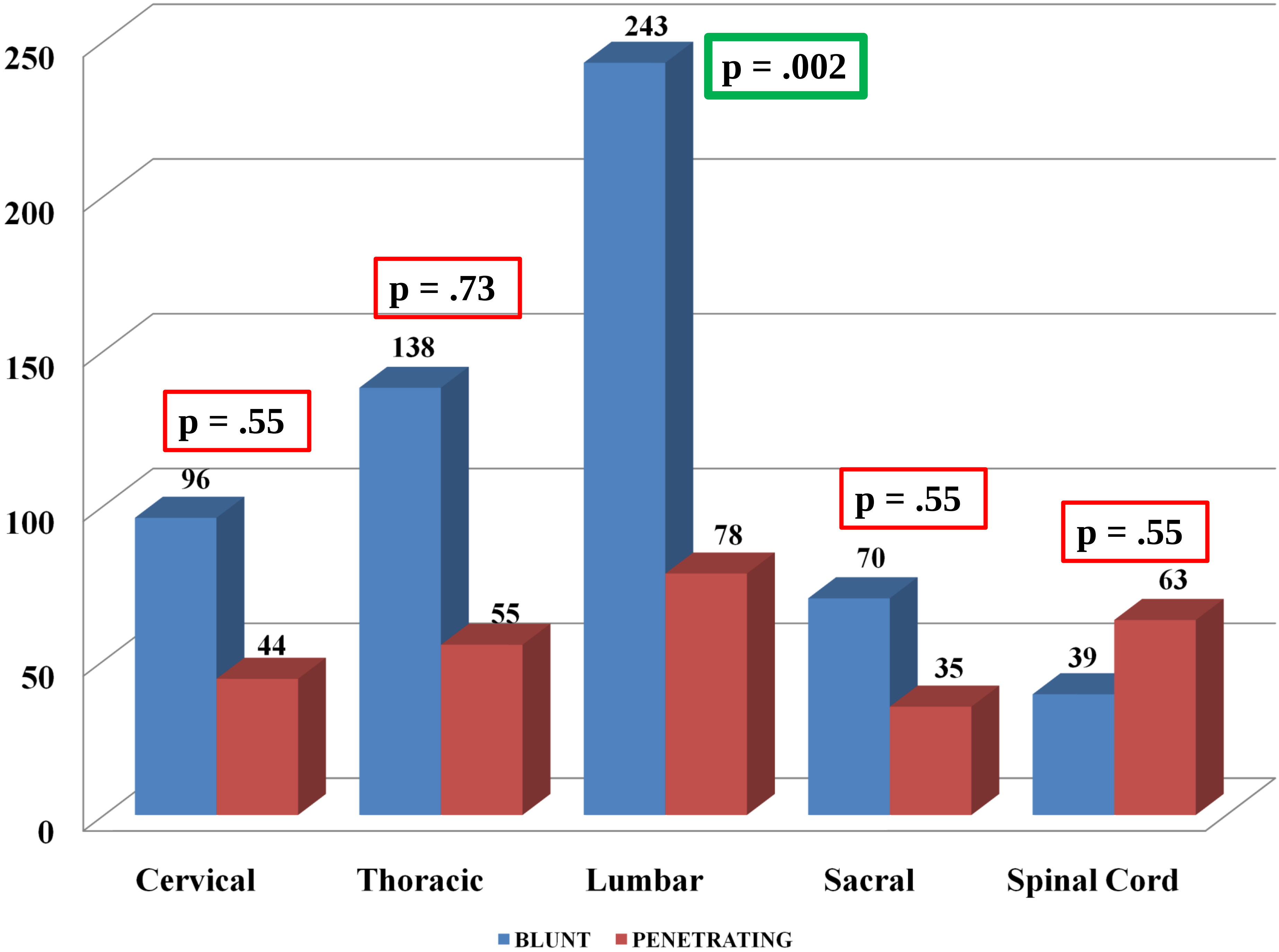

250
200
150
100
50
0
p = .55
96
44
p = .73
138
55
243
78
p = .002
p = .55
70
35
p = .55
39
63
Cervical
Thoracic
Lumbar
Sacral
Spinal Cord
BLUNT
PENETRATING

Characterization

104 **SPINAL CORD INJURIES (17% OF ALL SPINE-INJURED SERVICEMEMBERS)**

- 38% blunt (n=39)
  - n=39/396
- 60% penetrating (n=63)
  - n=63/165

p<.0001

Ch

ELSEVI

NAL

The … flict

USA TODAY

Home | News | Travel | Money | Sports | Life | Tech | Weather

Become a member TODAY

Log in | Bec

News » World ▪ War casualties

Spinal injuries up among troops

Updated 11/4/2009 9:29 AM | Comments 1707 | Recommend 25

E-mail | Save | Print | Reprints

Enlarge — By Dima Gavrysh, AP

A U.S. soldier unloads 50-caliber rounds from an MRAP vehicle after an IED attack in Wardak province on Aug. 3 in Afghanistan.

TROOPS AT RISK

By Gregg Zoroya, USA TODAY

BAGRAM, Afghanistan — Afghan insurgents are using roadside bombs powerful enough to throw the military's new 14-ton, blast-resistant vehicles into the air, increasing broken-back injuries among U.S. troops.

Doctors at the U.S. military hospital here say more than 100 U.S. servicemembers have suffered crushed or damaged spinal columns from being thrown around inside armored Mine Resistant Ambush Protected (MRAP) vehicles in the last five months.

TROOP DEATHS: American casualties in Afghanistan, Iraq and beyond

This "significant increase" in spinal injuries was not seen in the Iraq war, says Air Force Col. Warren Dorlac, director of trauma care for both conflicts. One in five wounded service members evacuated from Afghanistan this summer and early fall suffered a spinal injury and at least 14 were left paralyzed or with loss of sensation, says Air Force Lt. Col. Dustin Zierold, a surgeon and the hospital's director of trauma care.

"Whatever the G-force (of the roadside bombs), it is very high and very destructive," Zierold says.

the Skeletal Trauma Research Consortium (STReC)

April 1, 2007

53%

472

60%

1347

Characterization

Fracture incidence (expressed per 10,000 years)

Type	M1	D1	M2	D2	T1	T2	p
All fractures	3.95	13.75					<.0001
All fractures			4.89	11.15			<.0001
All fractures					17.7	16.0	.098

M1, Mounted in Time Period 1; D1, Dismounted in Time Period 1; M2, Mounted in Time Period 2; D2, Dismounted in Time Period 2.

Characterization

Statistical analysis for fractures

Fracture type	M1	D1	M2	D2	p
Denis/major	61/226 (27%)	173/786 (22%)			<.0005
Denis/major			86/246 (34%)	193/561 (34%)	.879
Denis/major	61/226 (27%)		86/246 (34%)		<.0005
Denis/minor	165/226 (73%)		159/246 (44%)		.05
Denis/minor		611/786 (78%)		362/561 (64%)	.003
All TL	1.28/10,000		1.73/10,000		.03
All TL		481/10,000		4.41/10,000	.84

M1, Mounted in Time Period 1; D1, Dismounted in Time Period 1; M2, Mounted in Time Period 2; D2, Dismounted in Time Period 2; TL, thoracolumbar.

Statistical analysis for fractures

Fracture type	M1	D1	M2	D2	p
Denis/major	61/226 (27%)	173/786 (22%)			<.0005
Denis/major			86/246 (34%)	193/561 (34%)	.879
Denis/major	61/226 (27%)		86/246 (34%)		<.0005
Denis/minor	165/226 (73%)		159/246 (44%)		.05
Denis/minor		611/786 (78%)		362/561 (64%)	.003
All TL	1.28/10,000		1.73/10,000		.03
All TL		481/10,000		4.41/10,000	.84

M1, Mounted in Time Period 1; D1, Dismounted in Time Period 1; M2, Mounted in Time Period 2; D2, Dismounted in Time Period 2; TL, thoracolumbar.

Chara

Statistical an

Fracture typ

TL (Denis/m

TL (Denis/m

TL (AO/Mag

TL (Denis m

T10–L3 (mo

T10–L3 (dis

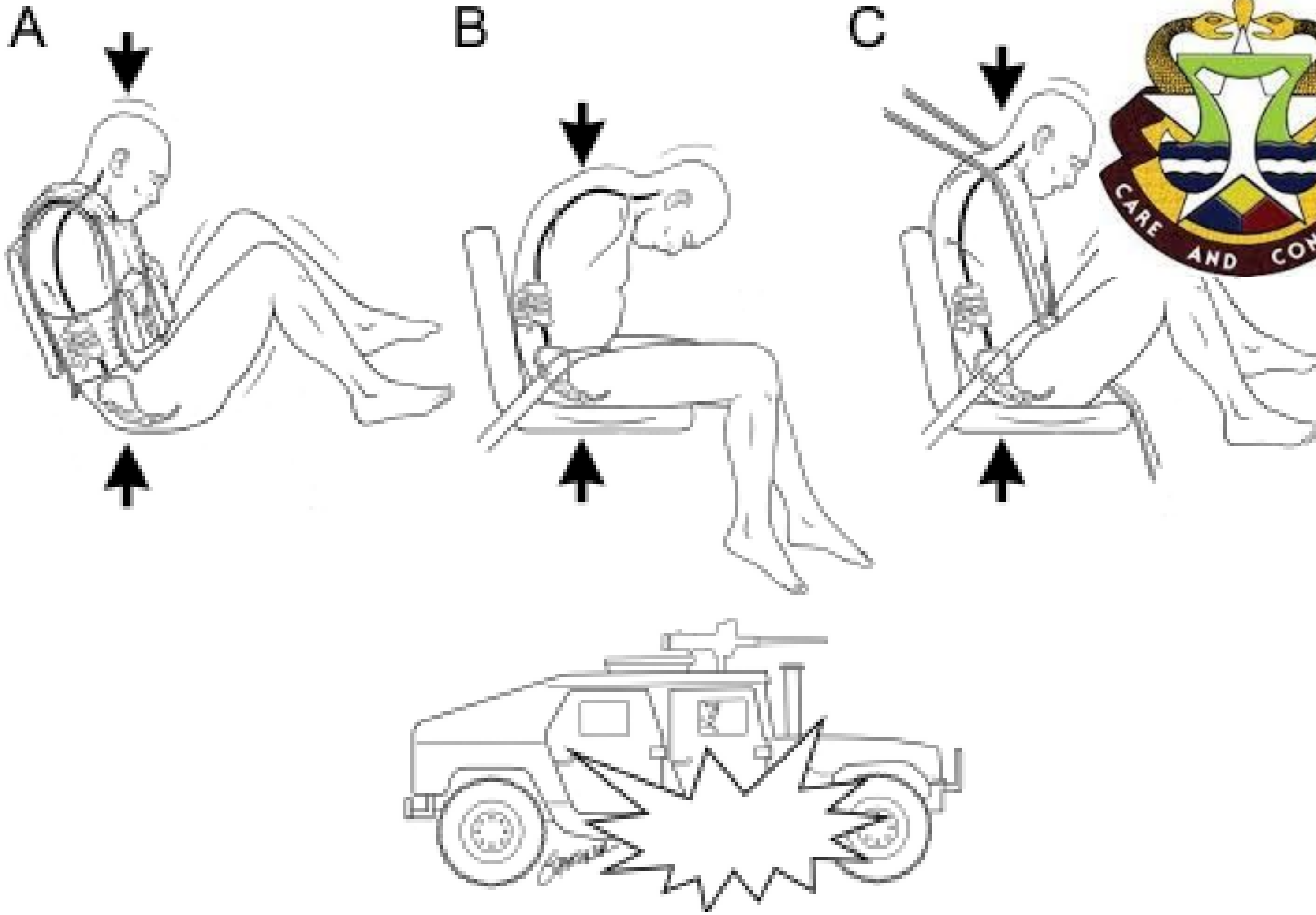

TL, thoracolumbar; AO, Arbeitsgemeinschaft fur Osteosynthesefragen.

Ragel BT, et al. Fractures of the thoracolumbar spine sustained by soldiers in vehicles attacked by improvised explosive devices. *SPINE* 2009;34(22):2400-5.

New data

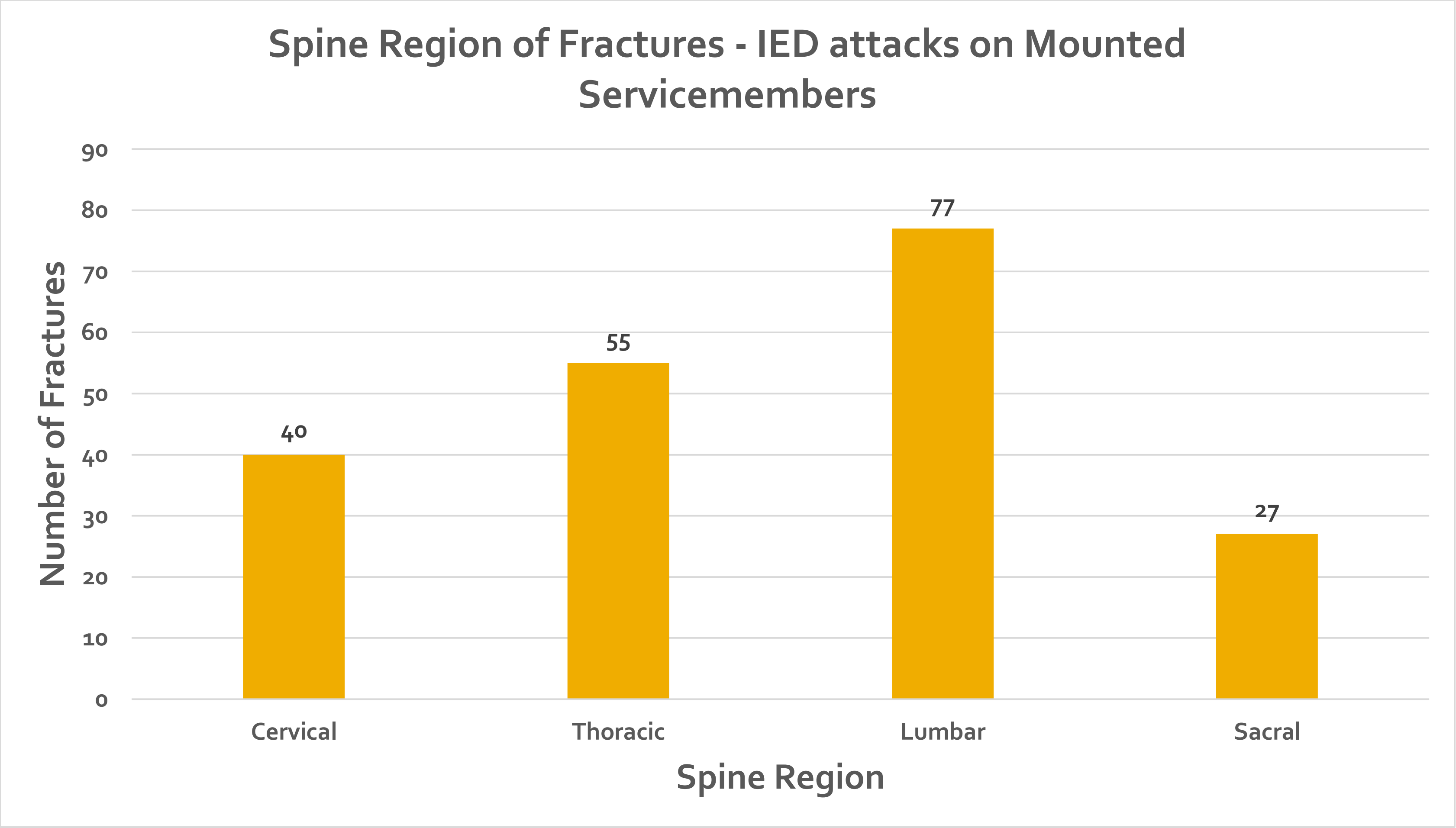

Spine Region of Fractures - IED attacks on Mounted Servicemembers
Number of Fractures
90
80
70
60
50
40
30
20
10
0
40
55
77
27
Cervical
Thoracic
Lumbar
Sacral
Spine Region

New data

Characterization of spinal injuries sustained by American service members killed in Iraq and Afghanistan: A study of 2,089 instances of spine trauma

Andrew J. Schoenfeld, MD, Ronald L. Newcomb, DO, Mark P. Pallis, DO, Andrew W. Cleveland, III, MD, Jose A. Serrano, MD, Julia O. Bader, PhD, Brian R. Waterman, MD, *and* Philip J. Belmont, Jr., MD, *El Paso, Texas*

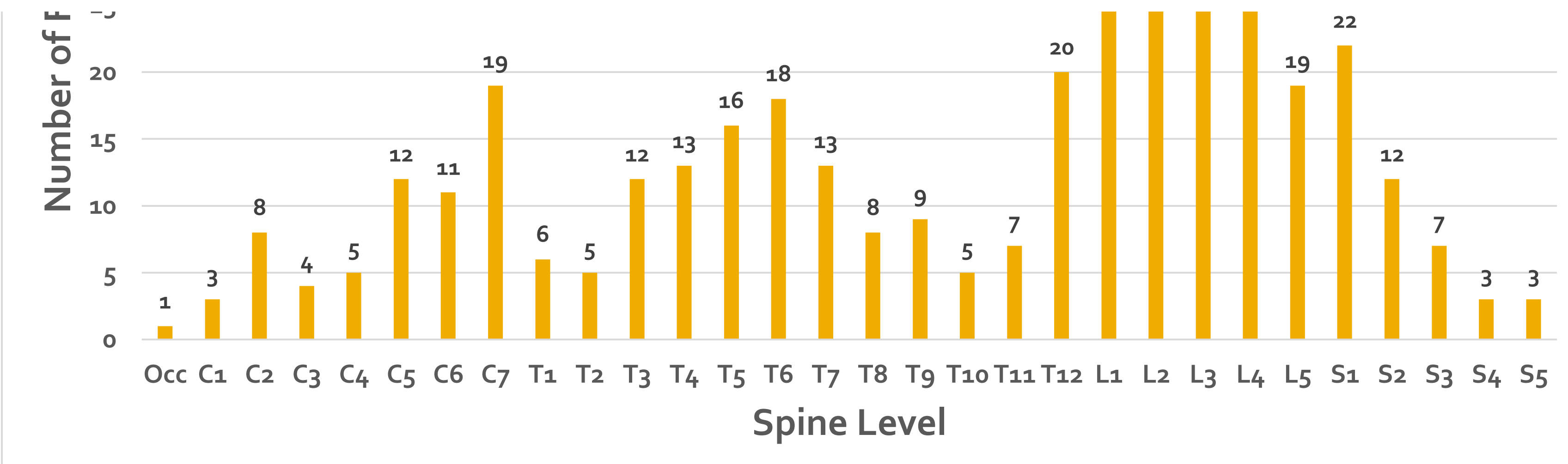

New data

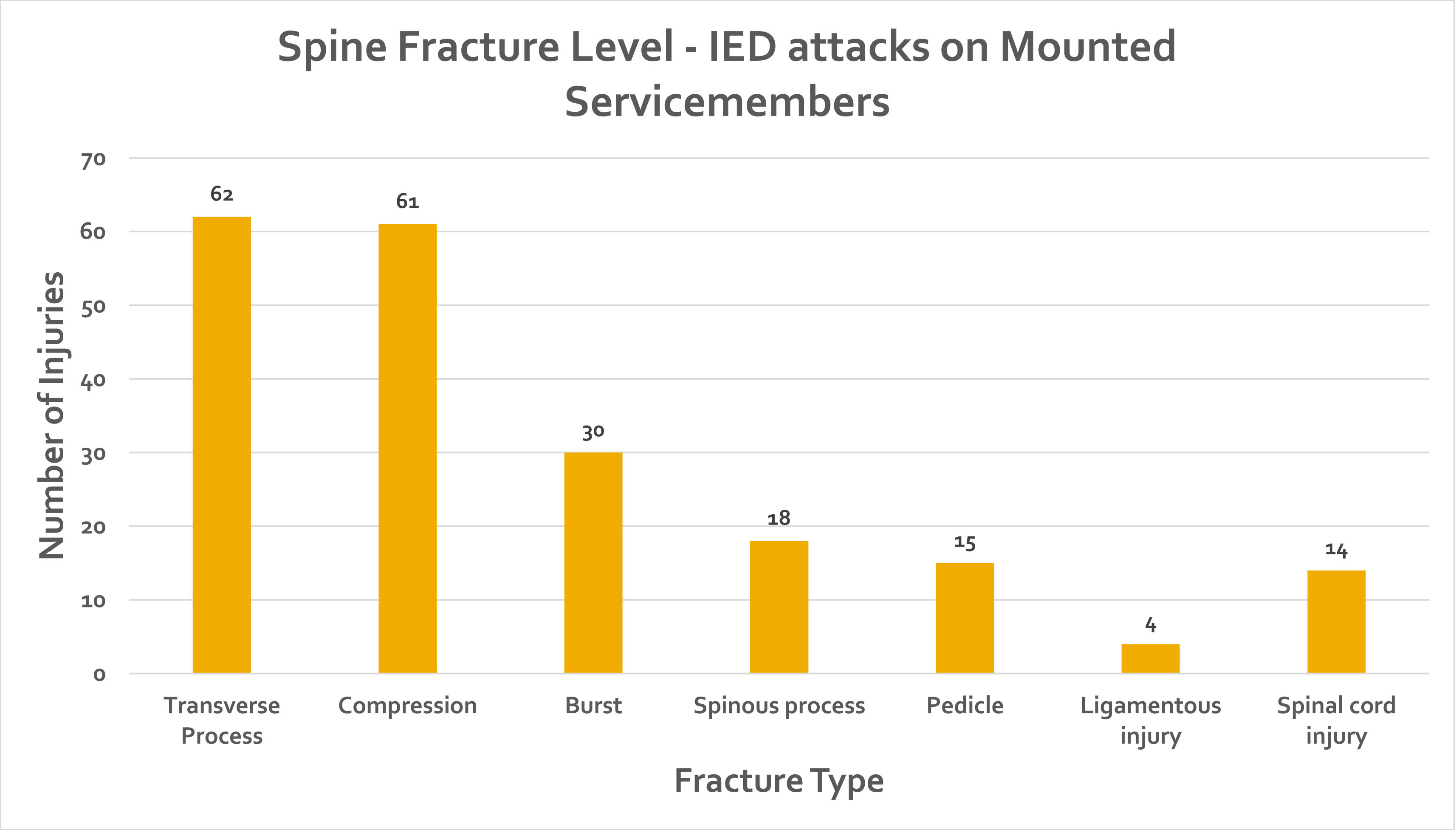
Spine Fracture Level - IED attacks on Mounted Servicemembers
Number of Injuries
70
60
50
40
30
20
10
0
62
61
30
18
15
4
14
Transverse Process
Compression
Burst
Spinous process
Pedicle
Ligamentous injury
Spinal cord injury
Fracture Type

Disability

Ranking of Unfitting Conditions by Average Percent Disability

Rank No.	Unfitting Condition	Average Percent Disability
1	Upper extremity amputation	72
2	Spine condition	60
3	Lower extremity amputation	56
4	Head condition	49
5	Abdomen/pelvis condition	38

ause

19:S

Ranking of Unfitting Conditions by Average Percent Disability

Ranking of Unfitting Conditions by Impact

Rank No.	Unfitting Condition	Impact[a]
1	Lower extremity amputation	3,150
2	Nerve: Loss of function	3,130
3	Degenerative arthritis	2,000
4	Spine condition	1,930
5	Posttraumatic stress disorder	1,930
6	Upper extremity amputation	1,795
7	Eye condition	1,570
8	Head condition	1,220
9	Hand condition	1,090
10	Abdomen/pelvis condition	1,050

Wish list

- 1. Stable soft tissues
- 2. Minimal contamination
- 3. Extra-articular fractures
- 4. Non-comminuted fractures

Daniel.r.possley.mil@mail.mil

U.S. ARMY TANK AUTOMOTIVE RESEARCH, DEVELOPMENT AND ENGINEERING CENTER

Assessment of Automotive Hybrid ATD Models for Prediction of Lower Extremity and Lumbar Spine Injuries under Mine Blast Loadings

Jai Ramalingam	Dmitriy Krayterman	Jianping Sheng
SE-Analytics	WMRD	SE-Analytics
TARDEC	ARL	TARDEC

2nd Workshop on Numerical Analysis of Human and Surrogate Response to Accelerative Loading,
Jan. 12~14, 2016

Near Term Under-Body Blast (NT-UBB) Program

Outline

- Background
- Objective
- Test Setup
- Test Case Selection
- LS-Dyna Model Assessment
- Madymo Model Assessment
- Conclusion

Background

- Either in the live fire tests, or in the underbody blast modeling and simulation for occupant survivability assessment, Hybrid III Anthropomorphic Test Devices (ATD) or dummies are used.
- However, the Hybrid III ATDs were originally developed, tested and validated specifically for occupant protection studies and assessments during automotive crashes, where occupants experience lateral loadings in most cases.
- In the underbody mine blast loading conditions, occupant injuries are caused by the severe vertical loading. There are also differences in the anatomical compatibility of these ATDs with the human body system especially at the lumbar spine geometry, and the complex neck region.
- WIAMan ATD is underway.

Background (cont.)

- **Questions:** Whether the current ATDs, both physical and computational, can accurately predict the injuries to the occupants when subjected to same loading conditions?
- (NTUBB) Modeling and Simulation Enhancement Program addresses this question for the understanding of the role and capability of the current ATD’s computational model in predicting the injuries to occupants.

NTUBB Computational M&S Enhancement Overview

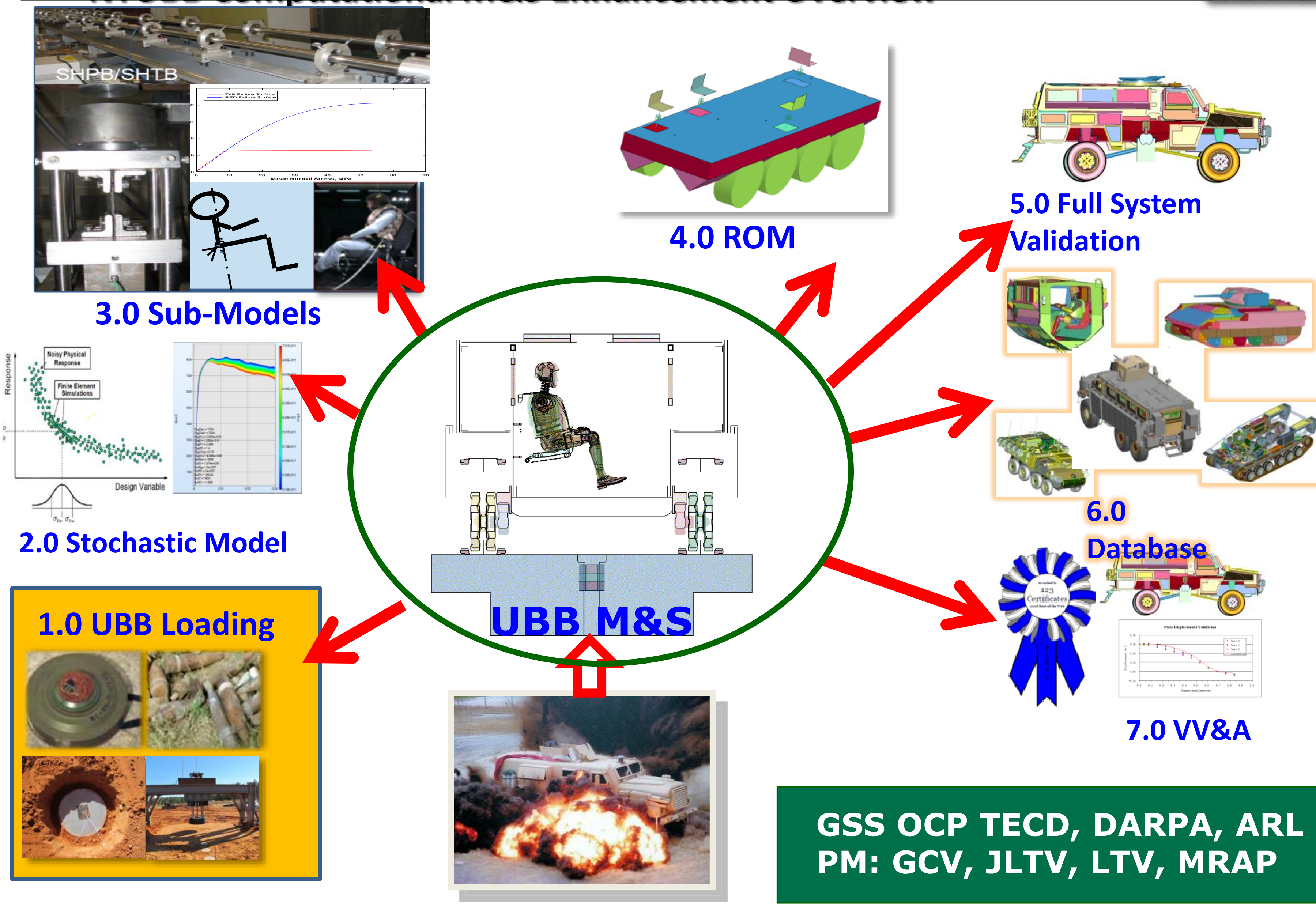

GSS OCP TECD, DARPA, ARL
PM: GCV, JLTV, LTV, MRAP

Objective

- The main objective of this study is to assess the capability of LS-Dyna ATD model and MADYMO ATD model to predict injuries (lower extremity and lumbar spine) as observed in the PMHS subjected to blast loading.
- To compare the performances of LS-Dyna and Madymo ATD Madymo model to that of Physical ATD in the ALF when subjected to same loading conditions.

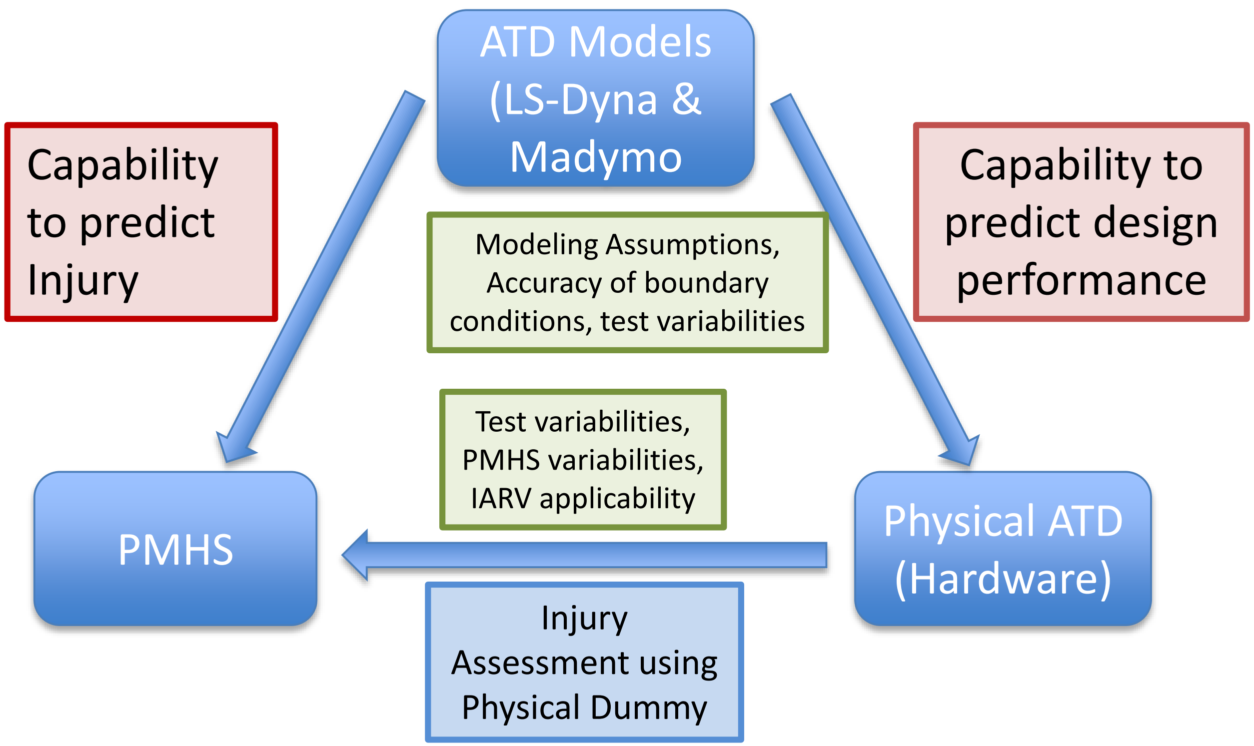

Experimental Setup (Accelerative Loading Fixture)

Inner Sled

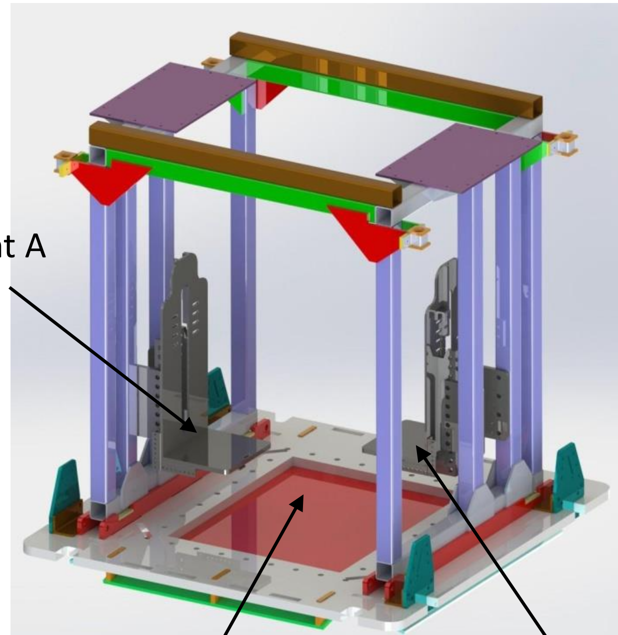

Occupant A (Crew 1)

Occupant B (Crew2)

Target plate

Floor instrumentation

boot print “would be” locations occ. **B**

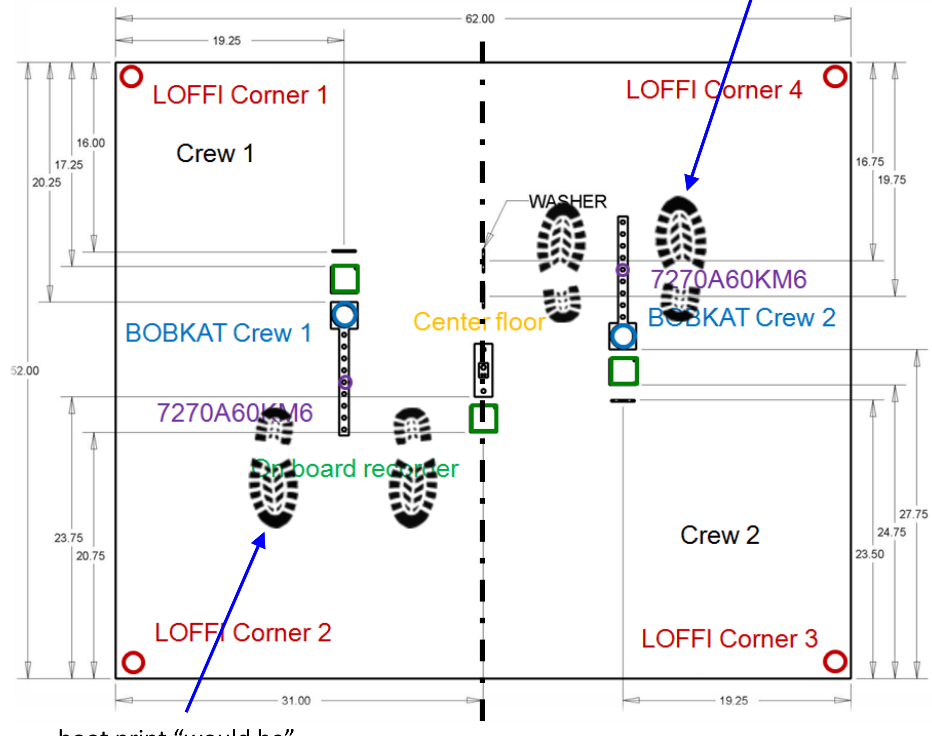

boot print “would be” locations occ. **A**

Experimental Setup

Examples of occupant placement in ALF

Occupant A (ATD, no PPE, knee angle 90°
Occupant A can be a PMHS, with or without PPE)

Occupant B (ATD, no PPE, knee angle 120°

Test Case Selection for Study

Test		Occupant A (1)								Occupant B (2)							
		Setup Matrix			Injury Matrix					Setup Matrix			Injury Matrix				
Matrix shot	Level	Type	Knee Angle (deg)	PPE	Ankle	Leg	Thigh	Pevis	Spine	Type	Knee Angle (deg)	PPE	Ankle	Leg	Thigh	Pevis	Spine
1	Enhanced	PMHS	90	no						ATD	90	no					
2	Enhanced	PMHS	120	no	L/R			X		ATD	120	no					
3	Enhanced	ATD	90	yes	L/R	L/R	L/R		X	ATD	90	no	L/R	L/R	L/R		X
4	Enhanced	PMHS	90	no	L/R			X	X	PMHS	120	no				X	X
5	Enhanced	PMHS	90	yes	R			X		PMHS	90	no				X	X
6	Enhanced	PMHS	120	yes	R			X	X	PMHS	120	no				X	X
7	Enhanced	PMHS	90	yes	L/R			X	X	PMHS	120	yes	L/R	R		X	X
8	Mild	ATD	90	no	L/R	L/R				ATD	120	no	L/R	R			X
9	Mild	ATD	90	yes	L/R	L/R				ATD	90	no	L/R	L/R	R		X
10	Mild	ATD	120	yes	L/R	L/R				ATD	120	no	L/R	R			
11	Mild	PMHS	90	no	L/R					PMHS	120	no					
12	Mild	ATD	90	yes	L/R	L/R				ATD	120	yes	L/R	L/R			
13	Enhanced	ATD	90	yes	L/R	L/R	L/R		X	ATD	120	yes					
14	Mild	PMHS	90	no	R					PMHS	120	yes					

- The tests can be grouped under three metrics. These are **knee angle** (90° or 120°), **PPE** (absence or presence), and **blast severity level** (mild or enhanced).
- The ATD is Hybrid III 50th percentile male. Variabilities in PMHS such as gender, age, stature (heights), and mass were ignored in this study because they have no applicability to the ATD.
- For this study, only tests with "no PPE" were considered in order to reduce additional variabilities and uncertainties arising out of PPE modeling. Similarly for the same reasons, preference was given to nominal leg (90^0) position.
- Since PMHS does not record loads in lumbar or tibia, test cases where injuries were observed in PMHS is selected as it provides a reasonable comparison point in the ATD responses.

Test Case Selection Summary

Test Case	Test metric		PMHS			equivalent ATD		
	blast level	leg angle	Matrix shot	Occupant	Injury	Matrix shot	Occupant	Injury
1	enhanced	90	4	A	LL/Spine	3	B	LL/Spine
2	enhanced	90	5	B	spine	3	B	LL/spine
3	mild	90	11	A	LL	8	A	LL
4	mild	90	11	A	LL	9	B	LL/Spine
5	mild	120	11	B	none	8	B	LL/Spine

Three groups of PMHS and equivalent ATD cases were identified:

- **GROUP 1: PMHS 4A (LL), 5B (Spine) – ATD 3B; CASE 1 – 4A (PMHS) vs. 3B (ATD), CASE 2 – 5B (PMHS) vs. 3B (ATD)**
- **GROUP 2: PMHS 11A (LL) – ATD 8A, 9B; CASE3 – 11A (PMHS) vs. 8A (ATD), CASE4 11A (PMHS) vs. 9B (ATD)**
- **GROUP 3: PMHS 11B (none) – ATD 8B; CASE5 – 11B (PMHS) vs. 8B (ATD),**

It should be noted that the Physical ATD (equivalent) does not always match the injuries observed in PMHS. It matches injury in cases 4A (PMHS) vs 3B (ATD) and 11A (PMHS) vs 8A (ATD).

It also should be noted that there are differences in injury between the PMHS cases themselves as observed in 4A vs 5B. This may be due to the variability in PMHS in terms of age, size and bone strengths.

Model Input Data Processing (summary)

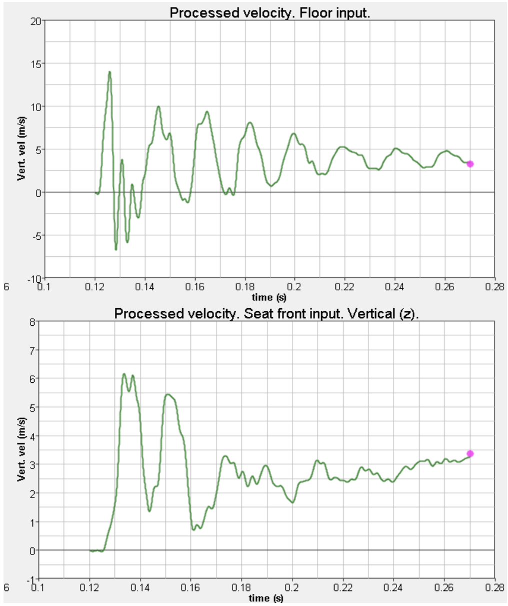

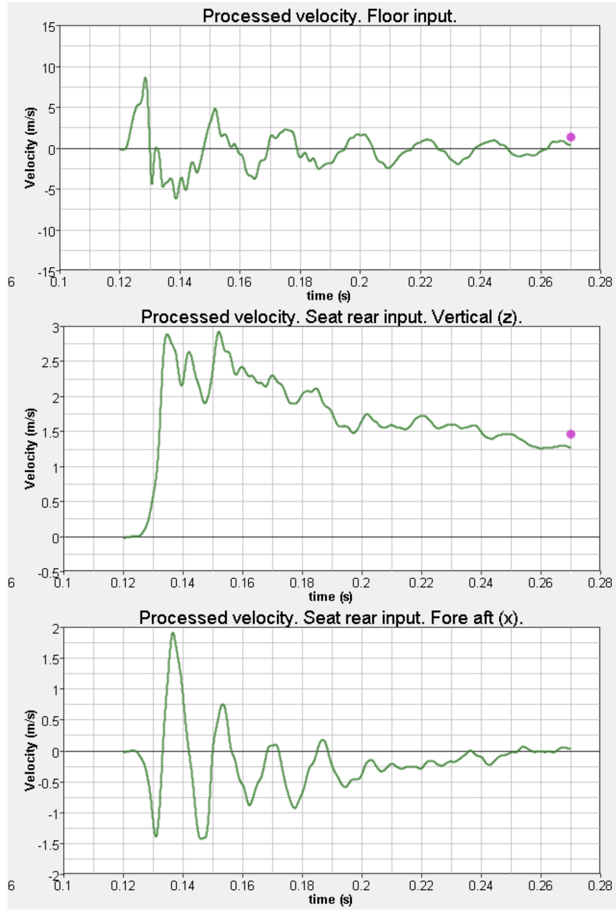

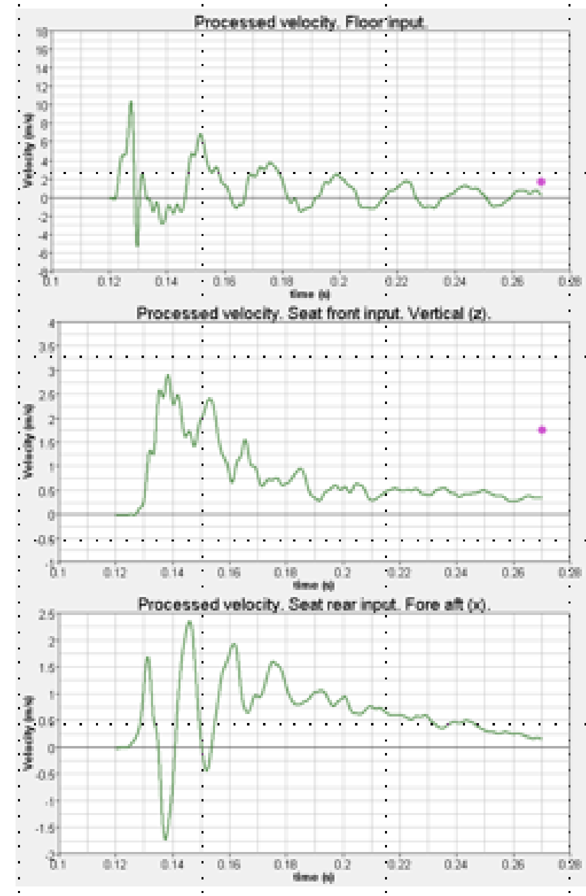

GROUP 1: 5B (PMHS input), 4A (PMHS input), 3B (equiv. ATD input)

GROUP 2: 11A (PMHS input), 8A (equiv. ATD input), 9B (equiv. ATD input)

GROUP 3: 11B (PMHS input), 8B (equiv. ATD input)

Finite Element (LS-Dyna) model setup.

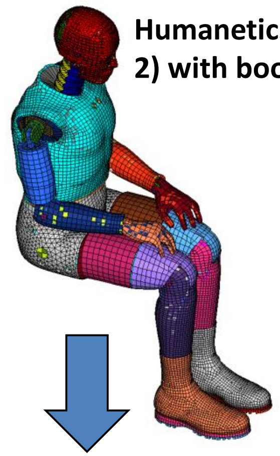

Humanetics Hybrid III ATD model (Gen 2) with boots (legs at 90º)

The Accelerative Loading Fixture (ALF) rigid model

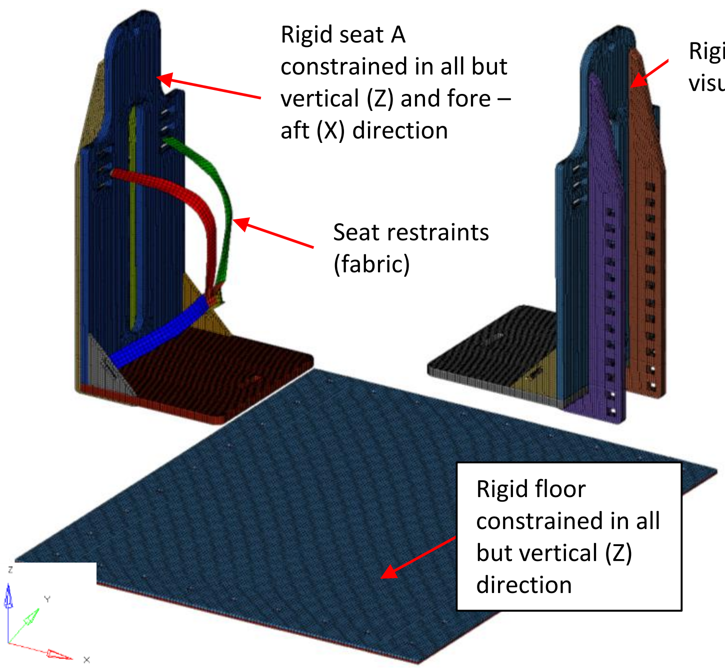

Humanetics Hybrid III ATD model (Gen 2) with boots (legs at 90º) placed on the rigid seat (before preload).

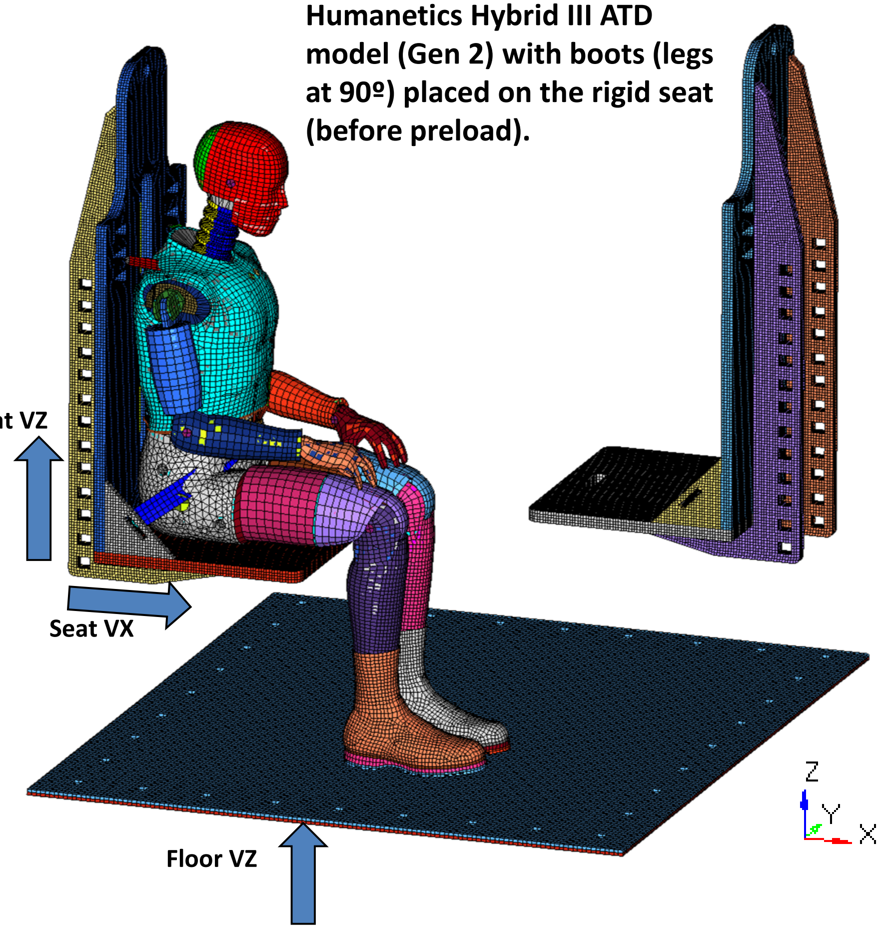

Humanetics Hybrid III ATD model (Gen 2) with boots (legs at 90º or 120º) is placed on the rigid seat and preload (120 ms) is applied. The pelvis is pushed down to simulate gravity preload and shoulders are pushed back to simulate belt tension. After preload phase is completed, the belts to body contact is initiated and the main pulse (velocity, integrated from acceleration data) is applied to the rigid floor in vertical (Z) direction and to the seat in vertical (Z) and for aft (X) directions (if data is available). The vertical pulse is also applied to the empty seat for proper motion visualization.

M&S vs Experimental Results –Test Cases 1 Tibia

CASE1: 4A (PMHS input) vs. 3B (equiv. ATD input) (PMHS lower extremity injury)

Test				Occupant A (1)								Occupant B (2)							
				Setup Matrix			Injury Matrix					Setup Matrix			Injury Matrix				
Matrix shot	Level	Charge Weight (kg)	Target Plate Thickness (mm)	Type	Knee Angle	PPE	Ankle	Leg	Thigh	Pevis	Spine	Type	Knee Angle	PPE	Ankle	Leg	Thigh	Pevis	Spine
3	Enhanced	2.25	12.7 RHA	ATD	90	yes	L/R	L/R	L/R		X	ATD	90	no	L/R	L/R	L/R		X
4	Enhanced	2.25	12.7 RHA	PMHS	90	no	L/R			X	X	PMHS	120	no				X	X

4A ATD Model tibia response (PMHS input)

3B Equiv. ATD experim. tibia response

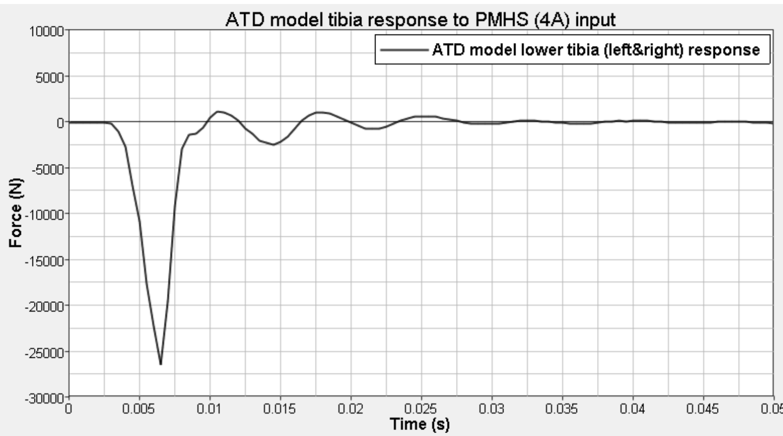

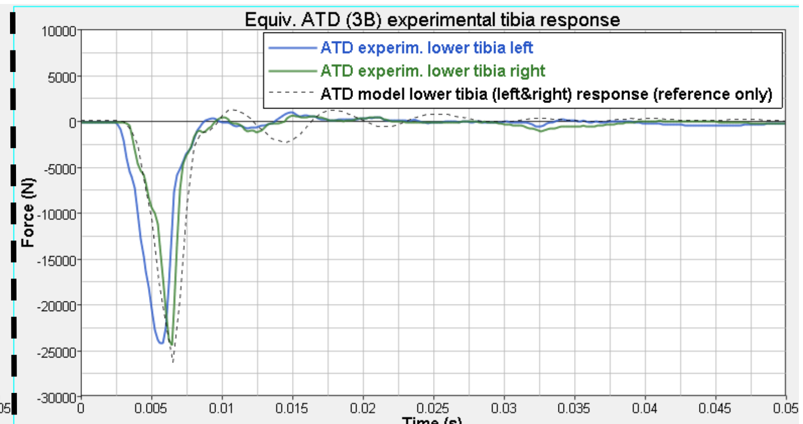

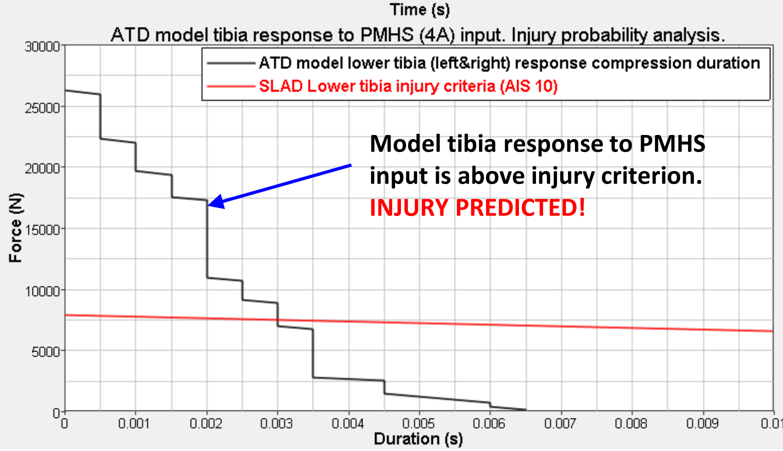

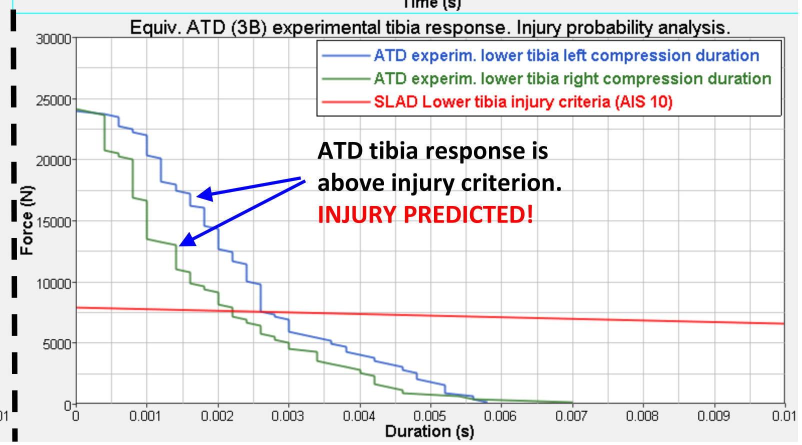

The ATD model **correctly predicts lower extremity injury** in PMHS (4A) .The equivalent ATD (3B) also predicts lower extremity injury.
No ATD model to equivalent ATD (3B) input comparison is performed due to the absence of ATD input data.

M&S vs Experimental Results –Test Cases 2 Spine

CASE 2: 5B (PMHS input) vs. 3B (equiv. ATD input) (PMHS lumbar spine injury)

Test				Occupant A (1)								Occupant B (2)							
				Setup Matrix			Injury Matrix					Setup Matrix			Injury Matrix				
Matrix shot	Level	Charge Weight (kg)	Target Plate Thickness (mm)	Type	Knee Angle	PPE	Ankle	Leg	Thigh	Pevis	Spine	Type	Knee Angle	PPE	Ankle	Leg	Thigh	Pevis	Spine
3	Enhanced	2.25	12.7 RHA	ATD	90	yes	L/R	L/R	L/R		X	ATD	90	no	L/R	L/R	L/R		X
4	Enhanced	2.25	12.7 RHA	PMHS	90	no	L/R			X	X	PMHS	120	no				X	X
5	Enhanced	2.25	12.7 RHA	PMHS	90	yes	R			X		PMHS	90	no				X	X

5B ATD Model lumbar spine response (PMHS input)

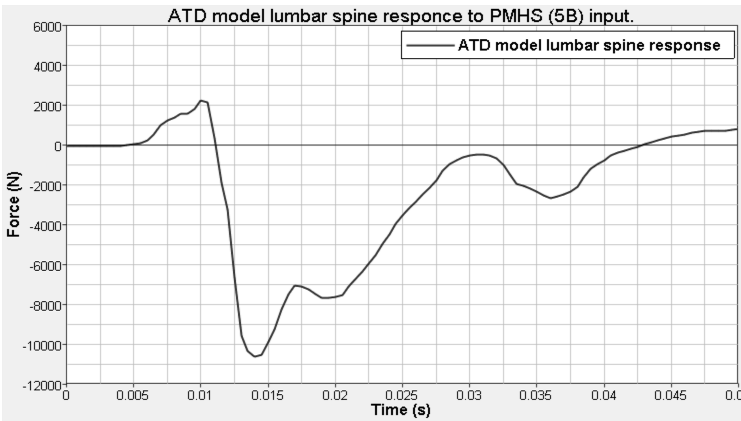

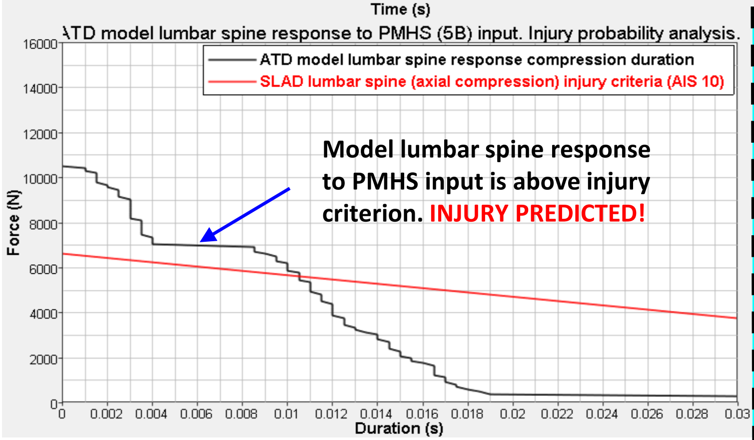

3B Equiv. ATD experim. lumbar spine response

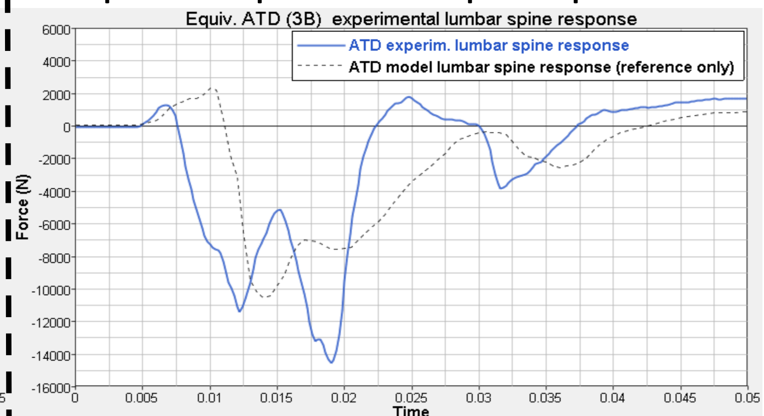

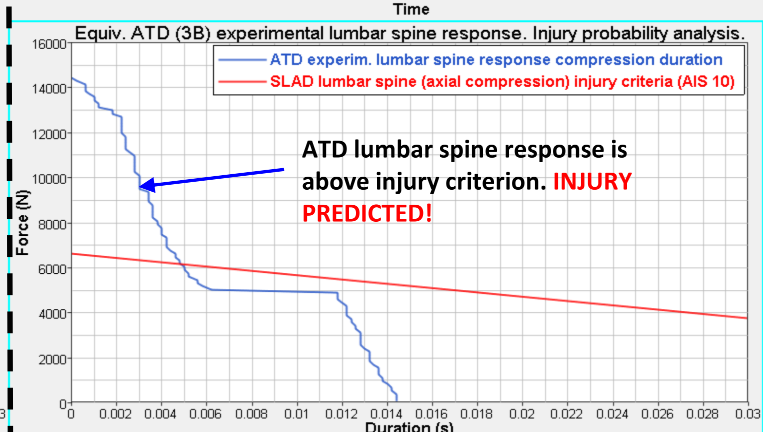

The ATD model **correctly** predicts lumbar spine injury in PMHS (5B) .The equivalent ATD (3B) also predicts lumbar spine injury.

No ATD model to equivalent ATD (3B) input comparison is performed due to the absence of ATD input data.

M&S vs Experimental Results –Test Cases 3 Tibia

The ATD model **correctly** predicts tibia injury in PMHS (11A). The model DOES NOT match the equivalent ATD injury prediction. The equivalent ATD (8A) also predicts tibia injury.

CASE 3: 11A (PMHS input) vs. 8A (equiv. ATD input) (PMHS lower extremity injury)

Test				Occupant A (1)								Occupant B (2)							
				Setup Matrix			Injury Matrix					Setup Matrix			Injury Matrix				
Matrix shot	Level	Charge Weight (kg)	Target Plate Thickness (mm)	Type	Knee Angle	PPE	Ankle	Leg	Thigh	Pevis	Spine	Type	Knee Angle	PPE	Ankle	Leg	Thigh	Pevis	Spine
8	Mild	1.125	6.35 RHA	ATD	90	no	L/R	L/R				ATD	120	no	L/R	R			X
11	Mild	1.125	6.35 RHA	PMHS	90	no	L/R					PMHS	120	no					

11A ATD Model tibia response (PMHS input)

8A ATD Model tibia response (equiv ATD input)

8A Equiv. ATD exper. tibia response

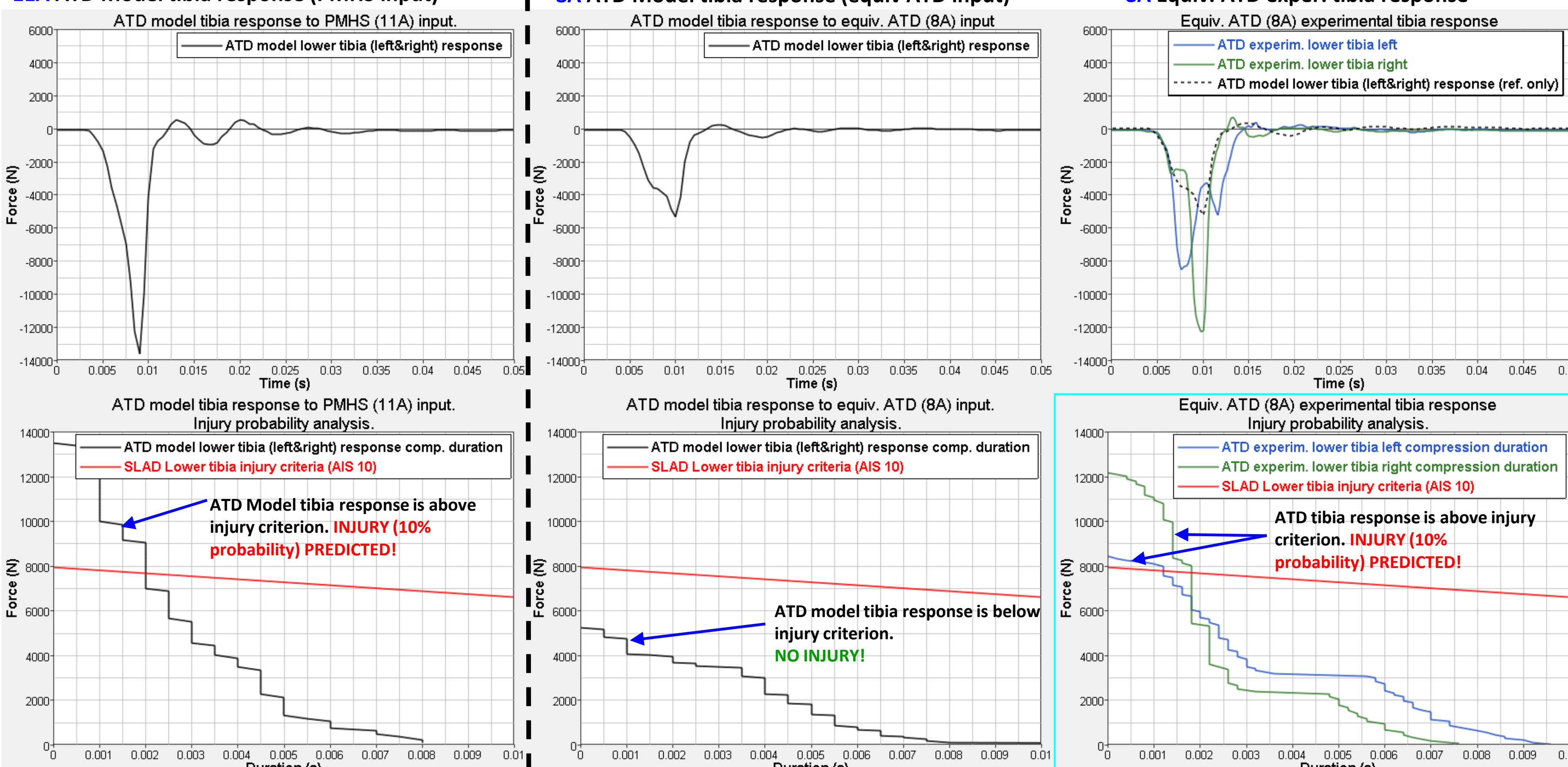

UNCLASSIFIED: Dist. A. Approved for public release

M&S vs Experimental Results –Test Cases 4 Tibia

The ATD model correctly predicts tibia injury in PMHS (11A). The model matches the equivalent ATD (9B) injury prediction.

CASE 4: 11A (PMHS input) vs. 9B (equiv. ATD input) (PMHS lower extremity injury)

Test				Occupant A (1)								Occupant B (2)							
				Setup Matrix			Injury Matrix					Setup Matrix			Injury Matrix				
Matrix shot	Level	Charge Weight (kg)	Target Plate Thickness (mm)	Type	Knee Angle	PPE	Ankle	Leg	Thigh	Pevis	Spine	Type	Knee Angle	PPE	Ankle	Leg	Thigh	Pevis	Spine
9	Mild	1.125	6.35 RHA	ATD	90	yes	L/R	L/R				ATD	90	no	L/R	L/R	R		X
11	Mild	1.125	6.35 RHA	PMHS	90	no	L/R					PMHS	120	no					

11A ATD Model tibia response (PMHS input)

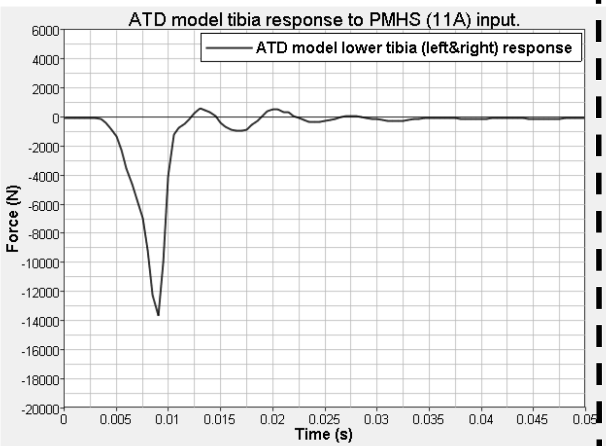

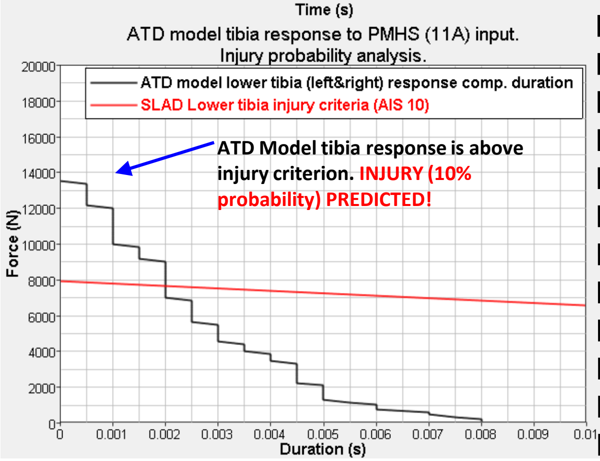

9B ATD Model tibia response (equiv ATD input)

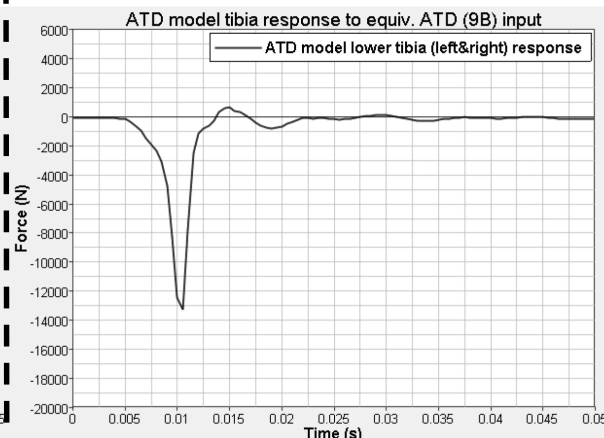

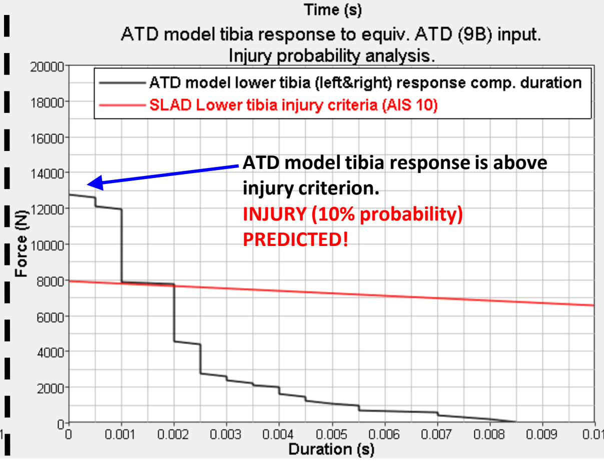

9B Equiv. ATD exper. tibia response

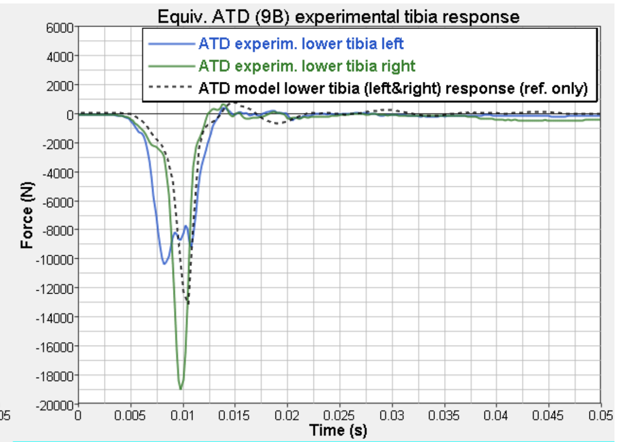

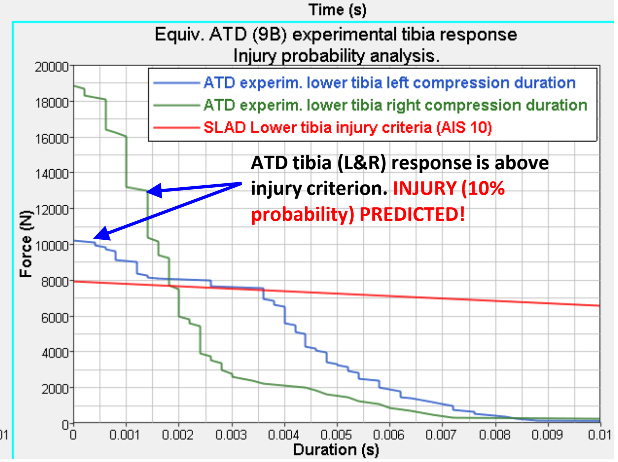

M&S vs Experimental Results –Test Cases 5 Tibia

CASE 5: 11B (PMHS input) vs. 8B (equiv. ATD input) (PMHS no lower extremity injury)

Test				Occupant A (1)								Occupant B (2)							
				Setup Matrix			Injury Matrix					Setup Matrix			Injury Matrix				
Matrix shot	Level	Charge Weight (kg)	Target Plate Thickness (mm)	Type	Knee Angle	PPE	Ankle	Leg	Thigh	Pevis	Spine	Type	Knee Angle	PPE	Ankle	Leg	Thigh	Pevis	Spine
8	Mild	1.125	6.35 RHA	ATD	90	no	L/R	L/R				ATD	120	no	L/R	R			X
11	Mild	1.125	6.35 RHA	PMHS	90	no	L/R					PMHS	120	no					

The ATD model predicts 10% tibia injury probability in PMHS (11A). No injury is observed in PMHS. The model partially matches (right leg only) the equivalent ATD (9B) injury prediction.

11B ATD Model tibia response (PMHS input)

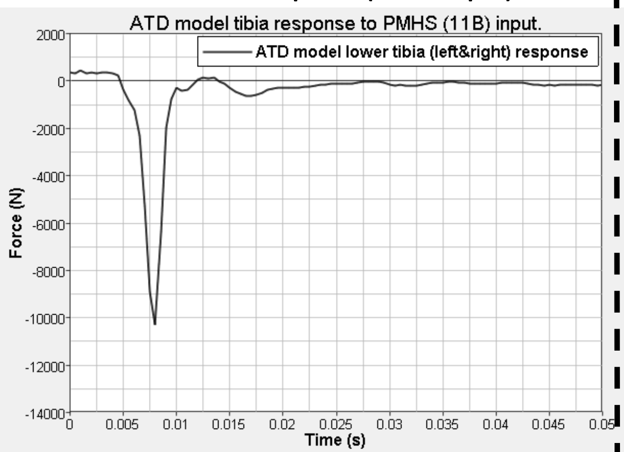

8B ATD Model tibia response (equiv ATD input)

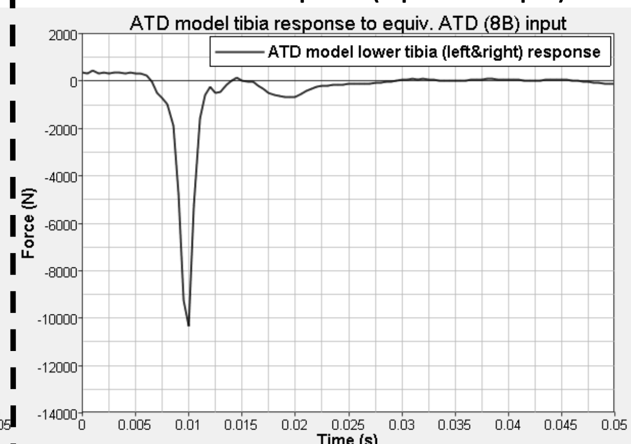

8B Equiv. ATD exper. tibia response

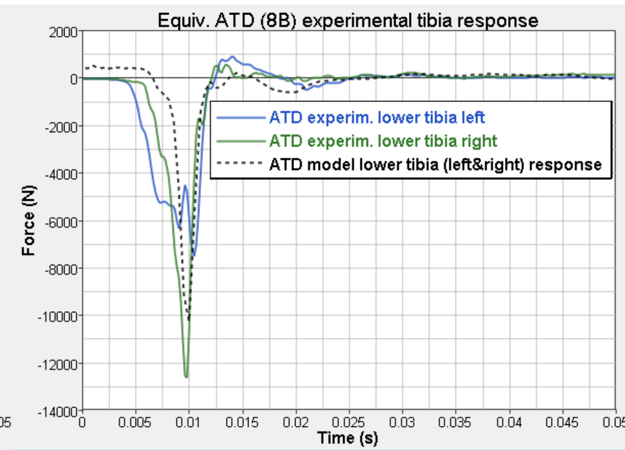

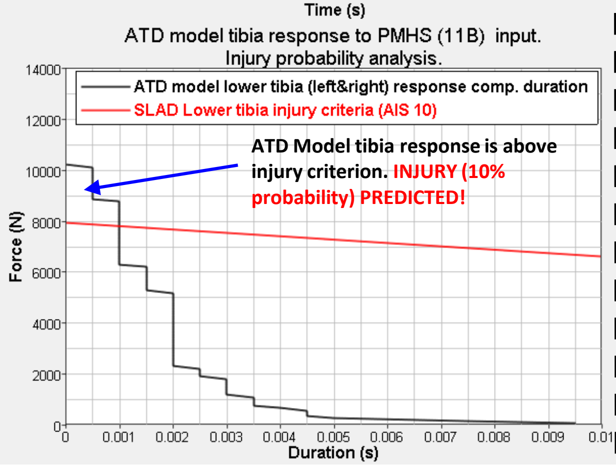

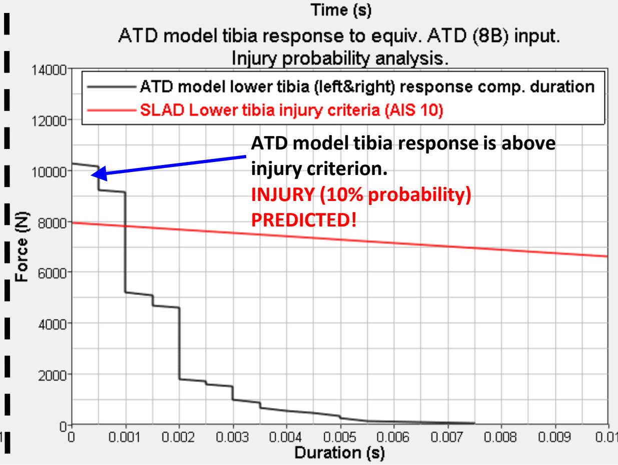

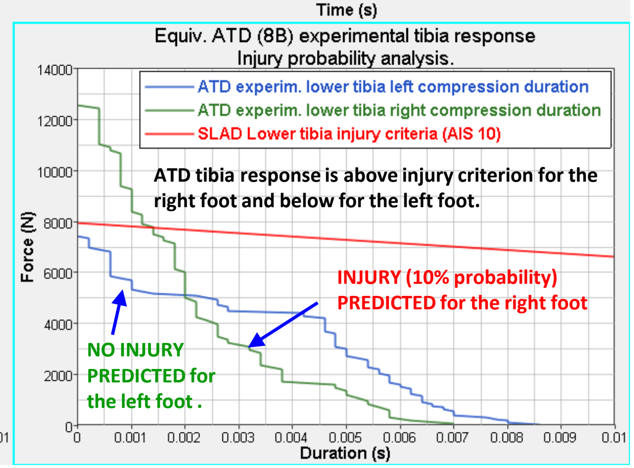

M&S vs Experimental Results –Test Cases 5 Spine

CASE 5: 11B (PMHS input) vs. 8B (equiv. ATD input) (PMHS no lumbar spine injury)

Test				Occupant A (1)								Occupant B (2)							
				Setup Matrix			Injury Matrix					Setup Matrix			Injury Matrix				
Matrix shot	Level	Charge Weight (kg)	Target Plate Thickness (mm)	Type	Knee Angle	PPE	Ankle	Leg	Thigh	Pevis	Spine	Type	Knee Angle	PPE	Ankle	Leg	Thigh	Pevis	Spine
8	Mild	1.125	6.35 RHA	ATD	90	no	L/R	L/R				ATD	120	no	L/R	R			X
11	Mild	1.125	6.35 RHA	PMHS	90	no	L/R					PMHS	120	no					

The ATD model does not predict lumbar spine injury in PMHS (11B). No injury is observed in PMHS. The model does not match the equivalent ATD (8B) injury prediction.

11B ATD Model spine response (PMHS input)

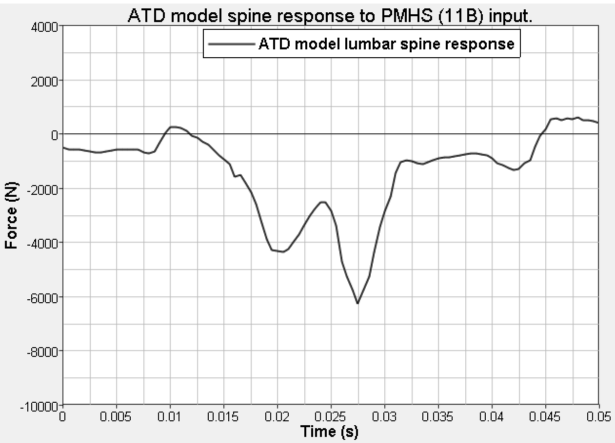

8B ATD Model spine response (equiv ATD input)

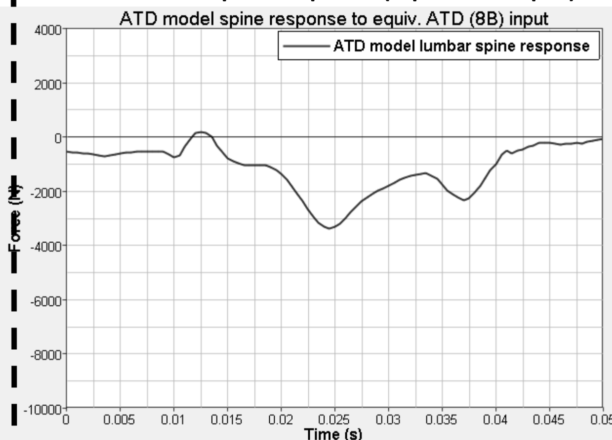

8B Equiv. ATD exper. spine response

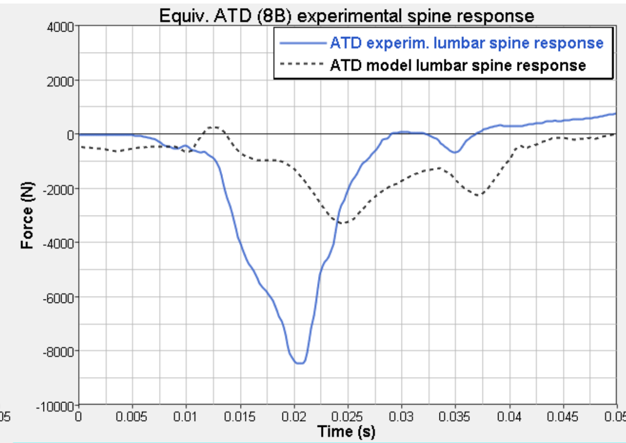

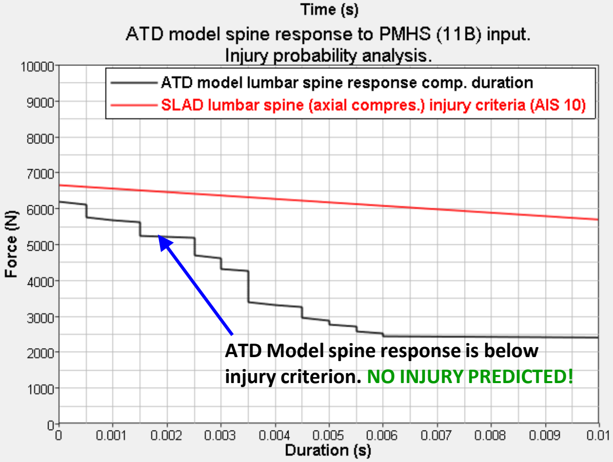

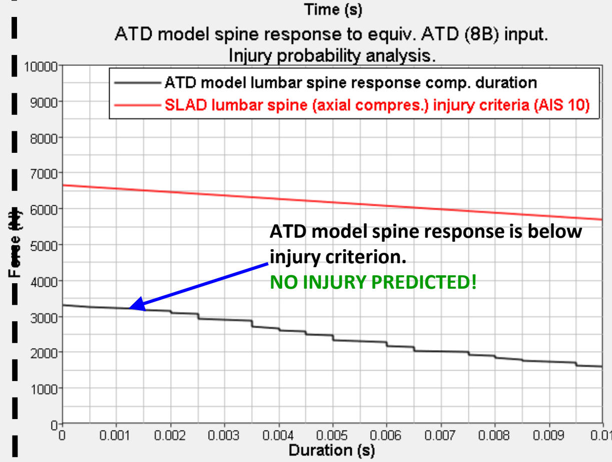

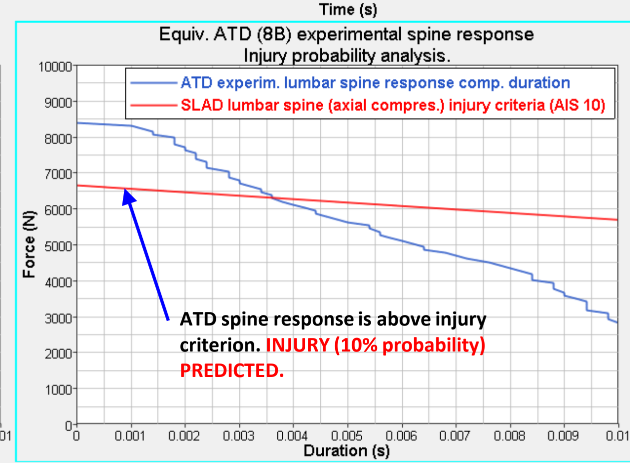

Results Analysis Summary (LS-Dyna ATD Model)

Group	Blast Level	Leg angle	Shot/ Occ. Pos.	Occ. Type	Injury observed		
					Experiment	M&S PMHS input	M&S eq. ATD input
I	Enhanced	90	4A	PMHS	LL	LL	NA
	Enhanced	90	5B	PMHS	SP	SP	NA
	Enhanced	90	3B	ATD	LL/SP	NA	NA
II	Mild	90	11A	PMHS	LL	LL	NA
	Mild	90	8A	ATD	LL	NA	None
	Mild	90	9B	ATD	LL	NA	LL
III	Mild	120	11B	PMHS	None (LL&SP)	LL, None	NA
	Mild	120	8B	ATD	LL/SP	NA	LL, None

Findings (from LS-DYNA ATD Model)

Based on the limited available data set analyses, the Humanetics Hybrid III ATD Ls Dyna model (GEN2) accurately predicted injury observed in PMHS in all but one analyzed event. In the case where no injury was observed in PMHS lower extremity, the model predicts lower leg injury (10% probability).

However, it is difficult to conclude that the model is reliably accurate in predicting injurious/non injurious events due to several reasons:

- the number of cases available to analyze is not large enough to warrant such a conclusion
- the modeling assumptions do not take into account cadaver's age, weight, instrumentation locations, etc (a younger person may not have been injured)
- the floor and seat inputs are assumed to be rigid (the floor (seat) input is constant and uniform throughout the floor)
- the injury prediction is based on AIS10 metric, which is only 10% probability of injury

In some cases the model correlates well with the "equivalent ATD" and in some cases it does not.
Again, there is not enough data to make any conclusion as to how well the model matches equivalent ATD responses.
The equivalent ATD responses match the PMHS responses in some cases analyzed (case 1, case2, case 3B), but do not
match in other cases (3A, 4).

MADYMO Model Setup

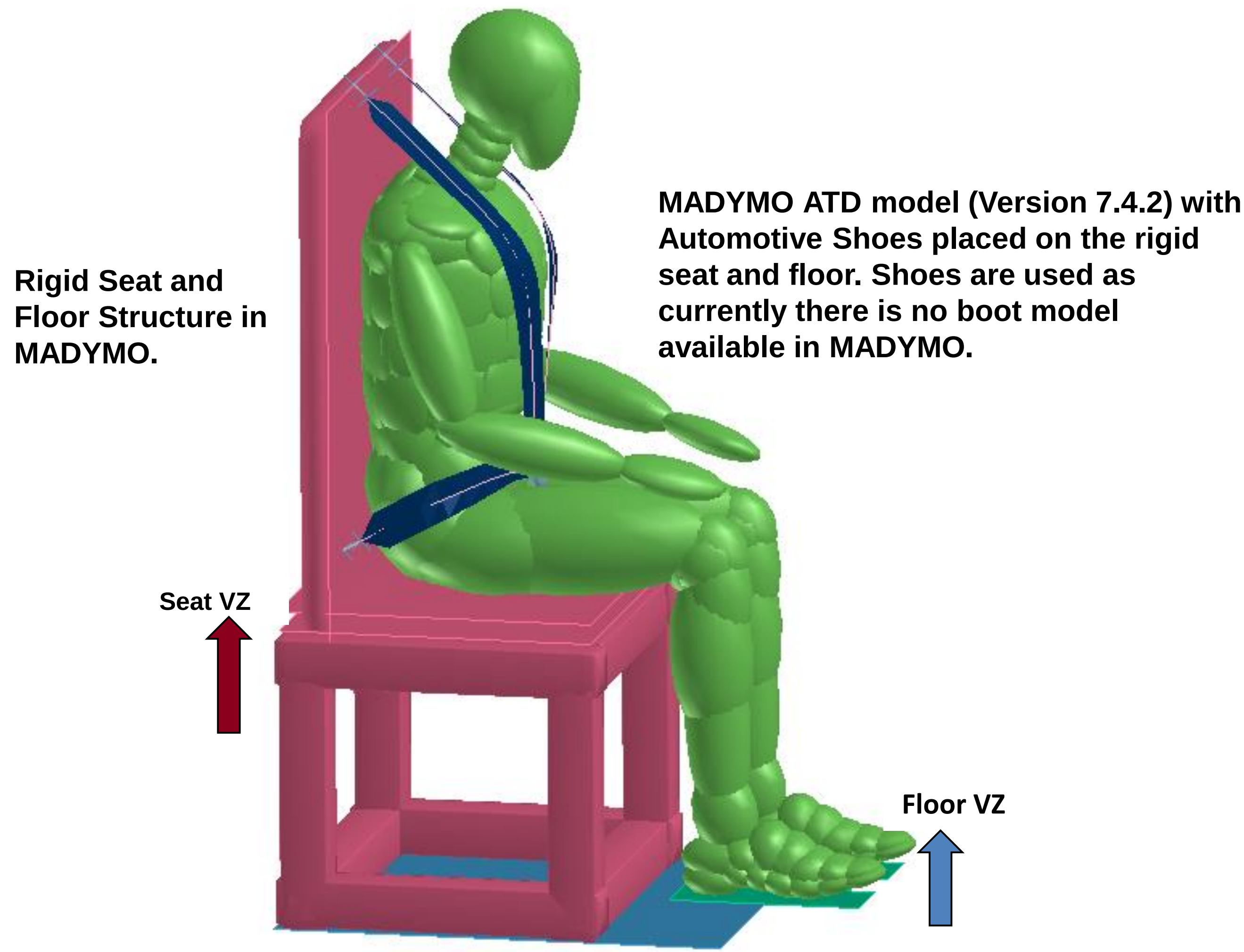

Seat Vertical Motion and Floor Motion were extracted from ALF Tests and included in MADYMO as boundary conditions

M&S vs Experimental Results – Test Cases 1 and 2

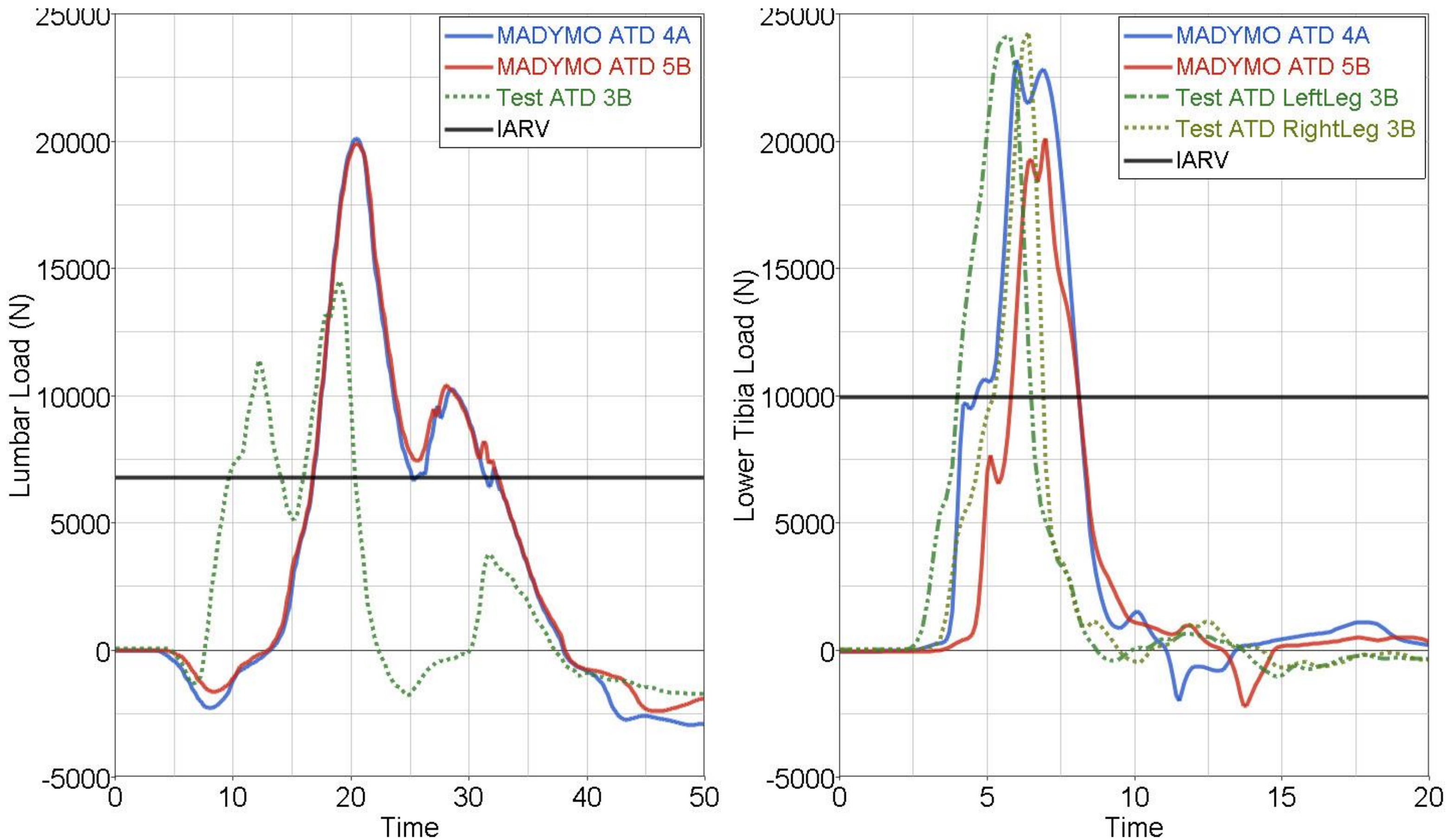

- Very good tibia peak load correlation between Madymo model and Experiment
- Lumbar load responses correlation is not good; however both model and experiment predict chance of failure

M&S vs Experimental Results – Test Cases 3 and 4

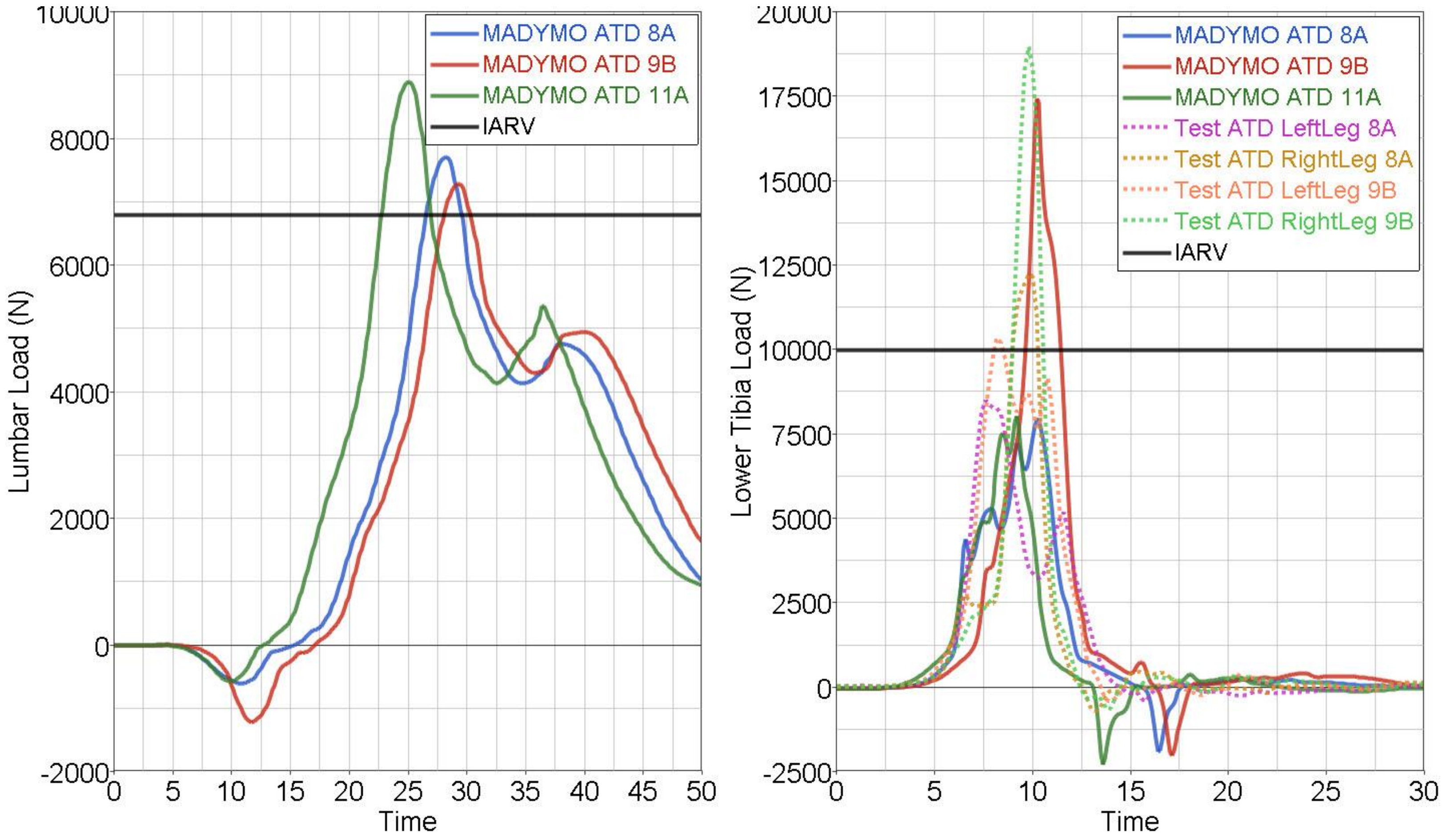

- Very good tibia peak load correlation between Madymo model and Experiment
- Lumbar load responses from experiment is not available; however all MADYMO runs are close and predict failure

M&S vs Experimental Results – Test Cases 5

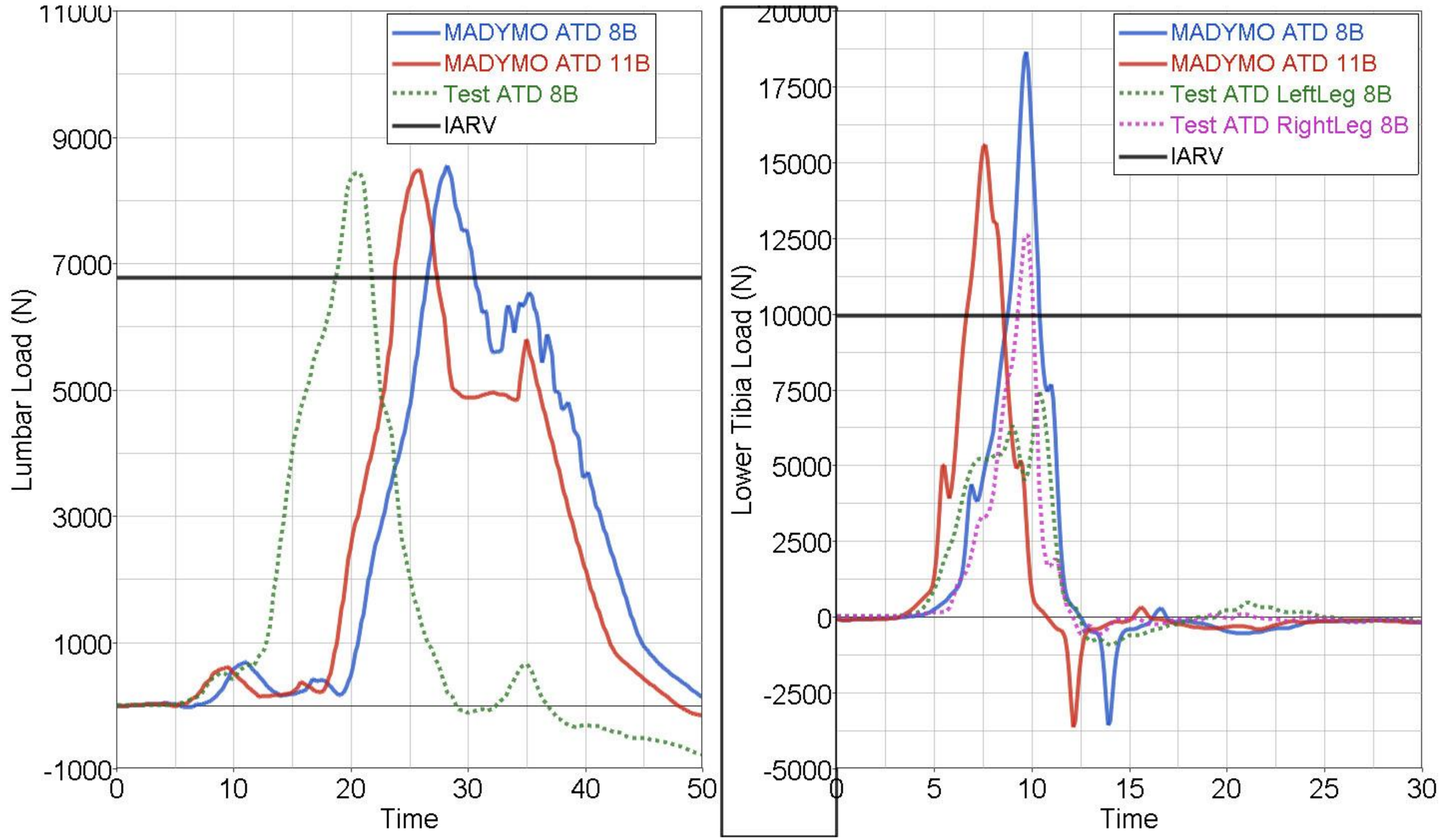

- Tibia load responses are similar between Madymo model and Experiment but peak values are not close; In the simulation, both left and right tibia record same loads, whereas in experiment, left and right tibia loads are different.
- Very good peak Lumbar load correlation between model and experiment with both predicting failure.

Summary of Analysis – (Madymo ATD)

Group	Blast Level	Leg Angle	Shot/ Occ. Pos.	Occ. Type	Injury Observed	
					Test	M&S
I	Enhanced	90	4A	PMHS	LL	LL
	Enhanced	90	5B	PMHS	Sp	Sp
	Enhanced	90	3B	ATD	LL/Sp	NA
II	Mild	90	11A	PMHS	LL	No
	Mild	90	8A	ATD	LL	No
	Mild	90	9B	ATD	LL	LL
III	Mild	120	11B	PMHS	No	LL/Sp
	Mild	120	8B	ATD	LL/Sp	LL/Sp

- Results are grouped under three categories based on the test metrics (Blast Level and Leg Angle)
- Each category has at least one PMHS and one ATD for comparison. Results from ATDs are highlighted.
- Tests 8A and 9B indicate differences that exist within the ATD experiments one showing Spine injury whereas the other one does not.
- ATD model injury predictions are same as experimental results excluding test case 8A.

Findings (from Madymo ATD Model study)

- Madymo ATD predicts the spine and lower extremity injury as observed from Physical ATD in all of the cases, however limited in number, analyzed. Therefore, its capability to predict PMHS injury stands similar to that of Physical ATD.

- Capability of ATDs (Model or Physical) to predict PMHS injury remains a mixed bag perhaps due to limited experimental data set available to compare the results. Within the limited set it was found that
  1) there are variations between one PMHS to another PMHS tests perhaps due to variability in PMHS characteristics (4A & 5B)
  2) Variations between repeat ATD test data (8A & 9B)
  3) The injury prediction from ATD is based on IARV (AIS10)
  4) Specific to M&S, it is assumed that the seat and floor measurements from ALF are accurate to be used as input to model and the materials are modeled as rigid.

Conclusions

Group	Blast Level	Leg Angle	Shot/ Occ. Pos.	Occ. Type	Injury Observed		
					Test	Madymo	LS-Dyna
I	Enhanced	90	4A	PMHS	LL	LL	LL
	Enhanced	90	5B	PMHS	Sp	Sp	Sp
	Enhanced	90	3B	ATD	LL/Sp	NA	NA
II	Mild	90	11A	PMHS	LL	No	LL
	Mild	90	8A	ATD	LL	No	NA
	Mild	90	9B	ATD	LL	LL	NA
III	Mild	120	11B	PMHS	No	LL/Sp	LL/No
	Mild	120	8B	ATD	LL/Sp	LL/Sp	NA

- Both MADYMO and LS-DYNA ATD models were able to predict the injuries in PMHS in general.
- It is difficult to conclude that the current ATD models can reliably and accurately predict injurious/non injurious events.

Thank You!
Q/A?

Second Workshop on Numerical Analysis of Human and Surrogate Response to Accelerative Loading

Hybrid III Crash-Dummy Lower Extremity under High Speed Vertical Loading: A Combined Experimental and Computational Study

Feng Zhu, Liqiang Dong, Xin Jin, Binhui Jiang, Anil Kalra, Ming Shen, King H. Yang

Bioengineering Center, Wayne State University

January 12, 2016

Aberdeen, MD

Wayne State University College of Engineering Bioengineering Center

Impact Biomechanics from Head to Toe Since 1939

Contents

- Introduction
- Calibration of three materials
- Full-body vertical loading: test and simulation
- Discussion
- Conclusions
- Acknowledgments

Introduction

- Axial loading of lower extremity → major cause of ankle and heel injuries (Morris et al. 1997; Sherwood et al. 1999)
  - Intrusion of the foot plate, caused by blast of AV landmines: 12 m/s in microseconds
- Current ATDs are not designed to take axial loading and no calibration procedures are available for the lower leg subjected to high-speed axial loading

Introduction

<u>Investigations into the effects of blasts on lower extremities:</u>

- PMHS data are scattered: Yoganandan et al. 1996, Mckay and Bir 2009, Dong et al. 2013
- HBIII, designed for automotive crash, has been used in axial loading mode because there is no military dummy available Yoganandan et al. 2014
- Current computational HBIII model does not include rate-dependency. Nilakantan and Tabiei 2009

Study goal

<u>**Improve the performance of HBIII lower leg FE model due to vertical loading**</u>

- Calibrate 3 soft materials in Hybrid III lower extremities: (1) heel-pad foam; (2) foot skin; (3) lower-leg flesh
- Identify material laws and optimal parameters
- Integrate new material models into LSTC Hybrid III dummy FE model
- Apply the model in high-speed vertical loading, and compare the predictions

Materials studied

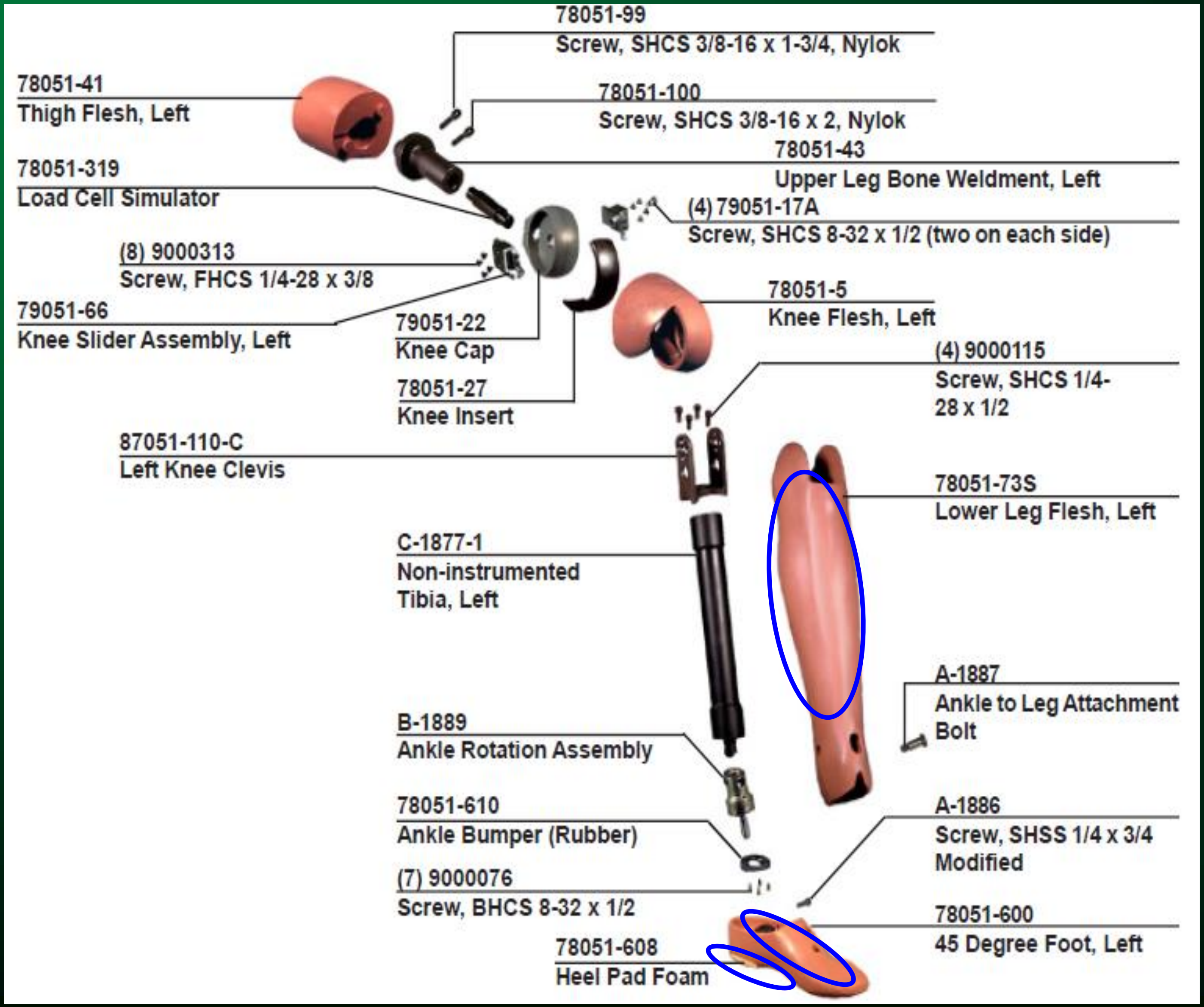

Contents

Calibration: Strategies

- Heel pad foam
  - The foam is cut into rectangular samples
  - Standard compressive tests
- Foot skin and lower leg flesh
  - The material samples in regular shape are not available
  - Material properties are calibrated using a reversed engineering (RE) based optimization method

Calibration: Heel-pad foam

- Uniaxial compression tests using Instron (rate: 0.01 to 600 s^{-1})
- Loading ram: 100 mm×100 mm

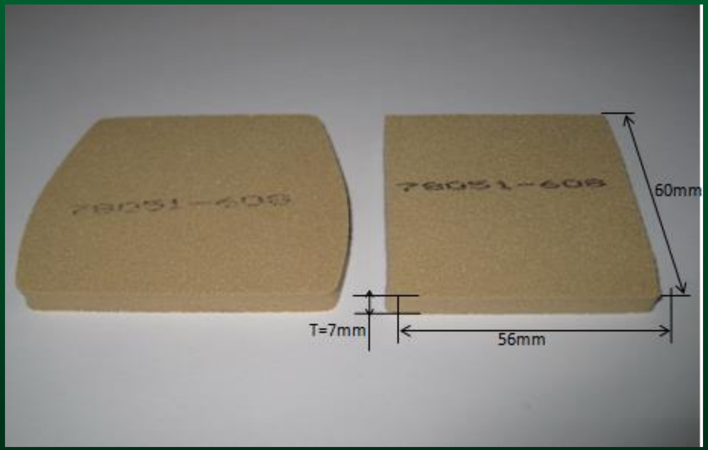

Sample: from Humanetics;
56 × 60 × 7 mm

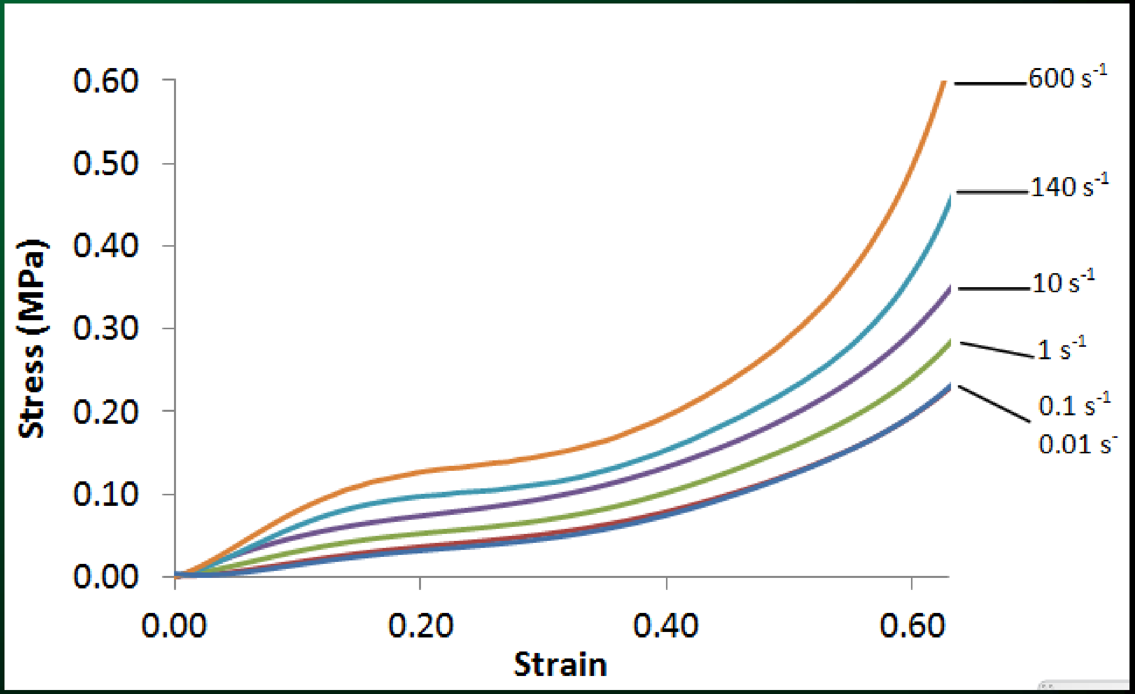

Stress – strain curves

Heel-pad foam material modeling

- Material model used by LSTC

  *MAT_57 (Low density foam)

- Material model used by WSU

  *MAT_83 (Fu_Chang foam)

Material parameters

Material	LS-DYNA material type, material properties (units: mm, kg, ms, GPa, kN)					
Heel-pad foam	*MAT_FU_CHANG_FOAM					
	RO	E	DAMP	TBID	BVFLAG	HU
	6.4E-7	0.15	0.05	Figure 3	1.0	1.0E-3

Heel-pad foam compression: test and simulations using LSTC, WSU materials

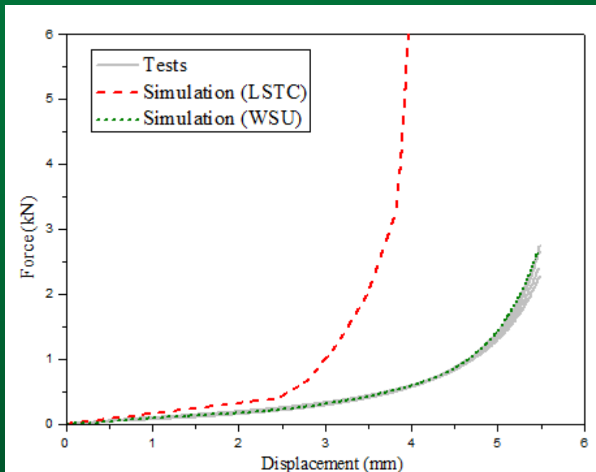

0. 1 s^{-1}

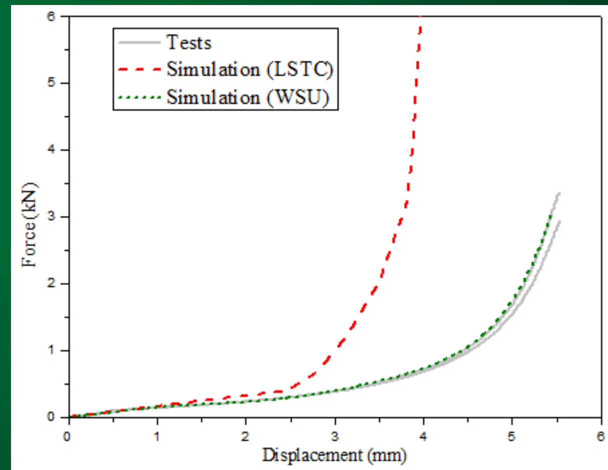

1 s^{-1}

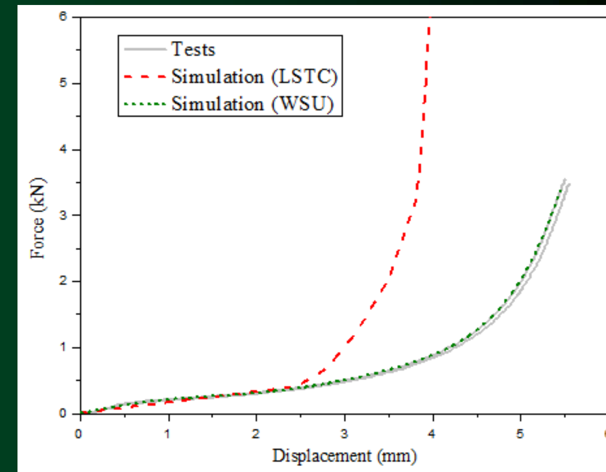

10 s^{-1}

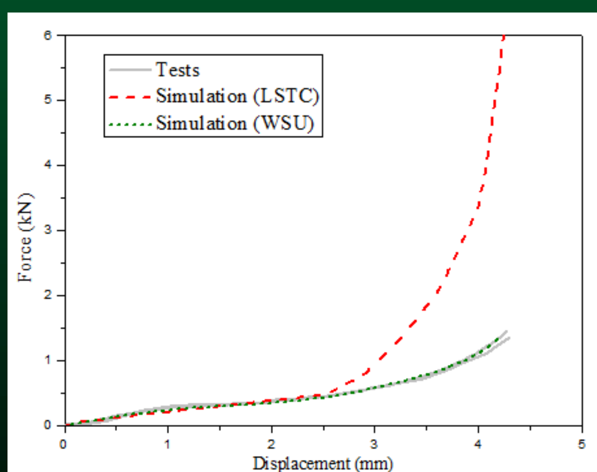

140 s^{-1}

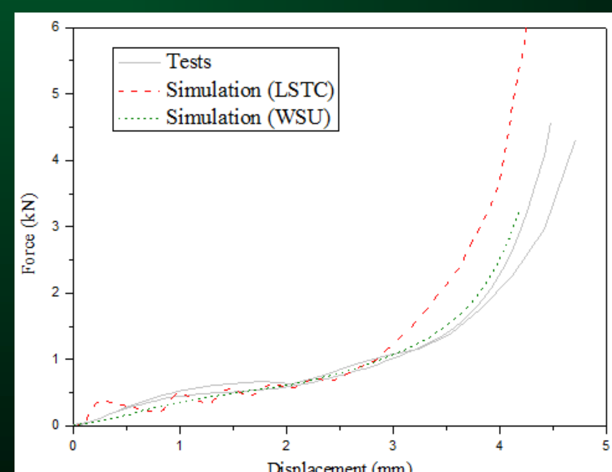

600 s^{-1}

Calibration: Foot skin

- Compressive test to dummy foot (speed: 1, 10 m/s for optimization, 5 m/s for validation)
- Impactor: rigid cylinder

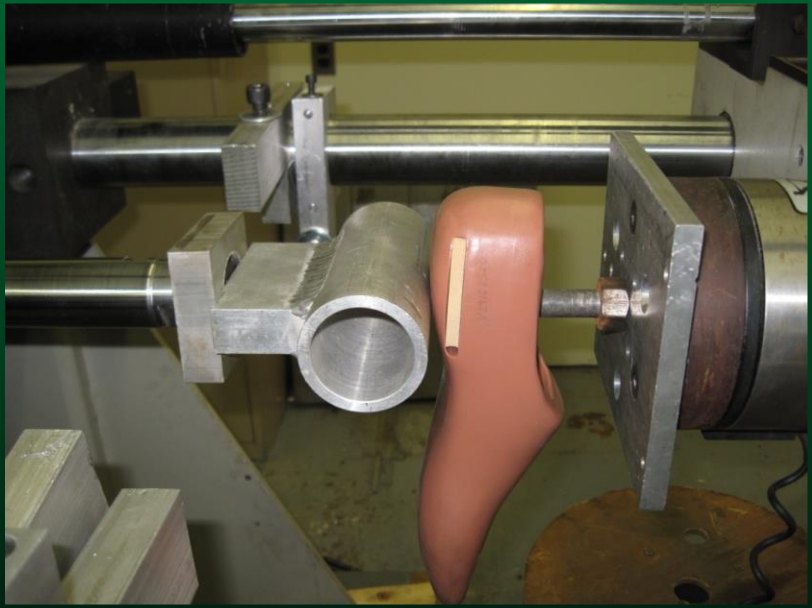

Test setup for foot skin behavior

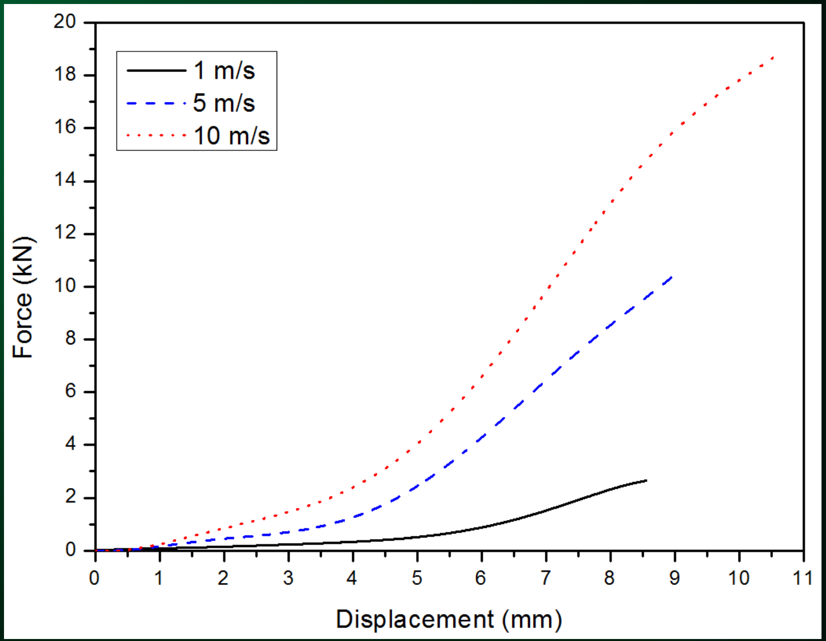

Force-displacement curves

Foot skin material modeling

- Material model used by LSTC

  *MAT_7 (Blatz-Ko rubber)
- Material model used by WSU

  *MAT_77_O (2nd order Ogden rubber)
- Constitutive equation:

$$\sigma_i = \sum_{j=1}^{n} \frac{\mu_j}{\alpha_j}\left[\lambda_i^{\alpha_j - 1} - \lambda_i^{-(\alpha_j/2)-1}\right] + \int_0^t (1-\lambda_i) \sum_{k=1}^{m} G_k e^{-\beta_k (t-\tau)} \lambda_i(t)\, d\tau$$

Hyper-elasticity **Visco-elasticity**

- Parameters to be determined by optimization
  - Hyper-elastic constants: $\mu_1, \alpha_1, \mu_2, \alpha_2$
  - Visco-elasticity: $G_1, G_2, G_3, \beta_1, \beta_2, \beta_3$

Flowchart of material optimization procedure

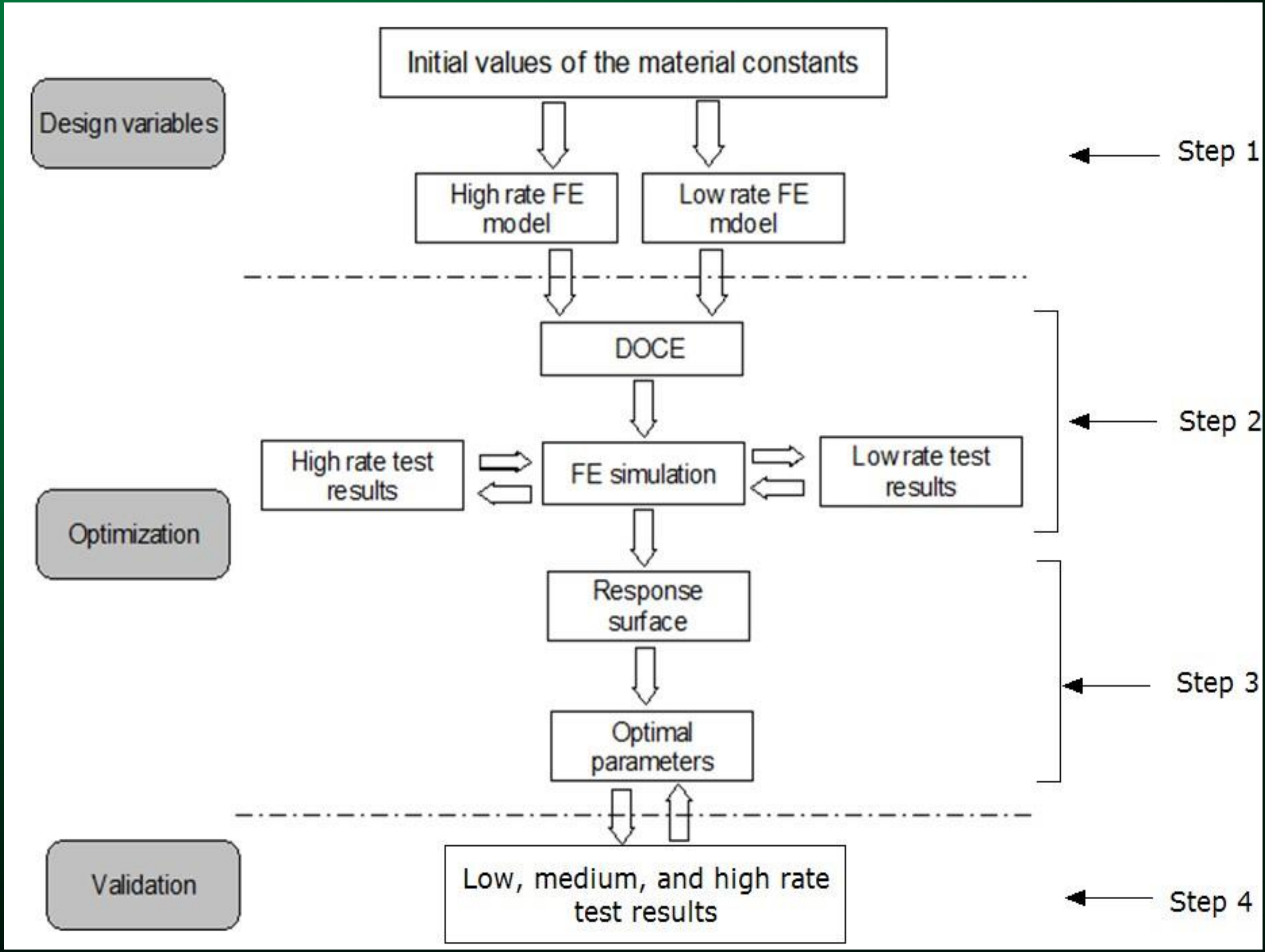

Foot skin material optimization

- Software: modeFRONTIER 4.1
- Sampling: Sobel algorithm → 100 parameter sets
- Shepard-k-Nearest method: Response surface
- Optimization target: least squares to curves
- Optimization algorithm: NSGA-II

Material parameters

Material	LS-DYNA material type, material properties (units: mm, kg, ms, GPa, kN)					
Foot skin	*MAT_OGDEN_RUBBER					
	RO	PR	MU1	MU2	ALPHA1	ALPHA2
	1.28E-6	0.49	2.0E-4	-1.0E-4	1.60	-1.30
	G1	G2	G3			
	0.022	0.0010	1.00E-4			
	BETA1	BETA2	BETA3			
	11.0	5.0	1.0			

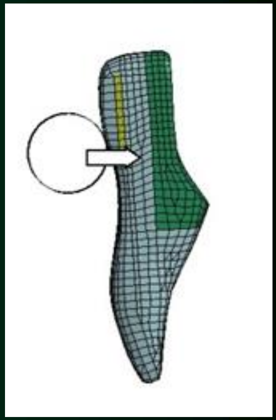

Simulation setup

Foot skin compression: test and simulations using LSTC, WSU materials

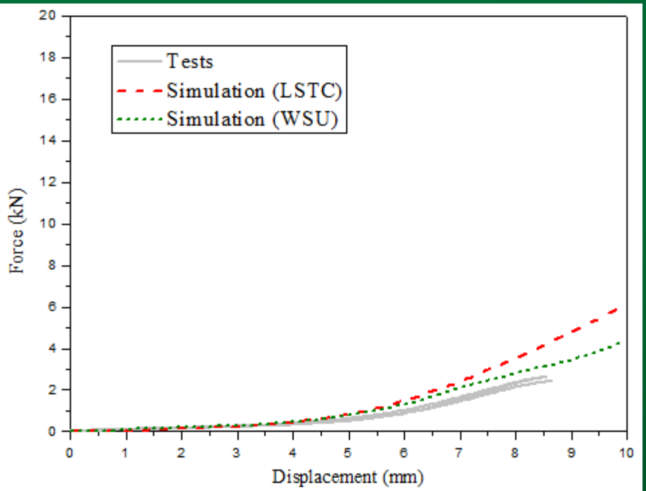

1 m/s

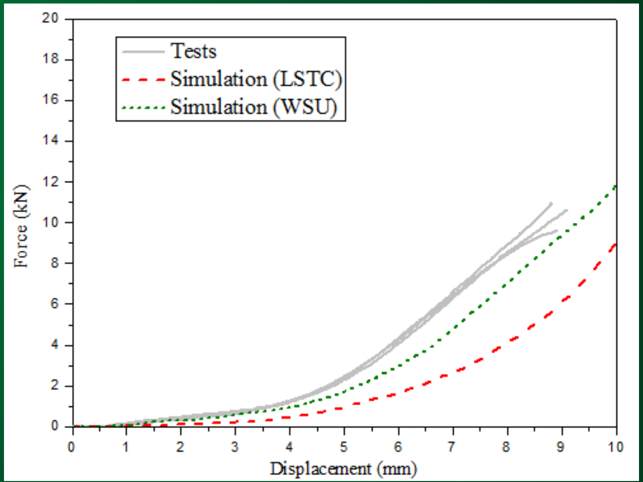

5 m/s

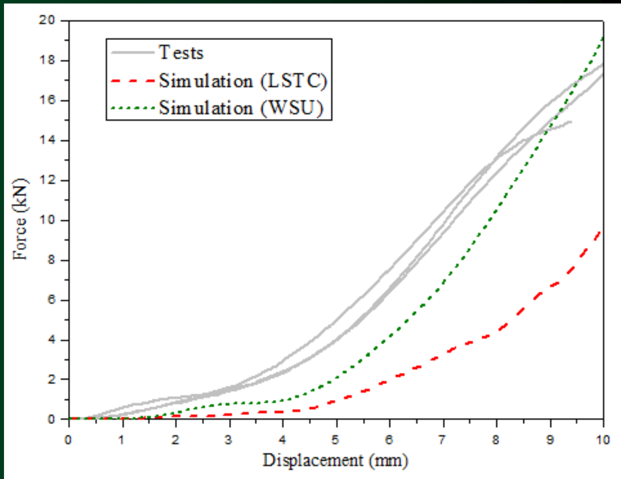

10 m/s

Comparison at displacement of 8 mm

Velocity (m/s)	Measured force (kN)	Simulation - LSTC		Simulation - WSU	
		Force (kN)	Discrepancy (%)	Force (kN)	Discrepancy (%)
1	2.4	3.5	45.8	2.8	16.7
5	8.8	4.1	53.4	7.0	20.5
10	13.3	4.4	66.9	11.4	19

Calibration: Lower leg flesh

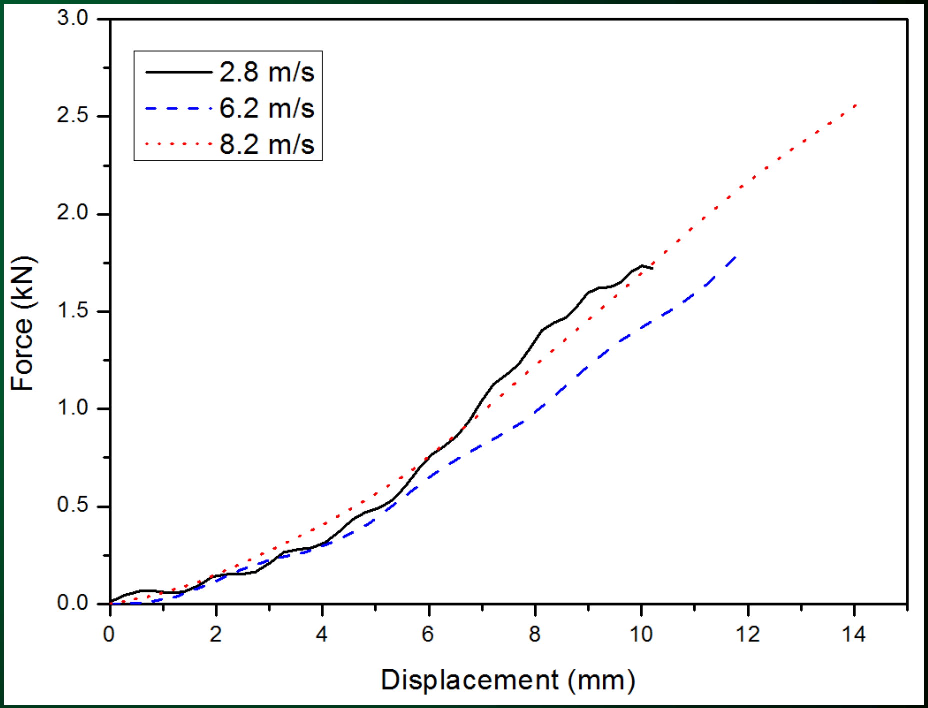

Force-displacement curves

Dynamic three-point bending

2.8 m/s and 8.2 m/s: used for optimization

6.2 m/s: used for validation

Material modeling

- Material law used by LSTC

  *MAT_57 (Low density foam)

- Material law used by WSU

  *MAT_77_O (2nd order Ogden rubber)

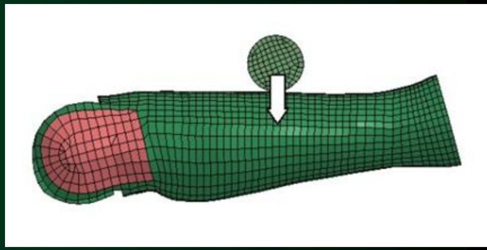

Simulation setup

Material parameters

Material	LS-DYNA material type, material properties (units: mm, kg, ms, GPa, kN)					
Lower leg flesh	*MAT_OGDEN_RUBBER					
	RO	PR	MU1	MU2	ALPHA1	ALPHA2
	8.6E-7	0.49	0.0028	-0.0025	0.2	-0.116

Lower leg bending: test and simulations using LSTC, WSU materials

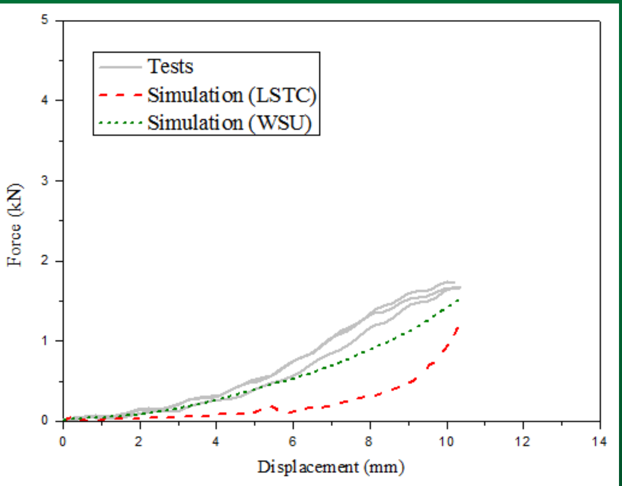

2.8 m/s

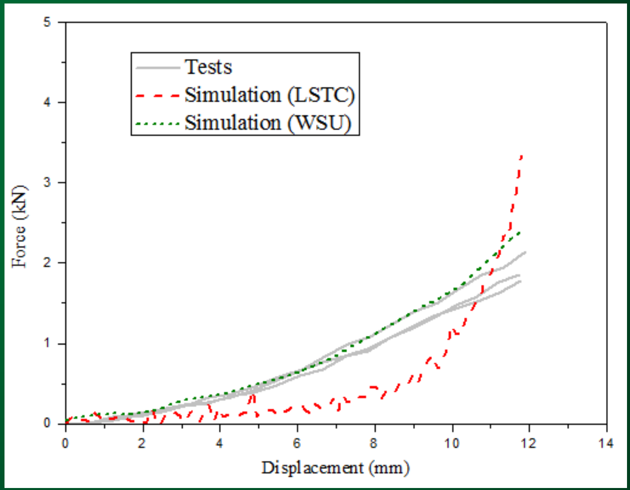

6.2 m/s

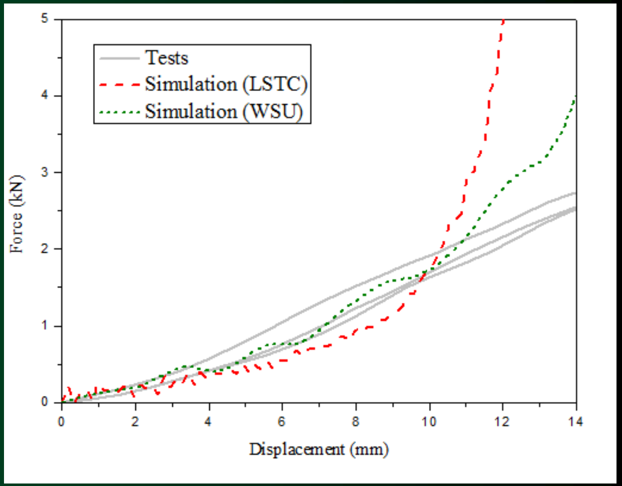

8.2 m/s

Comparison at displacement of 8 mm

Velocity (m/s)	Measured force (kN)	Simulation - LSTC		Simulation - WSU	
		Force (kN)	Discrepancy (%)	Force (kN)	Discrepancy (%)
2.8	1.5	0.5	66.7	1.1	26.7
6.2	1.3	0.5	61.5	1.4	7.7
8.2	1.5	1.1	26.7	1.6	6.7

Contents

- Introduction
- Calibration of three materials
- <u>**Full-body vertical loading: test and simulation**</u>
- Discussion
- Conclusions
- Acknowledgments

Full-body vertical loading: test

- Test bench: based on shock-generation tank
- Dummy posture: 90-90-90;
- Nominal peak velocity: 5, 8 and 12 m/s
- Output: M_y at upper tibia; F_z at lower tibia

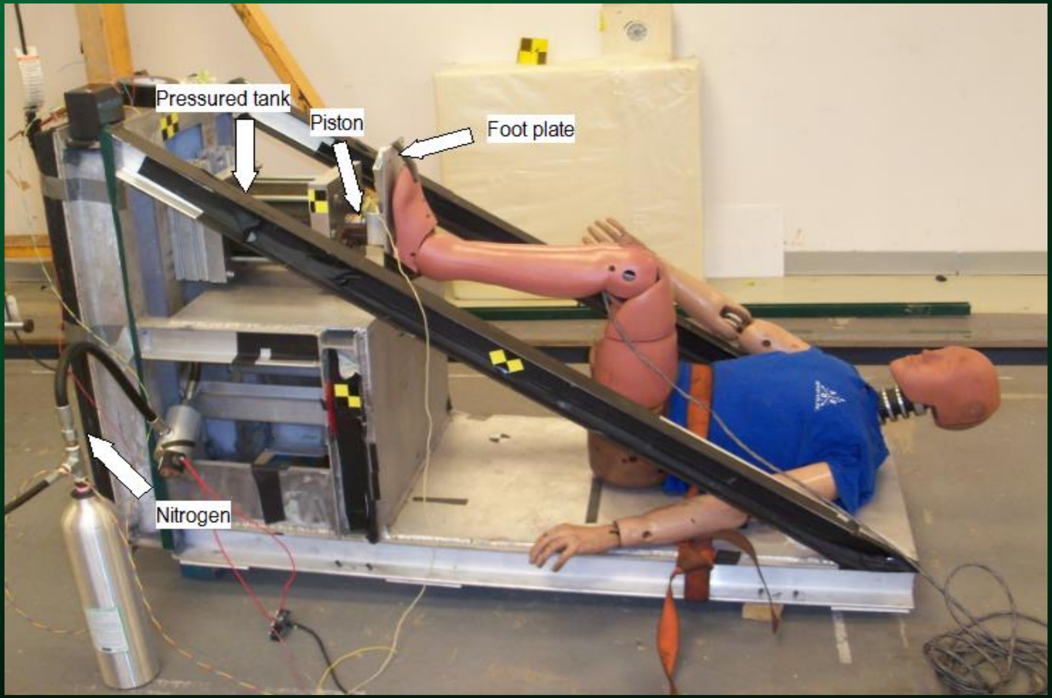

Test setup of full-body high-speed vertical loading

Test results

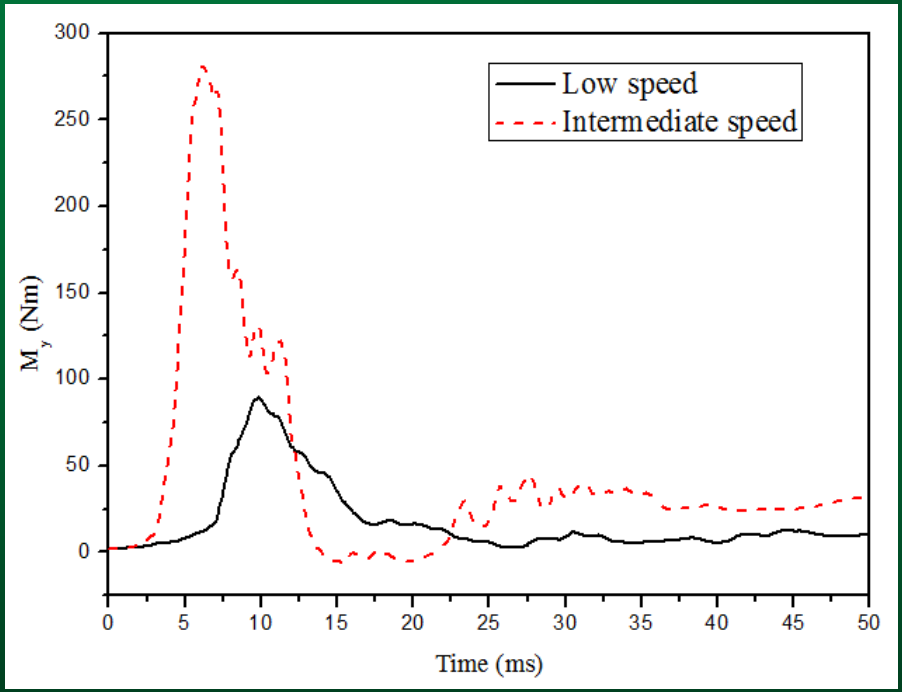

Bending moment at upper tibia (M_y)

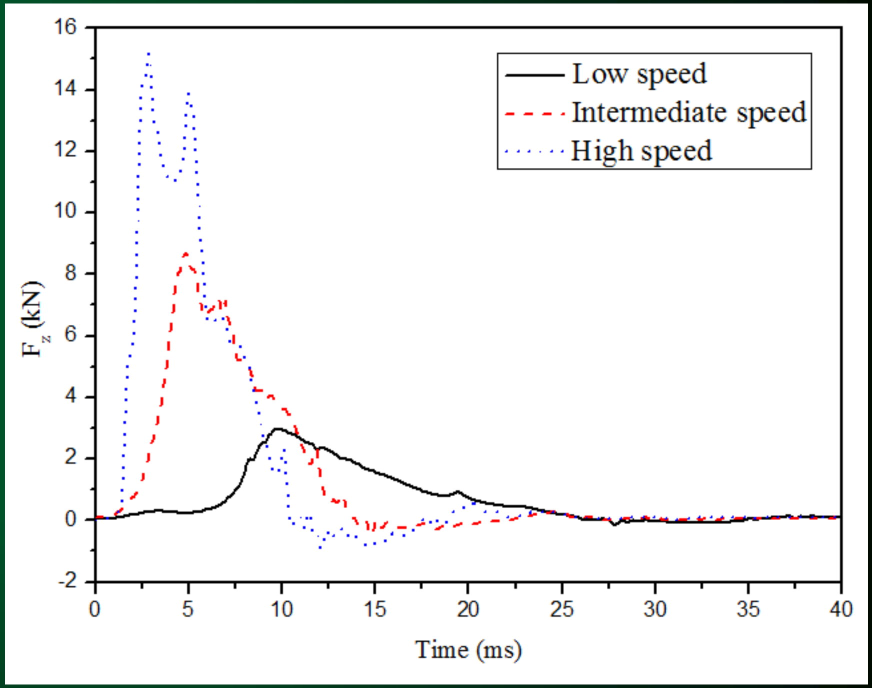

Axial force at lower tibia (F_z)

Note: The upper tibia load cell failed in the high-speed case

Full-body vertical loading: simulation (using improved material models)

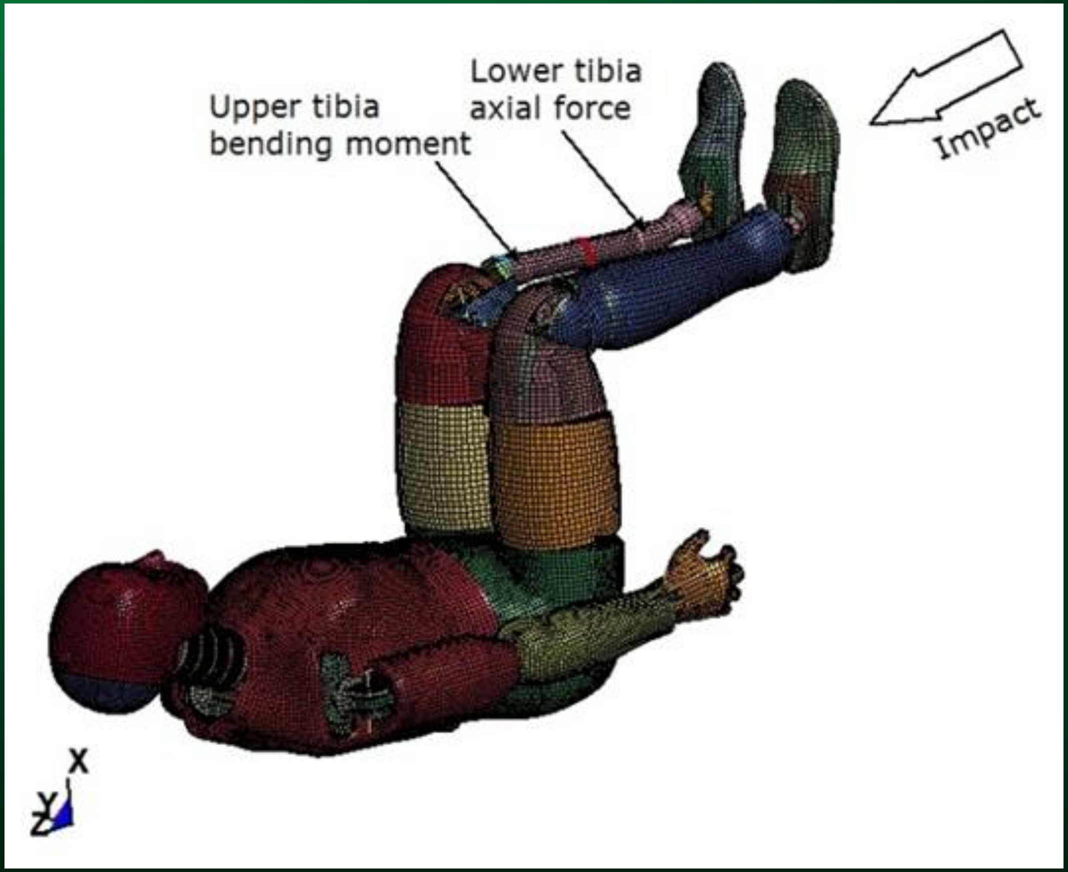

Simulation results: M_y

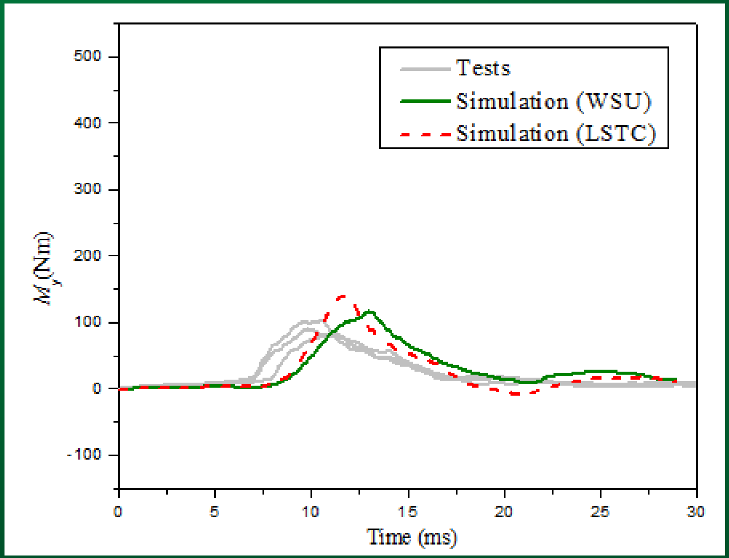

Low speed

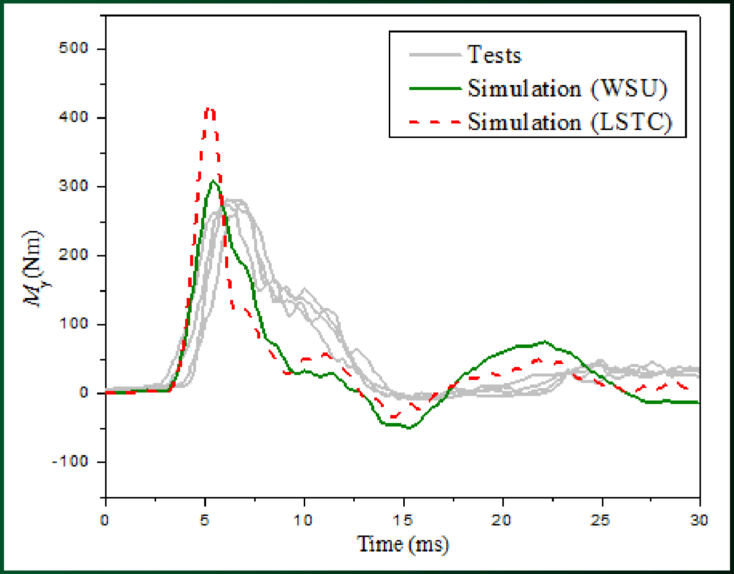

Intermediate speed

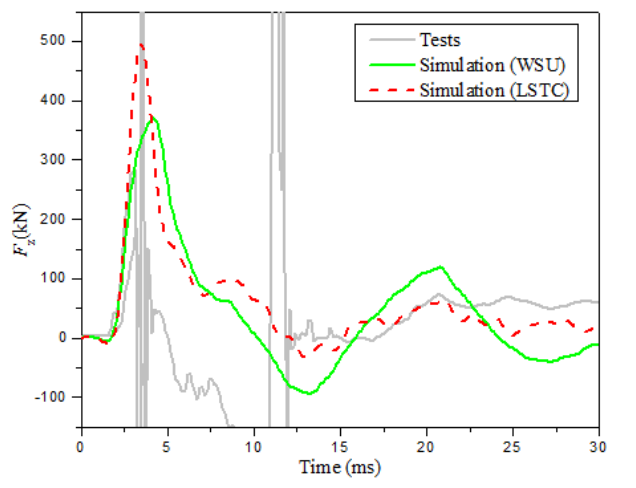

High speed
(load cell failed)

Simulation results: F_z

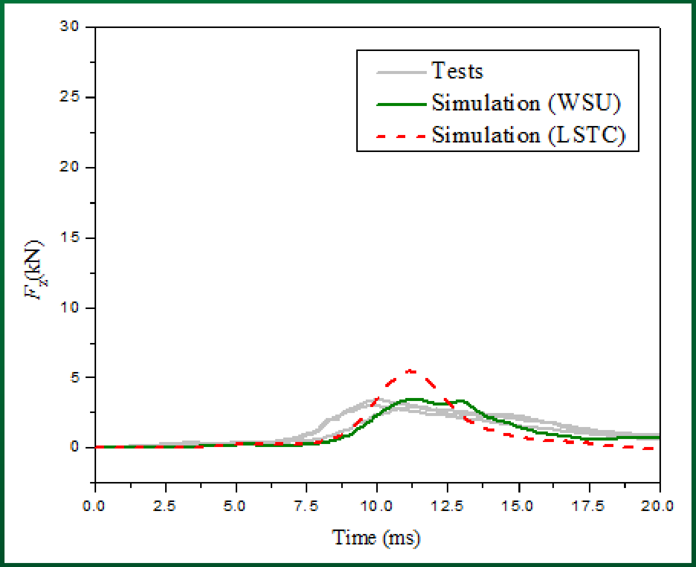

Low speed

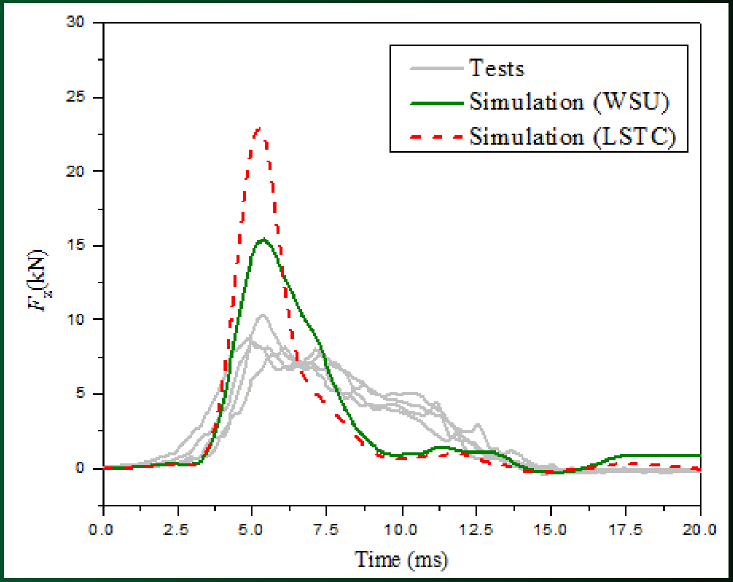

Intermediate speed

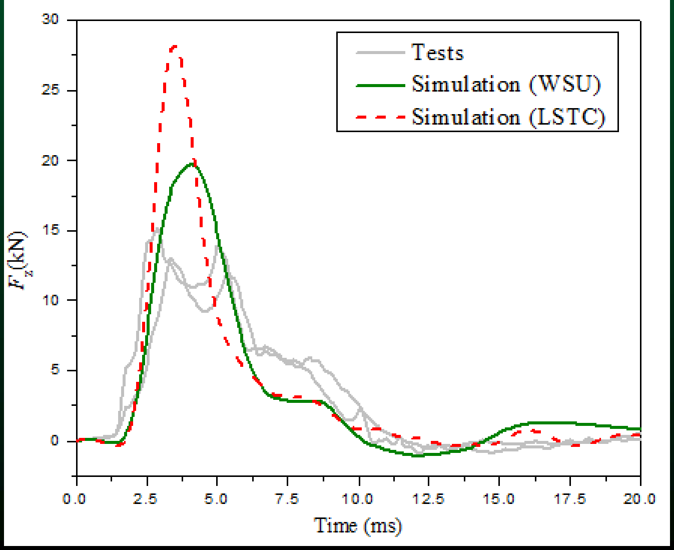

High speed

Contents

- Introduction
- Calibration of three materials
- Full-body vertical loading: test and simulation
- Discussion
- Conclusions
- Acknowledgments

Discussion

- Objective: to calibrate crash dummy in vertical loading → Not to build surrogate/FEM with high biofidelity
- LSTC Hybrid III whole-body FEM: never calibrated under high-speed vertical loading
- The improvement of prediction is significant
- Discrepancies occurred between the experimental data and the predicted results

Where the discrepancies come from??

Discussion

- The boundary conditions in tests for components and full-body dummy were well controlled and consistent
- The force and moment responses in full-body loading were not sensitive to the angles within the range of 90±5°
- Possible causes of discrepancies:
  - Joint stiffness
  - Mass accuracy
  - Friction between tibia-flesh
  - …

Future work

Discussion

- Inertial compensation:
  - Heel-pad & foot skin: (no) load cell on fixed side
  - Lower leg flesh: (no need) force from acc.
  - Whole body: (no) → Okay for load comparison
- Computational costs for the improved material models are greater than original ones
- Instrumented ATD legs, such as Thor-Lx (Choi et al. 2005) and Mil-Lx (Pandelani et al. 2010) can be used, with the same methodology
- Booted responses would be also interesting

Limitations

- Lack of quantitative comparison of curve (CORA)
- Lack of assessment of local / global optimums
- Lack of sensitivity studies on individual parameter of a material, individual material
- Calibration not identical to real-world loading
  - Foot skin (cylinder impactor): not plate
  - Lower leg (AP bending): not vertical

Contents

- Introduction
- Calibration of three materials
- Full-body vertical loading: test and simulation
- Discussion
- <u>Conclusions</u>
- Acknowledgments

Conclusions

- Three soft materials from lower leg of Hybrid III dummy were tested and calibrated
  - Heel-pad: from stress-strain curves
  - Foot skin and lower-leg flesh: using reverse engineering and optimization
- Improved material models were integrated to the full-body FEM
- The full-body tests and simulations (5, 8 and 12 m/s) were conducted to evaluate the performance
- Closer match was observed based on new material models

Acknowledgements

- This work was supported in part by BAE Systems and Wayne State University Bioengineering Center

Thank you

modeFRONTIER workflow

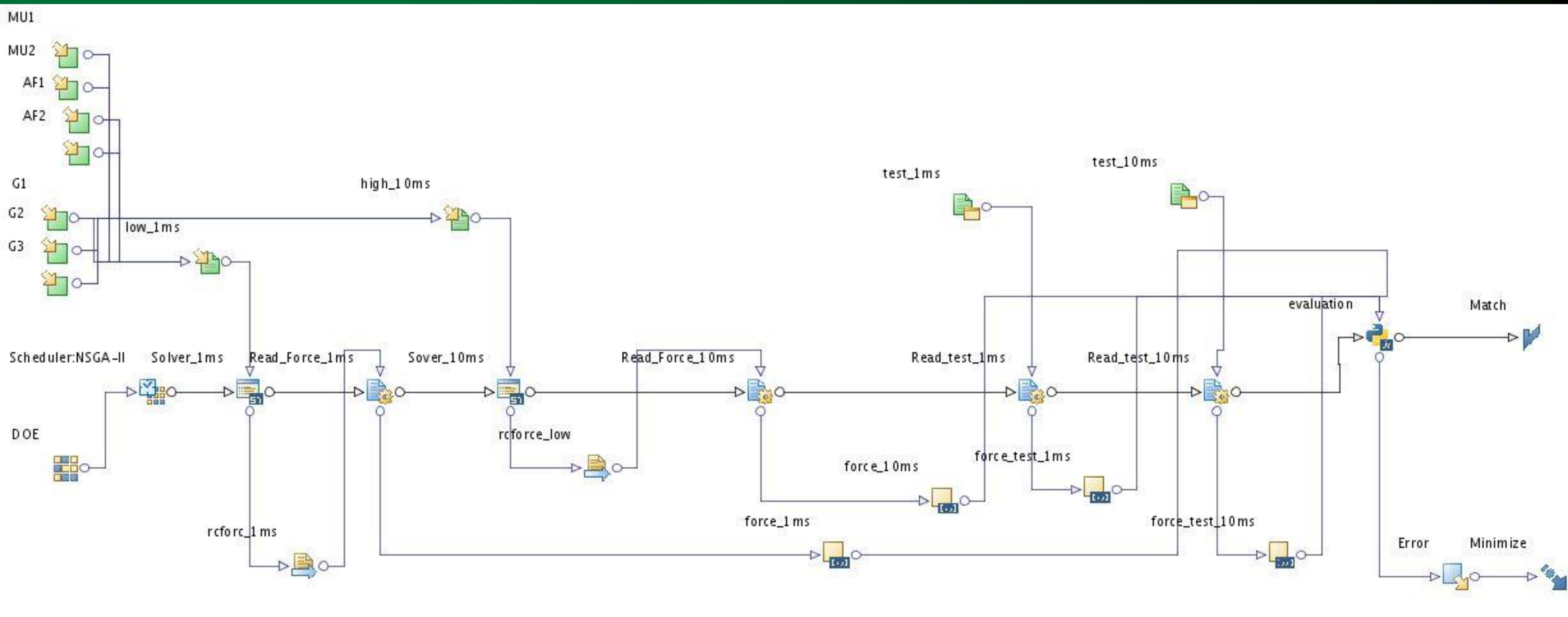

Input of high-speed vertical loading

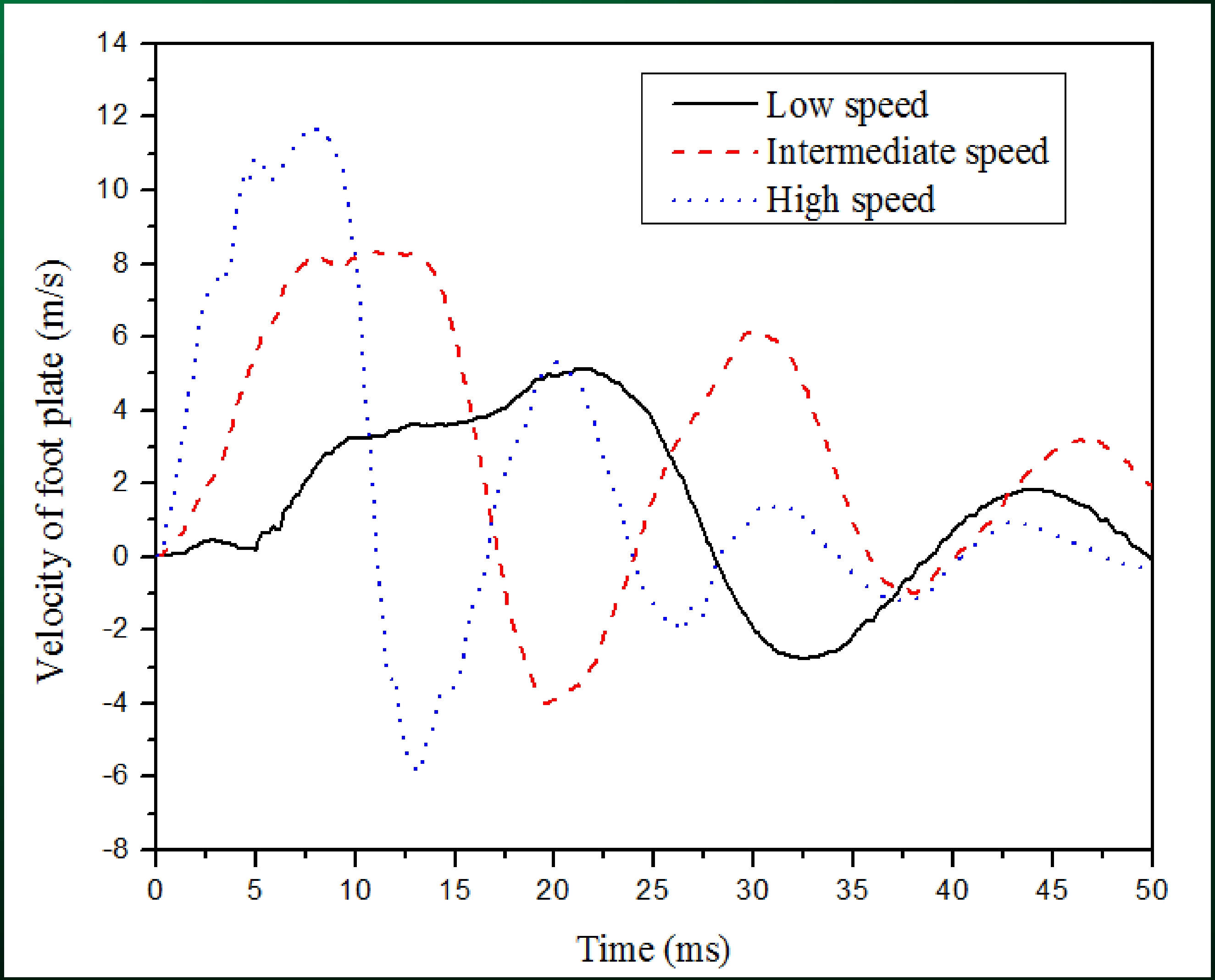

Material law of Fu-Chang foam

- An unified, constitutive equation for a low-to-medium density isotropic foam
- Compression: strain-rate dependency
- Tension: elastic-plastic
- No Poisson’s ratio & viscoelasticity effect
- Non-linear strain <-> stress and state variable

Material law of Ogden

$$\sigma_i = \sum_{j=1}^{n} \frac{\mu_j}{\alpha_j}\left[\lambda_i^{\alpha_j - 1} - \lambda_i^{-(\alpha_j/2)-1}\right] + \int_0^t (1-\lambda_i) \sum_{k=1}^{m} G_k e^{-\beta_k (t-\tau)} \lambda_i(t) d\tau$$

Hyper-elasticity　　Visco-elasticity

- Wood et al. 2010: for ATD head flesh
- i =1, 2, and 3: the normal directions.
- λ: the stretch ratio; n: 2 (2nd order); m: 0 or 3
- G and β were time-dependent, unknown parameters.

Modeling and Sensitivity Analysis of the WIAMan ATD Head and Neck: A Finite Element Study

Matthew L. Davis[1,2], Jeremy M. Schap[1,2], Michael P. Boyle[3], Robert S. Armiger[3], M. Chowdhury[4], F. Scott Gayzik[1,2]

[1]Wake Forest School of Medicine
[2]Wake Forest University Center for Injury Biomechanics
[3]Johns Hopkins Applied Physics Laboratory
[4]U.S. Army Research Lab, WIAMan Engineering Office

Background

– The Goal of the **WIAMan project** is to develop a new anthropomorphic testing device with biofidelic capabilities specific to the underbody blast environment.

– During the model development process, **computational modeling** is being used to:
  - Inform design
  - Evaluate design modifications
  - Assess strength of design

– Unique attributes of the Head and Neck
  - Primary vertical, increasing trend[1]
  - Tested in loading modes relevant to field data (flexion/extension, compression in sagittal plane)

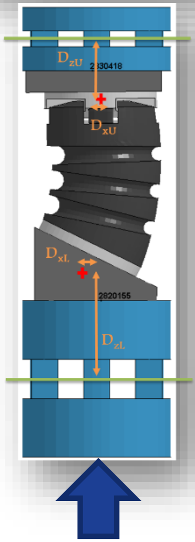

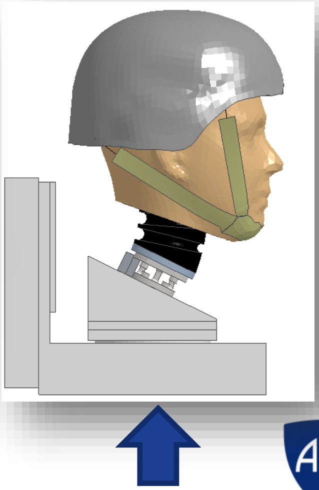

1. Yogandan et al. Clin. Biomech. 2013

Wake Forest School of Medicine

CORVID TECHNOLOGIES

The Nation's Premier Laboratory for Land Forces

Background

- The Goal of the **WIAMan project** is to develop a new anthropomorphic testing device with biofidelic capabilities specific to the underbody blast environment.
- During the model development process

Objective: Provide an overview our team's work on modeling (validation) and sensitivity analysis of the WIAMan ATD Head and Neck

- Unique attributes of the Head and Neck
  - Primary vertical, increasing trend[1]
  - Tested in loading modes relevant to field data (flexion/extension, compression in sagittal plane)

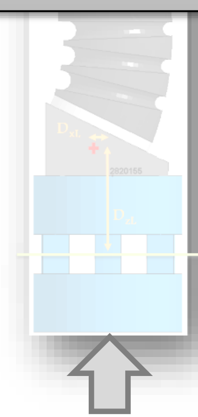

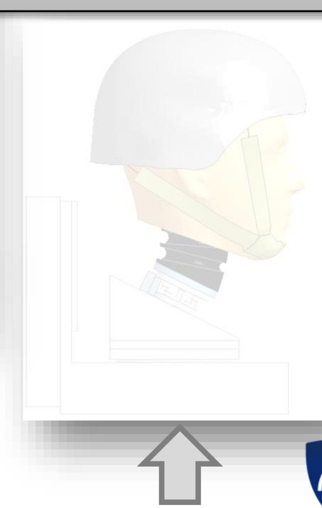

1. Yogandan et al. Clin. Biomech. 2013

Wake Forest School of Medicine

CORVID TECHNOLOGIES

The Nation's Premier Laboratory for Land Forces

M&S Team Overview

M&S Team

- WIAMan Engineering Office
- Johns Hopkins Applied Physics Lab
- Corvid Technologies
- Wake Forest University
- Virginia Tech

M&S Codes

- LS-Dyna
- Velodyne

Why two codes?

- Increased reliability
- Leverage unique strengths
- Broader user base for product

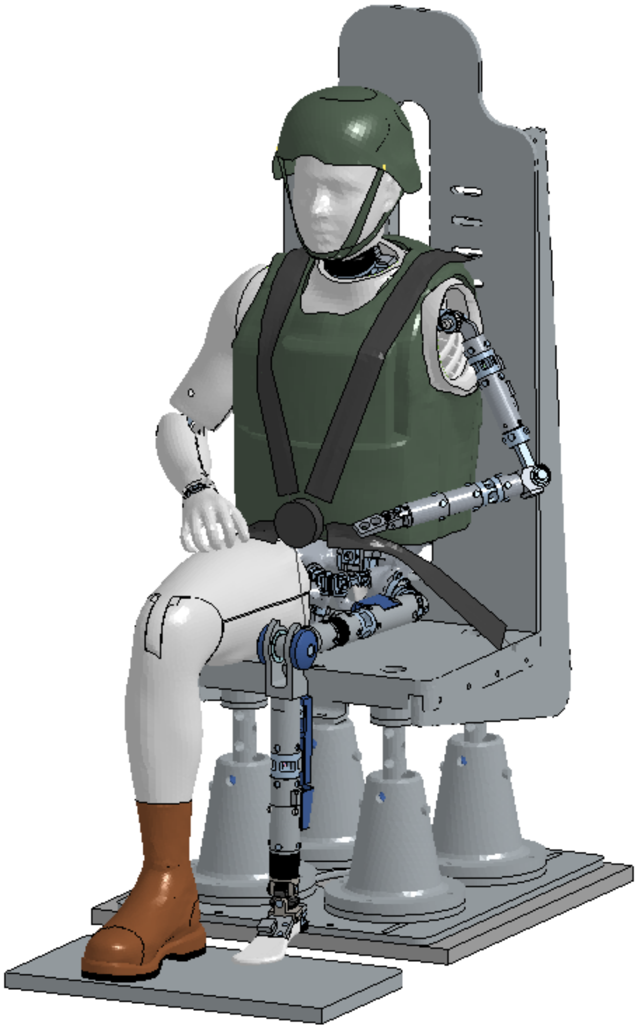

Wake Forest School of Medicine

CORVID TECHNOLOGIES

APL

Talk Overview

- Methods
  - Geometry, Mesh
  - Validation
    - Hierarchical approach
    - Material, component, system
    - Experimental and sensitivity study setups
- Results
  - Validation
  - Sensitivity
  - Future work
- Discussion and Conclusions

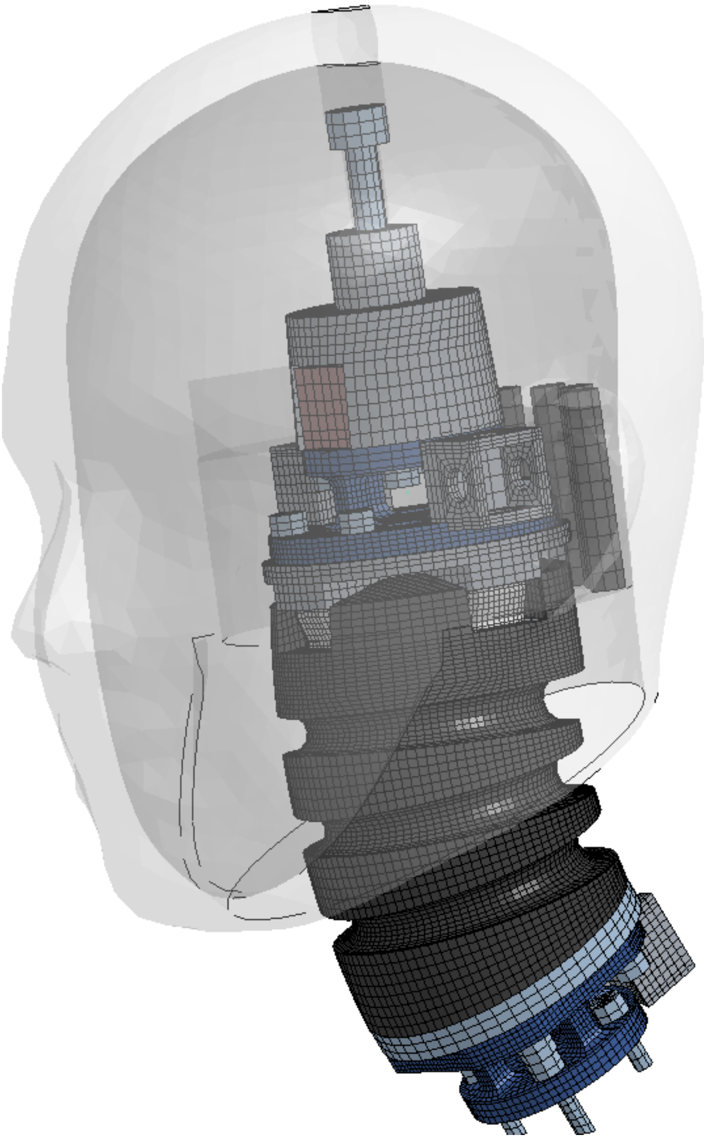

Methods - Geometry

Pre-Generation 1 Design

- Humanetics
- Molded rubber neck
- Flexion/extension buffers

Focus

- The M&S team is focused on modeling and validating the originally-proposed design
- Follow baseline TDP
- Staging for continued studies from this starting point
  - Design mods
  - Parametric studies

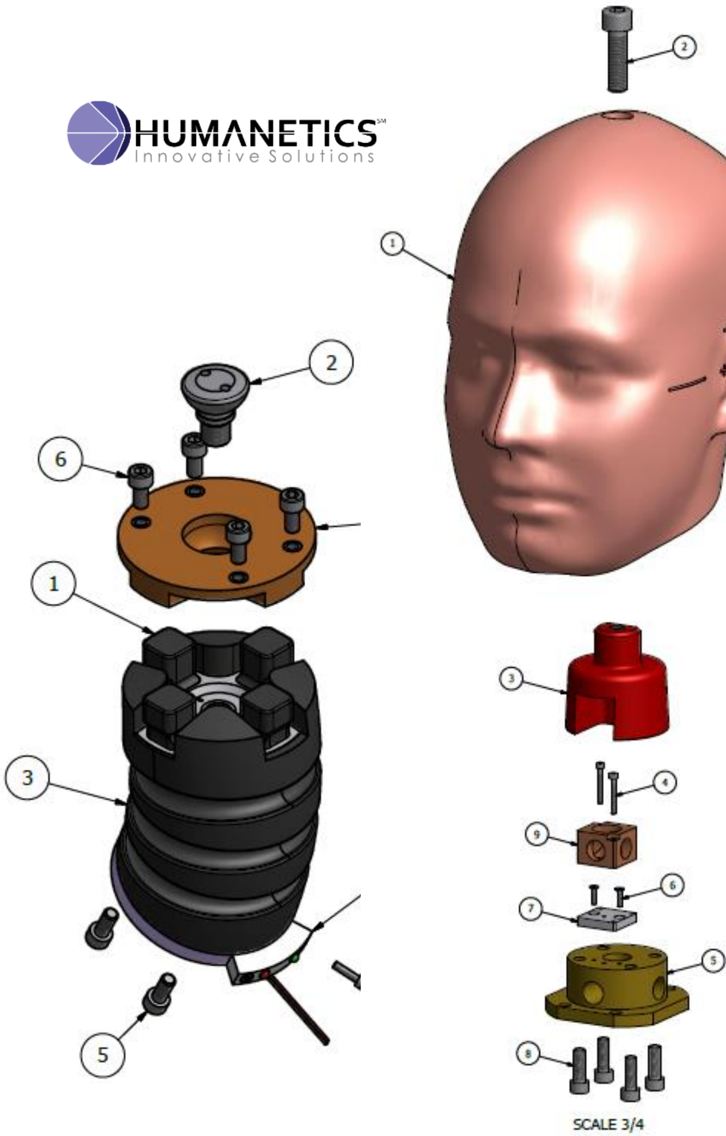

Wake Forest School of Medicine

Mesh Overview

- 207k elements, 195k nodes
- 100% solid elements
- 72% hex (28% tet face/skull)
- Single point integration with stiffness hourglass control
- Bolted interfaces use tied contacts, 1 single surface contact for remainder
- Minimum time step: ~0.1 μs Intersection/penetration removed
- Units: mm, ms, kg

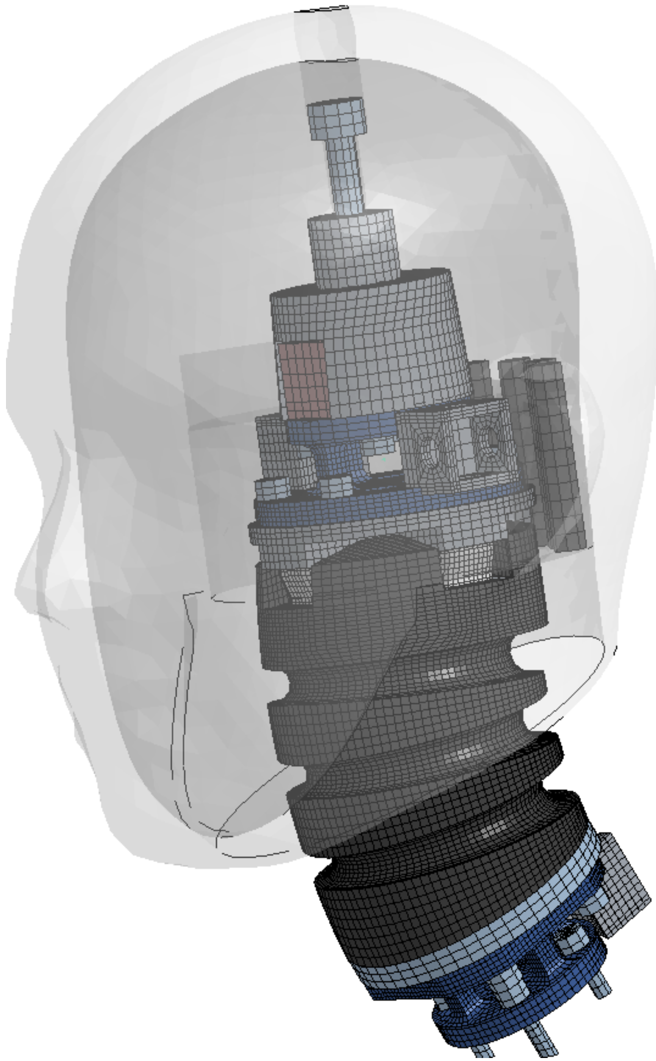

Model Overview

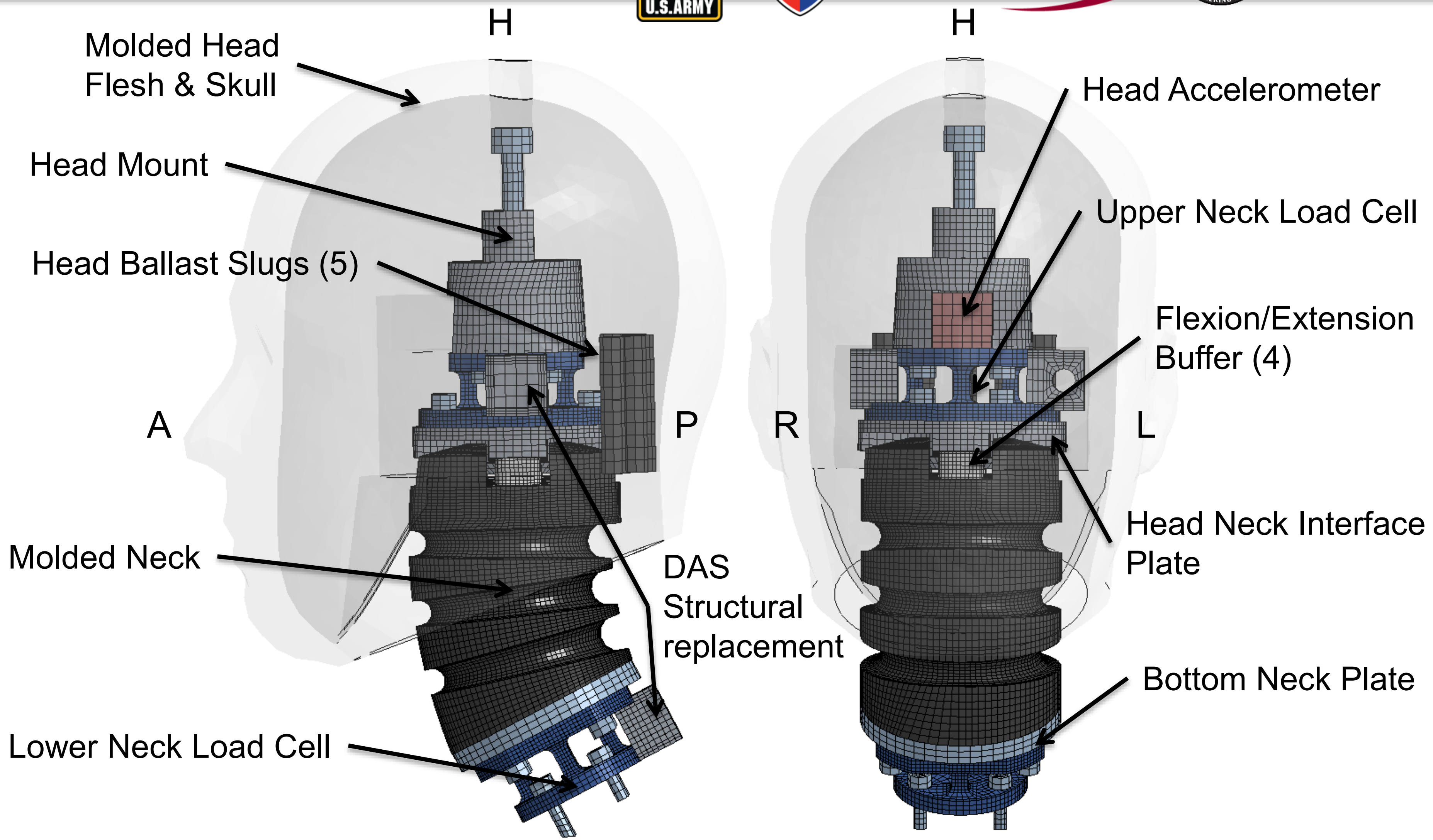

Wake Forest School of Medicine

Materials Overview

Steel & Aluminum

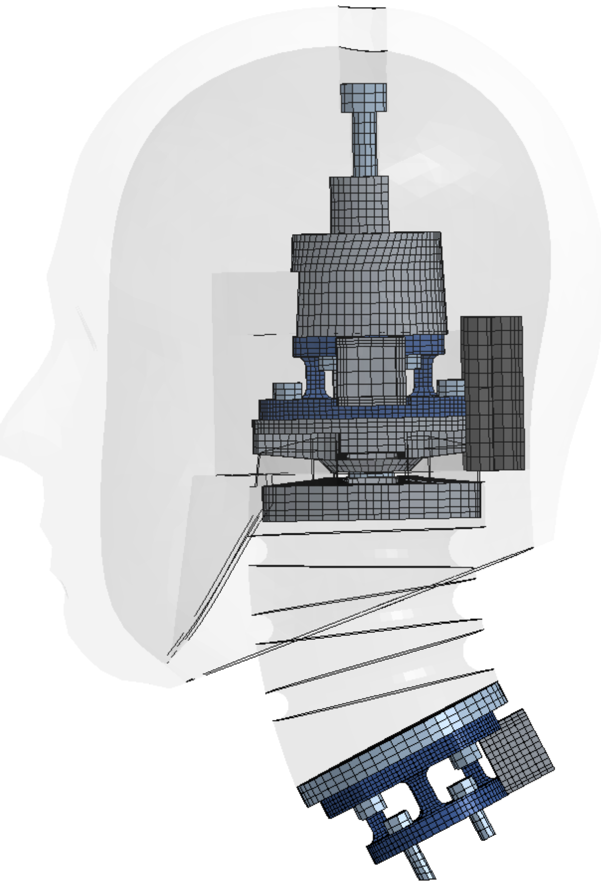

*Mat_Elastic

Polyuerthane (skull)
(Durometer 75 ± 5, Shore D)
Polyurethane (face flesh)
(Durometer 31 ± 10, Shore A)

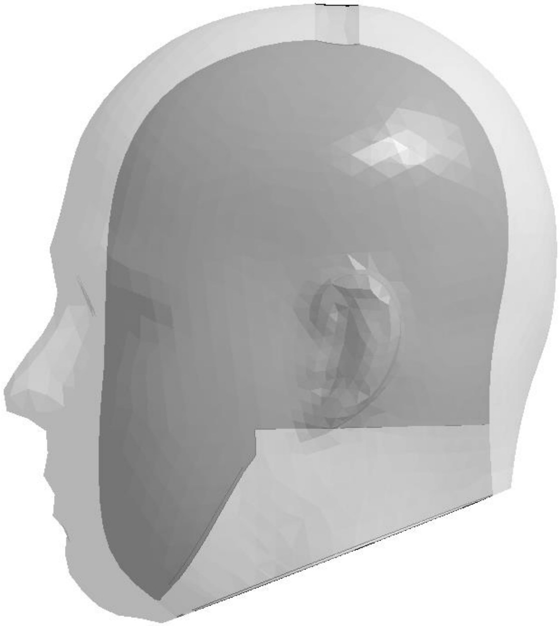

*Mat_Blatz-Ko_Rubber

*Mat_Bergstrom_Boyce_Rubber

Buytl Rubber
(Durometer 75 ± 10, Shore A)

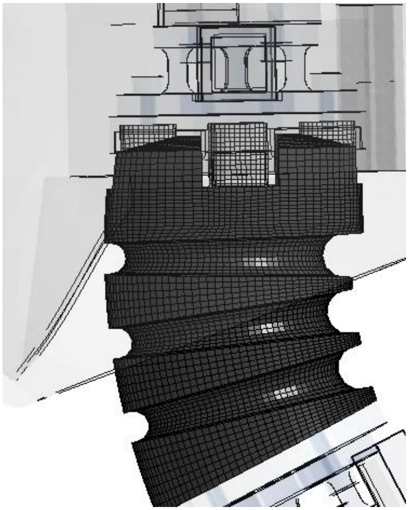

*Mat_Bergstrom_Boyce_Rubber

Wake Forest School of Medicine

The Nation's Premier Laboratory for Land Forces

Neck and Buffer Material

- First level in hierarchical approach
- Bergstrom-Boyce material model
  - Hyperelastic & rate dependent
- Tested sample is from same batch as actual test article
- Mcalibrate software from Veryst
- Two cyclic tests at and strain rates in compression
  - 1.0 s^{-1}
  - 0.1 s^{-1}
- Three monotonic tensile tests
  - 0.1 s^{-1}
  - 55 s^{-1}
  - 100 s^{-1}
- Use of high-rate compression tests in fit generates overly stiff response for moderate rates at strain < 5%

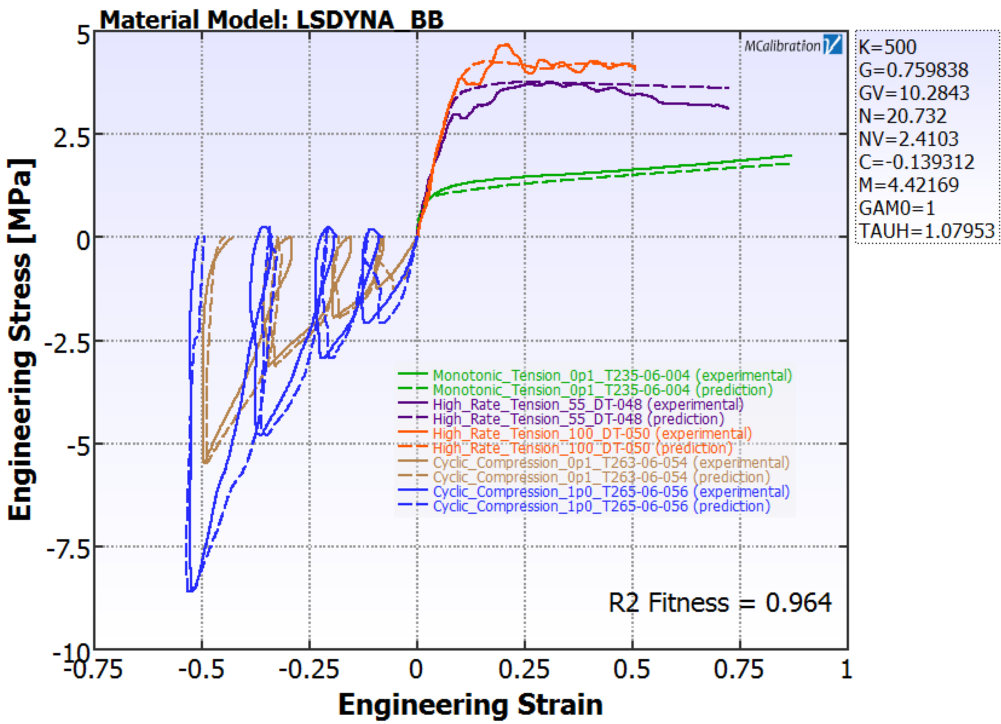

Wake Forest School of Medicine

Component Experiment

- Second level in hierarchical approach
- Vertical compression test of the tech demonstrator WIAMan ATD neck conducted at Duke University
- Tests conducted at 3 speeds
  - 200 N/ms
  - 400 N/ms
  - 600 N/ms
- Superior and inferior of molded neck were fixed to the rig
- Tests consisted of fixed crosshead with an applied displacement to T1 using a pneumatic ram

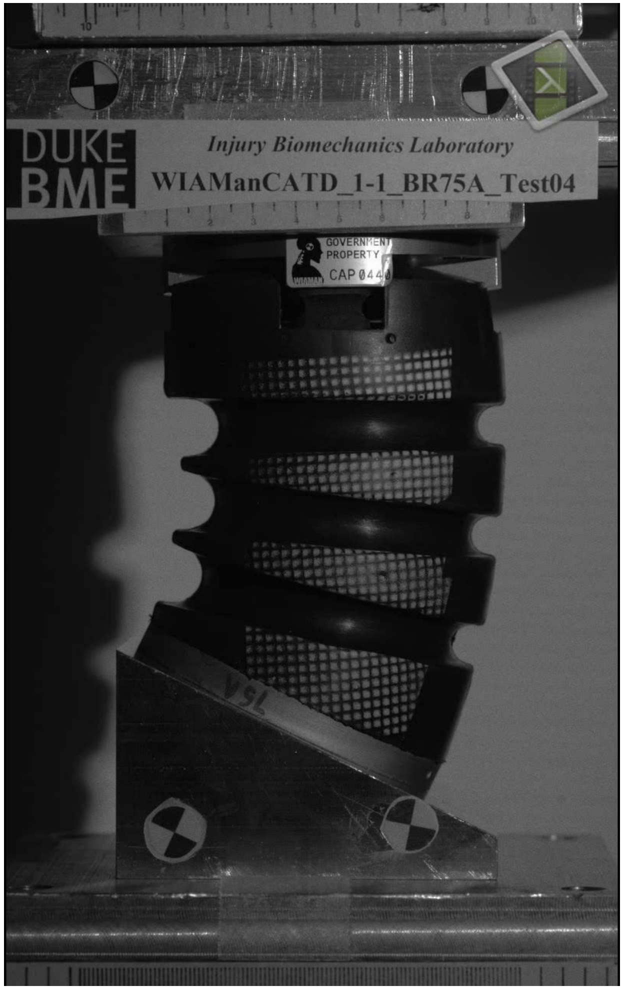

DUKE BME

Wake Forest School of Medicine

Overview of Experiments

- 3rd level in hierarchical approach
- Head-Neck accelerated using the Vertical Accelerator at Medical College of Wisconsin
  - HN03 PMHS test
  - Isolated Hybrid III helmeted Tests conducted at 3 speeds
    - 1 m/s
    - 2 m/s
    - 3 m/s
  - Current run for robustness and pre-test prediction
- For the 3 m/s test, the head-neck system made contact with an instrumented roof to evaluate roof contact forces

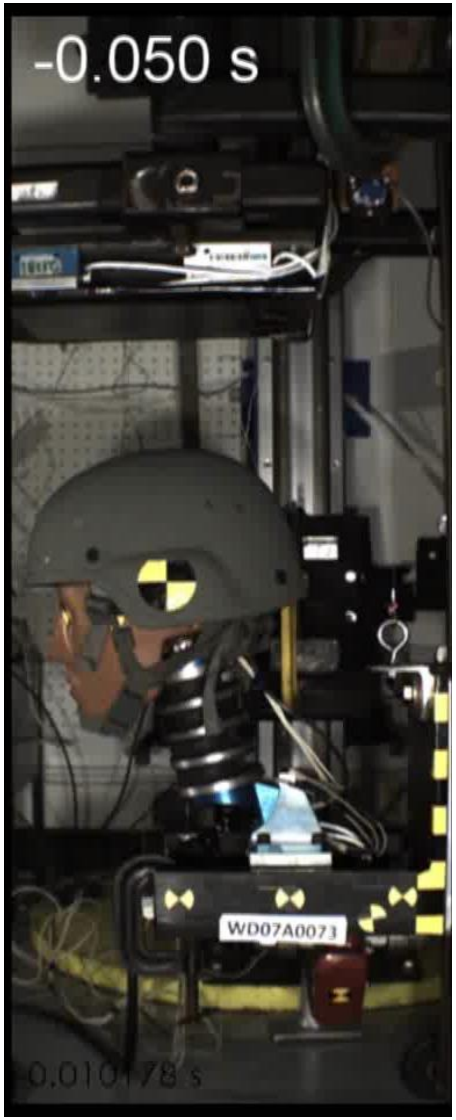

Wake Forest School of Medicine

Virtual Instrumentation

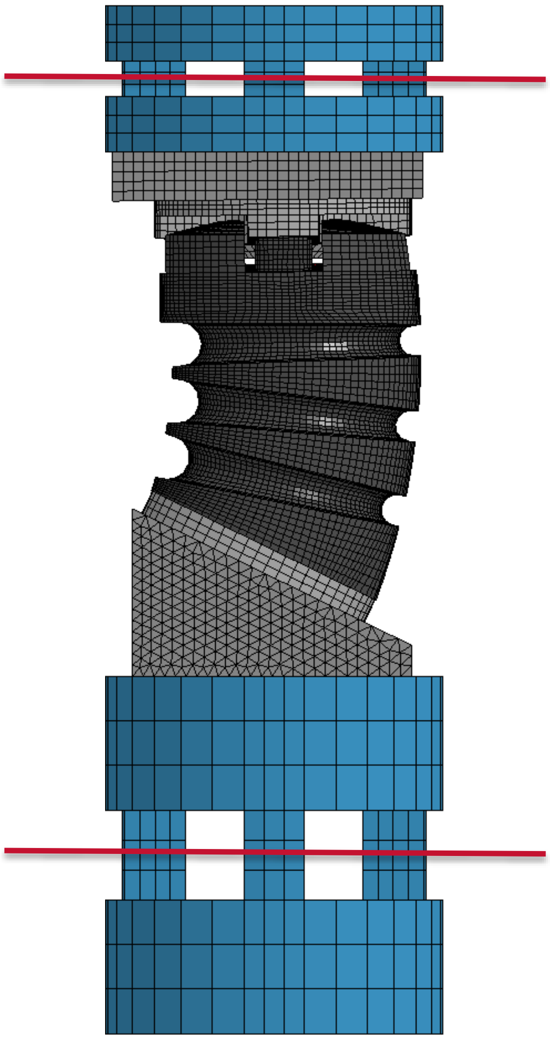

Converted (Output from LS-PP):

Red Planes Representing Section Outputs

Blue Circle Represents Head Accelerometer

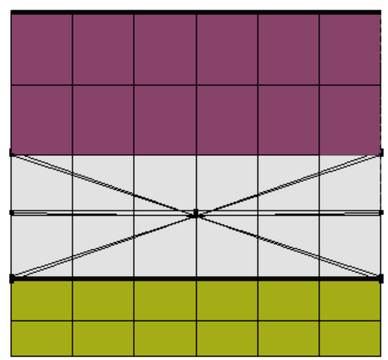

All Model Outputs Filtered Using SAE CFC 600 Hz Filter

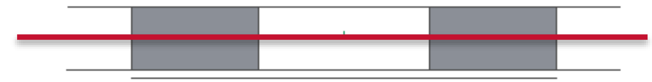

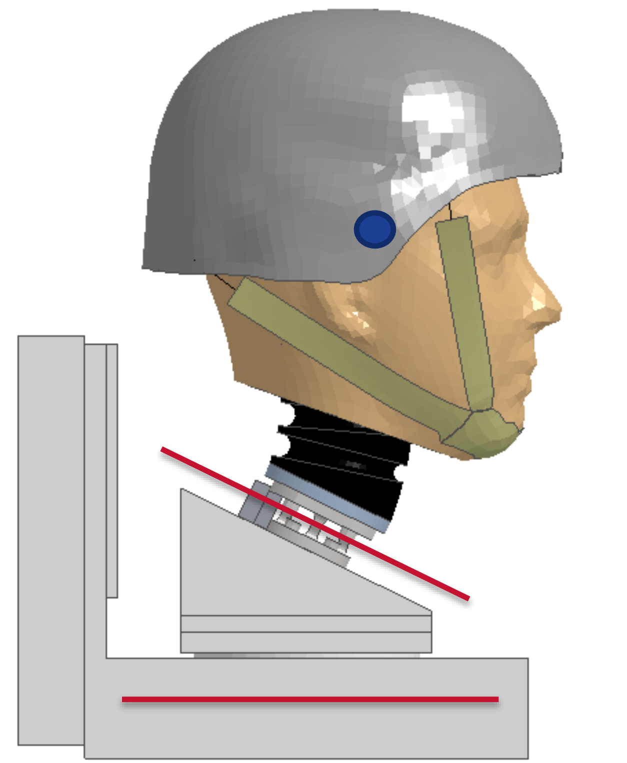

Wake Forest School of Medicine

CORA: Objective Eval.

Corridor Method, C_{cor}

C_{cor}= 1 is within inner band	C_{cor} = 0 is outside of outer band

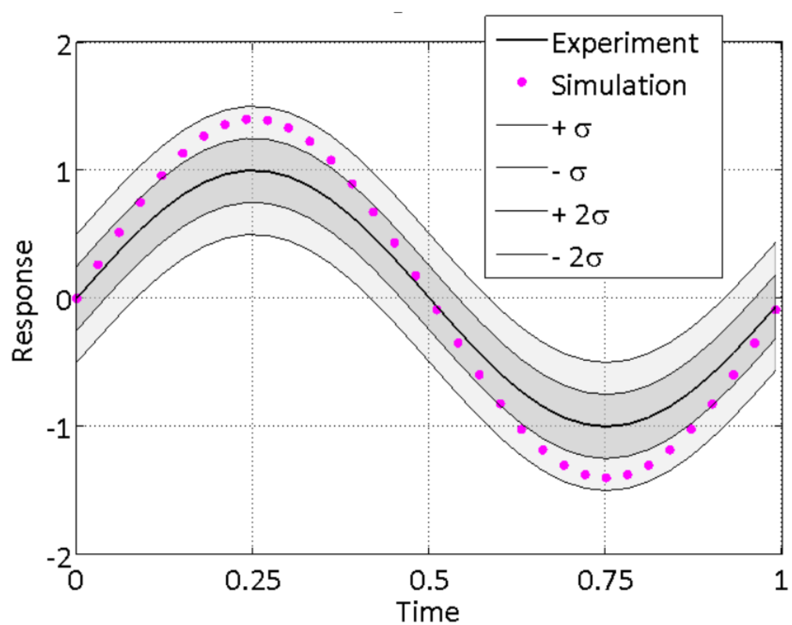

Current Study:
Inner corridor is 1 standard deviation
Outer corridor is 2 standard deviations

Gehre et al., *Objective rating of signals using test and simulated responses*. Enhanced Safety of Vehicles, 2009, no. 09-0407

CORA: Objective Eval.

Cross Correlation Method, C_{Phase}, C_{Size}, C_{shape}

C_{phase} = 1 if less than min shift, C_{phase} = 0 if greater than max shift	C_{size} = 1 if areas are equal, $C_{size} \rightarrow 0$ if areas are very different	C_{shape} = 1 if shape is similar, C_{shape} = 0 if shape is different

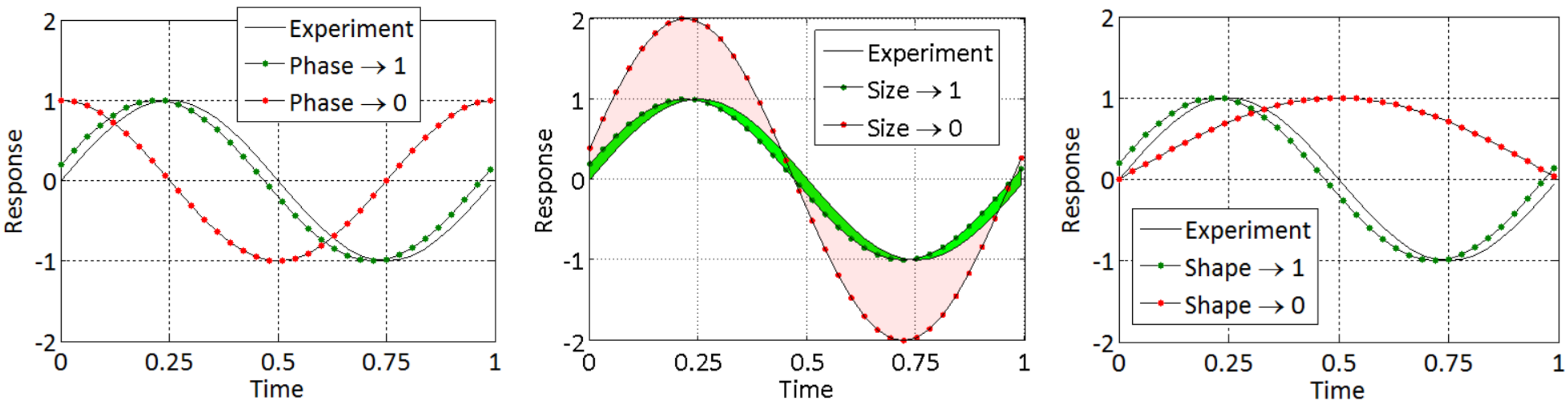

Gehre et al., *Objective rating of signals using test and simulated responses*. Enhanced Safety of Vehicles, 2009, no. 09-0407

Duke Compression Results

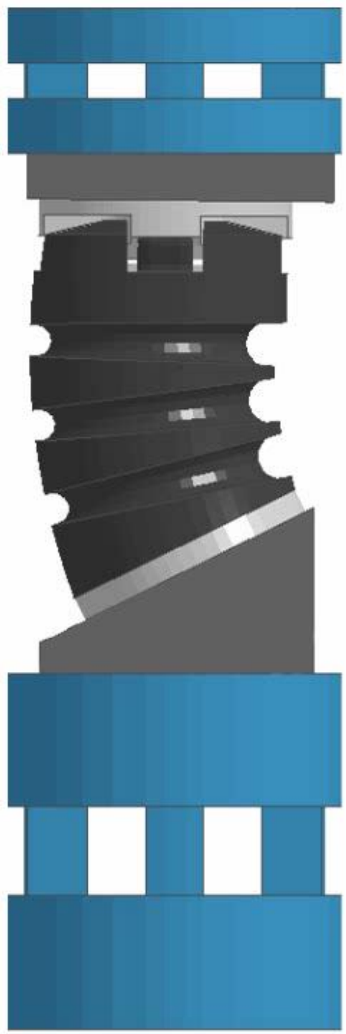

Wake Forest School of Medicine

Primary Signals: Converted

Horizontal lines represent the PMHS BRC +/- 1 σ

CORA: 0.77
ΔPeak: 0.01

CORA: 0.77
ΔPeak: 0.01

CORA: 0.80
ΔPeak: -0.04

Z-Force Upper

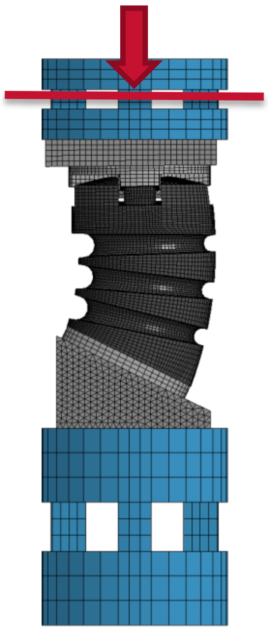

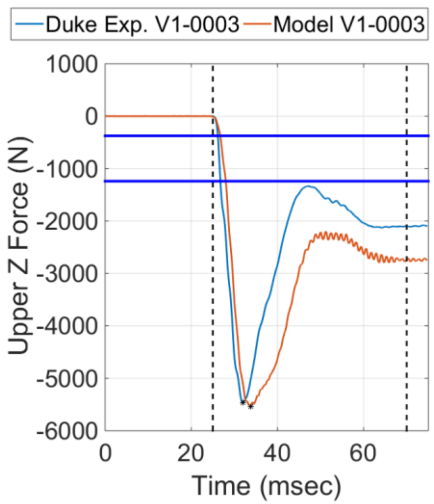

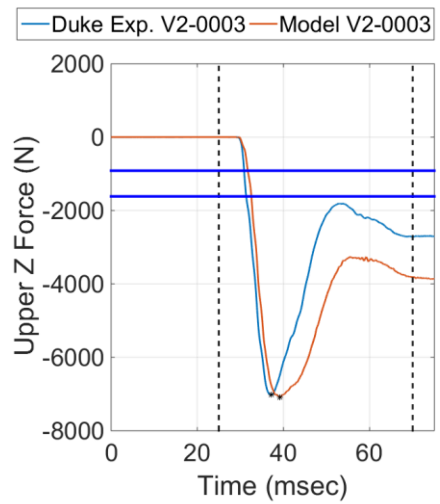

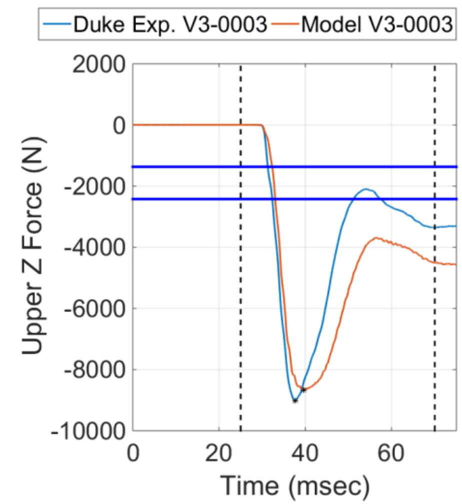

Increasing rate →

$$\Delta peak = \frac{Max\ Model - Max\ Experiment}{Max\ Experiment}$$

Take Home: Model closely matches peak compressive forces and rate of force in loading.

Wake Forest School of Medicine

Primary Signals: Converted

Y-Moment Upper

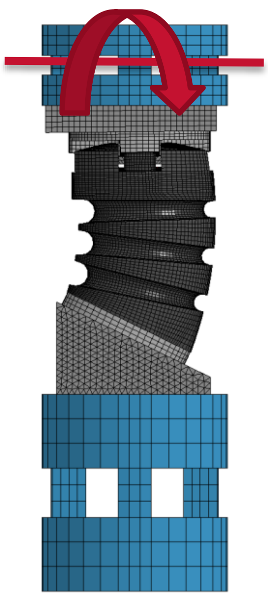

CORA: 0.83
ΔPeak: 0.07

CORA: 0.90
ΔPeak: -0.11

CORA: 0.82
ΔPeak: -0.23

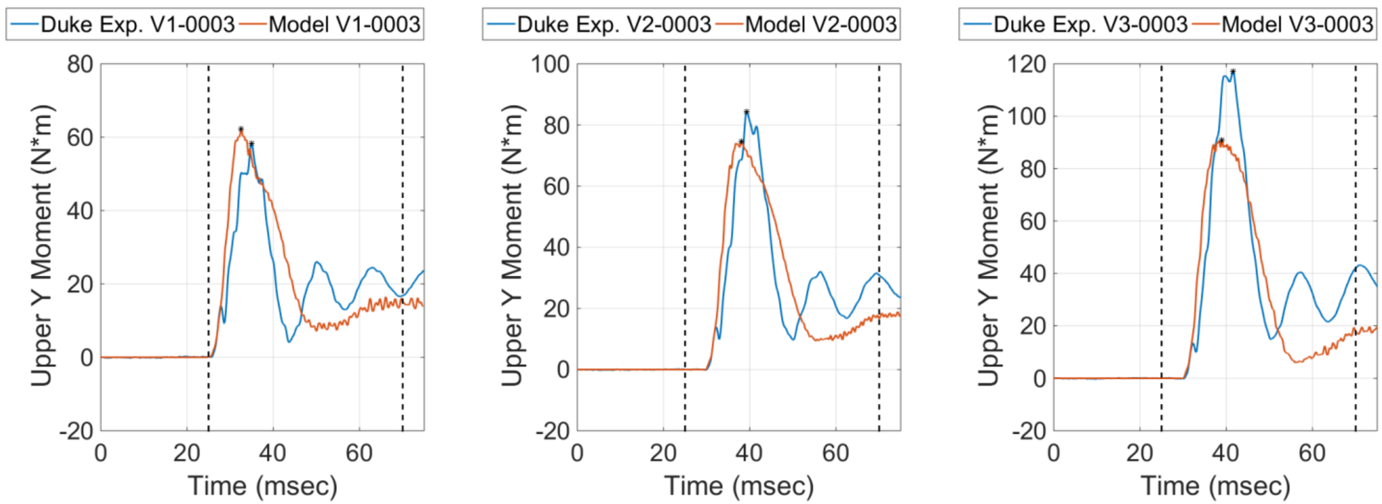

Increasing rate →

$$\Delta peak = \frac{Max\ Model - Max\ Experiment}{Max\ Experiment}$$

Take Home: Model closely matches peak sagittal plane moments and shows reasonable agreement with hold phase

Wake Forest School of Medicine

CORA Summary of HN02 LS-Dyna Validation

- CORA specifications harmonized
  - Corvid and APL/WFU
- CORA: 1 best, 0 worst
- Δ peak: 0 best, 1 worst
- Definition:
  - Converted signals are in engineering units, in this case filtered to SAE CFC 600
  - Processed signals are filtered and transformed to the location of interest for comparison with BRC

Velocity (N/ms)	Abscissa	Ordinate	Shape	Magnitude	Phase	Total	% Difference Peak
200	Fz, upper	Time	0.94	0.64	0.73	0.77	0.01
400	Fz, upper	Time	0.92	0.64	0.74	0.77	0.01
600	Fz, upper	Time	0.92	0.71	0.78	0.80	-0.04
200	My, upper	Time	0.67	0.82	1.00	0.83	0.07
400	My, upper	Time	0.74	1.00	0.97	0.90	-0.11
600	My, upper	Time	0.73	0.78	0.96	0.82	-0.23
200	Fz, lower	Time	0.94	0.66	0.65	0.75	0.12
400	Fz, lower	Time	0.92	0.66	0.66	0.75	0.07
600	Fz, lower	Time	0.92	0.74	0.70	0.79	0.02
200	My, lower	Time	0.78	0.98	1.00	0.92	0.04
400	My, lower	Time	0.51	0.79	0.98	0.76	-0.10
600	My, lower	Time	0.04	0.87	0.76	0.56	-0.20
200	Disp	Time	1.00	1.00	1.00	1.00	0.00
400	Disp	Time	1.00	1.00	1.00	1.00	0.00
600	Disp	Time	1.00	1.00	1.00	1.00	0.00
Average (equal weighting all signals)			**0.80**	**0.82**	**0.86**	**0.83**	**-0.02**

Wake Forest School of Medicine

CORA Summary of HN02 LS-Dyna Validation

CORA specifications harmonized

- Corvid and APL/WFU

CORA: 1 best, 0 worst

Δ peak: 0 best, 1 worst

Definition:

- Converted signals are in engineering units, in this case filtered to SAE CFC 600
- Processed signals are filtered and transformed to the location of interest for comparison with BRC

Weights from W0032

Converted	200 N/ms	400 N/ms	600 N/ms
Weighted CORA Score	**0.82**	**0.81**	**0.81**
Weighted Peak Difference	**0.11**	**0.09**	**0.10**

Highest weighted signals:

- Vertical force
- Sagittal moment
- Input displacement

Wake Forest School of Medicine

Sensitivity Analysis

Purpose:

- Determine **effect of load cell alignment** on measured force and moment

Caveats:

- Experiment is well documented, but we can use the model to illustrate the effect of tech demonstrator placement in the rig

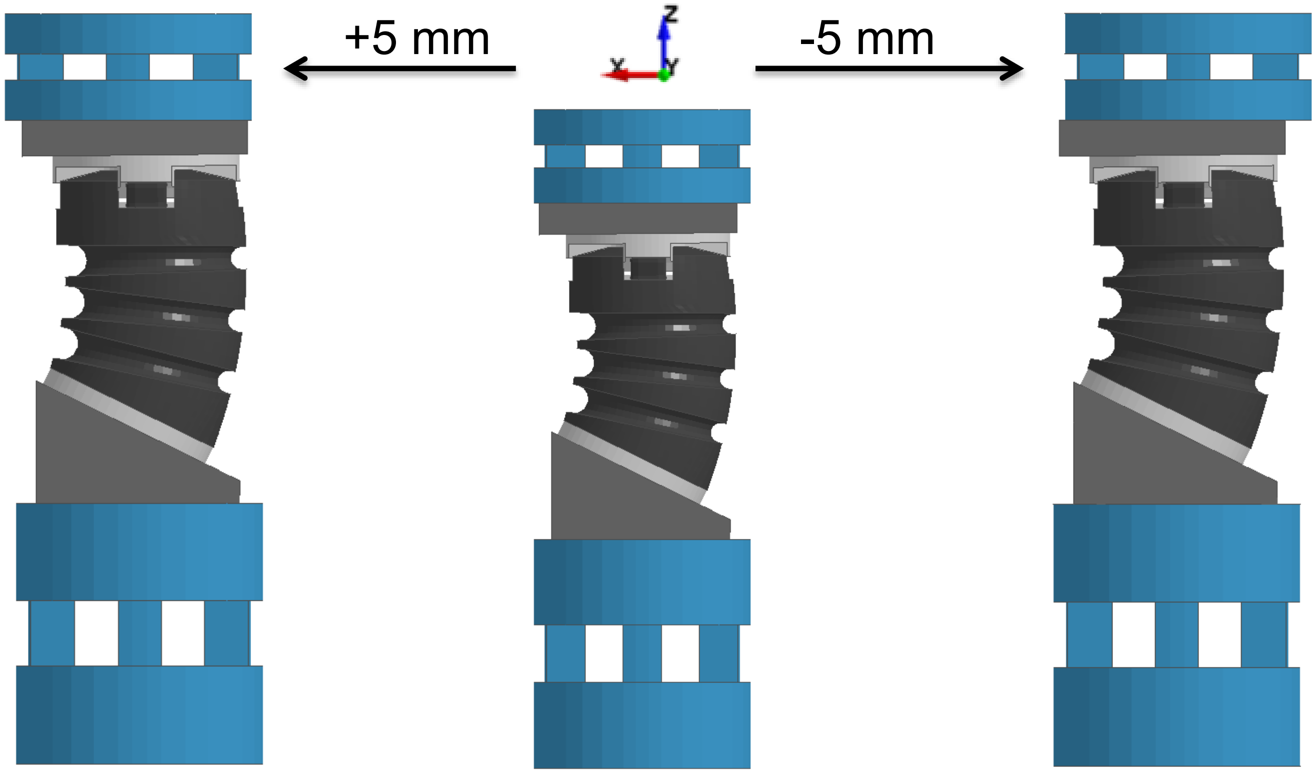

Wake Forest School of Medicine

Sensitivity Analysis

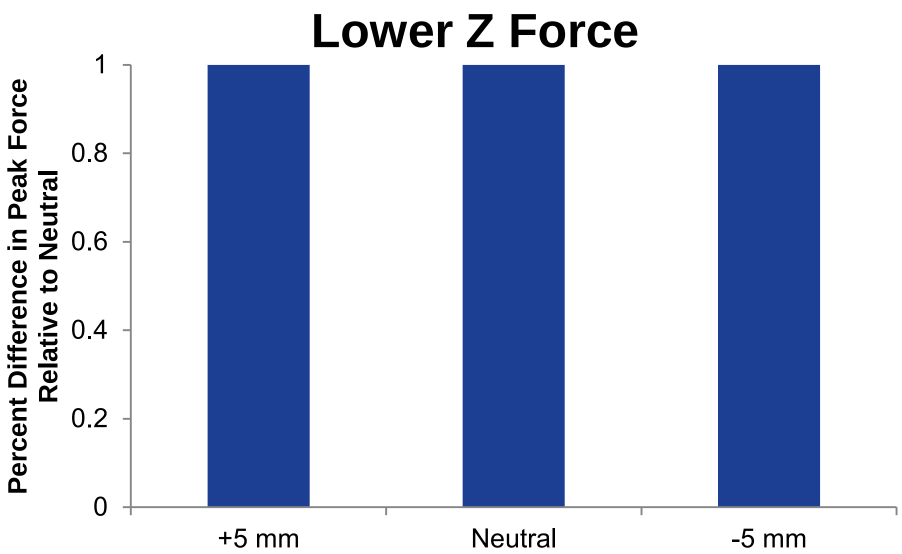

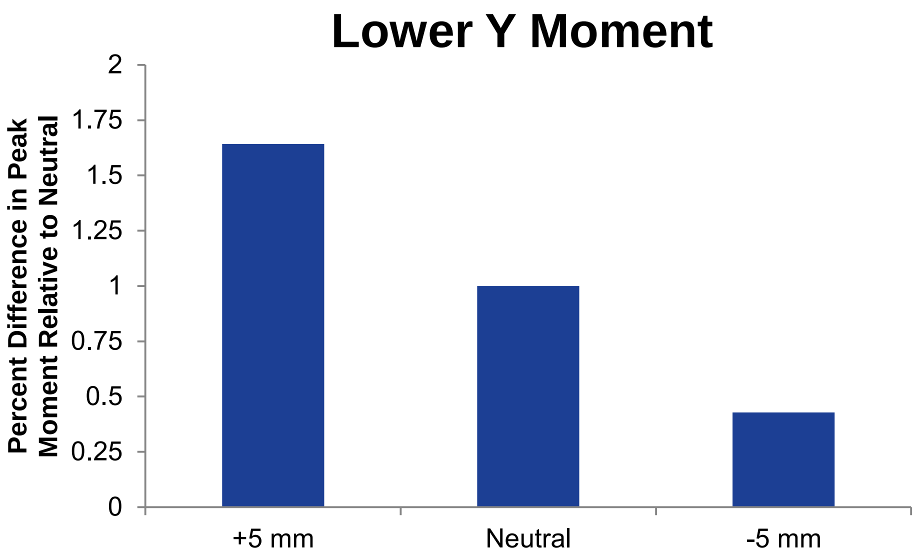

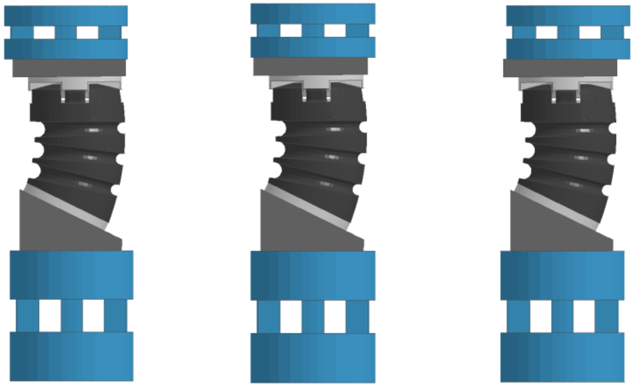

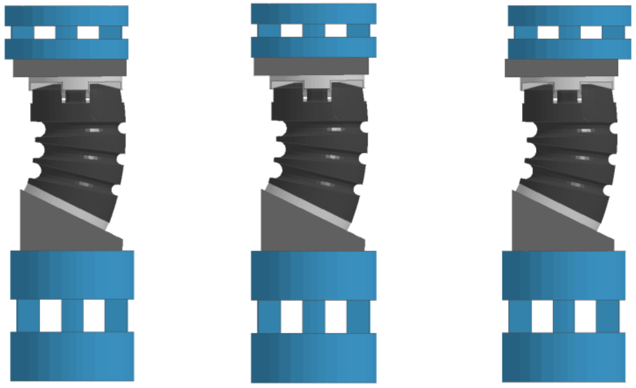

Take Home: Load cell position had little effect on the peak compressive force, but had significant effect on the peak sagittal plane moments

Wake Forest School of Medicine

Sensitivity Analysis

Purpose:

- Determine effect of neck curvature on output

Caveats:

- Displacement vs. time for these tests is different than displacement vs. time for data above
- Fixtures are different and pre-date Duke ATD spine testing

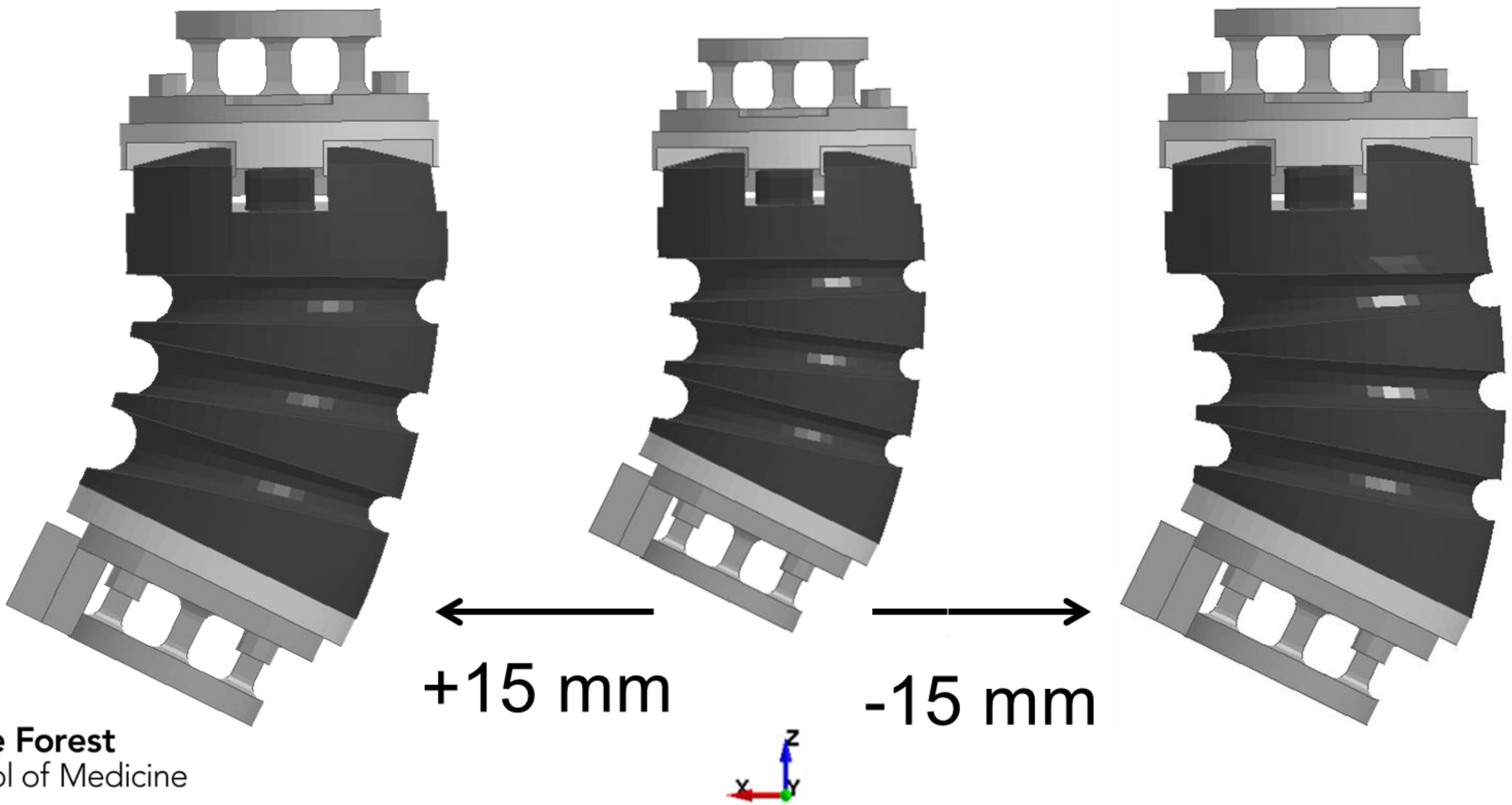

Wake Forest School of Medicine

Sensitivity Analysis

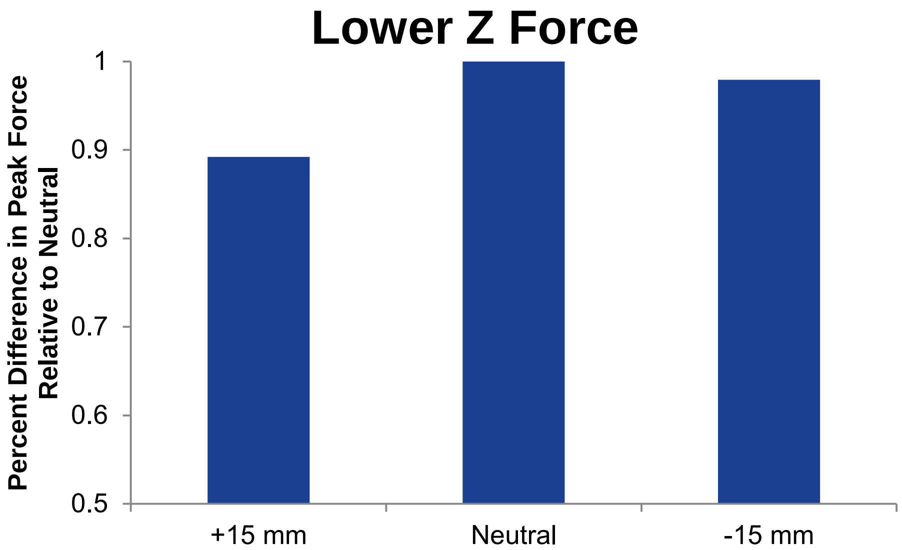

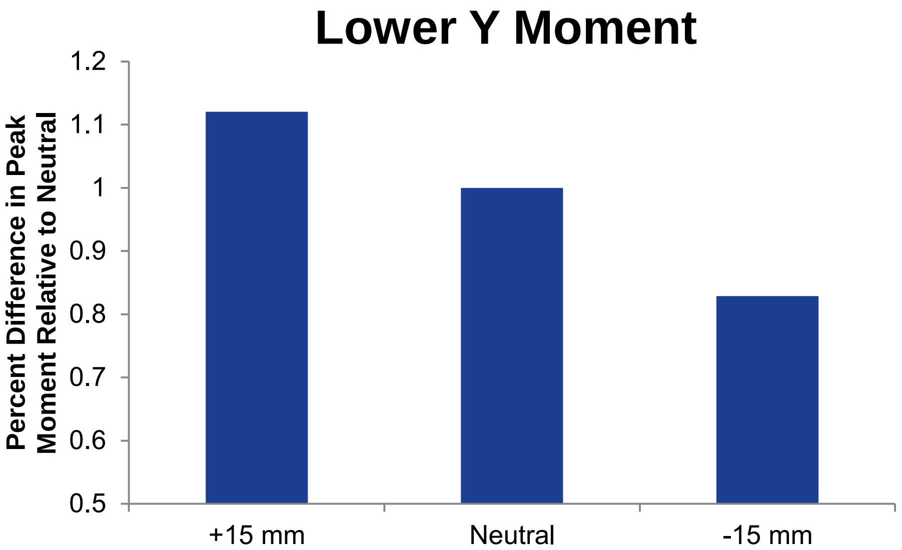

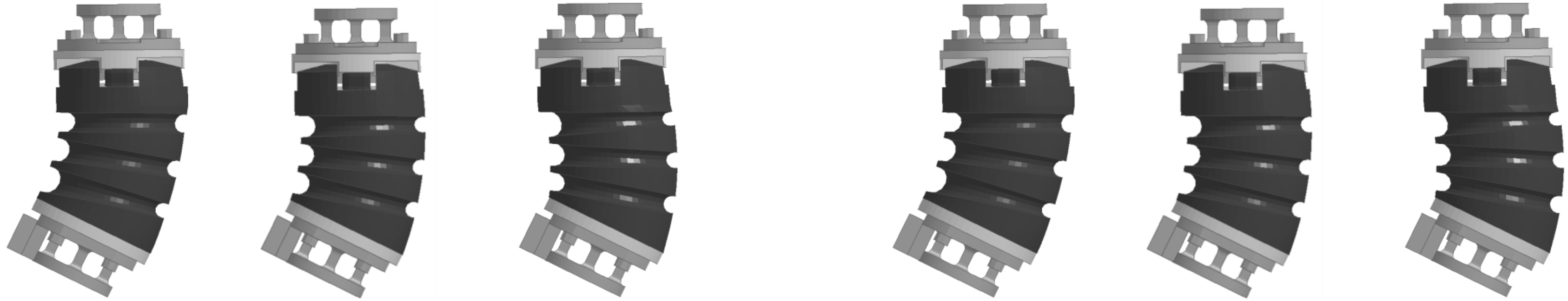

Take Home: Increasing neck curvature caused a decrease in peak compressive force and an increase in the moment. Shifting the neck anteriorly had little effect on compressive forces, but decreased the peak moment.

Geometry Evaluations: Ovals

Oval, Tet: Large holes	Oval, Tet: Medium holes	Oval, Tet: Small holes

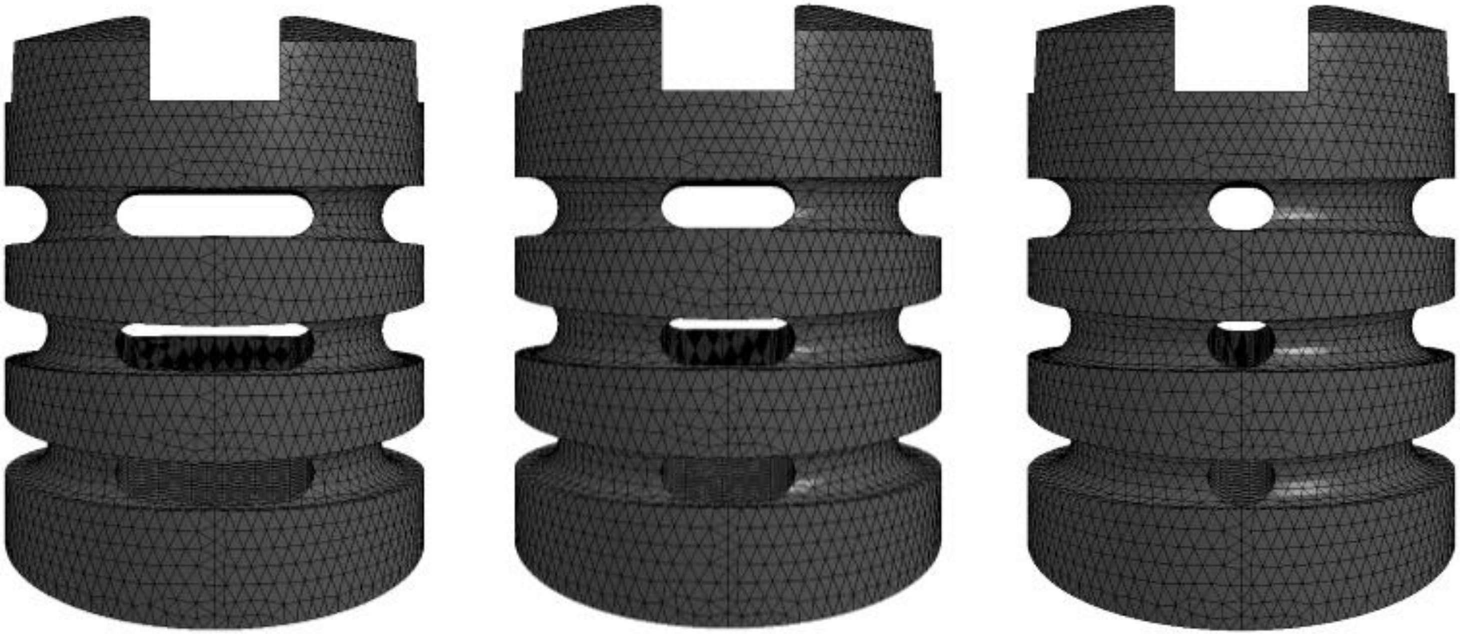

Wake Forest School of Medicine

Geometry Evaluations: Ovals

Take Home: Iterative reduction of material in the molded neck via oval cuts had a greater effect on peak axial force than peak moment.

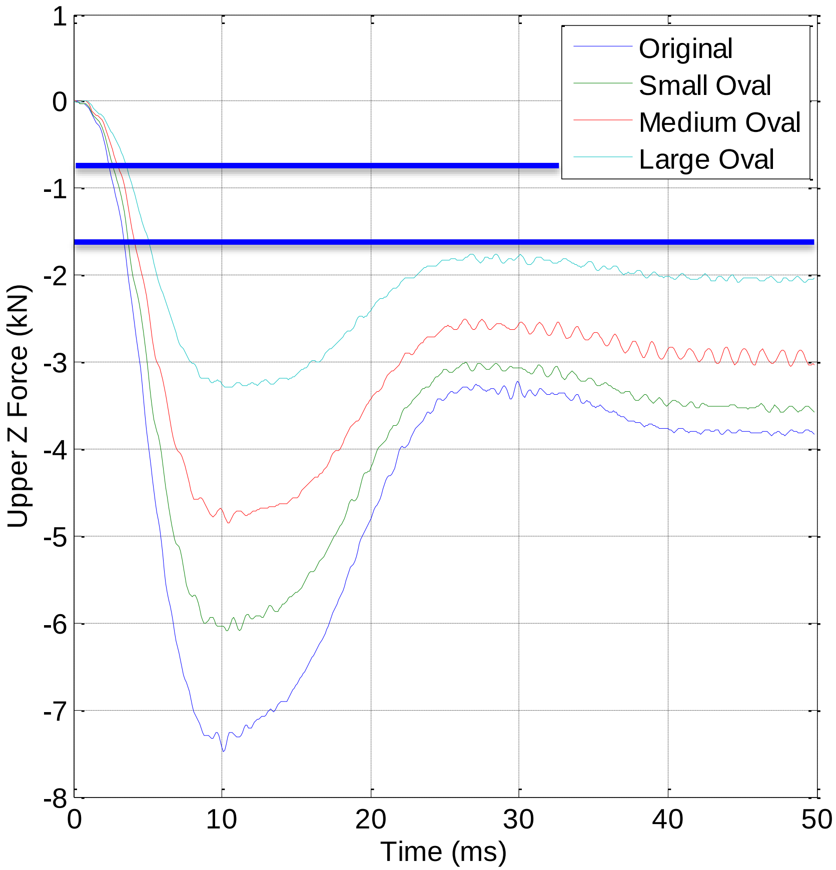

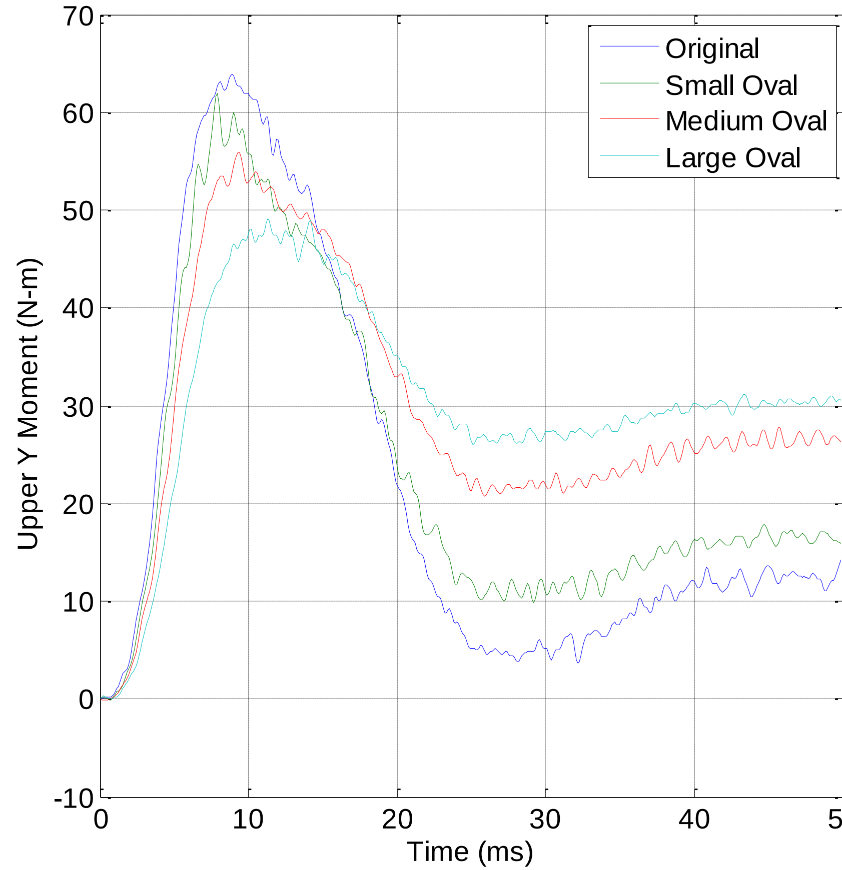

Wake Forest School of Medicine

Geometry Evaluations: Notches

Notches, Tet (0250): 194,069 elements

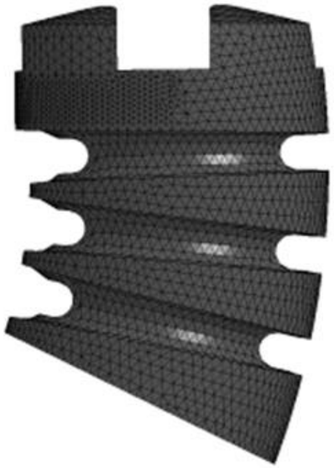

Notches, Tet (0375): 159,710 elements

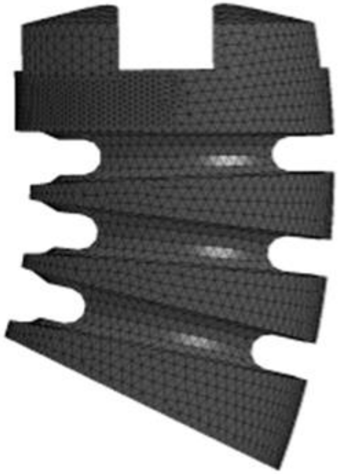

Notches, Tet (0500): 140,119 elements

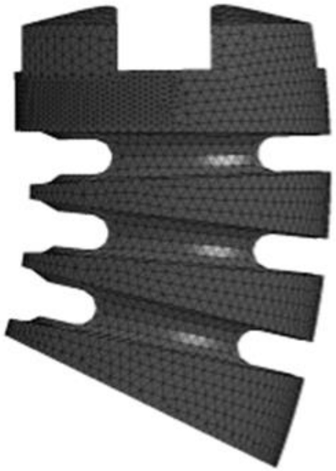

Notches, Tet (0625): 133,855 elements

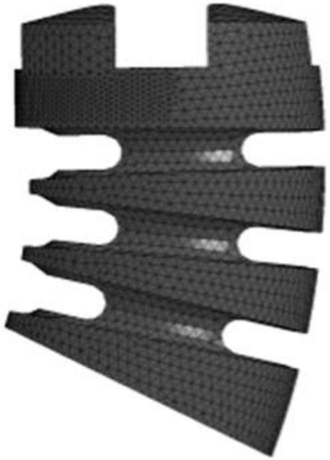

Wake Forest School of Medicine

Geometry Evaluations: Notches

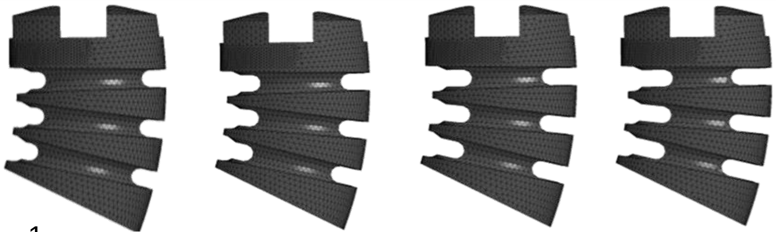

Take Home: Reduction of material in the molded neck via notched cuts reduced peak compressive forces but had little effect on moments.

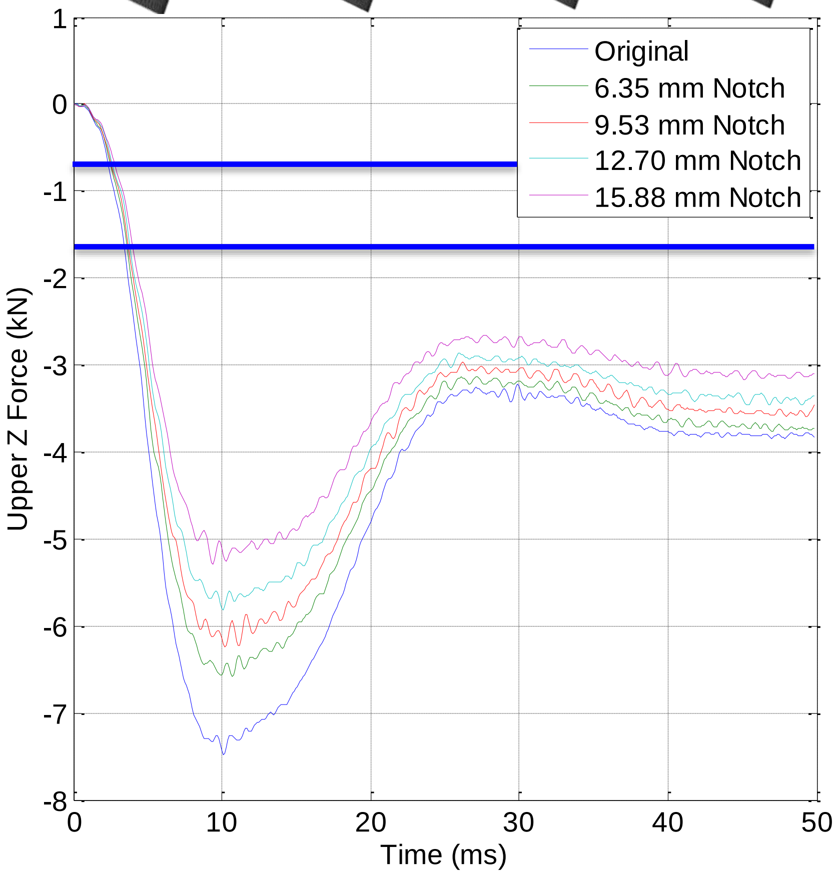

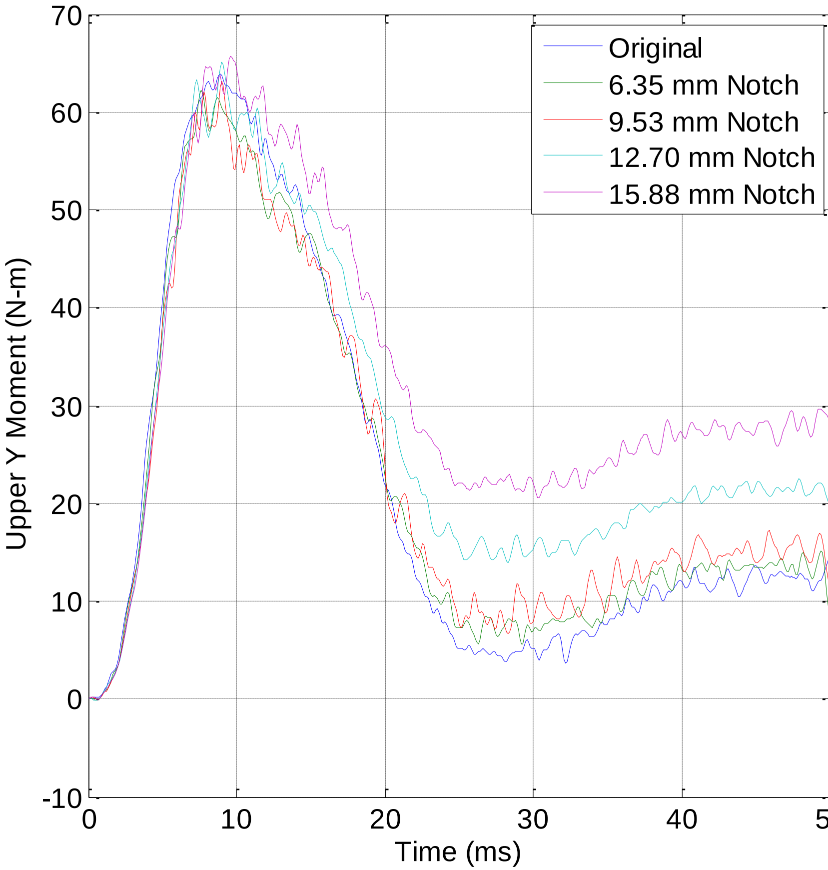

Wake Forest School of Medicine

Comparison of Geometry Evaluations

- Comparing peak upper Z force as function of volume change
- The linear decrease in volume due to the oval cuts led to a linear decrease in peak Z force
- Oval cuts also had larger effect on overall model volume

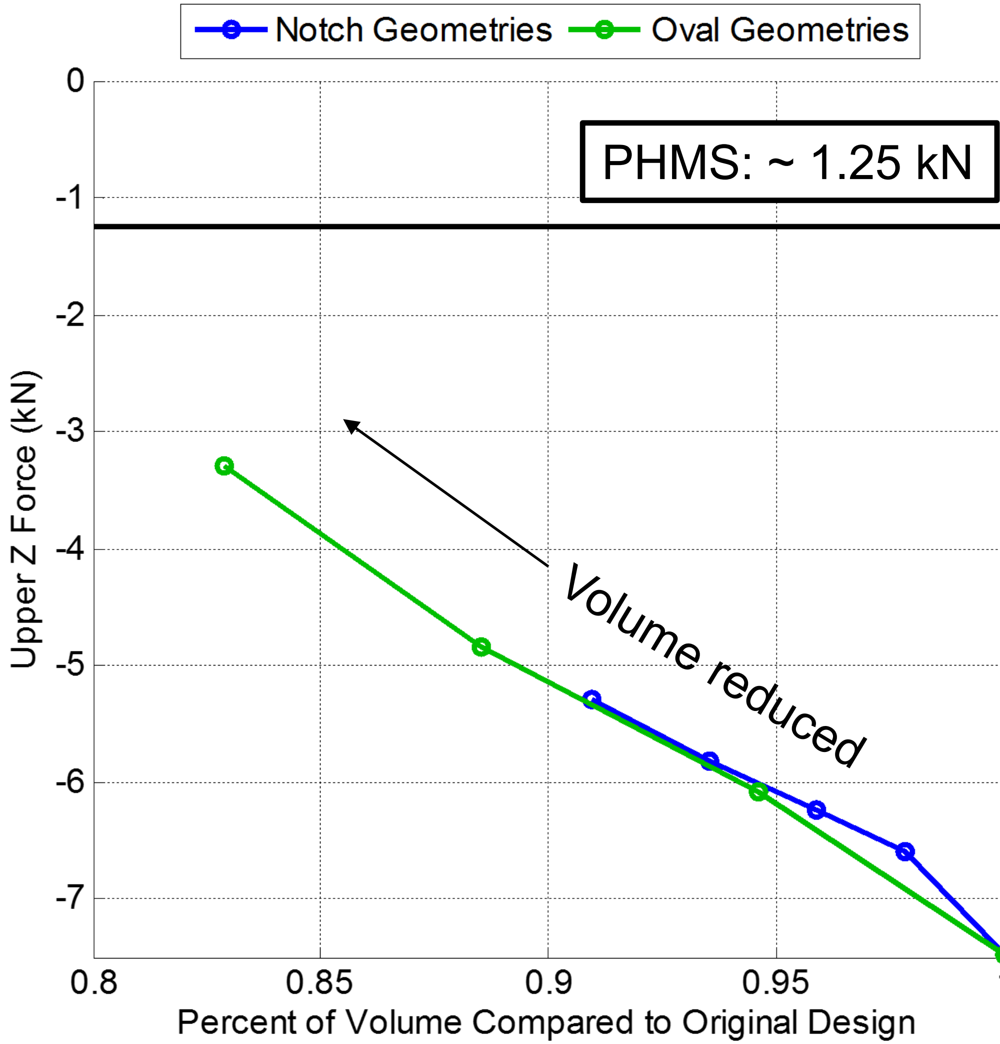

Wake Forest School of Medicine

MCW: Roof Contact Force

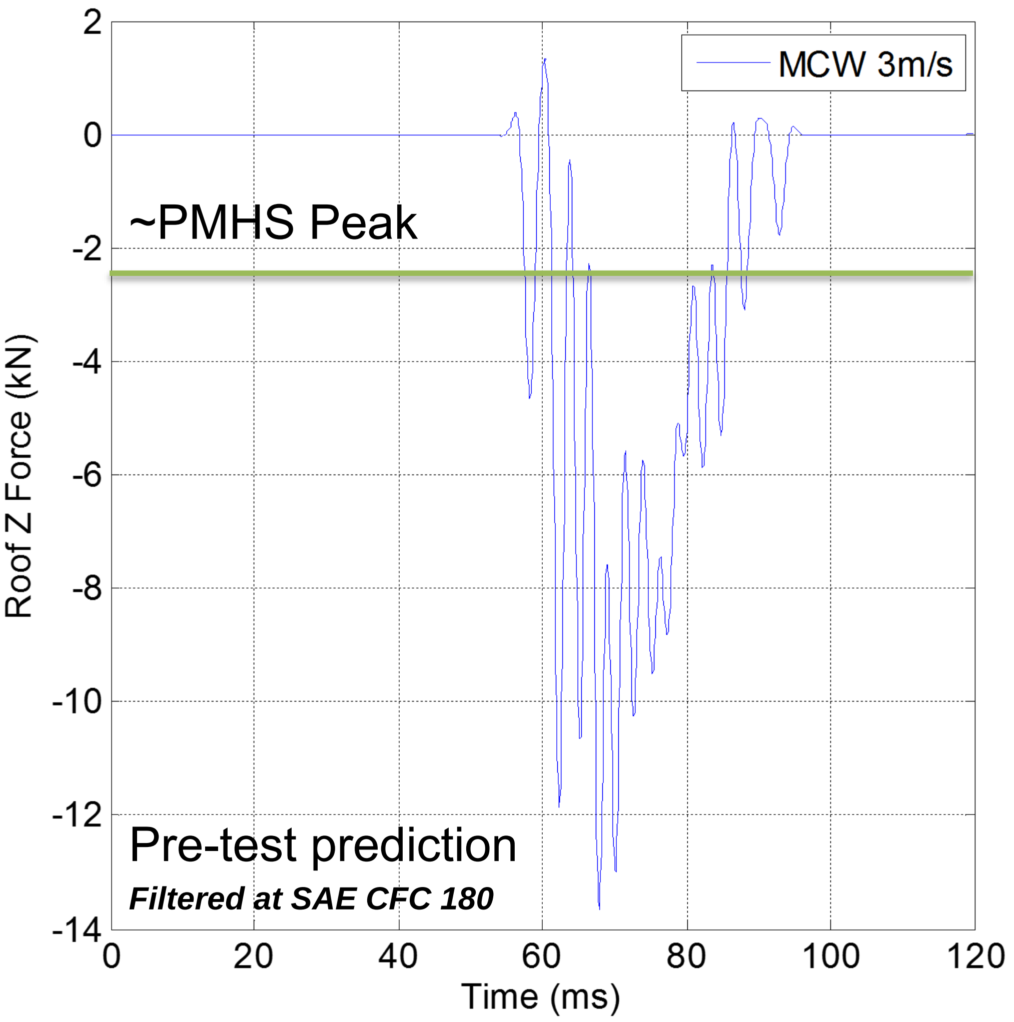

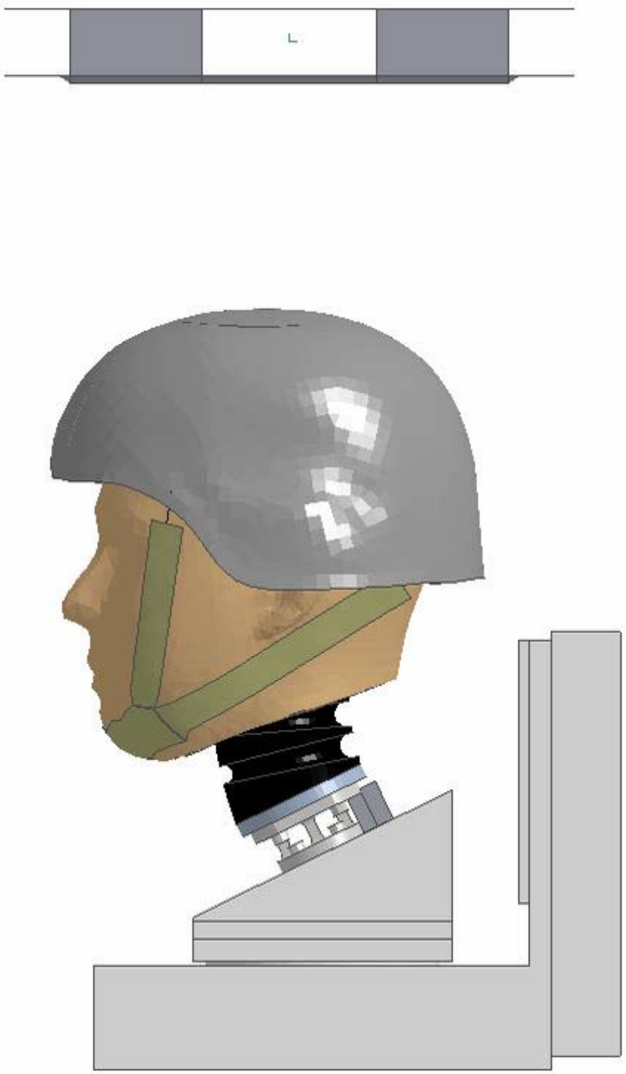

Wake Forest School of Medicine

MCW: Lower Load Cell

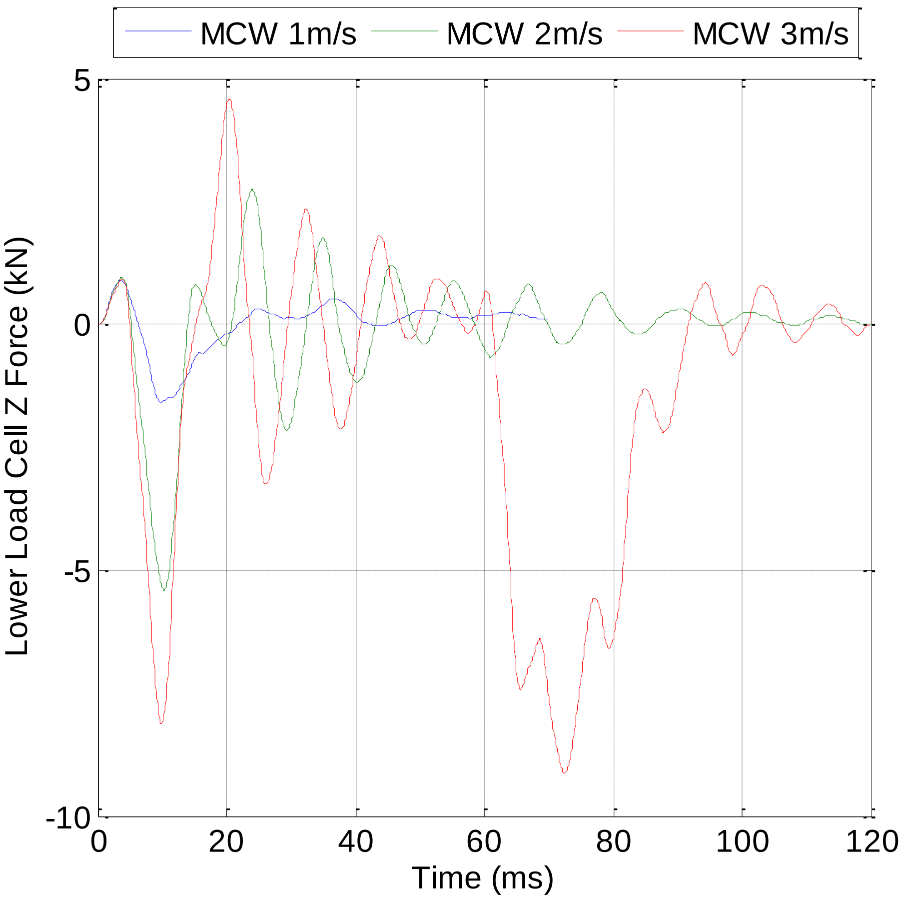

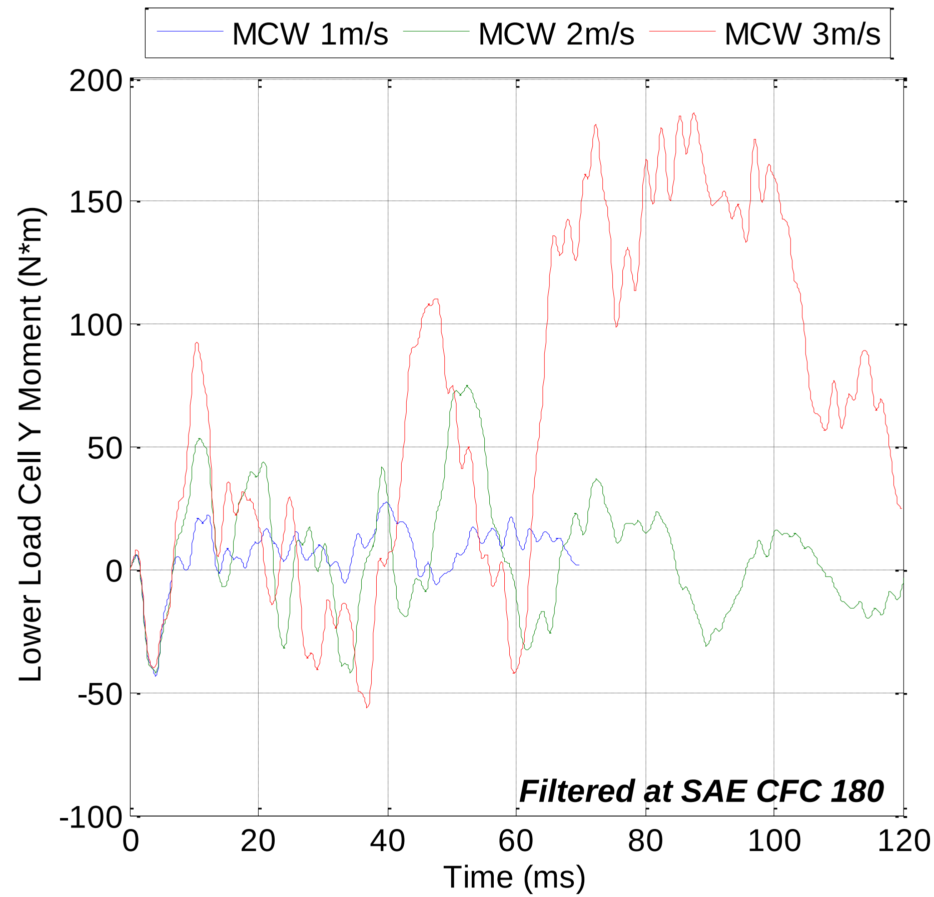

Take Home: Pre-test prediction summary compared to neck compression component test: The forces are similar, moments slightly greater when impact occurs

Wake Forest School of Medicine

Discussion & Caveats

- Preliminary ATD validation is to develop confidence in the model
- Ultimately for use in evaluating designs against BRCs
  - Challenge: Match experimental transforms used in BRC development
  - “Converted” data shown, “Processed” is forthcoming
- Alignment is key for moments
- HN03 validation is forthcoming, design concepts MUST be evaluated in multiple testing scenarios

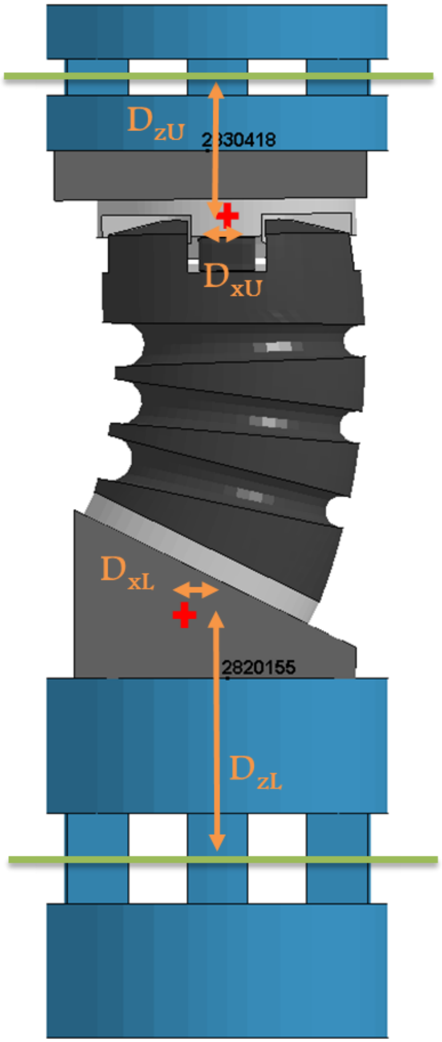

Wake Forest School of Medicine

Discussion: Sensitivity

U.S. ARMY RDECOM ARL

Summary: How sensitivity studies affected force and moments

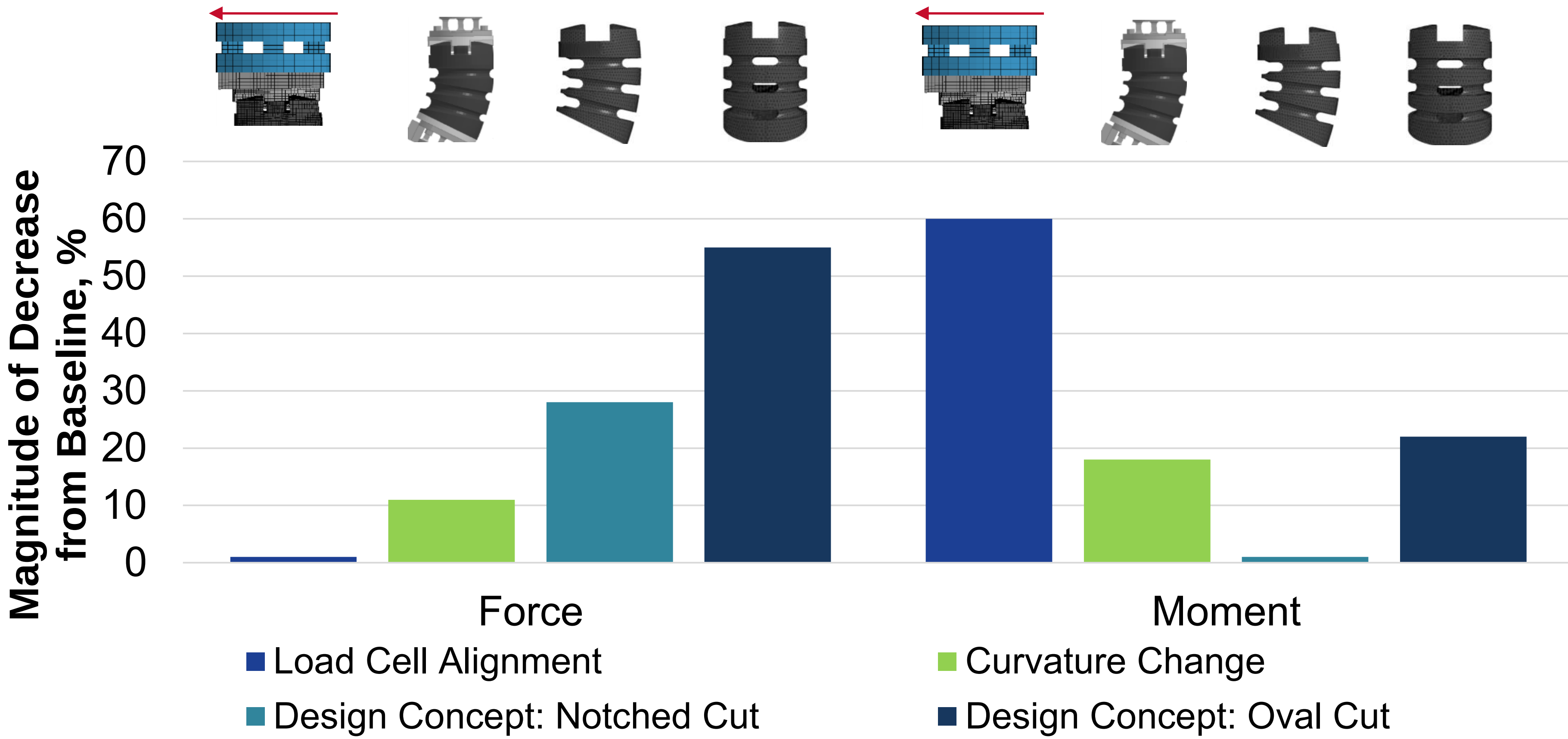

Take Home: Oval cuts had the most significant effect on peak compressive force. Load cell sensitivity (5mm posterior shift) had the most significant effect on moments

Wake Forest School of Medicine

APL

Summary & Conclusions

- M&S is performing modeling work for the WIAMan program using LS-Dyna and Velodyne
- First Wiaman ATD Tech Demonstrator validated (NH02 condition)
  - 3 rates ~ 0.8 CORA, given weighting on key measures
  - Processed data is pending for comparison to BRCs
  - HN03 simulations have begun, pending physical testing
- Set precedent for validation reporting procedures
- Key component of the model, molded rubber neck and buffers incorporates strain rate dependency from material testing
- Design evaluations showed dependence of peak load and moment on curvature and bore designs
- M&S activities are informing design, evaluate design modifications and assess strength of design

Wake Forest School of Medicine

Acknowledgements

Sponsor:

U.S. Army Research Lab, WIAMan Program Office (N00024-13-D-6400)

Johns Hopkins Applied Physics Laboratory (No. 117216)

Thanks to Modeling and Simulation Partners:

Corvid Technologies

Virginia Tech

Medical College of Wisconsin

Duke U.

Wake Forest School of Medicine

Modeling and Sensitivity Analysis of the WIAMan ATD Head and Neck: A Finite Element Study

Matthew L. Davis[1,2], Jeremy M. Schap[1,2], Michael Boyle[3], Robert Armiger[3], M. Chowdhury[4], F. Scott Gayzik[1,2]

[1]Wake Forest School of Medicine
[2]Wake Forest University Center for Injury Biomechanics
[3]Johns Hopkins Applied Physics Laboratory
[4]U.S. Army Research Lab, WIAMan Engineering Office

Supplemental Slides

Validation Report Format

WFU format, mature, currently internal rev. 3

Verifying processed data
before finalizing

Validation Data Summary

LS-Dyna Simulation Results:

WIAMan ATD neck compression (HN02, Shore 75A)
Experiments performed by Duke U. (Bass et al.)

Date: Rev. 1: 10/28/2015
Rev. 2: 11/17/2015
Rev. 3: 11/30/2015

Authors:

Matthew L. Davis, Jeremy M. Schap, Nicholas R. Williams, F. Scott Gayzik
Wake Forest University Center for Injury Biomechanics, Winston-Salem, NC

Matthew Shanaman, Michael Boyle, Robert Armiger
Johns Hopkins Applied Physics Lab, Laurel, MD

1

3. CORA Summary

CORA was used to objectively compare model output to the experiment. This compared the computational model to the ATD tech demonstrator. We compared a single trace to the model output so no variability in the experimental system is considered. This variability was found to be minimal. For this reason no corridor scores are presented. Converted data taken at the load cell location is presented first, followed by processed data.

Table 2. CORA Data Summary

Objective (Compares A to B)	A: ATD FEA model	To	B: Single ATD Physical Test
Code Version	3.5		
Configuration file name, date	Cora_settings_CSvalidation.cps, 11/2/15		
Time window for CORA evaluation	25 to 70 ms		
CORA notes	Corridor score dropped because we are comparing model output to a single curve (Test 0003)		

3.1. Converted Comparison Data

The converted data form the LS-Dyna model has been filtered using SAE CFC 600 filter to match the experimental data.

Table 3. Primary Response Data, CORA scores, Converted. Color coding corresponds to scale from worst (red) to best (green). Note CORA scores are best at 1 and peak difference scores are best at 0.

Velocity (N/ms)	Abscissa	Ordinate	Shape	Magnitude	Phase	Total	% Difference Peak
200	Fz, upper	Time	0.94	0.64	0.73	0.77	0.02
400	Fz, upper	Time	0.92	0.64	0.74	0.77	0.01
600	Fz, upper	Time	0.92	0.71	0.78	0.80	-0.04
200	My, upper	Time	0.59	0.74	0.98	0.77	-0.12
400	My, upper	Time	0.66	0.61	0.94	0.74	-0.28
600	My, upper	Time	0.65	0.47	0.94	0.69	-0.38
200	Fz, lower	Time	0.94	0.66	0.65	0.75	0.12
400	Fz, lower	Time	0.92	0.66	0.66	0.75	0.08
600	Fz, lower	Time	0.92	0.74	0.70	0.79	0.01
200	My, lower	Time	0.72	0.75	1.00	0.82	-0.06
400	My, lower	Time	0.37	0.61	0.96	0.65	-0.19
600	My, lower	Time	0.01	0.80	0.73	0.51	-0.26
200	Disp	Time	1.00	1.00	1.00	1.00	0.00
400	Disp	Time	1.00	1.00	1.00	1.00	0.00
600	Disp	Time	1.00	1.00	1.00	1.00	0.00
Average (equal weighting all signals)			0.77	0.74	0.85	0.79	0.10

1. See Eq. 8

4.7. Moment Y, Upper, 200 N/ms (V1-In sagittal plane)

Model Revision & Upload Date	Wiaman ATD Neck v 2.0 10/26/15
LS-Dyna Version	ls-dyna_mpp_s_Dev_101757_intel_linux86-64_platformmpi
Execution File	RIG_MAIN_v1.dyn
Termination	Normal @ t_{total} = 50 ms (plot is time shifted to match experiment zero)
Simulation Type	Boundary Prescribed Motion (MTS Compression)
System Mass	9.43 kg
Velocity	200 N/ms
Validated Component Material	Butyl Rubber (75A) modeled as Bergstrom Boyce Rubber (see pg. 4)

Experimental Data	Performer	N	Test No.	Material	Shore Hardness	Time Shift	Filter
	Duke U.	1	0003	Butyl Rubber	75A	NA	CFC 600

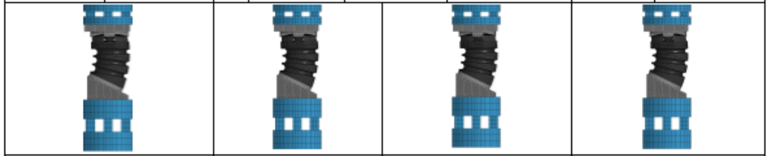

t = 0	t = 1/3 t_{total}	t = 2/3 t_{total}	t = t_{total}

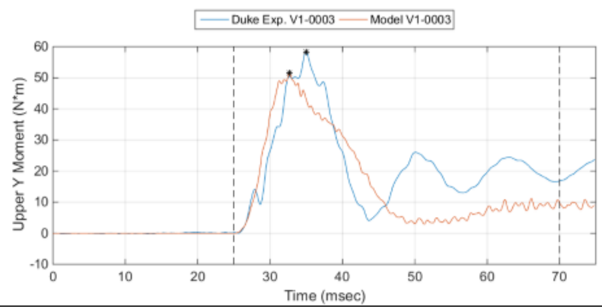

Figure 10. Moment Y (sagittal) vs. Time, Converted.

Filter for Force Data (LS-Dyna)	Mass gained (%)	Mass scaled time step	Hourglass ratio at peak force	CORA (CFC 600)	% Peak Diff
CFC 600	1.99E-4 kg (0.002%)	0.09 µs	2.8%	0.77	-0.12

Time method	Force Method
Simulation time was reduced by setting time zero at 24.8 ms of simulation. Pre-simulation time added back in to compare to experimental data.	Secforc branch 2: Upper LC, Raw untransformed
Time transform:	**Force transform:**
None	None

Wake Forest
School of Medicine

The Nation's Premier Laboratory for Land Forces

Shore 45A Material Change

- Study uses PBD-45A material model
  - Ogden Viscoelastic
  - Validated against APL lumbar spine demonstrator investigation
- Significant reduction in axial force and moments brings CS response closer to the desired BRC
- M&S recommended manufacture of BR-45A cervical spine, although questions of durability remains
  - Recommend testing in MCW HN03 condition to achieve larger strains

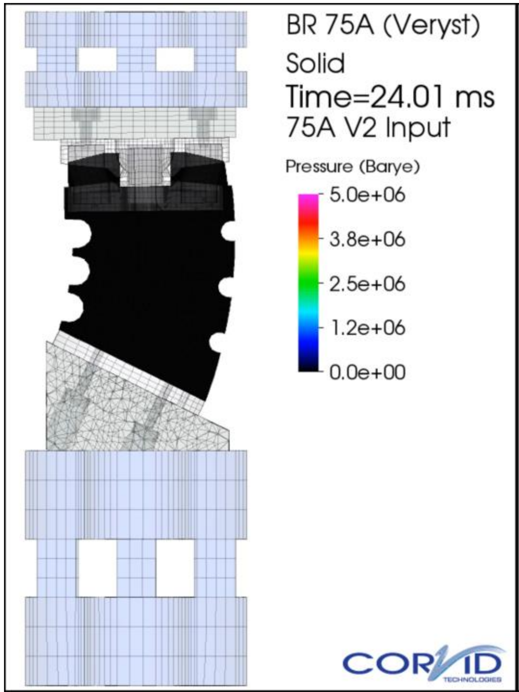

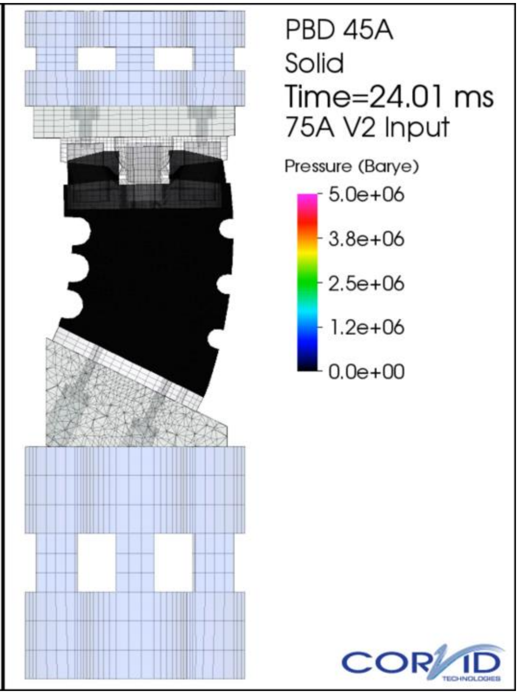

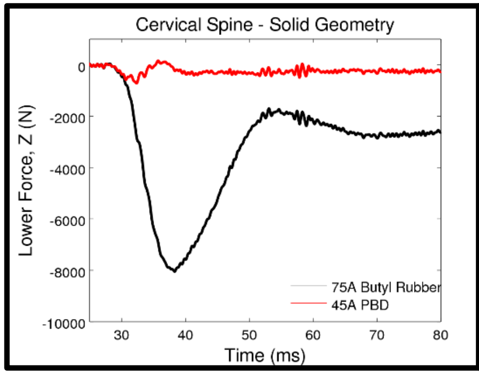

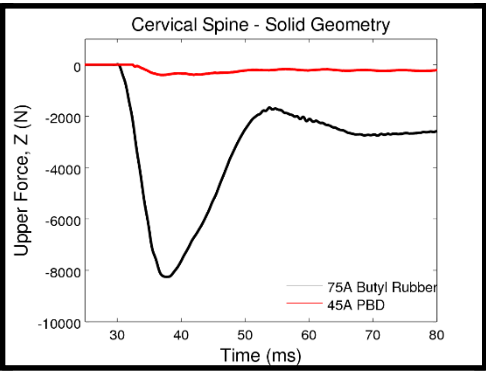

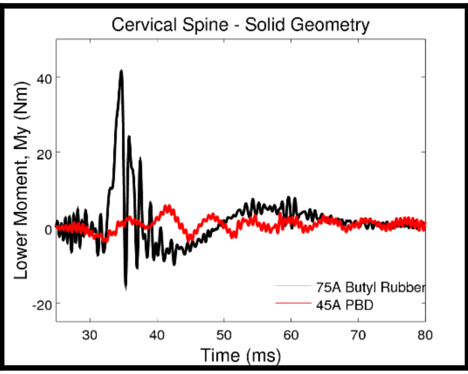

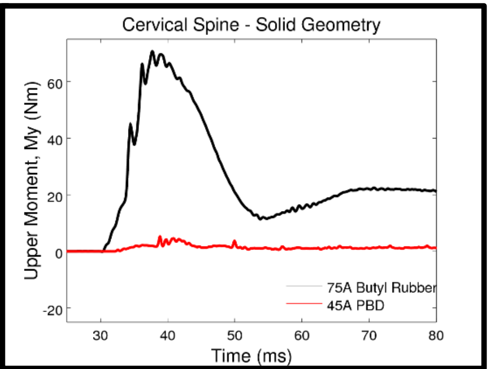

45A Butyl Rubber cervical spine has been manufactured and will be tested at Duke

New Geometries Provided

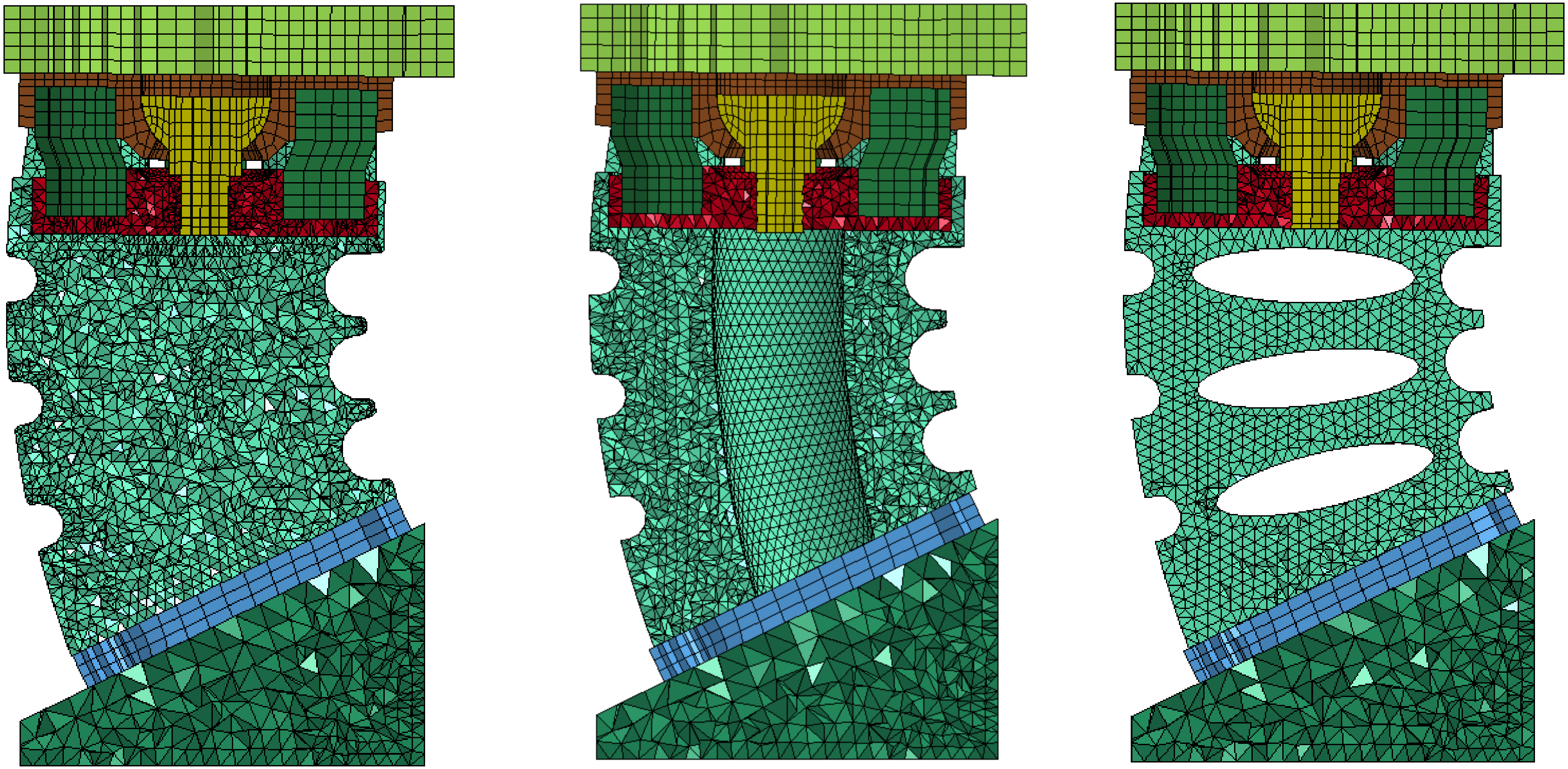

Original Geometry

Bore

Oval

Wake Forest School of Medicine

Run Outputs- V2-0004

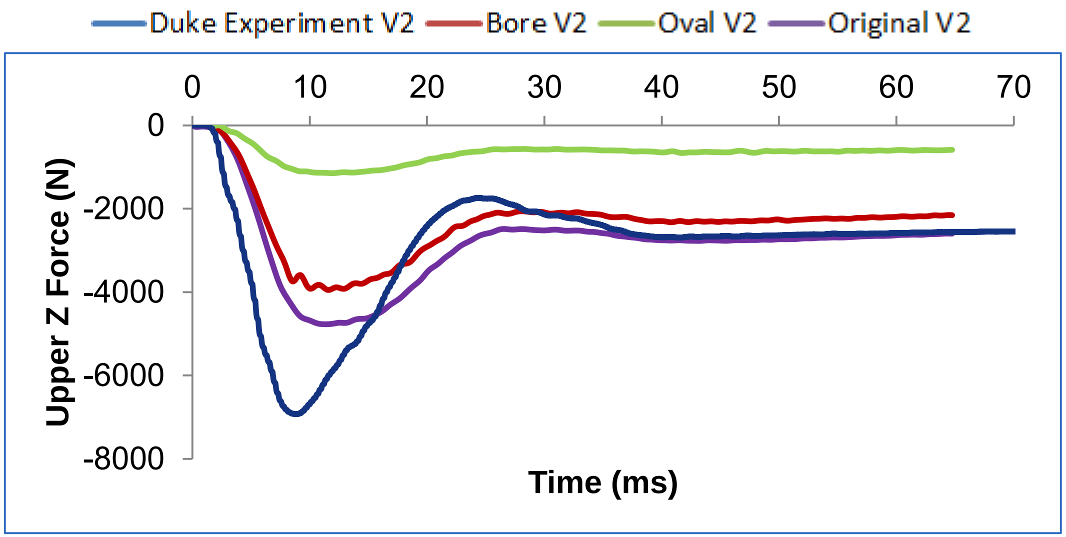

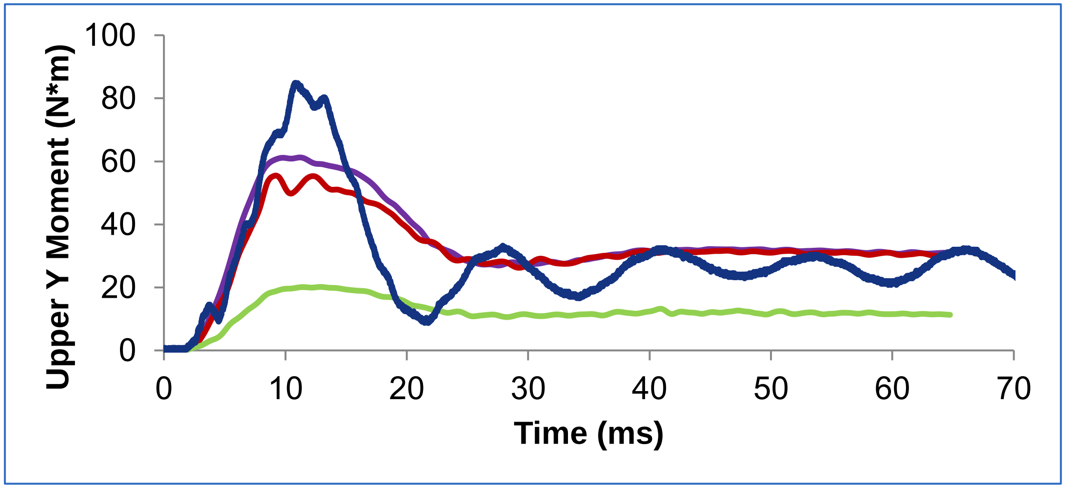

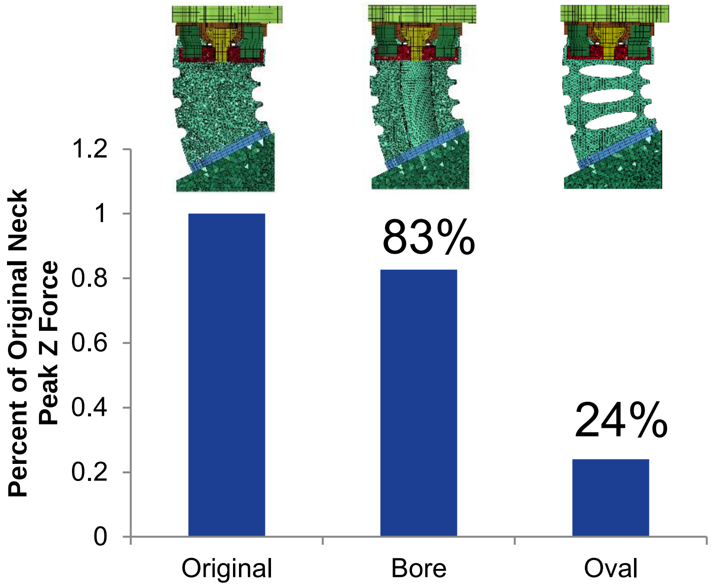

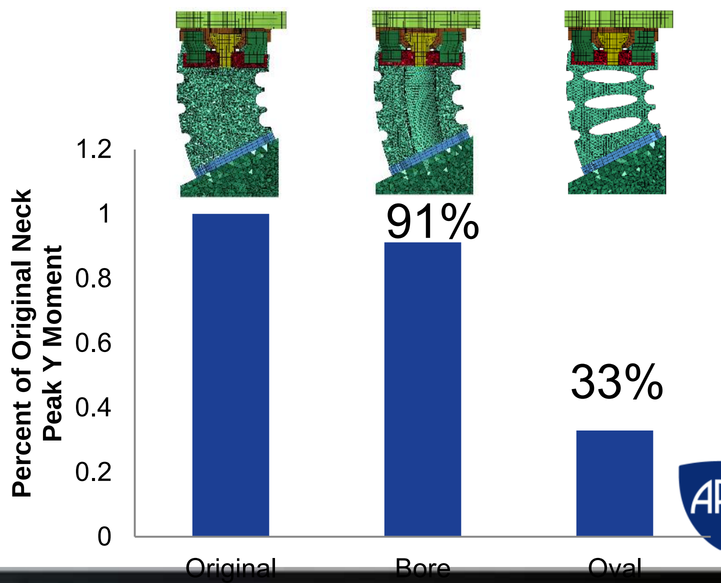

The bored and oval cut versions reduce the peak load by 17% and 76%, respectively. Moments were reduced by 9% and 67%.

PMHS Data Comparison

U.S. ARMY RDECOM ARL

- Peak force and moment comparison for the V2 simulations to PMHS data
- The blue bars indicate the peaks for the simulated upper neck Z force and upper neck Y moment
- The orange lines represent the 1 standard deviation for force and moment respectively in the PMHS tests from the BRC delivery

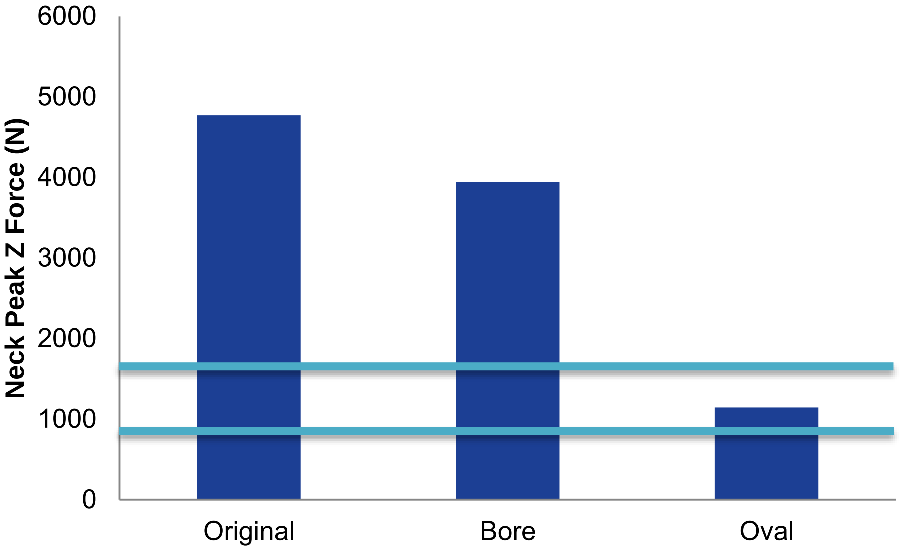

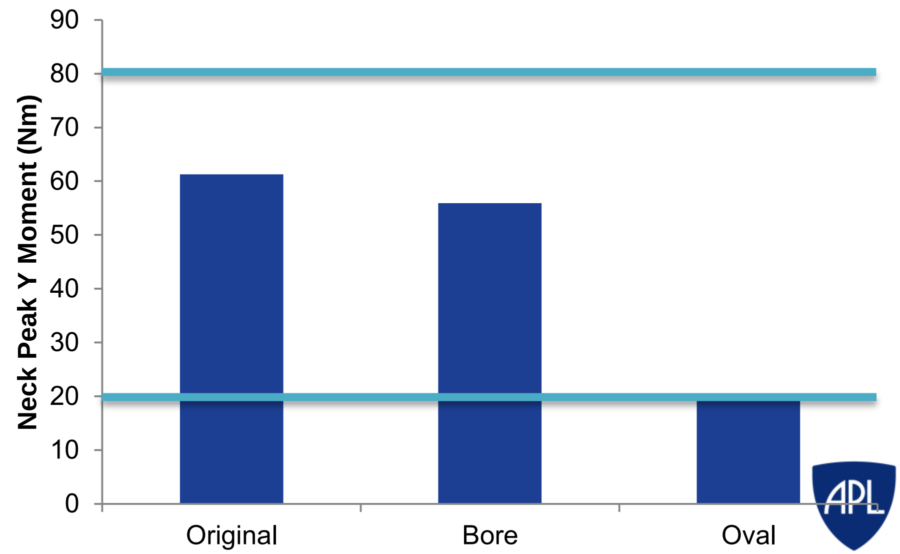

In comparison to PMHS 1 standard deviation response ranges, the oval design was the closest to peak force.

Both designs were reasonable for peak moment.

(At this point, interpret the results with caution.)

WIAMan Pelvis Finite Element Model Application and Testing

January 12, 2016

Cameron Bell[1], Adam Kareem[1], Garrett Kiessling[1], Kevin Lister[1], Horacio Nochetto[1], Corbin Robeck[1], Allen Shirley[1], Caleb Yow[1], Mostafiz Chowdhury[2]

[1]Corvid Technologies, [2]WIAMan EO

WIAMan Pelvis Design

- The pelvis is the **primary load path** for vertical seat loads resulting from under body blast (UBB)
  - Injuries sustained directly to the pelvis resulting from UBB events are not uncommon
- The TD WIAMan pelvis design represents a **major step forward in the amount of data** that can be captured within the pelvis as compared to the current seat occupant surrogate.
  - 6 Load Cells
  - 1 6DX Accelerometer
- Greatly **enhanced injury localization** potential

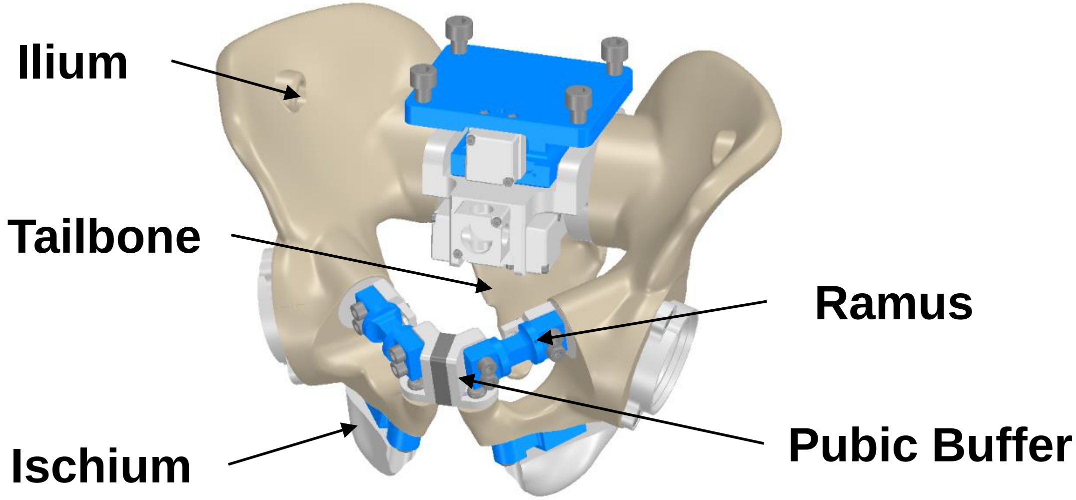

Preliminary Model: Structural

CAD

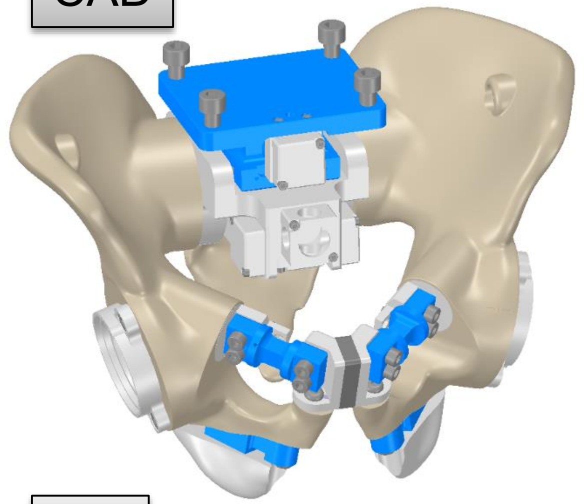

FE

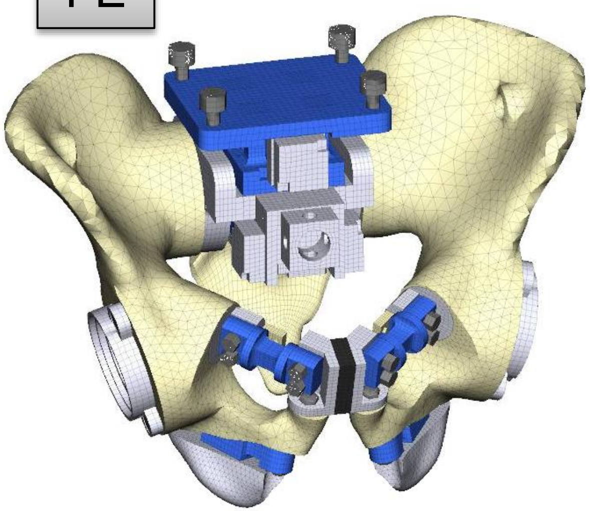

WIAMan Pelvis Mesh

- **High fidelity meshing** approach to support SoD
- **Explicit modeling** of bolts, inserts, joints, etc.

	Hex	Tet	Total
Elements	63374	116690	**180064**
Parts	56	4	**60**

Material	Constitutive Model
Metals	Johnson Cook
Polymer Tailbone	Johnson Cook (Lexan)
Polymer Ilium	Johnson Cook (Lexan)
Pubic Buffer	Blatz-Ko (Butyl Rubber 80A)

*Placeholder materials (prior to mat'l testing)

Category	Mass (kg)
Skeletal	2.31
Compliance	0.01
Data Acquisition	1.35
Hardware	0.32
Misc.	0.09
Total	**4.08**

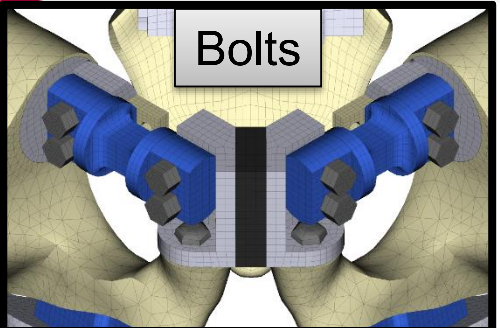

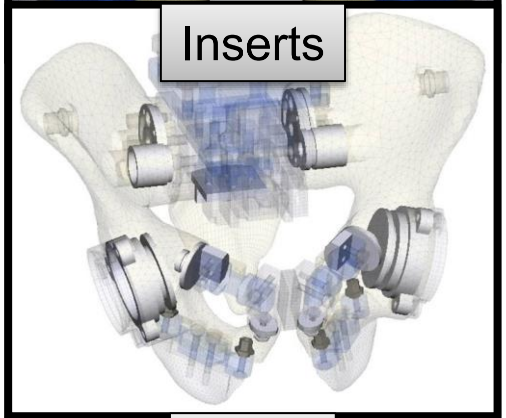

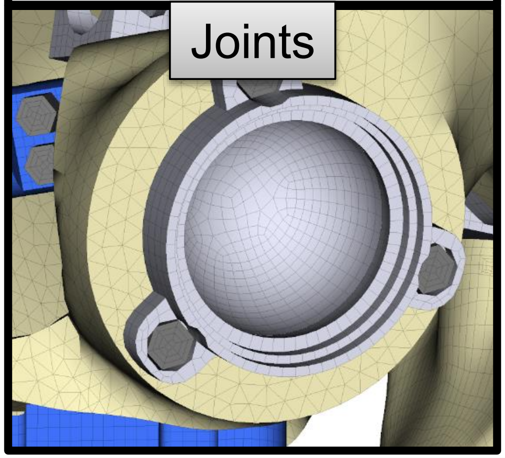

Preliminary Model: Flesh

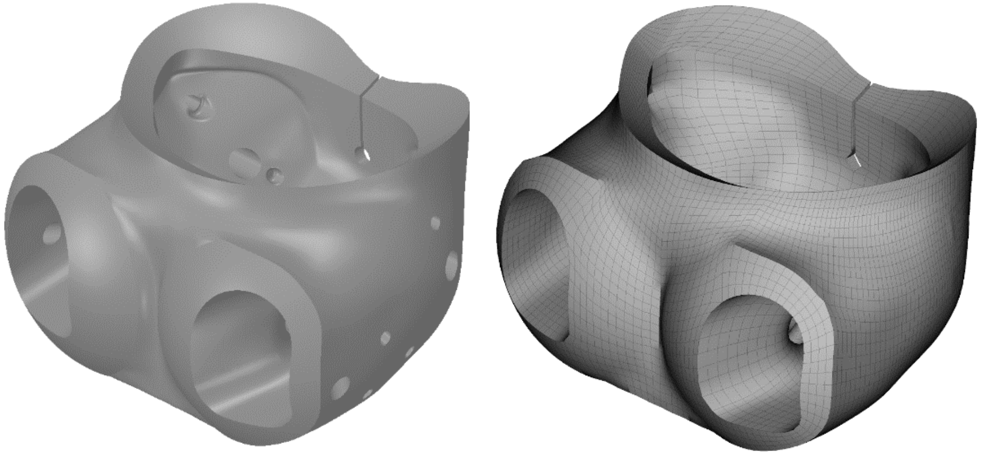

	Hex	Tet	Total
Elements	101774	116690	**218464**
Parts	57	4	**61**

Material	Constitutive Model
Pelvis Flesh	Blatz-Ko (Shore 32A estimate)

*Placeholder materials (prior to mat'l testing)

STEP 1: Pump

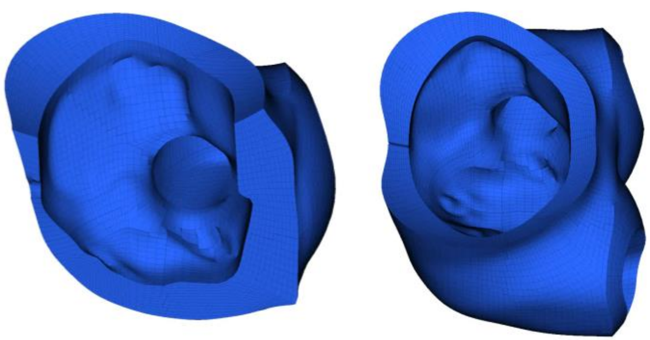

STEP 2: Release

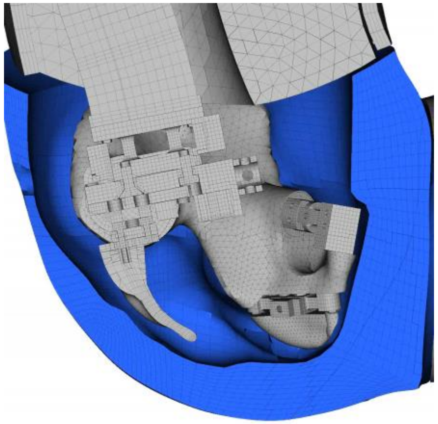

Category	Mass (kg)
Skeletal	2.31
Compliance	0.01
Data Acquisition	1.35
Hardware	0.32
Misc.	0.09
Flesh	9.98
Total	**14.06**

Good agreement between CAD and FE mass

WIAMan SoD: Whole Body

- VALTS vertical acceleration rig used for early analysis of WIAMan ATD
    - **Input:** 2,4,6,8,10m/s peak velocities over 4ms (scaled from 4m/s HIII test)
      Note: 10 m/s is known to be an extreme loading case
- SoD analysis highlighted all components that undergo permanent deformation

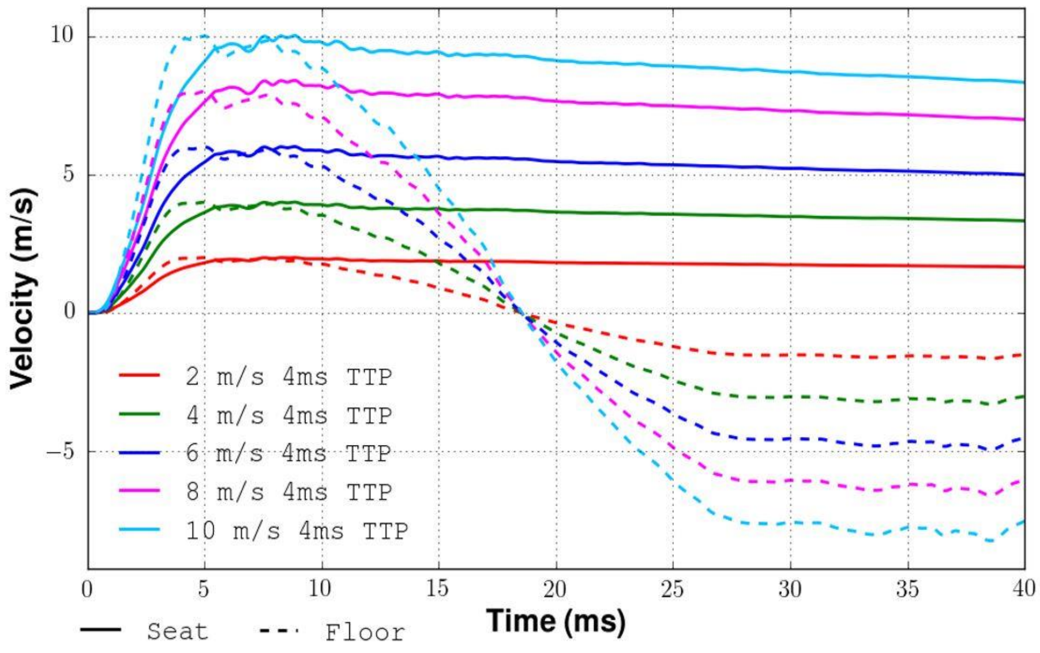

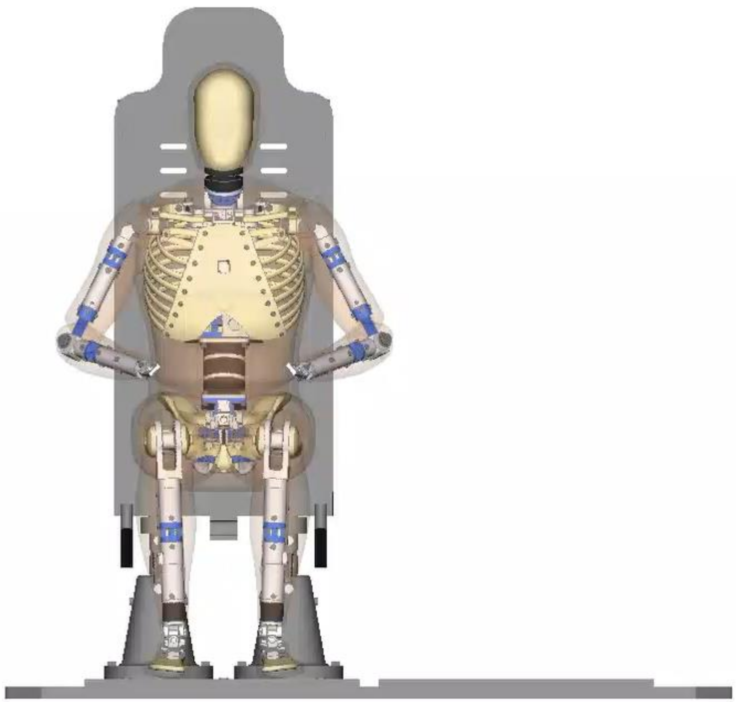

Pelvis SoD: WB VALTS

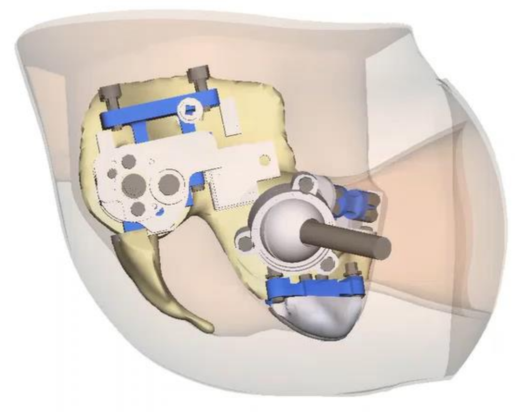

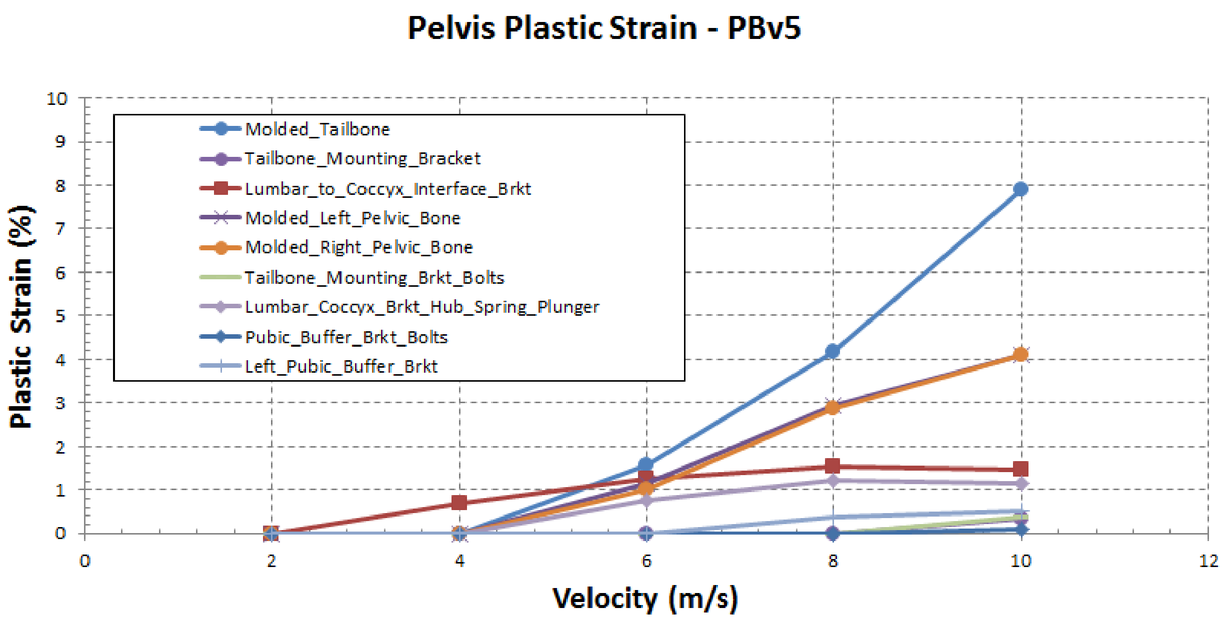

- **Plastic strain was tracked** on each component
- This approach establishes a **“weakest link” for the pelvis** component in a realistic loading, whole body loading environment
    - Intended to **inform TD design**

Pelvis SoD: VALTS 8 m/s

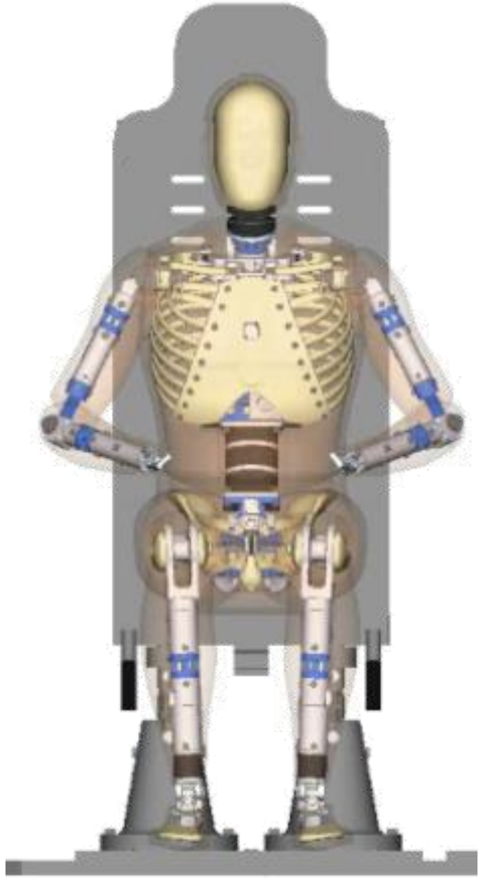

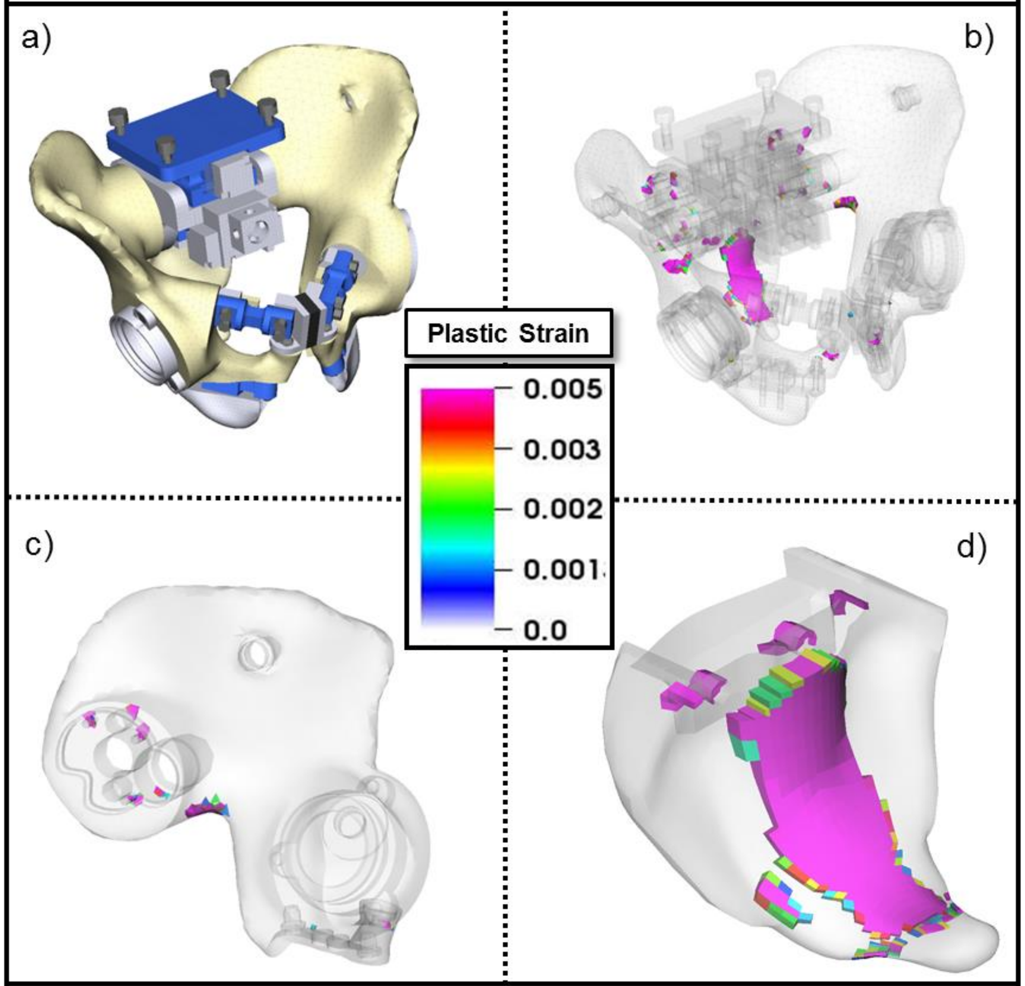

a) Pelvis assembly, b) Plastic deformation observed during 8m/s VALTS impact. All plastic deformation is observed in the c) pelvic bones and d) the molded tailbone

All permanent deformation limited to thermoplastic components

UVA Telemachus Model

- The pelvis rig modeling approach follows our standard for Velodyne FE model development
  - Bolted together with explicitly modeled hardware
  - Slider and rail system are explicitly modeled for upper and lower sleds, including friction
  - More accurately captures rig dynamics

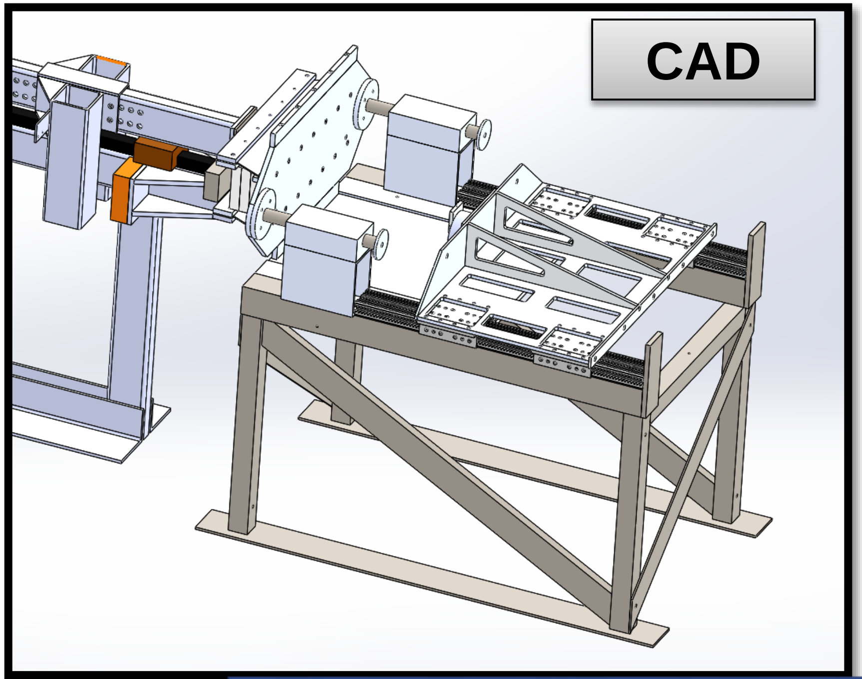

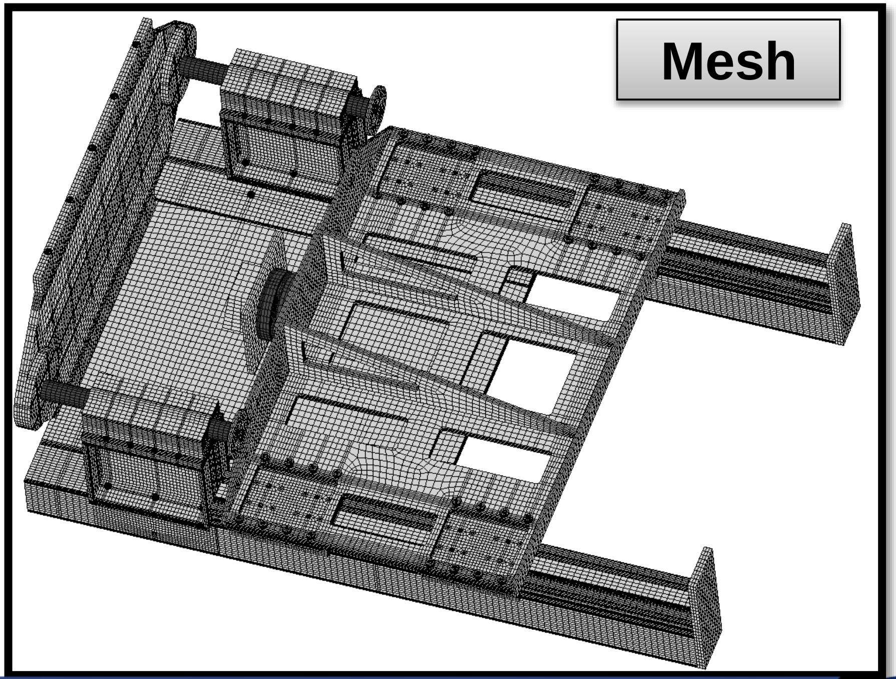

Employed same high fidelity modeling approach as the WIAMan Model

UVA Rig: Check-out

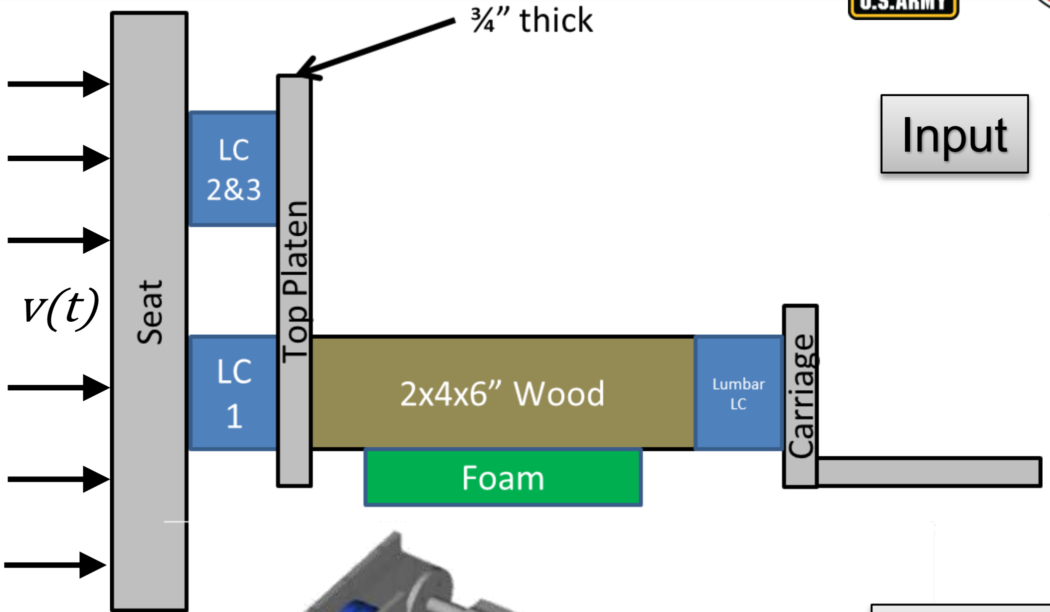

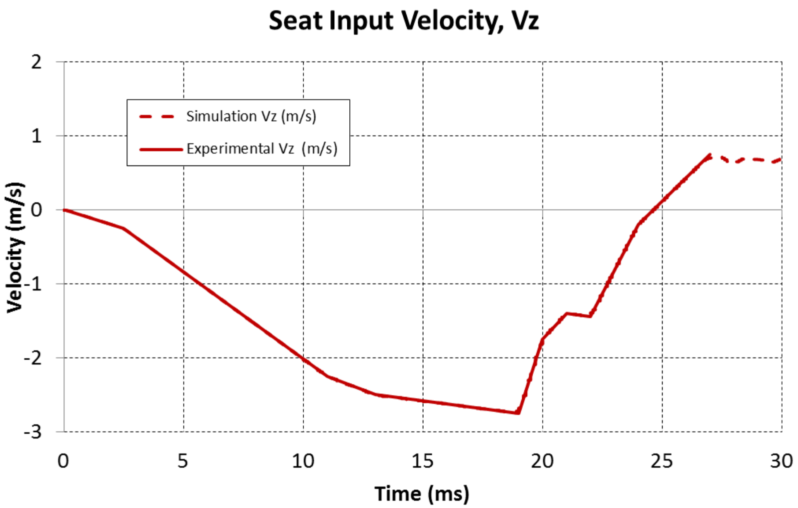

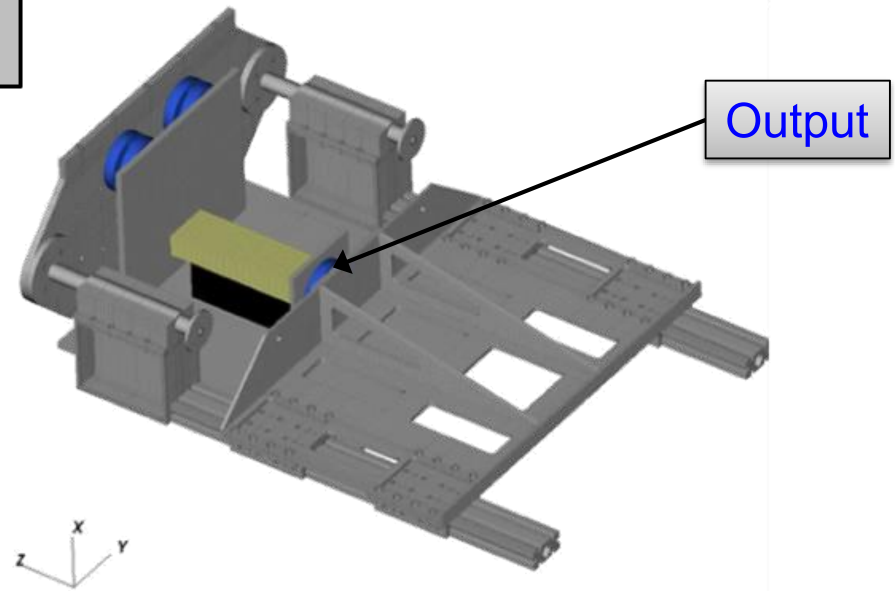

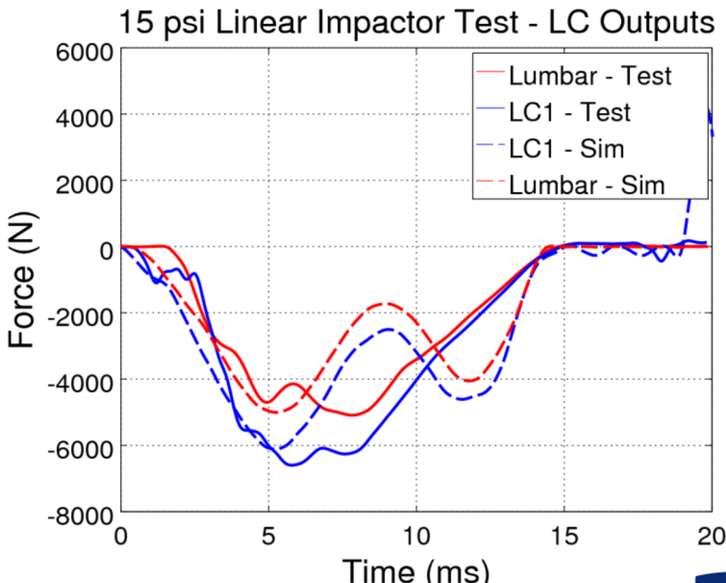

Models compares well to the “wood block” checkout case

Pelvis Material Characterization

- Material characterization testing carried out at Veryst Engineering including:
  - **Quasi-static:** Tension and Compression
  - **High Rate:** Tension and Compression
  - **Failure:** V-notch Shear or Type C Tear Strength

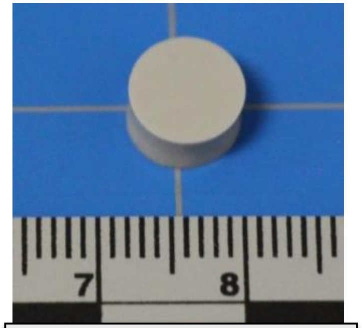

Pelvis Flesh

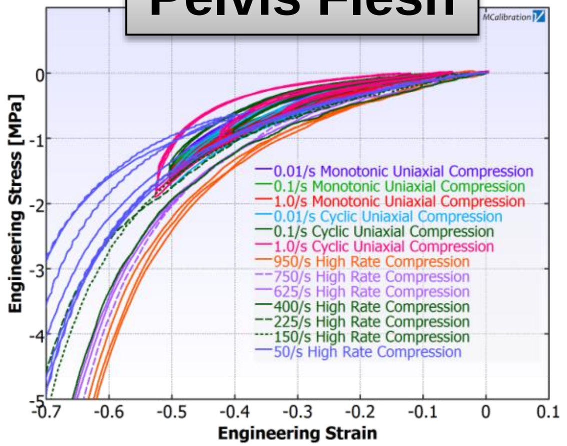

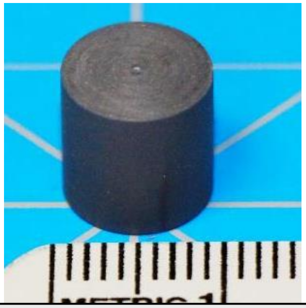

Ilium Bone

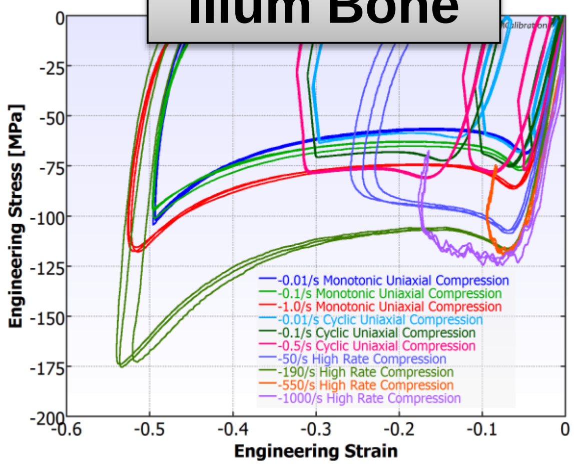

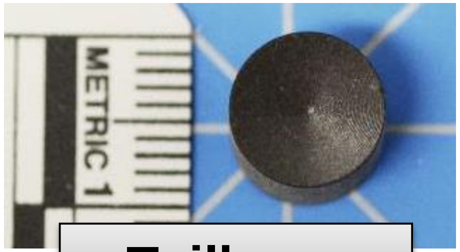

Tailbone

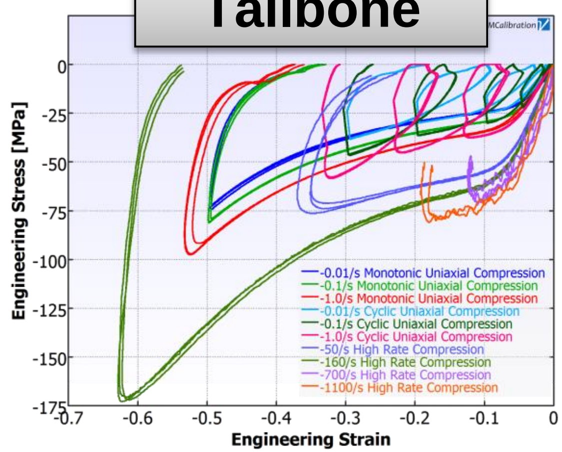

Material Parameterization

- 3 compliant materials fit to Ogden hyper-viscoelastic material constitutive model
- 2-step inverse FEA approach to parameterize Velodyne material models
  - i. **Hyperelastic** fit to quasi-static testing
  - ii. **Viscoelastic** fit to high-rate testing (w/ hyperelastic parameters locked)

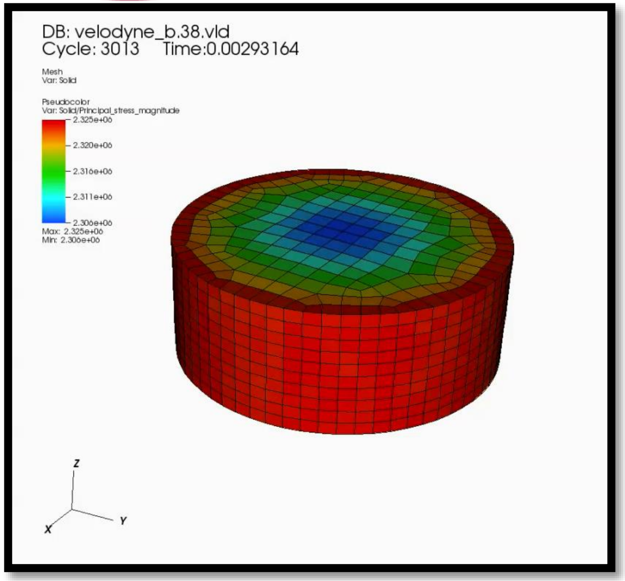

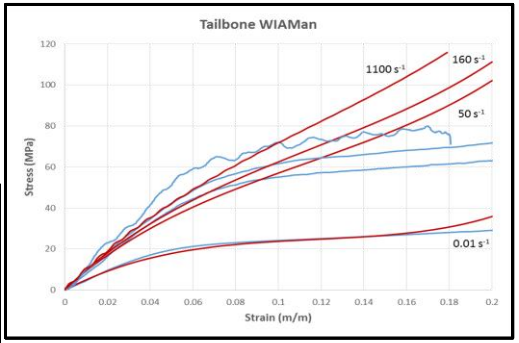

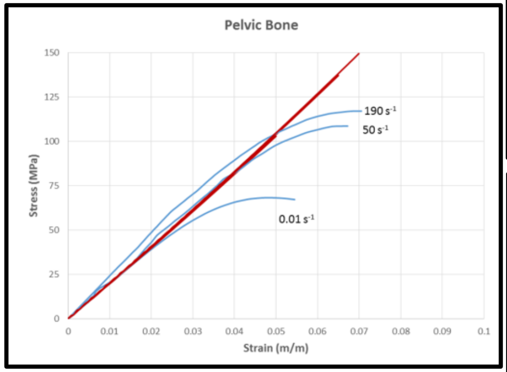

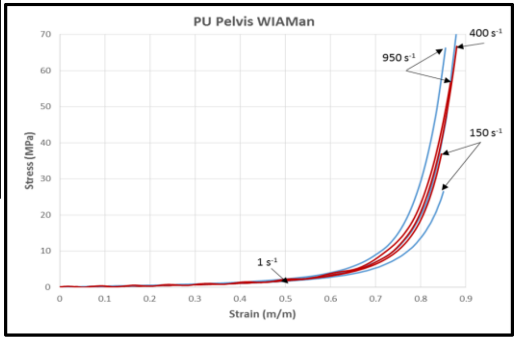

Hyperelastic:

$$\psi_{Ogden} = \sum_{m=1}^{n}\left\{\frac{\mu_m}{\alpha_m}\left[J^{-\alpha_m/3}\left(\lambda_1^{\alpha_m}+\lambda_2^{\alpha_m}+\lambda_3^{\alpha_m}-3\right)\right]\right\}+\frac{K}{2}(J-1)^2$$

Viscoelastic

$$\sigma_{visco} = \frac{1}{J}F\left\{\int_0^t \underbrace{\left[A_1 + A_2(I_2-3)\right]}_{\text{non-linear viscoelasticity}}\left[\sum_{i=1}^{6} G_i e^{-(t-\tau)/\tau_i}\right]\dot{E}(\tau)\,d\tau\right\}F^T$$

PV02 & PV12 Modeling

Post-test Model Validation

1. Seat input velocity profile from testing:
   - V1: Test 1.07 (2 m/s) – Fleshed
   - V2: Test 1.06 (3 m/s) – Fleshed
   - V1: Test 1.11 (2 m/s) – Defleshed
   - V2: Test 1.13 (3 m/s) – Defleshed

Material	Constitutive Model
Metals	Johnson Cook
Recast 6425 (Tailbone)	Ogden Visco
TC892 (Ilium)	Elastic-Plastic
Butyl Rubber 75A (Pubic Buffer)	Ogden Visco
Proflex 30 (Pelvis Flesh)	Ogden Visco

Higher-order fit in progress.

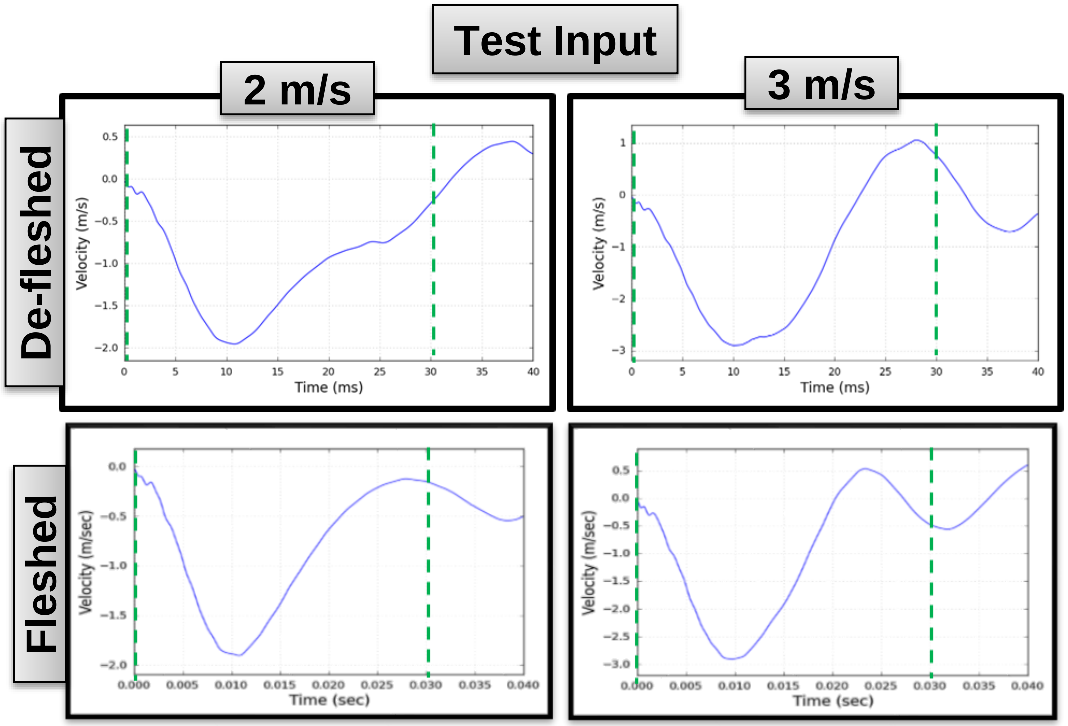

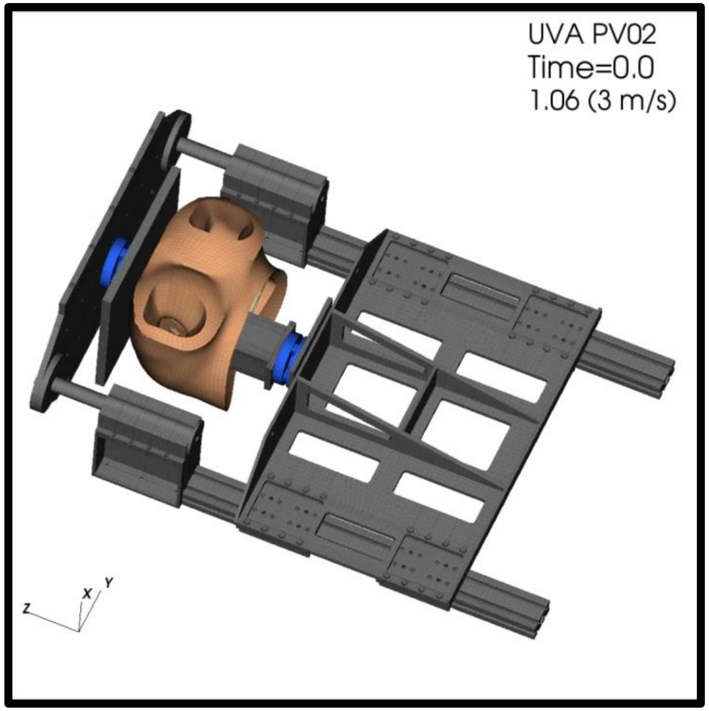

PV02: 2 m/s Comparison

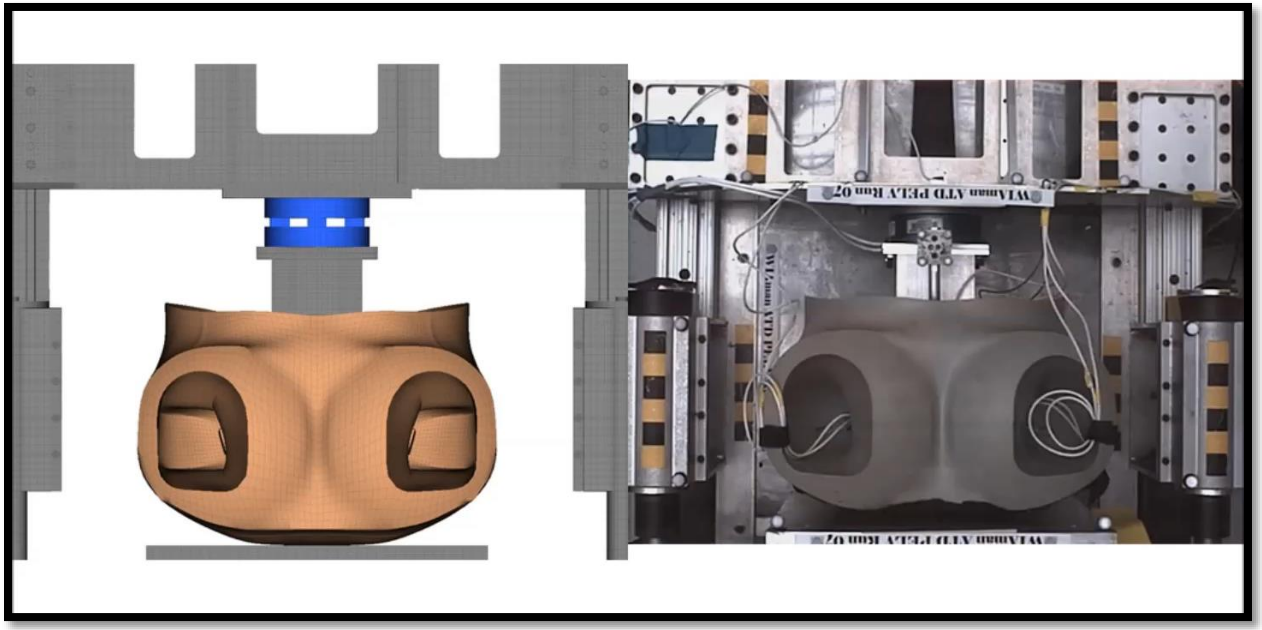

Upper Rig Load Cell

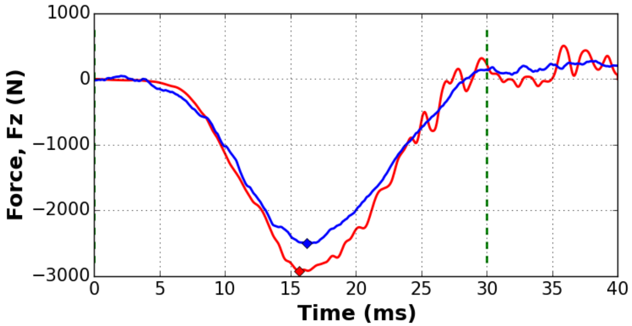

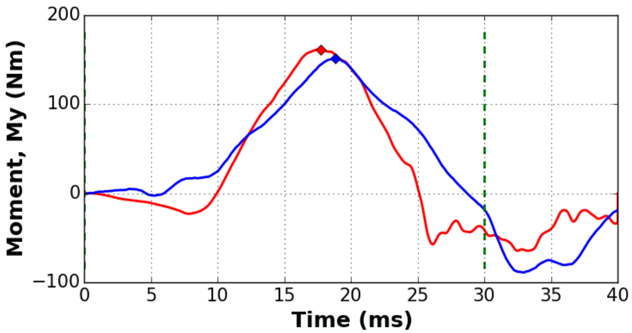

Seat Load Cell

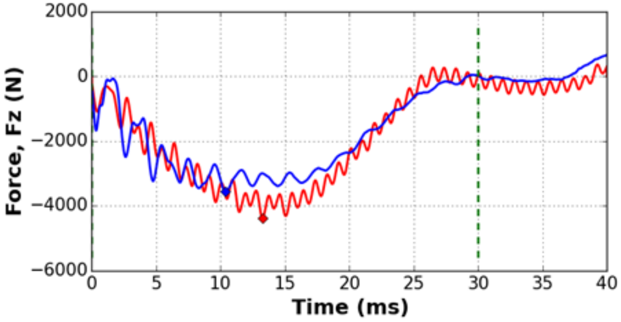

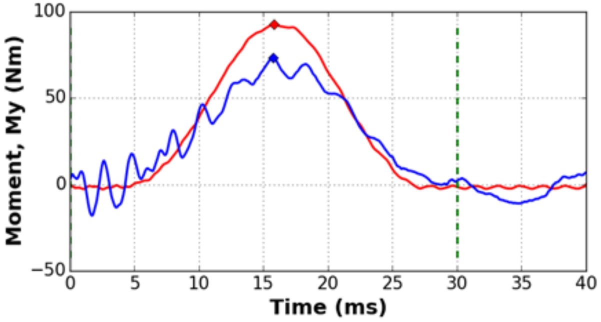

Test
Simulation

PV02: 3 m/s Comparison

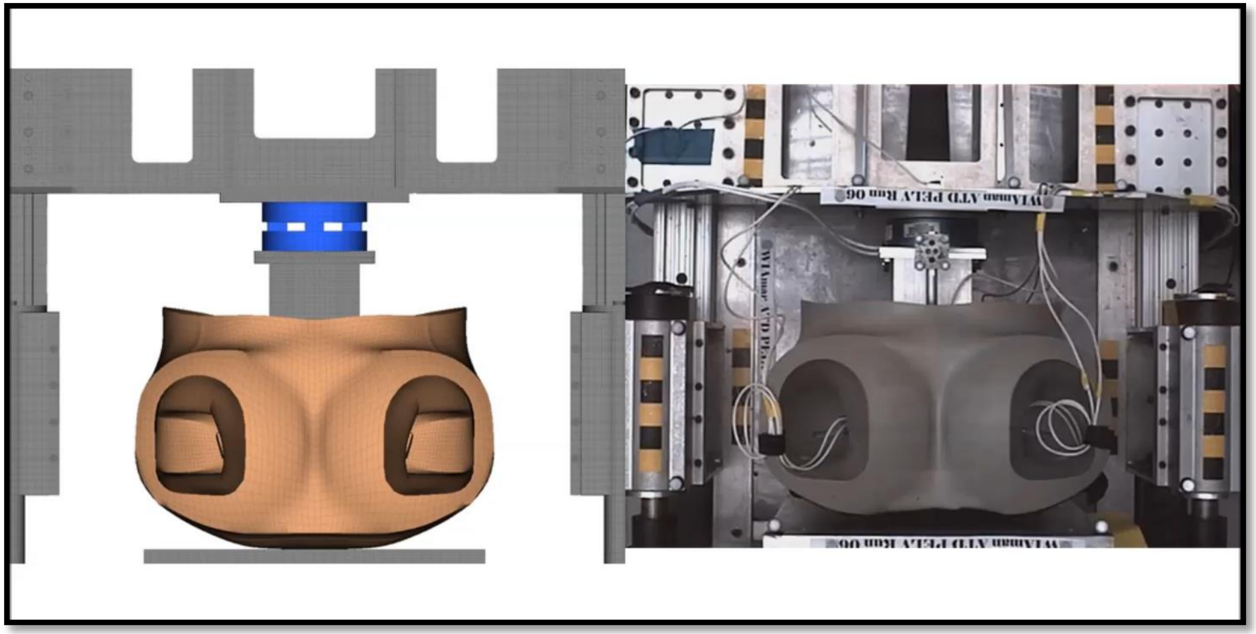

Upper Rig Load Cell

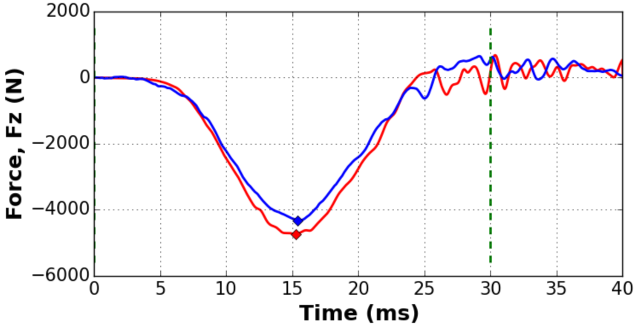

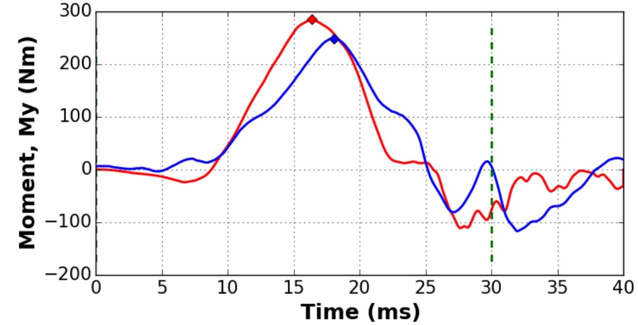

Seat Load Cell

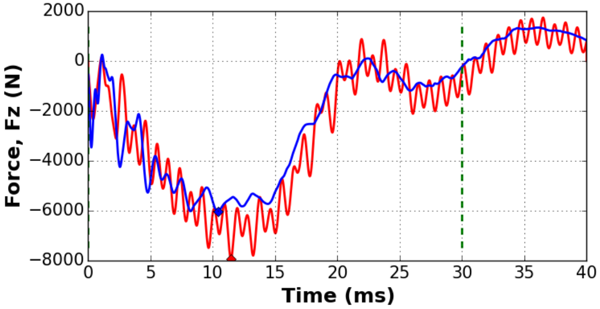

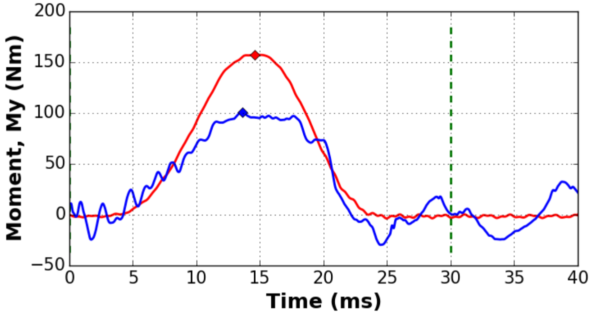

Test
Simulation

PV12: 2 m/s Comparison

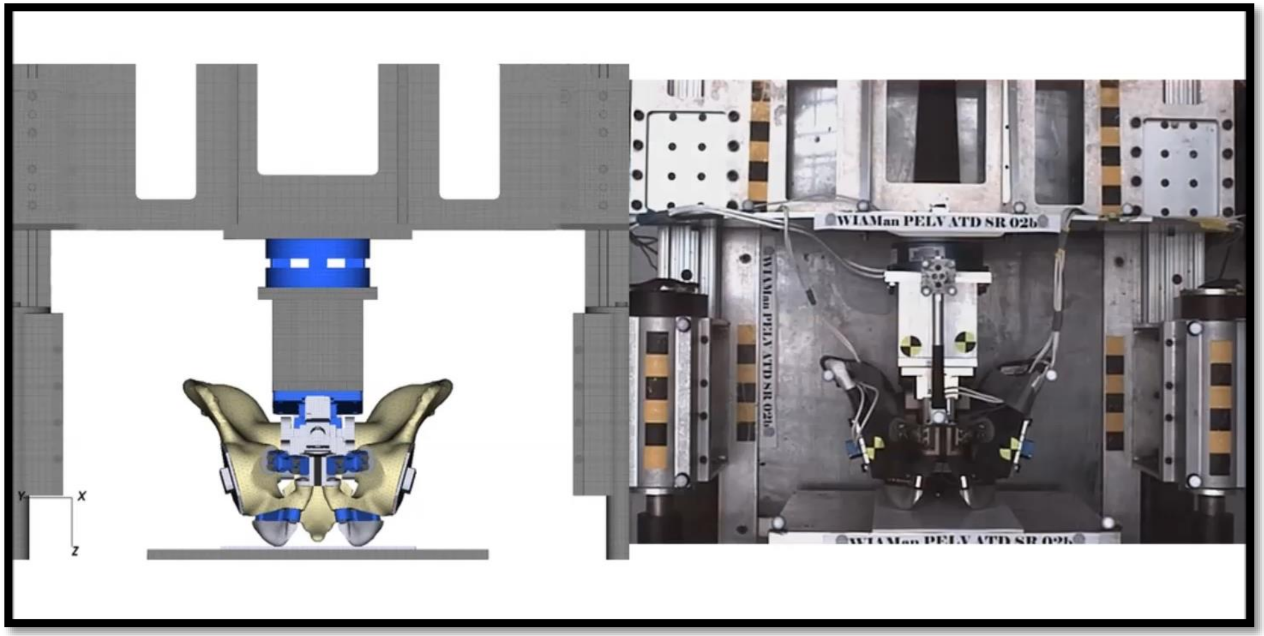

Upper Rig Load Cell

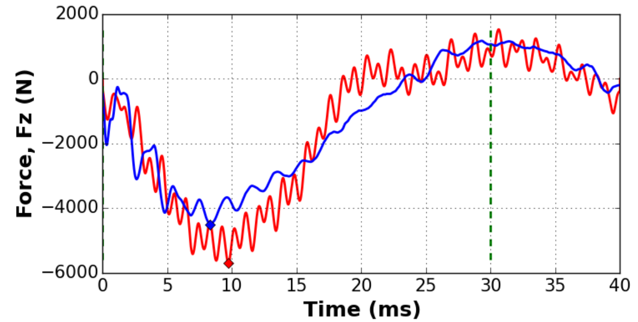

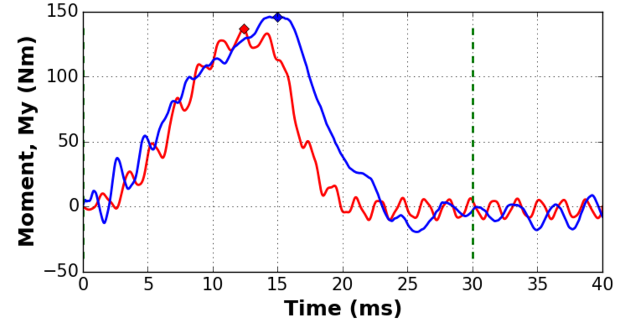

Seat Load Cell

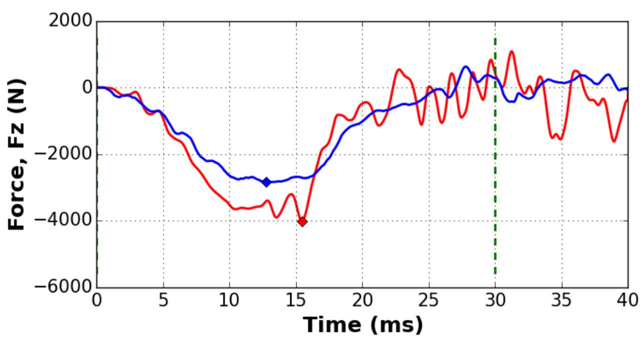

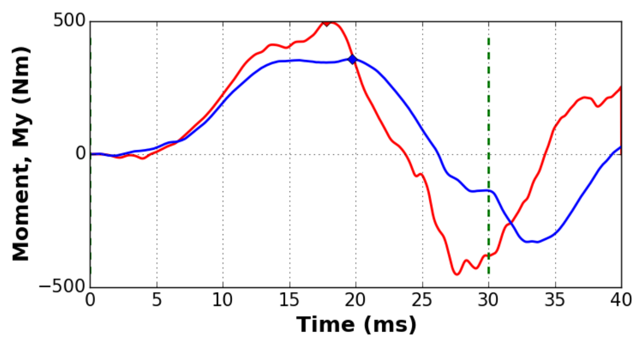

Test
Simulation

PV12: 3 m/s Comparison

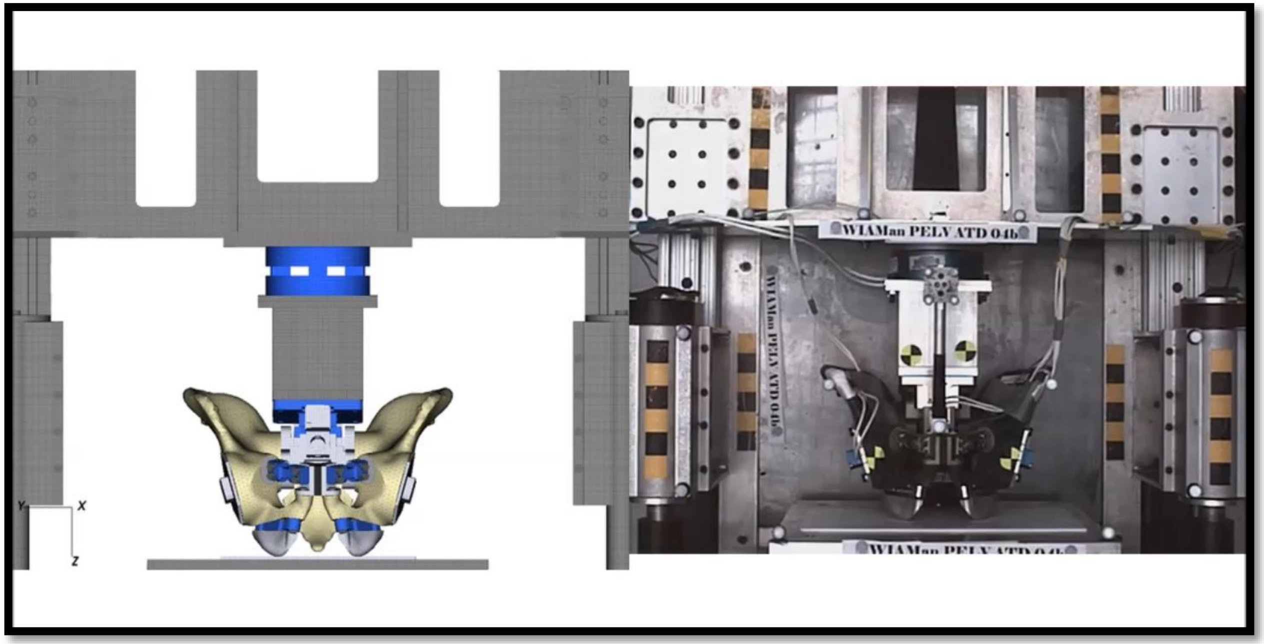

Upper Rig Load Cell

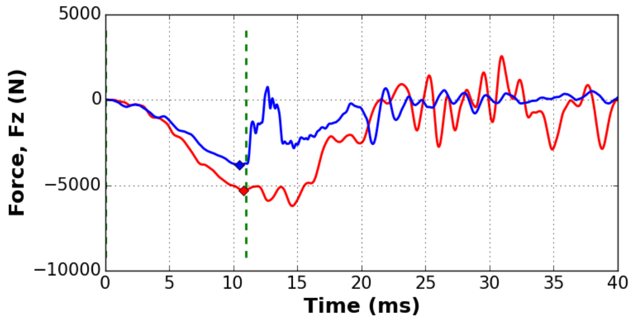

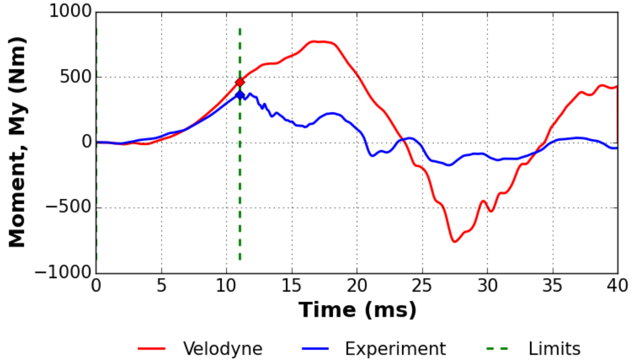

Seat Load Cell

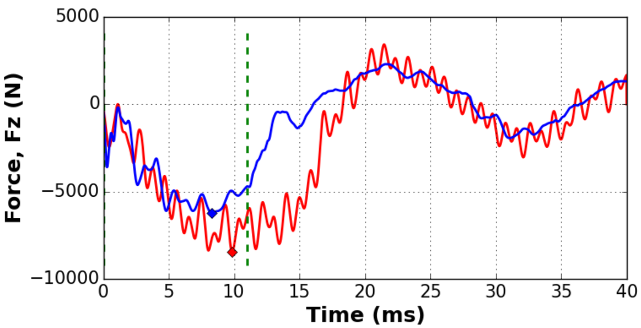

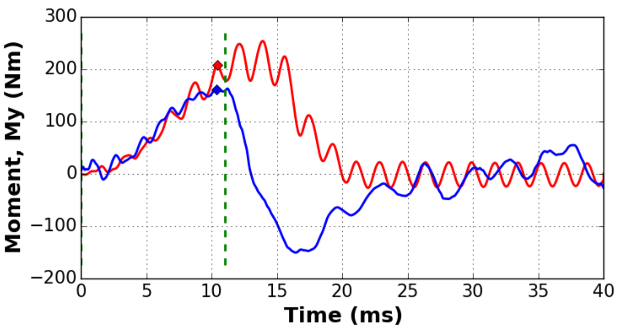

Test
Simulation

The model and test responses diverge post fracture

CORA Setup

- Default values recommended by CORA documentation
- **Fixed Time Interval:** 0 ms to 30 ms
  - Due to component failure during the 3m/s de-fleshed experiment, the analysis of this run is on the interval of 0 ms to 11 ms
- **Signal Weight Factors:**
  - Corridor Method: 0
  - Cross Correlation Method: 1
    - Size: 0.333
    - Shape: 0.333
    - Phase: 0.333
- **Overall Simulation Weight Factors:**
  - All **12 signals** are equally weighted

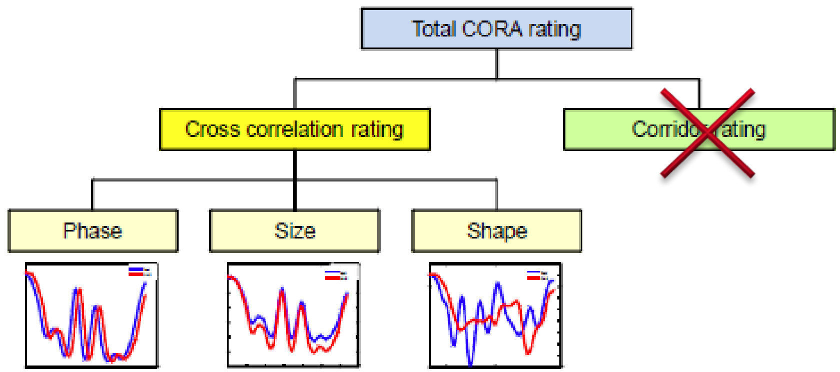

Measure	UVA Channel	Velodyne
Pelvis Compression (carriage to seat Z disp.), Dz	BP-60z	Disp. between upper and lower plates Dz
Right Hip Acceleration, Az	C0022	Sacrum 6DX Az
Right Hip Rotation Rate, Ry_dot	C0024	Right Hip Flange 6DX Ry_dot
Right Hip Rotation, Ry	Int(C0024)	Right Hip Flange int(6DX Ry_dot)
Sacrum Acceleration, Az	C0028	Sacrum 6DX Az
Upper Rig (Carriage) Accelerometer, Az	C0038	Upper Rig LC Az
Seat Load Cell Force, Fx	C0006	Seat LC Fx
Seat Load Cell Force, Fz	C0008	Seat LC Fz
Seat Load Cell Moment, My	C0010	Seat LC My
Upper Rig Load Cell Force, Fx	C0032	Upper Rig LC Fx
Upper Rig Load Cell Force, Fz	C0034	Upper Rig LC Fz
Upper Rig Load Cell Moment, My	C0036	Upper Rig Load Cell Moment, My

CORA Summary

2 m/s

Fleshed

Velocity	Abscissa	Shape	Magnitude	Phase	Total
1.07	Pevlis Compression, Dz	0.947	0.799	0.709	0.818
1.07	Right Hip Accel, Az	0.560	0.586	0.985	0.710
1.07	Right Hip Rotation Rate, Ry_dot	0.914	0.876	1.000	0.930
1.07	Right Hip Rotation, Ry	0.967	0.863	0.864	0.898
1.07	Sacrum Accel, Az	0.780	0.620	1.000	0.800
1.07	Upper Rig Accel, Az	0.928	0.561	0.991	0.827
1.07	Seat Load, Fx	0.816	0.902	0.936	0.885
1.07	Seat Load, Fz	0.911	0.806	0.955	0.891
1.07	Seat Moment, My	0.911	0.638	0.991	0.847
1.07	Upper Rig Force, Fx	0.535	0.325	0.812	0.557
1.07	Upper Rig Force, Fz	0.986	0.768	1.000	0.918
1.07	Upper Rig Moment, My	0.719	0.951	0.673	0.781
	Average (equal weighting all signals)	**0.831**	**0.725**	**0.910**	**0.822**

De-fleshed

Velocity	Abscissa	Shape	Magnitude	Phase	Total
1.11	Pevlis Compression, Dz	0.748	0.568	0.042	0.453
1.11	Right Hip Accel, Az	0.061	0.300	0.000	0.120
1.11	Right Hip Rotation Rate, Ry_dot	0.937	0.756	0.579	0.757
1.11	Right Hip Rotation, Ry	0.841	0.879	0.497	0.739
1.11	Sacrum Accel, Az	0.205	0.458	0.448	0.370
1.11	Upper Rig Accel, Az	0.514	0.481	0.888	0.628
1.11	Seat Load, Fx	0.444	0.457	0.527	0.476
1.11	Seat Load, Fz	0.818	0.755	0.945	0.839
1.11	Seat Moment, My	0.889	0.717	0.709	0.772
1.11	Upper Rig Force, Fx	0.539	0.376	0.061	0.325
1.11	Upper Rig Force, Fz	0.876	0.654	0.891	0.807
1.11	Upper Rig Moment, My	0.747	0.661	0.394	0.601
	Average (equal weighting all signals)	**0.635**	**0.589**	**0.498**	**0.574**

3 m/s

Fleshed

Velocity	Abscissa	Shape	Magnitude	Phase	Total
1.06	Pevlis Compression, Dz	0.925	0.982	0.761	0.889
1.06	Right Hip Accel, Az	0.387	0.465	0.609	0.487
1.06	Right Hip Rotation Rate, Ry_dot	0.807	0.988	0.927	0.907
1.06	Right Hip Rotation, Ry	0.983	0.840	0.927	0.917
1.06	Sacrum Accel, Az	0.719	0.609	0.776	0.701
1.06	Upper Rig Accel, Az	0.935	0.578	0.885	0.799
1.06	Seat Load, Fx	0.798	0.858	0.979	0.878
1.06	Seat Load, Fz	0.881	0.782	0.924	0.862
1.06	Seat Moment, My	0.881	0.500	1.000	0.794
1.06	Upper Rig Force, Fx	0.583	0.491	0.927	0.667
1.06	Upper Rig Force, Fz	0.969	0.796	1.000	0.922
1.06	Upper Rig Moment, My	0.764	0.751	0.779	0.765
	Average (equal weighting all signals)	**0.803**	**0.720**	**0.875**	**0.799**

De-fleshed

Velocity	Abscissa	Shape	Magnitude	Phase	Total
1.13	Pevlis Compression, Dz	1.000	0.759	0.810	0.856
1.13	Right Hip Accel, Az	0.310	0.323	0.455	0.363
1.13	Right Hip Rotation Rate, Ry_dot	0.999	0.947	0.868	0.938
1.13	Right Hip Rotation, Ry	0.999	0.998	0.802	0.933
1.13	Sacrum Accel, Az	0.843	0.354	0.149	0.449
1.13	Upper Rig Accel, Az	0.924	0.479	1.000	0.801
1.13	Seat Load, Fx	0.177	0.431	0.000	0.203
1.13	Seat Load, Fz	0.889	0.597	0.000	0.495
1.13	Seat Moment, My	0.954	0.806	0.678	0.813
1.13	Upper Rig Force, Fx	0.992	0.481	0.909	0.794
1.13	Upper Rig Force, Fz	0.992	0.528	1.000	0.840
1.13	Upper Rig Moment, My	0.991	0.237	0.000	0.409
	Average (equal weighting all signals)	**0.839**	**0.578**	**0.556**	**0.658**

Color coding corresponds to scale from 0 (worst) to 1 (best)

Good overall agreement between test and simulation

De-fleshed 3m/s Fracture

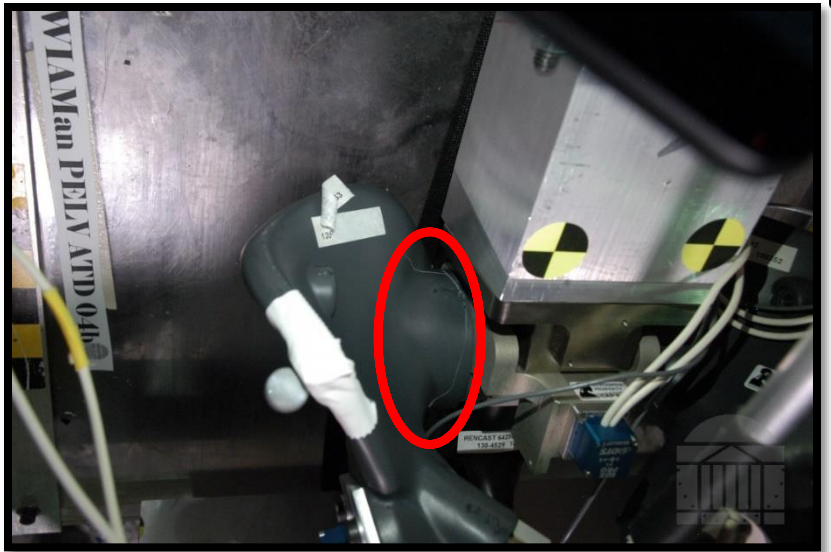

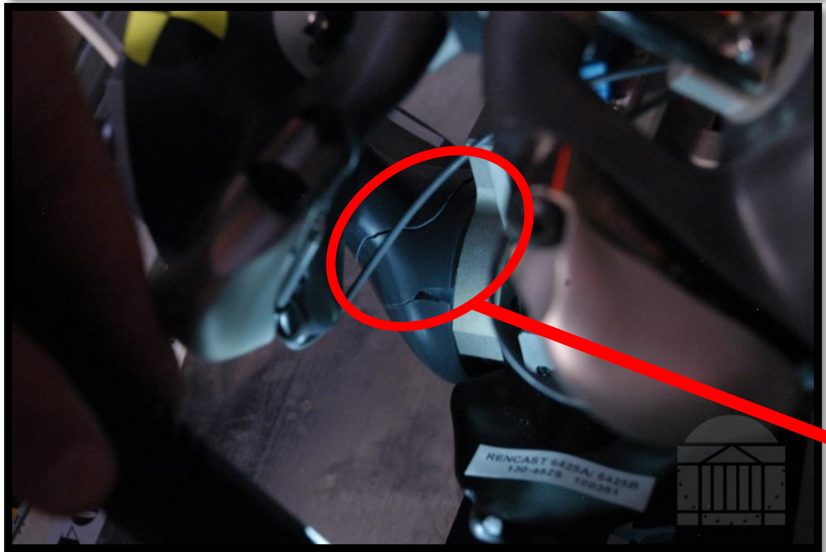

- Molded pelvic bone (ilium) fracture on 1st 3m/s de-fleshed impact
  - Brittle-type fracture
- Failure is believed to have initiated from the sciatic notch
  - M&S identified this as a high risk area from very early whole-body SoD simulations

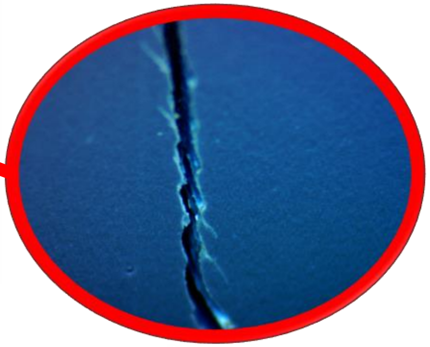

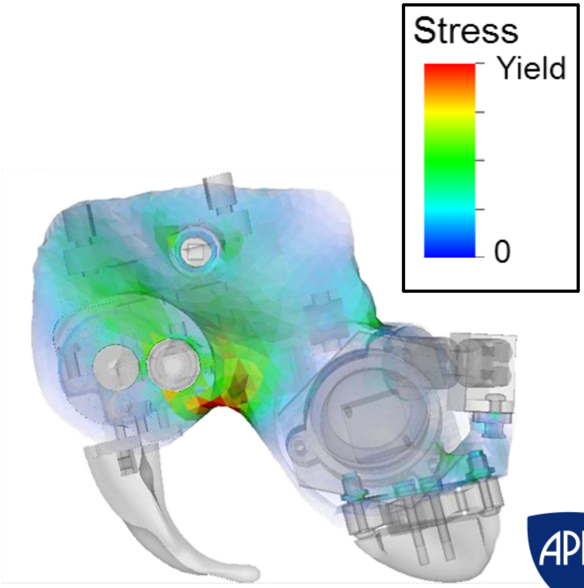

Ilium Material Swap

- The brittle fracture resulting from a de-fleshed 3m/s impact prompted **concern over ilium durability**
- WIAMan M&S was tasked to investigate **reducing risk of ilium fracture** in Tech. Demonstrator (TD) testing by swapping the ilium bone material (TC892) for the tailbone material (Rencast 892)
    - Ilium material is significantly more compliant with much greater ductility

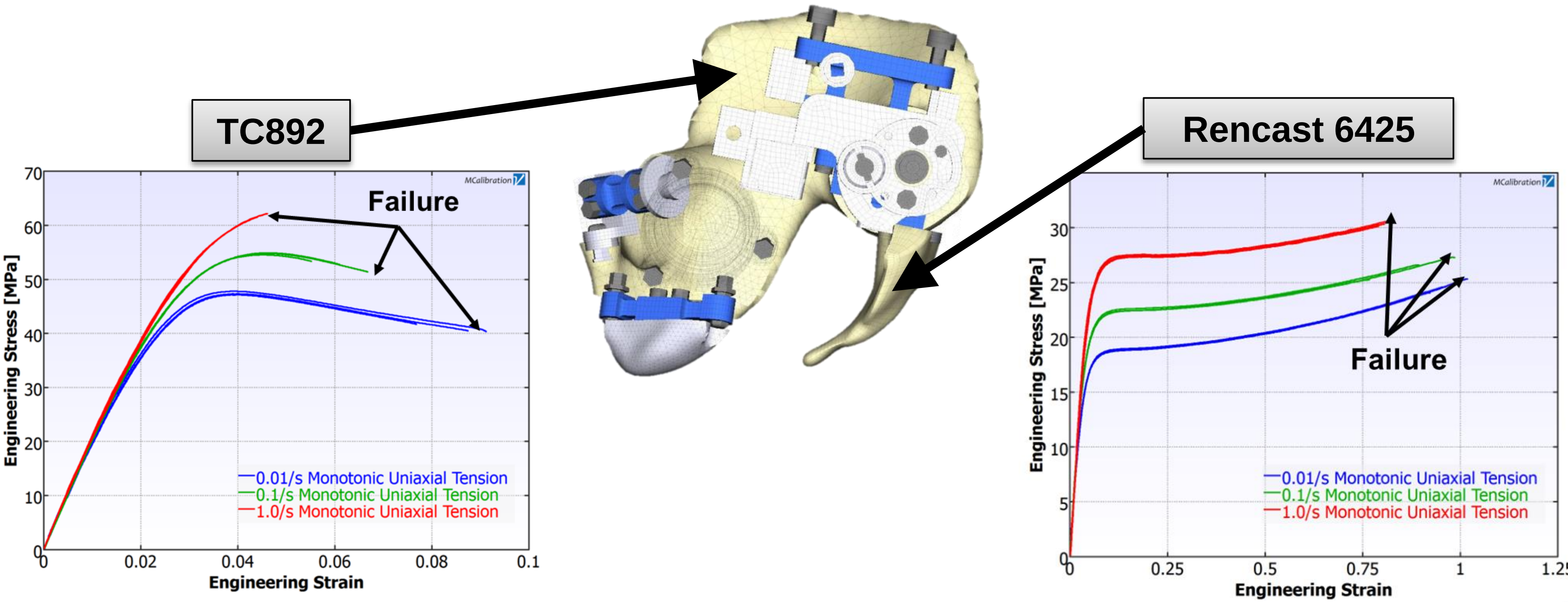

Source: Veryst, Material Characterization Report

Ilium Mat'l: Fleshed Case

Coccyx, Fz

Ischial Force

2 m/s

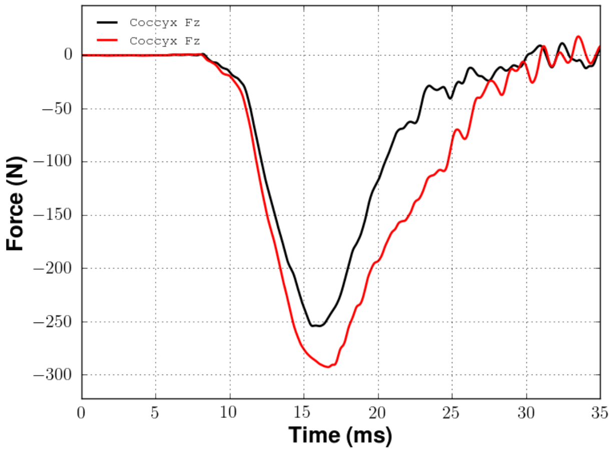

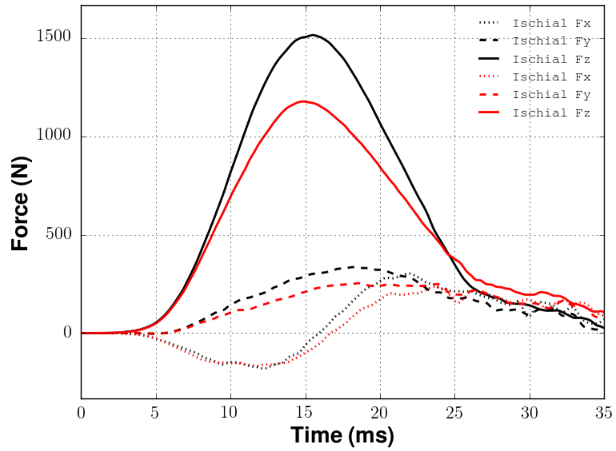

3 m/s

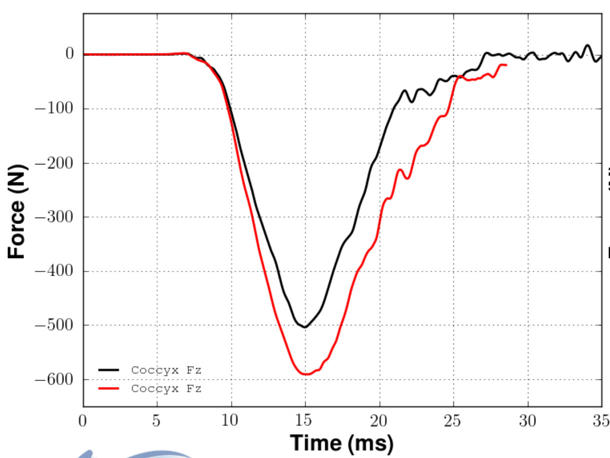

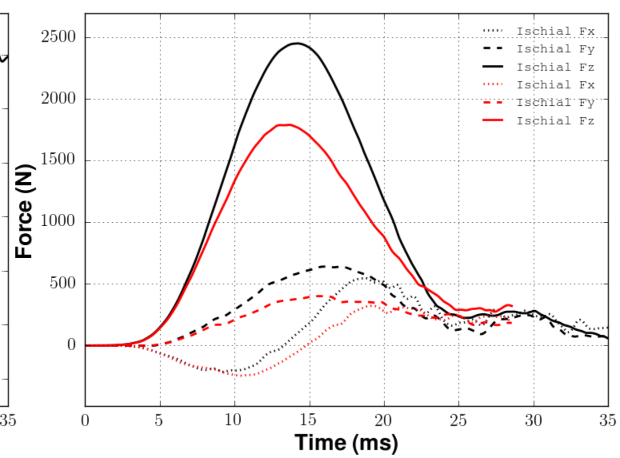

Observations:

- The ischial tuberosity forces are lower by ~25% in the Rencast case due to the more compliant pelvic bone material
- The coccyx load is increased by ~ 20% as it must support more load as the pelvic bone deflects further
- A comparable decrease in rig LC Fz is observed as well

Baseline
Alt (Rencast)

Ilium Mat'l: Fleshed 3m/s

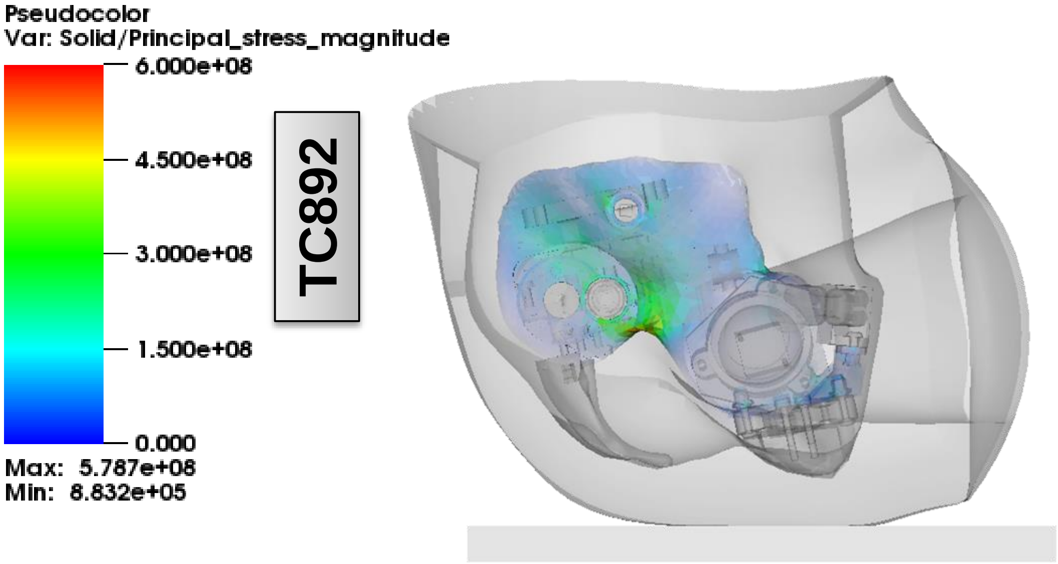

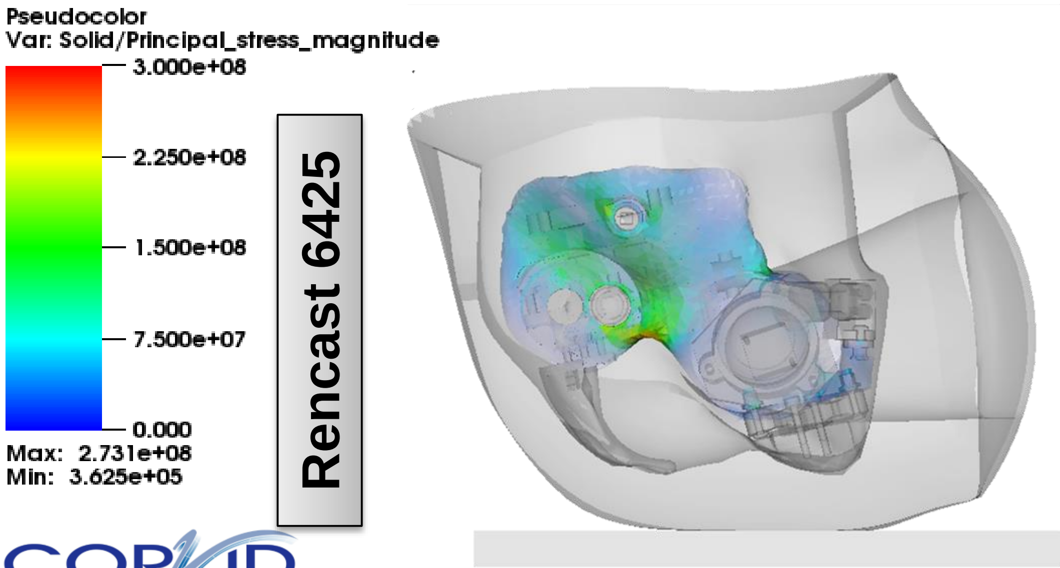

Observations:

1. In both cases, the sciatic notch stresses approach the material strength limits
   - **Note:** The max for each scale is set at the approx. material strength
2. Tailbone stresses are much lower than the pelvic bone in both cases and thus were not visualized
   - 3 m/s is only a moderate impact rate and excessive tailbone loading may become an issue at higher loading rates

Ilium Mat'l: Deflished Case

U.S. ARMY RDECOM ARL

Coccyx, Fz | **Ischial Force**

2 m/s

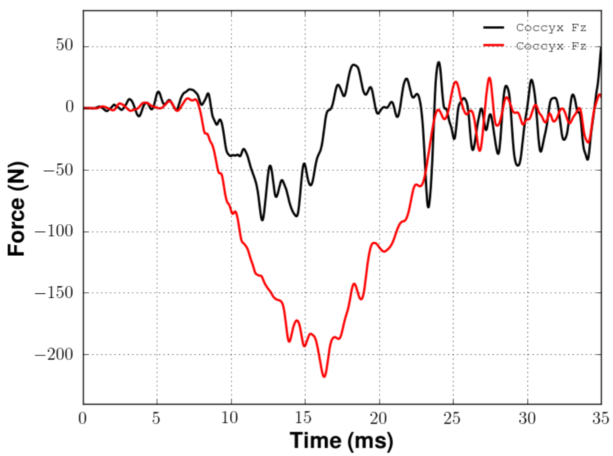

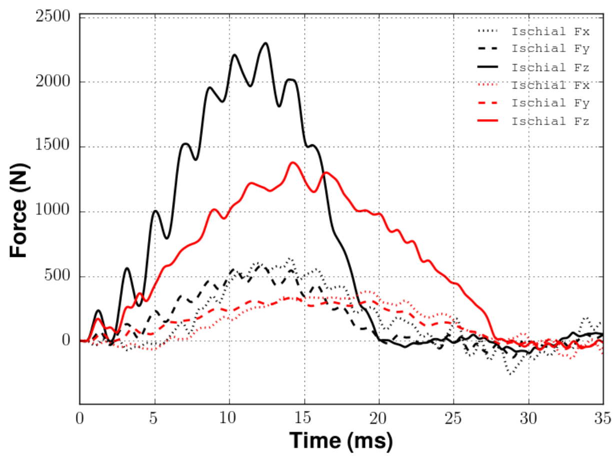

3 m/s

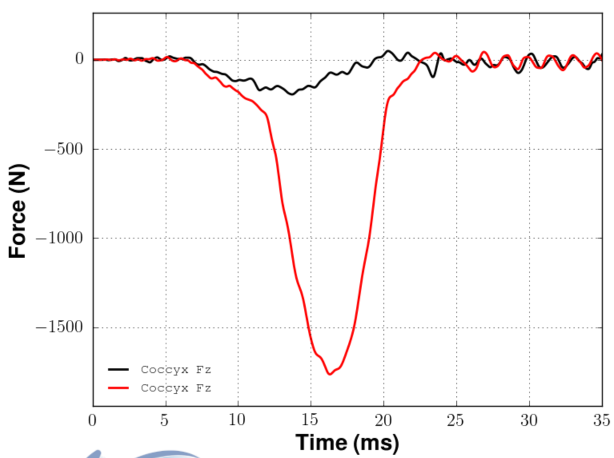

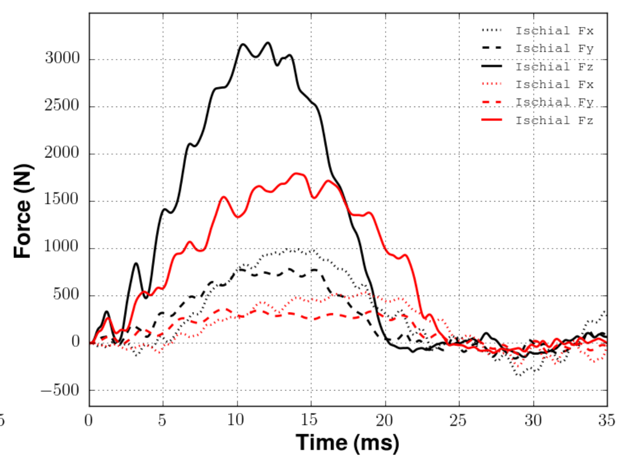

Observations:

- The ischial tuberosity forces are lower by ~50% in the Rencast case due to the more compliant pelvic bone material
- The coccyx load is increased by ~ 300-800% as it must support more load as the pelvic bone deflects further

Baseline
Alt (Rencast)

CORVID TECHNOLOGIES

APL

The Nation's Premier Laboratory for Land Forces

Ilium Mat'l: Defleshed 3m/s

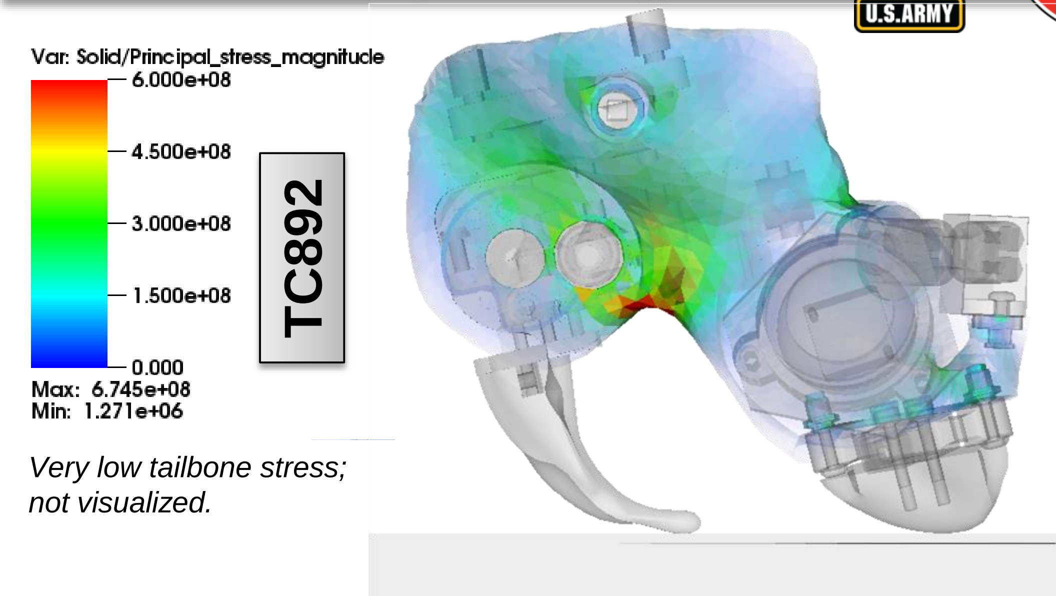

Very low tailbone stress; not visualized.

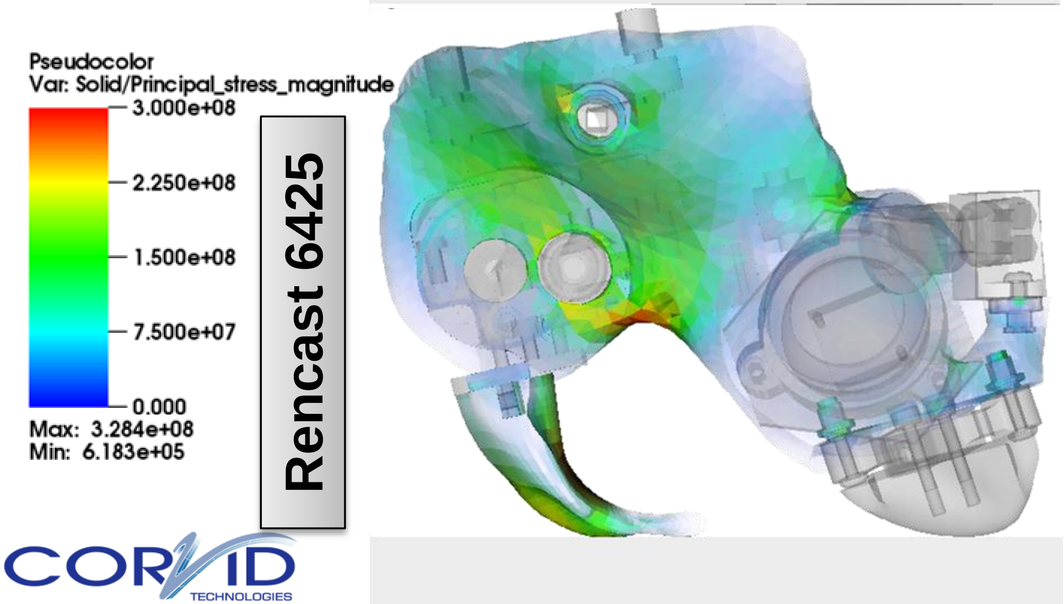

Observations:

1. In both cases, the sciatic notch stresses approach (if not exceed) the material strength limits
   - Note: The max for each scale is set at the approx. material strength
2. The tailbone deflects significantly further and is subjected to higher loads due to the increased rotation/ bending of the pelvic bone

Minimal performance improvement from material change

Ilium Mat'l: Conclusions

1. The alternate ilium material marginally **decreases pelvis loads**, while **increasing total deflection/rotation** under the UVA rig test conditions
2. Rencast 6425 material is **not believed to be an ideal solution** to solve the pelvic bone SoD concerns
   - "Failure" is still immanent in the 3m/s defleshed case
   - Only a minimal factor of safety in the 3m/s fleshed case
   - However if failure were achieved, it would be expected to occur much more gradually with significant plastic deformation due to the relatively high ductility of Rencast relative to TC892

WIAMan Pelvis: Summary and Path Forward

- M&S has demonstrated successful validation of the WAIMan Tech. Demonstrator pelvis model
- The UVA Telemachus rig testing is only one component of a full WIAMan pelvis performance assessment
  - Pelvis is **very rigidly mounted** with limited lumbar compliance and pelvis rotation
  - Early whole body simulations presented here indicate that the **tailbone may actually be the highest risk (weakest)** area from a SoD perspective in a whole body testing environment
- The extent of necessary Gen 1 modifications will be more clear after whole body testing
  - M&S work indicates that a material change to Rencast 6425 may not be a sufficient solution
  - Further M&S can investigate material strength needs in order to inform future material selection
  - M&S is capable of quickly investigating the effect of potential geometry changes or introduction of sacroiliac (SI) joint compliance if necessary

Modeling and Simulation of Lumbar Surrogate Response for UBB Loading

C. Pyles, M. Boyle, R. Armiger, J. Zhang,
F. Pintar, N. Yoganandan, J. Moore,
M. Chowdhury, A. Merkle

Lumbar Surrogates for UBB

- **Underbody blast (UBB) events result in devastating injuries to the seated occupant's lower extremities, pelvis, and lumbar spine**
  - Lumbar spine is principal structural anatomy linking upper and lower body
  - Of UBB casualties, 18% WIA, and 26% KIA sustain lumbar fractures
    - Alvarez, 2011
- **WIAMan Lumbar Spine Finite Element Model (FEM)**
  - Design tool
    - BRC comparisons
    - Strength of design (SOD)
    - Risk assessment and mitigation
- **Requires hierarchical model validation**
  - Material → Component (Lumbar) → System (Whole Body)

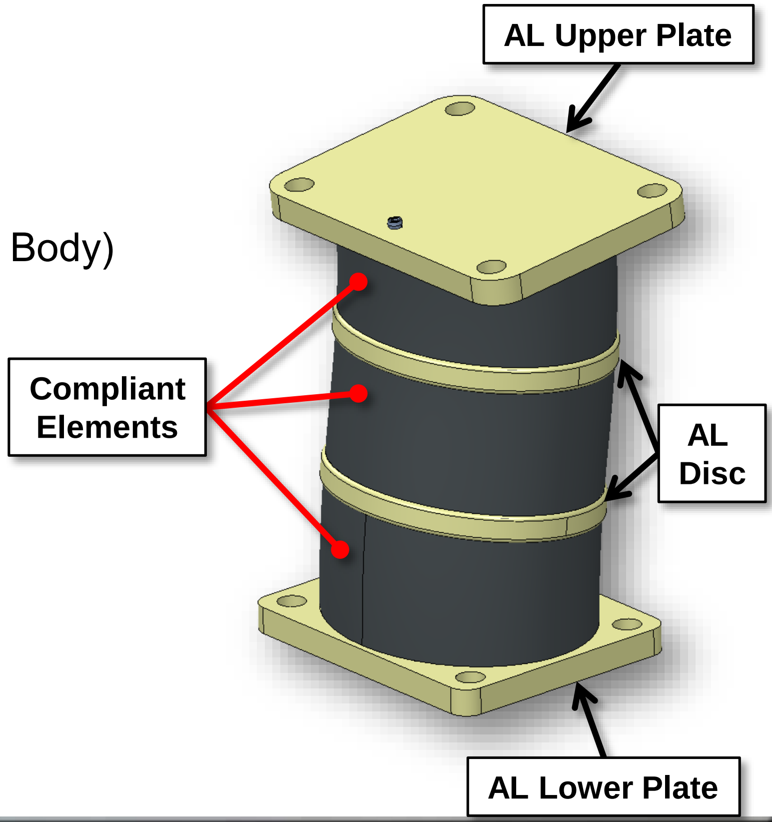

Model Development Process

U.S. ARMY RDECOM ARL APL CORVID TECHNOLOGIES

VertAc Rig Validation

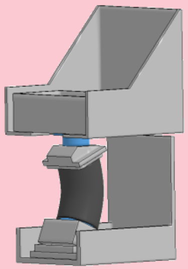

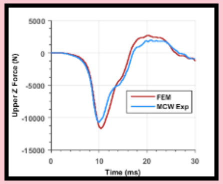

WIAMan Lumbar Spine FEM Developed

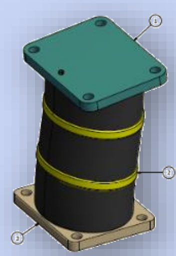

Polymer Characterization

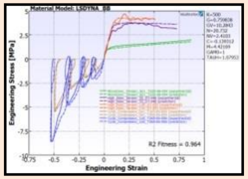

Lumbar Characterization and Validation

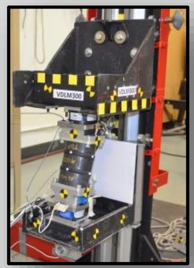

MEDICAL COLLEGE OF WISCONSIN

Design Analysis

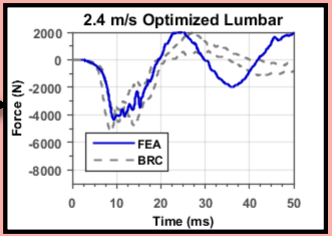

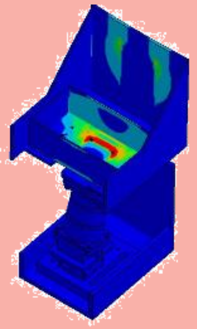

Whole Body Integration

VertAc FEM Validation

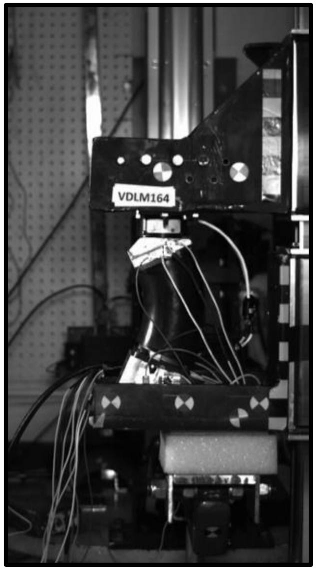

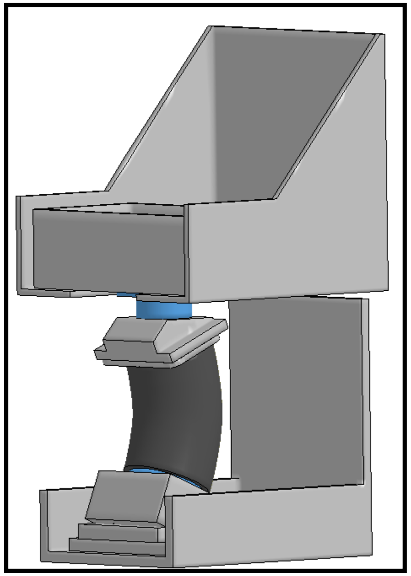

MEDICAL COLLEGE OF WISCONSIN

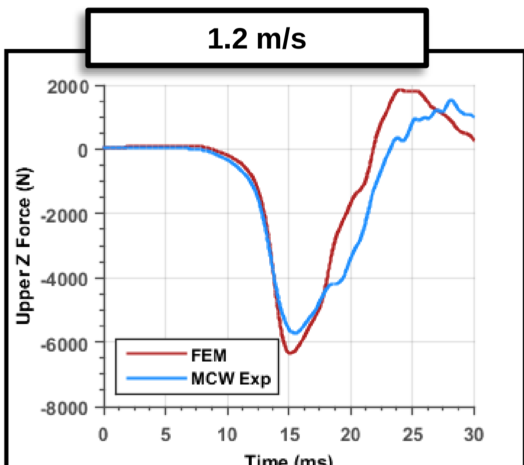

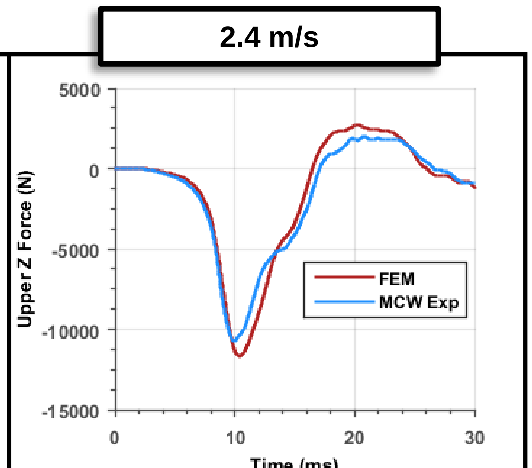

- **VertAc FEM:** Developed from MCW CAD and physical measurements
- **Hybrid-III Lumbar FEM**: Open-source LSTC model
  - Polymer material updated to reflect 85 Shore A hardness
- **Validation metric:**
  - Transmitted axial force compared to experiments at 1.2 m/s and 2.4 m.s
  - CORA scores calculated
    - See appendix for weights

	L1 Force (+Z) CORA Score
1.2 m/s	0.862
2.4 m/s	0.924

Validation of VertAc test system builds confidence in predictions

BR75A Constitutive Model

- **Bergstrom-Boyce material model**
  - Viscoelasticity physically accounted for based on polymer chain entanglement
  - Produced best fits across variety of loading conditions

- **Optimized using MCalibrate (Veryst)**
  - Single element loading
  - Parameter fitting bases on least squares regression

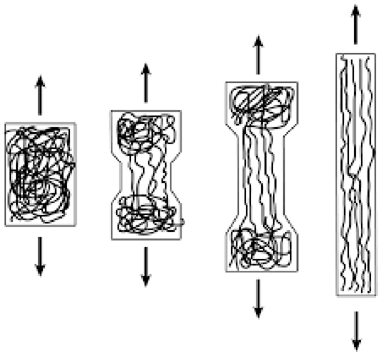

MCalibrate Model Fit

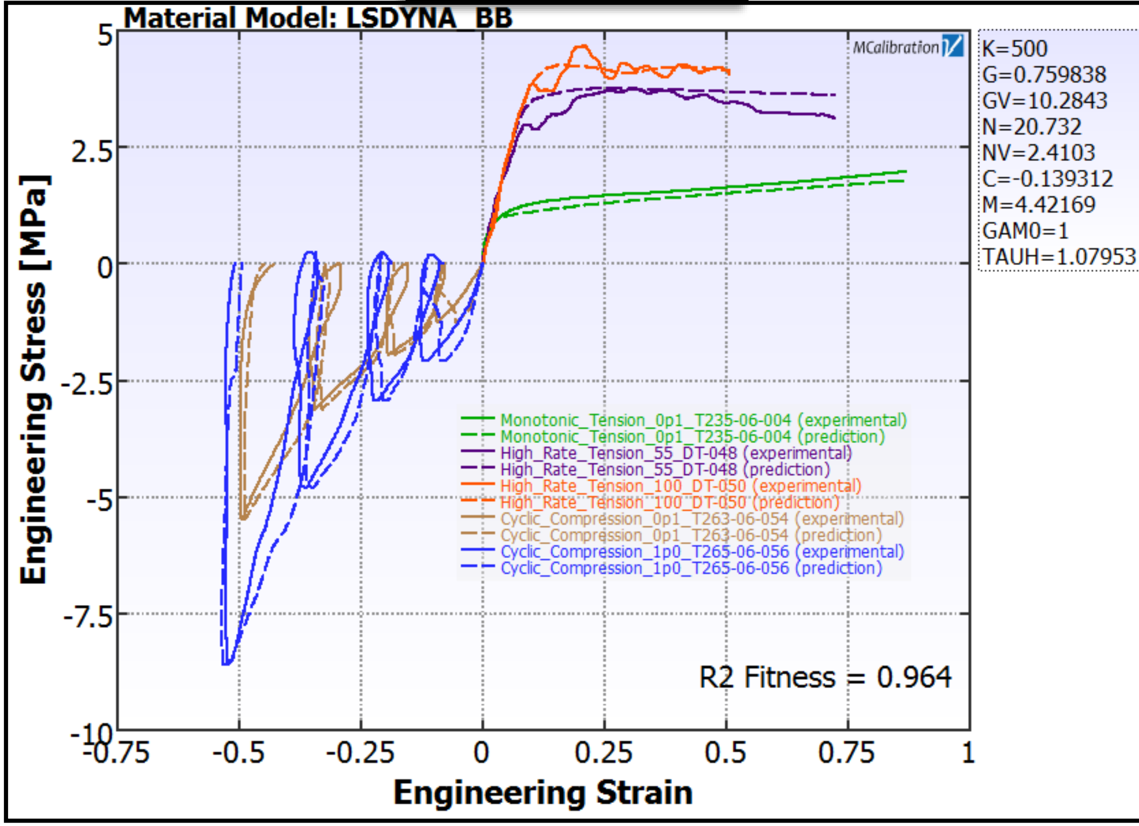

Optimization at material level allows for un-trained validation at component level

VertAc Setup

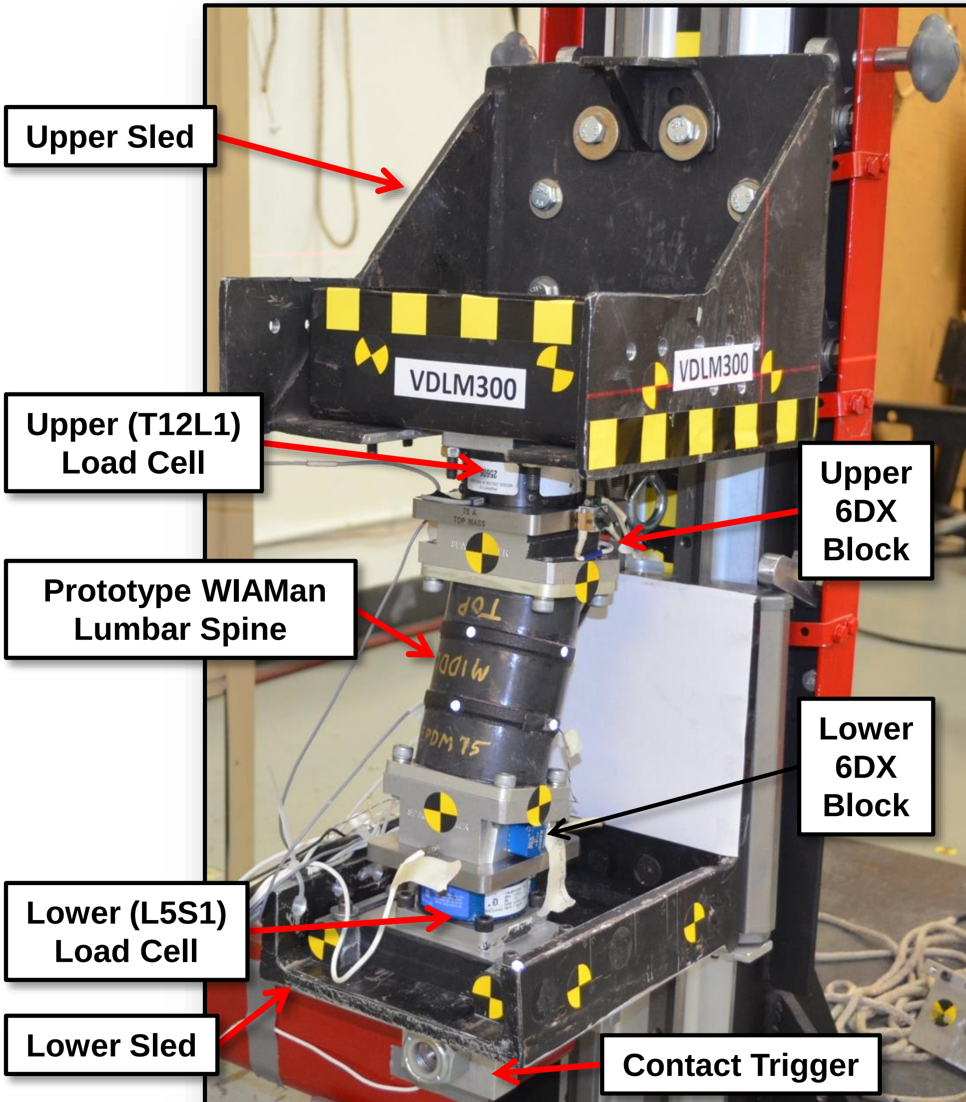

V = 2.4 m/s

V = 6.0 m/s

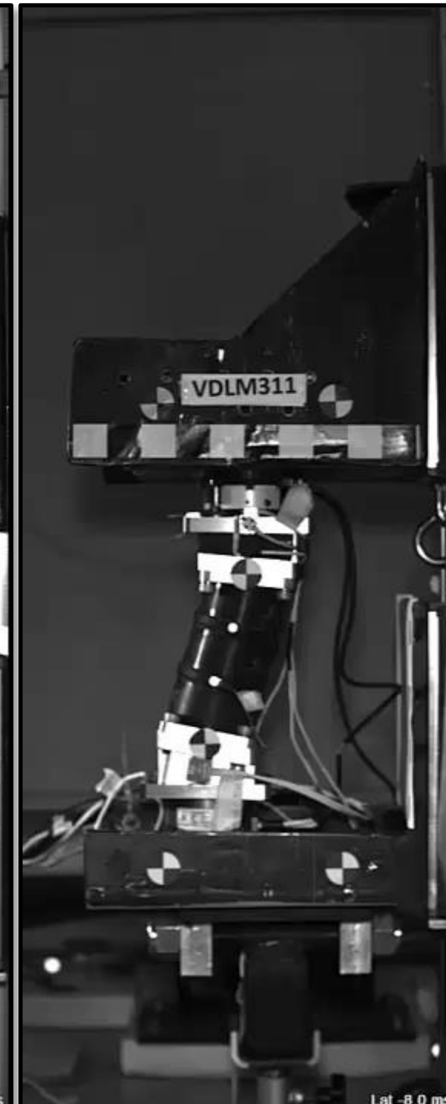

WIAMan Lumbar FEM

- **FEA Code:** LS-DYNA
- **Element Count:** 210,293
- **Element Formulation:** Hexahedral
- **Constitutive Models:**
  - Metals: Johnson-Cook
  - Molded Rubber: Bergstrom-Boyce
- **Boundary Conditions:**
  - Prescribed velocity applied to lower sled
  - Posterior carriage bearings constrained to slide vertically
- **Outputs:**
  - Forces/Moments: Load cell cross-sections
  - Nodal Accelerations: Constrained-interpolation method at 6DX blocks
- **Post-processing**
  - CFC 600 filter for forces and moments
  - CFC 1000 filter for accelerations
  - Force and moment transformations to joint centers (PMHS comparisons only)

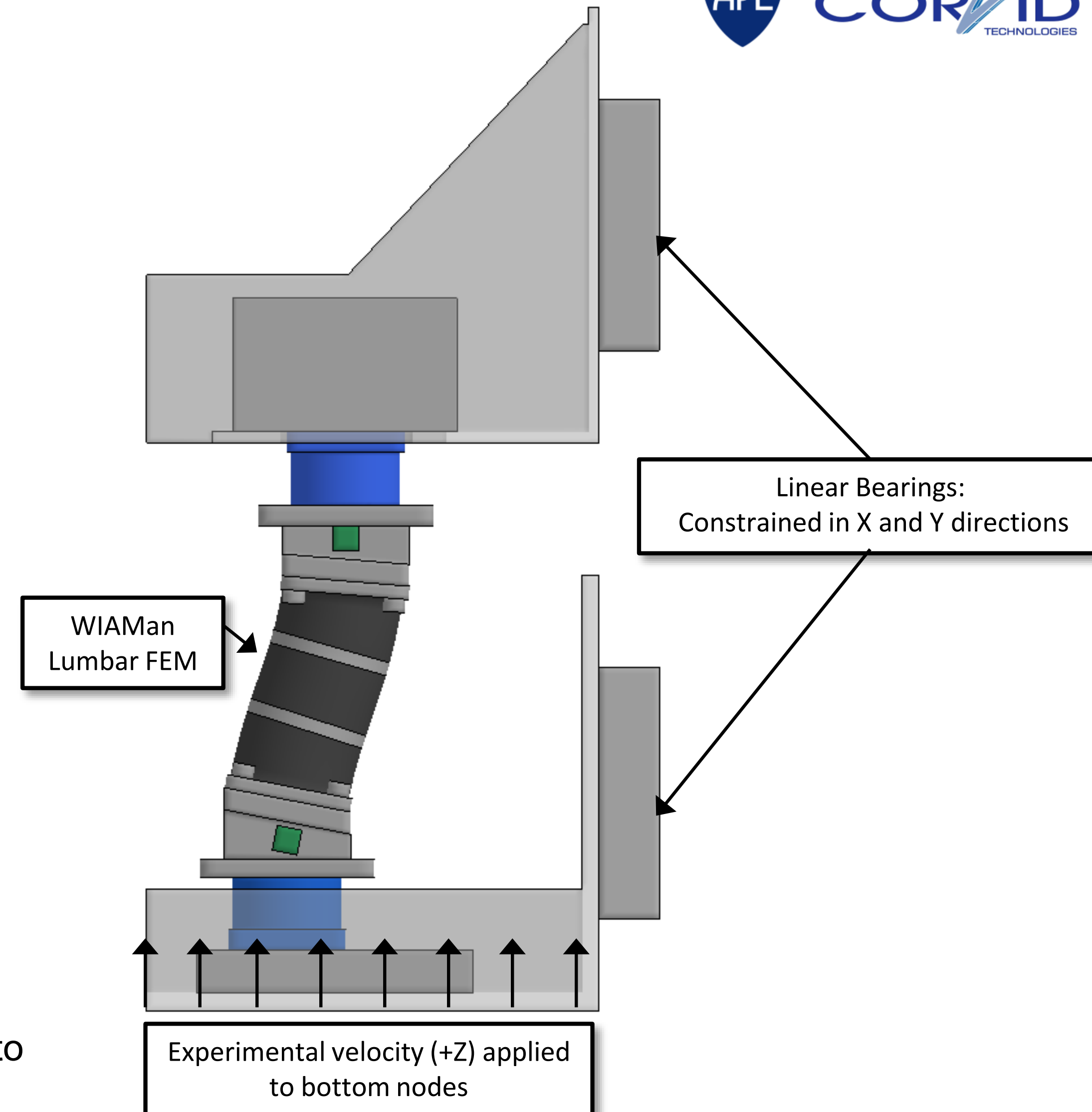

LS02: Validation Summary

- **Physical test series**
  - **BR 75A, Pre-Gen 1**
- **Simulation inputs**
  - **Bergstrom-Boyce Material Model:** Calibrated against Veryst test data at multiple loading rates
  - **Input Condition**
    - **Integrated accelerometer from MCW testing**
    - **Velocity input condition terminated according to contact trigger**

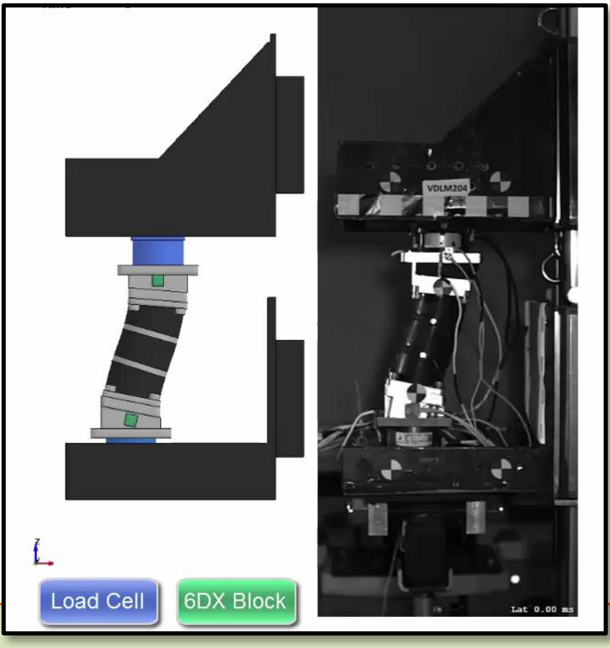

Velocity Inputs

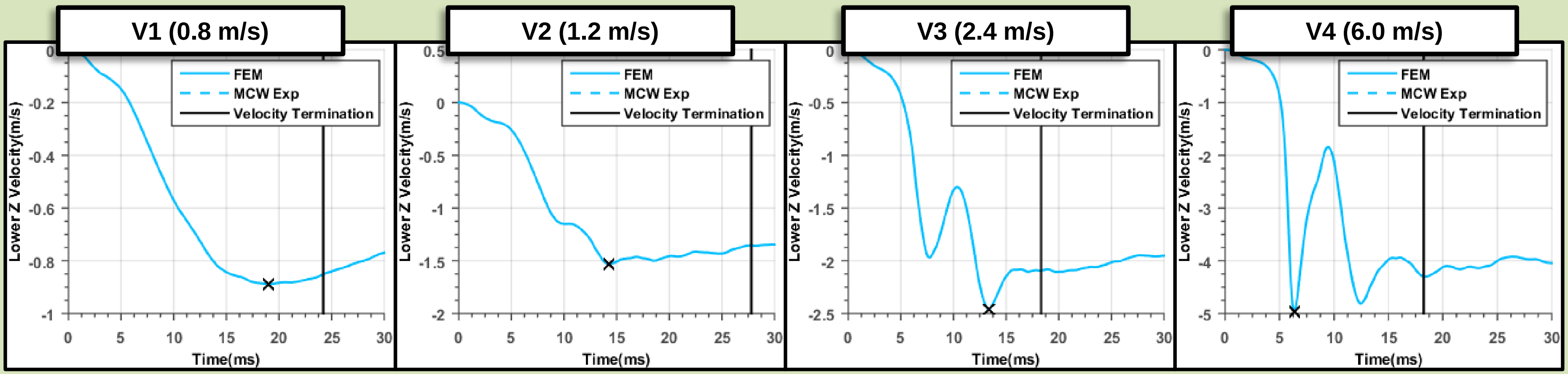

The Nation's Premier Laboratory for Land Forces

0.8 m/s Response Comparison

Upper Z Force

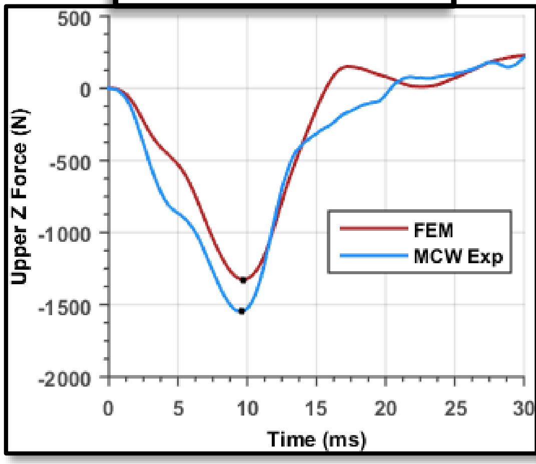

Upper Z Accel

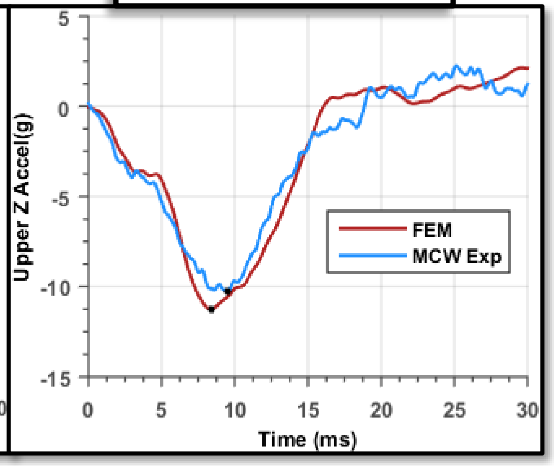

Upper Y Moment

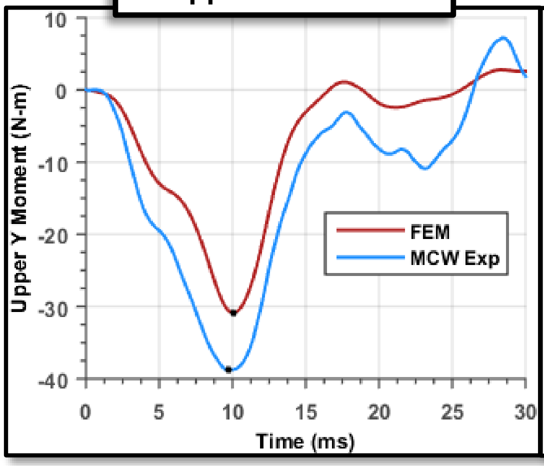

Compression

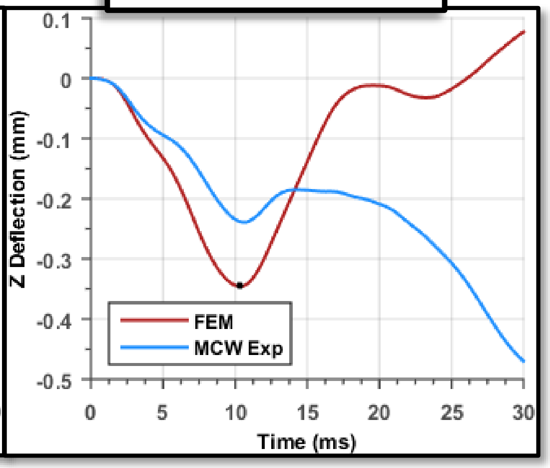

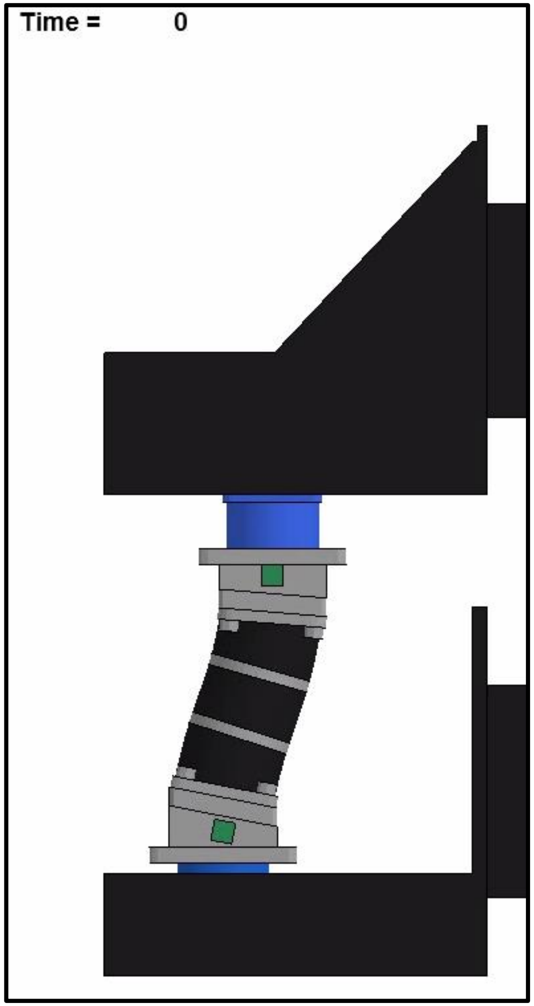

The Nation's Premier Laboratory for Land Forces

1.2 m/s Response Comparison

Upper Z Force

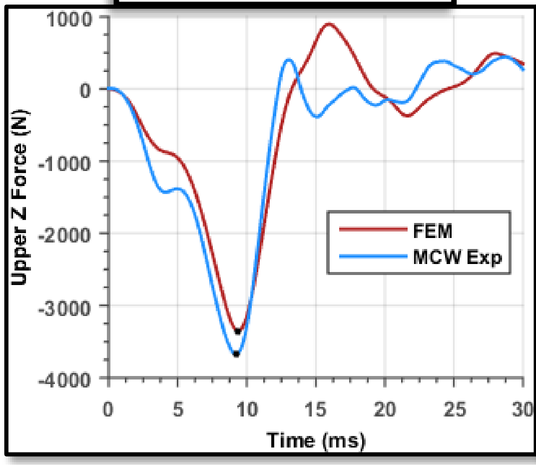

Upper Z Accel

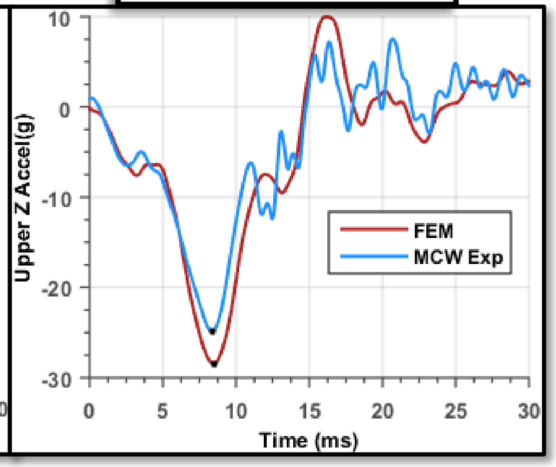

Upper Y Moment

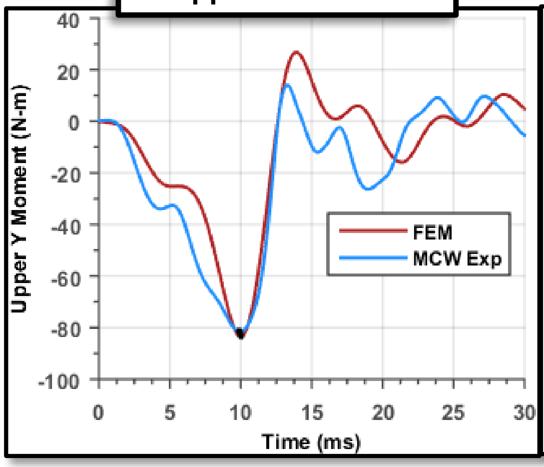

Compression

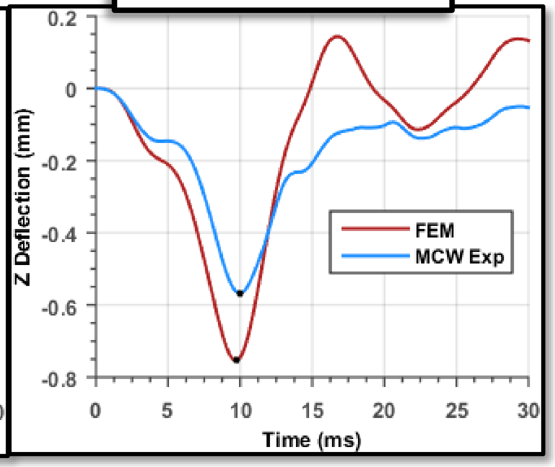

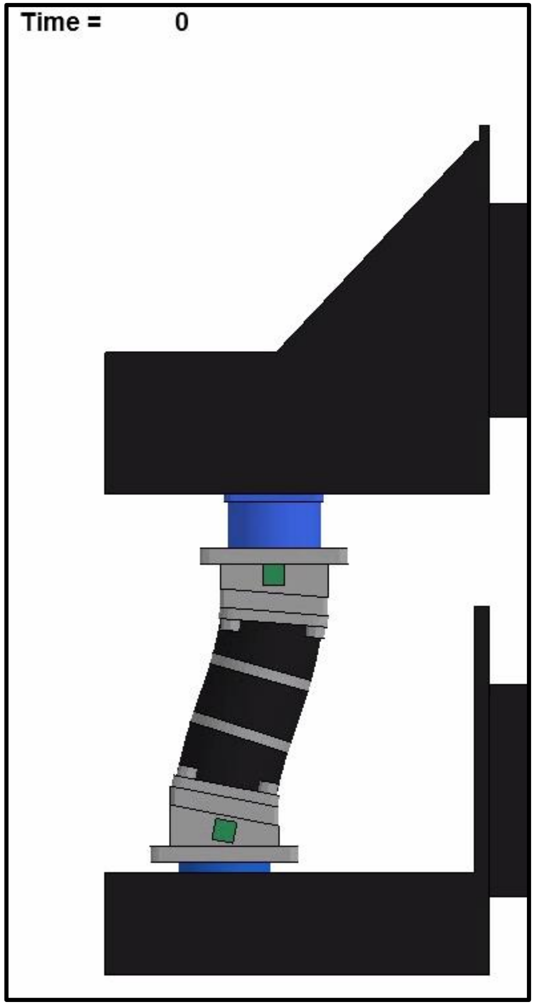

The Nation's Premier Laboratory for Land Forces

2.4 m/s Response Comparison

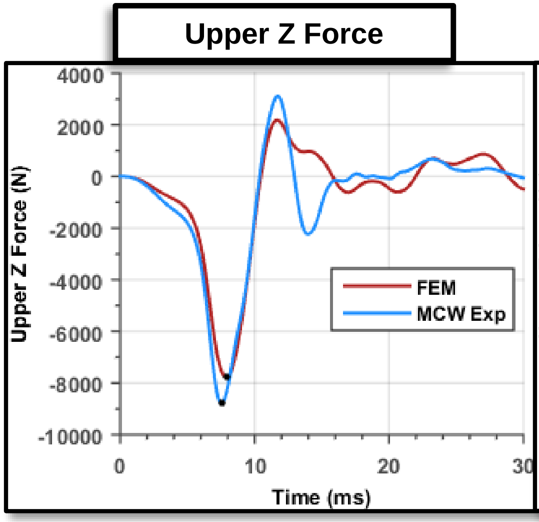

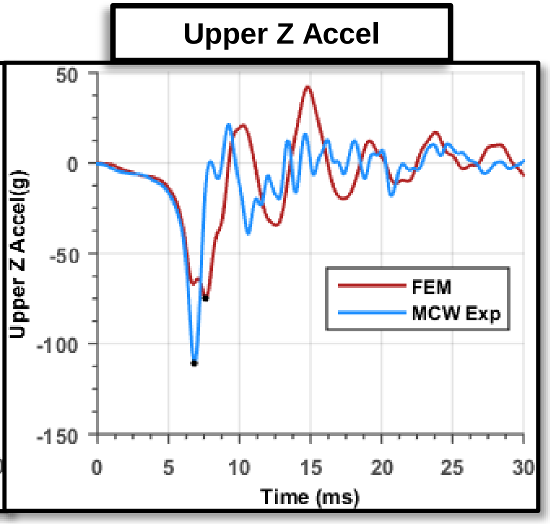

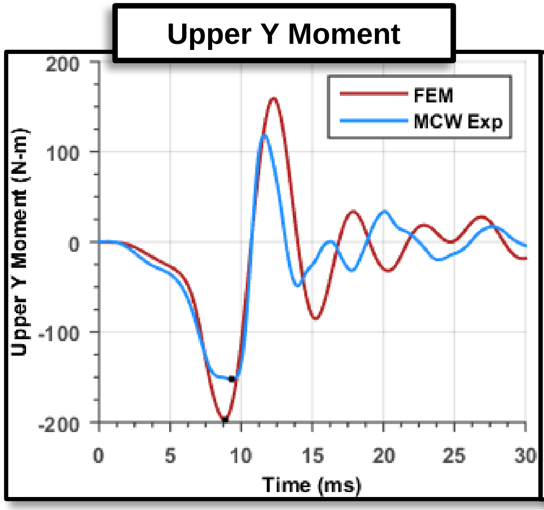

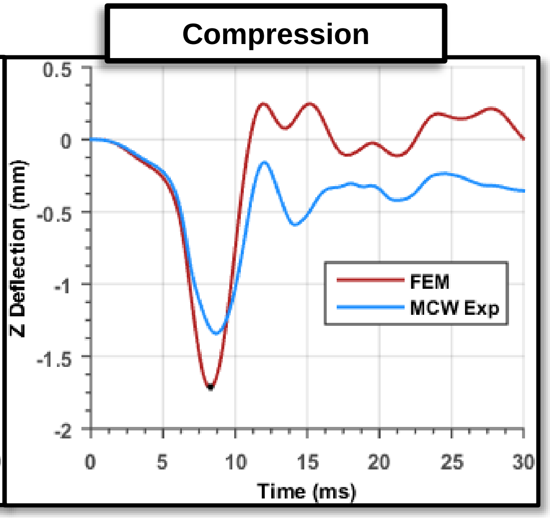

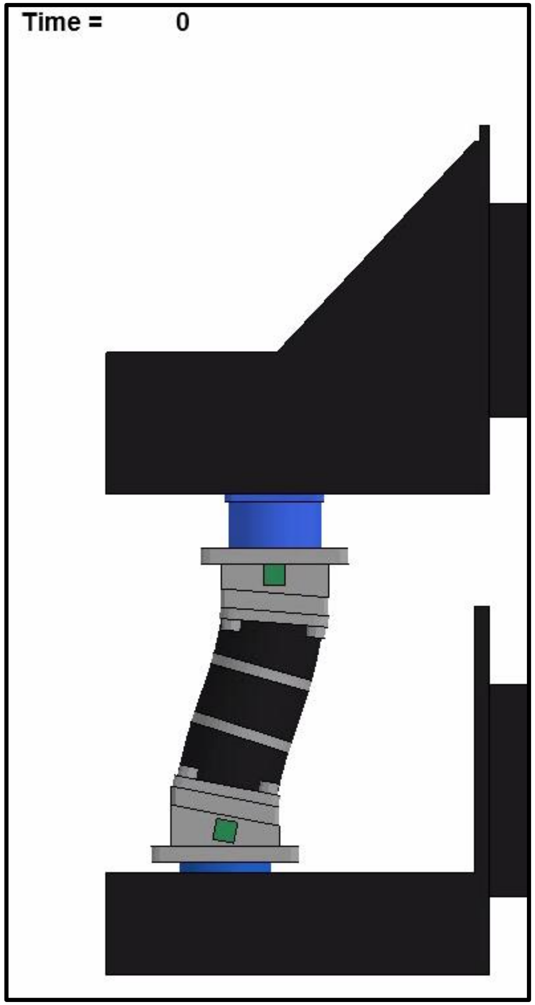

6.0 m/s Response Comparison

U.S. ARMY RDECOM ARL APL CORVID TECHNOLOGIES

Upper Z Force

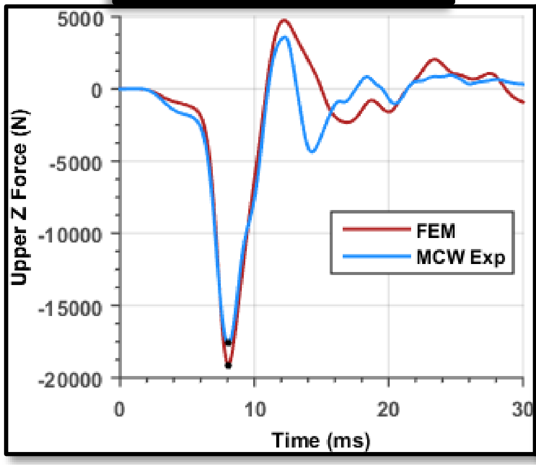

Upper Z Accel

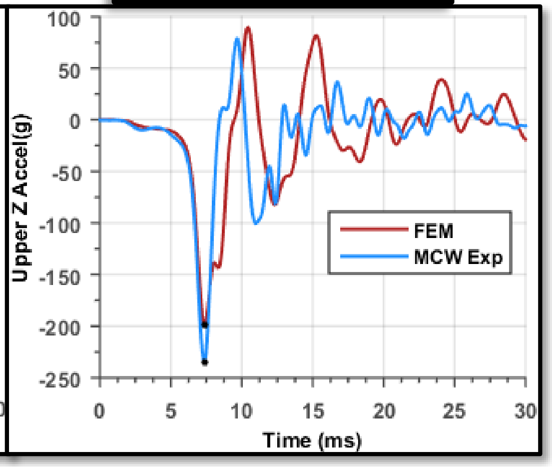

Upper Y Moment

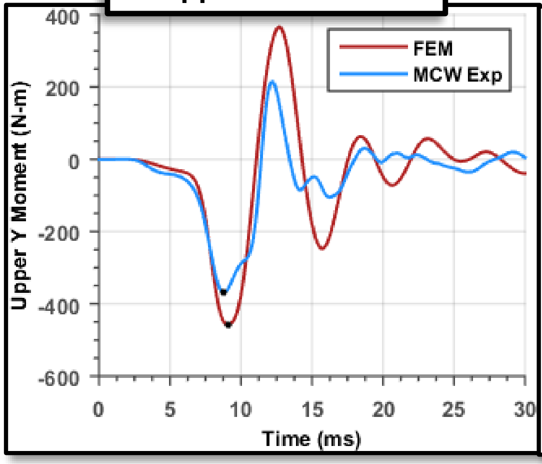

Compression

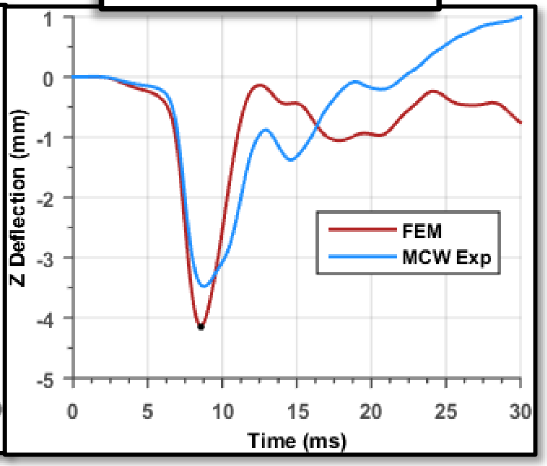

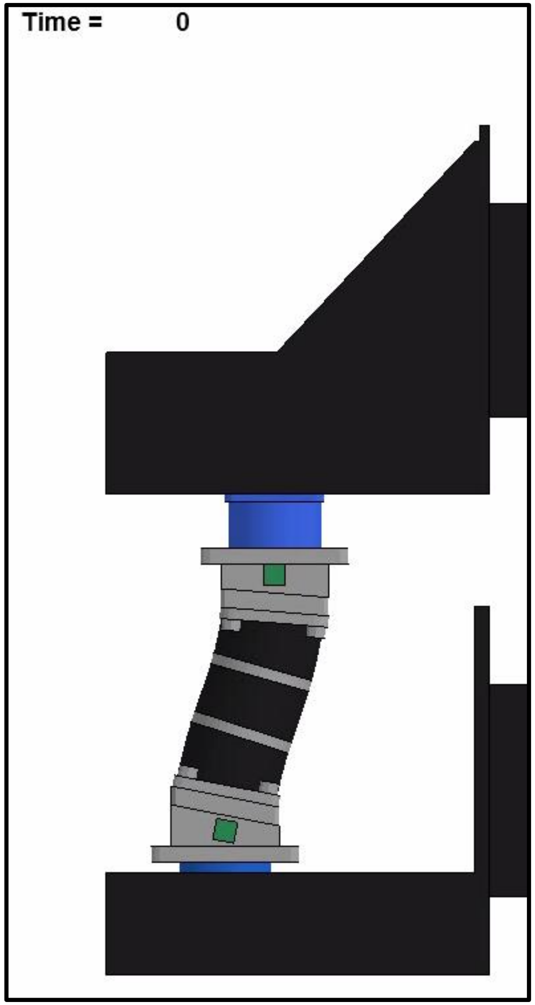

Validation CORA Results

Velocity	Response	Shape	Size	Phase	Total
V1	Az, upper				
V2					
V3					
V4					
V1	Fz, upper				
V2					
V3					
V4					
V1	My, upper				
V2					
V3					
V4					
V1	Az, lower				
V2					
V3					
V4					
V1	Fz, lower				
V2					
V3					
V4					
V1	Compression	N/A	N/A	N/A	N/A
V2					
V3					
V4					
V1	My, lower				
V2					
V3					
V4					
V1	Fx, upper				
V2					
V3					
V4					
V1	Fx, lower				
V2					
V3					
V4					

CORA Scale

0 — 1

Signal	W0032 CORA Weight Factor			
	V1 (0.8 m/s)	V2 (1.2 m/s)	V3 (2.4 m/s)	V4 (6.0 m/s)
Fz, upper	10	10	10	10
Compression	10	10	10	10
Az, lower	10	10	10	10
My, upper	8	8	8	8
Fz, lower	8	8	8	8
Az, upper	8	8	8	8
My, lower	2	2	2	2
Fx, upper	2	2	2	2
Fx, lower	2	2	2	2

	V1 (0.8 m/s)	V2 (1.2 m/s)	V3 (2.4 m/s)	V4 (6.0 m/s)
Weighted CORA Score	0.895	0.873	0.818	0.769

Lumbar Spine FEM Validated Across All Loading Velocities

PMHS Comparisons

2.4 m/s LS02 BRC Comparison

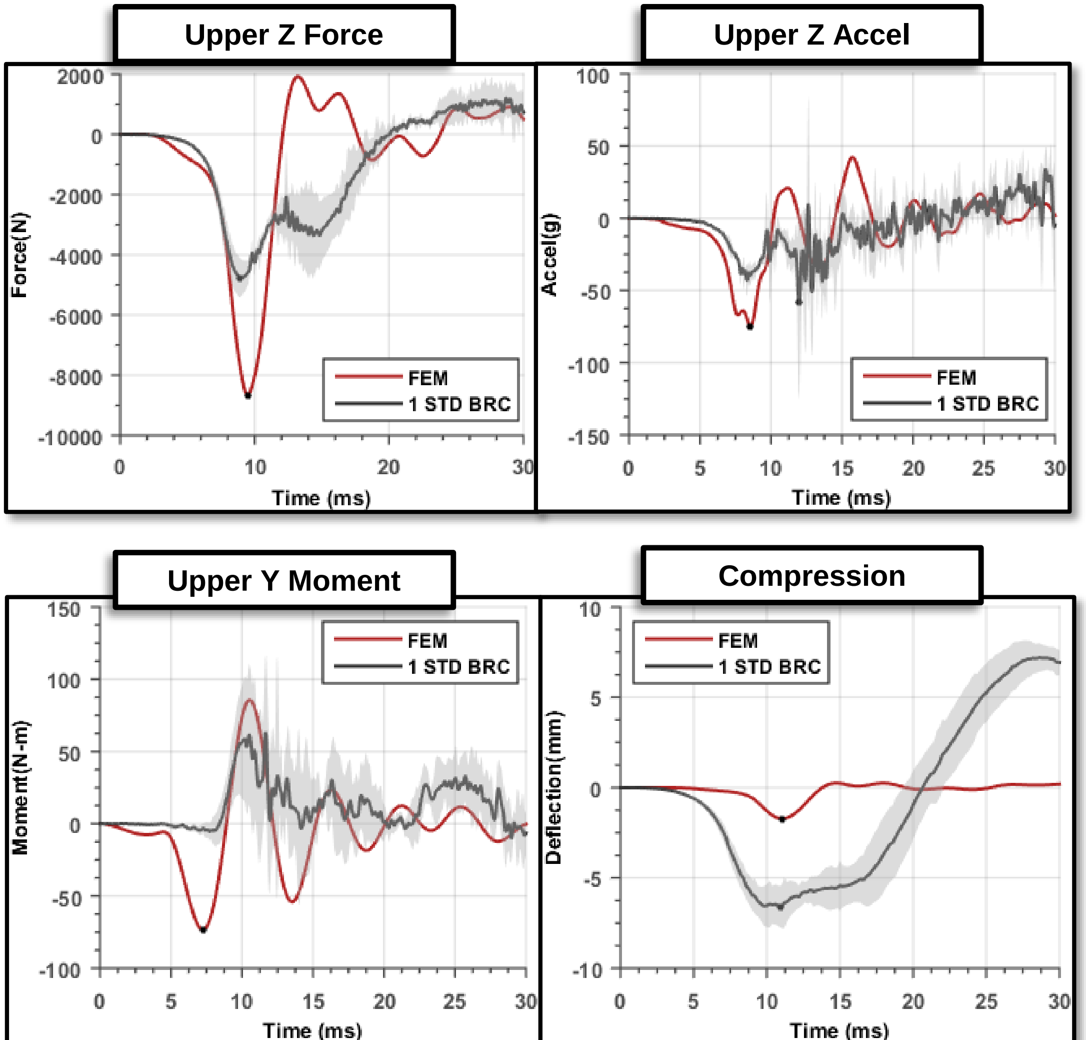

- **Validated lumbar spine FEM used to compare ATD vs PMHS response**
  - **Boundary conditions from ATD tests used**
  - **Results transformed to align with anatomical joint centers**
  - **Stiffness mismatch between ATD and PMHS**

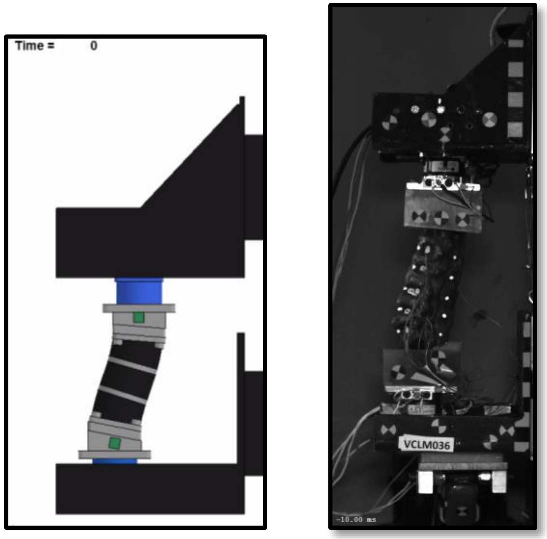

LS02: BRC Optimization

- Validated model used inform material selection
  - Polymer hardness varied from 30-85 Shore A
  - CORA ran to compare predicted force transmission to preliminary BRCs
- Optimized polymer
  - 60-65 Shore A Hardness (compare to 79 A for PreGen1)
  - Agrees with prototype lumbar testing

	L1 Force (+Z) CORA Overall
0.8 m/s	0.748
1.2 m/s	0.827
2.4 m/s	0.738

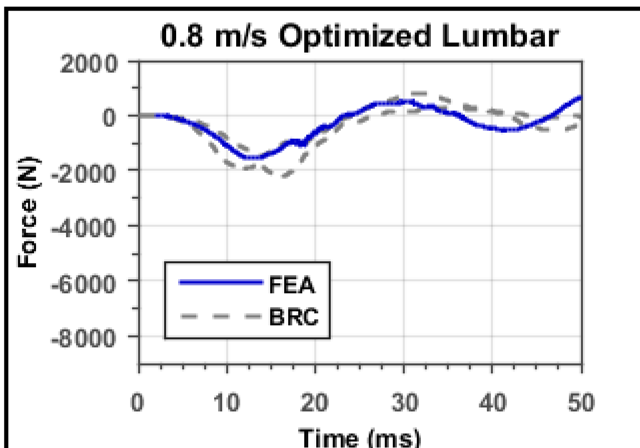

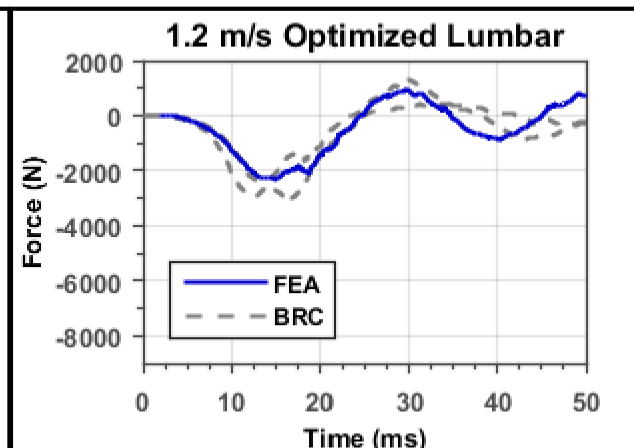

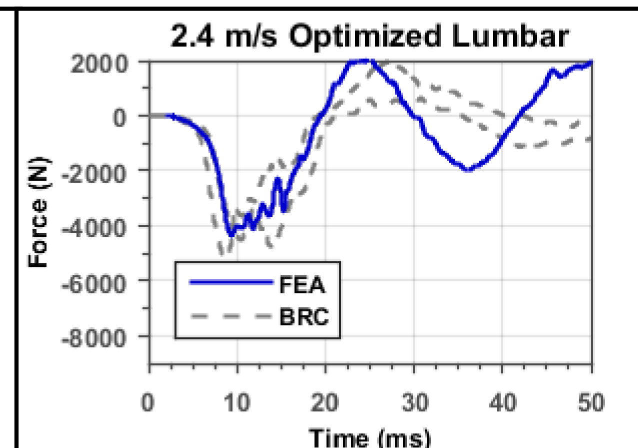

Strength of Design

LS02: SOD Assessment

- Potential rig yield at higher velocities
- No damage to lumbar discs anticipated

Material	Component	Yield Strength
6061 Aluminum	Rig Carriage	276 Mpa
1018 Steel	Ballast Box	310 MPa
7075-T6 Aluminum	Lumbar Discs	503 MPa

250 MPa

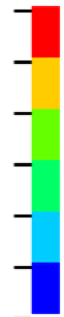

0 MPa

V04 V05 V06 V07

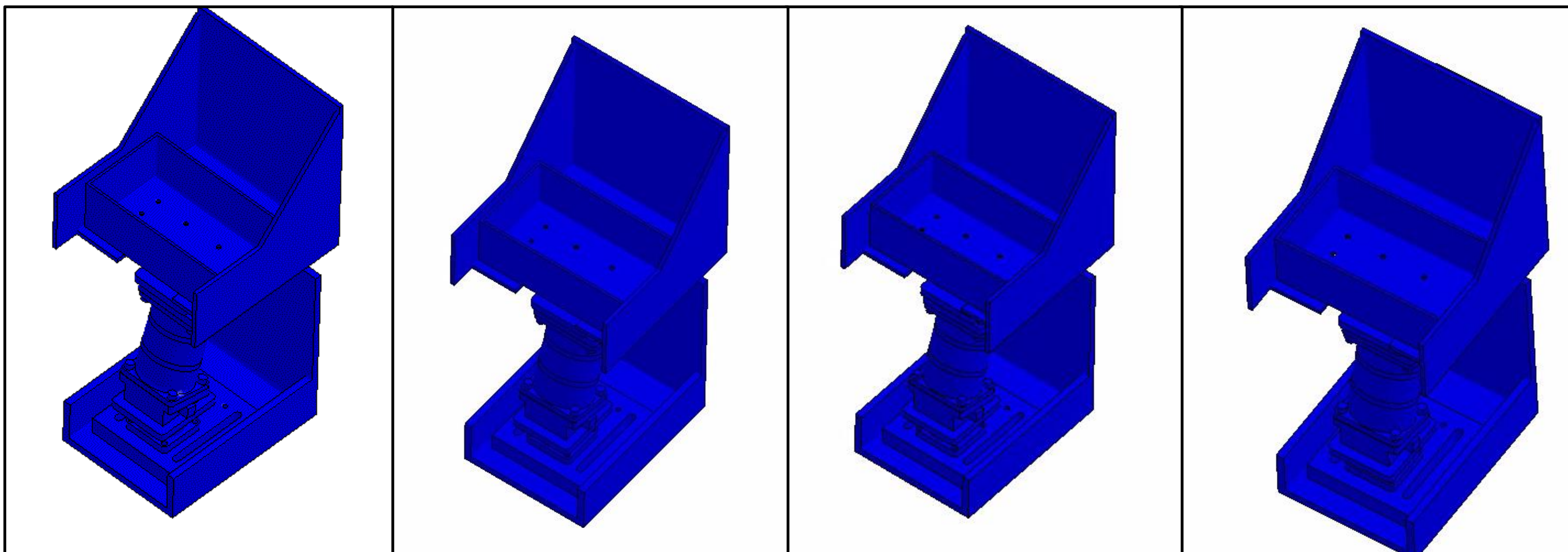

Load Cell SOD Assessment

- **10, 15, and 20 m/s overload velocity pulses generated as inputs for SOD**
- **WIAMan load cells included in simulations**
- **Stress concentrations located during 20 m/s impact**
  - No apparent risk for load cell failure

Part	Material	Max Von Mises Stress (MPa)	Min Yield Stress (MPa)
Lower Load Cell	4140 Steel	132.3	1310
Upper Load Cell	2024-T6 Aluminum	23.8	345
Bottom Plate	7075-T6 Aluminum	12.1	503
Top Plate	7075-T6 Aluminum	13.8	503
Lumbar Discs	7075-T6 Aluminum	22.5	503

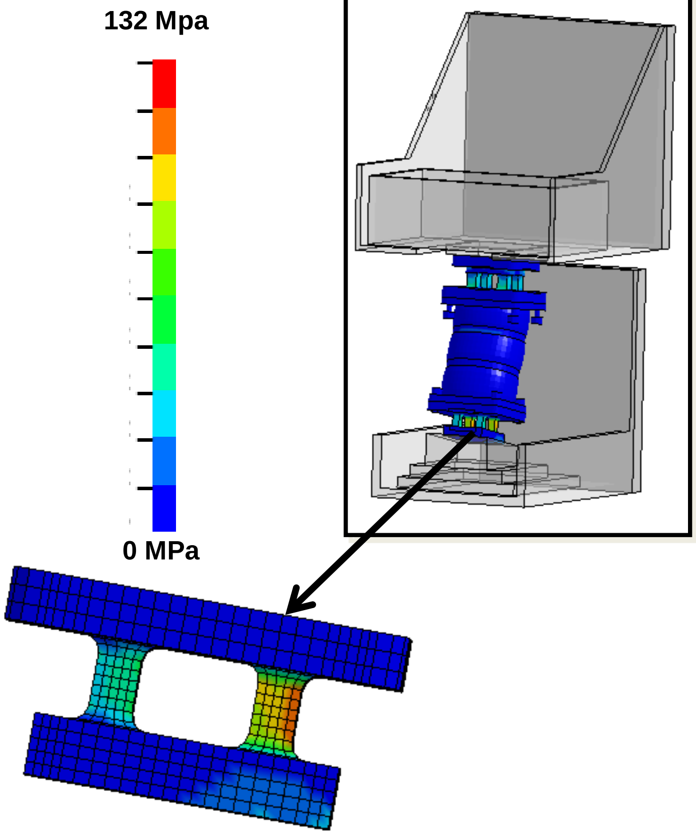

LS02: Bond Failure

- WIAMan lumbar rubber planned to be molded in place
  - Any potential redesigns require expensive and time-consuming mold creation
- Prototypes may be bonded
  - Shear-lap testing conducted to measure bond strength of Chemlok and Hysol on verious rubber types
  - Simulations in VertAc rig predict maximum shear above failure threshold
    - Consistent with observed failure of bonded prototypes

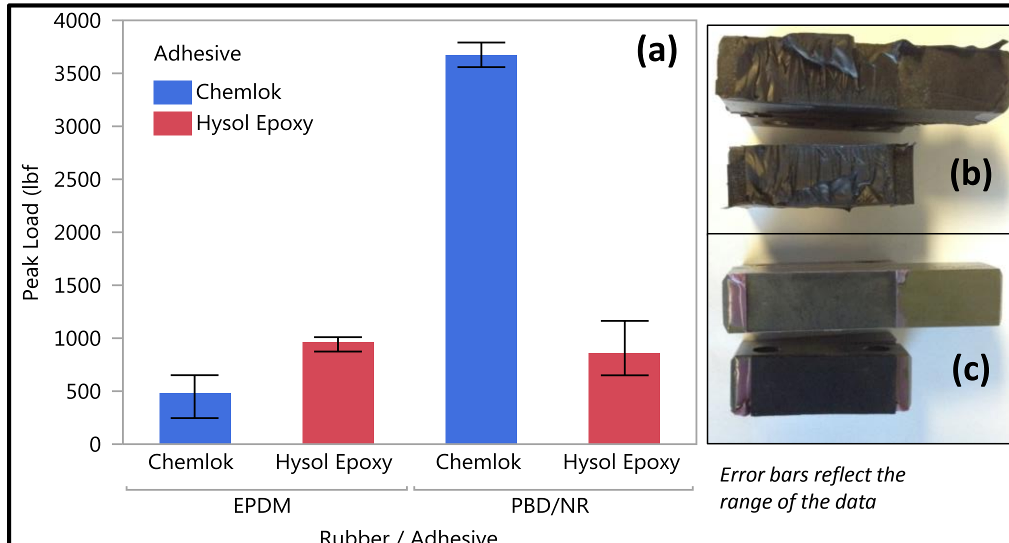

Error bars reflect the range of the data

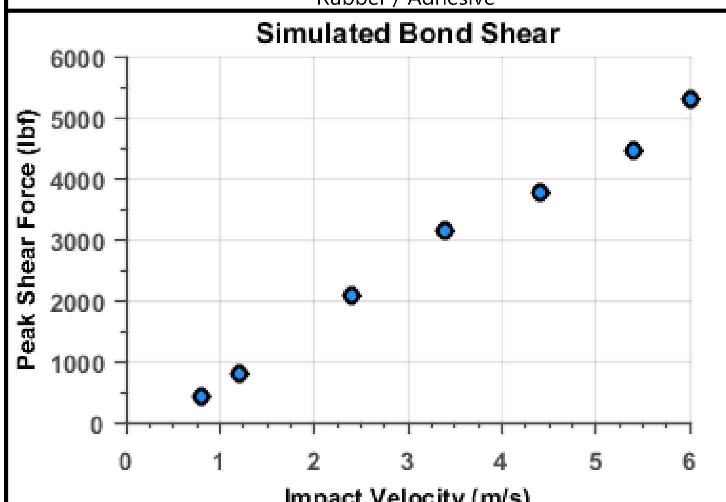

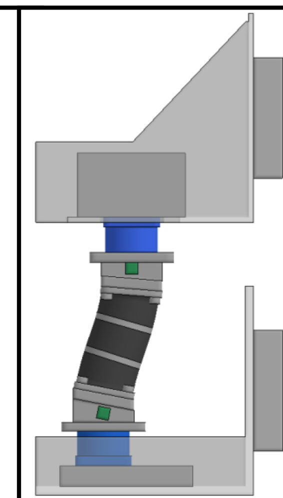

LS02: Strain Rate Study

Veryst Butyl 75A Characterization

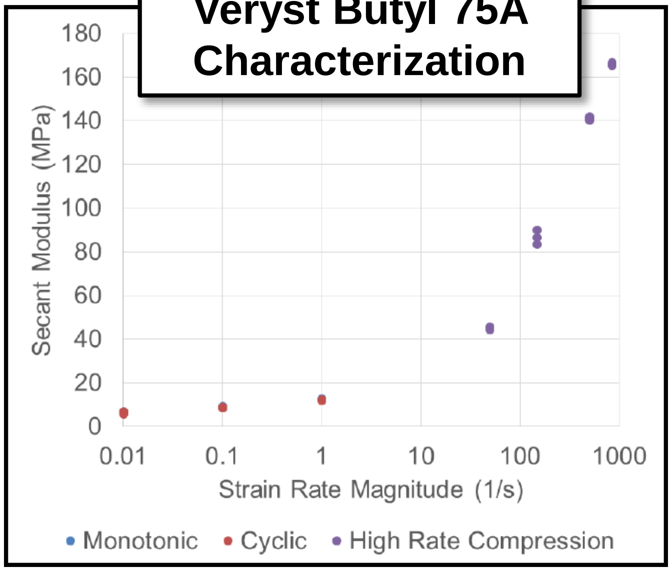

Strain Rate Histogram: 6 m/s Simulation

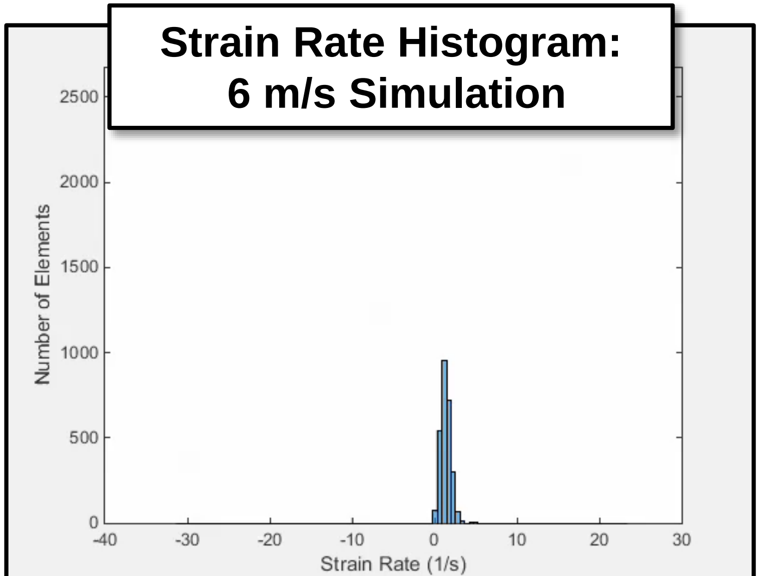

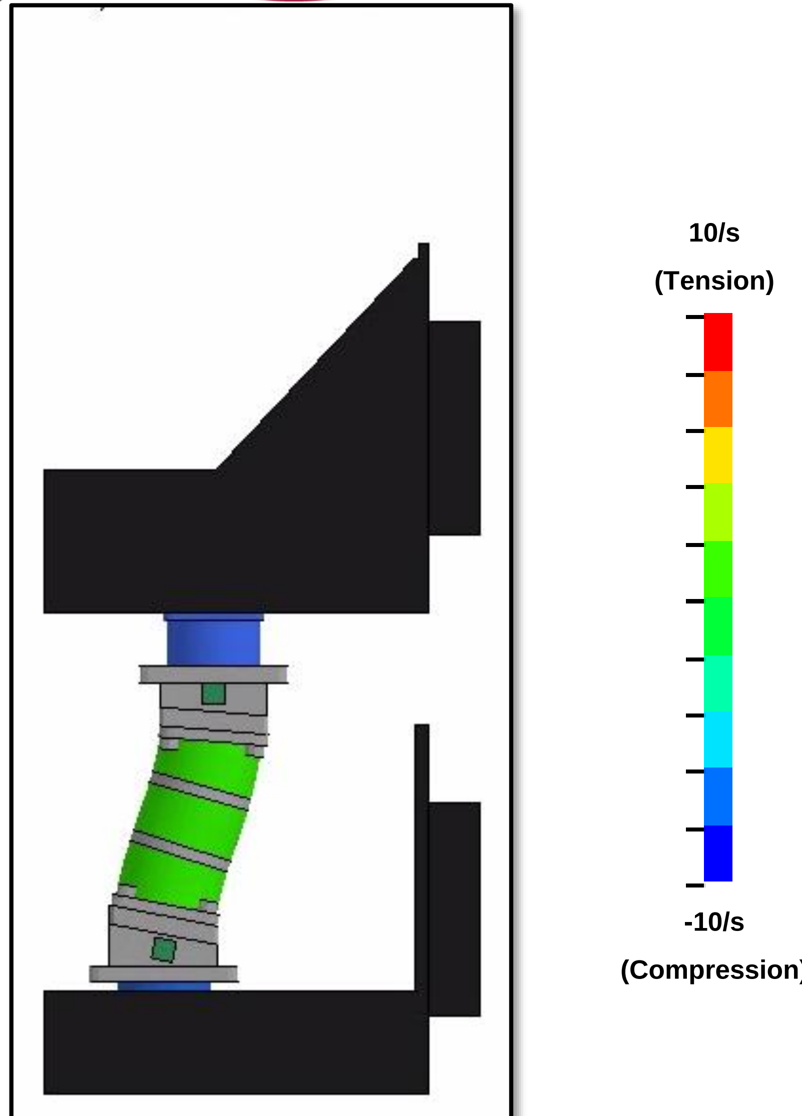

Whole Body Integration

- Lumbar spine characteristics have significant impact on whole body response
- Specifically, bending stiffness determines overall kinematics
  - Pelvis rotation, torso accelerations
  - FEM can inform design in absence of relevant experimental tests

VALTS – Whole Body

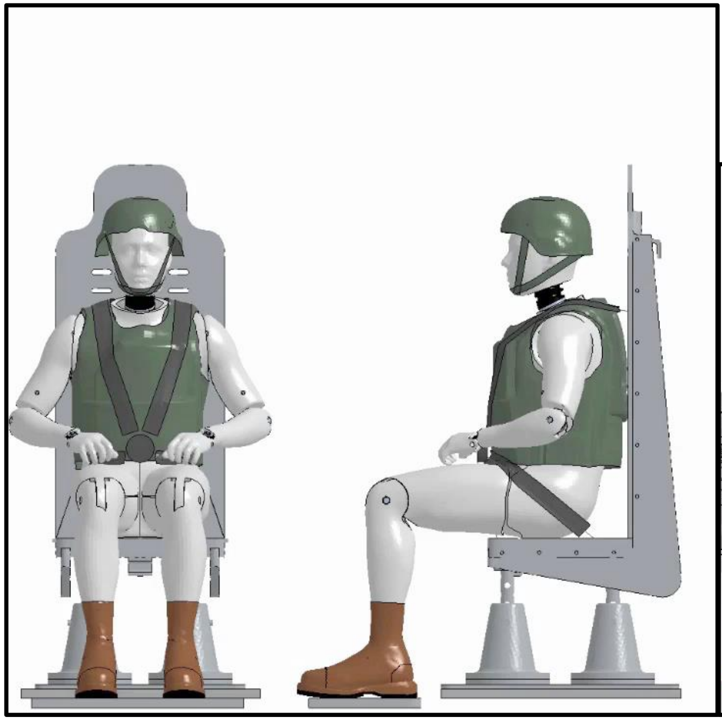

VALTS – Whole Body

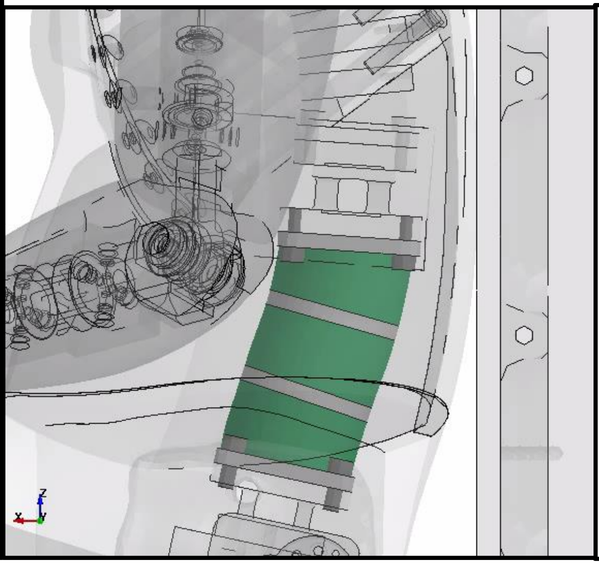

VertAc – Lumbar

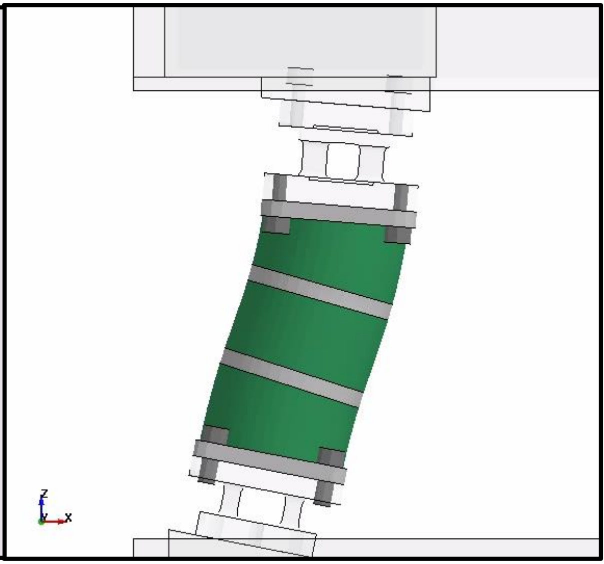

Conclusion and Next Steps

- **Mature WIAMan ATD Lumbar Spine FEM**
  - Material level characterization
  - Fully validated across range of impact velocities
- **SOD assessments**
  - Rig and lumbar failure, including overload cases
- **BRC assessments performed**
  - Optimal polymer hardness determined
- **Validated lumbar spine FEM well situated to…**
  - Explore design alternatives
    - Balance BRC response with SOD
  - Assess injury risk during untested loading scenarios
    - Altered environment, posture, etc.
  - Test potential injury mitigation systems
    - PPE
    - Vehicle design

Questions?

CORA Review

- **Inputs**
  - Reference curve(s)
    - e.g. experimental
  - Comparison curve
    - e.g. model
- **Outputs**
  - Ratings at each level
  - Total CORA rating is weighted average of 4

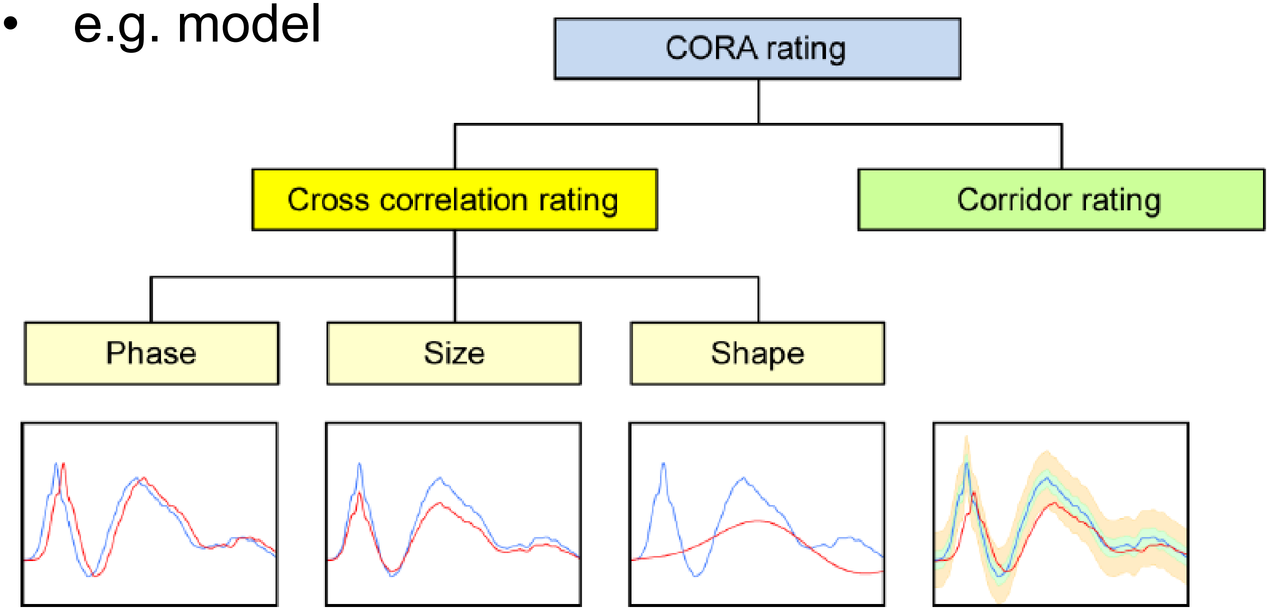

Goal: Reduce subjectivity by comparing all signals with the same level of objectivity

CORA Review

Phase Rating: Amount of shift required to maximize correlation

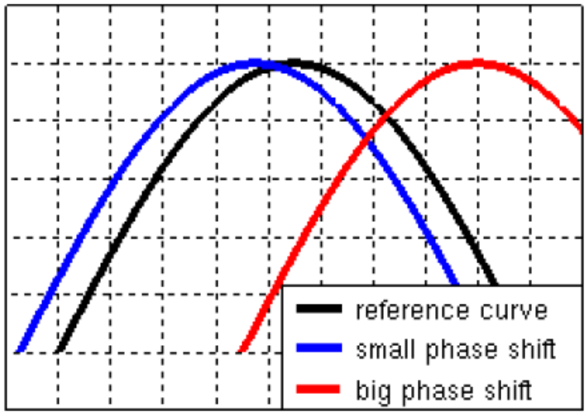

Size Rating: Area under the curve ratio

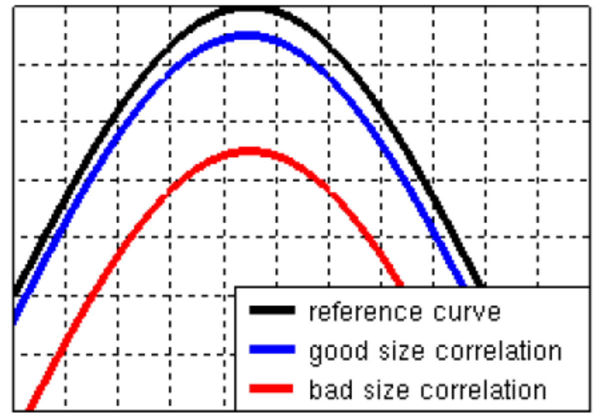

Shape Rating: Correlation

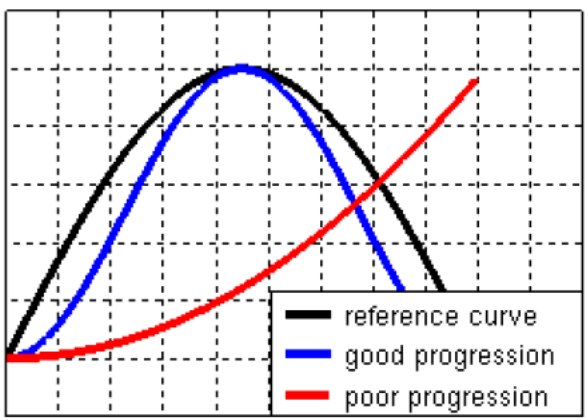

Corridor Rating: Fit in corridor

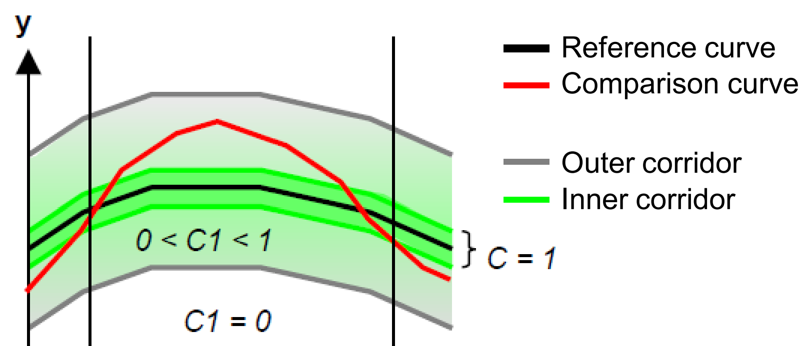

CORA user manual

Each metric is used to compensate the others' disadvantages

CORA Settings

- **Default values recommended by CORA sensitivity analysis**
- **Interval of evaluation: 0-30ms**

- **Signal Weight Factors**
  - Corridor: 0.5 (0 for comparison to single curve)
  - Cross Correlation: 0.5 (1 for comparison to multiple curves)
    - Size: 0.333
    - Shape: 0.333
    - Phase: 0.333

0.8 m/s LS02 BRC Comparison

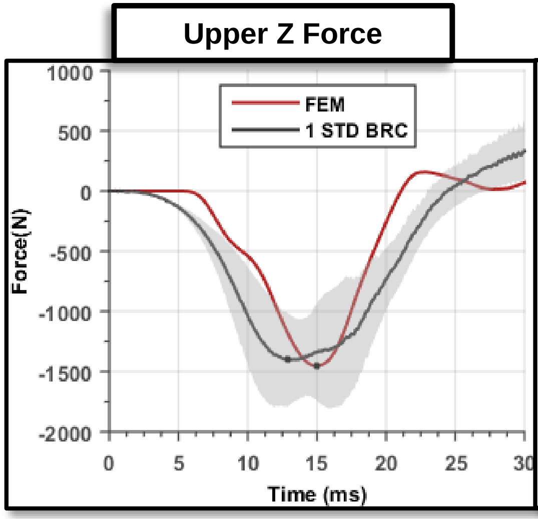

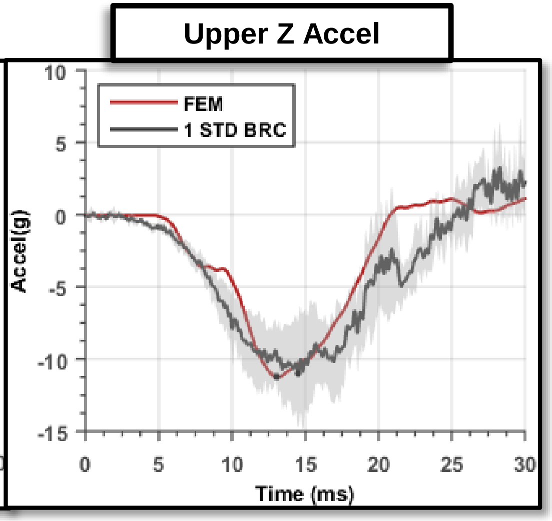

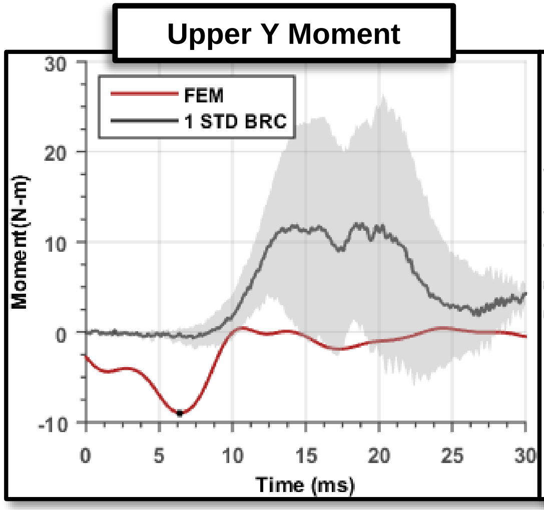

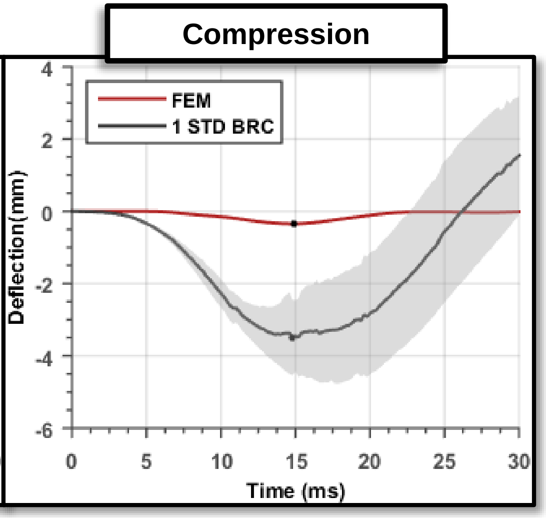

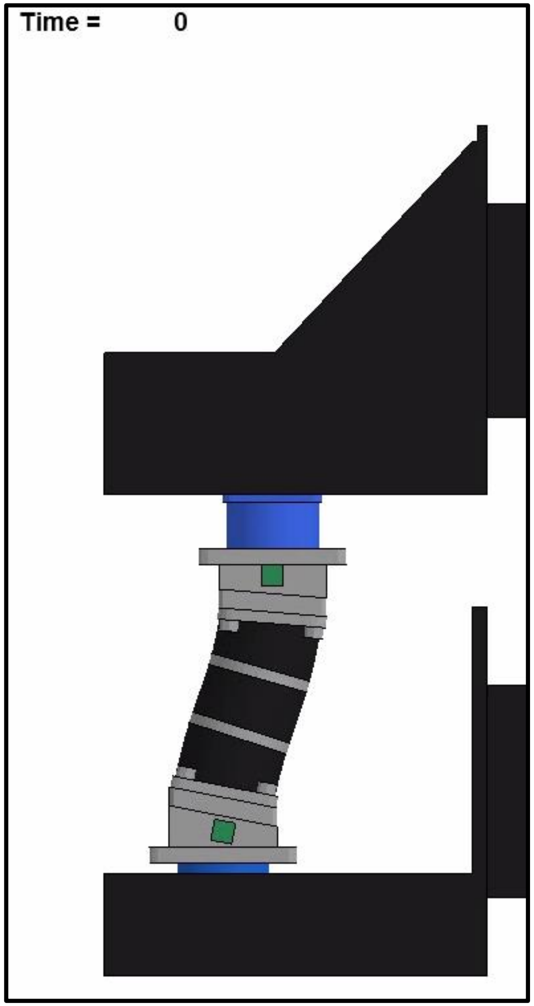

1.2 m/s LS02 BRC Comparison

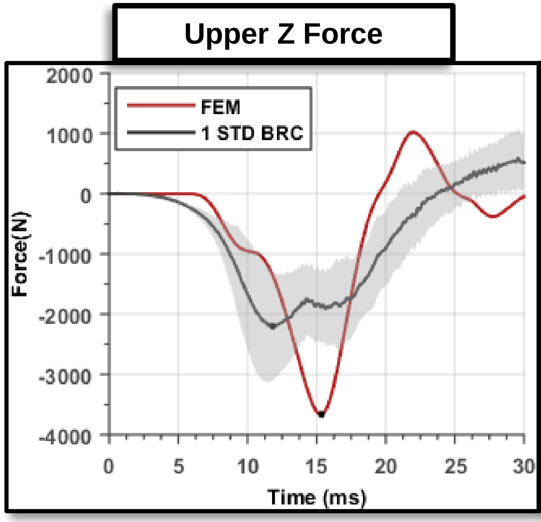

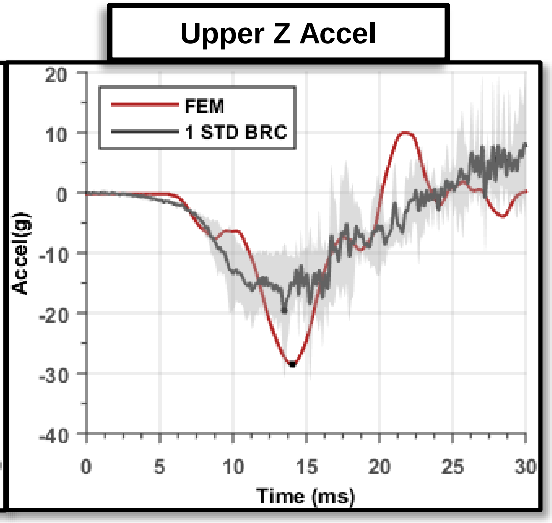

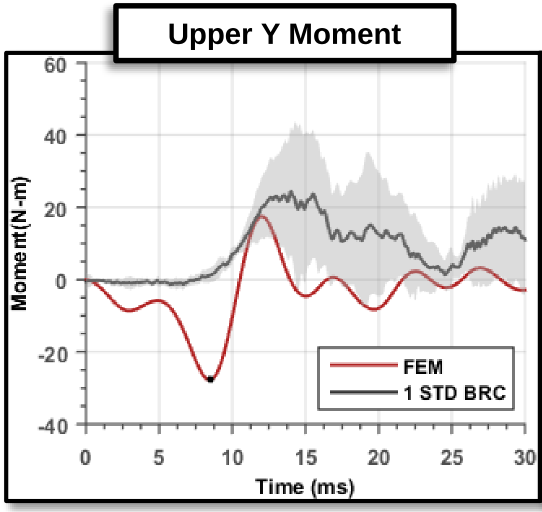

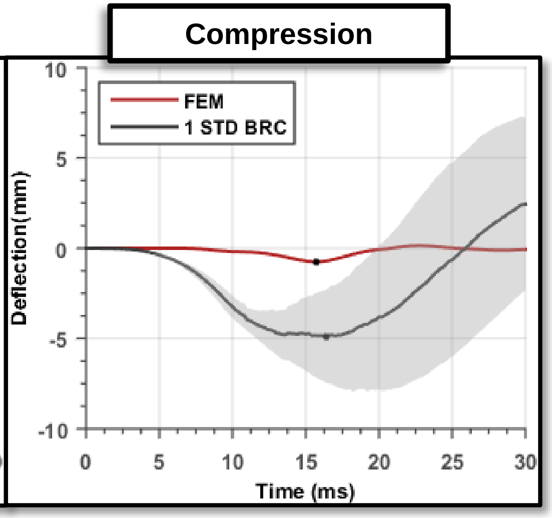

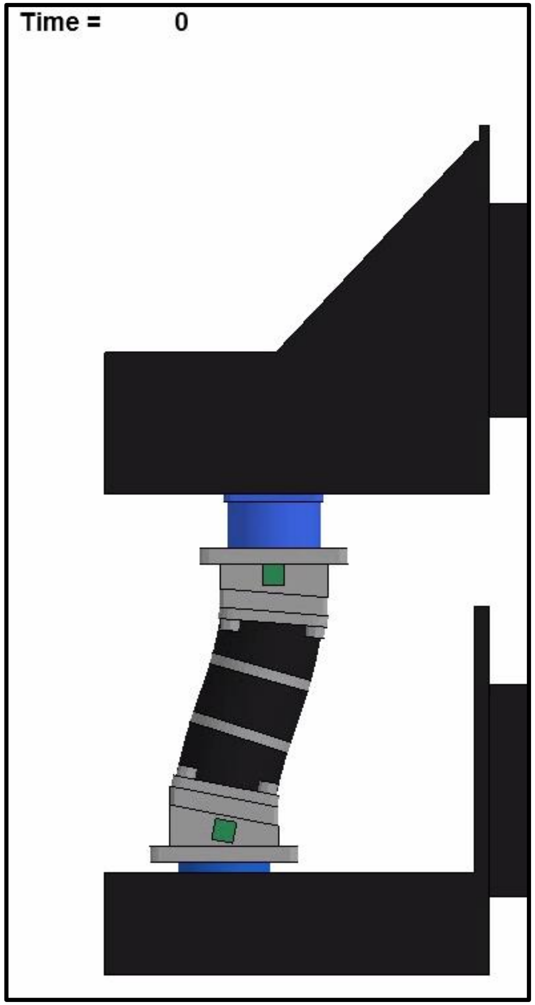

Preliminary Development of a finite element model of WIAMan lower extremity, sensitivity analysis to impact loading conditions

Wade Baker[1], Costin D. Untaroiu[1],
Mostafiz Chowdhury[2], Randy Coates[2]

[1]Virginia Tech, [2]US Army Research Laboratory

Overview

- Introduction: Underbody-blast impact loading & Military injuries
- Introduction: Anthropometric Test Devices & FE Modeling
- WIAMan Lower Limb: *Development & Preliminary Validation*
- GHBMC Lower Limb Model: *Development & Preliminary Validation*
- Limitations and Future work
- Conclusions
- WIAMan Lower Leg Strength of Design and Soft Materials Sensitivity Study using Design of Experiments (APL)

Introduction

(Youtube.com)

Under-body blast impact loading

The improvised explosive devices (IED) – the leading cause of injury and death for service members (more than **50,000 coalition forces** injured or killed)

(Champion et al. 2009,Belmont et al. 2010)

Vehicle Occupant injury mechanisms

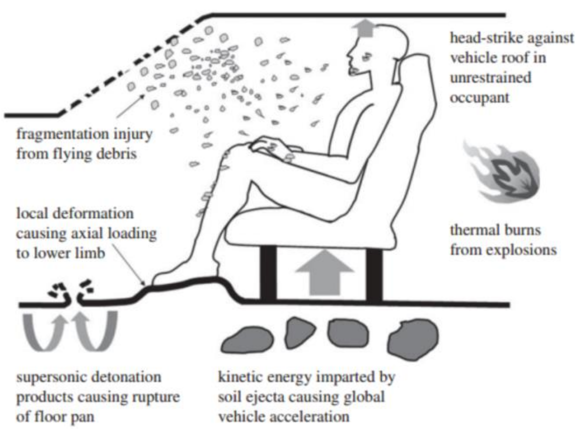

(Ramasamy et al. 2010)

Time sequence of Events during an Anti-Vehicular Mine Detonation

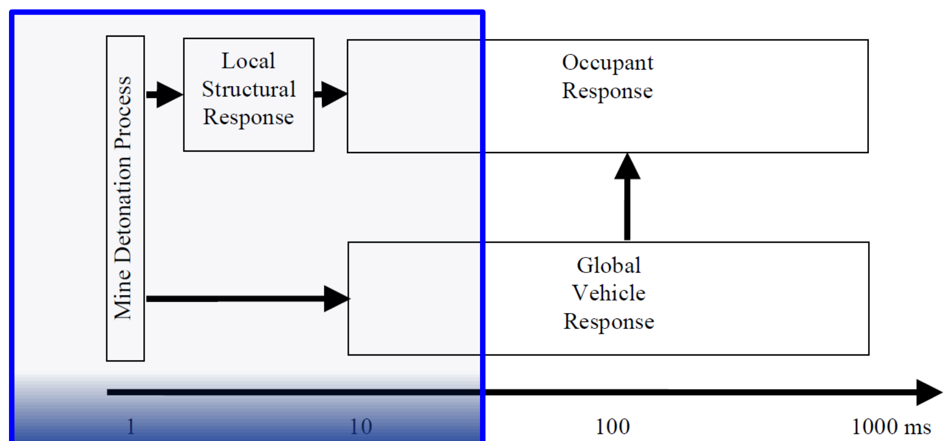

(NATO 2007 Report)

Introduction

U.S. ARMY RDECOM ARL

Injury Distribution per body region

- U.K. Army (2006-2008)
- 63 service personnel injured from under-body IED explosion
- 26 ± 5.7 years

- Lower limb: the most severely injured body region
- 89 foot/ankle injuries

(Ramasamy et al. 2013)

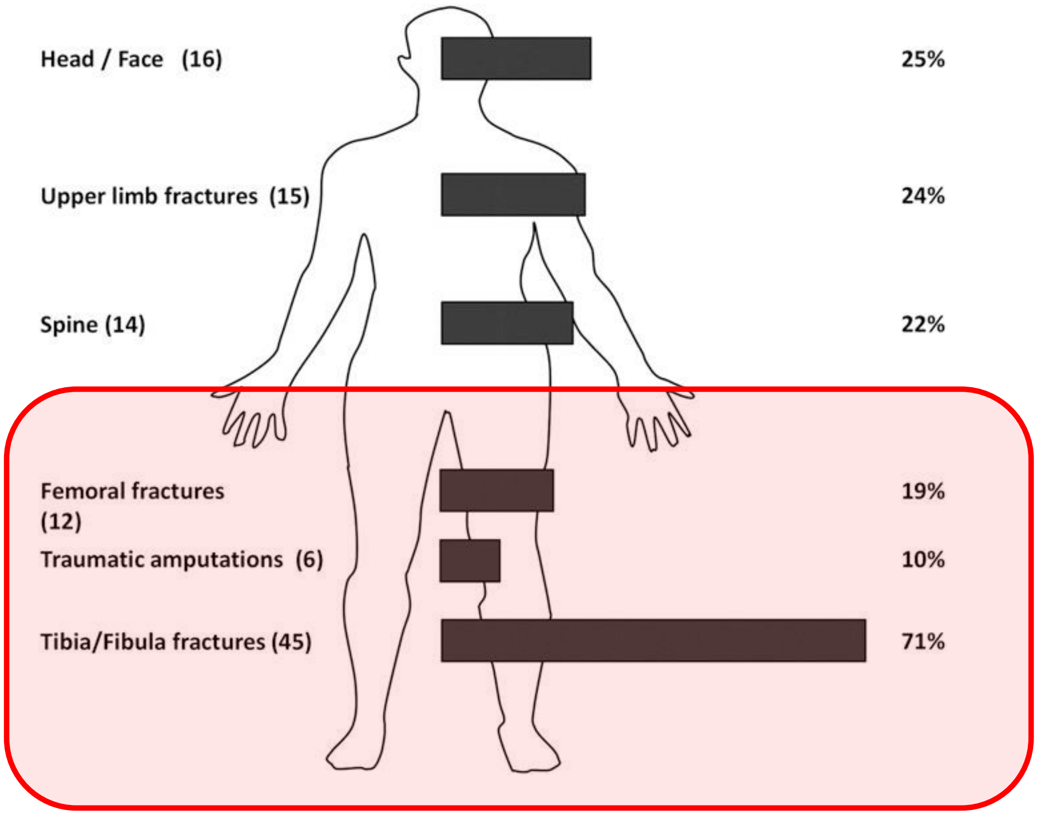

VirginiaTech Invent the Future

CORVID TECHNOLOGIES

APL

Introduction

Anthropometric Test Devices (ATD)/Dummies

50th male ATDs (dummies)

Hybrid III

THOR dummy

Dummies designed for frontal automotive crashes, so their applicability in under-body impact scenarios is questionable

WIAMan (Warrior Injury Assessment Manikin) ATD

WIAMan Lower Limb FE Model

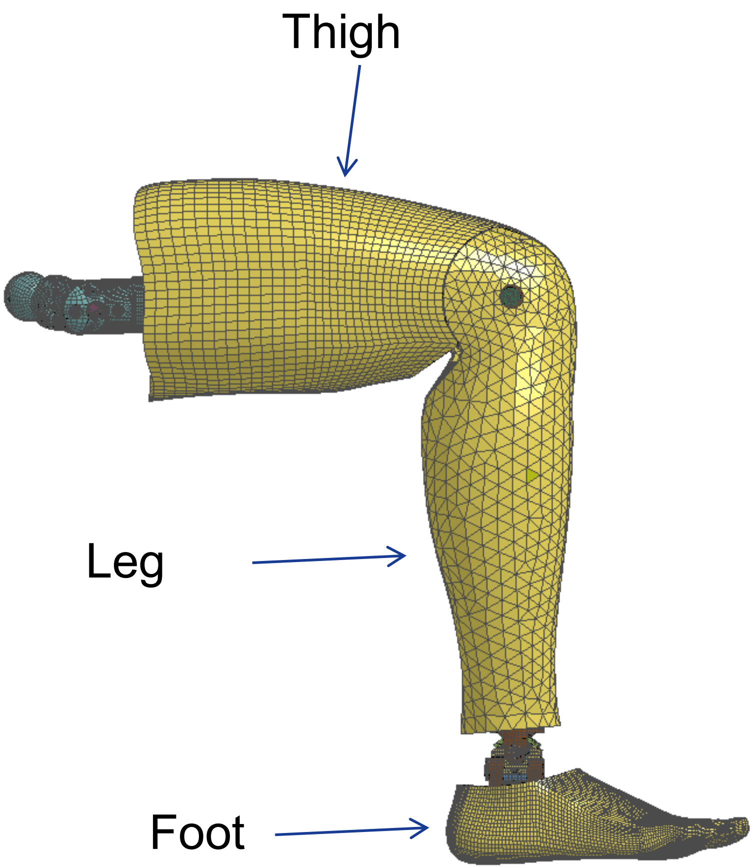

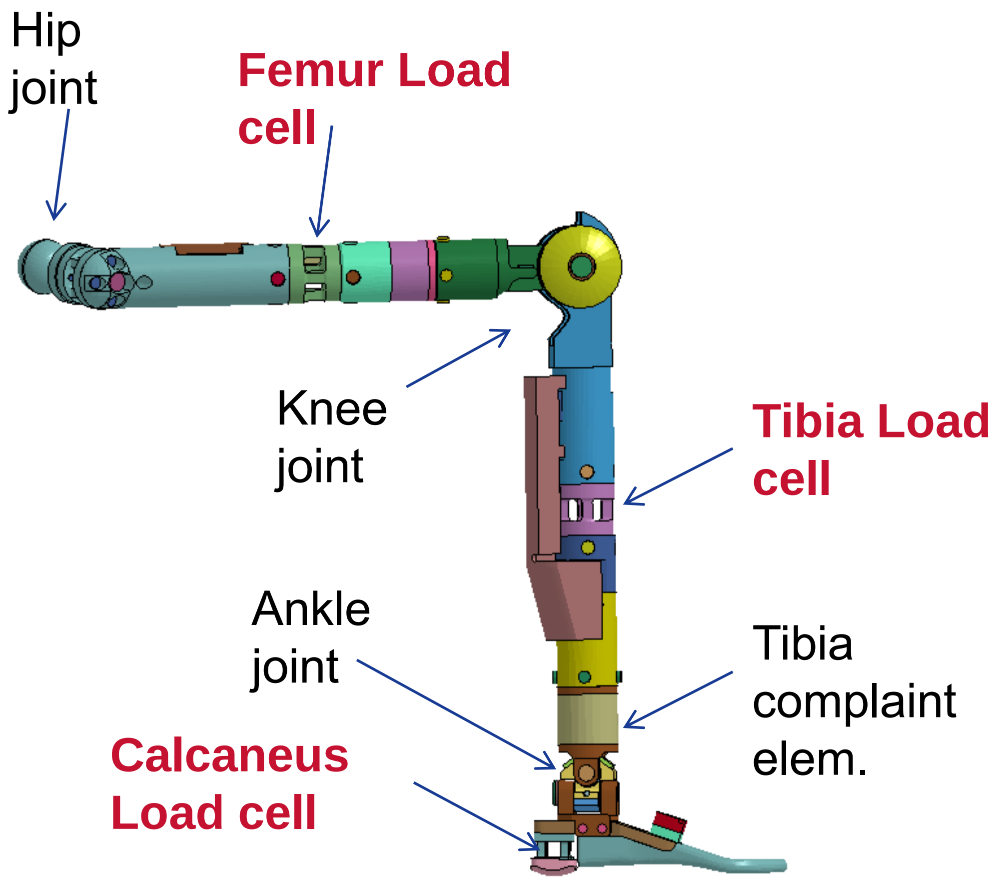

98 parts
381,235 nodes
338,855 elements (deformable)
5.4 kg (lower leg)

WIAMan Lower Limb FE Model

Meshing the model

Material testing and Development of material model

Definition of contacts, sections, hourglass etc.

Preliminary Model Validation

Sensitivity Studies

Material Modeling

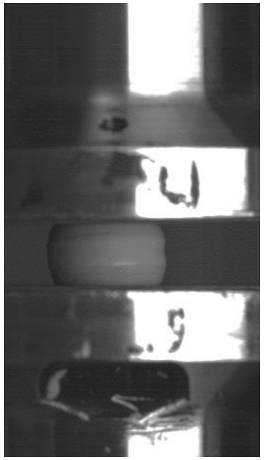

Tension/compression material testing tests

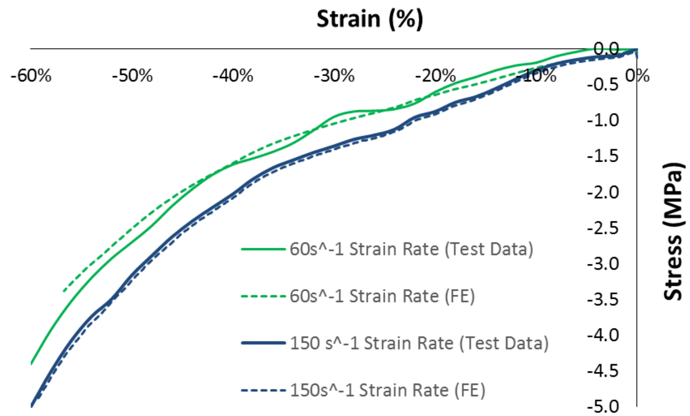

The Nation's Premier Laboratory for Land Forces

WIAMan Model Validation

Outputs:

- Loadings
  - Tibia LC forces & moments
  - Calcaneus Forces
  - Knee LC forces & moments
- Kinematics
  - Tibia accelerations
  - Foot accelerations

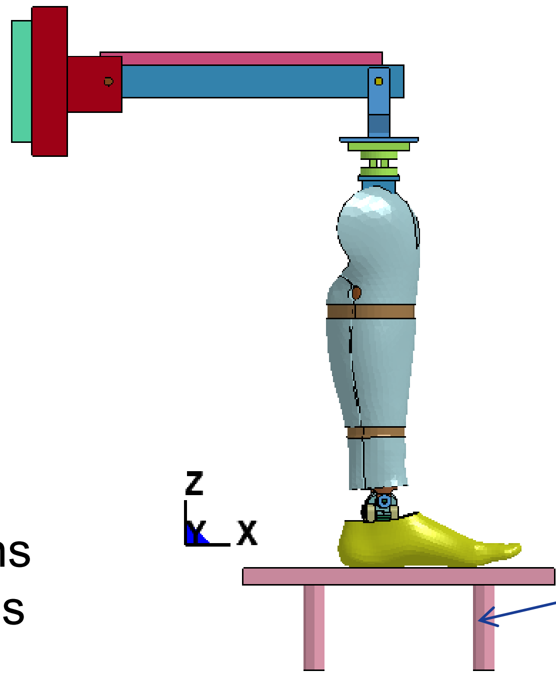

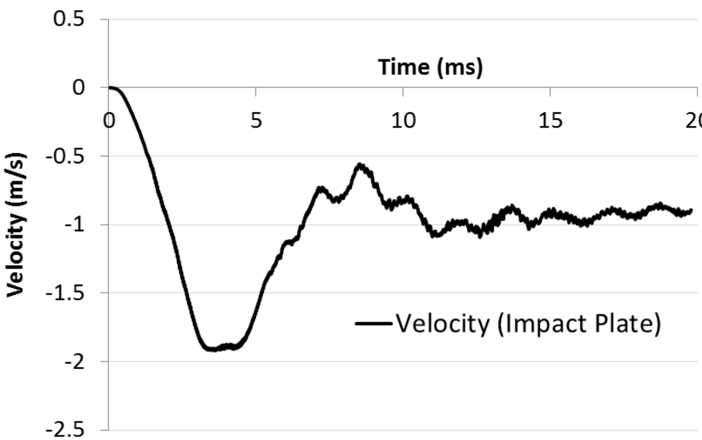

Input: Time history of impact plate velocity

WIAMan Model Validation

U.S. ARMY RDECOM ARL

Knee force (z-direction)

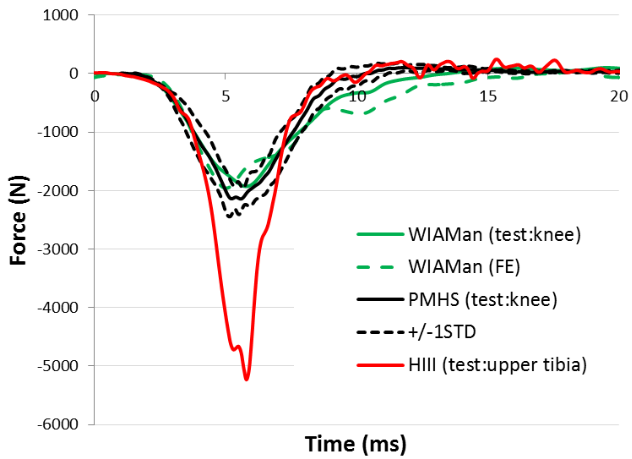

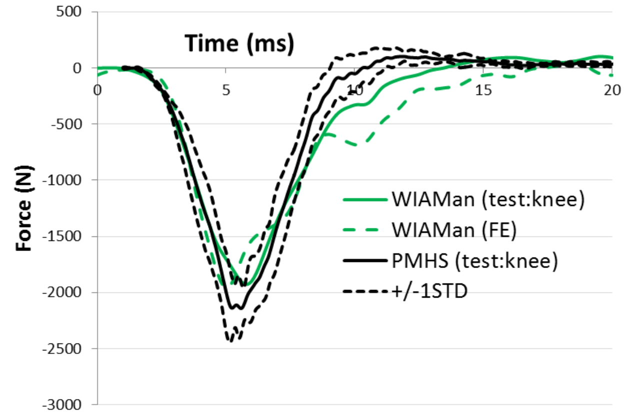

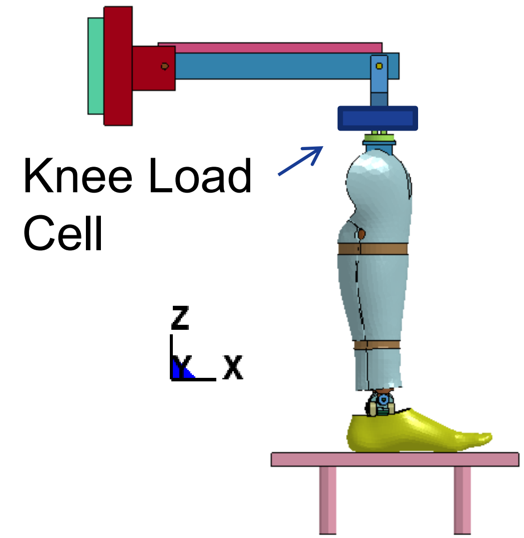

Knee moment (z-direction)

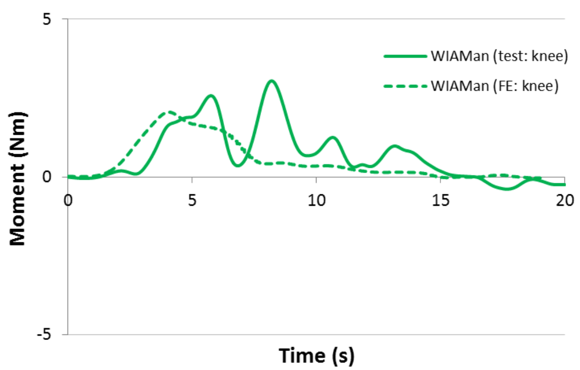

Knee moment (y-direction)

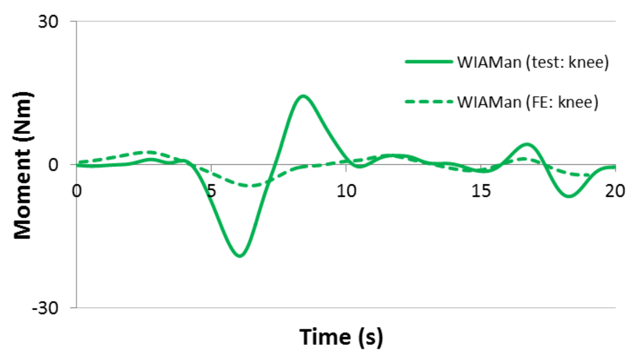

Knee force (x-direction)

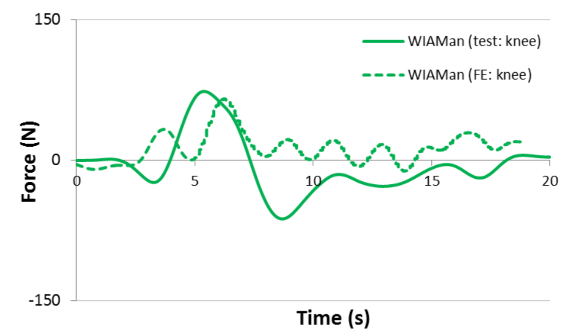

VirginiaTech Invent the Future

CORVID TECHNOLOGIES

APL

WIAMan Model Validation

Tibia force (z-direction)

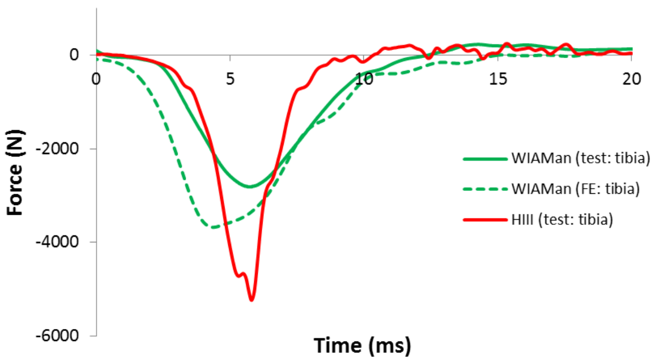

Tibia force (y-direction)

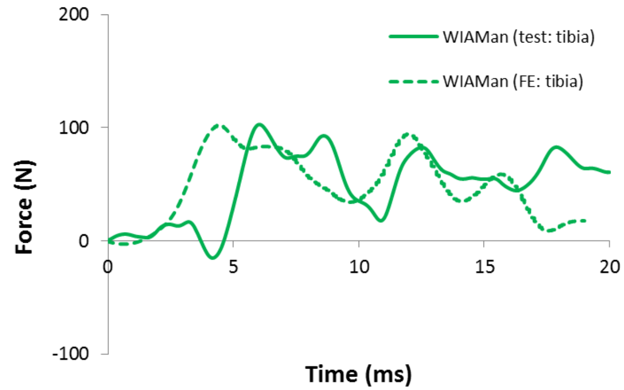

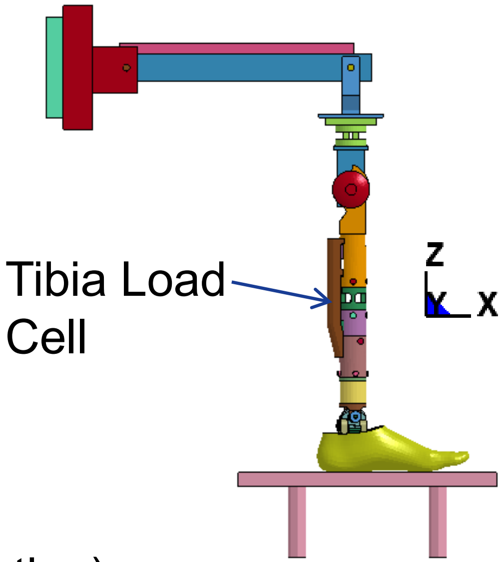

Tibia moment (y-direction)

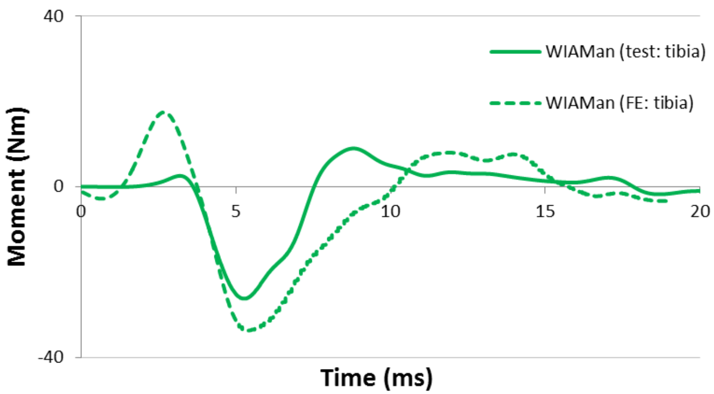

Tibia moment (x-direction)

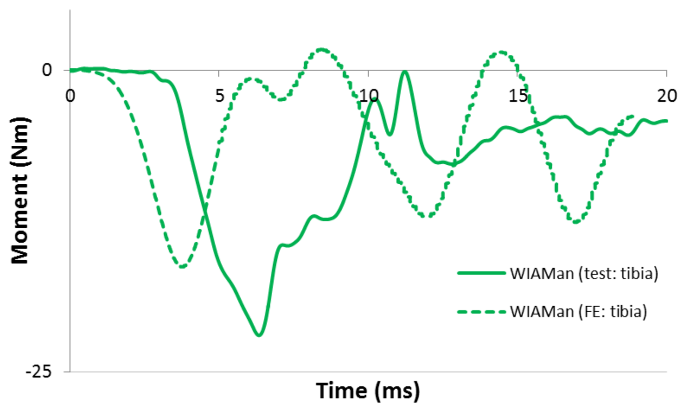

WIAMan Model Validation

Calcaneus force (z-direction)

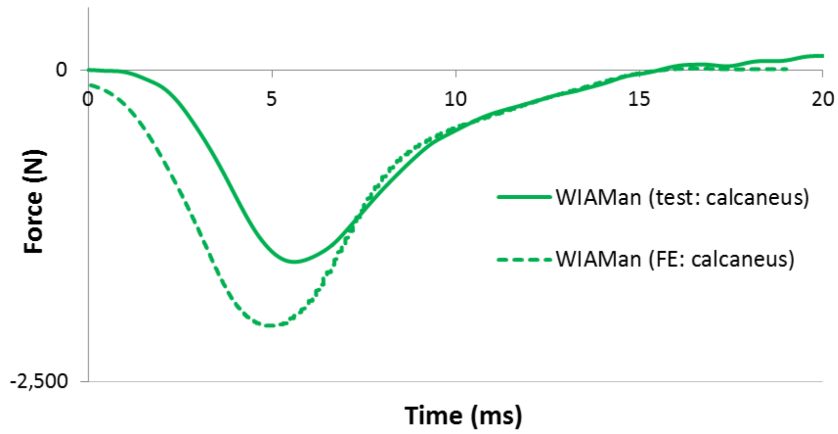

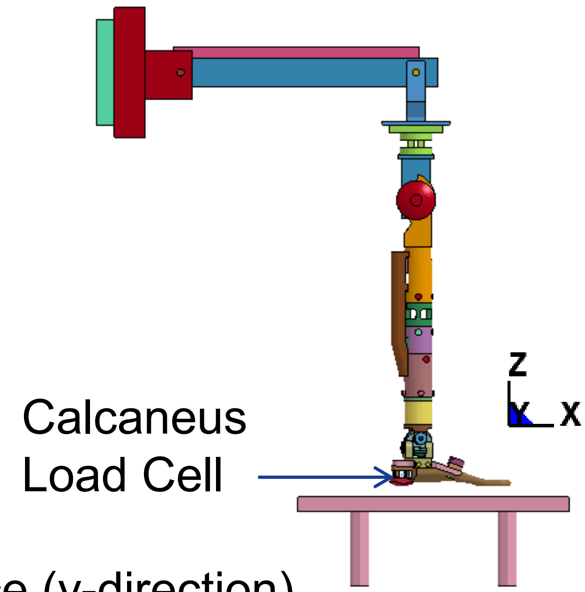

Calcaneus force (x-direction)

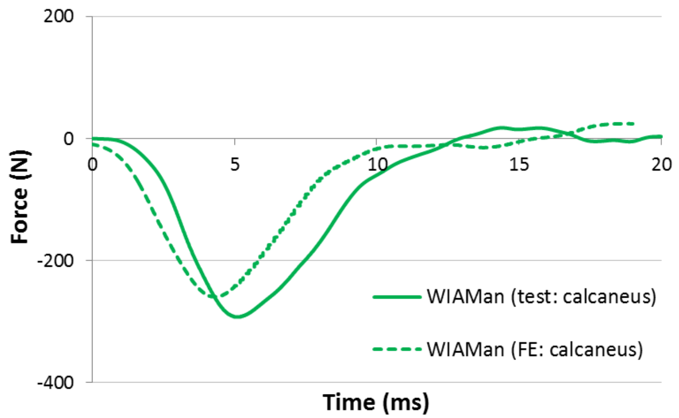

Calcaneus force (y-direction)

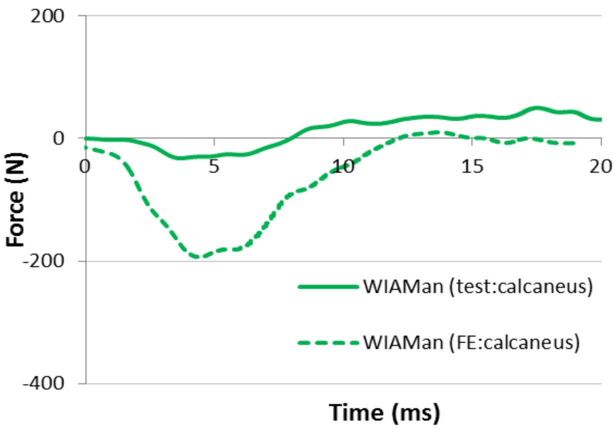

WIAMan Model Validation

Foot ang. rotation (x-direction)

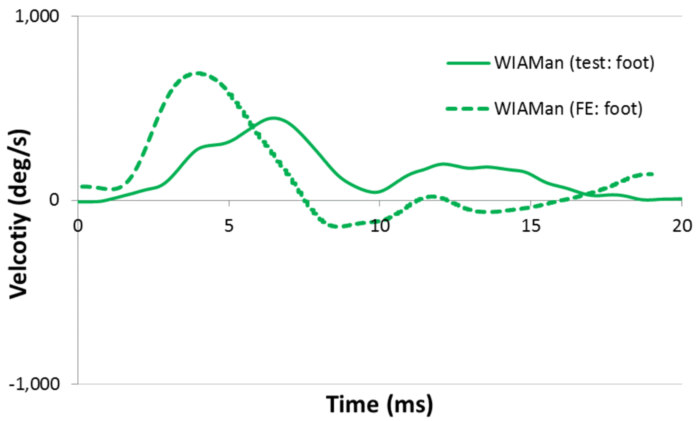

Foot ang. rotation (y-direction)

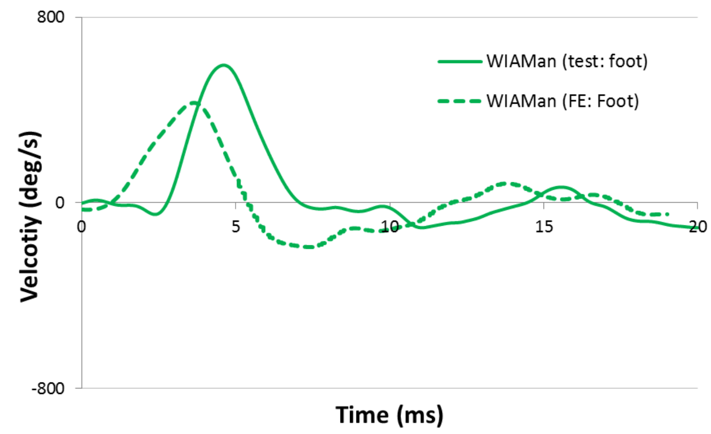

Foot ang. rotation (z-direction)

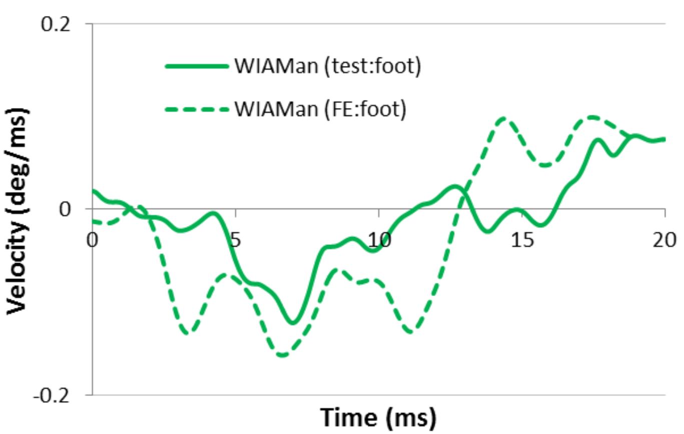

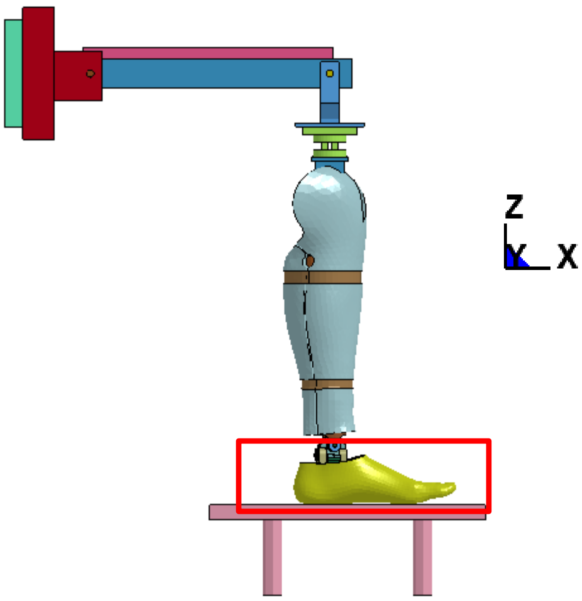

WIAMan Model Validation

Tibia ang. rotation (x-direction)

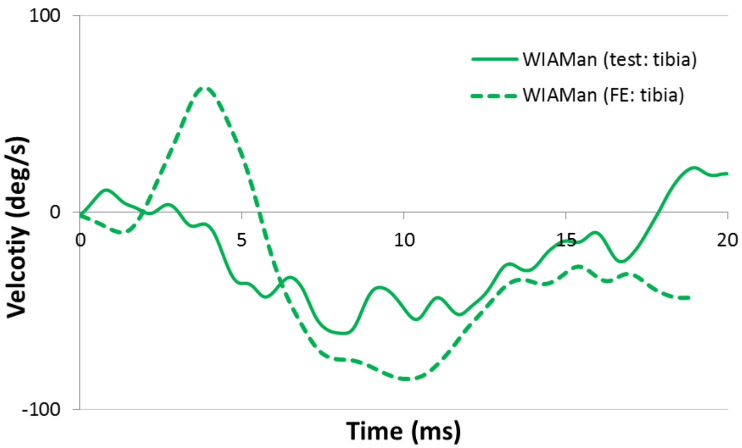

Tibia ang. rotation (y-direction)

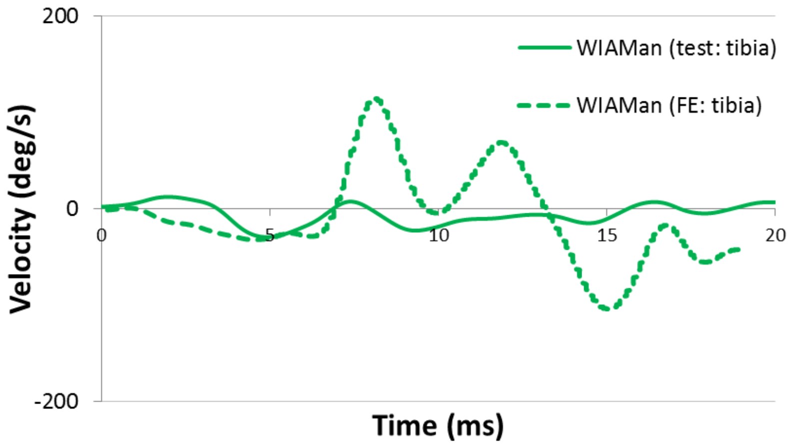

Tibia ang. rotation (z-direction)

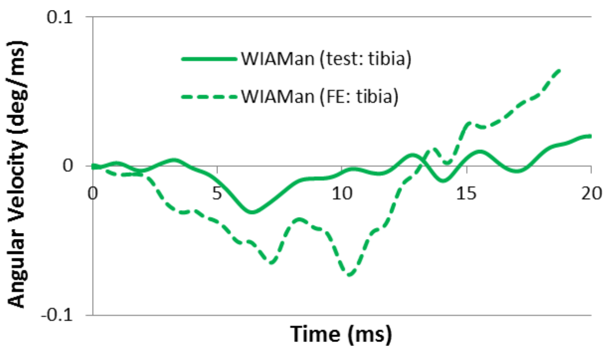

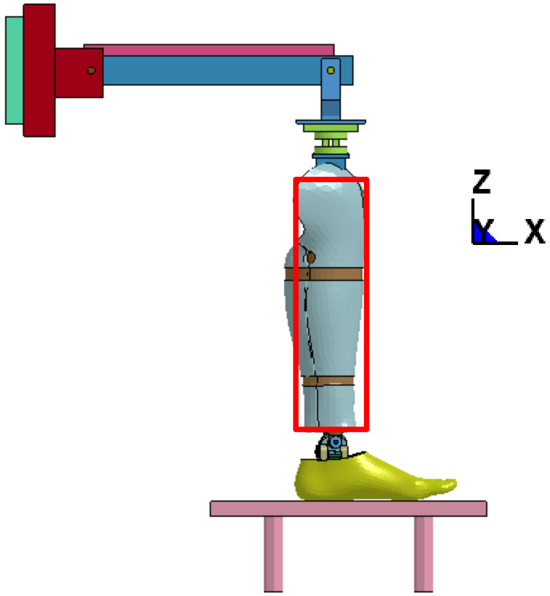

FE Modeling

ATD

Dummy FE Model **Human FE Model**

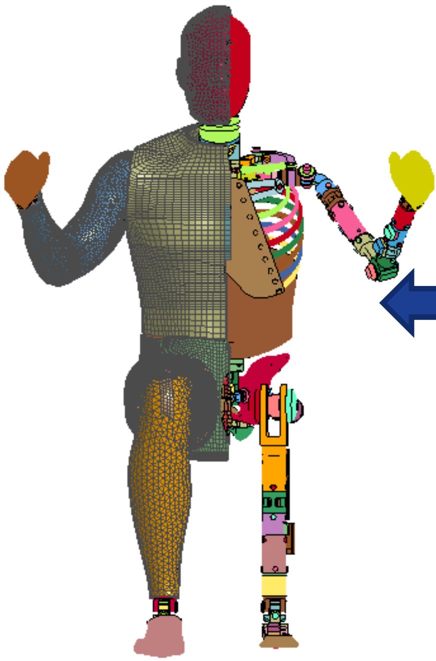

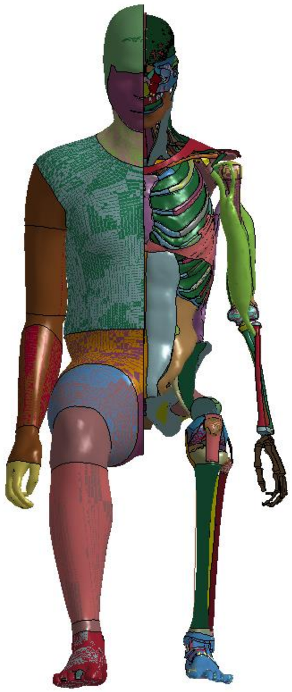

Biofidelity?
Durable
Expensive

Inexpensive
Unlimited "Testing"
Accurate?

Biofidelic
Testing Limitations
PMHS Issues

FE based-Injury surfaces

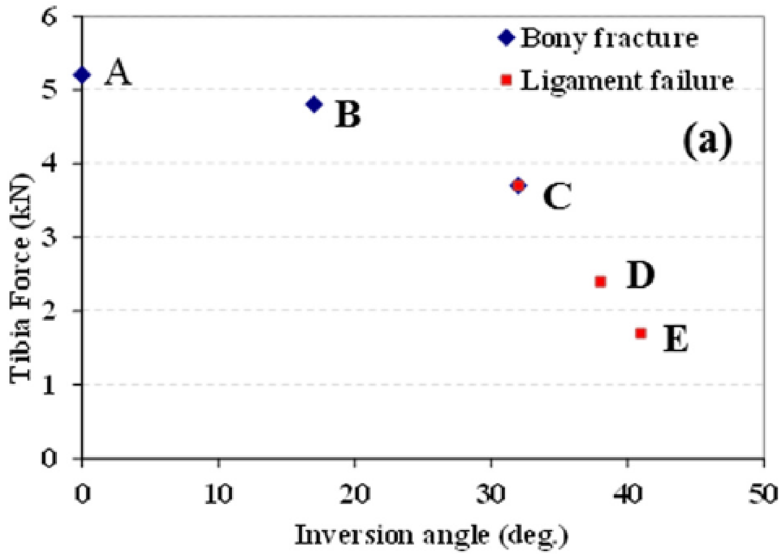

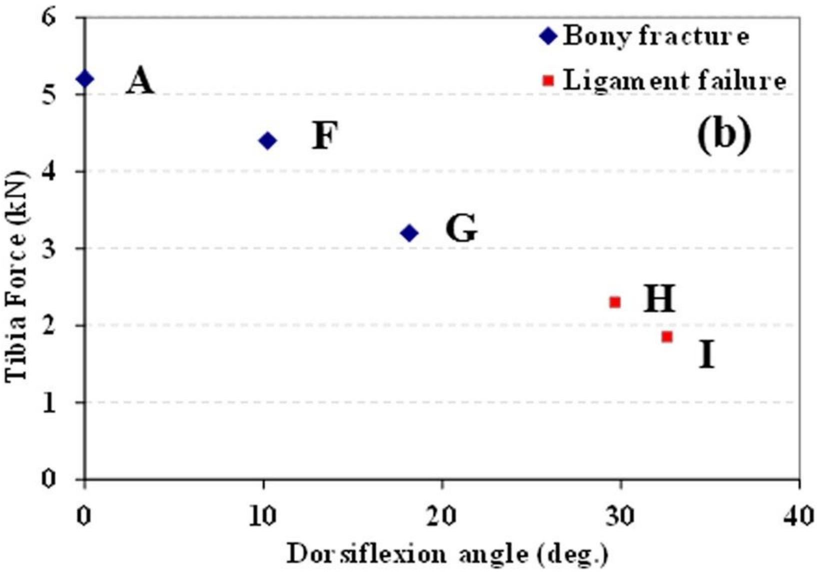

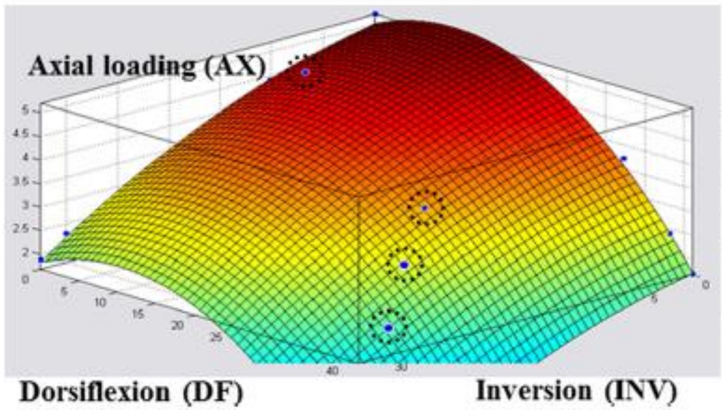

Injury Surface equation :

$f(x,y) = a + b\,x + c\,y + d\,x^2 + e\,x\,y + f y^2$

$a = 5.006E+00$, $b = -3.942E-02$,

$c = 8.004E-02$, $d = -1.769E-03$,

$e = 1.694E-06$, $f = -3.913E-03$

Goodness of fit: $R^2 = 0.9511$

VirginiaTech *Invent the Future*

CORVID TECHNOLOGIES

GHBMC Model Validation & Further Improvements

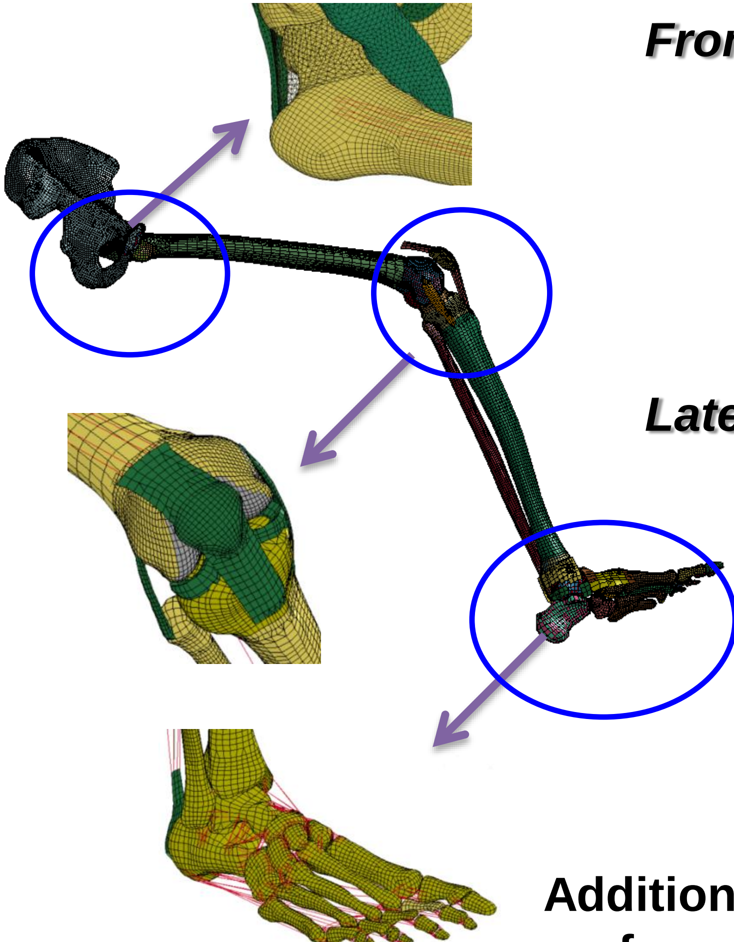

Frontal Impact Validations

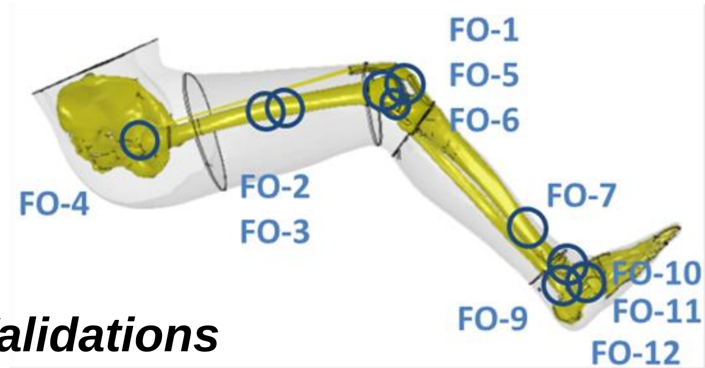

Lateral Impact Validations

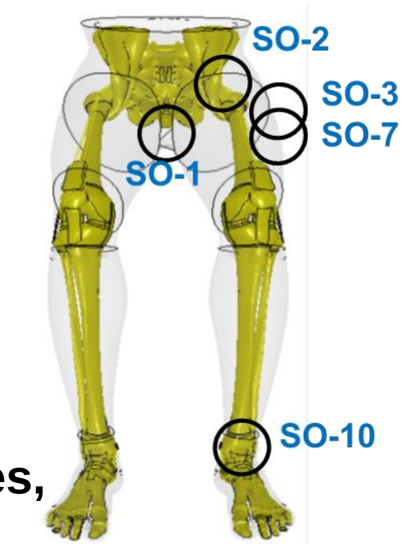

References

1) Shin et al. 2012
2) Untaroiu et al. 2013
3) Shin & Untaroiu 2013
4) Kim et al. 2014
5) Yue & Untaroiu 2014

Additional updates of the model were performed in terms of material properties, contacts, hourglass definition, etc.

VirginiaTech Invent the Future

CORVID TECHNOLOGIES

GHBMC FE Model Validation

Outputs:

- Loadings
  - Upper Tibia (knee) LC forces & moments
- Kinematics
  - Lower 1/3 tibia acceleration
  - Medial calcaneus acceleration
  - Flesh and rig markers for video tracking

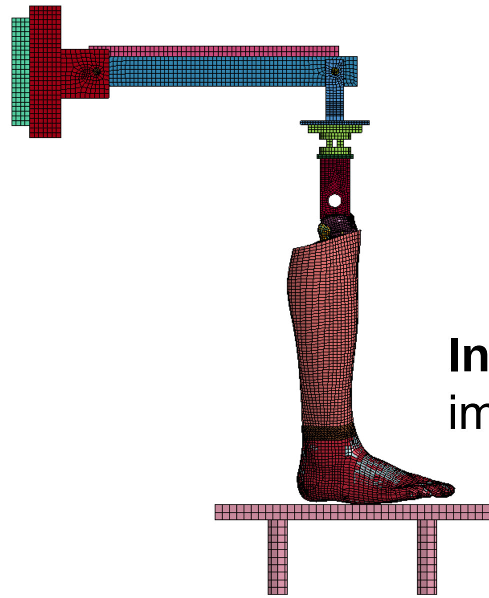

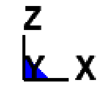

Input: Time history of impact plate velocity

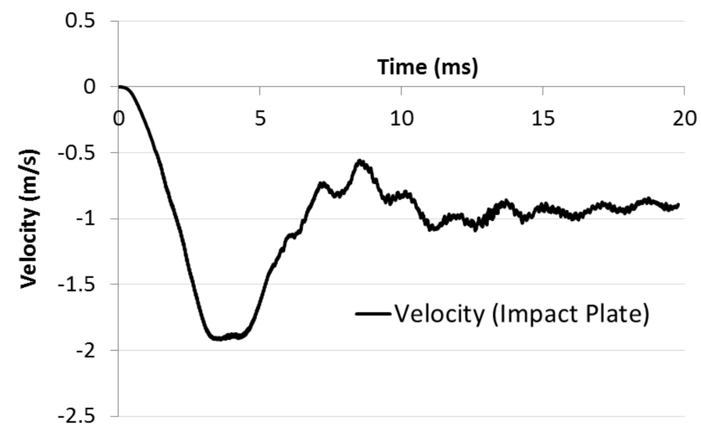

GHBMC FE Model Validation

Upper Tibia (knee) Force (z-direction)

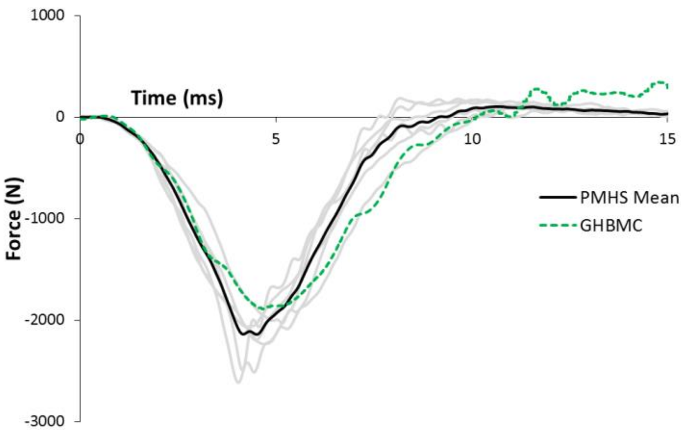

1/3 Tibia Acceleration(z-direction)

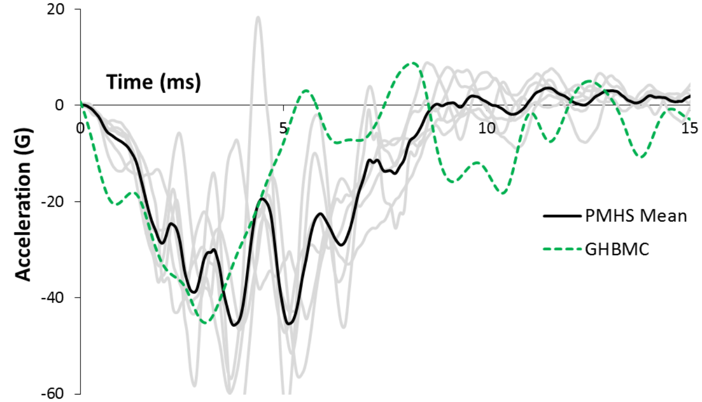

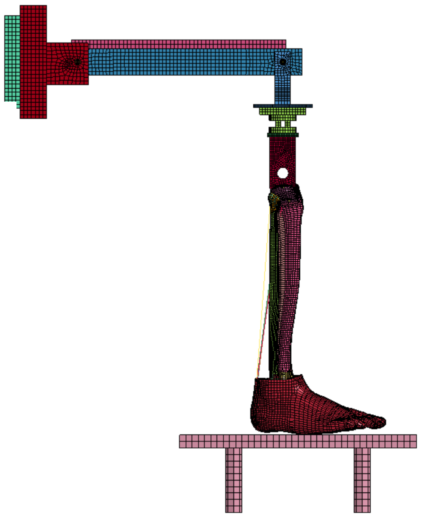

Upper Tibia (knee) Force (x-direction)

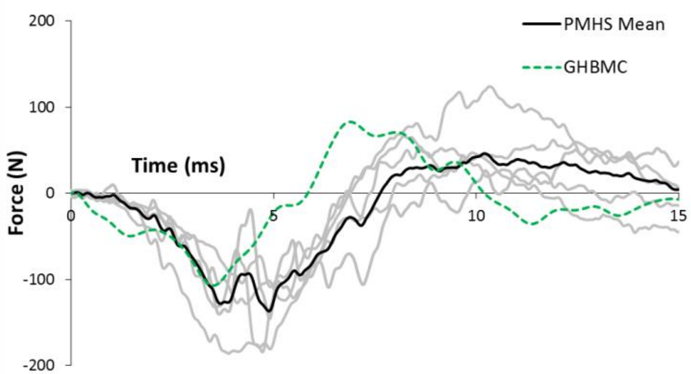

Tibia Angular Rotation (y - axis)

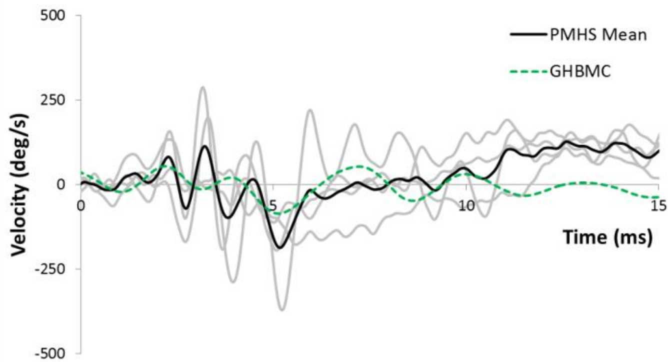

GHBMC FE Model Validation

Calcaneus Accel. (z-direction)

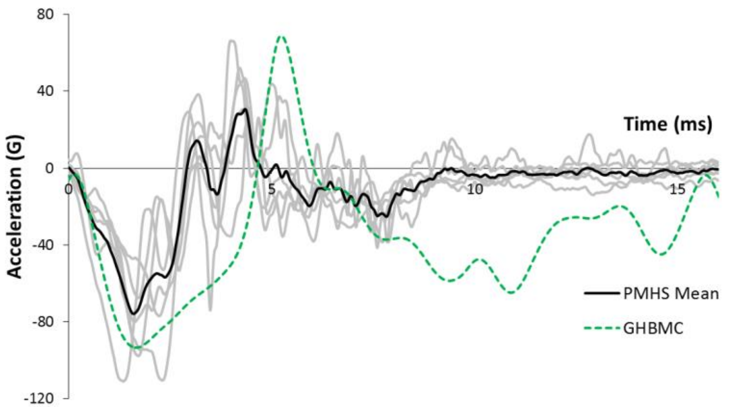

Heel Displacement. (z-direction)

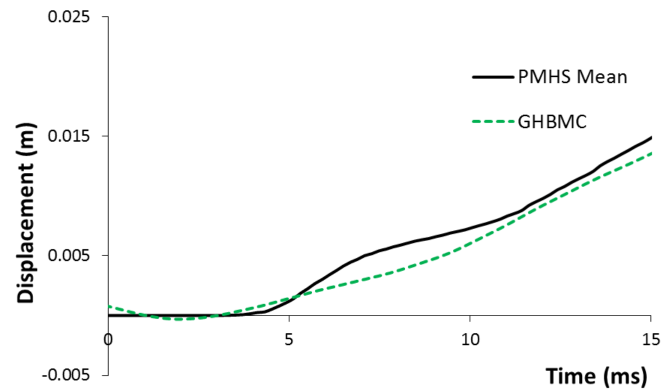

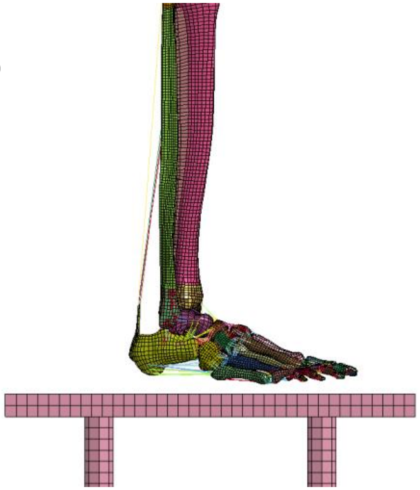

Heel Displacement. (x-direction)

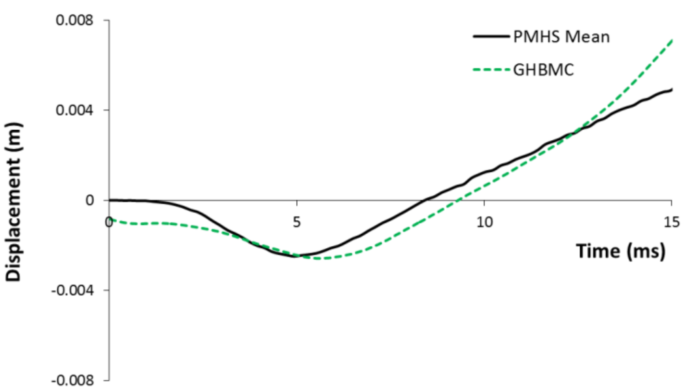

Ankle Compression. (z-direction)

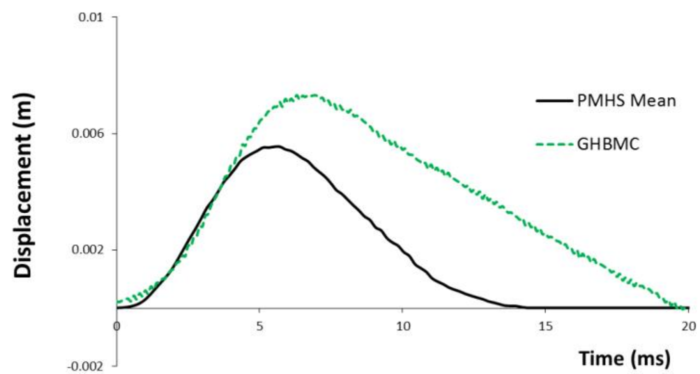

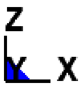

Limitations & Future work

- The WIAMan lower limb FE model was developed based on CAD data and mostly assumed mass densities. In future, the inertial properties of the whole lower limb model will be verified against corresponding measured properties of physical dummy. If mass discrepancies will be observed, the model will be updated and its results compared to test data
- The FE model was verified only against test data recorded in one impact configuration. To increase the confidence in the model, more verifications of the lower limb FE model against various impact conditions will be performed.

- The current verification of the dummy model was performed mostly by visual comparisons. Objective rating systems (e.g. CORA) will be used in future during the process of model improvement.
- The current lower limb model tries to replicate the physical WIAMan dummy. However, to quantify the injury risk based on the dummy responses, dummy-human transfer functions should be developed by using PMHS data and simulations with human FE models.

Conclusions

- A FE model of WIAMan Lower Limb was developed based on the CAD data.
- The material properties were assigned based on material testing and literature data.
- The model was verified by simulating of an axial impact test performed on the physical dummy.
- Overall, the model response showed good correlation to test data and PMHS leg data
- Further improvements of the model are currently performed and the final validation will be presented in a research paper.

WIAMan Lower Leg Strength of Design and Soft Materials Sensitivity Study using Design of Experiments

Michael Boyle[1], Thomas Magee[1], Andrew Lennon[1], Robert Armiger[1], Mostafiz Chowdhury[2]

[1]Johns Hopkins University Applied Physics Laboratory
[2]U.S. Army Research Lab, WIAMan Engineering Office

Strength of Design

Lower Leg Pretest Modeling

Series ID #	PPE	Posture	Test Type	Velocities (m/s)	Model Image
LL01, LL03, LL04	Booted	90-90	Slap	4, 6, 8	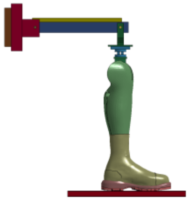
LL08	Unbooted	90-90	In-Contact	2, 4, 6, 8	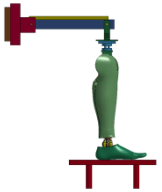
LL11	Booted	Dorsi-flexion Ankle angle = 75 degrees	In-Contact	2, 4, 6, 10	
LL12	Booted	Plantar-Flexion Ankle Angle = 110 degrees	In-Contact	2, 4, 6, 10	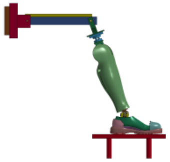

VirginiaTech Invent the Future

CORVID TECHNOLOGIES

APL

Model Conditions

- ARL Boot Model
- Foot is settled into boot
- Plate velocity is prescribed from BRC test data previously performed for this series

- Boot upper fabric was not modeled because of fitment issues
- Original Leg flesh is used
- Compliant element is uncompressed
- Material properties for “soft” materials are derived from Veryst test data

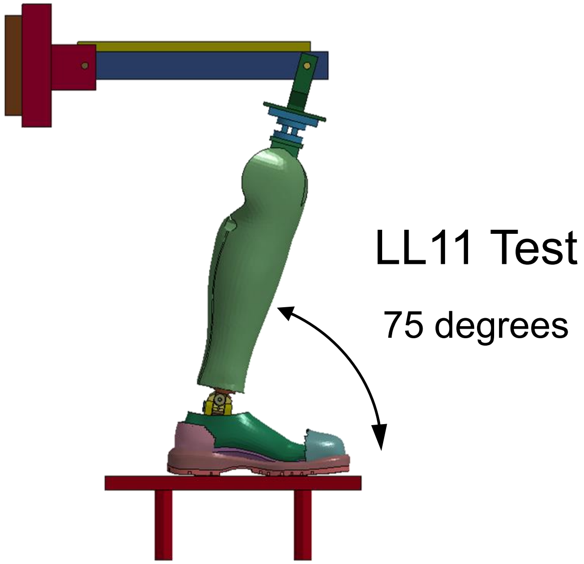

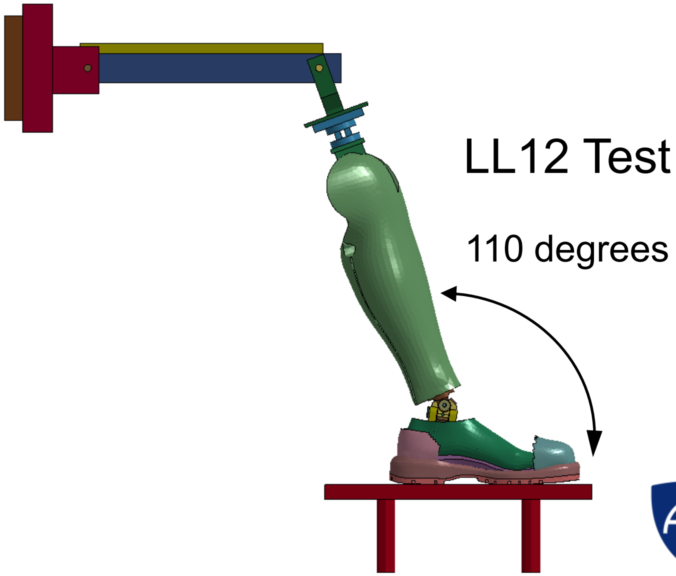

LL11 Animation, 10 m/s

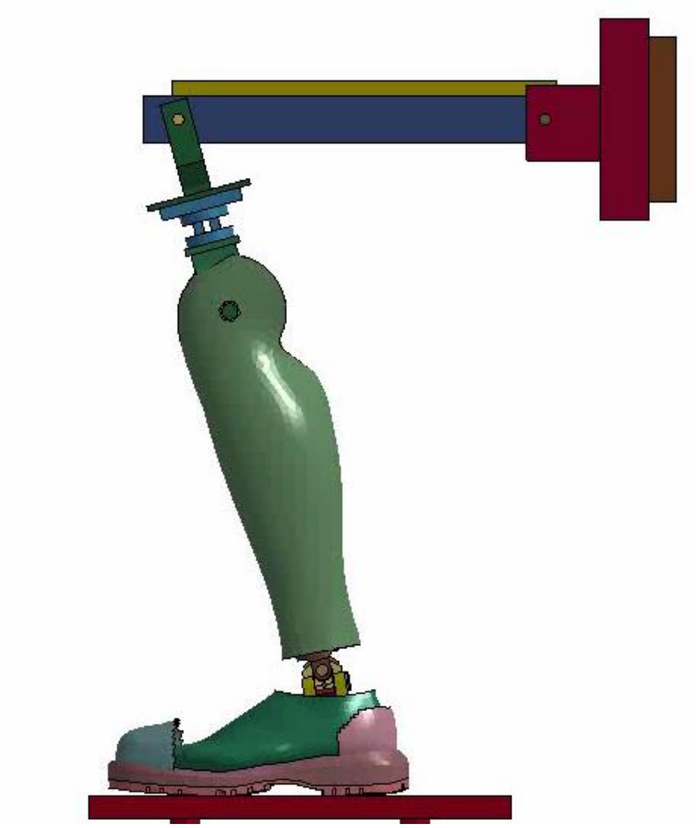

Full view showing 30 msec of impact after settling is complete

Cutaway flesh View with upper boot and flesh turned off showing 20 msec of settling then 30 msec of impact.

Foot Plate Strength of Design

- Maximum strain rate from analysis = 24/sec
- Closest test curve is 75/sec
  - Yield Strength ~ 0.032 GPa
  - Ultimate Strength ~ 0.035 GPa
- Expected to Fail at 10 m/s
  - FS_ult = 0.035/0.048 = 0.73
  - Less than 1 means failure

Result shown is at 28.4 msec for LL11 at 10 m/s

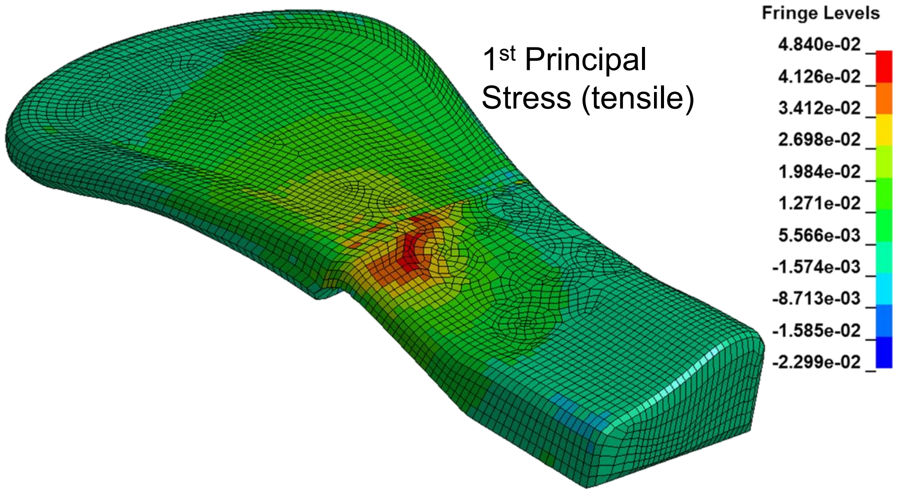

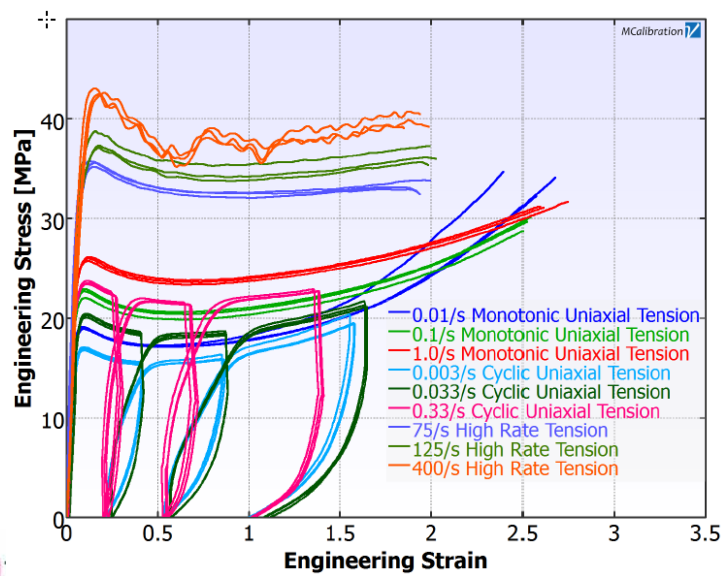

Virginia Tech
Invent the Future

Section view of Foot Plate at high stress location at the thinnest area near the metal insert

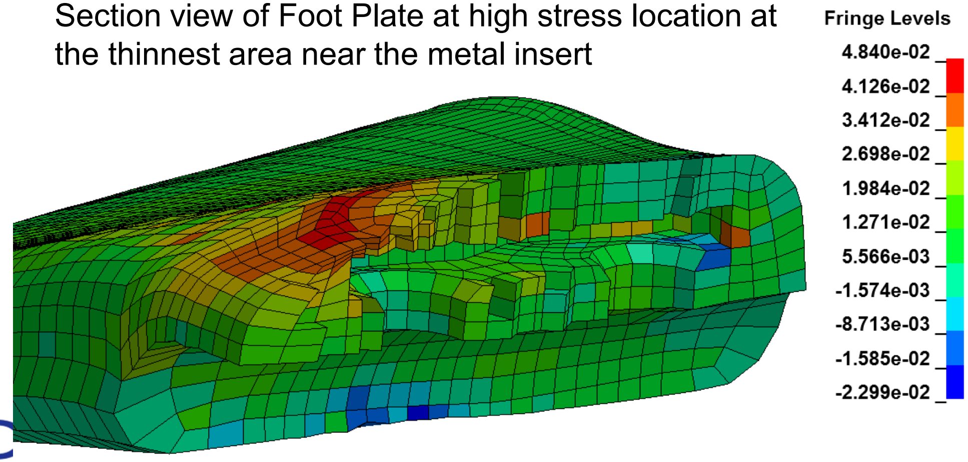

Factor of Safety for LL11

- At 6 m/s the Screws, Delrin Sleeve, and Upper Rotating Groove may see failure
  - Footplate survives at this velocity
- Footplate and Calcaneus Cap may fail at 10 m/s
- Titanium parts should survive 10 m/s

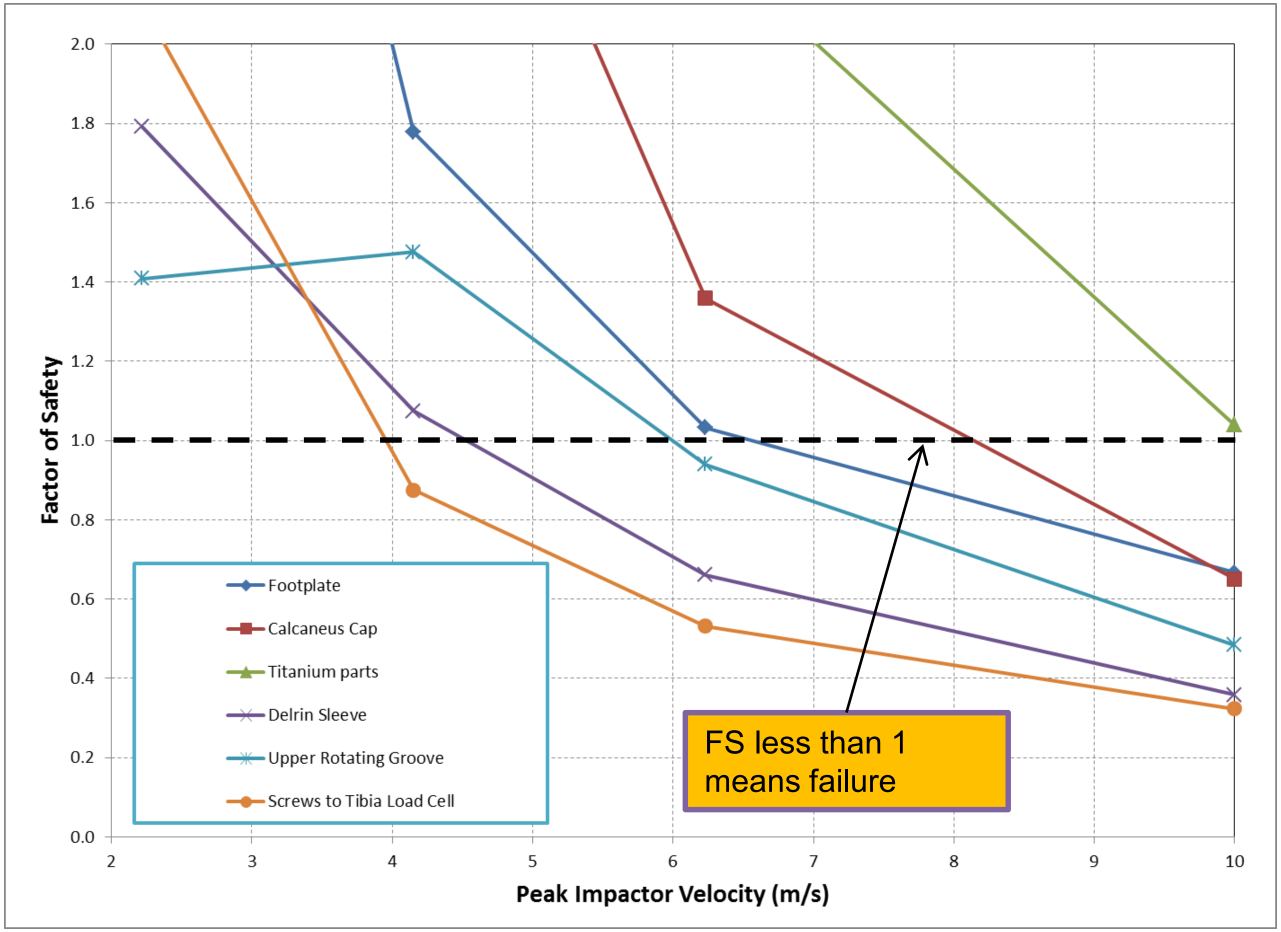

VirginiaTech Invent the Future

CORVID TECHNOLOGIES

APL

The Nation's Premier Laboratory for Land Forces

Conclusions for SOD

- Some parts may experience failure during upcoming proposed tests
  - Posture LL11 appears to be more severe for the upper leg parts while LL12 is more stressing on the Footplate
  - The LL08 90-90 posture without a boot could also fail the footplate at 6 m/s
  - Between 6 and 10 m/s appears to be the threshold of damage
  - Lower velocity tests should be safe
- Inspection of damage will be difficult
  - Footplate is inside of foot flesh and cannot easily be inspected
    - Suggest flexibility testing before and after each test or CT/X-ray
  - Some parts may undergo plastic strain but not fail
    - Suggest to inspect gaps and looseness between parts before and after each test
      - Particularly for the pin joint and compliant element in bending
    - Check for screws bending
      - Perhaps loosen and retighten screws as an inspection method between tests

Soft Materials Sensitivity Study using Design of Experiments

Sensitivity DOE

- Statistical Design of Experiments (DOE) was used to determine sensitivity of LL response to the stiffness of the compliant materials
  – 4 continuous parameters (2 rubbers and 2 plastics)
  – One categorical "Boot" parameter to determine how presence of the boot affects the influence of the compliant materials
  – 2nd order effects and 2-factor interactions are included in DOE
  – Total of 29 simulations performed

Parameter	Low	Middle ("TDP")	High
Tibia Damper Durometer (Shore A)	60	75	85
Foot Flesh Hardness (Shore A)	15	30	45
Calcaneus Modulus (GPa)	2.2	3.2	4.2
Foot Plate Modulus (GPa)	0.26	0.38	0.50
Boot	Booted		Unbooted

FEM Simulation Results – Knee Axial Force (Fz)

- Knee Fz histories are shown for each simulation run
- Presence of the boot dominates peak Fz and time to peak
  - Unclear from this plot if there are important boot interactions
- Booted tests show relatively narrow range of peak compressive force
  - Despite large variation in the other compliant materials

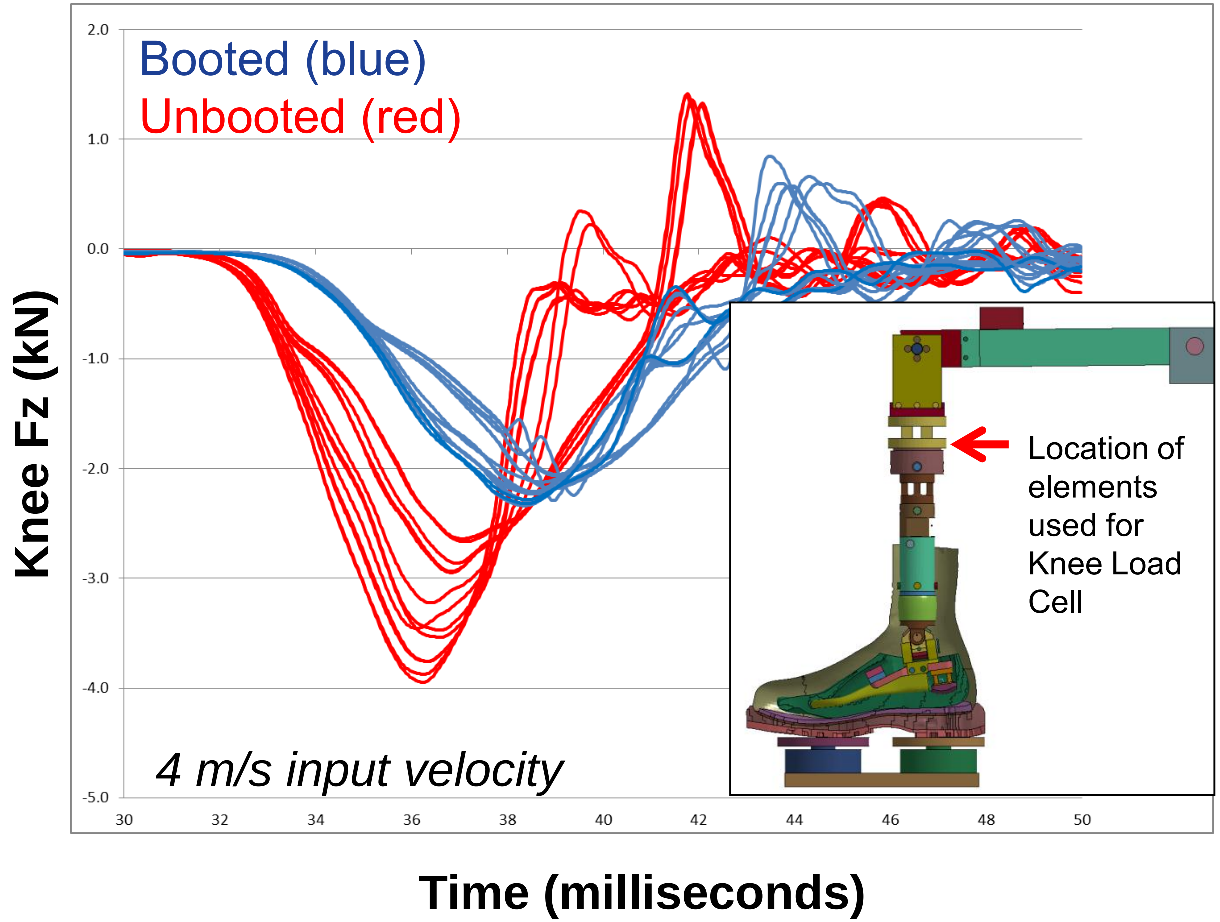

Significant Model Effects – Compressive Peak Knee Fz

- Five of the model effects appear to be significant (FDR LogWorth > 2):
  - Boot
  - Tibia Damper Hardness (TDH)
  - Interaction of TDH and Boot
  - Foot Flesh Hardness (FFH)
  - Interaction of FFH and Boot
- Note that the Boot interaction with the Tibia Damper is more significant than the Foot Flesh

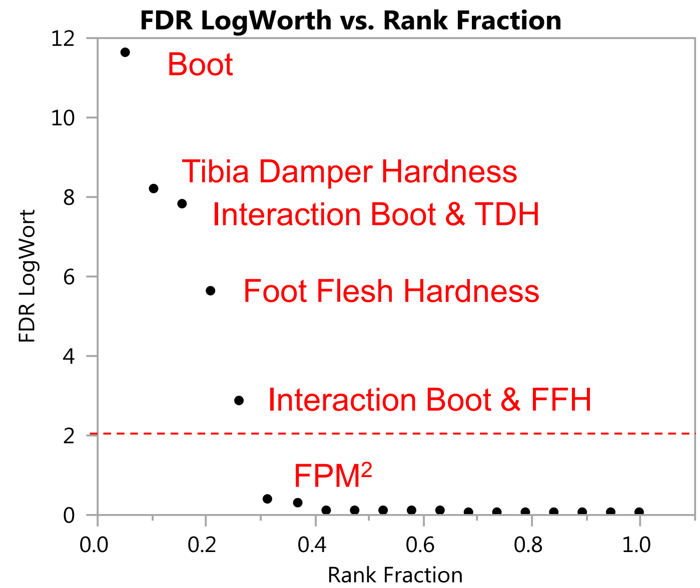

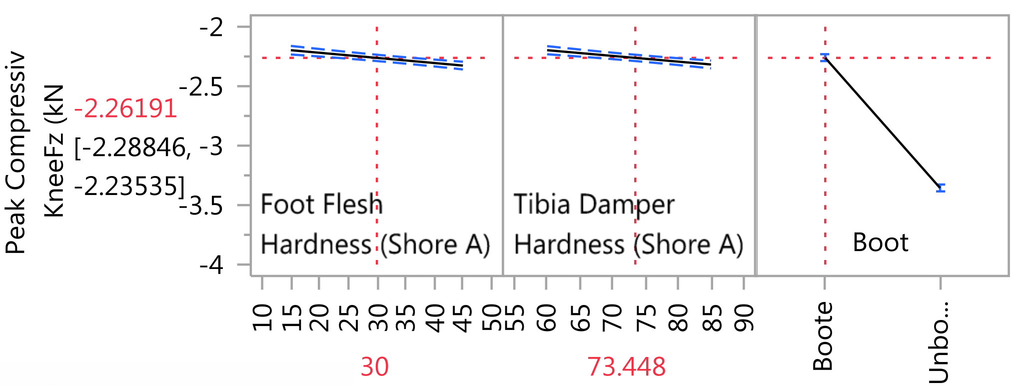

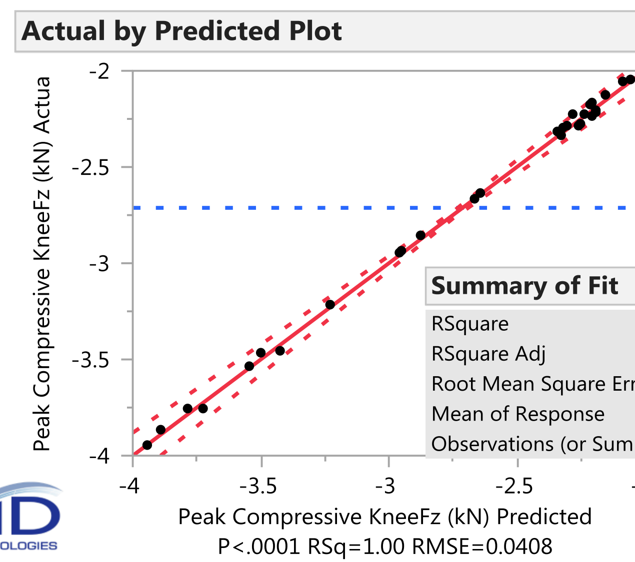

Summary of Fit

RSquare	0.998662
RSquare Adj	0.995838
Root Mean Square Error	0.040839
Mean of Response	-2.71206
Observations (or Sum Wgts	29

Significant Model Effects – Peak +Y-Moment

- Foot Plate Modulus is the most significant effect for the +Y-Moment response at the knee
  - Interaction of the Boot and Tibia Damper Hardness is also highly significant
- Note that the maximum FDR LogWorths are lower for the Peak +Y-Moment than for the Peak Compressive Force
  - Indicates that influence is spread more evenly over the model effects

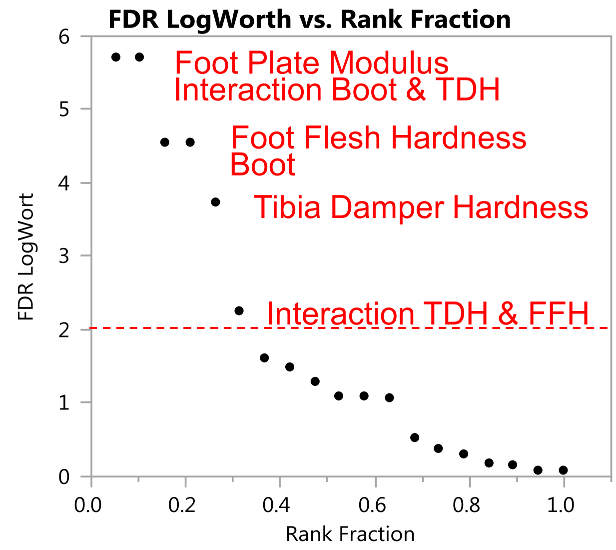

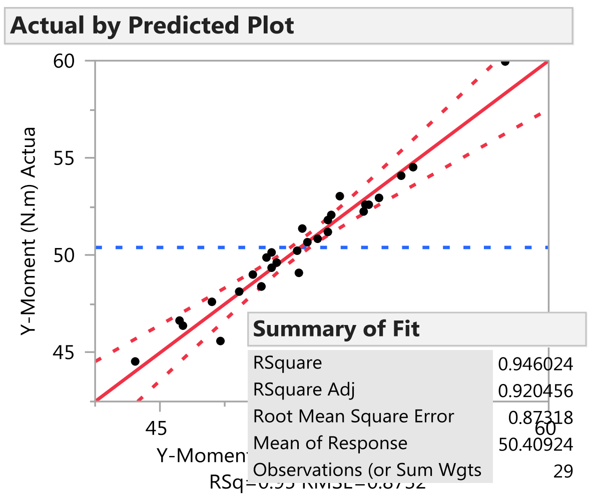

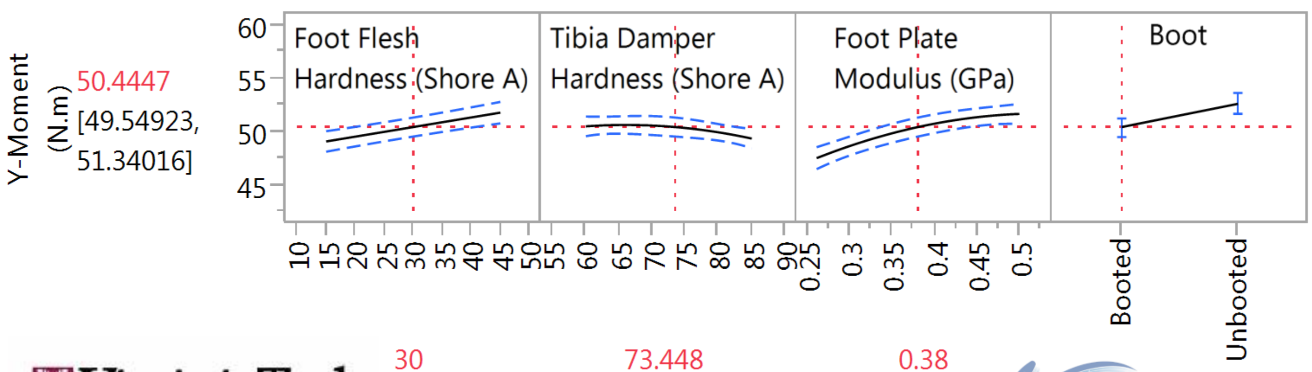

Conclusions for DOE

- The boot, tibia damper, and foot flesh have a significant effect on the responses of the lower leg assembly
- In addition, the foot plate modulus has a significant effect on the +Y-moment at the knee
- Calcaneus cap has negligible effect on the responses studied
- For the range of "reasonable properties" for the compliant materials that were simulated in the FEA, the effect on the lower leg responses measured was smaller than expected
  - For example, based on DOE model predictions, for a booted lower leg, the maximum variation in peak compressive force at the knee over the range of properties simulated is 16%
  - Maximum variation in time to peak compression is 10%
  - Maximum variation in +Y-moment at the knee over the range of properties simulated is 20%

WIAMan Finite Element Model Development and Application

January 12, 2016

Cameron Bell[1], Adam Kareem[1], Garrett Kiessling[1], Kevin Lister[1], Horacio Nochetto[1], Corbin Robeck[1], Allen Shirley[1], Caleb Yow[1], Mostafiz Chowdhury[2]

[1]Corvid Technologies, [2]WIAMan EO

WIAMan Modeling

High fidelity modeling approach provides the detail required for the complete performance evaluation for WIAMan through explicit modeling of:

- **Structural bolts and pins** to assess strength of all connections
- **Joints** motion based on explicit contact which allows for damage assessment within the joint itself
- **Load cells** modeled with a four-post design to mimic the physical system for superior accuracy and strength of design evaluation
- **6DX blocks** modeled for assessment of acceleration and angular rotation traces

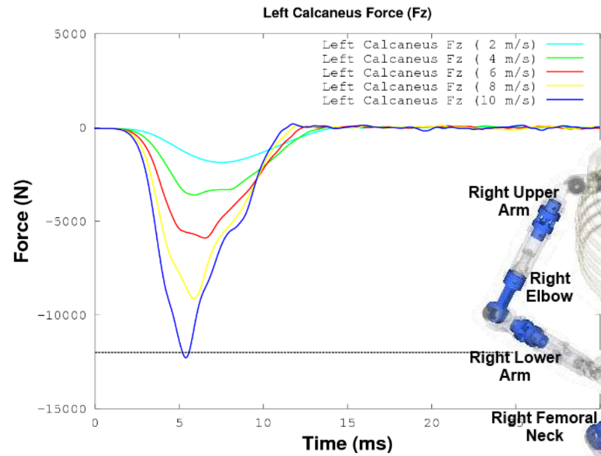

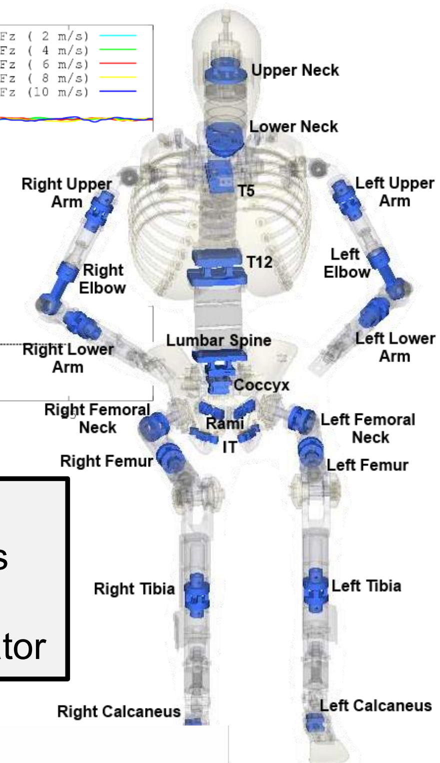

WIAMan ATD model includes all load cells contained in the Technology Demonstrator

Detailed modeling of all structural components of the WIAMan ATD down to the hardware level

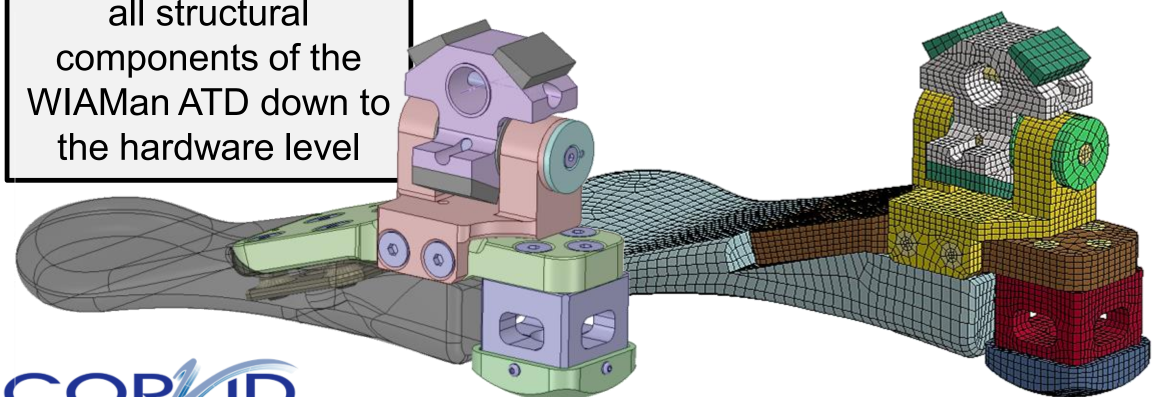

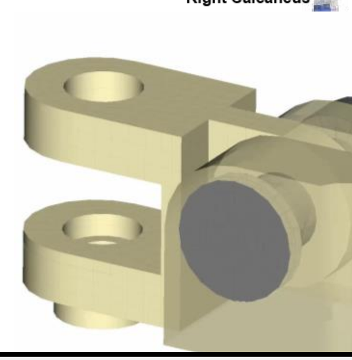

All joints modeled and **verified**

The Nation's Premier Laboratory for Land Forces

Whole Body: Mesh

- **Geometry (526 Parts):**

Type	Count
Solid	518
Shell	8

- **Mesh (1.5M Elements):**

Type	Count	Elem Type
Solid	1.49M	Hex 1.13M
		Tet 367k
Shell	8k	Quad

Tet: Flesh, Pelvic Bone Skull

- **Materials (29):**

Type	Count
Metal	11
Polymer	18

- **Time Step:** 5.25e-8s

TDP CAD

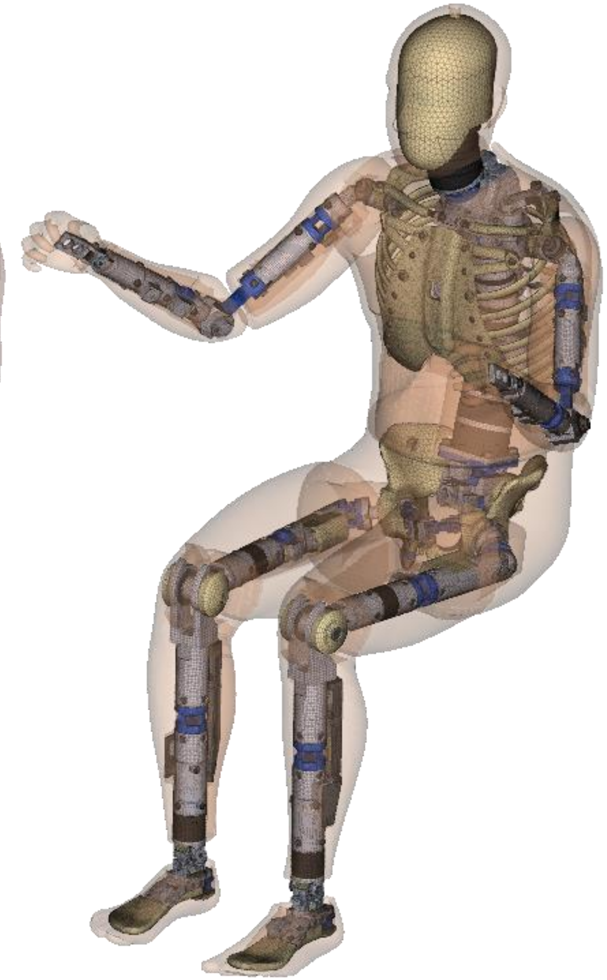

Tech Demonstrator Mesh

Whole Body: Mass

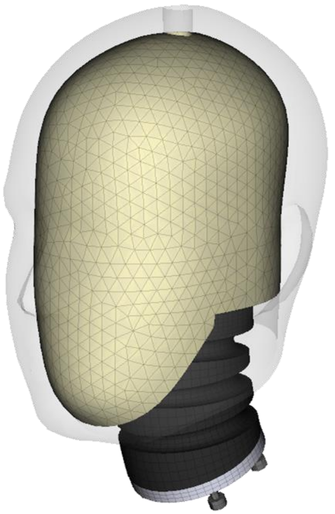

Subsystem	Mass (kg)
Head	6.1
Thorax	24.7
Left Arm	5.1
Right Arm	5.1
Pelvis	14.1
Left Leg	13.1
Right Leg	13.1
Total	**81.3**

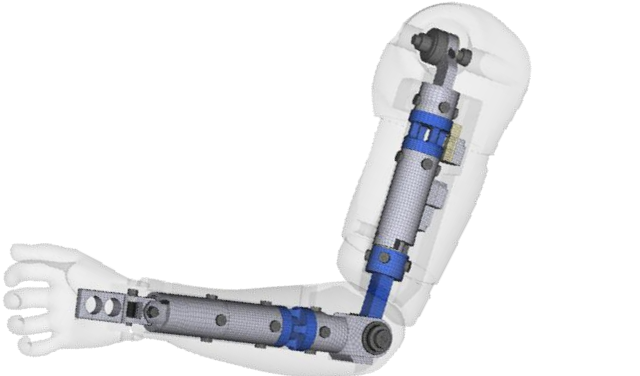

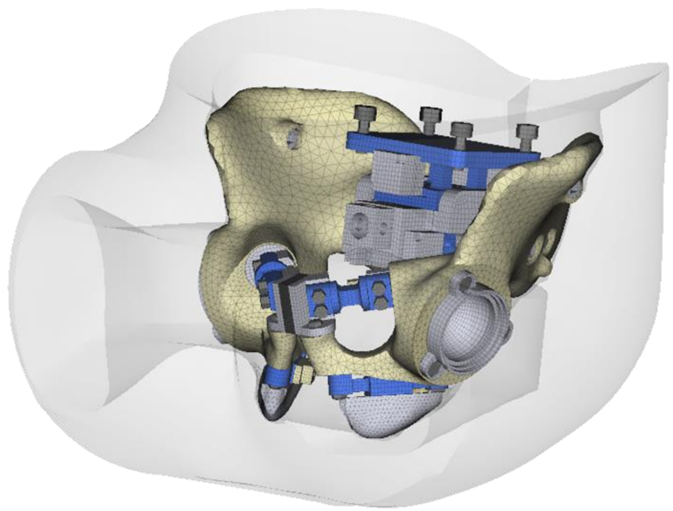

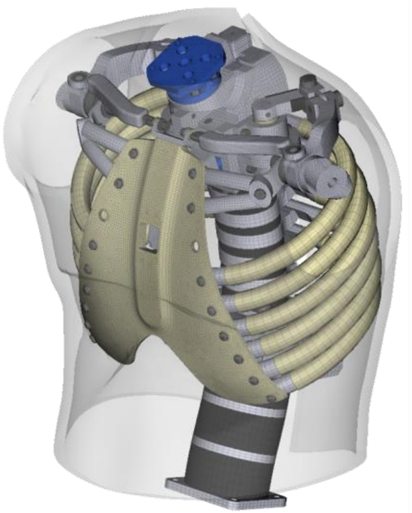

Tech. Demonstrator is 2.9kg light of 84.2kg target mass as well

WIAMan Model Development

- Initial testing of subsystem models:
  - Lower Leg, Pelvis and Lumbar Spine
- Component level simulations achieved two goals:
  - i. **Model verification** while exploring the WIAMan model response in a realistic loading environment
  - ii. **Highlighted high risk areas** within the WIAMan design which resulted in changes to the TDP

MCW Test Rig (Pelvis Configuration)

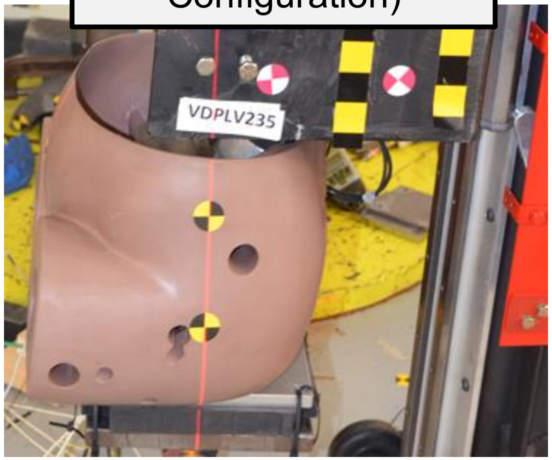

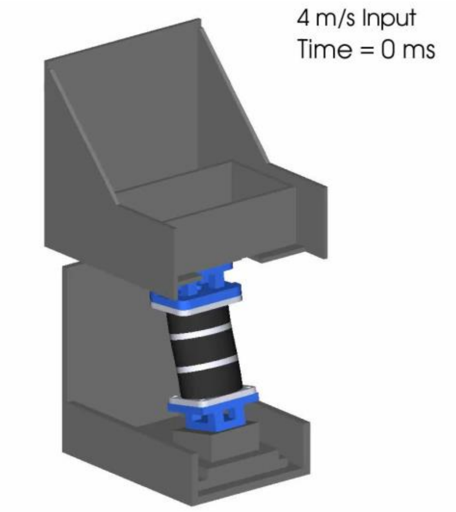

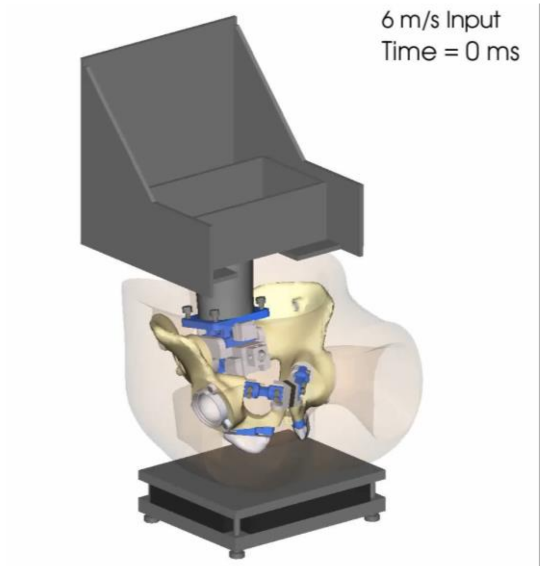

Early Lower Leg Model Testing

Von. Mises Stress

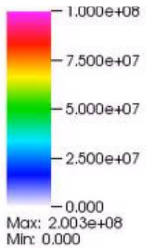

Excessive motion in the tibia compliance element and ankle resulted in design modifications

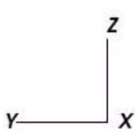

Lower Leg Design Modifications

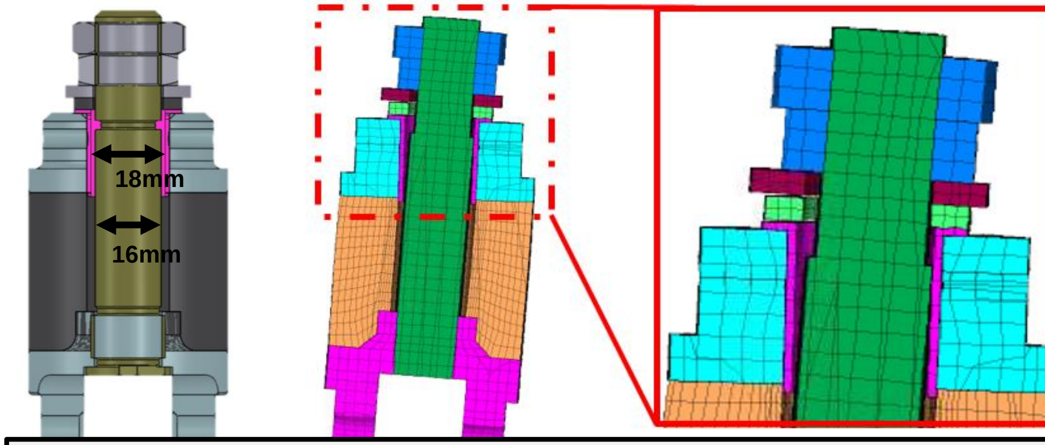

Gap between bushing and central shaft resulted in addition of unwanted tibia bending. Shaft and bushing were resized.

Contact between ankle and stops differed from design intent. Talus dimensions were changed to achieve proper response.

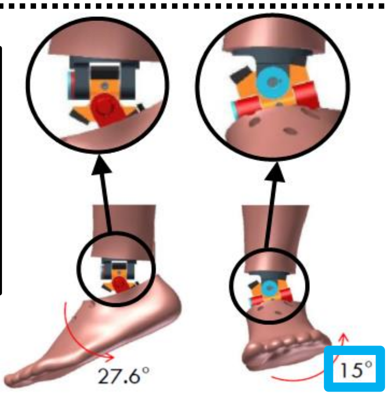

Analysis of WIAMan Lower Leg highlighted design issues in the tibia and ankle. Findings **impacted TD -> TDP design changes**.

Al Compliance Element Testing

- Aluminum compliance element for VALTS tibia rig validation
  - Served as the **first validation test** for the WIAMan lower leg structural model (April 2015)
  - **Builds confidence** in the meshing and material modeling of the metallic components

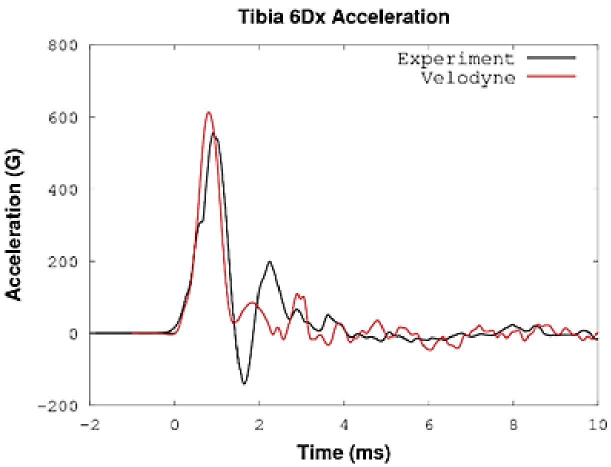

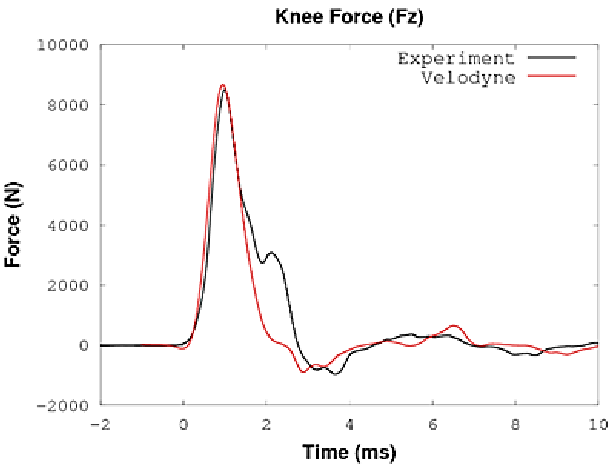

	Experimental	Simulation	% Difference	Filter
Force (N)	8490.4	8673.6	2.2	CFC 600
Acceleration (Gs)	556.25	612.79	10.2	CFC 1000

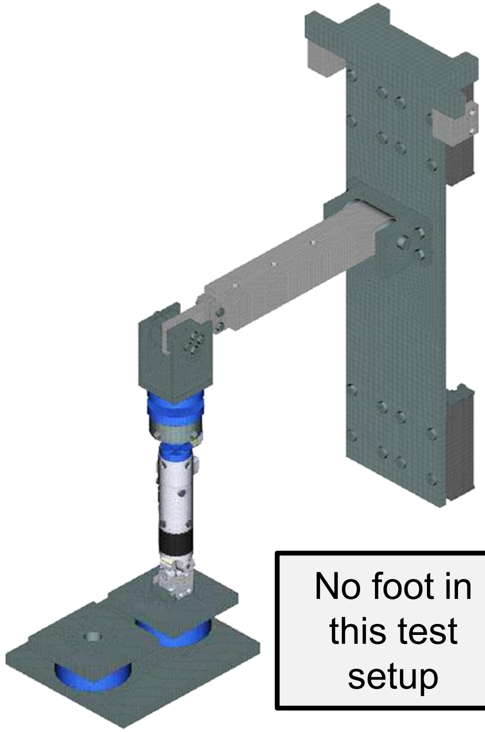

No foot in this test setup

Blind prediction showed excellent agreement without need for any modifications. Builds confident in the **predictive modeling process**

Pelvis Component Investigation

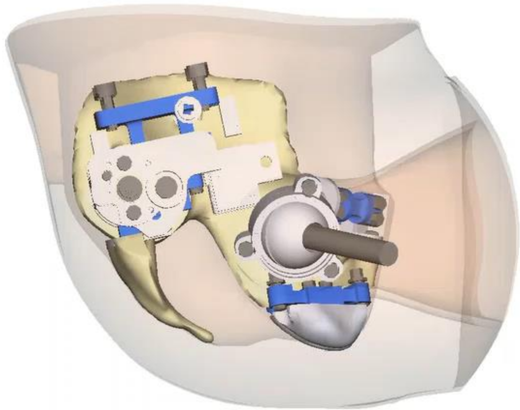

Coccyx Force, Fz

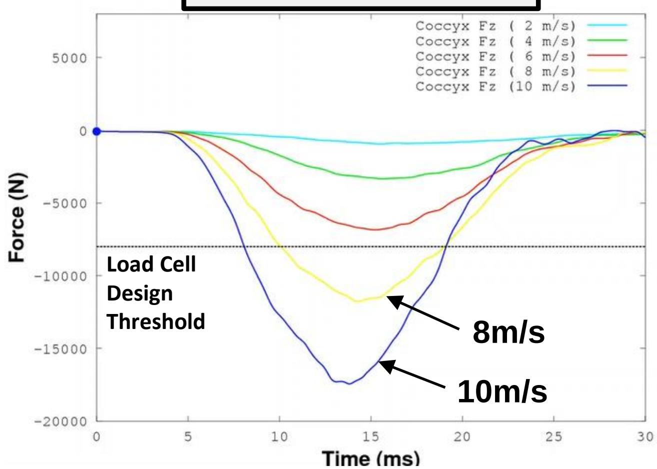

Severe pelvis loading in rigid VALTS seat.
Permanent deformation isolated to thermoplastics

Pelvis Plastic Deformation

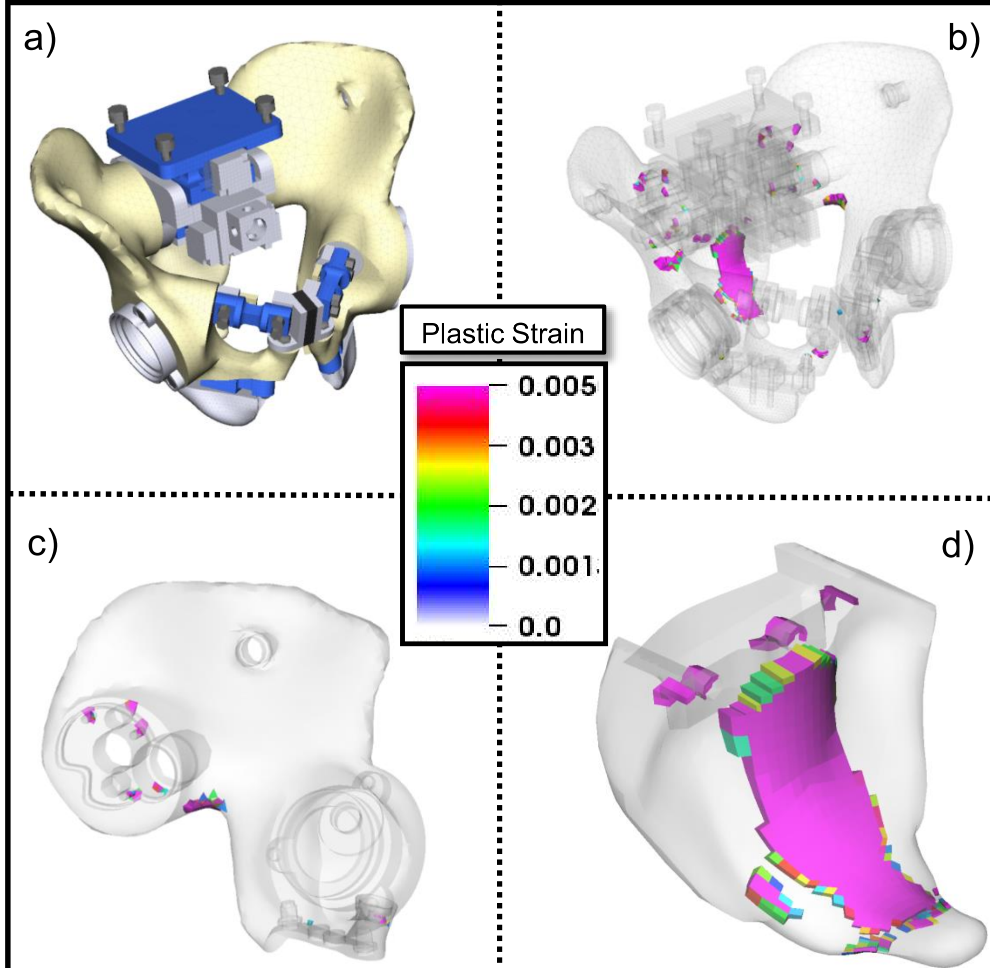

a) Pelvis assembly, b) Plastic deformation observed during **8m/s** VALTS impact. All plastic deformation is observed in the c) pelvic bones and d) the molded tailbone

Lumbar Spine Demonstrator

- Parameterized a rate-dependent material model based on **EPDM 75A** characterization data
- **High degree of correlation** throughout entire test duration
  - Captured damping effects
- **Verification** of meshing approach and material modeling
  - Demonstrates the “plug-n-play” capabilities of the model that readily accommodates material changes
- Lumbar spine demonstrator process produced a **suite of validated rubber material models** which can be utilized throughout the WIAMan ATD moving forward

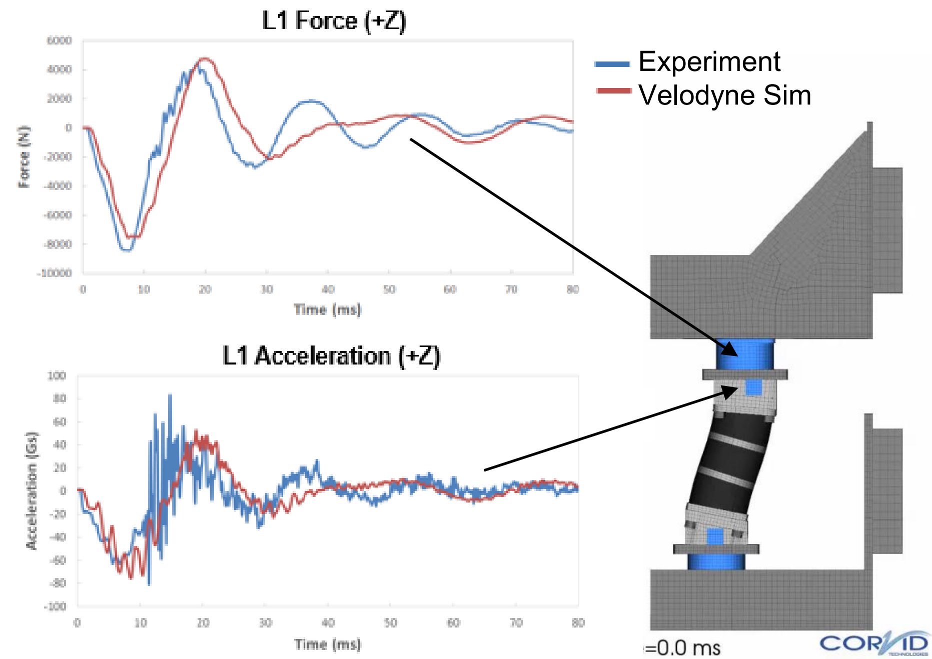

EPDM 75A CORA Evaluation				
	Corridor	Cross Correlation	Size	**Total**
0.8 m/s	0.529	0.637	0.672	**0.592**
1.2 m/s	0.589	0.701	0.855	**0.684**
2.4 m/s	0.713	0.856	0.974	**0.814**
3.4 m/s	0.825	0.926	0.987	**0.891**
4.4 m/s	0.864	0.947	0.975	**0.913**
5.4 m/s	0.903	0.954	0.996	**0.939**
6.0 m/s	0.911	0.961	0.956	**0.935**

Blind prediction of lumbar spine response over entire loading region **demonstrates model maturity**

WIAMan SoD: Whole Body

- Simulation of **VALTS environment**: 2,4,6,8,10m/s Peak, 4ms TTP
- **Strength of design (SoD)** analysis has highlighted all components that undergo **permanent deformation** over the range of loading conditions
  - Highlighted additional areas of concern for the WIAMan program that were not part of component level testing (i.e. **shoulder design**)

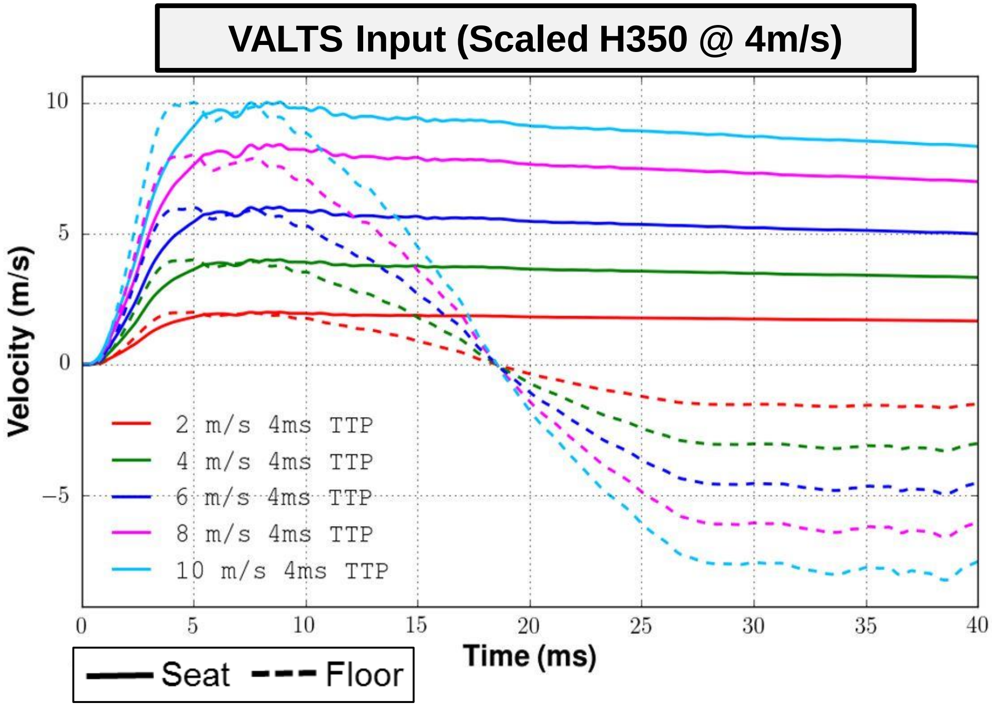

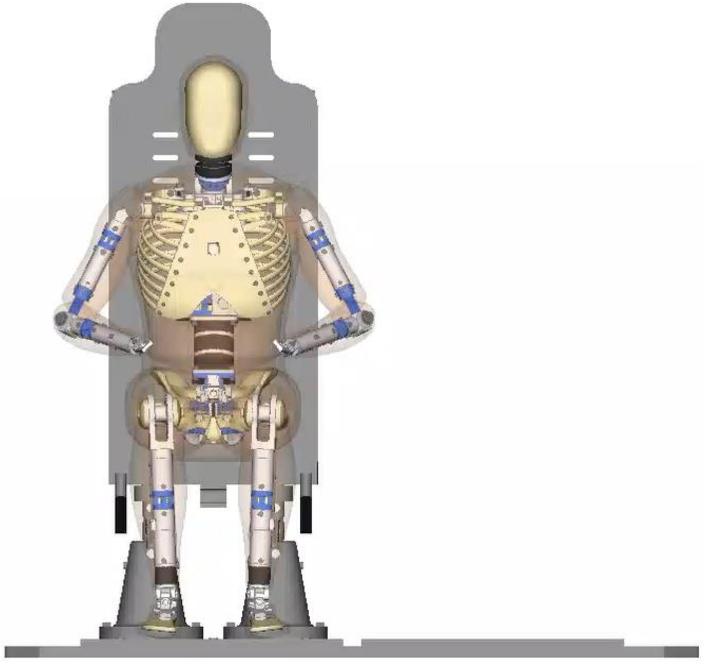

A 10m/s VALTS impact is a very server case, perhaps beyond design limit

Leg Plastic Strain

2 – 10 m/s VALTS (Whole Body) Analysis

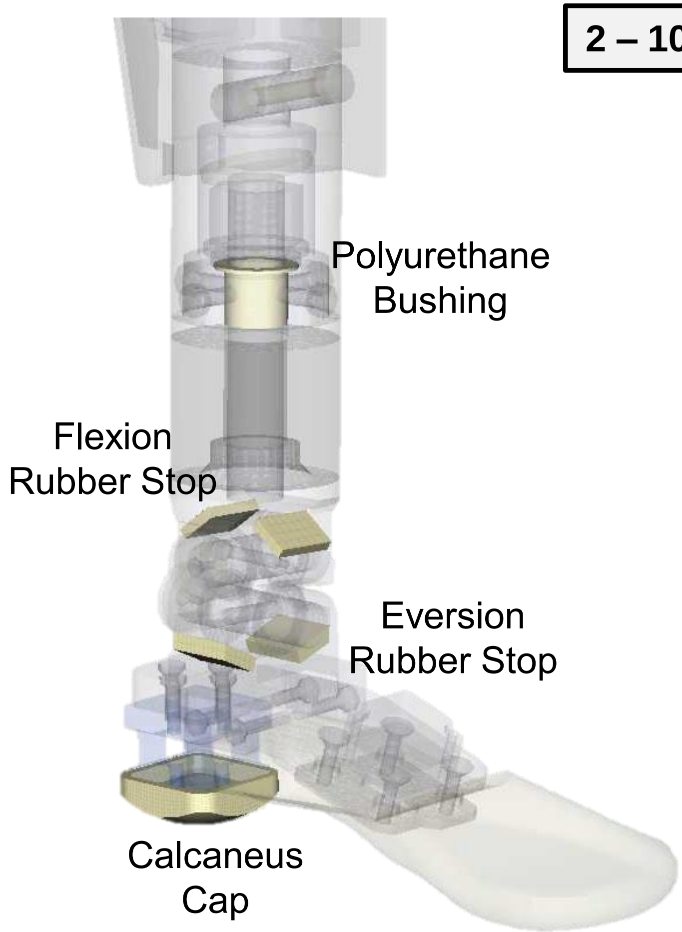

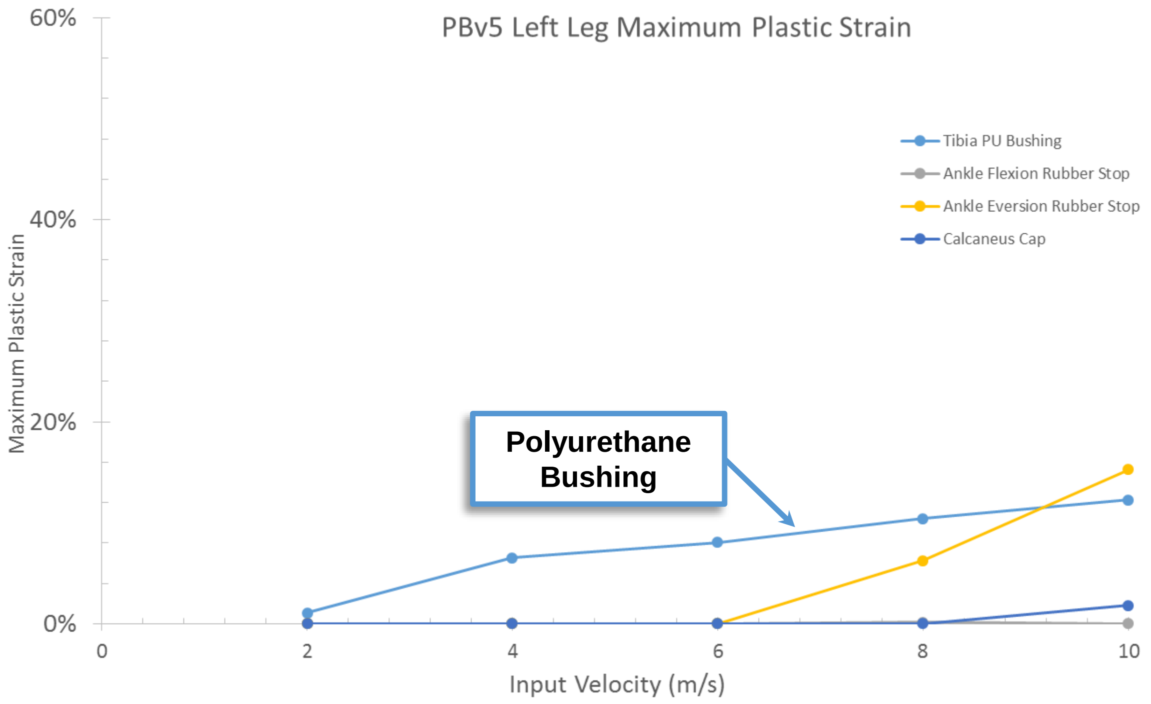

Component	% Plastic Strain @ 2 m/s	% Plastic Strain @ 4 m/s	% Plastic Strain @ 6 m/s	% Plastic Strain @ 8 m/s	% Plastic Strain @ 10 m/s
Tibia PU Bushing	1.1%	6.5%	8.1%	10.4%	12.3%
Ankle Flexion Rubber Stop	0.0%	0.0%	0.0%	0.1%	0.0%
Ankle Eversion Rubber Stop	0.0%	0.0%	0.0%	6.2%	15.2%
Calcaneus Cap	0.0%	0.0%	0.0%	0.0%	1.8%
Femur PU Bushing	0.0%	0.0%	0.8%	4.4%	6.1%

WB Plastic Strain Analysis

2 – 10 m/s VALTS (Whole Body) Analysis

- Strength analysis completed for each body region
- Identified focus areas:
  i. FE model refinement
  ii. Physical model weaknesses

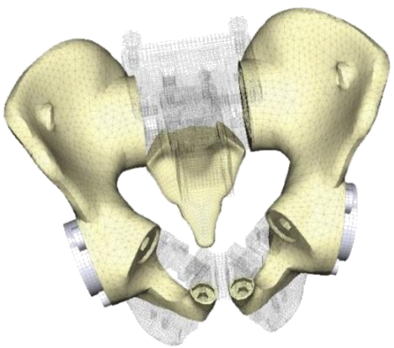

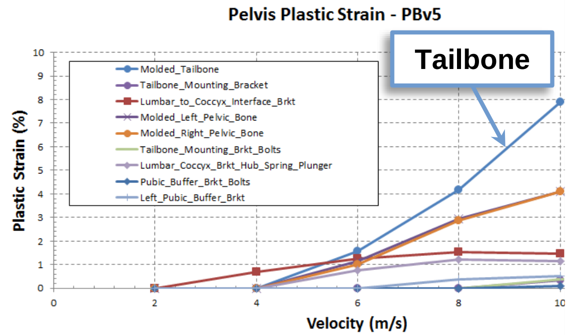

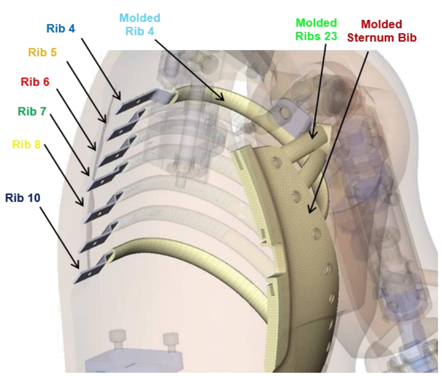

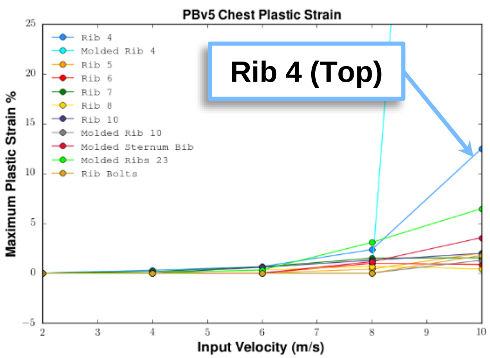

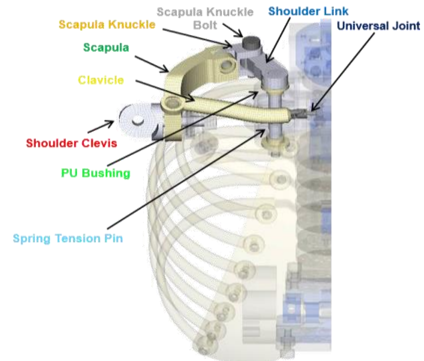

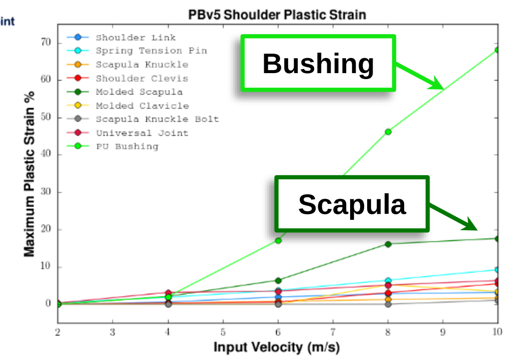

Highlighted areas of highest risk throughout the body

Preliminary Load Cell Analysis

Comparison of maximum force values to **TDP LC design threshold**:

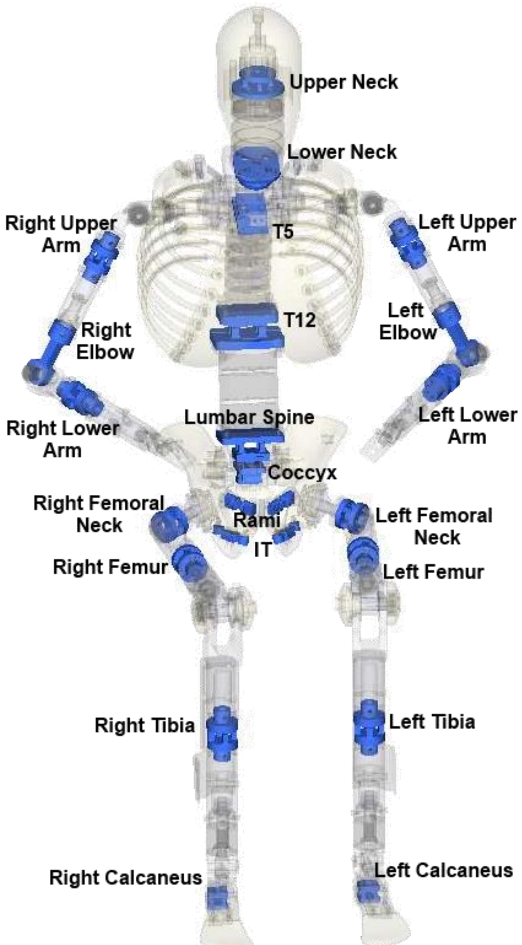

		Force Rating				
Load Cell Location		2m/s	4m/s	6m/s	8m/s	10m/s
Left Leg	Left Calcaneus	14%	26%	42%	67%	89%
	Left Tibia	8%	15%	22%	36%	49%
	Left Femur	2%	3%	5%	9%	13%
	Left Femoral Neck	6%	9%	14%	20%	23%
Right Leg	Right Calcaneus	14%	27%	43%	66%	90%
	Right Tibia	8%	14%	22%	35%	48%
	Right Femur	5%	3%	5%	9%	13%
	Right Femoral Neck	6%	9%	14%	18%	24%
Pelvis	**Coccyx**	11%	38%	78%	**123%**	**176%**
	Left Ischial	22%	35%	49%	63%	72%
	Right Ischial	21%	35%	49%	62%	73%
Spine	**Lumbar**	24%	49%	80%	**113%**	**138%**
	T12	19%	39%	60%	79%	98%
	T5	26%	54%	86%	**113%**	**143%**
	Lower Neck	16%	32%	57%	80%	**104%**
	Upper Neck	12%	26%	45%	63%	85%
Left Arm	Left Upper Arm	5%	12%	16%	17%	19%
	Left Lower Arm	1%	3%	6%	10%	11%
Right Arm	Right Upper Arm	5%	11%	16%	17%	19%
	Right Lower Arm	1%	4%	5%	9%	11%

Load cell design limits base on TDP.

Early VALTS simulations indicated potential LC risk areas

WIAMan SOD: Shoulder

- SoD analysis highlighted the **TDP shoulder design as a high risk area** of focus
  - Damage onset @ 4m/s case
  - Scapula knuckle bolt and rib 4 interference
  - Use of low strength steel called out in the TDP for the spring tension pin

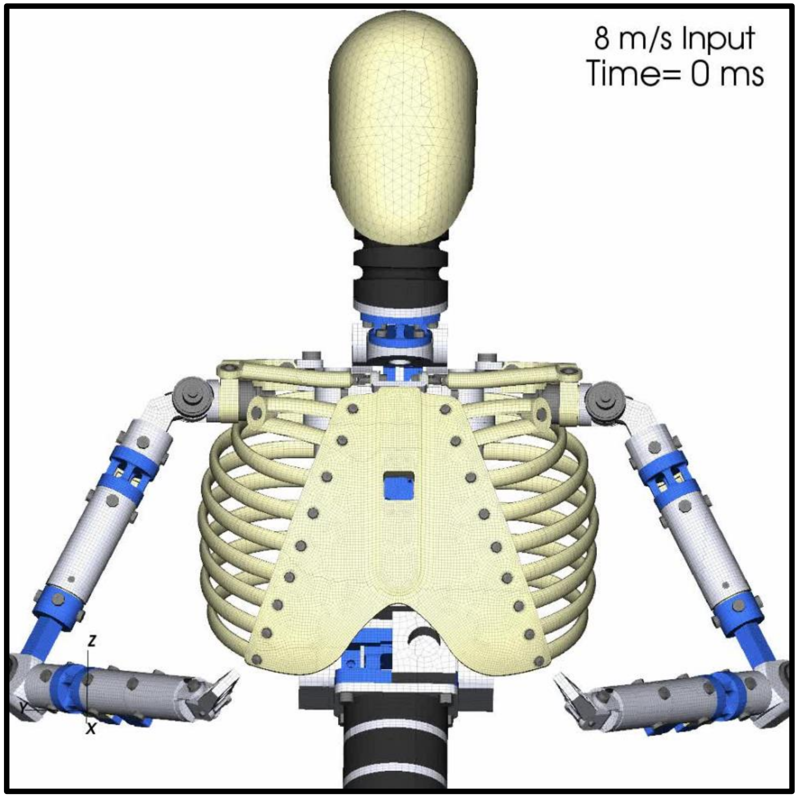

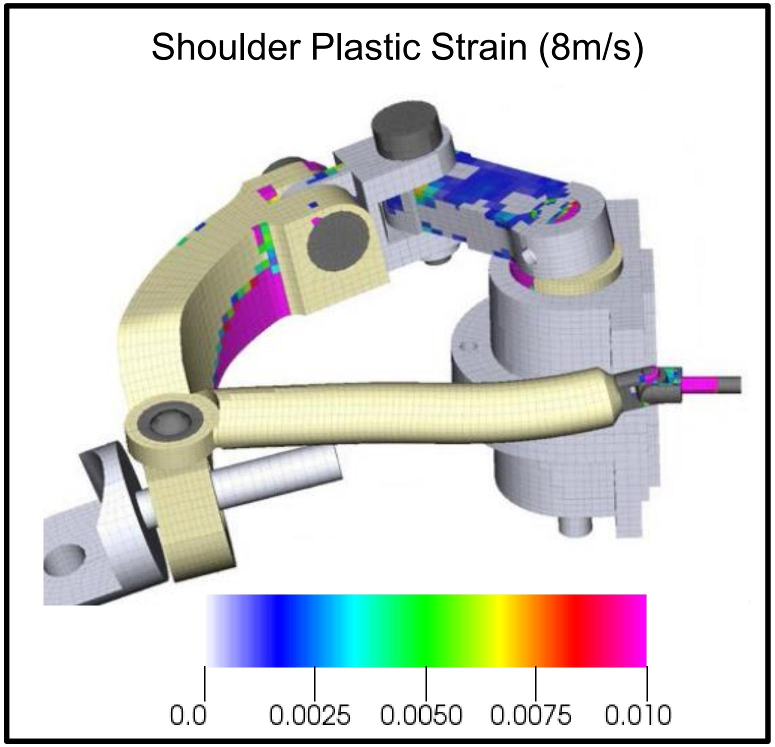

Analysis identified shoulder performance risk prompting design modifications

WIAMan SOD: Rib Impact

WB VALTS loading case: **undesirable upper arm to rib interaction**

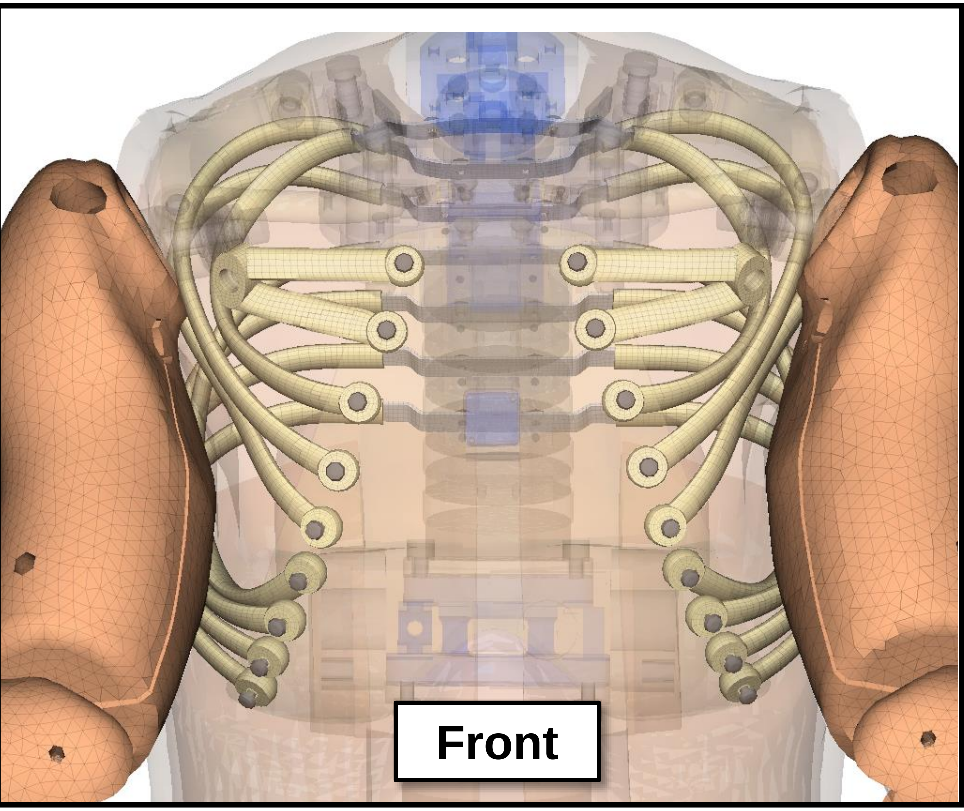

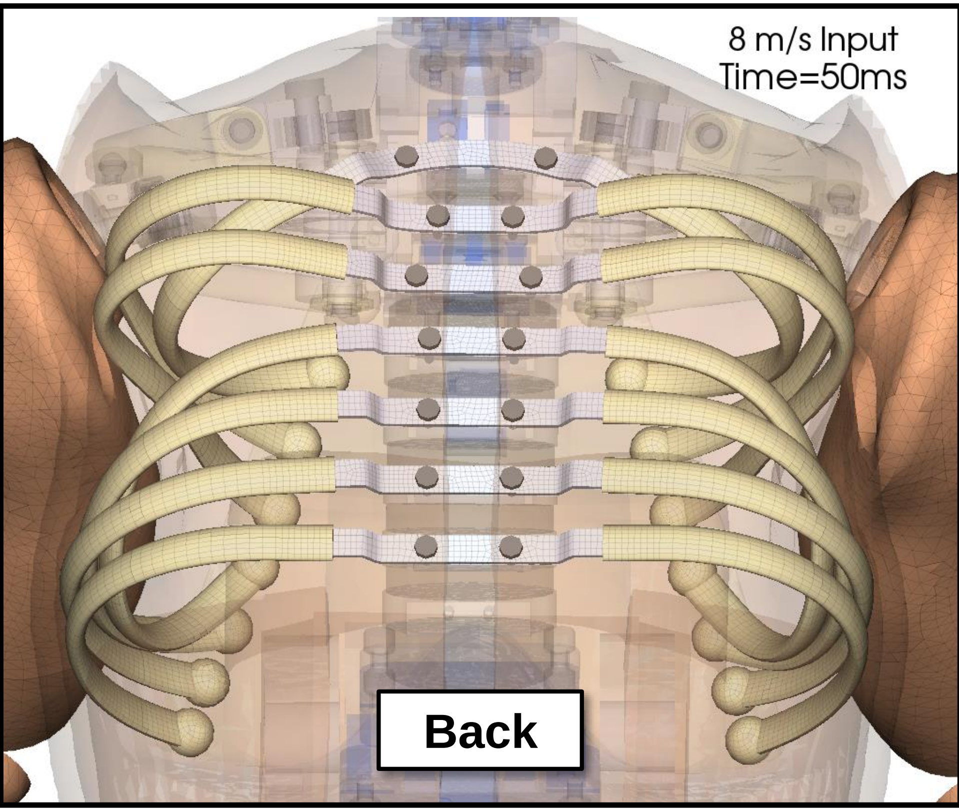

Ribs are impacted by arms from the side in addition to Scapula from above

WIAMan SOD: Shoulder Study

- Study into shoulder system material changes:
  - Leveraged the SoD test case to determine if a simple material change could alleviate the shoulder design limitation
  - Advanced into whole body analysis of system level sensitivity to the applied design modifications
- Proactive investigations into steel ribs
  - Increased strength
  - Added needed upper body mass
  - No major changes within the whole body system

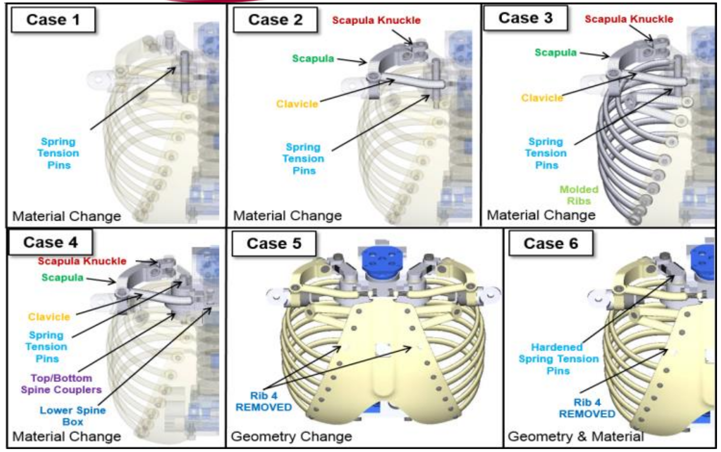

Run	2 m/s	4 m/s	6 m/s	8 m/s	10 m/s
PBv3	TDP Materials	TDP Materials	TDP Material s	TDP Materials	TDP Material s
Case 1		Hardened Steel Spring Pin		Hardened Steel Spring Pin	
Case 2		Steel Shoulder Assembly*		Steel Shoulder Assembly*	
Case 3		All Torso Component s† Steel		All Torso Components † Steel	
Case 4		Case 2 + Steel Coupler/Spi ne Box		Case 2 + Steel Coupler/Spin e Box	
Case 5		TDP - Rib 4 Removed		TDP - Rib 4 Removed	
Case 6		Case 1 - Rib 4 Removed		Case 1 - Rib 4 Removed	

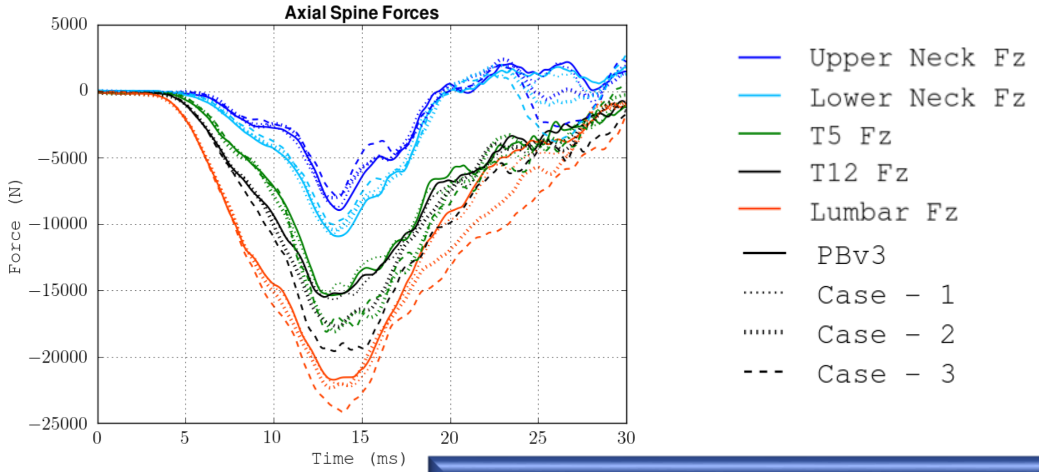

M&S-based shoulder study impacted TD -> TDP design changes

LFT&E Loading Condition

LFTE SEVERE LOADING CONDITION

Whole Body SoD Environment

LFT&E Loading Condition: MCW Pelvis

Idealized 12 m/s Input

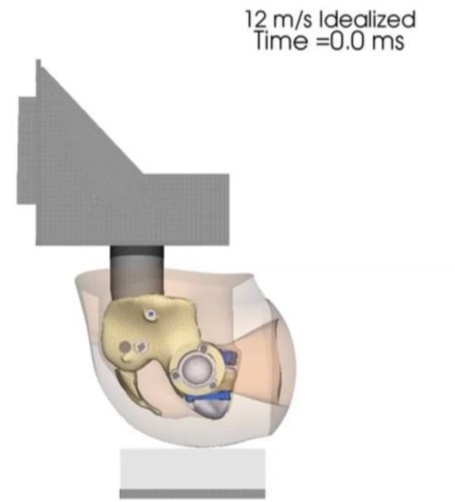

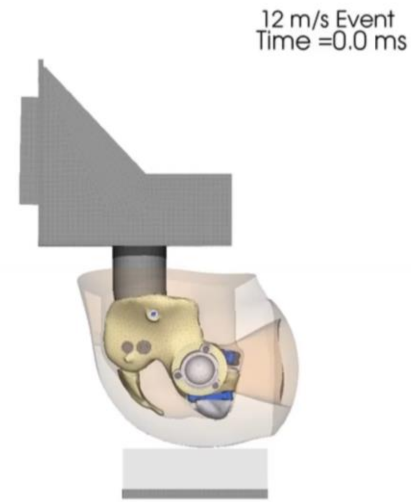

Vehicle Event (scaled)

Seat Input Velocities

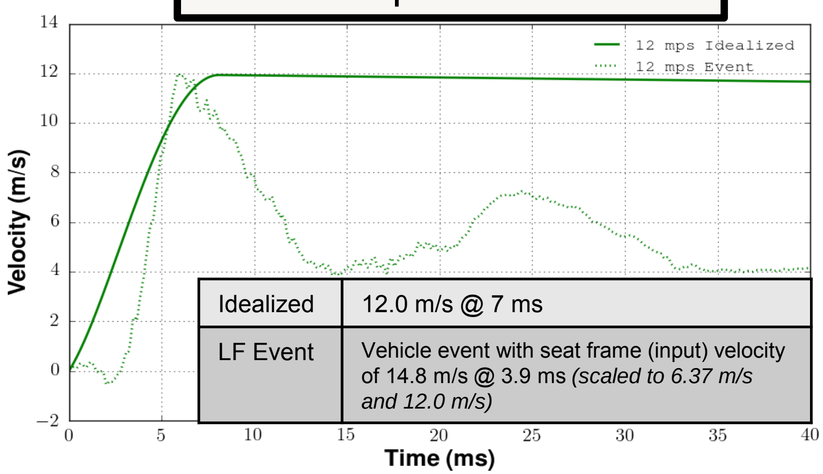

Idealized	12.0 m/s @ 7 ms
LF Event	Vehicle event with seat frame (input) velocity of 14.8 m/s @ 3.9 ms *(scaled to 6.37 m/s and 12.0 m/s)*

Lumbar/Coccyx Forces

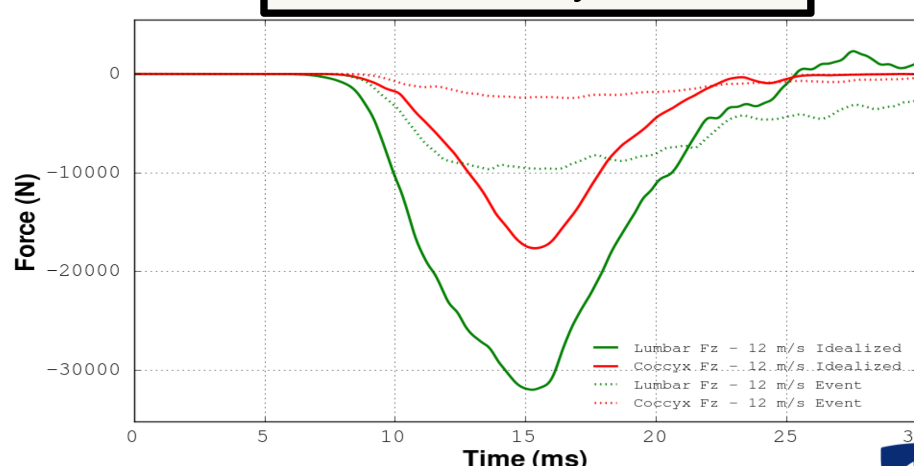

Pelvis loads very sensitive to seat input profile even after peak

LFT&E Loading Condition: VALTS

8 m/s VALTS

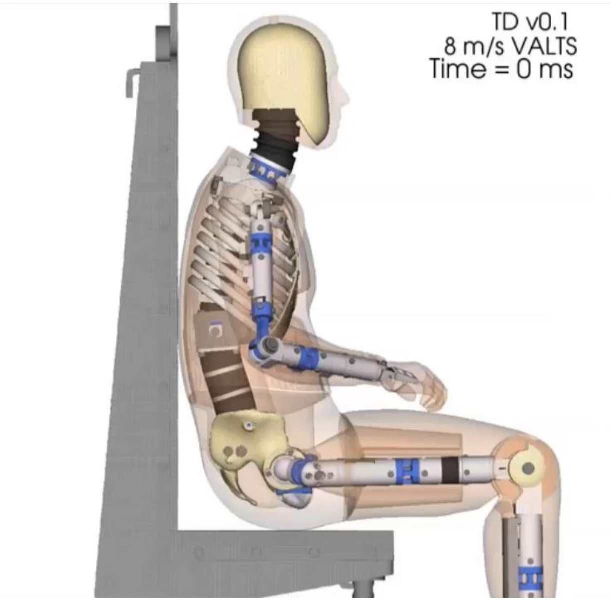

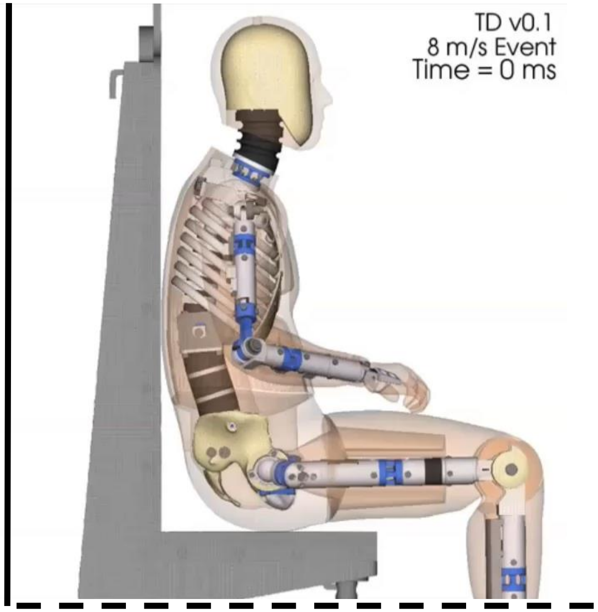

8 m/s Vehicle Event

Seat Input Velocities

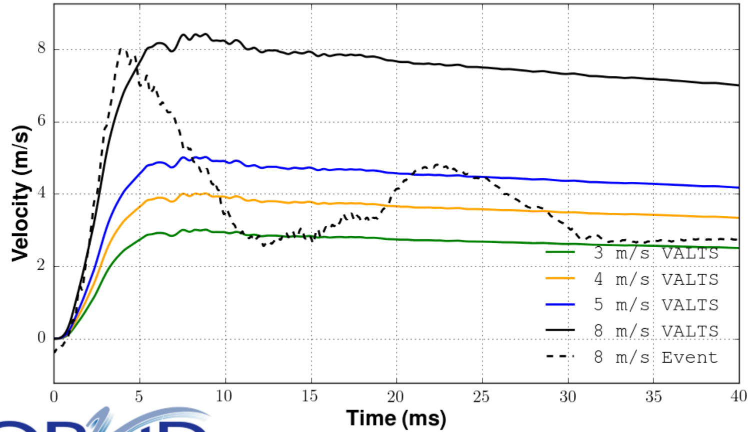

Lumbar Forces

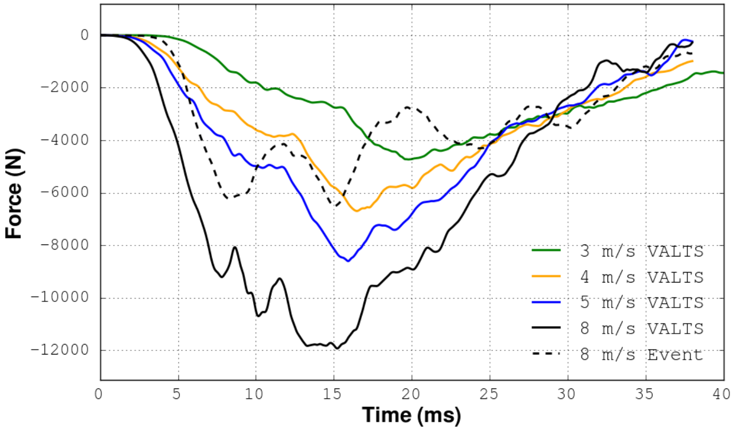

The Nation's Premier Laboratory for Land Forces

LFT&E Loading Condition: Input Pulse

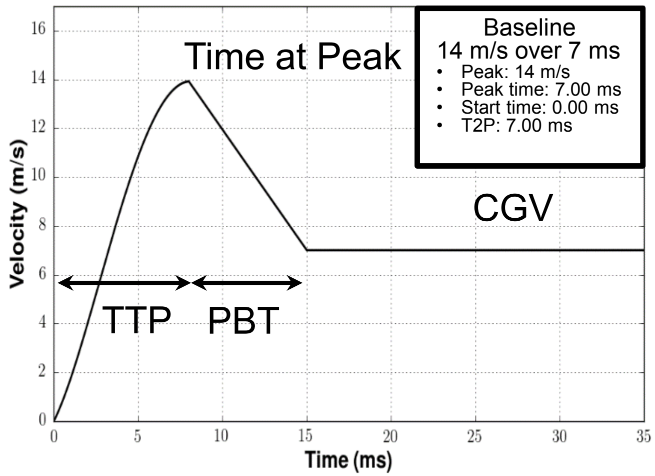

Input Profile Parameters:

Time to Peak (TTP): 7ms

Peak Velocity:14m/s

CG Velocity (CGV): 6, 7, 8 m/s

Pull Back Time (PBT): 7 ± 5 msec

Time at Peak(TAP): 0, 5, 10 msec

Proposed Additional Parameters

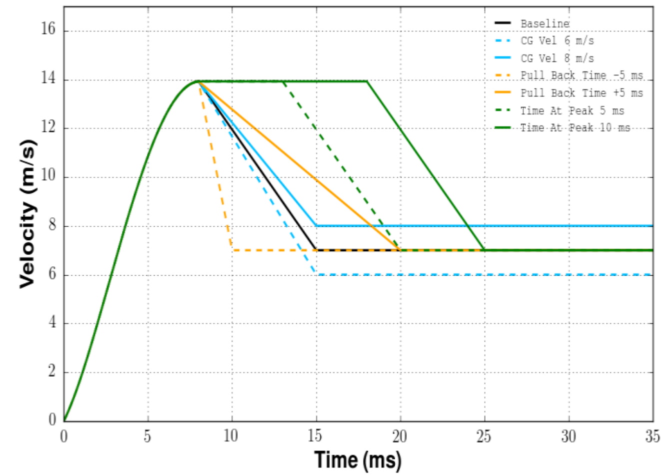

Lumbar Forces

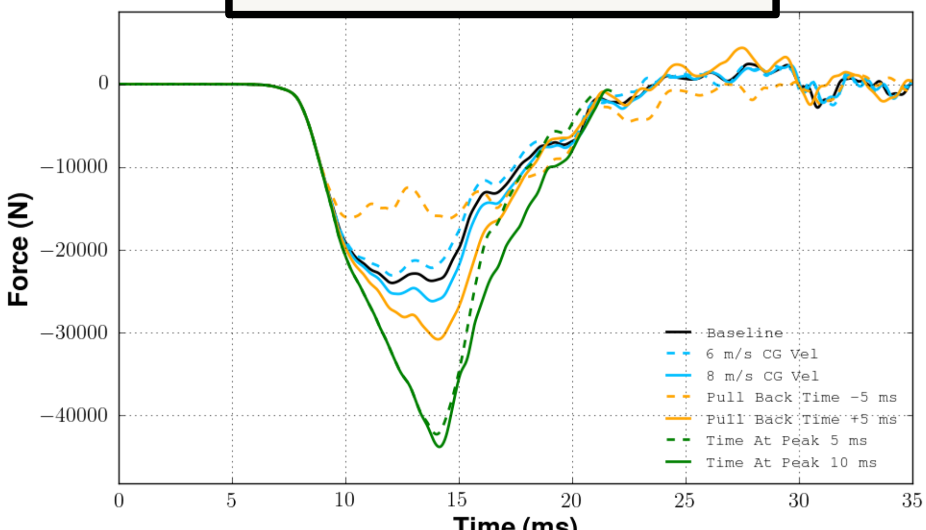

Lumbar Moments

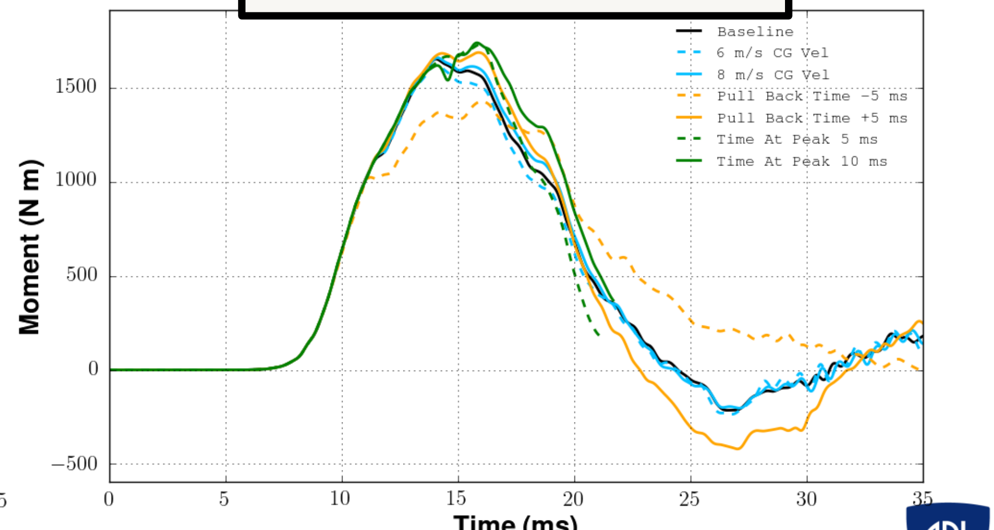

Lumbar forces sensitive to proposed additional parameters

WIAMan PPE: WH1A Input

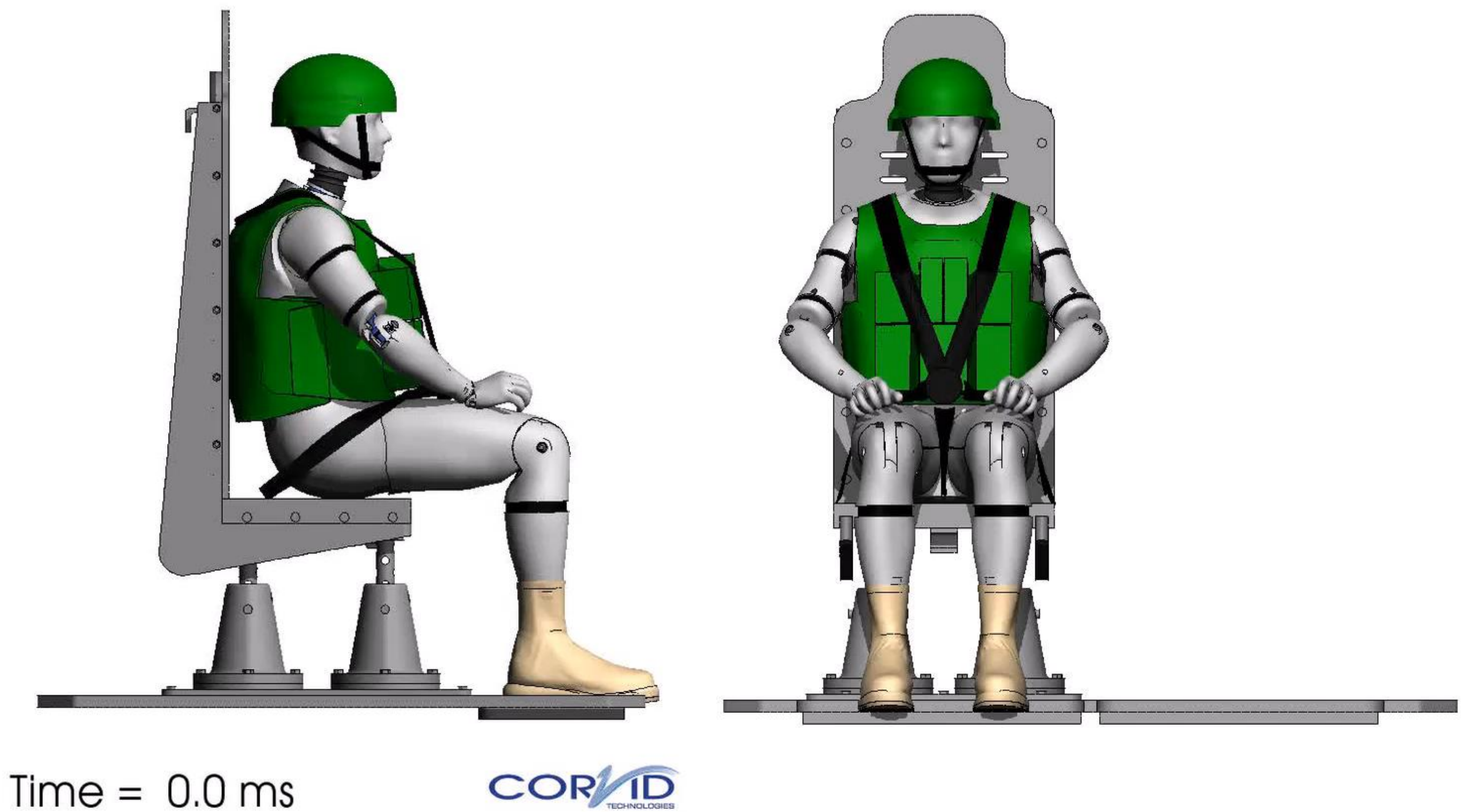

Full PPE finite element models are complete for DA boots, IOTV and ACH

M&S Influence on TD/GEN1 Design

- **Accomplishing the mission of the M&S team → reducing cost, schedule, and performance risk by providing insights prior to TD testing:**
  - PU bushing redesign (Tech Demonstrator)
  - Ankle stop redesign (Tech Demonstrator)
  - Material change for steel shoulder components (Tech Demonstrator)
  - Adoption of change to steel ribs (Tech Demonstrator)
  - Removal of rib 4 to prevent interference with bolt head (Tech Demonstrator)
  - Insight into abdomen redesign (Tech Demonstrator)
  - Insight into upper arm flesh redesign (Tech Demonstrator)
- **M&S will continue to investigate requests from the ATD PT, at minimal risk, which will aid in:**
  - Improvements to WIAMan ATD biofidelity (Gen 1)
  - Enhancement to WIAMan ATD pelvis strength (Gen 1)
  - Other component redesign as required based on WIAMan ATD testing (Gen 1)

Response Corridors of Cadaveric Human Head-neck under Accelerative Loading

Liming Voo*, Frank Pintar[+], Scott Gayzik[@], John Humm[+], Daniel Fama[+], Narayan Yoganandan[+], Andrew Merkle*

***Johns Hopkins University Applied Physics Laboratory**
[+]Medical College of Wisconsin
[@]Wake Forest University

Second Workshop on Numerical Analysis of Human and Surrogate Response to Accelerative Loading
January 12-14, 2016

Introduction

- Head and cervical spine injuries are a significant threat to the survivability of mounted soldiers (Possley 2012, Schoenfeld 2013) as the accelerative loading could induce rapid head motion or head contact with vehicle interior
- The WIAMan ATD serving as the human surrogate would need to include injury prediction capability for those anatomies when being used for vehicle protection assessment
- The reliability of such injury risk prediction depends largely on how the surrogate could accurately represent the anatomic structures in those application environments: Biofidelity of this ATD is therefore essential for this purpose
- ATD Biofidelity by design: matching degrees of freedom, dimensions, inertial properties; structural properties
- ATD Biofidelity by validation: response data from human anatomies, matched-pair ATD responses, design revisions
- Biofidelity Response Corridors:
  - Relevant anatomy
  - Relevant test model
  - Relevant test conditions
  - Procedures for quality assurance and corridor development

Objectives

- Develop Biofidelity Response Corridors (BRCs) that account for the following factors:
  - Anatomy relevance
  - Test conditions relevance
  - Specimen quality control
  - Test condition repeatability
  - Essential biomechanical parameters (BPs)
  - Data scaling
  - Procedure for response corridor development
- Determine Effect of Anatomic Posture
  - Nominal posture
  - Pre-flexed posture
  - Pre-extended posture
- Determine Effect of Head Impact

Methods: Specimen and Setup

- Specimen:
  - Male cadaveric Head-T1
  - Acceptance criteria based on (W0062; ANSUR II):
    - Whole body anthropometry: 50% male military population, Mean+/- 1.5SD
    - Or head circumference 327-610mm; neck length 88-129mm
    - Absence of prior damage, surgery, or anatomic anomalies
- Test model:
  - PMMA-potted at T1 and below and attached with a 6-axis load cell and allowed to move vertically
  - Combat helmet fitted to the head
  - Head unrestrained but initially supported

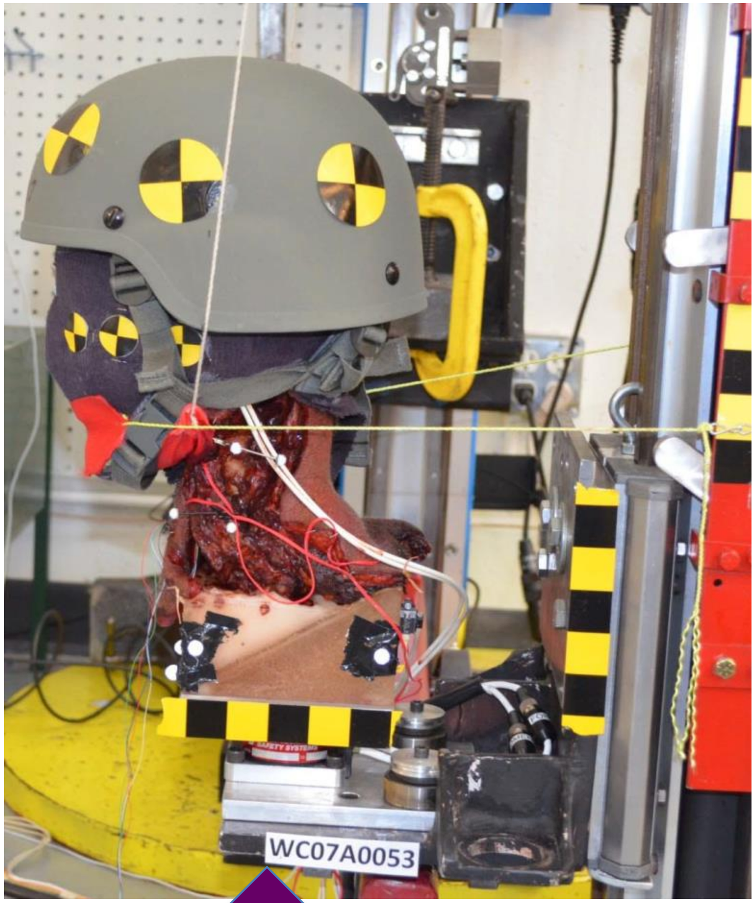

Accelerative Loading

Methods: Biomechanical Parameters

Anatomy	Measured (or Calculated) Parameters	ITM Reference: Biomechanical Parameters	Biofidelity Importance
Head	Roof Impact Force in Z	BP-65	Secondary
	Head CG Acceleration Z	BP-1	Primary
	Head CG Acceleration Resultant	BP-2	Primary
	Head Rotation relative to T1 (ARS-Y)	BP-3	Primary
	Head Rotation relative to T1 (ARS-X)	BP-4	Secondary
	Head Rotation relative to T1 (ARS-Z)	BP-5	Secondary
Neck	Lower Neck Force FZ (C7-T1)	BP-7-L	Primary
	Lower Neck Force FX (C7-T1)	BP-8-L	Secondary
	Lower Neck Moments MY (C7-T1)	BP-9-L	Primary
	C3 Motion (Ry)	BP-12	Secondary
	C5 Motion (Ry)	BP-15	Secondary
	Spine Compression (OC-T1 Distance Change)	BP-16	Secondary
	Neck X Deformation (OC Relative to T1 Displacement X)	BP-16x	Secondary
	Neck Z Deformation (OC Relative to T1 Displacement Z)	BP-16z	Secondary
	T1 Z acceleration	BP-18*	N/A
T1	T1 Velocity in Z (Test Input)	Input Condition	N/A

* Accelerometer mounted to potting block and used to produce input condition, therefore not considered for a BRC.

Methods: Instrumentation

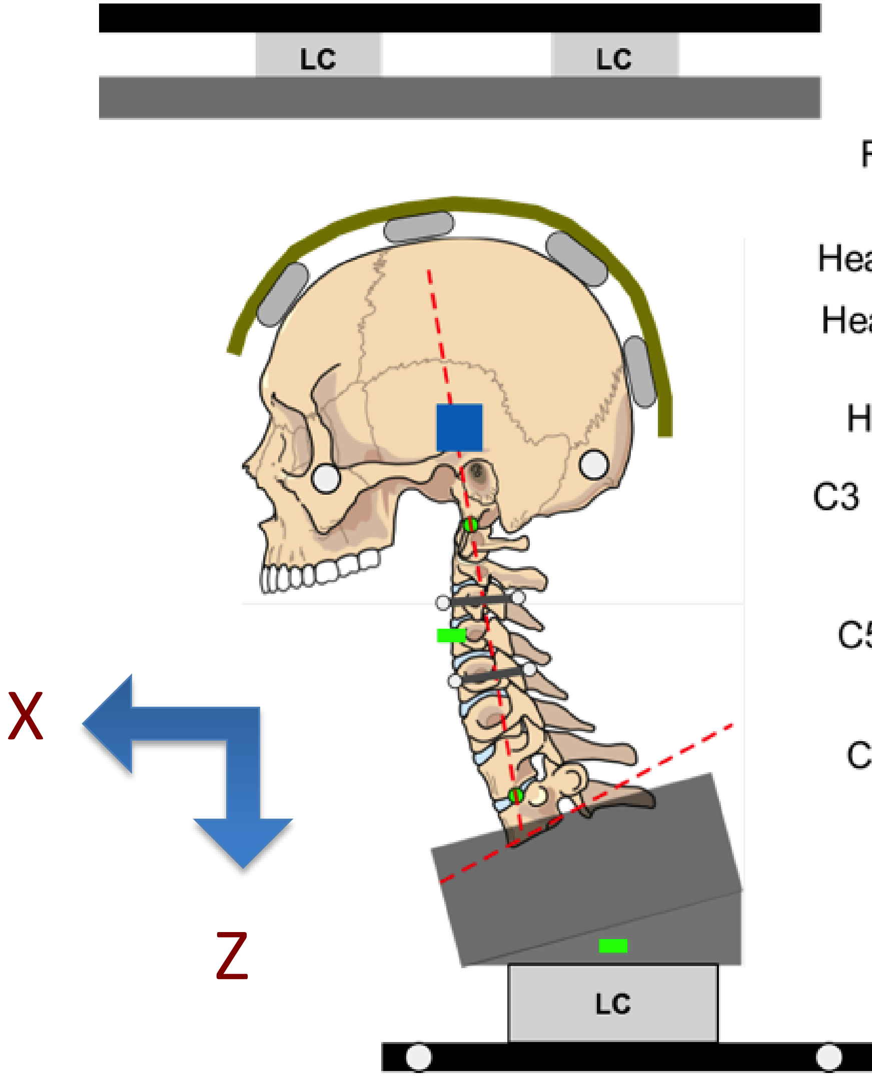

Roof Load Cells (BP-65)

Roof contact switch

Head 3-axis Accels (BP-1, 2)

Head 3-axis ARS (BP-3)

Head Motion Targets (BP-4, 5)

C3 Motion Targets (BP-12)

C4 Z-Accel (BP-14)

C5 Motion Targets (BP-15)

C3, C5 Strain Gages and/or Acoustic Sensors

3-Accels on T1 base

Lower Neck 6-axis LC (BP-7, 8, 9)

T1 Motion Targets

Methods: Testing

- Data quality controls
  - Helmet fitting procedure
  - Head and neck posture specifications
  - Load pulse tuning and control
  - Instrumentation protocol
  - Injury assessment between and after tests

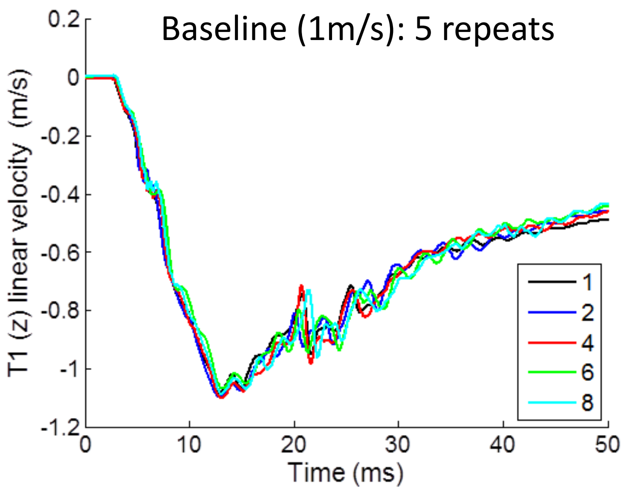

- Loading conditions
  - Accelerative loading to the neck base
  - Velocities: 1, 2, 3 m/s
  - Time to peaks: nominal 10ms
  - Posture specifications (neutral posture):
    - C7-T1 disc 31-deg to horizontal; head Frankfort plane horizontal; neck angle 7-deg
- Sample size
  - 6-8 specimen in each test series and test condition

Methods: Positioning Posture

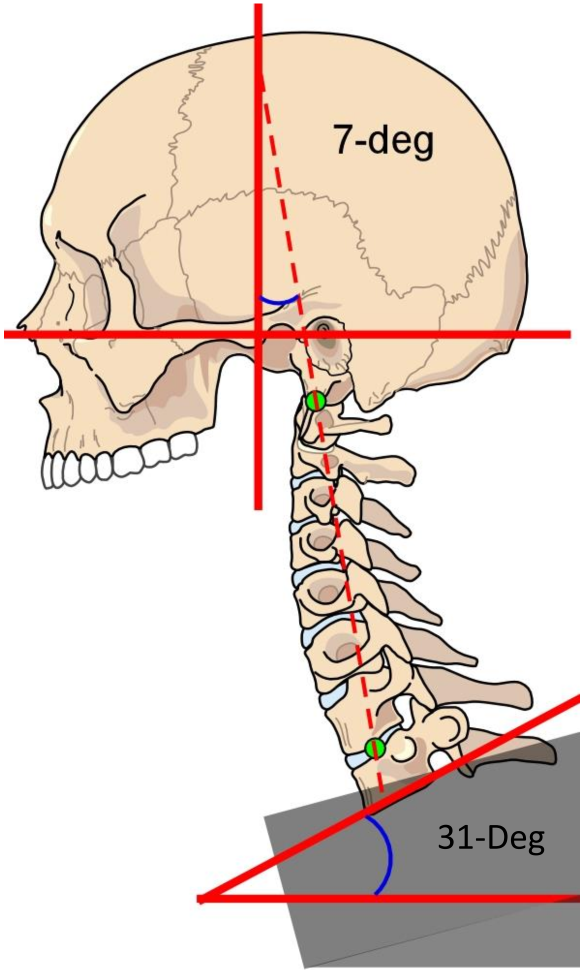

Posture data based on UMTRI Seated Soldier Study; Reed et al. 2013

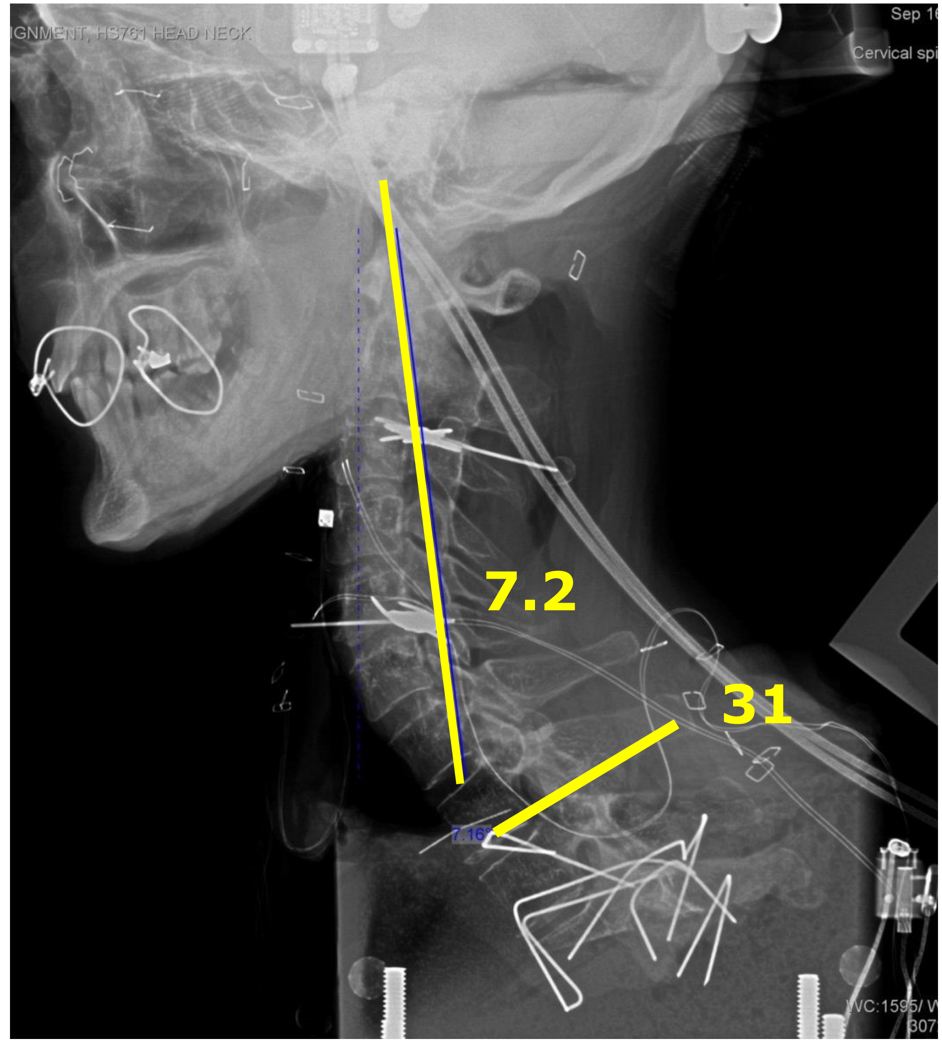

Methods: Test Matrix

Velocity (m/s)	1 no roof	1 no roof	2 no roof	1 no roof	3 no roof	1 roof	2 roof	1 roof	3 roof	1 roof	5 roof
HN03-1	01-001	01-002	01-003	01-004	01-005	01-006			01-007	01-008	01-009
HN03-2	02-001	02-002	02-003	02-004	02-005	02-006		02-007	02-008		
HN03-3				03-001	03-002	03-003	03-004	03-005	03-006	03-007	03-008
HN03-4				04-001	04-002	04-003	04-004	04-005			04-006
HN03-5				05-001	05-002	05-003	05-004	05-005	05-006		
HN03-6				06-001	06-002	06-003	06-004	06-005	06-006		
HN03-7				07-001	07-002						
HN03-8						08-001	08-002	08-003	08-004		

BRC data sources

V1 V2 V3

RED Text=Injury; BLACK Text=No Injury; Yellow Shade=BRC input

Methods: Data Treatment

- Data sampling and filtering
  - High-speed video sampled data at 5000 frame/sec
  - Sampled data at 1000 kHz with 300 kHz AA filter
  - Post-test filtered data with a 4-pole Butterworth,
    - 3 kHz roll-off for accelerometer and load cell data
    - 1.65 kHz roll-off for angular rate sensor
- Data conversion to anatomic locations
  - Head acceleration to head CG
  - Neck forces and moments to C7-T1 disc center
- Data normalization (Scaling)
  - Equal stress equal velocity (Eppinger 1984)
  - Based on mass ratio
  - **Normalized to the WIAMan ATD population**
- BRC generation
  - Signal alignment
  - Representative curve (RC) +/- 1 SD of the RC

Methods: Conversion to Anatomy

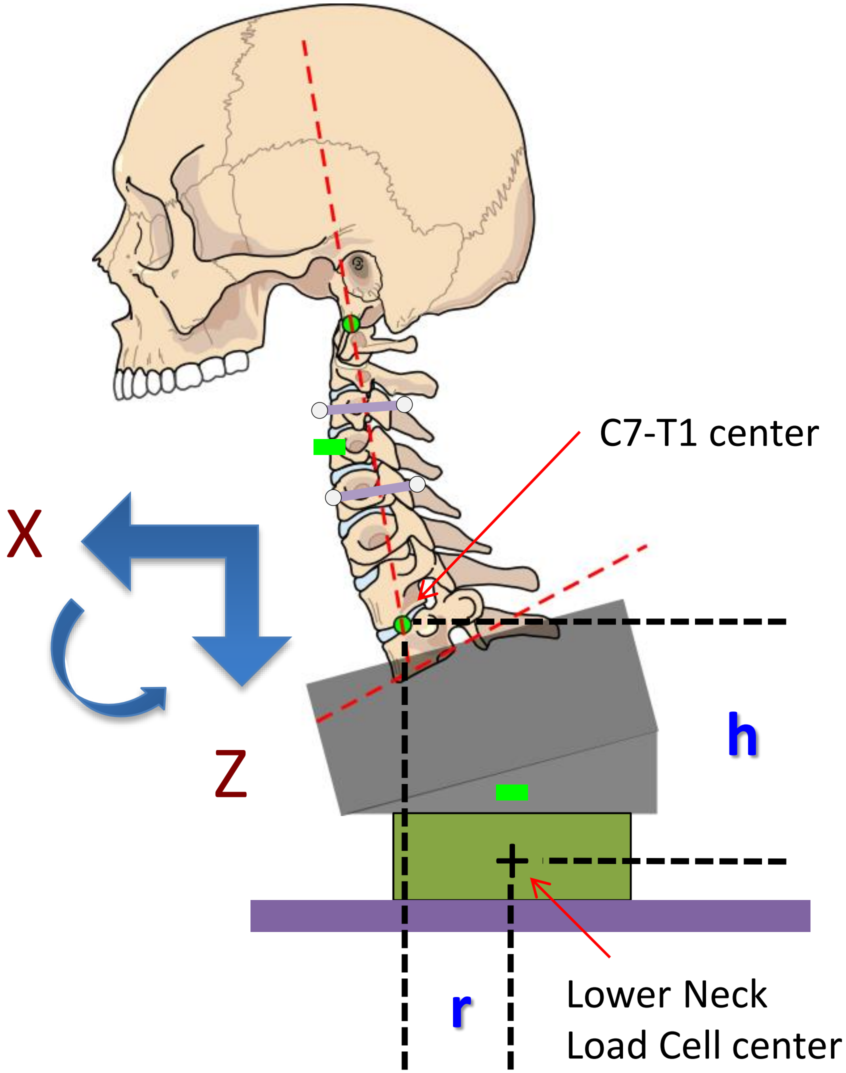

Translate the forces and moment at the load cell to the C7-T1 joint center:

- Record offsets ‘h’ and ‘r’
- Apply calculations to based on equations of motion using mass, acceleration, force, moment, and force times off-set distances

Specimen	r (m)	h (m)
HN03-1	0.0396	0.112
HN03-2	0.027	0.113
HN03-3	0.033	0.134
HN03-4	0.051	0.1422
HN03-5	0.023	0.119
HN03-6	0.056	0.146
HN03-8	0.0177	0.0998

Methods: Data Normalization

Population of postmortem human surrogate for biomechanical testing

Measure	Mean +/- 1.5 Standard Deviation
Sex	Males
Age	18-80 years
Height	65 – 73 inches (165-186 cm)
Weight	141 – 233 lbs. (64-106 kg)
BMI	18 - 35
DEXA BMD	-1.0 < T-score <+2.5 (Whole Body)
General Skeleton	No abnormalities beyond average population
Ethnicity	Any

WIAMan Target Population

Methods: Data Normalization

- Force: equal stress
- Displacement: equal strain
- Moment: force x displacement
- Head acceleration: Equal-Stress Equal-Velocity Method (Eppinger 1984)

Force: $F_{ref,i}(t) = (F_i(t)/\text{Mid IVD area}_{ref\ i})* \text{Mid IVD area}_{ref}$

Displacement: $D_{ref,i}(t) = (D_i(t)/L_{ref\ i}) * L_{ref}$

Moment: $M_{ref,i}(t) = (M_i(t)/(\text{Mid IVD area}_{ref\ i} * L_{ref\ i})) * \text{Mid IVD area}_{ref} * L_{ref}$

Head Acceleration: $A_{ref,i} = \lambda^{-1/3} A_i$

Time: $T_{ref,i} = \lambda^{1/3} T_i$

Head Rotation: $R_{ref,i} = R_i$

Where: $\lambda_i = M_{ref}/M_i$

Head Velocity: $V_{ref,i} = V_i$

Definition:

- "Ref" = Reference: quantity normalized to the WIAMan ATD equivalent
- Index "i" indicates individual specimens

	Acceleration	Acceleration	Force	Displacement
Target WIAMan Values	WIAMan Head	WIAMan Head, Neck, & Helmet	Average Mid Disc Cross Sectional Area	Average Neck Length
	4.5 kg	7.071 kg	3.44 cm^2	161.7 mm

JOHNS HOPKINS UNIVERSITY
Applied Physics Laboratory

Methods: Scaling Factors

MEDICAL COLLEGE OF WISCONSIN

Normalization Factors for each Specimen

Specimen	Head Accel. Normalization Time	Head Accel. Normalization Accel	T1 Accel. Normalization Time	T1 Accel. Normalization Accel	Force	Moment	Disp.
HN03-1	1.06	0.94	0.96	1.04	1.07	1.19	1.11
HN03-2	1.07	0.93	1.00	1.00	1.10	1.05	0.95
HN03-3	1.11	0.90	1.01	0.99	0.99	0.95	0.95
HN03-4	1.09	0.92	0.99	1.01	0.95	0.96	1.01
HN03-5	1.06	0.94	0.98	1.02	1.02	0.97	0.95
HN03-6	1.04	0.96	0.94	1.06	0.90	0.86	0.96
HN03-8	1.06	0.94	0.98	1.02	1.00	1.08	1.09

Note: Time is not normalized unless noted.

Results

- Head kinematics
- Force Fz at C7-T1 joint
- Head CG Acceleration Az
- Separate BRCs before and after roof contact

Kinematics: High-speed Video

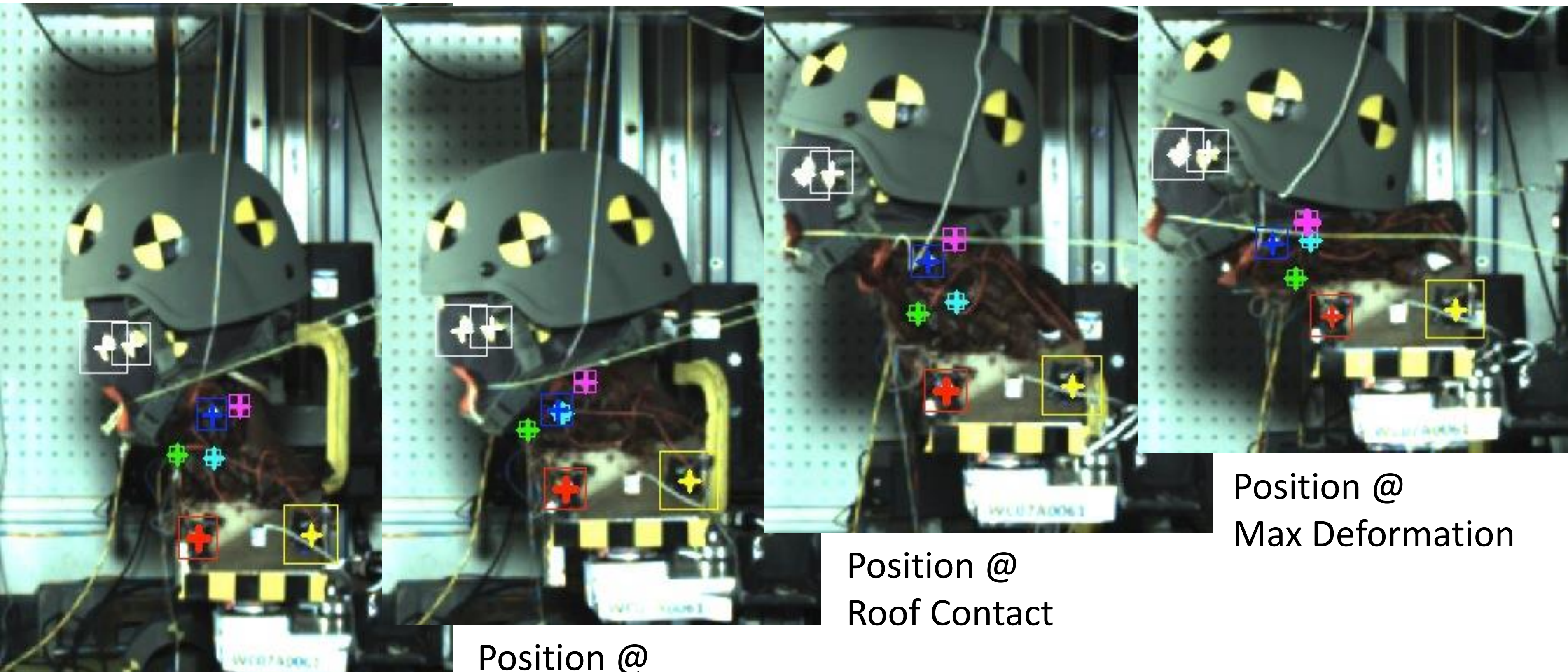

Position @ T=0

Position @ Thrust Phase

Position @ Roof Contact

Position @ Max Deformation

V = 3m/s

<u>Thrust to Roof Contact Timing:</u>
V1: No roof contact
V2: Contact @106 +/- 8 ms
V3: Contact @53 +/- 8 ms

Head Kinematics: Forward Motion

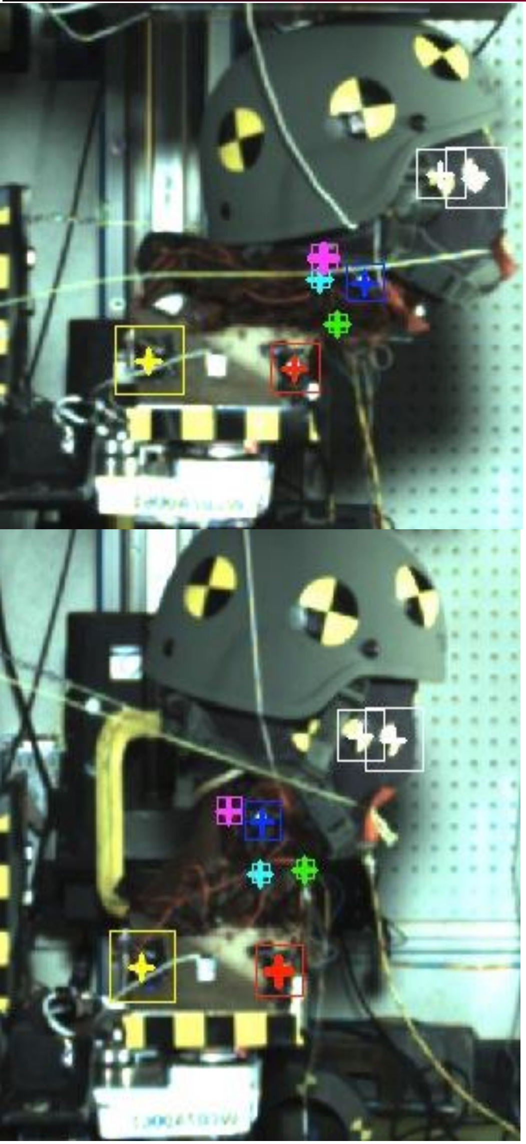

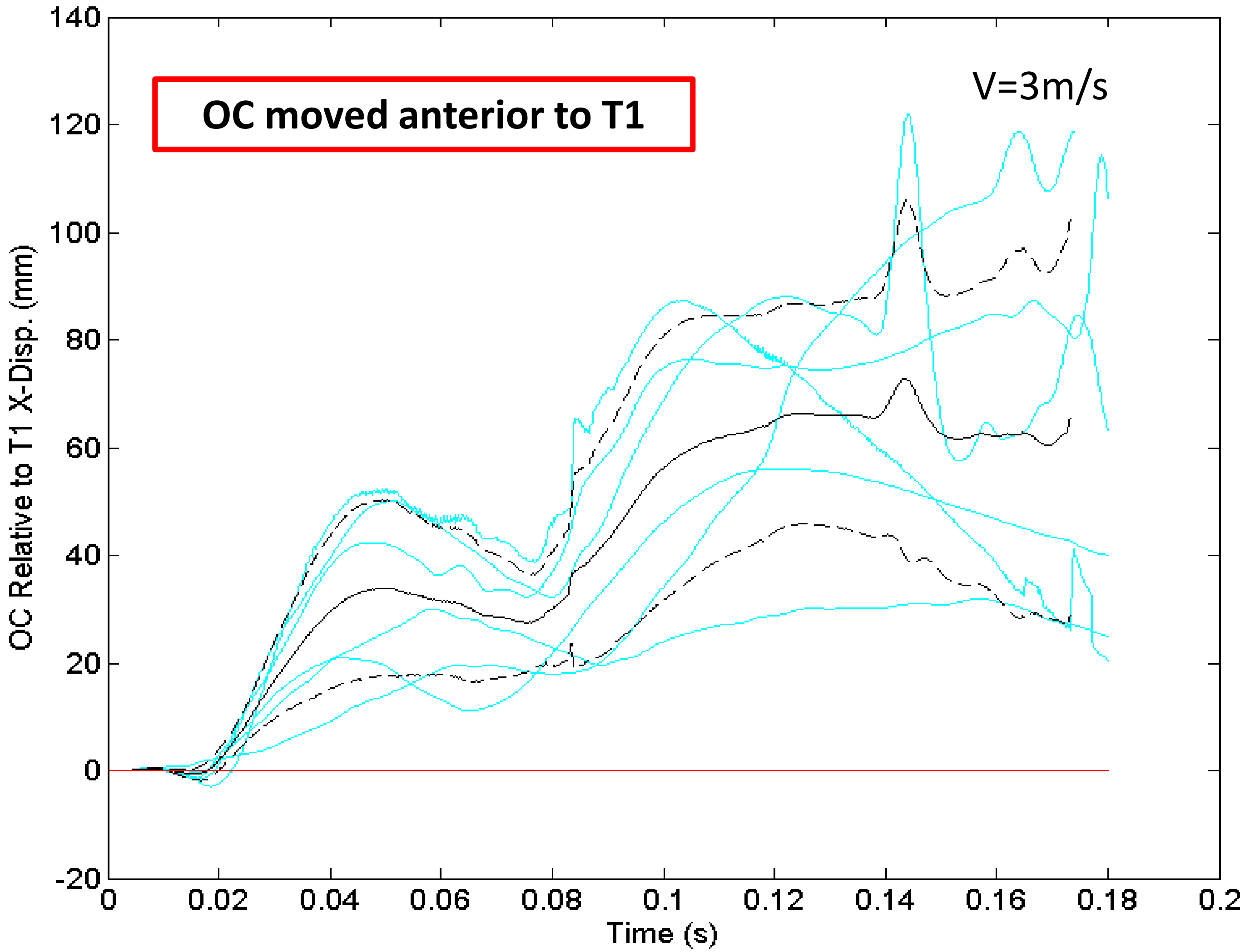

Lower Neck Force Fz

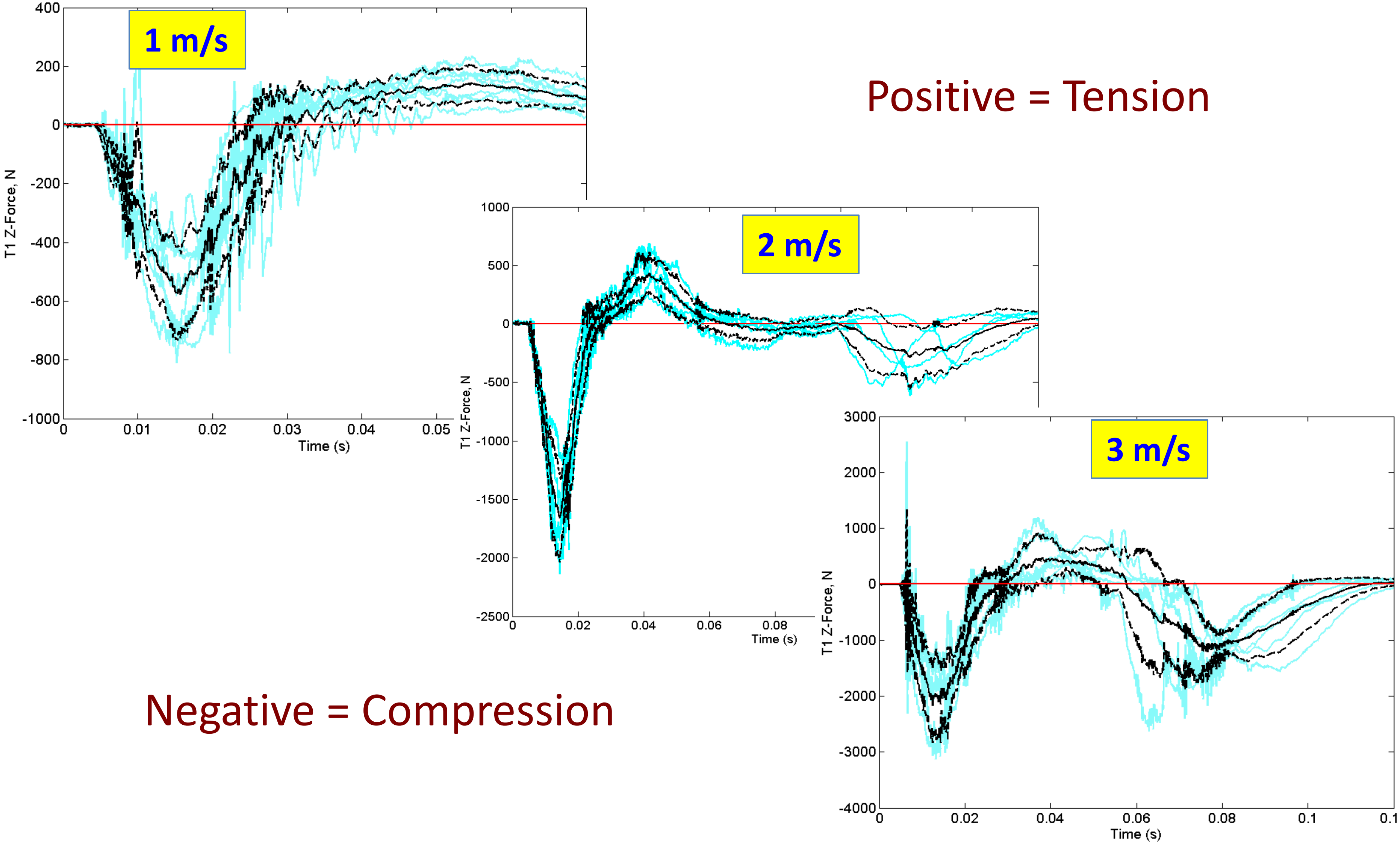

Positive = Tension

Negative = Compression

Lower Neck Fz at 2m/s

Before roof contact

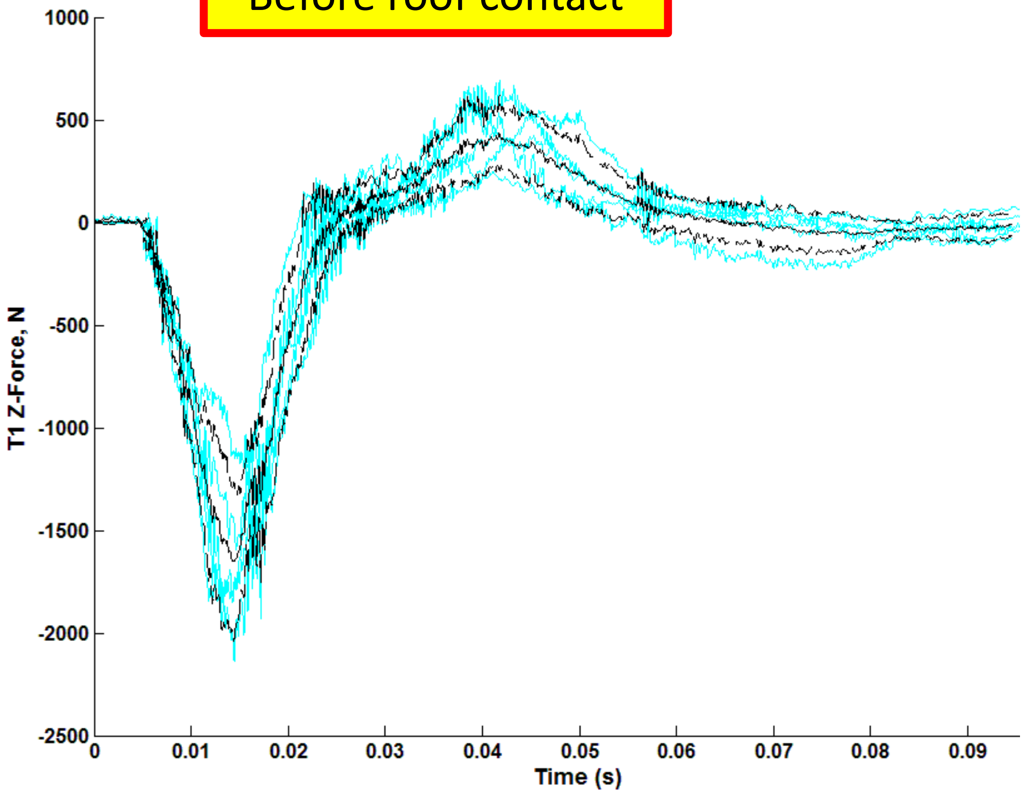

After roof contact

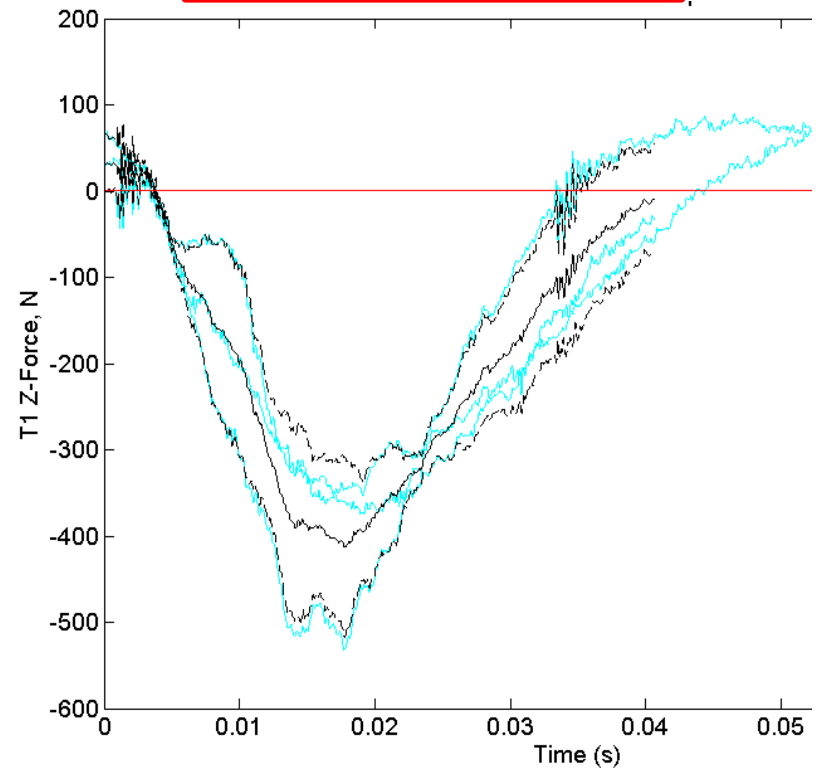

Caveats Noted:

Time zero defined as roof contact time for signals; BRC begins instant prior to roof contact Initial position of C-spine not controlled

Lower Neck Fz at 3 m/s

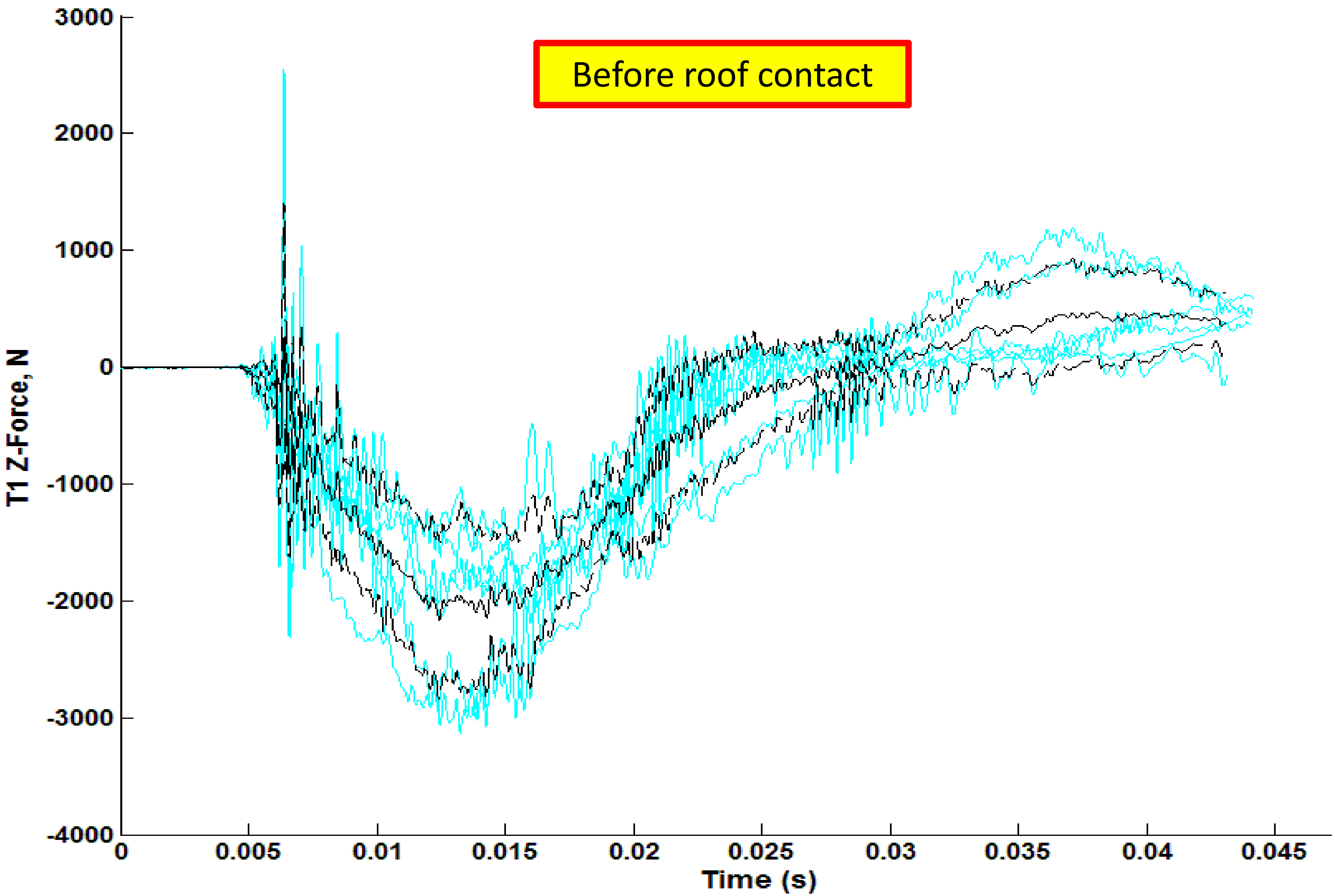

Head CG Accel Az at 1m/s

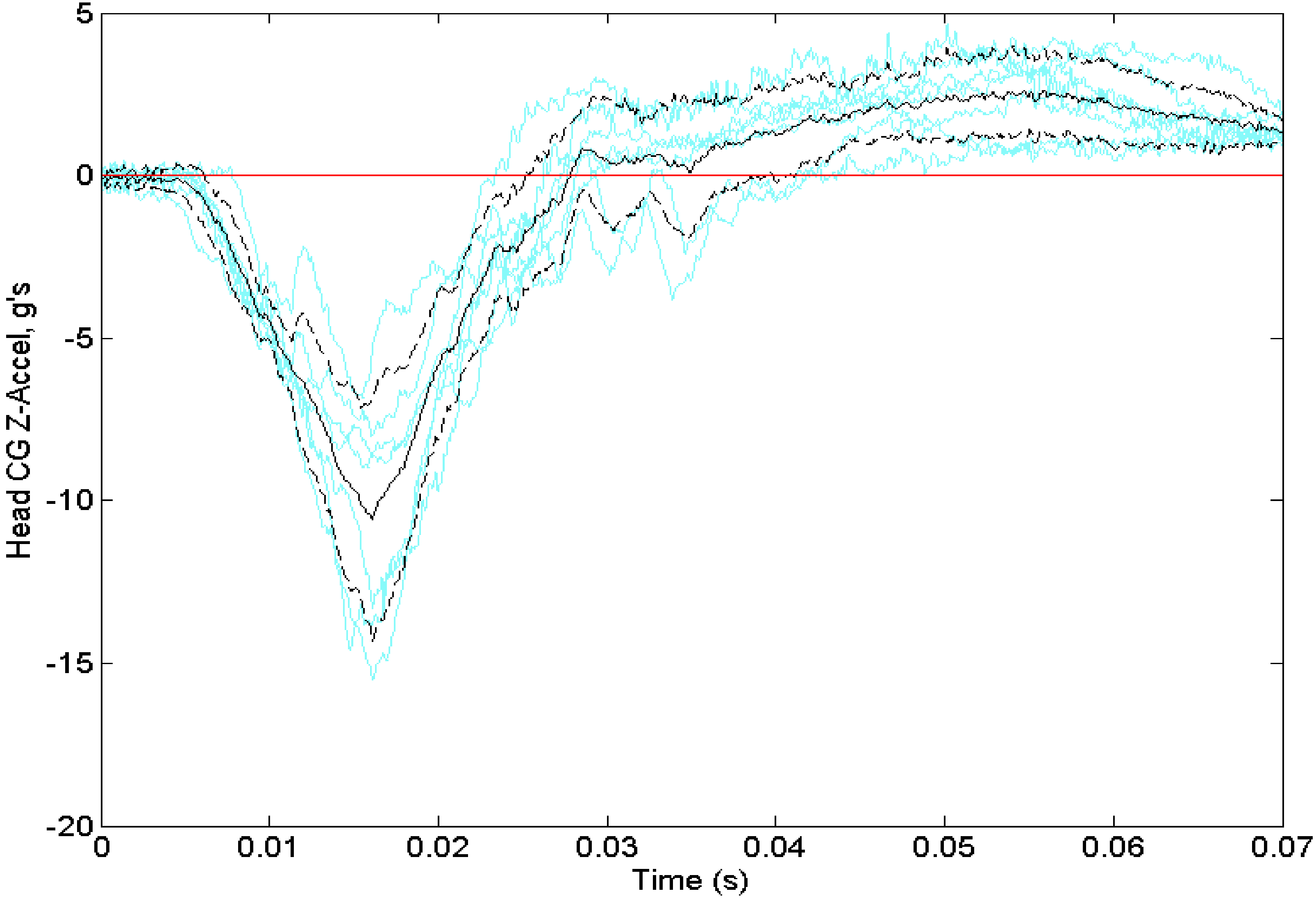

Head CG Accel Az at 2m/s

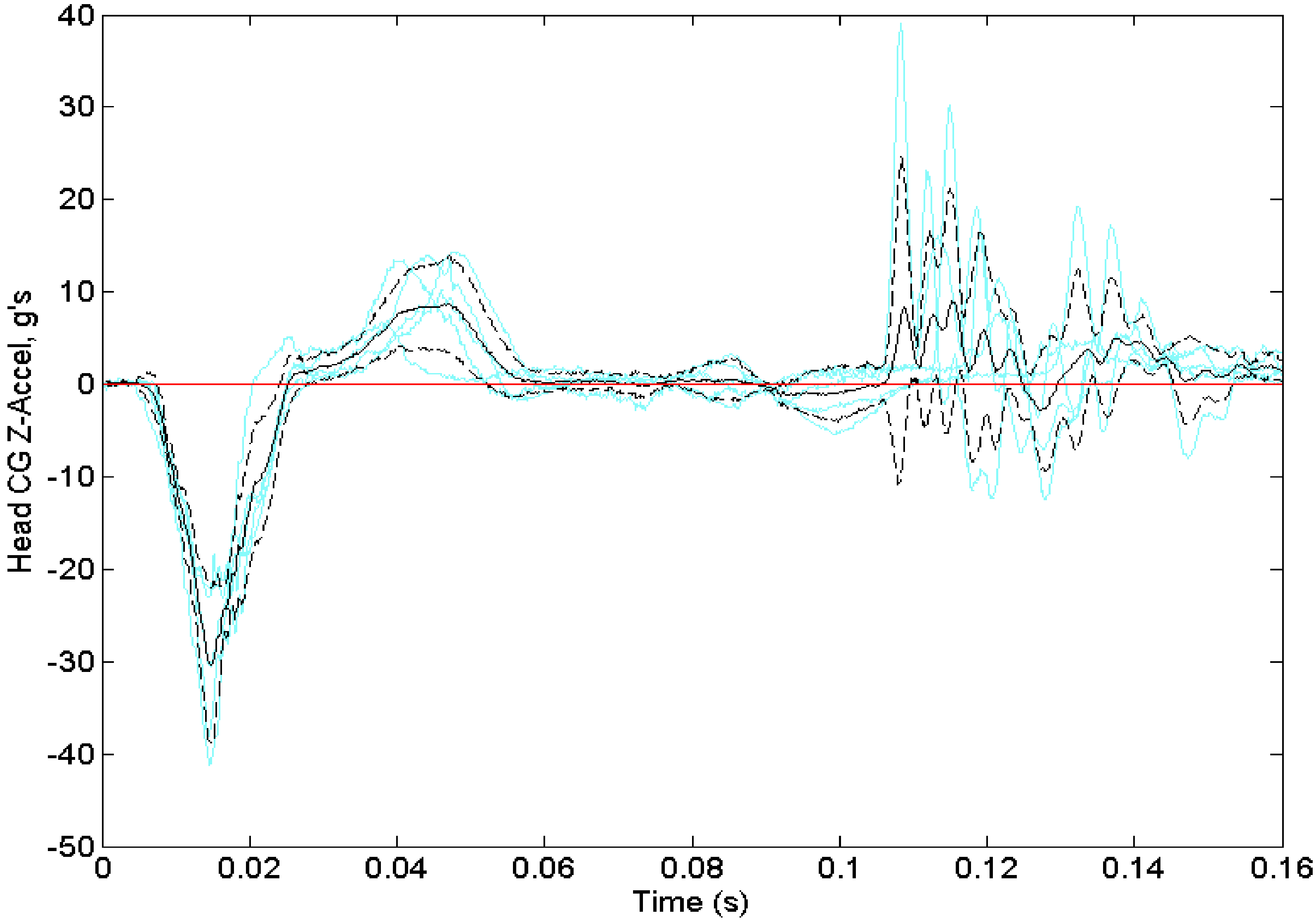

Head CG Accel Az at 2m/s

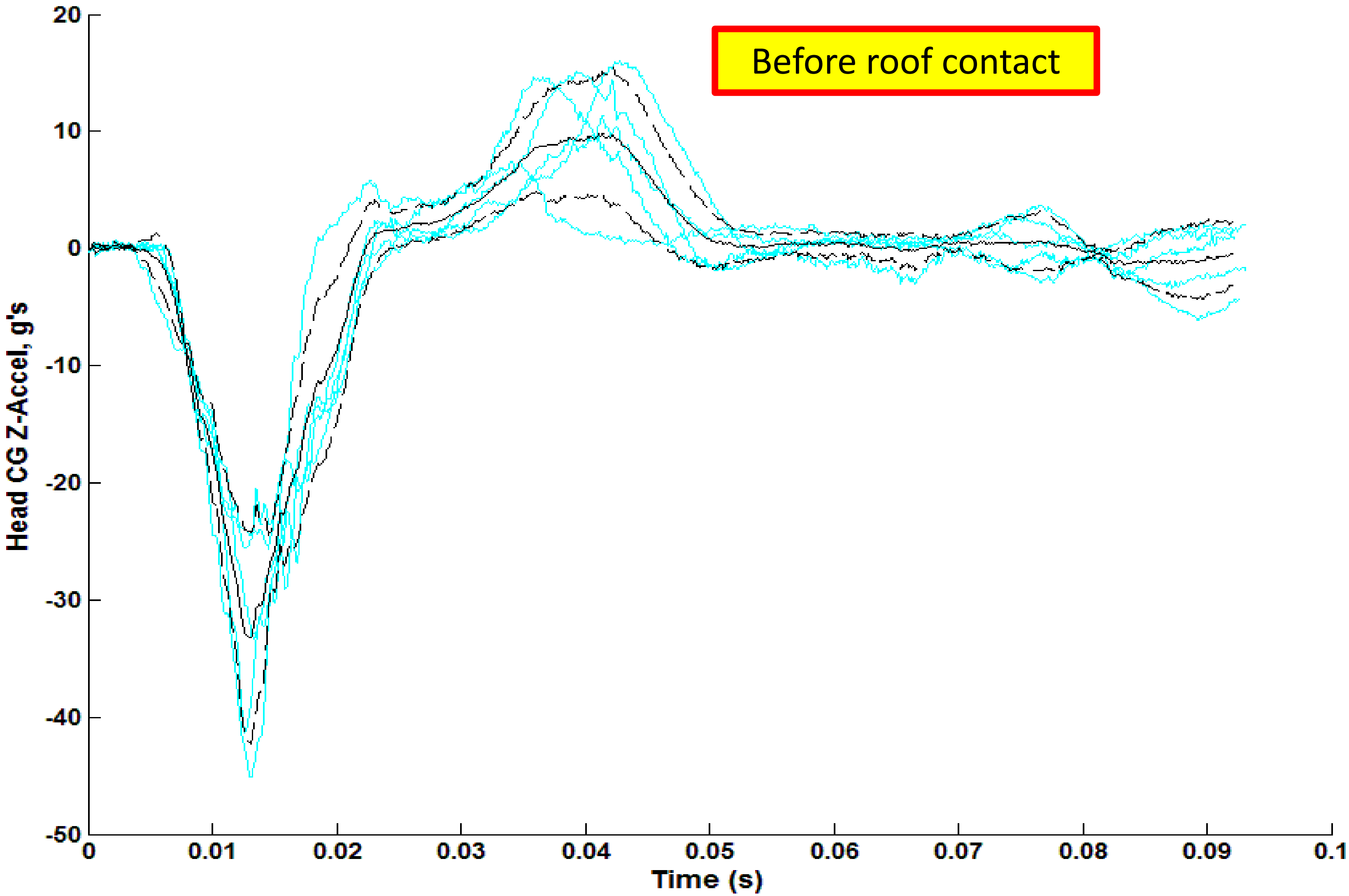

Head CG Accel Az at 2m/s

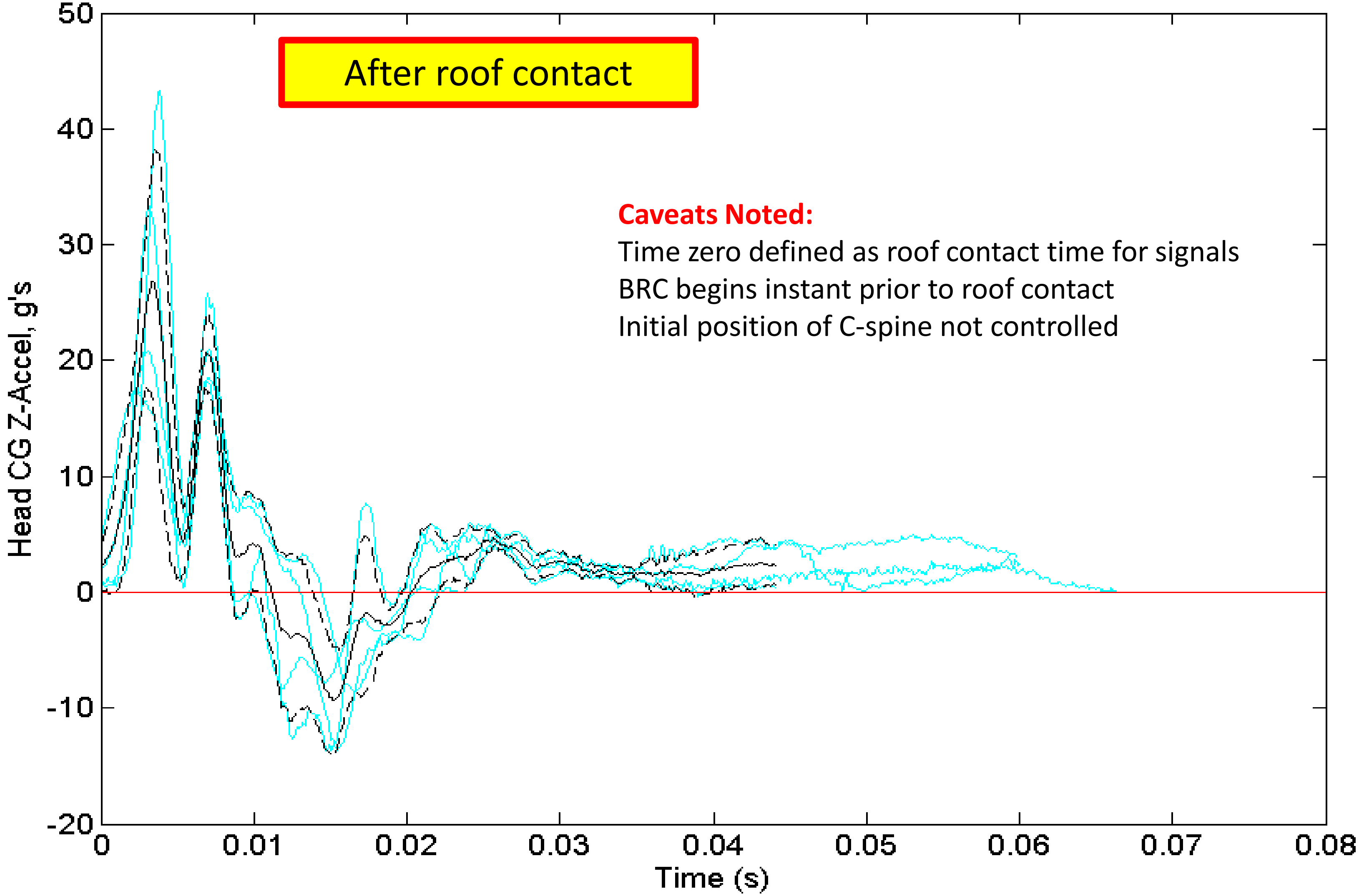

Head CG Accel Az at 3m/s

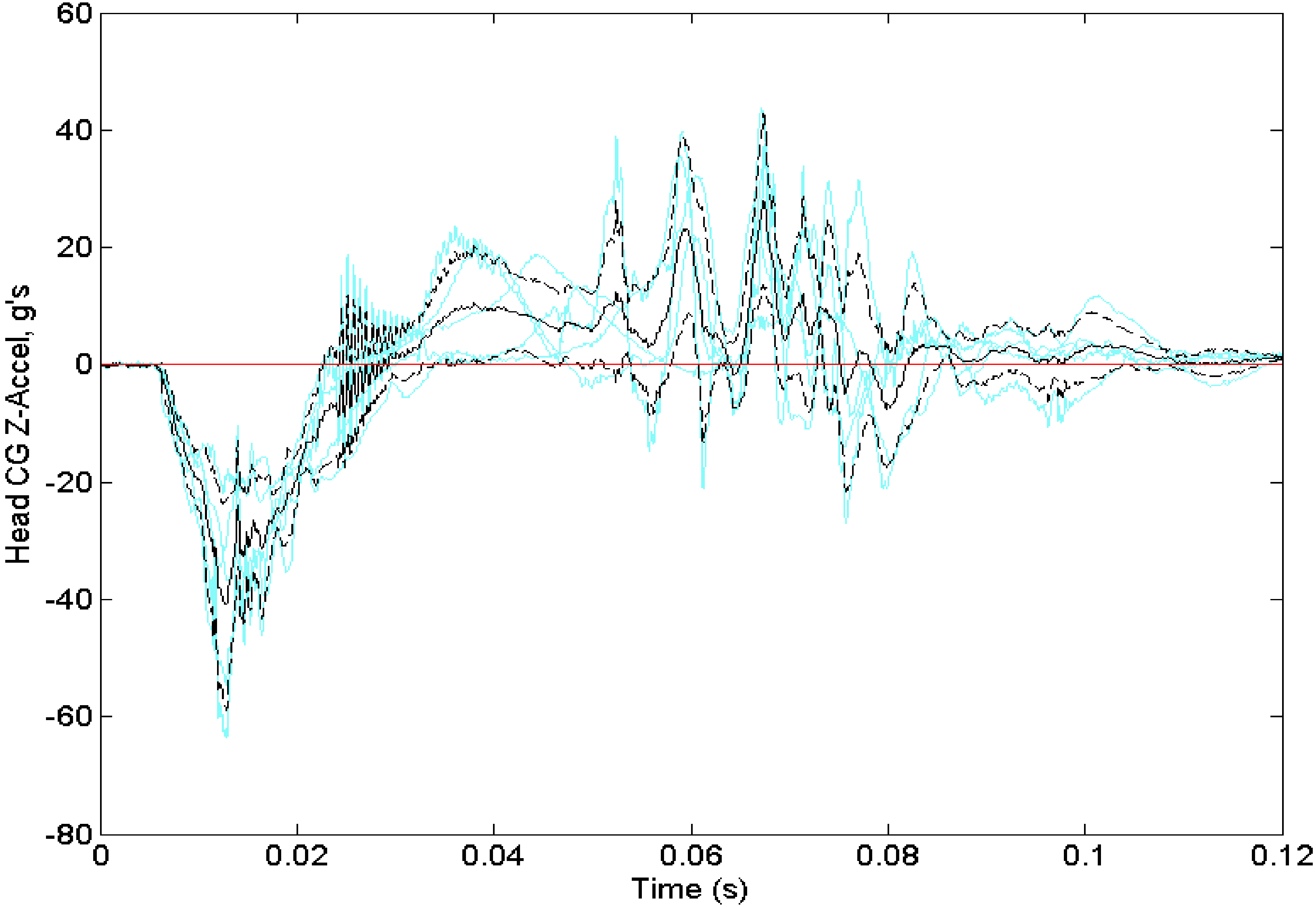

Head CG Accel Az at 3m/s

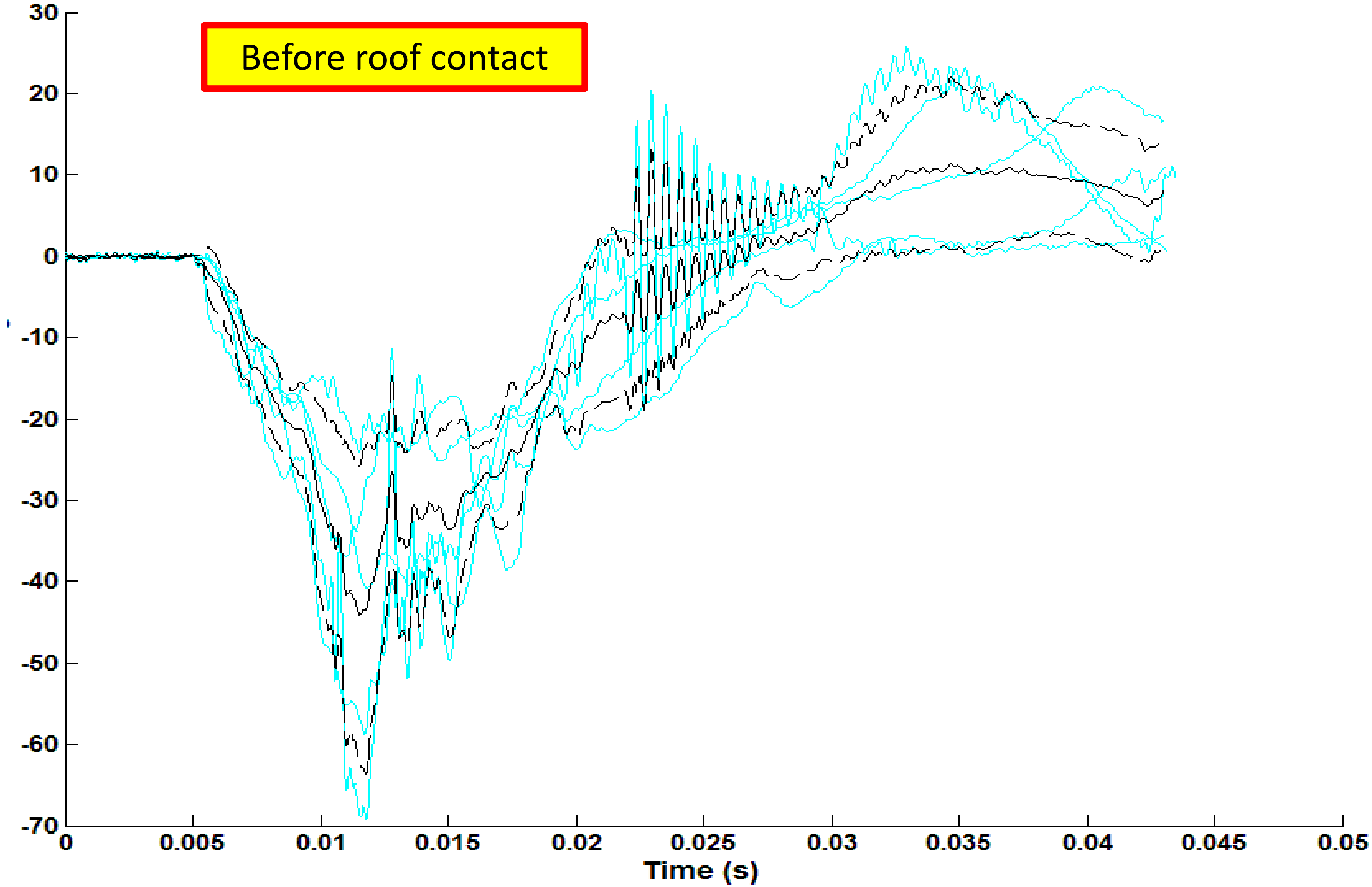

Summary

- Rigorous BRC development process
- All relevant information included in BRC packages
  - Fixtures: dimensions, materials, mass, coupling
  - Boundary condition
  - Initial posture
  - Input corridors

- Total of 81 BRCs available for model validation
  - Two series completed: head-neck and cervical spine in neutral posture
  - Four series on-going: pre-flexed and pre-extended postures
  - Additional 148 BRCs are in the pipeline

- Significant anterior excursion of the head when head contact with roof structure

Acknowledgment

This effort was funded by contract #N00024-13-D-6400, U.S. Army Research, Development and Engineering Command.

The content included in this work does not necessarily reflect the position or policy of the U.S. government.

Lower Neck Fz at 2 m/s

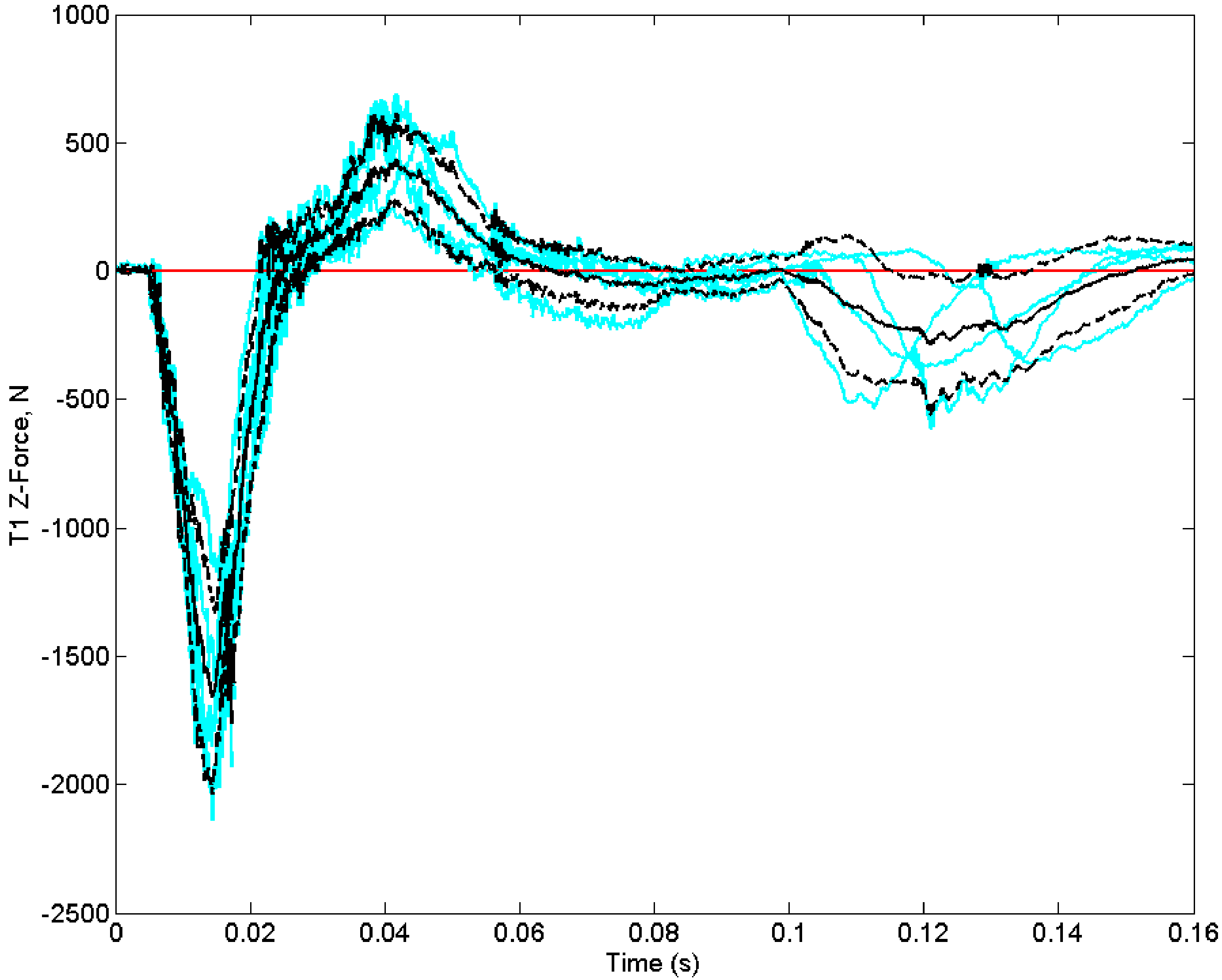

Lower Neck Fz at 3 m/s

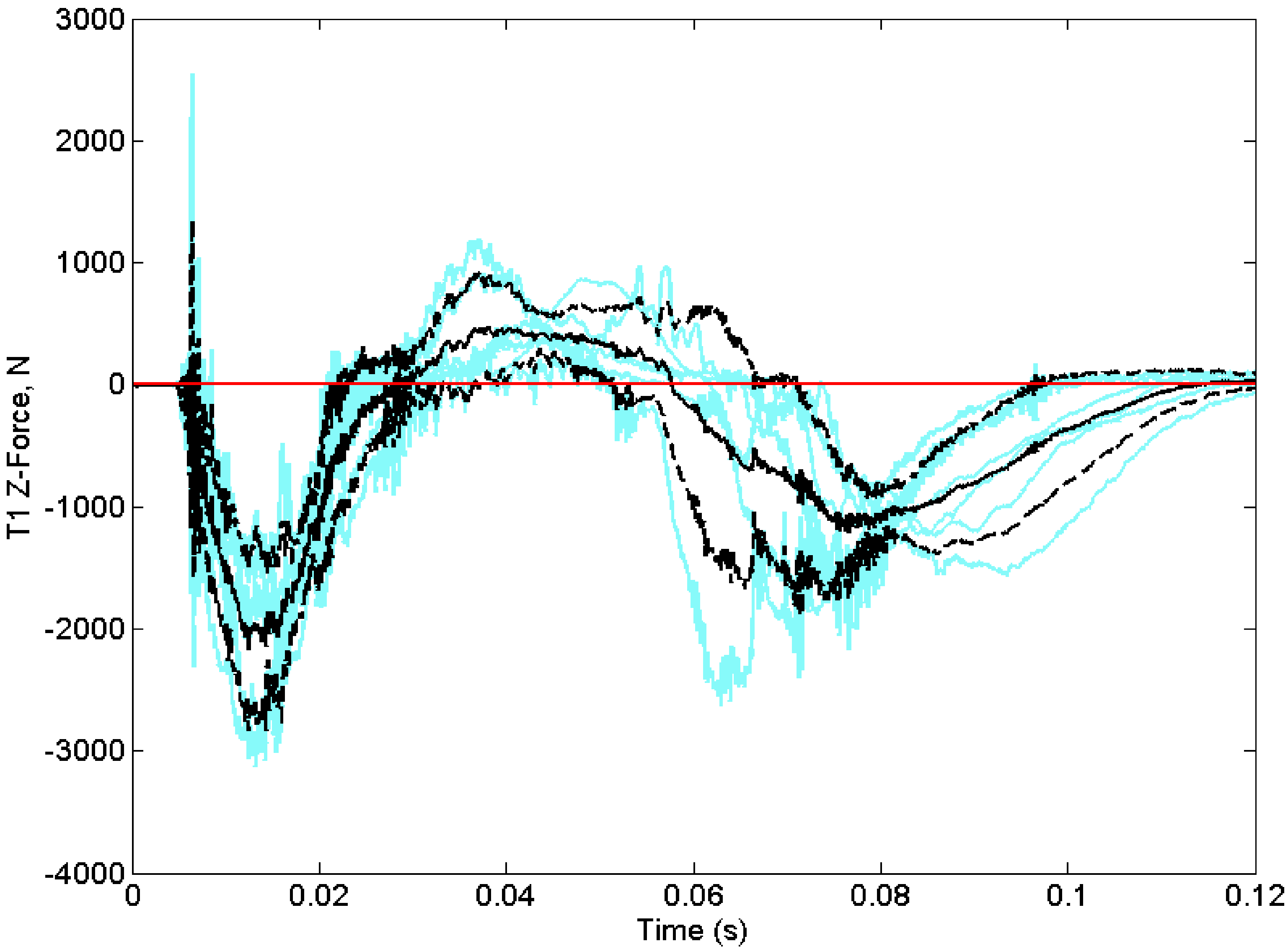

Lower Neck Fz at 2m/s

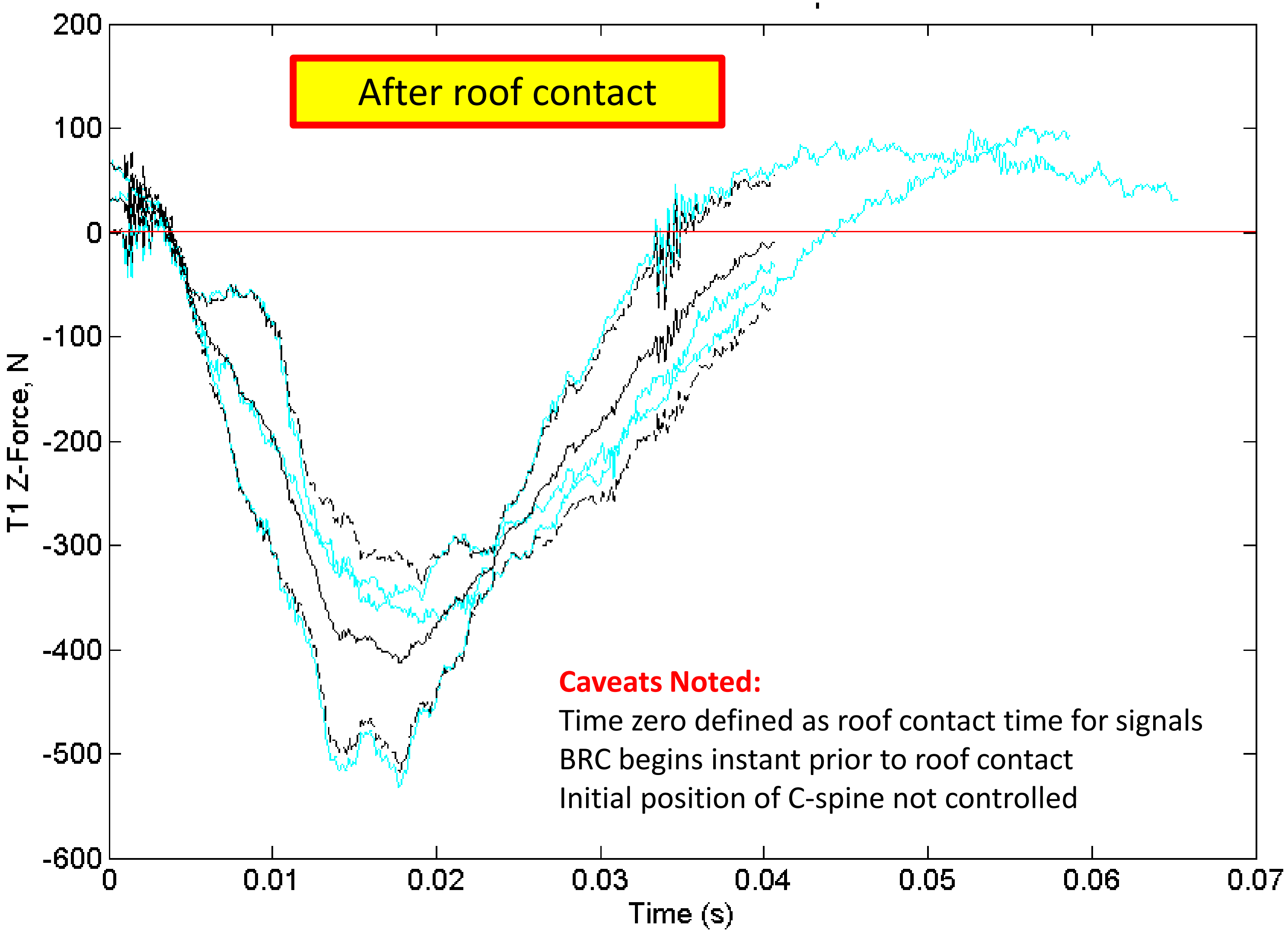

Effects of Lordosis on Lumbar Spine Biomechanical Responses

JiangYue Zhang[1], Jason Moore[2],
Frank Pintar[2], Narayan Yoganandan[2], Andrew Merkle[1]

1. Johns Hopkins University, Applied Physics Laboratories
2. Dept. of Neurosurgery, Medical College of Wisconsin

Second Workshop on Numerical Analysis of Human and Surrogate Response to Accelerative Loading
Aberdeen Proving Ground, MD
January 12-14, 2016

WARRIOR INJURY ASSESSMENT MANIKIN
RDECOM
ENGINEERING OFFICE

MEDICAL COLLEGE OF WISCONSIN

APL
The Johns Hopkins University
APPLIED PHYSICS LABORATORY

Background

UBB Lumbar Spine Injuries

- **IED—A major threat to ground vehicles**
  (Gondusky et al., 2005)
- **UBB – High rate, large amplitude, vertical loading (Cameron et al, 2011)**
- **Lumbar spine sustains various types of injuries created from different mechanisms**
  (Ragel et al., 2009)

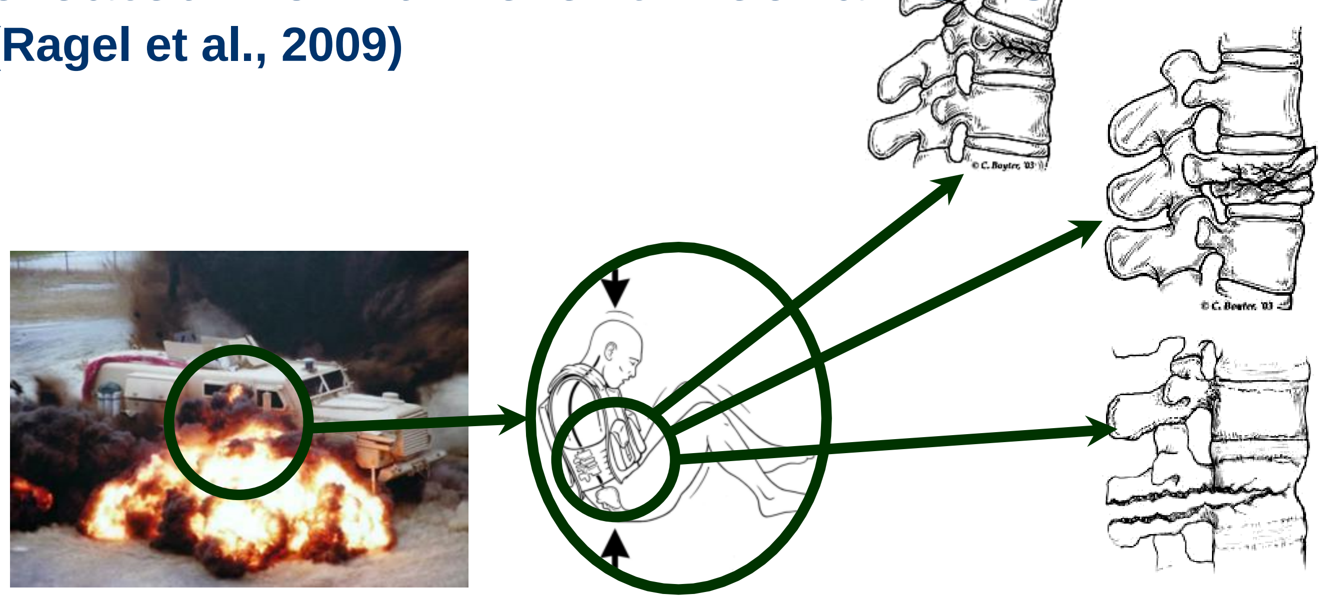

MEDICAL COLLEGE OF WISCONSIN

APL

Objectives

WIAMan Dev. & FEM Validation

- **Obtain biomechanical response data from PMHS under simulated UBB loading**
  - To guide WIAMan development
  - Provide validation data for FEM under accelerative loading in vertical direction

Methods

MCW Vertical Accelerative Device

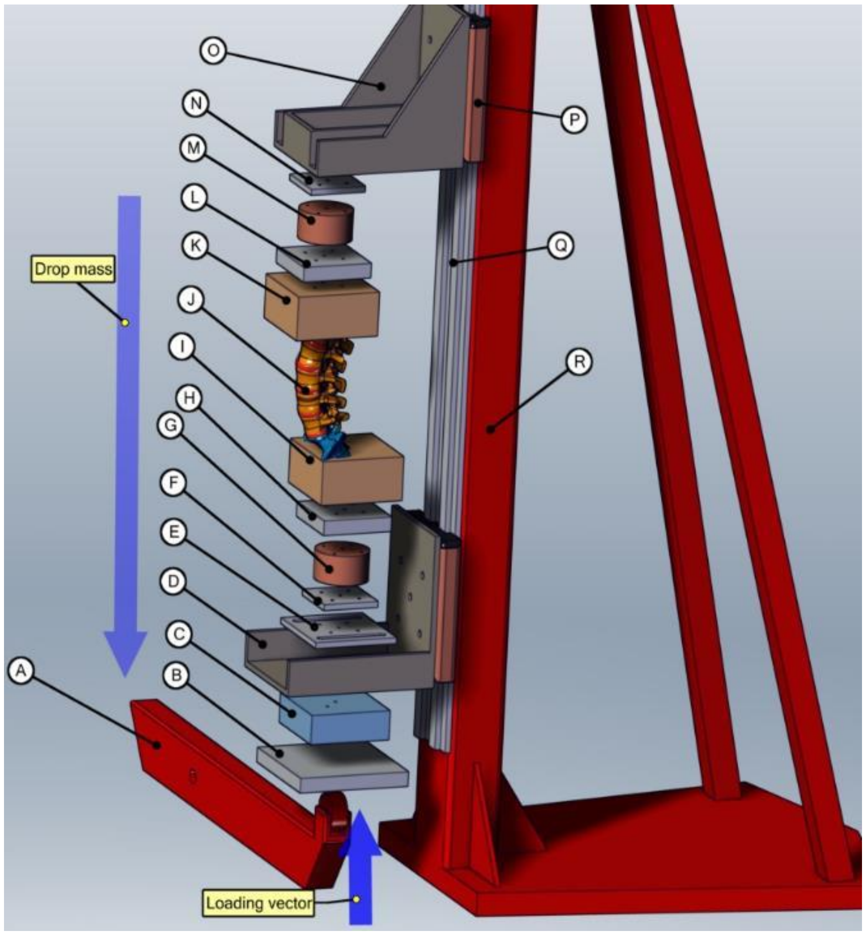

Simulated UBB loading to

- Loading
  - Simulated UBB loading were applied to the specimen through a drop mass that were amplified through a 1:2 lever arm
- Specimen & Potting
  - Whole lumbar spine from T12 to S1
  - Specimen were rigidly potted at T12 & S1 without interference with T12/L1 and L5/S1 joint, leaving everything in between free
- Posture
  - Nominal lumbar spine posture from UMTRI seated soldier study
  - T12 potted at 4.7º from horizontal; Spine column angle at 11.6º (5.1).

Lumbar Testing Conditions

- Specimen:
  - Whole lumbar spine with T12 & S1 attached
- Potting
  - Rigidly potted at T12 & S1 without interference with T12/L1 & L5/S1 joint
- Posture
  - Nominal lumbar spine posture from UMTRI seated soldier study
  - T12 potted at 4.7° from horizontal; Spine column angle at 11.6° (5.1).

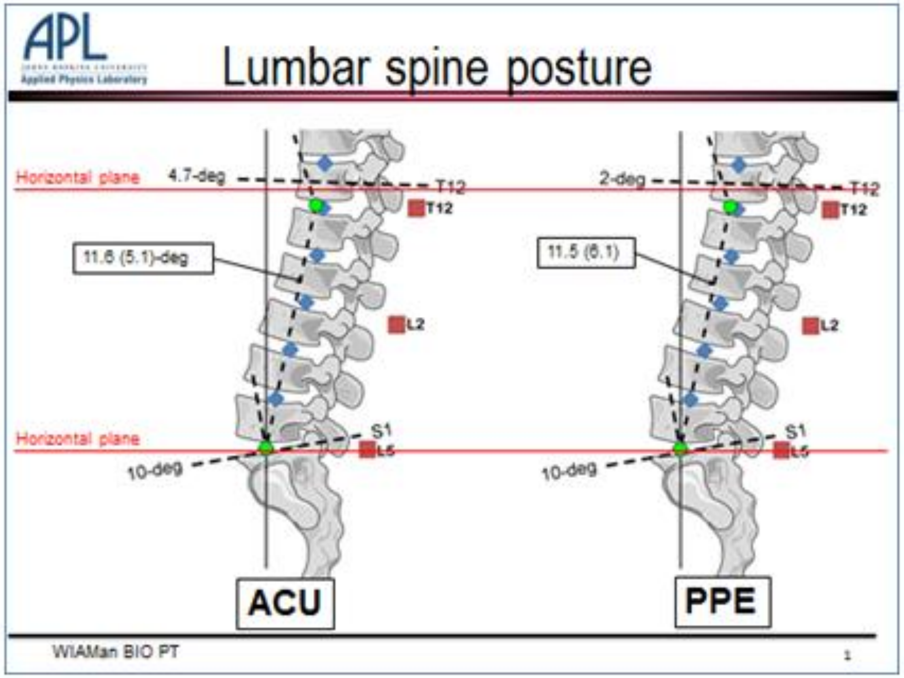

Methods

Specimens Tested

Performer	Specimen	Age	Race	Gender	Height (cm)	Weight (kg)	BMI
MCW	LS02-01	51	Caucasian	M	175	76	22.2
MCW	LS02-02	66	Caucasian	M	178	75	21.5
MCW	LS02-03	65	Caucasian	M	188	67	19.2
MCW	LS02-04	79	Caucasian	M	173	86	28.9
MCW	LS02-05	41	Caucasian	M	188	99	28.0
MCW	LS02-06	64	Caucasian	M	183	94	28.1

WIAMan Acceptance Range

WIAMan	Age	Gender	Height (cm)	Weight (kg)	BMI
Acceptance Range	18-80	M	165-186	64-106	18-35

Methods

Completed Tests

Performer	Specimen	BRC Test Sequence						Injury Test
		V1 (0.8 m/s, 10 ms TTP)	V1 (0.8 m/s, 10 ms TTP)	V2 (1.2 m/s, 10 ms TTP)	V1 (0.8 m/s, 10 ms TTP)	V3 (2.4 m/s, 10 ms TTP)	V1 (0.8 m/s, 10 ms TTP)	
MCW	LS02_01	✓	✓	✓	✓	✓	✓	X
MCW	LS02_02	✓	✓	✓	✓	✓	✓	X
MCW	LS02_03	✓	✓	✓	✓	✓	✓	X
MCW	LS02_04	✓	✓	✓	✓	X		
MCW	LS02_05	✓	✓	✓	✓	✓	✓	X
MCW	LS02_06	✓	✓	✓	✓	X*	✓	X

✓ = non-injurious test (BRC)
X = injurious test (HIPC)
***subtle injury at L1 endplate @ v3, subsequent injury run @ 9 m/s**

Methods

Detailed instrumentation

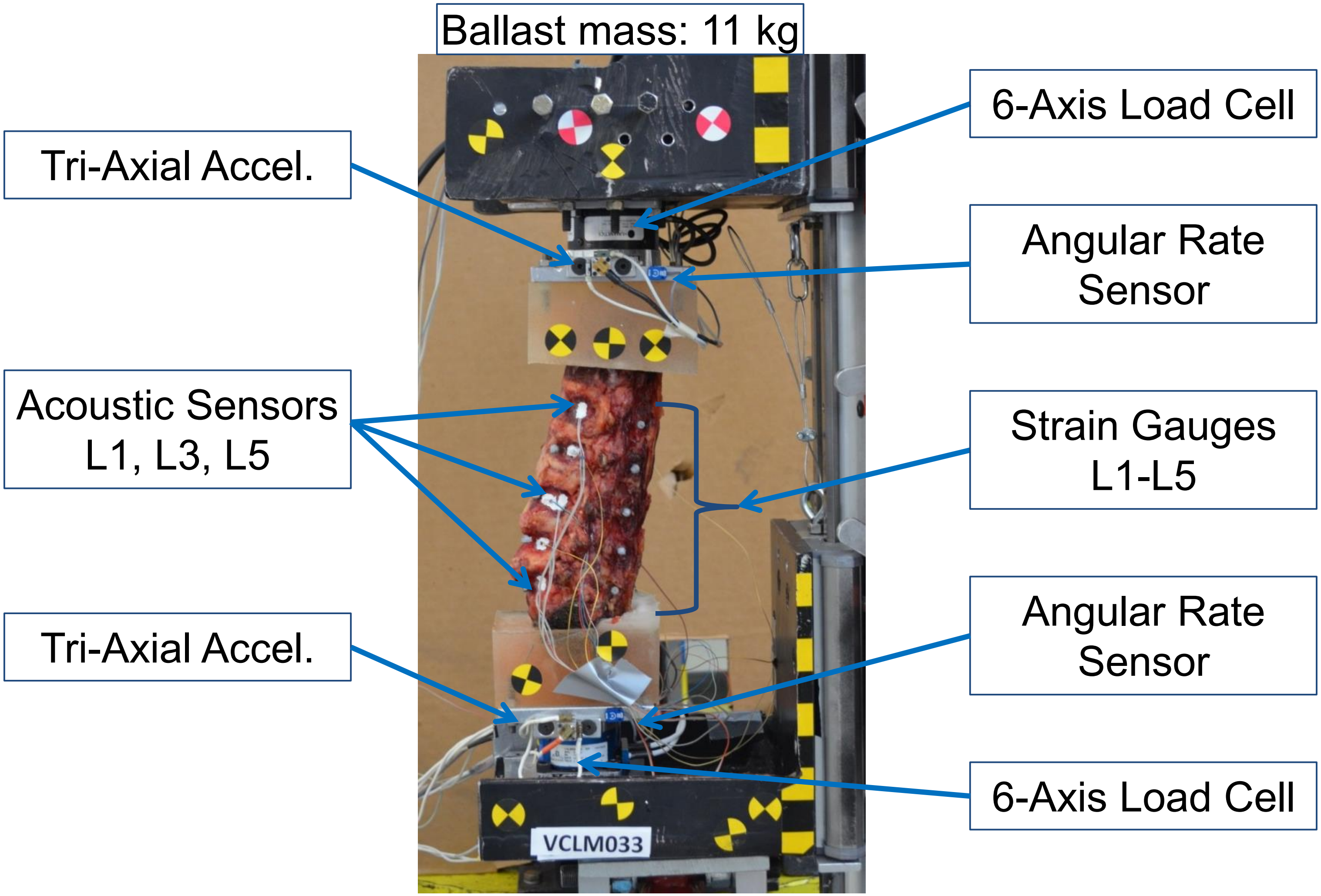

Methods

Collected Data

BP	Measure	# Specs @ each Velocity			Comments
		V1	V2	V3	
69	S1 Velocity in Z	6	6	4	From integration of S1 Accelerometer
30-U	Upper Lumbar Force Z	6	6	4	From upper lumbar load cell
30-L	Lower Lumbar Force Z	6	6	4	From lower lumbar load cell
31-U	Upper Lumbar Force X	6	6	4	From upper lumbar load cell
31-L	Lower Lumbar Force X	6	6	4	From lower lumbar load cell
32-U	Upper Lumbar Moment Y	6	6	4	From upper lumbar load cell
32-L	Lower Lumbar Moment Y	6	6	4	From lower lumbar load cell

Methods

Collected Data

WIAMan BIO PT

BP	Measure	# Specs @ each Vel			Comments
		V1	V2	V3	
33	T12 Potting Accel. Z	6	6	4	T12 accelerometers
35x	L1 motion in X	6	6	4	Video target
35z	L1 motion in Z	6	6	4	Video target
36	L3 acceleration Z	6	6	4	Accelerometers
37	L3 spine rotation	6	6	4	ARS mounted on L3
38z	L3 motion in Z	6	6	4	From high-speed video
38x	L3 motion in X	6	6	4	From high-speed video
39	S1 acceleration Z	6	6	4	From accelerometer on S1 potting
41z	L5 motion in Z	6	6	4	Video target on L5
41x	L5 motion in X	6	6	4	Video target on L5
58	T12 to S1 overall compression	6	6	4	Integration of T12 & S1 accelerometers

Results

Compensated Axial Force Fz

Measured Load Cell Forces compensated to L5/S1 and T12/L1 joint center

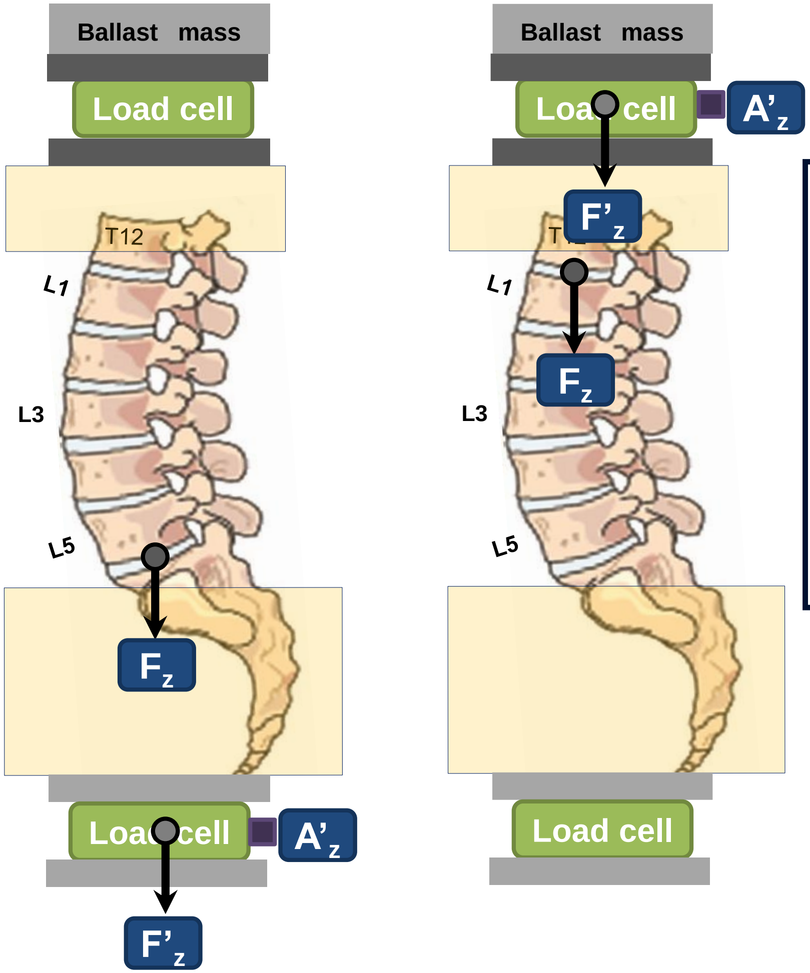

Compensation mass:

$$M_{Comp} = M_{Potting} + 0.5*M_{load\ cell}$$

Compensation:

$$F_z = F'_z + M_{comp} * A'_z$$

Results

Compensated Axial Fz Raw Data

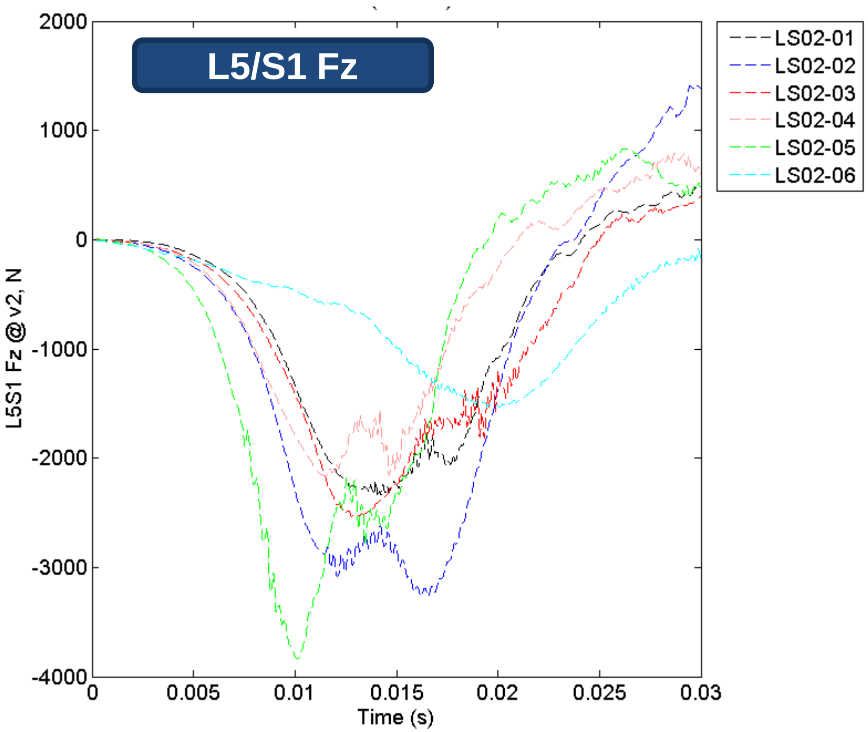

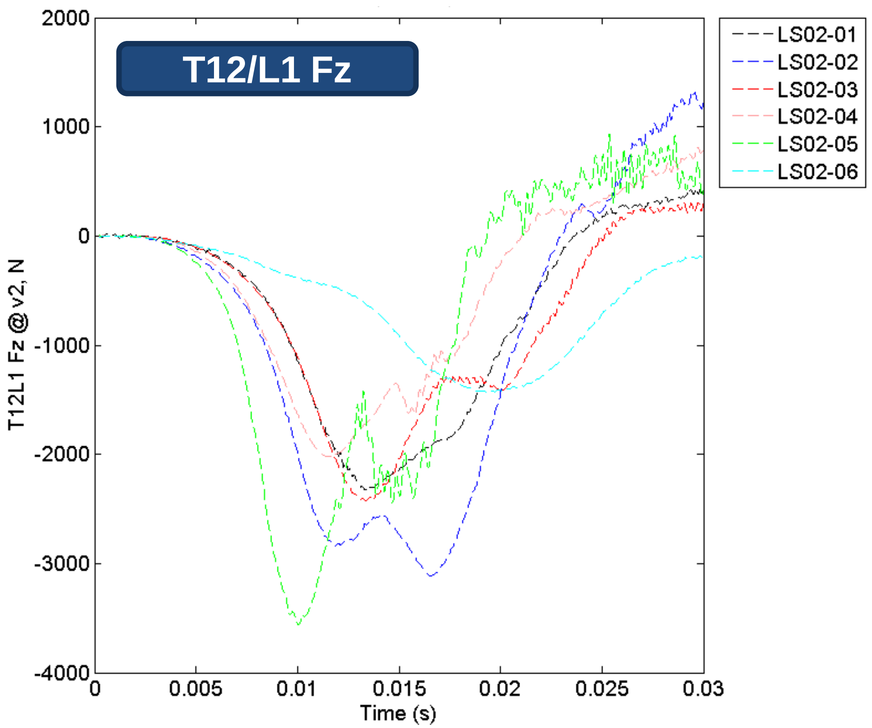

BRC Generation

Gayzik et al., J. Biomech, 2015

$$p(x_1, x_2, h) = 1 - \frac{1}{L}\sum_{i=1}^{L} \frac{\sqrt{\left(x_{1,i} - x_{2,i+h}\right)^2}}{\sqrt{{x_{1,i}}^2} + \sqrt{{x_{2,i+h}}^2}}$$

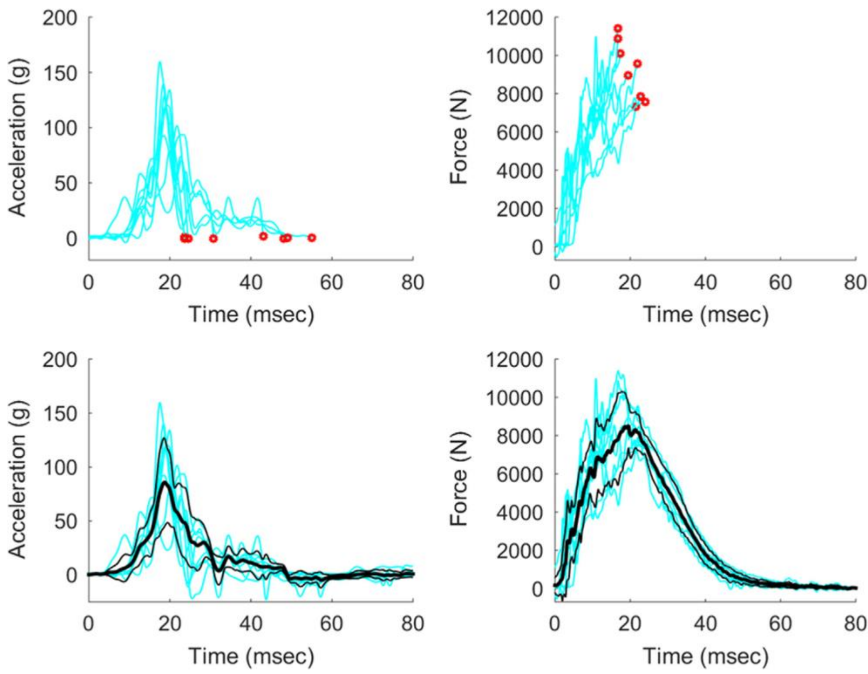

Gayzik, J. Biomech, 2015

- **Goal: Find *h (time shift)* that maximizes p**
- **A normalized least squares correlation coefficient**
  - L: Number of data points in the length of the time signal allowed to overlap
  - Numerator: sum of squares difference at a given time point (i) for a given shift (i+h)
  - Denominator: the largest difference possible at a given time point and shift (sum of absolute value)
  - Ratio is subtracted from 1 so that good match will be 1 not 0
  - Normalizes the difference on a point by point basis, i.e. all time points are treated equally (not weighted at peaks)

BRC Generation

Maximize CCC to calculate RC

1. Calculate CCC and time shifts between all curves
2. ID the two signals with the highest CCC
3. Shift one signal based on the calculated time shift
4. Find the next signal with the highest CCC between it and the first two and time shift it
5. Repeat finding signals one at a time until all have been shifted
6. **Calc. Mean (1st iteration of RC)**
7. Calculate the CCCs and time shifts between all the signals and the mean, sum the CCCs
8. Align the signals to the mean based on the time shifts
9. Average the aligned signals to get the new mean

RC – Representative Curve, CCC – Cross Correlation Coefficients

BRC Generation

Maximize CCC to calculate RC

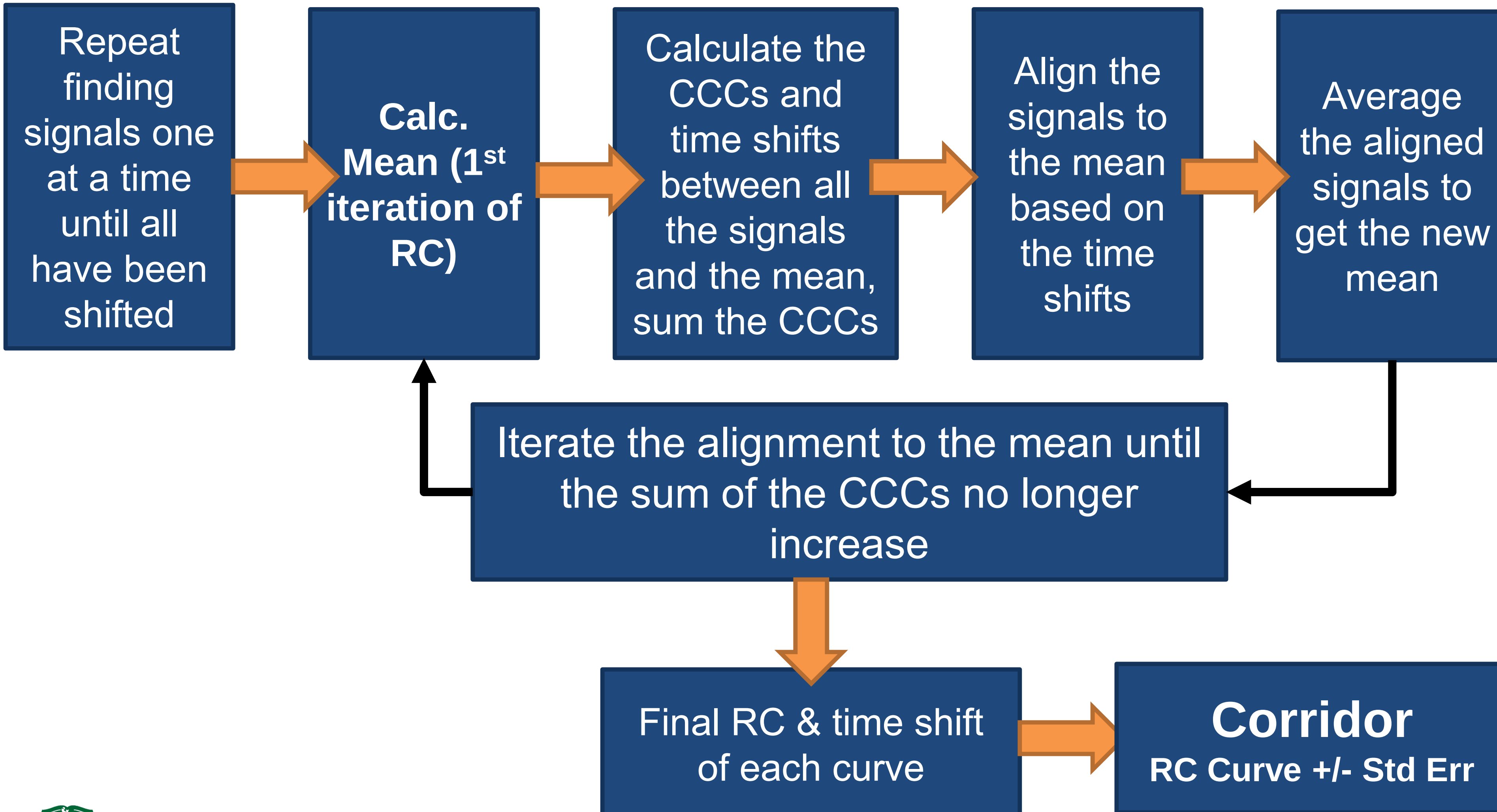

RC – Representative Curve, CCC – Cross Correlation Coefficients

Results

Compensated Axial Fz Corridor

L5/S1

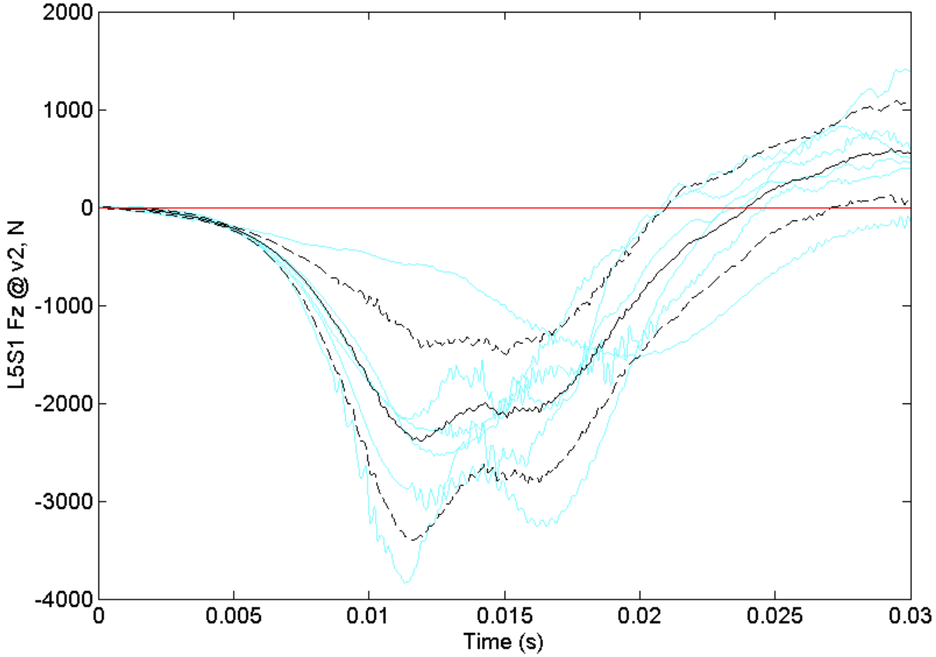

T12/L1

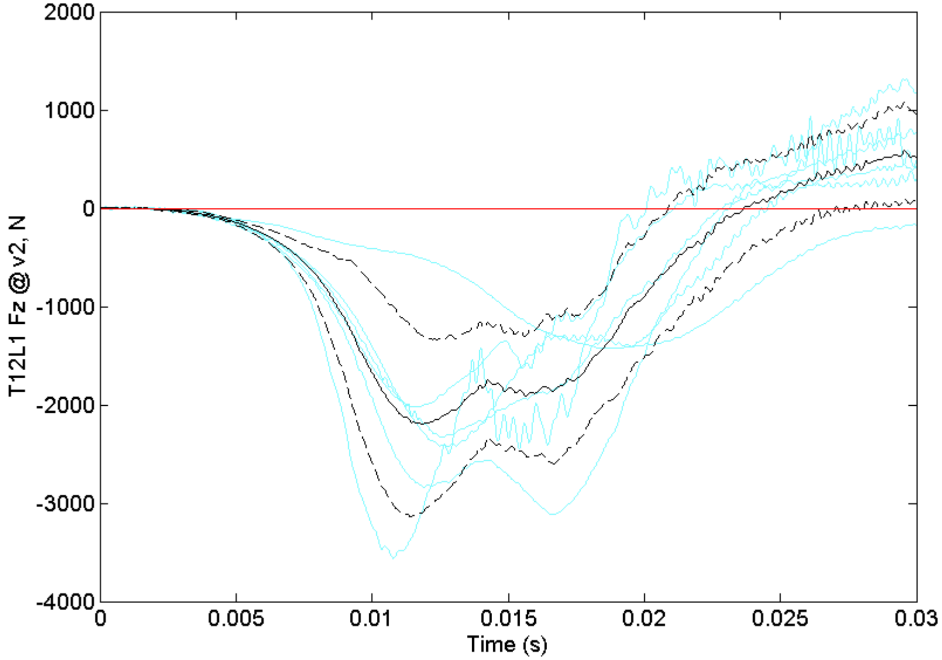

MEDICAL COLLEGE OF WISCONSIN

APL

Results

Transformed Moments

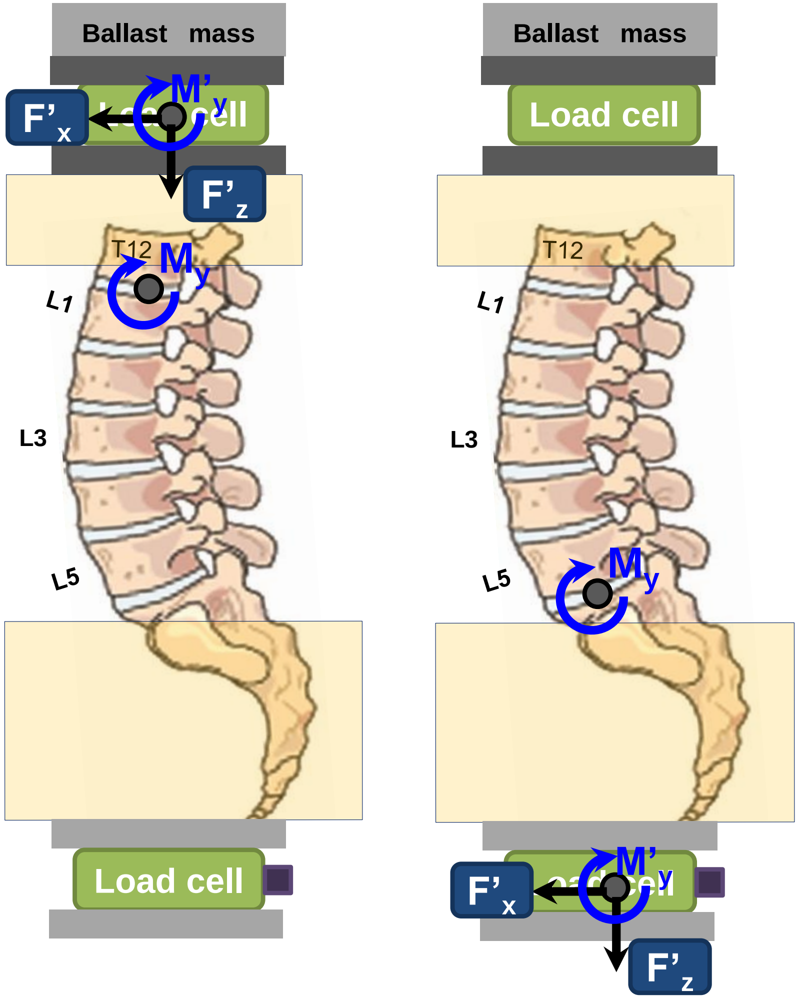

Moment Y Transformation:

$$\mathbf{M_y} = \mathbf{M'_y} + \vec{\mathbf{F}} \times \vec{\mathbf{D}}$$
$$= \mathbf{M'_y} + \mathbf{F_z D_x} - \mathbf{F_x D_z}$$

Results
Transformed Moments Raw Data

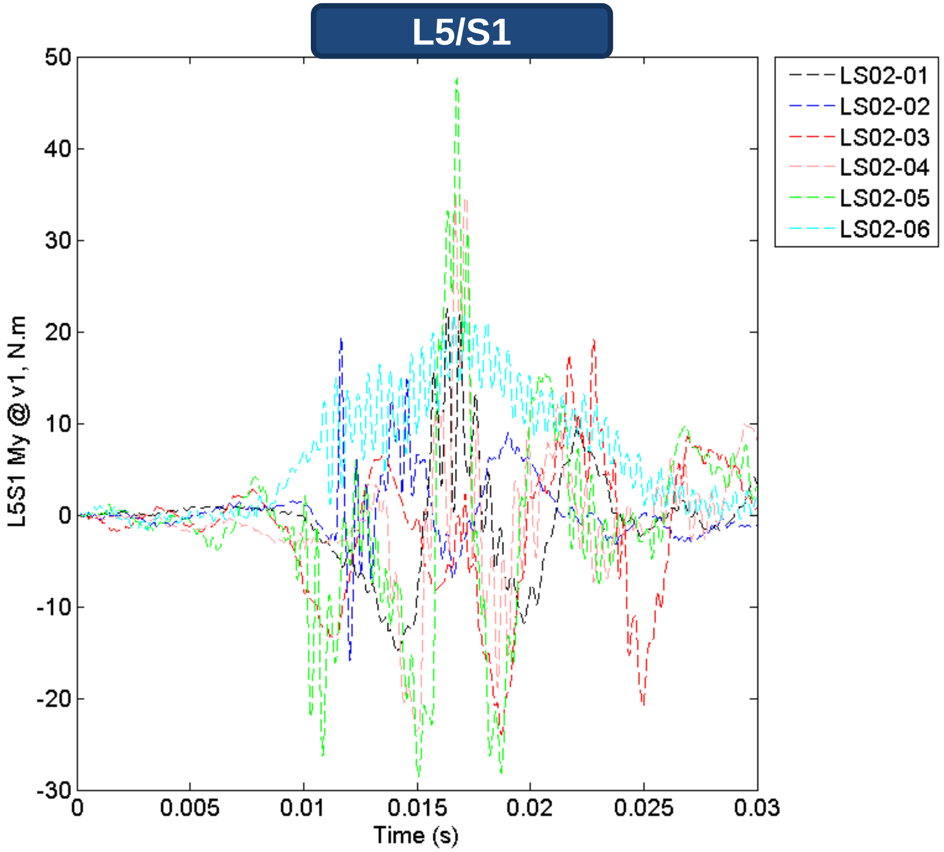

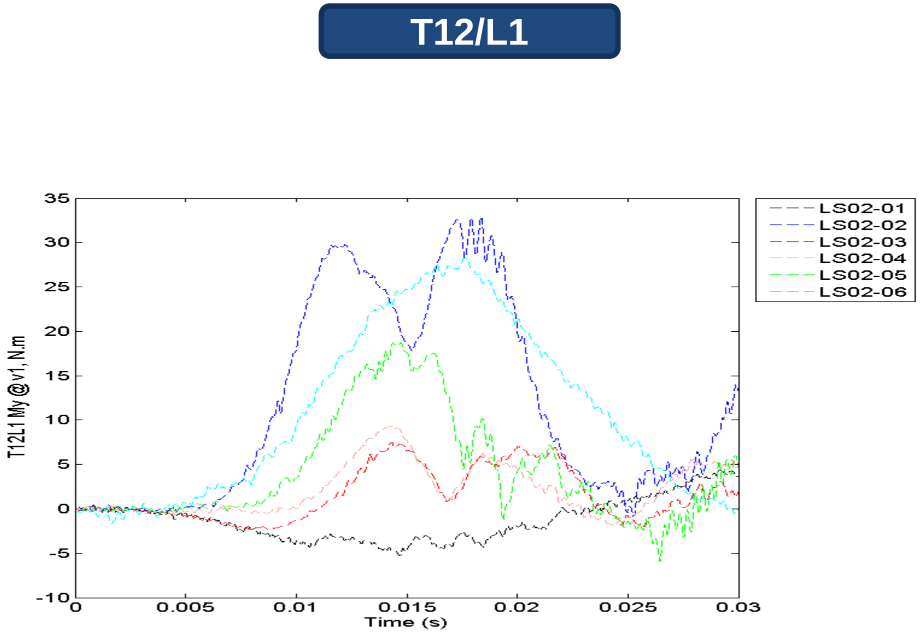

Results

Transformed Moments Corridor

L5/S1

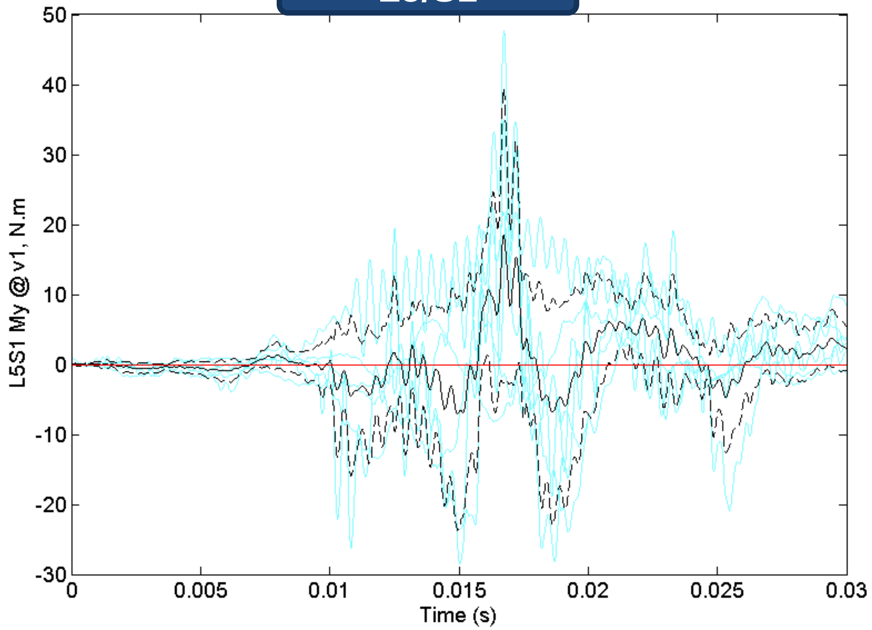

T12/L1

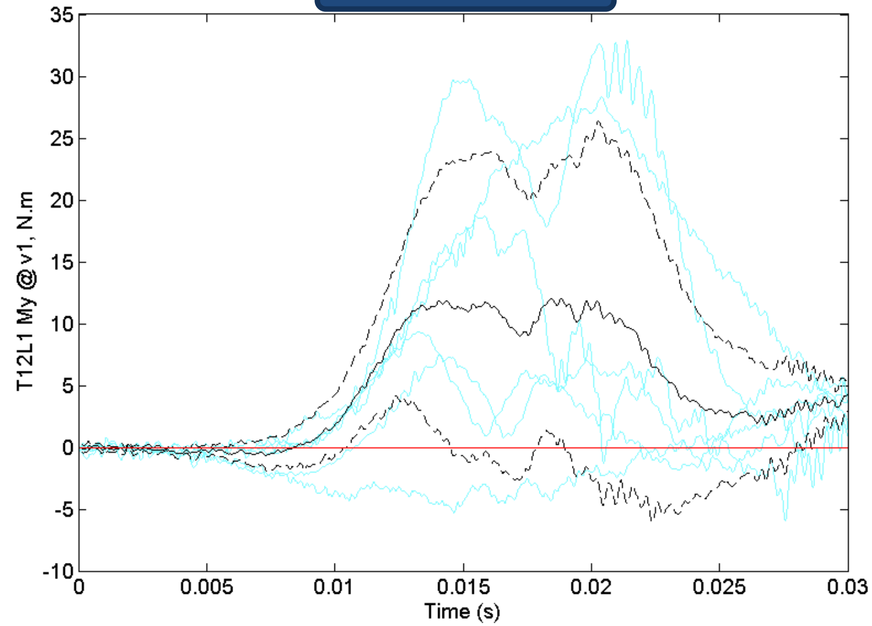

Results

Discrepancy in Transformed Moments

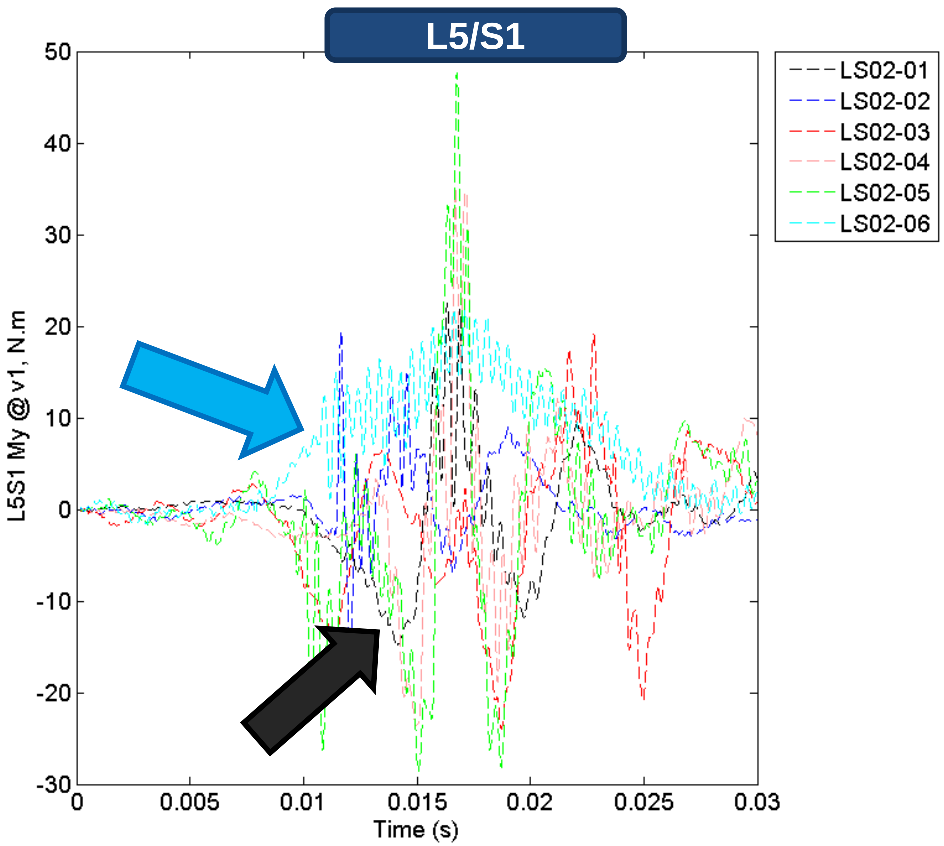

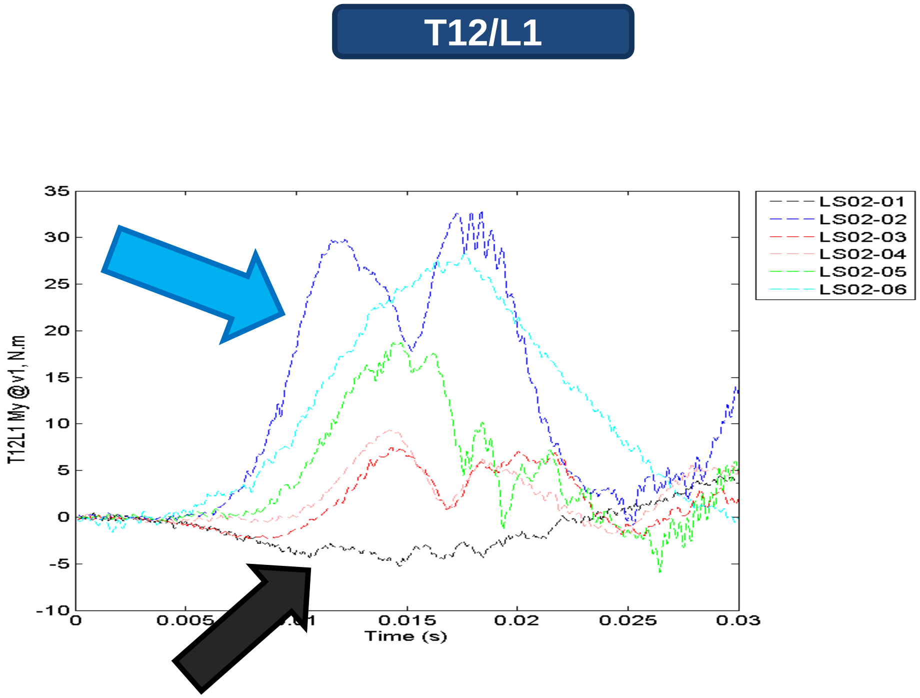

Discussion

Specimen Lordosis as Received

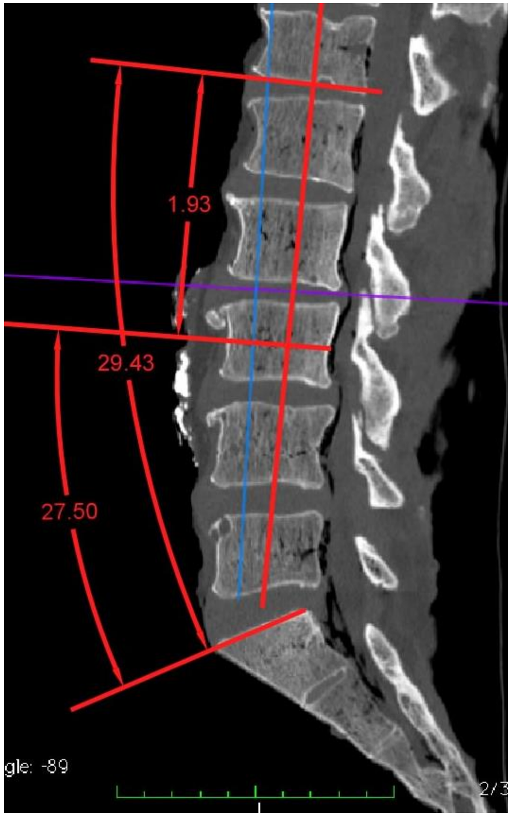

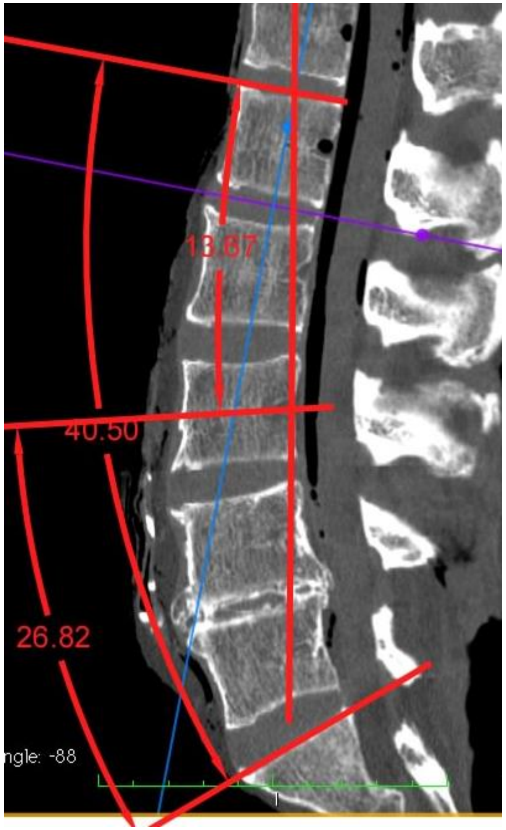

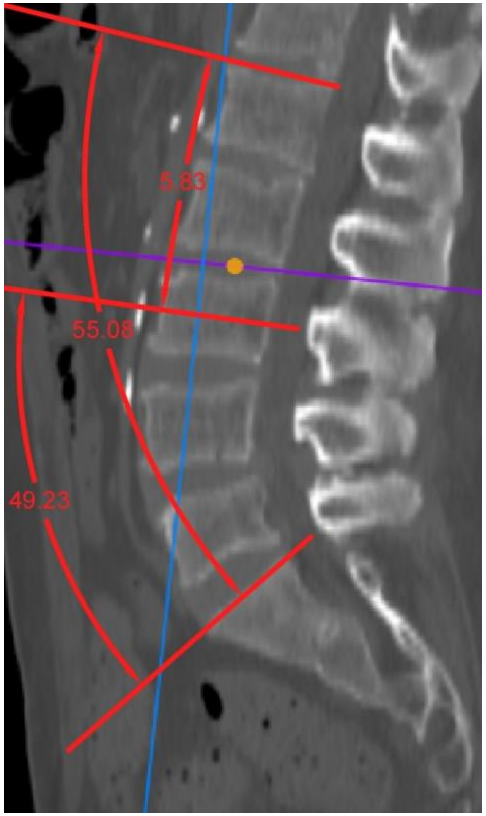

Discussion

Specimen Lordosis as Received

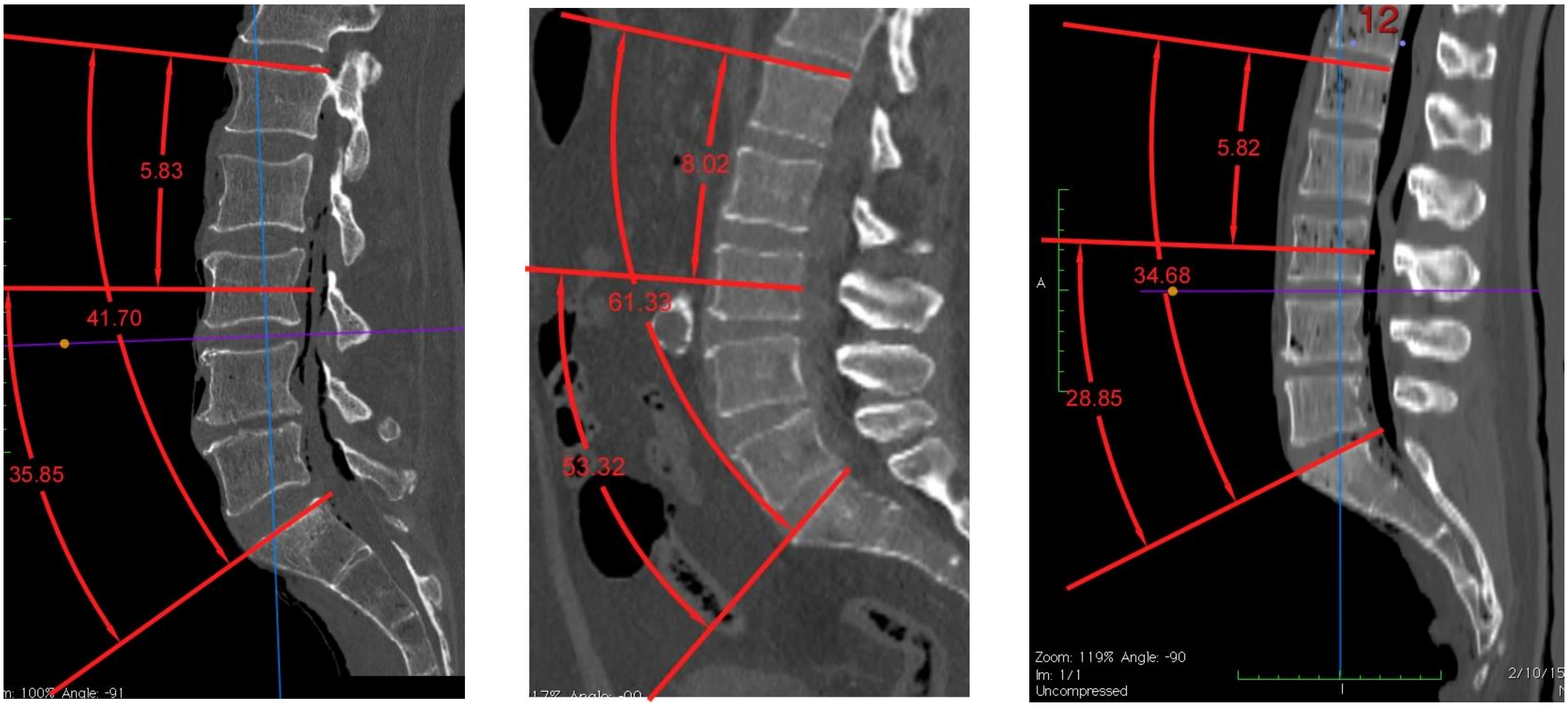

MEDICAL COLLEGE OF WISCONSIN

APL

Discussion

Specimen Lordosis in Position

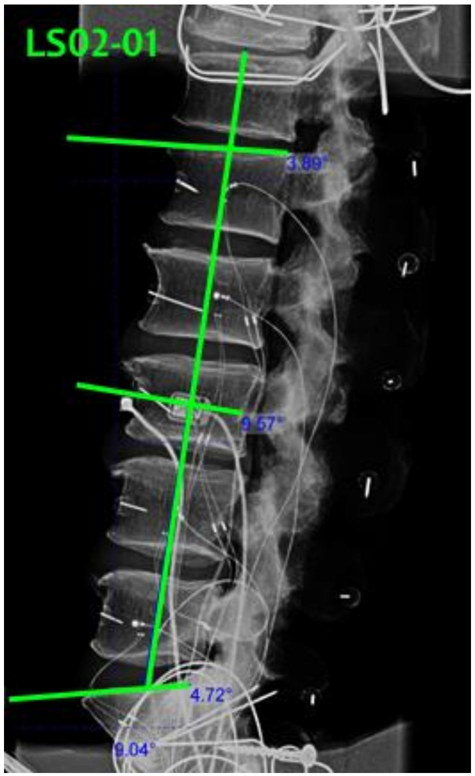

Discussion

Specimen Lordosis in Position

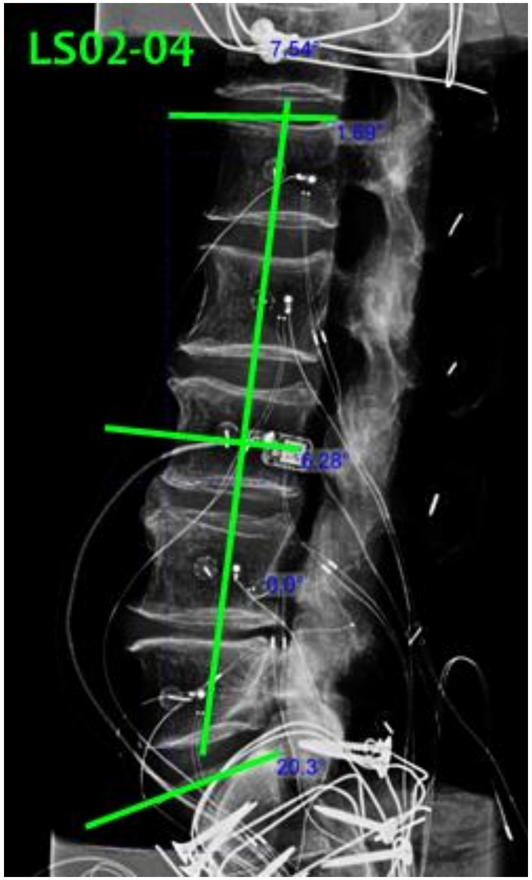

Discussion

Spine Angles as Received & In Position

	Lumbar Tilt	L1--S1 Cobb Angle			L1--L3 Cobb Angle			L3--S1 Cobb Angle		
	In Position	@ Recd	In Position	Change	@ Recd	In Position	Change	@ Recd	In Position	Change
LS02-01	9.04	29.43	8.61	20.82	1.93	-5.68	7.61	27.5	14.29	13.21
LS02-02	11.28	40.5	32.55	7.95	13.67	-2.02	15.69	26.82	34.57	-7.75
LS02-03	10.1	55.08	15.2	39.88	5.83	-9.1	14.93	49.23	24.3	24.93
LS02-04	7.54	41.7	21.99	19.71	5.83	-4.59	10.42	35.8	26.58	9.22
LS02-05	10.79	34.68	28.98	5.7	5.82	-1.5	7.32	28.85	30.48	-1.63
LS02-06	9.51	61.13	39.56	21.57	8.02	1.09	6.93	53.32	38.47	14.85

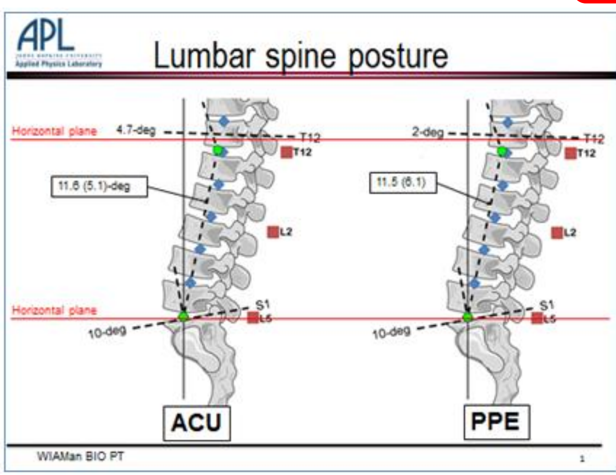

- **Spines had initial subject variations**
- **Spines were prepositioned according to UMTRI nominal posture with <40 N.m preloading to align T12 & spine column angle**
- **There are still differences in spine lordosis from T12 to S1 after preposition**
- **These difference can contribute to the variations in biomechanical response**

Discussion

Comparison of Specimen #1 vs. #6

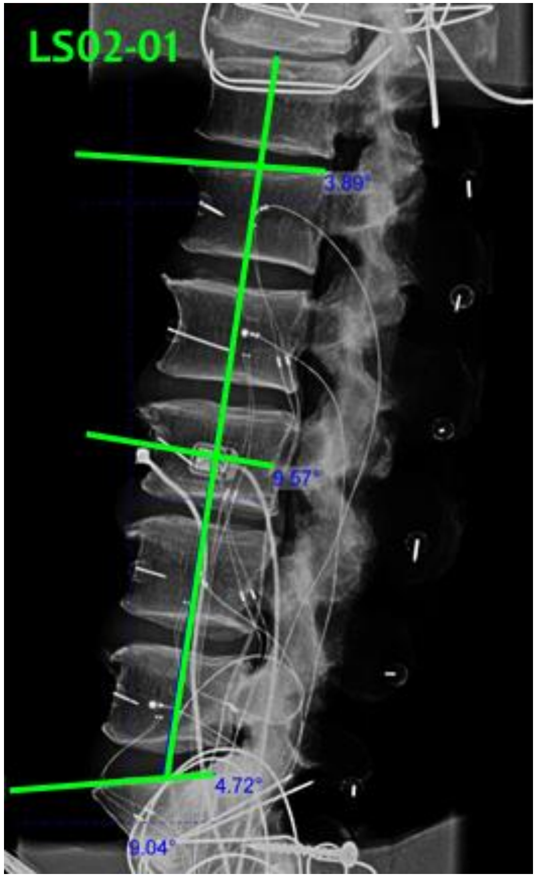

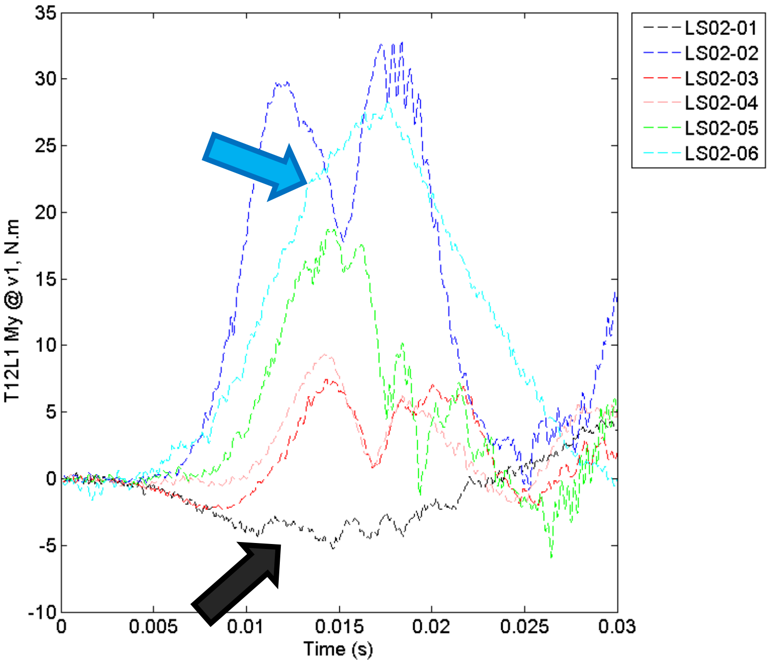

Discussion

Comparison of Specimen #1 vs. #6

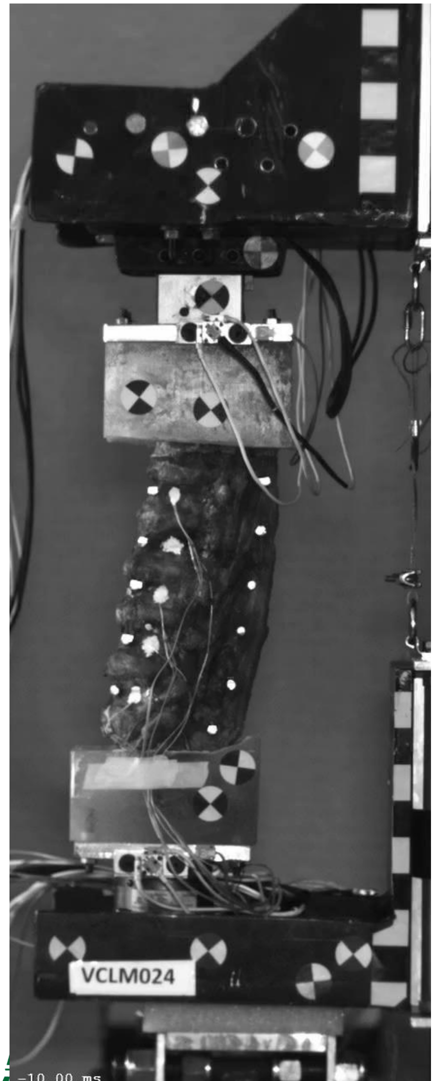

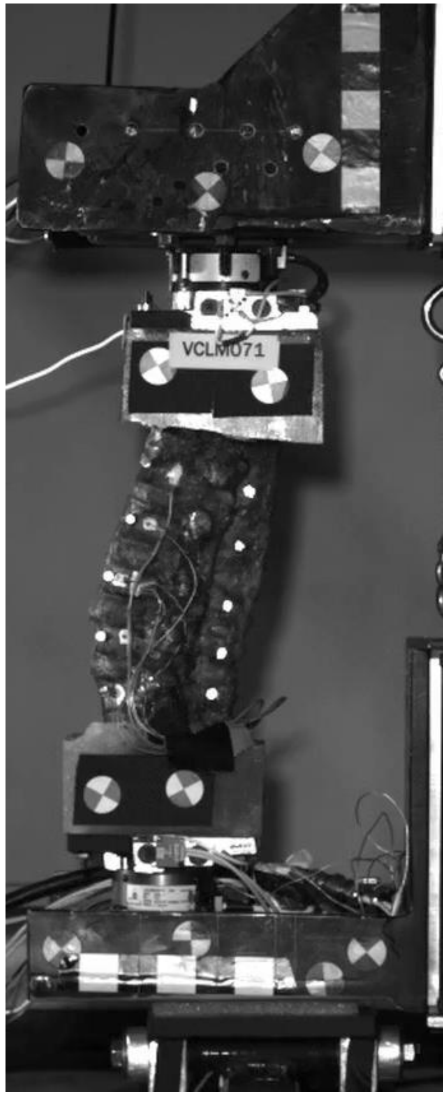

Comparison of specimen 1 & 6

- **Subject variation**
  - Specimen #1 is straight, with smallest cob angles
  - Specimen #6 has largest lordosis with largest cob angles
- **Spine kinematics**
  - Specimen #1 was loaded axially with limited amount of bending
  - Specimen #6 bent continuously in “C” shape during the loading
- **T12/L1 joint motion**
  - Specimen #1 has limited amount of bending
  - Specimen #6 was clearly in flexion

Discussion

Comparison of Specimen #1 vs. #6

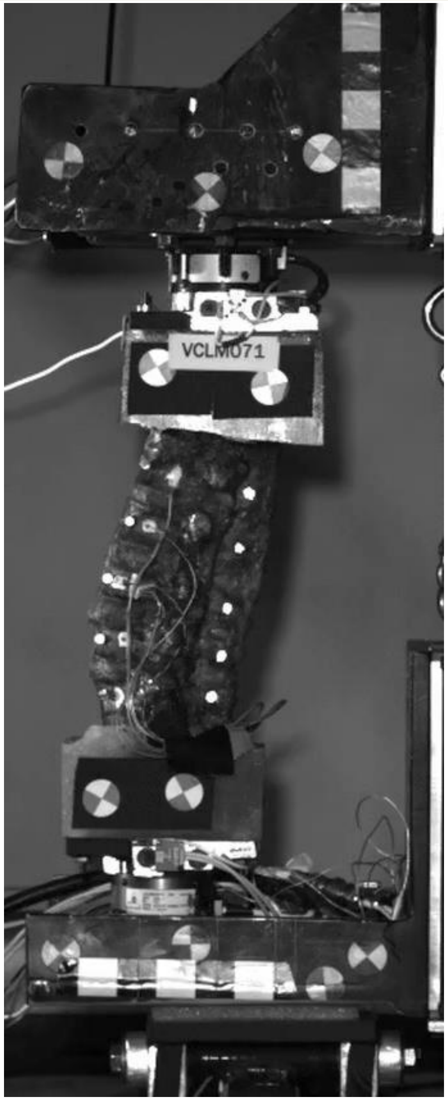

Comparison of specimen 1 & 6

- **L5/S1 joint**
  - L5 of Specimen #1 rocks back & forth
  - L5 of Specimen #6 was clearly in flexion

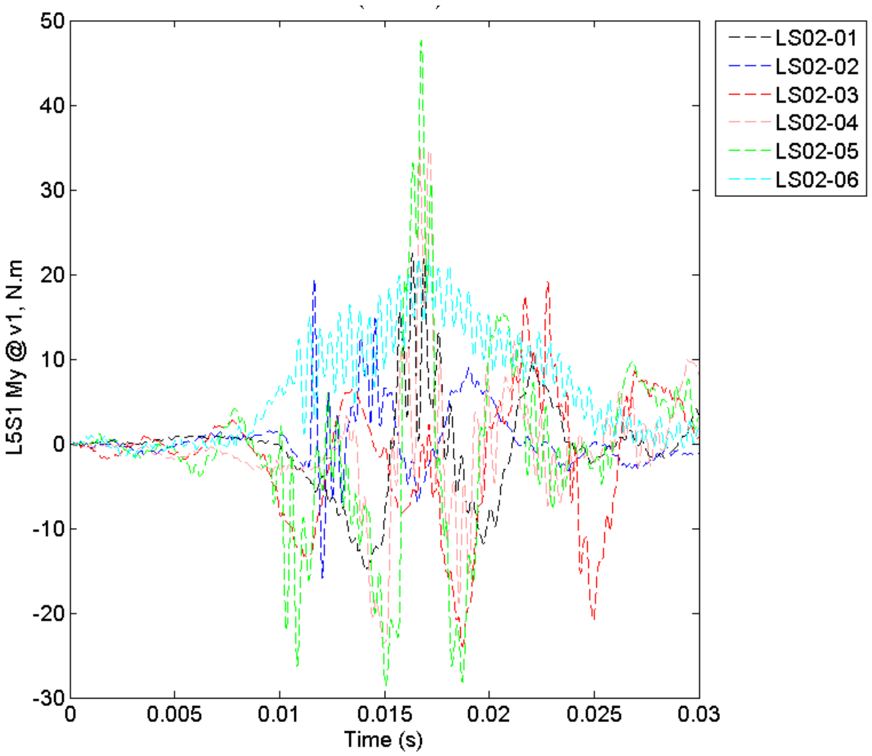

Summary

- **A total of 26 tests has been conducted on 6 PMHS lumbar spines which produced**
  - 3 input loading corridor corresponding to 3 loading severity
  - 51 biomechanical response corridors normalized and transferred to anatomical locations
  - Primary response corridors can be used to guide WIAMan design and FEA validation
  - Variation in off axis responses (shear forces and bending moments) can be attributed to subject variation in initial spine lordosis
- **These valuable PMHS data can be used for**
  - Validation of FE human lumbar spine model under accelerative loading in the vertical direction
  - Provide guidance to WIAMan design to ensure biofidelity of the surrogate
- **Future studies**
  - Lumbar spine BRCs in preflex (completed) and pre-extended posture
  - Effect of time-to-peak (loading rate) on lumbar response

Acknowledgement

This research was conducted as part of the Biomechanics Product Team led by the Johns Hopkins Applied Physic Laboratory for the WIAMan Project under contract #N00024-13-D-6400, U.S. Army Research, Development and Engineering Command.

The content included in this work does not necessarily reflect the position or policy of the U.S. government.

Effects of Lordosis on Lumbar Spine Biomechanical Responses

JiangYue Zhang[1], Jason Moore[2], Frank Pintar[2], Narayan Yoganandan[2], Andrew Merkle[1]

1. Johns Hopkins University, Applied Physics Laboratories
2. Dept. of Neurosurgery, Medical College of Wisconsin

Second Workshop on Numerical Analysis of Human and Surrogate Response to Accelerative Loading
Aberdeen Proving Ground, MD
January 12-14, 2016

WARRIOR INJURY ASSESSMENT MANIKIN
RDECOM
ENGINEERING OFFICE

MEDICAL COLLEGE OF WISCONSIN

APL
The Johns Hopkins University
APPLIED PHYSICS LABORATORY

Methods

Sign Conventions

- **Global coordinate definition:**
  - **+X**: posterior → anterior;
  - **+Y**: left → right;
  - **+Z**: superior→ inferior
- **Displacement, velocity and acceleration were defined same as above**

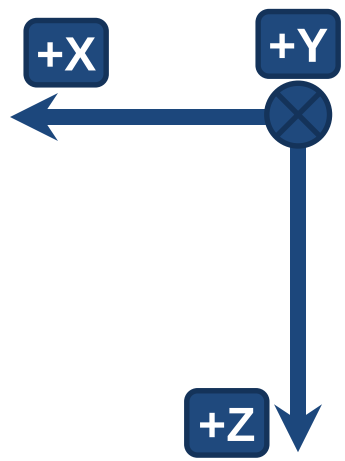

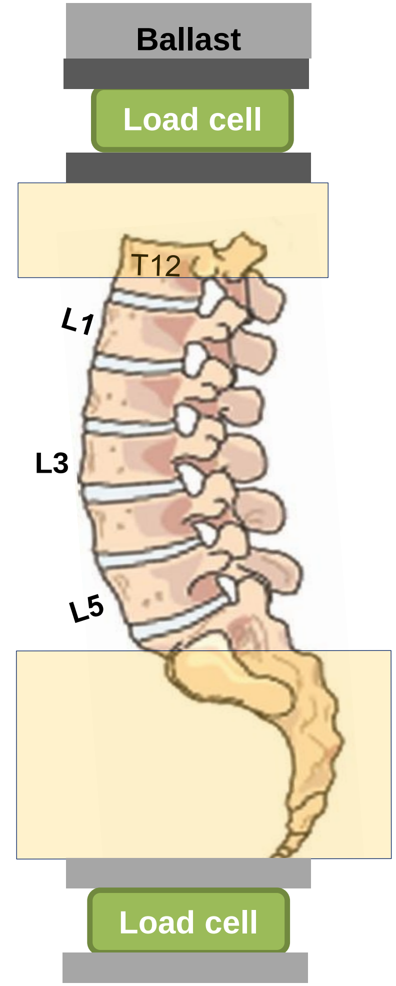

Methods

Sign Conventions

- **T12/L1 joint Force & Moment (Assuming T12 stationary)**
    - **+Fx** L1 forward;
    - **+Fy** L1 rightward;
    - **+Fz** L1 downward
    - **+Mx** L1 left lateral process toward T12 left lateral process;
    - **+My** Lumbar toward sternum; T12/L1 joint in flexion;
    - **+Mz** L1 left lateral process rotate toward anterior of spine, L1 right lateral process rotation toward posterior of spine
  - – Rotational displacement, velocity and acceleration were defined in same direction as the moment

*** Forces/moment causing same relative T12/L1 motion as mentioned above will be of the same sign**

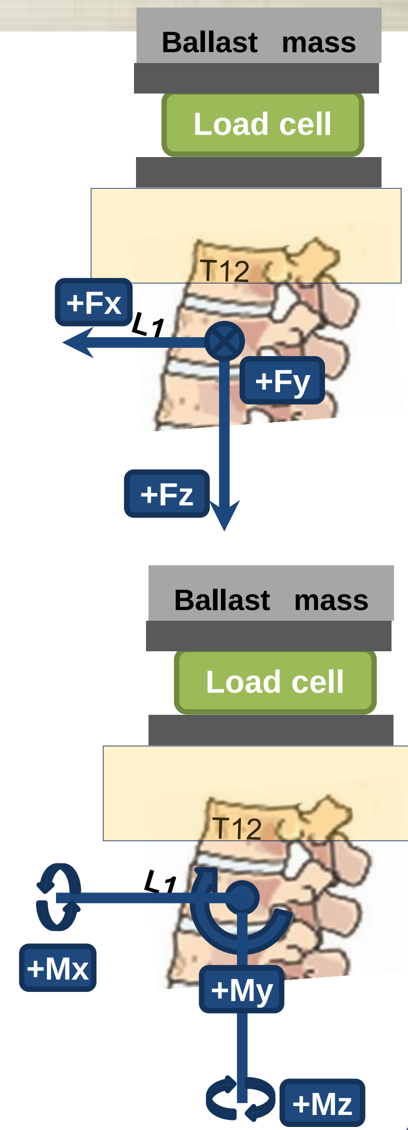

Methods

Sign Conventions

L5/S1 joint force and moment (L5 stationary):

- **+Fx** S1 forwardward;
- **+Fy** S1 rightward;
- **+Fz** S1 downward
- **+Mx** S1 left lateral process toward L5 left lateral process
- **+My** Pelvis rotate toward lumbar spine; L5/S1 joint in flexion
- **+Mz** S1 left lateral process rotate toward anterior of spine, S1 right lateral process rotation toward posterior of spine
  - Rotational displacement, velocity and acceleration were defined in same direction as the moment

*** Forces/moment causing same relative L5/S1 motion as mentioned above will be of the same sign**

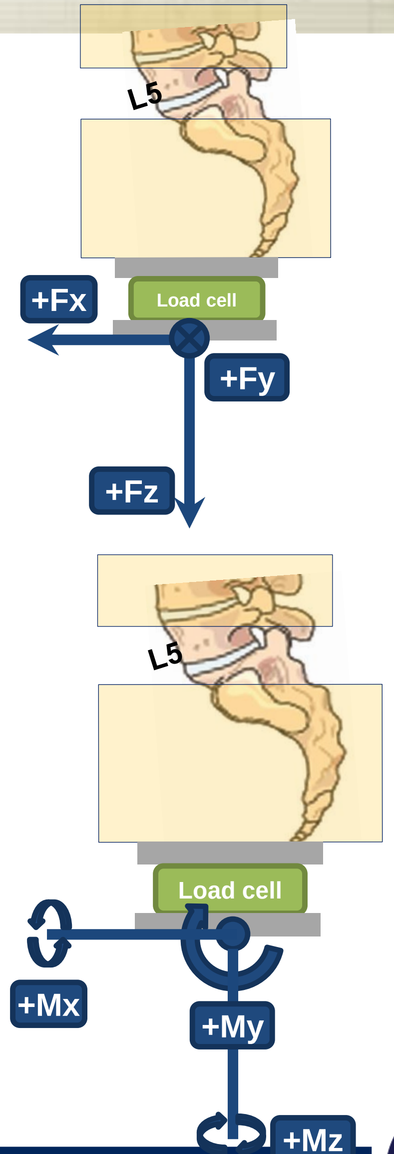

Effects of Flesh on Pelvis Biomechanical Responses

JiangYue Zhang[1], Robert Salzar[2], Brandon Perry[2], Meade Spratley[2], Andrew Merkle[1]

1. Johns Hopkins University, Applied Physics Laboratories
2. Center for Applied Biomechanics, University of Virginia

Second Workshop on Numerical Analysis of Human and Surrogate Response to Accelerative Loading
Aberdeen Proving Ground, MD
January 12-14, 2016

Background

UBB Pelvis Injuries

- **IED—A major threat to ground vehicles**
  (Gondusky et al., 2005)
- **UBB – High rate, large amplitude, vertical loading (Cameron et al, 2011)**
- **Pelvis sustains various types of injuries created from different mechanisms**
  (Ragel et al., 2009)

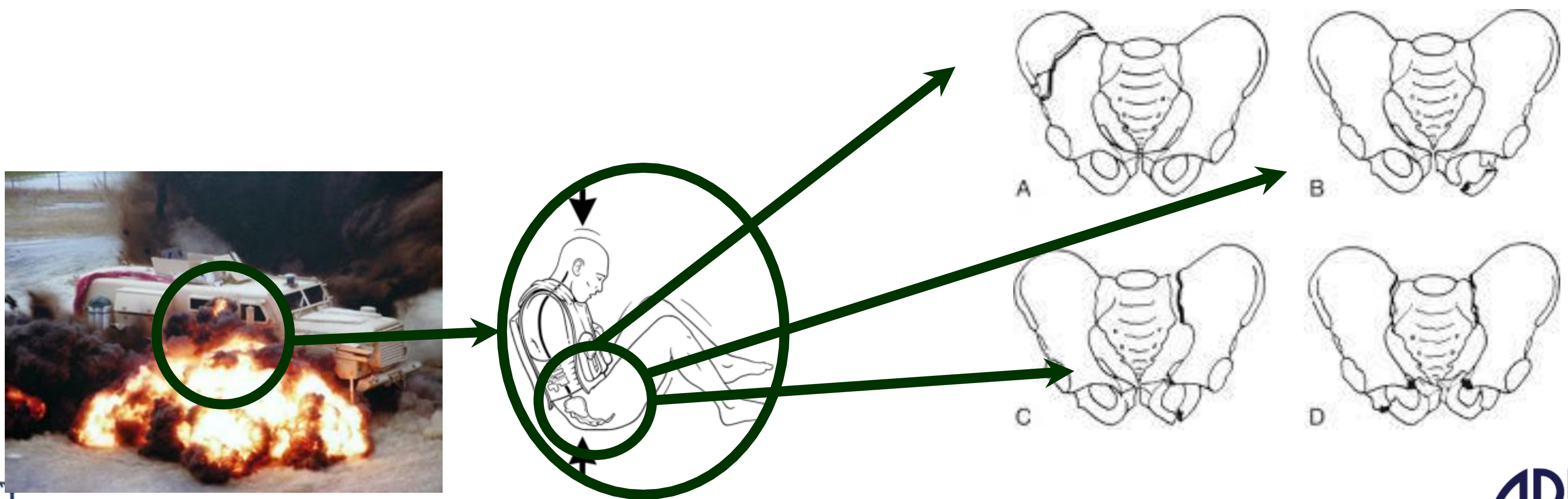

Objectives

WIAMan Dev. & FEM Validation

- **Obtain biomechanical response data from intact and defleshed PMHS pelvis under simulated UBB loading**
  - To guide WIAMan pelvis (skeleton + flesh) development
  - Provide validation data for pelvis (skeleton only and intact) FEM under accelerative loading in vertical direction

Methods

Pelvis Testing Conditions

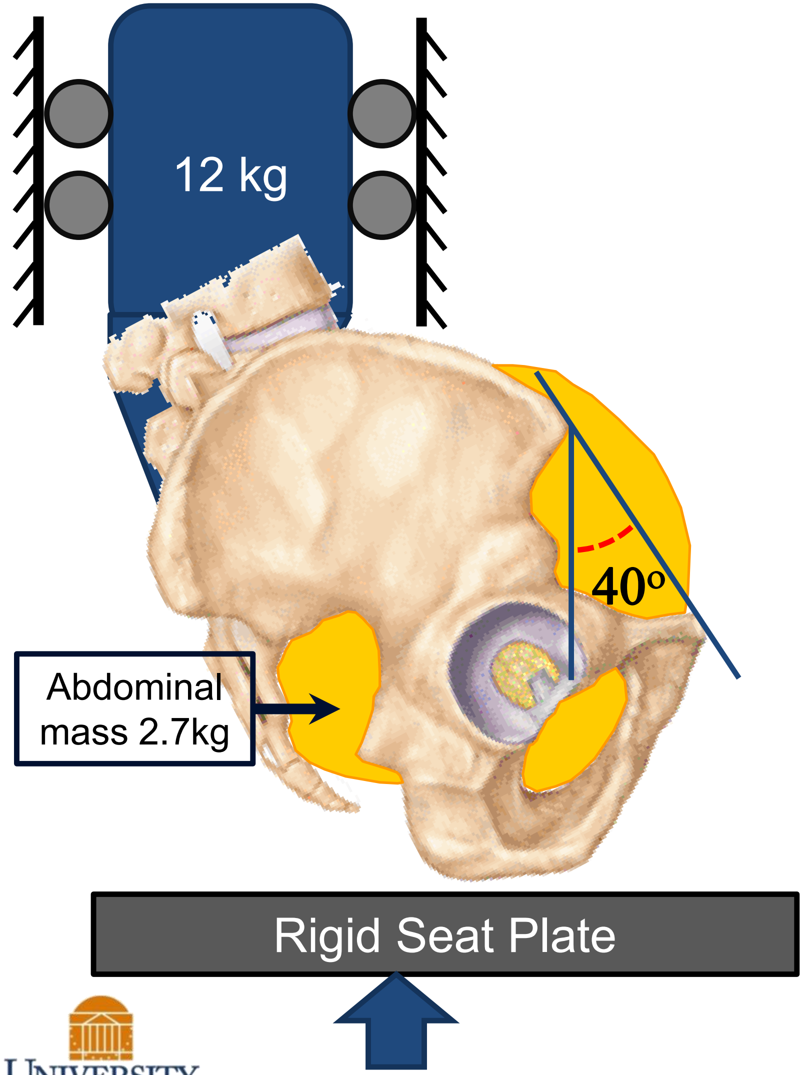

- ❑ Specimen:
  - Pelvis with lumbar spine up to L4 vertebra with femurs detached
- ❑ Potting
  - Rigidly potted from L4-S2 levels without interference with SI joint.
- ❑ Ballast mass
  - 2.7 kg ballistic gel as abdominal mass
  - 12 kg rigid mounted to sacrum potting, constrained to allow in SAE-J211 Z motion only
- ❑ Posture
  - aligned atop a seat plate with a pelvic angle at 40º
- ❑ Boundary & Initial condition
  - Left & right ischial tuberosity in contact with seat plate
  - Initial pre-compression (12kg+specimen weight)

Methods

UVA Pelvis Testing Setup

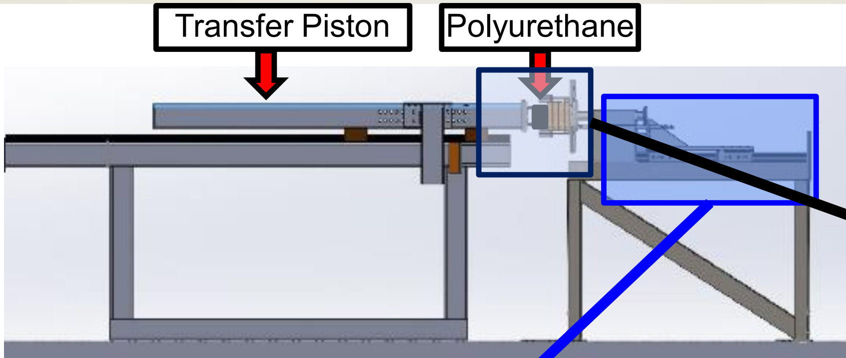

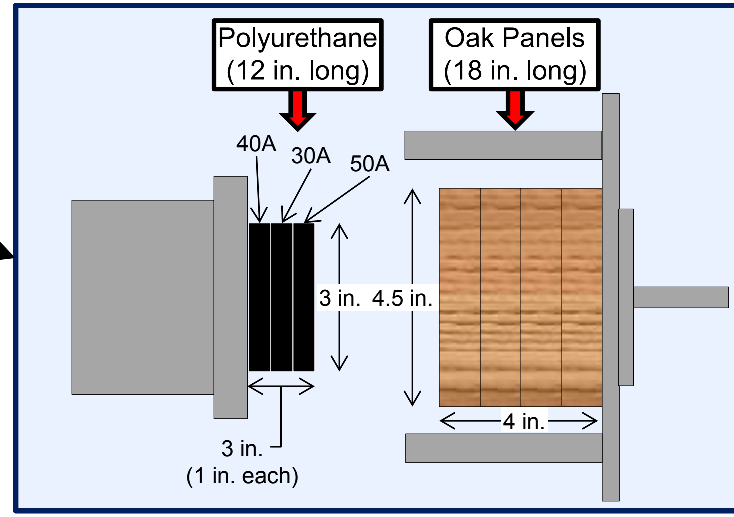

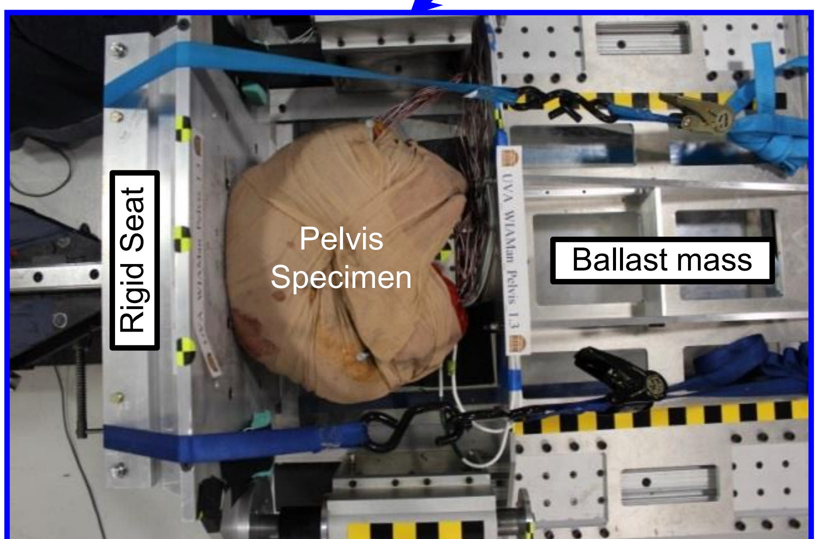

Top view of Carriage

Setup Description

- A pneumatically driven transfer piston delivers impact energy to the system
- Varying durometers of polyurethane are used to achieve desired pulse shape and time-to-peak velocity
- Piezoelectric load cells were fitted to the seat platen to measure impact force
- Pelvis is potted at sacrum and rigidly attached to guided ballast mass and carriage
- Preloading equivalent to the weight of specimen and ballast mass is applied to the pelvis using ratchet straps and immediately released at impact

Methods

Specimens Tested

Performer	Specimen	Age	Gender	Height (cm)	Weight (kg)	BMI
UVA	PV02-1	60	M	162	63	24
UVA	PV02-2	47	M	173	68	23
UVA	PV02-3	57	M	183	94	28
UVA	PV02-4	54	M	185	103	30
UVA	PV02-5	62	M	168	78.5	28
UVA	PV02-6	71	M	185	100	29

Avg (stdev)		58.5 (8)		176 (9.8)	84.4 (17.0)	27(2.8)
WIAMan Range		18-80		165-186	64-105	18-35

WIAMan BIO PT

Methods

Completed Tests

V1: 2 m/s, 10 ms TTP; V2: 3 m/s, 10 ms TTP; V3: 4 m/s, 10 ms TTP

Performer	Specimen	PV02: BRC Tests w/ Flesh						PV12: BRC Test w/o Flesh						Last Injury Tests**		
		V1	V1	V2	V1	V3	V1	V1	V1	V2	V1	V3	V1	Outcome	PeakForce (N)	Peak Moment (N.m)
UVA	PV02-1	✓	✓	✓	✓	✓	✓							Sacrum fractures at S2/S3, Sacral ala fractures – bilateral, SI joint disruption – bilateral	937	29
UVA	PV02-2	✓	✓	✓	✓			✓	✓	✓				bilateral sacroiliac joint laxity	2153	153
UVA	PV02-3	✓	✓	✓	✓			✓	✓	✓	✓			bilateral sacroiliac joint laxity, sacral comminution at S1/S2	11416	413
UVA	PV02-4	✓	✓	✓	✓			✓	✓	✓	✓			S4 transverse fracture	5657	138
UVA	PV02-5	✓	✓	✓	✓			✓	✓	✓	✓			Sacral ala, sacral, and coccyx fractures	6075	224
UVA	PV02-6	✓	✓	✓	✓			✓	✓	✓	✓			S2 and sacral ala fractures	4614	218

*Specimen was injured in de-fleshed state

** Peak force and peak moment are from processed data after mass compensation, transformation and normalization.

Methods

Detailed instrumentation

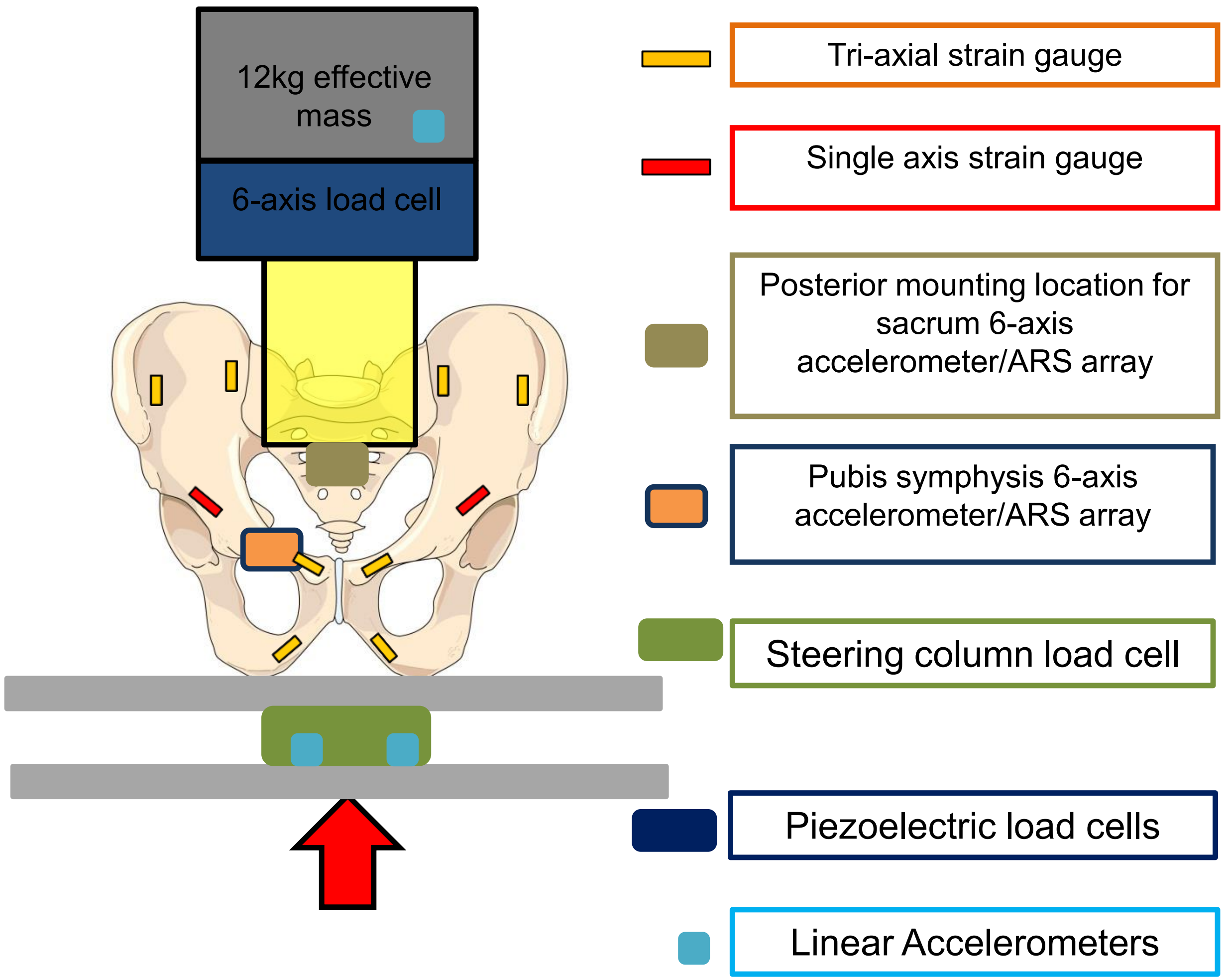

Methods

Collected Data

BP	Measure	# Specimens @ each Velocity		Comments
		V1	V2	
42	Sacrum Z acceleration	6	6	Due to high probability of injury at v3, decision was made not to pursue BPs at v3
43	Sacrum resultant acceleration	6	6	
45	Pelvis to seat contact Fz	3	3	Implemented only at later phase of testing
46	Fz at sacrum potting	6	6	Due to high probability of injury at v3, decision was made not to pursue BPs at v3
60	Sacrum potting to seat disp. x, y, z	6	6	x, y not N/A due to guided boundary
70	Moment at sacrum potting in y	6	6	Pelvis bending response
72	Pelvis rotational velocity about Y axis	6	6	Pelvis rotation
73	Pelvis rotation about Y axis	6	6	Pelvis bending response
74	Potting carriage Z acceleration	6	6	Pelvis axis compression response
75	Seat platen Z acceleration	6	6	Acceleration loading to the pelvis
102	Seat platen velocity history in z	6	6	Defines input to specimen
102r	Redundant seat platen velocity history in z	6	6	Defines input to specimen

Pelvis Local Anatomical Coordinate

Rupp et al.,2014

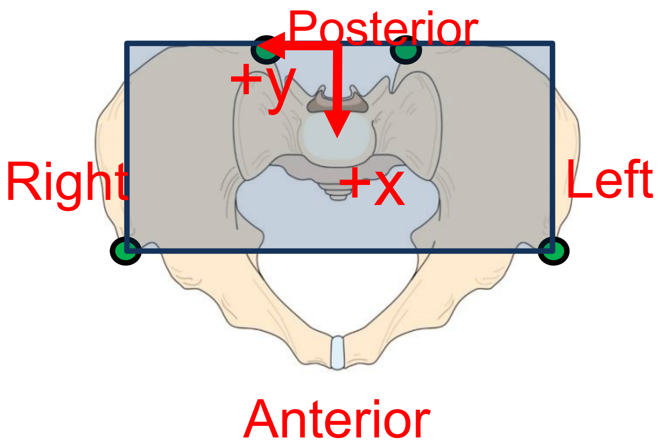

- **Pelvis local anatomical coordinate is defined as:**
  - +Y defined as left ASIS → right ASIS
  - +X: Vector from Midpoint of two PSIS perpendicular to +Y vector in the Wu plane
  - +Z: Cross product of X vector and Y vector
- **ASIS & PSIS are clearly identifiable landmarks on CTs.**
- **Once the local coordinates are defined, the coordinates are rigidly attached to, and move with regions of interest, such as sacrum and public symphysis etc. The coordinates will NOT be redefined based on new locations of ASIS & PSIS during the test.**

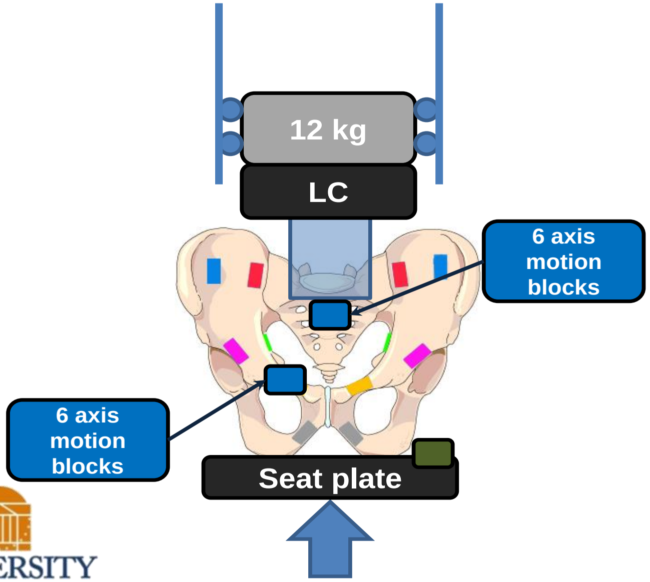

- Data transformation
  - Pubic rami 6 axis motion block: transferred to center of pubic symphysis in local pelvis coordinates rigidly attached to pubis as defined above
  - Sacrum 6 axis motion block: transfer to mid-point of two PSIS in local pelvis coordinates rigidly attached to sacrum as defined above

Signal Conversion Tiger Team (SCoTT) *Rupp et al.,2014*

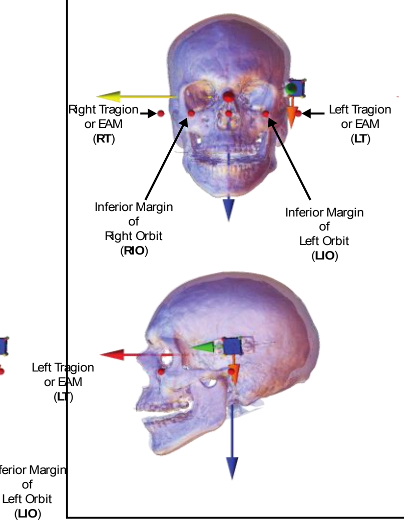

- Landmarks
  - Left and right tragion (effectively EAM)
  - Inferior margin of left and right orbit
- Local Coordinate System
  - **Y:** Vector connecting left to right tragion
  - **Z:** Vector between left tragion to midpoint between left and right orbits cross Y-Axis
  - **X:** Y-axis cross Z-axis
- Anatomical Origin
  - Head CG as calculated from pretest CT scan using methods defined in W0084.
- Transformation to ATD: None (6DX in ATD is at head CG)

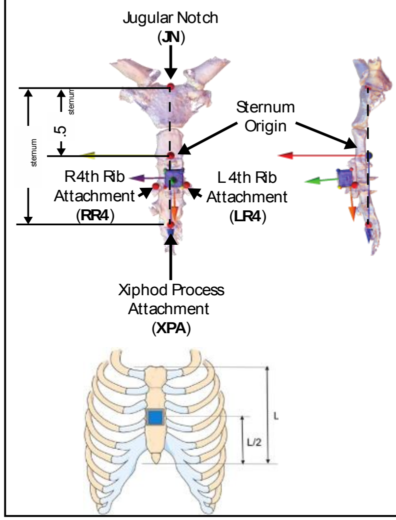

- Landmarks
  - Suprasternal notch
  - Xiphoid process attachment
  - Rib 4 insertion point (right anterior)
  - Rib 4 insertion point (left anterior)
- Local Coordinate System
  - **Z:** Vector connecting suprasternal notch to xiphoid process attachment
  - **X:** Z-axis cross vector connecting rib 4 right insertion point to rib 4 left insertion point
  - **Y:** Z-axis cross X-axis
- Anatomical Origin
  - Midpoint between suprasternal notch and xiphoid process attachment along Z-axis

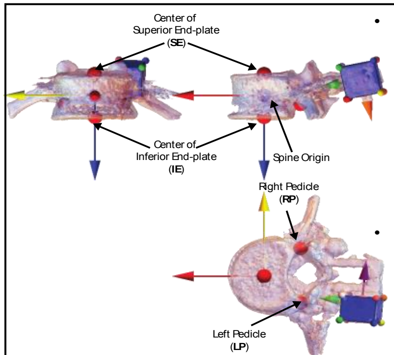

- Landmarks
  - Similar landmarks on left and right pedicle
    - Use left and right transverse process if pedicles are obscured by hardware
  - Area centroids of end plates
    - Vertebral body center is the midpoint between the superior and inferior endplate area centroids.
- Local Coordinate System
  - **Y:** Vector connecting left pedicle landmark to right pedicle landmark
  - **X:** Y-axis cross vector connecting area centroids of upper and lower endplates
  - **Z:** X-axis cross Y-axis
- Anatomical Origin
  - Volumetric centroid of vertebral body determined from CT scan or midpoint between area centroids of endplates (locations are effectively equivalent)

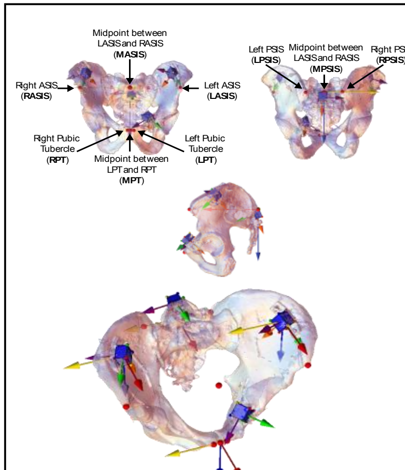

- Landmarks
  - Left and right ASIS
  - Left and right PSIS
  - Most anterior point of left and right pubic tubercles
- Local Coordinate System
  - **Y:** Vector connecting left ASIS to right ASIS
  - **Z:** Vector connecting midpoint between left and right PSIS to midpoint between left and right ASIS cross Y-Axis
  - **X:** Y-axis cross Z-axis
- Anatomical Origins
  - Sacrum: Midpoint between Left and Right PSIS
  - Pubic Symphysis: Midpoint between most anterior point of left and right pubic tubercles (center of Pubic Symphysis)
  - IW: Use installation location

University of Virginia

The Ohio State University | Medical College of Wisconsin | University of Virginia | APL | UMTRI | Wayne State | Duke BME | WF

APL

SCoTT

Rupp et al.,2014

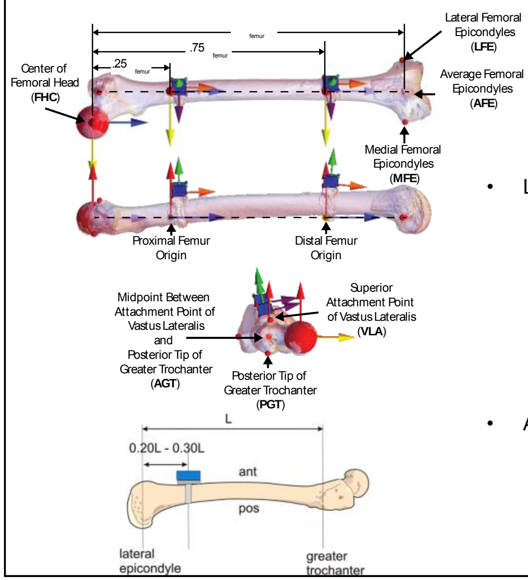

- Landmarks
  - Lateral Epicondyle
  - Medial Epicondyle
  - Attachment point of the vastus lateralus (VL) along the greater trochanter superior surface
  - Posterior tip of greater trochanter
  - Hip joint center
- Local Coordinate System
  - **Z:** Vector connecting midpoint between VL attachment point and posterior tip of greater trochanter cross midpoint of epicondyles
  - **X:** (Right Femur) Z-axis cross Vector connecting Lateral Epicondyle to Medial Epicondyle
  - **X:** (Left Femur) Z-axis cross Vector connecting Medial Epicondyle to Lateral Epicondyle
  - **Y:** Z-axis cross X-axis
- Anatomical Origins
  - Distal Femur: Proximal knee joint center 25% of the distance between knee and hip joint center.
  - Proximal Femur: Proximal knee joint center 75% of the distance between knee and hip joint center.

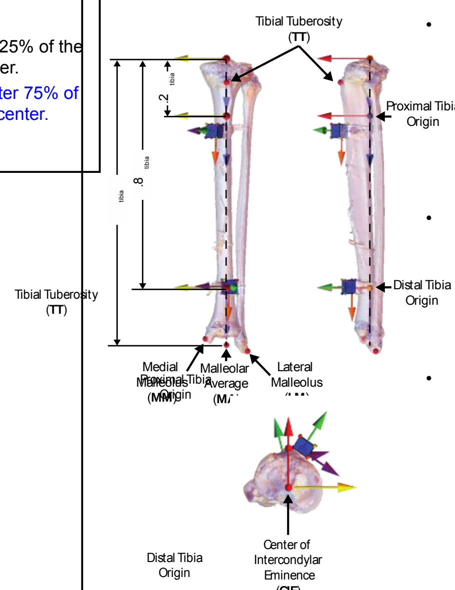

- Landmarks
  - Center of Tibial Intercondylar Eminence
  - Tibial Tuberosity
  - Lateral Malleolus
  - Medial Malleolus
  - Ankle joint center (midpoint between lateral and medial malleoli)
- Local Coordinate System
  - **Z:** Vector connecting center of tibial intercondylar eminence to midpoint between lateral and medial malleolus
  - **Y:** Z-axis cross vector connecting center of tibial intercondylar eminence to tibial tuberosity
  - **X:** Y-axis cross z-axis
- Anatomical Origins
  - Distal Tibia: Proximal of the ankle joint center equal to 20% of the distance between the ankle joint center and center of tibial intercondylar eminence along Z-axis
  - Proximal Tibia: Proximal of the ankle joint center equal to 80% of the distance between the ankle joint center and center of tibial intercondylar eminence along Z-axis

Medial Malleolus (MM) Malleolar Average (MA) Lateral Malleolus (LM)

Results

Input Seat Velocity Vz

$$\mathbf{V}_{\mathbf{z}_2}(\mathbf{t}) = \int_0^{t} A_{z_2}(t)\,dt$$

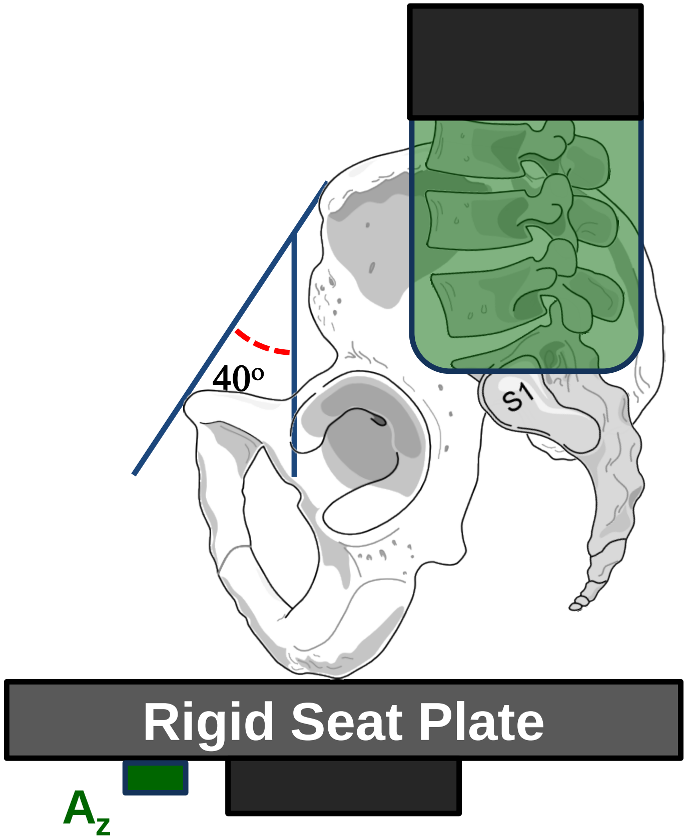

Results

Input Seat Velocity Vz Corridor

Intact Seat Vz

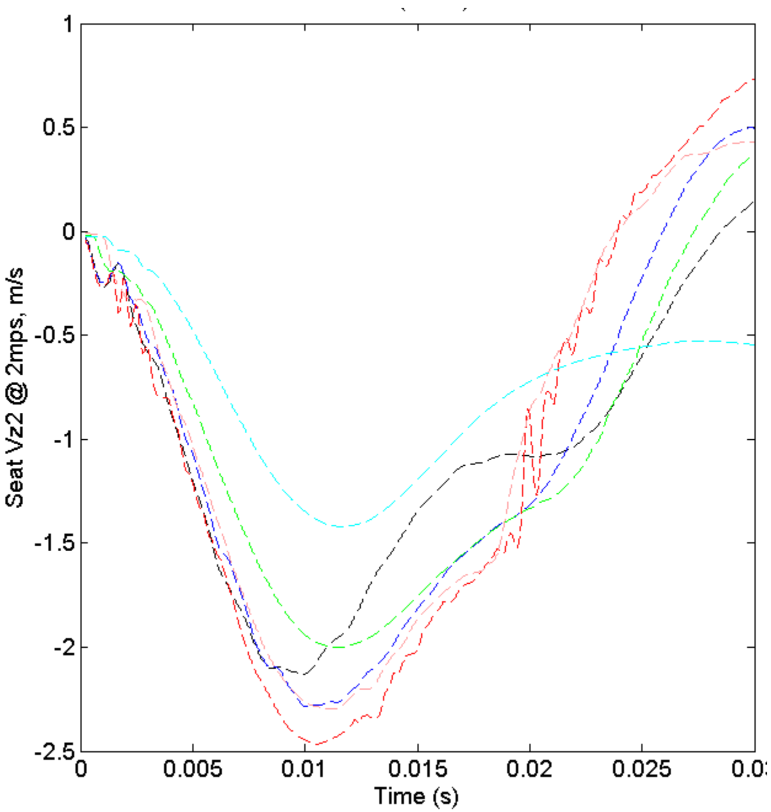

Defleshed Seat Vz

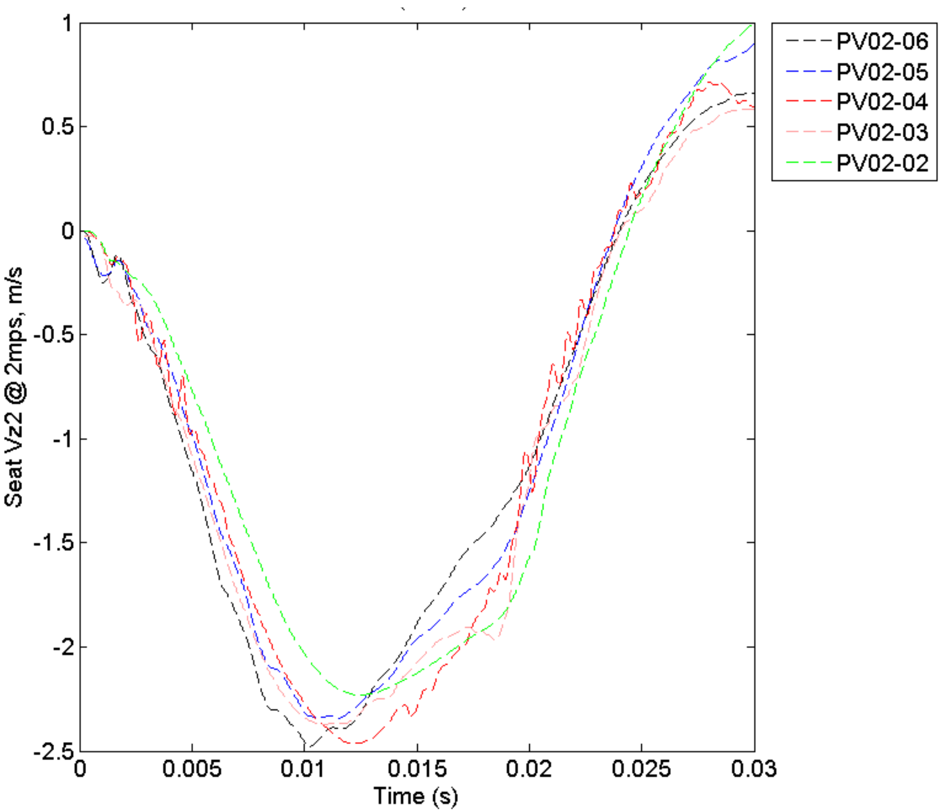

UNIVERSITY of VIRGINIA

APL

Results

Input Seat Velocity Vz Raw Data

Intact Seat Vz

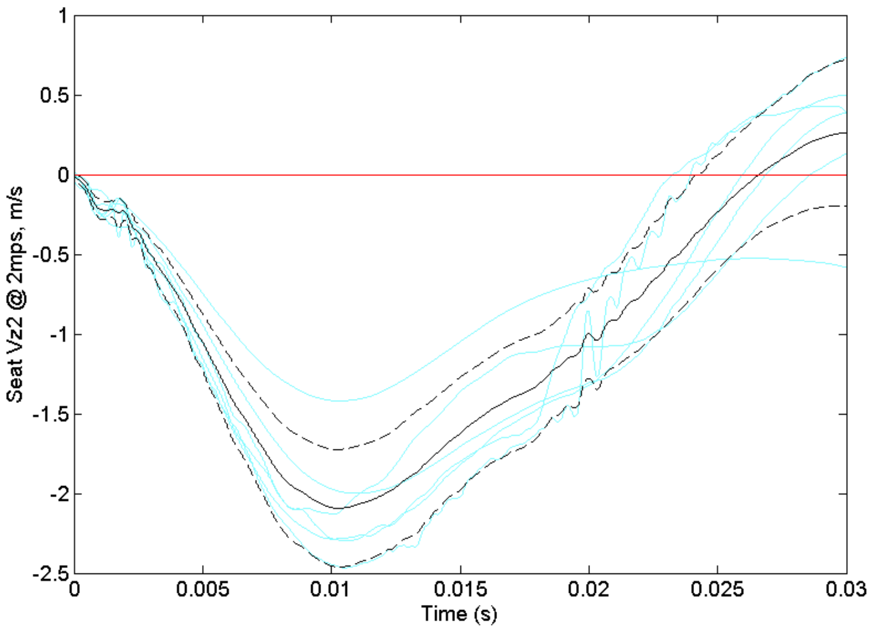

Defleshed Seat Vz

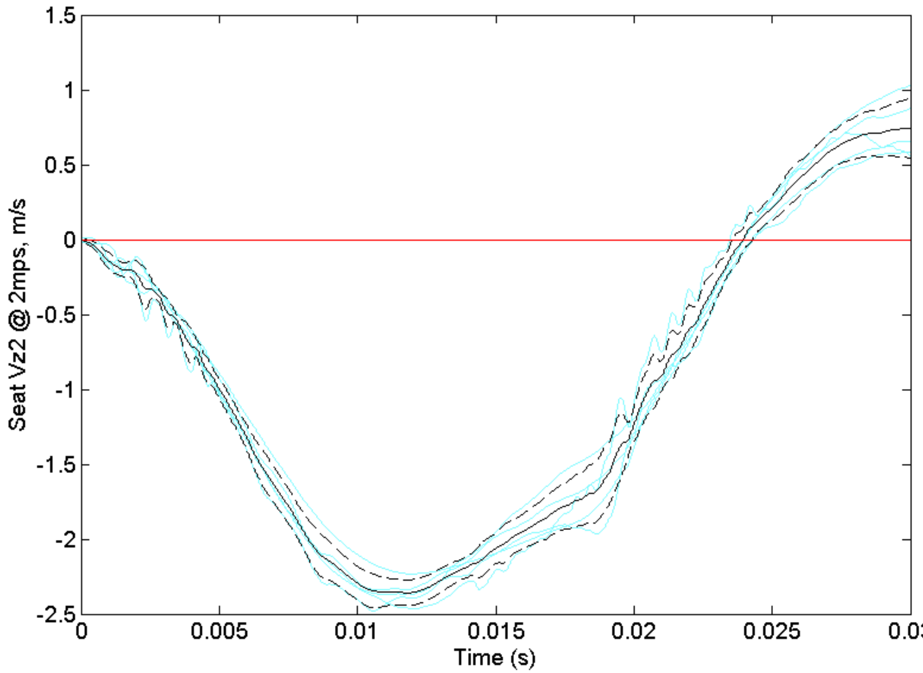

University of Virginia

APL

Results

Mass Compensated Force Fz

Transfer forces from load cell to L5/S1 joint center:

Compensate mass: $M_{Comp} = M_{Potting} + 0.5*M_{load\ cell}$

Fx at L5/S1 joint center: $F_x = F'_x$

Fz at L5/S1 joint center: $F_z = F'_z + M_{comp} * A_z$

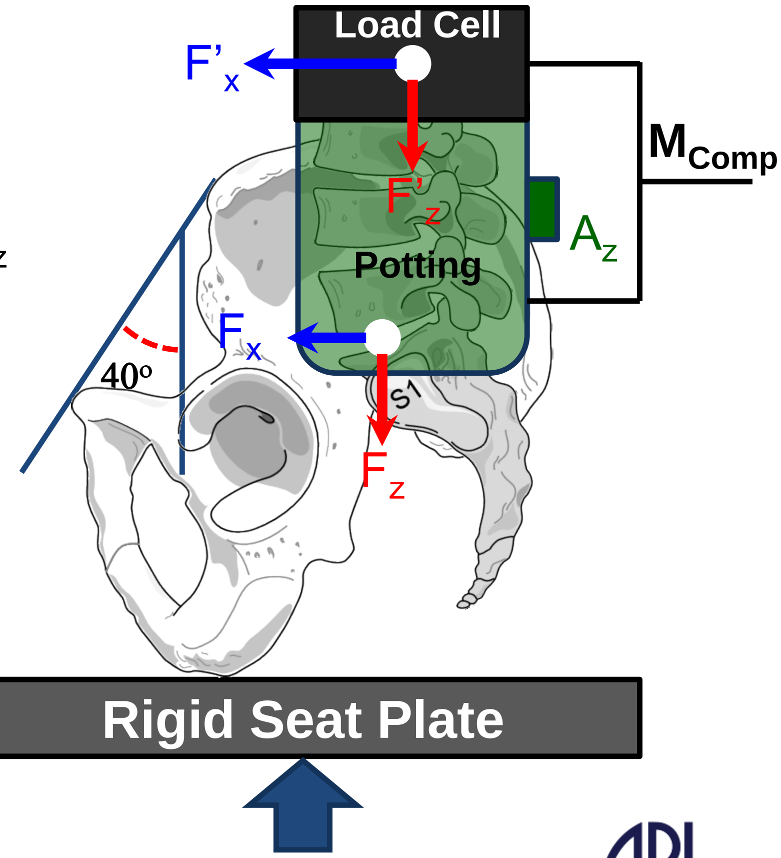

Results

Mass Compensated Force Fz Raw Data

Intact L5/S1 Fz

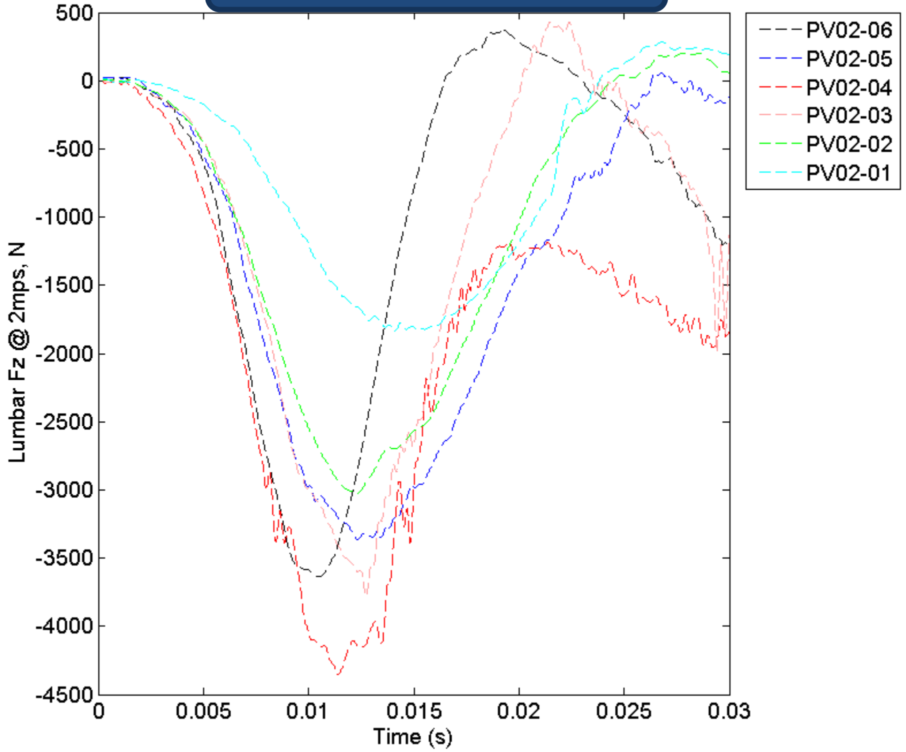

Defleshed L5/S1 Fz

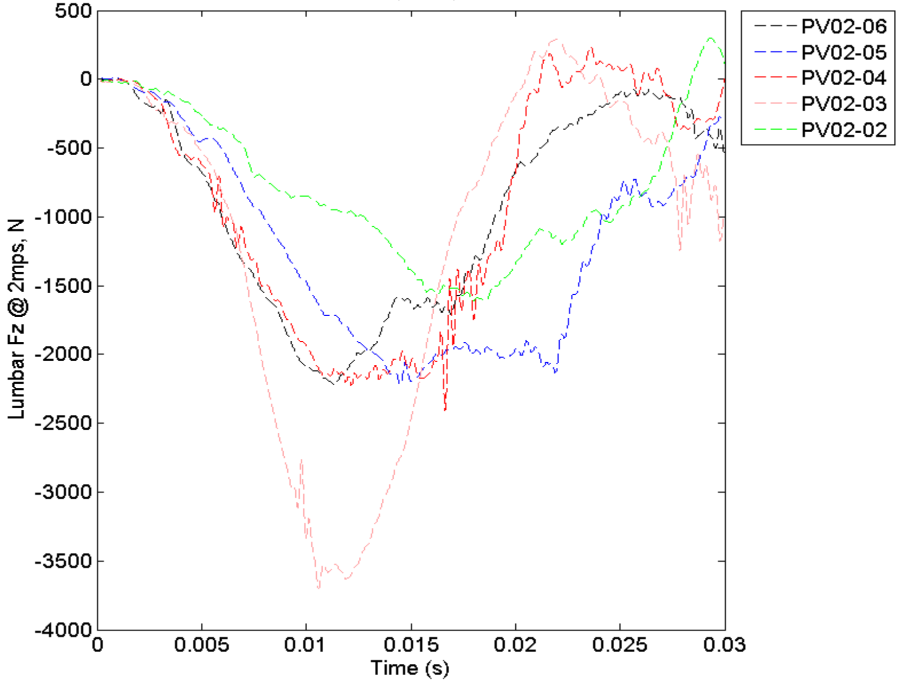

Results

Mass Compensated Force Fz Corridor

Intact L5/S1 Fz

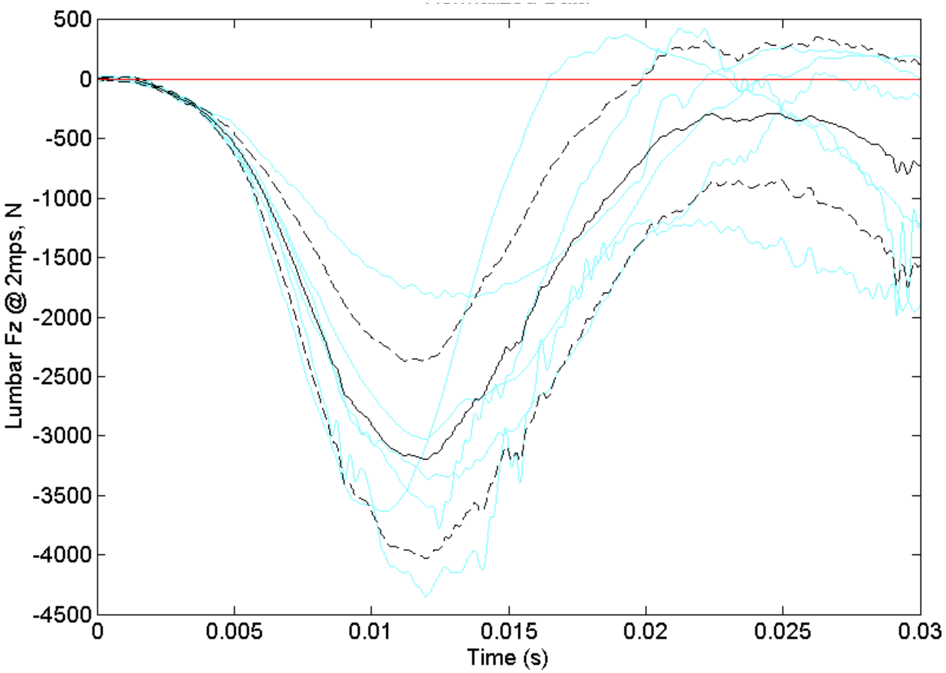

Defleshed L5/S1 Fz

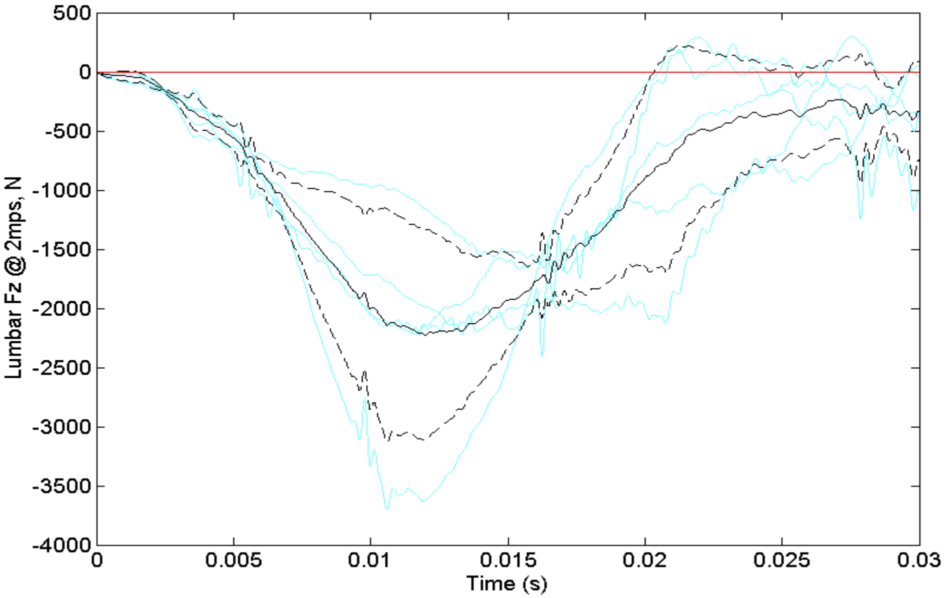

Results

Transferred Moment My

Transfer moments from load cell to L5/S1 joint center:

Moment Y at L5/S1 joint center:

$$\mathbf{M_y = M'_y + \vec{F} \times \vec{D} = M'_y + F_z D_x - F_x D_z}$$

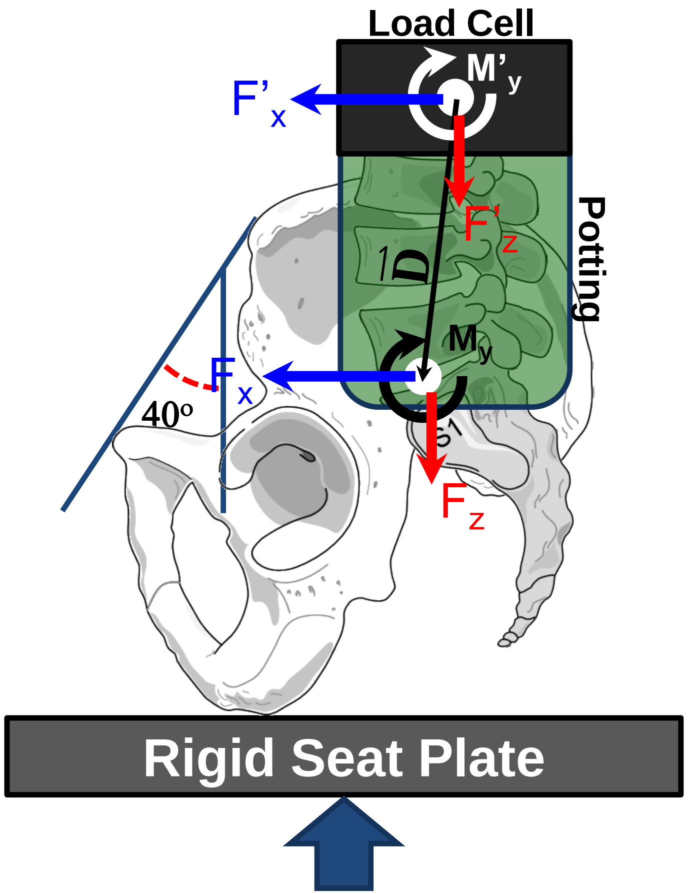

Results

Transferred Moment My Raw Data

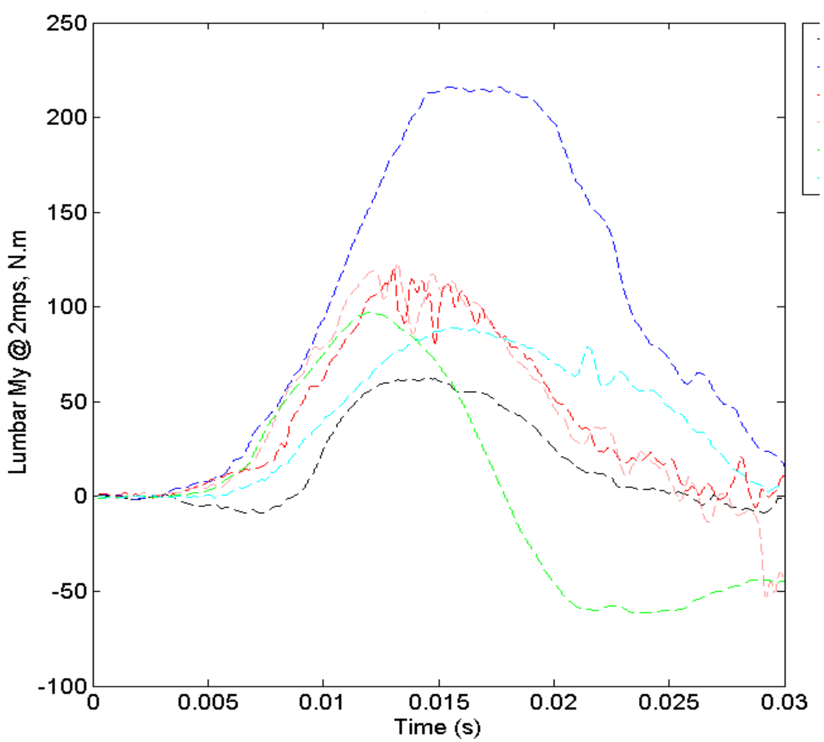

Intact

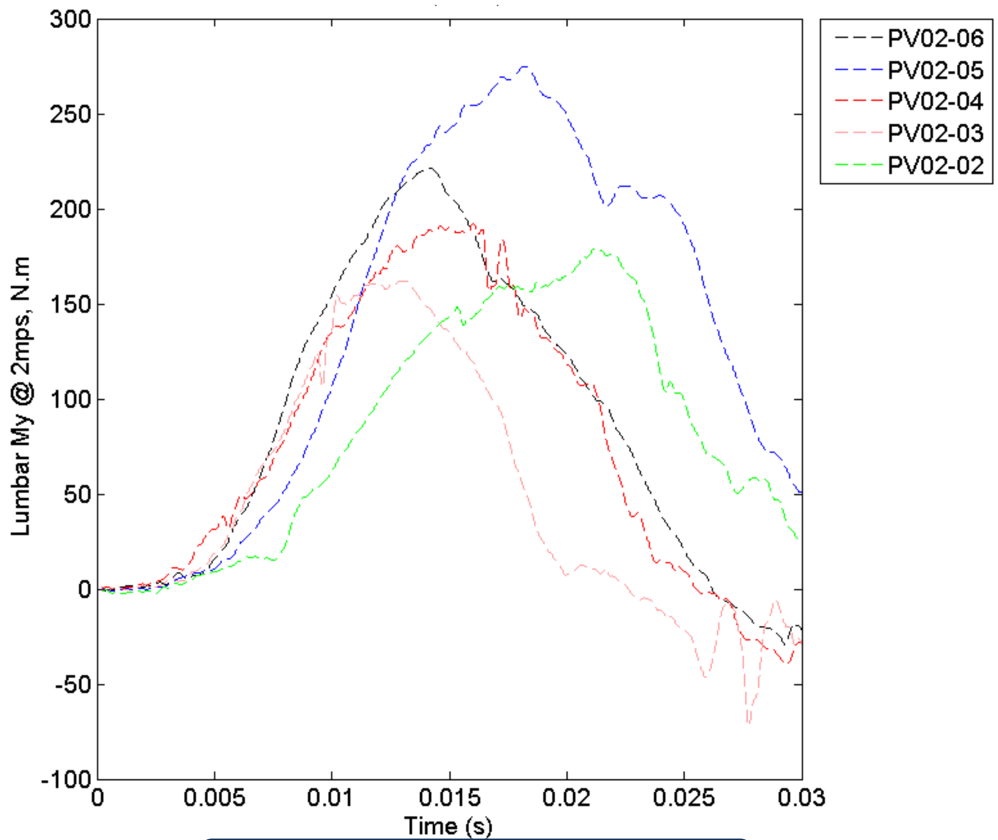

Defleshed

Results

Transferred Moment Corridor

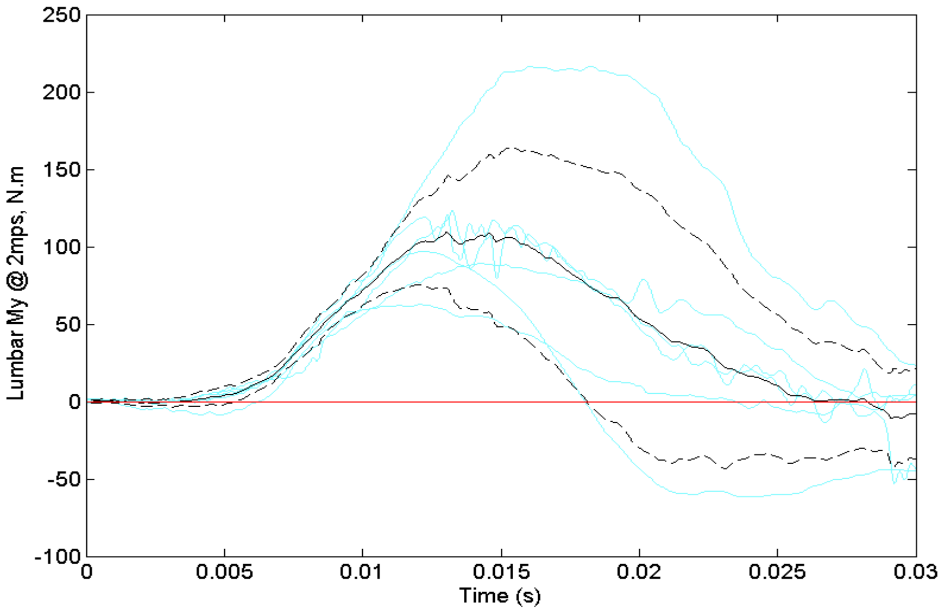

Intact

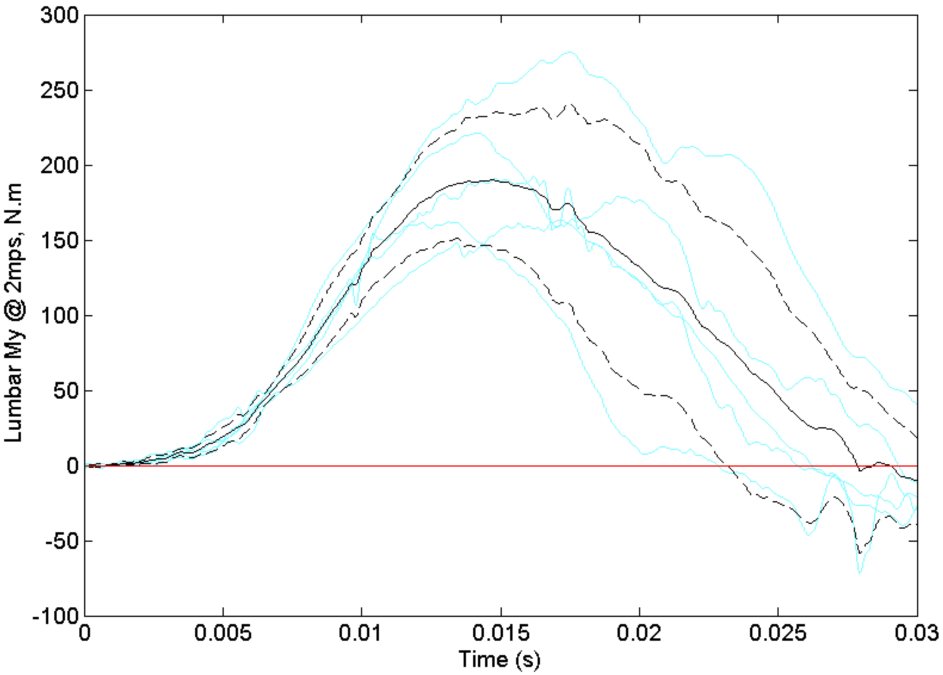

Defleshed

Results

Pelvis Rotation ω_y

ω_y

- Angular rate sensor measurements transformed to pelvic-local coordinates

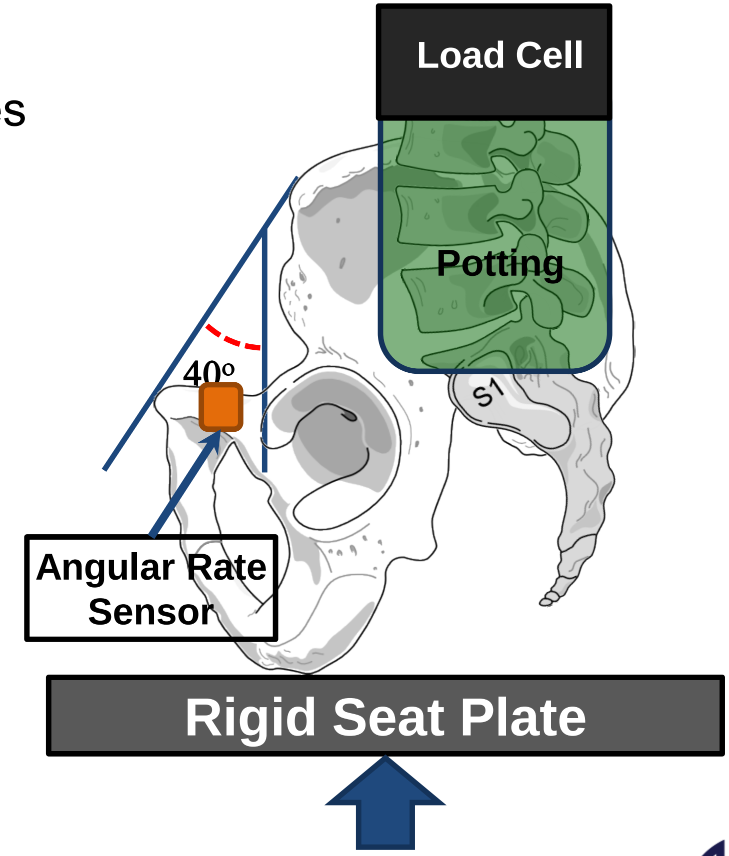

Results

Pelvis Rotation ω_y Raw Data

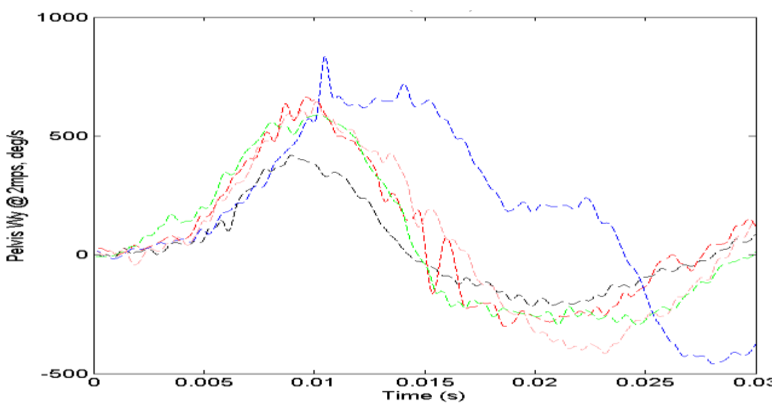

Intact

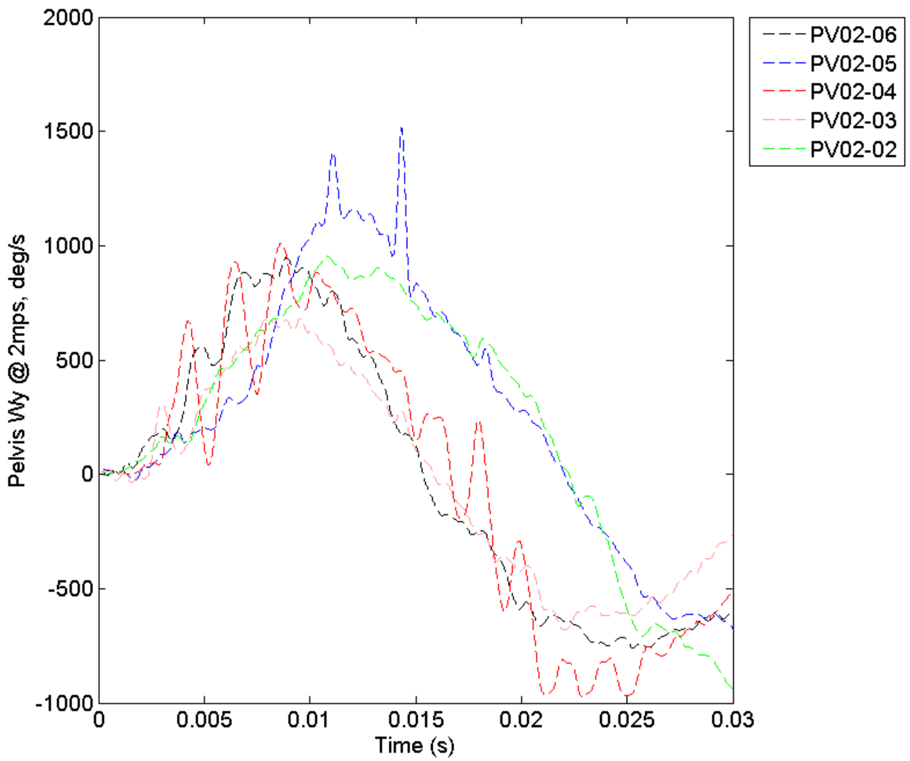

Deflesched

Results

Pelvis Rotation ω_y Corridor

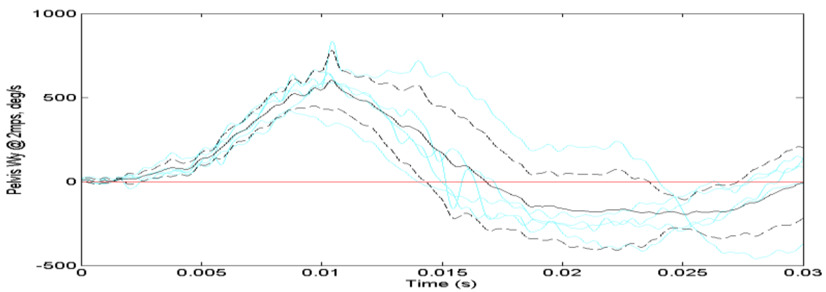

Intact

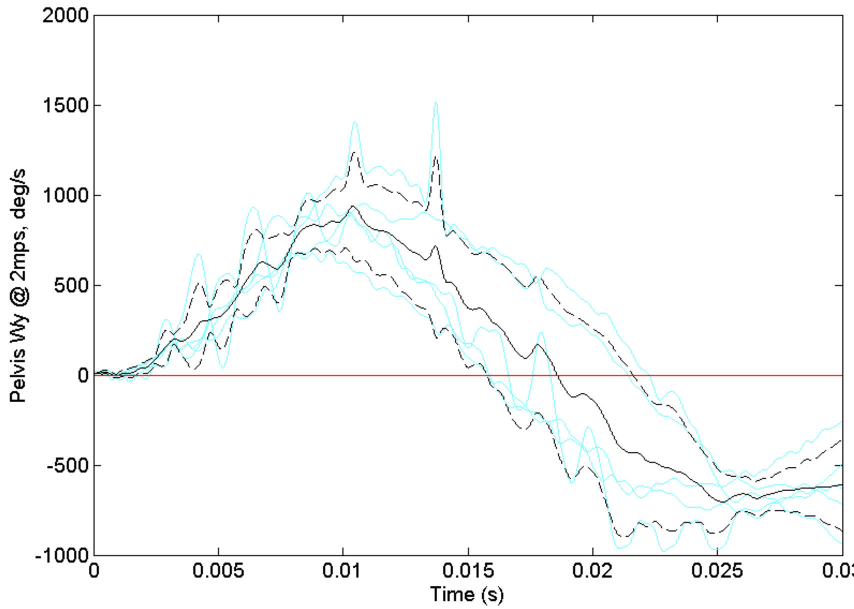

Deflished

Discussion

Comparison of Intact vs. Deflesh

With approximately same seat loading velocity comparing biomechanical responses from intact specimen to deflesh:

- Axial Fz dropped from ~3200N to ~2200N
- Bending moment increased from ~100 N.m to ~200 N.m
- Pelvic rotation velocity increase from ~500 deg/s to ~900 deg/s

These results indicated pelvis flesh will:

- Help in axial transmitting of vertical UBB loading downstream into spine
- Resist pelvis rotation

Summary

- **A total of 48 tests has been conducted on 6 PMHS pelvis which produced**
  - 2 input loading corridor corresponding to 2 loading severity
  - 2 specimen conditions, intact & defleshed
  - 56 biomechanical response corridors normalized and transferred to anatomical locations
  - Defleshed specimens responded with reduced axial loads and increased bending moments indicating the effects of pelvis flesh in helping to transmit axial loads up through the spine while resisting pelvic rotation
- **These valuable PMHS data can be used to**
  - Individually validation the skeleton and flesh part of the human pelvis FEM under accelerative loading in the vertical direction
  - Provide guidance to WIAMan skeleton+flesh pelvis design to ensure biofidelity of the surrogate
- **Future studies**
  - Pelvis BRCs in anterior (partially completed) and posterior till posture
  - Effect of time-to-peak (loading rate) on pelvic response

Acknowledgement

This research was conducted as part of the Biomechanics Product Team led by the Johns Hopkins Applied Physic Laboratory for the WIAMan Project under contract #N00024-13-D-6400, U.S. Army Research, Development and Engineering Command.

The content included in this work does not necessarily reflect the position or policy of the U.S. government.

Effects of Flesh on Pelvis Biomechanical Responses

JiangYue Zhang[1], Robert Salzar[2], Brandon Perry[2], Meade Spratley[2], Andrew Merkle[1]

1. Johns Hopkins University, Applied Physics Laboratories
2. Center for Applied Biomechanics, University of Virginia

Second Workshop on Numerical Analysis of Human and Surrogate Response to Accelerative Loading
Aberdeen Proving Ground, MD
January 12-14, 2016

Response Corridors of Cadaveric Human Leg-foot under Accelerative Loading: Effect of Posture and Input Rise Time

Liming Voo*, Frank Pintar+, Kyle Ott*, Mike Schlick+, Chris Dooley*, Narayan Yoganandan+, Andrew Merkle*

***Johns Hopkins University Applied Physics Laboratory**
+Medical College of Wisconsin

Second Workshop on Numerical Analysis of Human and Surrogate Response to Accelerative Loading
January 12-14, 2016

WARRIOR INJURY ASSESSMENT MANIKIN
RDECOM
ENGINEERING OFFICE

MEDICAL COLLEGE OF WISCONSIN

APL
The Johns Hopkins University
APPLIED PHYSICS LABORATORY

Introduction

- Fractures in the foot, ankle and leg are the most common orthopedic injuries in the UBB environment (Ramasamy 2011*)
- The WIAMan ATD serving as the human surrogate would need to include injury prediction capability for those anatomies when being used for vehicle protection assessment
- The reliability of such injury risk prediction depends largely on how the surrogate could accurately represent the anatomic structures in those application environments: Biofidelity of this ATD is therefore essential for this purpose
- ATD Biofidelity by design: matching degrees of freedom, dimensions, inertial properties; structural properties
- ATD Biofidelity by validation: response data from human anatomies, matched-pair ATD responses, design revisions
- Biofidelity Response Corridors:
  - Relevant anatomy
  - Relevant test model
  - Relevant test conditions
  - Procedures for quality assurance and corridor development

*Ramasamy A, et al.: In-vehicle extremity injuries from improvised explosive devices, Phil Trans R Soc, 2011

Objectives

- Develop Biofidelity Response Corridors (BRCs) that account for the following factors:
  - Anatomy relevance
  - Test conditions relevance
  - Specimen quality control
  - Test condition repeatability
  - Essential biomechanical parameters
  - Data scaling
  - Procedure for response corridor development

- Determine Effect of Anatomic Posture

- Determine Effect of Input Velocity Time-to-Peak (TTP)

Methods: Specimen and Setup

- Specimen:
  - Male cadaveric leg-foot
  - Acceptance criteria based on (W0062; ANSUR II):
    - Whole body anthropometry: 50% male military population, Mean+/- 1.5SD
    - Absence of prior damage, surgery, or anatomic anomalies
- Test model:
  - PMMA-potted at proximal tibia with knee replaced by a 6-axis load cell
  - Metal bar representing femur;
  - Pin joints representing knee and hip in sagittal plane
  - Hip joint attached to a mass that slides vertically on a rail
  - Foot in contact with a floor plate
- Test Sites:
  - APL VALTS
  - MCW VerTec

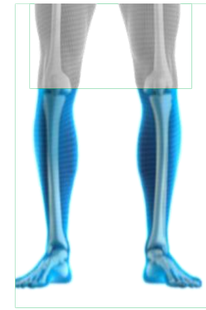

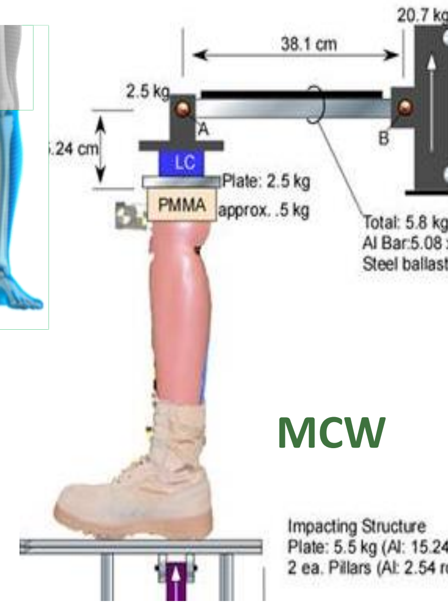

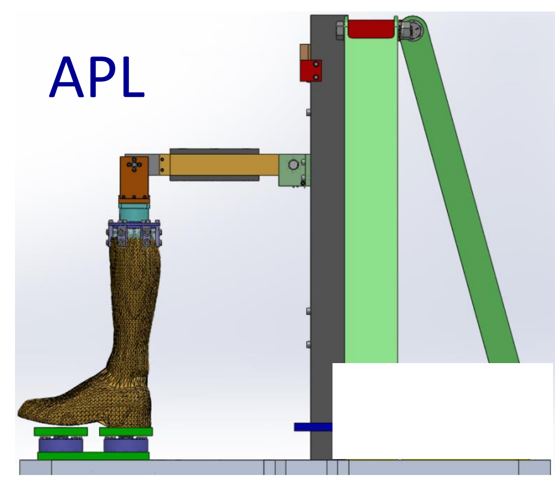

Methods: BPs and Instrumentation

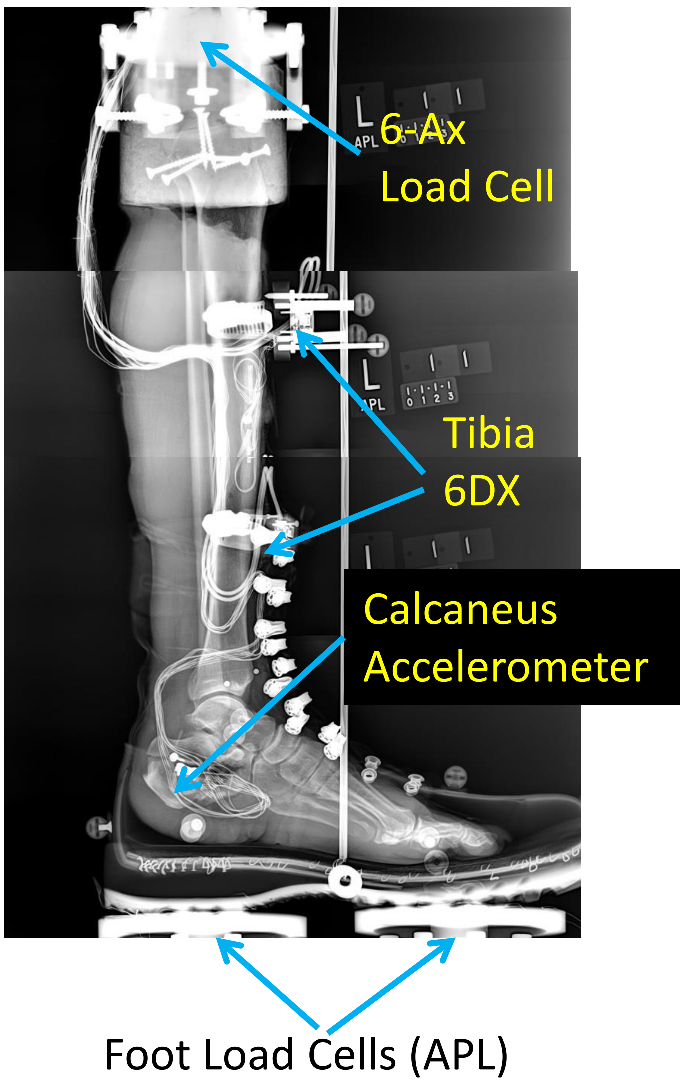

BP	Measure	Comments
101	Floor Plate Linear Velocity Z	From integral of floor plate acceleration
50x	Tibia Linear Acceleration X	From lower tibia 6DX
50z	Tibia Linear Acceleration Z	From lower tibia 6DX
68	Tibia Angular Velocity Y	From lower tibia 6DX
51	Tibia Force Z	From upper tibia load cell
52	Tibia Force X	From upper tibia load cell
71	Tibia Moment Y	From upper tibia load cell
53	Foot Lin Acceleration Z	From medial calcaneus acceleration
54x	Motion of feet – heel X	From video – Boot heel marker
54y	Ankle angle change Y	From video – Angle between foot and tibia
54z	Motion of feet – heel Z	From video – Boot heel marker
55	Booted Ankle Compression Z	From video – PMMA/Plate

Methods: Testing

- Data quality controls
  - Boot donning procedure
  - Positioning procedure
  - Load pulse tuning and control
  - Instrumentation protocol
  - Injury assessment between and after tests
- Loading conditions
  - Accelerative loading to the floor plate
  - Velocities: 2, 4, 6 m/s
  - Time to peaks: 2, 5, 8ms
  - Postures:
    - Neutral 90-90; Dorsiflexion 75-75; Plantar-flexion 110-110
- Sample size
  - 6-8 specimen in each test series and test condition

Positioning Postures

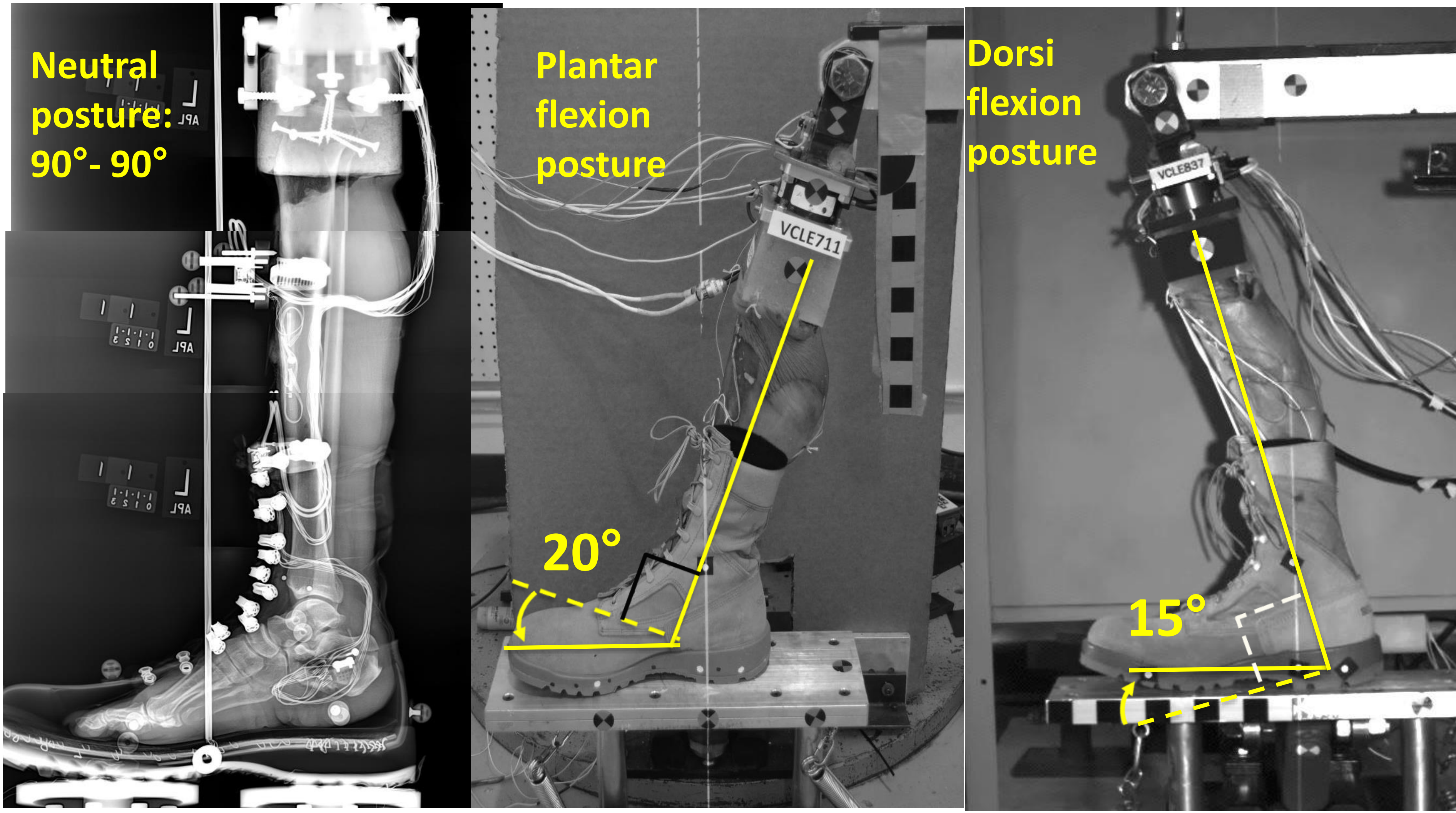

Methods: Test Sequence

Specimen	Floor Velocity (m/s)	2	4	2	6	2	10-14
APL ##	2 ms TTP	X	X	X	X	X	
	8 ms TTP	X	X	X	X	X	Injury Test
MCW ##	5 ms TTP	X	X	X	X	X	Injury Test

Methods: Data Treatment

- Data sampling and filtering
  - High-speed video sampled data at 1000 frame/sec
  - Sampled data at 1000 kHz with 300 kHz AA filter
  - Post-test filtered data with a 4-pole Butterworth,
    - 3 kHz roll-off for accelerometer and load cell data
    - 1.65 kHz roll-off for angular rate sensor
- Data normalization (Scaling)
  - Equal stress equal velocity (Eppinger 1984)
  - Based on mass ratio
  - **Normalized to the WIAMan ATD population**
- BRC generation
  - Signal alignment
  - Representative curve (RC)
  - Corridor: +/- 1 SD of the RC

Methods: Data Normalization

- Equal-Stress Equal-Velocity Method (Eppinger 1984)
- Normalization Equations
  - Acceleration
  - Force
  - Moment
  - Displacement
  - Rotation
  - Time
  - Velocity

$\lambda_i = M_{ref}/M_i$

Acceleration: $A_{i,ref} = \lambda_i^{-1/3} A_i$

Force: $F_{i,ref} = \lambda_i^{2/3} F_i$

Displacement: $D_{i,ref} = \lambda_i^{1/3} D_i$

Moment: $M_{i,ref} = \lambda_i M_i$

Rotation: $R_{i,ref} = R_i$

Time: $T_{i,ref} = \lambda_i^{1/3} T_i$

Velocity: $V_{i,ref} = V_i$

Definition:

- "Ref" = Reference: quantity normalized to the WIAMan ATD equivalent
- Index "i" indicates individual specimens

Target WIAMan Mass	WIAMan Foot	WIAMan Leg
	1.1 kg	3.64 kg

Results

- Kinematics
- Selected Biofidelity Response Corridors
- Effect of Posture
- Effect of TTP

Leg-Foot Kinematics

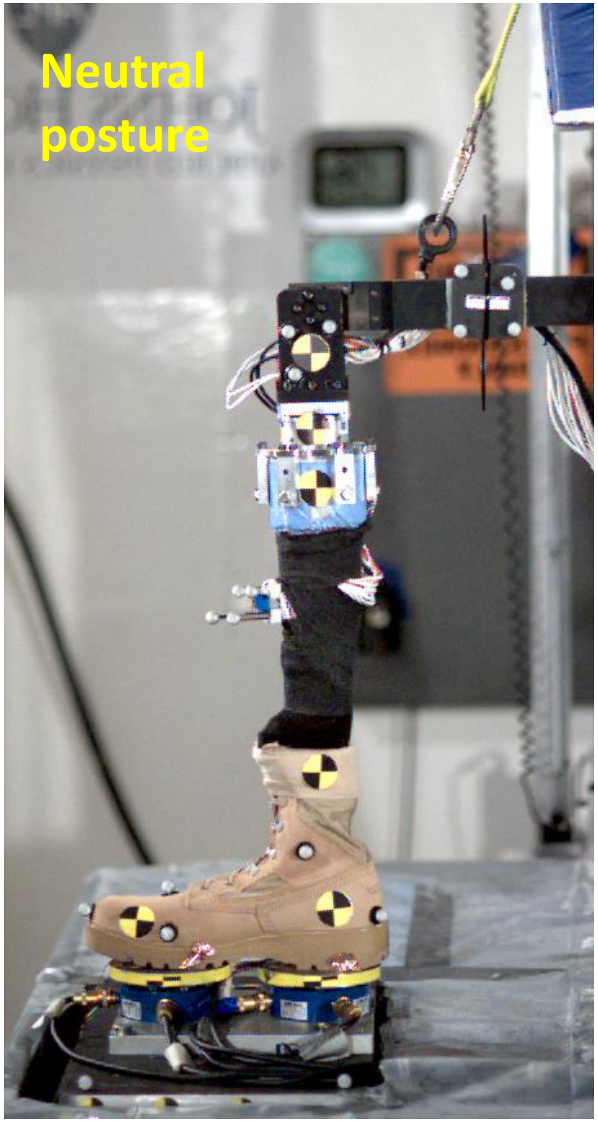

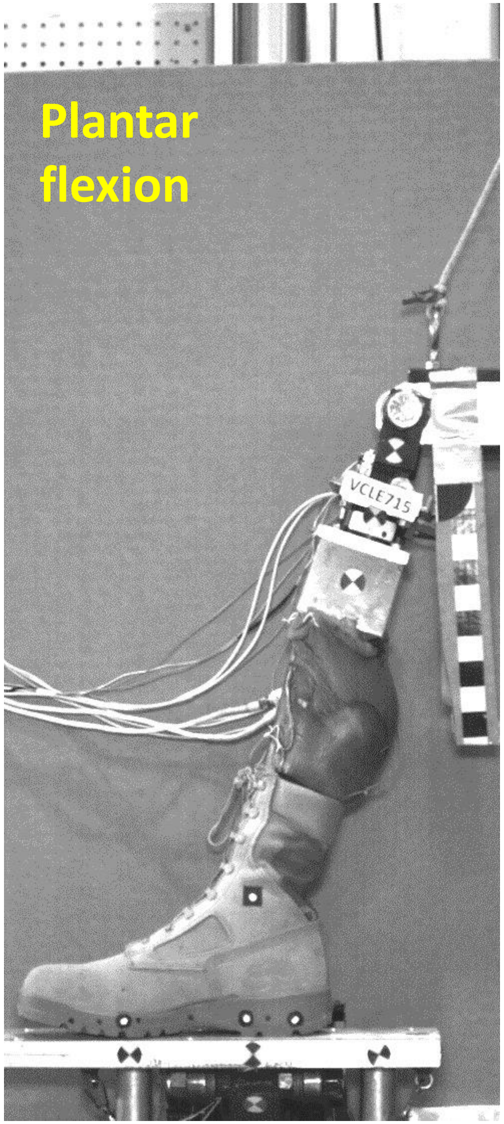

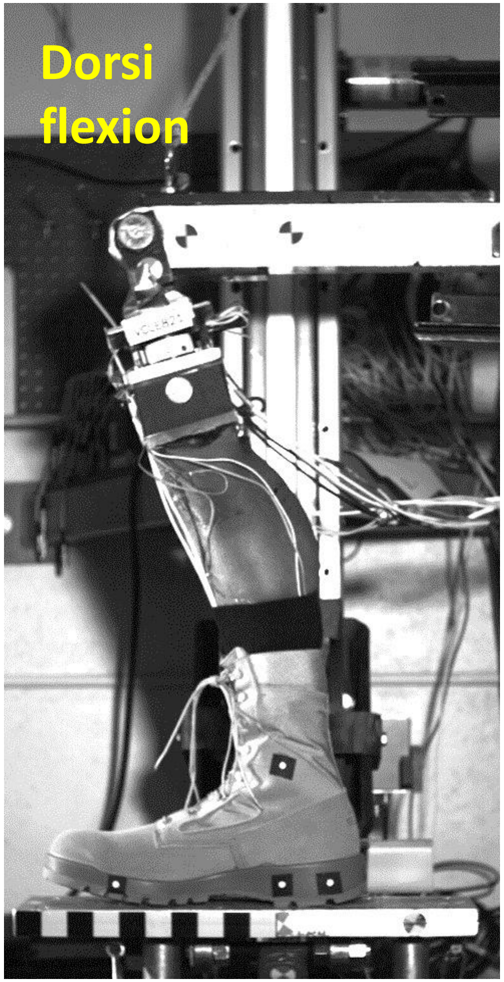

Leg-Foot Kinematics

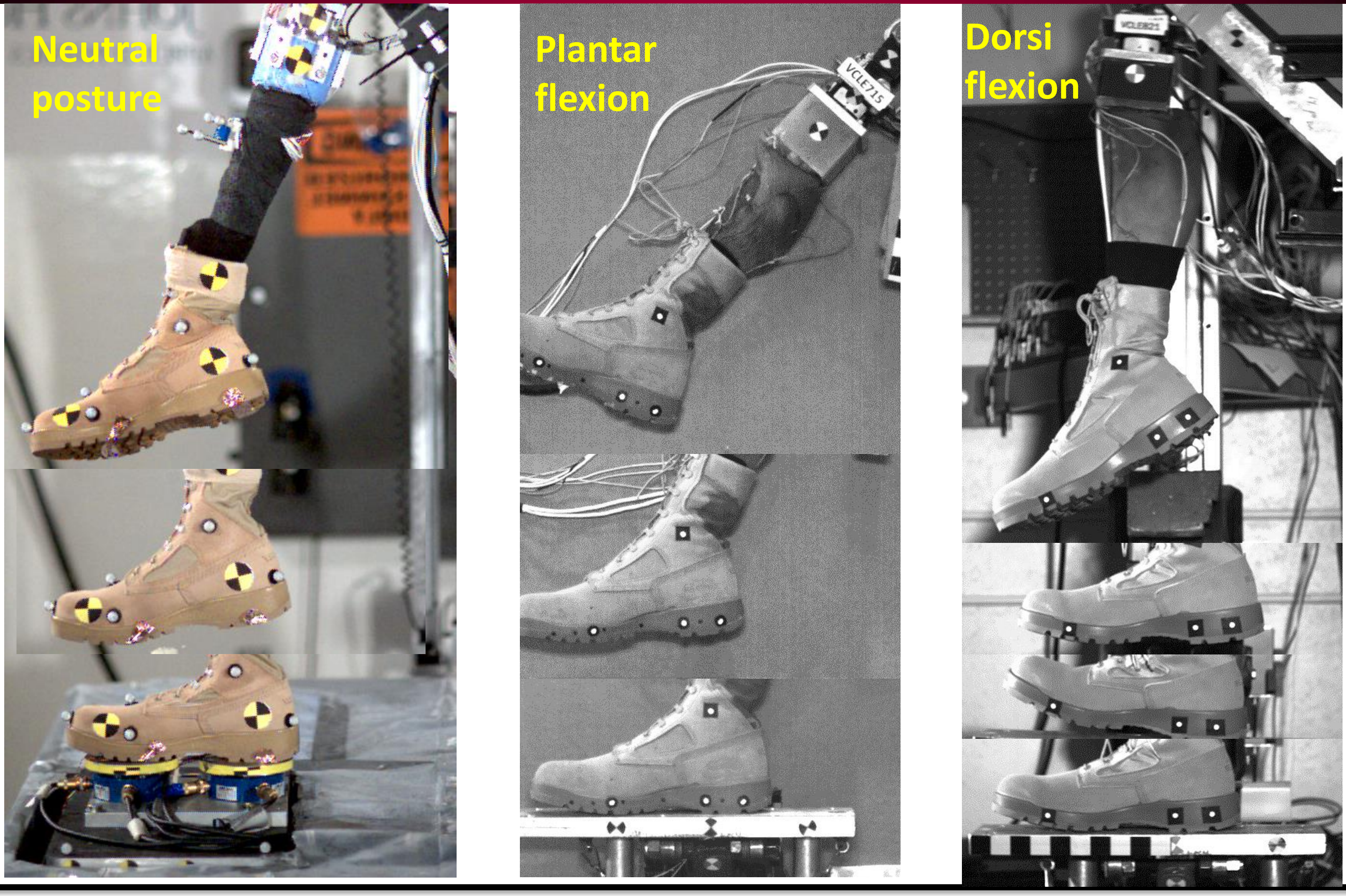

Selected Biofidelity Response Corridors

Representative Curve & +/- 1SD

BRC Time Windows:

- Sensor data:
  - 30 ms
- Video kinematics:
  - 50 ms

BRC: Calc. Acceleration

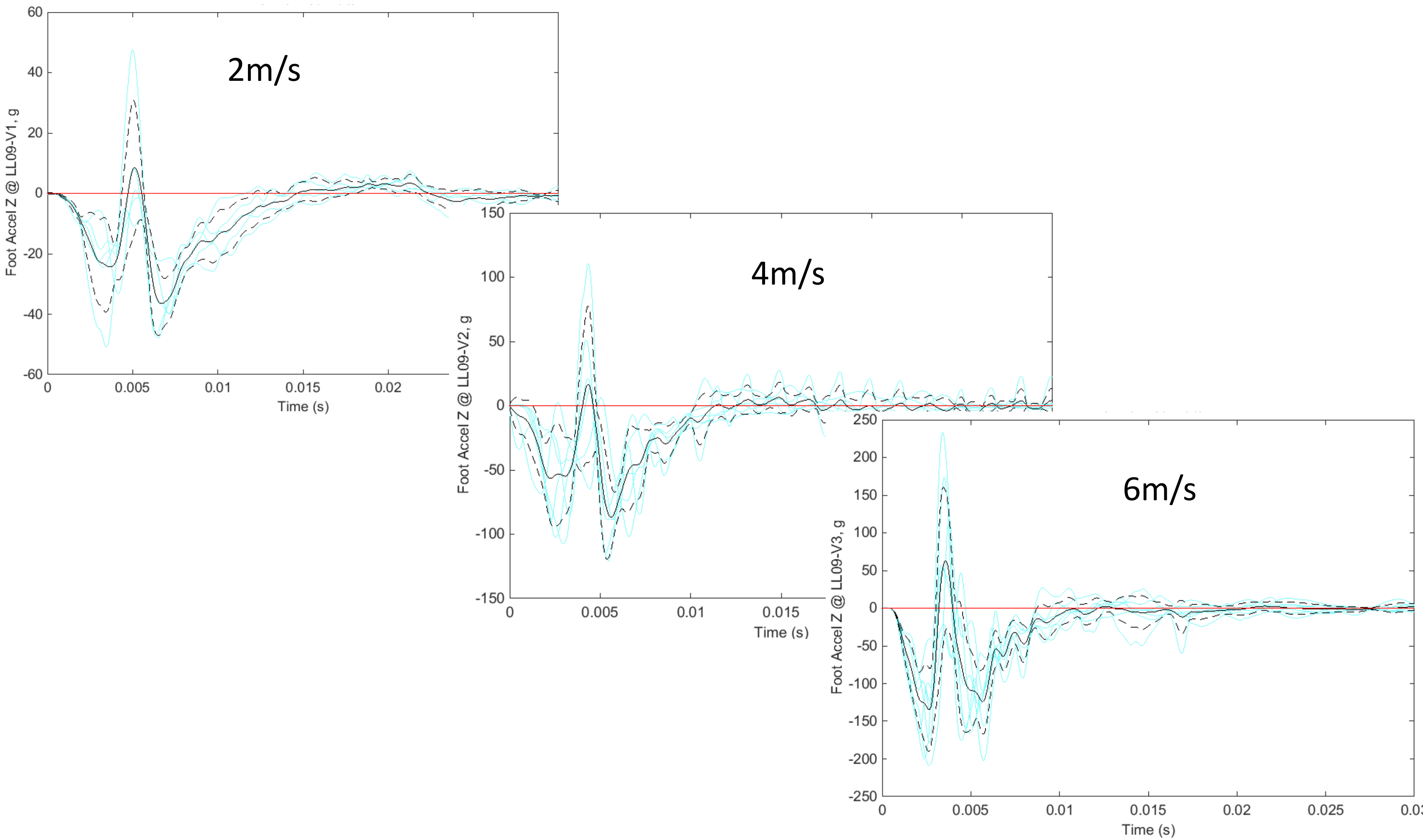

BRC: Knee Force Fz

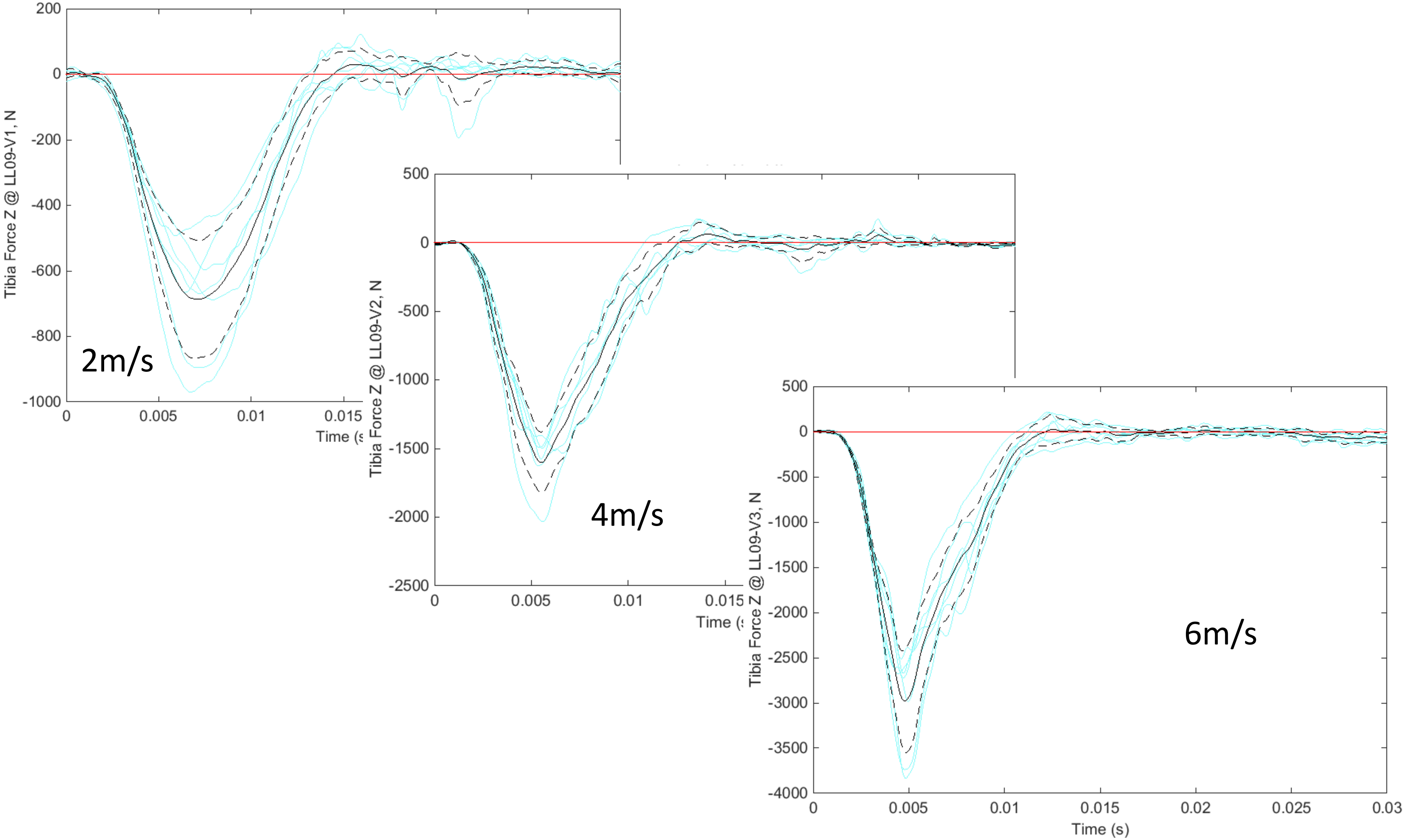

Effect of Leg Posture
on
Biofidelity Responses

Effects of Posture: Calc. Accel

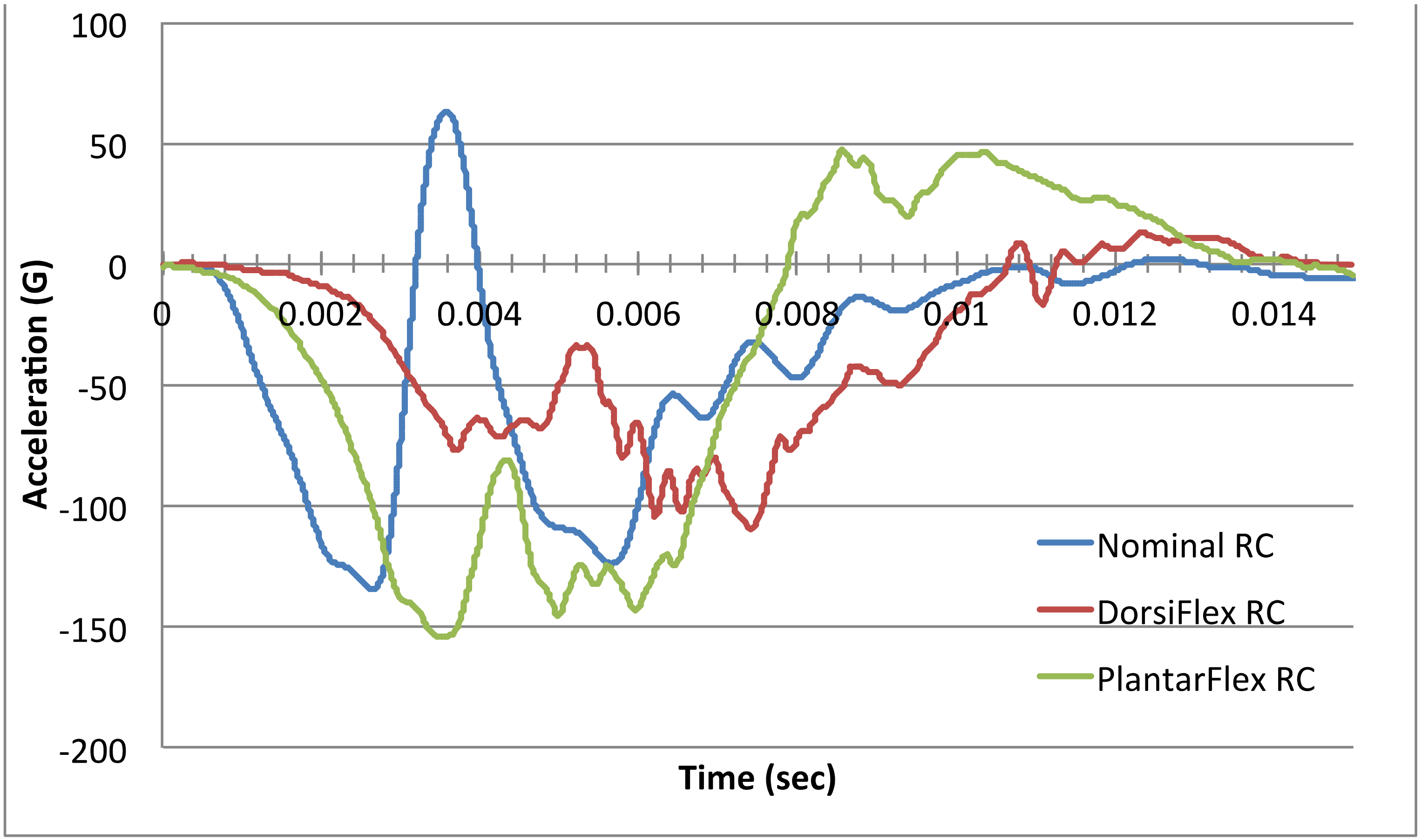

Effects of Posture: Distal Tibia Accel

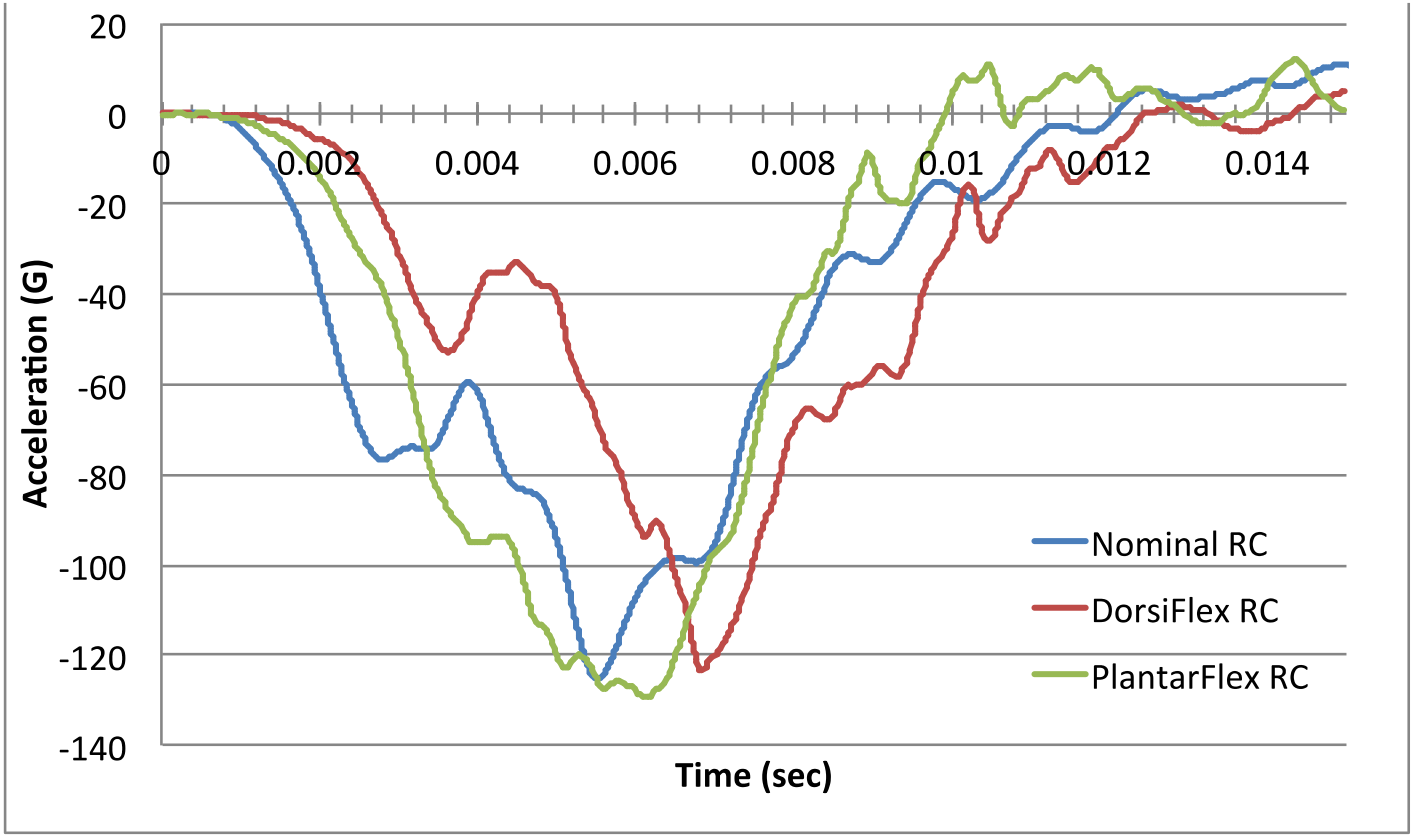

Effects of Posture: Tibia Fx

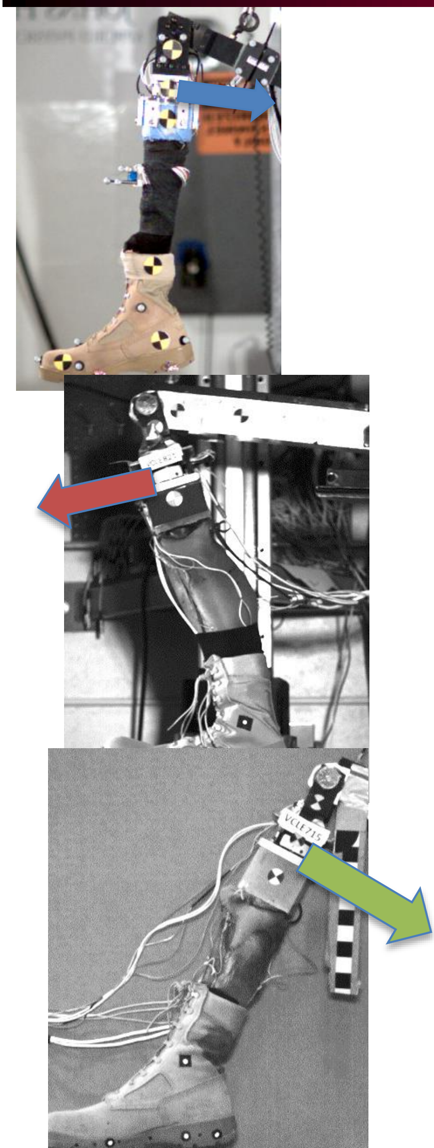

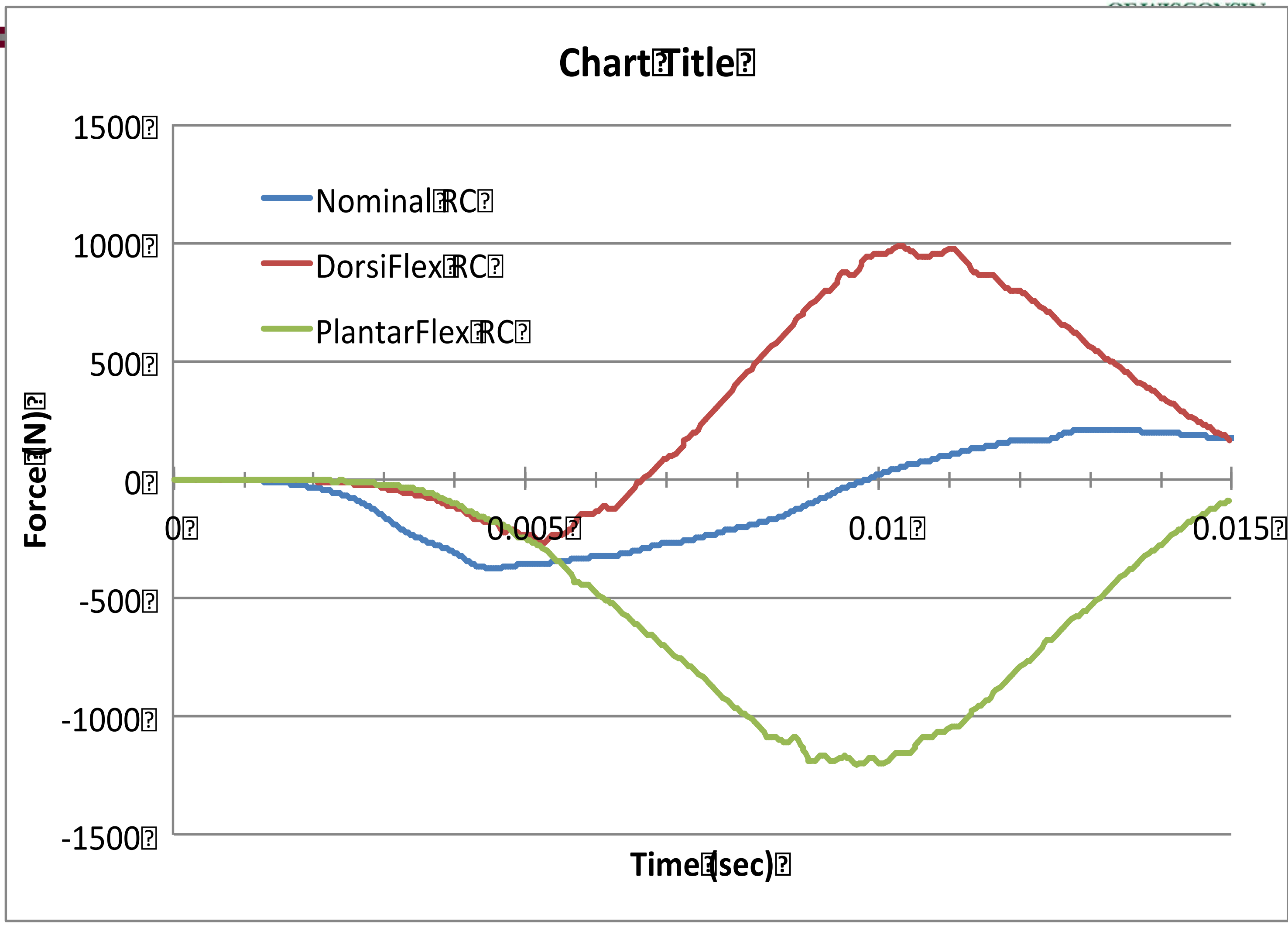

Effects of Posture: Tibia Fz

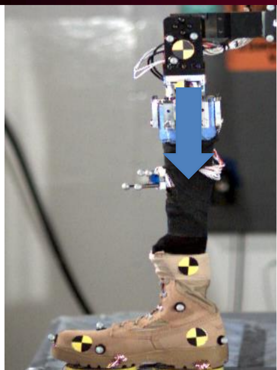

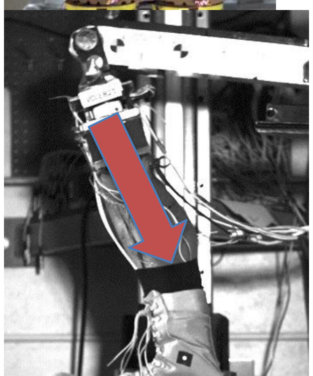

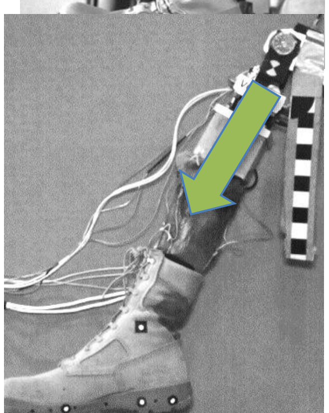

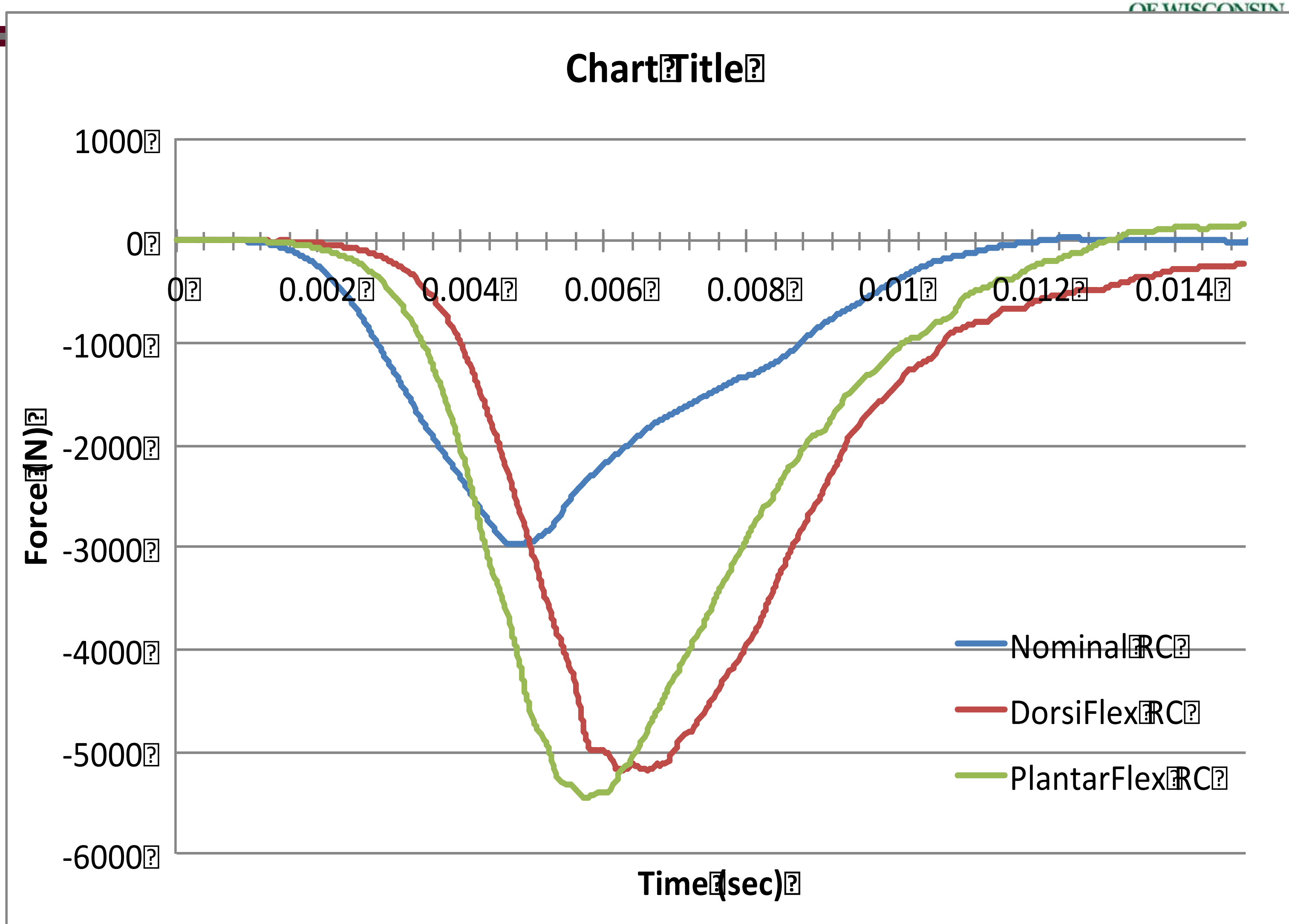

Effects of Posture: Tibia My

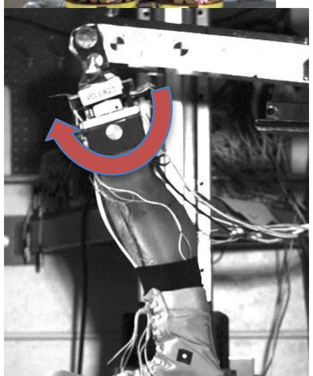

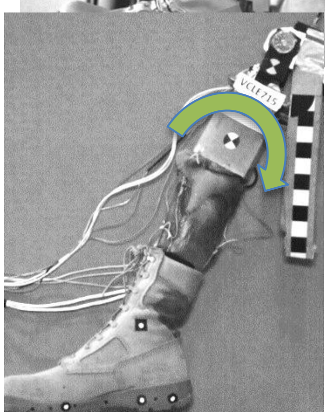

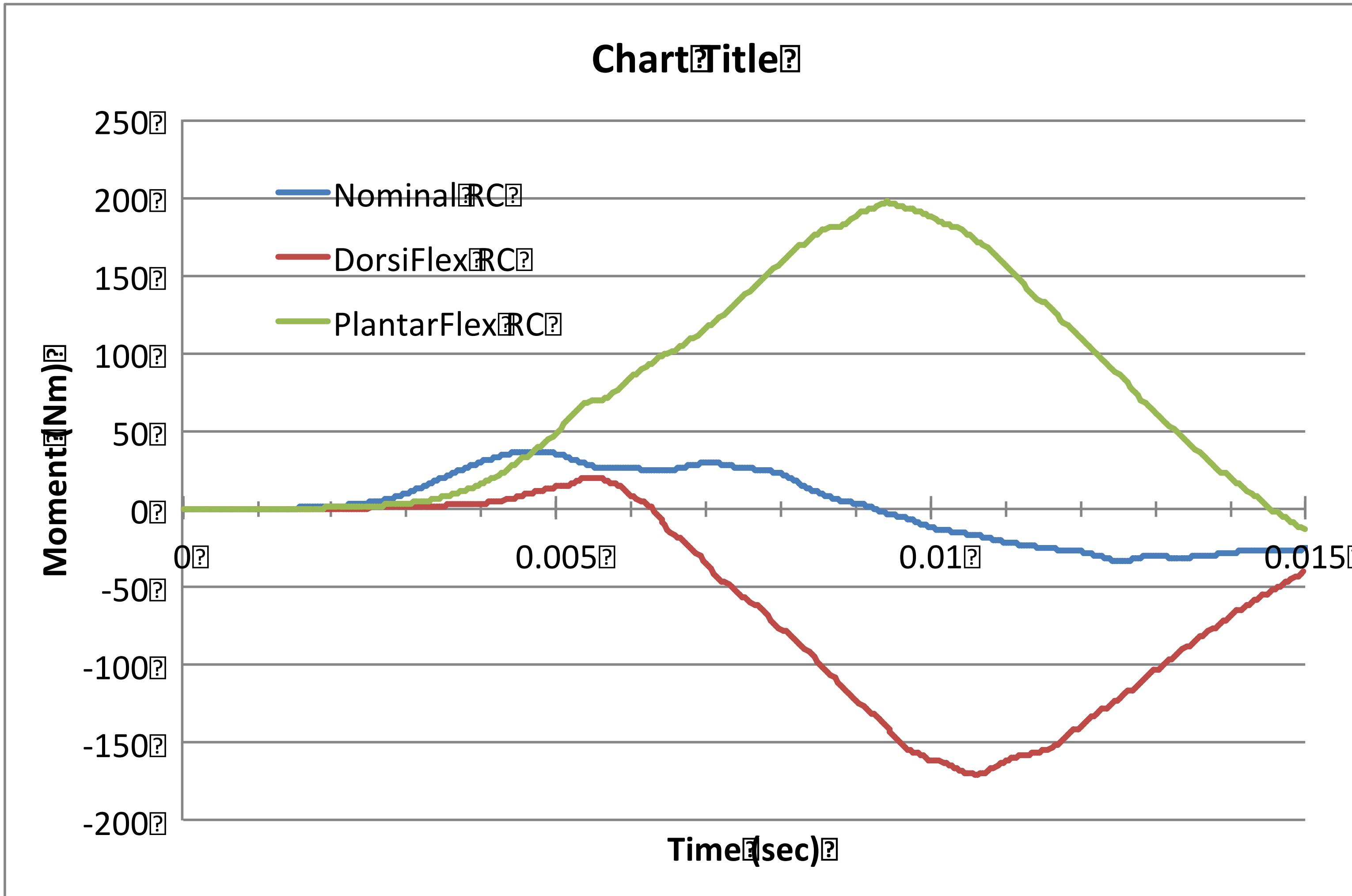

Effect of Velocity Time-to-Peak
on
Biofidelity Responses

Effects of TTP on Responses

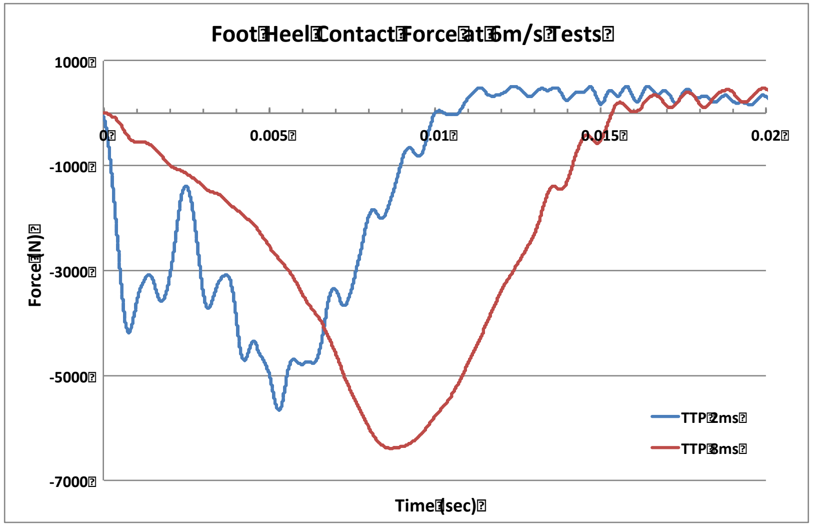

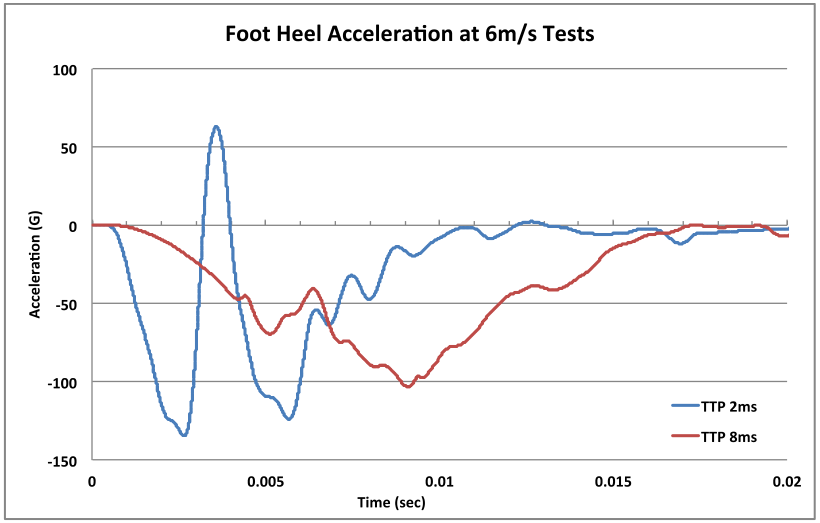

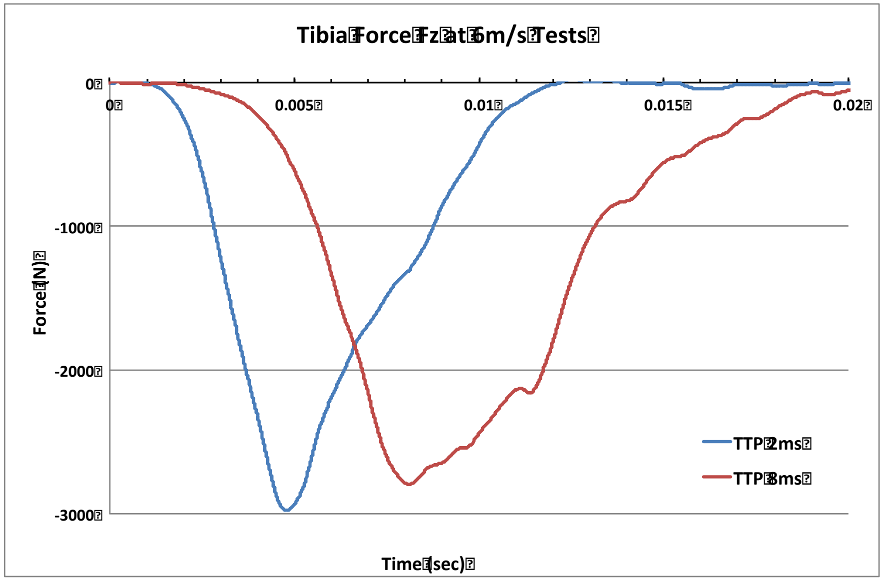

Summary

- Rigorous BRC development process
- All relevant information included in BRC packages
  - Fixtures: dimensions, materials, mass, coupling
  - Boundary condition
  - Initial posture
  - Input corridors
- Total of 184 BRCs available for model validation
  - Six test series
  - Booted: 2, 4, 6, 8m/s velocity; 2, 5, 8ms TTP; 3 postures
  - Bare-foot: 2m/s, 5ms TTP in 90-90 posture
- Posture affects axial and off-axis loads in tibia
- TTP affects near site responses but not far site responses

Acknowledgment

This effort was funded by contract #N00024-13-D-6400, U.S. Army Research, Development and Engineering Command.

The content included in this work does not necessarily reflect the position or policy of the U.S. government.

BACK UP SLIDES

Axial Compression: 3D vs. 2D

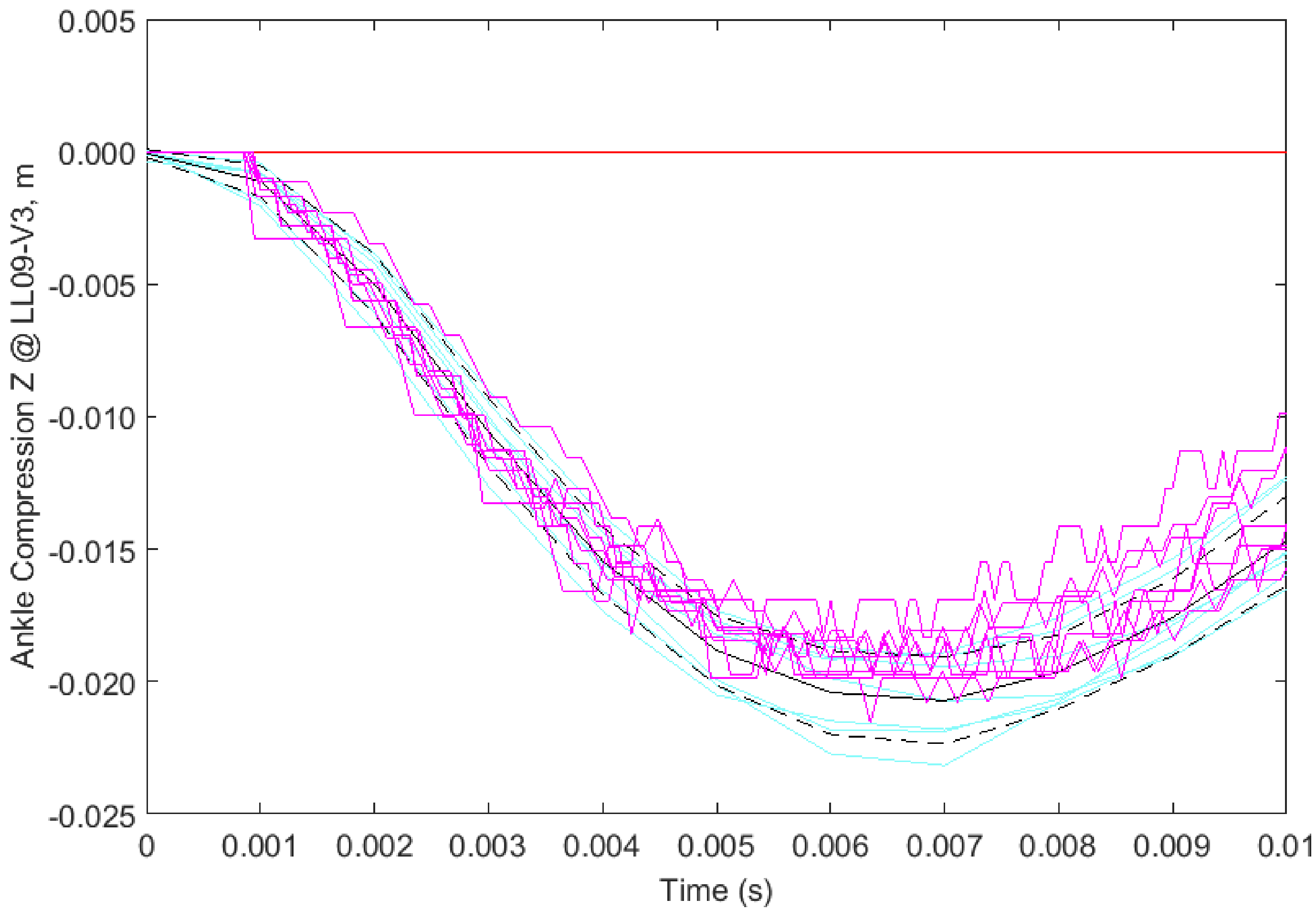

21 January 2016

Ministry of Defence

The use of numerical techniques to identify the key factors associated with in-vehicle, lower leg response to underbody mine-blast loading

J Cordell, D Pope, Dstl

A Sokolow, Army Research Laboratory (USA)

S Masouros, Imperial College London

Page Intentionally Left Blank

U.S. ARMY RDECOM

ARL

Effect of Boots on Leg Injury Mitigation in Underbody Blast Loading Events

Carolyn E Hampton, Ph.D
Michael Kleinberger, Ph.D.
U.S. Army Research Laboratory

13 JAN 2016

Importance of Leg Injuries

Musculoskeletal Injuries in the Army (2005-2009)
3.56 injuries per 1000 personnel per year
82% of injuries caused by explosive blast

Belmont et al 2013 J Orthopaedic Trauma 27(5)

6,092 casualties

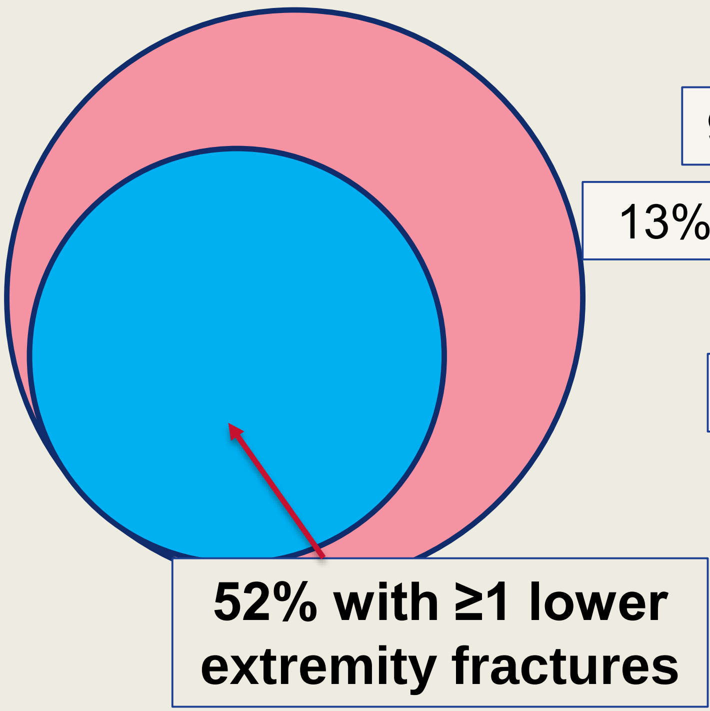

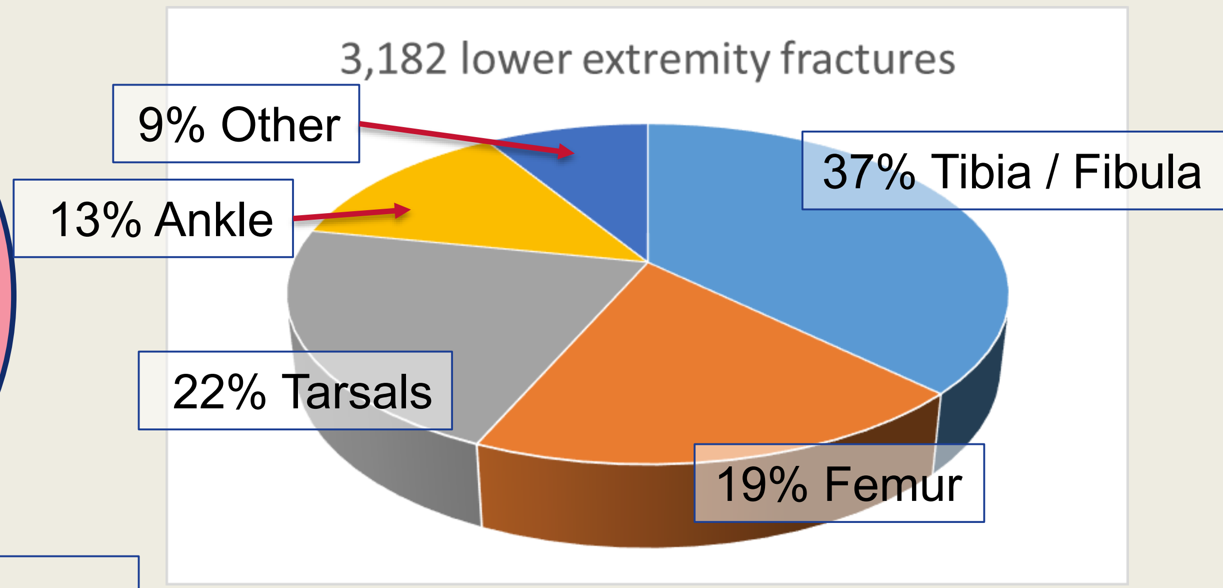

Finite Element Leg

- Lower leg model (400,000 tetrahedral elements) adapted from ARL leg created from Zygote geometry data
- Tibia and fibula potted in PMMA cement
- Posterior cruciate ligament (PCL) insertion on tibial plateau above the malleoli midpoint

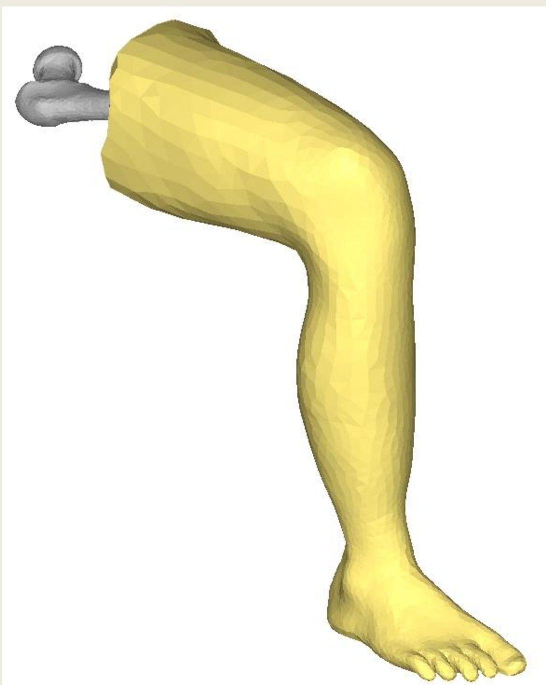

ARL Leg

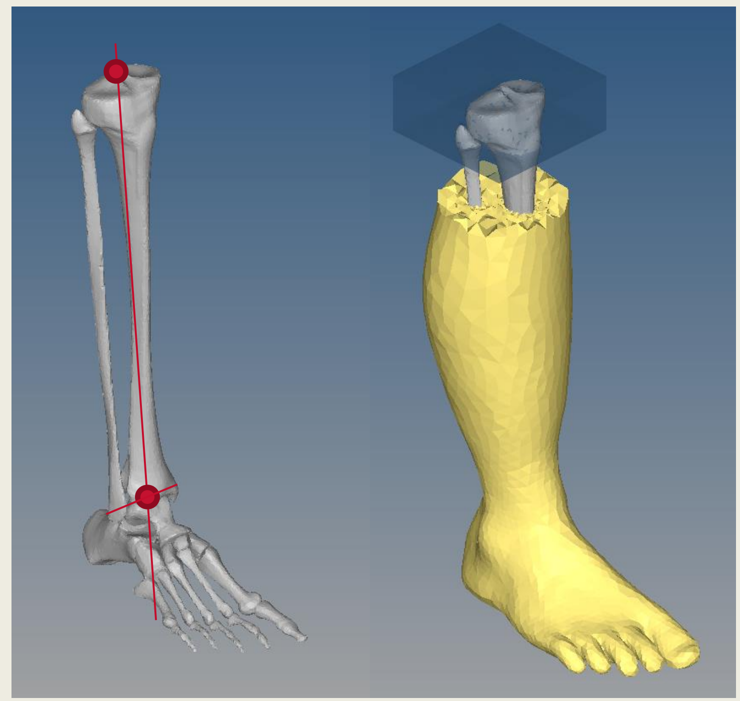

Isolated Lower Leg

Finite Element Solvers

- **Simulated in LS-DYNA on Excalibur cluster**
- **1 – 2 hours on 32 processors**

Linear Elastic (Lynch et al 2015 ARL-TR-7310)

	Density [kg/m^3]	Modulus [GPa]	Poisson's Ratio
Cortical Bone	1850	15	0.3
Trabecular Bone	650	0.15	0.3
Aluminum	2700	68.9	0.33
Steel	7850	190	0.28

Viscoelastic Hyperelastic (Untaroiu et al 2005 Stapp 49)

	Density [kg/m^3]	Bulk Modulus [MPa]	Coefficient C1 [Pa]	Coefficient C2 [Pa]
Flesh	1300	37.5	120	250
	Relaxation S1	**Relaxation S2**	**Time T1 [ms]**	**Time T2 [ms]**
	1.2	0.8	23	63

Experimental Setup

- Barefoot post-mortem human subject (PMHS) legs subjected to axial pendulum impact
- Impact speed of 2 – 9 m/s
- Pendulum mass of 3.3 – 9.1 kg
- Leg weighted to 11.5 kg (includes instrumentation)

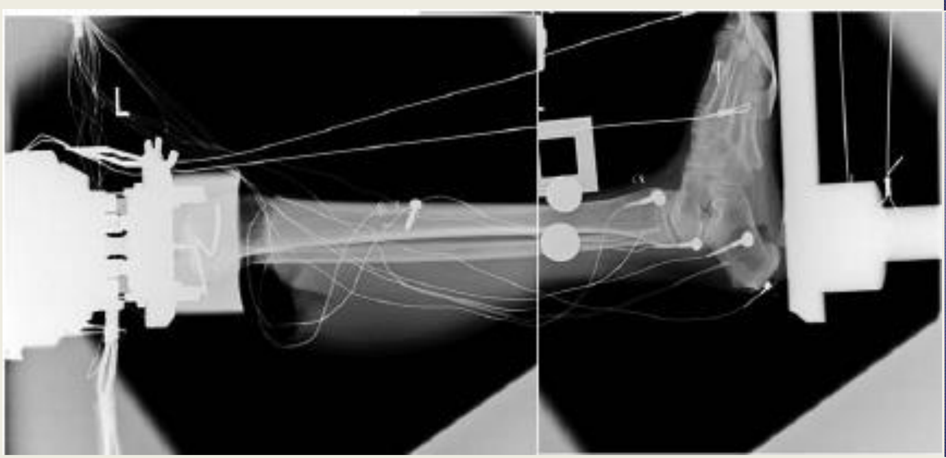

Gallenberger et al 2013

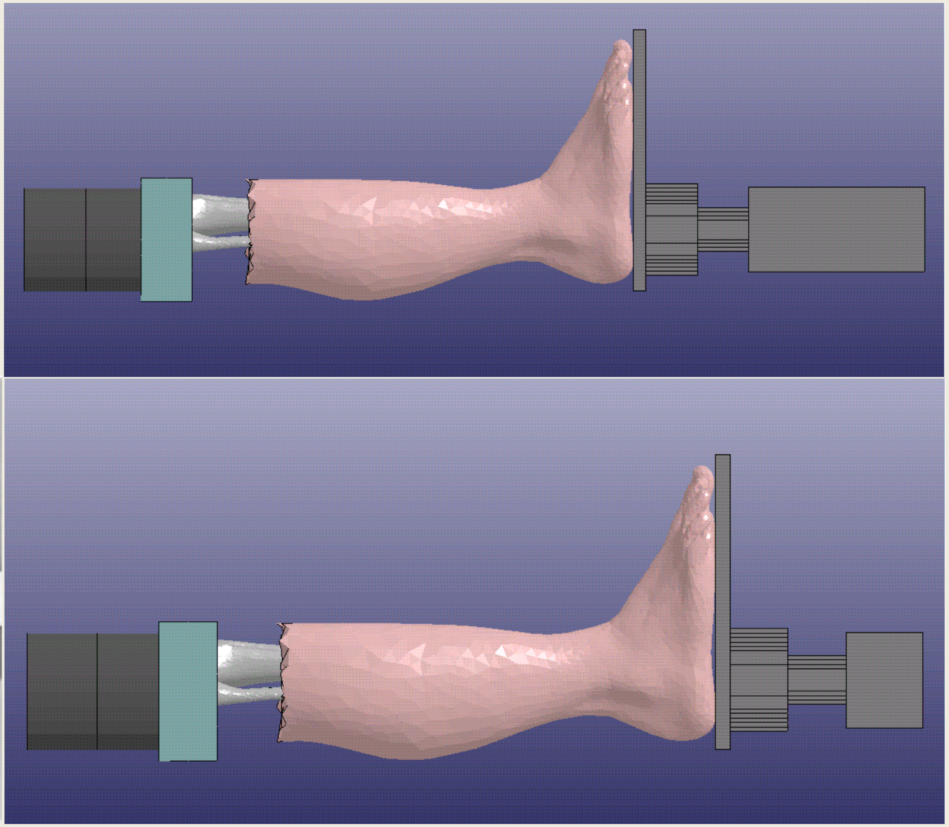

Finite element representation

Mesh Matched Potting

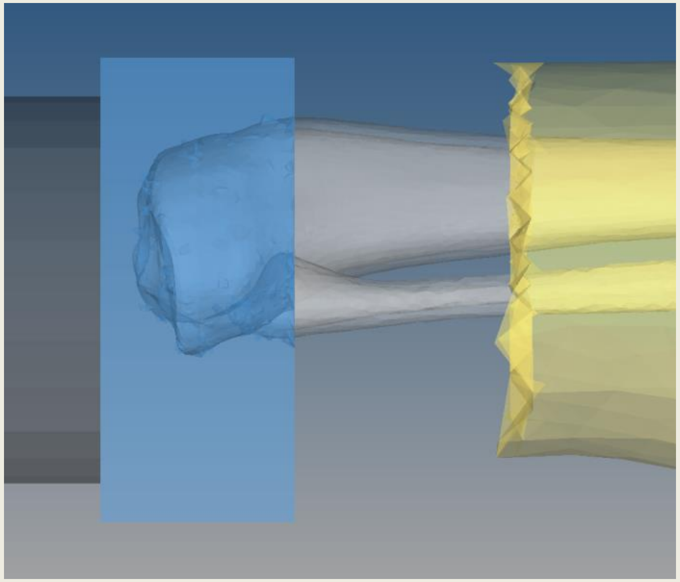

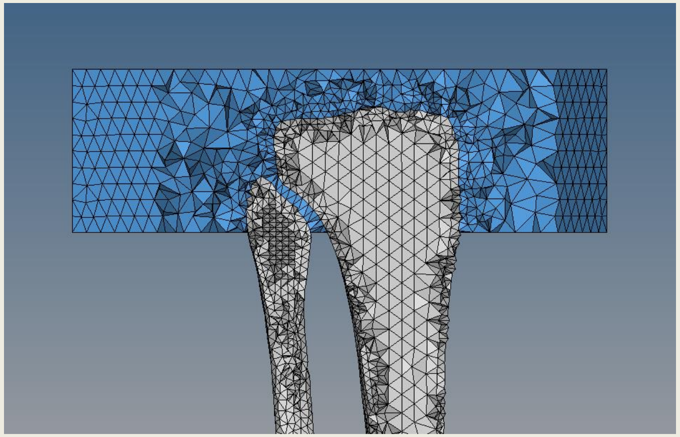

Simulated Impact

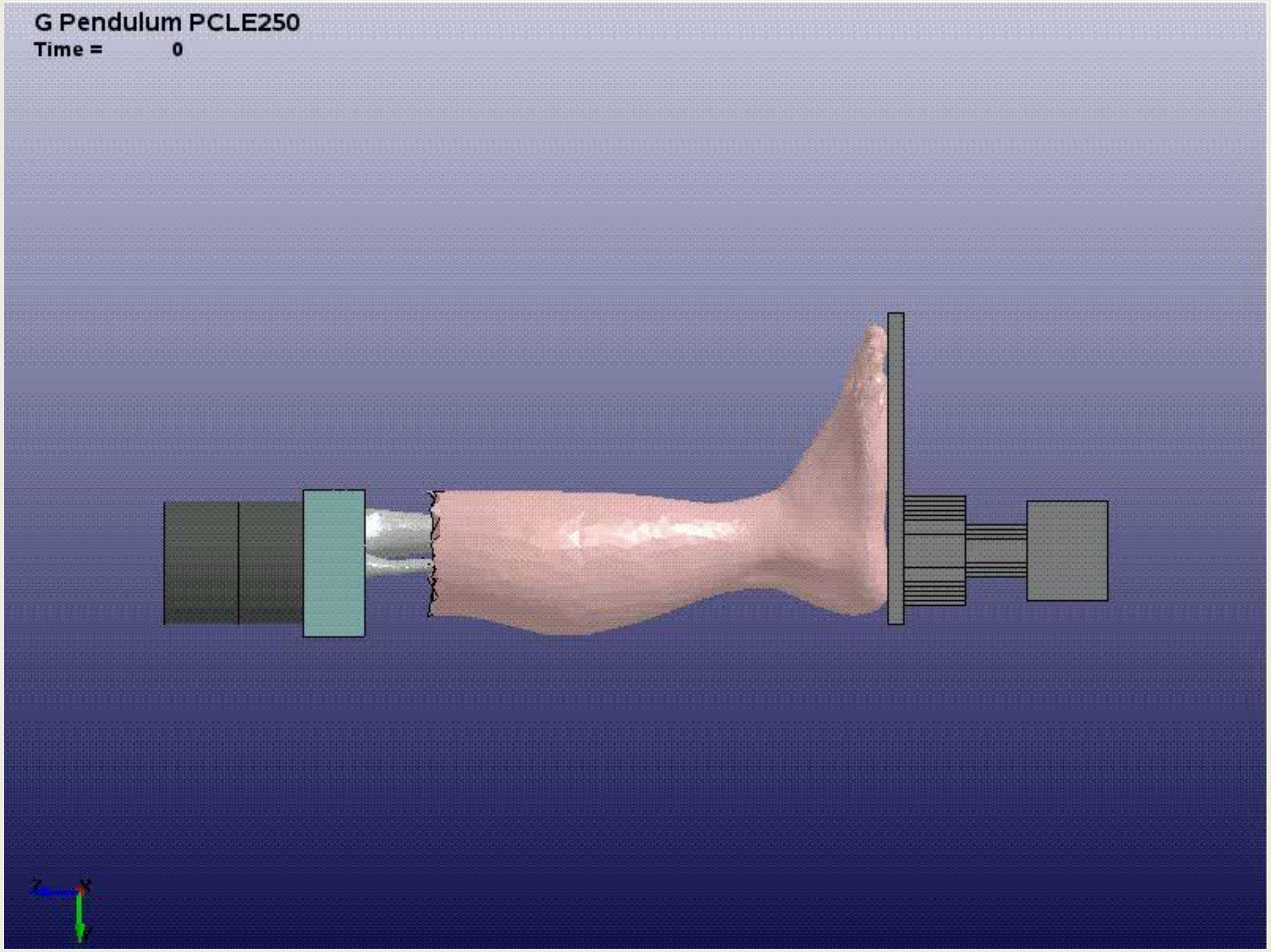

Experimental Results to Match

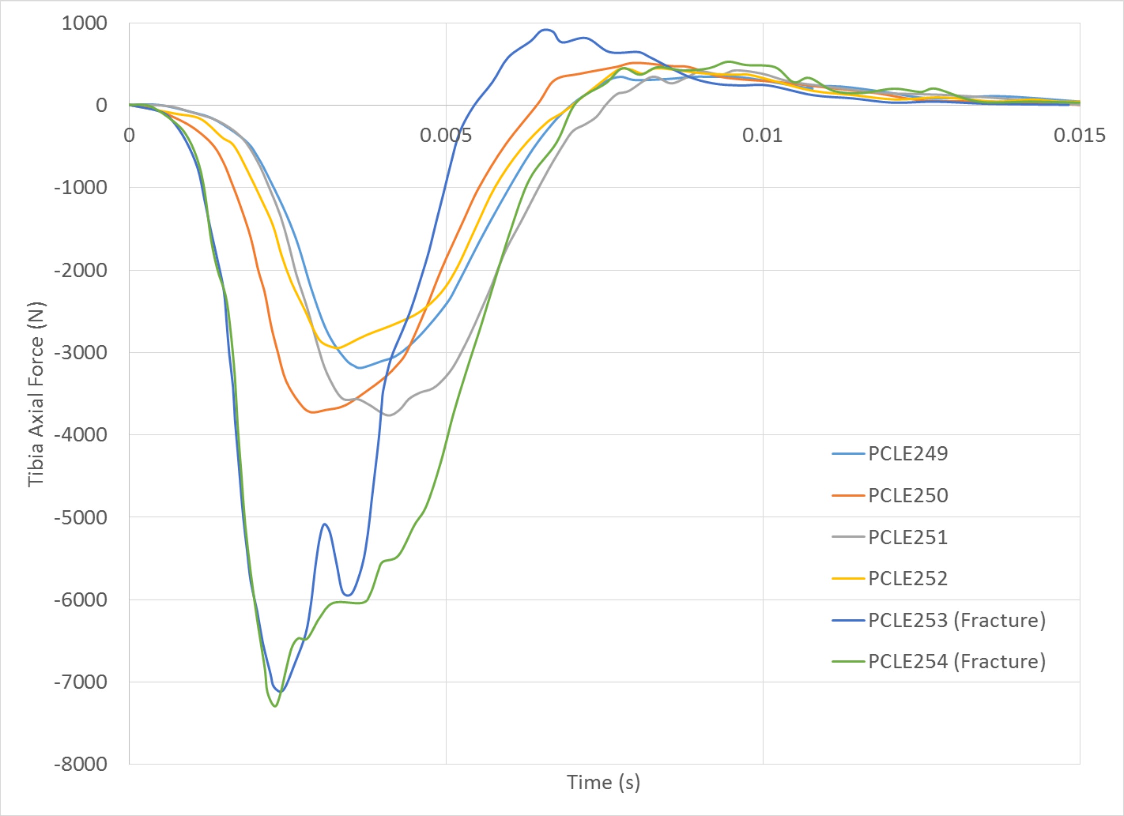

Using PCLE249 through PCLE254

PCLE249/252:	3.36 kg pendulum	4.88 m/s impact speed
PCLE250:	3.36 kg pendulum	5.67 m/s impact speed
PCLE251:	5.76 kg pendulum	4.65 m/s impact speed
PCLE253/254:	5.76 kg pendulum	8.99 m/s impact speed

Simulation Results

ARL

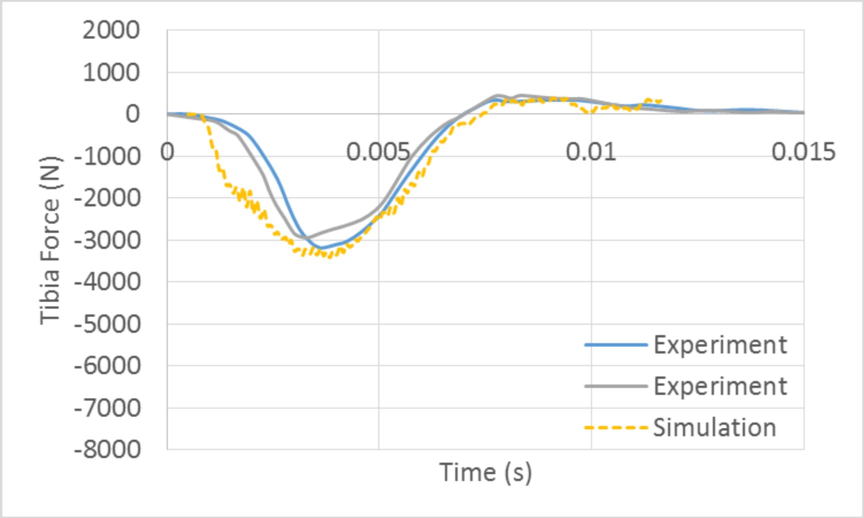

PCLE249/252: 3.36 kg at 4.88 m/s

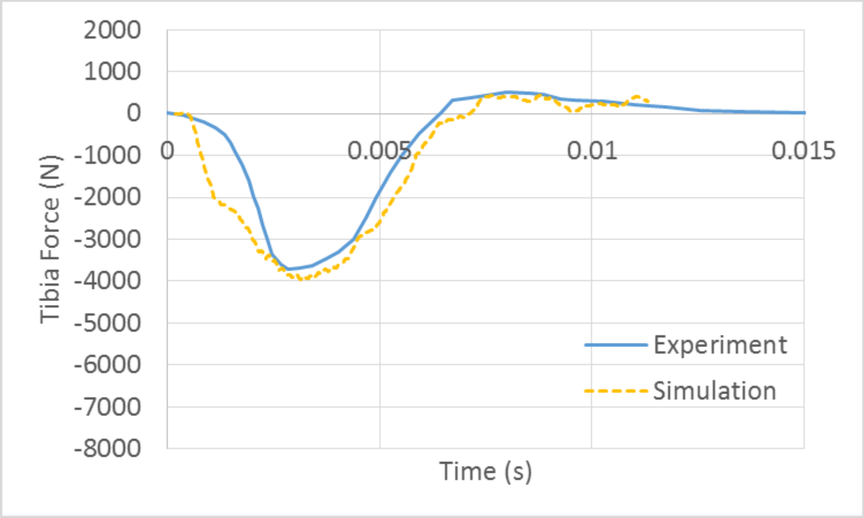

PCLE250: 3.36 kg at 5.67 m/s

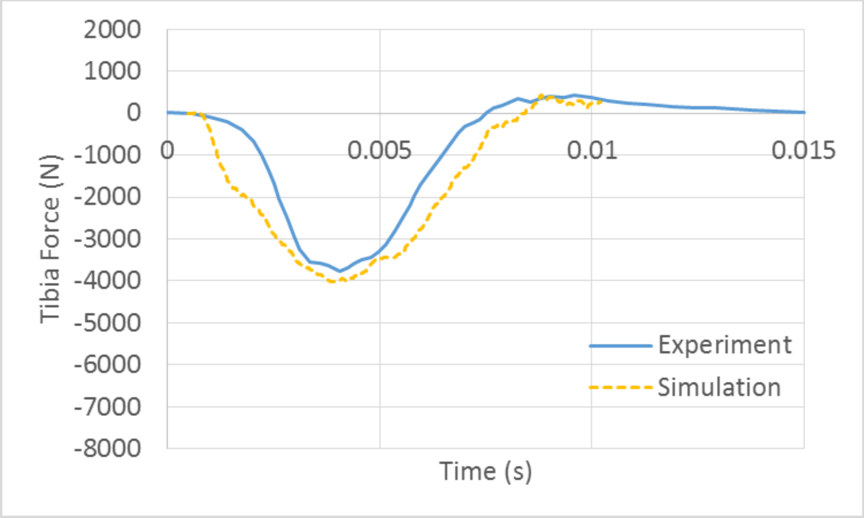

PCLE251: 5.376 kg at 4.65 m/s

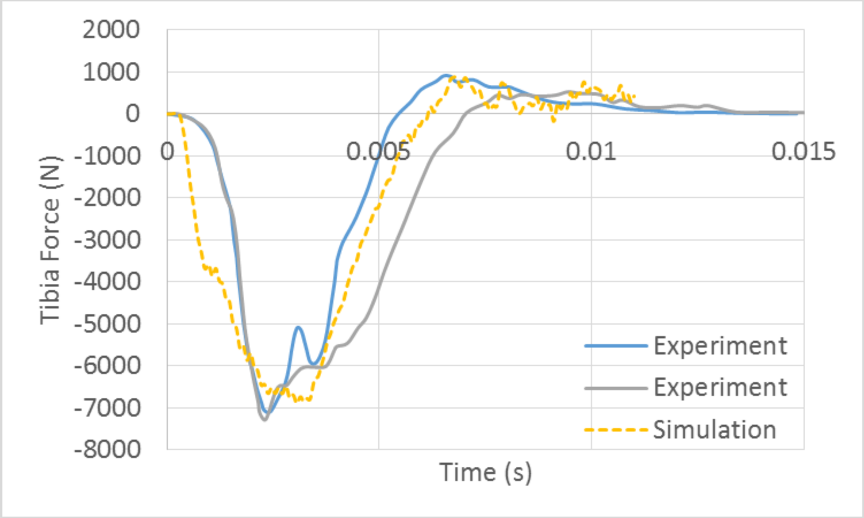

PCLE253/254: 3.36 kg at 8.99 m/s

Tibia-Fibula Load Sharing

- Dynamic PMHS testing
- Fibula sustains 6-33% of axial load
- Very high variability between specimens

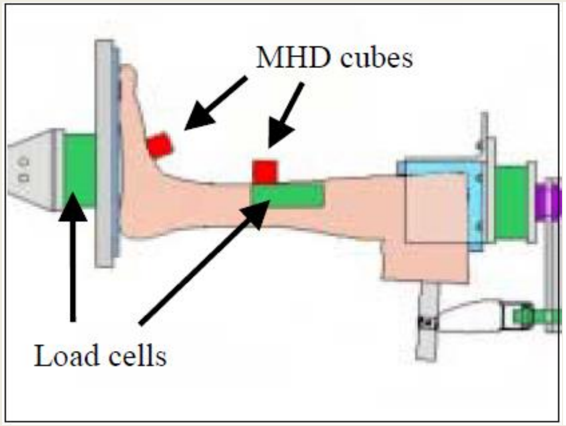

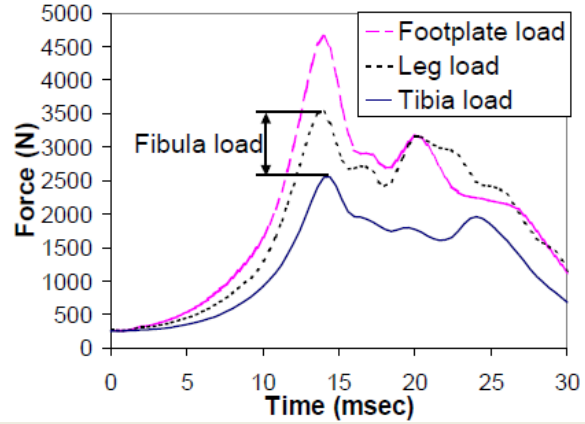

Funk et al 2000 Am Soc Biomech

- Quasistatic PMHS testing
- In neutral posture the fibula carries ~6.0 ± 4.6% of the axial load
- Fibula load share increases with ankle eversion to 15.9% ± 3.0%

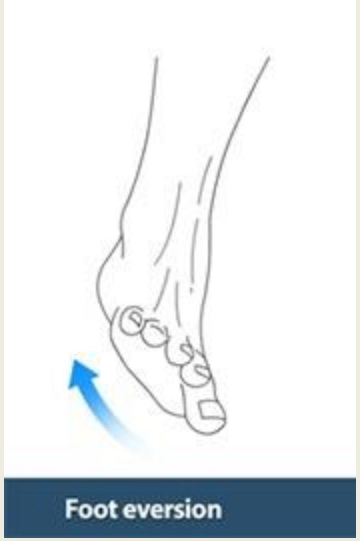

Funk et al 2007 J Biomech

Dynamic Simulation Load Sharing

- **From Funk 2000**
  23.0% ± 7.6% load share if no injury
  16.2% ± 7.4% when injured

- **From simulation**
  22% load share if no injury

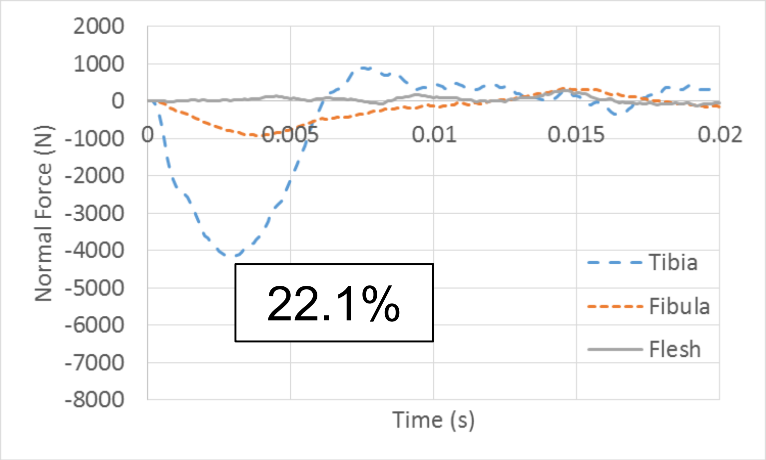

PCLE250 Simulation

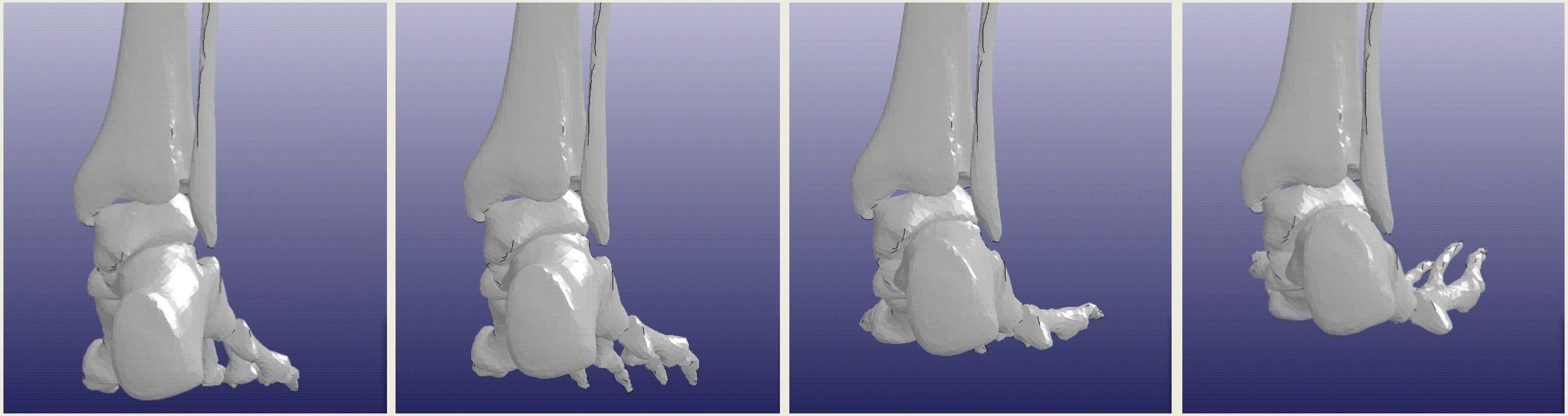

t = 0 ms t = 1 ms t = 2 ms t = 3 ms

Ankle Motion (3x magnification)

Boot Model

Finite element model of Altama size 11 military boot

~1 cm of insole over ~2 cm soft rubber under heel

Matched booted H-III UBB tests at 6 – 12 m/s within 12%

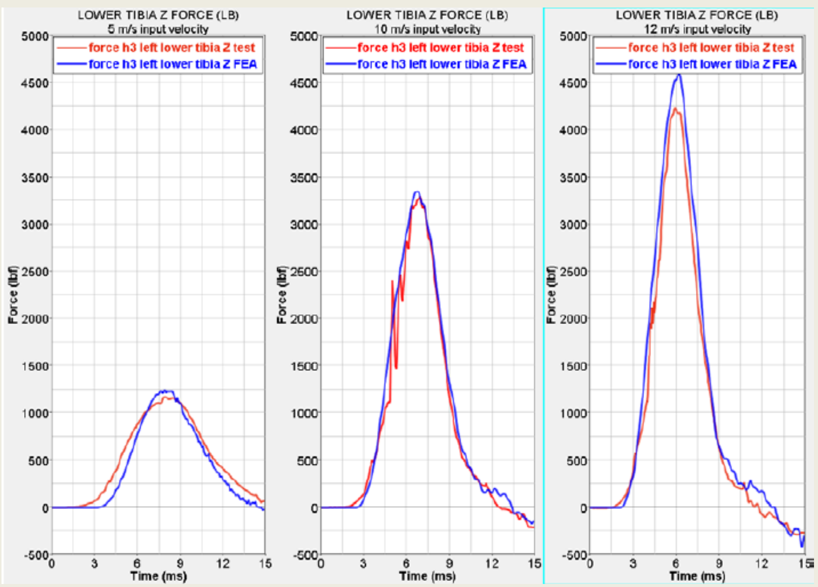

D Krayterman, ARL-TR-7359

Foot Reshaping

- Leg FE model obtained from person standing on hard surface
- Use gravity load and dynamic relaxation to reshape foot to initial contours of boot
- Replace original mesh with the reshaped mesh
- All booted simulations use the reshaped foot geometry

PMHS Paired Boot – No Boot Tests

- Left and right legs from the same PMHS specimen subjected to multiple sub-injury impacts
  - Low severity: 3.4 kg pendulum at 5 m/s
  - Medium severity: 5.7 kg pendulum at 7 m/s
  - High severity: 5.7 kg pendulum at 10 m/s
  - High severity unbooted test resulted in calcaneus fracture

- Neutral leg posture
- PMHS weight matches 50th percentile male target weight

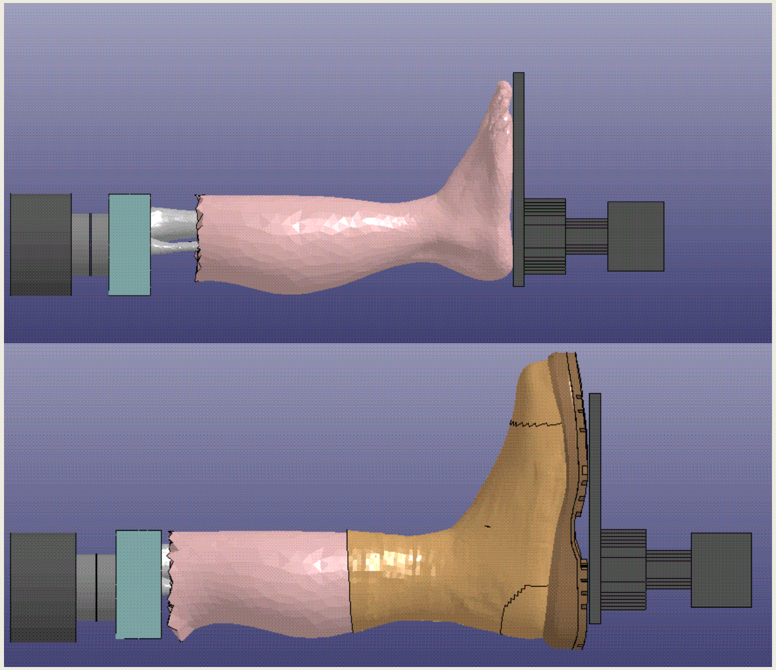

Schlick, Pintar 2015 Email correspondence

Simulated Impact

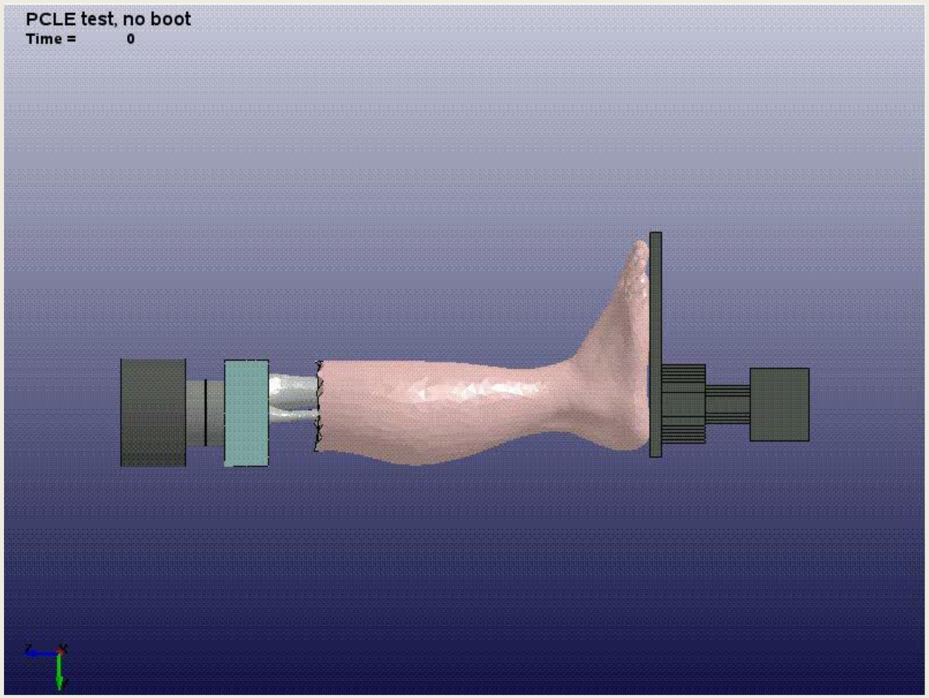

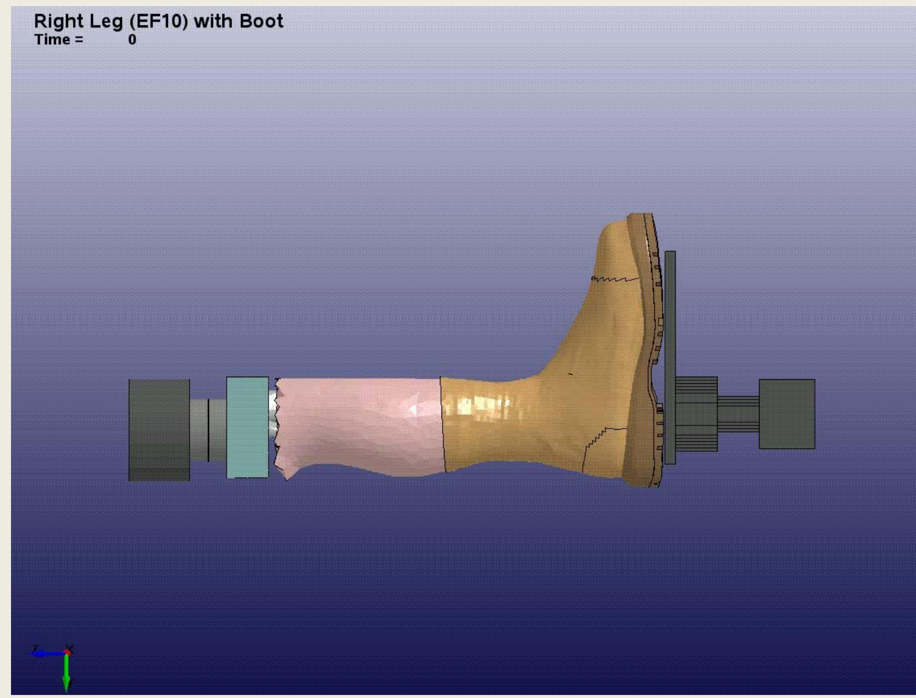

Load Cell Forces

- Simulation is best at emulating booted or low severity unbooted tests
- Boot mitigates peak force
  - -39.8% mean experimentally
  - -34.0% in lower severity simulation

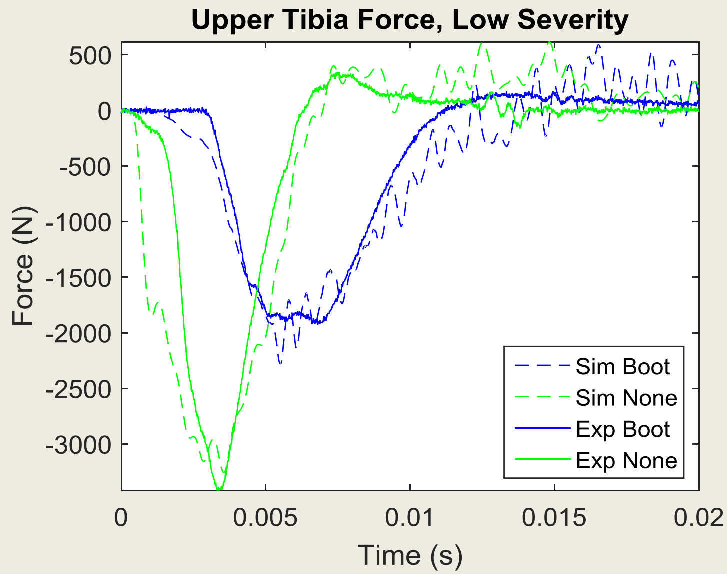

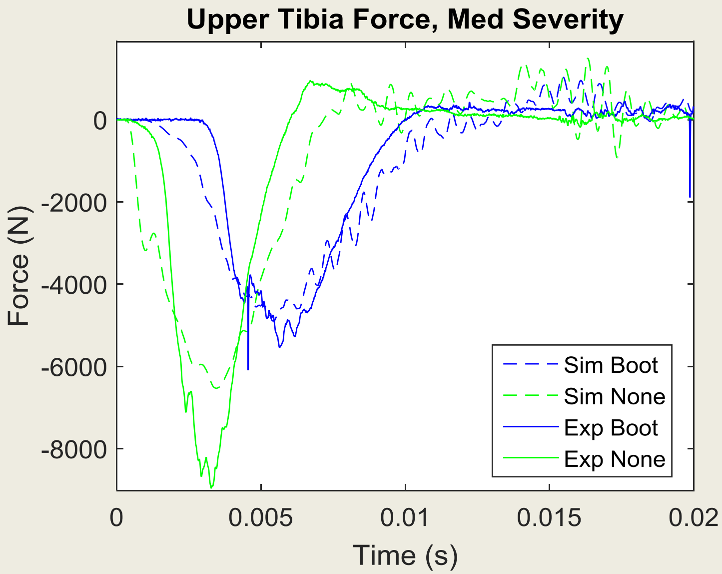

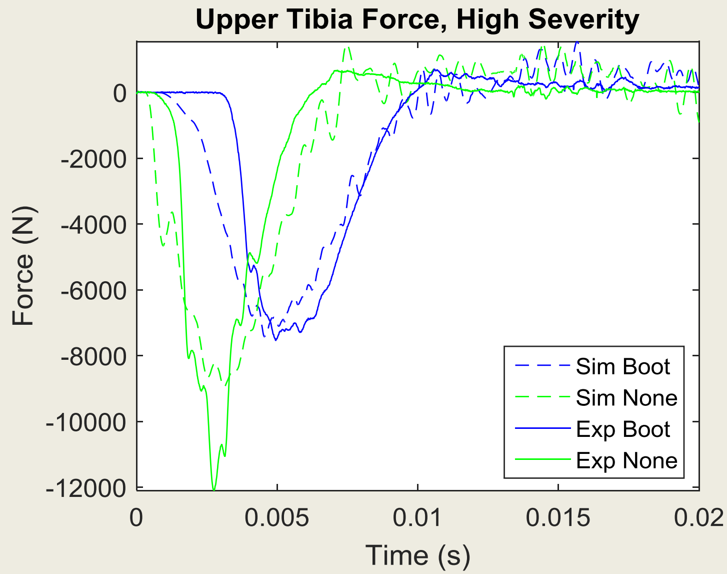

Supplemental PMHS Tests with Boots

- Flyer plate impacts into booted legs at 4, 6, 8 m/s
- Pin joint in place of knee allows more realistic response
- Mostly non-injurious

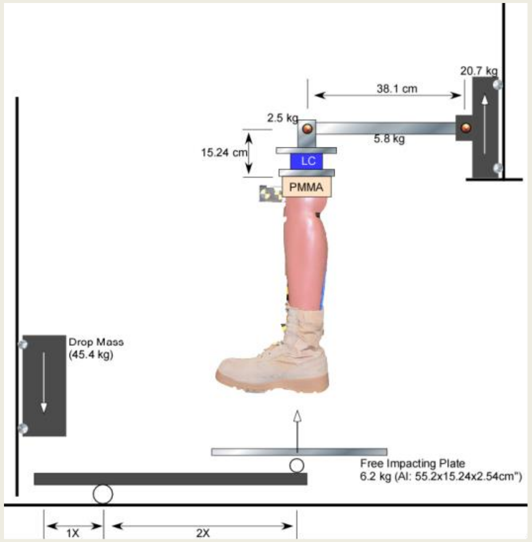

- Upper tibia force
- Plate velocity
- Peak force

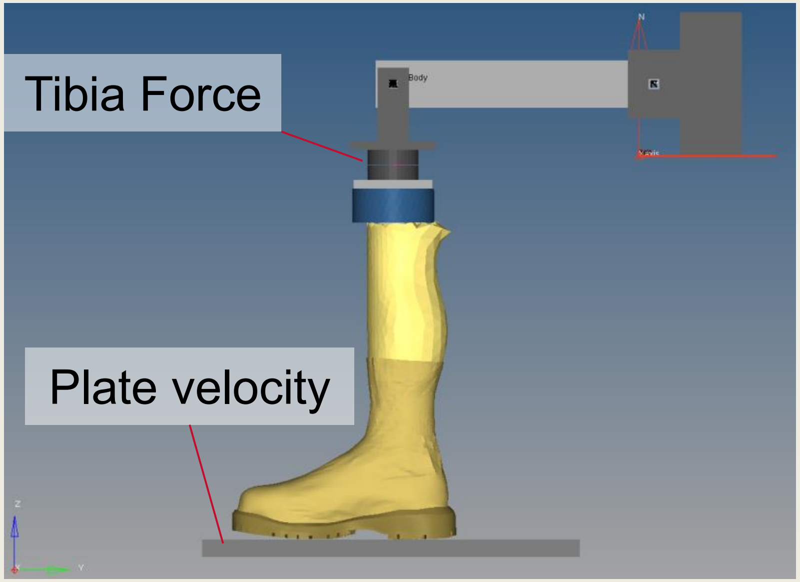

WIAMan Project Biofidelity Response Corridors (BRC): Leg (90-90) 2014

Plate Velocity

- Simulated impacts show more elasticity

- Plate velocity during impact tracks within corridor

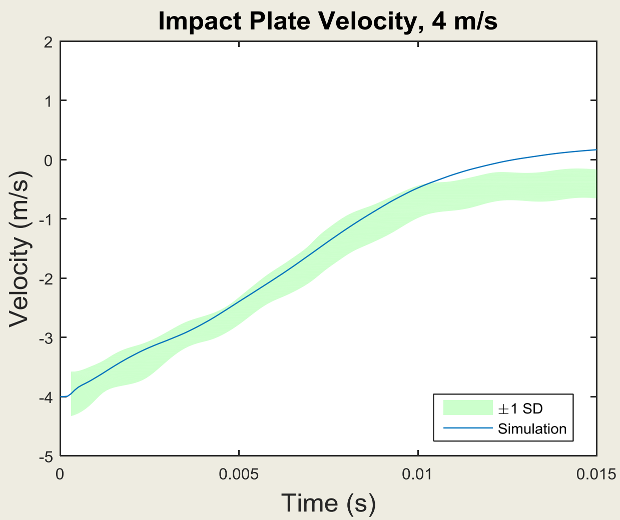

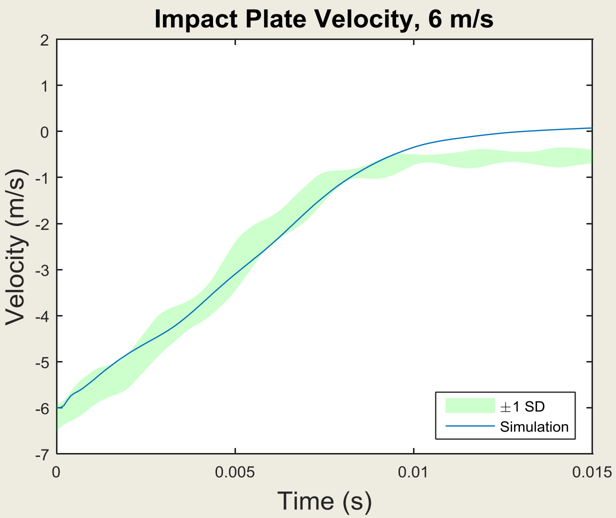

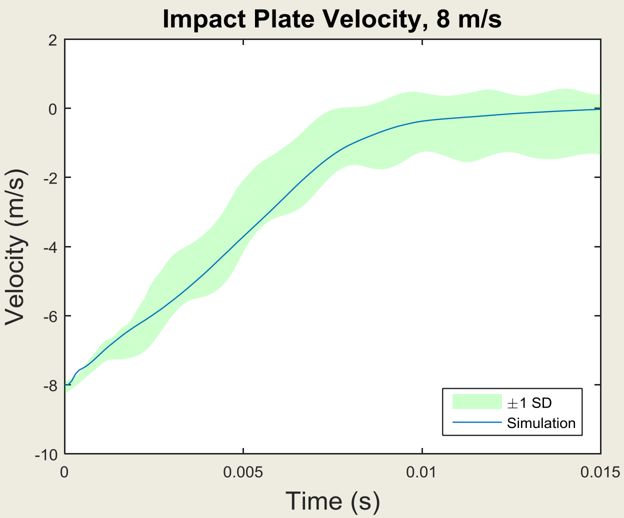

Upper Tibia Force

ARL

- Real leg more compliant in early phase
- Simulated leg missing hardening effects in higher velocity impacts
- Mitigation of peak force with boots is comparable to pendulum simulations

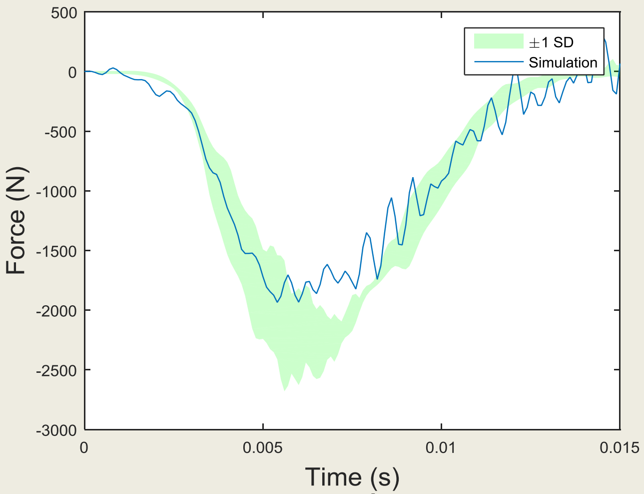

4 m/s

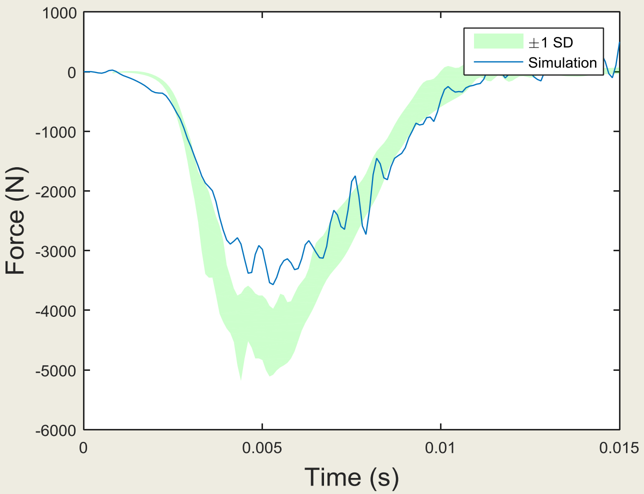

6 m/s

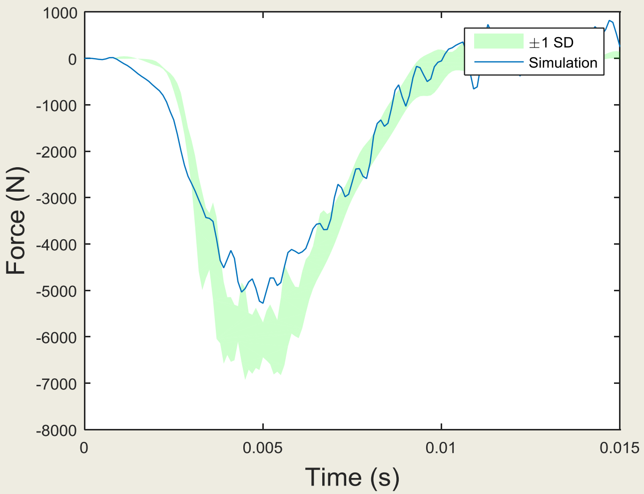

8 m/s

Limitations & Future Work

- Source geometry based on < 50th percentile male volunteer
- Homogenous flesh model doesn't capture ligament & muscle attachments or muscle activity
- Simulation doesn't capture fracture behavior

- Future work:
  - Transition to newer leg model with musculature and ligaments
  - Improved flesh material with reduced elasticity, improved stability under high loading rates
  - Scaling of the boot or foot to other sizes
  - Failure models for bones

Acknowledgements

Mike Schlick, Frank Pintar (Medical College of Wisconsin) for sharing experimental data from the PMHS PCLE/VCLE test series

Department of Defense (DoD) High Performance Computing Modernization Program (HPCMP) for access and hours on the computer clusters

Blast Protection for Platforms and Personnel Institute (BP3I) and Oak Ridge Institute for Science and Education (ORISE) for funding for this study

References

- PJ Belmont et al 2013 The nature and incidence of musculoskeletal combat wounds in Iraq and Afghanistan (2005-2009), Journal of Orthopaedic Trauma 27(5) e107-e113
- Gallenberger 2013 Foot and ankle injuries in variable energy impacts, Master's Thesis from Marquette University
- C Untaroiu, K Darvish, J Crandall 2005 A finite element model of the lower limb for simulating pedestrian impacts, Stapp Car Crash Journal 49 157-181
- JR Funk, LJ Tourret, JR Crandall 2000 Estimation of fibula load-sharing during dynamic axial loading of the lower extremity, Proceedings of the 24th American Society of Biomechanics, Chicago IL
- JR Funk et al 2007 The line of action in the tibia during axial compression of the leg, Journal of Biomechanics 40 2277-2282
- D Krayterman 2015 Development and validation of the lower leg finite element model of the H-III anthropometric test device for vehicle underbody blast protection applications, ARL-TR-7359
- M Schlick, F Pintar 2015 Email correspondence
- WIAMan Project Biofidelity Response Corridors (BRC): Leg (90-90), John Hopkins Applied Physics Laboratory, Feb 28 2014

Effect of Boots on Leg Injury Mitigation in Underbody Blast Loading Events

Carolyn E Hampton, Ph.D

Michael Kleinberger, Ph.D.

U.S. Army Research Laboratory

13 JAN 2016

THE UNIVERSITY OF MELBOURNE

UNCLASSIFIED

Australian Government
Department of Defence
Defence Science and Technology Group

Second Workshop on Numerical Analysis of Human and Surrogate Response to Accelerative Loading
Aberdeen Proving Ground, MD, January 12-14, 2015

Development of a computational method to predict pelvic fractures for military vehicle underbelly blast events

Dale Robinson[1], Kwong Ming Tse[1], Peter Lee[1], Melanie Franklyn[2]

[1] Department of Mechanical Engineering, University of Melbourne

[2] Defence Science and Technology Group, Australian Department of Defence

University of Melbourne

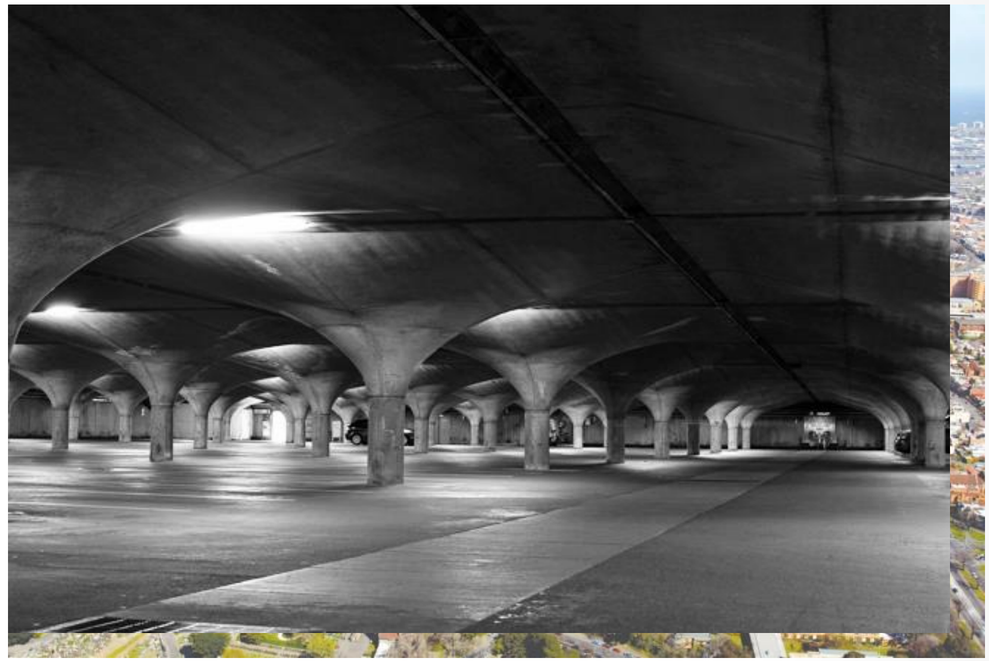

- Role in WIAMan project:

  Contribute to injury criteria for underbelly blasts for:

  - Pelvis
  - Lumbar spine

Agenda

- Background
- Aim
- Full-body musculoskeletal model
  - Introduction
  - Methods
  - Results
  - Discussion
- Pelvis finite element model
  - Methods
  - Results
  - Discussion

Background

- Military vehicle underbelly blast (UBB) impose high accelerations over short times:
  - Seat and floor pan accelerations[1]: 290-740 g, 230-860 g, respectively.
  - Floor pan velocities[2]: 30 ms^{-1} within 6-10 ms
- Fractures include: pubic rami, ischium, sacral ala, acetabulum, sacroiliac joints[3]
- Previous study on pelvic injuries at high loading rate:
  - Automotive ➔ injuries different to UBB[3]
  - Aviation ejection seat ➔ typically spinal injuries[4]
- Relationship between loading variables and pelvic fractures not well understood for UBB

[1] Bailey et al. (2015). *Ann Biomed Eng* 43(8):1907-1917
[2] Ramasamy et al. (2010). *J R Soc Interface* 8(58):689-698
[3] Tegtmeyer, M., (2012). *The WIAMan Development Program Objectives and Rationale*
[4] Salzar et al. (2009). *Aviat. Space Envir Med* 80(7):621-628

Aim

- To develop musculoskeletal models and finite element models to examine how pelvic fracture relates to different loading variables

- Loading variables include:
  - The contribution of muscle forces ➔ How to get these?
  - Variations in bone density (i.e., young male versus older cadaver)
  - Postural differences
  - Seat materials
  - Soft tissue of buttocks

Introduction - Full-body musculoskeletal model

- Aim: To predict muscle forces prior and during UBB

- Musculoskeletal software available:

Opensim[1] - Open-source software
- Static-optimization (muscle forces for static equilibrium)
- Forward dynamics (predict kinematics by forward integration)
- Model muscle excitation and activation dynamics
- No published combined spine and legs models

Anybody[2] - Licensed software
- Validated full-body model
- Performs static-optimization only

- Question: Are muscle forces constant during UBB? ➔ Need forward dynamics

[1] Delp et al. (1990). *IEEE Trans Biomed Eng 37(8):757-767*
[2] Damsgaard et al. (2006). *Simul Model Pract Th 14(8) 1100-1111*

Methods - Full-body musculoskeletal model

- Opensim full-body model ➔ visible human male[1]
- Segmented skin and skeleton:

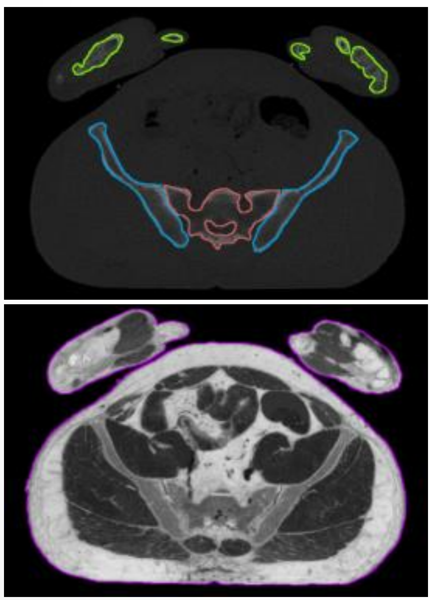

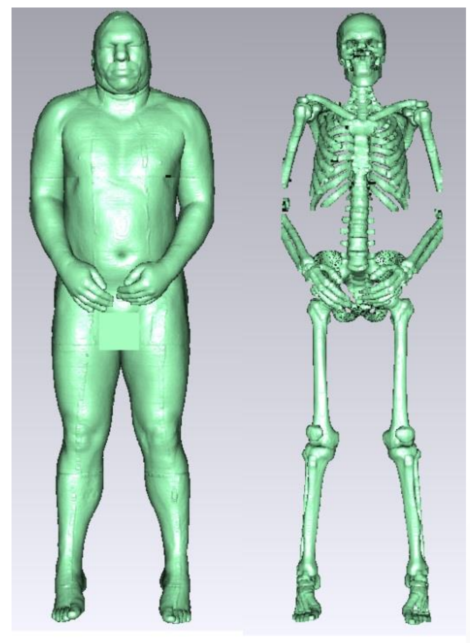

[1] Spitzer et al. (1996). *J Am Med Inform Assoc* 3(2):118-130

Methods - Full-body musculoskeletal model

- Model based on three validated models:

Lumbar model[1]

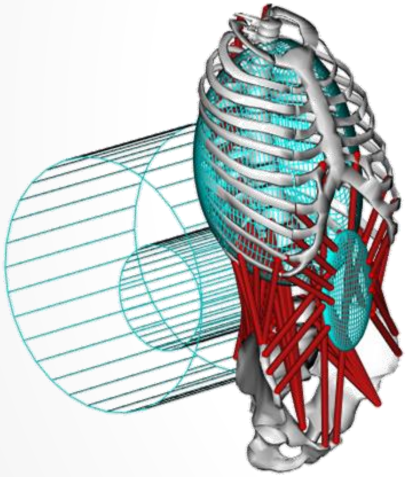

210 muscles
7 segments

Custom hip model[2]

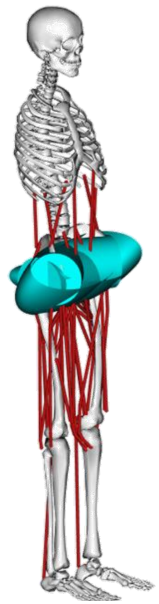

72 muscles
12 segments

Hamner full-body model[3]

Used arms segments
- 8 segments
- Joint actuators (i.e., no muscles)

[1] Christophy et al. (2012). *Biomech Model Mechanobiol* 11(1):19-34
[2] Shelburne et al. (2010). *Trans 60th ORS Meeting*
[3] Hamner et al. (2010). *J Biomech* 43(14):2709-2716

Methods - Full-body musculoskeletal model

- Each model scaled (anisotropic, linear) to visible human male
- Set to same posture and united

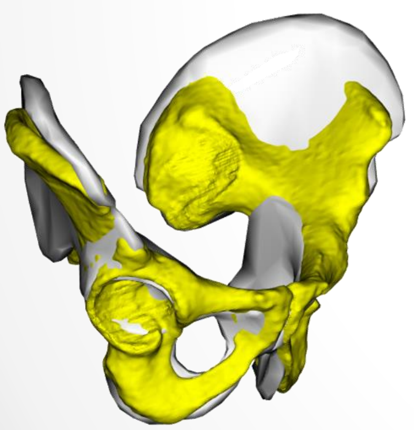

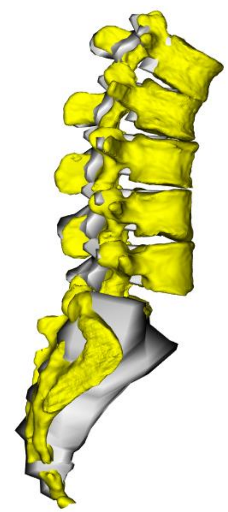

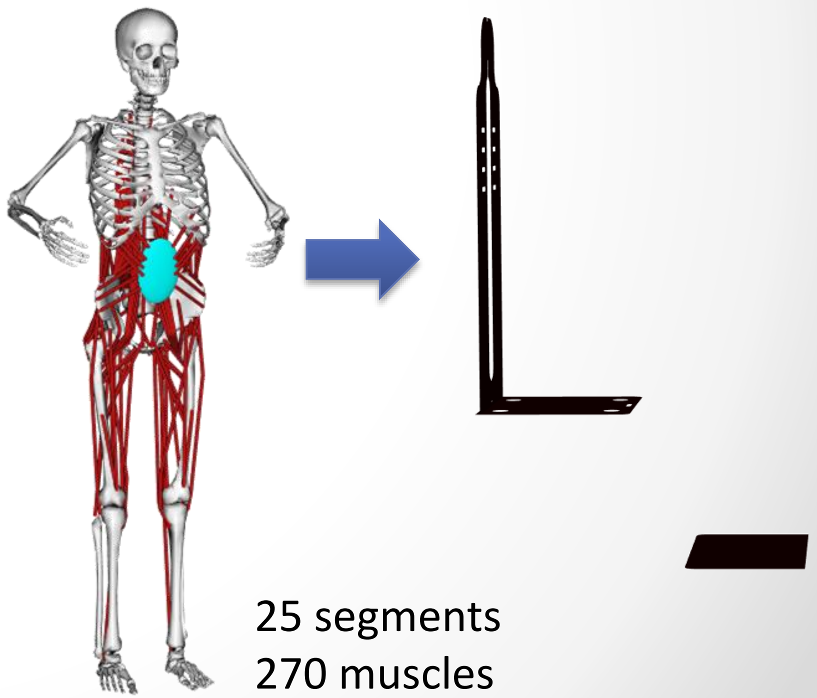

Methods - Full-body musculoskeletal model

- Posture set to WIAMan anthropometry target[1] (i.e., 40^{o} pelvic tilt, 9^{o} S5 angle etc.)

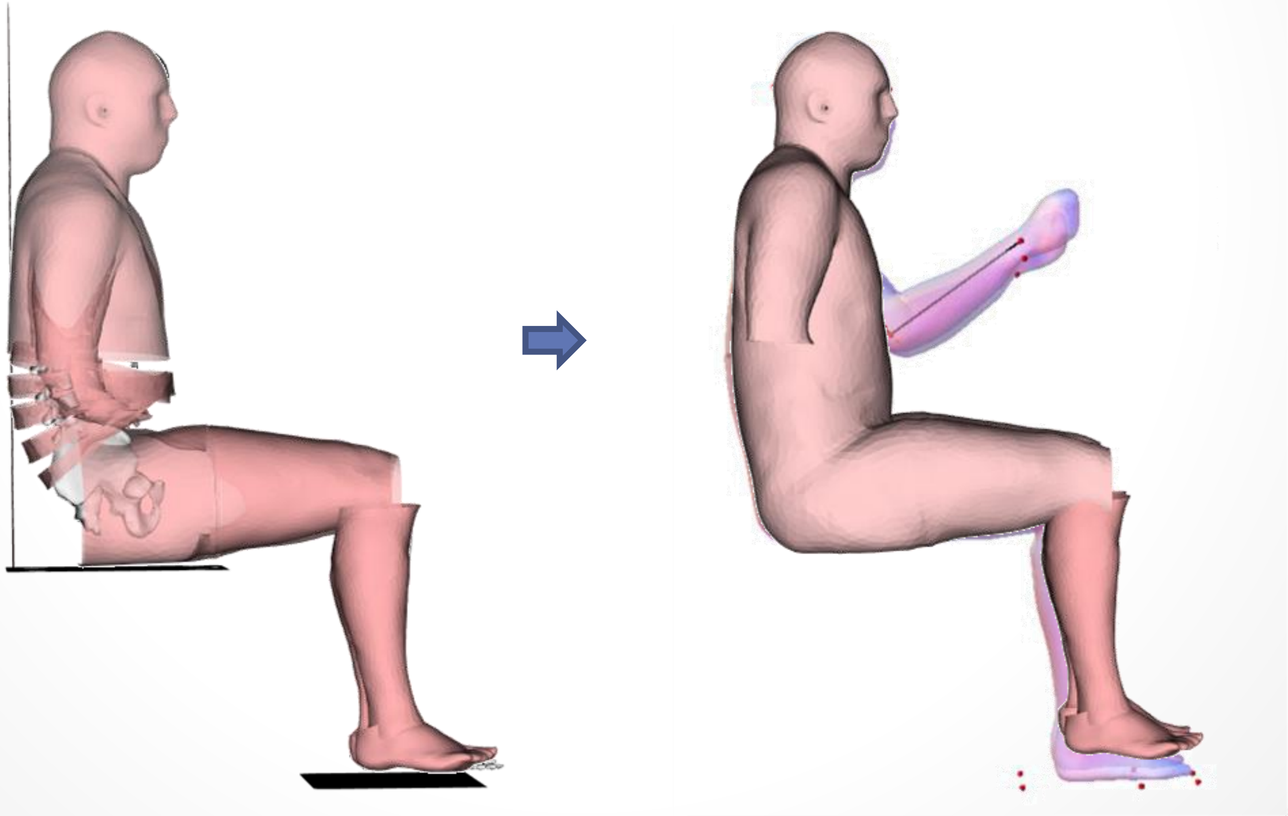

[1] Reed, MP (2013). *Dev. of Anthro. Specs. for WIAMAN, Final Report*

Methods - Full-body musculoskeletal model

Interactions: Contact model

- Hertzian contact:
  - Spheres for soft tissue[1] (E=20 MPa, ν=0.46)
  - Flat plates for VALTS seat (E=70 GPa, ν=0.33)
- Initial penetration set to satisfy static equilibrium in sagittal plane
- To solve indeterminacy assumed:
  - Coefficient of friction for the torso of 0.1[2]
  - The feet supported 30% of the total body mass[3]
  - Equal frictional forces at seat and feet

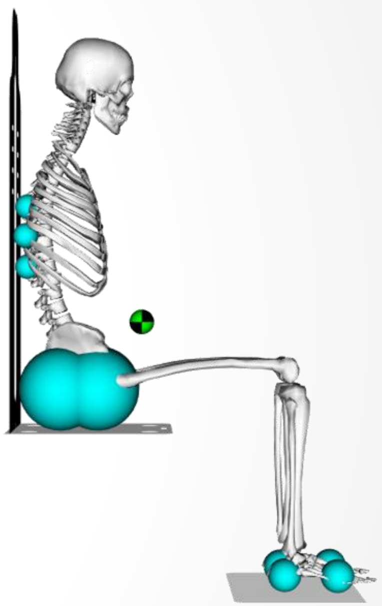

[1] Grujicic et al. (2009). *Mater Des* 30(10):4273-4285
[2] Bush and Hubbard (2010). *J Biomech Eng* 129(1):58-65
[3] Nag et al. (2008). *Int J Ind Ergonom* 38(5):539-545

Methods - Full-body musculoskeletal model

- Analysis: Relaxed sitting
  - Static optimization to determine muscle forces and activations
  - Objective function: $$J = \sum_{m=1}^{nm} (a_m)^2$$
- Analysis: Blast simulation
  - Assume initially steady-state (muscle excitations = muscle activations)
  - Then accelerate vertically according to VALTS data for 50 ms
  - Excitations assumed constant

Question: Are muscle excitations constant over this interval?

- Force disturbance shoulder, elbow and wrist, reflex delay[1]: 29-39 ms
- Sternocleidomastoid reflex delay[2] : 36-61 ms
- Feline paraspinal muscle delay[3]: 2.5-2.8 ms

[1] de Vlugt et al. (2006). *J Neruosci Methods* 155(2):328-349
[2] Stemper et al. (2005). *Spine* 30(24):2794-2798
[3] Stubbs et al. (1998). *J Electromyogr Kinesiol* 8(4):197-204

Results - Full-body musculoskeletal model

- Relaxed sitting

Group	Muscle	F_o^M (N)	Act.	Force (N)
Iliocostalis lumborum	IL_R11	45.7	0.60	27.4
Iliocostalis lumborum	IL_R10	38.6	0.51	19.7
Iliocostalis lumborum	IL_R12	46.3	0.51	23.6
Internal abd oblique	IO3	92.9	0.49	45.5
Longissimus thoracis	LTpT_T9	32.2	0.37	11.9
Multifidus	MF_m2t_3	38.9	0.36	14.0
Multifidus	MF_m2t_2	34.7	0.34	11.8
Longissimus thoracis	LTpT_T10	27.5	0.32	8.8
Longissimus thoracis	LTpt_R11	27.7	0.31	8.6
Longissimus thoracis	LTpT_R10	26.8	0.31	8.3

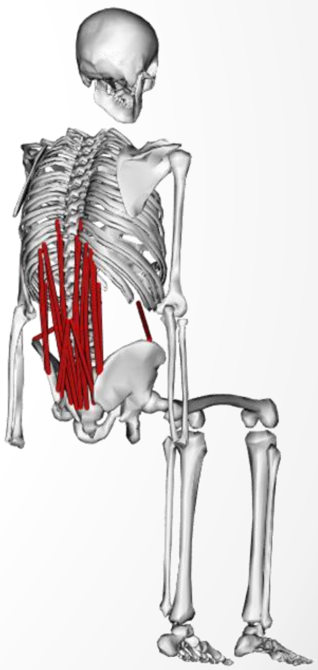

Results - Full-body musculoskeletal model

- Blast simulation

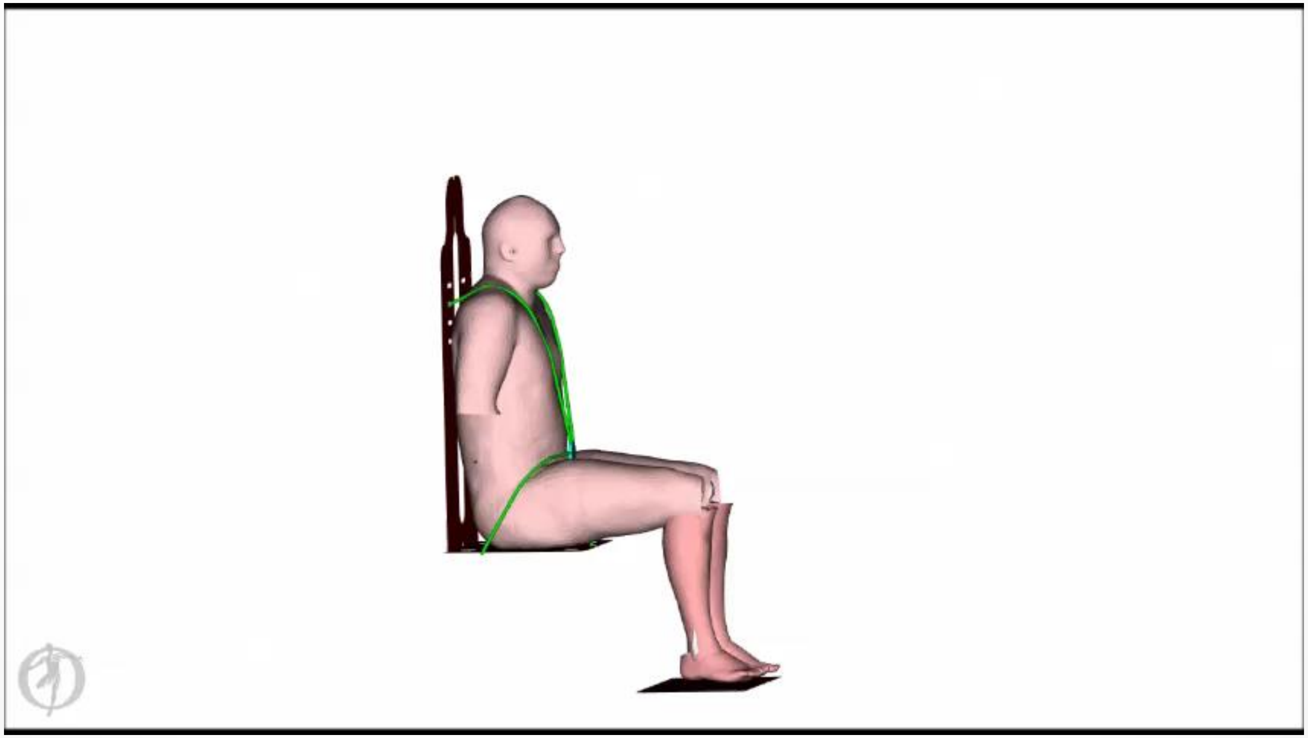

Results - Full-body musculoskeletal model

- Blast simulation

Forces of 10 muscles with highest initial activation

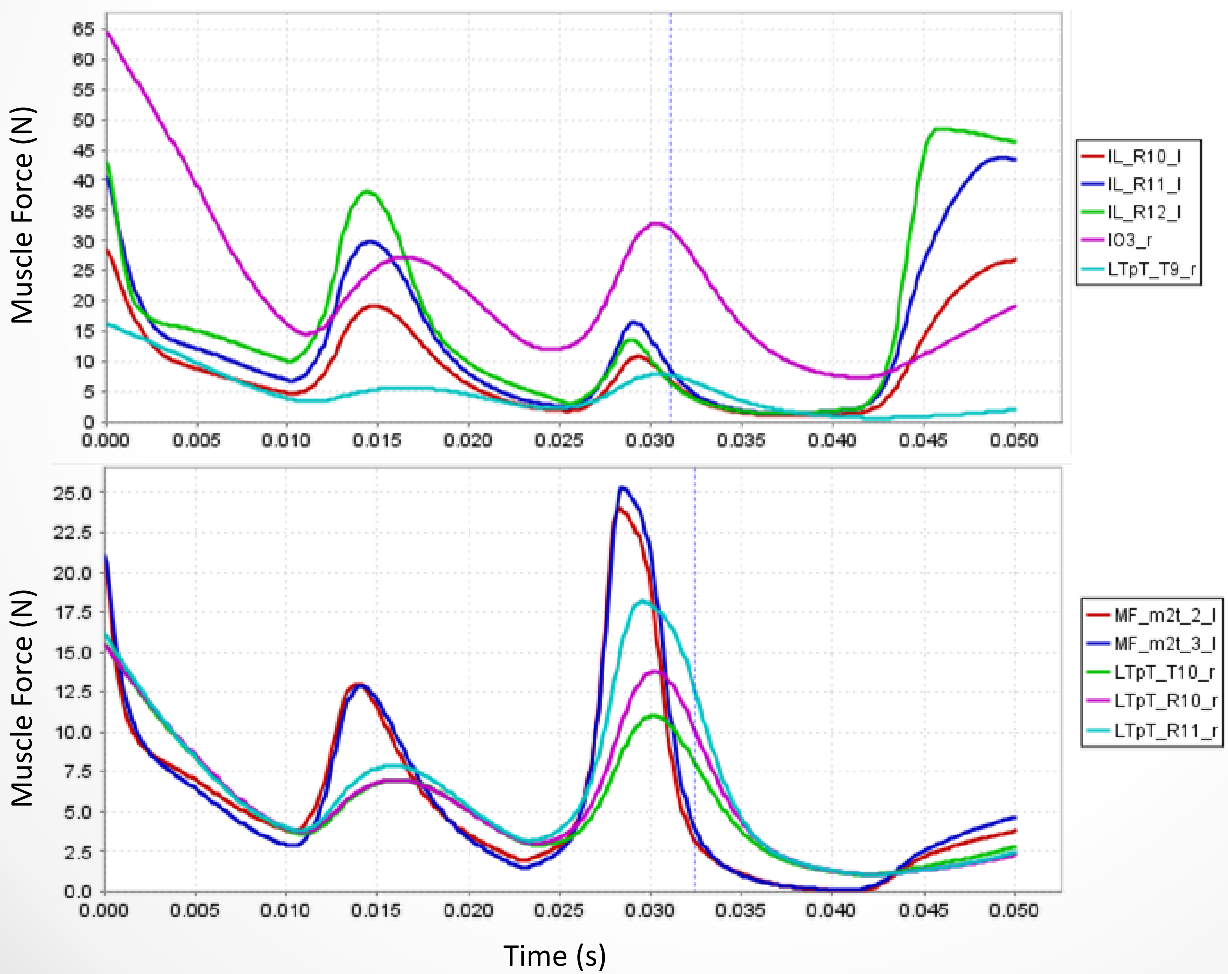

Discussion - Full-body musculoskeletal model

- Relaxed sitting
  - Model appears to over-estimate spine extensor muscle force
  - Do not have ligaments, intervertebral discs, intra-abdominal pressure
  - **Future work:** Use Anybody for relaxed sitting problem

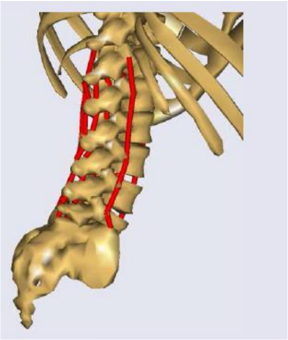

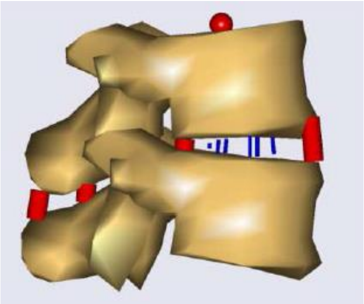

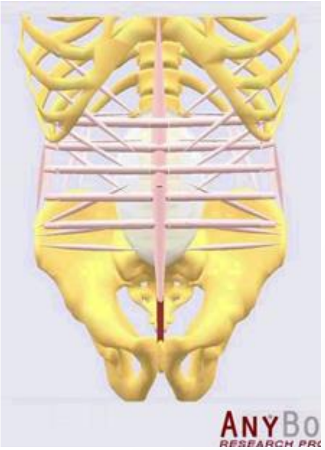

Discussion - Full-body musculoskeletal model

- Blast simulation
  - Passive muscle forces change
  - Most changes are below the initial value

  ➔ Conservatively assume constant muscle force during UBB

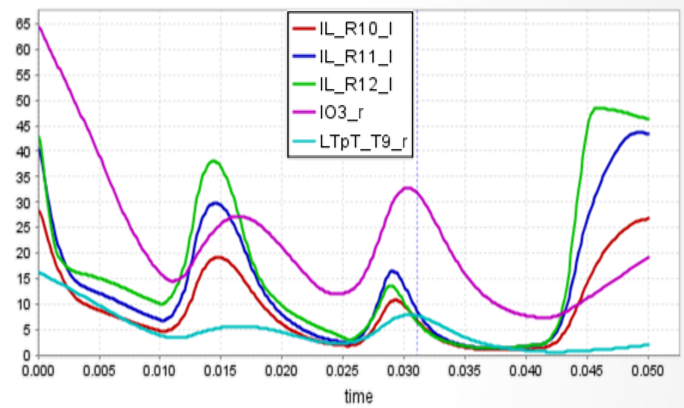

Methods - Pelvis finite element model (FEM)

- FEM of visible human male pelvis created in Abaqus

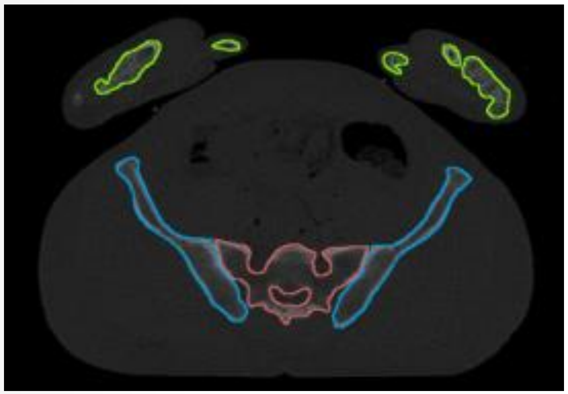

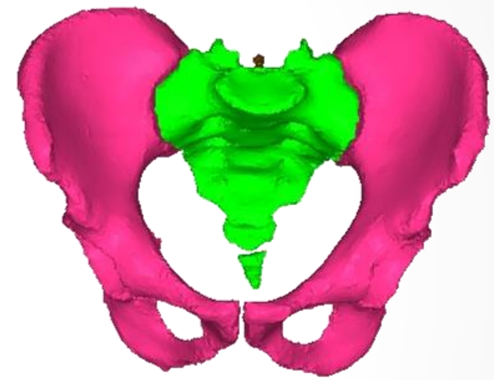

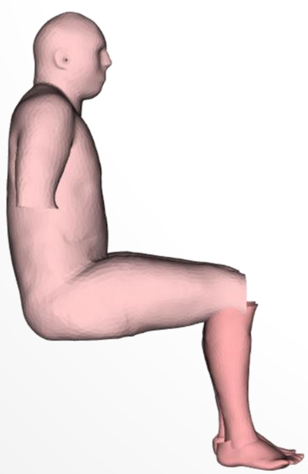

Skin layer added for sitting

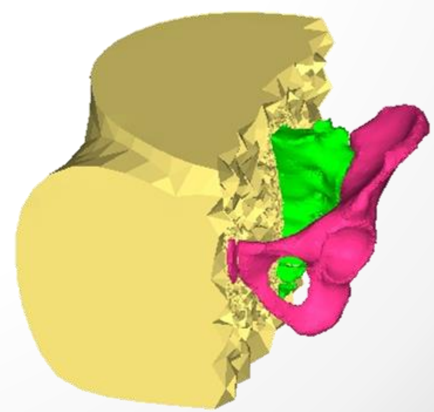

Methods - Pelvis FEM

Material properties

- 1-1.2 mm cortical bone thickness[1]
- Cortical bone[2]: E=16.7 GPa, ν = 0.3
- Trabecular bone[3]: E=1 GPa, ν = 0.2
- **Future work:** Use MAP client[4] to apply *in vivo* bone properties for normal and older males

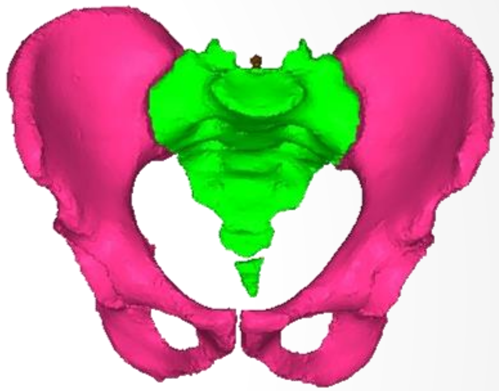

Interactions

- Sacroiliac joint rigidly tied
- Pubic symphysis rigidly tied
- Buttocks tissue rigidly connected to bone via conforming mesh

[1] Dalstra et al. (1995). *J Biomech Eng* 117(3): 272-278
[2] Majunder et al. (2008). *Int J Crashworthiness* 13(3): 313-329
[3] Fernandez et al. (2014). *Int J Numer Method Biomed Eng* 30(1): 28-41
[4] Zhang et al. (2014). *Comput Methods Biomech Biomed Eng Imaging Vis* 2(3): 176-185

Methods - Pelvis FEM

Loads and boundary conditions

➔ Pelvic tilt tests performed at UVA

- Pelvic tilt of 40^o
- Potted to S2 using tie
- Ischial tuberosity pressed against flat plate
- Abdominal mass of 2.7 kg tied to L & R hemipelvis
- 12 kg mass added to potting fixture
- Enforced velocity applied to seat plate

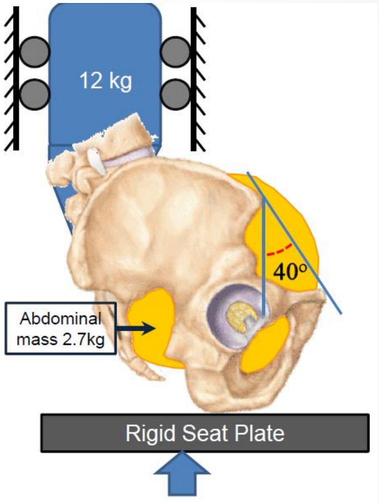

Simulations

- Defleshed at V1 (2 m/s)

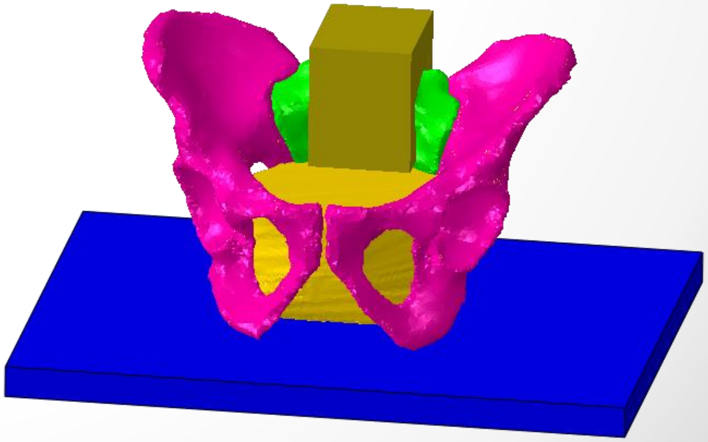

Results - Pelvis FEM

Force

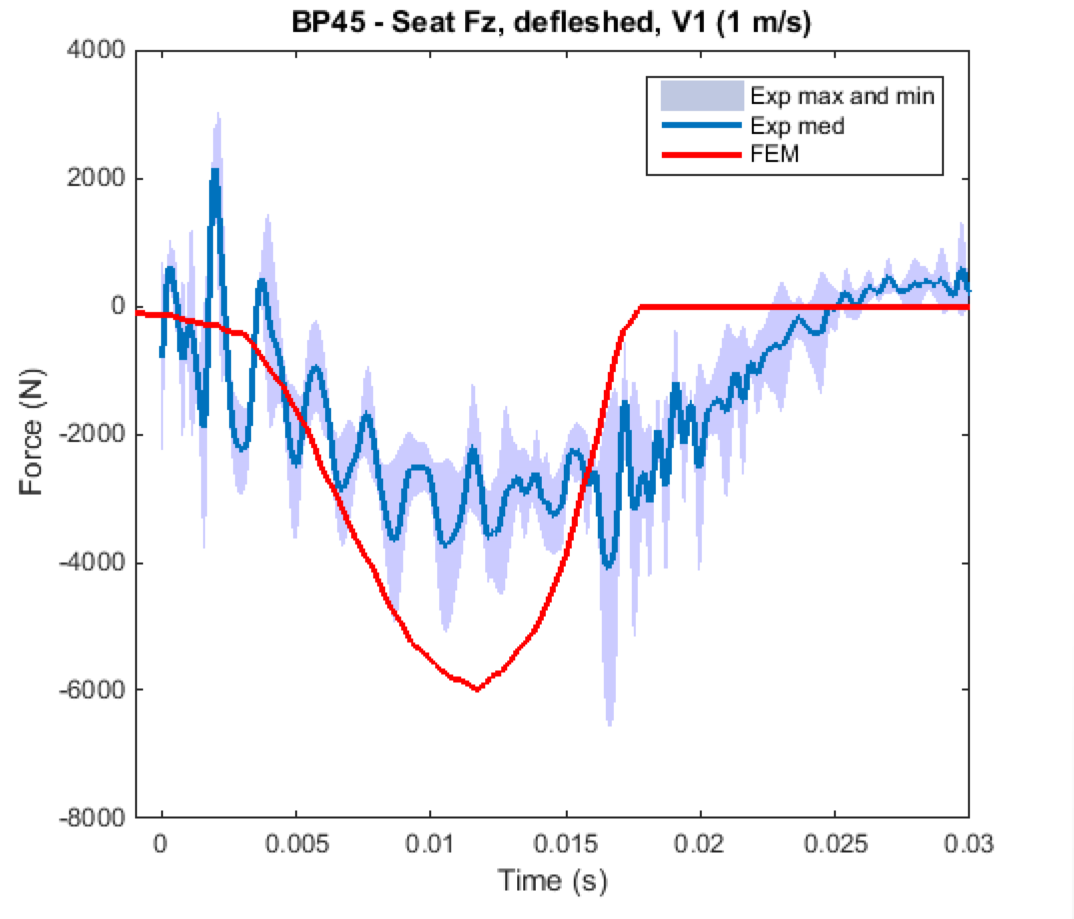

Results - Pelvis FEM

Compression

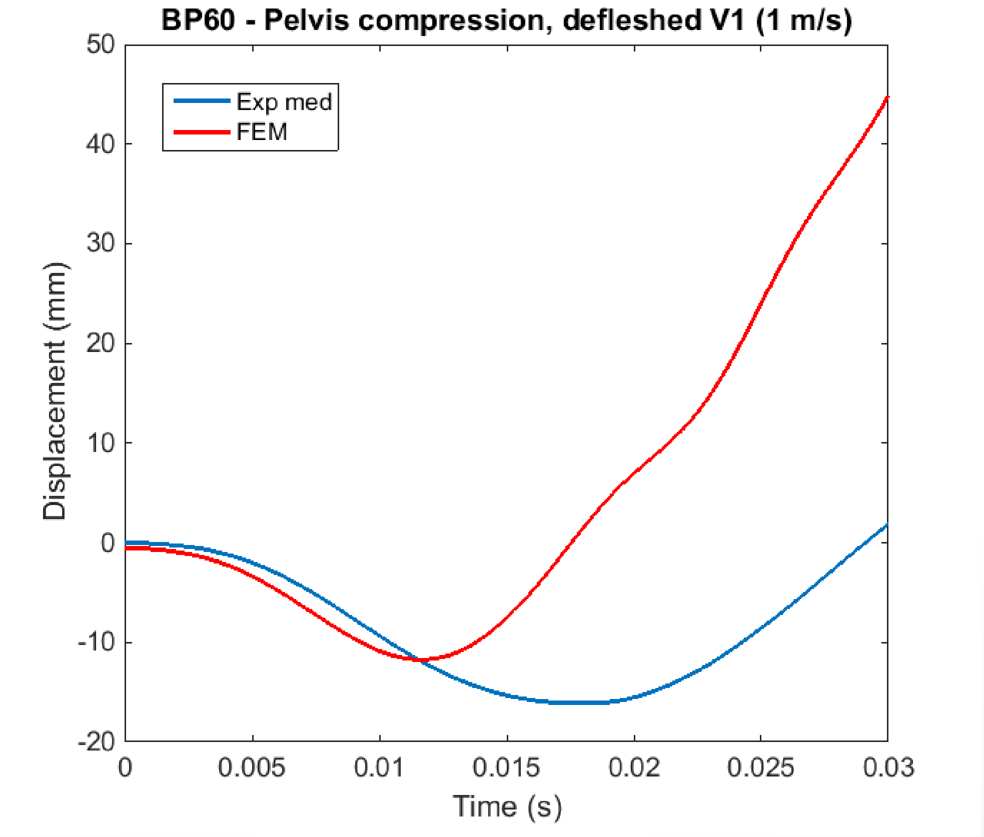

Results - Pelvis FEM

Principal stresses

Yield limits[1]: σ_{tens} = 83.9 MPa σ_{comp} = -153.0 MPa

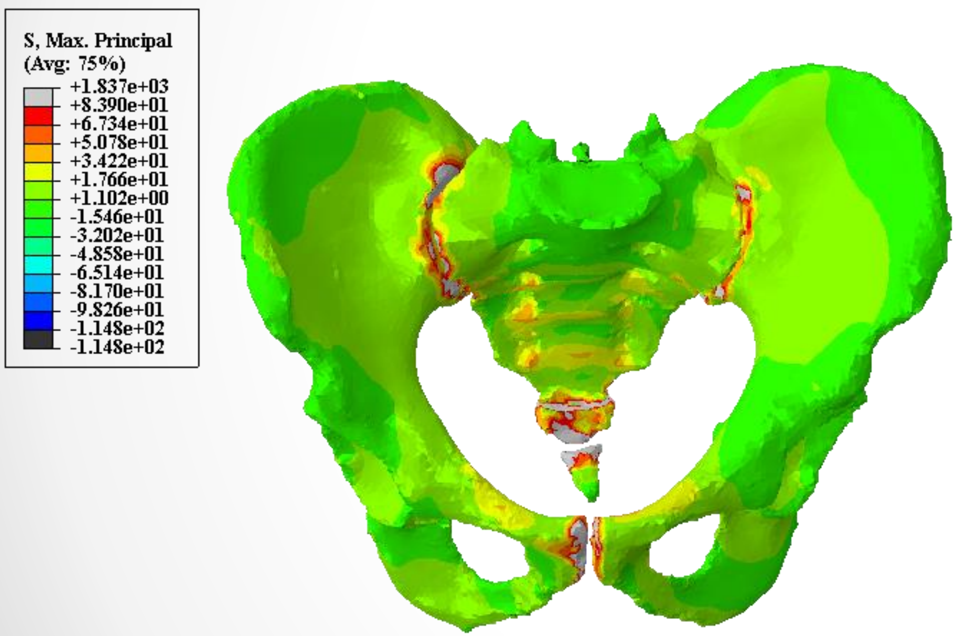

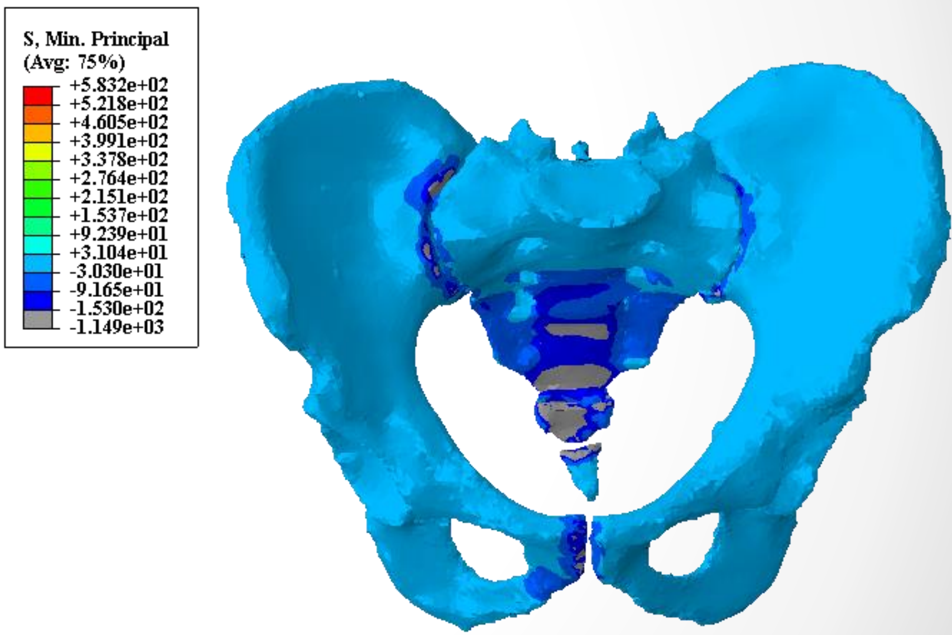

[1] Kaneko et al. (2003). *Med Eng Phys* 25(6): 445-454

Results - Pelvis FEM

Principal strains

Yield limits[1]: $\varepsilon_{tens,yield}$ = 0.57% $\varepsilon_{comp,yield}$ = -0.86%

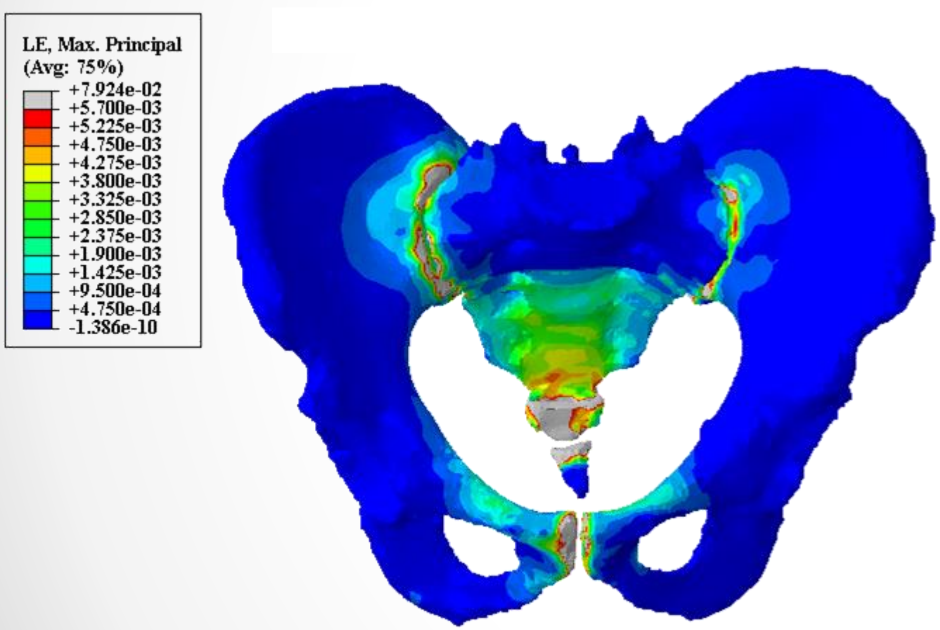

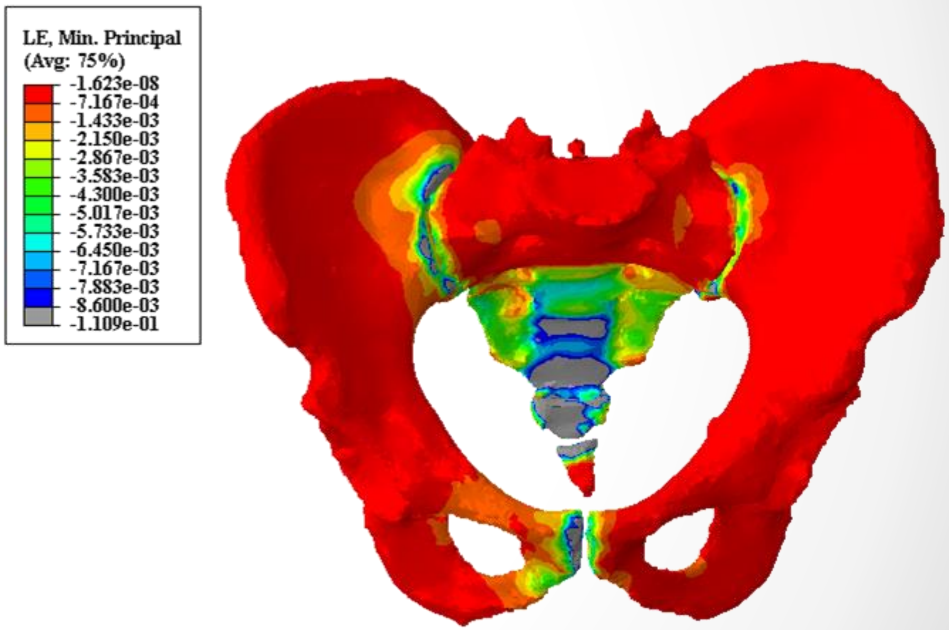

[1] Kaneko et al. (2003). *Med Eng Phys* 25(6): 445-454

Discussion - Pelvis FEM

- Model is too stiff!
- Fracture predicted at sacrum, coccyx and SI joint
  - ➔ Qualitatively consistent with experiment
  - ➔ Due to large flexion moment at SI joint

Future work:

- Validate strain predictions
- Softening the model: mapped bone properties, contact model, compliance at SI joint, quadratic elements
- Add ligaments
- Add muscle forces
- Sensitivity analysis (posture, abdominal mass, bone density, seat stiffness)

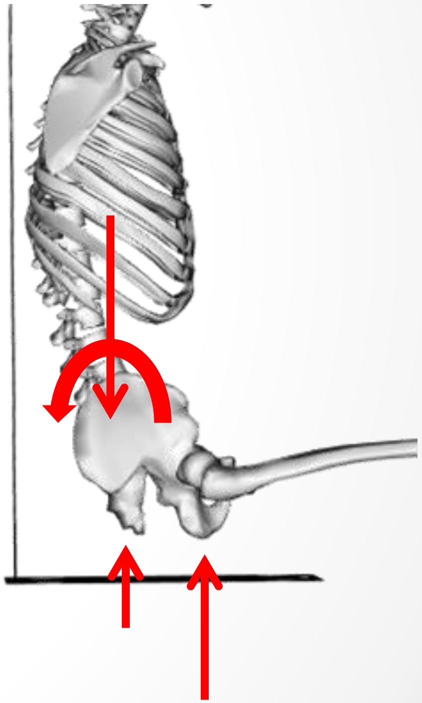

In vivo reduced by a number of factors

Questions?

Pelvic Response of a Total Human Body Finite Element Model During Simulated Under Body Blast Impacts Using Cross-Sectional Force as a Metric

Caitlin M. Weaver and Joel D. Stitzel

2016 Workshop on Numerical Analysis of Human and Surrogate Response to Accelerative Loading
Army Research Lab
Aberdeen Proving Ground, MD

13 January 2016

Center for Injury Biomechanics

Wake Forest School of Medicine

CIB

Virginia Tech Wake Forest University
School of Biomedical Engineering and Sciences

Problem of Interest

Challenge: Injury prediction for UBB events

Limited UBB test studies

Lack of UBB injury response data

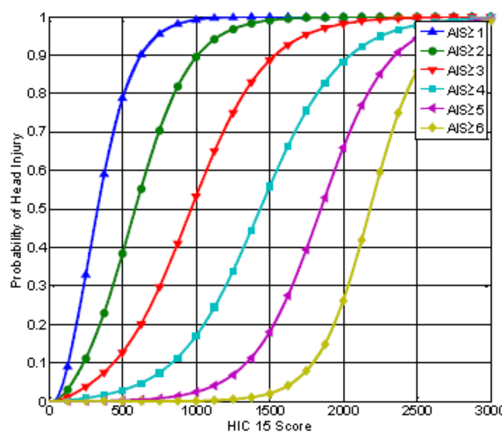

Hybrid III currently not designed for extreme vertical loading conditions

Problem of Interest

Challenge: Injury prediction for UBB events

To date, no standardized LFT&E prediction method for UBB injury prediction

Impact of Problem

Injury Mechanism From Previous US Wars

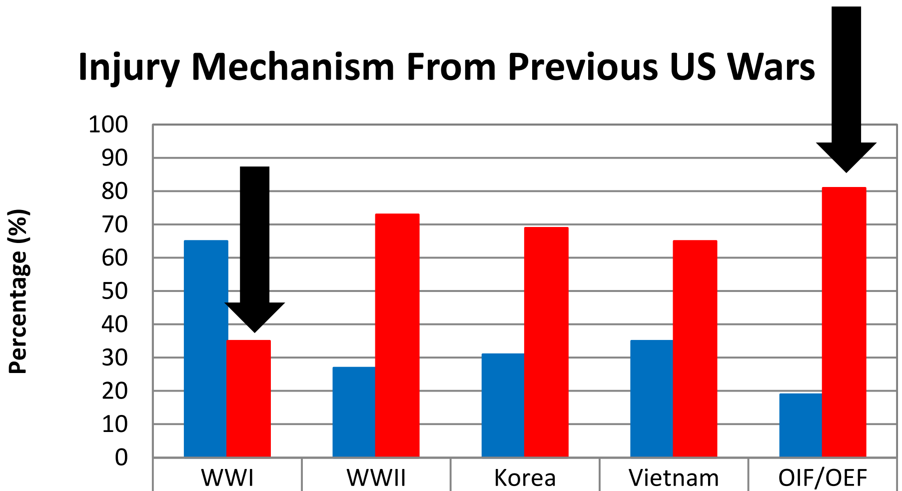

	WWI	WWII	Korea	Vietnam	OIF/OEF
GSW	65	27	31	35	19
Explosion	35	73	69	65	81

Mechanism of Injury (Explosive)

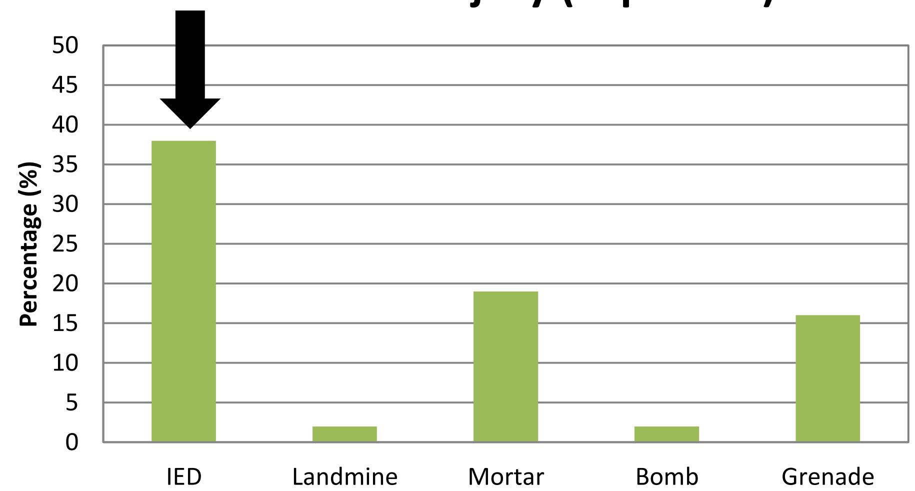

Owens, B. D., Kragh Jr, J. F., Wenke, J. F., Macaitis, J., Wade, C. E., and Holcomb, J.B. Combat Wounds in Operation Iraqi Freedom and Operation Enduring Freedom. *The Journal of Trauma Injury, Infection, and Critical Care*, 2008, 64(2):295-299.

Impact of Problem

Pelvic injuries are often debilitating, resulting in increased healthcare expenses and a reduced quality of life

- Largest total median in-hospital charge cost
- Higher rate of indirect costs:
  - Inability/delay return to work and pre-injury activities
  - Mood disorders - depression

Impact of Problem

Partially/unstable pelvic fractures

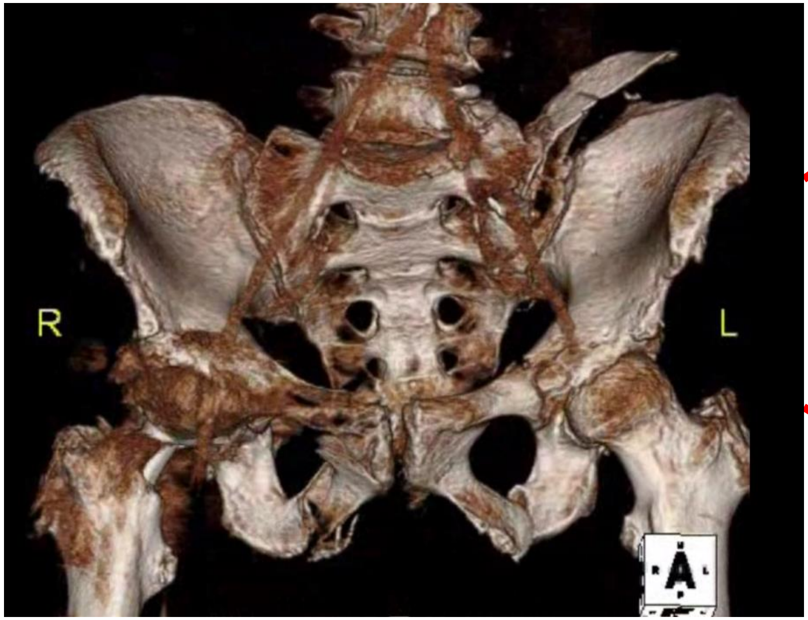

CIREN, WFU

Quick/safe vehicle evacuation

Combat Casualty Care (CCC)

US Army Warrior Injury Assessment Manikin (WIAMan) Project

Purpose: To create an enhanced capability to assess risk to soldiers in the UBB environment for use in LFT&E and protection technology development

Creation of a soldier-representative, biomechanically-validated ATD

Wake Forest School of Medicine · UMTRI · Medical College of Wisconsin · Duke University · Wayne State · The Ohio State University · University of Virginia · APL The Johns Hopkins University Applied Physics Laboratory

Project Overview

- Focus: Pelvic response to high impact loading scenarios in a FE environment.
  - Model: Global Human Body Models Consortium (GHBMC) 50th percentile seated FE human body model (v4.3)
  - Input data: Experimental testing performed by:
    - Bouquet et al. (lateral)
    - Biomechanics Product Team (BIO PT) for WIAMan (UBB/vertical)

ARL

SMART
SCIENCE, MATHEMATICS & RESEARCH FOR TRANSFORMATION
PART OF THE NATIONAL DEFENSE EDUCATION PROGRAM

Wake Forest School of Medicine | UMTRI | Medical College of Wisconsin | Duke University | Wayne State | The Ohio State University | University of Virginia | APL The Johns Hopkins University Applied Physics Laboratory

M50 Detailed Occupant Model (v4.3)
Mass – 76.8 kg
Parts – 978
Elements – 2.2 Million
Nodes – 1.3 Million

Project Overview

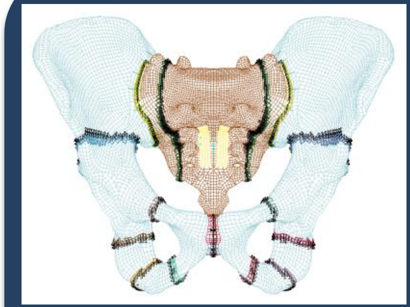

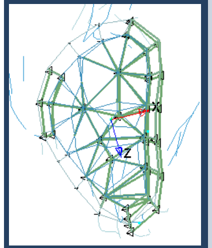

Specific Aim 1: Develop virtual load cell instrumentation to analyze pelvic injury response

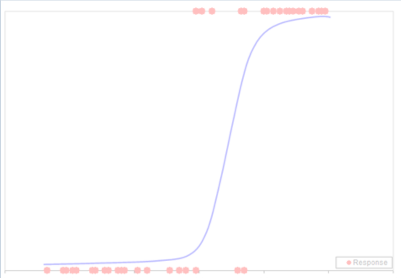

Specific Aim 2: Validate tissue level metrics in FE pelvis using whole body and isolated pelvis tests to develop injury metrics and risk curves

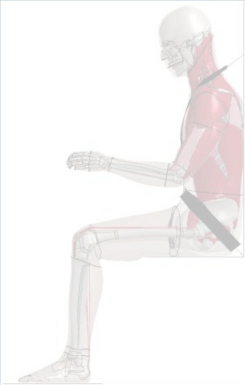

Specific Aim 3: Investigate injury risk of UBB events based on vehicle environment and occupant position

Pre-Programmed ATD Location Outputs

Head:
- CG

Neck:
- C0/C1 Nij

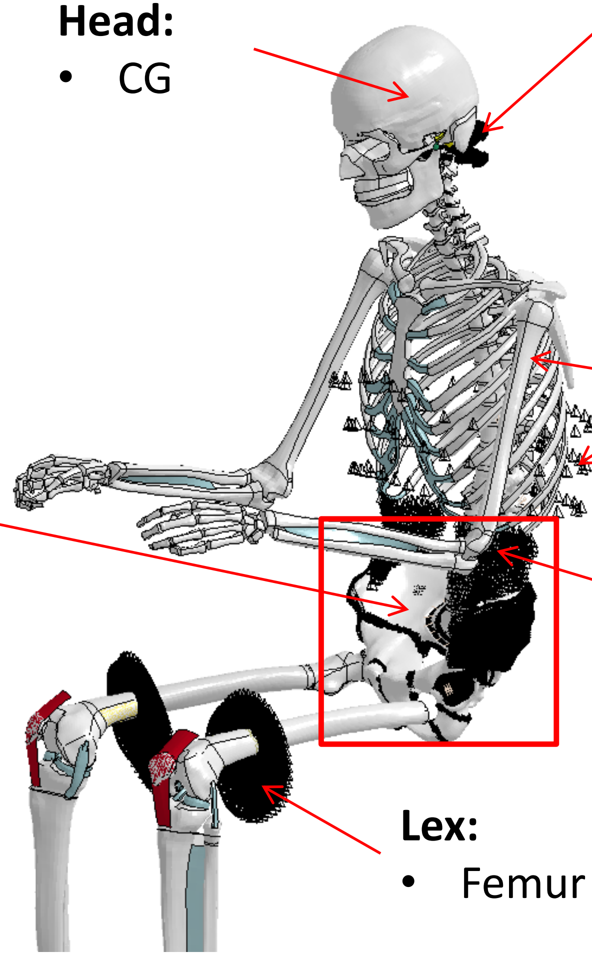

Thorax:
- Thorax accelerometer
- Chest band (U/M/L)

Pelvis:
- CG
- Pubic Sym. force
- Iliac force
- Acetabulum force

Abdomen:
- Lateral load cell

Lex:
- Femur force

User Programmed Pelvis Instrumentation

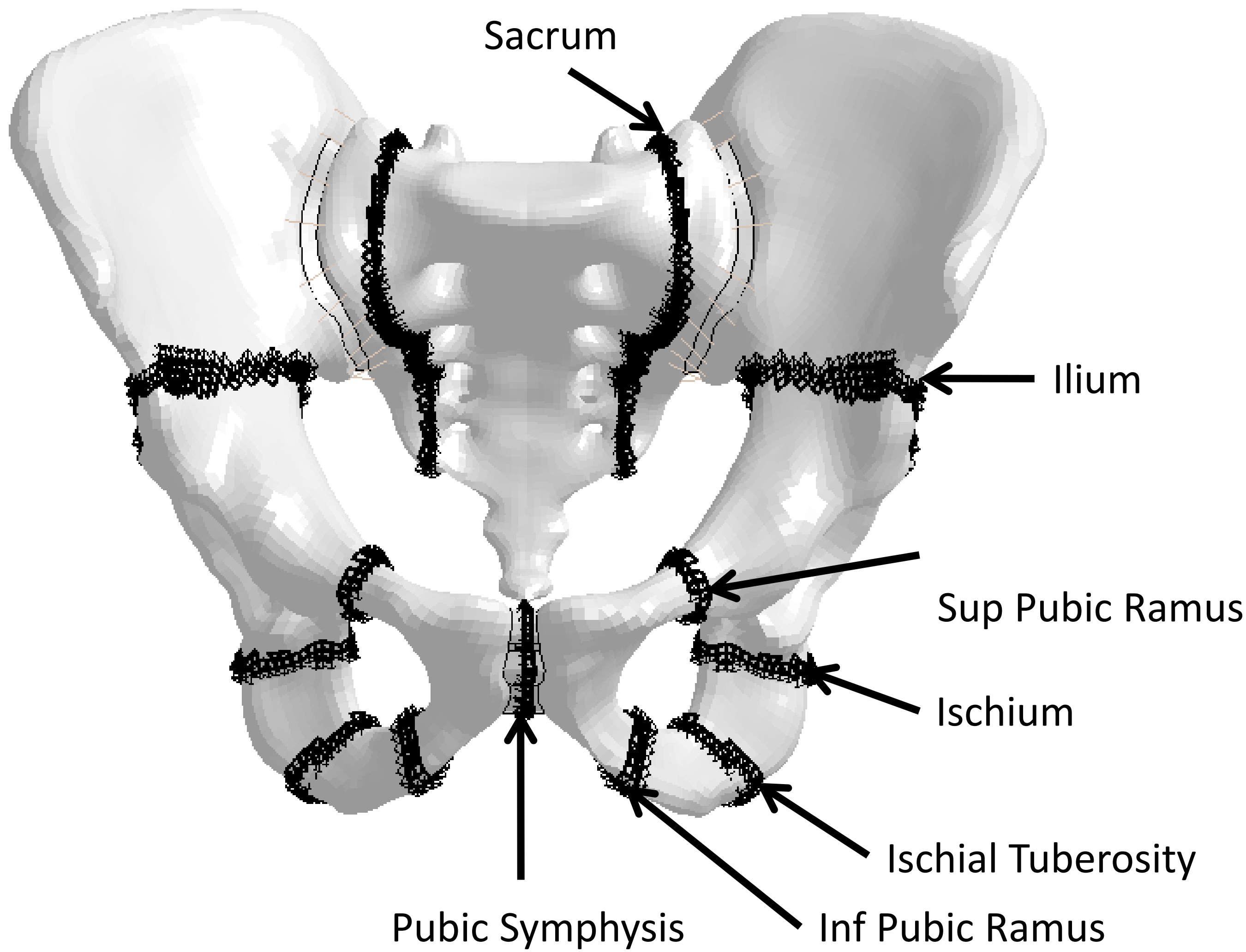

Cross-Section Creation

- LS-DYNA Keyword Input
  - *DATABASE_CROSS_SECTION_SET
    - Uses a node set to define the cross-section
    - Uses element set(s) for force by summing all the forces of the elements in the specified sets

Cross-Section Creation

- GHBMC M50-O (detailed) pelvis bones are specified as two parts to represent the cortical and cancellous portions of the bone
  - Layers are not symmetric
  - Composed of different element types

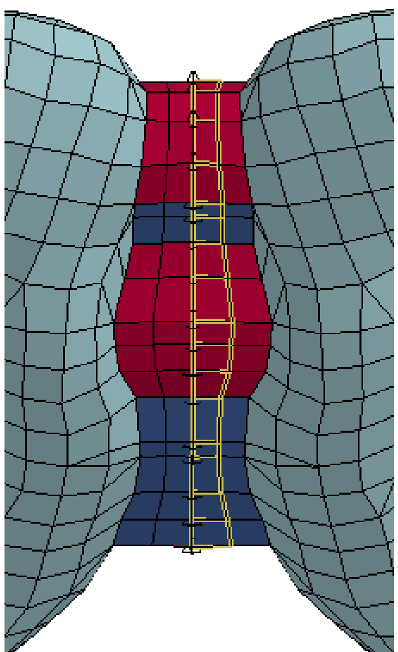

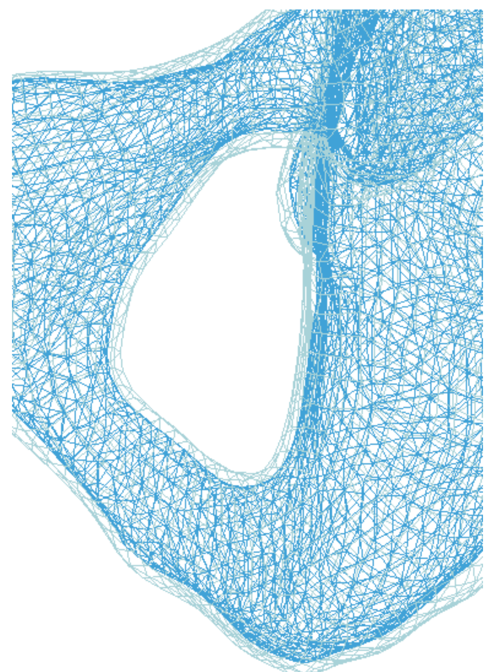

Cross-Section Plane

- LS-DYNA Keyword Input
  - *DATABASE_CROSS_SECTION_PLANE
- Method
  - Create a plane in area of interest
  - Run simulation for a single time step
  - Obtain node and element sets for cross-section from cross-sectional interfaces in D3HSP file

Cross-Section Creation

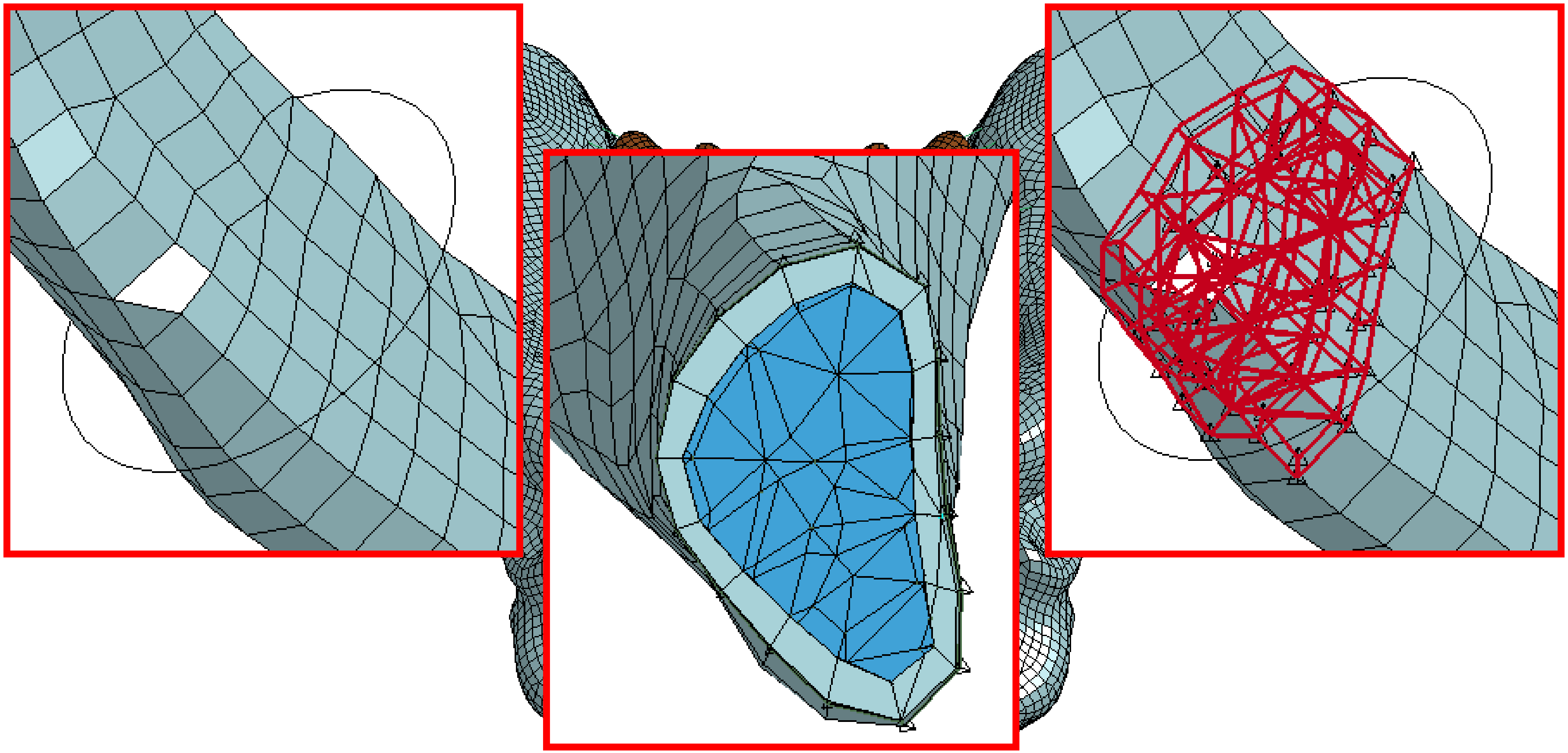

Cross-Section Creation

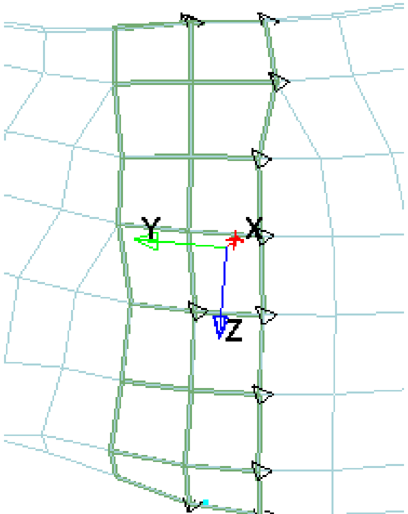

- Local Coordinate System Creation
  - DYNA Keyword input: *DEFINED_COORDINATE_NODES
  - Node 1: Cross-Section Centroid (X,Y,Z)
  - Node 2: Anterior to face
  - Node 3: Inferior to face
- Constrained Interpolation used to attach coordinate nodes to model

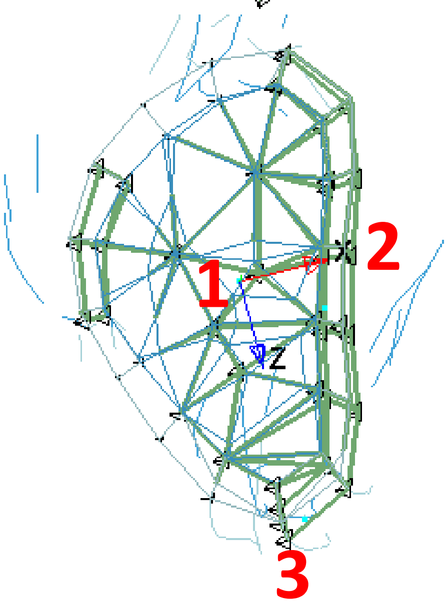

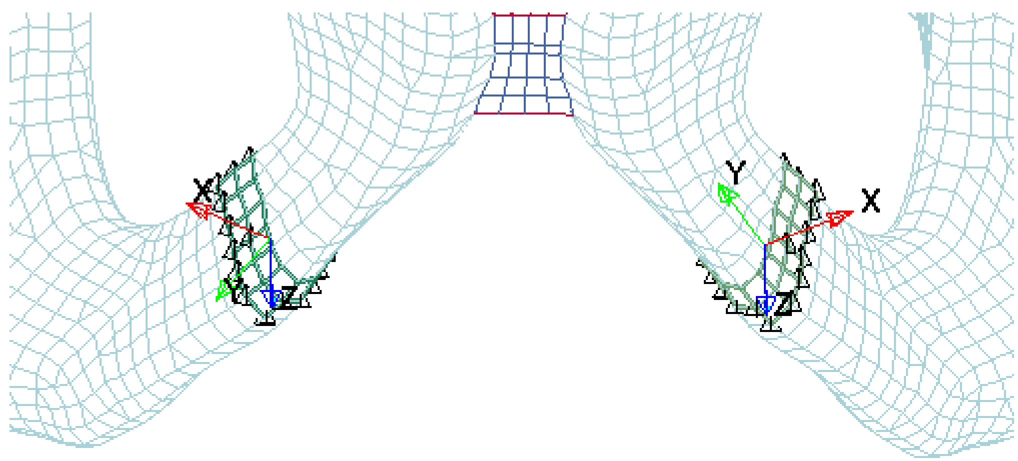

Project Overview

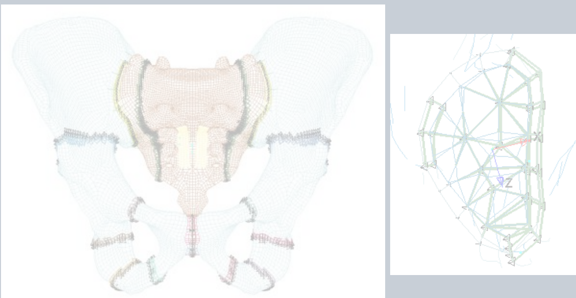

Specific Aim 1: Develop virtual load cell instrumentation to analyze pelvic injury response

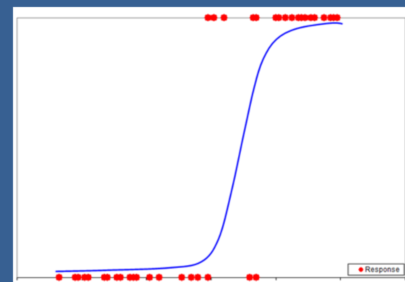

Specific Aim 2: Validate tissue level metrics in FE pelvis using whole body and isolated pelvis tests to develop injury metrics and risk curves

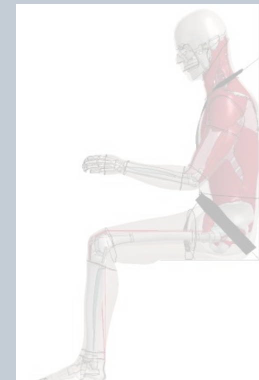

Specific Aim 3: Investigate injury risk of UBB events based on vehicle environment and occupant position

Bouquet et al.

Lateral Load Testing:
- 25 simulations
  - 9 non-injurious
  - 18 injurious

Performed using an initial velocity recorded in experimental testing

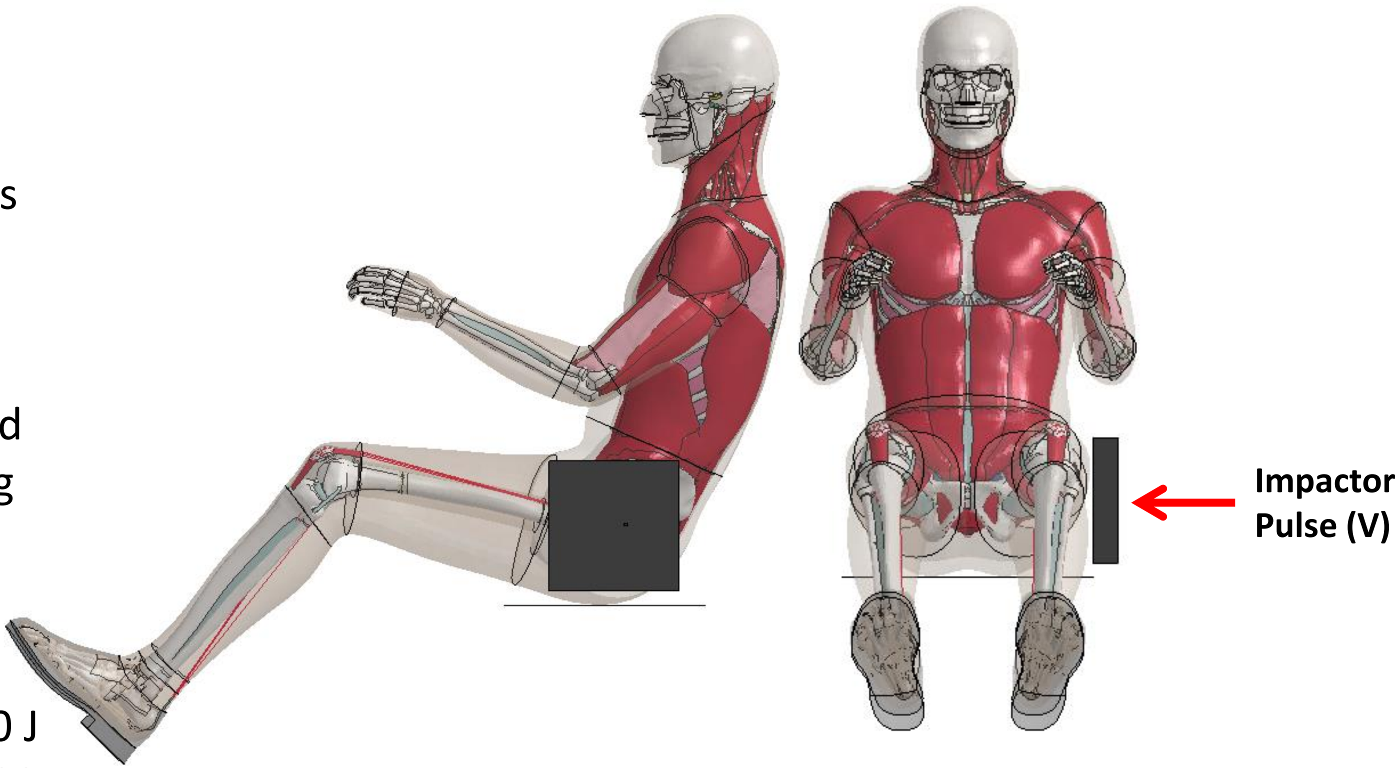

Energy levels:
- Non-Injurious – 130 J
- Injurious – 500 J, 600 J, 800 J, 1100 J

Impactor Type:
- 200x200mm, 12 kg
- 200x200mm, 16 kg
- 100x200mm, 23.4 kg

Bouquet et al.

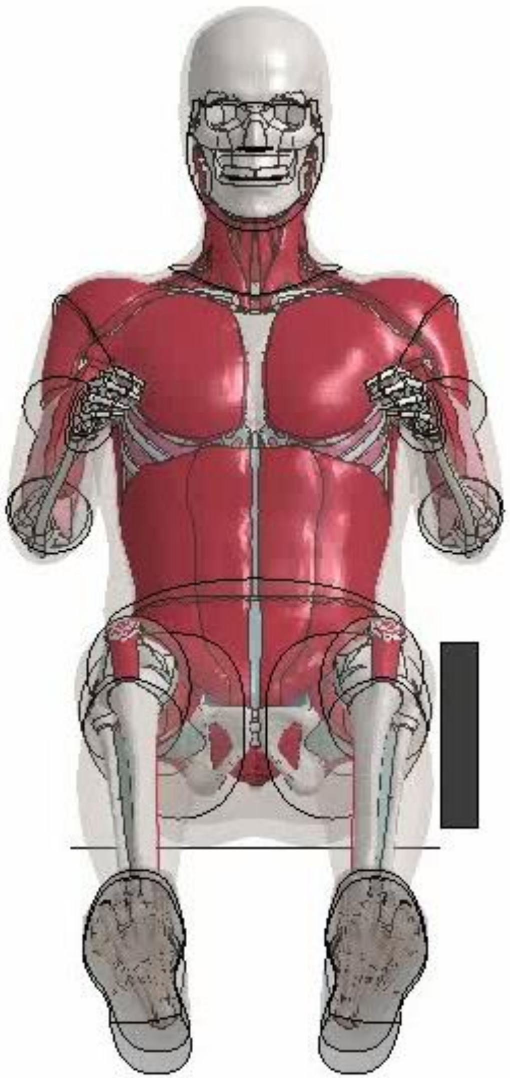

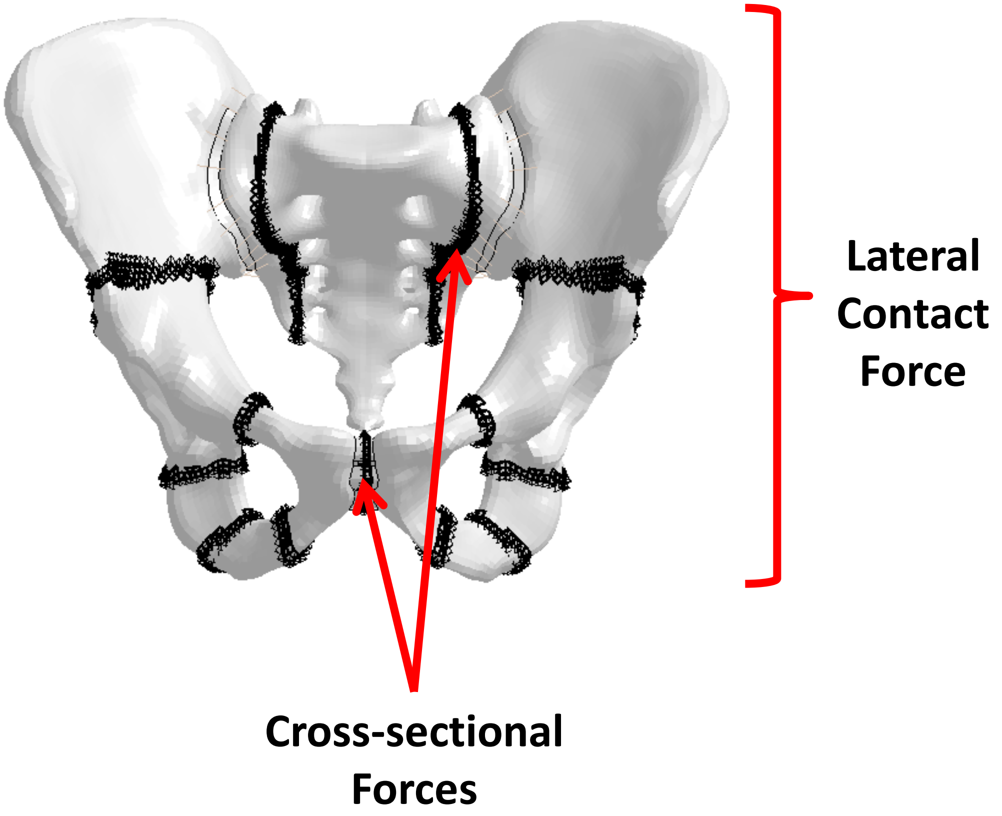

Injury Prediction

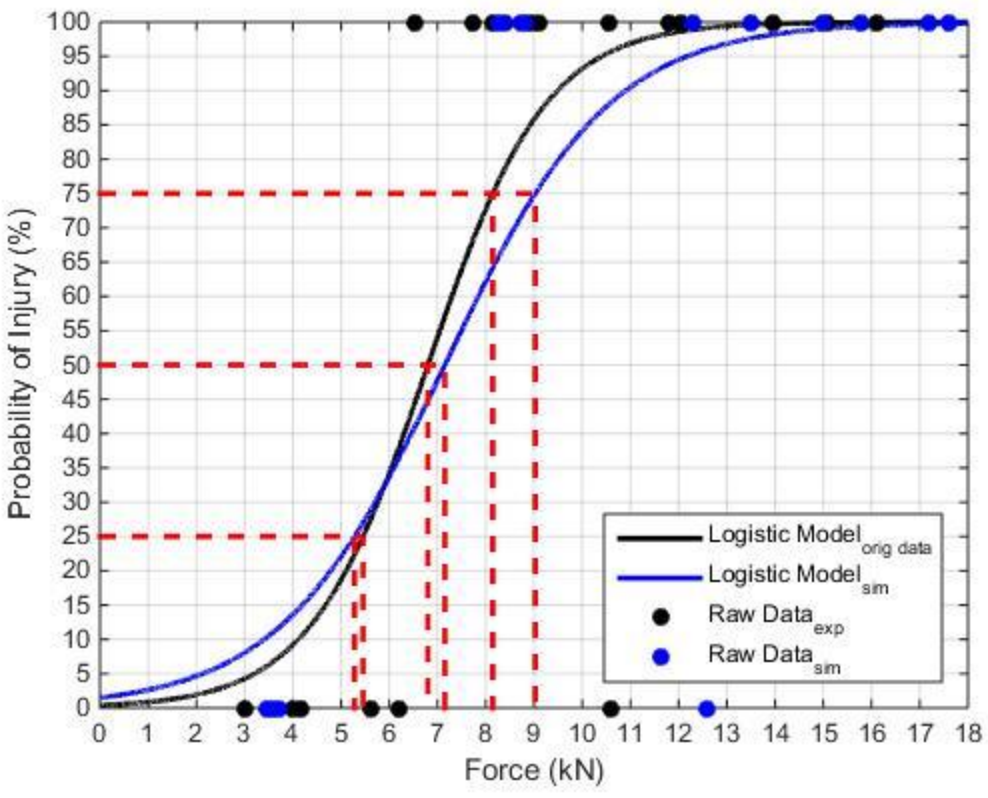

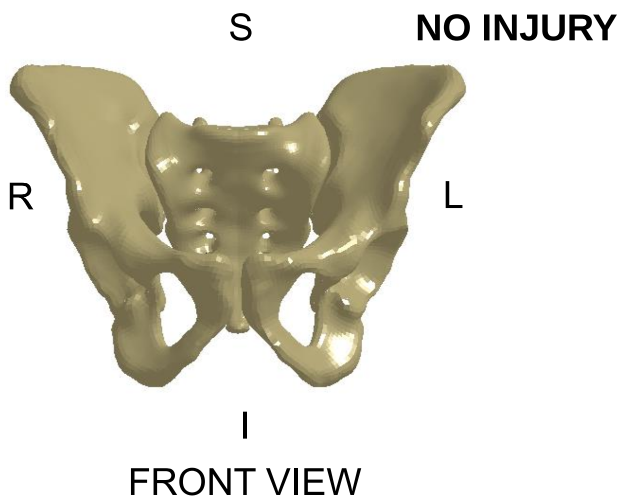

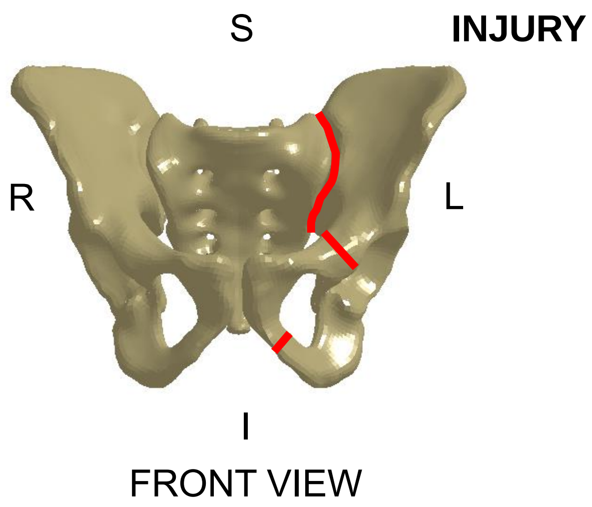

- Injury analysis: Logistic regression using force and presence/absence of pelvic injury
  - Experimental and simulation results
  - Simulation results show under prediction of injury risk

Injury Prediction – Specific Areas

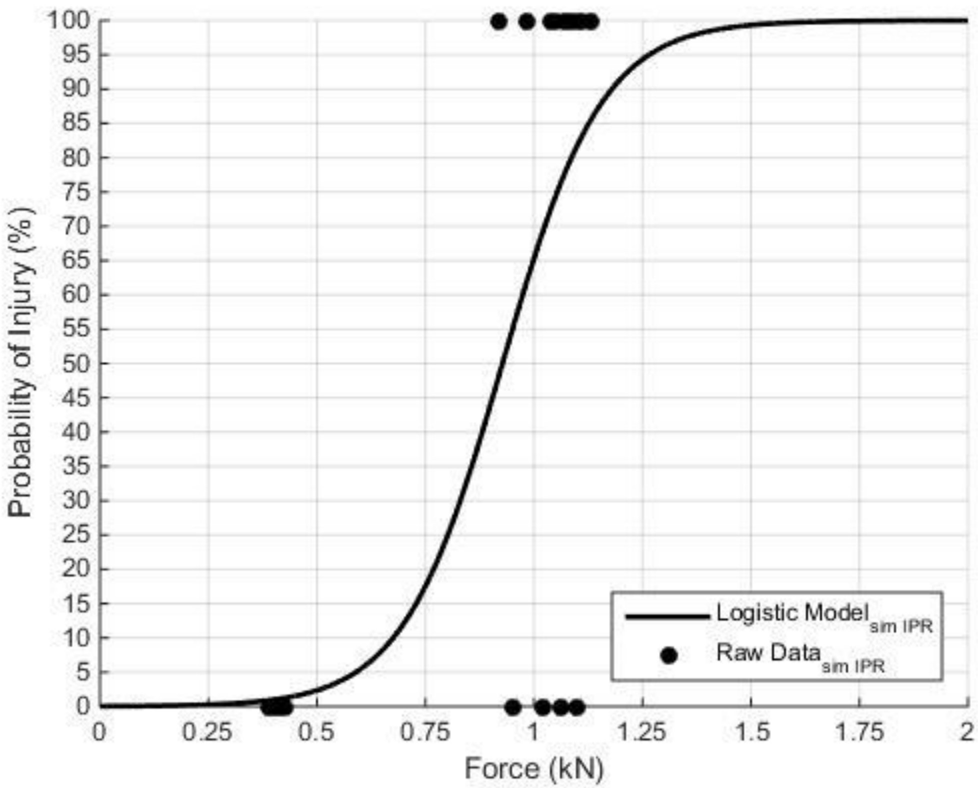

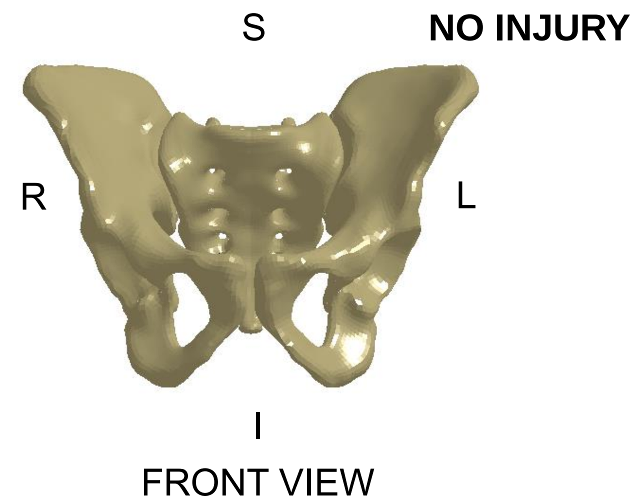

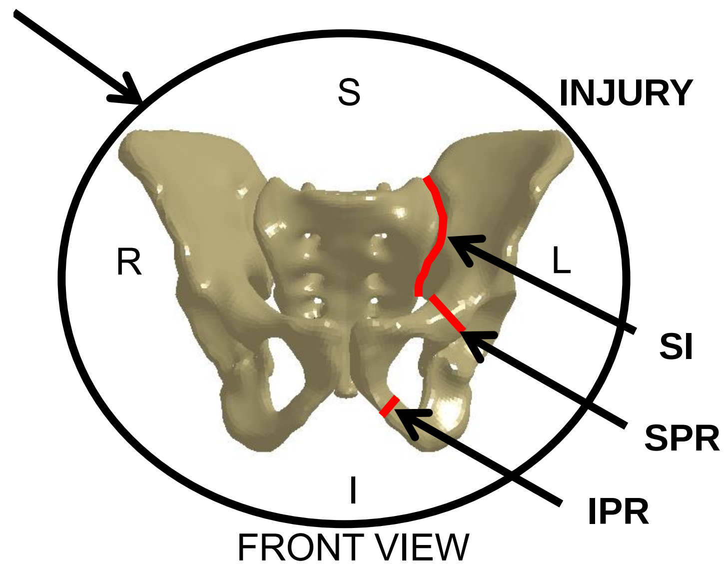

- Injury analysis: Logistic regression using force and presence/absence of pelvic injury
  - Experimental and simulation results
  - Simulation results show under prediction of injury risk

Injury Prediction – Specimen Size

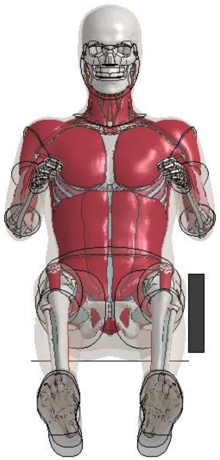

PMHS Specimen
Mass = 54.5 kg
Pelvis Width = 311 mm
Force = 13,940 N

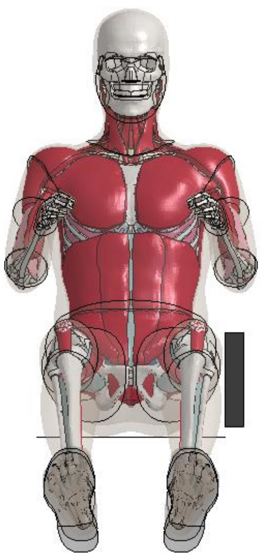

GHBMC M50
Mass = 78.6 kg
Pelvis Width = 268 mm
Force = 15,000 N

Scaling Methods

- ESEV (Eppinger et al.)
- Impulse Momentum Characteristic Length (Mertz et al.)
- Impulse Momentum Cubed Root (Mertz et al.)
- Impulse Momentum Effective Mass (Davis et al.)
- Linear Scaling in LS-DYNA

Injury Prediction – Specimen Size

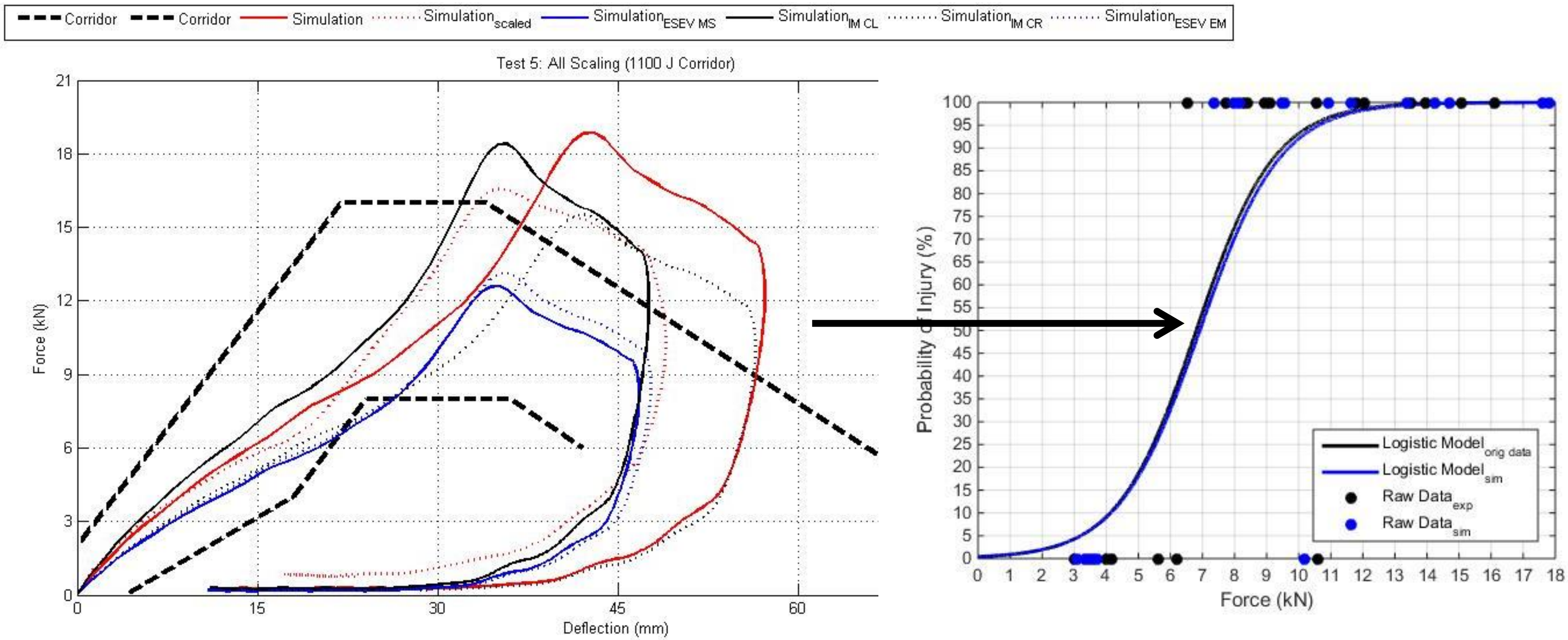

Use scaling methods to determine best force model force response → finalize injury risk prediction curves for the model

Vertical Load Testing

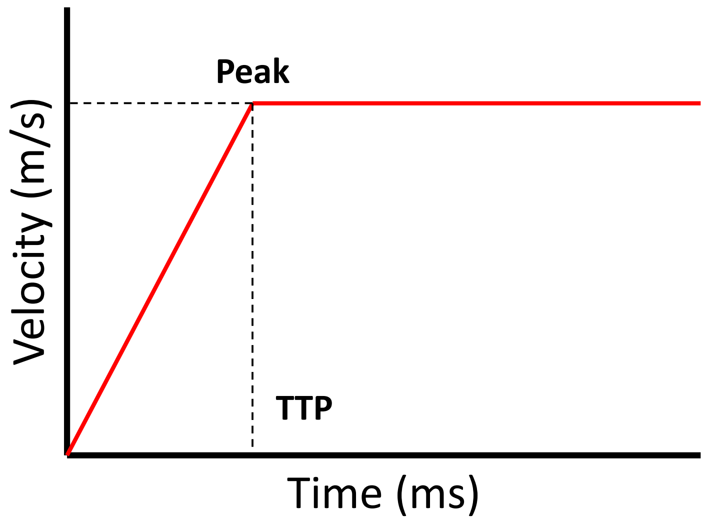

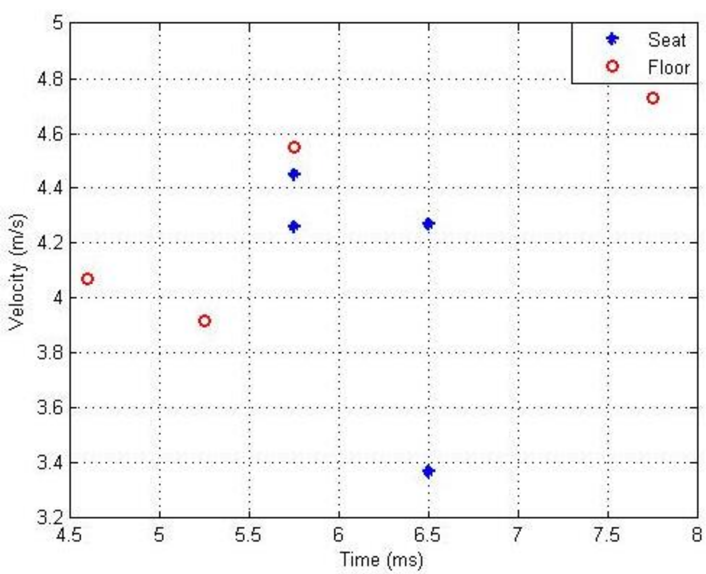

All Test: 4 m/s (non injurious)

Independent pulse (seat/floor)
Performed on PMHS

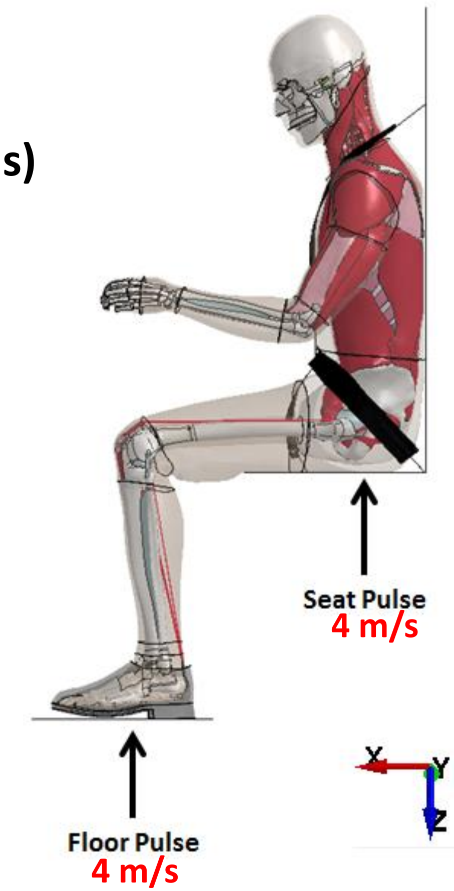

Performers:

UMTRI · Wayne State · University of Virginia · APL The Johns Hopkins University Applied Physics Laboratory

Repositioning of GHBMC - Legs

- The default position of the seated GHBMC for a civilian motor vehicle (approx. 120°)
- Repositioning to fit position of experimental test step:
  - *BOUNDARY_PRESCRIBED_MOTION_NODE
  - x, y, z translation to achieve desired position

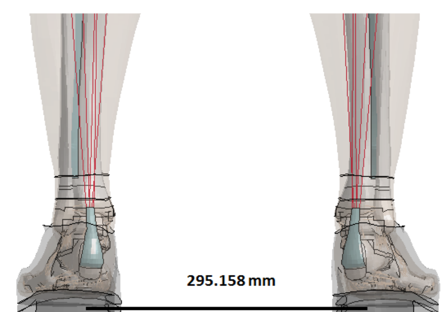

Repositioning of GHBMC - Pelvis

- Pelvis angle is determined by the position of specific landmarks of the pelvis
  - ASIS, PSIS, PS
  - Angle: line created by the ASIS and PS
- Repositioning to fit position of experimental test step:
  - *BOUNDARY_PRESCRIBED_MOTION_SET
  - y-axis at center of mass of the pelvis
  - pelvis angle approx. 21° to approx. 36°

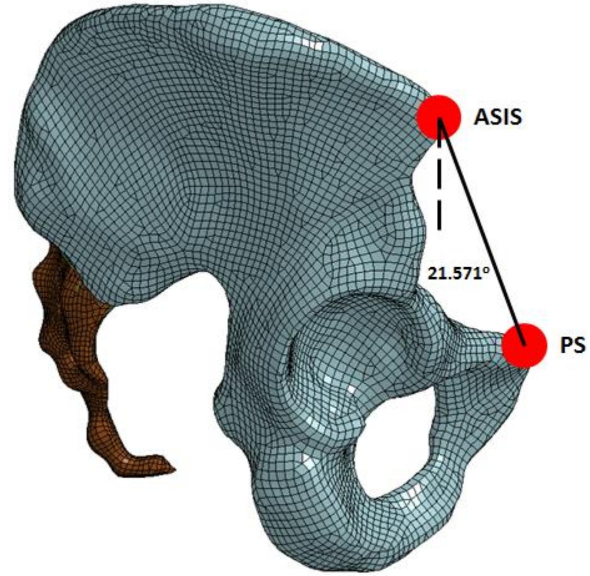

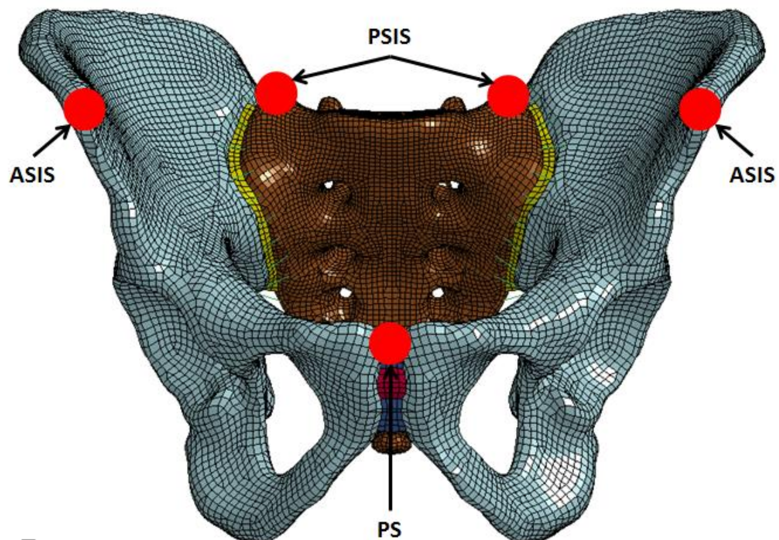

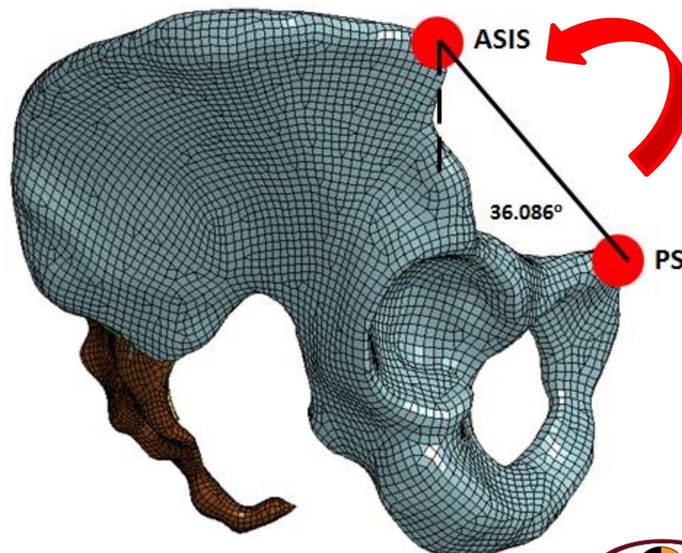

Development of FE Rig

- FE simplified rig consists of:
  - (1) a seat with a seat back and head rest
  - (2) a floor plate, and
  - (3) a five-point harness
- The acceleration pulse curves are used to move the seat and the floor plate independently along the Z-direction using *BOUNDARY_PRESCRIBED_MOTION_RIGID

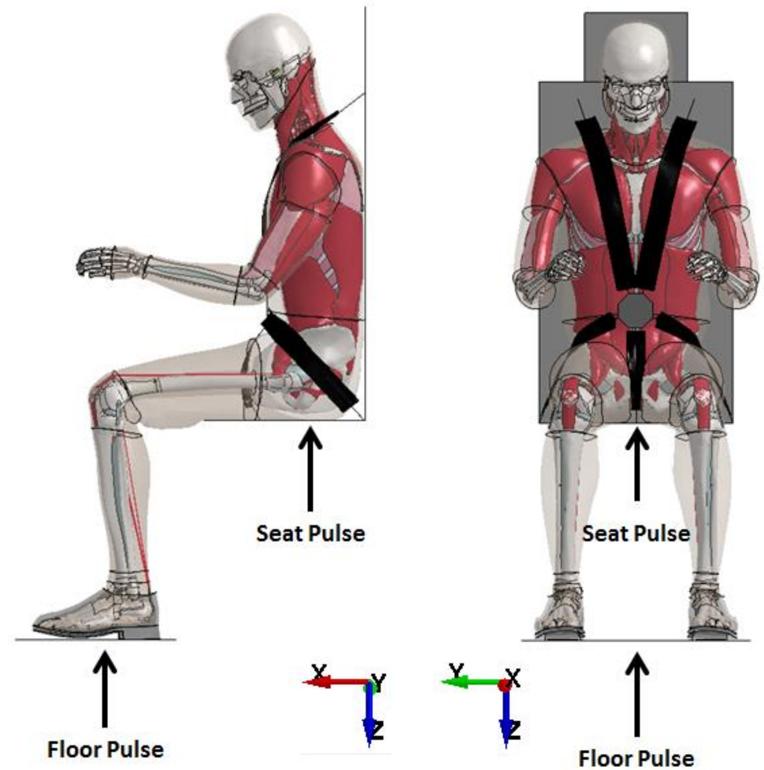

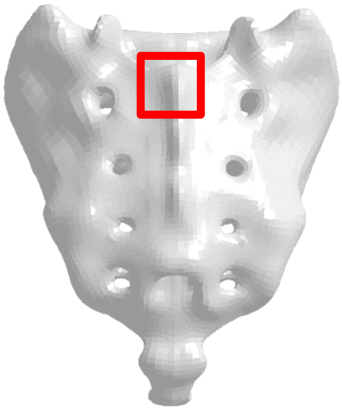

Vertical Load Testing

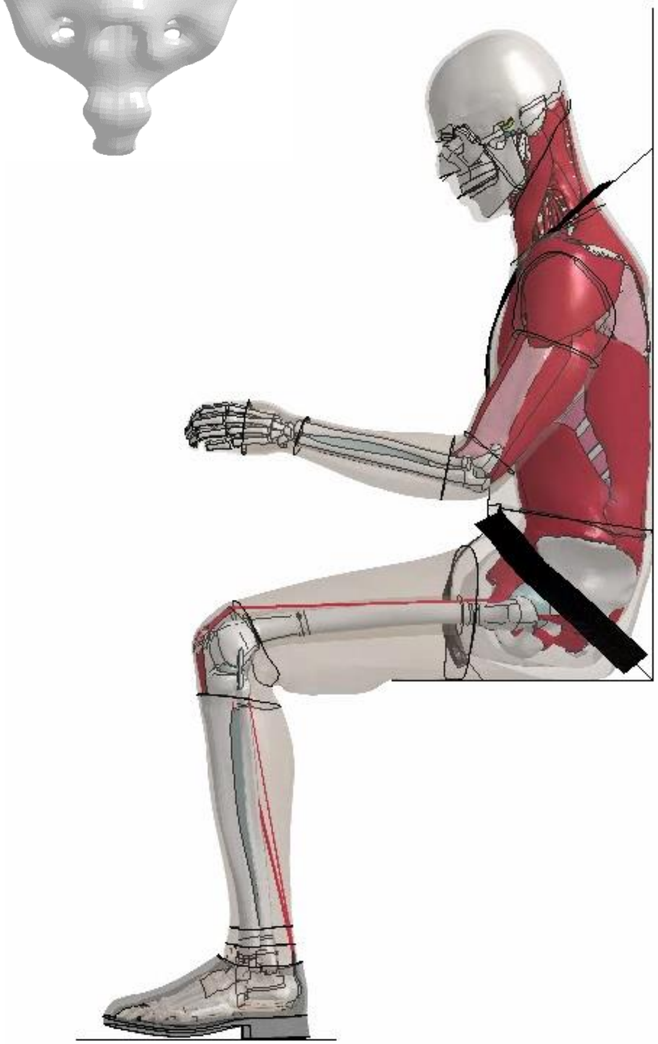

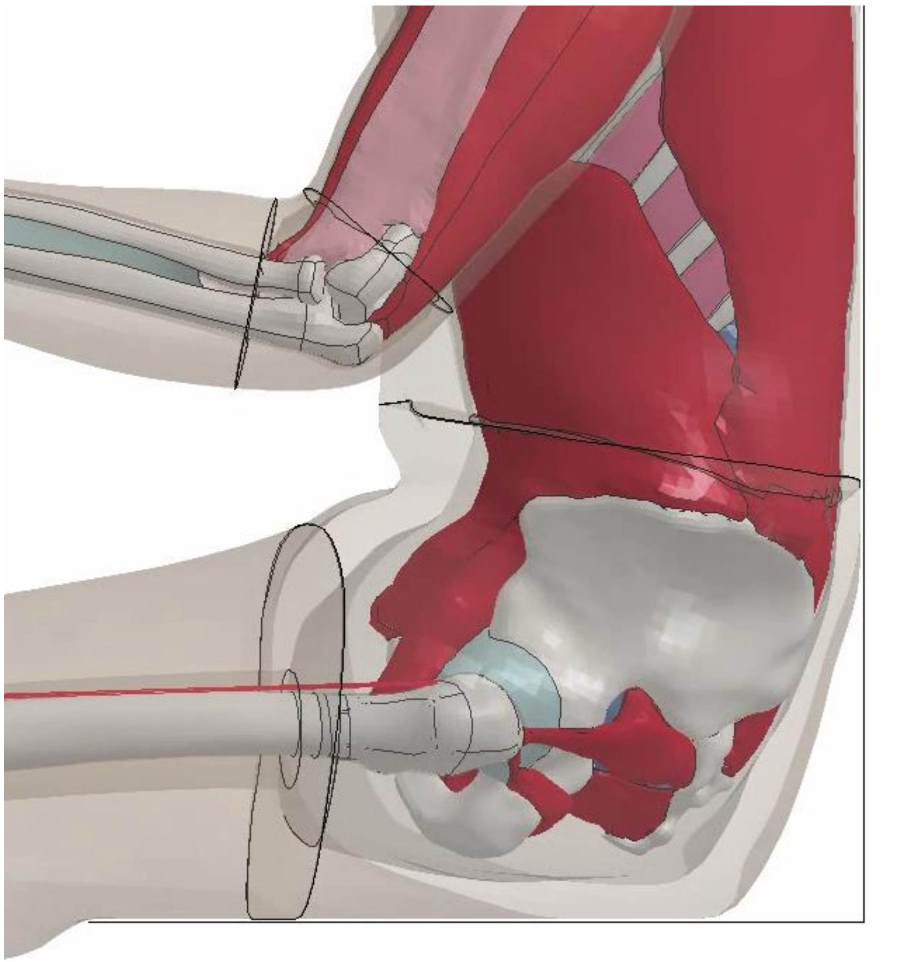

Wake Forest
School of Medicine

S1 Acceleration Extraction

- S1 acceleration data was extracted from GHBMC model and compared to S1 data recorded from accelerometers used in PMHS testing
  - Acceleration data from 133 nodes
  - Same surface area as the DTS 6DX PRO accelerometer used in PMHS experimental testing

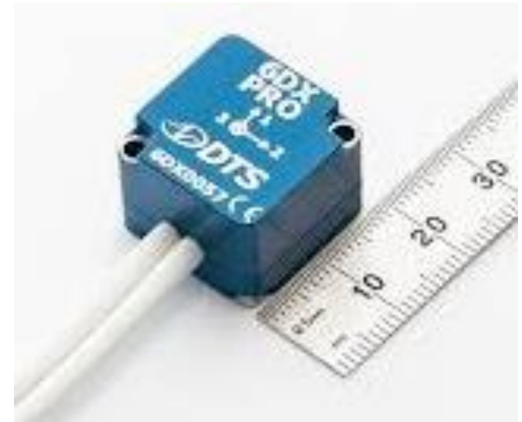

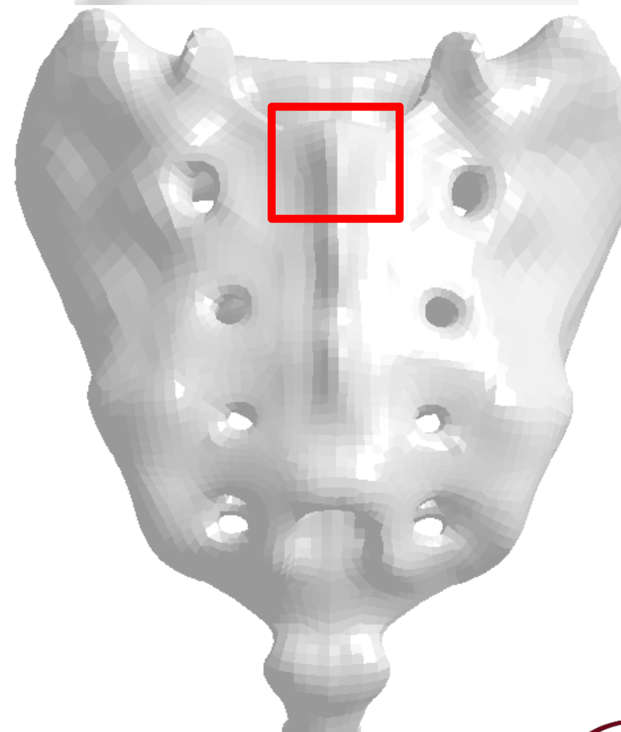

Filtering Method

- The frequency value used to filter data for this study was determined from preliminary work performed by the Signal Analysis Working Group (SAWG) for the WIAMan project

- Filter Method: Four pole, zero-phase Butterworth filter
  - For this study, 1050Hz filter was used

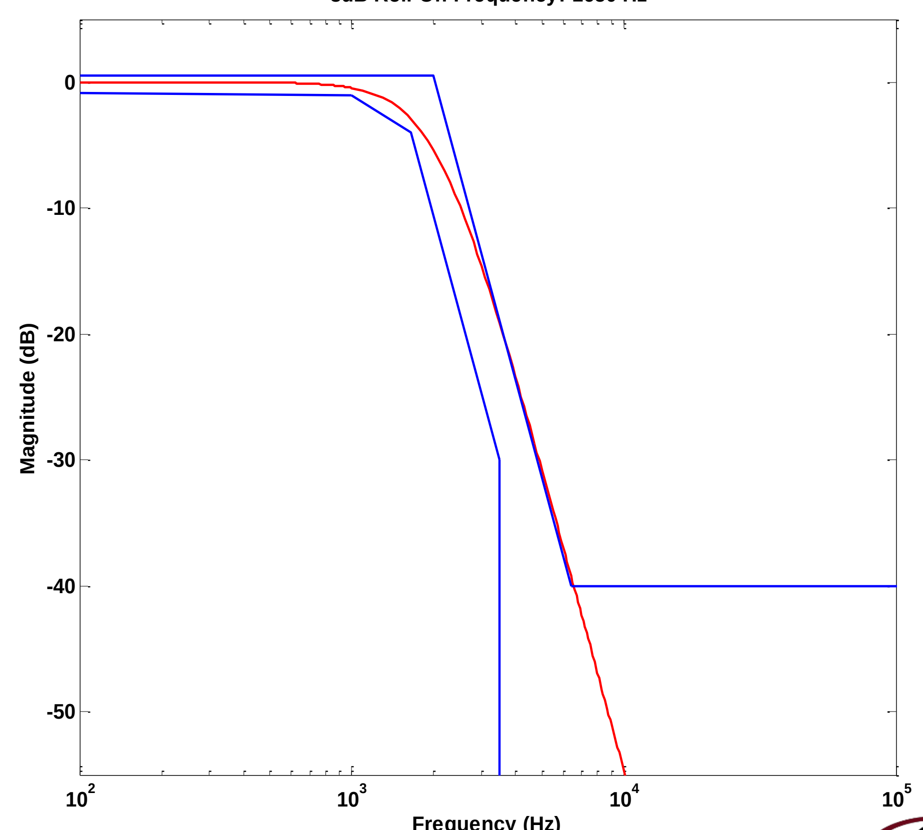

CORrelation and Analysis (CORA)

Weighted average of corridor and cross correlation methods

Simulation Data

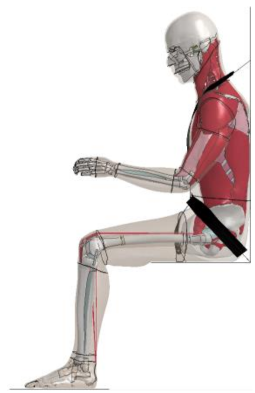

Experimental Data

Corridor fit, phase shift, and size and shape differences

Gehre et al. (CORA)

Scores range from 0 (lowest) to 1(highest)

C_{Cor} | C_{Phase} | C_{Size} | C_{Shape}

Preliminary Biofidelity Corridors

- Constructed using PMHS test data
- Standard approach determined by the Biofidelity Response Corridor (BRC) working group for the WIAMan BIO PT
  - Nusholtz et al. 2013
  - Transforms signals to principal component space using eigenvectors and eigenvalues
  - Alignment based on maximized correlation of signals iteratively
  - Output: Representative curve (RC) or cross-correlation reference and ±1 and ±2 standard deviation equivalent corridors

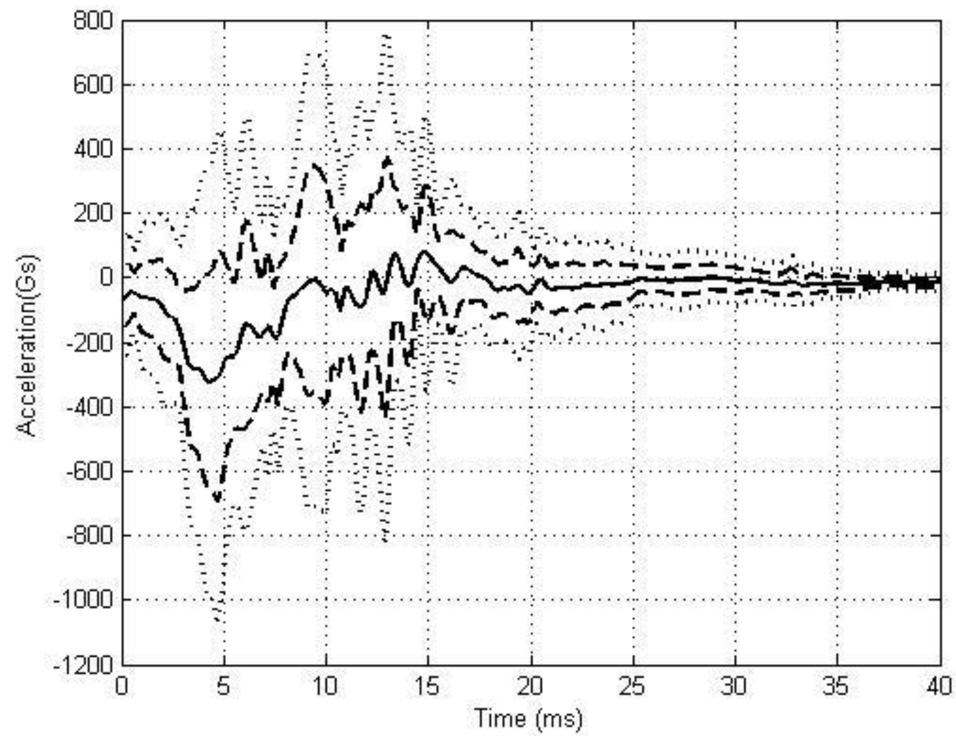

BRC Comparison and CORA Analysis

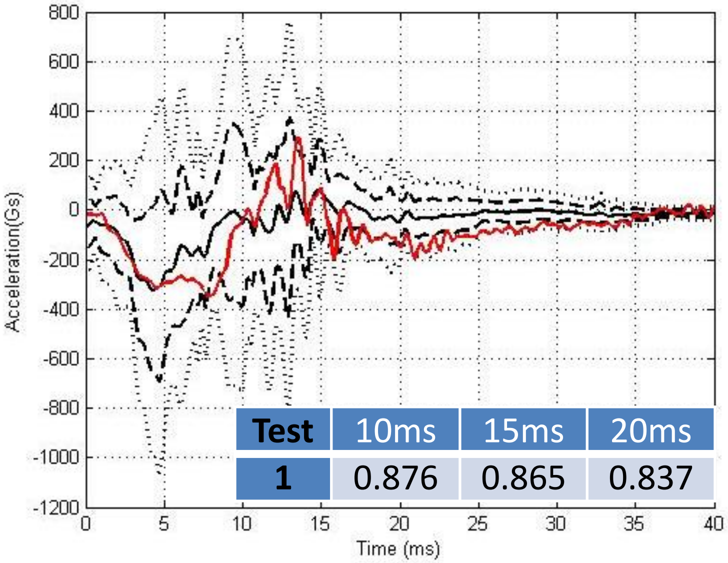

Test	10ms	15ms	20ms
1	0.876	0.865	0.837

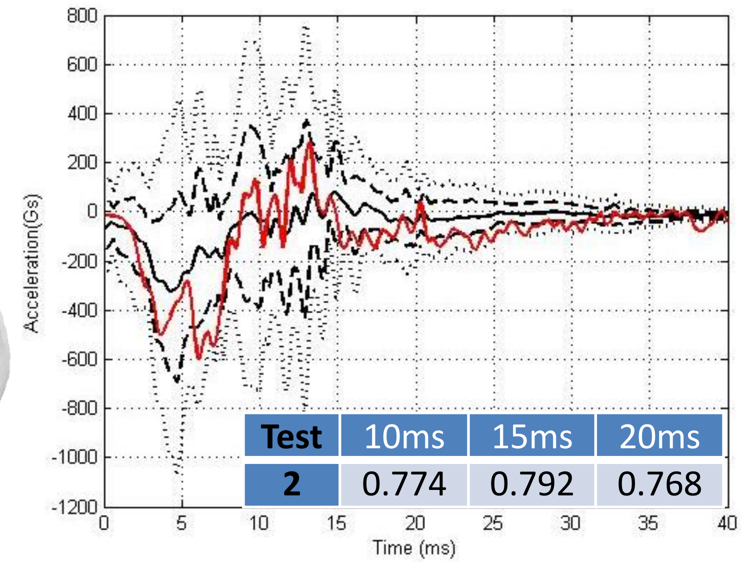

Test	10ms	15ms	20ms
2	0.774	0.792	0.768

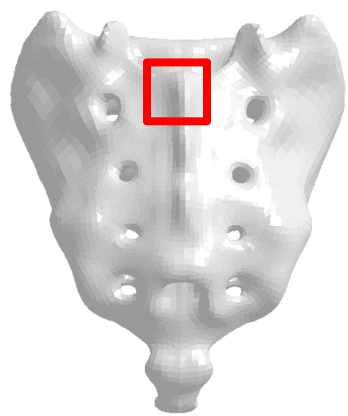

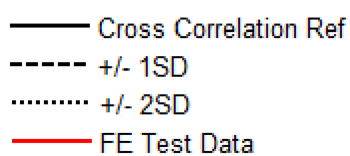

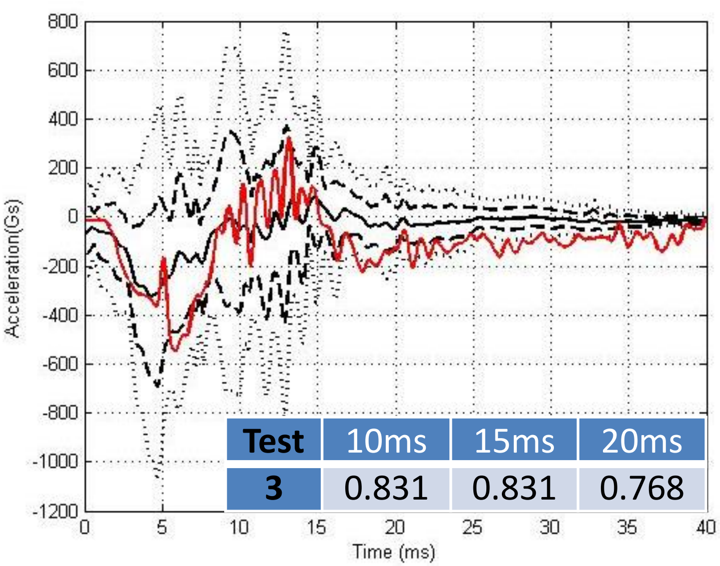

Test	10ms	15ms	20ms
3	0.831	0.831	0.768

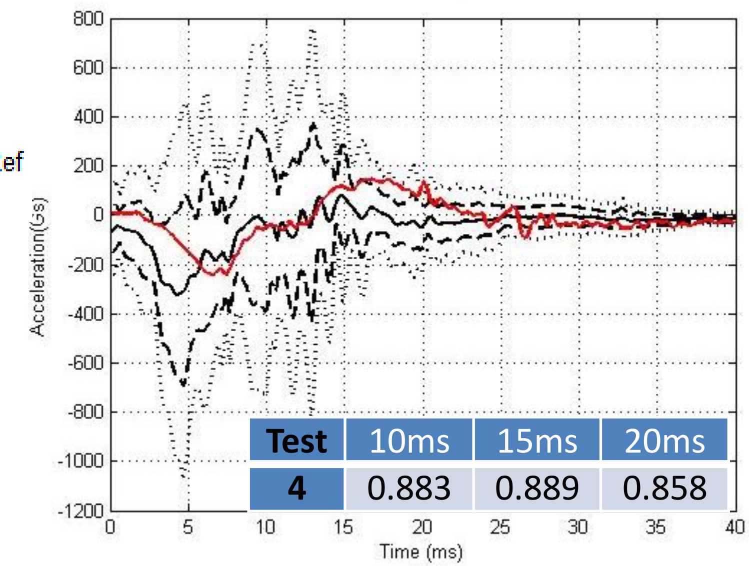

Test	10ms	15ms	20ms
4	0.883	0.889	0.858

Cross-Sectional Forces

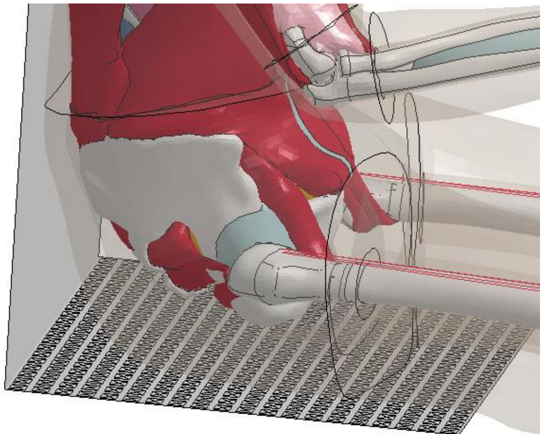

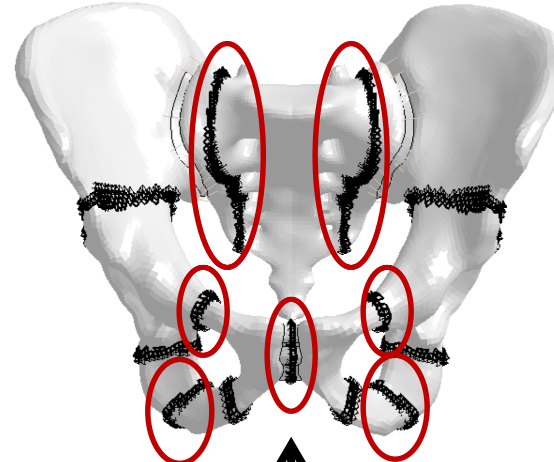

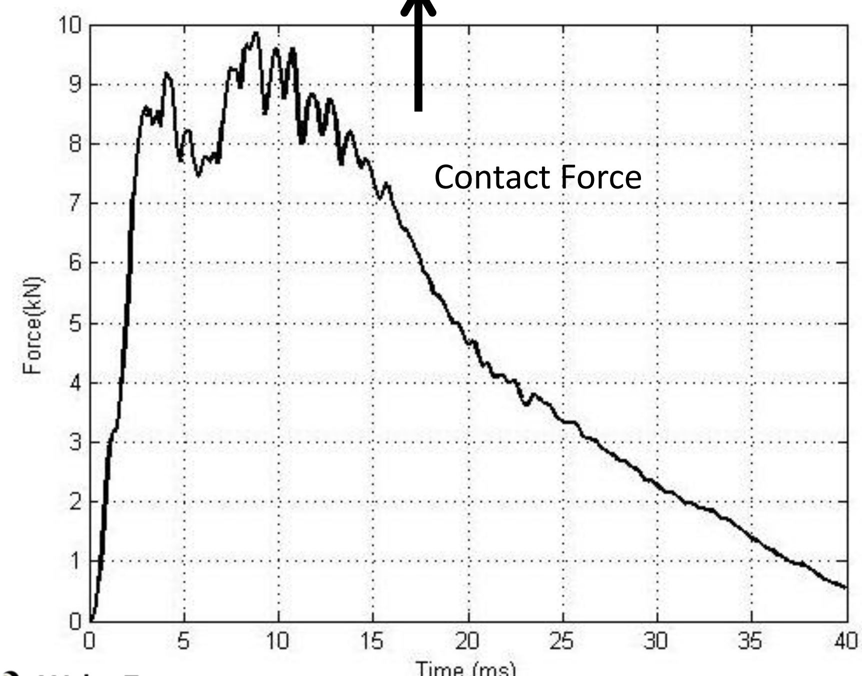

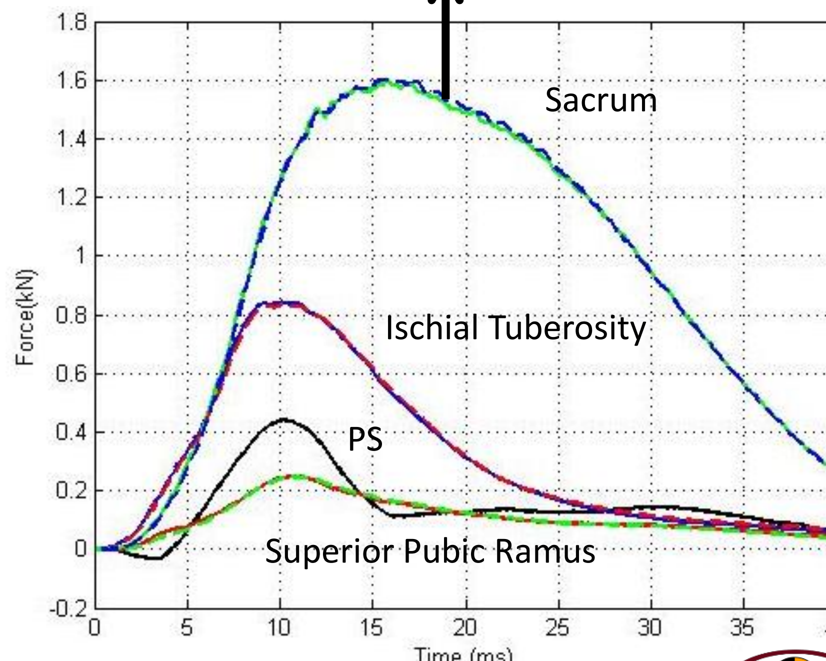

Pubic Symphysis

Pubic Symphysis

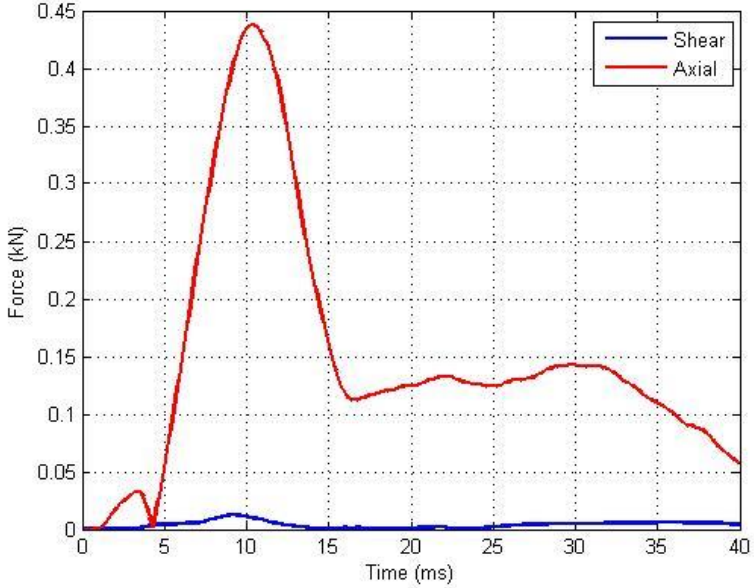

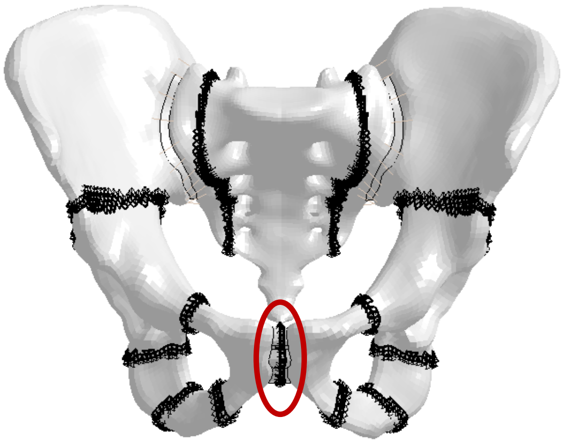

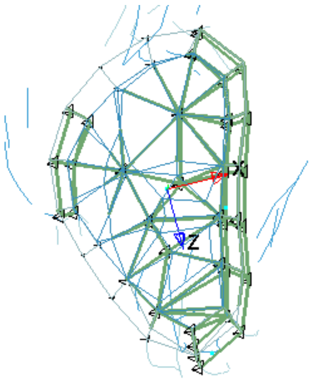

Shear: X,Z
Axial: Y

Inferior Pubic Ramus

Right Inferior Pubic Ramus

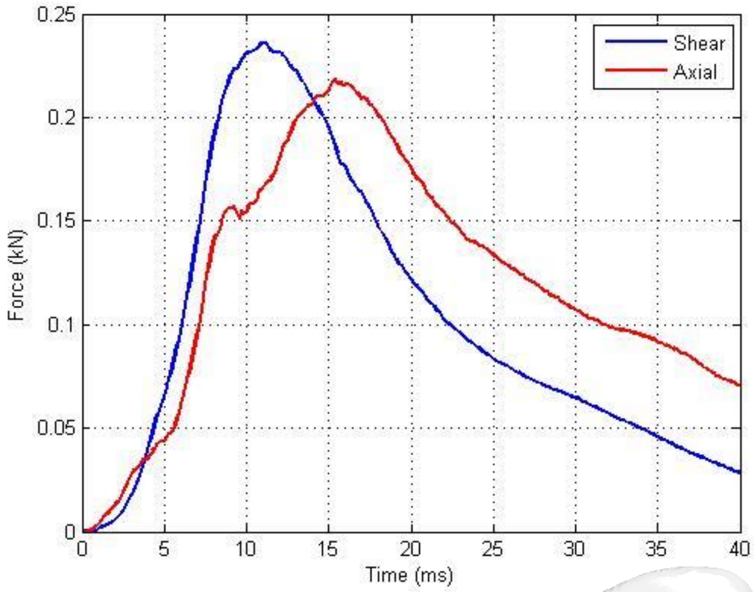

Left Inferior Pubic Ramus

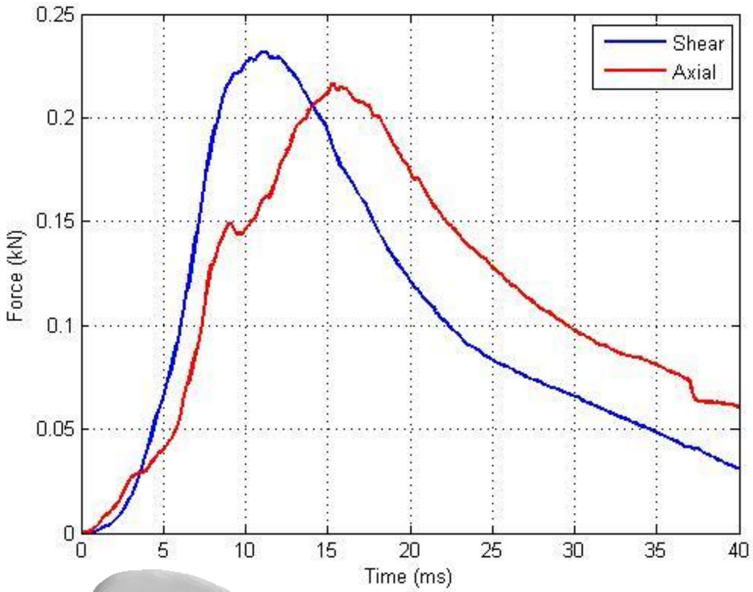

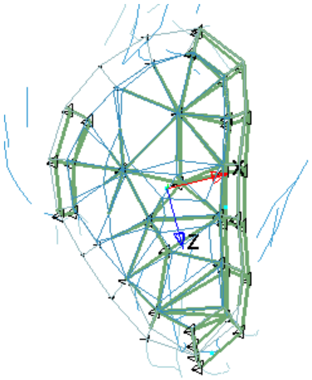

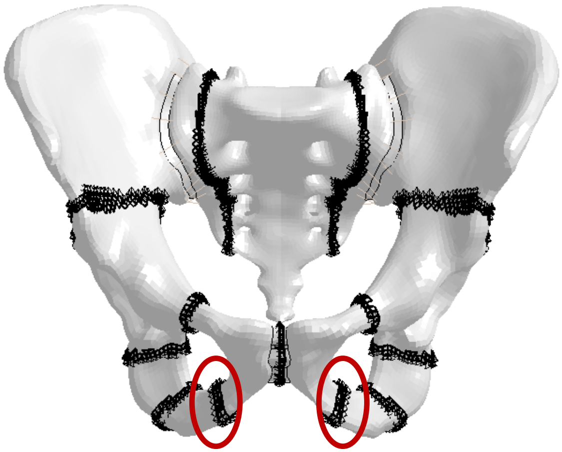

Shear: X,Z
Axial: Y

Ischial Tuberosity

Right Ischial Tuberosity

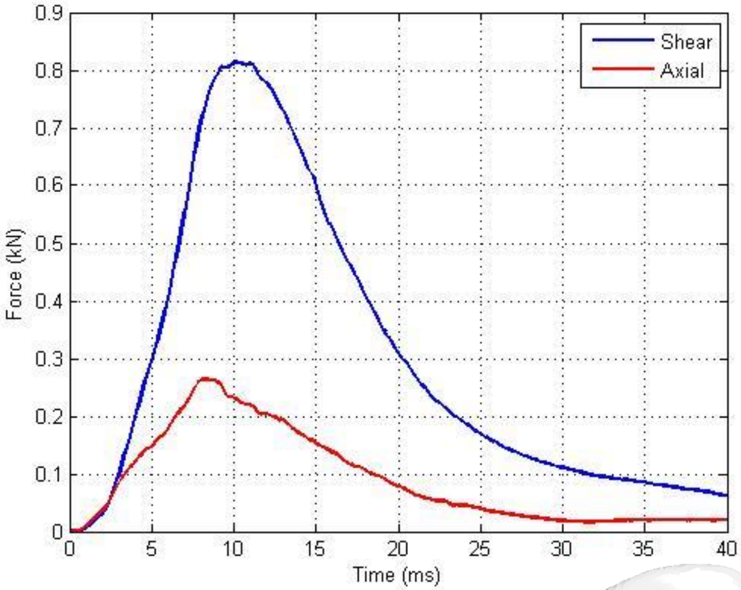

Left Ischial Tuberosity

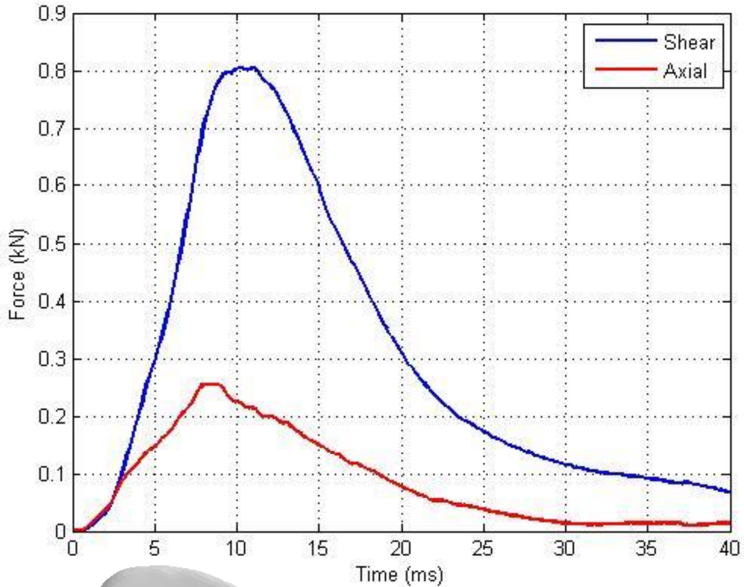

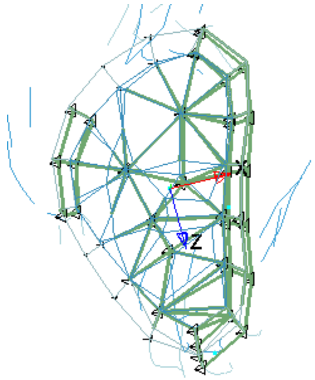

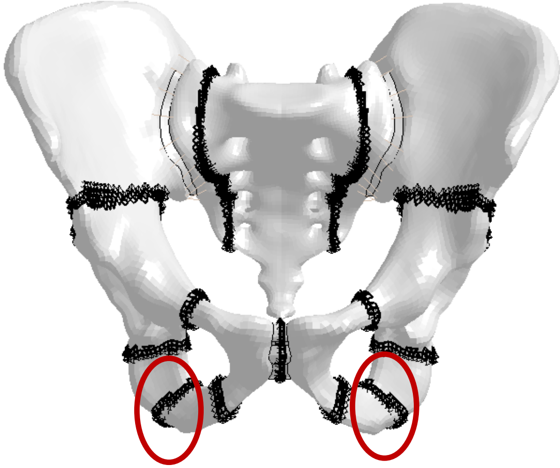

Shear: X,Z
Axial: Y

Ischium

Right Ischium

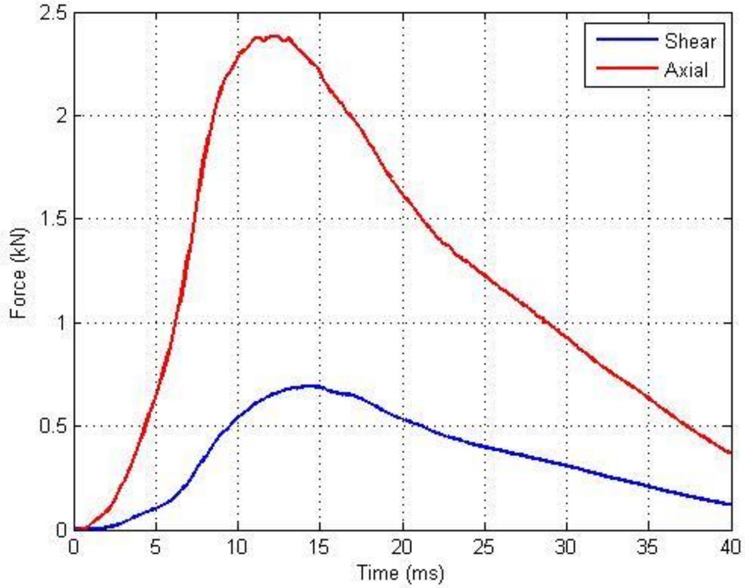

Left Ischium

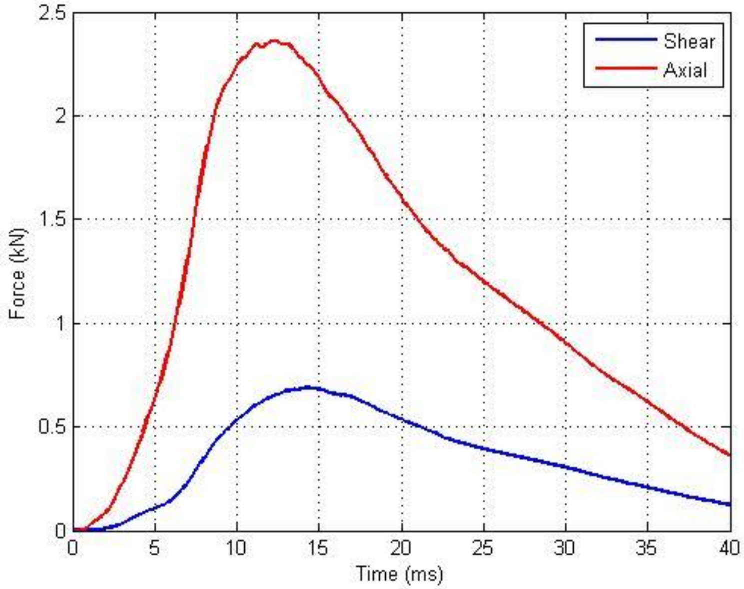

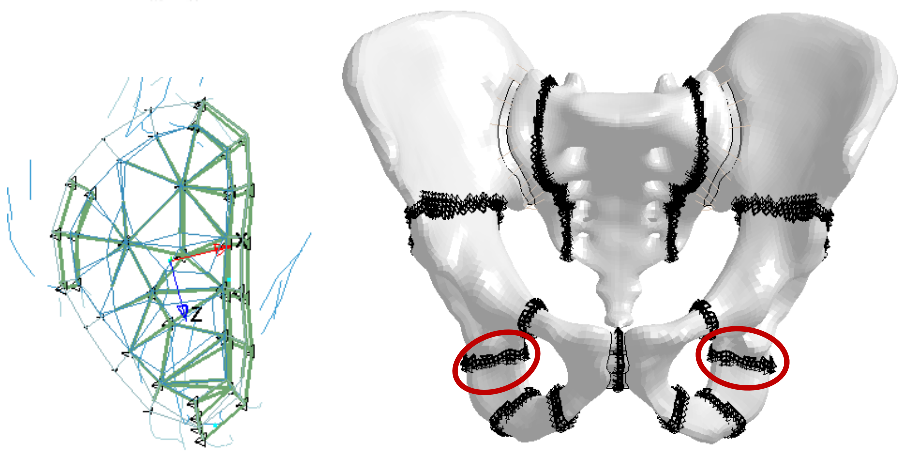

Shear: X,Z
Axial: Y

Superior Pubic Ramus

Right Superior Pubic Ramus

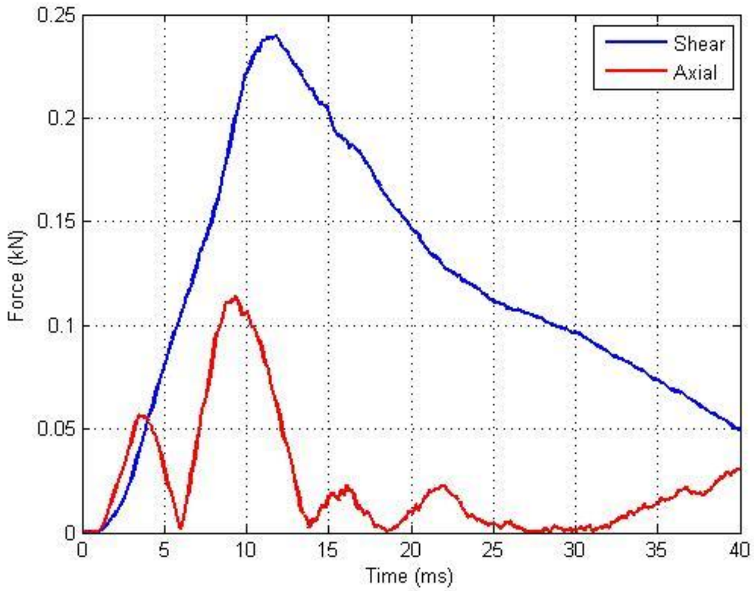

Left Superior Pubic Ramus

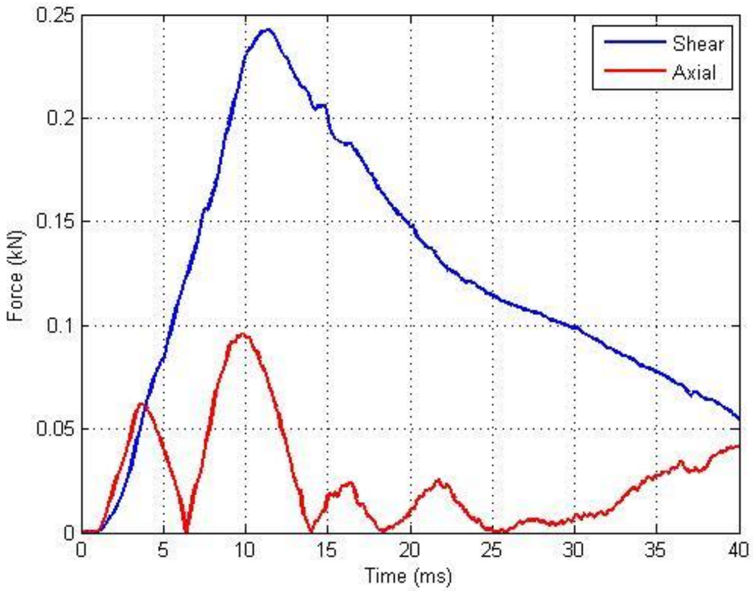

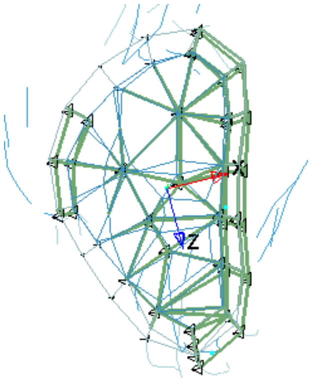

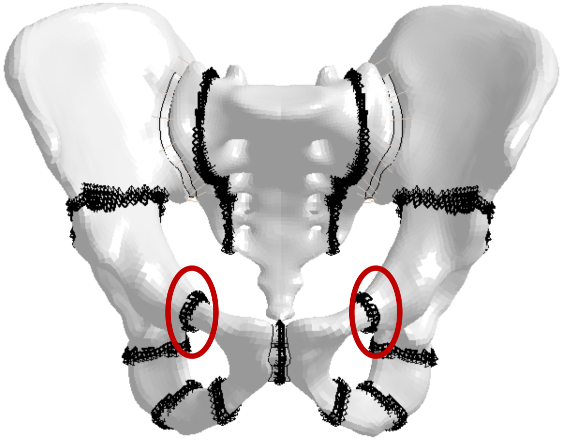

Shear: X,Z
Axial: Y

Ilium

Right Ilium

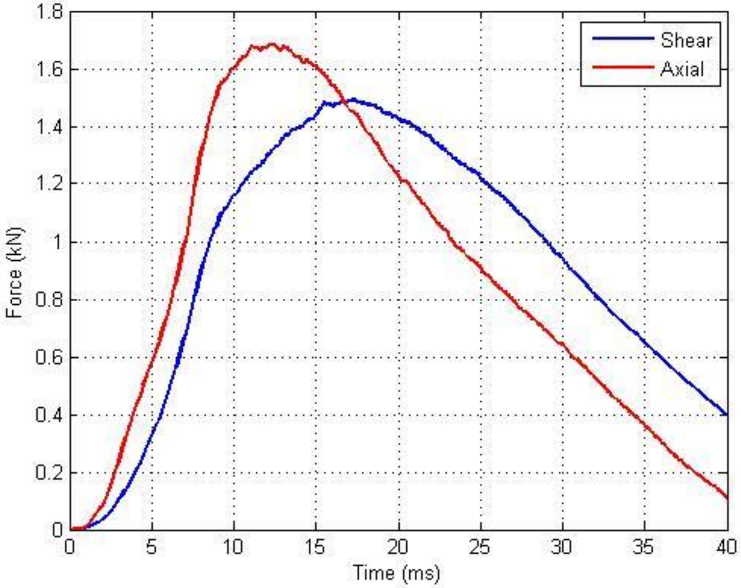

Left Ilium

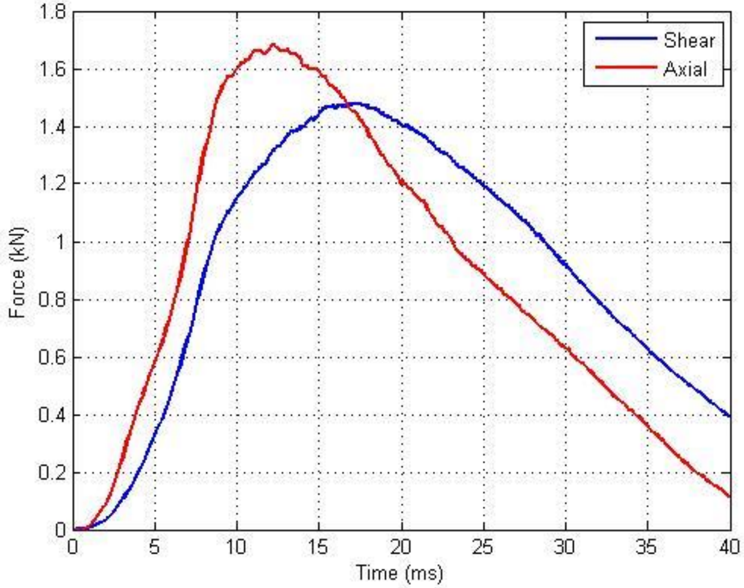

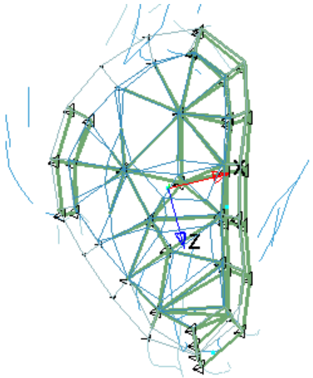

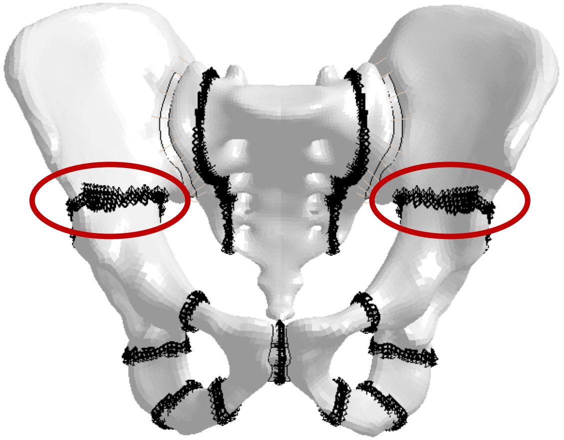

Shear: X,Z
Axial: Y

Sacrum

Right Sacrum

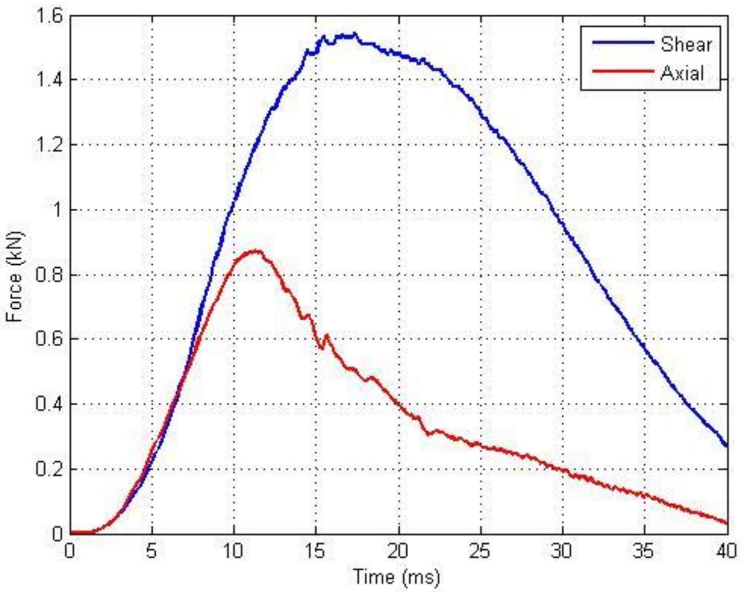

Left Sacrum

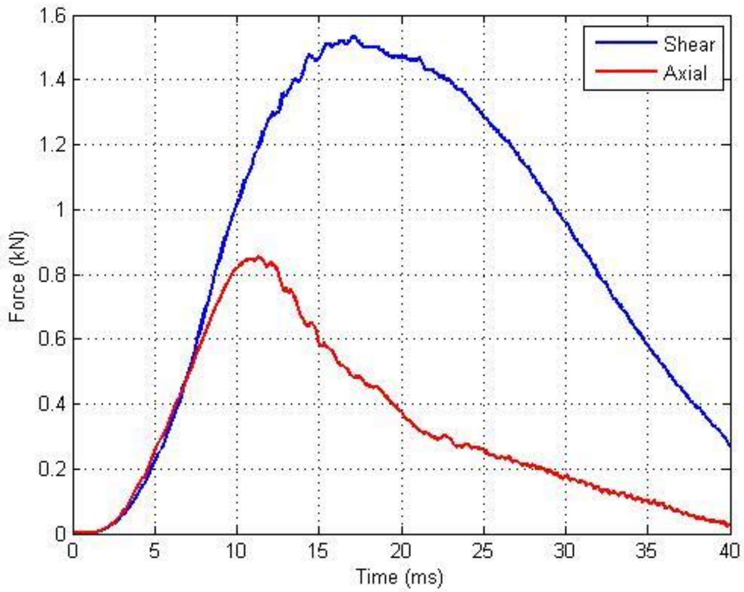

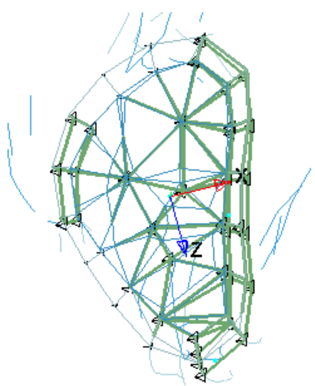

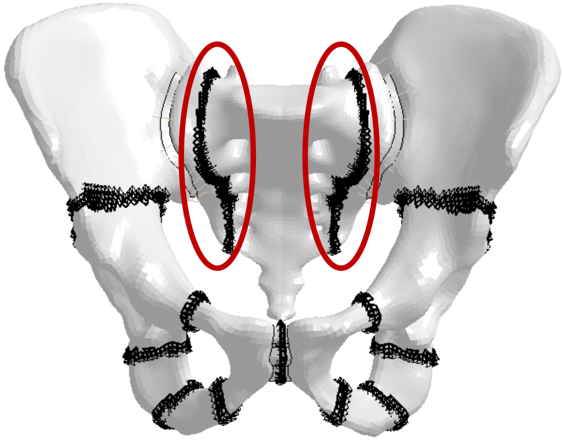

Shear: X,Z
Axial: Y

Shear and Axial Forces

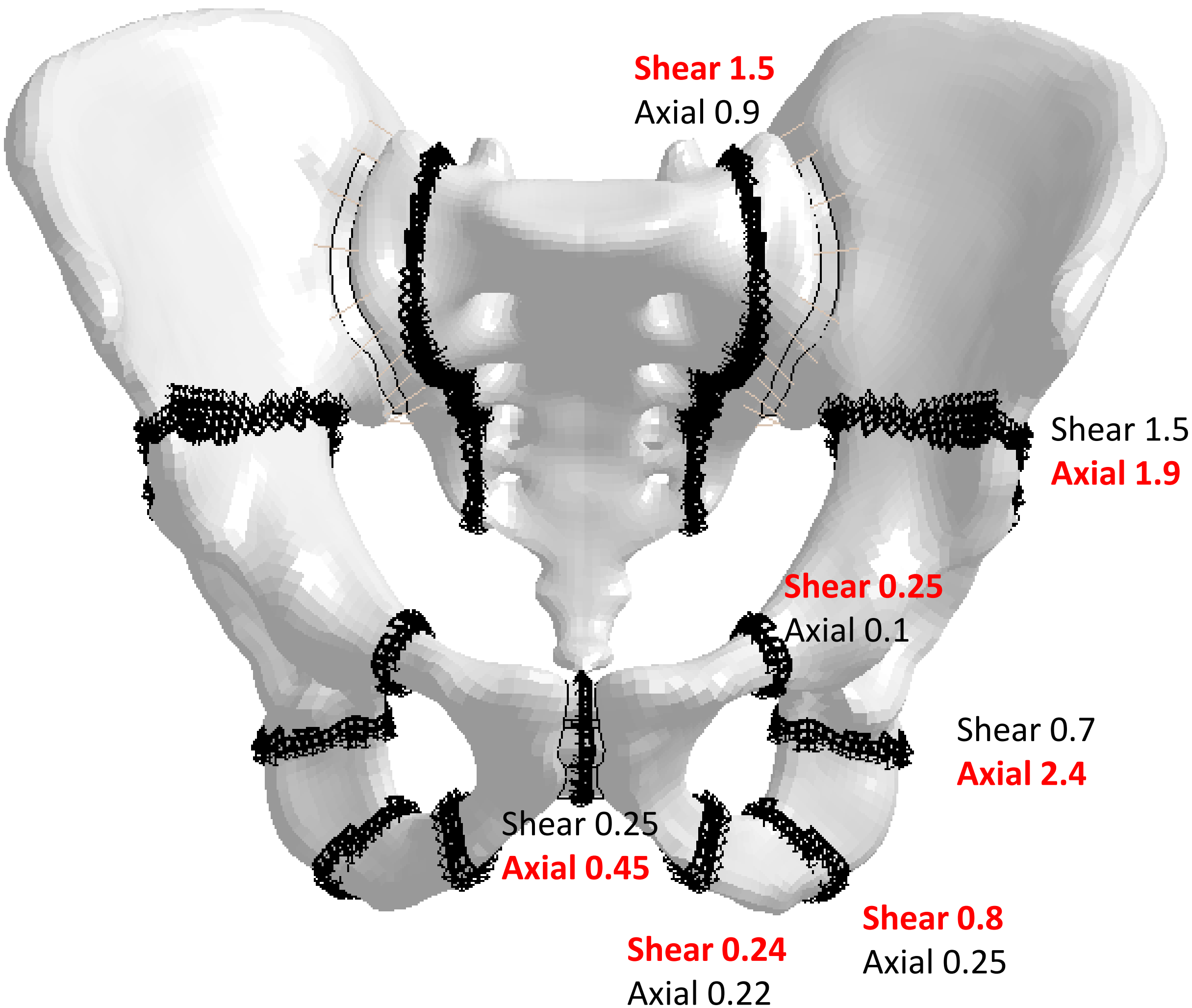

On Going Efforts and Future Work

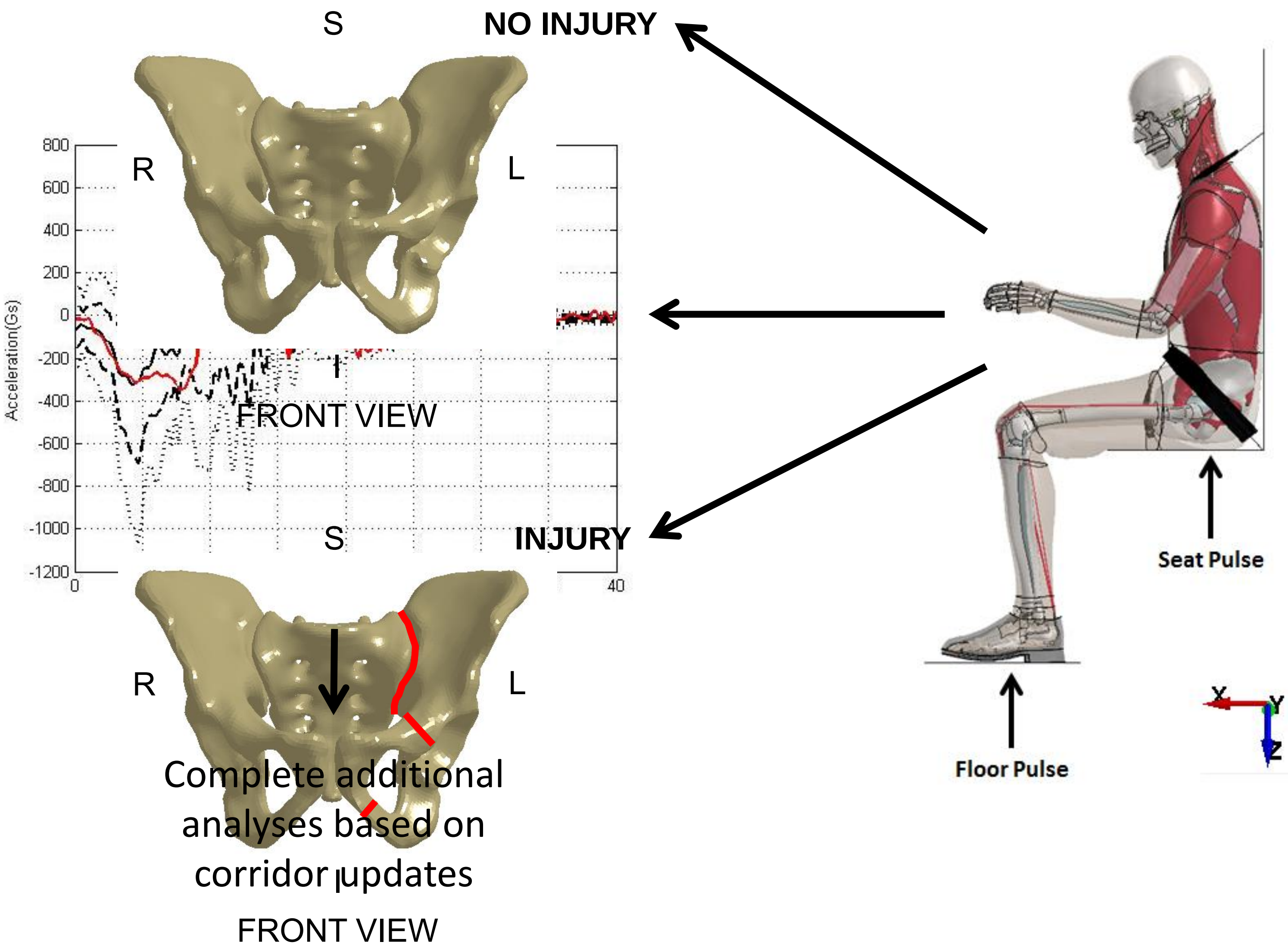

Complete additional analyses based on corridor updates

On Going Efforts and Future Work

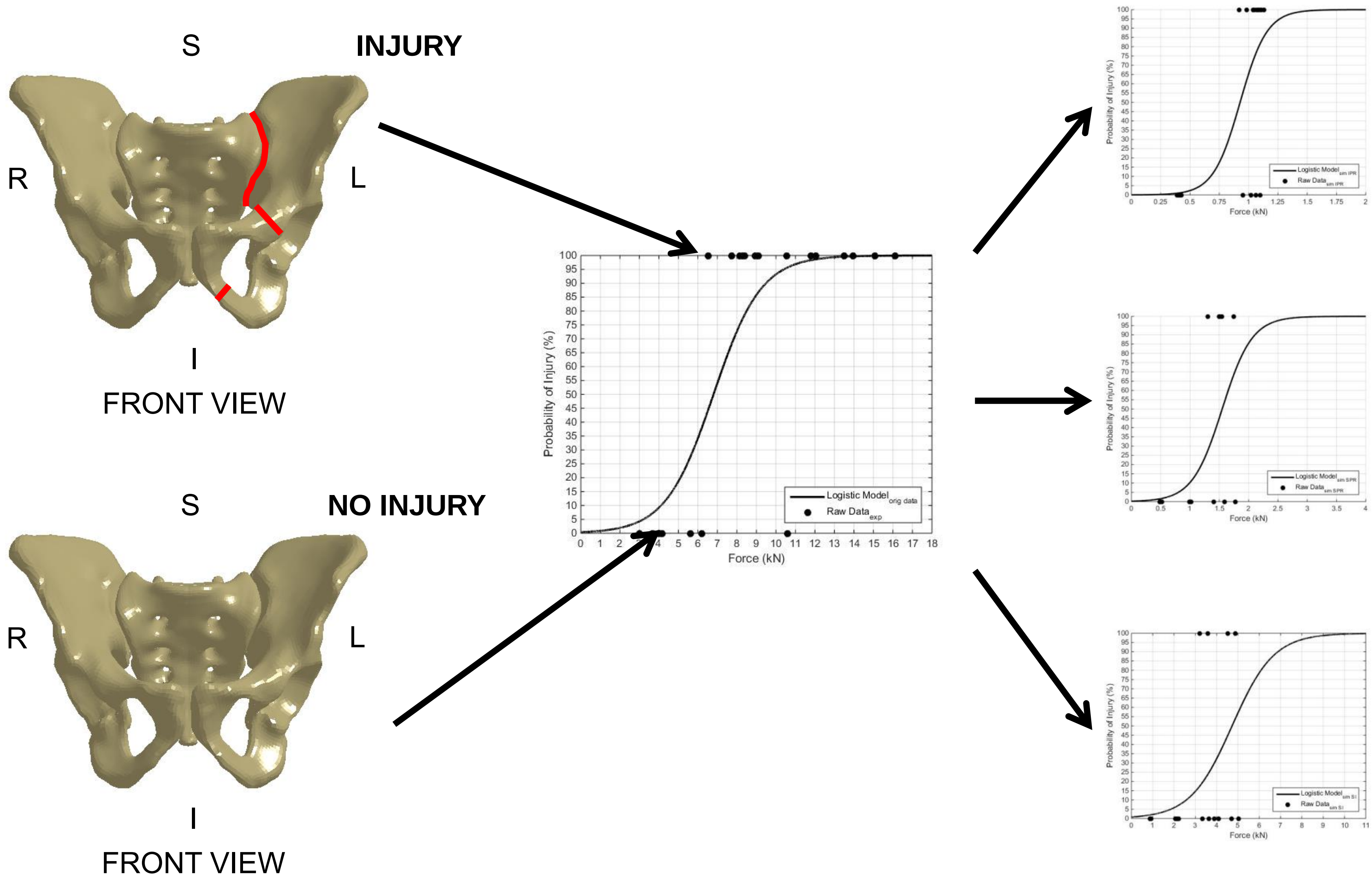

Tool for Injury Risk Analysis Using GHBMC WIAMan BIO PT Reconstructions

Select WIAMan cases

Pelvis fx

No pelvis fx

Reposition GHBMC based on pre-positioning data

Perform UBB simulations

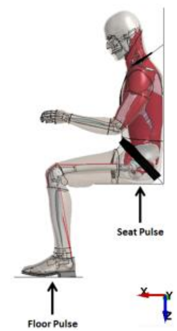

Analyze Injury Risks

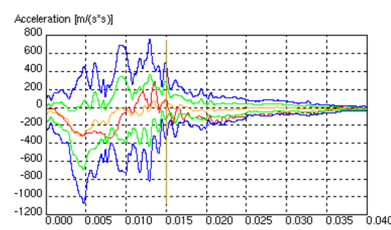

Develop Injury Risk Curves & Thresholds for GHBMC Pelvis

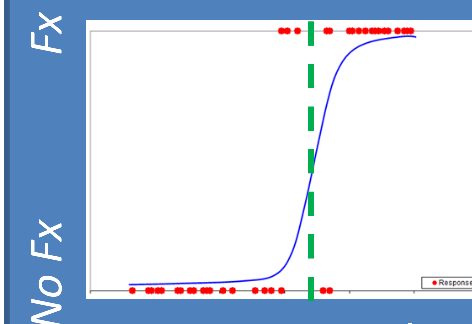

Cross-sectional force (N)

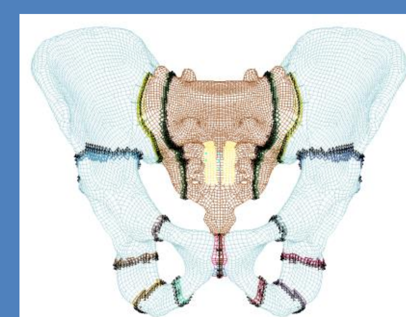

Discussion

- Results should be considered preliminary
  - Number of tests used
  - Corridors
  - Filter frequency
  - One injury metric (S1 acceleration)

On-Going Efforts

- Finalized corridors
- Updated filtering method
- Additional metrics
  – i.e. Strain
- Further Characterization
  – i.e. Cross-sectional force

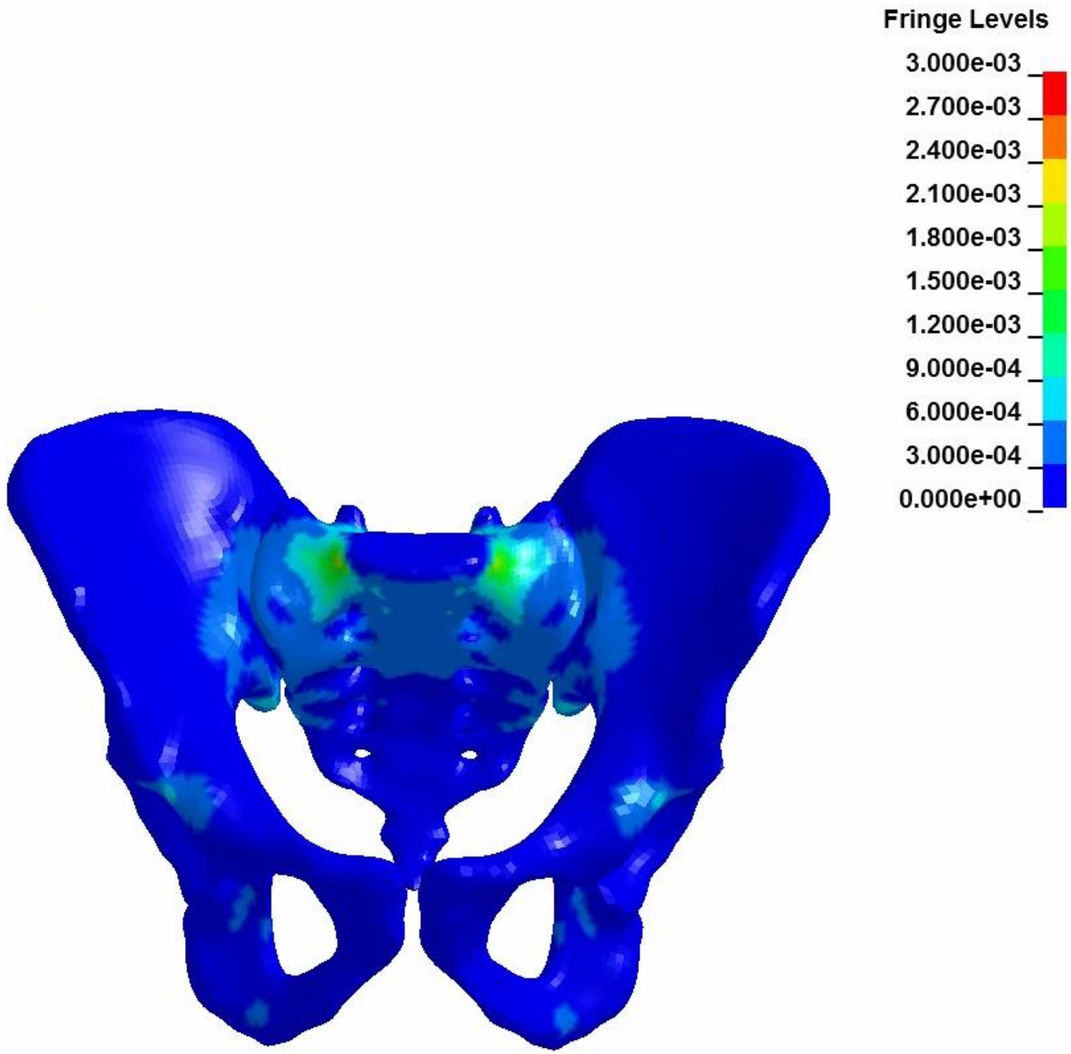

Summary

- Prevention of pelvic injuries in a military environment is crucial because they can lead to an increased risk of mortality.
- The work performed in this study will help lead to a better understanding of the causation and mechanism of UBB pelvic injuries.
- This knowledge will be useful for future development of injury risk criteria for UBB loading conditions using total human body finite element modeling.
- The resulting model will be used to assess injury potential and explore load paths and potential countermeasures (positioning, energy absorption and cushioning)

Acknowledgements

GHBMC

Global Human Body Models Consortium

SMART
SCIENCE, MATHEMATICS & RESEARCH FOR TRANSFORMATION
PART OF THE NATIONAL DEFENSE EDUCATION PROGRAM

ARL

Wake Forest School of Medicine
UMTRI
Medical College of Wisconsin
Duke University
Wayne State
The Ohio State University
University of Virginia
APL The Johns Hopkins University Applied Physics Laboratory

Joel D. Stitzel, Ph.D. (Advisor)

F. Scott Gayzik, Ph.D.

Andrew R. Kemper, Ph.D.

Anna N. Miller, M.D.

Ashley A. Weaver, Ph.D.

Center for Injury Biomechanics

Wake Forest School of Medicine

CIB

Virginia Tech Wake Forest University

School of Biomedical Engineering and Sciences

Thank you!

Caitlin M. Weaver and Joel D. Stitzel

13 January 2016

Center for Injury Biomechanics

Wake Forest School of Medicine

CIB

Virginia Tech Wake Forest University

School of Biomedical Engineering and Sciences

Backup Slides

Caitlin M. Weaver and Joel D. Stitzel

10 September 2015

Center for Injury Biomechanics

Wake Forest School of Medicine

Virginia Tech
Wake Forest University
School of Biomedical Engineering and Sciences

Project Overview

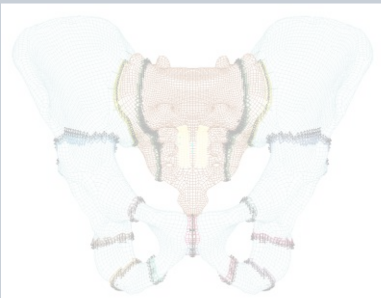

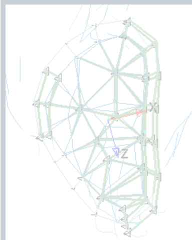

Specific Aim 1: Develop virtual load cell instrumentation to analyze pelvic injury response

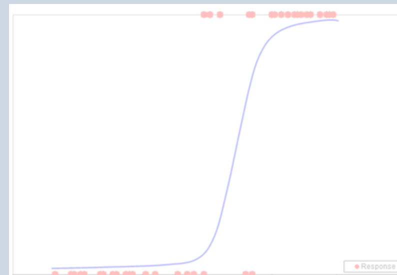

Specific Aim 2: Validate tissue level metrics in FE pelvis using whole body and isolated pelvis tests to develop injury metrics and risk curves

Specific Aim 3: Investigate injury risk of UBB events based on vehicle environment and occupant position

Proposal Overview

Investigate injury risk using different occupant position and vehicle/seat conditions

Determine appropriate parameters and boundary conditions for testing → Design optimal Latin Hypercube study to test impact of boundary conditions → Evaluate the injury risk associated with these boundary conditions

Test Matrix

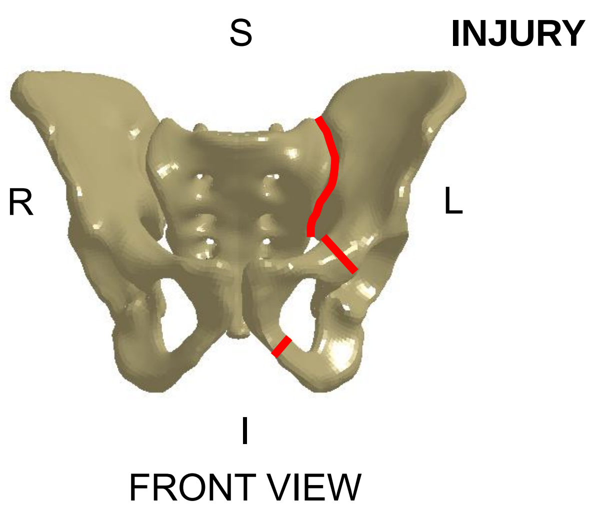

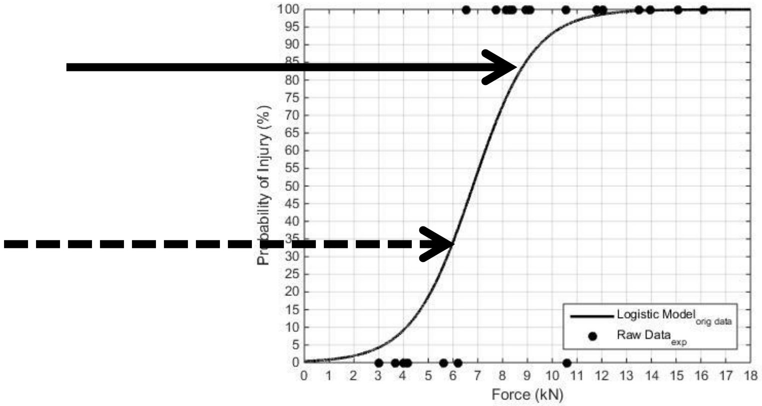

Table 1. Range for boundary conditions for Latin Hypercube design of experiments.			
Pelvis Angle Range (degrees)	Knee Angle (degrees)	PPE	Seat Material
35 to 45	30 to 120	None, head, upper torso, lower torso, combination	Steel, Foam varieties

Results Analysis

LHD Simulations

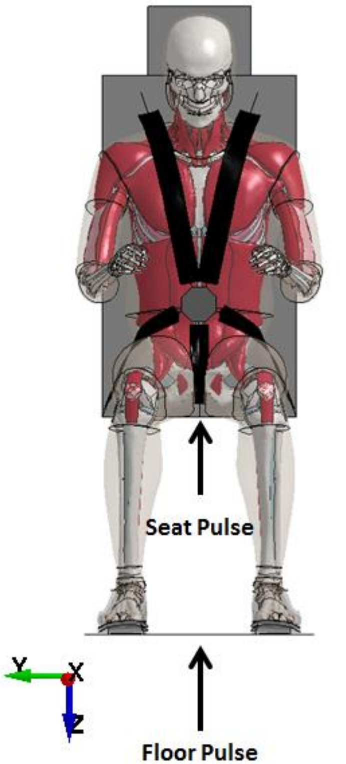

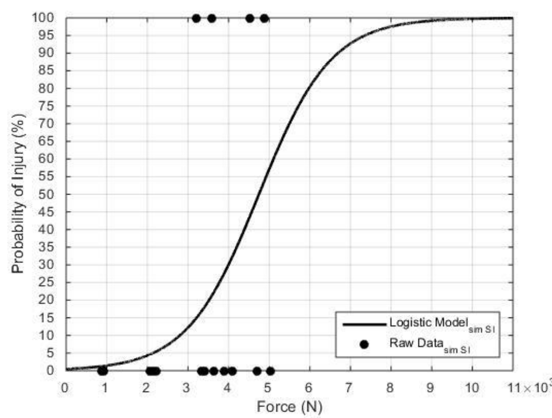

Expected injury risk based on the boundary conditions used

Determine conditions resulting in the lowest and highest risk of injury

Determine if certain conditions are more important in risk mitigation than others

Previous Research

The majority of reported LEX UBB injury evaluation studies focus on region below the knee

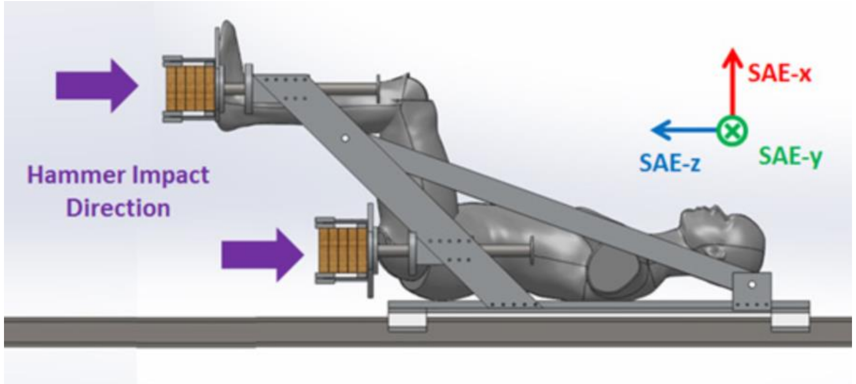

Bailey et al. Pelvis injury, whole body PMHS, sled blast simulator of UBB-type loading

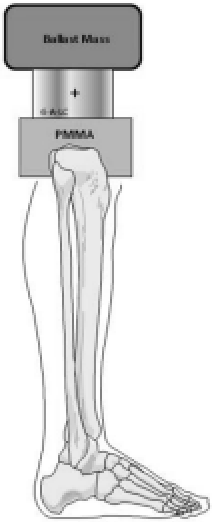

Zhang et al. FE UBB, lumbar spine

Pintar et al. FE UBB, cervical spine

Cross-Section Creation

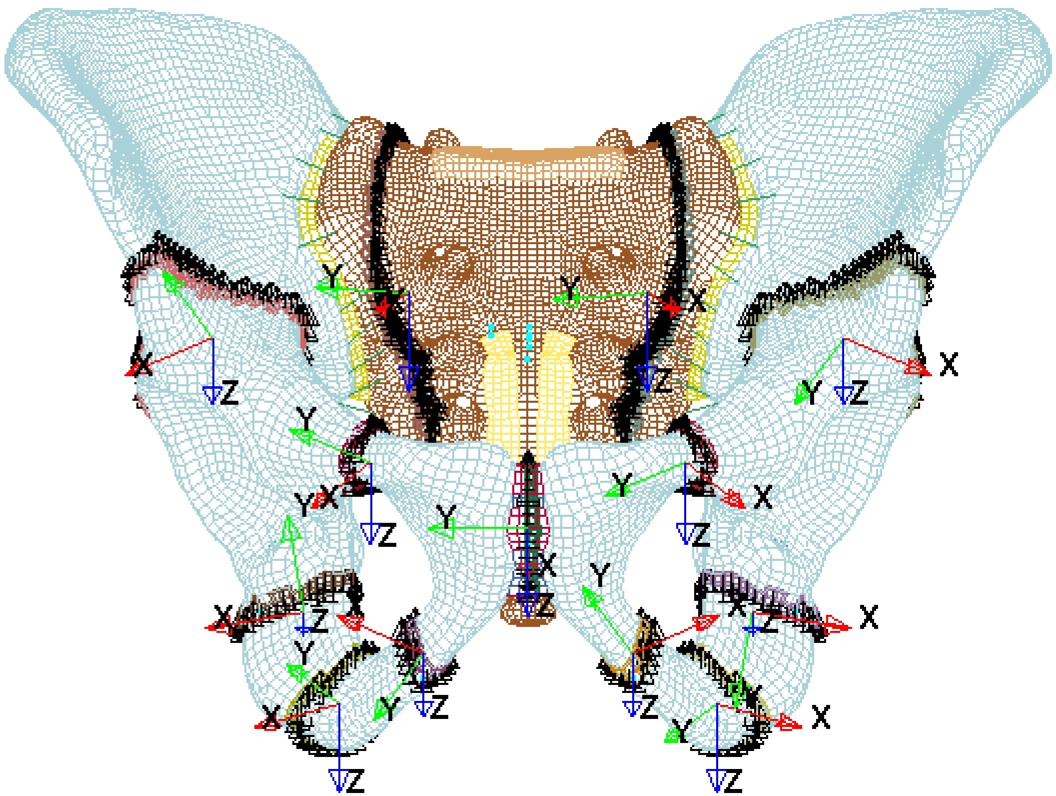

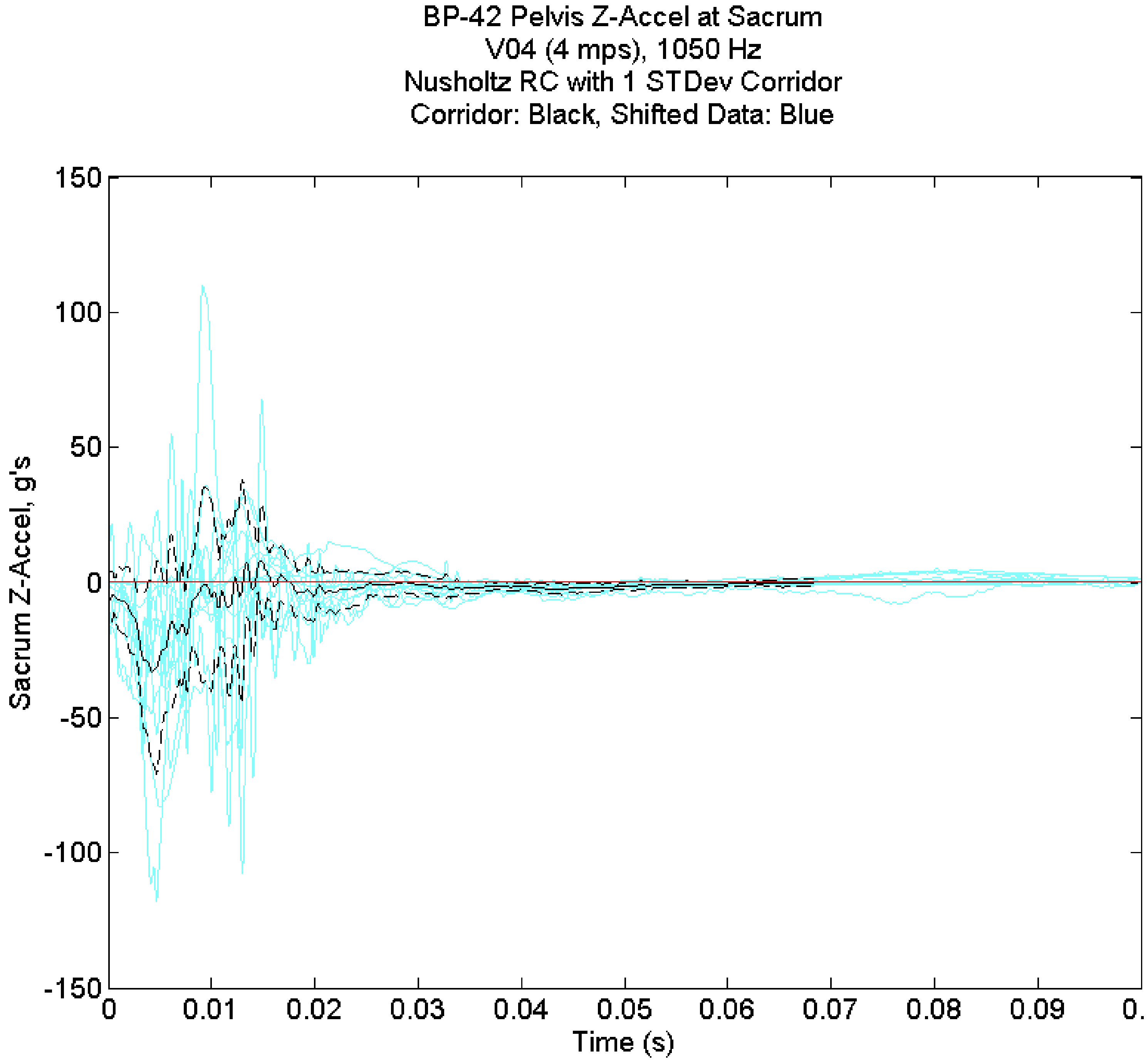
BP-42 Pelvis Z-Accel at Sacrum
V04 (4 mps), 1050 Hz
Nusholtz RC with 1 STDev Corridor
Corridor: Black, Shifted Data: Blue
Sacrum Z-Accel, g's
Time (s)
150
100
50
0
-50
-100
-150
0
0.01
0.02
0.03
0.04
0.05
0.06
0.07
0.08
0.09
0.1

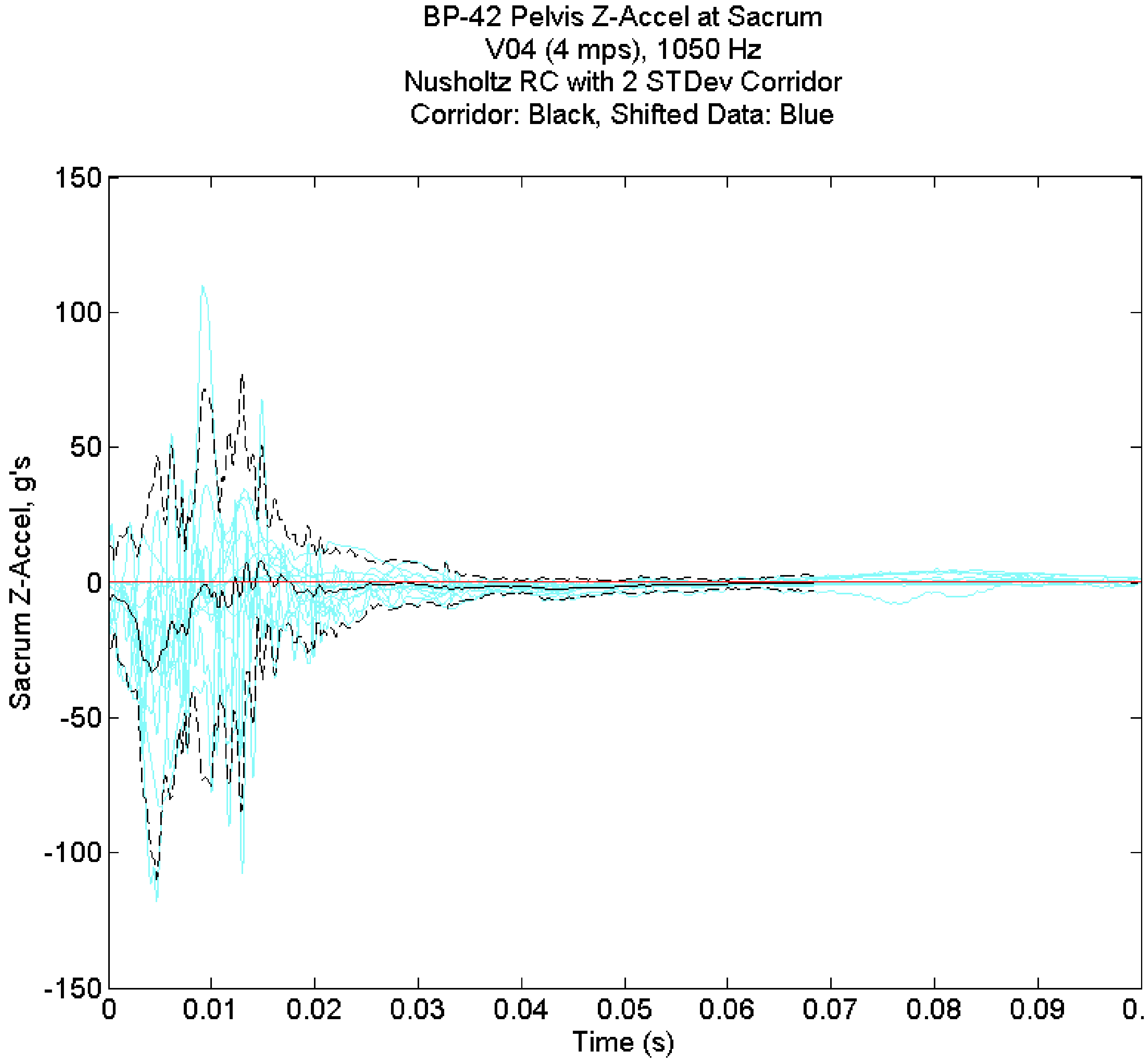
BP-42 Pelvis Z-Accel at Sacrum
V04 (4 mps), 1050 Hz
Nusholtz RC with 2 STDev Corridor
Corridor: Black, Shifted Data: Blue
Sacrum Z-Accel, g's
Time (s)
150
100
50
0
-50
-100
-150
0
0.01
0.02
0.03
0.04
0.05
0.06
0.07
0.08
0.09
0.1

Vertical Load Testing

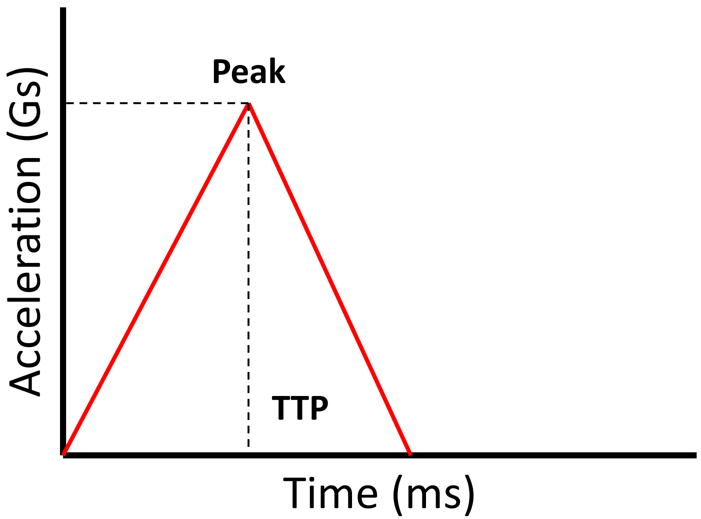

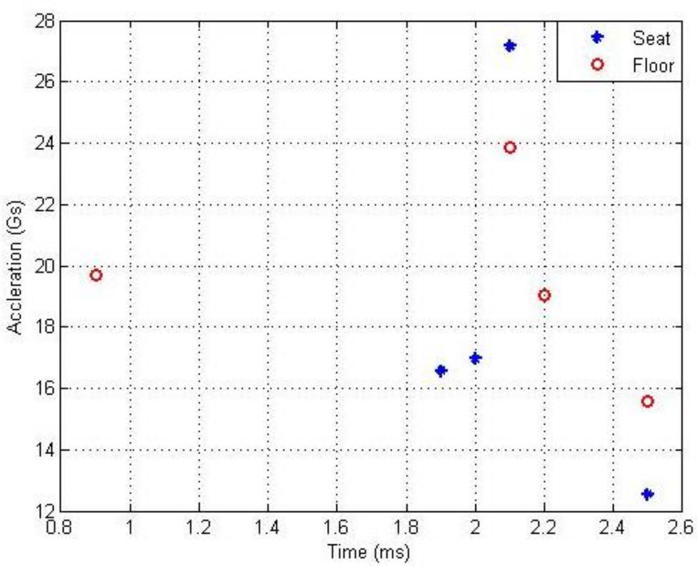

All Test: 4 m/s (non injurious)

Independent pulse (seat/floor)
Performed on PMHS

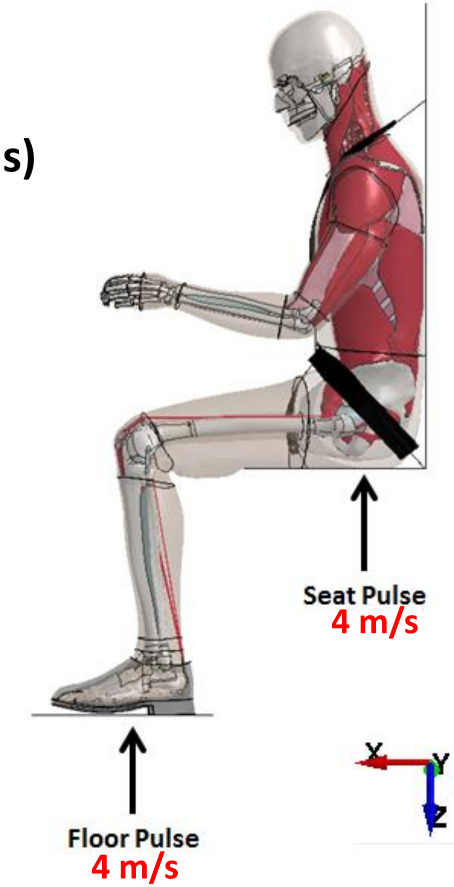

Performers:

Cross-Sectional Forces

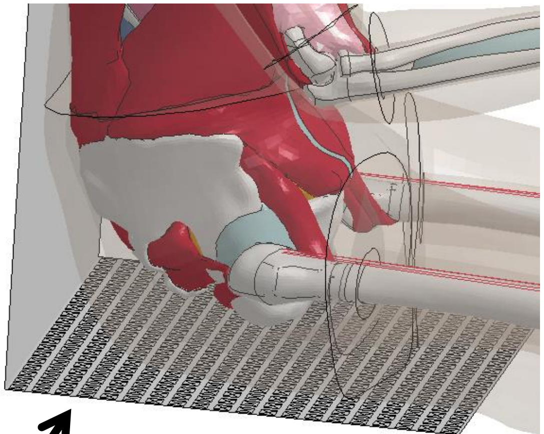

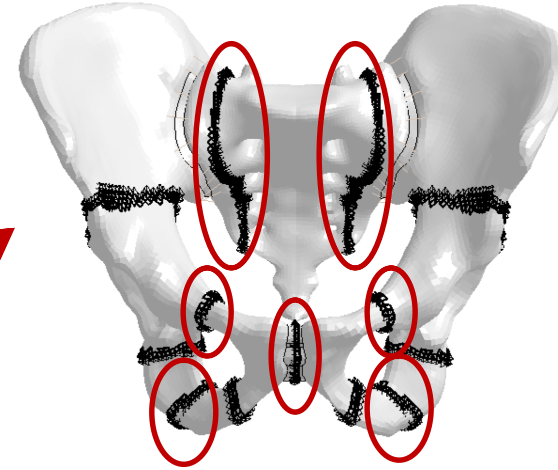

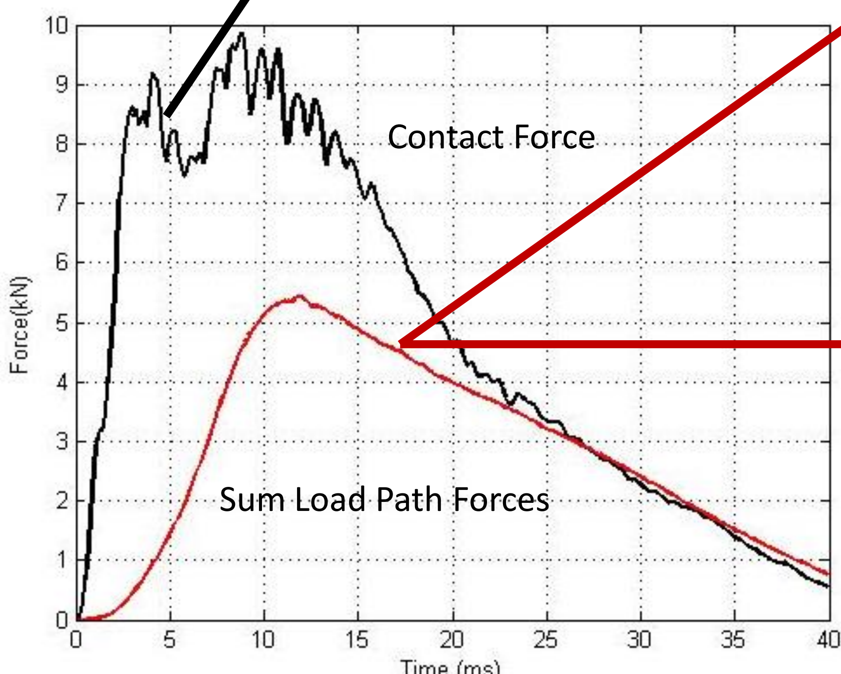

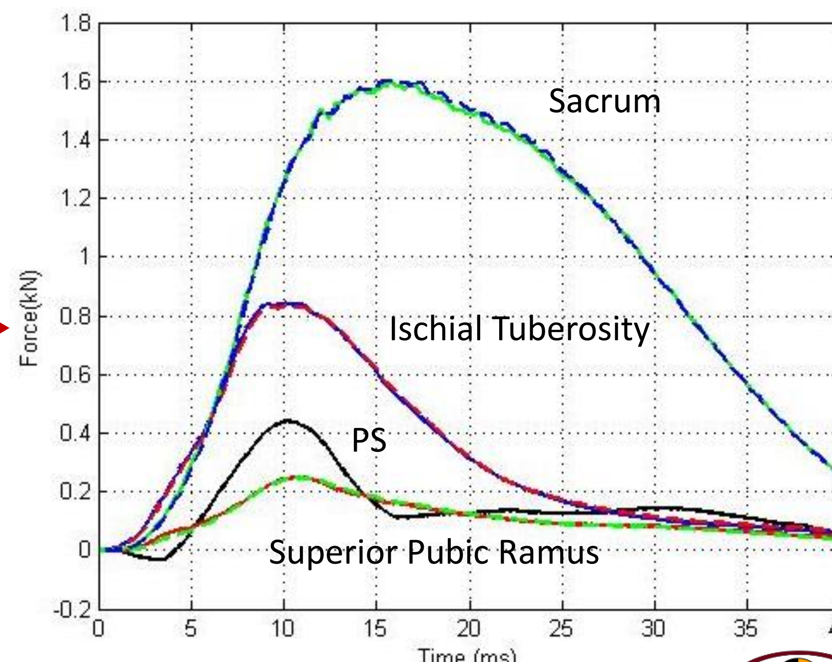

Validation of a 50th Percentile Lumbar FEM for Vertical Loading

C. Pyles, R. Armiger, C. Demetropoulos,
J. Zhang, A. Merkle

JOHNS HOPKINS
APPLIED PHYSICS LABORATORY

Human Computational Modeling

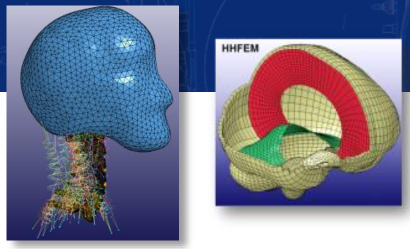

- APL is developing human models for understanding blast, ballistic, and accelerative loading environments
- Focused on end-to-end approach for model development and hierarchical validation
- Collaborative development:
  - Surrogate Modeling
  - Vasculature Modeling
  - Parametric Probabilistic

APPLIED RESEARCH ASSOCIATES, INC.

CFDRC

SwRI

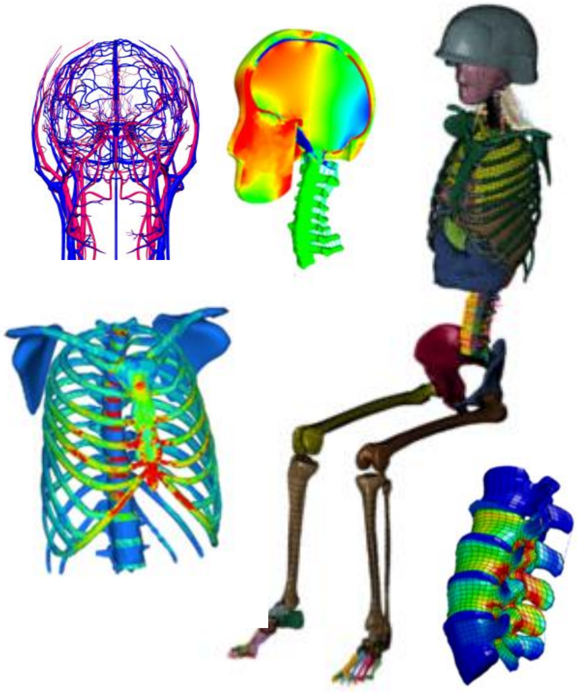

- Validate and apply models in relevant loading environments

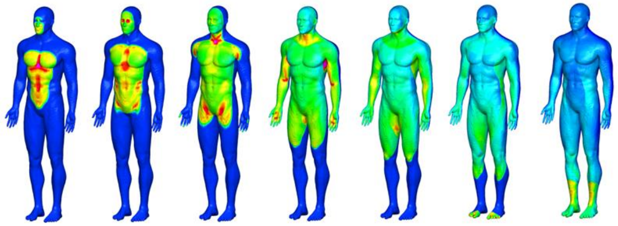

High-rate Human Lumbar Spine Model

- **Underbody blast (UBB) events result in devastating injuries to the seated occupant's lower extremities, pelvis, and lumbar spine**
  - **Lumbar spine is principal structural anatomy linking upper and lower body**
  - **Of UBB casualties, 18% WIA, and 26% KIA sustain lumbar fractures**
    - **Alvarez, 2011**
- **High Fidelity Lumbar Spine Finite Element Model (FEM)**
  - **Risk assessment and injury mitigation**
- **Requires hierarchical model validation**
  - **Material → Component (Lumbar) → System (Whole Body)**

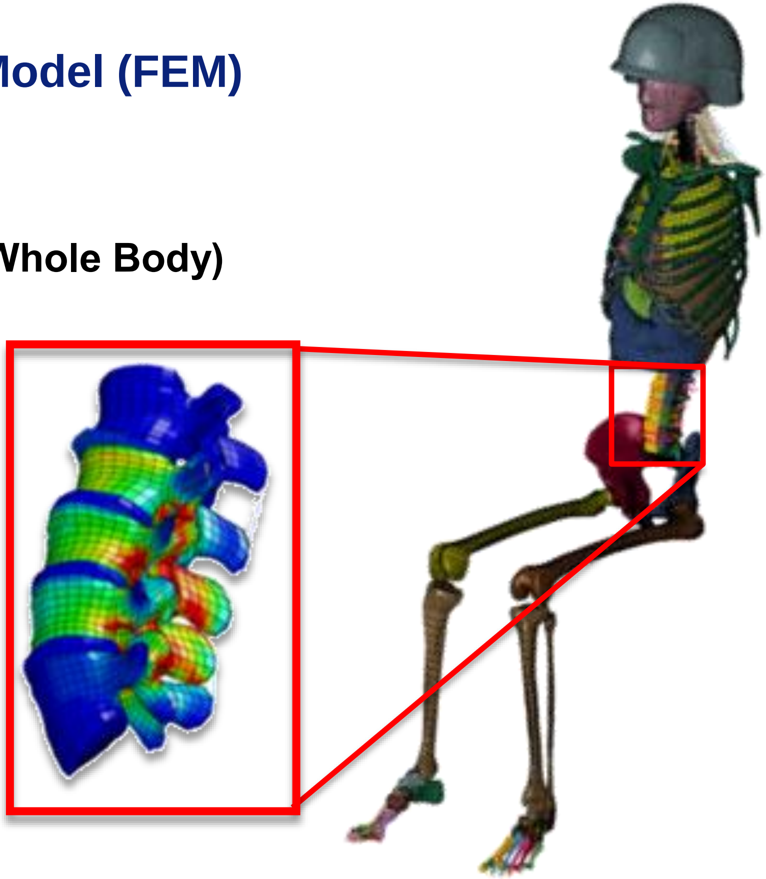

Human Lumbar Spine Model Summary

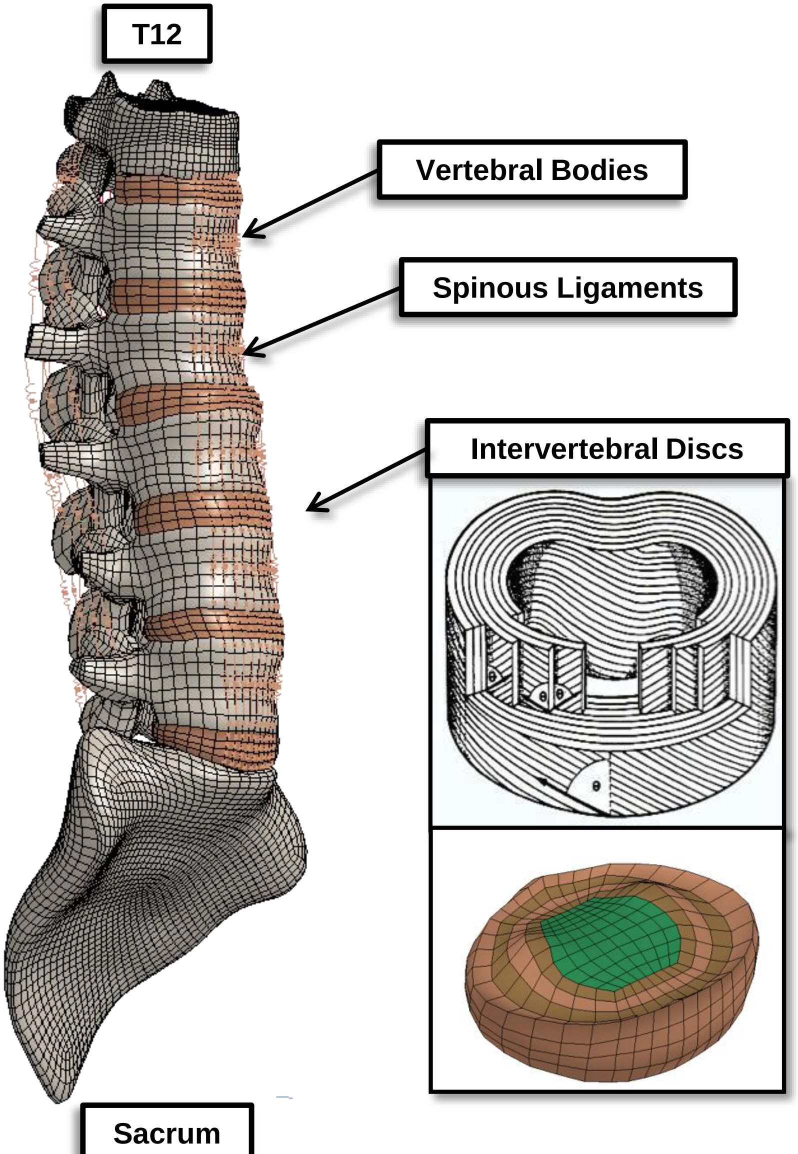

- **LS-DYNA FEM (LSTC)**
- **Anatomical mesh**
  - **Reconstructed using CT scans from Visible Human Project**
  - **Scaled to size of 50th percentile male soldier**
  - **Mirrored to induce symmetry**
  - **Repositioned from supine to seated posture**
  - **~30,000 solid hexahedral elements**
- **Biological tissue properties**
  - **Nucleus:** Mooney-Rivlin, incompressible, hyperelastic
  - **Annulus:** Fiber reinforced Mooney-Rivlin
  - **Spinous ligaments:** 2D, non-linear elastic
  - **Bone:** Elastic
    - Cortical shell
    - Trabecular bone

Material Level Characterization

Tissue-Level Characterization

- **Delineate contribution of individual soft tissue components on lumbar response**
  - **Approach:** Sequential Dissection
- **2 primary experimental loading cases**

Quasi-Static Bending (Hueur et al., 2006)

- **Applied pure bending moment up to 10 N-m in flexion or extension**
- **Range of motion (ROM) measured**

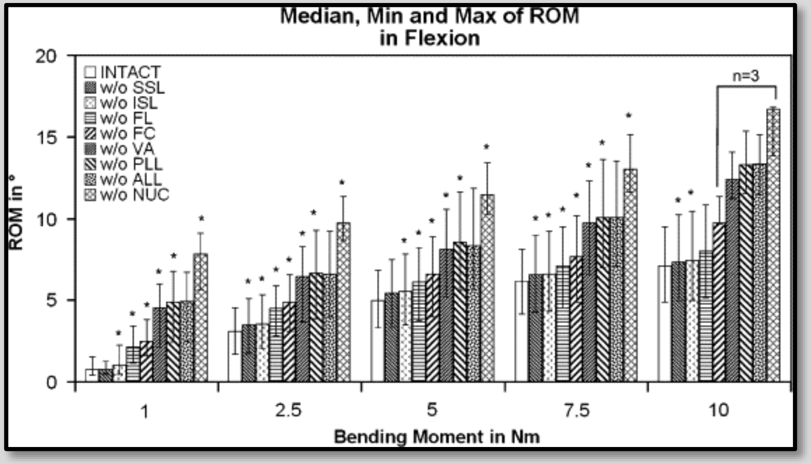

High-Rate Combined Compression and Bending (Bradfield et al., 2015)

JOHNS HOPKINS
APPLIED PHYSICS LABORATORY

- **Static pre-compression of 36.2 kg**
- **Dynamic 4300 N axial load at various moment arm lengths**
  - **Peak moments > 40 N-m**
- **Compression and range of motion measured**

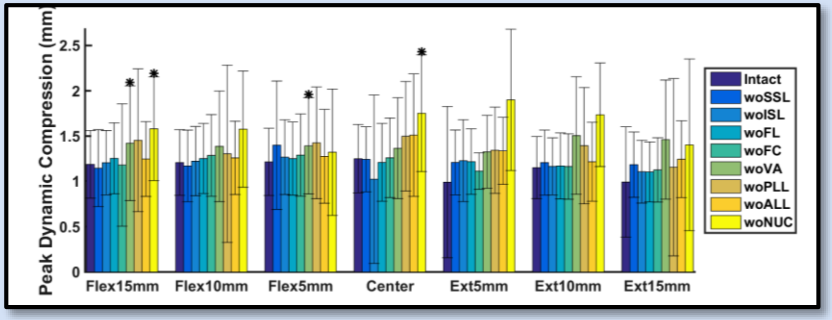

Methods
Sequential Dissection

Intact State

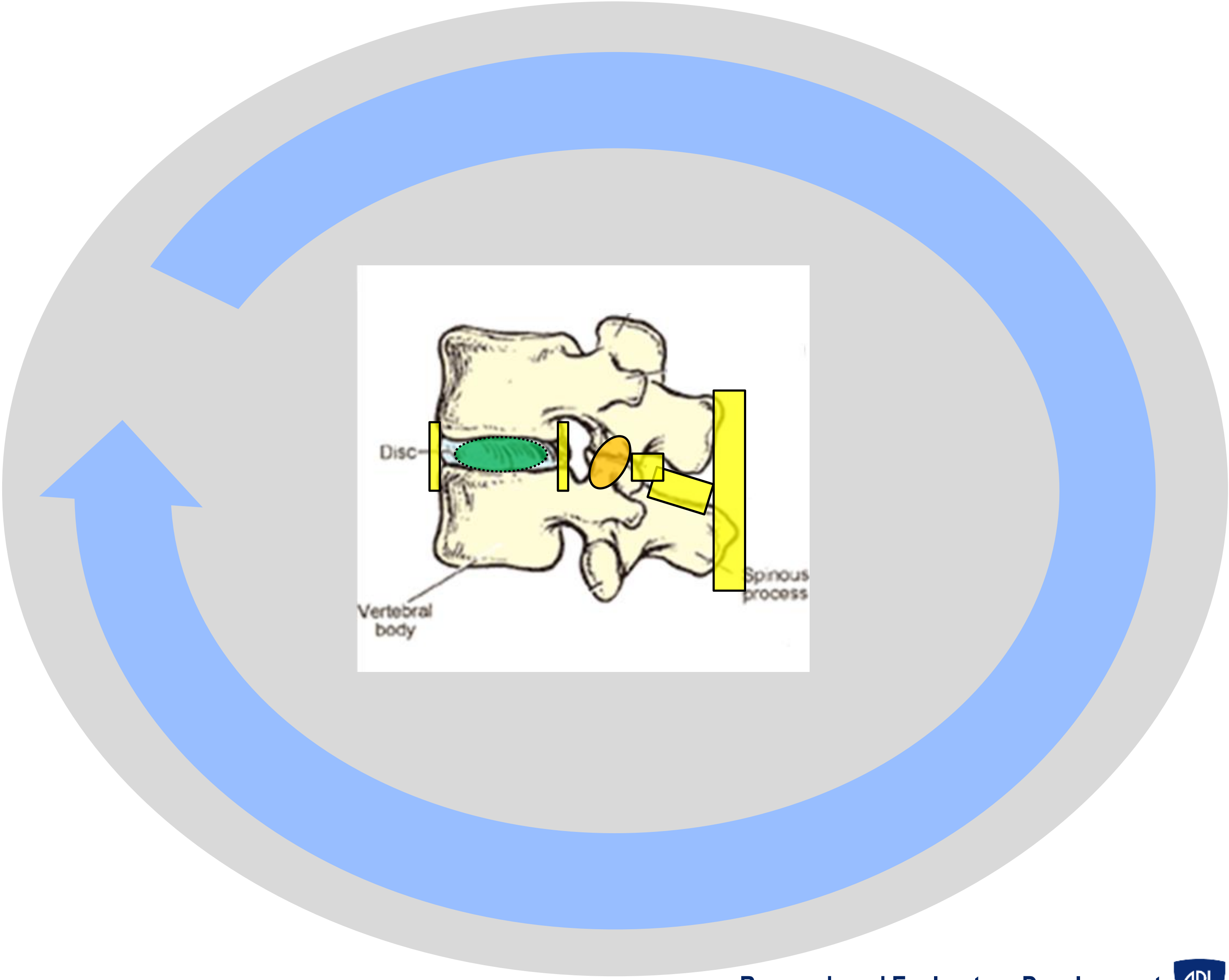

Methods
Sequential Dissection

Intact State

Supraspinous Ligament Removed

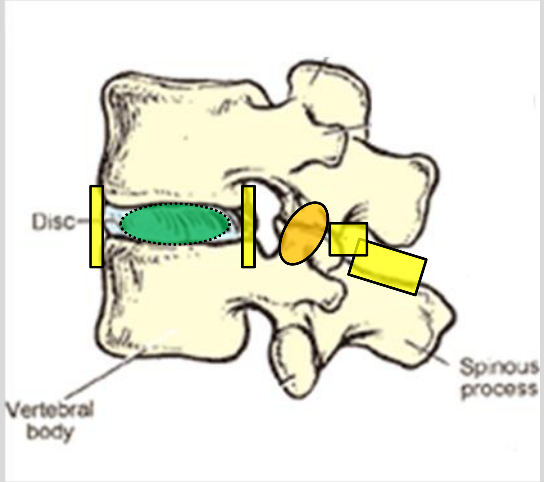

Methods
Sequential Dissection

Intact State

Supraspinous Ligament Removed

Interspinous Ligament Removed

Methods
Sequential Dissection

Intact State

Supraspinous Ligament Removed

Interspinous Ligament Removed

Ligamentum Flavum Removed

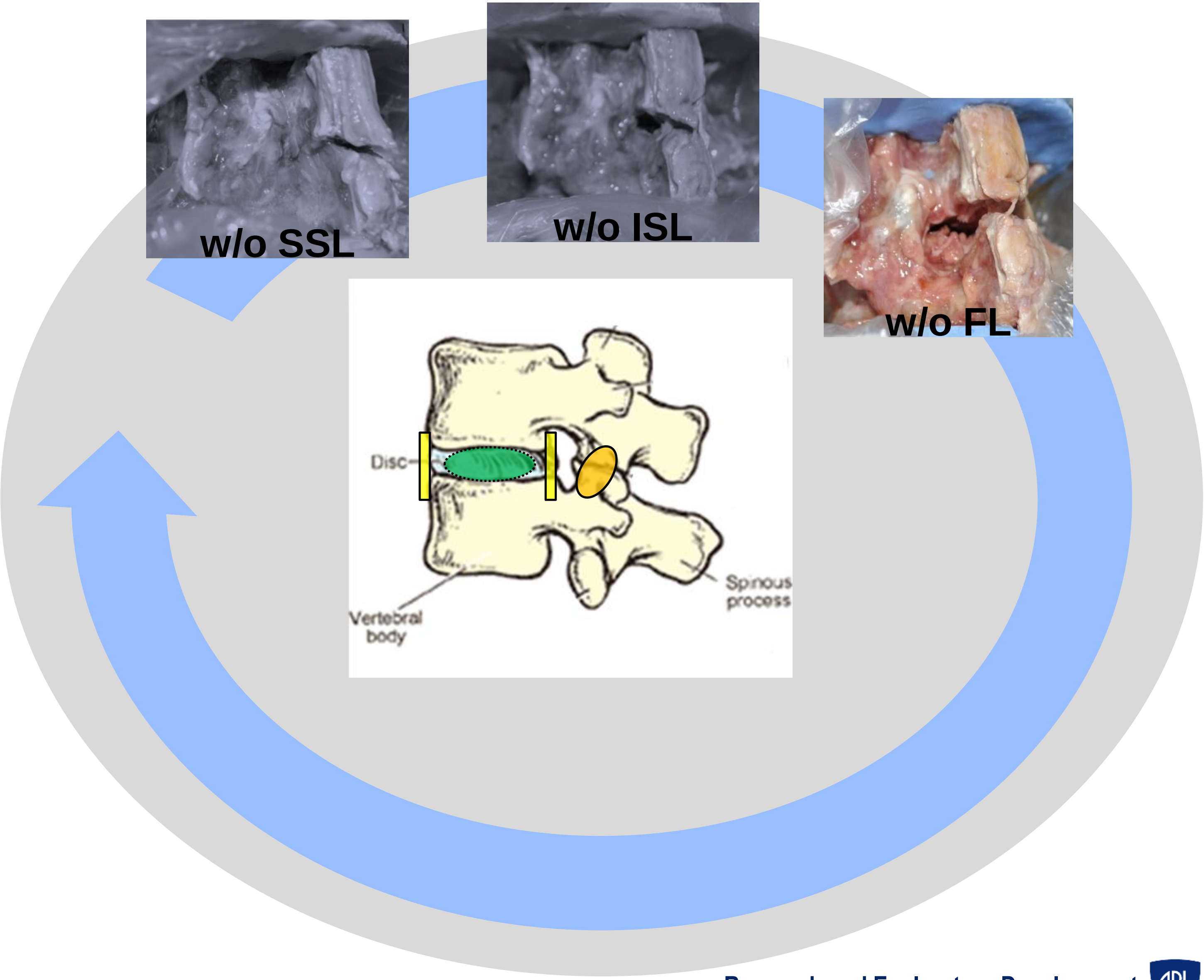

Methods
Sequential Dissection

Intact State

Supraspinous Ligament Removed

Interspinous Ligament Removed

Ligamentum Flavum Removed

Facet Capsules transected

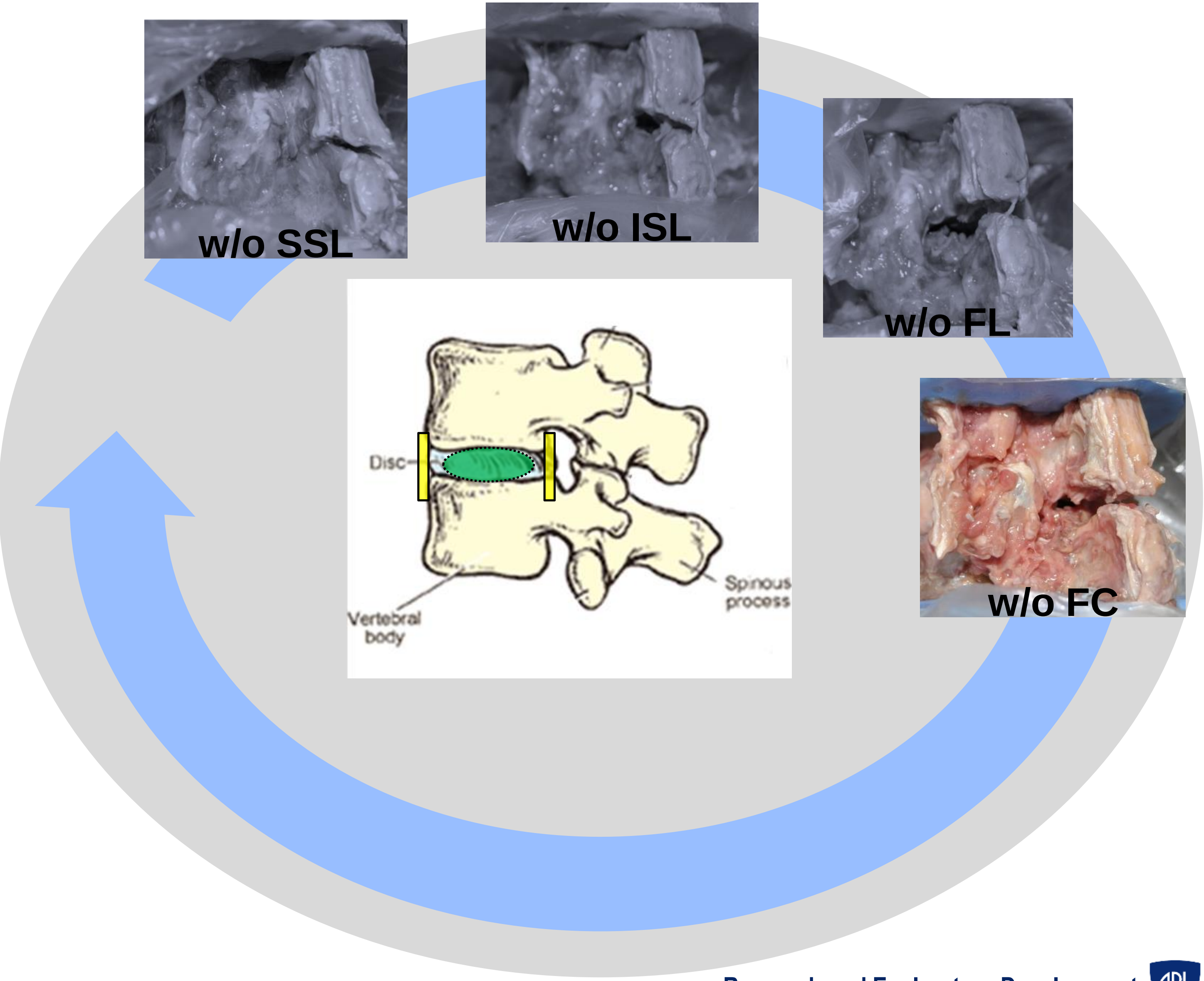

Methods
Sequential Dissection

Intact State

Supraspinous Ligament Removed

Interspinous Ligament Removed

Ligamentum Flavum Removed

Facet Capsules transected

Posterior Elements Removed

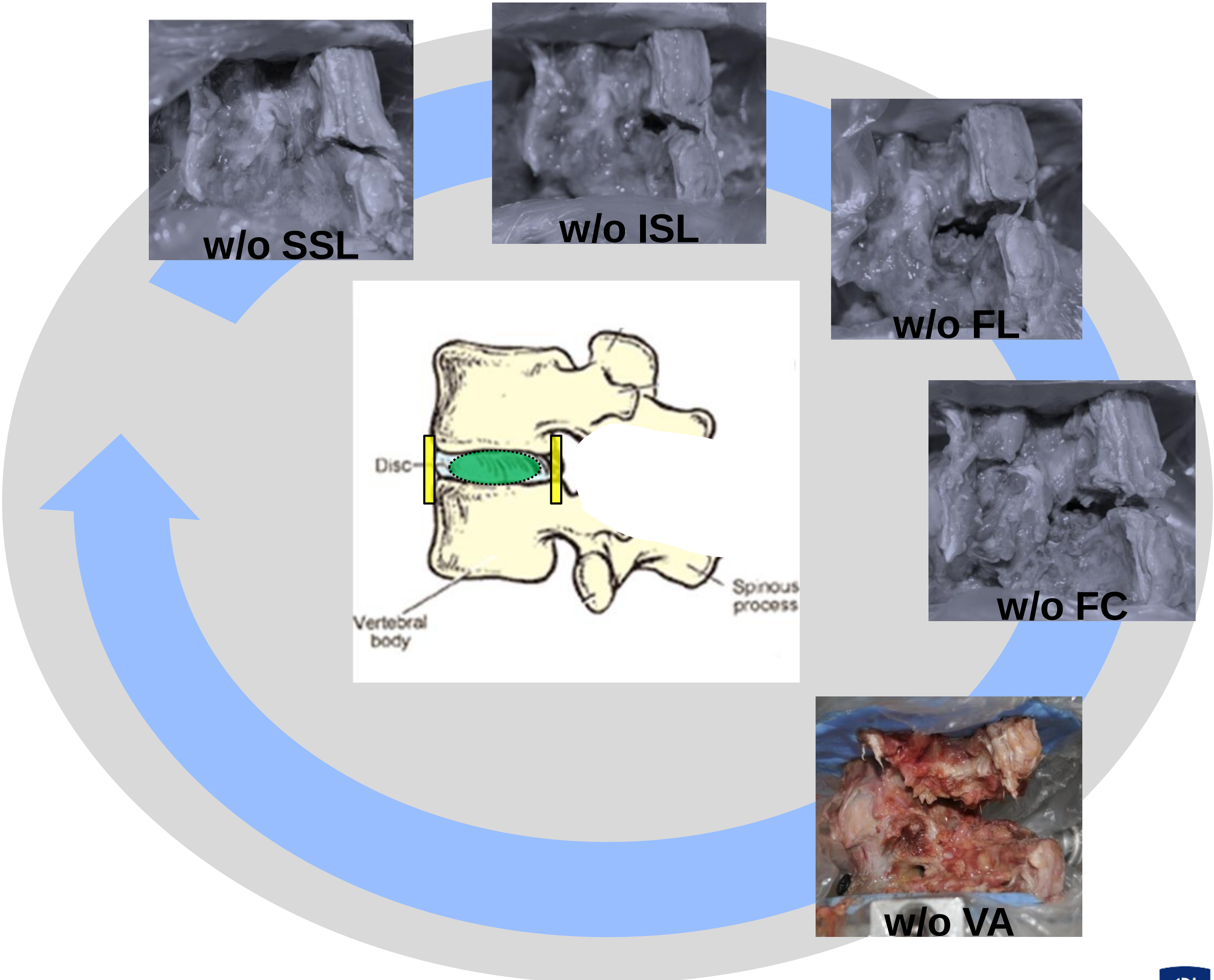

Methods
Sequential Dissection

- Intact State
- Supraspinous Ligament Removed
- Interspinous Ligament Removed
- Ligamentum Flavum Removed
- Facet Capsules transected
- Posterior Elements Removed
- Posterior Longitudinal Ligament Transected

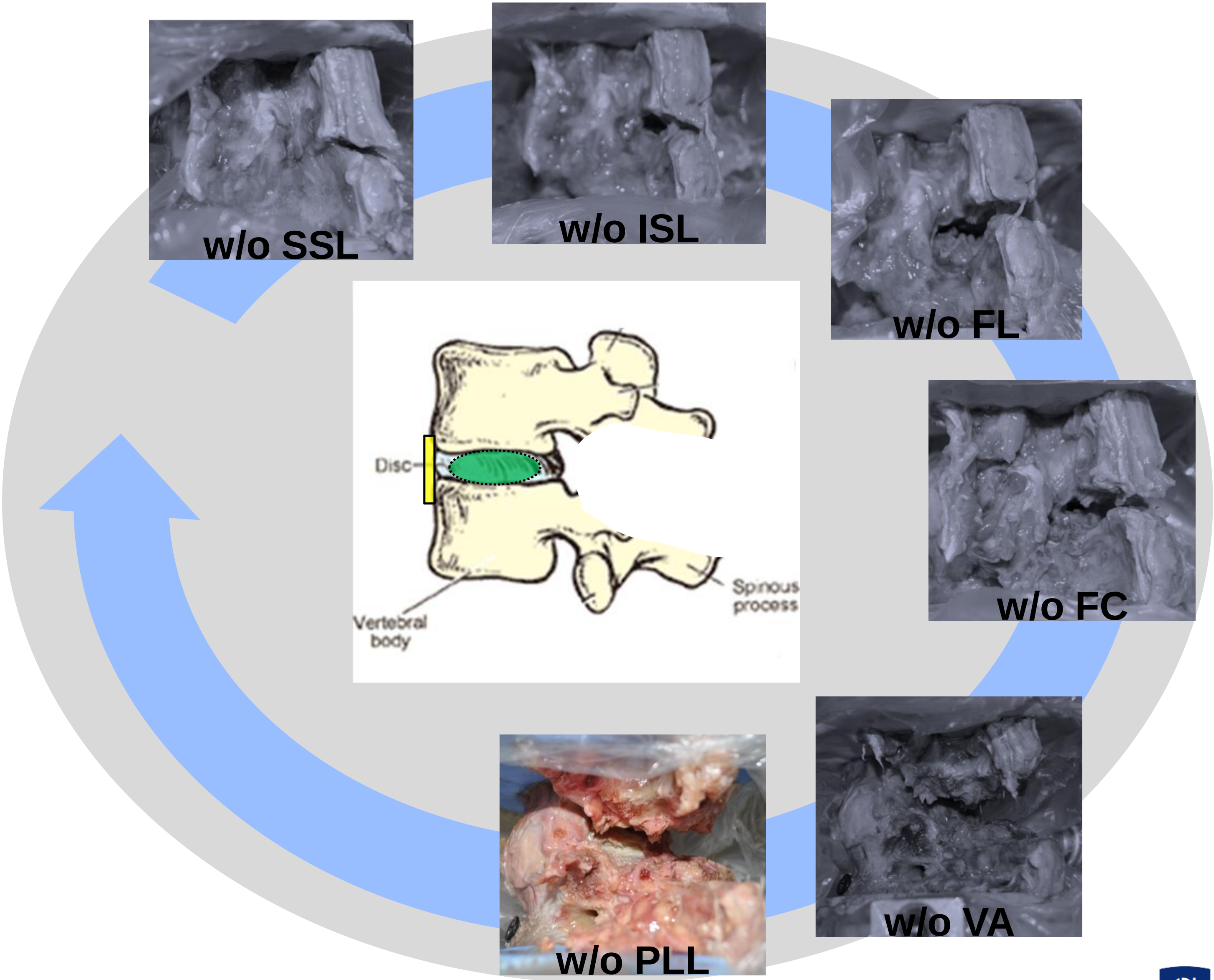

Methods
Sequential Dissection

- Intact State
- Supraspinous Ligament Removed
- Interspinous Ligament Removed
- Ligamentum Flavum Removed
- Facet Capsules transected
- Posterior Elements Removed
- Posterior Longitudinal Ligament Transected
- Anterior Longitudinal Ligament Transected

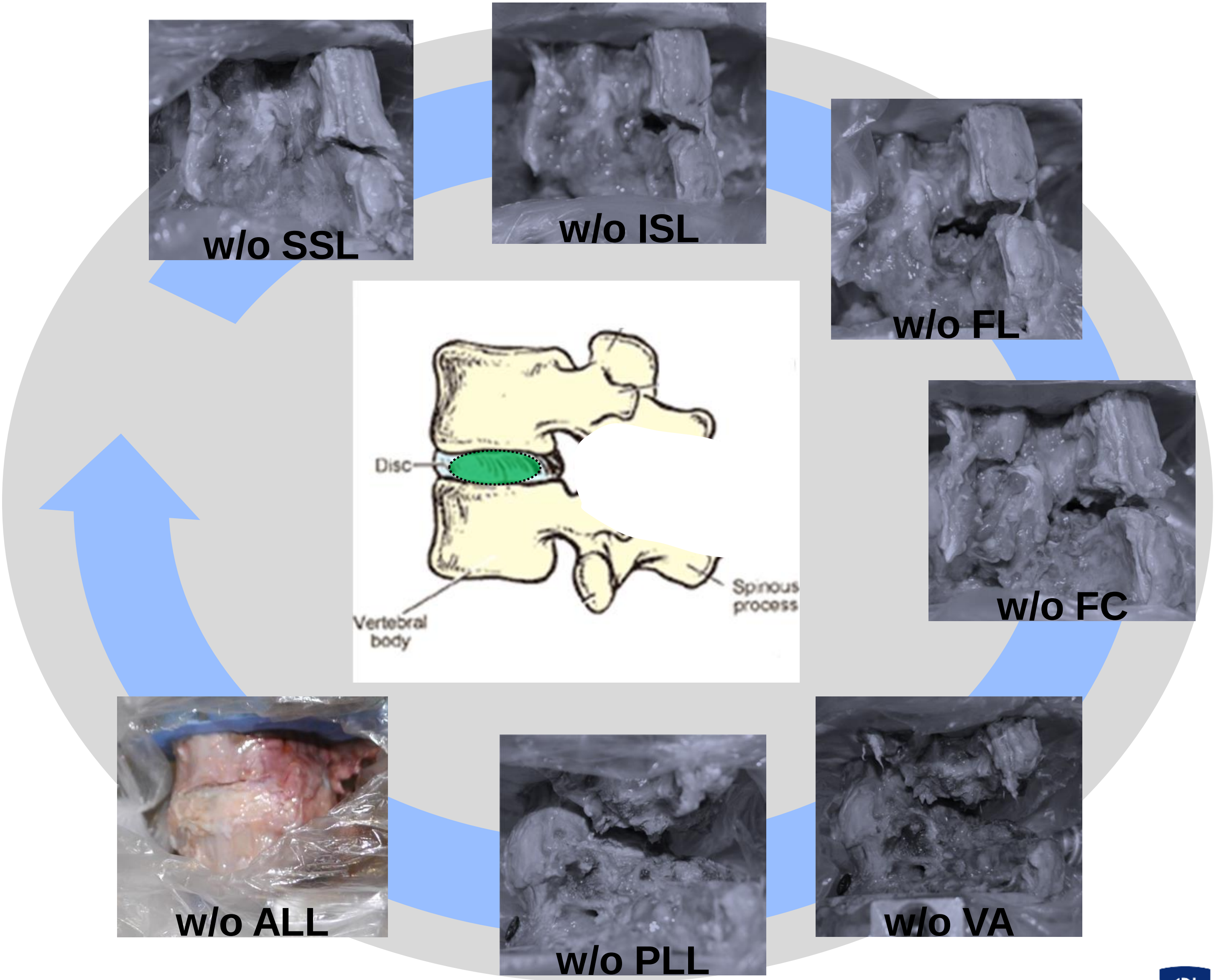

Methods
Sequential Dissection

Intact State

Supraspinous Ligament Removed

Interspinous Ligament Removed

Ligamentum Flavum Removed

Facet Capsules transected

Posterior Elements Removed

Posterior Longitudinal Ligament Transected

Anterior Longitudinal Ligament Transected

Nucleus Pulposus Removed

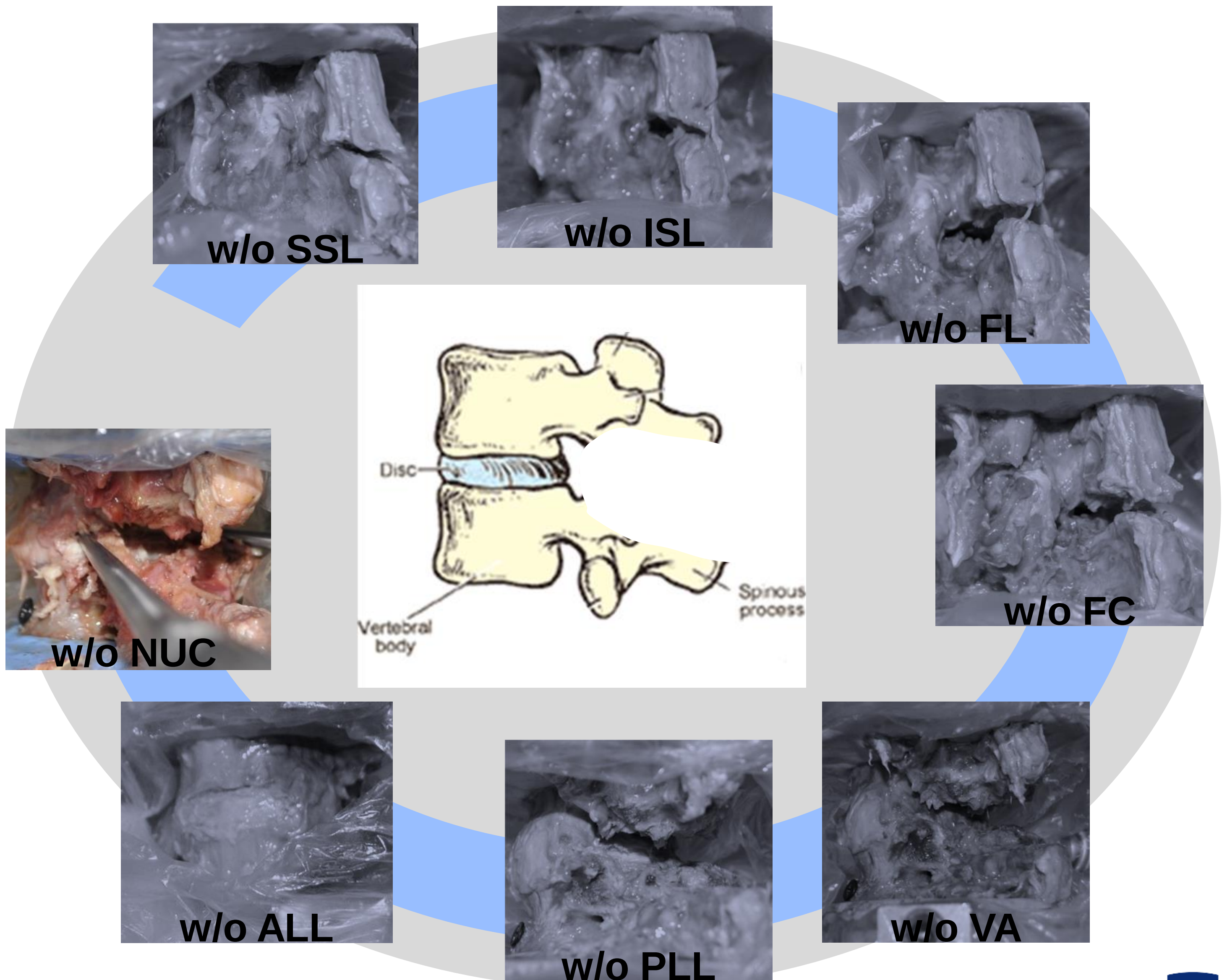

Material Parameter Determination: Quasi-Static Bending

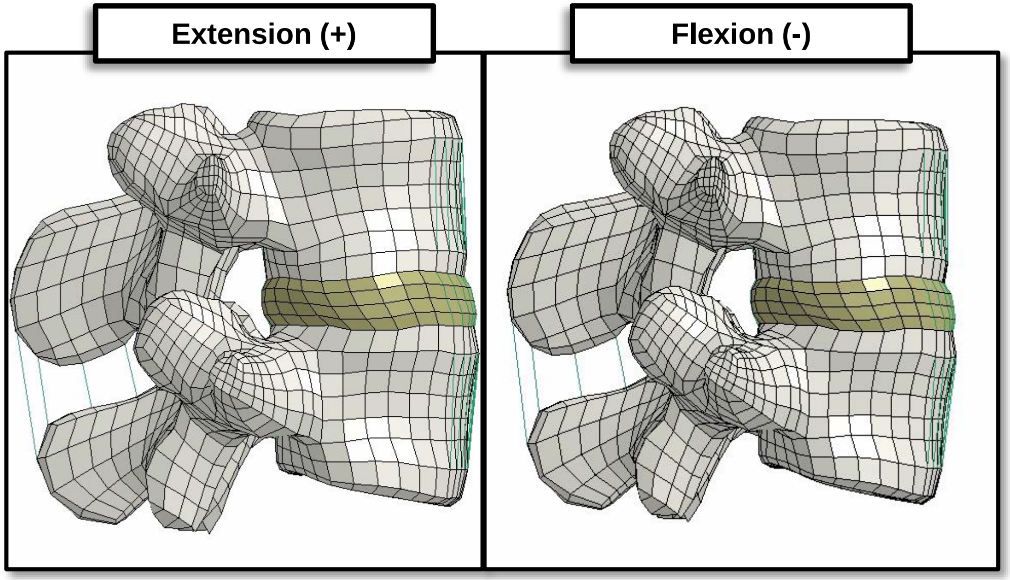

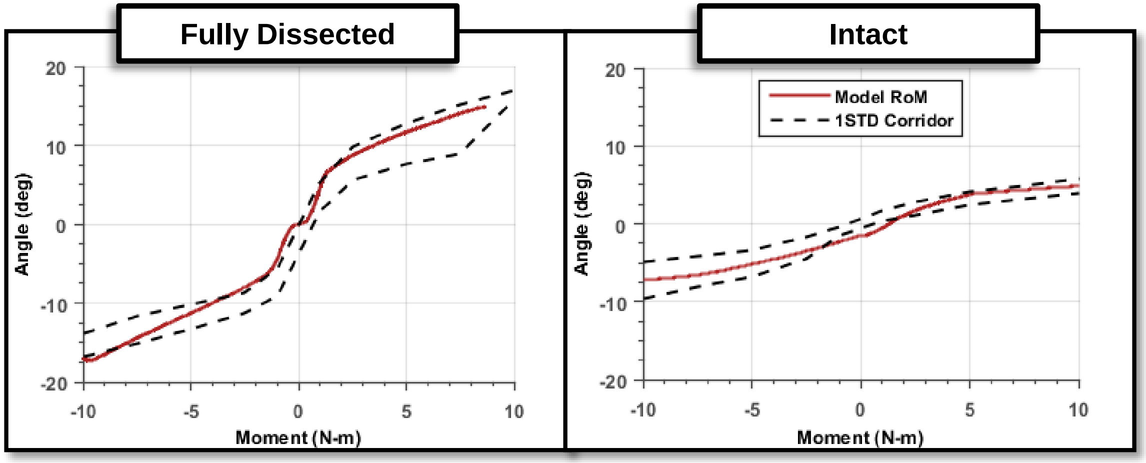

- **Rationale**
  - Add soft tissue components in reverse of sequential dissection experiments
  - Optimize constitutive properties
- **Boundary Conditions**
  - Statically ramped bending moment applied to upper (L4) vertebra
  - Lower (L5) vertebra constrained in all degrees of freedom
- **Outputs**
  - Resulting range of motion compared against experiments at each dissection stage
- **Quasi-statically optimized motion segment allows for proper settling for high-rate compression**

Material Parameter Determination: High-Rate Compression

- **Rationale**
  - Determine high-rate material properties of lumbar spine leveraging sequential dissection experiments
- **Boundary Conditions**
  - Static pre-compression (36.2 kg)
  - High-rate compression according to experimental loads (~4.3 kN over 5 ms)
- **Outputs**
  - Resulting compression compared against experiments at each dissection stage

Material	Constitutive Model	Optimized Dynamic Parameters (MPa)
Annulus matrix	Fiber-Reinforced Mooney-Rivlin	$C_1 = 0.60$ $C_2 = 0.15$ ($E \approx 4.5$)
Annulus fibers		$C_5 = 317.9$
Nucleus	Mooney-Rivlin	$C_1 = 0.43$, $C_2 = 0.10$ ($E \approx 3.18$)

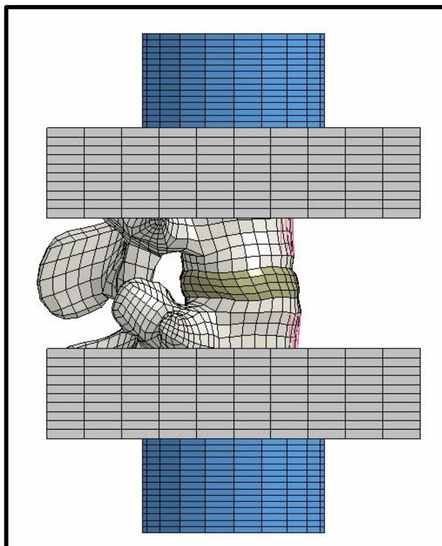

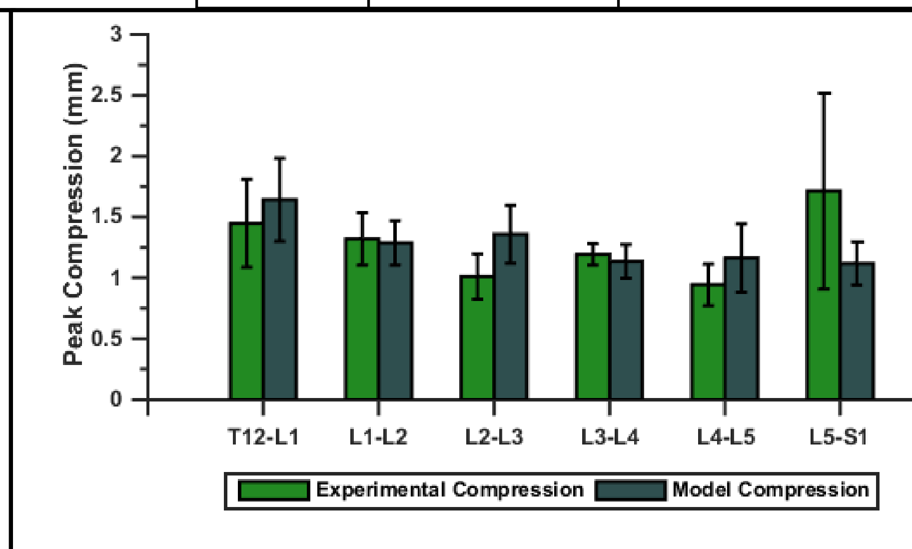

Component-Level Validation

Human Lumbar Spine FEM: VertAc Rig Validation

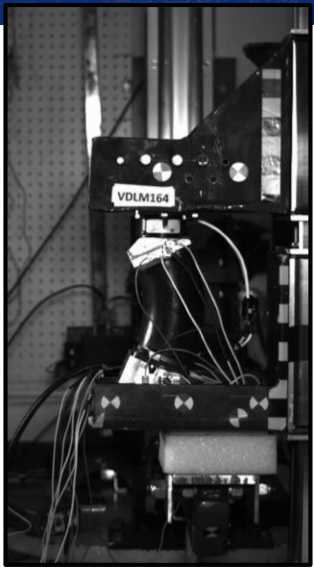

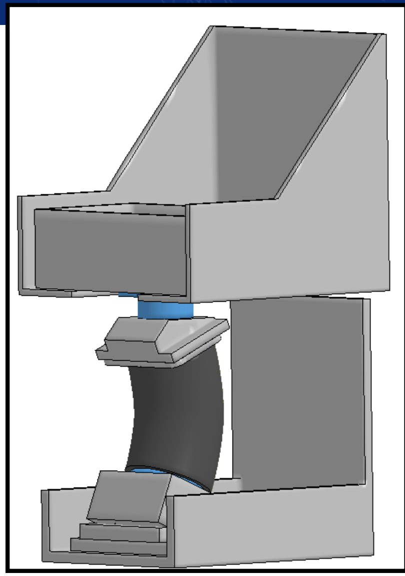

- **VertAc FEM:** Developed from MCW CAD and physical measurements
- **Hybrid-III Lumbar FEM**: Open-source LSTC model
  - Polymer material updated to reflect 85 Shore A hardness
- **Validation metric:**
  - Transmitted axial force compared to experiments at 1.2 m/s and 2.4 m/s
  - CORA scores calculated
    - See appendix for weights

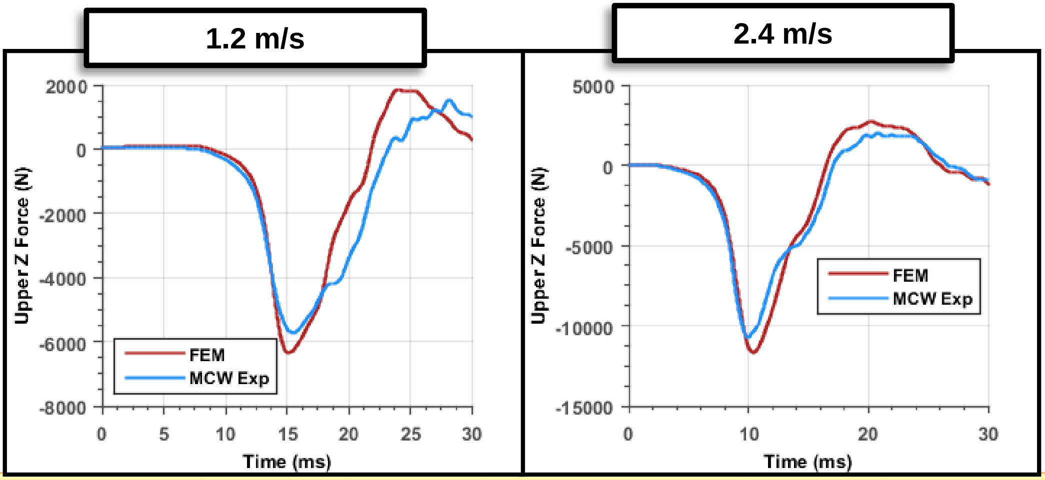

VertAc test system simulation validates boundary conditions

	L1 Force (+Z) CORA Score
1.2 m/s	0.862
2.4 m/s	0.924

Transition from Supine to Seated Posture

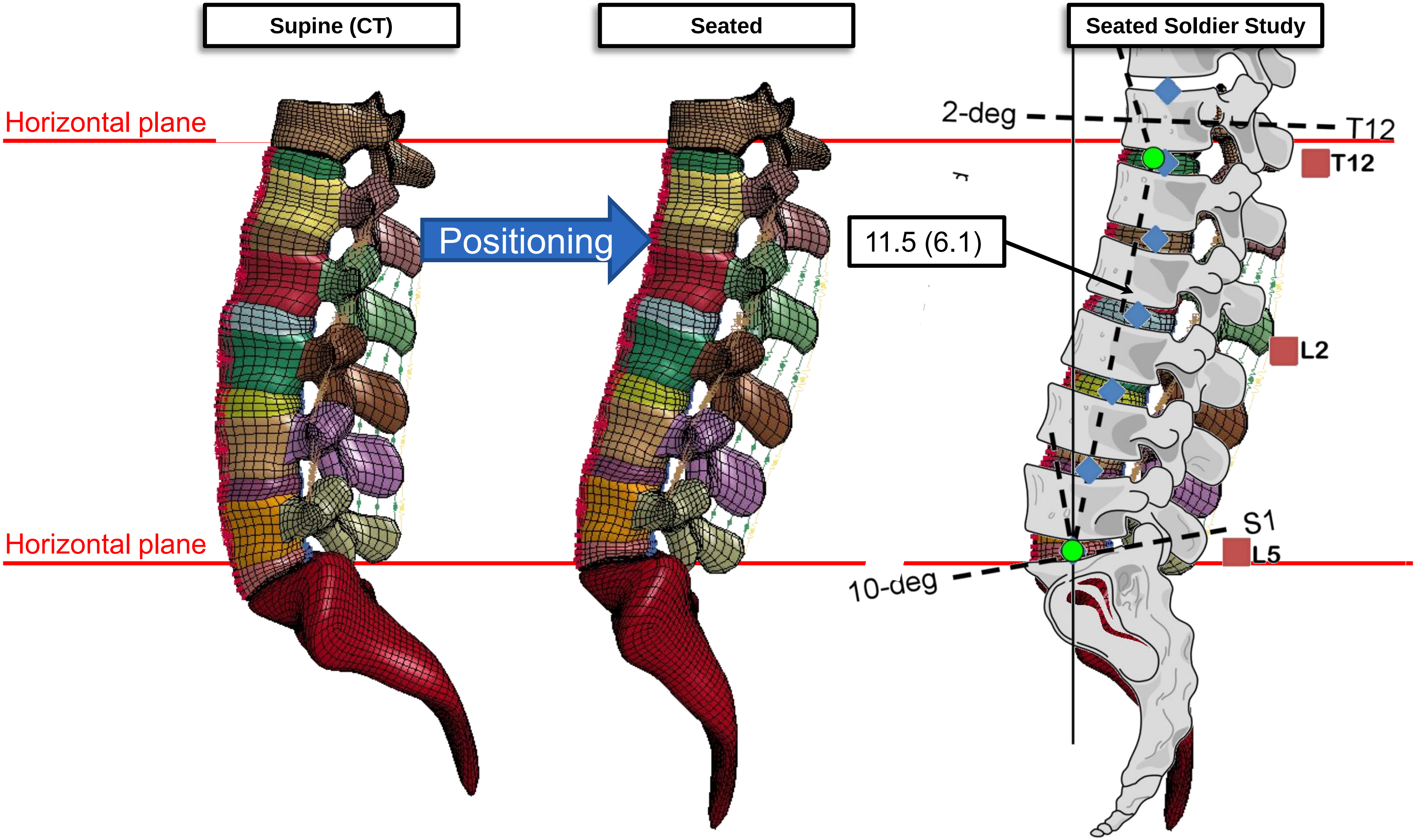

Vertical Impact Validation Overview

- **Model:**
  - **VertAc test rig**
    - Validated with HIII loading cases
  - **Human high fidelity lumbar FEM**
    - Tissue level characterization
    - Repositioned according to seated soldier study
- **Boundary Conditions:**
  - **Prescribed velocity applied to lower sled**
  - **Posterior carriage bearings constrained to slide vertically**
- **Outputs:**
  - **Forces/Moments: Load cell cross-sections**
  - **Nodal Accelerations: Constrained-interpolation method at 6DX blocks**
- **Post-processing:**
  - **CFC 1000 filter for forces and moments**
  - **3kHz filter for accelerations**
  - **Force and moment transformations to joint centers**

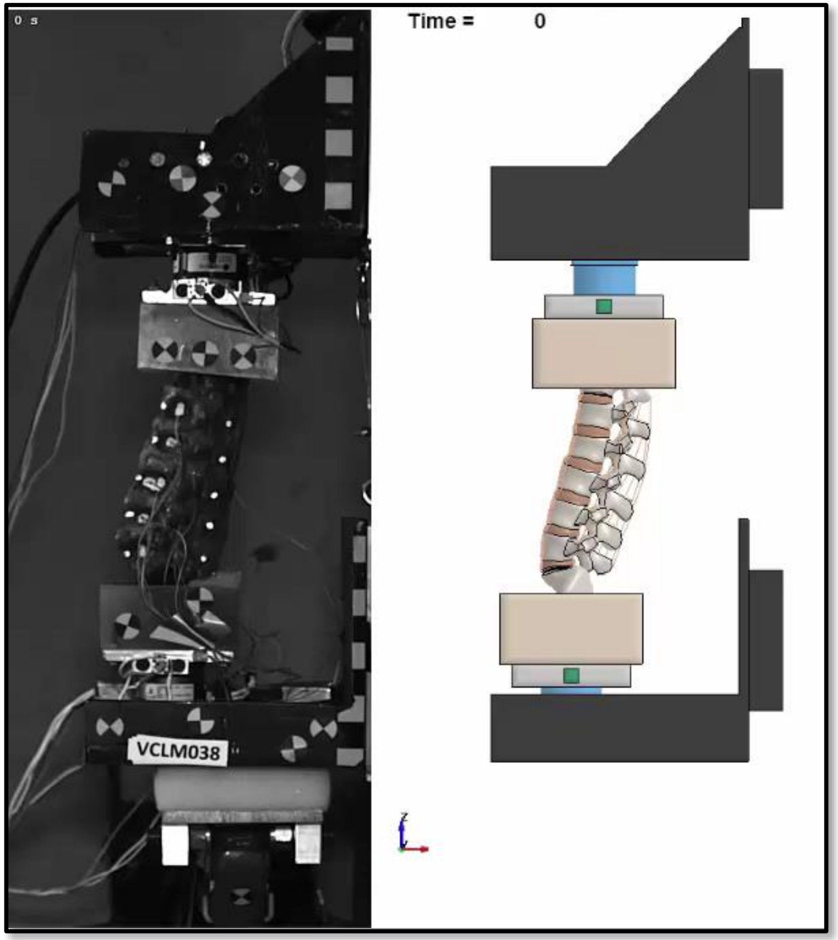

Human Lumbar Spine FEM: 0.8 m/s BRC Comparison

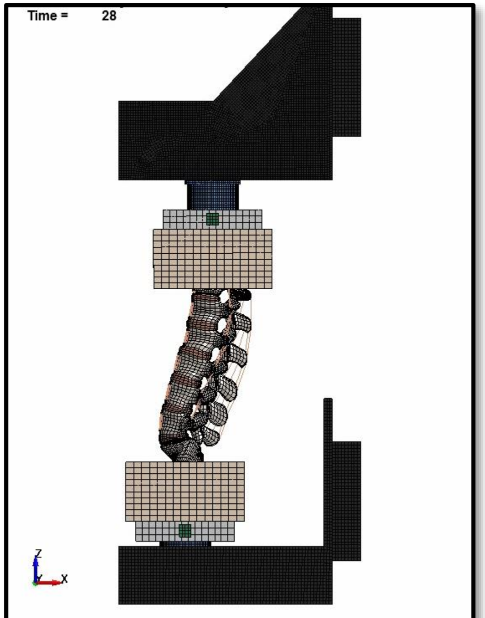

- ***Excellent agreement for force and acceleration***
- ***Peak moment under-predicted***
  - ***Large variation within PMHS (posture, facet engagement, tissue variation, etc.)***

CORA Scale

Velocity	Response	Shape	Magnitude	Phase	Corridorr	Total
V1	Az, upper	0.962	0.678	1.00	0.71	0.795
V1	Fz, upper	0.978	0.849	1.00	0.722	0.722
V1	My, upper	0.651	0.129	0.97	0.846	0.715

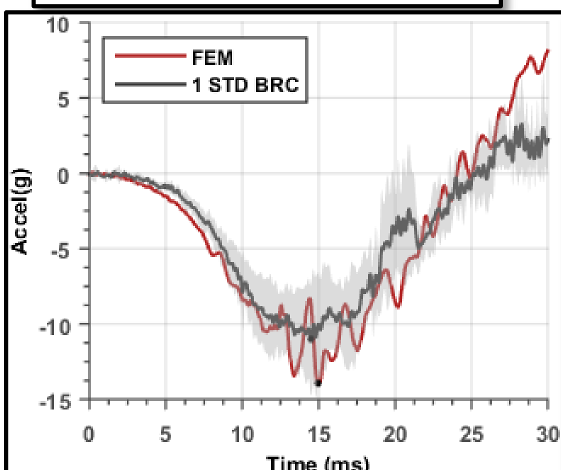

Upper Acceleration

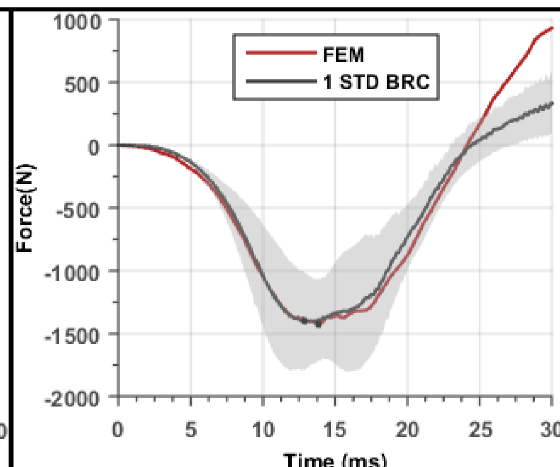

Upper Force

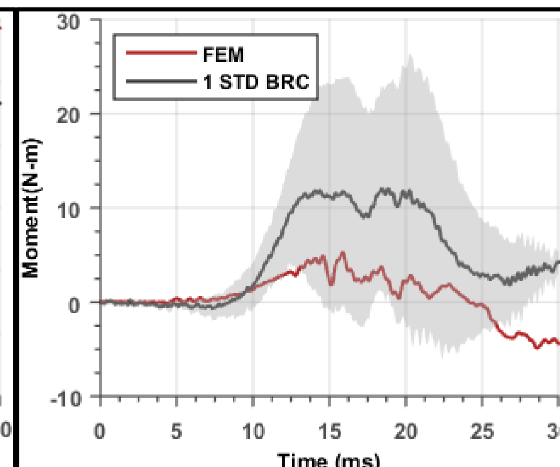

Upper Moment

Human Lumbar Spine FEM: 1.2 m/s BRC Comparison

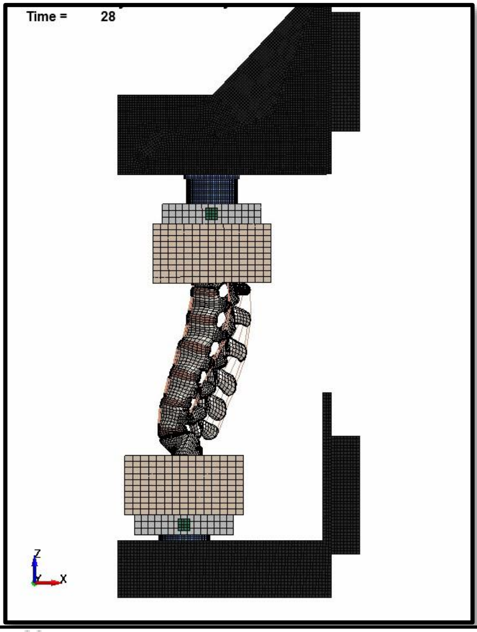

- ***Excellent agreement for force and acceleration***
- ***Peak moment under-predicted***
    - ***Large variation within PMHS (posture, facet engagement, tissue variation, etc.)***

CORA Scale

0 — 1

Velocity	Response	Shape	Magnitude	Phase	Corridorr	Total
V2	Az, upper	0.936	0.531	1.00	0.601	0.712
V2	Fz, upper	0.963	0.646	1.00	0.574	0.722
V2	My, upper	0.500	0.18	0.00	0.632	0.429

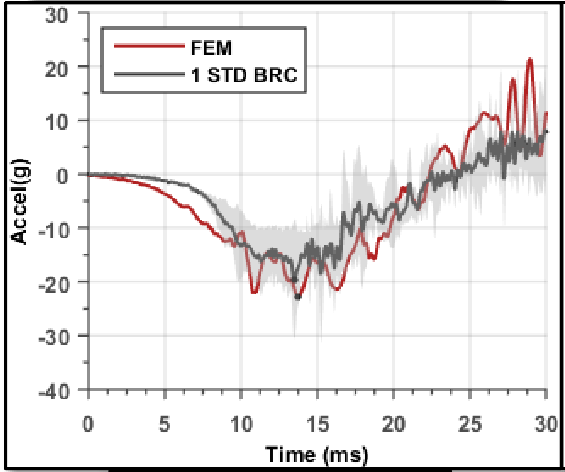

Upper Acceleration

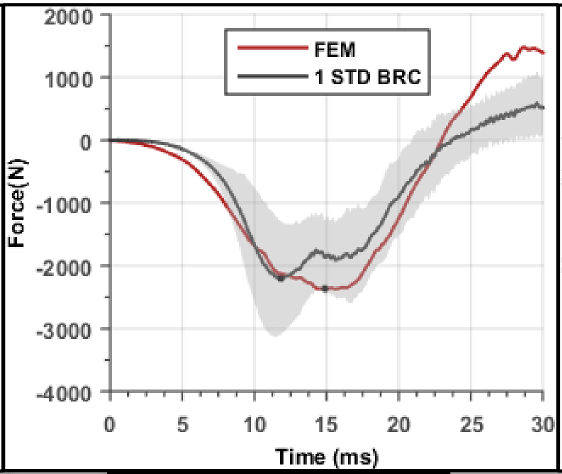

Upper Force

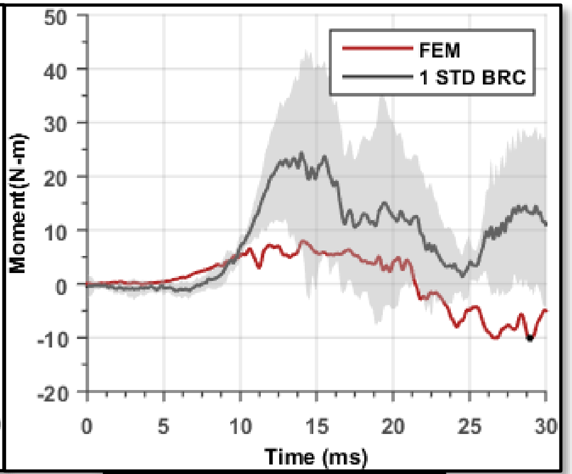

Upper Moment

Human Lumbar Spine FEM: 2.4 m/s BRC Comparison

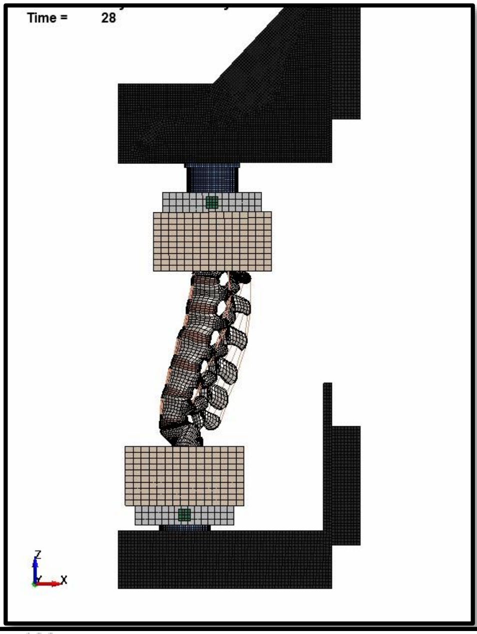

- ***Excellent agreement for force and acceleration***
- ***Peak moment under-predicted***
  - ***Large variation within PMHS (posture, facet engagement, tissue variation, etc.)***

CORA Scale

Velocity	Response	Shape	Magnitude	Phase	Corridorr	Total
V3	Az, upper	0.839	0.858	1.00	0.629	0.764
V3	Fz, upper	0.921	0.754	1.00	0.395	0.643
V3	My, upper	0.633	0.226	0.00	0.747	0.517

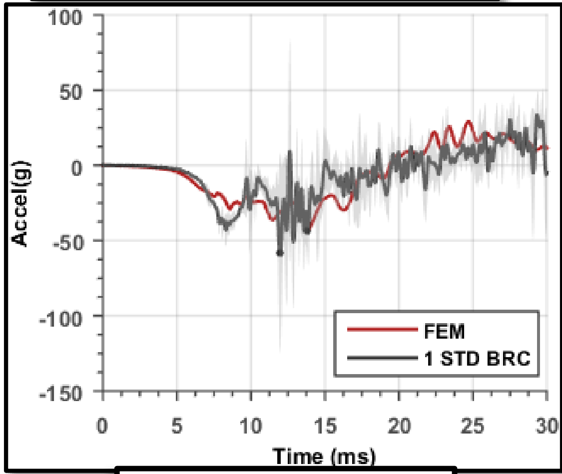

Upper Acceleration

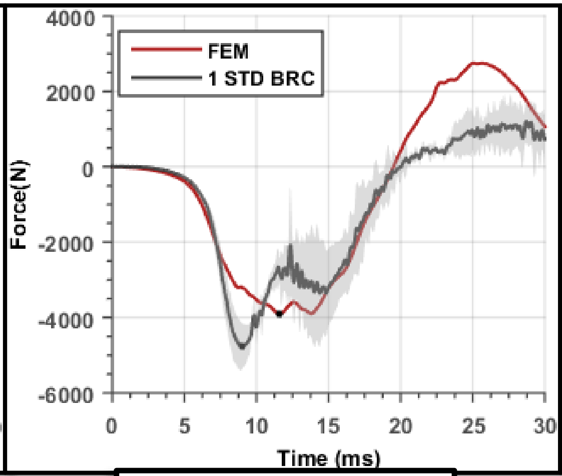

Upper Force

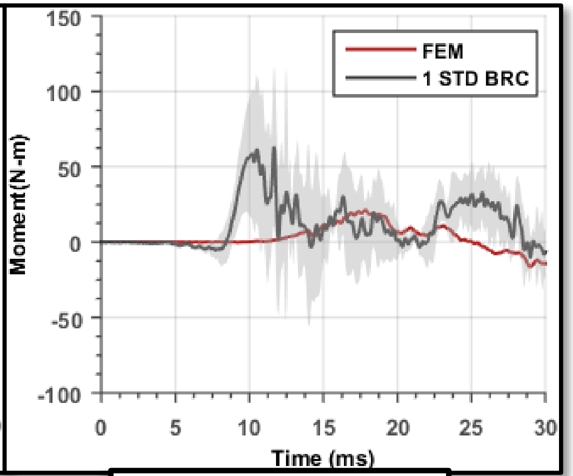

Upper Moment

Summary and ongoing work

- **Developed human lumbar spine model for dynamic investigations**
  - Focus on multi-level validation
  - Validation ranges for blast exposure, ballistic impact, and accelerative loading
- **Groundwork for Injury prediction modeling**
  - Develop local injury criteria through simulations of failure tests
    - Vertebral body crush
    - 3-vertebra motion segment fracture studies
  - Explore changes in injury mechanism
    - Effect of loading rate
    - Posture
  - Integration into full human body model
    - System level validation

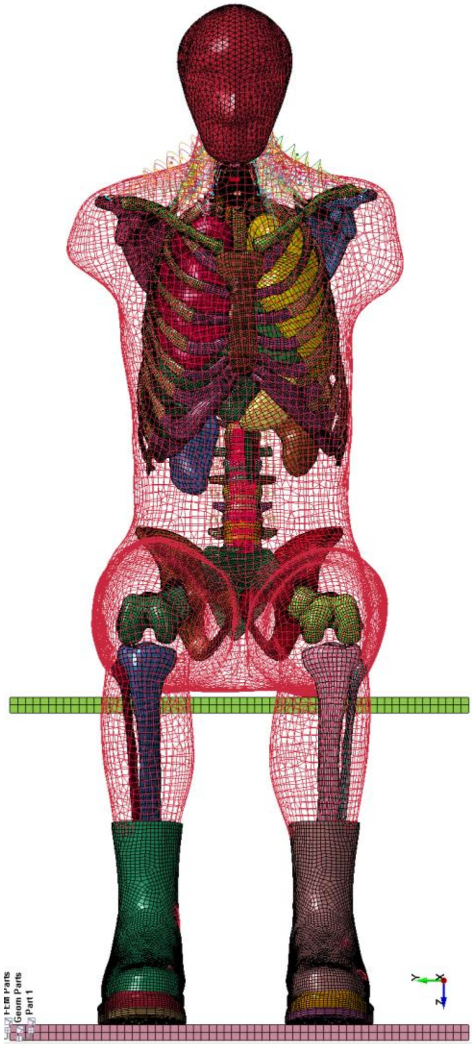

Acknowledgements

The U.S. Army Medical Research Acquisition Activity, 820 Chandler Street, Fort Detrick MD 21702-5014 is the awarding and administering acquisition office.

The content included in this work does not necessarily reflect the position or policy of the U.S. government.

JOHNS HOPKINS
APPLIED PHYSICS LABORATORY

CORA Review

- **Inputs**
  - **Reference curve(s)**
    - **e.g. experimental**
  - **Comparison curve**
    - **e.g. model**
- **Outputs**
  - Ratings at each level
  - Total CORA rating is weighted average of 4

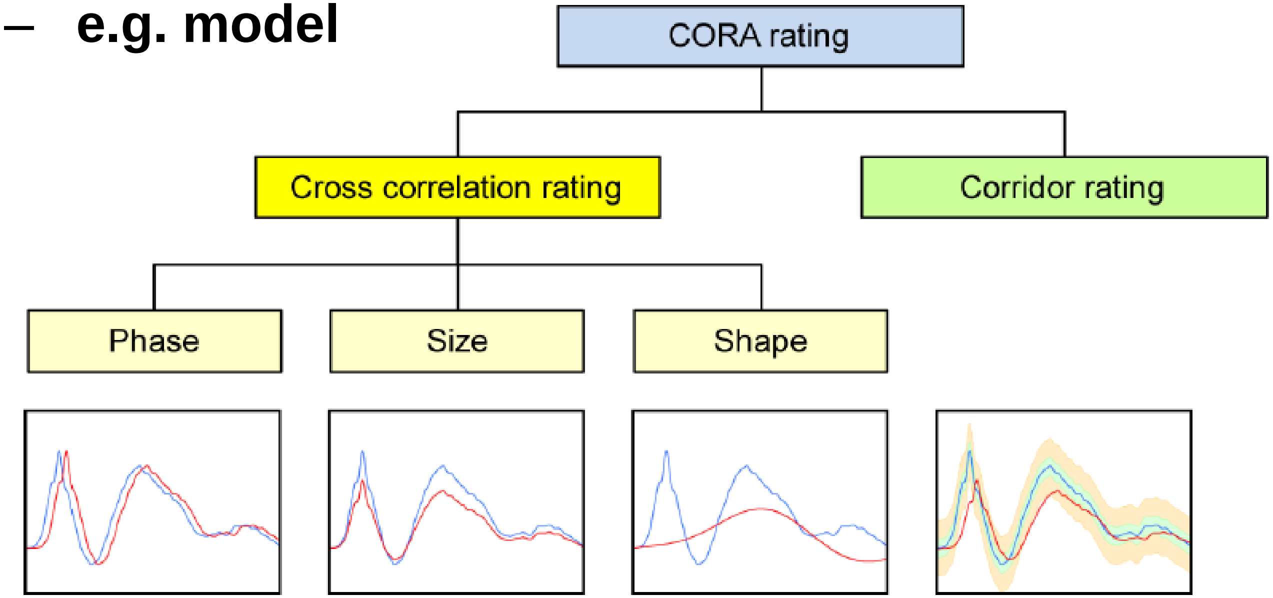

Goal: Reduce subjectivity by comparing all signals with the same level of objectivity

Phase Rating: Amount of shift required to maximize correlation

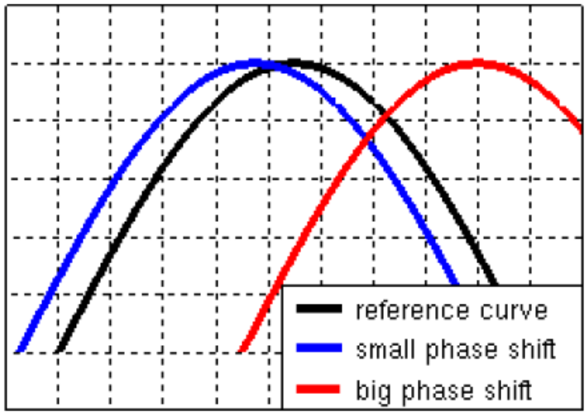

Size Rating: Area under the curve ratio

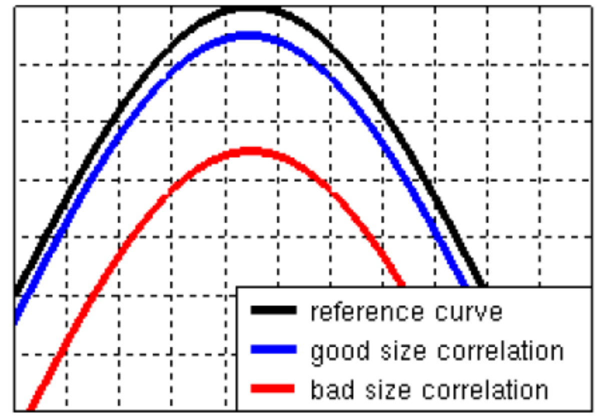

Shape Rating: Correlation

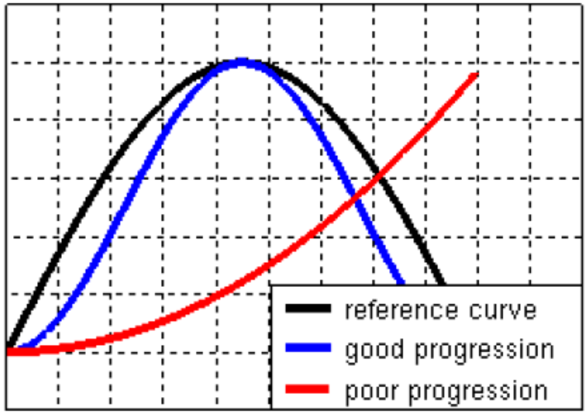

Corridor Rating: Fit in corridor

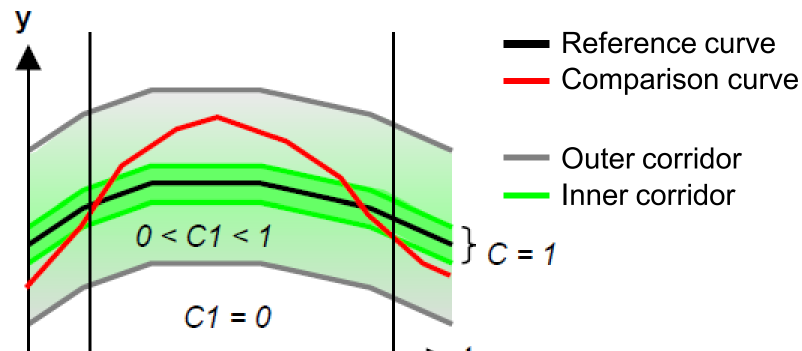

CORA user manual

Each metric is used to compensate the others' disadvantages

CORA Settings

```
###############################################################################
#
#   Global Parameters
#
###############################################################################
BEGIN GLOBAL_PARAMETERS
  DES_MOD            CORA Curve Compare       ; Header of the evaluation
  DES_GLO            CORA Curve Compare       ; Sub-header of the evaluation
#
# Global settings to define the interval of evaluation
  A_THRES            0.030                  ; Threshold to set the start of the interval of evaluation [0,...,1]
  B_THRES            0.075                  ; Threshold to set the end of the interval of evaluation [0,...,1]
  A_EVAL             0.010                  ; Extension of the interval of evaluation [0,...,1]
  B_DELTA_END        0.200                  ; Additional parameter to shorten the interval of evaluation (width of the corridor: A_DELTA_END*Y_NORM) 0 = disable
  T_MIN/T_MAX        0 30             ; Manually defined start (time) and end (time) of the interval of evaluation (automatic = calculated for each channel)
  T_UNIT             ms                      ; Unit of T_MIN, T_MAX, t_min and t_max
#
# Global settings of the corridor method
  K                  2                      ; Transition between ratings of 1 and 0 of the corridor method [-] (1 = linear, 2 = quadratic ...)
  G_1                0.50                   ; Weighting factor of the corridor method [-]
  a_0/b_0            0.05     0.50          ; Width of the inner and outer corridor [-]
  a_sigma/b_sigma    0        0             ; Multiples of the standard deviation to widen the inner and outer corridor [-]
# Global settings of the cross correlation method
  D_MIN              0.01                   ; delta_min as share of the interval of evaluation [0,...,1]
  D_MAX              0.12                   ; delta_max as share of the interval of evaluation [0,...,1]
  INT_MIN            0.8                      ; Minimum overlap of the interval [0,...,1]
  K_V                2                    ; Transition between ratings of 1 and 0 of the progression rating [-] (1 = linear, 2 = quadratic ...)
  K_G                1                      ; Transition between ratings of 1 and 0 of the size rating [-] (1 = linear, 2 = quadratic ...)
  K_P                1                      ; Transition between ratings of 1 and 0 of the phase shift rating [-] (1 = linear, 2 = quadratic ...)
  G_V                0.33                   ; Weighting factors of the progression rating [-]
  G_G                0.33                   ; Weighting factors of the size rating [-]
  G_P                0.33                   ; Weighting factors of the phase shift rating [-]
  G_2                0.50                   ; Weighting factors of the cross correlation method [-]
# Normalisation of the the weighting factors
  WF_NORM            YES                    ; Normalisation of the weighting factors [YES/NO]?
# Signal settings
  ISONAME_1-2/11-12  YES YES                ; Consideration of the position 1/2 (test object, seating position) and 11/12 (fine location 3 - dummy) of the ISO c
  MIN_NORM           0.00                   ; Threshold (as fraction of the global absolute maximum amplitude) to start special treatment of secondary axis [0,.
  Y_NORM             extremum               ; Type of calculation of Y_NORM (extremum or value)
```

Human Lumbar Spine FEM: Data Transformations

Move force and moments from top and bottom load cell to T12/L1 or L5/S1

$$\mathbf{F}_{\mathbf{z,top,transformed}} = \mathbf{F}_{\mathbf{z,top,collected}} + \mathbf{m}_{(\mathbf{T12-LC\ neutral\ axis})} * \mathbf{a}_{\mathbf{z,top}}$$

$$\mathbf{F}_{\mathbf{z,bot,transformed}} = \mathbf{F}_{\mathbf{z,bot,collected}} - \mathbf{m}_{(\mathbf{S1-LC\ neutral\ axis})} * \mathbf{a}_{\mathbf{z,bot}}$$

$$\mathbf{M}_{\mathbf{y,top,transformed}} = \mathbf{M}_{\mathbf{y,top,collected}} + \mathbf{F}_{\mathbf{z,top,transformed}} * \boldsymbol{D}_{\boldsymbol{x,top}} - \mathbf{F}_{\mathbf{x,top,collected}} * \boldsymbol{D}_{\boldsymbol{z,top}}$$

$$\mathbf{M}_{\mathbf{y,bot,transformed}} = \mathbf{M}_{\mathbf{y,bot,collected}} + \mathbf{F}_{\mathbf{z,bot,transformed}} * \boldsymbol{D}_{\boldsymbol{x,bot}} - \mathbf{F}_{\mathbf{x,bot,collected}} * \boldsymbol{D}$$

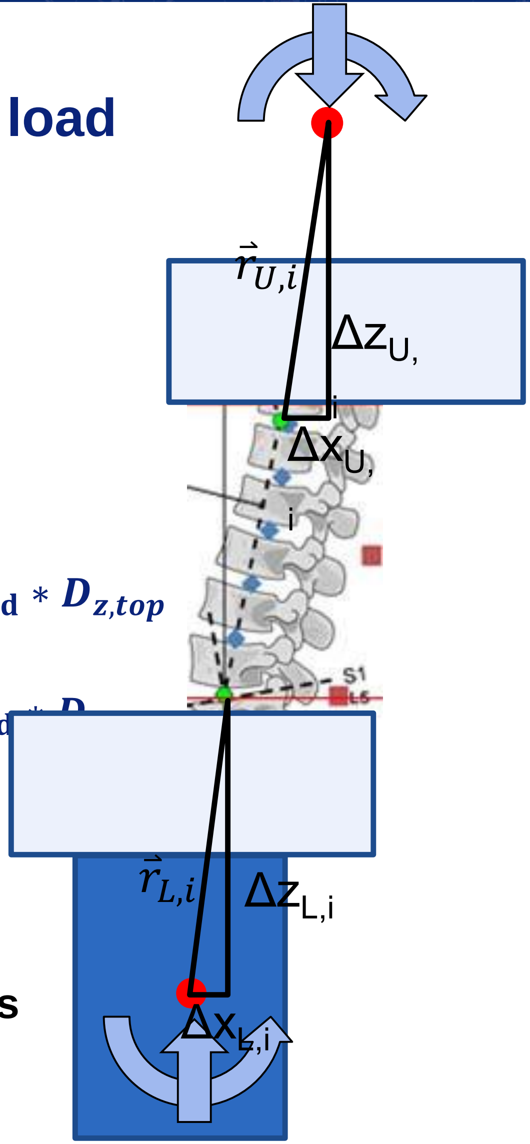

Transformation applied using virtual accelerometers

- Not directly coupled to experimental transformations

Numerical Model of the Porcine and Human Head

January 13, 2016

Kimberly Thompson, Timothy Zhang, Sikhanda Satapathy
Army Research Laboratory
Aurelie Jean, Martin Hautefeuille, Adrian Rosolen, Raul Radovitzky
Massachusetts Institute of Technology

Project Overview

Traumatic brain injury (TBI) has been a common injury for Soldiers in recent wars

Animal Model

Link ballistic load to head injury in <u>animal head models</u>

Human Model

<u>Develop transfer function</u> from animal model to human head model

PPE

Characterize <u>role of helmet and pads</u> in load transfer to head

Approach: Bump Study

- Exercise and analyze the Porcine Head Model
  - 1. Assess different bump velocities
  - 2. Assess different bump locations
  - 3. Assess interfacial effects (Skin-Skull, Skull-Brain)
  - 4. Compare between different codes (working with MIT)
    - LS-Dyna and Summit (MIT)
- Exercise and analyze the Human Head Model
  - Compare results to porcine model
- Important Assumptions:
  - Material models and parameters are the same for porcine and human model (taken from the literature)

Geometry Comparison

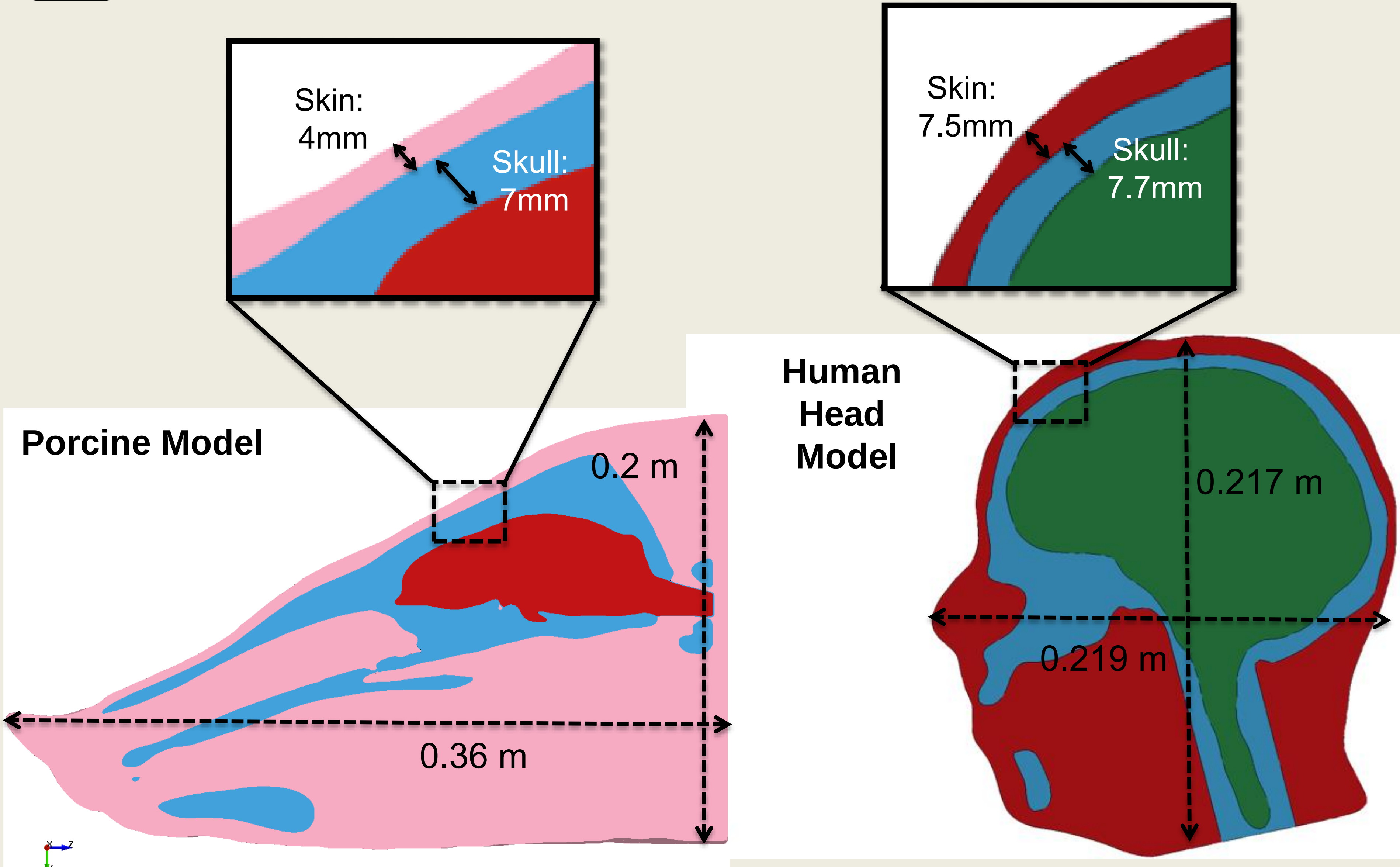

Material Models

Component	Model	Properties
Brain	Viscoelastic	Density = 1040 kg/m^3, Bulk Modulus = 2.19 GPa, G0 (short term shear) = 41 kPa, G1 (long term shear) = 7.8 kPa, B (decay constant) = 700 /s
Skull	Elastic	Density = 1710 kg/m^3, Young's Modulus = 5.37 GPa Poisson = 0.19
Skin	Elastic	Density = 1130 kg/m^3, Young's Modulus = 16.7 MPa, Poisson = 0.499

<u>Properties obtained from the literature:</u>

T. G. Zhang and S. S. Satapathy. Effect of Helmet Pads on the Load Transfer to the Head Under Blast Loadings. Proceedings of ASME 2014 International Mechanical Engineering Congress & Exposition, Nov. 14-20, 2014.

Bump Study

Simulation Details:

- 10 ms simulation time
- 64 processors
- 15 million linear tetrahedral elements
- Use LS-Dyna for simulations
- Free Boundary Conditions

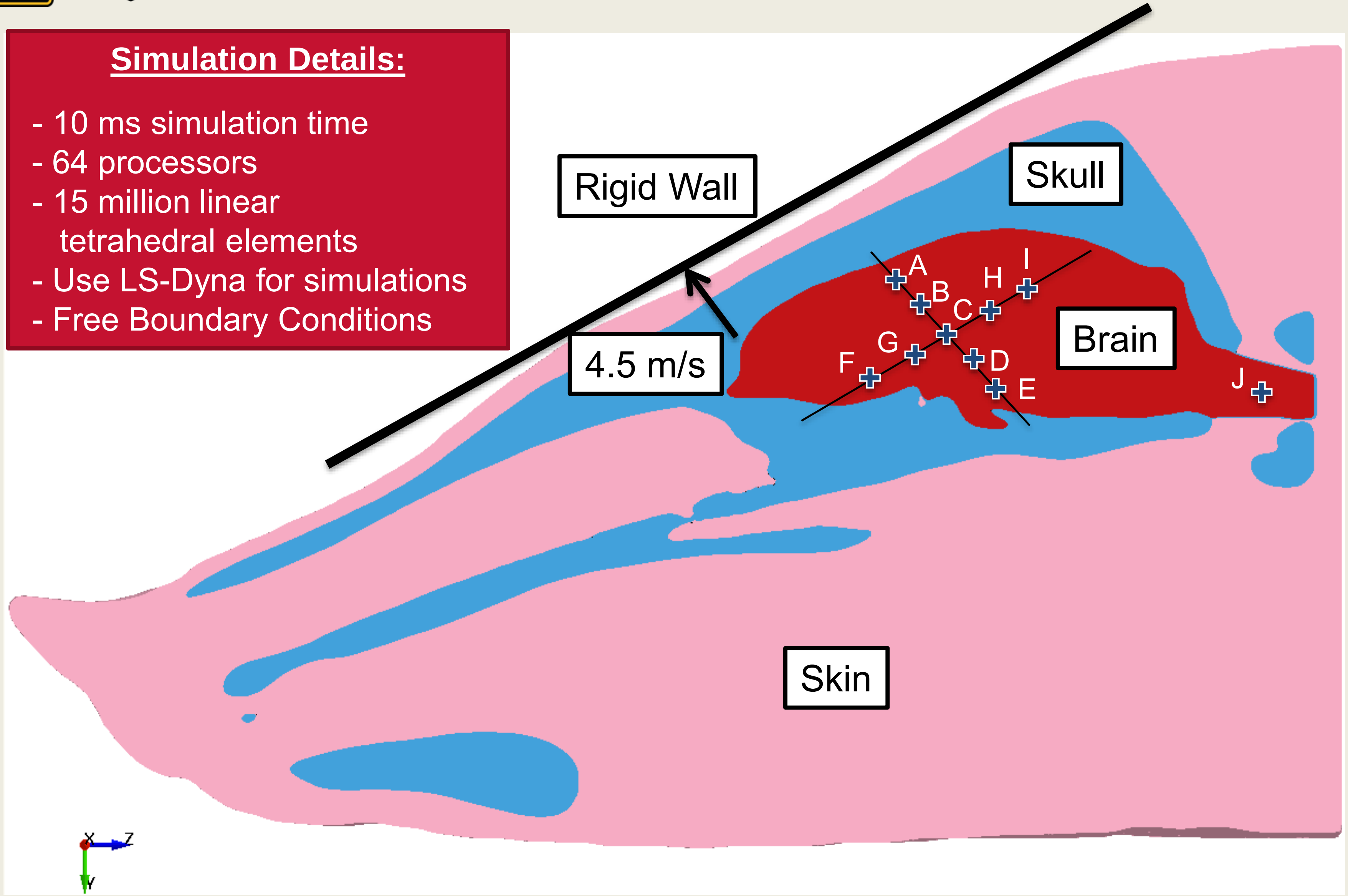

1. Bump Velocity

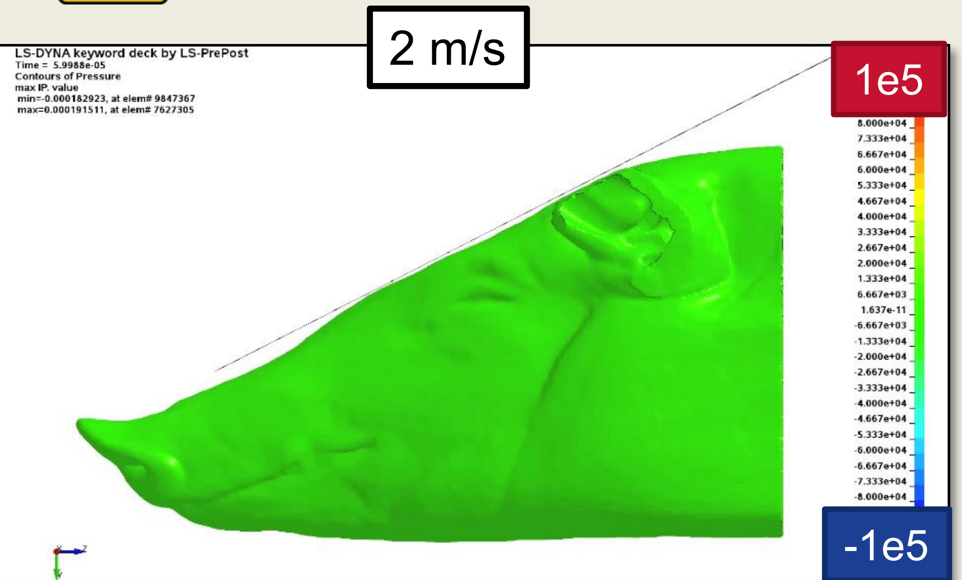

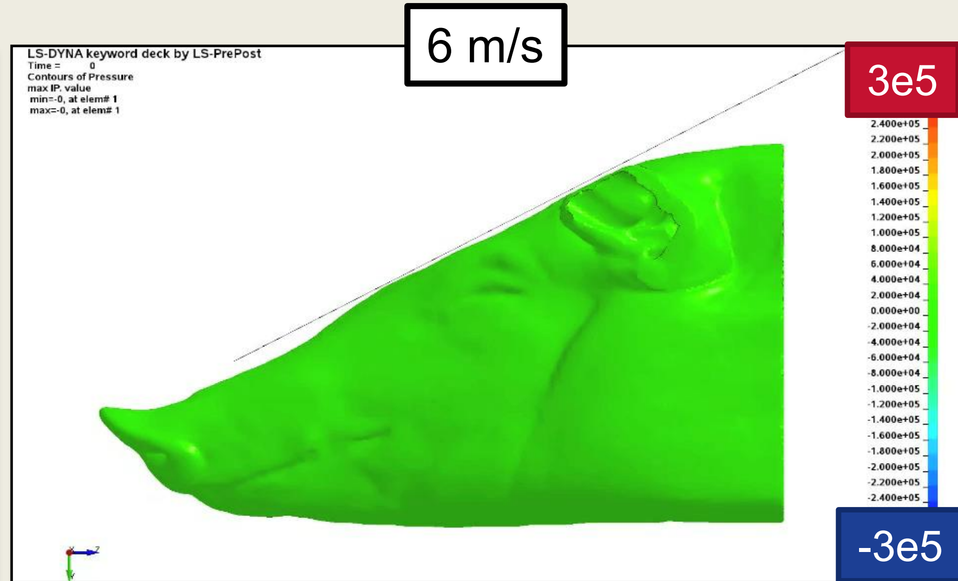

Simulation Time:
10 ms

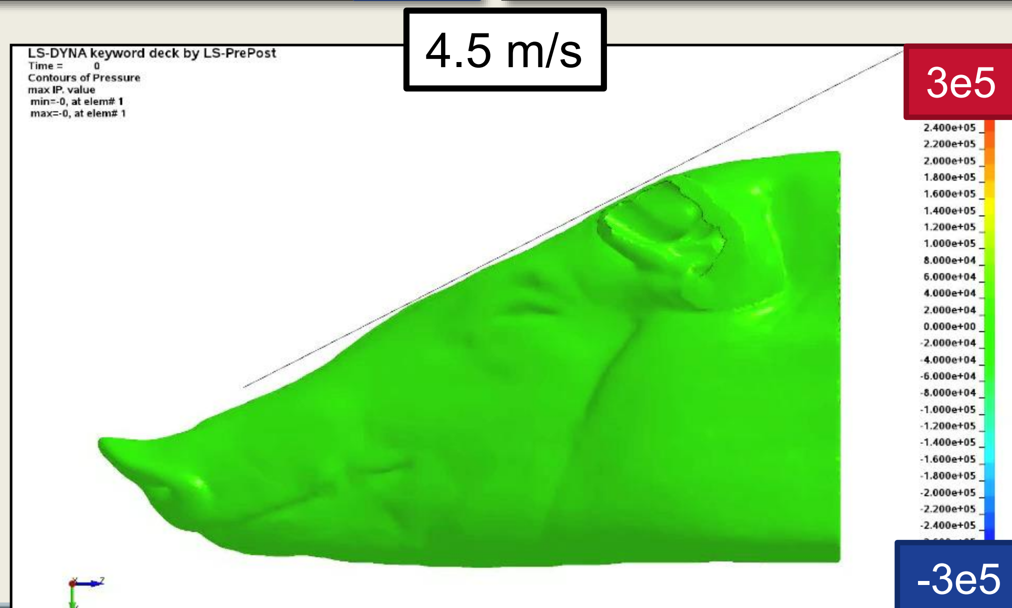

1. Bump Velocity

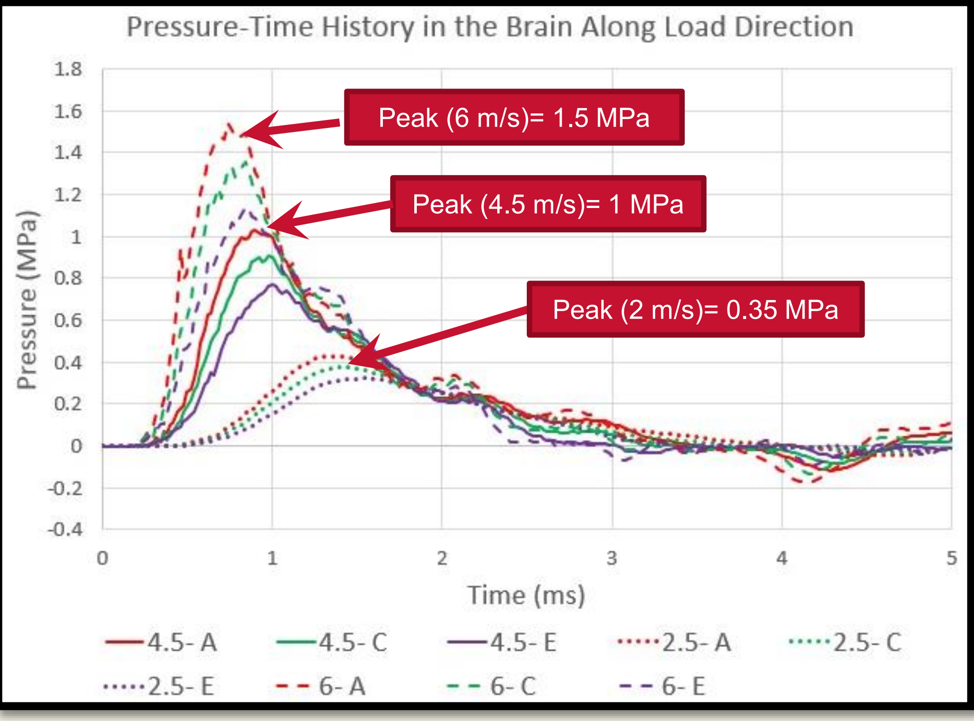

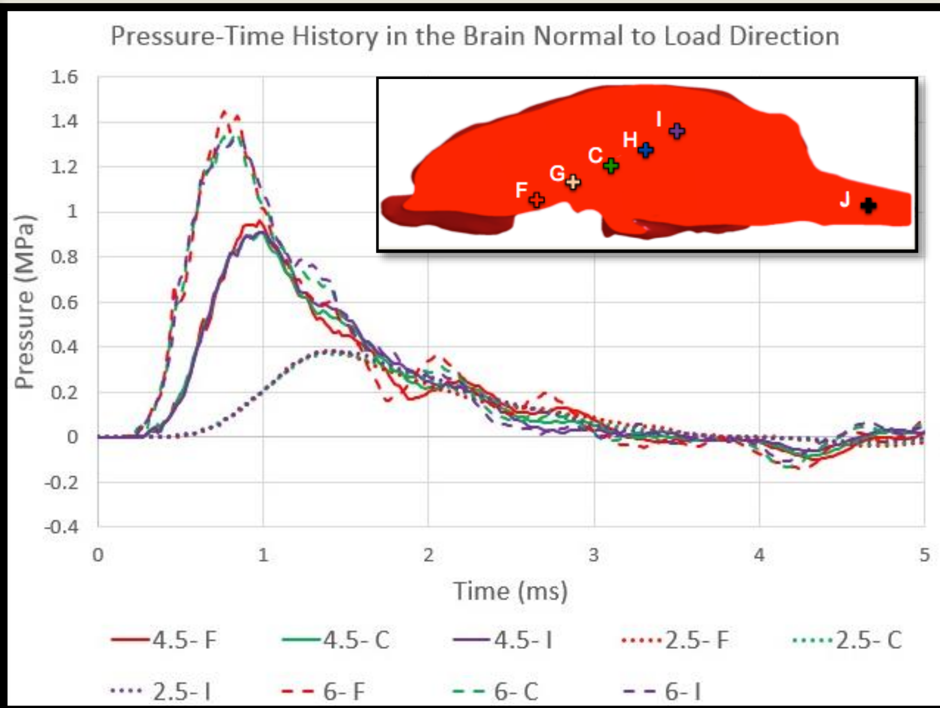

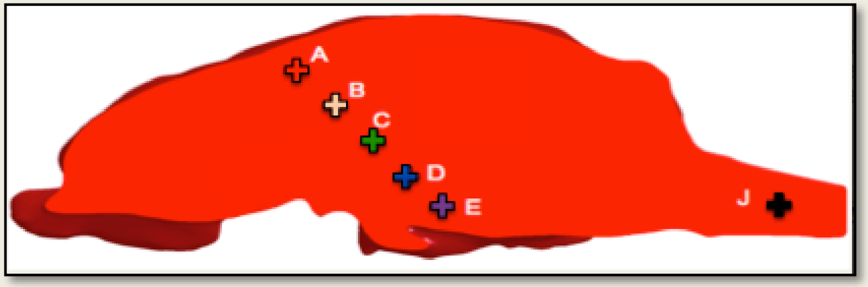

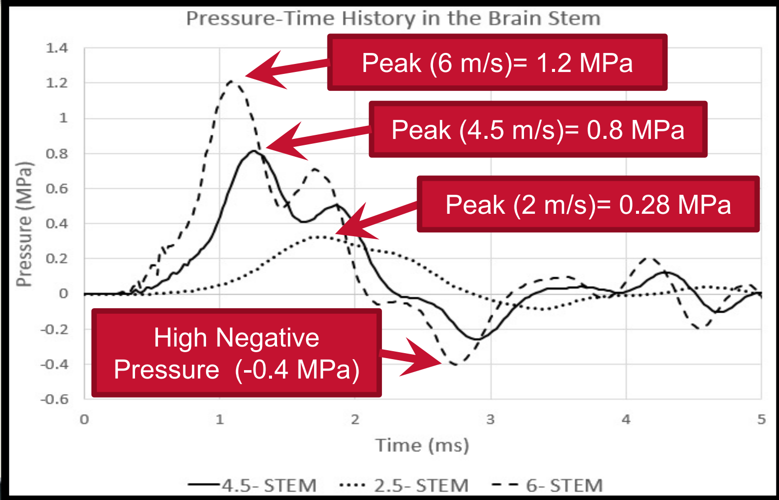

Brainstem area experiences high negative pressure

U.S. ARMY RDECOM

2. Bump Location

ARL

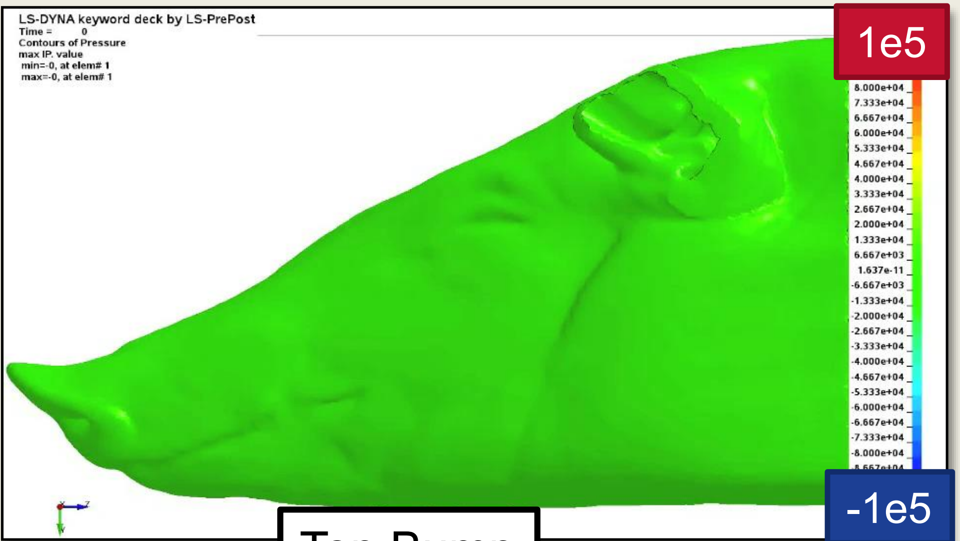

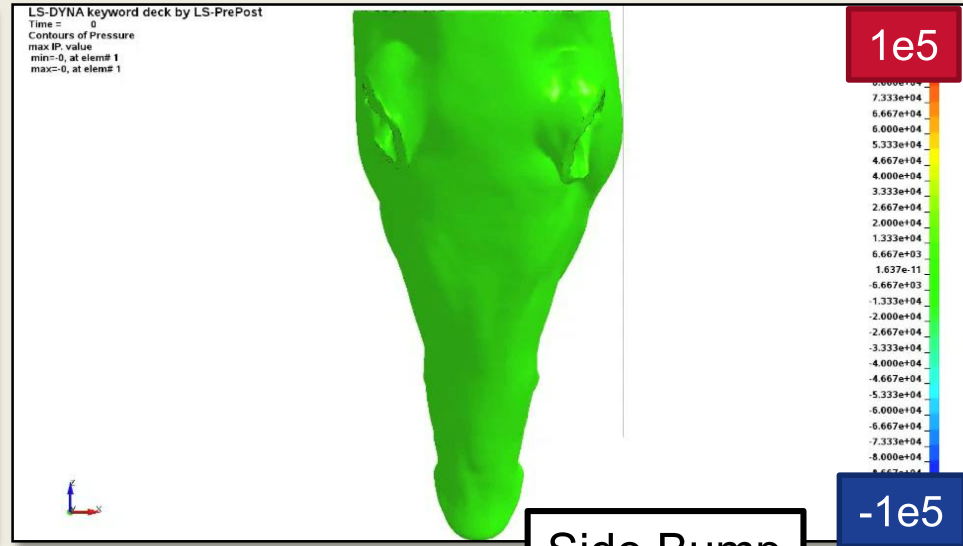

Velocity: 4.5 m/s

NOTE: Rigid body rotation for Top and Side Bump is not accurate due to no BC at neck to incorporate full body mass.

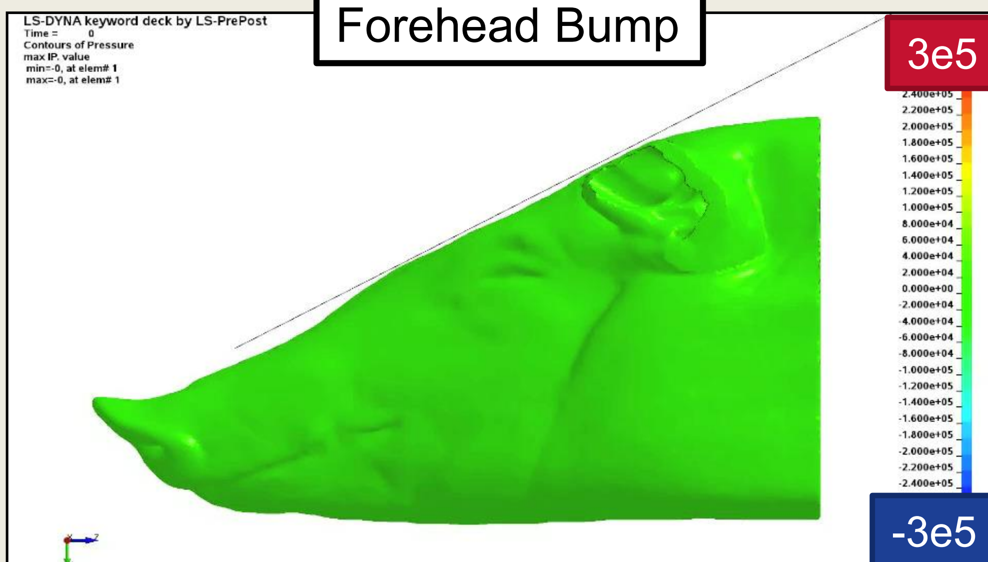

U.S. ARMY RDECOM

2. Bump Location

ARL

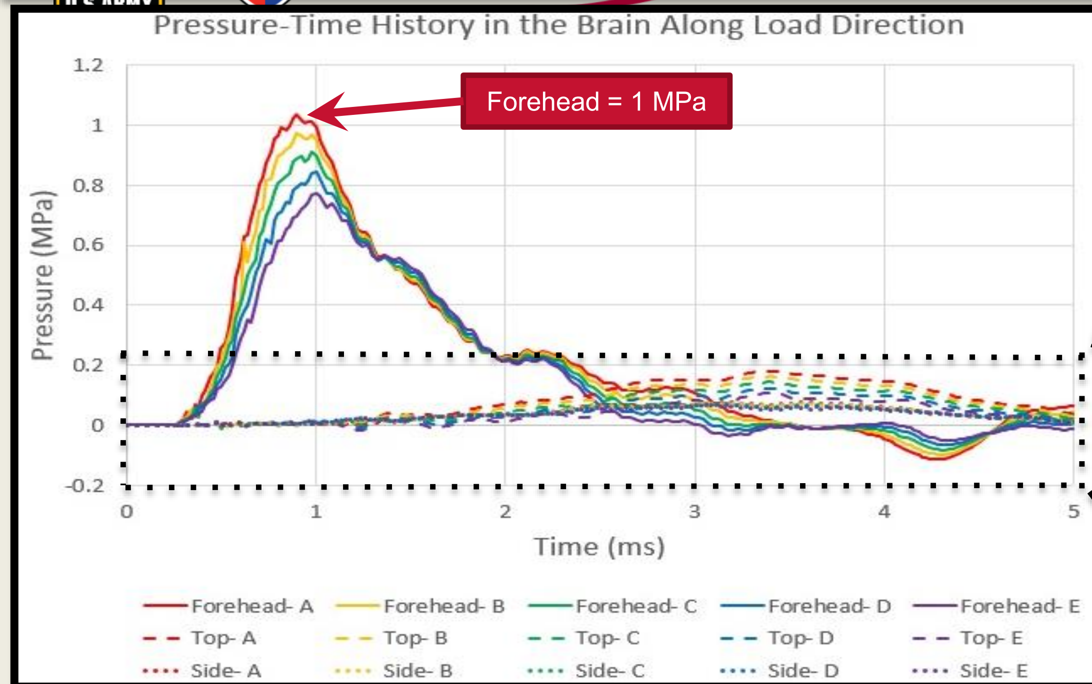

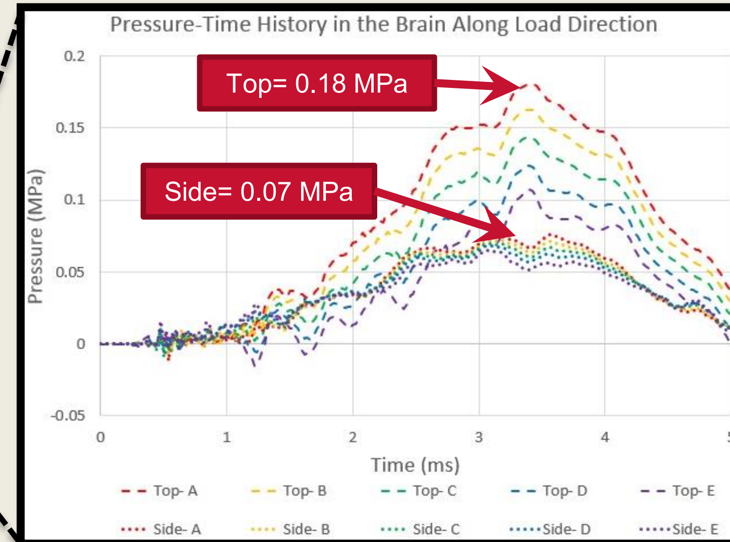

The forehead bump is an order of magnitude larger than the top bump, which is double the magnitude of the side bump. More analysis needs to be done to understand the effects of different loading directions.

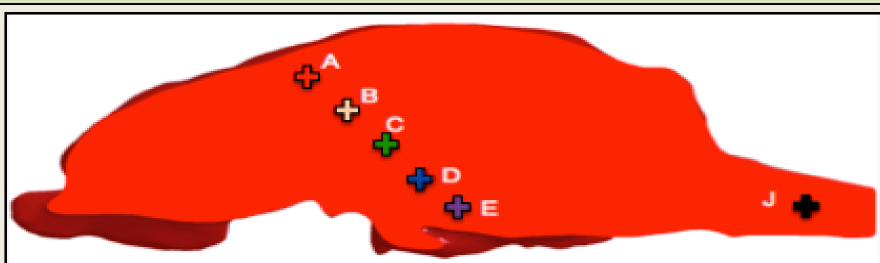

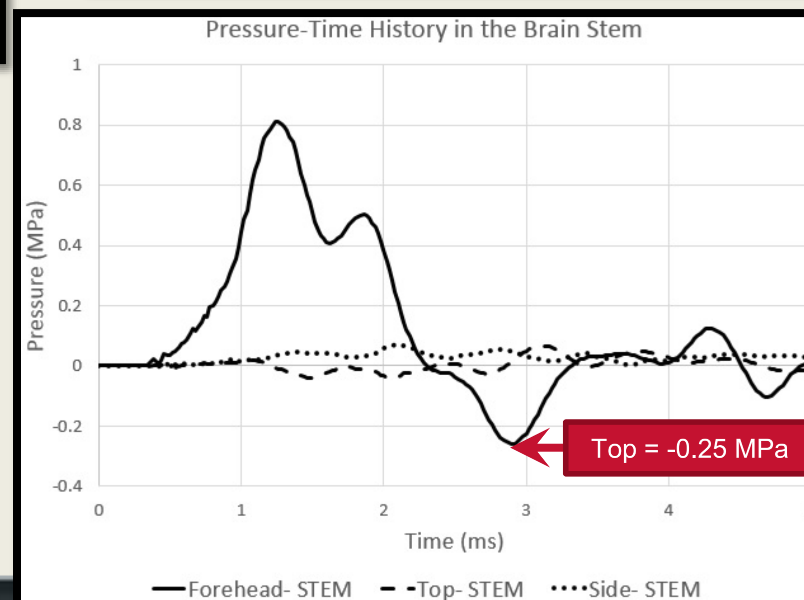

U.S. ARMY RDECOM

3. Interfacial Effects

ARL

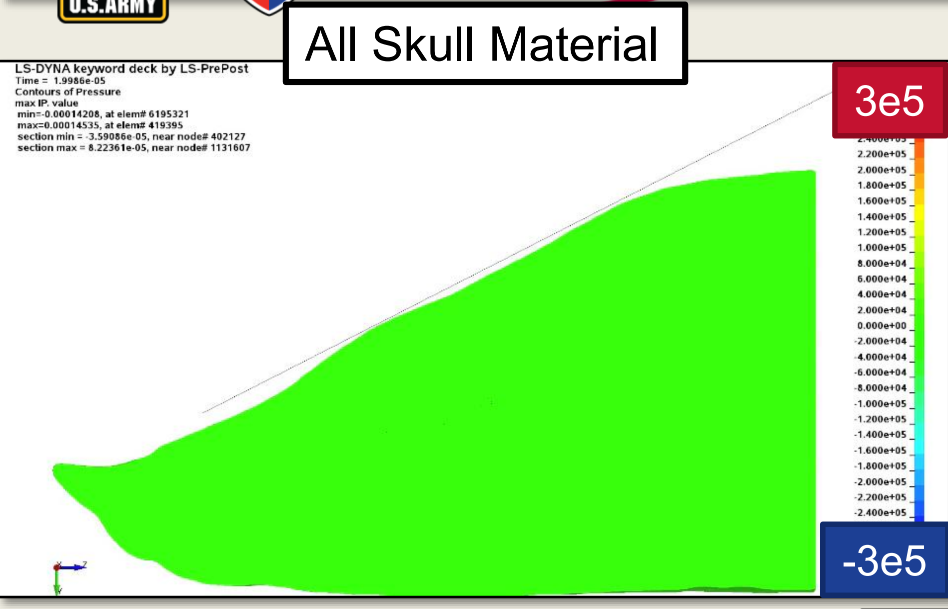

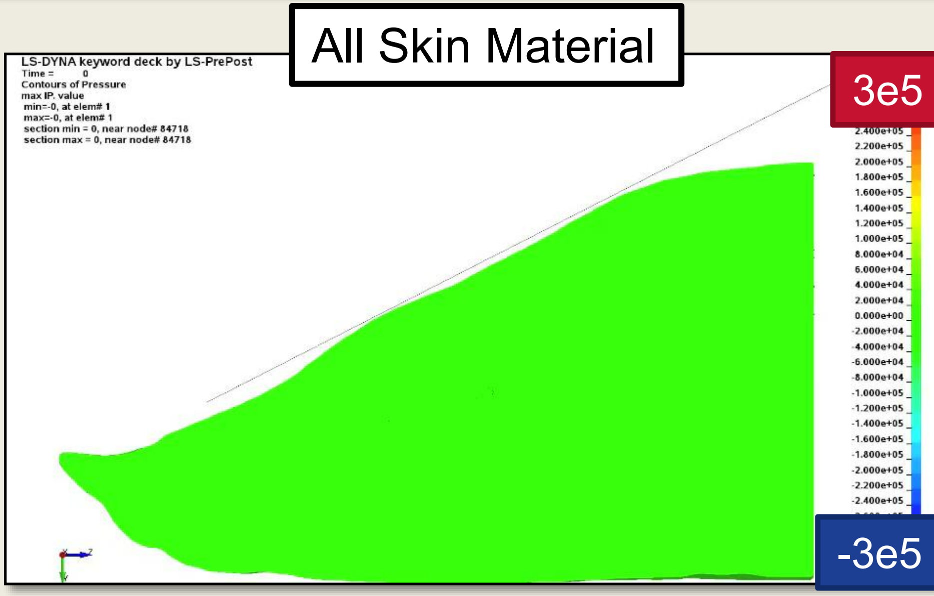

Velocity: 4.5 m/s

Interfaces introduce complexity to the stress wave structure. The role of interface strength and possible interface separation needs further evaluation.

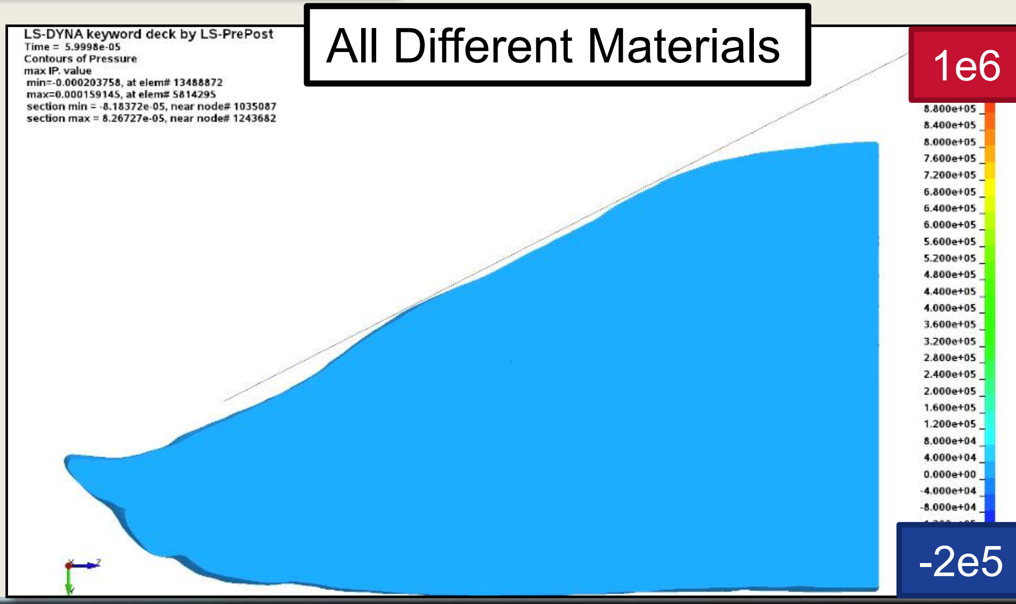

3. Interfacial Effects

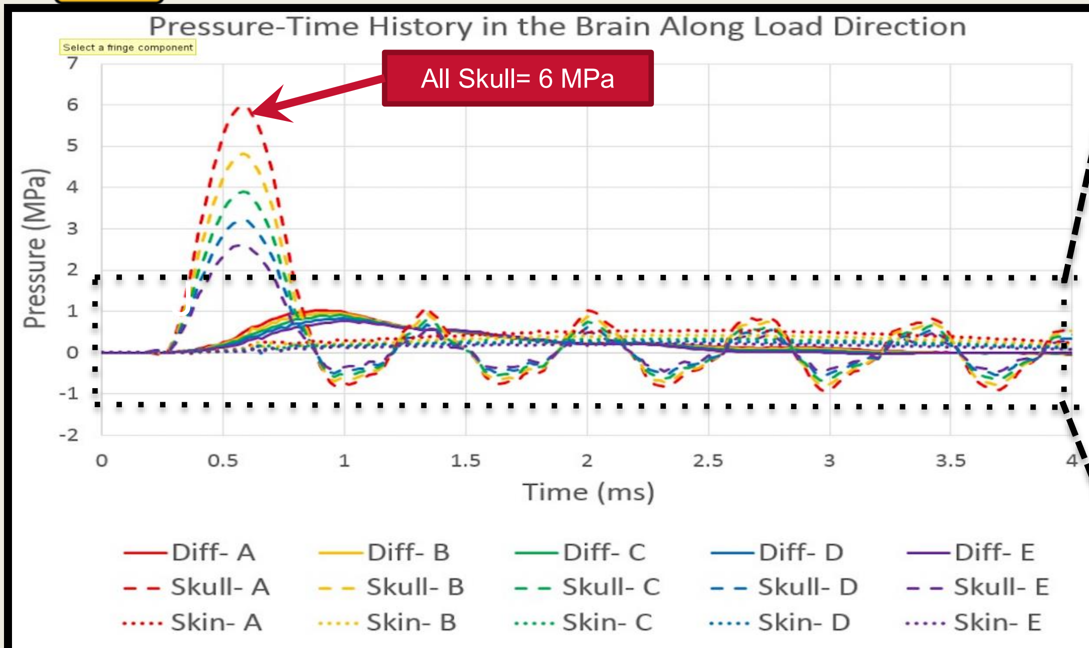

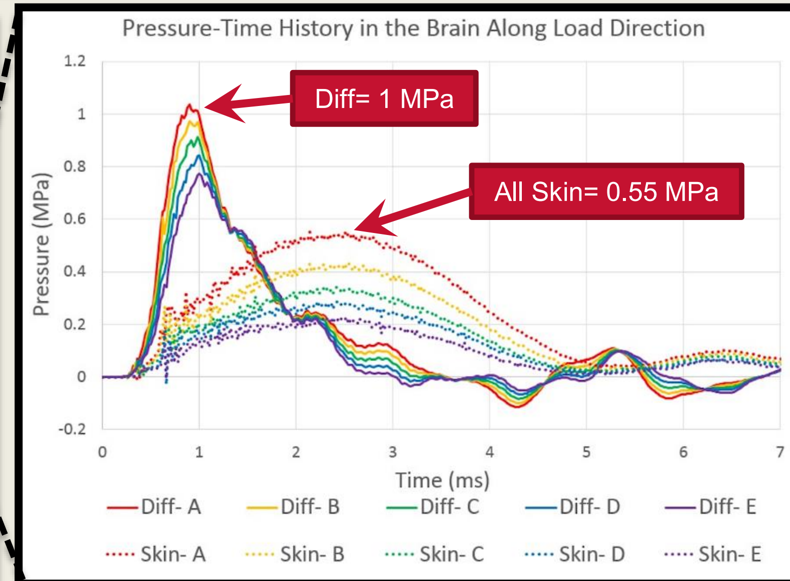

The response is monotonic in absence of interfaces, as expected. Presence of interfaces makes the wave structure more complex and results in higher negative pressure in the brain stem area.

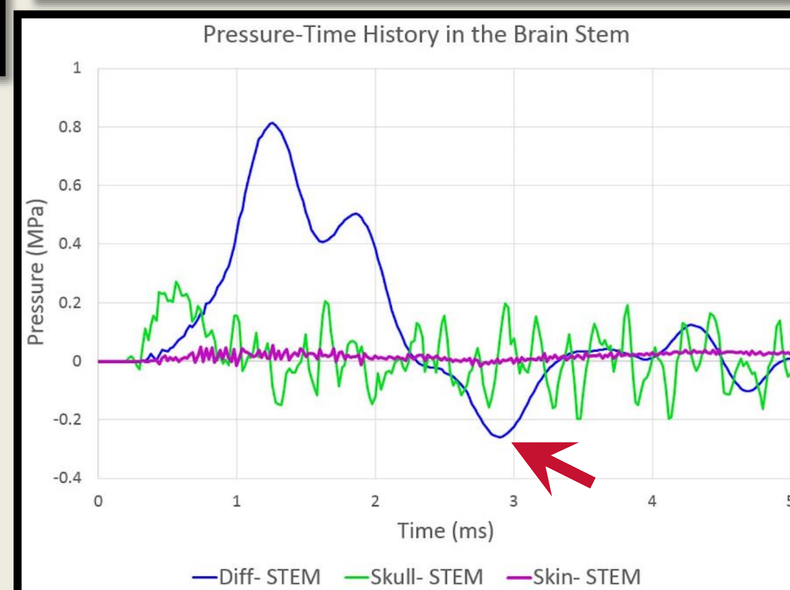

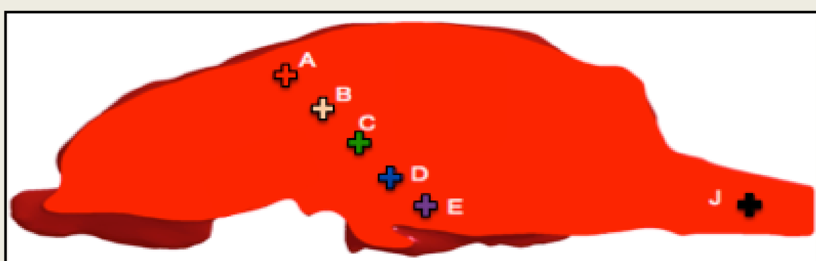

LS-Dyna and Summit

LS-Dyna

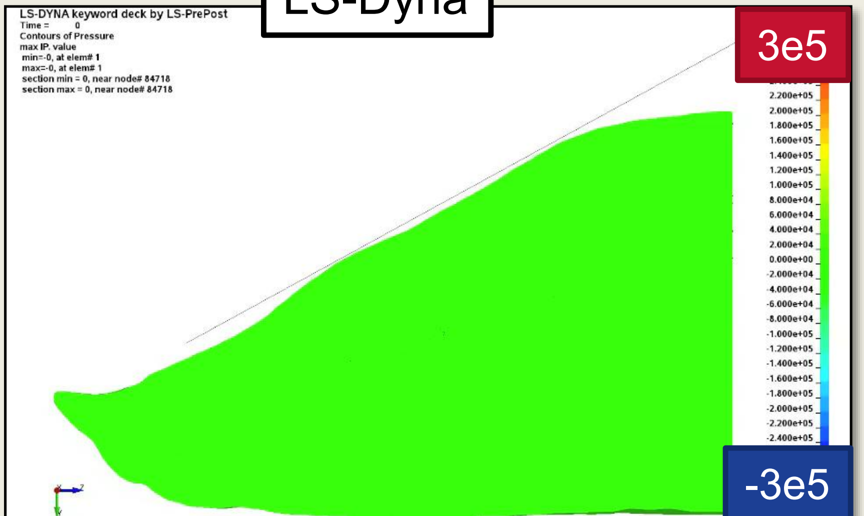

Summit

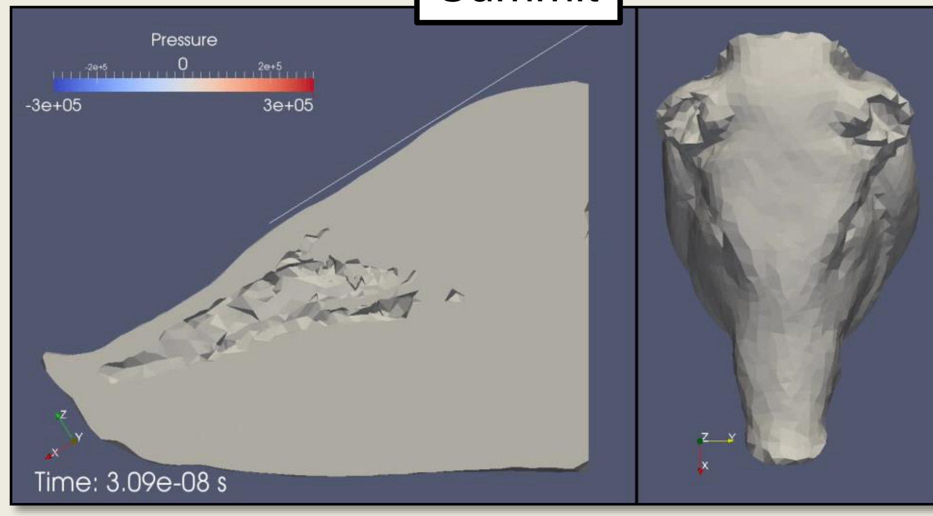

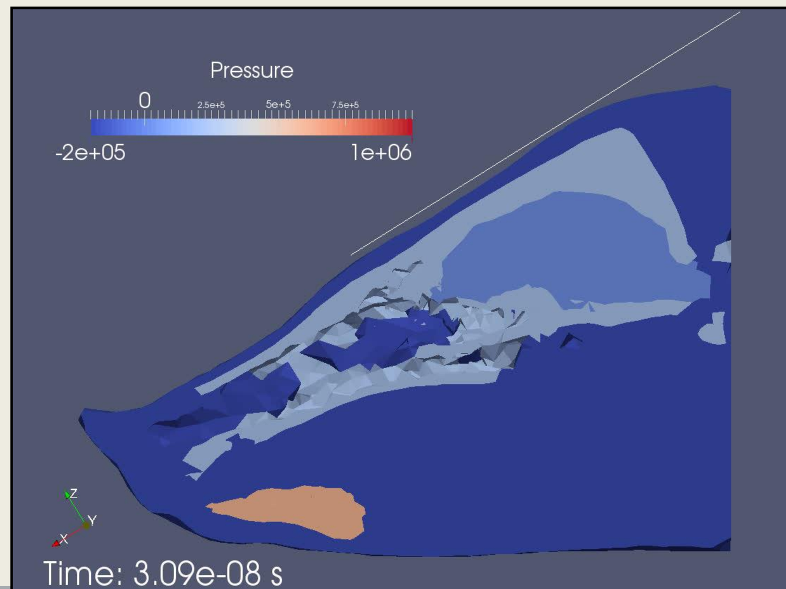

LS-Dyna and Summit

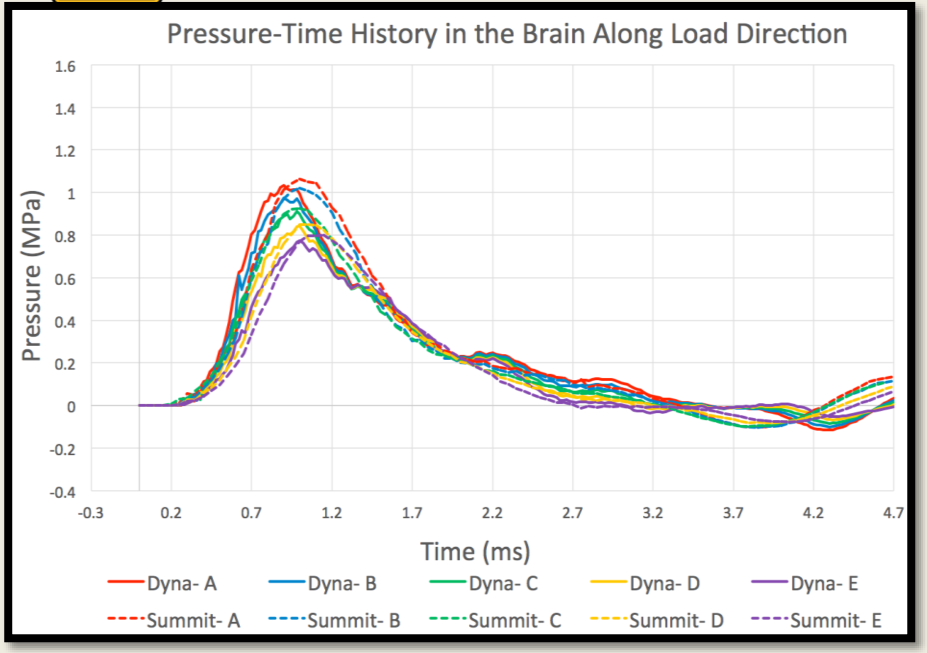

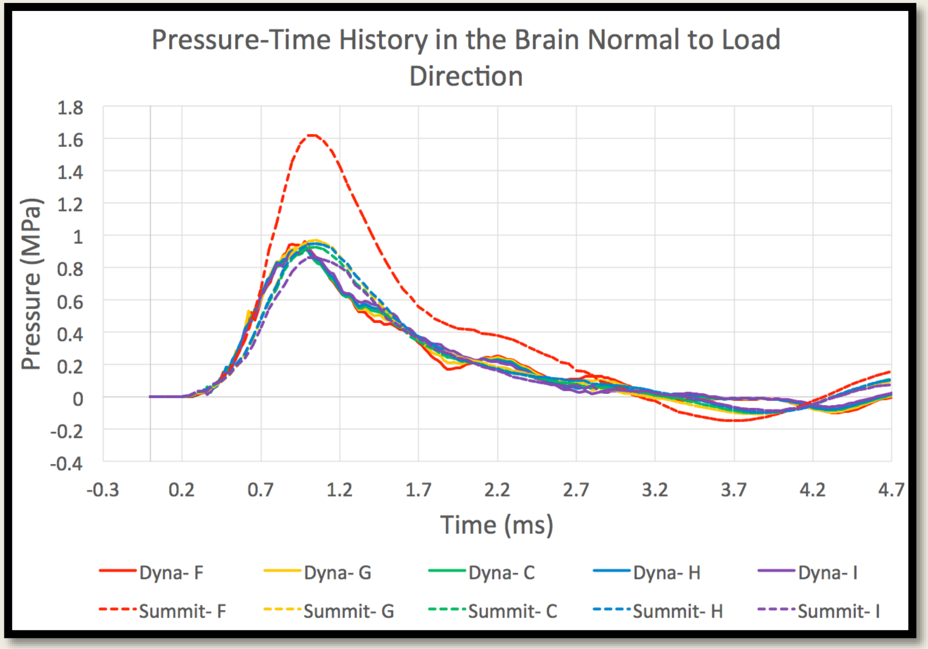

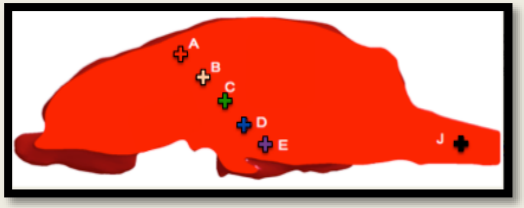

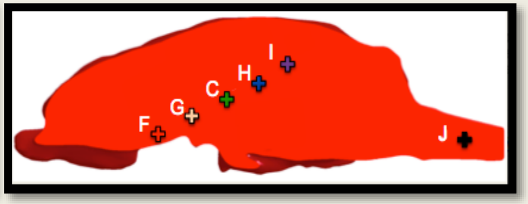

- The pressure profiles are similar between codes for along and normal to load directions
- Both codes show large negative pressure in the brain stem

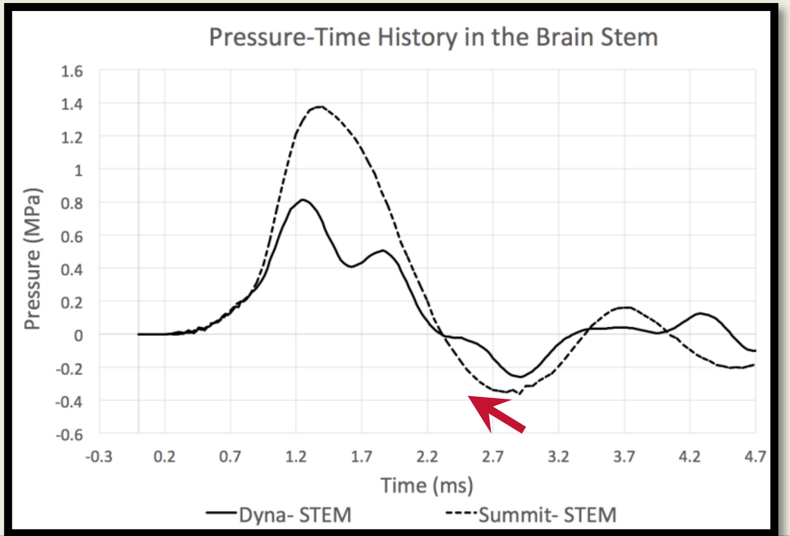

Compare Porcine and Human

-Rigid wall force on the pig is triple that of the human due to greater impact area
-Pulse width is similar due to similar head height

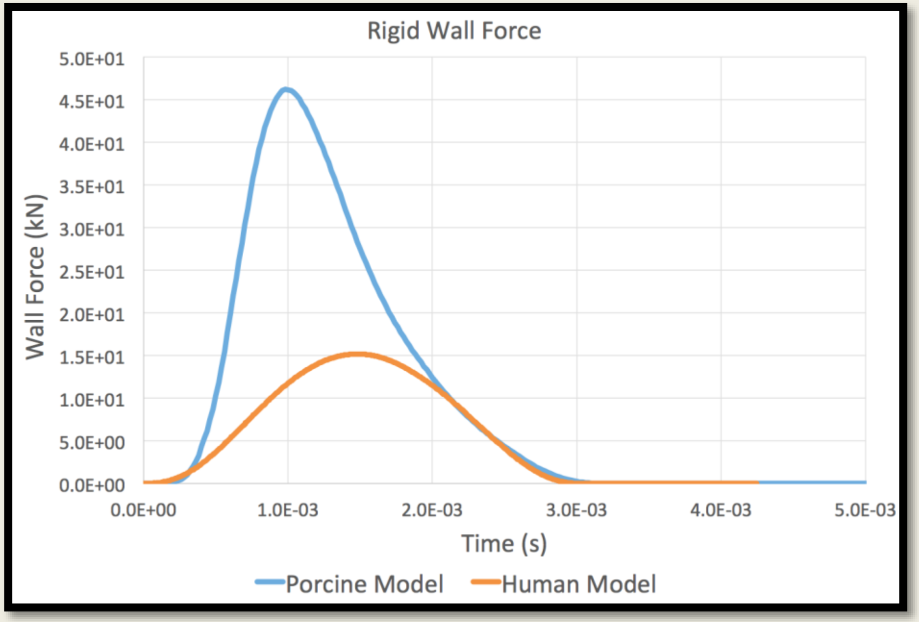

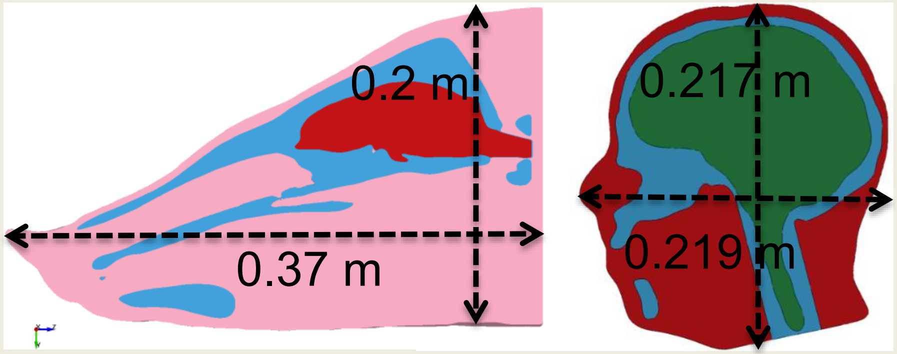

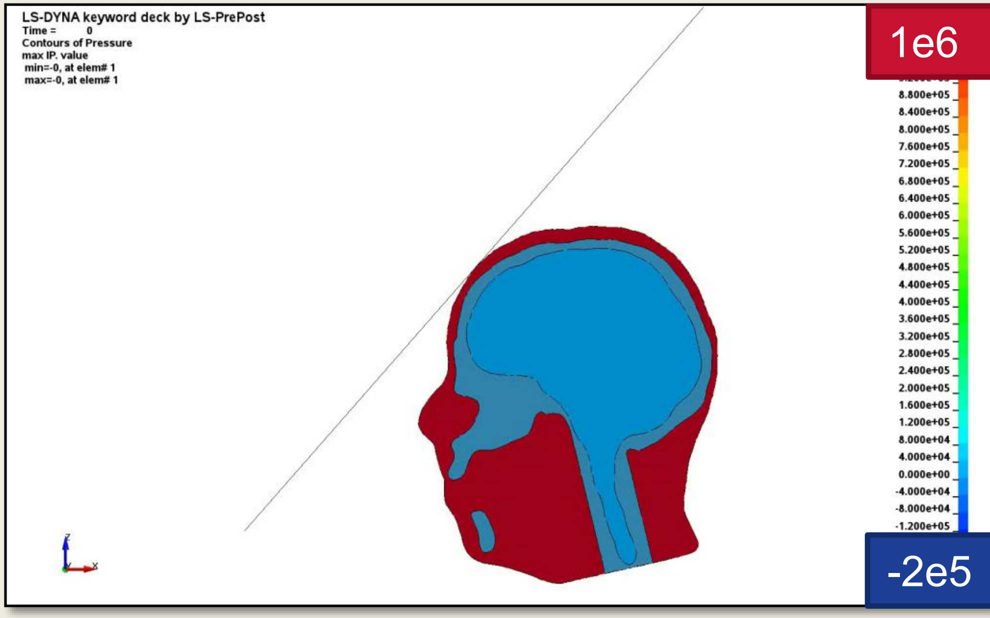

Compare Porcine and Human

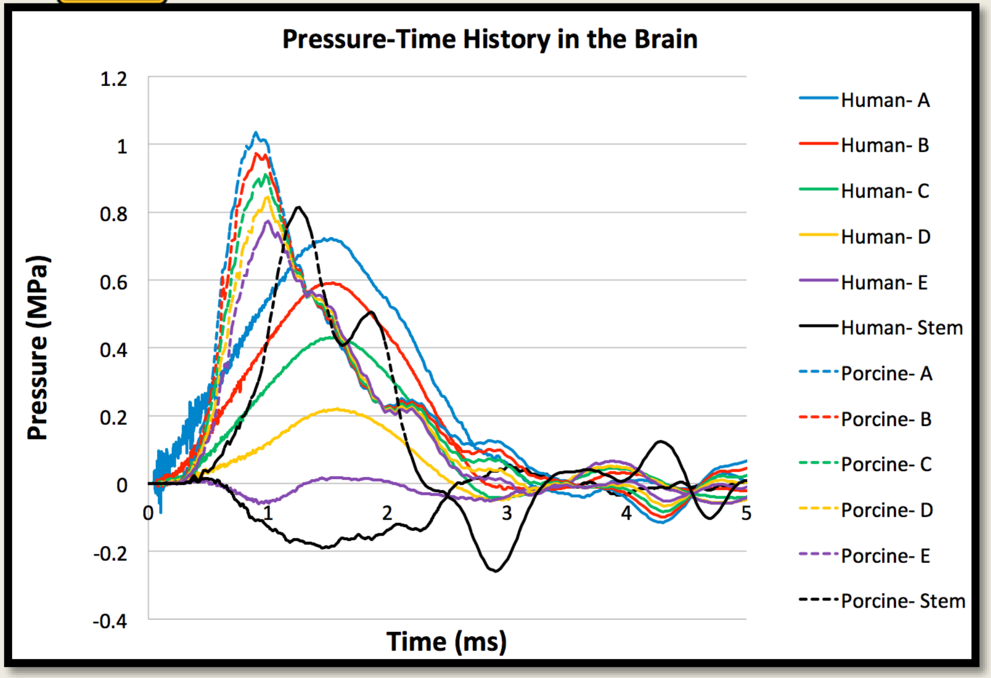

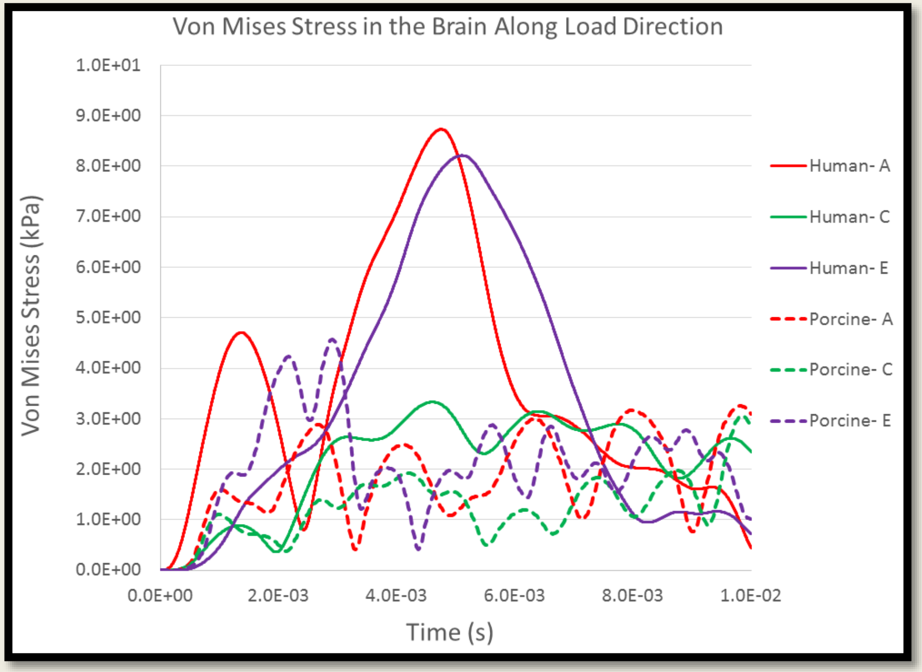

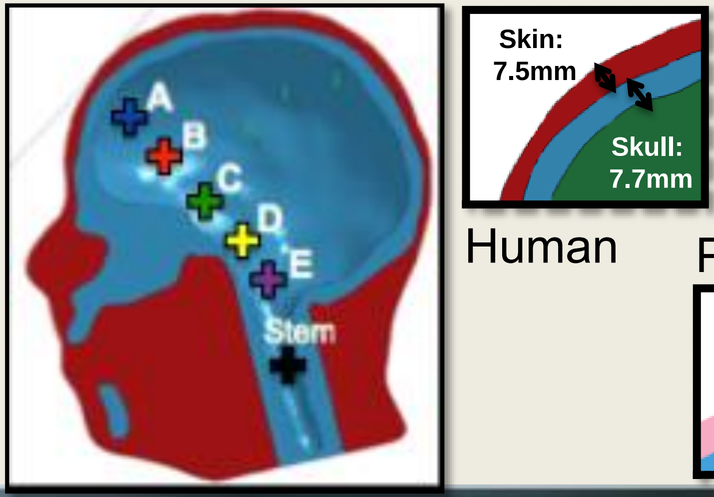

- Head topology plays an important role in the stress wave structure.
- Porcine data is not directly transferable to human head.

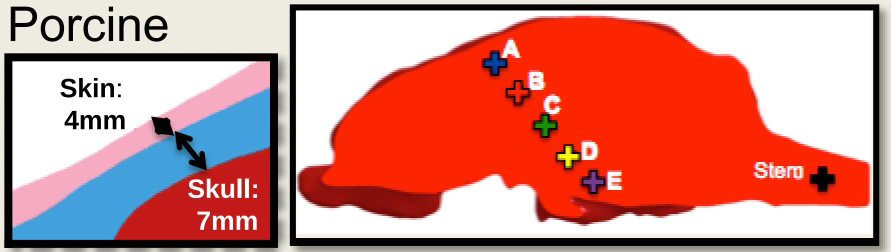

Conclusion & Future Work

Summary:

- ❑ Animal models are a convenient means of understanding high-rate load transfer to the head
- ❑ The brain stem area of the porcine model experiences high negative pressure and is susceptible to injury
- ❑ Even though the computed pressure in porcine and human head models are similar, the pulse shapes are different.
  - ❖ Porcine data is not directly transferable to human head.

Future Work:

- ❑ Investigate the effects of material interfaces
- ❑ Investigate injury indicators in porcine and human models
- ❑ Develop transfer function for load transfer to human head

Thank you!

EXTRA SLIDES

Transfer Function (TF)

	EXPERIMENT	COMPUTATIONAL MODEL
Porcine Head	v_1 → Injury Detected	v_1 → $I_1 = I_1(\sigma_m, \varepsilon_m, p_m, \ldots)$; correlates with injury
Human Head	v_2 →	v_2 → $I_1 = I_2$: **Predicted Injury** (Animal results directly apply to the human)
Species #2	**With Limited Knowledge of the Experiment …**	→ **Can we PREDICT the injury??**

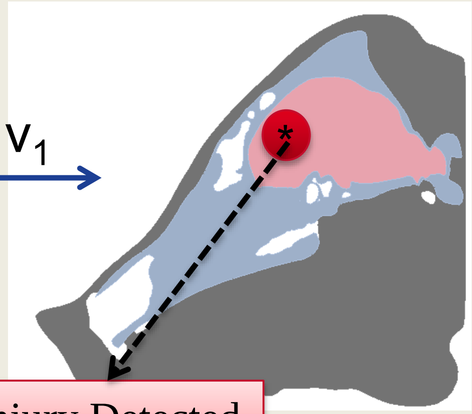

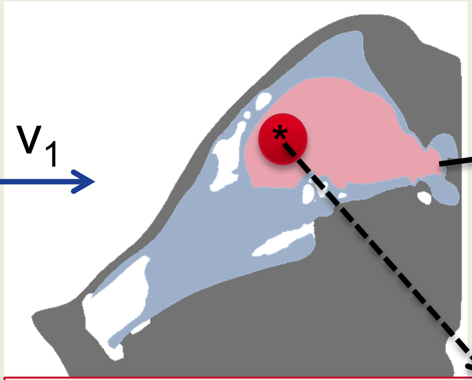

Computed Stress, Strain, Pressure Profiles, etc., over time

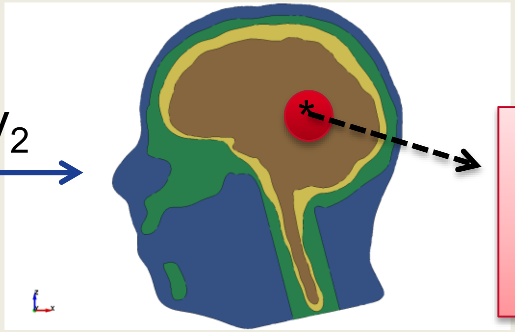

U.S. ARMY RDECOM

Background

ARL

- **Animal models offer a convenient means of studying pathogenesis and epidemiology of traumatic brain injury arising from high-rate loading conditions**
- **Cell and tissue-level studies commonly use mice or rats (lower species) as these structures are similar among species**
- **To understand more complex structure with higher functionality (e.g. brain) requires use of species with higher order structural and functional similarities**
  - Porcine brain is similar in structure to human brain
- **Important to consider differences between animal and human models**
  - Skull thickness and sinus cavity location and size (these characteristics change with weight)
- **Working towards a transfer function between animal and human models to evaluate injury to the human head**

Challenges

- **Biofidelic geometry and mesh**
  - What are the critical features to retain in the model and how to retain complex features.
  - Tet vs. hex mesh
    - Higher order mesh vs computational cost
- **Material Characterization**
  - High rate properties of soft and hard tissues
  - Injury criteria and threshold
  - Interface properties

IDENTIFYING TRAUMATIC BRAIN INJURY (TBI) THRESHOLDS USING ANIMAL AND HUMAN FINITE ELEMENT MODELS BASED ON IN-VIVO IMPACT TEST DATA

Keegan Yates, Costin Untaroiu, Wade Baker, Elisabeth Fievisohn, Warren Hardy

Center for Injury Biomechanics

Background

- At least 1.4 million TBIs each year in the US
- Some types of TBIs can be prevented/reduced in severity through design changes
- Injury metrics are available as a design criterion (HIC, BrIC, etc.)

Langlois, J.A., W. Rutland-Brown, and K.E. Thomas, *Traumatic brain injury in the United States: emergency department visits, hospitalizations, and deaths*. 2006: Department of Health and Human Services, Centers for Disease Control and Prevention, National Center for Injury Prevention and Control.

VIRGINIA TECH WAKE FOREST UNIVERSITY
School of Biomedical Engineering and Sciences

Background

- Human data insufficient
- Injury metrics rely heavily on animal test data
- Data are scaled using simple mathematical relationship
  - Typically only use density, length, elastic modulus, etc.
  - Originally developed to scale non-human primate data
- Scaling could be done on a per species basis

Ommaya, A.K., et al., *Scaling of experimental data on cerebral concussion in sub-human primates to concussion threshold for man*. 1967, DTIC Document.

Overview

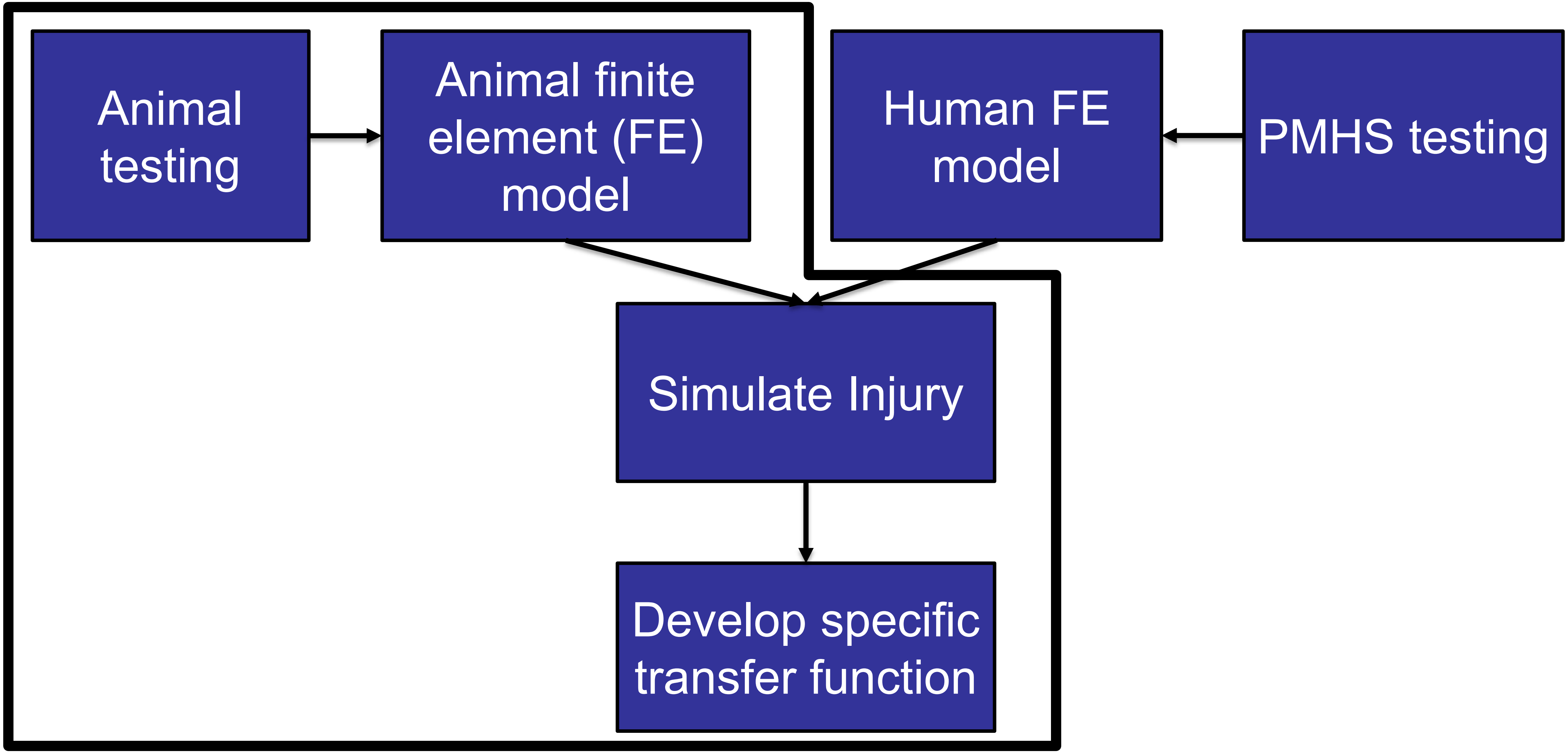
Animal testing
Animal finite element (FE) model
Human FE model
PMHS testing
Simulate Injury
Develop specific transfer function

Overview

- **Pig impact testing**
- **Pig brain finite element (FE) model from MRI/CT scans**
- **Apply testing kinematics**
- **Validate with neutral density target (NDT) motion**
- **Prepare validated human FE model**
- **Repeat loading conditions in human model**
- **Develop methodology for creating a pig-human transfer function –*in progress***

VIRGINIA TECH WAKE FOREST UNIVERSITY
School of Biomedical Engineering and Sciences

Introduction

- **Tests performed on Göttingen mini-pigs**
- **VT tests**
  - **Neutral density target (NDT) tracking**
  - **Drop height constant**
- **WFU tests**
  - **Histology performed**
  - **Drop height varying**

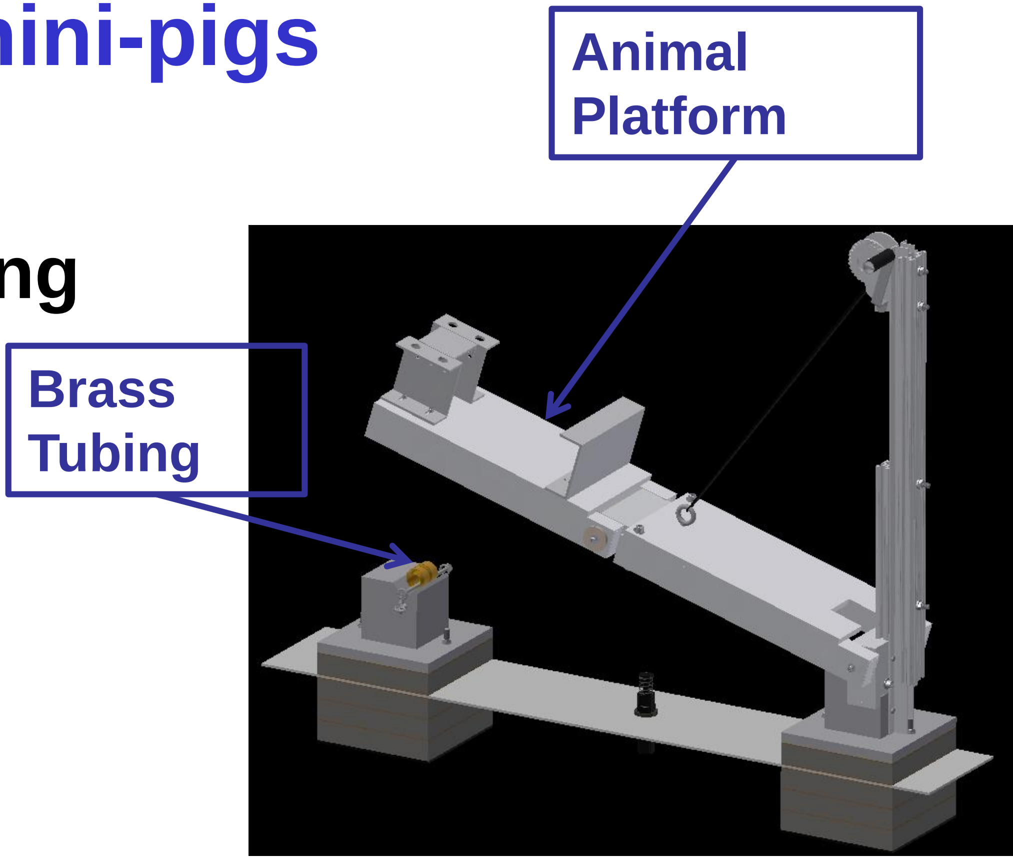

Injury Device

Fievisohn, E.M., et al., *Evaluation of impact-induced traumatic brain injury in the Göttingen Minipig using two input modes.* Traffic injury prevention, 2014. **15**(sup1): p. S81-S87.

Impact

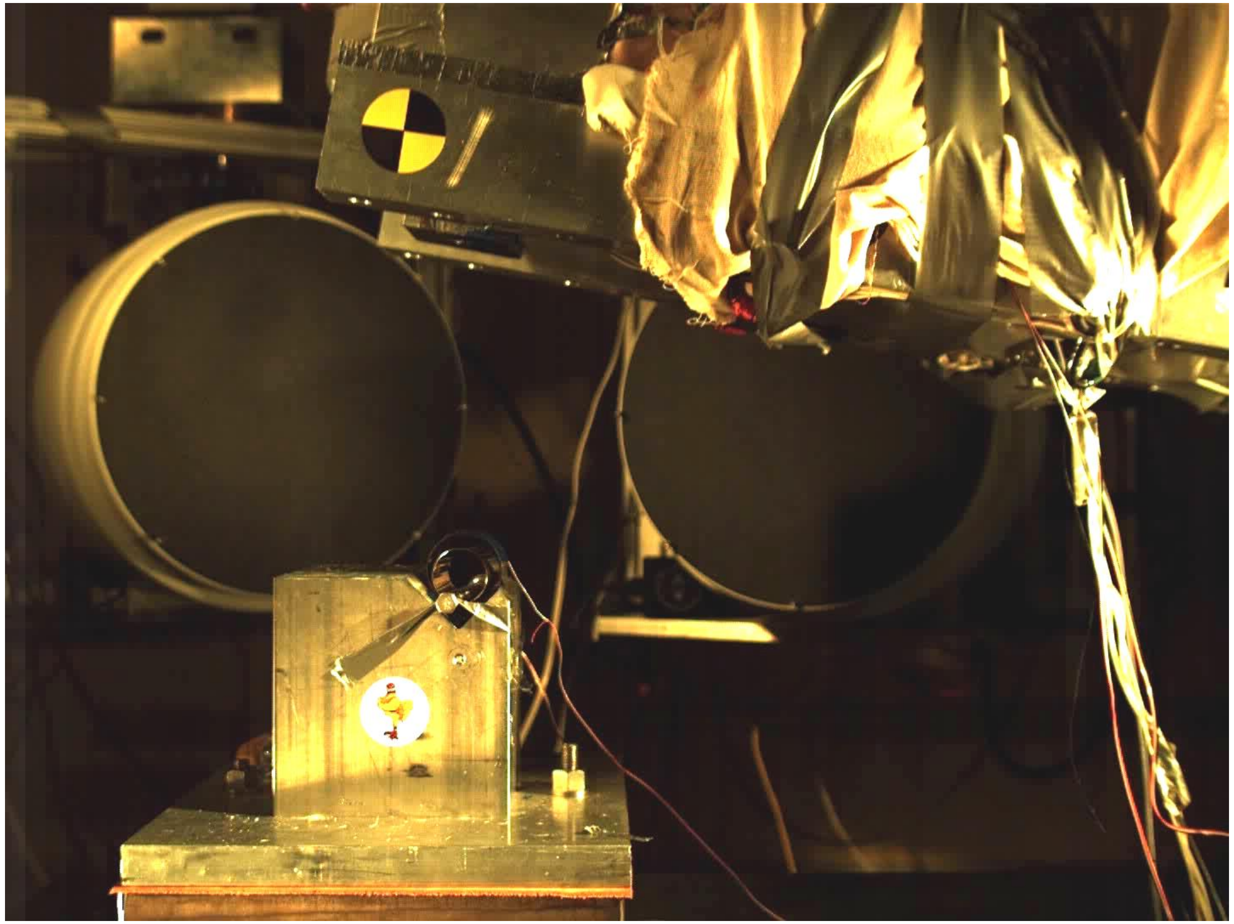

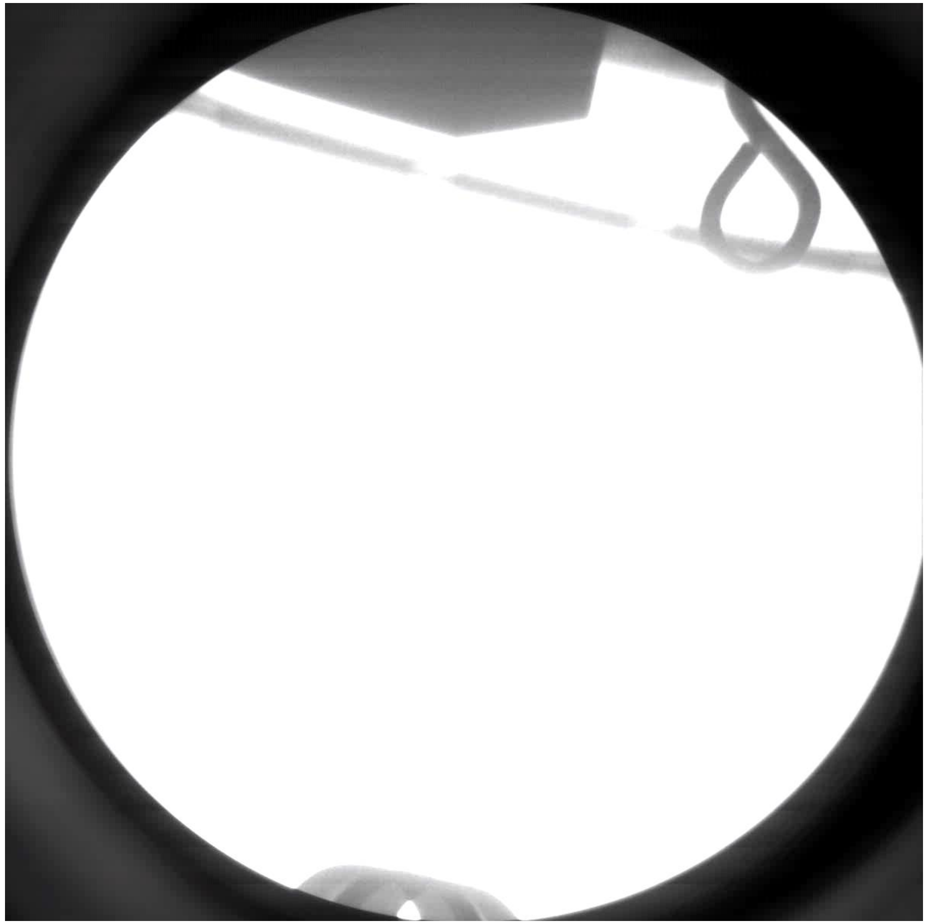

Injury

- Injuries quantified by immunohistochemistry and proton magnetic resonance spectroscopy
- Increase in light and heavy neurofilament ≈11%
- Changes in several metabolite concentrations indicate glutamate excitotoxicity

Range of Peak Kinematics Parameters (at accelerometer array)	
Impact Speed (m/s)	2.6-4.3
Impact Duration (ms)	13.6-19.9
Linear Acceleration (g)	40.1-95.9
Angular Acceleration (rad/s^2)	1014.5-3814.9
Angular Speed (rad/s)	7.2-10.8

VIRGINIA TECH WAKE FOREST UNIVERSITY
School of Biomedical Engineering and Sciences

Kinematics

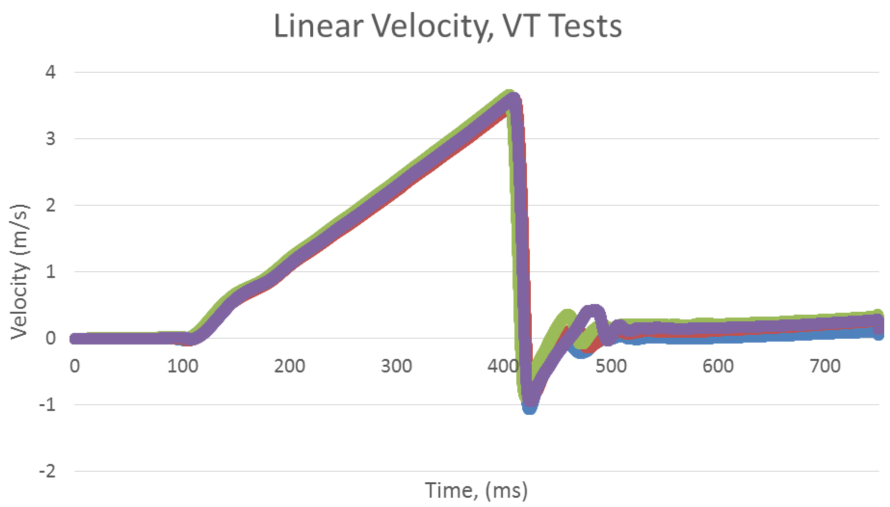

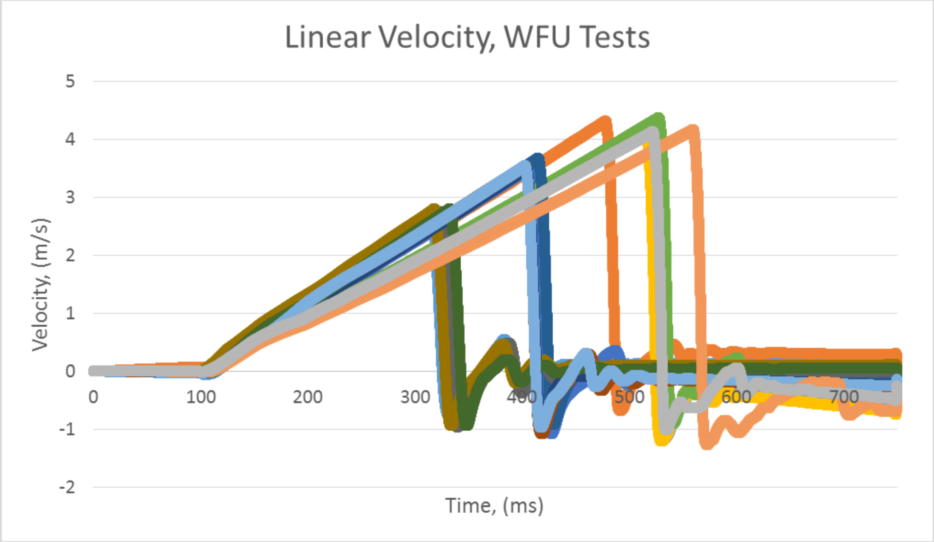

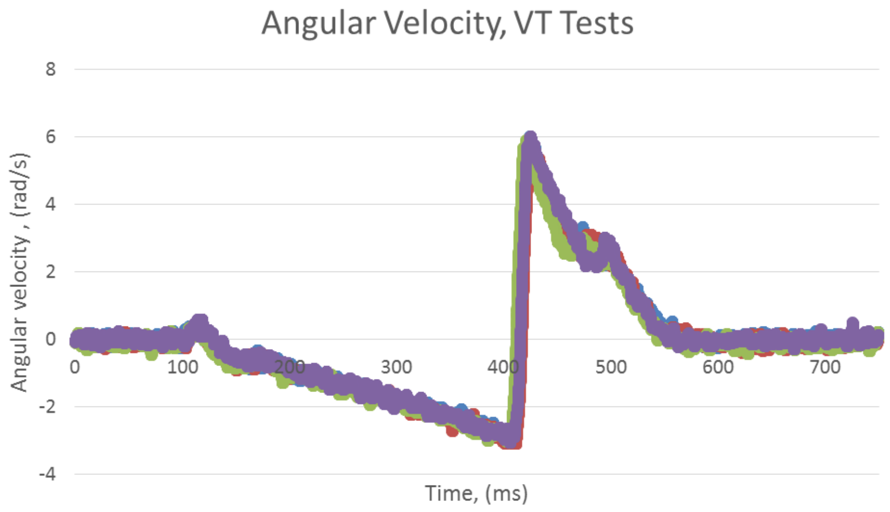

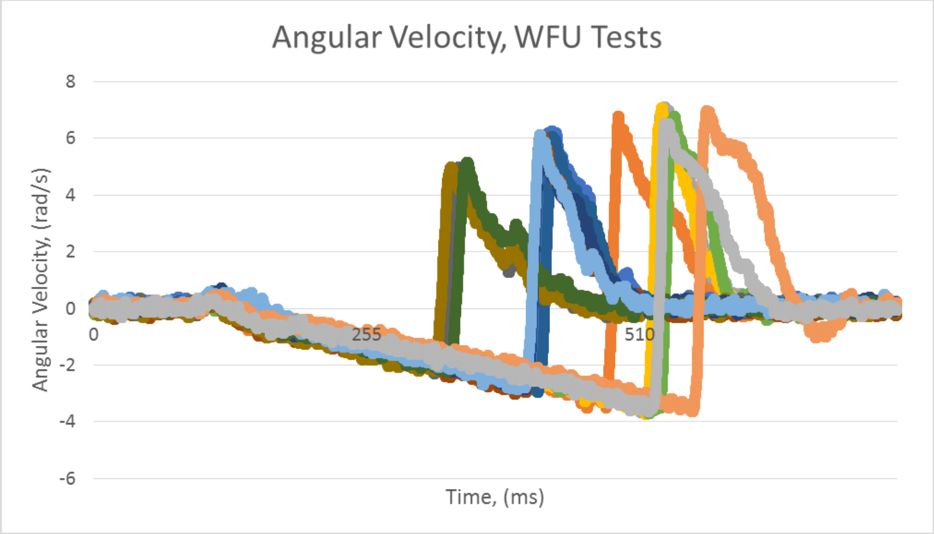

FE Model Creation – Geometric Reconstruction

Medical images from Gottingen Minipig

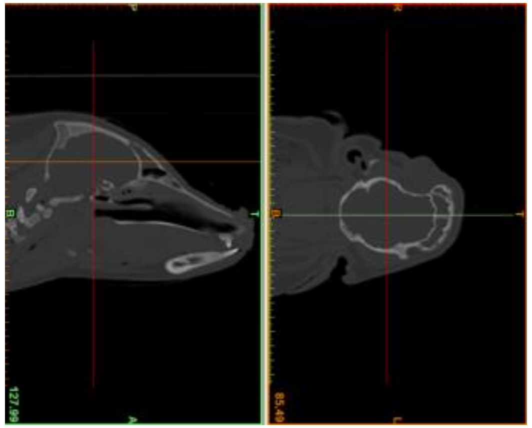

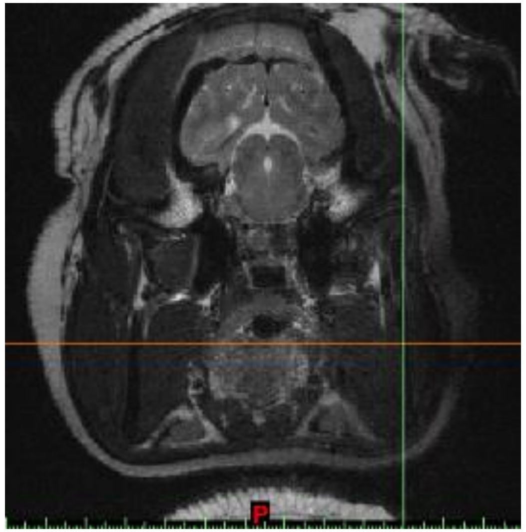

Segmentation (Materialise Mimics)

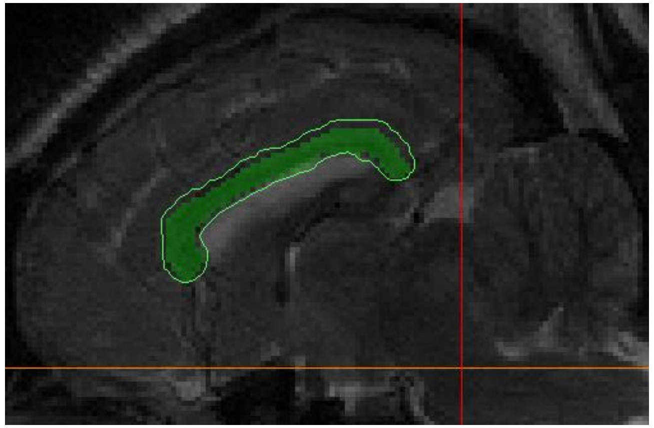

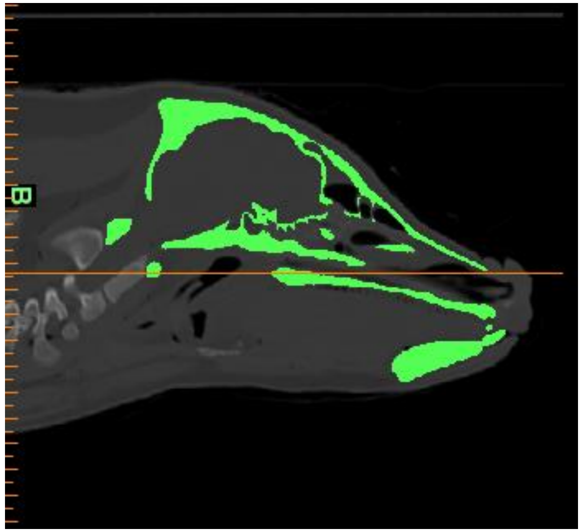

Creation of surface geometry from segments (Rhinoceros)

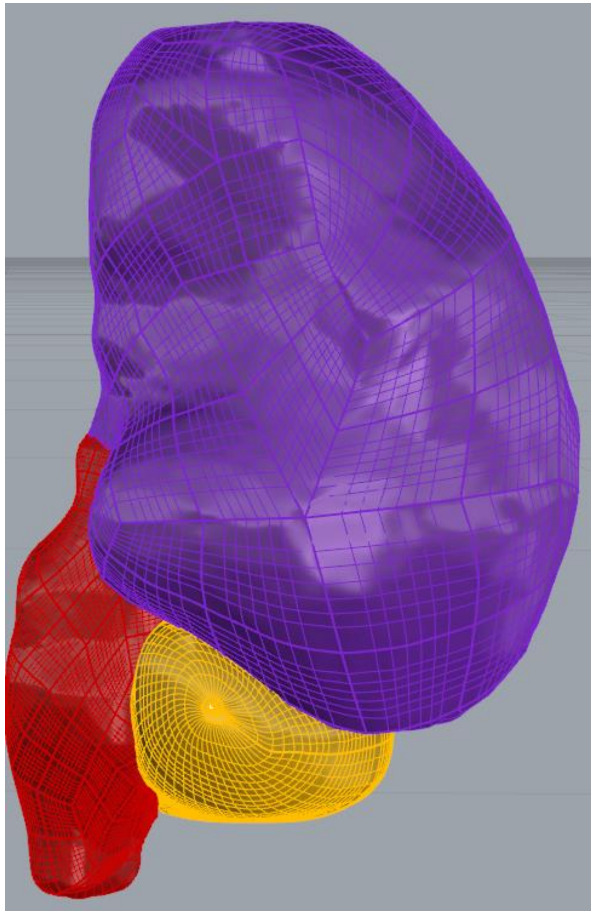

FE Model Creation – Meshing

- The brain was meshed with deformable hex elements
- The skull was meshed with rigid plate elements
- Brain modeled as Kelvin-Voight viscoelastic

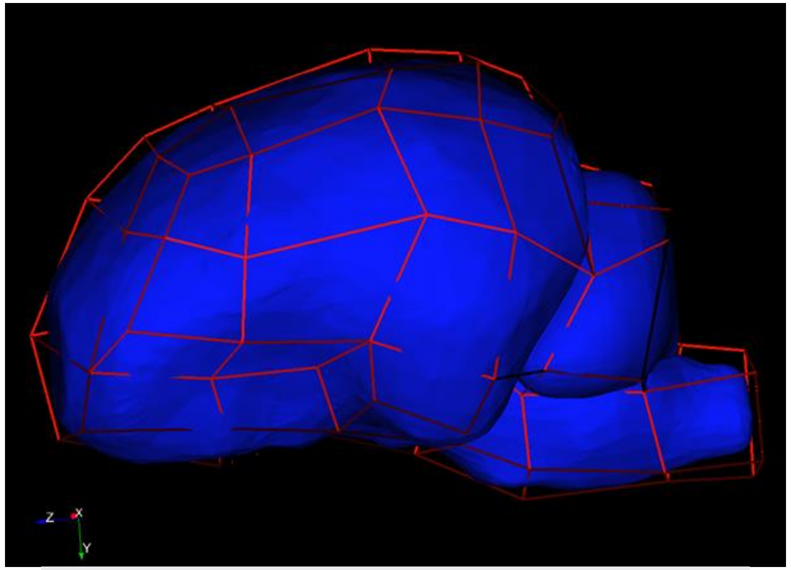

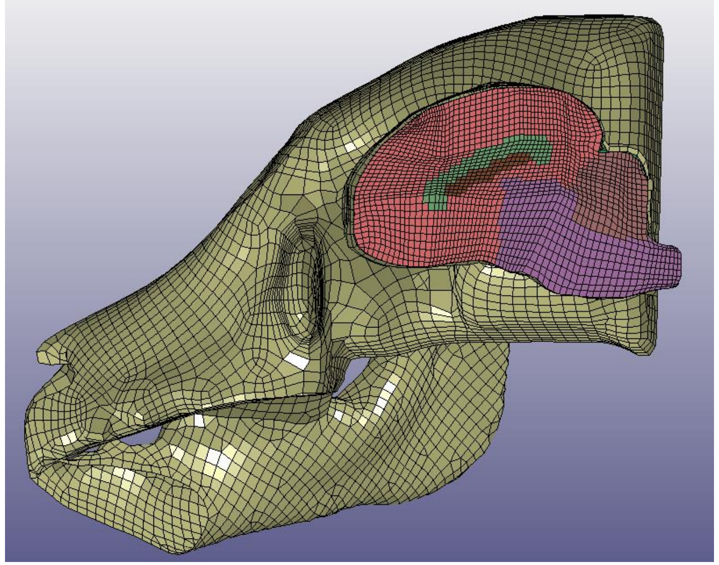

FE Model Creation – Boundary Conditions

- Skull-brain interface modeled as sliding contact
- Accelerometer data applied to skull

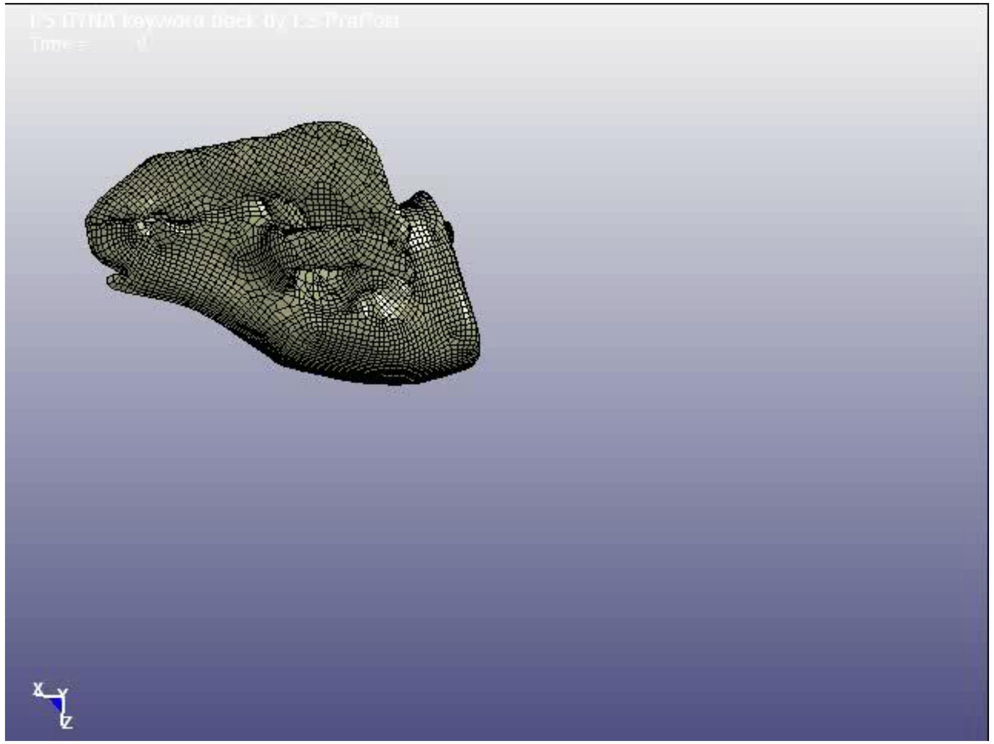

Results

- Nodes were chosen at the marker locations

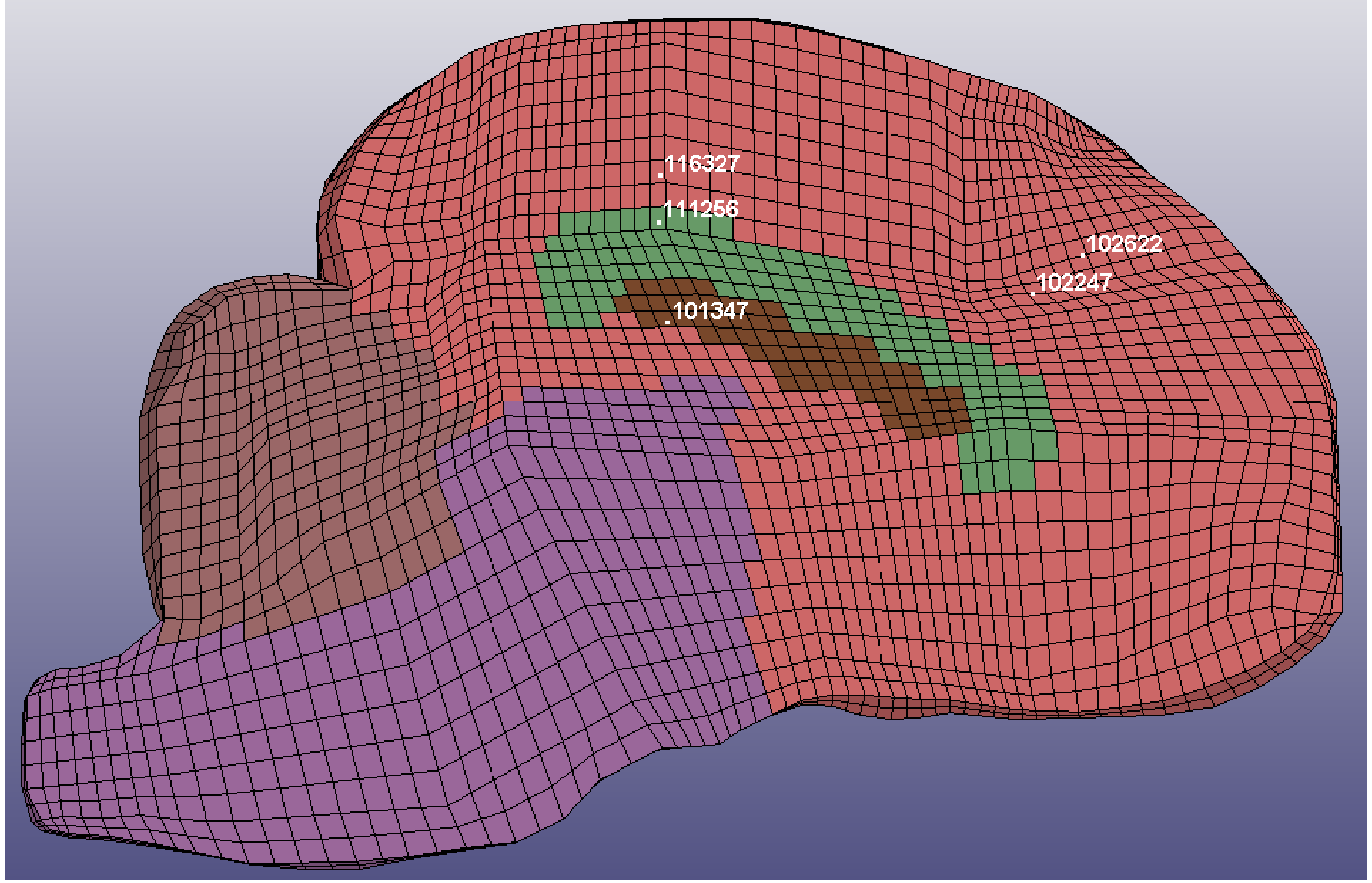

Results

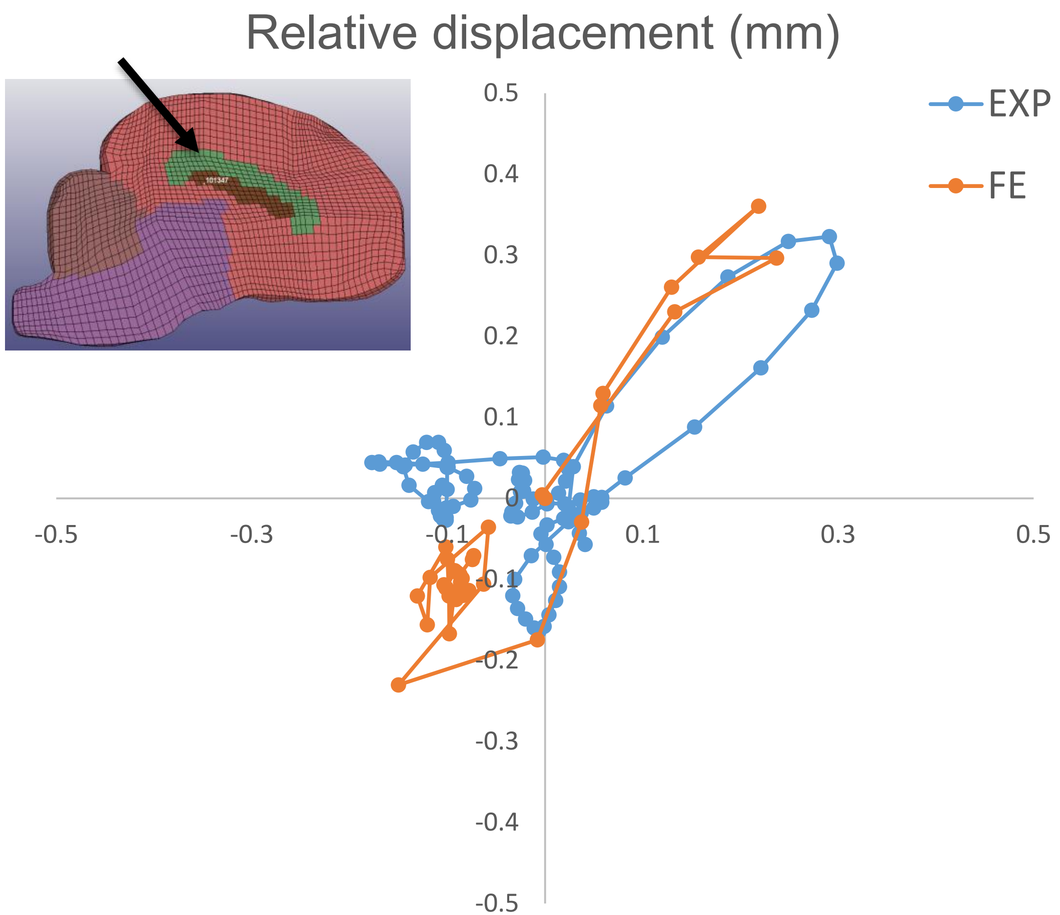

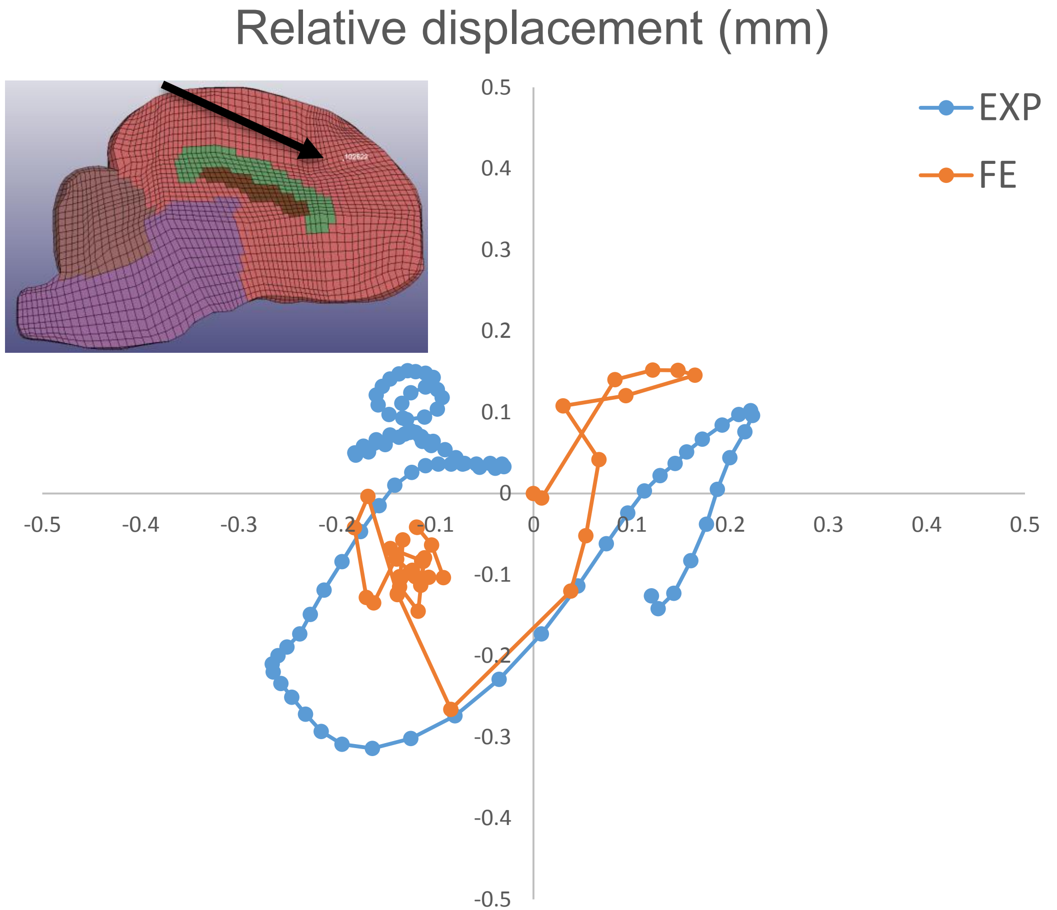

Model simulation compared to one experimental test

VIRGINIA TECH WAKE FOREST UNIVERSITY
School of Biomedical Engineering and Sciences

Results

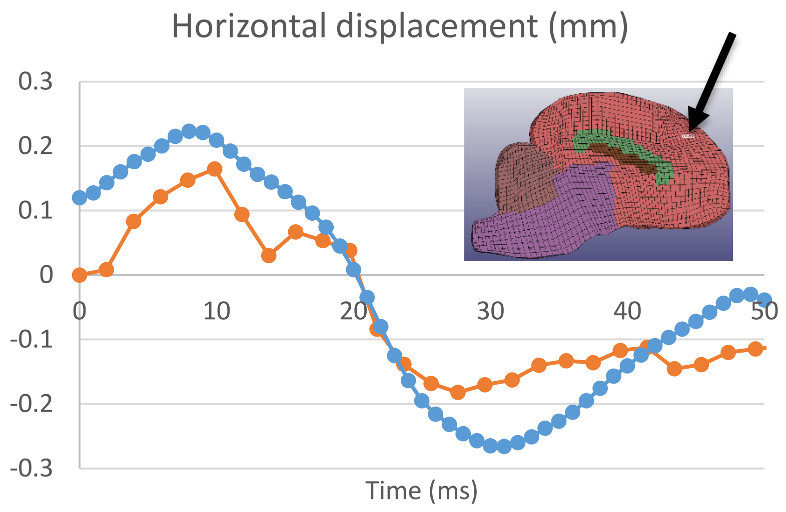

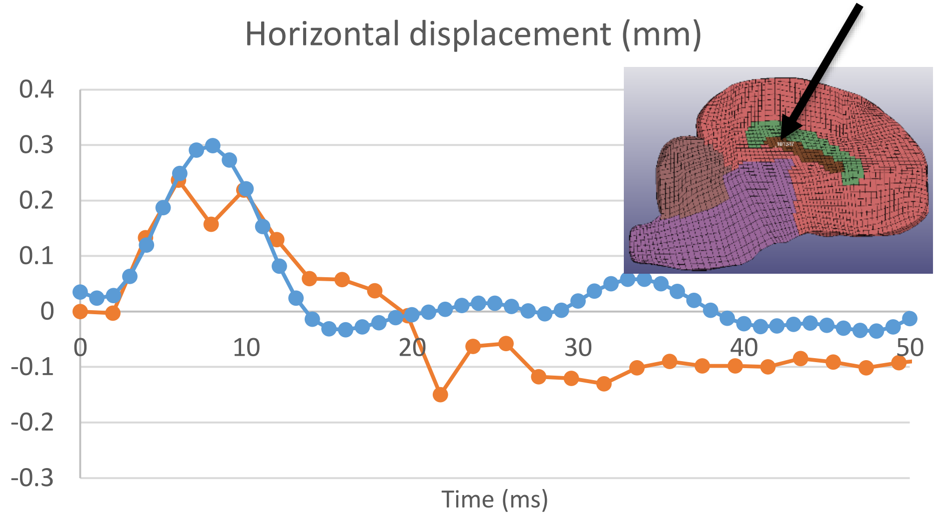

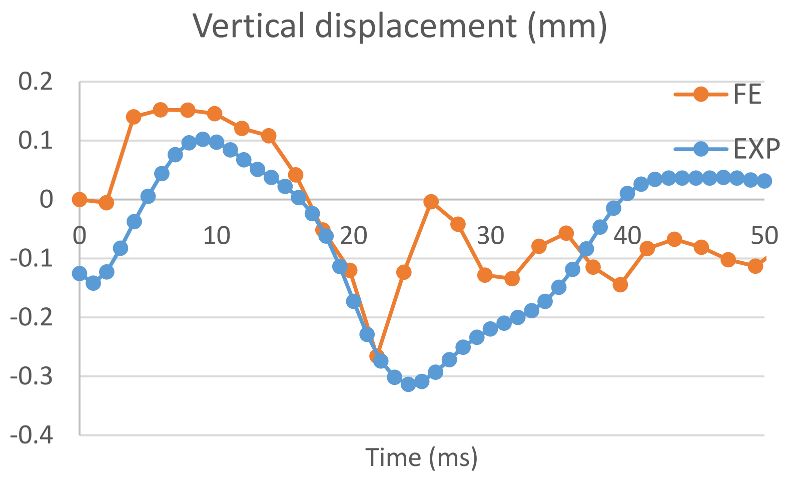

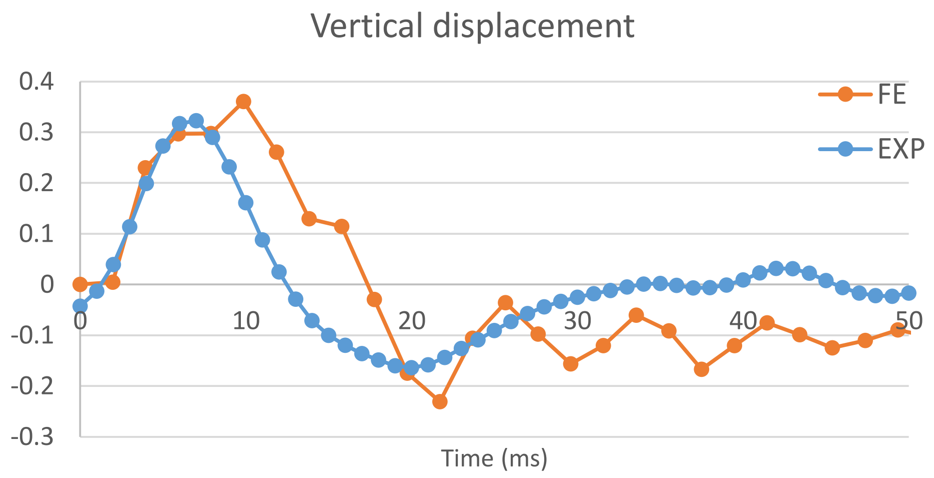

GHBMC Model

- **GHBMC skull modified with rigid outer shell**
- **Boundary conditions identical to pig**

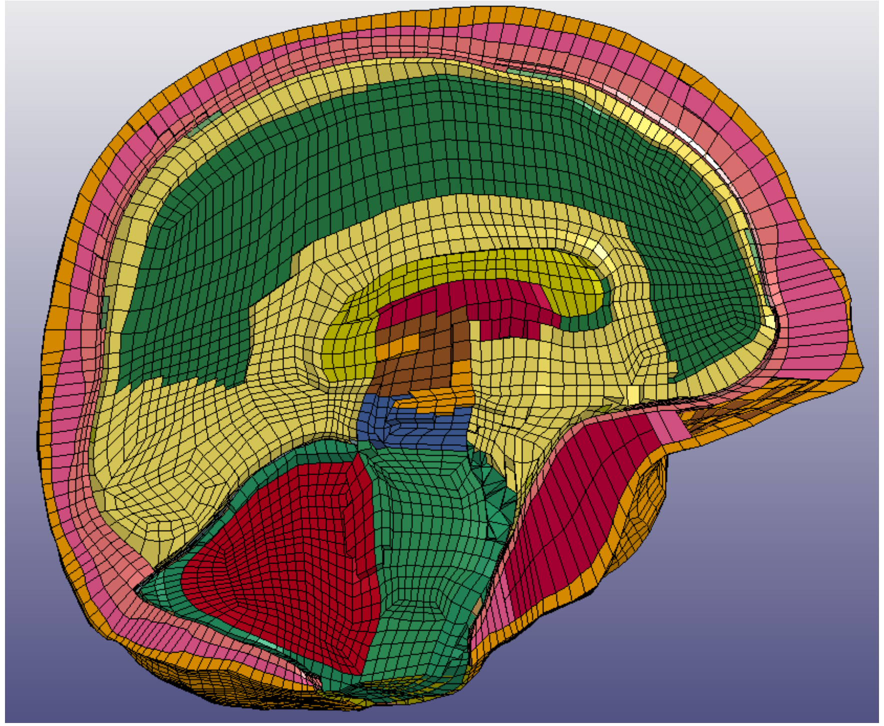

Mao, H., et al., *Development of a finite element human head model partially validated with thirty five experimental cases.* Journal of biomechanical engineering, 2013. **135**(11): p. 111002.

Results

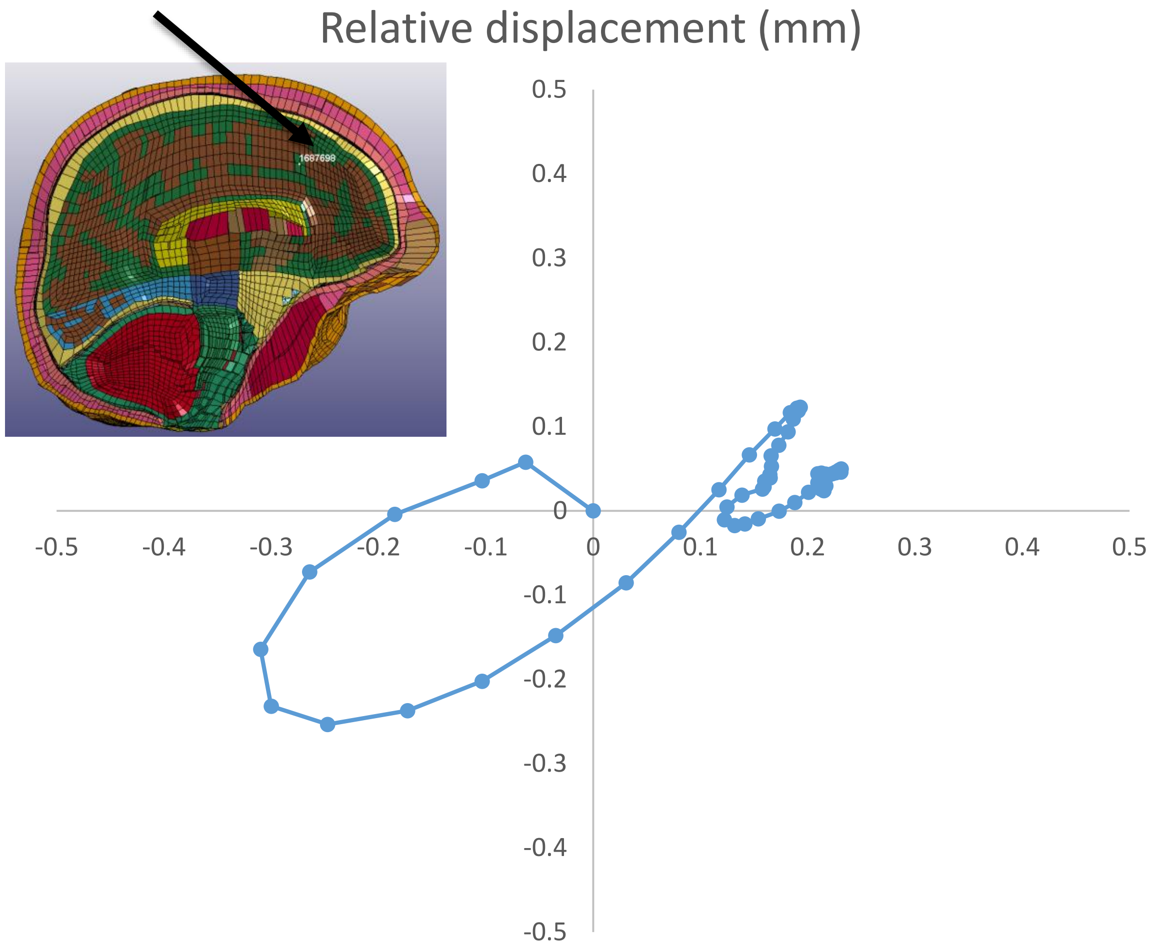

Relative displacement (mm)
0.5
0.4
0.3
0.2
0.1
0
-0.1
-0.2
-0.3
-0.4
-0.5
-0.5 -0.4 -0.3 -0.2 -0.1 0 0.1 0.2 0.3 0.4 0.5

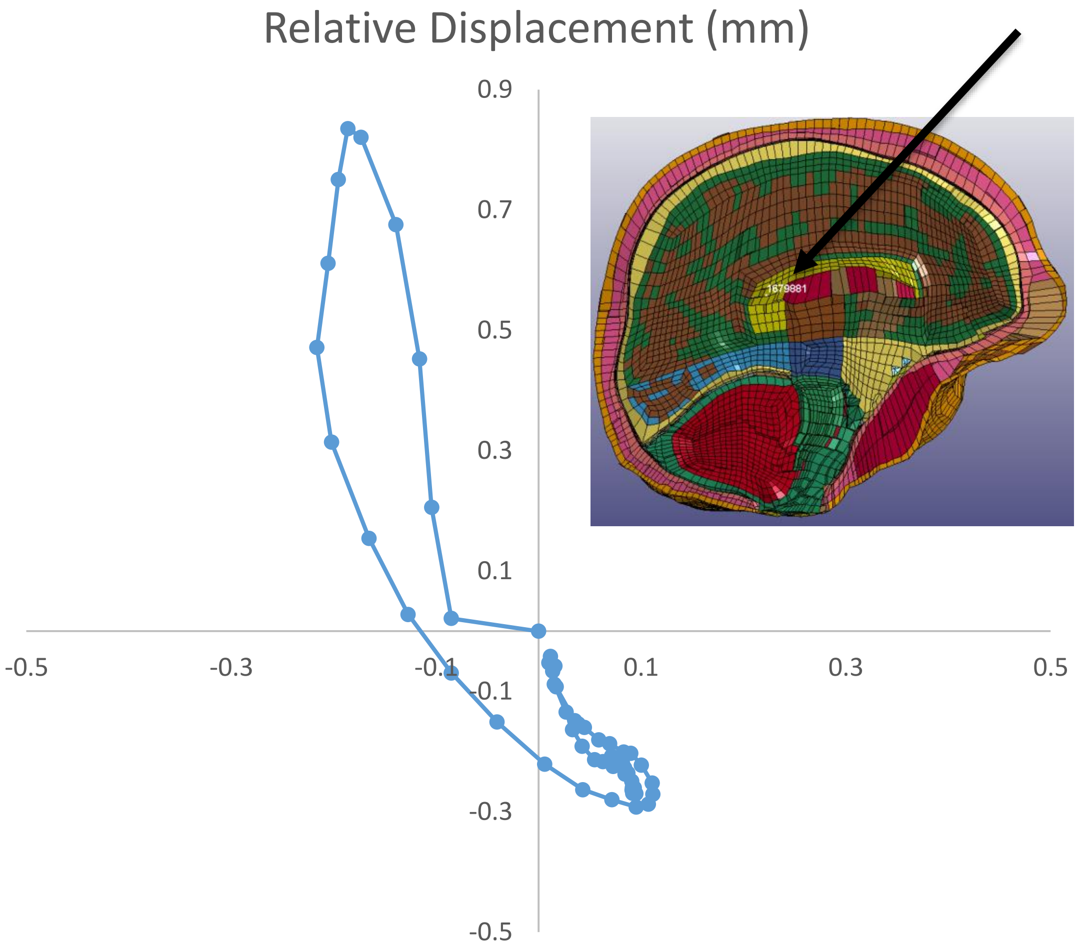

Relative Displacement (mm)
0.9
0.7
0.5
0.3
0.1
-0.1
-0.3
-0.5
-0.5 -0.3 -0.1 0.1 0.3 0.5

SIMon Model

- Simulated Injury Monitor (SIMon) prepared
- Identical boundary conditions to pig

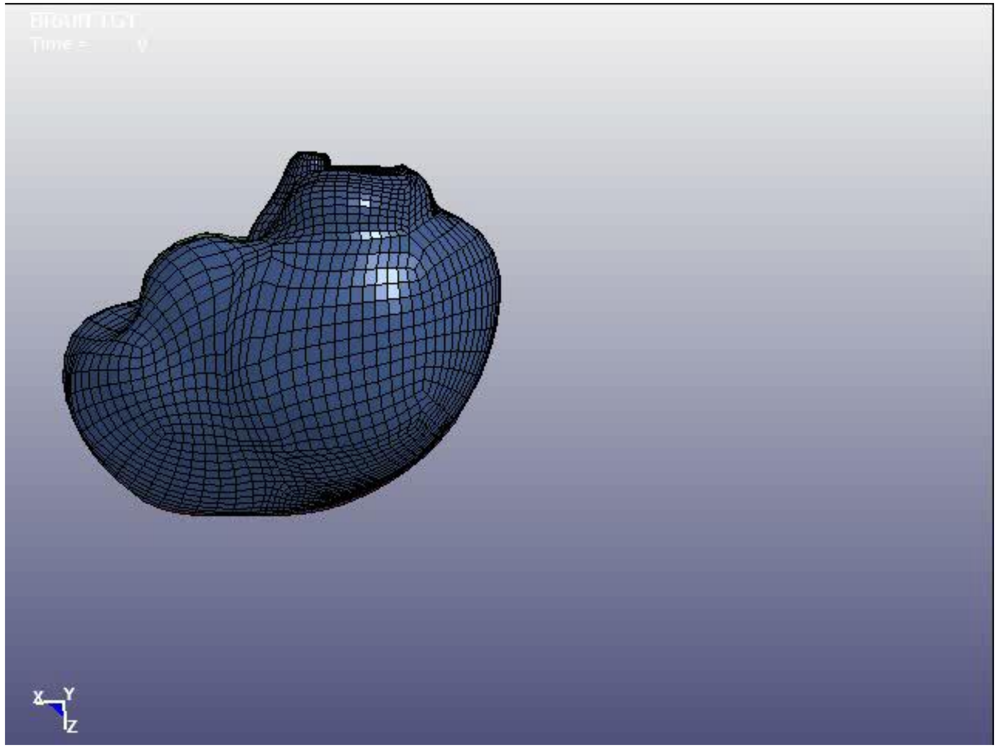

Takhounts, E.G., et al., *Investigation of traumatic brain injuries using the next generation of simulated injury monitor (SIMon) finite element head model.* Stapp Car Crash J, 2008. **52**: p. 1-31.

Cumulative Strain Damage Measure

- Cumulative percentage of elements above a threshold strain level

Model	CSDM .025
Pig Brain	.40
GHBMC	.74
SIMon	.68

Future Work

- Calculate analytical injury metrics
- Human kinematics adjusted to match pig injuries
- Change pig kinematics
- Empirical formula to scale pig to human

Acknowledgement

- NHTSA
- Takata

- Questions?

kmyates@vt.edu

FE Model Creation – Mesh Quality

	Pig Brain	GHBMC Brain	SIMon Brain
Number of 3D elements	51,664 hexa 0 penta 0 tetra	80,764 hexa 106 penta 631 tetra	40,203 hexa 493 penta 12 tetra

	Quality Threshold	Failed Elements in Pig Brain Model (%)	GHBMC Brain Model (%)	SIMon Brain Model (%)
Jacobian	< 0.4	.728	0.498	.151
Aspect Ratio	> 5	.178	1.011	.465
Min. Angle (deg)	< 25	.484	.576	.354
Max. Angle (deg)	> 160	.705	.645	.013
Skew (mm)	>60	0.821	0.675	.642

Funded by National Institute for Neurological Disorders and Stroke

A Multiscale Virtual Human Head Model Validated Using 3D Dynamic Deformations in Live Human Brain

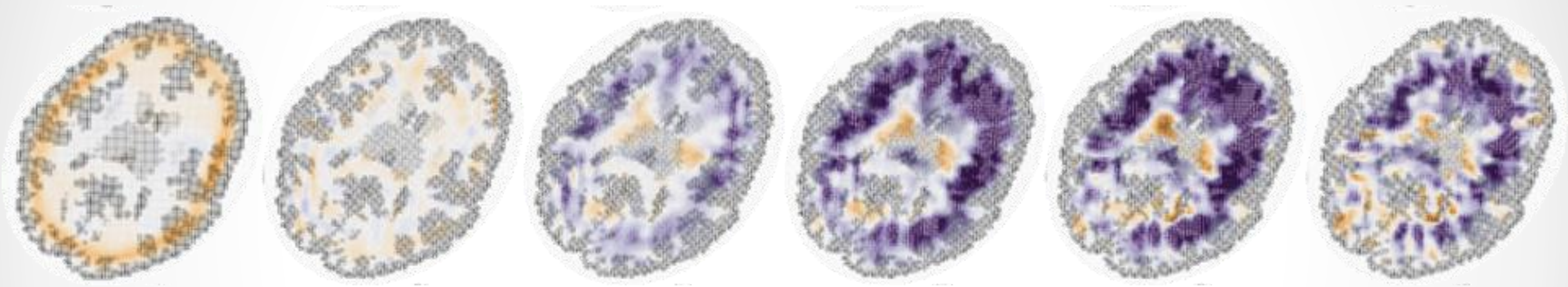

S. Ganpule, N.P. Daphalapurkar, K.T. Ramesh, J. Prince.
Johns Hopkins University.

D. Pham, A. Knutsen.
Henry Jackson Foundation.

P. Bayly.
University of Washington, St. Louis.

Shearing Deformations in Brain

Tagged MRI imaging for measurement of strains

- Full-field measurements of in-plane strain components using tagged Magnetic Resonance Imaging (MRI) and Harmonic phase (HARP) algorithm. Osman, Kerwin, McVeigh, Prince, Magn. Reson Med. 1999.
- Application of tagged MRI and HARP to live human brain

  Bayly, Cohen, Leister, Ajo, Leuthardt, Genin, J Neurotrauma 2005.
- Temporal Resolution: ~6 ms. Knutsen et al. J biomechanics 2015.
- Spatial Resolution: ~8 mm. Communication with Bayly and Prince.

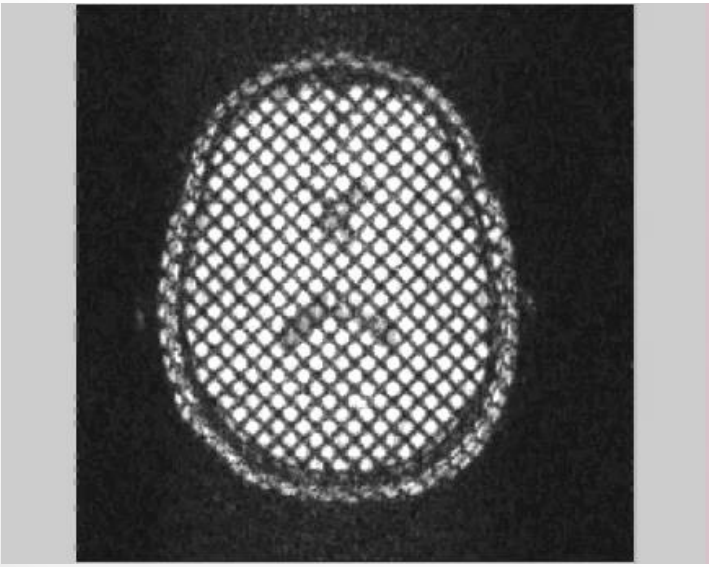

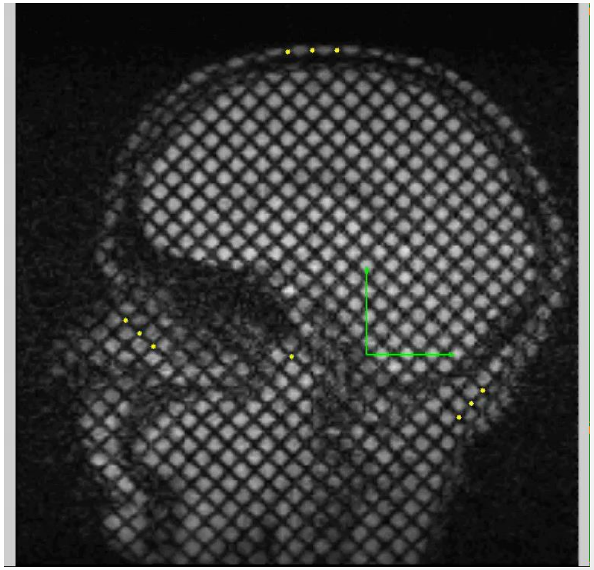

Courtesy: Drs. Jerry Prince, Dzung Pham, Philip Bayly

Dynamics of Brain tissue

- Low shearing stiffness → low shear wave speeds, c_s ~ 1 mm/ms (wave speeds in polymers is 1000x).
- Large difference between the bulk wave speed (~10^3 mm/ms) and shear wave speed (~ 1 mm/ms).
- White matter is anisotropic and nonlinear mechanical response.
- For axial head rotation the dominant mode of deformation is shearing induced by slow moving shear waves.

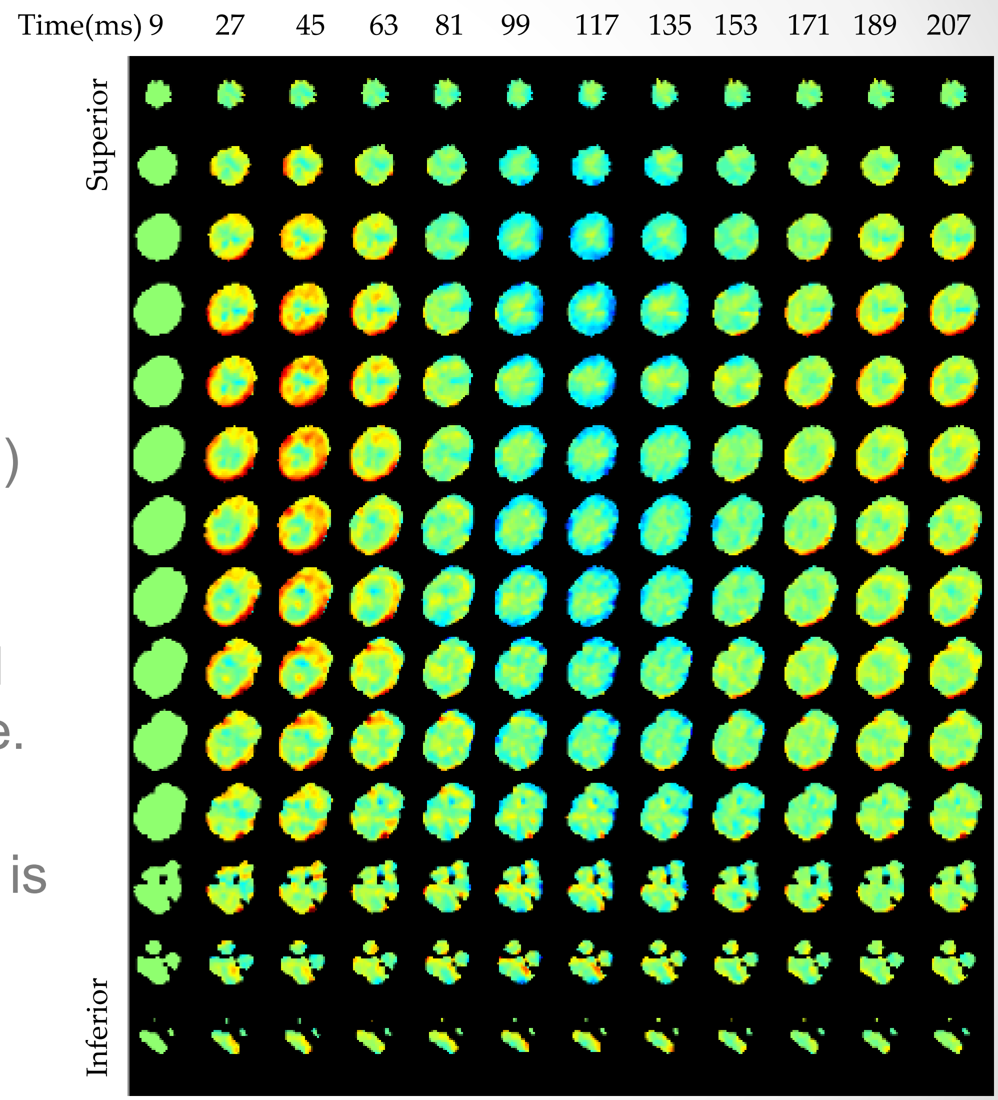

MPM and Shearing Deformations

Material Point Method (MPM) is a particle-based method (Sulsky+1995)

Advantages:

- an ability to model large deformations, without mesh lockup or mesh degeneration.
- no-slip contact is natural
- a combination of advantages from Lagrangian and Eulerian methods.
- excellent scaling for simulations on a computing clust

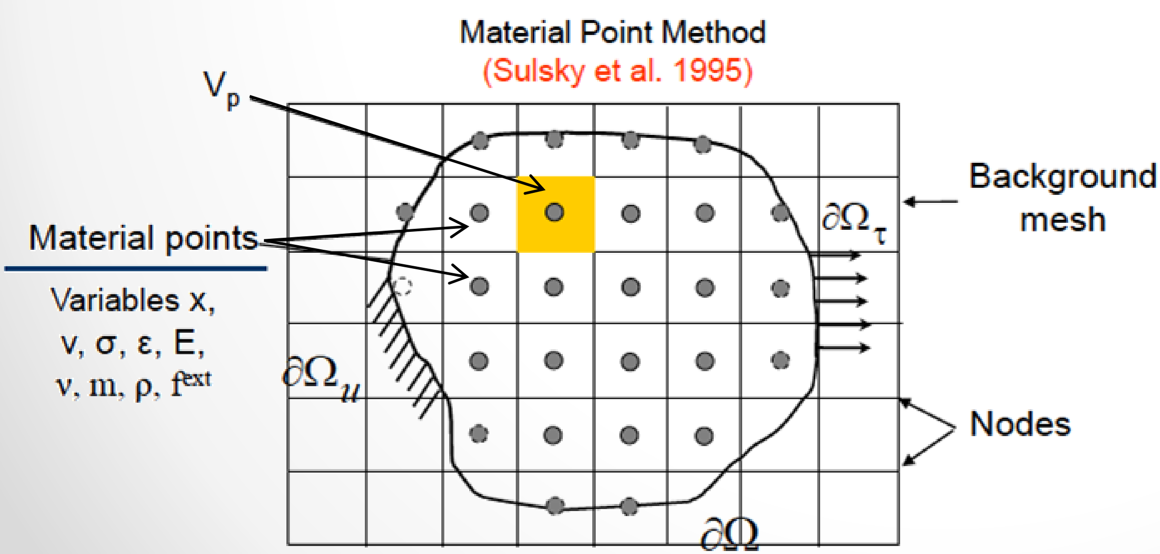

Brannon+ 2013; Verification: Generalized Vortex

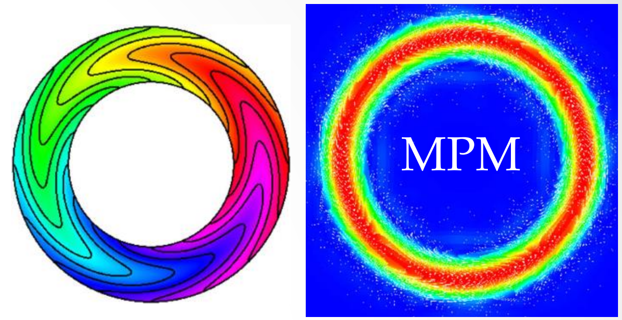

Ionescu, Weiss+ 2006

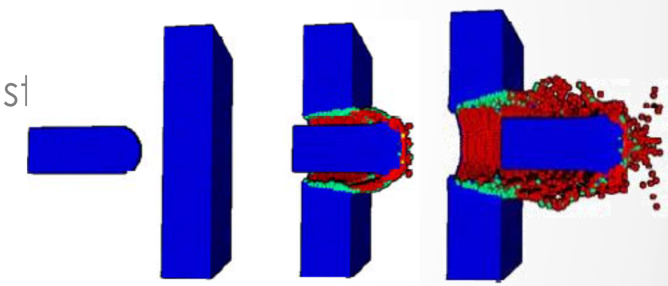

Segmented MRI to MPM

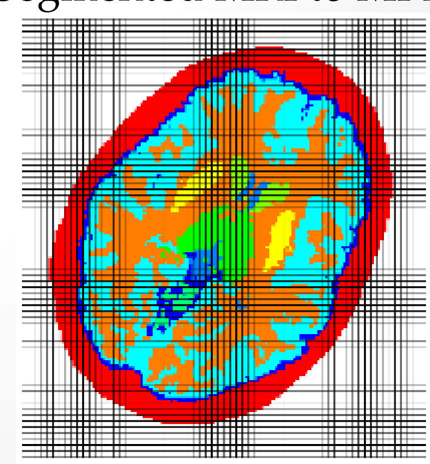

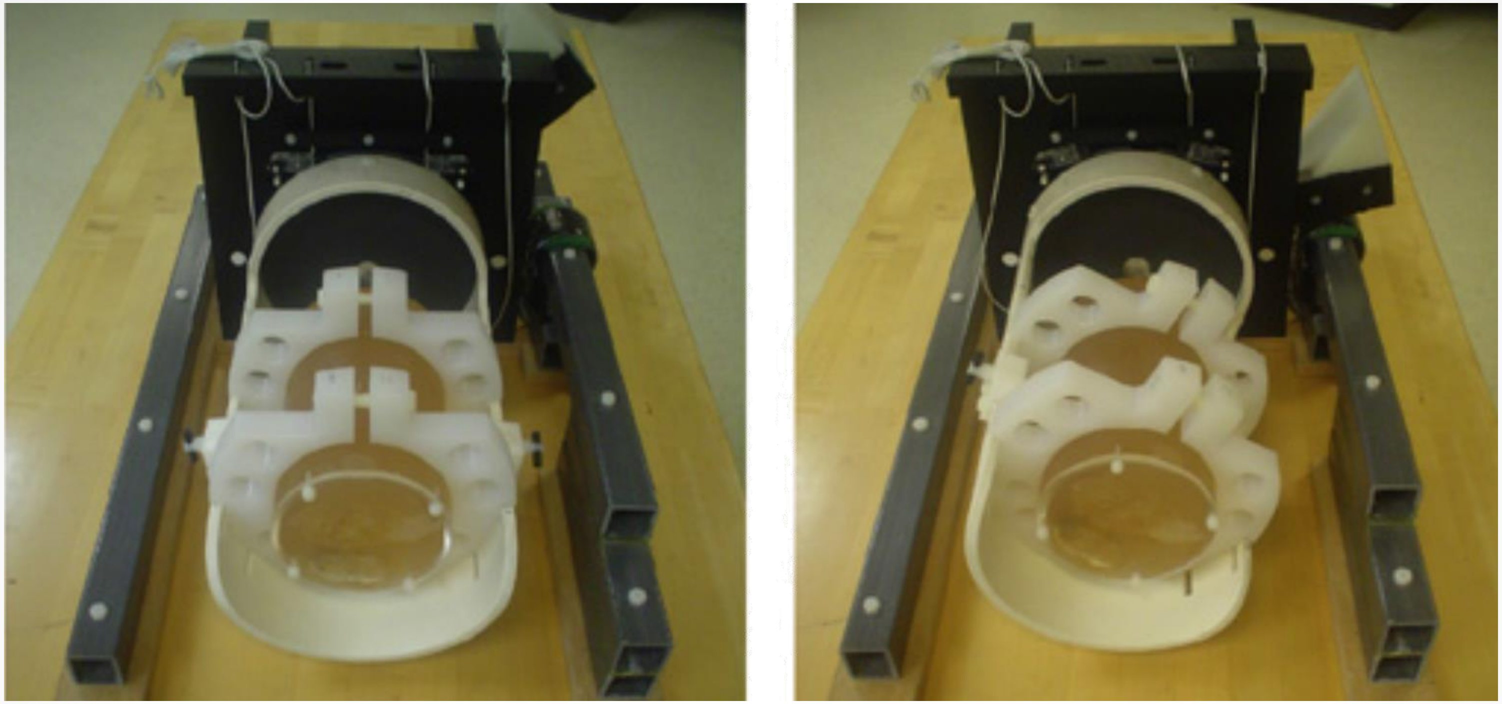

Experiments on Gelatin Cylinder

Experiments on Gel

Experimental Setup

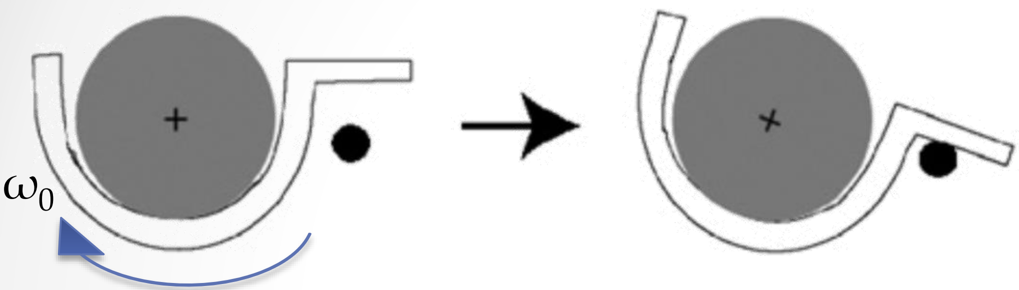

Cylinder: radius 56 mm; length 203 mm

Initial Conditions

ω_0= 6.37 rad/s

Boundary Conditions

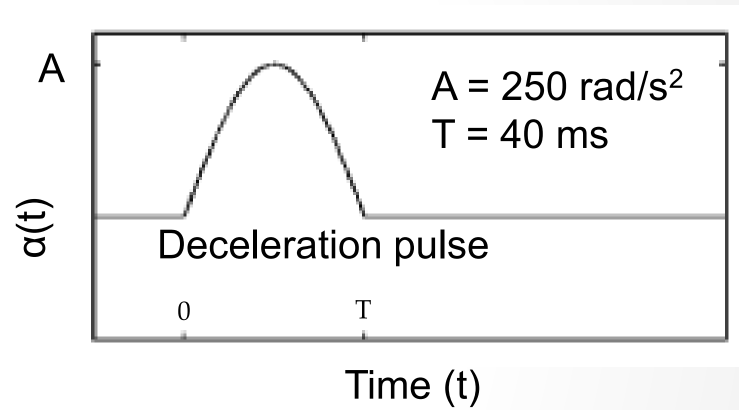

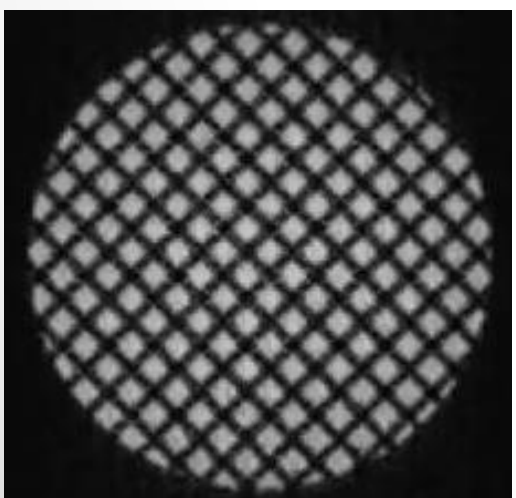

Measurements of deformation in gel

Tagged MRI Displacements Strain, $E_{r\theta}$

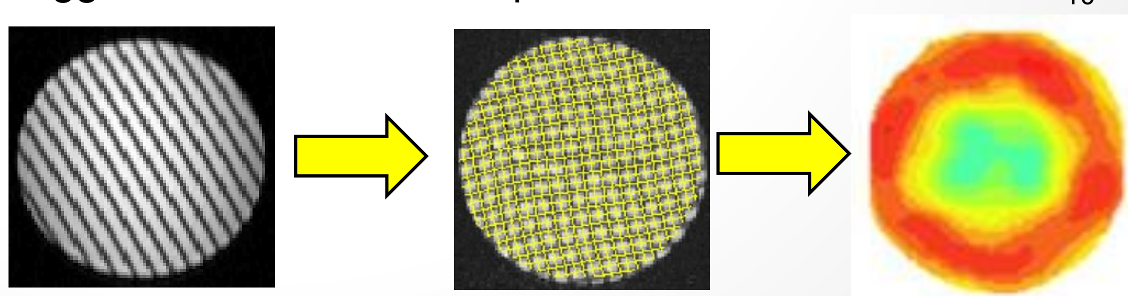

Courtesy: Dr. Andy Knutsen; Henry Jackson Foundation.

Verification & Validation of Predictions from Gel Simulations

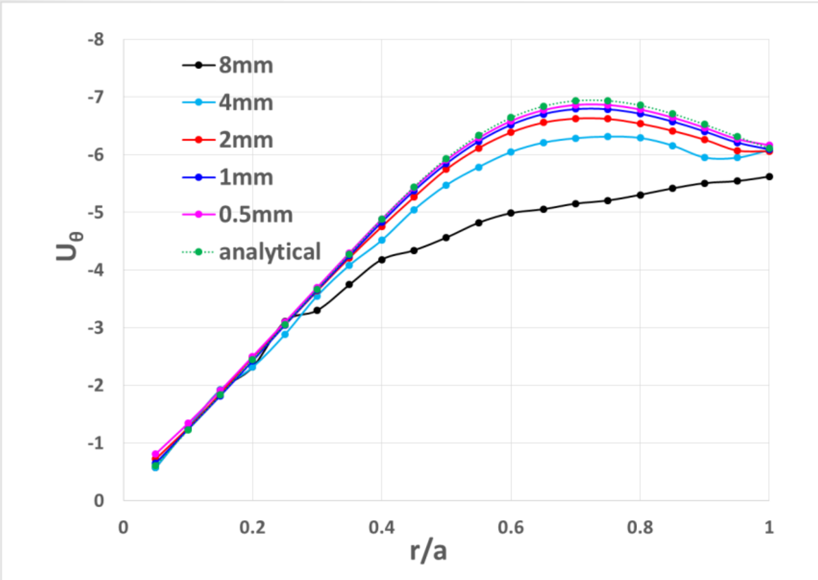

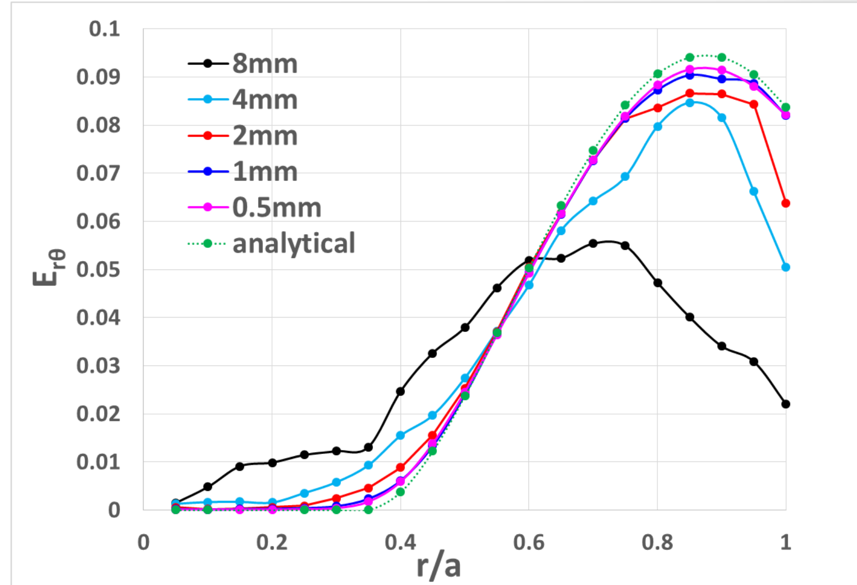

A shearing wave (+ $E_{r\theta}$) travels to the center at speed c_s, and reflects back (- $E_{r\theta}$) as a shearing wave travelling outwards.

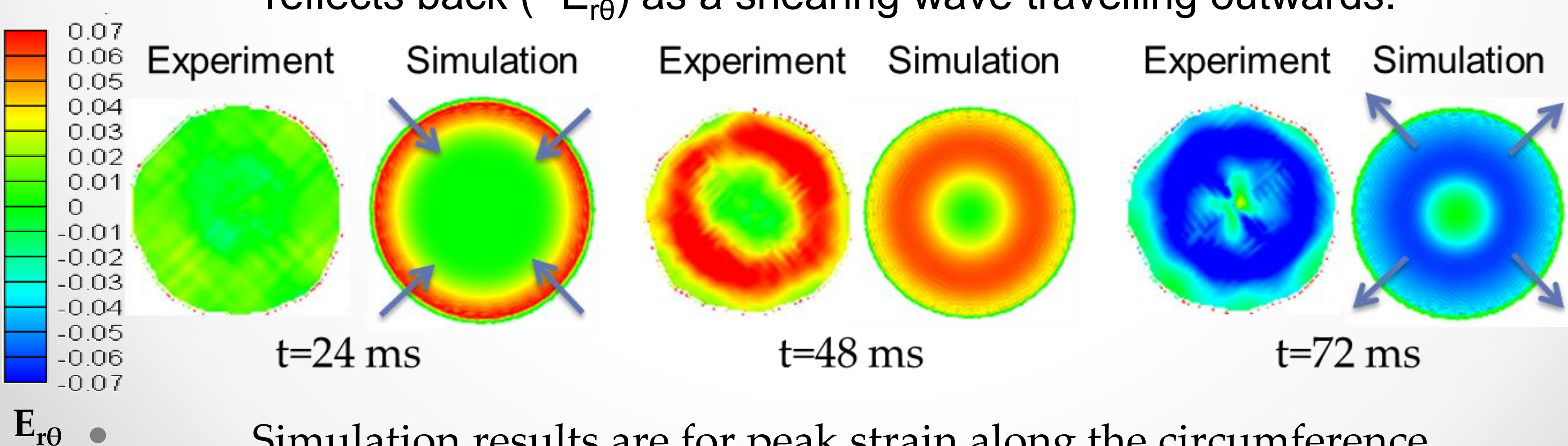

Simulation results are for peak strain along the circumference

Measurement of Brain Deformations using Tagged MRI

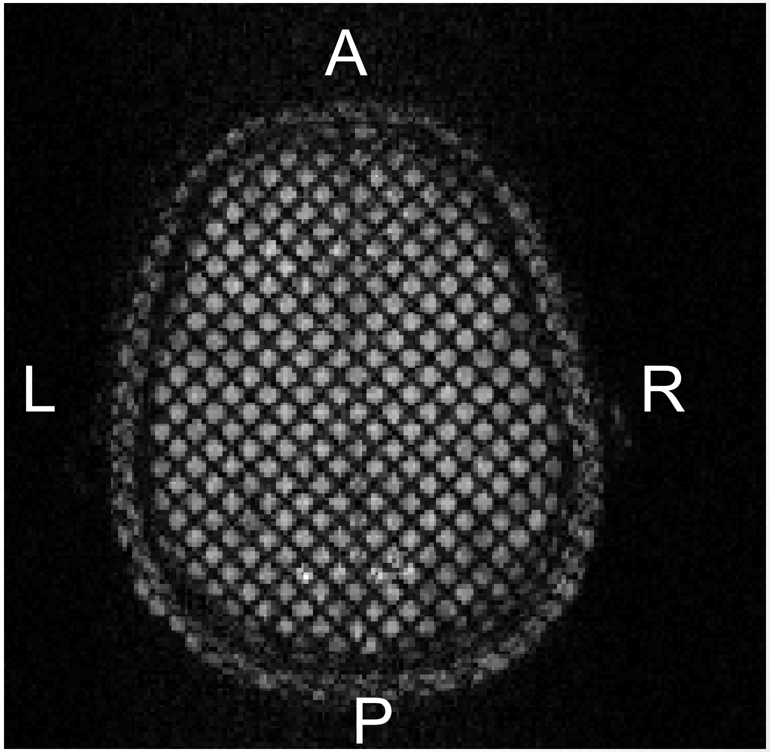

Courtesy: Dr. Andy Knutsen; Formerly at Henry Jackson Foundation.

How well do brain tissue properties predict the measured brain response?

Virtual Human Brain

Voxelated data

Segmented data

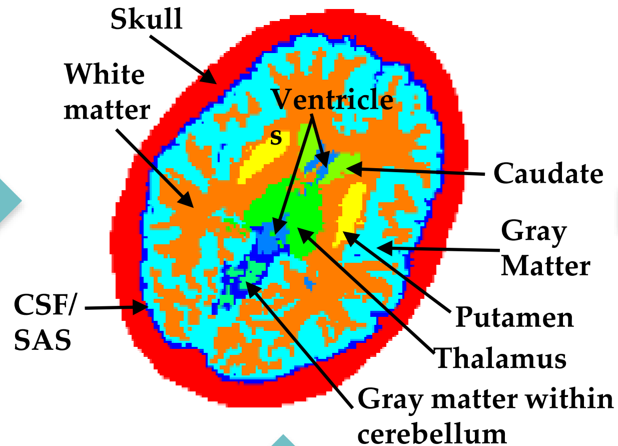

MPM model

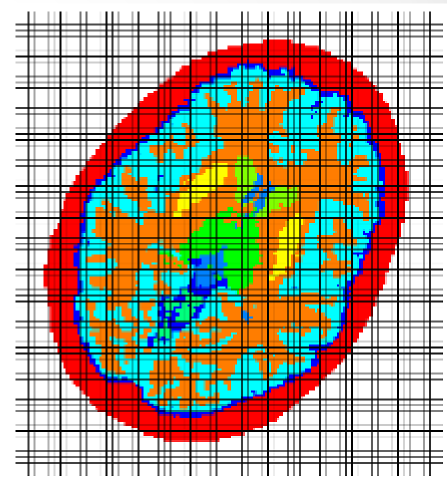

Discretization:
2 voxel = 1 MP

MRI

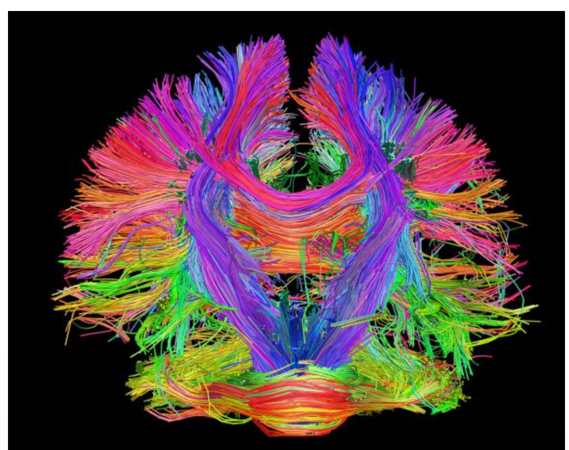

A representative DT image

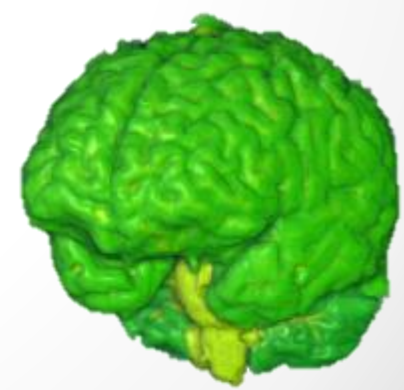

3D brain
1 voxel = 1 mm^3

Constitutive Model – White Matter

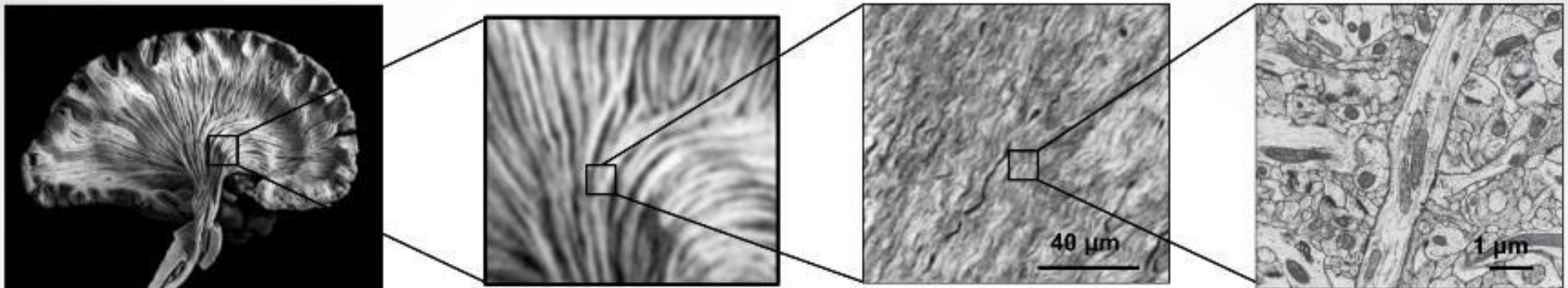

Bammer and Moseley (2002) | Bammer and Moseley (2002) | Bain, Meaney (2000) | Peters, Palay, Webster (1991)

Anisotropic Hyper-viscoelastic Framework

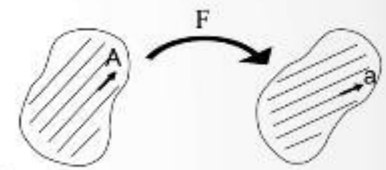

$$W(\overline{I}_1,\overline{I}_2,\ldots\overline{I}_5) = W_{iso}(\overline{I}_1,\overline{I}_2,J) + W_{aniso}(\overline{I}_4,\overline{I}_5)$$

Invariants

Isotropic Response:

$$\overline{I}_1 = tr(\overline{\mathbf{C}})$$

$$\overline{I}_2 = \frac{1}{2}\left\{(tr\overline{\mathbf{C}})^2 - (tr\overline{\mathbf{C}}^2)\right\}$$

$$J = \det \mathbf{F}$$

Anisotropic Response:

$$\overline{I}_4 = \mathbf{A}\cdot\overline{\mathbf{C}}\mathbf{A}$$

$$\overline{I}_5 = \mathbf{A}\cdot\overline{\mathbf{C}}^2\mathbf{A}$$

Stretch: $\lambda = \dfrac{\text{final length}}{\text{initial length}}$ **Right Cauchy-Green Deformation Tensor:** $\overline{\mathbf{C}} = \overline{\mathbf{F}}^T\overline{\mathbf{F}}$ $\overline{\mathbf{F}} = J^{-1/3}\mathbf{F}$

Constitutive Model for the Brain Tissue

- Gasser, T.C., Ogden, R.W., and Holzapfel, G.A. (2006). Hyperelastic modelling of arterial layers with distributed collagen fibre orientations. J. R. Soc. Interface 3, 15–35.

$$W = \frac{\mu}{2}(\bar{I}_1 - 3) + \frac{k_1}{2k_2}\left\{e^{\langle k_2(\kappa(\bar{I}_1-3)+(1-3\kappa)(\bar{I}_4-1))^2\rangle} - 1\right\} + U_J$$

$$\bar{I}_1 = tr(\bar{C});\ \bar{I}_4 = A \cdot \bar{C}A;\ \bar{C} = J^{-2/3}F^T F$$

$$\langle x \rangle = \frac{1}{2}(|x| + x)$$

$$\kappa = \frac{1}{2}\frac{1 - 6 + FA^2 + 2\sqrt{3FA^2 - FA^4}}{-9 + 6FA^2} \qquad 0 < FA < 1$$

(gray) (white)

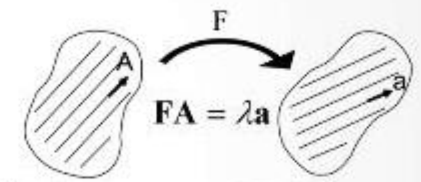

- Volumetric strain energy function is chosen such that it satisfies all mathematical requirements and physical conditions (Doll and Schweizerhof 1999). Specifically,
  - $U_{J\to+0} \to +\infty$; $\partial_J U_{J\to+0} \to -\infty$ $\qquad \neq \frac{K}{2}(J-1)^2$
  - $U_{J\to+\infty} \to +\infty$; $\partial_J U_{J\to+\infty} \to +\infty$ $\qquad \neq \frac{K}{2}(lnJ)^2$
  - $\partial^2_{JJ} U \geq 0$ $\qquad \neq \frac{K}{2}(lnJ)^2$
  - $U_J = \frac{K}{2}\left(\frac{J^2-1}{2} - \ln(J)\right)$

Material Properties Inputs to Constitutive Models

Bulk modulus (K) at high rate (unpublished)
Cerebellum: 1.19 GPa Cerebrum: 1.46 GPa

Sub-structure	Material Properties source	Properties
White matter**	Velardi et al., Biomech Model Mechanbiol 2006 *(pig)*	G_{inf}= 286 Pa; G_0= 1906 Pa
Skull	McElhaney, J Biomech, 1970	E= 8 GPa; ν=0.22
CSF/SAS	Jin et al., Stapp Car Crash J. 2006 *(bovine)*	E= 9.85 GPa; ν=0.45
Caudate and Putamen	Lee et al., Mech. Beh. Biomed. Materials 2014 *(rat)*	G_{inf}= 110 Pa; G_0= 700 Pa
Gray matter	Lee et al., Mech. Beh. Biomed. Materials 2014 *(rat)*	G_{inf}= 385 Pa; G_0= 2750 Pa
Thalamus	Domelen et al., Mech. Beh. Biomed. Materials 2010 *(pig)*	G_{inf}= 943 Pa; G_0= 6700 Pa
Ventricle	Cole, Underwater Explosions	K= 1.46 e9; n= 7.15

**Constitutive model for WM is a transversely isotropic with linear viscoelasticity. Parameters in the strain energy function are fitted to data reported in Velardi et al. (2006).

Loading and Boundary Conditions

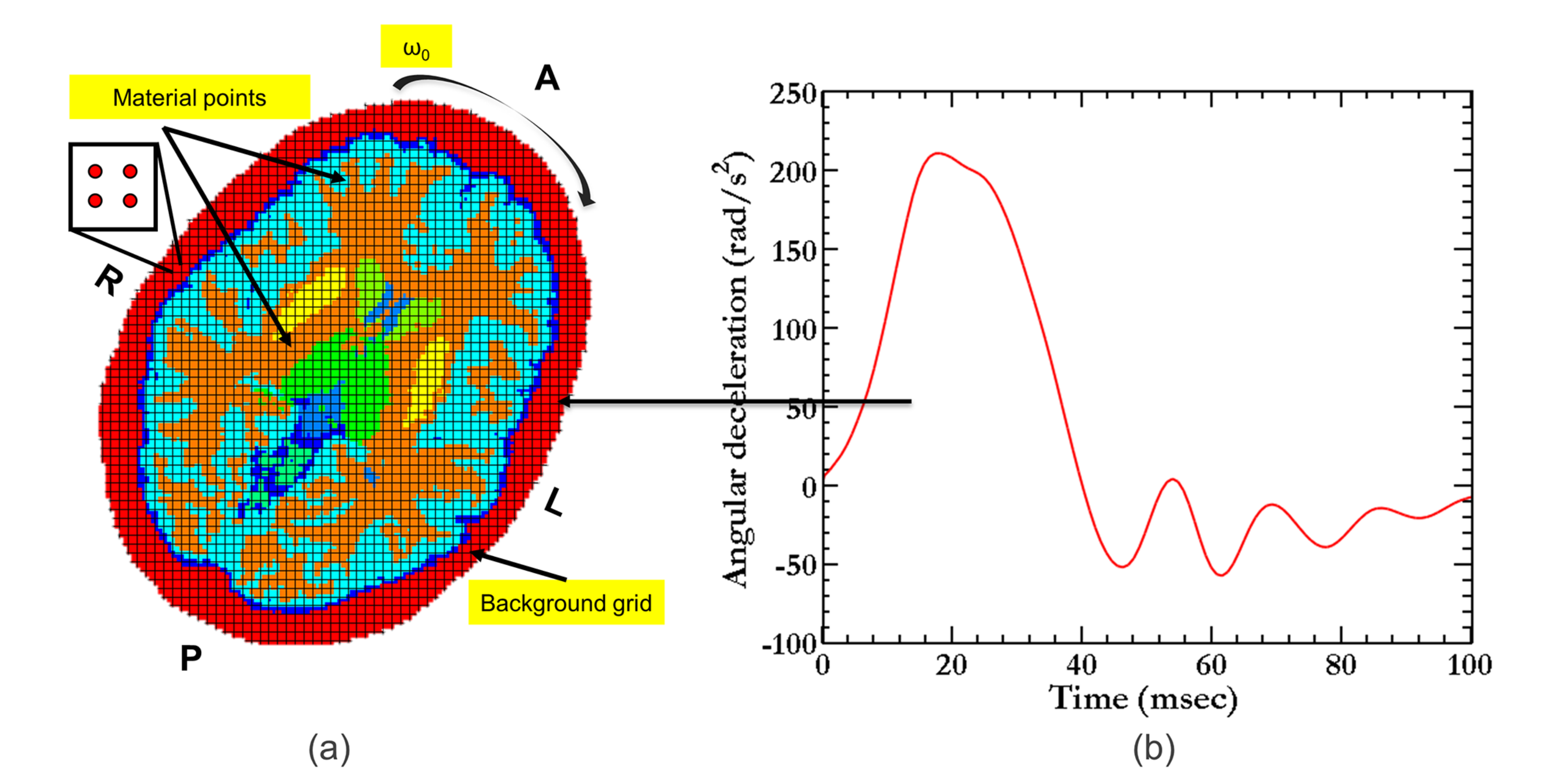

Deformations in 3D

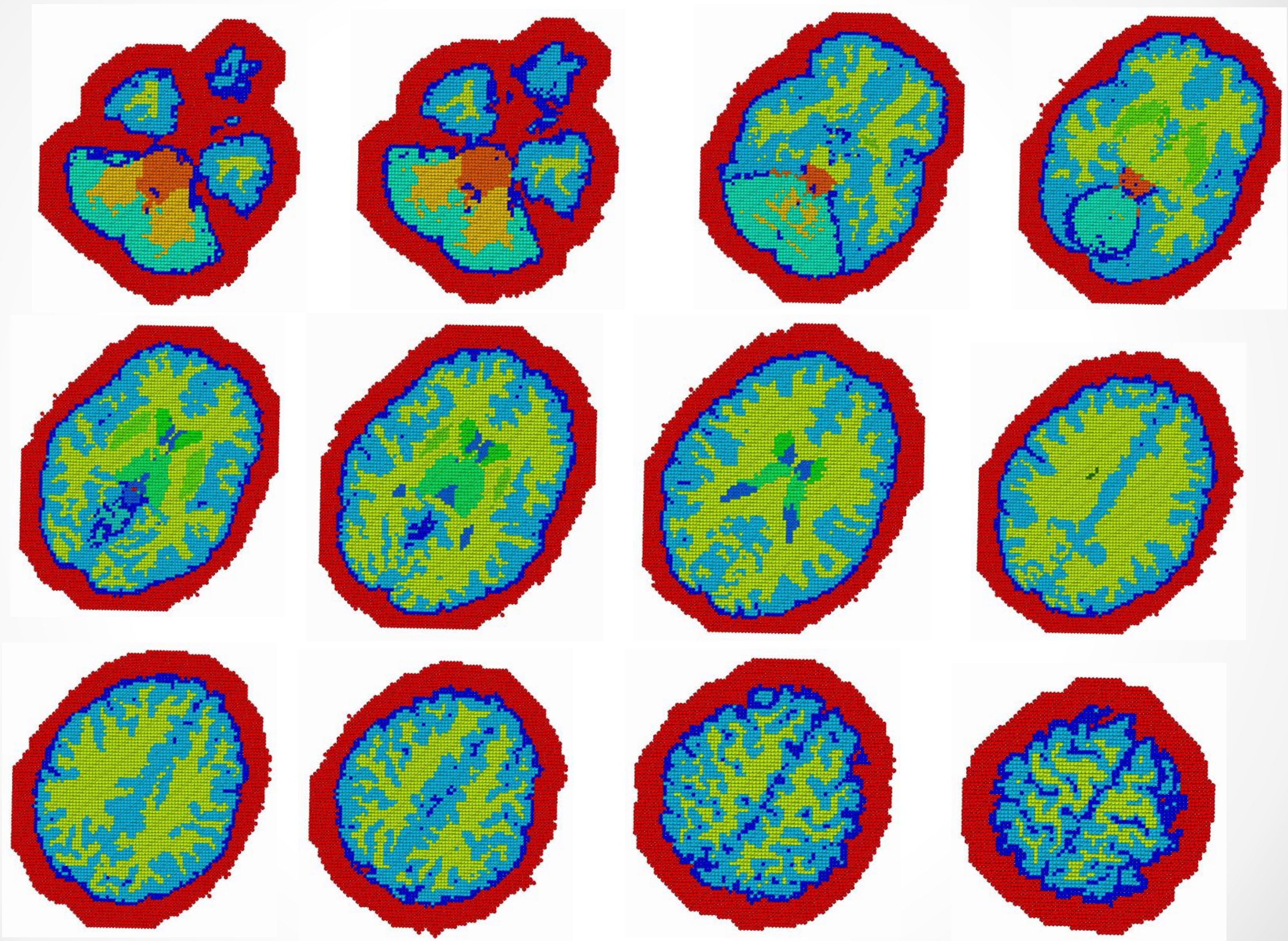

Transverse slices of a brain

Representative Comparison of Dynamic Shearing Strain

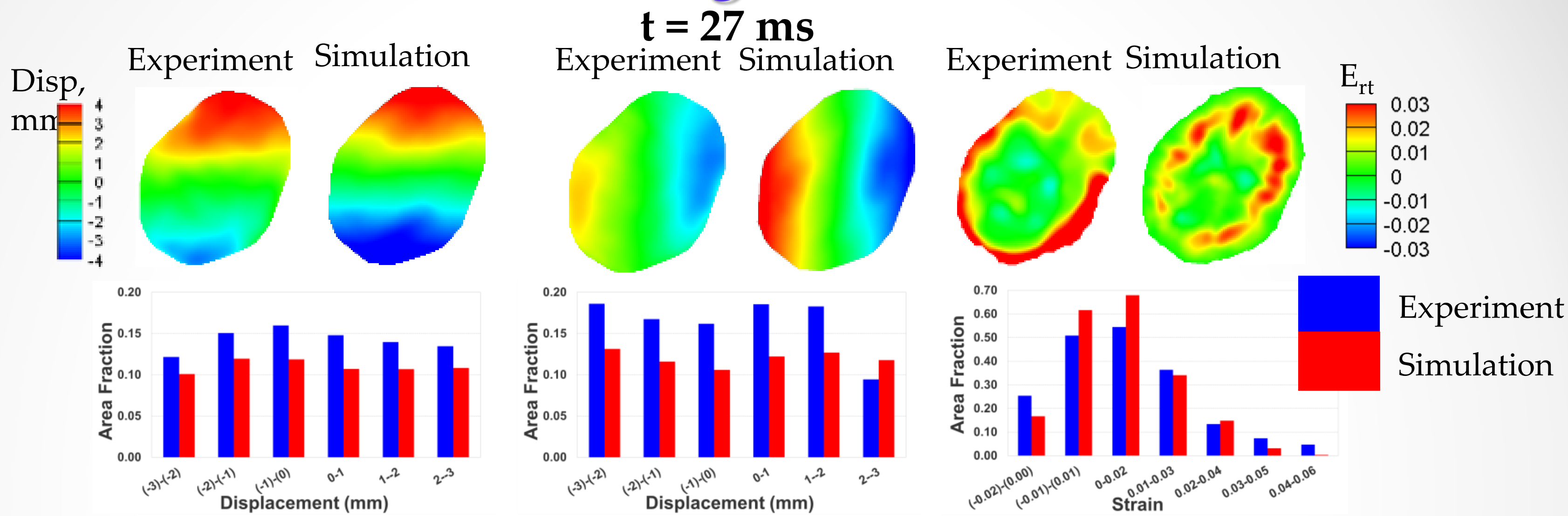

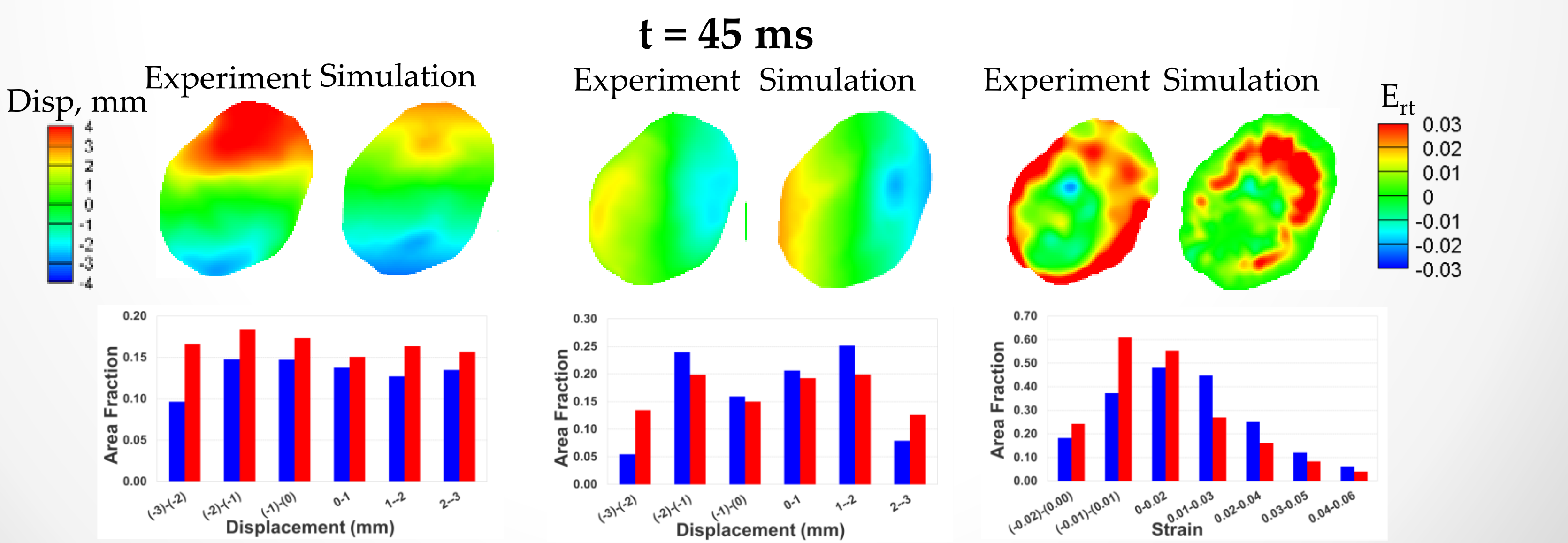

Predictions without any stiff membranes, such as Falx

Effect of Properties for Sub-Arachnoid Space and Falx on Shear Strain Patterns

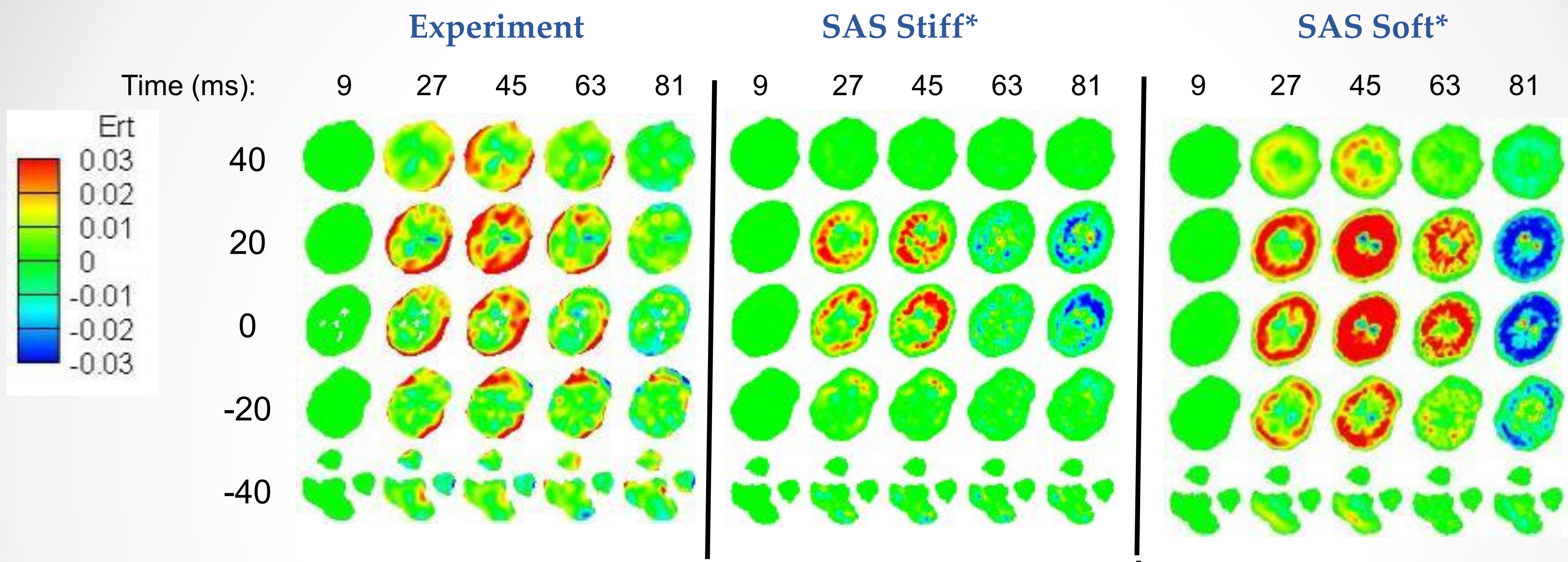

Identified a range of material properties for SAS and Falx that give agreeable results with experiments.

SAS stiff ~ 3.4 MPa
SAS soft ~ 0.5 KPa
Falx ~ 21 MPa

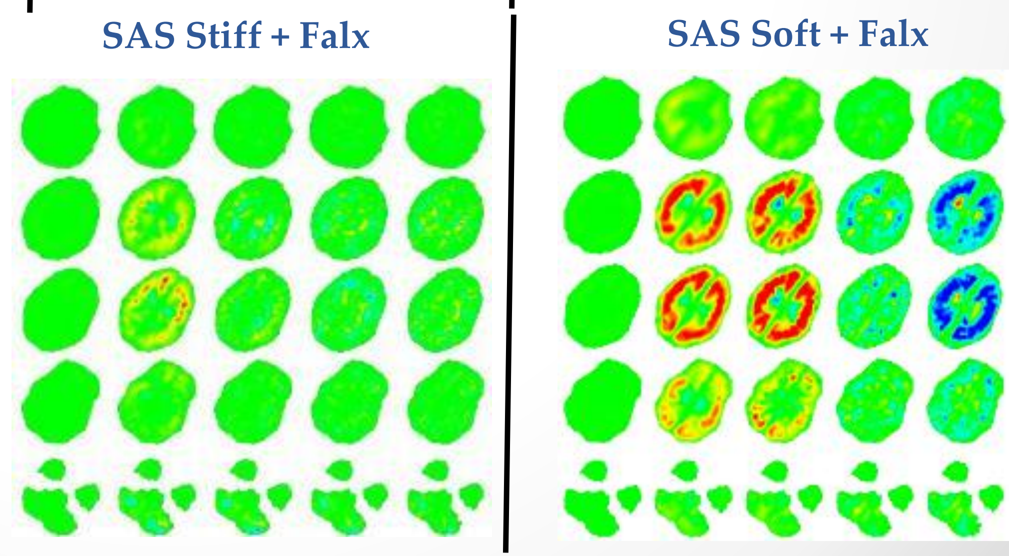

Subject-to-Subject Variability

Subject #1; t = 27 ms

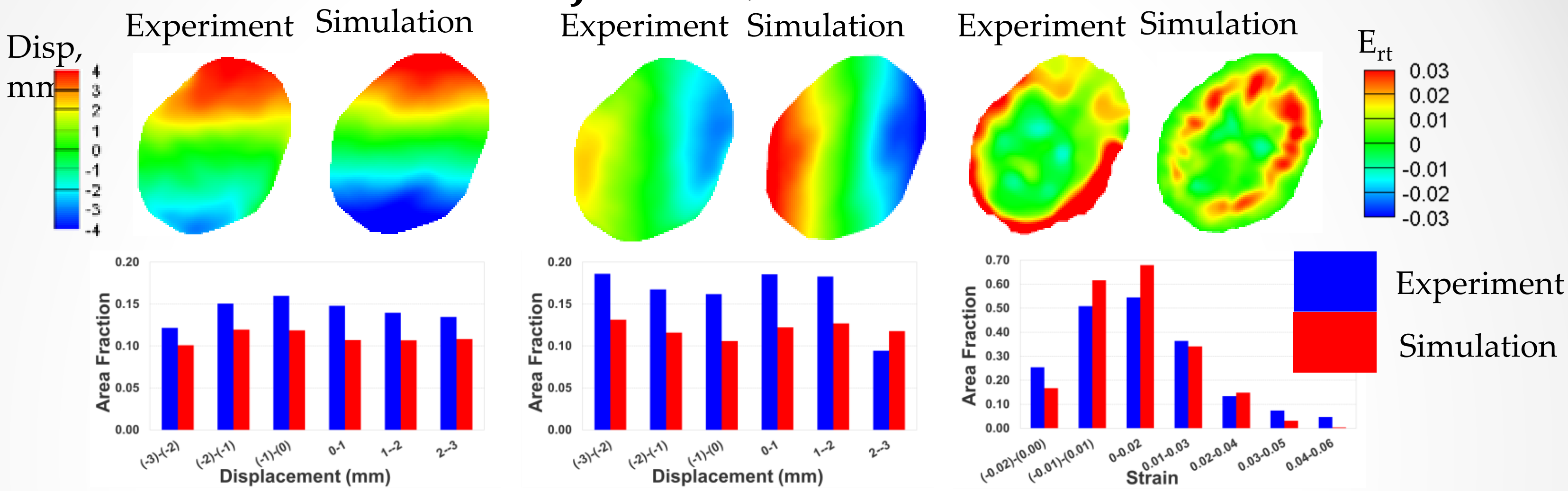

Subject #2; t = 27 ms

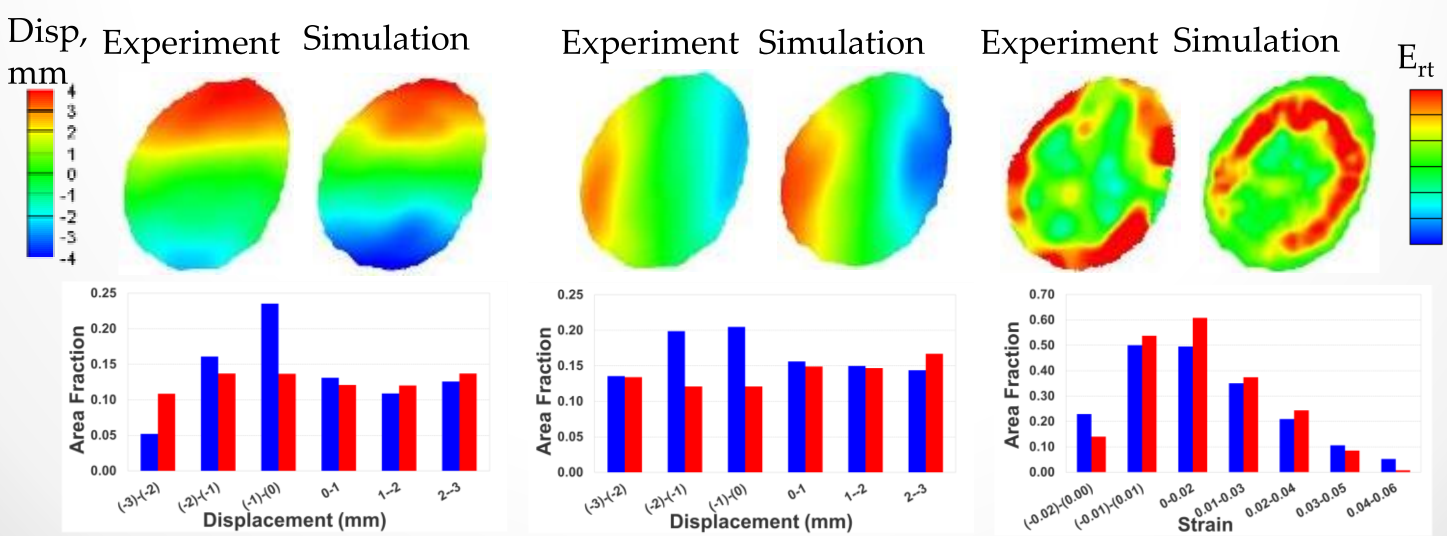

Summary

1. Material Point Method is capable of simulating large shearing deformations and can resolve anatomical differences in within the brain.

2. Predicted shear strain distribution is fairly heterogeneous (at ~10 mm length scale), attributed to various sub-structures in the brain.

3. Area-weighted analysis method allows comparison of strains in sub-structures of the brain.

4. Realistic bulk modulus is crucial to correct predictions of shearing strains observed in experiments.

Radial circumferential shear strain (E_{rt}) pattern across subjects

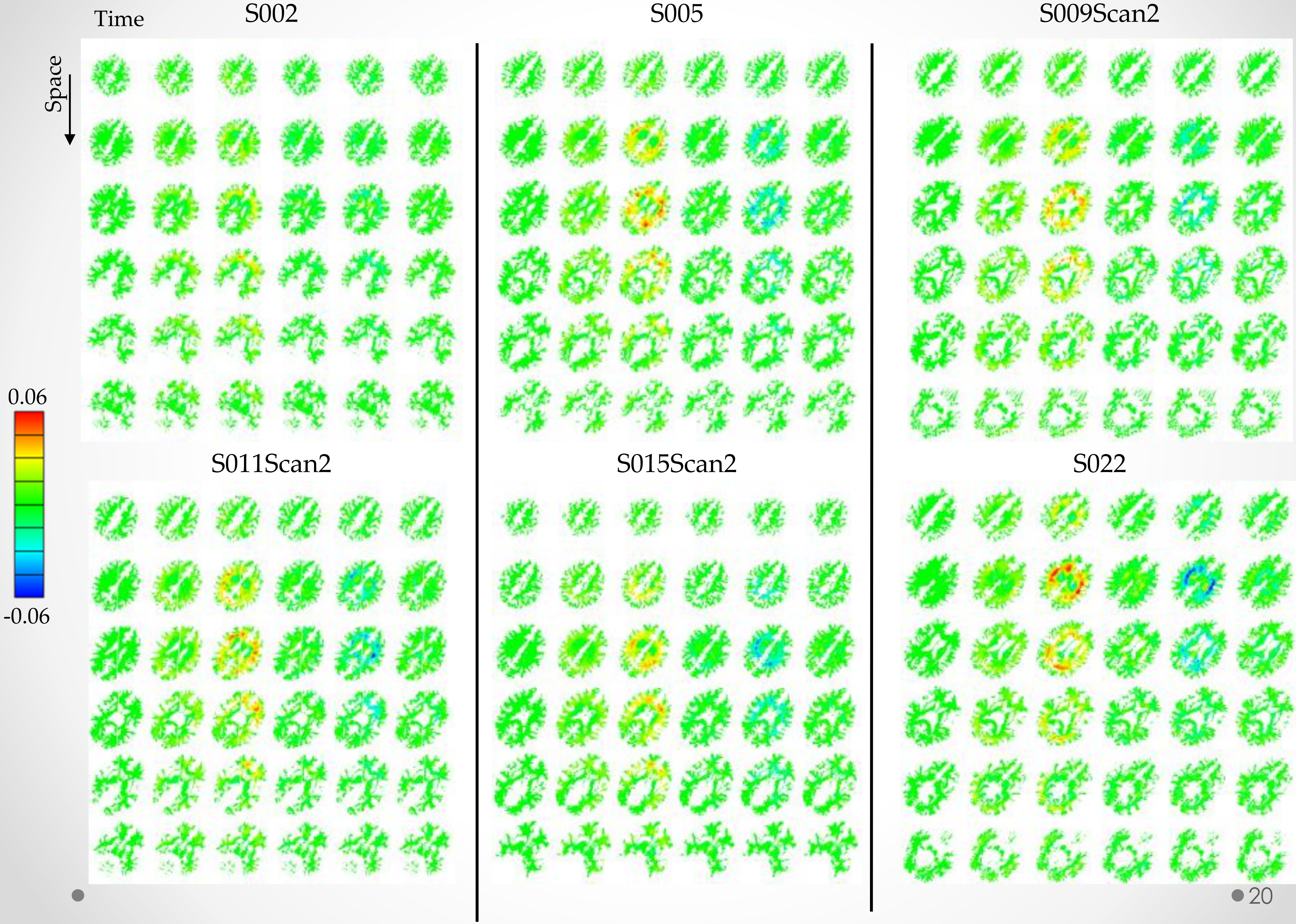

Deformation Patterns

Shear strain E_{rt}:

Time (ms): 9 27 45 63 81 99

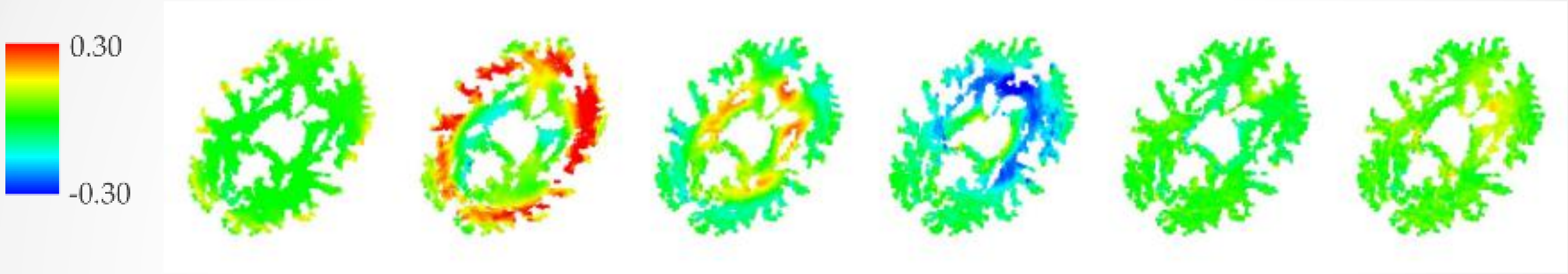

Predicted locations of axonal damage:

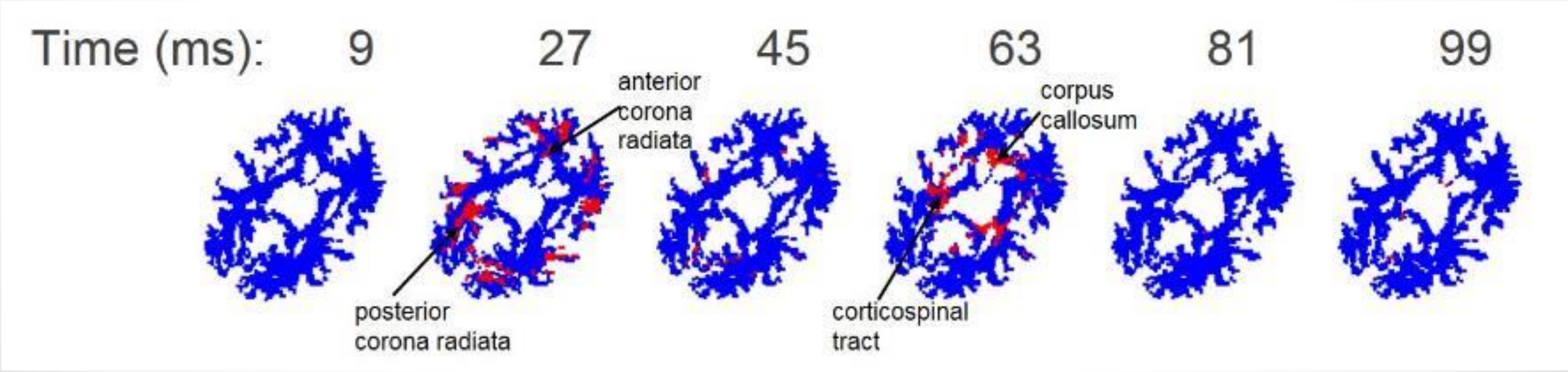

ASI: Axial strain of 18 % (tensile) in fiber tracts (Bain and Meaney, 2000)

Verification and Validation of Predictions from Phantom Simulations

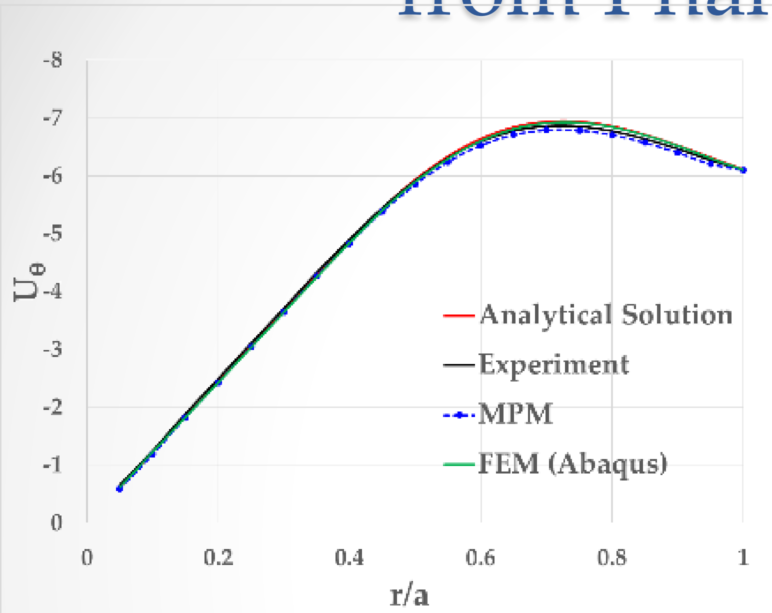

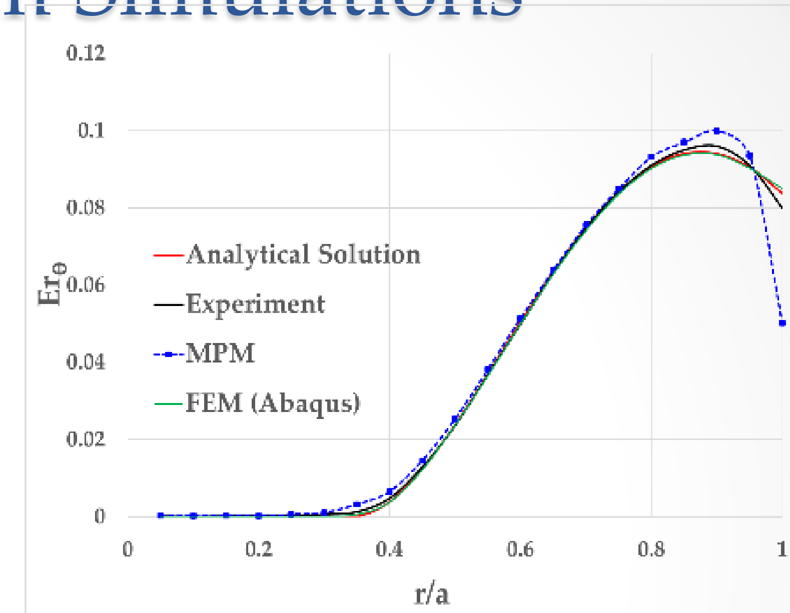

A shearing wave (+ $E_{r\theta}$) travels to the center at speed c_s, and reflects back (- $E_{r\theta}$) as a shearing wave travelling outwards.

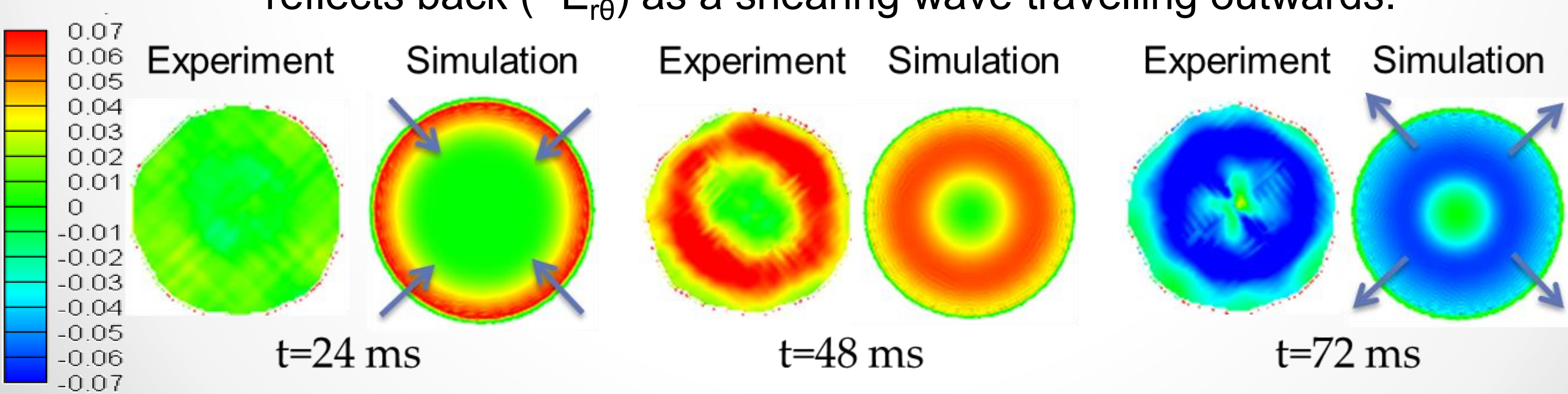

$E_{r\theta}$

Simulation results are for peak strain along the circumference

Detection of Load-Induced Structural Changes to Neurons and the Brain using X-ray Diffraction

Joseph Orgel (IIT), Rama Madhurapantula (IIT), Mamie Wang (IIT), Dean Modrich (IIT), Paval Dutov (IIT), Jason McDonald (ARL), Sikhanda Satapath (ARL).

Joseph P.R.O. Orgel

Associate Professor: Departments of Biology, Physics and Biomedical Engineering and Pritzker Institute of Biomedical Science and Engineering, Illinois Institute of Technology

Associate Director: Biophysics Collaborative Access Team,
an NIH National Research Resource at the Advanced Photon Source, Argonne Lab, IL.

Section Editor for Biochemistry: Public Library of Science ONE
Board of Directors National Museum of Health and Medicine, Chicago

Financial support:
National Institutes of Health #RR-08630
US Army #W911NF-11-2-0018-P00002-AWARD Modification

Traumatic Brain Injury

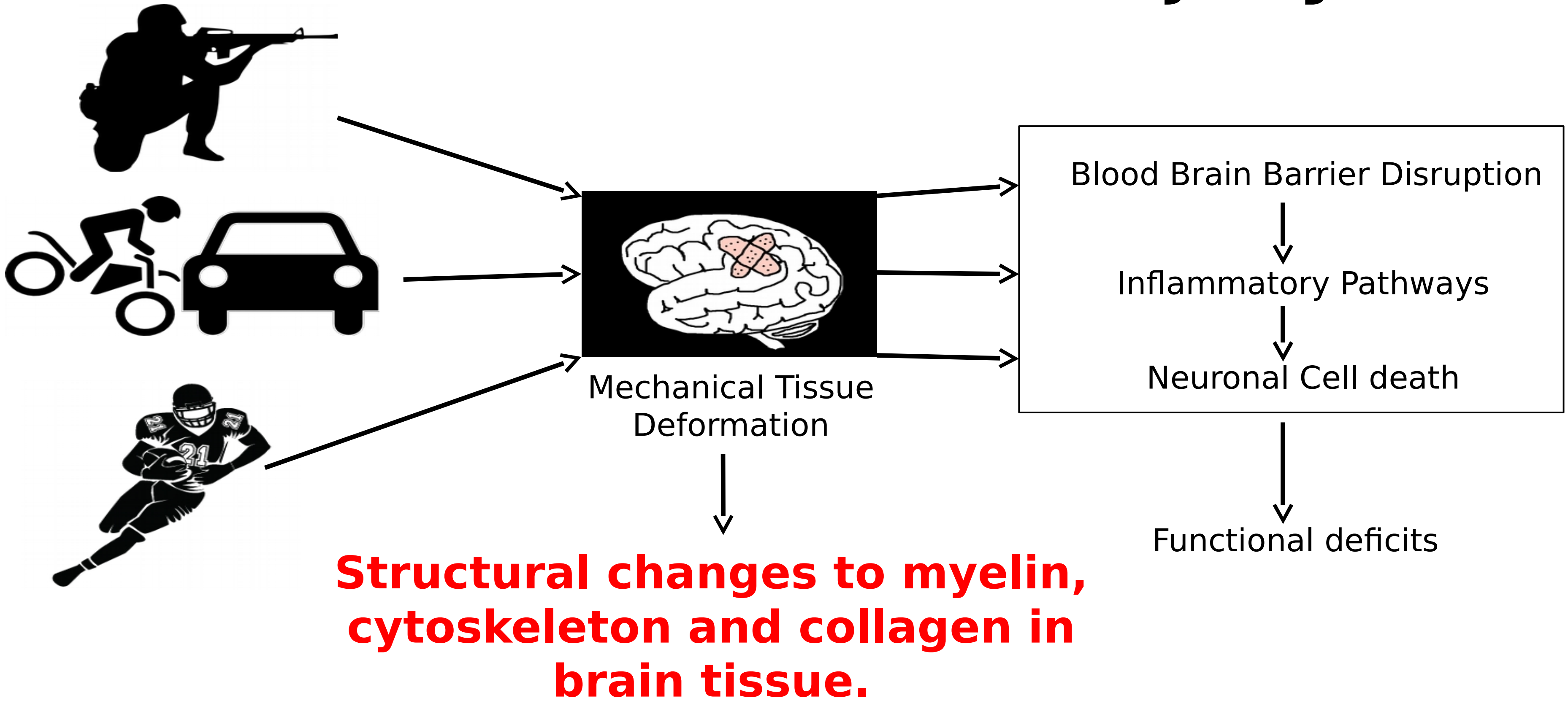

Background in: X-ray diffraction based studies of connective tissues, amyloid, prion and strange fibril based brain diseases

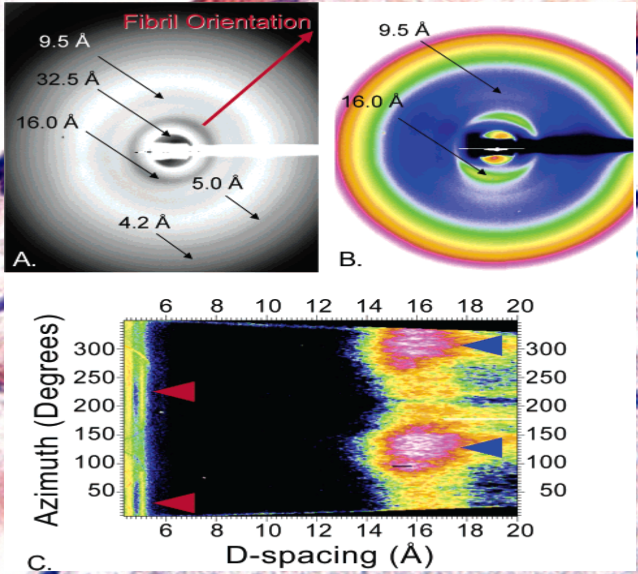

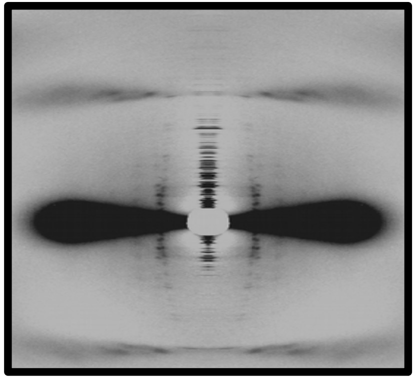


http://www.fadeeva.com

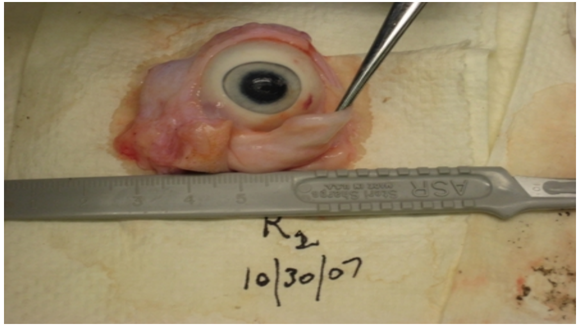
10/30/07

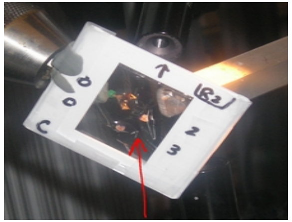

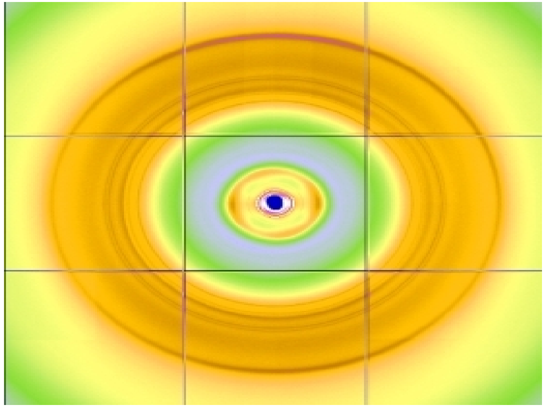


18 ID-C

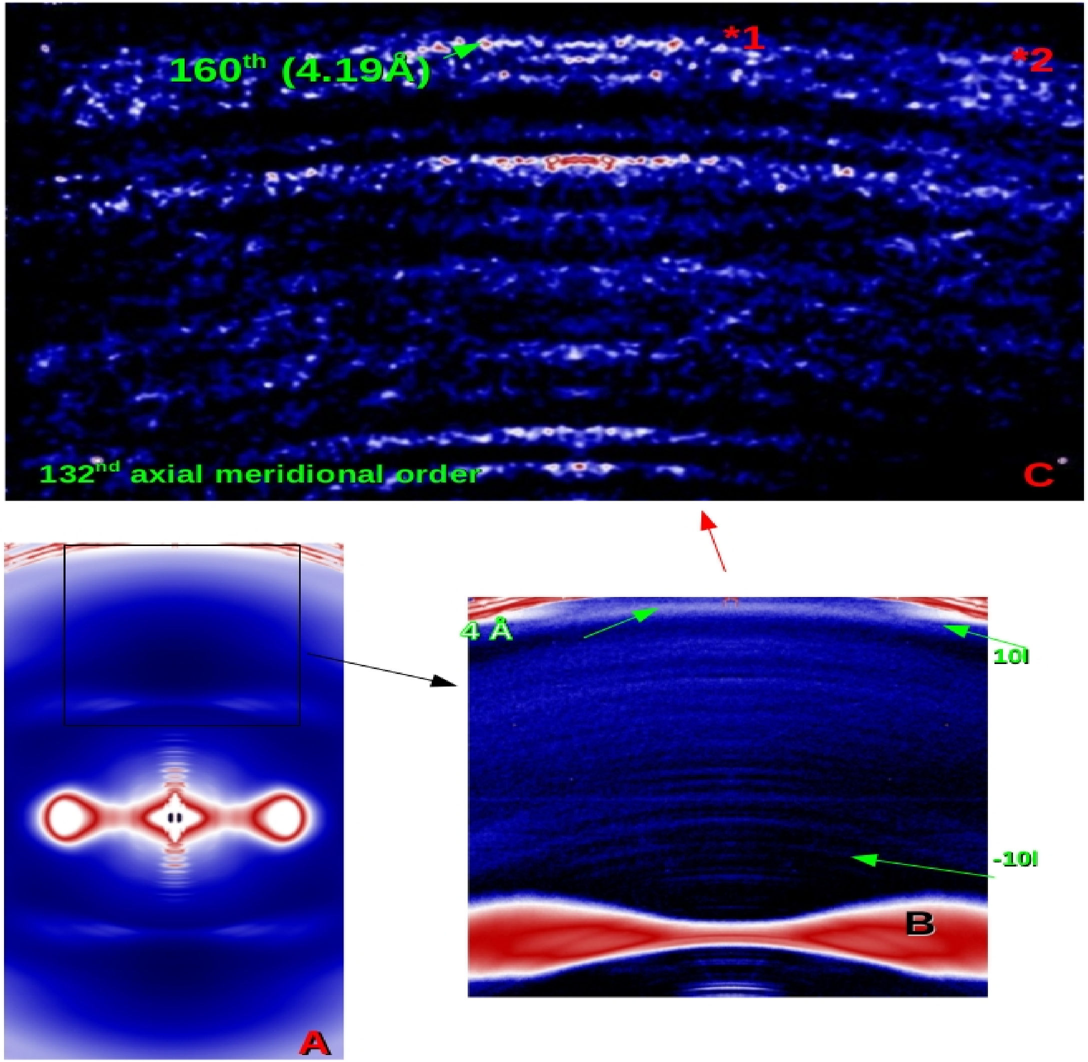

X-ray Micro-Diffraction Studies on Biological Samples at the BioCAT Beamline 18-ID at the Advanced Photon Source.

R A. Barrea, O. Antipova, D. Gore, R. Heurich, M. Vukonich, Naresh G. Kujala, T. C. Irving and J.P.R.O. Orgel

J. Synchrotron Rad. 21 (5) (2014).
doi:10.1107/S1600577514012259

CSRRI
CENTER FOR SYNCHROTRON RADIATION RESEARCH & INSTRUMENTATION

Collagen type I sub-fibrillar structure

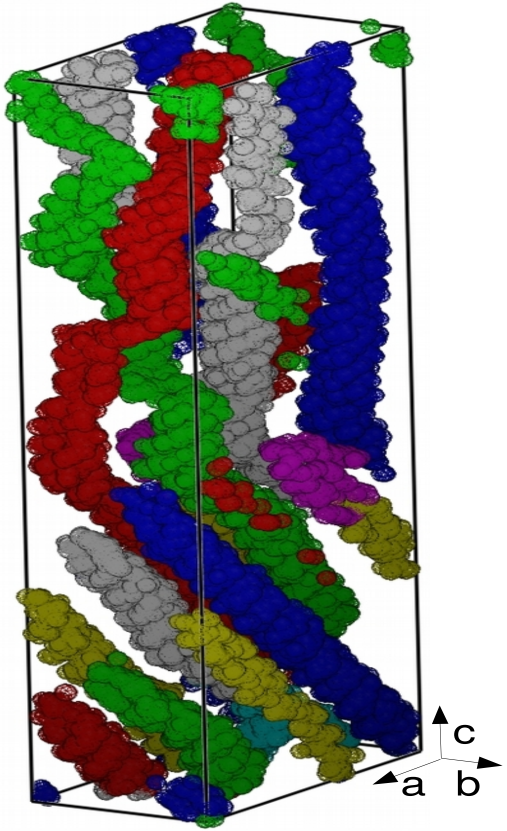

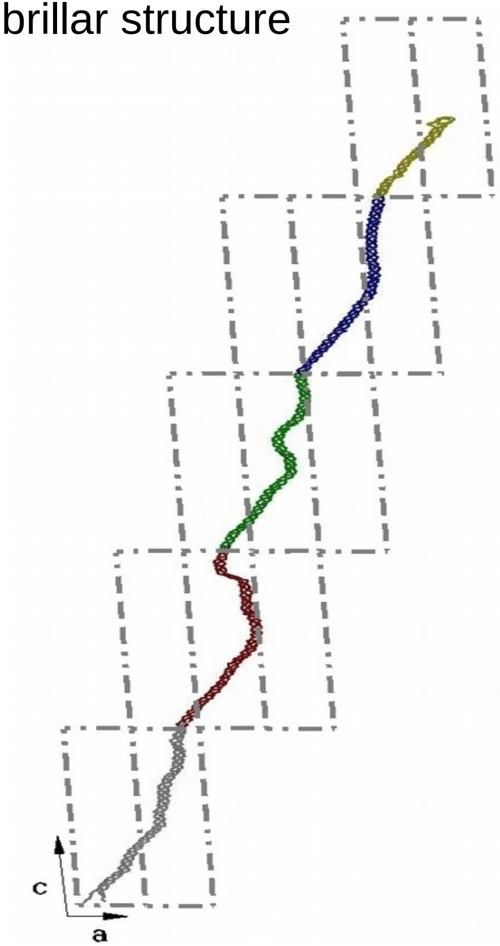

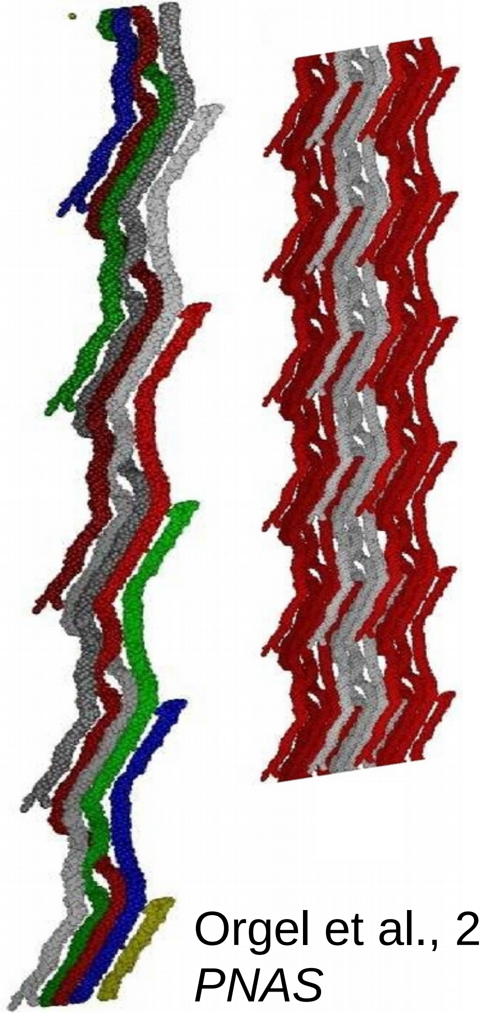

Orgel et al., 2006
PNAS

Resolution ~ 11 /5.16 Å

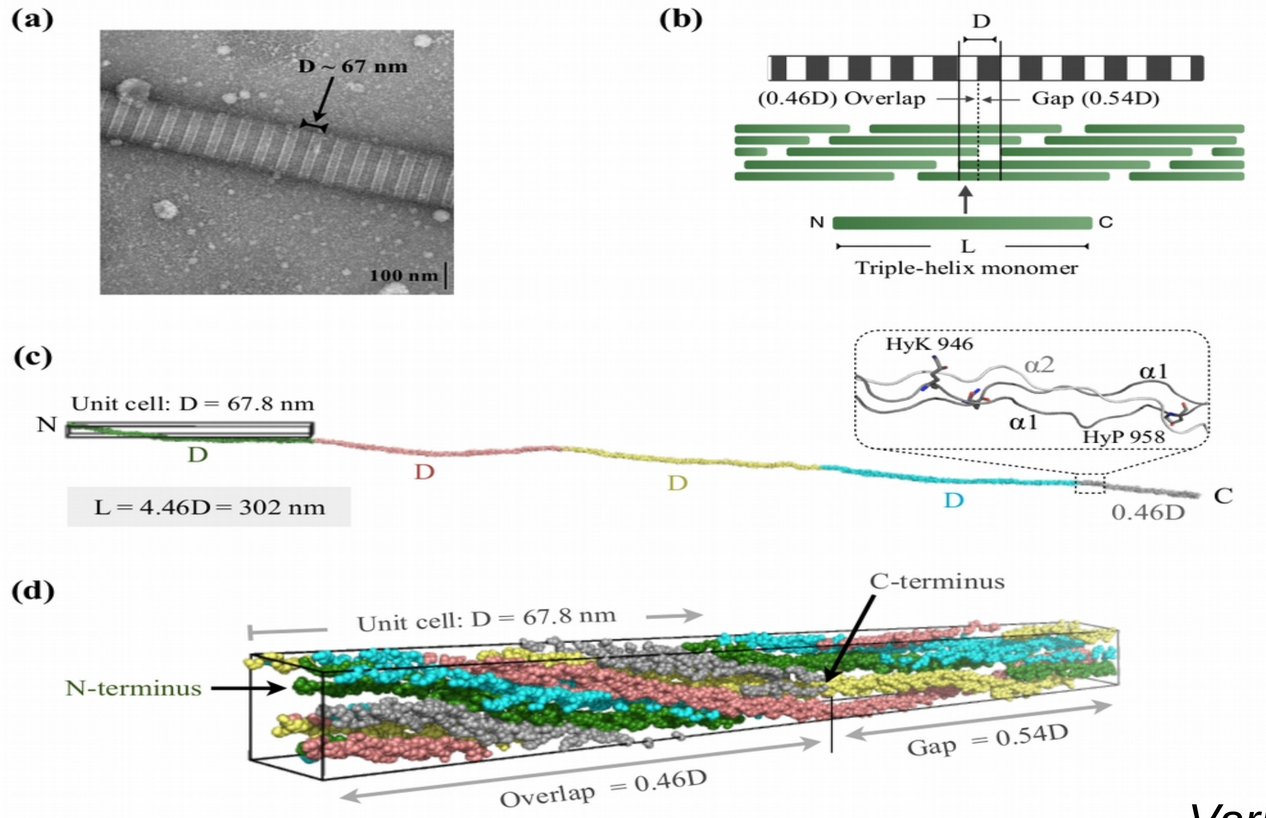

Varma et al 2015

Proteins: Structure, Function, and Bioinformatics

Animal models

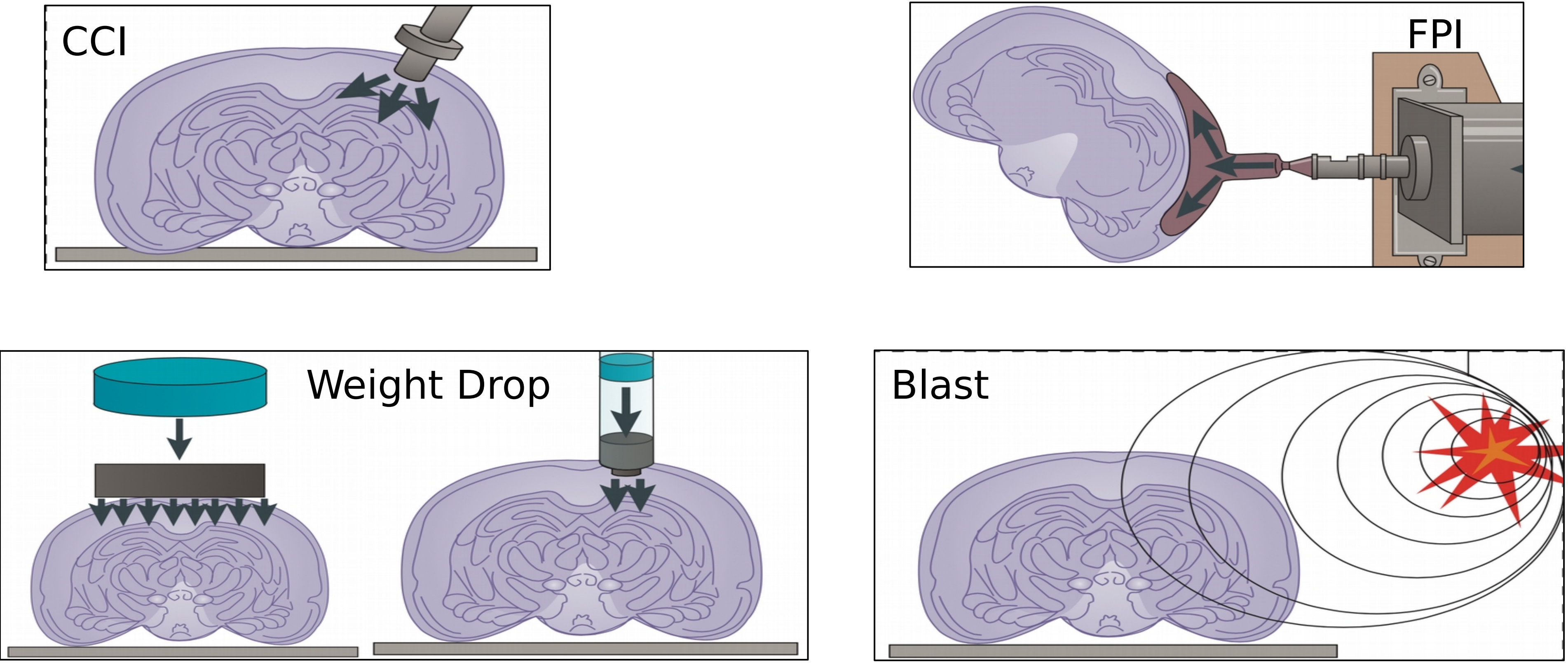

Xiong et al; Nature Reviews Neuroscience 2013

Myelin organization

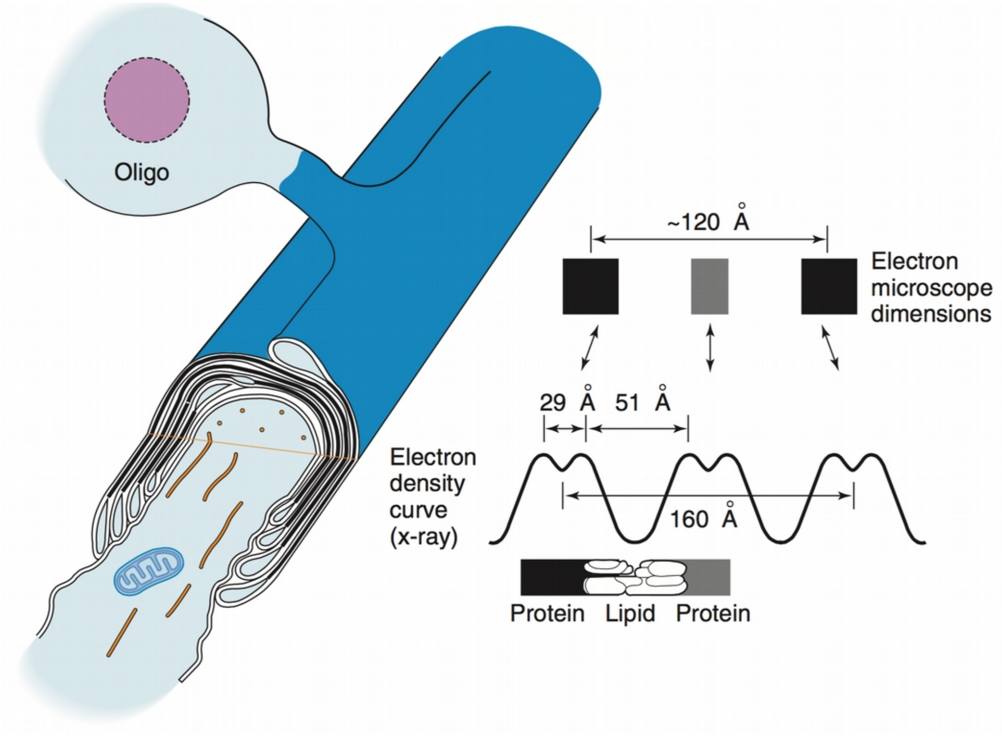

	D (Å)	c_p/c_ℓ	c_w	d_p (Å)	d_ℓ (Å)	d_w (Å)	d_{hc} (Å)
CNS	154	0.32	0.10	25.0	113.0	16.0	81.0
PNS	175	0.42	0.15	33.8	113.0	28.2	81.0

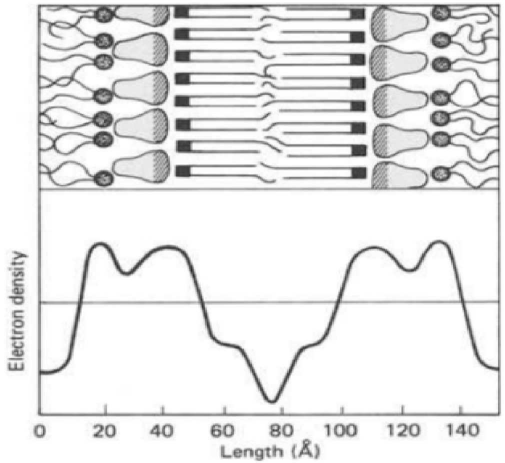

Membrane Spectroscopy Edited: E. Grell (from MBBB series), 1981

Myelin and diffraction

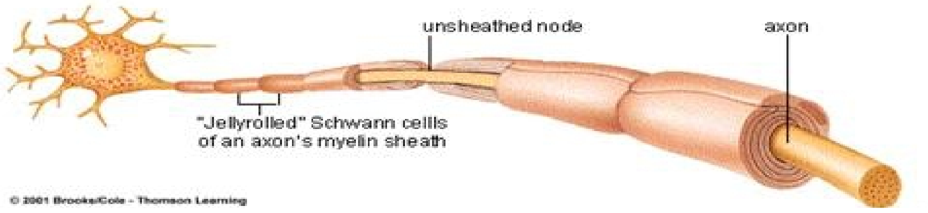

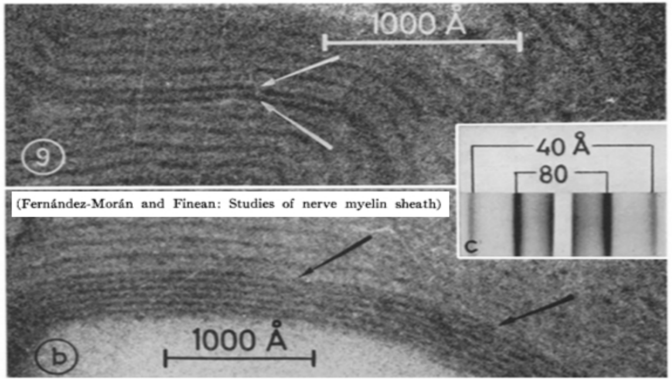

1957

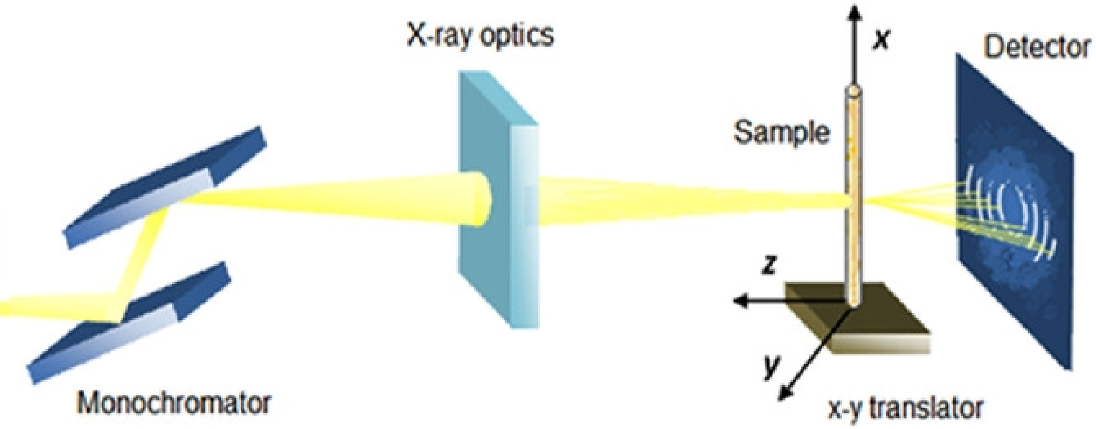

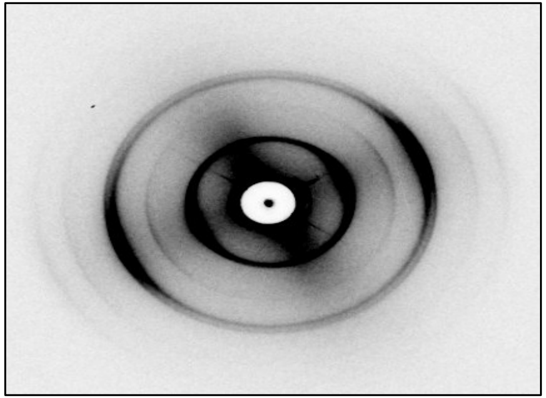

Link

Poccia et al 2014

2015

Our TBI apparatus- CCI

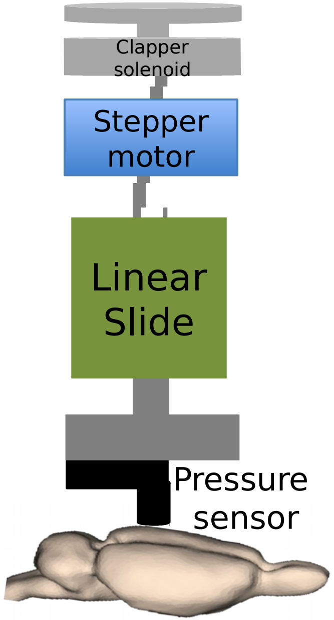

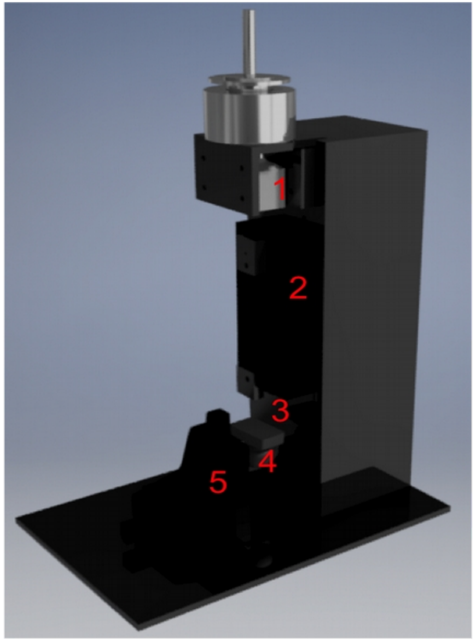

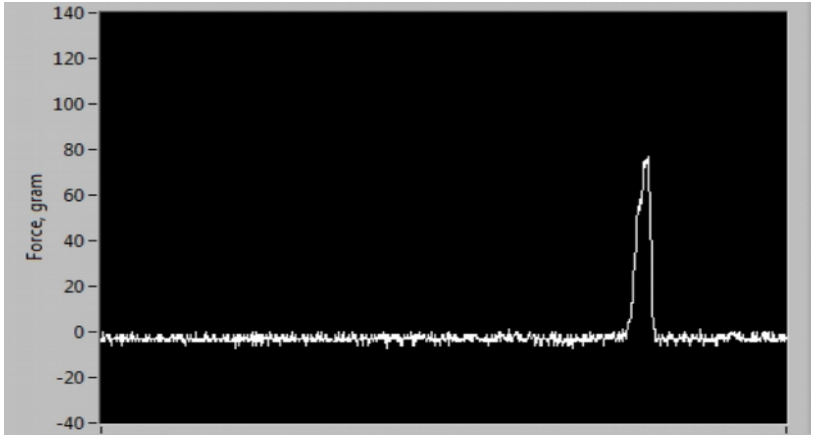

Impact Profile

Experimental Protocol

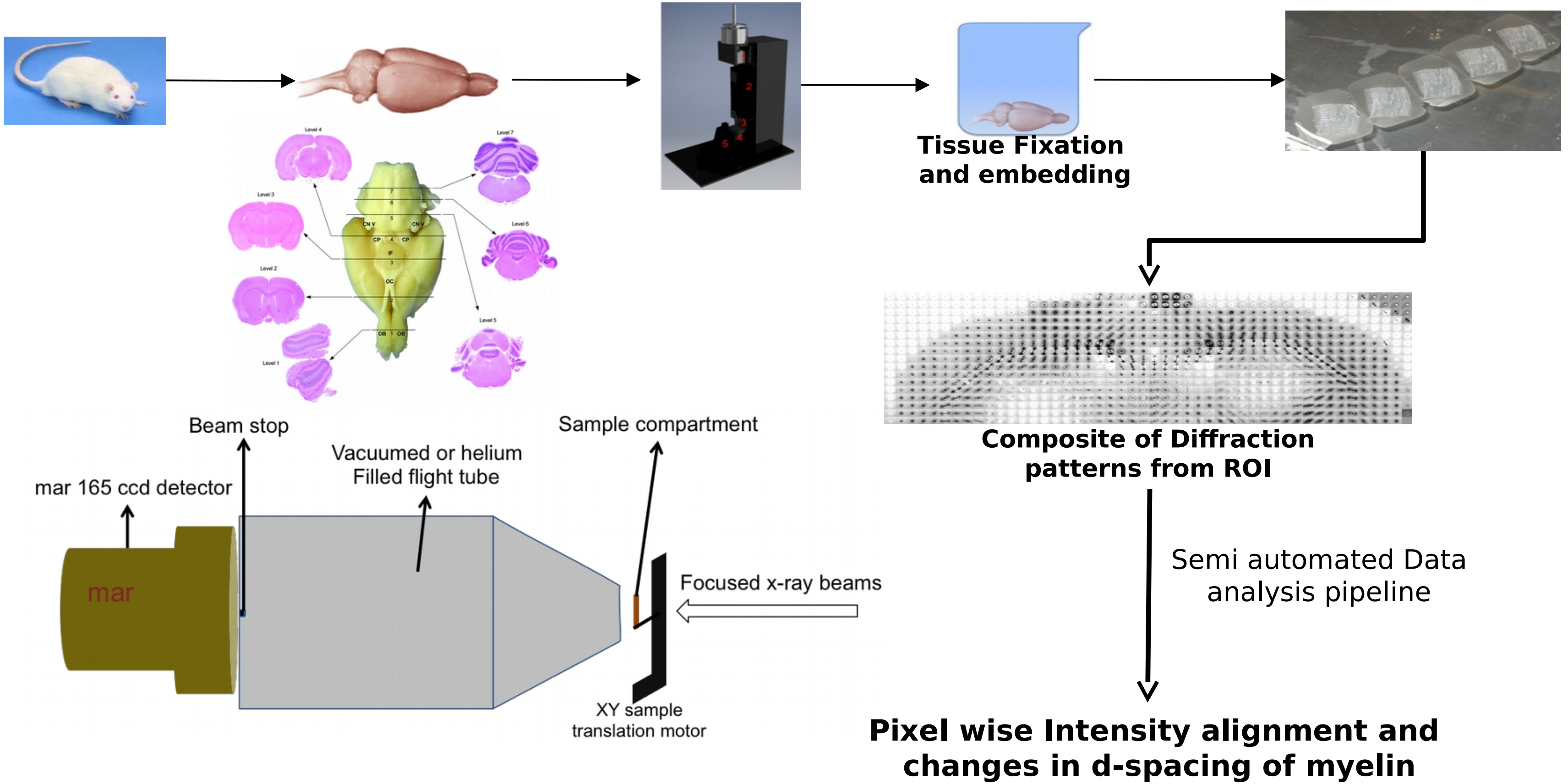

TBI-Results

Post mortem
impacted
Fresh optic nerve
(Static load)

Fixed, post-mortem, static impact brain scans

Mylein 2nd order, D-space change

Control

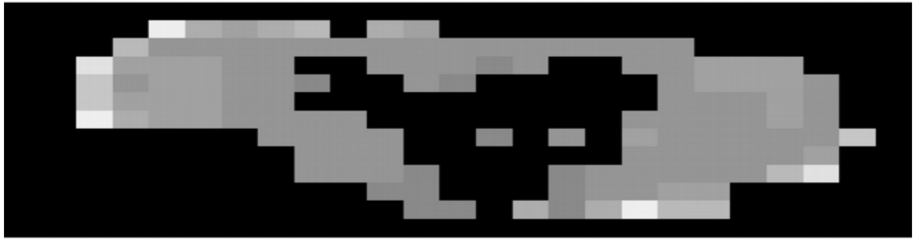

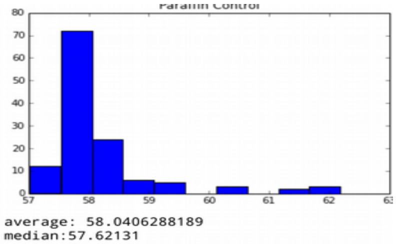

15gm

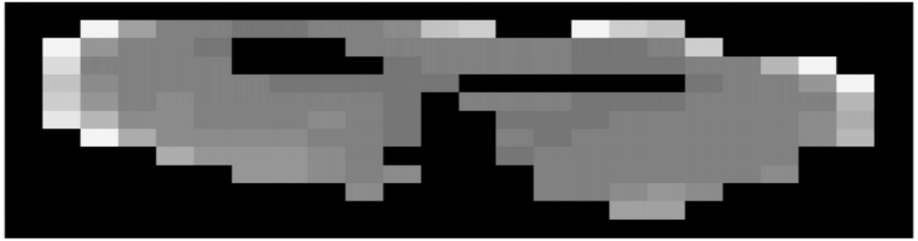

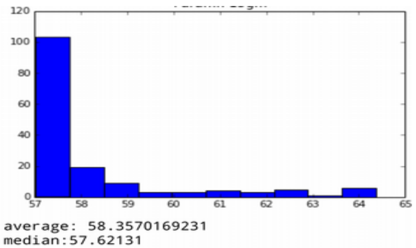

30 gm

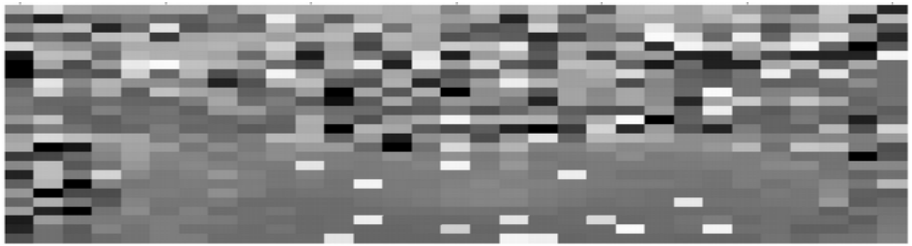

Dynamic loading

Post-mortem freshly extracted optic nerve

and

live TBI animal models,

X-ray diffraction section scans

Post-mortem freshly extracted optic nerve

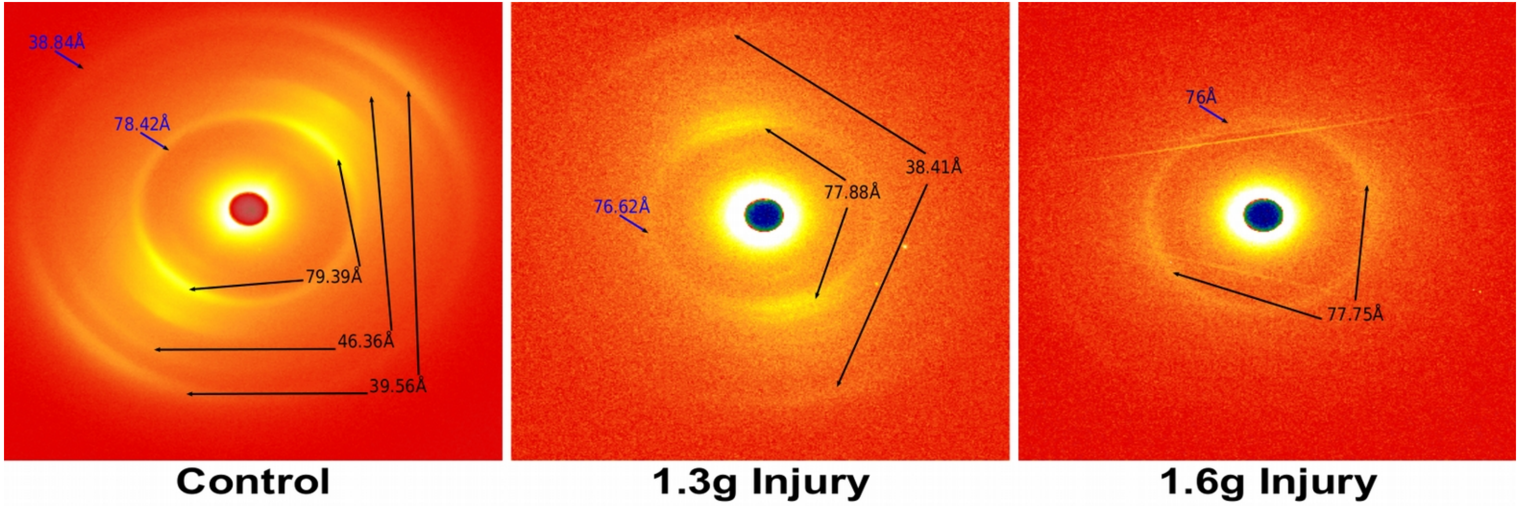

Comparison of x-ray diffraction patterns collected from freshly dissected injured (*1.3g and 1.6g*) rat optic nerves against uninjured (*Control*). Reflections from myelin are marked in black and from cytoskeleton are marked in blue. A clear loss in signal from both diffracting series is observed post injury.

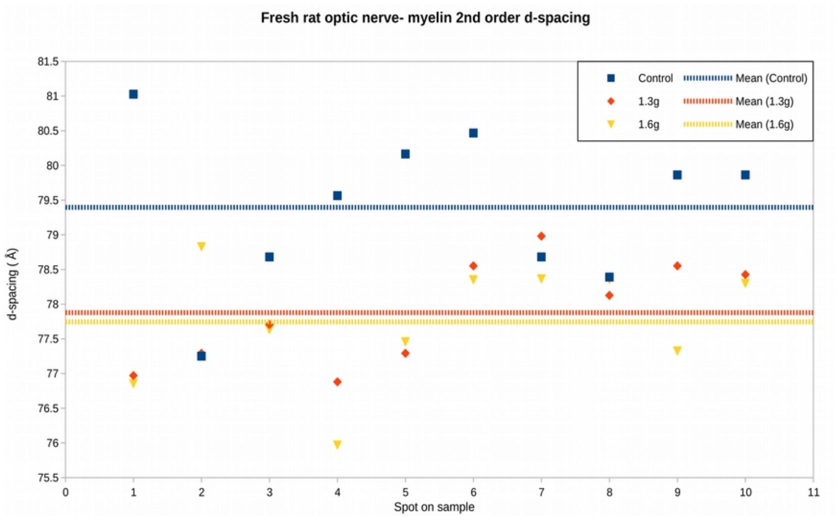

Fresh rat optic nerve- myelin 2nd order d-spacing
d-spacing (Å)
Spot on sample
Control
Mean (Control)
1.3g
Mean (1.3g)
1.6g
Mean (1.6g)
81.5
81
80.5
80
79.5
79
78.5
78
77.5
77
76.5
76
75.5
0 1 2 3 4 5 6 7 8 9 10 11

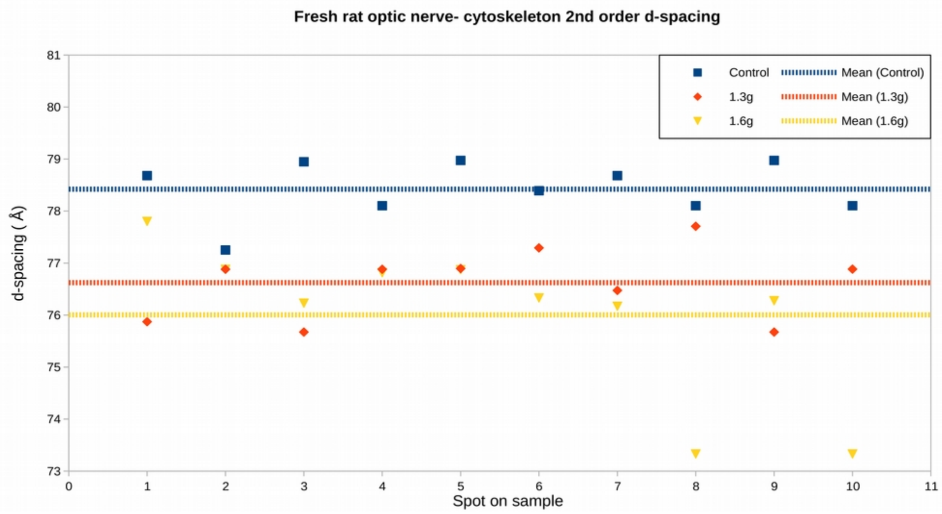

Fresh rat optic nerve- cytoskeleton 2nd order d-spacing
d-spacing (Å)
Spot on sample
Control
Mean (Control)
1.3g
Mean (1.3g)
1.6g
Mean (1.6g)
81
80
79
78
77
76
75
74
73
0 1 2 3 4 5 6 7 8 9 10 11

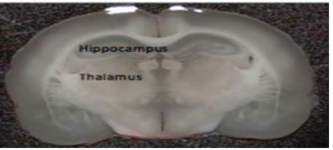

Accelerated impact, 2g

Control | 3 days post injury | 30 days post injury

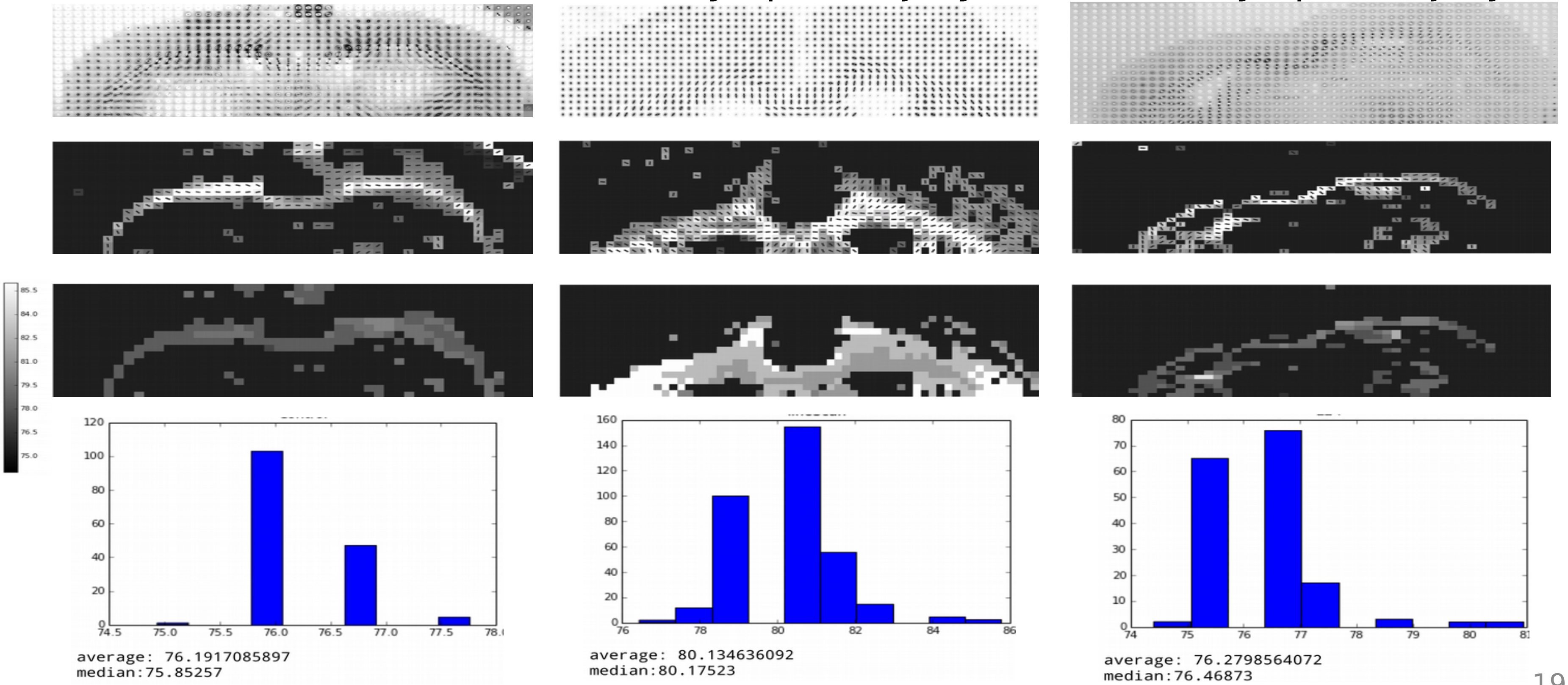

Acknowledgements

- Orgel Group
  - Dr. Rama Madhurapantula
  - Dr. Pavel Dutov
  - Meng ‘Mamie’ Wang
  - Mary Thomas
  - Sarah Kirby
  - Gina Qualter
  - Berenice Morfin
  - Charles Dean Modrich

- BioCAT
  - Dr. Olga Antipova
  - Dr. Weifeng Shang
  - Richard Heurich
  - Mark Vukonich
  - Scientific and administrative staff
- Dr. Dorothy Kozlowski
  - DePaul University
- Dr. David McCormick
  - IITRI
- Dr. Peiter de Tombe
  - Loyola University

Overview of Occupant Protection Research at NASA

J. Somers[1], N. Newby[1], J. Wells[2]

[1]Wyle Science, Engineering and Technology Group, Houston, TX

[2]Lockheed Martin Information Systems and Global Solutions, Houston, TX

Overview

- **Background and Introduction**
- **NASA Environment**
- **Injury Risk Considerations**
- **Current Approach to Implementing Requirements**
- **Future Work**

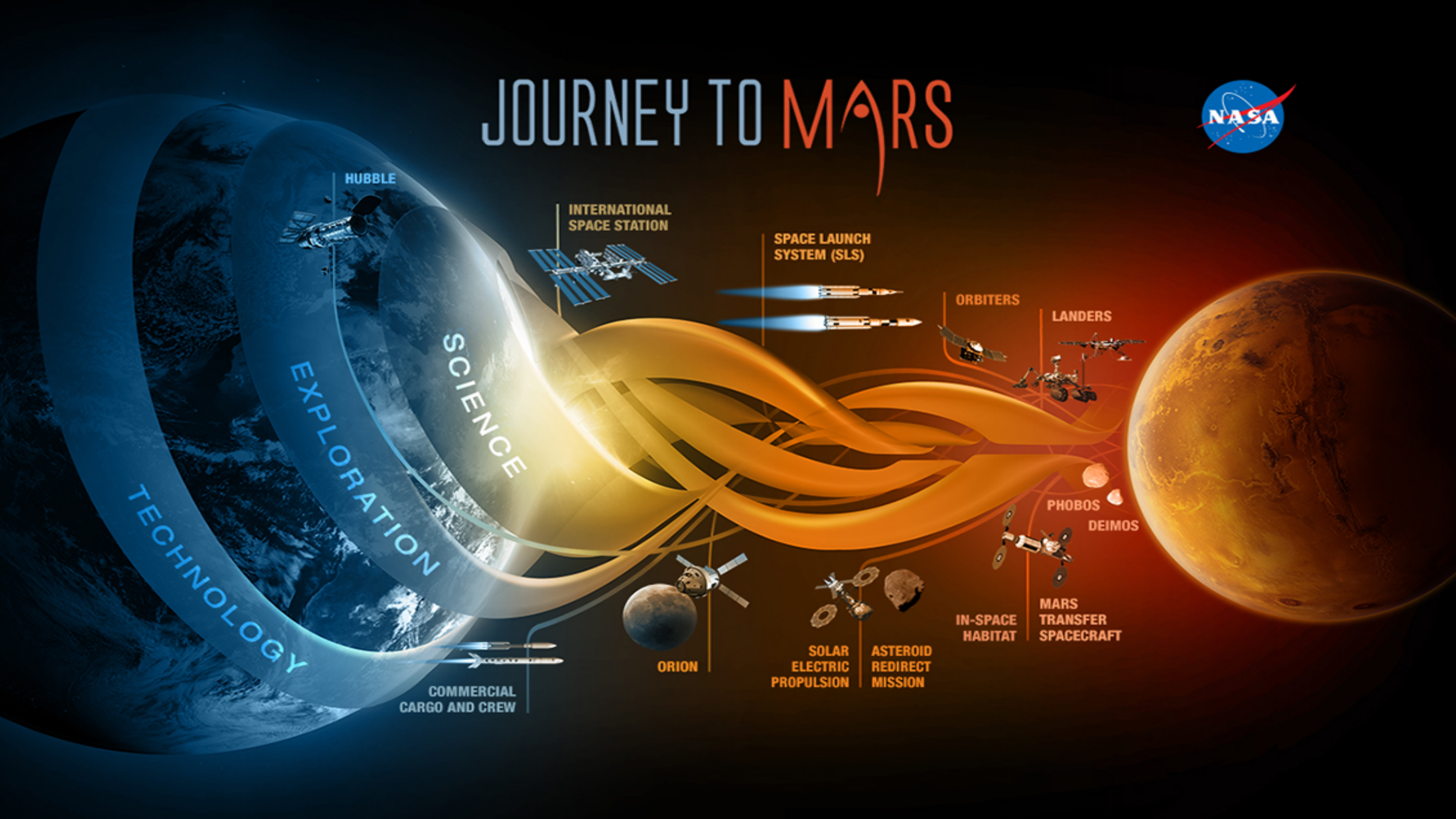
JOURNEY TO MARS
NASA
HUBBLE
INTERNATIONAL SPACE STATION
SPACE LAUNCH SYSTEM (SLS)
ORBITERS
LANDERS
SCIENCE
EXPLORATION
TECHNOLOGY
PHOBOS
DEIMOS
COMMERCIAL CARGO AND CREW
ORION
SOLAR ELECTRIC PROPULSION
ASTEROID REDIRECT MISSION
IN-SPACE HABITAT
MARS TRANSFER SPACECRAFT

NASA Environment

Crew Vehicle Comparison

Current System

Soyuz TMA-M

Multi-purpose Crew Vehicle Program

Orion

Commercial Crew Program

SpaceX Dragon

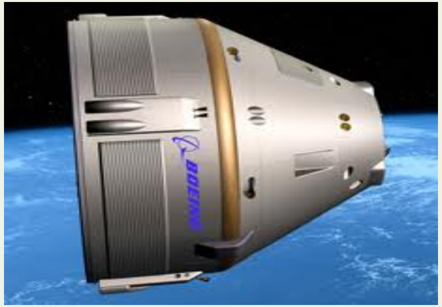

Boeing CCT-100

Dynamic Phases of Flight

- Launch
  - All proposed vehicles launch with crew laying on their backs (eyeballs in accelerations)
- Abort
  - Primarily X-axis loads (Eyeballs in)
  - May have significant oscillatory components
- In-Orbit
  - Very benign loads
- Reentry
  - Primarily X-axis loads (Eyeballs in)
  - May have transient dynamics due to parachute deploy
- Landing
  - The landing mode is specific to the vehicle design
    - Water Landing
    - Land Landing

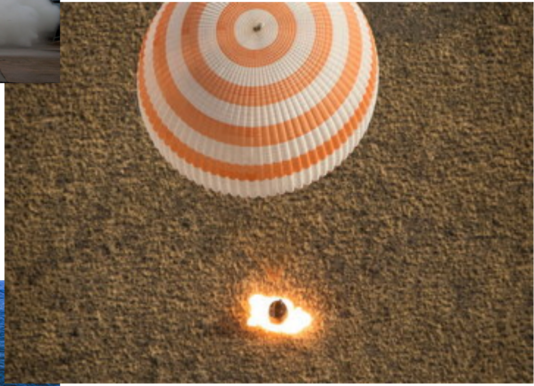

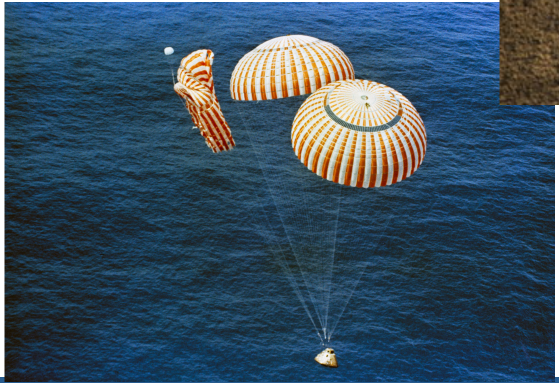

Vehicle Loading Considerations

- **Unlike automotive impacts, which are typically frontal or side impact, spacecraft landings are multi-axial and complex – more akin to vehicle rollover cases**
- **Depending on the design, may factors greatly influence spacecraft dynamics**
  - Primary landing location (water vs. land)
  - Parachute configuration and vehicle hang angle
  - Vehicle mass and shape
  - Wind and wave conditions
  - Crew orientation within the vehicle
  - Energy absorbing devices
- **Spacecraft experience the equivalent of a minor (to moderate) car accident every time they fly, so the probability of injury in these conditions must be very low**

Suit Considerations

- **Helmet Mass**
  - Helmet can increase neck loads and moments
  - Without proper padding, head can impact interior of helmet
- **Rigid Elements**
  - Previous research has shown that rigid suit elements such as mobility bearing can case injury
- **Suit Pressurization**
  - Although the suit should not be inflated at landing, residual pressure may exist and could interfere with the restraints
  - Previous pressurized suit testing during Apollo resulted in injury to the subject

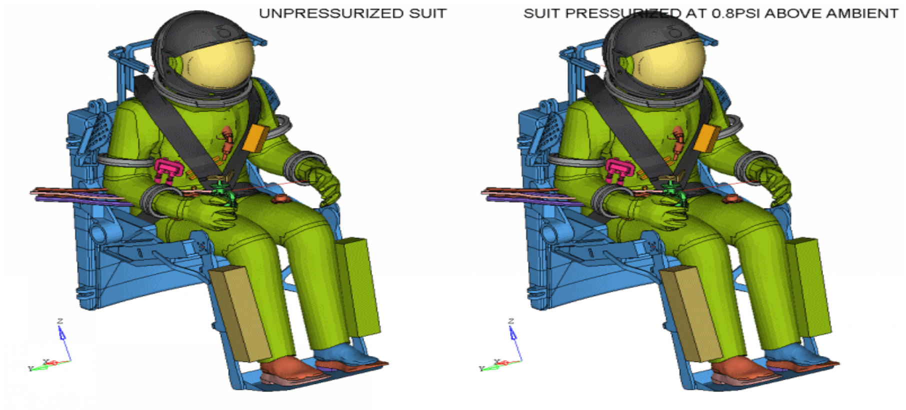

Spaceflight Deconditioning

- **Prolonged exposure to reduced gravity affects bone and muscle**
- **Bone mineral density (BMD) has been shown to decrease by ~1% per month**
- **Recent improvements to exercise have reduced the loss of BMD**
- **Even so, there are significant changes in bone architecture, particularly in the trabecular bone**
- **<u>Varies significantly by subject</u>**
- **Unclear how these changes affect returning crewmember's tolerance to impact**

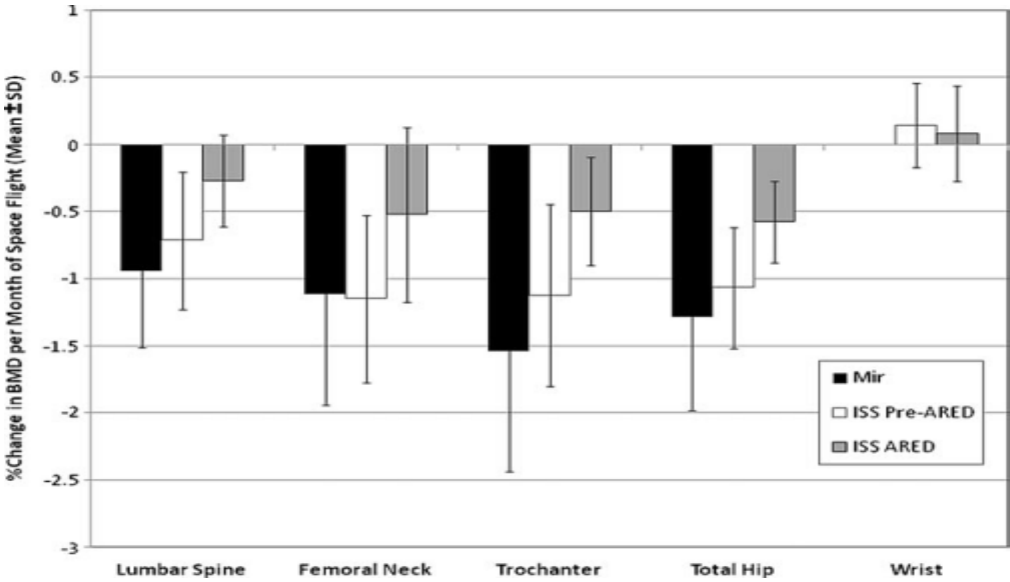

Figure reproduced from J. D. Sibonga, "Spaceflight-induced bone loss: is there an osteoporosis risk?," Curr Osteoporos Rep, vol. 11, pp. 92-8, Jun 2013.

Injury Risk

Environment	P(impact)	P(inj)	P(total)
Military	Low	Medium	Low
Automotive	Remote	Med-High	Low
Race Car	Low	Medium	Low
Spaceflight	Certain	Low	Low

- **Current ATD injury assessment reference values (IARVs) are based on automotive injury risk functions**
  - These functions are optimized for more severe and higher probabilities of injury than are needed for NASA use
  - Less information is available between the range of known human tolerance and injury risk

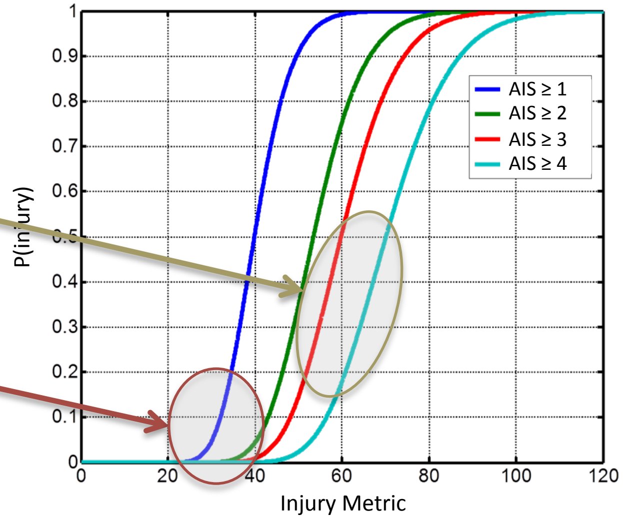

Probabilistic Approach to Certification

- **Unlike the automotive world, each vehicle design can have completely different operating environments**
- **Defining a standard test to certify a vehicle has drawbacks:**
  - For vehicles with low landing loads, a standard test may result in unnecessary additional mass
  - For vehicles with higher landing loads, a standard test may result in a design that is insufficient to protect crewmembers
- **Instead, the analysis and test method is based on a probabilistic approach to determining the appropriate critical loading cases**

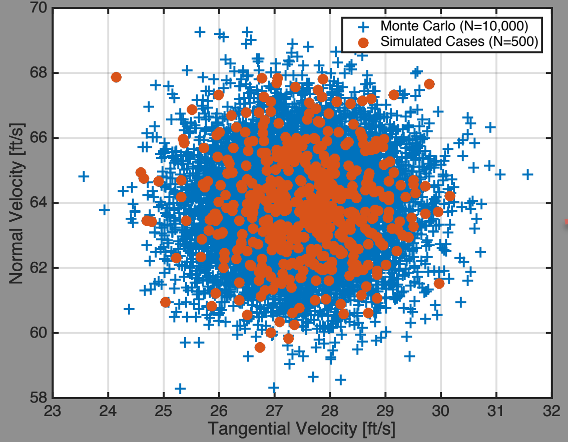

10,000 Monte Carlo Landing Cases

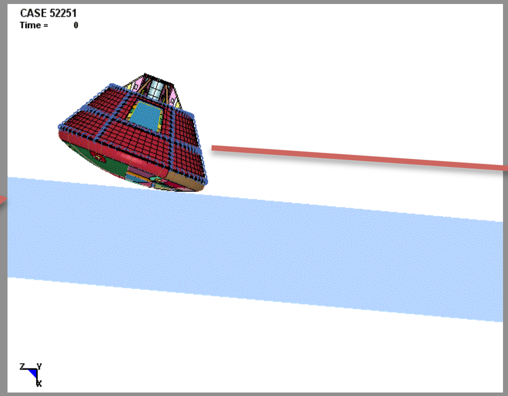

Simulate Selected Cases

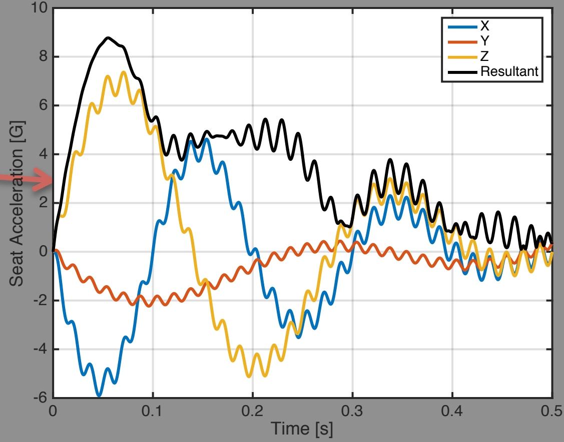

Recover Seat Accelerations

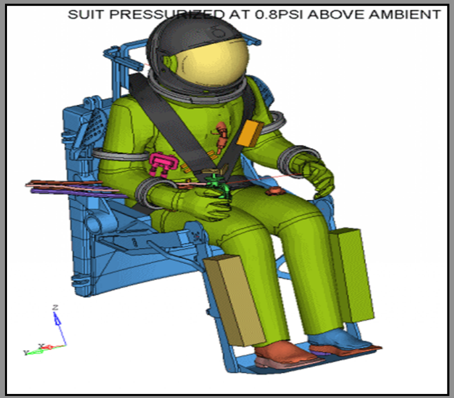

Suit &
Seat FEM

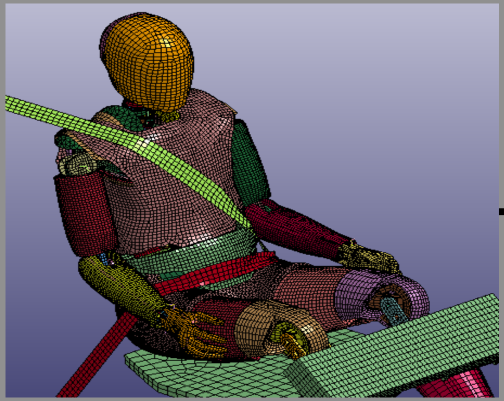

ATD FEM

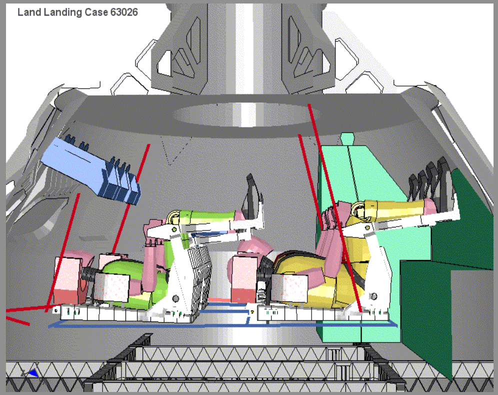

Landing
Simulation

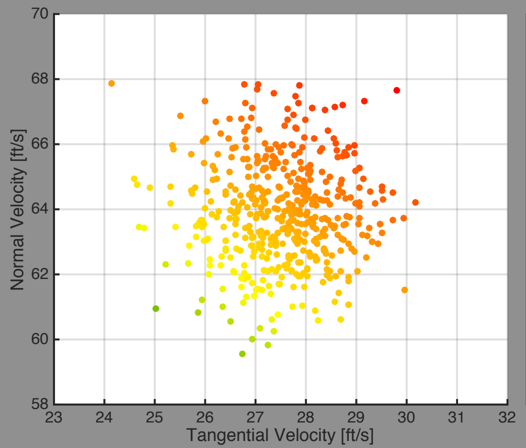

Create Response Surface

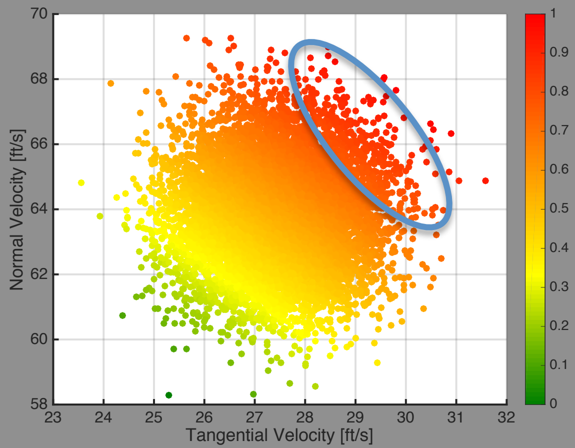

Determine Driving Cases

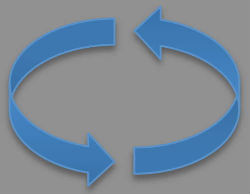

Iterate Design

Seat &
Suit

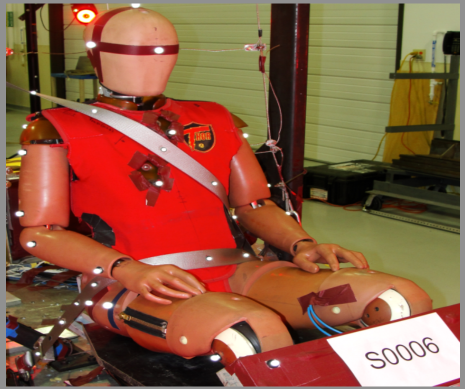

Physical
ATD

Physical
Testing

Future Work

- **Current requirements do not adequately address all of the risk factors (red boxes)**
- **NASA research is directed at addressing these areas**
  - Investigating the use of the THOR ATD
  - Conducting testing and simulation to evaluate suit design
  - Developing injury risk functions to address low probability of injury and sex differences
  - Conducting research to assess spaceflight deconditioning, and its effect on impact tolerance of the spine

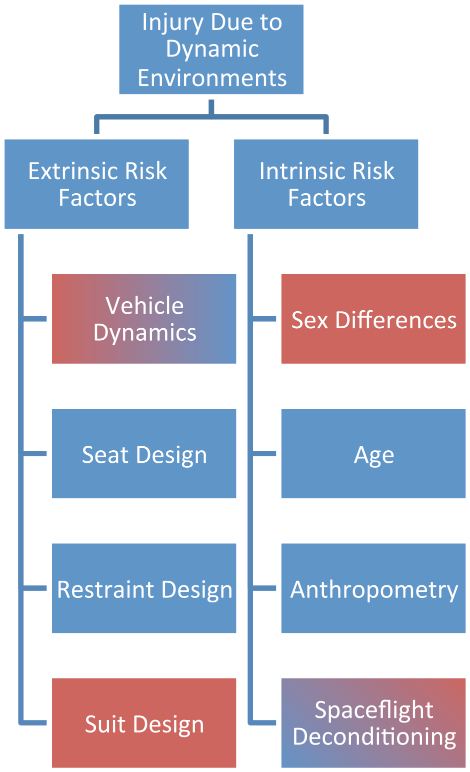

Mars Path to Risk Reduction

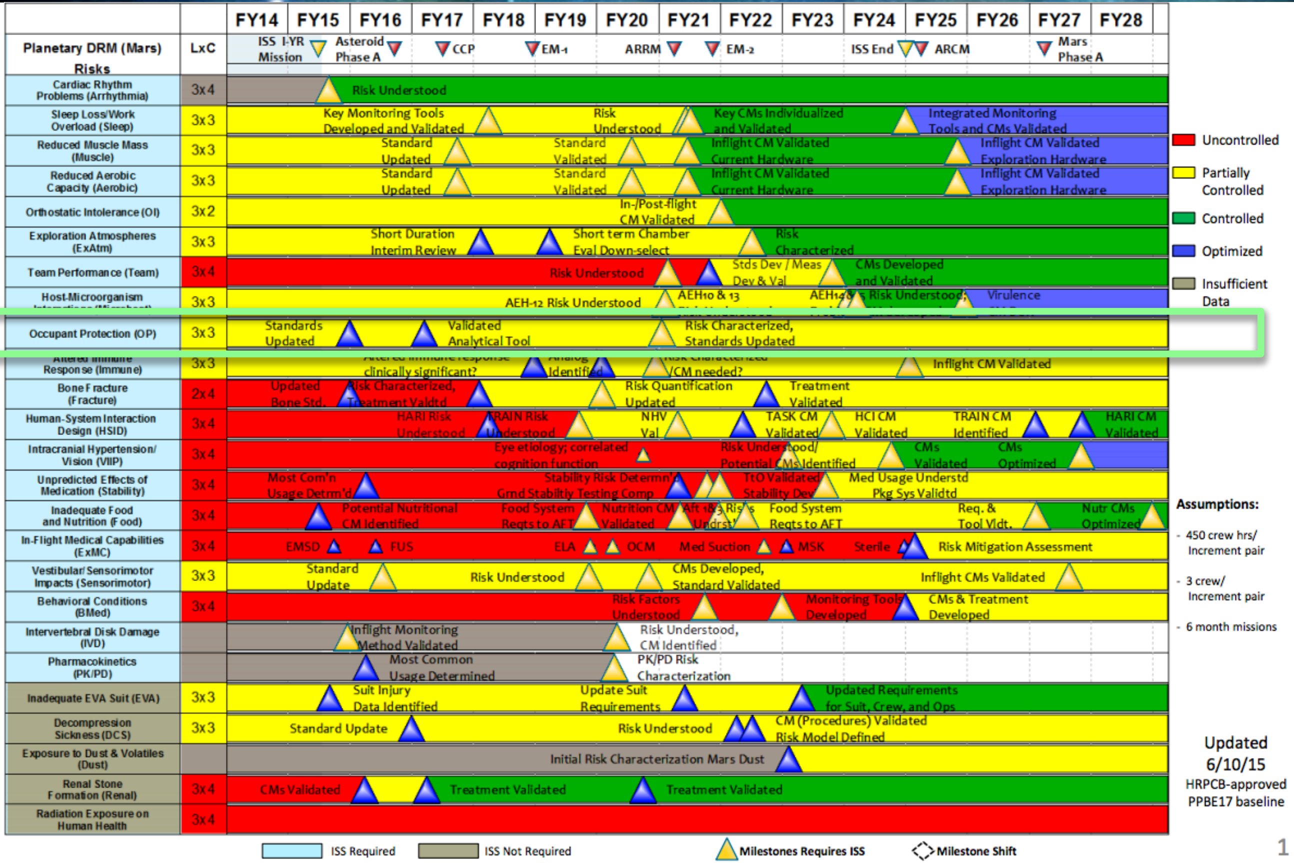

Summary

- **NASA's ultimate goal is to send Astronauts to Mars**
- **NASA is currently involved in the development of 3 crewed capsules**
- **The spaceflight dynamic environment is unique and has some unique challenges**
- **NASA uses a probabilistic approach to mitigate occupant injury and certify a design for human flight**
- **The NASA Human Research Program is conducting targeted research in injury biomechanics to address spaceflight specific needs**

Acknowledgements

- **The NASA Team**
  - Nate Newby
  - Jessica Wells
- **Funding for this work is provided by:**
  - NASA Human Research Program
- **We are also grateful for the assistance and guidance from the following Groups:**
  - Federal Aviation Administration
  - National Highway Traffic Safety Administration
  - NASA Engineering and Safety Center
  - NASA Space Medicine Division
  - NASA Biomedical Research and Environmental Division
  - NASA Astronaut Office

Quantitative Validation of High Fidelity Human Injury Finite Element Models using a Quantitative Probabilistic Error Metric

Dan Nicolella, Ph.D., Jessica Coogan, Ph.D., Travis Eliason, Ben Thacker, Ph.D.

Southwest Research Institute

San Antonio, TX

Computational Modeling for Biomechanical Analysis

- Relatively easy to construct high fidelity models from high quality 3D image data
  - powerful geometry modeling and meshing software
  - high performance computational resources
  - Resulting models “looks” almost identical to the actual biological system.
- Non-linear material constitutive models with properties either derived from experimental data or reported in the literature
- Large deformation, and motion defined by sliding contact between complex, deformable articulating surfaces

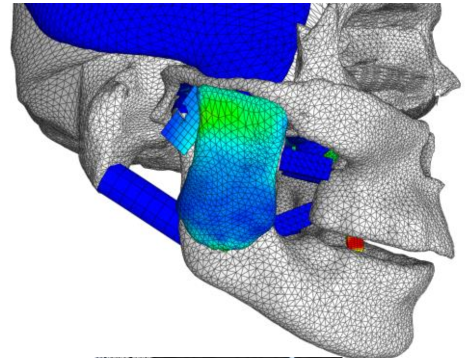

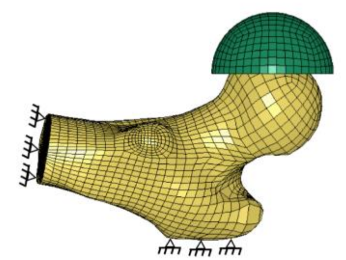

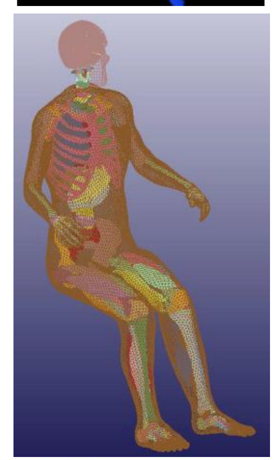

Model Verification and Validation (V&V)

- High fidelity should not be confused with model credibility
- High fidelity is necessary but not sufficient
  - Fidelity is the result of modeling tools (pre-processor, FE code, etc.) computational speed, etc.
- Model credibility is the result of specific and rigorous model V&V

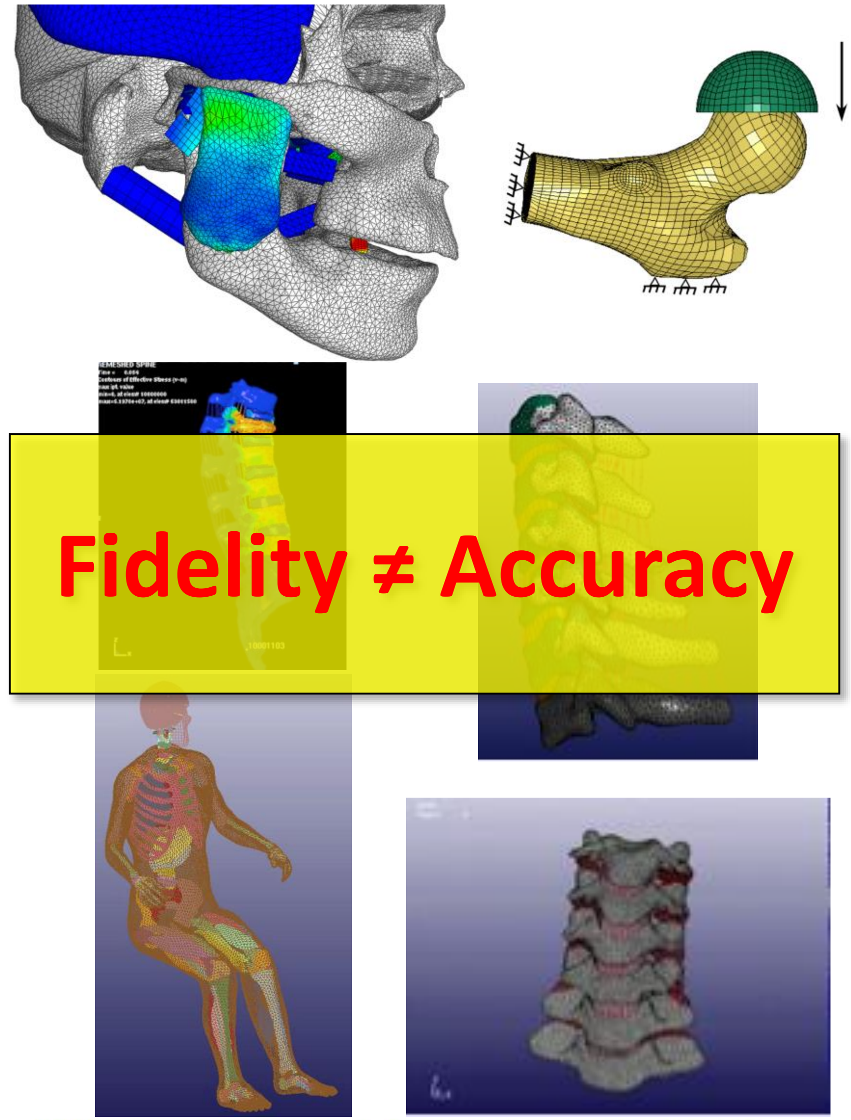

Fidelity ≠ Accuracy

Introduction

Why Model Verification and Validation (V&V)

- Fidelity does not mean accuracy
- Decision makers want to know:
  - What is the **error** between the model and tests?
  - How much **confidence** do we have in the model predictions?
  - Can we use these models to predict occupant injury?
  - Can we design safer systems using these models?
  - How accurate are these models for decision making?
- Model Verification and Validation can help answer these questions

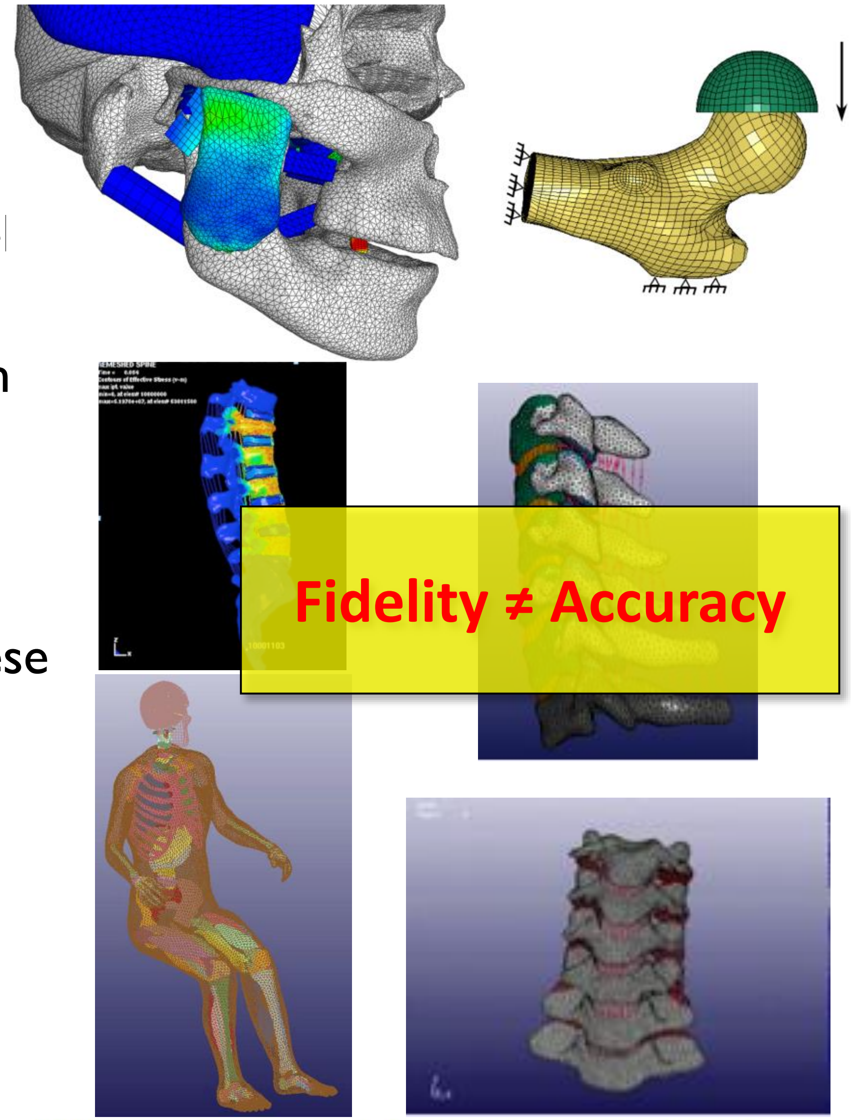

Establishing a Predictive Capability

- Verification
  - Credibility from understanding the mathematics
  - Are the equations being solved correctly?
  - Compare computed results to known solutions
- Validation
  - Credibility from understanding the physics
  - Are the correct equations being solved?
  - Compare computed results to experimental data
- Uncertainty Analysis
  - Credibility from understanding the uncertainties
  - How accurate is the model prediction?
  - Quantify uncertainty & variability from all sources

Mathematical Evidence

Experimental Evidence

Statistical Evidence

Model Verification & Validation

- Verification: Process of determining that a model implementation accurately represents the developer's conceptual description of the model and the solution to the model
    - Math issue: "Solving the equations right"
- Validation: Process of determining the degree to which a model is an accurate representation of the real world from the perspective of the intended uses of the model
    - Physics issue: "Solving the right equations"

Model Validation?

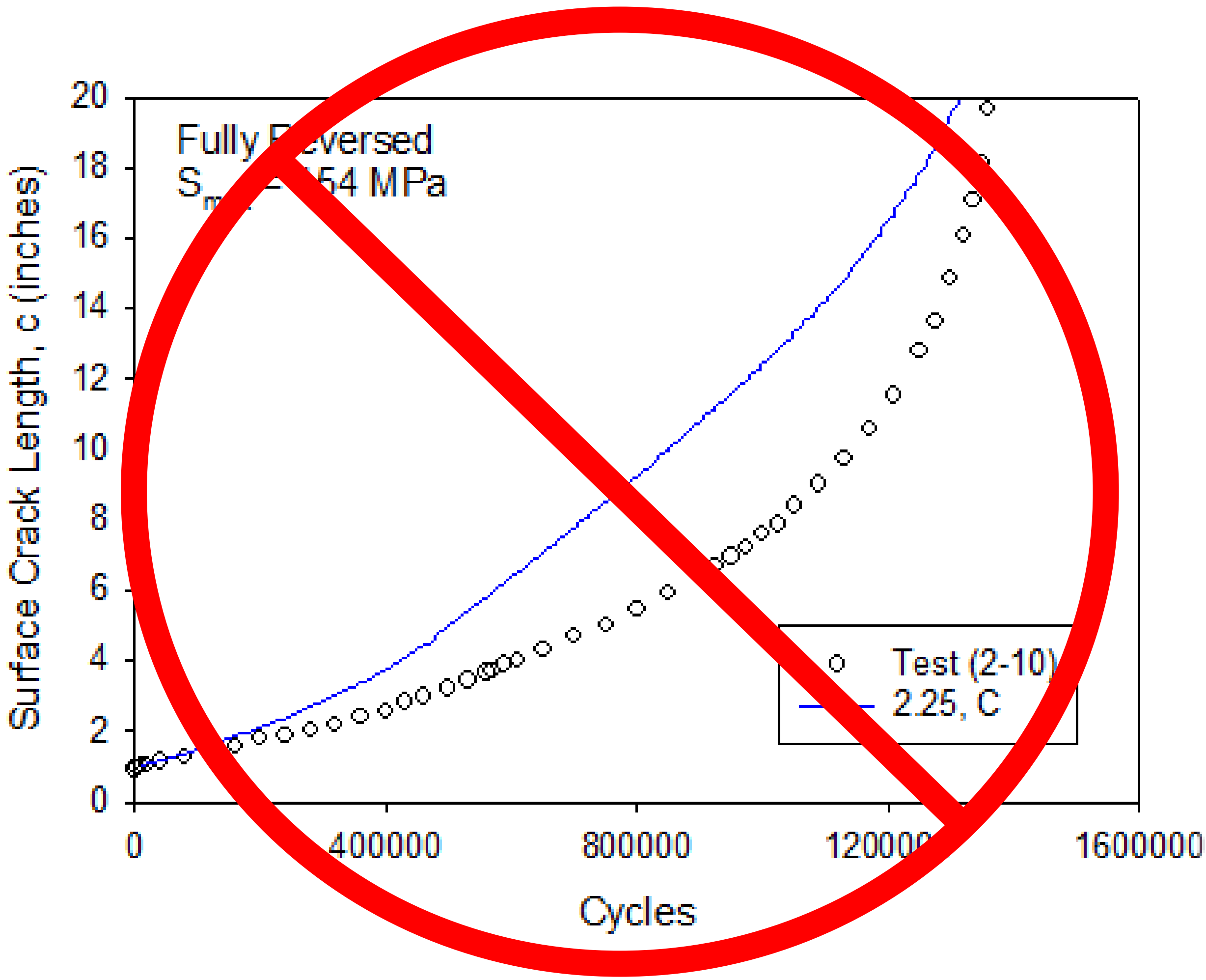

Model Validation Example

Typical Approach

- Common approach: model is valid if prediction falls within experimental corridors
- Issues
  - Mismatch not quantified
  - Corridor limits are arbitrary ($\pm 1\sigma$?)
  - Reducing the quality of the experimental data improves the chance that the model is valid (not good!)

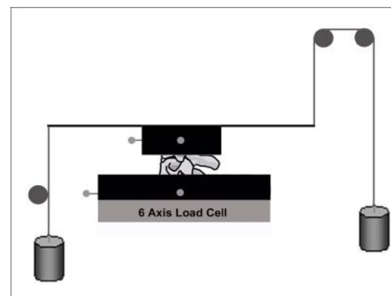

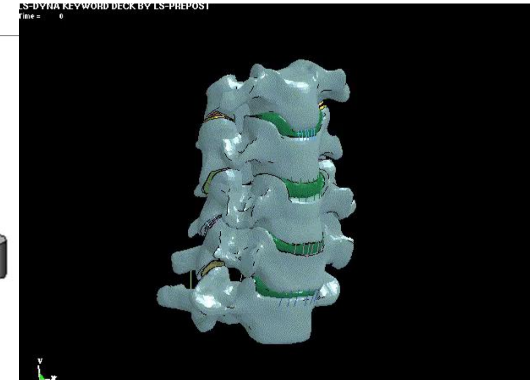

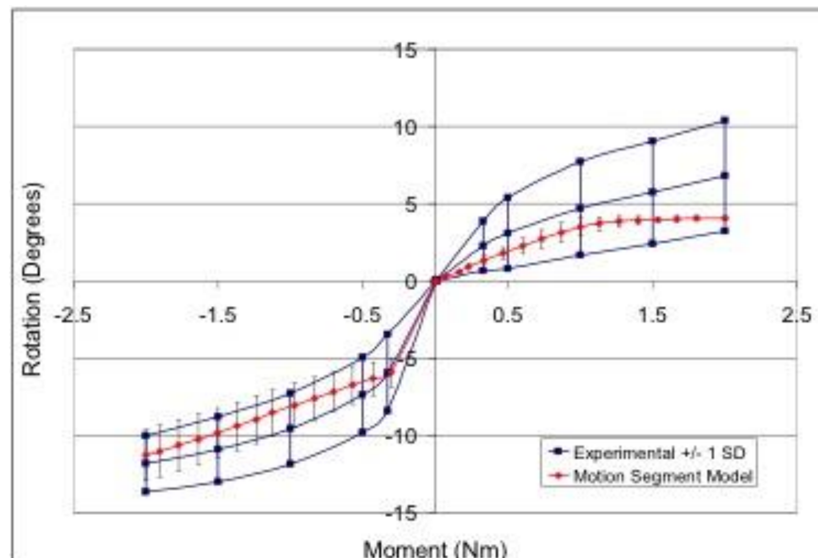

Validation Process

- The validation process has the goal of assessing the predictive capability of the model by quantitatively comparing the predictive results of the model with validation experiments.
- Three key elements of Validation:
  - Validation Experiments
    - Defined by validation hierarchy
  - Uncertainty Quantification
    - Experiment
    - Model
  - Validation Metrics
    - Quantification of error

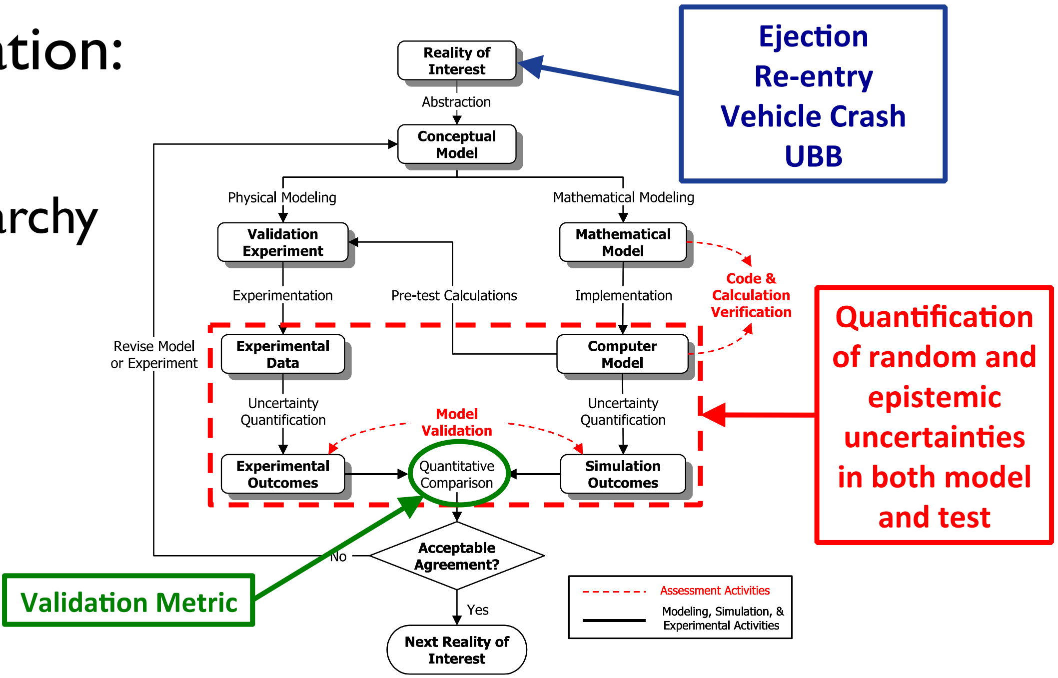

Approach based on ASME V&V 10-2006 "Guide for V&V in Computational Solid Mechanics"

V&V Plan

What is the question, and how good of an answer is needed?

- **Intended use of the model**
- Driven by customer/stakeholder
- Description of the top level model (what we ultimately want to predict)
- System response quantities (SRQs)
- Validation hierarchy (physical and phenomena decomposition of the problem) – validation experiments and modeling
- Validation metrics and requirements
- Phenomenon identification and ranking table (PIRT)
- Cost and schedule constraints and expectations
- Programmatic assumptions and limitations (for example, availability and adequacy of other experiments, testing, models, etc.)

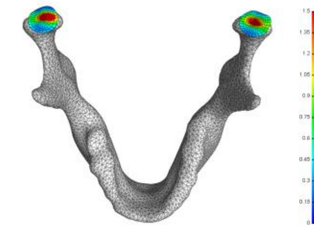

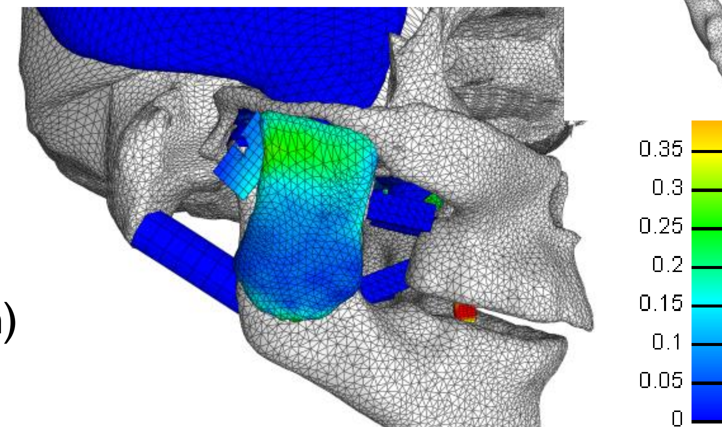

No.	Phenomenon	Importance (R-high, Y-med, G-low)	Adequacy (R-low, Y-med, G-high)
1	Linear behavior		
2	Nonlinear behavior		
3	Quasi-static		
4	Linear dynamic		
5	Non linear dynamic		
6	Sliding contact		
7	Friction		
8	Muscle activation		
9	Thermal transient		
10	Anthropomorphics		

Hierarchical Model V&V Approach

ASME V&V-10 Guidelines

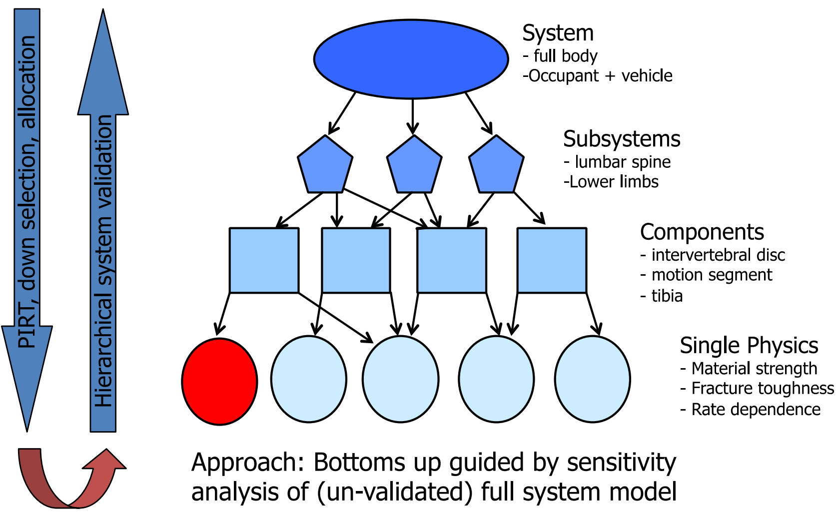

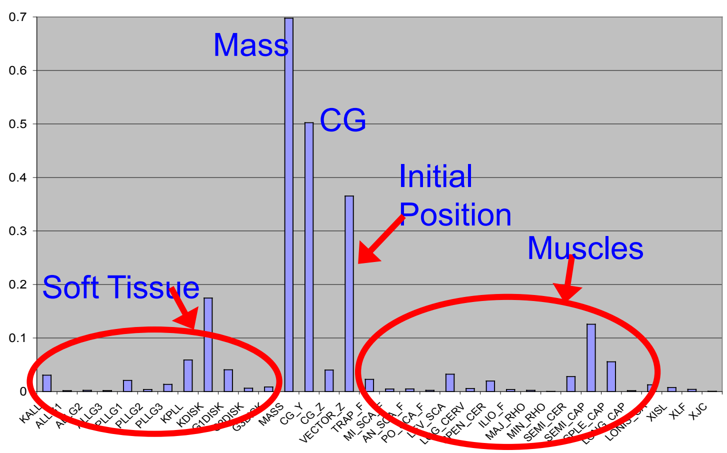

- Validation hierarchy
  - Breaks the problem into smaller parts
  - Validation process employed for every element in the hierarchy (ideally)
  - Allows the model to be challenged (and proven) step by step
  - Dramatically increases likelihood of <u>right answer for the right reason</u>
- Customer/stakeholder establishes intended use and top-level validation requirement
- Validation team constructs hierarchy, establishes sub-level metrics and validation requirements
  - Modeling and experiment teams work closely together to define hierarchy and experiments/simulations
  - Experiments are designed expressly for model validation
- In general, validation requirements will be increasingly more stringent in lower levels
- Full system (un-validated) sensitivity analysis can provide guidance

Validation Experiments

- A validation experiment is a physical realization of an initial boundary value problem
- Purpose is to produce data that the model is expected to predict
  - Redundancy of the Data – repeat experiments to establish experimental variation
  - Supporting Measurements – redundant measurements to ensure data integrity and to serve as inputs to model (actual loads, for example)
  - Uncertainty Quantification – model is also expected to predict measured variability
- Validation experiments are designed by both the experimentalists and the modelers
  - What's hard in the lab is easy in the model…and vice versa
- Must carefully assess whether or not existing data are suitable for validation (usually not)
- Experiment is modeled and the results quantitatively compared

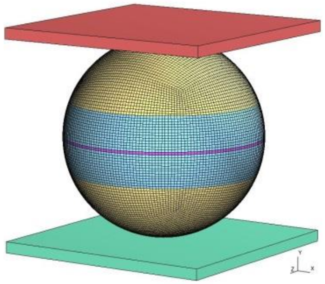

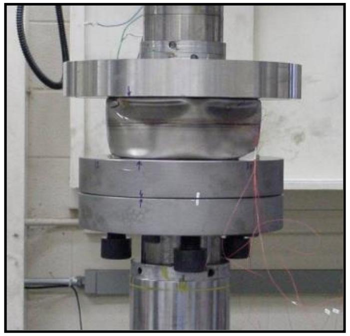

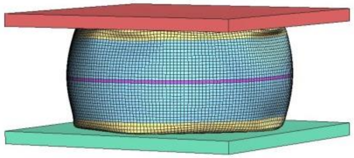

Uncertainty Quantification

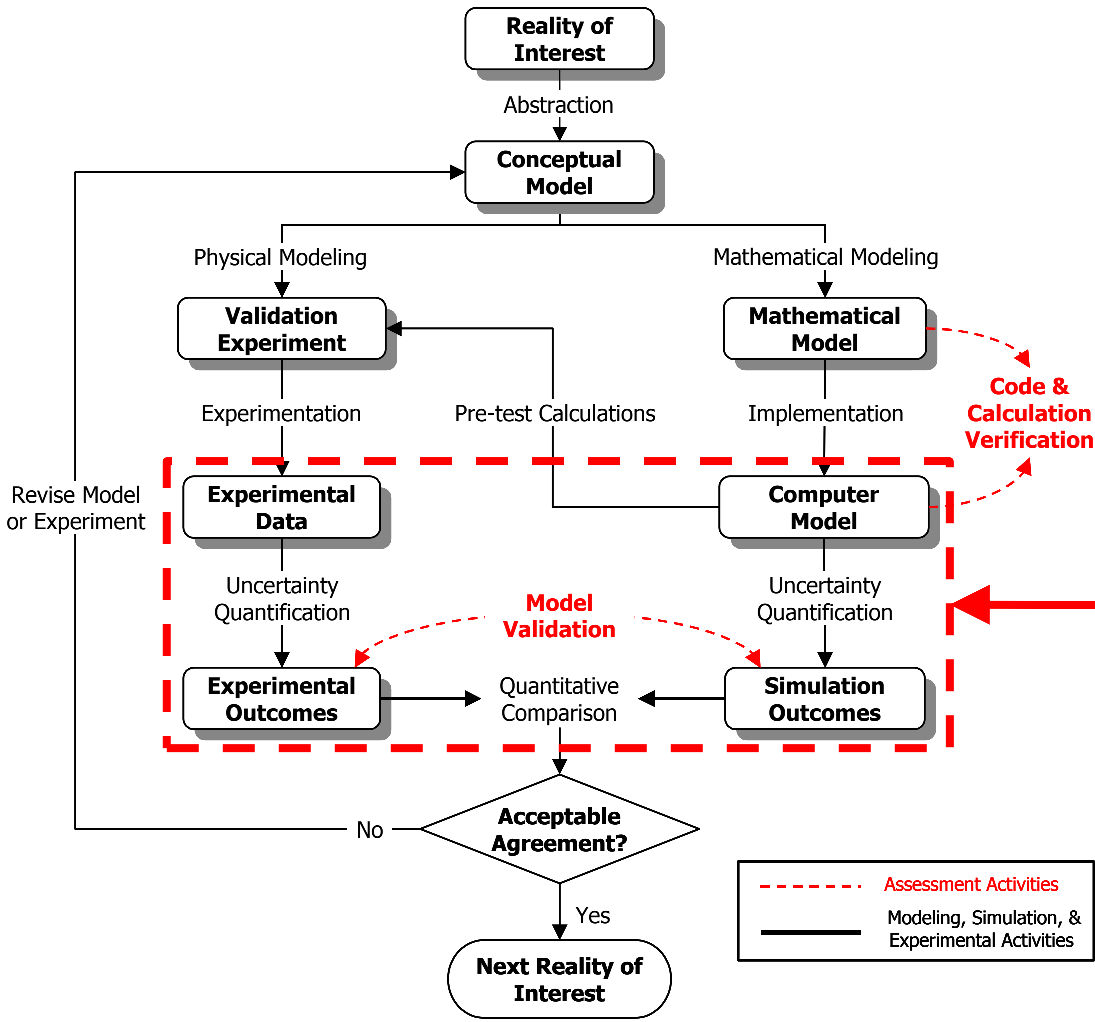

Quantification of random and epistemic uncertainties in both model and test

Uncertainty Quantification

- Quantify all sources of significant uncertainty
  - ***Exist in both the model and experiment***
  - Reducible uncertainty (epistemic uncertainty)
    - Deficiencies that result from a lack of complete information
  - Irreducible uncertainty (aleatory uncertainty)
    - Inherent property of all physical systems
- Help design validation experiments (what to control, what not to control, what to measure, and what to let vary)
- Validation metrics will also operate on uncertain quantities

Characterizing Uncertainties: *Experiment*

CONDUCT EXPERIMENT

Values of Young's modulus (GPa)

206.0	221.7	216.9	196.4
202.8	210.6	205.2	211.6
207.7	203.9		

PERFORM STATISTICAL ANALYSIS

Average (μ) = 208.3 GPa

Standard deviation (σ) = 7.3 GPa

Coefficient of Variation (COV) = σ/μ = 3.7%

CONSTRUCT HISTOGRAM

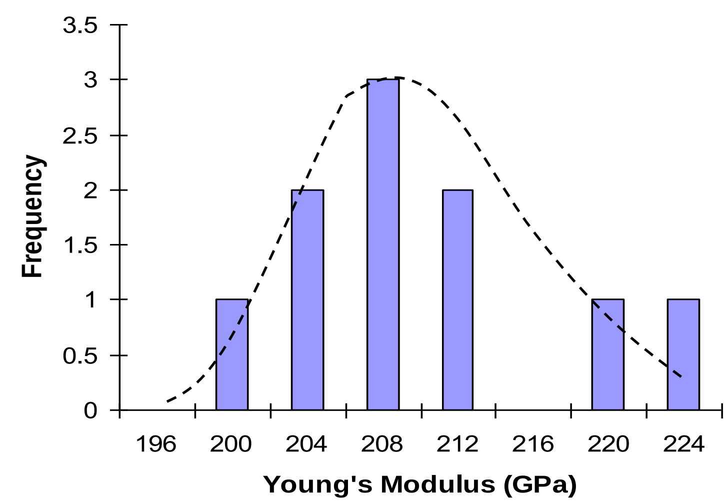

SELECT PROBABILITY DISTRIBUTION

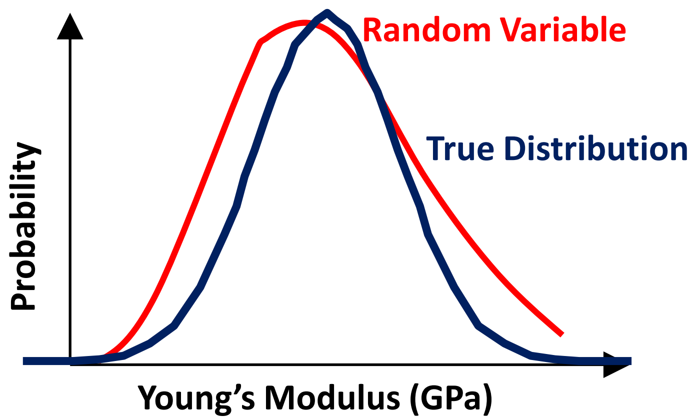

Characterizing Uncertainties

Probabilistic Computational Model

Aleatory uncertainty
Operational Conditions
Population Group

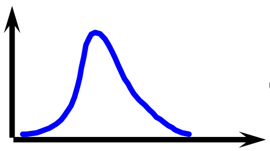

COV's~100%

Material Property

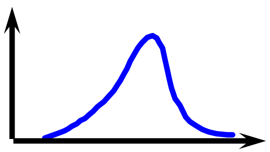

unknown & variable

Forces

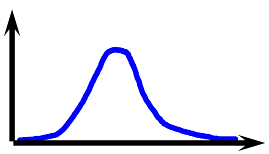

unknown & variable

Boundary Conditions

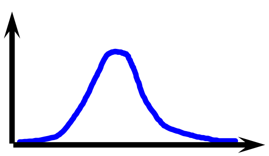

COV's~20%

Geometry

Finite Element Model

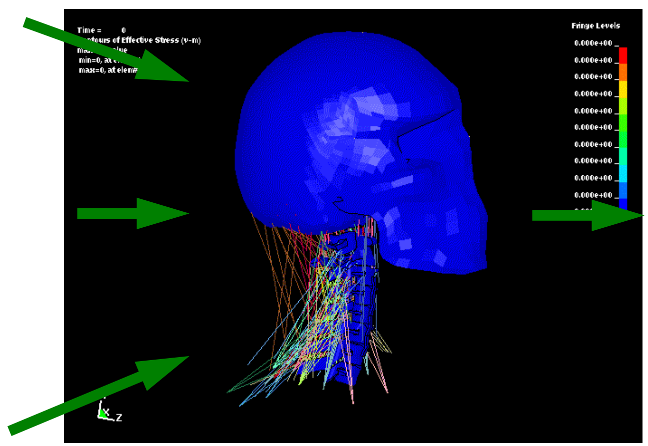

Predicted Probabilistic Response

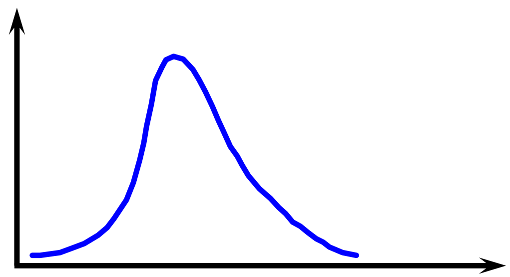

Model Response
Forces, Stress, Strain, Deflections, etc.

Probabilistic Methods

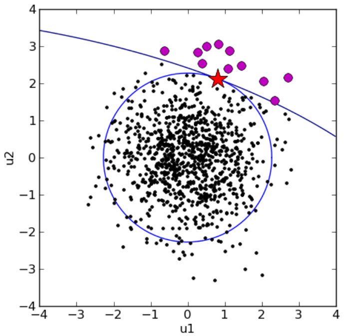

Basic Monte Carlo

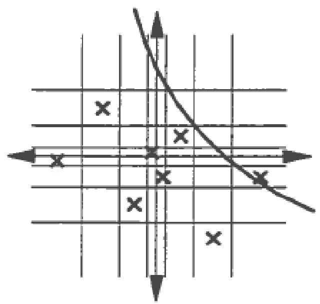

LHS

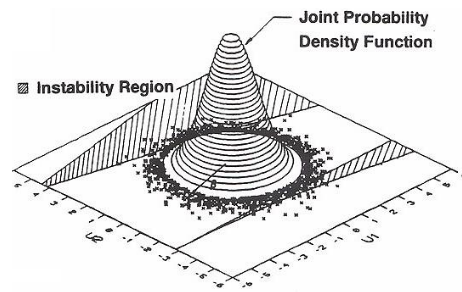

Sphere Based IS

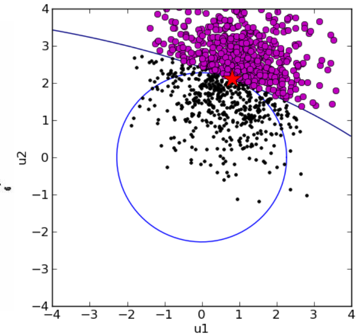

MPP Based IS

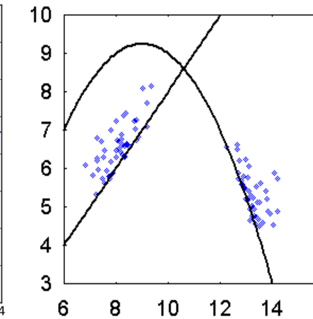

Adaptive IS

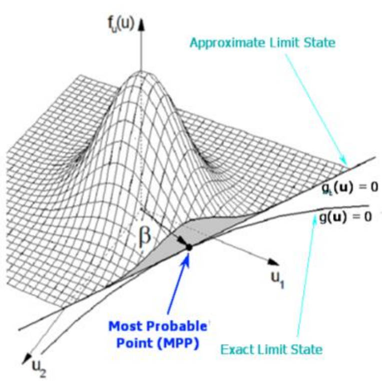

MPP Based Methods
FORM/SORM

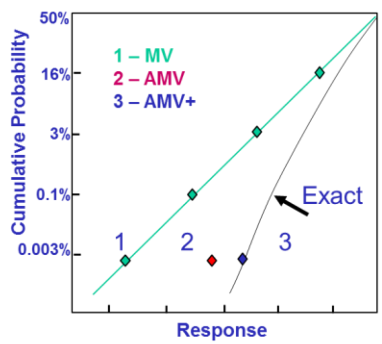

AMV+

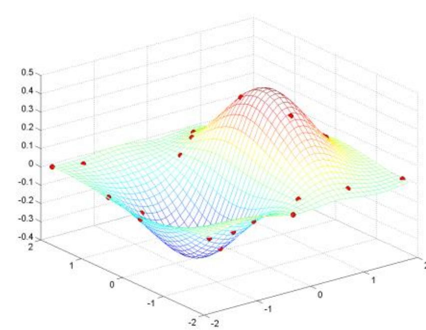

Surrogate Models
Gaussian Process Models

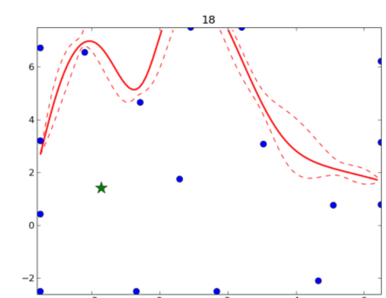

EGRA

Validation Metrics

How do you define valid?

- A metric is the quantitative *measure* of the mismatch between model predictions and experimental data
- Typically some type of a difference measure in system response quantities (statistics, probability distributions, etc.)
- Generally, multiple response quantities and associated metrics are better than one (right answer for the right reason)
- Desired features of a validation metric
  - **Consider uncertainties in both the model and the experiment – *implies a statistical comparison***
  - Reflect only the comparison (not the adequacy)

Probabilistic Validation Metric

- Absolute error between a model prediction and an experimental response quantity
  - Model prediction and experimental measurement are uncertain
  - Normalized by the experimental mean value (to simplify solution)

$$Z = \frac{Y^{\mathrm{mod}} - Y^{\exp}}{E\left[Y^{\exp}\right]}$$

$$p = P\left(|Z| \le z\right)$$ Probability that the error will not be exceeded

  - Validation Requirement

$$p < p_r,\ \text{or}\ z < z_r$$

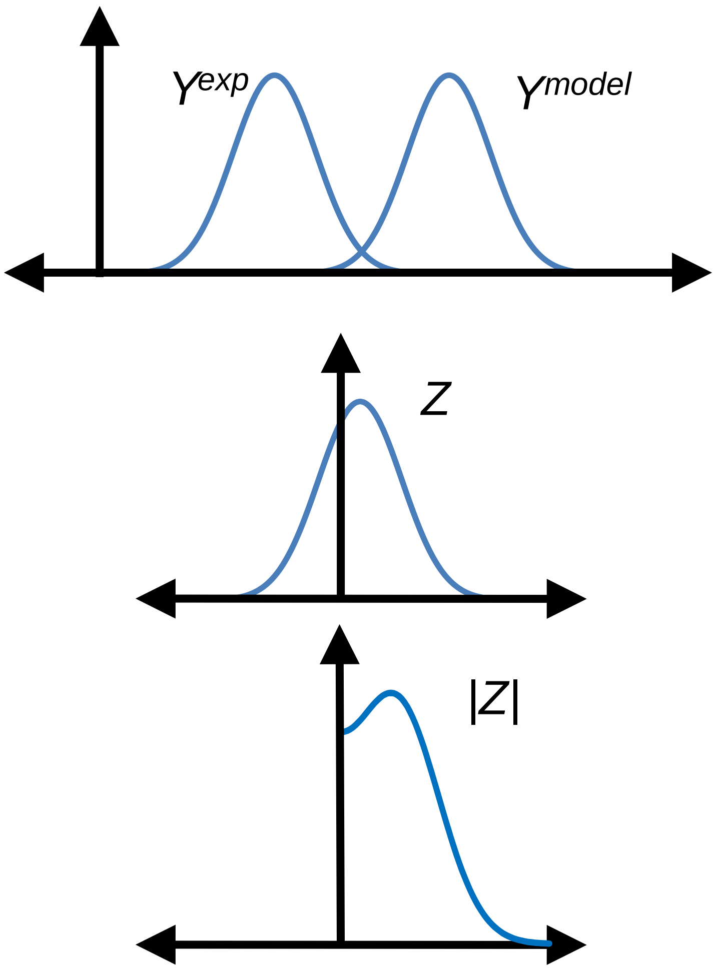

Probabilistic Validation Metric
Interpretation

- CDF (integration of PDF) of Z
  - X-axis is error - Z
  - Y-axis is probability level - p
- 90% probability that the error will not be greater than 15.6%
- 61% probability that the error will not be greater than 10%
- The error between the model and the experiment is fully defined
- Sensitivity analysis indicates which variables are driving the error

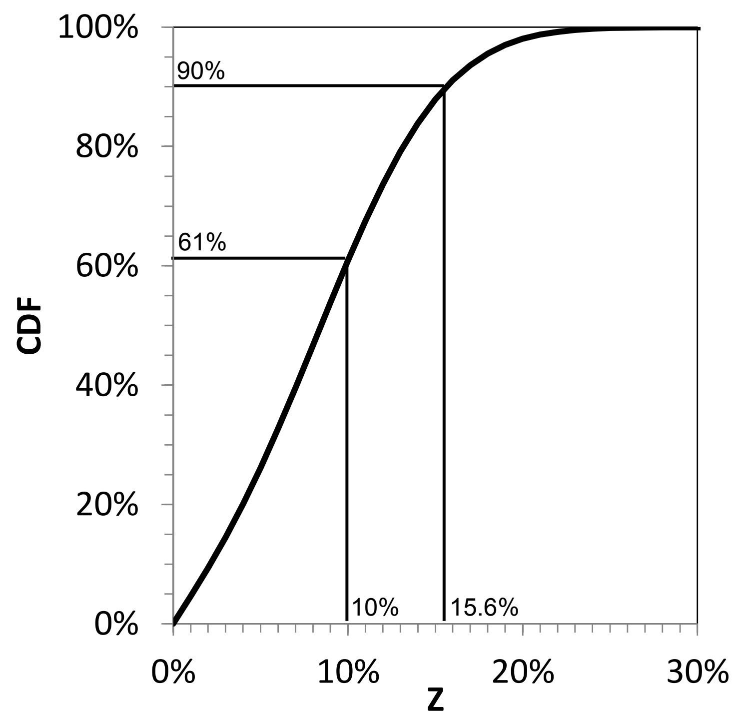

(b)

Z = error between model and experiment

Model Validation Example

Sensitivity of Error to Model and Experiment Uncertainties

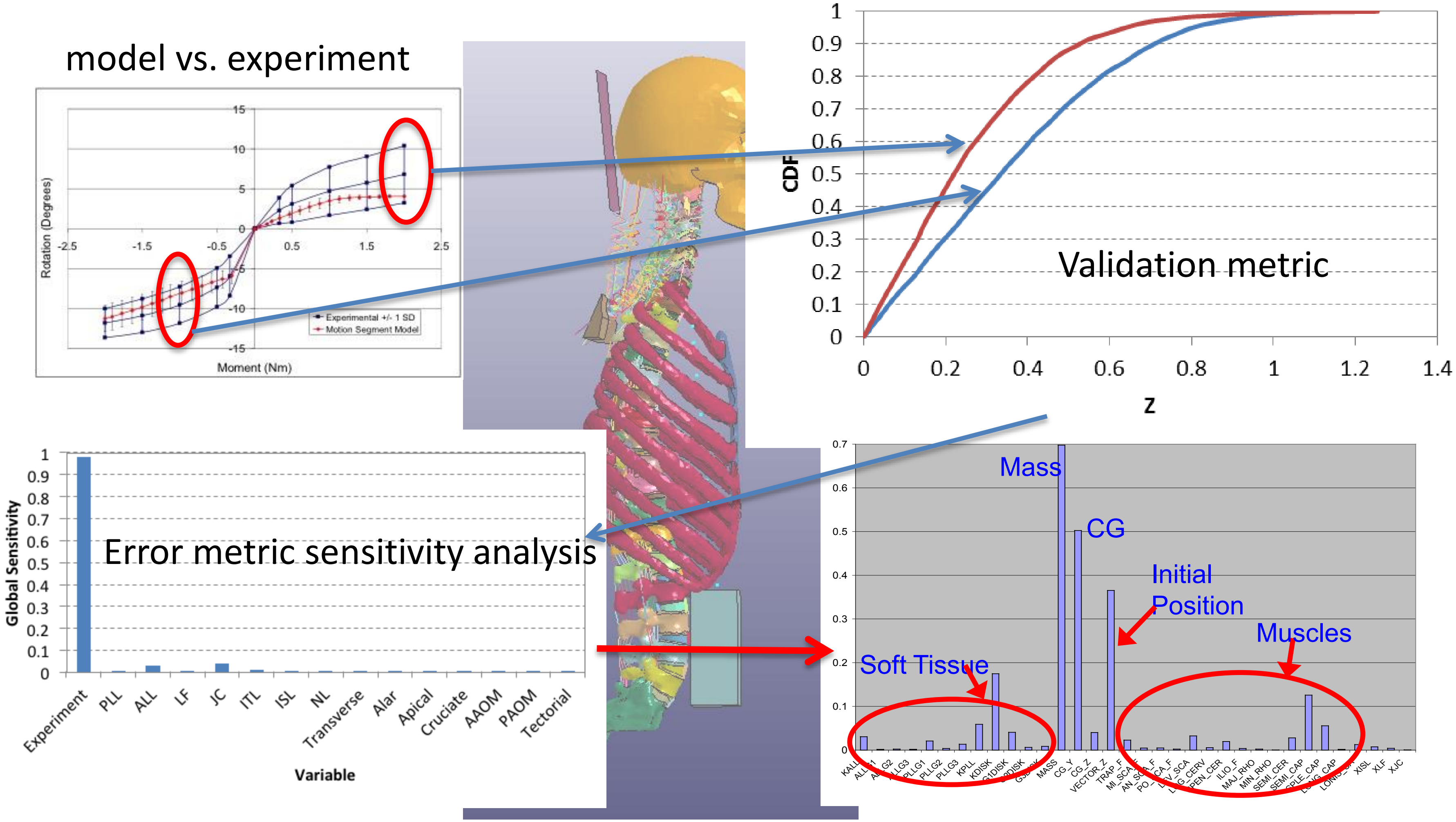

Summary

- Modeling tools allows the development of complex, high fidelity models
  - Model fidelity ≠ model validity
- Ubiquitous use of computational modeling requires a model validation plan
  - How much **confidence** do we have in the model predictions?
- Modeling and experiment teams need to work together
  - Experiments should be designed for model validation
- Development of a validation plan is recommended
- Hierarchical approach (ASME V&V-10 Committee)
  - Breaks the problem into smaller parts
  - Validation process employed for every element in the hierarchy (ideally)
  - Allows the model to be challenged (and proven) step by step
  - Dramatically increases likelihood of right answer for the right reason
- **Account for uncertainty in both model and experiment**
- Validation metric is the *measure* of the mismatch between model and experiment - Quantitative


Thank You
Southwest Research Institute®
Benefiting government, industry and the public through innovative science and technology

SPINAL INJURY RISK ASSESSMENT MODEL FOR THE 5TH AND 95TH PERCENTILE OCCUPANT

ARL - Second Workshop on Numerical Analysis of Human and Surrogate Response to Accelerative Loading | Tim Westerhof, Jeroen Broos, Mat Philippens

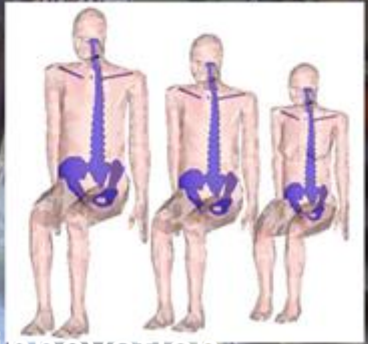

innovation for life

Unclassified

SCOPE

- Test procedure of STANAG 4569 – AEP 55, qualification for vehicle IED/Mine protection, provides method for injury risk assessment of the lumbar spine for a 50th percentile occupant:
  - Dutch MoD: what are the injury risk consequences for 5th and 95th percentile occupant, when seated on a 50th percentile ATD qualified seat?

- Industry is working on active protective seat systems for real time controlled damping:
  - Prototype magnetorheological fluid damper (30% less stroke required for same injury criteria).
  - Can a damper optimized for 50th % HIII ATD, be used for 5th, 50th or 95th percentile real human.

INJURY CRITERIA

- Test procedure of STANAG 4569 – AEP 55 , qualification for vehicle IED/Mine protection, requires the Dynamic Response Index (DRI) to assess of injury risk to the lumbar vertebral column.
- DRI has its flaws (Thyagarajan *et al*, 2014), meanwhile the need for 5th and 95th is there. DRI will be used here for 5th and 95th occupant injury risk assessment to be in line with the current STANAG 4569.
- *Future injury criteria in a next version of STANAG 4569 can originate from different research, e.g. the WIAMan project (ARL-USA).*

STANAG Injury criteria $\xrightarrow{2006}$ ~~DRI~~ (50th %ile) $\xrightarrow{2016}$ ~~DRI~~ (5th & 95th %ile) $\xrightarrow{future}$ WIAMan criteria?

GOAL

- *To develop an engineering method to asses spinal injury risk, induced by vertical accelerative loading for a 5th and 95th percentile occupant, in line with STANAG 4569 – AEP-55.*

- The following steps are taken to achieve this goal:
  - Development of a lumbar spine model, based on a human body model (HBM) (Happee et al, 1998, 2000) for the 5th, 50th and 95th percentile anthropometry.
  - Determination of force tolerance for the 50th percentile lumbar spine model, based on STANAG DRI tolerance of 17.7 (STANAG 4569 – AEP 55 , Brinkley et al, 1971).
  - Scaling the force tolerance of the 50th percentile lumbar spine model to the 5th and 95th lumbar spine model assuming: a constant failure stress (Ebbenese 1999) and a correlation between the cross sectional area of vertebrae and body weight (Riggs 2004).

MADYMO HUMAN BODY MODEL (HBM)

SCALABLE MODELS

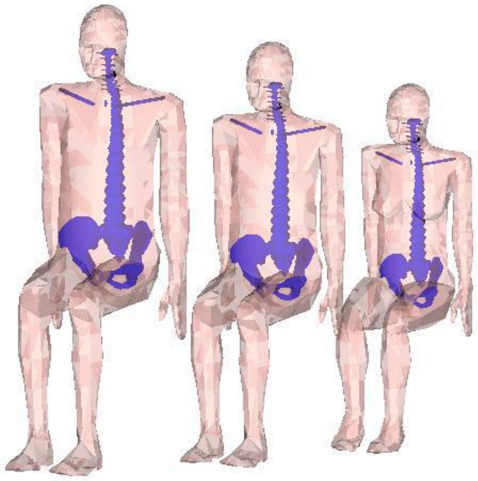

- 50th male HBM (Happee *et al*, 1998, De Lange *et al*, 2005)
  - Anthropometry from RAMSIS (measurements on civilian population)
  - Joint and contact characteristics based on literature and validation data
- 5th female HBM (Happee *et al*, 2000)
  - Anthropometry of short and slim female (RAMSIS, scaled to 5th female)
  - Joint and contact parameters scaled from 50th male HBM using generic scaling methods
- 95th male HBM (Rodarius *et al*, 2007)
  - Anthropometry of tall male with large waist (RAMSIS, scaled to 95th male)
  - Joint and contact parameters scaled from 50th male HBM using generic scaling methods

Table 2.1 Anthropometry of the adult facet occupant models.

Parameter	Small female	Mid-size male	Large male
Standing height [m]	1.52 m	1.74 m	1.91 m
Sitting height [m]	0.81 m	0.92 m	1.00 m
Weight [kg]	49.8 kg	75.7 kg	101.1 kg

LUMBAR SPINE MODEL

- The lumbar spine and upper torso vertical parameters were taken from the HBM to create a MDOF mass spring damper model for the 5th, 50th and 95th percentile anthropometry.
- The lumbar vertebrae and upper torso are represented by rigid bodies with their specific mass, springs and dampers connect the rigid bodies with each other.
- Input acceleration is applied at the pelvis on spring k_5 and damper c_5, resulting in a load (F_5) on m_5.
- Model determines the force exhibited on the rigid bodies, due to the spring compression and damper loading.

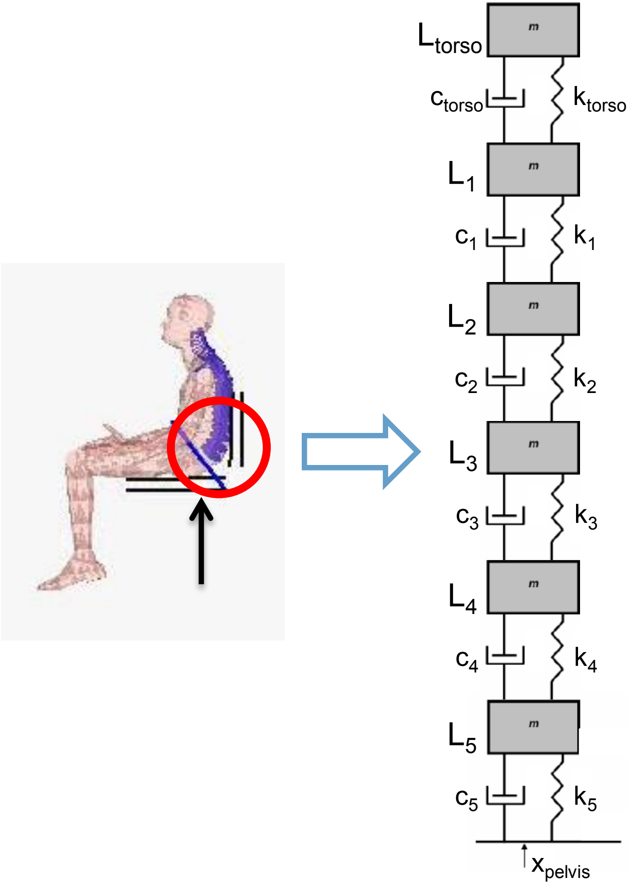

LUMBAR SPINE MODEL

- $\boldsymbol{M}$ = body mass matrix (kg)
- $\ddot{\vec{x}}(t)$ = vertical acceleration (m/s²)
- $\boldsymbol{C}$ = damping coefficient matrix (kg·m/s)
- $\dot{\vec{x}}(t)$ = vertical velocity (m/s)
- $\boldsymbol{K}$ = spring constant matrix (N/m)
- $\vec{x}(t)$ = vertical displacement (m)
- $\vec{F}_{ext}(t)$ = applied external force (N)

$$F_5(t) = c_5 \cdot \dot{x}_{pelvis}(t) + k_5 \cdot x_{pelvis}(t)$$

$$\boxed{\boldsymbol{M} \cdot \ddot{\vec{x}}(t) + \boldsymbol{C} \cdot \dot{\vec{x}}(t) + \boldsymbol{K} \cdot \vec{x}(t) = \vec{F}_{ext}\,(t)}$$

- Force on vertebrae:

$$\boxed{\vec{F}_{int}(t) = \boldsymbol{K} \cdot \vec{x}(t) + \boldsymbol{C} \cdot \dot{\vec{x}}(t)}$$

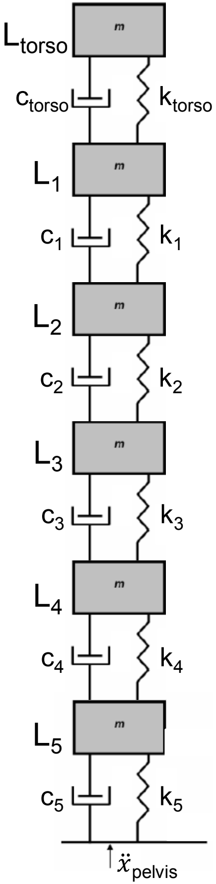

SIMULATION EXAMPLE RESULT

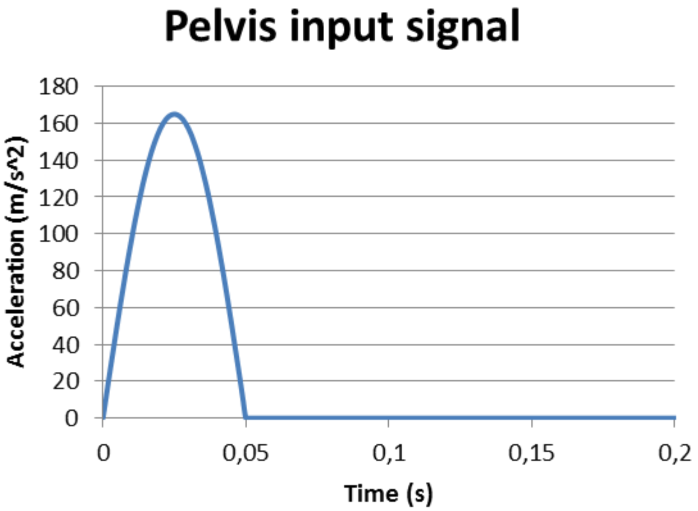

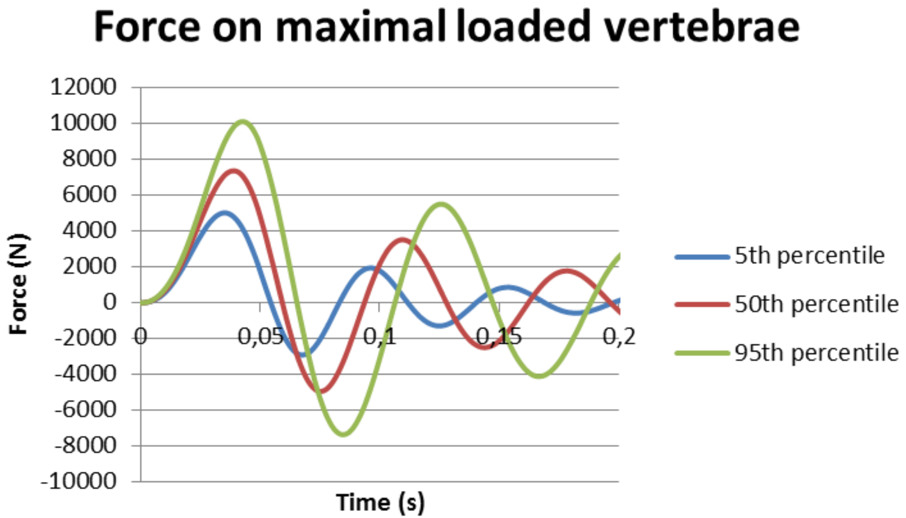

- These results show a increasing maximum simulated force for the 5th to 95th percentile anthropometry, for the same input signal, due to the inertia

TOLERANCE VALUE

- To asses lumbar spine injury with the lumbar spine model, a tolerance value is required.

Maximum $\vec{F}_{int}$?

- Tolerance DRI = 17.7 , 10% risk of spinal injury is used to define a force tolerance for the 50th lumbar spine model.

- The maximum of all forces between all rigid bodies is selected as the criterion.

FORCE TOLERANCE VALUE – 50TH PERCENTILE

DRI = 17.7 → 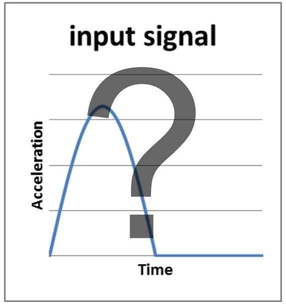

→ 50th lumbar spine model → force tolerance

- Input signals of a half sine pulse is used to simulate a DRI of 17.7.
  - Amplitude is adjusted to get DRI = 17.7
  - Repeated for range of frequencies
- Tolerance for 50th percentile lumbar spine model is determined using the found input signal
- Force limit is assumed to be frequency dependant.

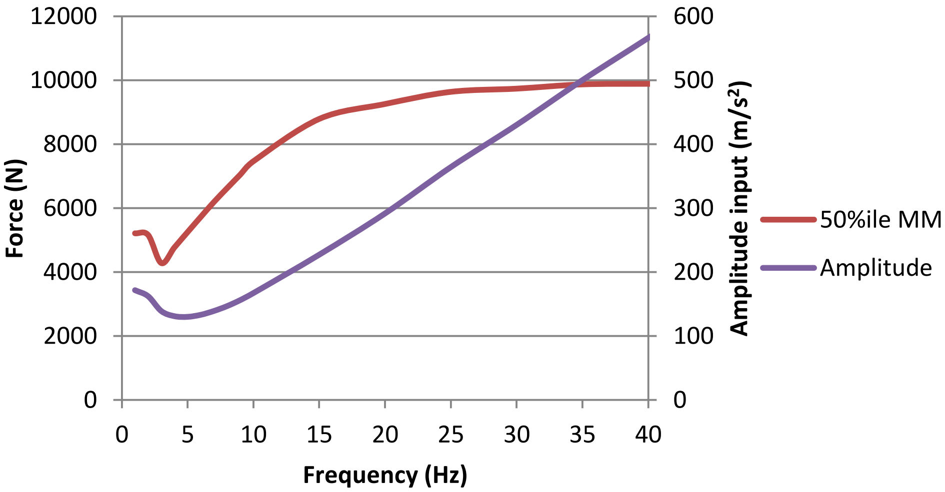

FORCE TOLERANCE VALUE – SCALING TO 5TH AND 95TH PERCENTILE

- Failure stress is equal for all sizes and sexes (Ebbenese *et al,* 1999a,1999b, Riggs *et al,* 2004)

- For similar bone quality (e.g. Bone Mineral content) cross sectional area of vertebrae correlates to body weight (Riggs *et al,* 2004)

$$F_5 = F_{50} \cdot \frac{A_5}{A_{50}} = F_{50} \cdot \frac{m_5}{m_{50}}$$

$$F_{95} = F_{50} \cdot \frac{A_{95}}{A_{50}} = F_{50} \cdot \frac{m_{95}}{m_{50}}$$

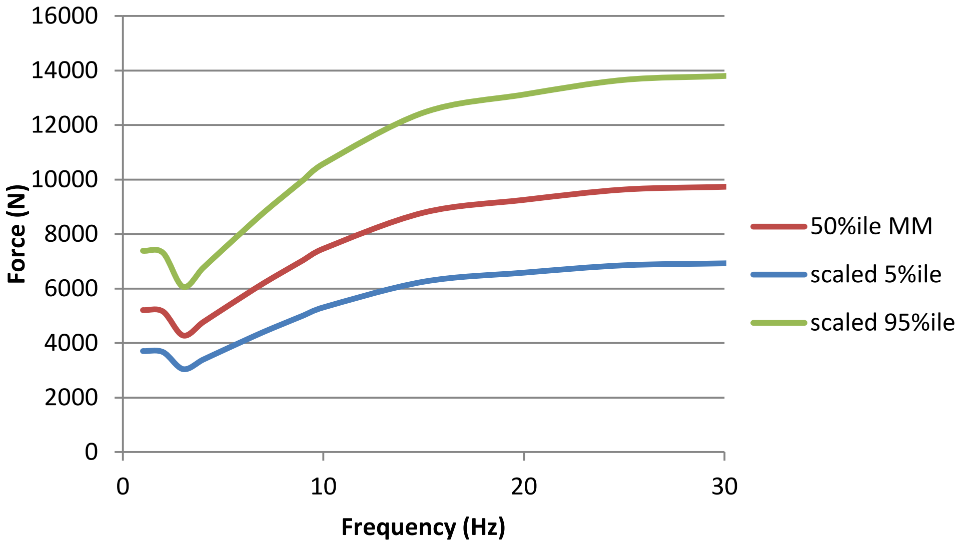

ROUTINE

- Due to input frequency dependency of tolerance values, frequency of input signal has to be known
  - Frequency spectrum
  - Shock response spectrum
- Force tolerance value is selected for the found frequencies
- Lumbar spine model simulations are performed to determine maximum force

- This procedure was tested on previously performed sled tests.
  - 5th, 50th and 95th percentile HIII ATD.
  - 50th percentile DRI was calculated for all tests.
  - Just presented routine for lumbar spine model is performed for these tests.

SLED TESTS COMPARISON

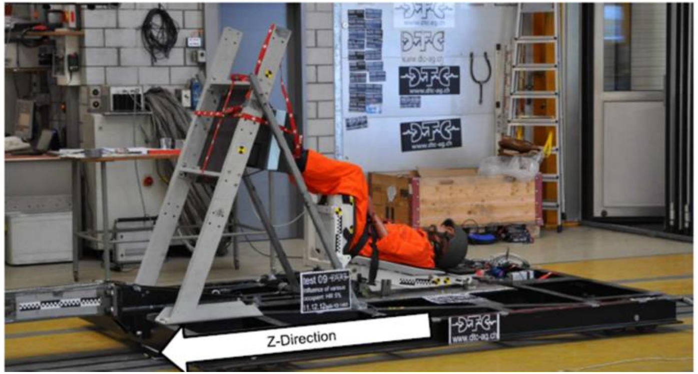

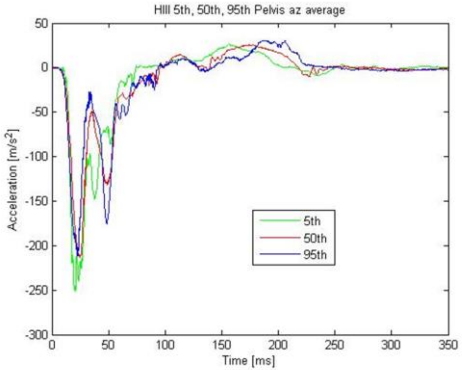

Spinal injury risk assessment model for the 5th and 95th percentile occupant

Test nr.	%tile	Max simulated force [N]	Freq [Hz]	Limit [N]	Pass?	DRIz 50th %ile
1	50	8774	10	7463	1311	20.821
2	50	6477	10	7463	-986	16.256
3	50	6585	11	7728	-1143	16.491
4	50	6699	10,5	7595	-896	16.498
5	50	6207	10,5	7595	-1389	15.219
6	50	6069	10	7463	-1394	14.604
7	5	5825	10	5309	516	18.7
8	5	5774	8	4710	1064	18.4
9	5	5812	10	5309	503	18.5
10	95	7443	8	9386	-1943	14.4
11	95	7329	8	9386	-2057	14.5
12	95	7333	8	9386	-2053	14.6
13	95	9621	8	9386	235	18.2

DISCUSSION

- Currently only **compression** fractures induced by a vertical load are included.
- **Wedge fractures** can occur, load direction and occupant positioning dependant (Zhang & Zhao, 2013).

- Reported **compression fracture tolerances vary significantly** (static 0.85 – 15.5 kN (Hutton *et al* 1979), dynamic 50% risk at 3.7 kN (Yoganandan *et al* 2013)).
- The presented force tolerances are **within ranges** reported as in literature and are considered a **realistic estimate** for a **minimum of 10%** fracture risk.
- Significant **out of position postures** and/or **additional weight** e.g. personal protective equipment **increase injury risk** significantly.

DISCUSSION

- **Bone mineral content** (BMC) is a **dominant factor** for bone strength (Ebbesen *et al,* 1999a, Hulme *et al* 2007, Hutton *et al* 1979) and is gender and age related. (Ebbesen *et al,* 1999b, Riggs *et al* 2004).
- BMC is **currently not included** in the injury criteria.

- The force tolerance is defined with a **half sine** acceleration signal.
- What is the **significant loading part** of an applied acceleration signal? (e.g. a high double peak signal)
- The **tolerance values** may need to be **redefined** for the specific scenario.

- **Further analysis** of active controlled protective seats is required.
- **Comparison** of responses of an **ATD** and **Human body** for adequate provided protection.

CONCLUSION

- A lumbar spine model was developed using the scalable MADYMO HBM as reference for the 5^{th}, 50^{th} and 95^{th} percentile human.

- DRI is used as a reference for spinal injury risk for the 50^{th} percentile lumbar spine model.

- Force tolerance is occupant size dependent and scaled by assuming that:

  - Compressive strength of bone is not occupant size dependent
  - Compressive pressure tolerance is the same for multiple size occupants
  - Cross section area of vertebrae is mass dependent

- This is a first step in developing a 5^{th} and 95^{th} percentile spinal injury risk, based on the current STANAG 4569 injury risk criteria. Future insight into injury criteria can continue this development.

ACKNOWLEDGEMENT

- Defensie Materieel Organisatie
  Dutch Ministry of Defence

- General Dynamics
  European Land Systems – MOWAG
  - Björn Schröder
  - Hans-Jörg List


THANK YOU FOR YOUR ATTENTION
TNO innovation for life

REFERENCES

- STANAG 4569 (edition 2), protection levels for occupants of armoured vehicles, NATO Standardization Organization, December 2012
- AEP-55, Procedures for evaluating the protection level of armoured vehicles, Allied Engineering Publication 55, NATO Standardization Organization, Volume 2, Mine threat, august 2011
- Brinkley, J.W., Staffer T.S., Dynamic simulation techniques for the design of escape systems: Current applications and future air force requirements. AMRL-TR-71-29, Aerospace Medical Research Laboratory, Aerospace Medical Div. Air Force Systems Command, Wright-Patterson Airforce Base, Ohio 45433, 1971
- Ebbesen, E.N., Thomsen J.S., Beck-Nielsen H., Nepper-Rasmussen H.J., Mosekilde L., Lumbar vertebral body compressive strength evaluated Dual-Energy X-ray Absorptiometry, Quantative Computed Tomography , and Ashing, Bone, Vol. 25 No. 6, December 1999, pp 713-724
- Ebbesen E.N., Thomsen J.S., Beck-Nielsen H, Nepper-Rasmussen H.J., Mosekilde L., Age- and Gender –Related differences in vertebral body Mass, Density and Strength, JOURNAL OF BONE AND MINERAL RESEARCH, Volume 14, Number 8, 1999, Blackwell Science, Inc.© 1999 American Society for Bone and Mineral Research
- Happee R., Hoofman H., van den Kroonenberg A.J., Morsink P., Wismans J. A mathemathical Human Body Modle for Frontal and rearward seated automotive impact loading, SAE 983150, 42th Stapp Car Crash Conference, (P-337), 1998, SAE 400 Commonwealth Drive, Warrendale, PA 15096-0001 USA
- Happee R.J., Ridella S., Nayef A., de lange R., Morsink P., Bours R., van Hoof J., Mathematical human body models representing a midsize male and a small female for frontal, lateral and rearward impact loading, IRCOBI Conference, 2000
- Hulme P.A., Boyd S.K., Ferguson S.J., Regional variation in vertebral bone morphology and its contribution to vertebral fracture strength. Bone 41, 2007

REFERENCES

- Hutton W.C., Cyron B. M. and Stott J.R., The compressive strength of lumbar vertebrae, J. Anat. (1979), 129, 4, pp. 753-758 753
- De Lange R., van Rooij, L., Mooi, H., Wismans, J., Objective Biofidelity Rating of a Numerical Human Occupant Model in Frontal to Lateral Impact, Stapp Car Crash Journal, Vol. 49, November 2005
- Riggs B.L., Melton L.J. 3rd, Robb R.A., Camp J.J., Atkinson E.J., Peterson J.M., Rouleau P.A., McCollough C.H., Bouxsein M.L., Khosla S., Population-based study of age and sex differences in bone volumetric density, size, geometry, and structure at different skeletal sites. J Bone Miner Res. 2004 Dec; 19(12):1945-54.
- Rodarius, C.,van Rooij, L., de Lange, R., Scalability of human models, The Proceedings of the 20th International Technical Conference on the Enhanced Safety of Vehicles (ESV), Lyon, France (2007)
- Stemper BD, Baisden JL, Yoganandan N, et al. Effect of loading rate on injury patterns during high rate vertical acceleration, *Proceedings of IRCOBI Conference*, 2012, Dublin, Ireland
- Thyagarajan R., Ramalingam J., Kulkarni K.B., Comparing the Use of Dynamic Response Index (DRI) and Lumbar Load as Relevant Spinal Injury Metrics, ARL Workshop on Numerical Analysis of Human and Surrogate Response to Accelerative Loading, Jan 09 201409
- Yoganandan N., Arun M.W.J., Stemper B.D., Pintar F.A., Maiman D.J., Biomechanics of Human Thoracolumbar Spinal Column Trauma from Vertical Impact Loading, Annals of Advances in Automotive Medicine, 57th AAAM Annual Conference, September 22-25, 2013
- Zhang N., Zhao J., Study of compression-related lumbar spine fracture criteria using a full body FE human model, 2013

An Objective Evaluation of Mass Scaling Techniques Utilizing Computational Human Body Models

Matthew Davis, F. Scott Gayzik

2nd Workshop on Numerical Analysis of Human and Surrogate Response to Accelerative Loading,

January 14, 2016, Aberdeen Proving Ground, MD

Center for Injury Biomechanics

Wake Forest School of Medicine

Virginia Tech
Wake Forest University
School of Biomedical Engineering and Sciences

Introduction

- In biomechanics, we frequently encounter the need to scale
- **Experimentalist:** Diverse specimens are typically scaled to a target mass for corridor development

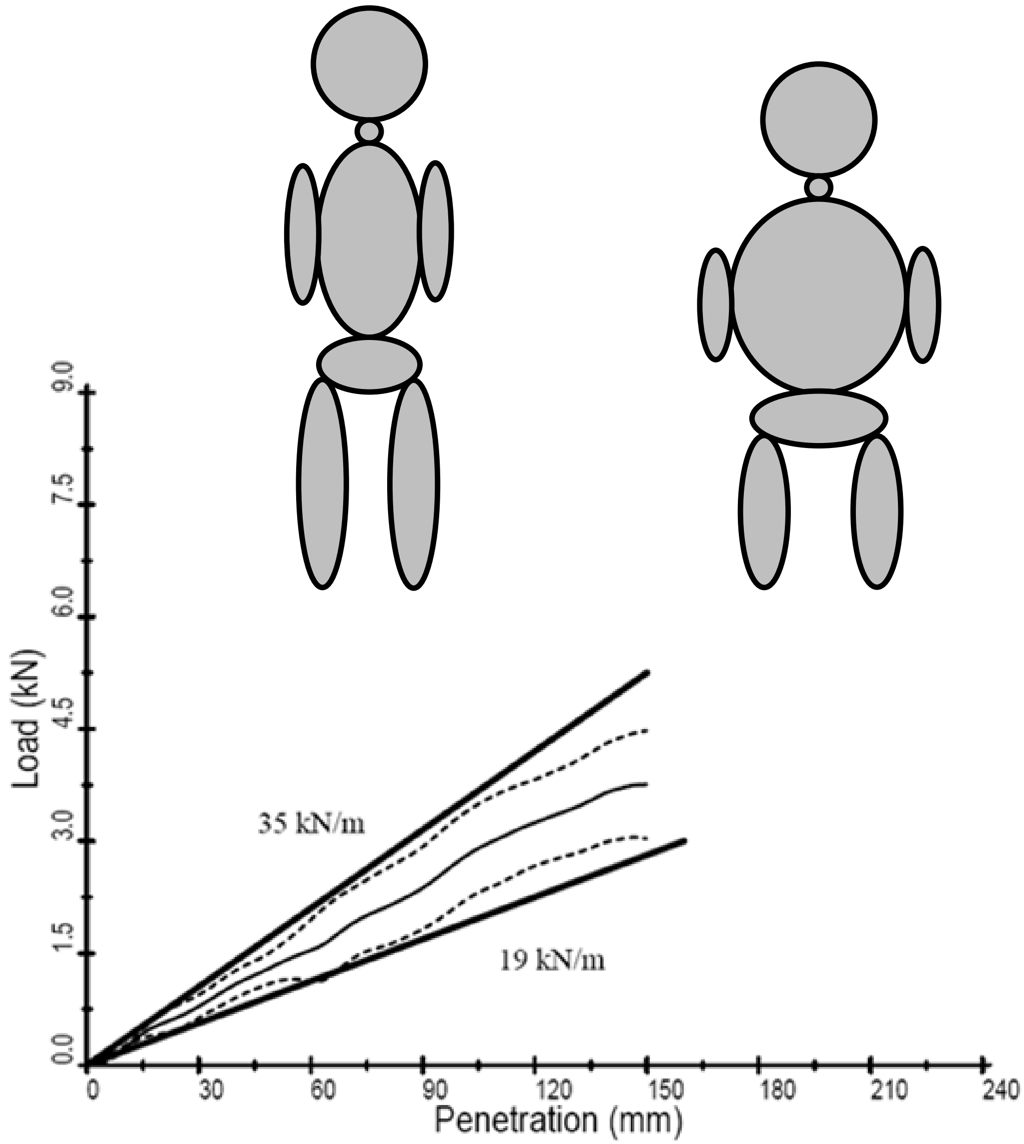

Hardy et al., 2001

Introduction

- In biomechanics, we frequently encounter the need to scale
- **Experimentalist:** Diverse specimens are typically scaled to a target mass for corridor development
- **Modeling:** This works well if your model represents an average male, but can be a challenge for validating models of varying anthropometry

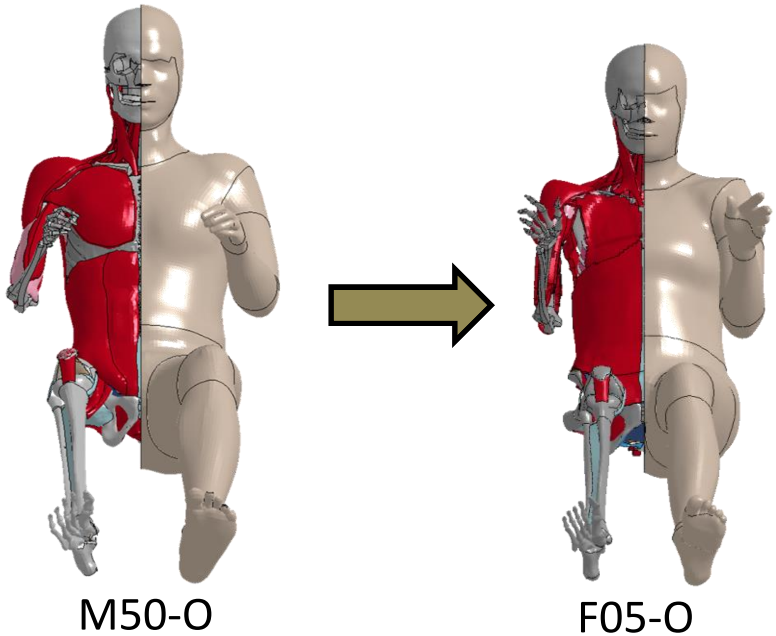

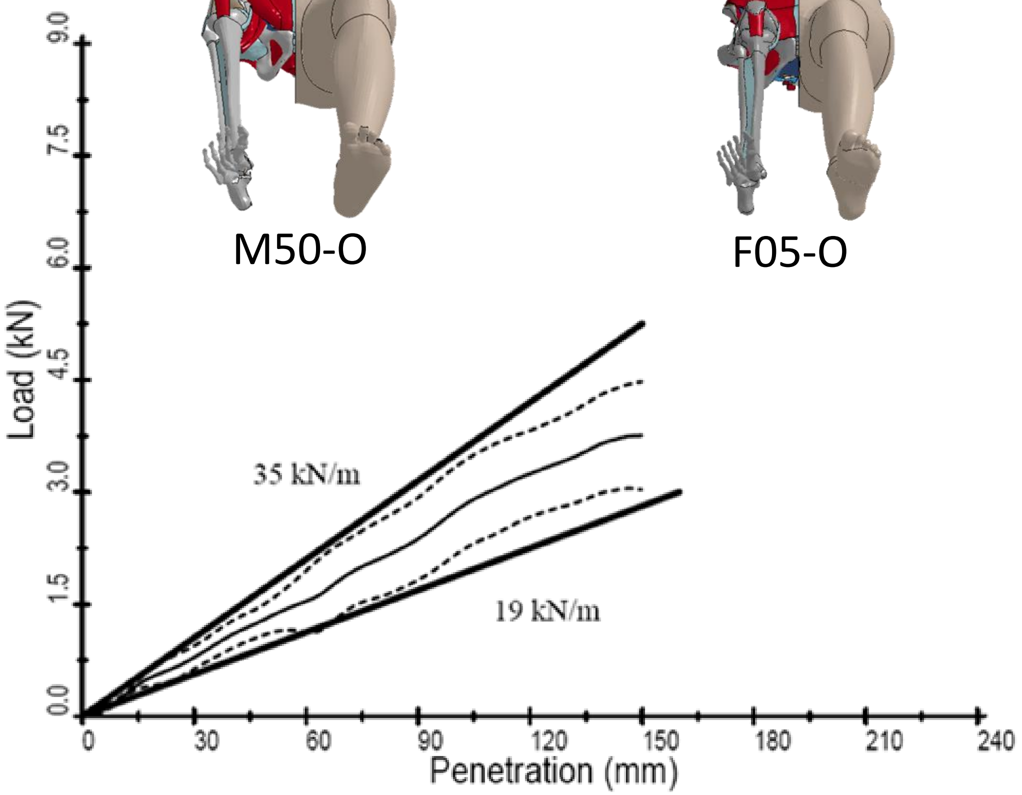

Hardy et al., 2001

Objective

- The goal of this study is to objectively evaluate several mass scaling techniques
- Determine which is the most effective at scaling response data from a reference to a target using quantitative comparison techniques

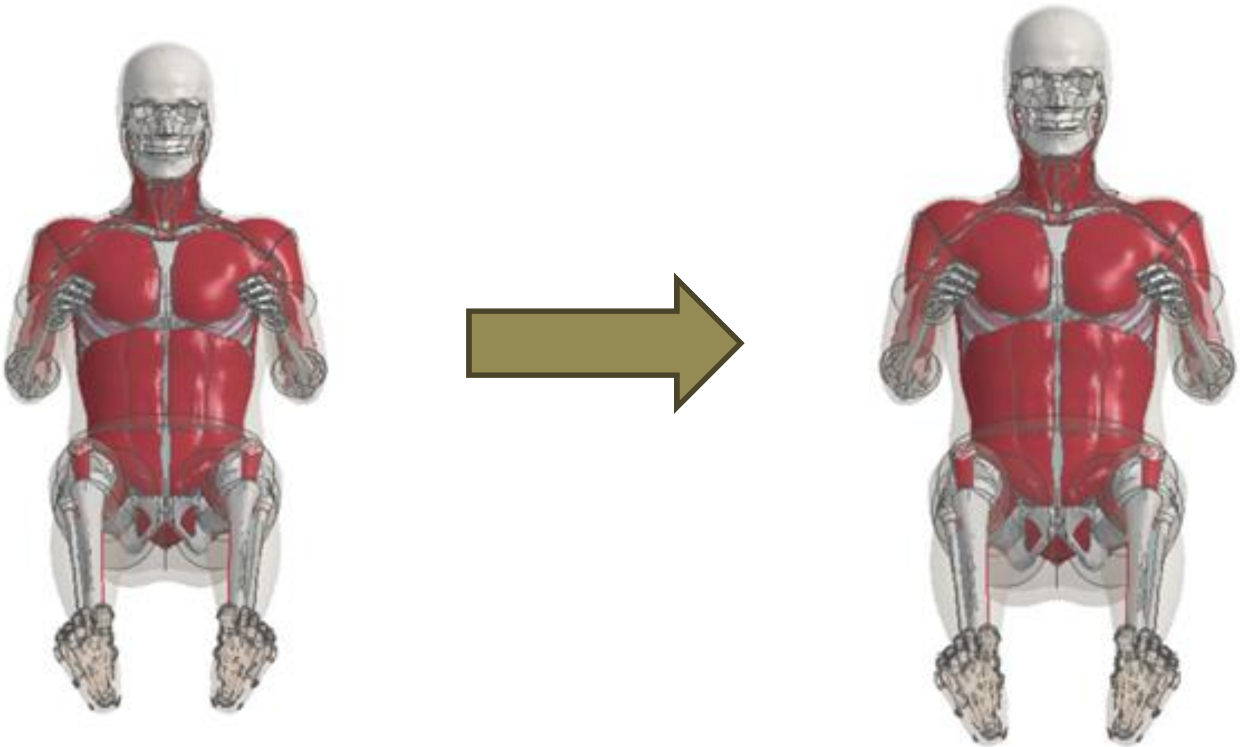

Why Use Models to Evaluate Scaling?

Small female

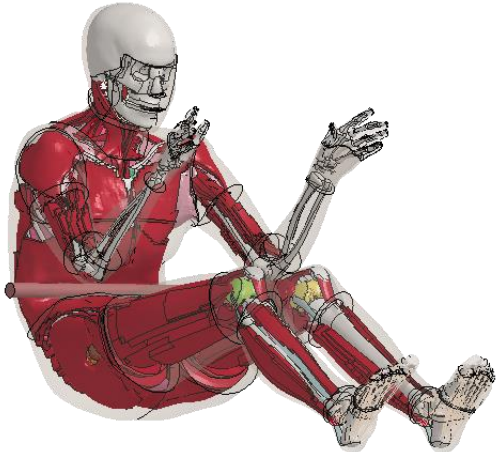

Data Scale

Average male

Scaling is the process by which a response can be transformed from one standard to another

Techniques / Assumptions

- Scaling Methods
  - Mass Scaling
    - Geometric Similitude
    - Equal Modulus
  - Impulse Momentum
    - Geometric Similitude
    - Equal Modulus

Why Use Models to Evaluate Scaling?

- **Review of the 2 main scaling techniques**
  - Equal-Stress Equal-Velocity
  - Impulse-Momentum
- **Three models were simulated**
  - GHBMC M50 v4.3
  - GHBMC M50 v4.3 scaled to F05 mass
  - GHBMC M50 v4.3 scaled to M95 mass
- **Evaluate performance using ISO/TS 18571 Standard**

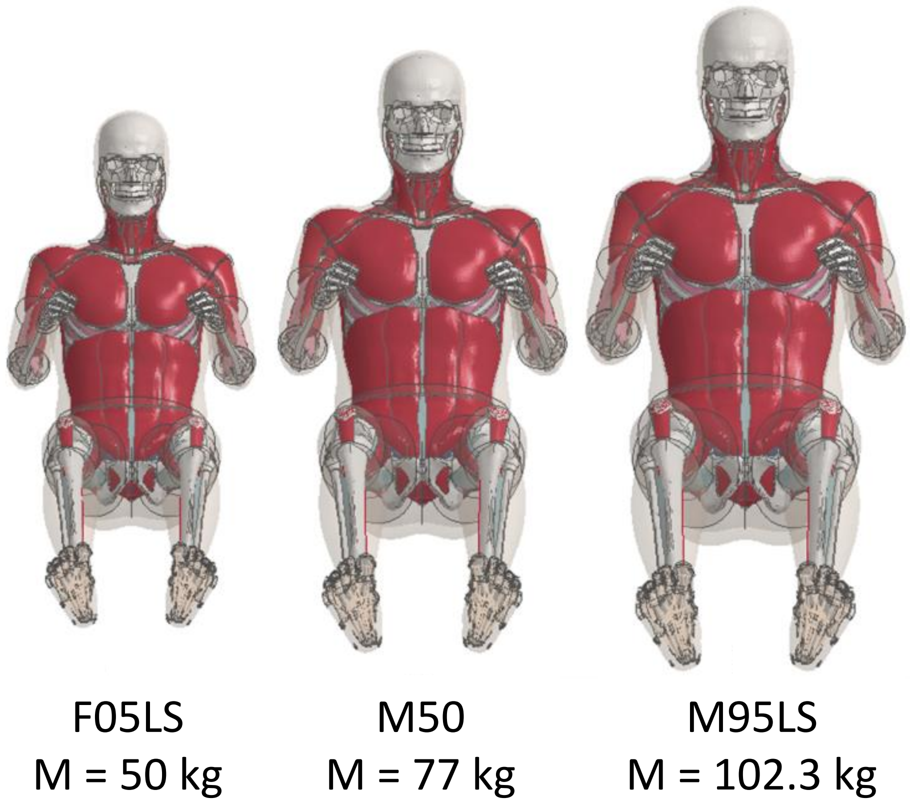

Simulations – Rigid Impactors

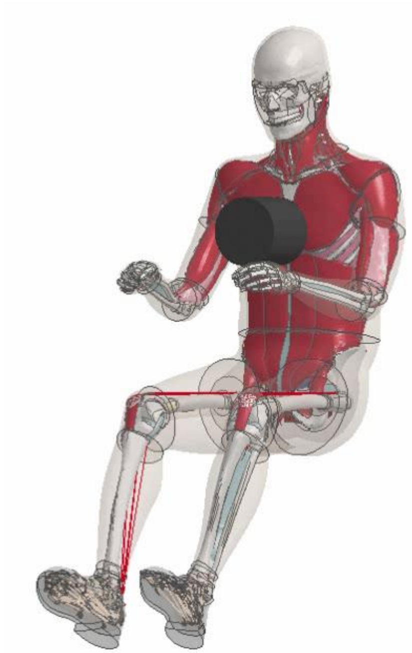

- Rigid impactor: 23.4 kg
- Impact Velocity: 6.7 m/s
- Simulation time: 60 ms

- Rigid impactor: 49 kg
- Impact Velocity: 6.0 m/s
- Simulation time: 100 ms

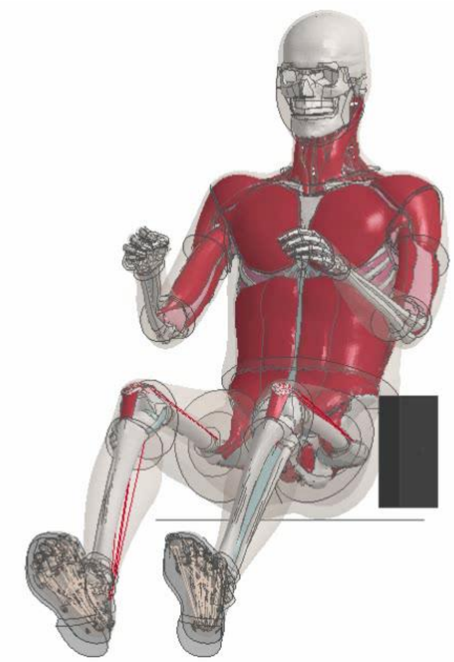

- Rigid impactor: 16 kg
- Impact Velocity: 10 m/s
- Simulation time: 40 ms

Simulations – Infinite Mass (Whole Body)

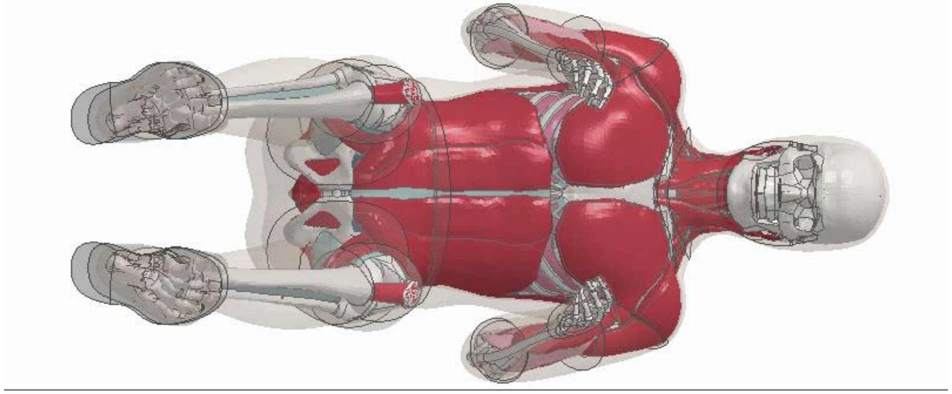

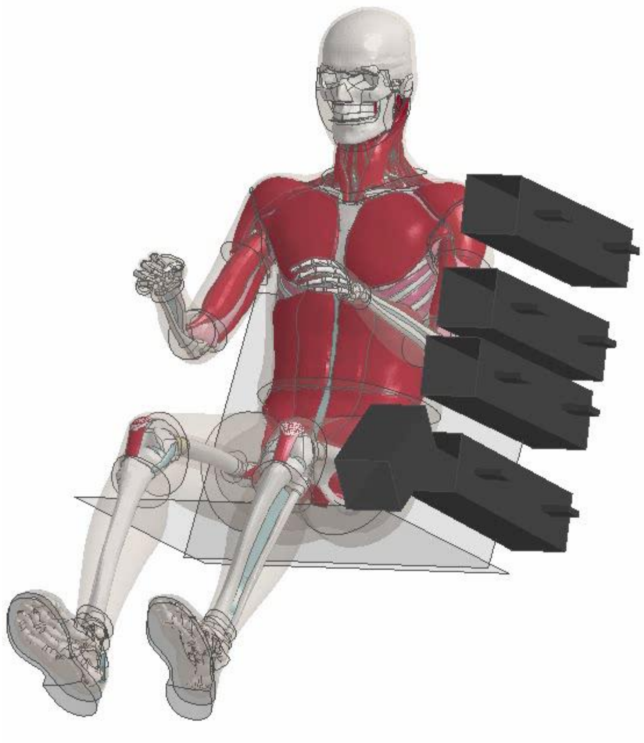

- Drop from 1 m onto instrumented floor
- Impact Velocity: 4.4 m/s
- Simulation time: 80 ms

- Lateral sled into fixed steel plates
- Impact Velocity: 6.7 m/s
- Simulation time: 80 ms

Equal Stress Equal Velocity

Required Data:
Full body mass of all subjects

- Scaling technique based purely on a mass ratio of the full body masses
- Assumes linear relationships between length, mass and time
- Assumes identical density and elastic modulus

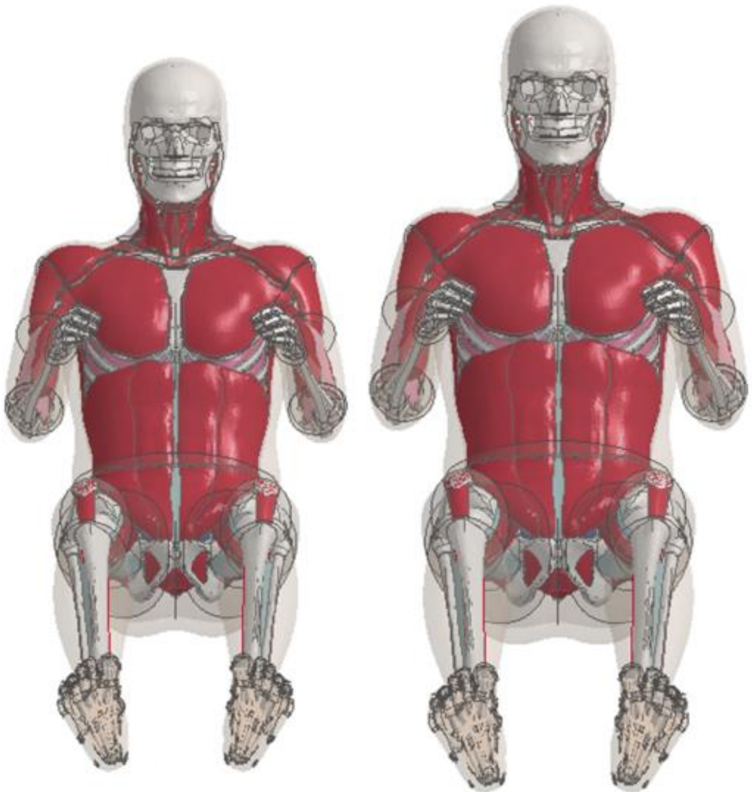

M50
M = 77 kg

M95R
M = 102.3 kg

$$\lambda = \frac{M_{M95}}{M_{M50}}$$

$Time\ Scale\ Factor = \lambda^{\frac{1}{3}}$
$Deflection\ Scale\ Factor = \lambda^{\frac{1}{3}}$
$Acceleration\ Scale\ Factor = \lambda^{\frac{-1}{3}}$
$Force\ Scale\ Factor = \lambda^{\frac{2}{3}}$
$Moment\ Scale\ Factor = \lambda$

Eppinger et al. (1976)

Impulse Momentum

Technique for accommodating specific body region characteristics of the impact test

Required Data:
- Force-Time Histories

Assumptions:
- Constant Modulus
- Geometric Similitude

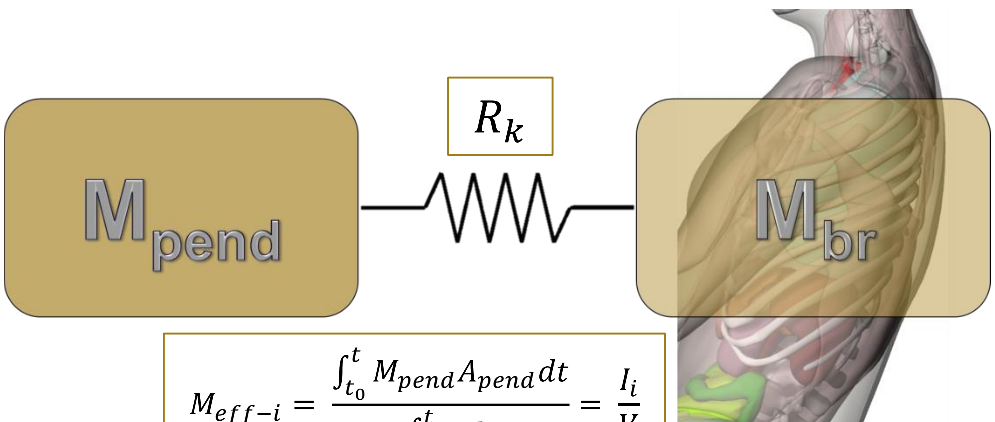

$$M_{eff-i} = \frac{\int_{t_0}^{t} M_{pend} A_{pend}\, dt}{\int_{t_0}^{t} A dt} = \frac{I_i}{V}$$

$$\text{Time Scale Factor} = \sqrt{\frac{R_m}{R_k} * \frac{M_{pend} + M_{\text{eff}-ref}}{M_{pend} + M_{\text{eff}-target}}}$$

$$\text{Deflection Scale Factor} = \sqrt{\frac{R_m}{R_k} * \frac{M_{pend} + M_{\text{eff}-ref}}{M_{pend} + M_{\text{eff}-target}}}$$

$$\text{Acceleration Scale Factor} = \sqrt{\frac{R_k}{R_m} * \frac{M_{pend} + M_{\text{eff}-ref}}{M_{pend} + M_{\text{eff}-target}}}$$

$$\text{Force Scale Factor} = \sqrt{R_m * R_k * \frac{M_{pend} + M_{\text{eff}-ref}}{M_{pend} + M_{\text{eff}-target}}}$$

Mertz (1984), Viano (1989)

Impulse Momentum- Stiffness Ratio

Characteristic Length	Cubed Root of Effective Mass	Effective Stiffness

Characteristic Length

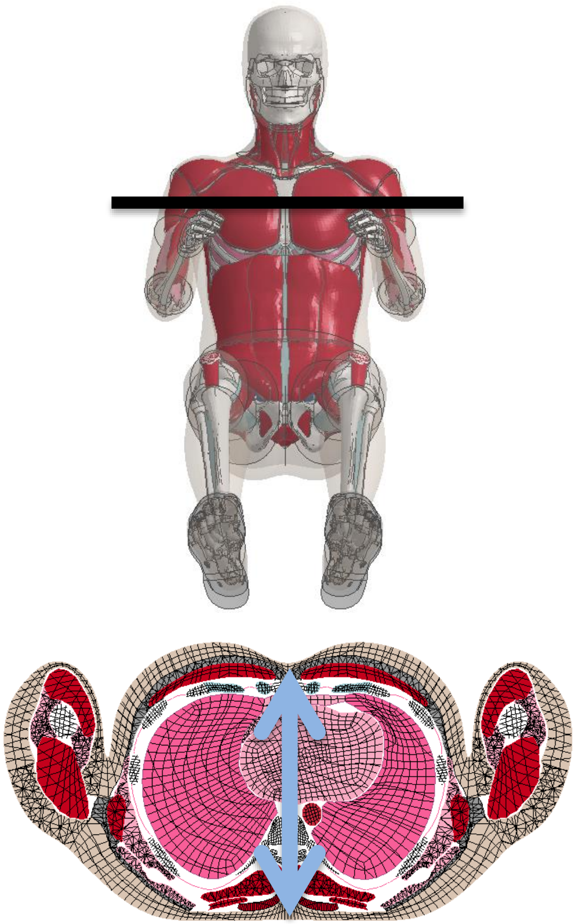

Cubed Root of Effective Mass

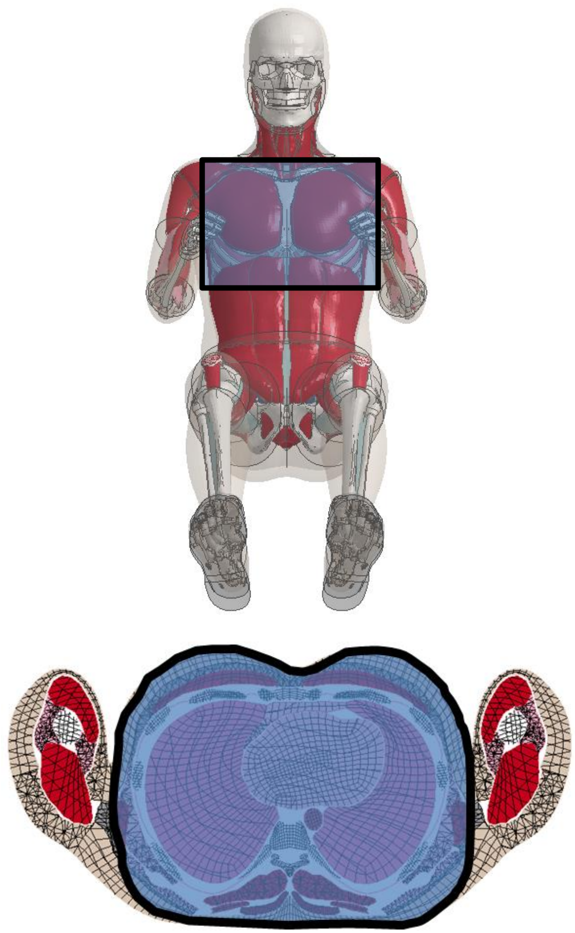

Effective Stiffness

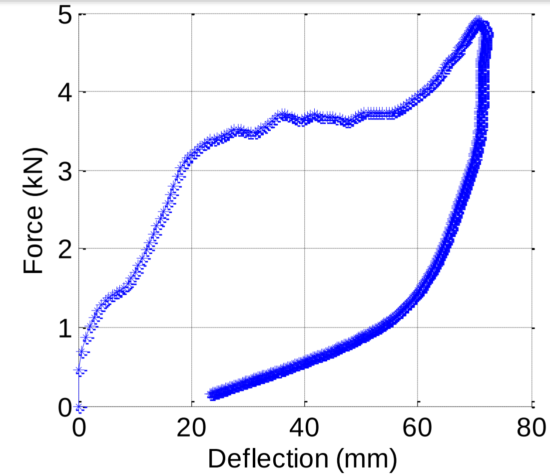

$$K_{eff} = \frac{2\int_{t_0}^{t} F\,dx}{xmax^2}$$

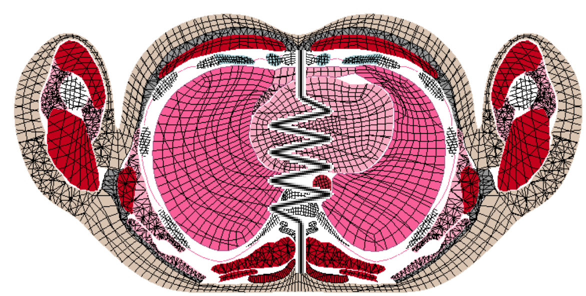

Moorhouse (2013)

Variation: ESEV + Effective Mass

Develop a mass ratio based on effective mass which takes physiological variation across specimens that is not included in a full body mass ratio into account

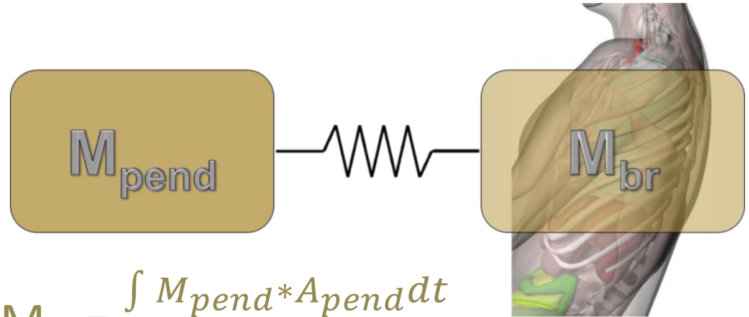

$$M_{eff} = \frac{\int M_{pend} * A_{pend}\,dt}{\int A\,dt}$$

$$\lambda = \frac{M_{eff-target}}{M_{eff-ref}}$$

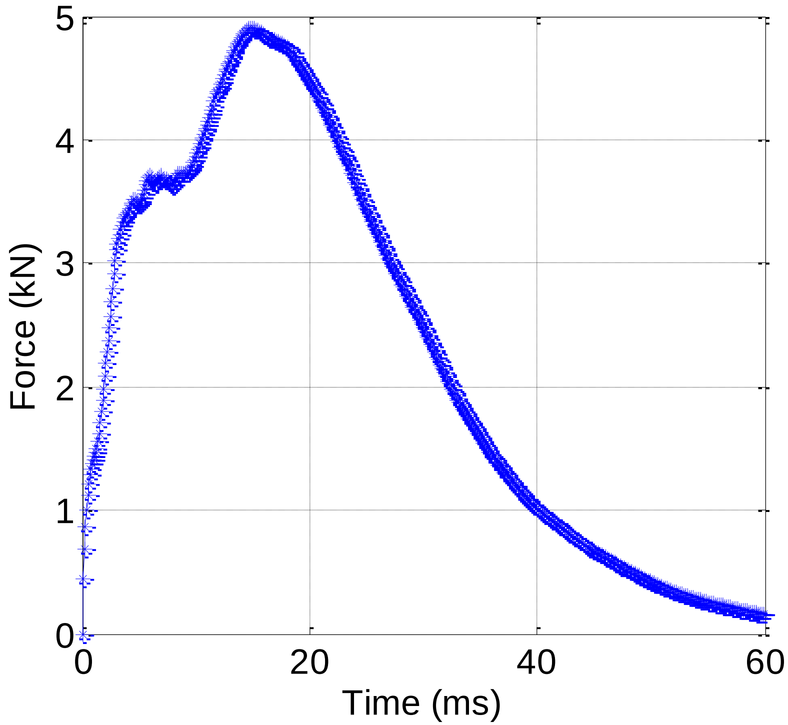

Time Scale Factor $= \lambda^{\frac{1}{3}}$
Deflection Scale Factor $= \lambda^{\frac{1}{3}}$
Acceleration Scale Factor $= \lambda^{\frac{-1}{3}}$
Force Scale Factor $= \lambda^{\frac{2}{3}}$
Moment Scale Factor $= \lambda$

Variation: ESEV + Kinetic Energy

Using force and deflection response data to relate the net work done to the FBM to the change in kinetic energy within the FBM

$$\Delta\left(\frac{1}{2}mv^2\right) = \int Fdx$$

$$M = \frac{2*\int Fdx}{\Delta V^2}$$

$$\lambda = \frac{M_{target}}{M_{ref}}$$

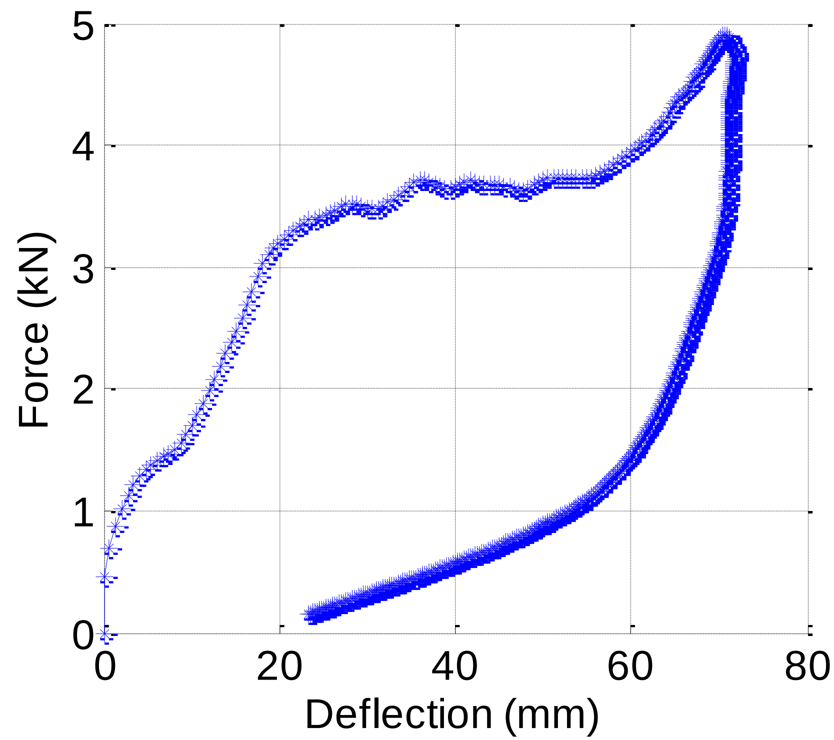

Time Scale Factor $= \lambda^{\frac{1}{3}}$
Deflection Scale Factor $= \lambda^{\frac{1}{3}}$
Acceleration Scale Factor $= \lambda^{\frac{-1}{3}}$
Force Scale Factor $= \lambda^{\frac{2}{3}}$
Moment Scale Factor $= \lambda$

Data Scaling

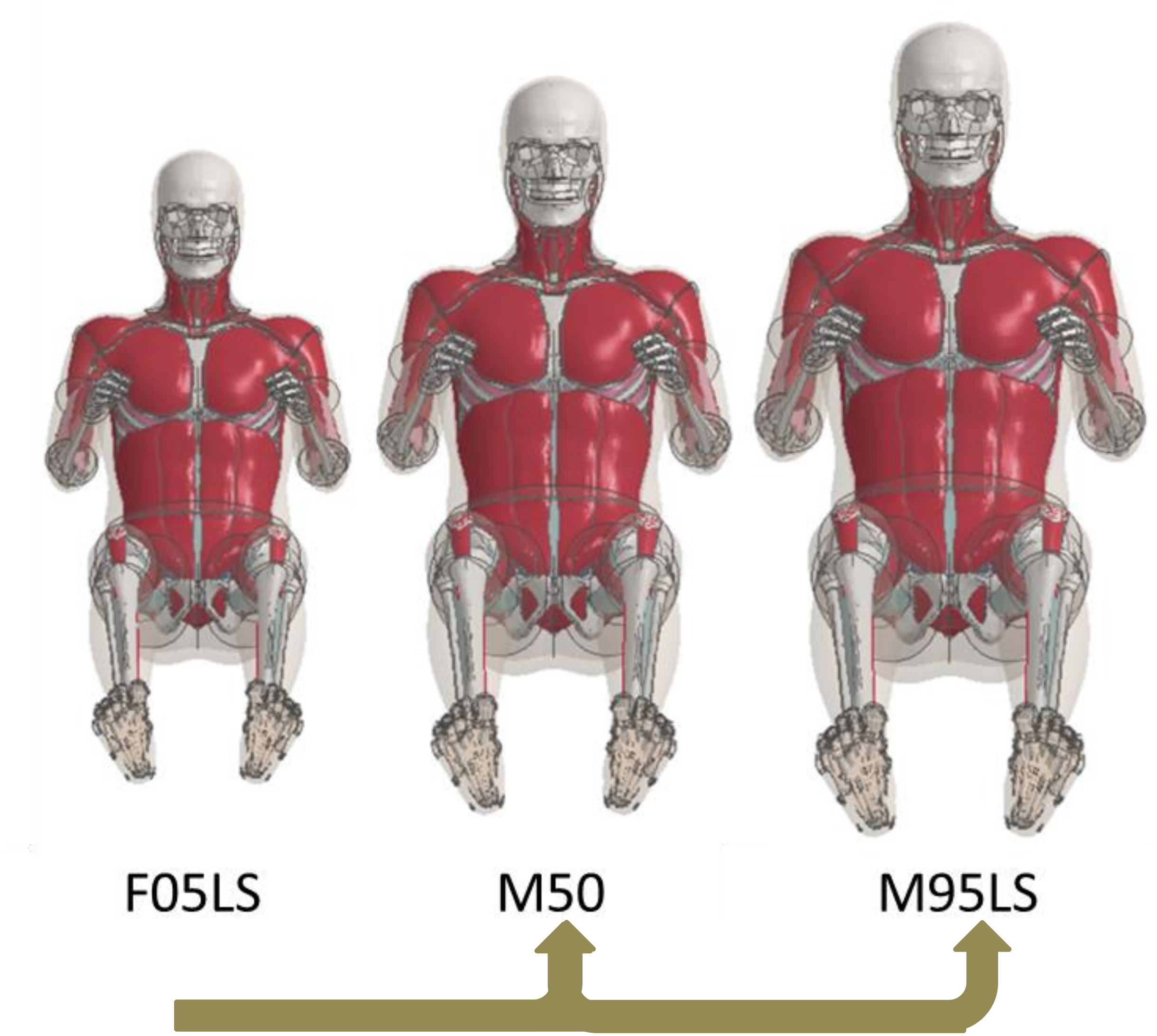

Results – Unmodified Impactors

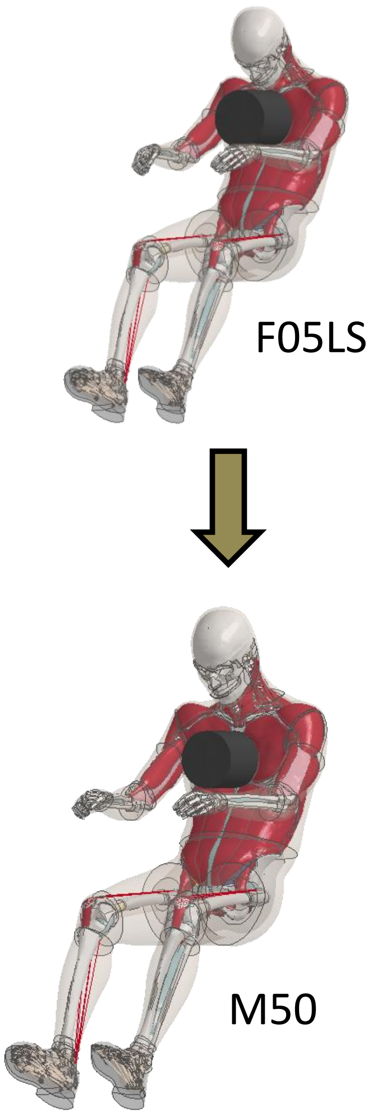

Example: Frontal Chest Impact Scaling F05LS to M50

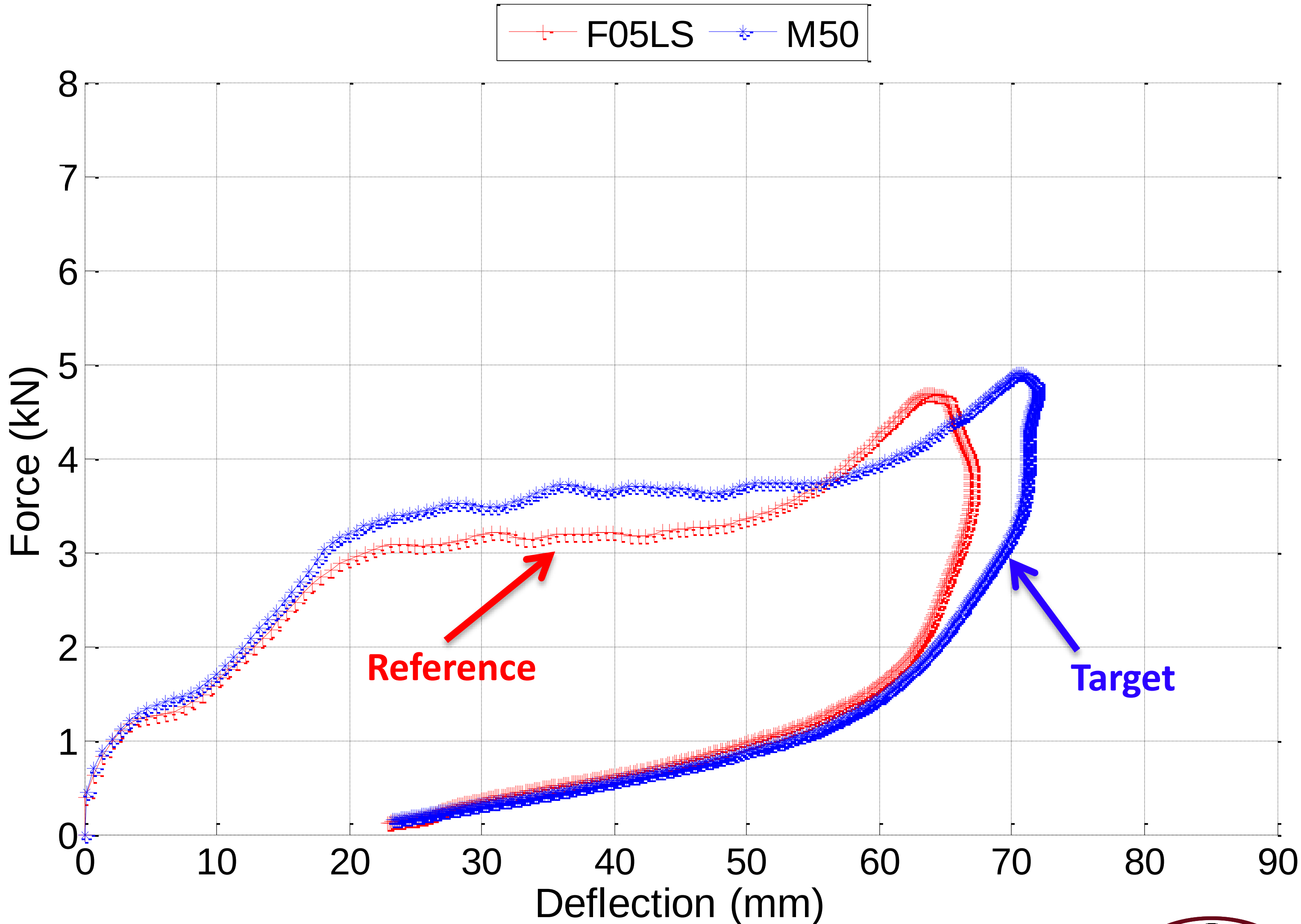

Results: Equal Stress Equal Velocity

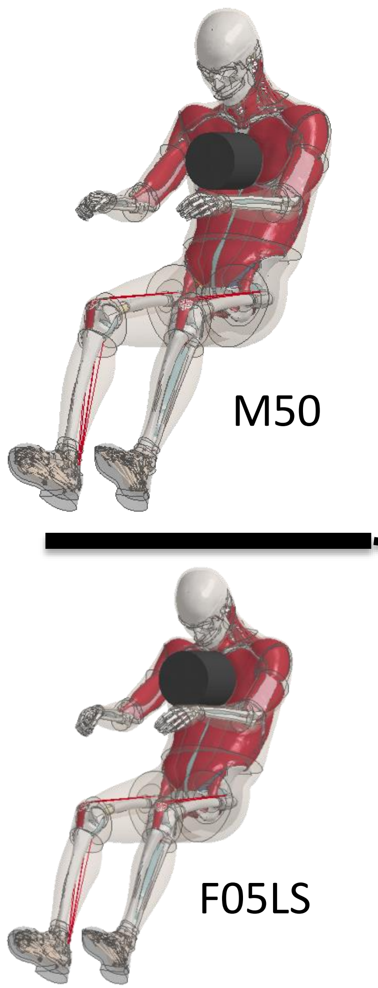

Example: Frontal Chest Impact Scaling F05LS to M50

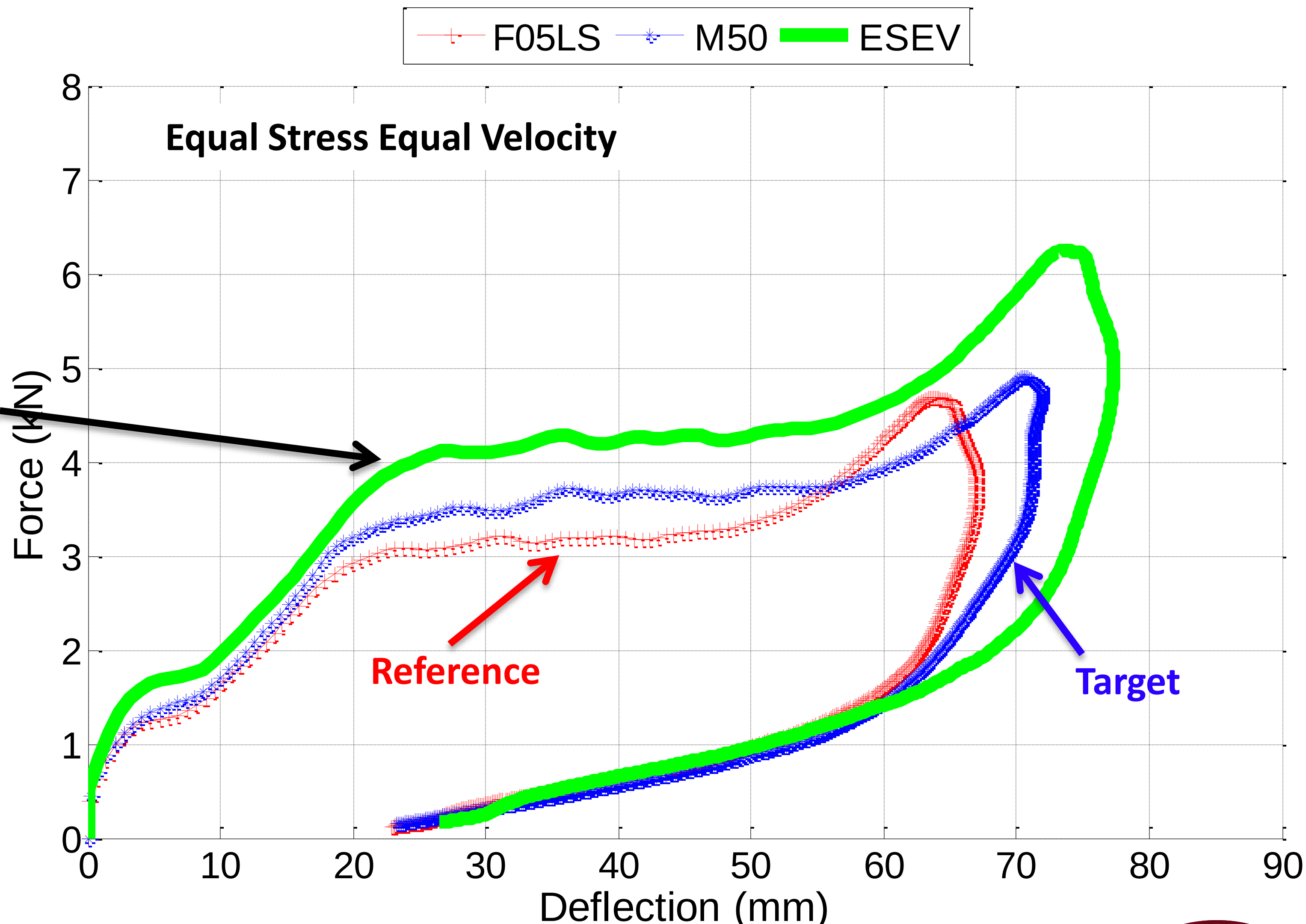

Wake Forest
School of Medicine

Results: Impulse Momentum

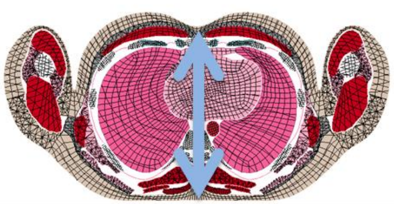

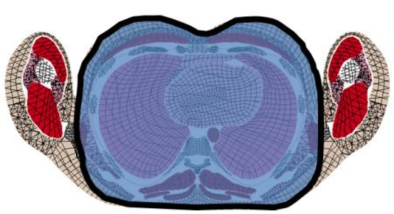

Example: Frontal Chest Impact Scaling F05LS to M50

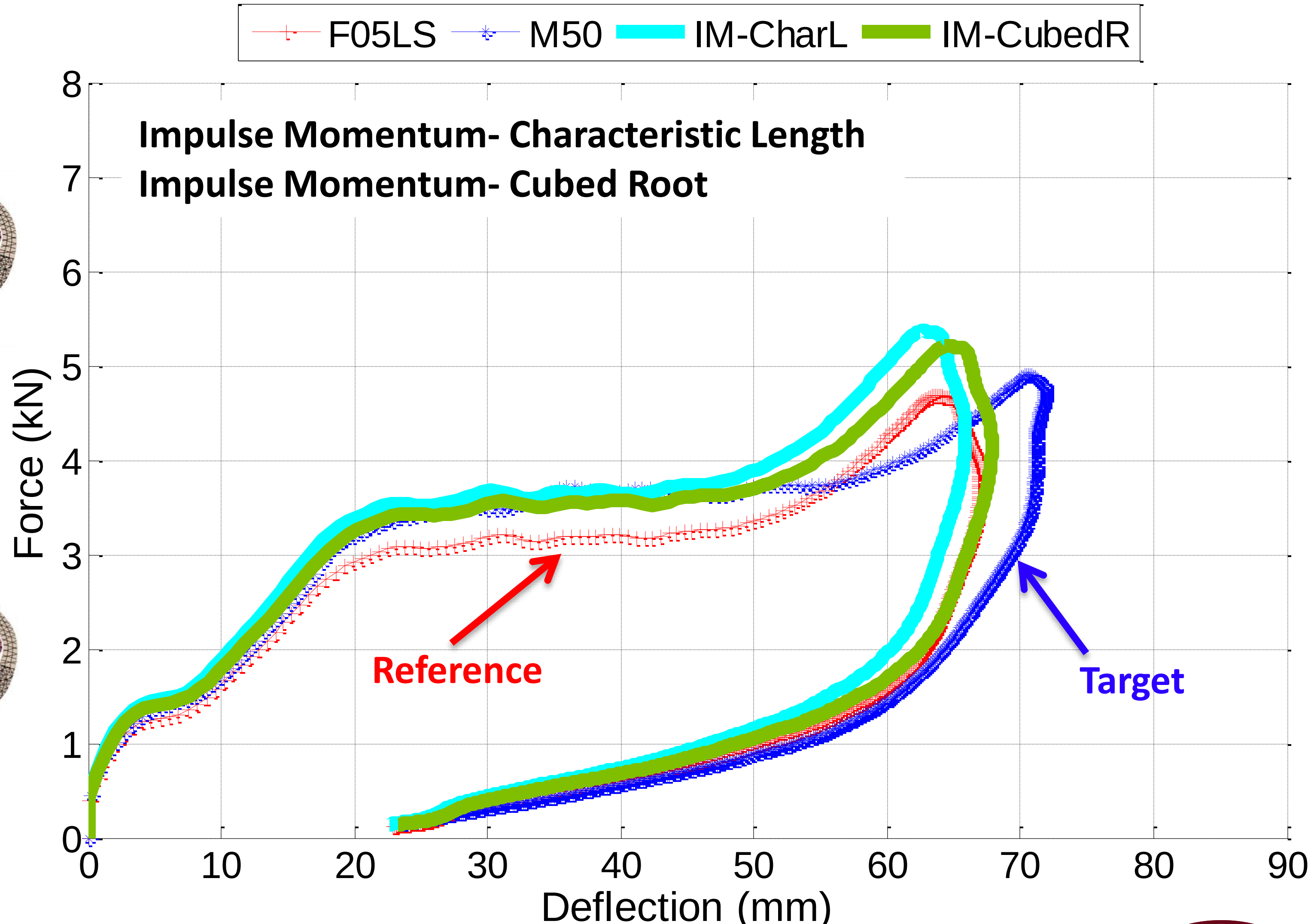

Results: Impulse Momentum

Example: Frontal Chest Impact Scaling F05LS to M50

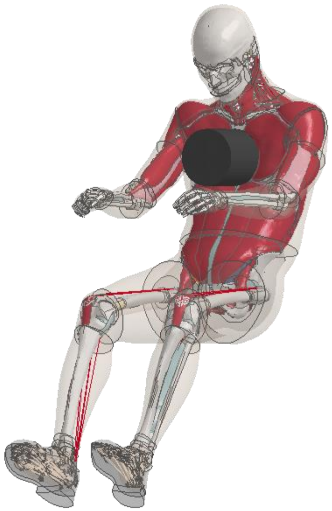

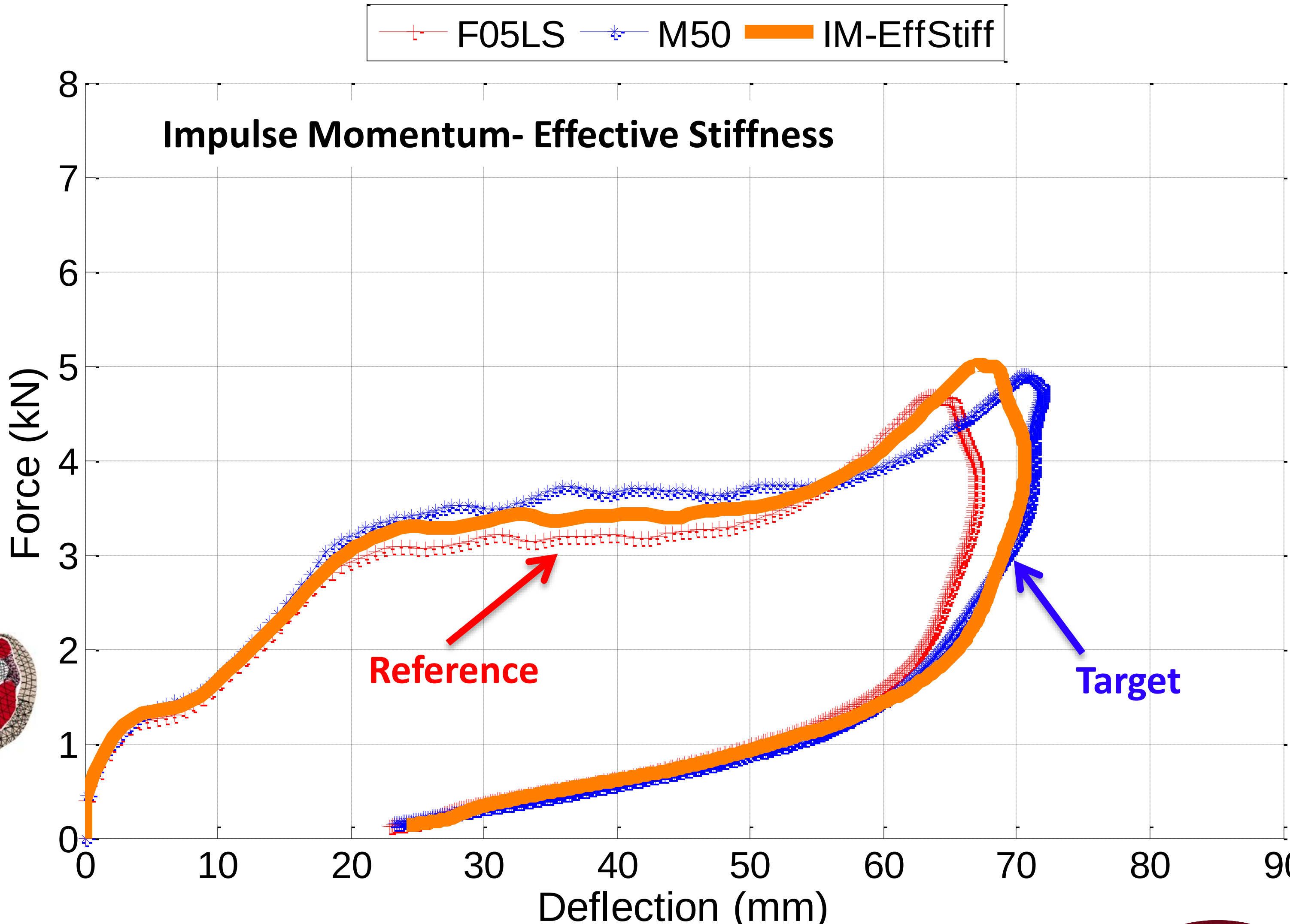

Results: ESEV Variations

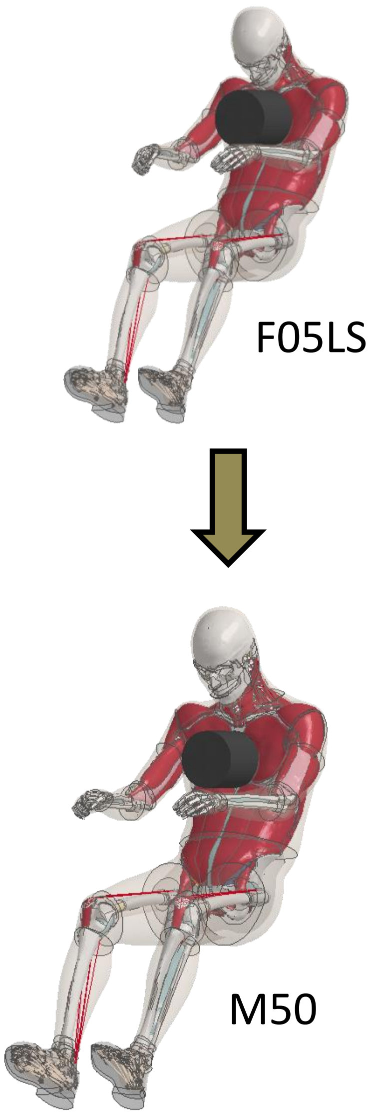

Example: Frontal Chest Impact Scaling F05LS to M50

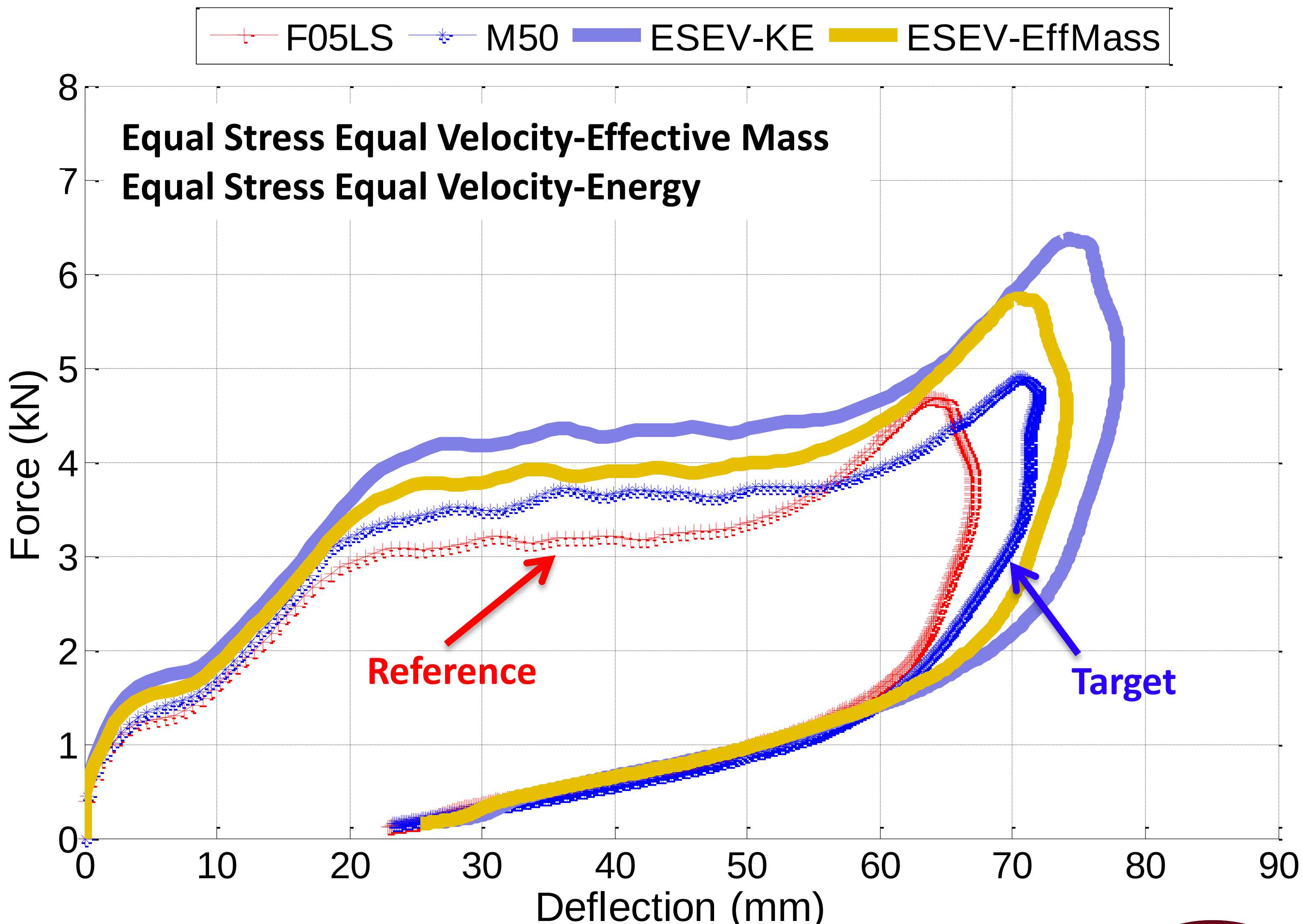

ISO/TS 18571 Standard

Standard regarding **objective rating metrics for dynamic systems**

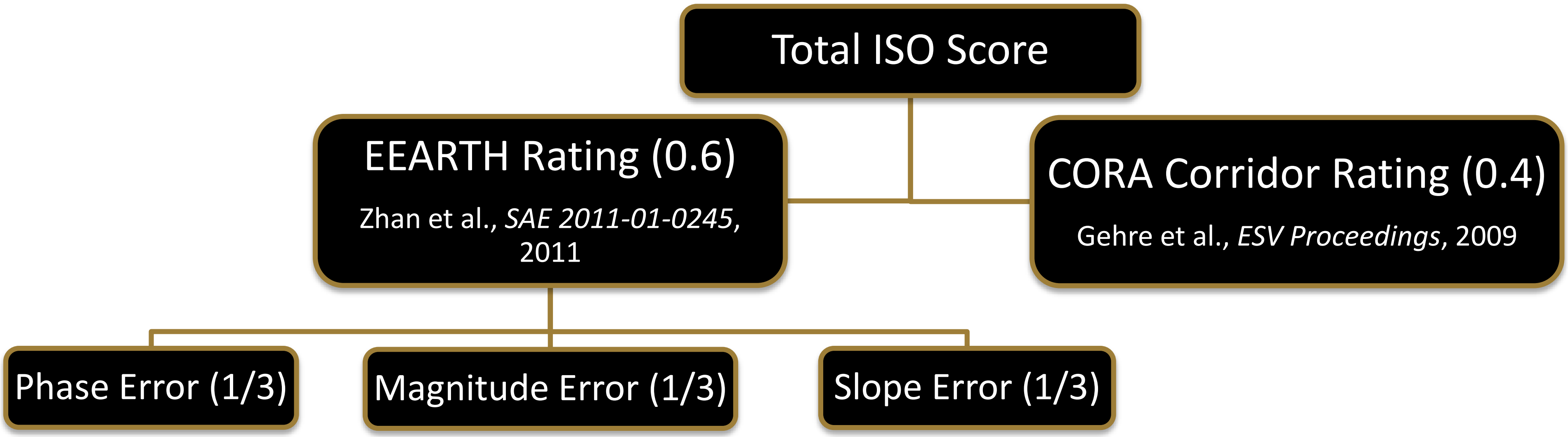

Recreated from ISO/TR 16250, Fig. 10-1

ISO-Results: Unmodified Impactors

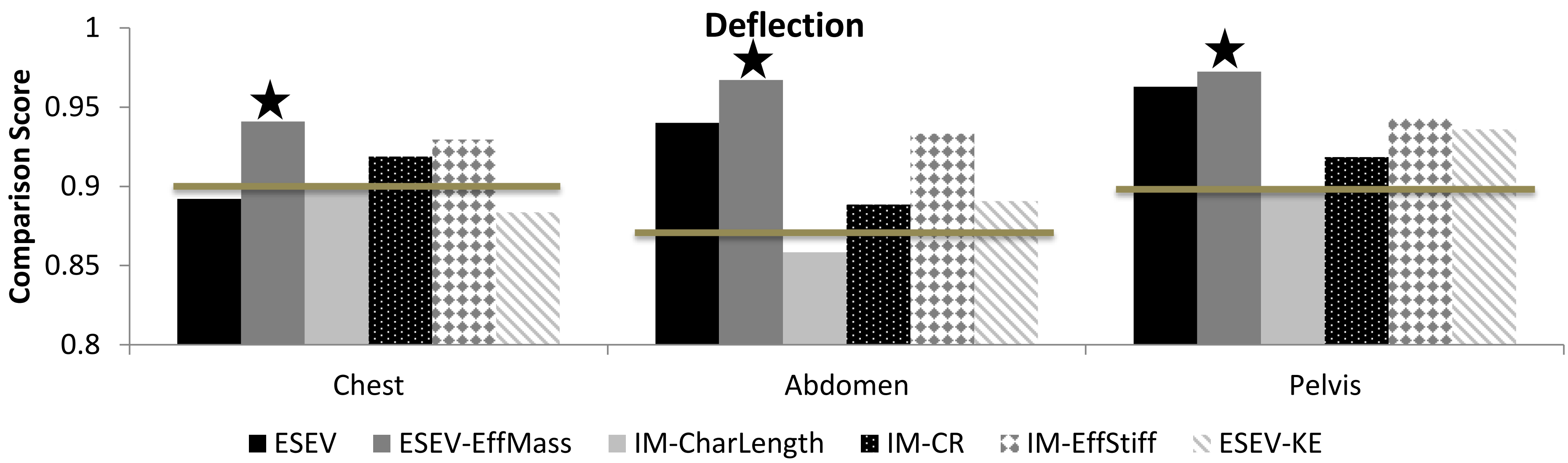

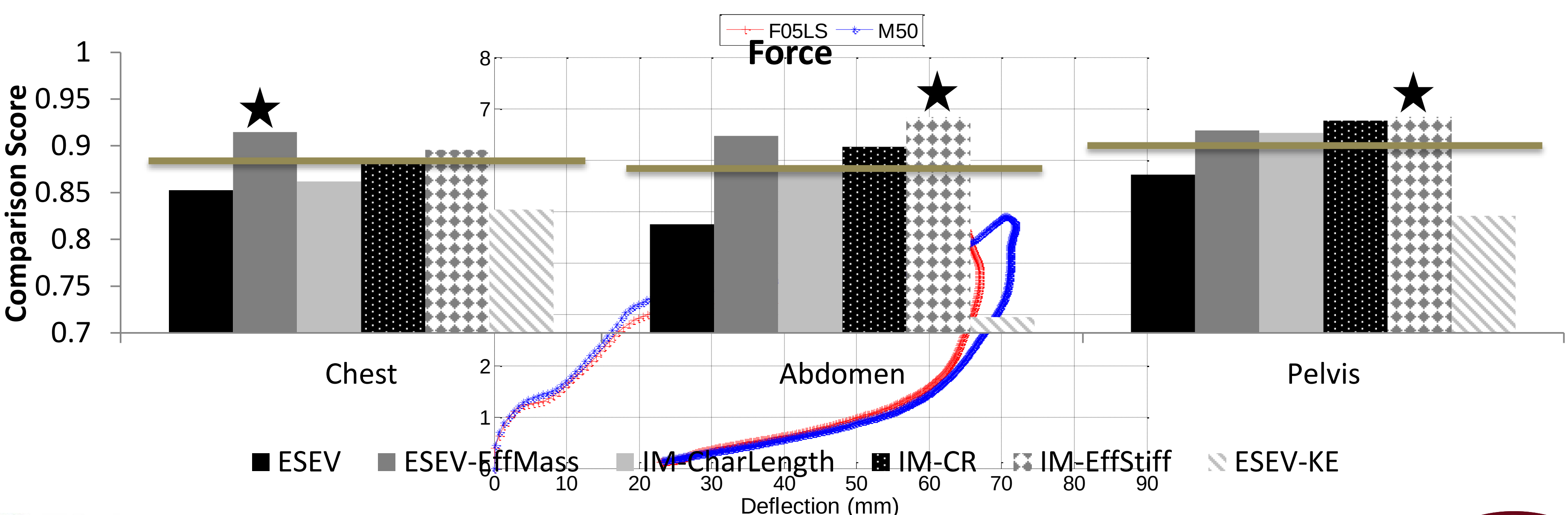

ISO-Results: Unmodified Impactors

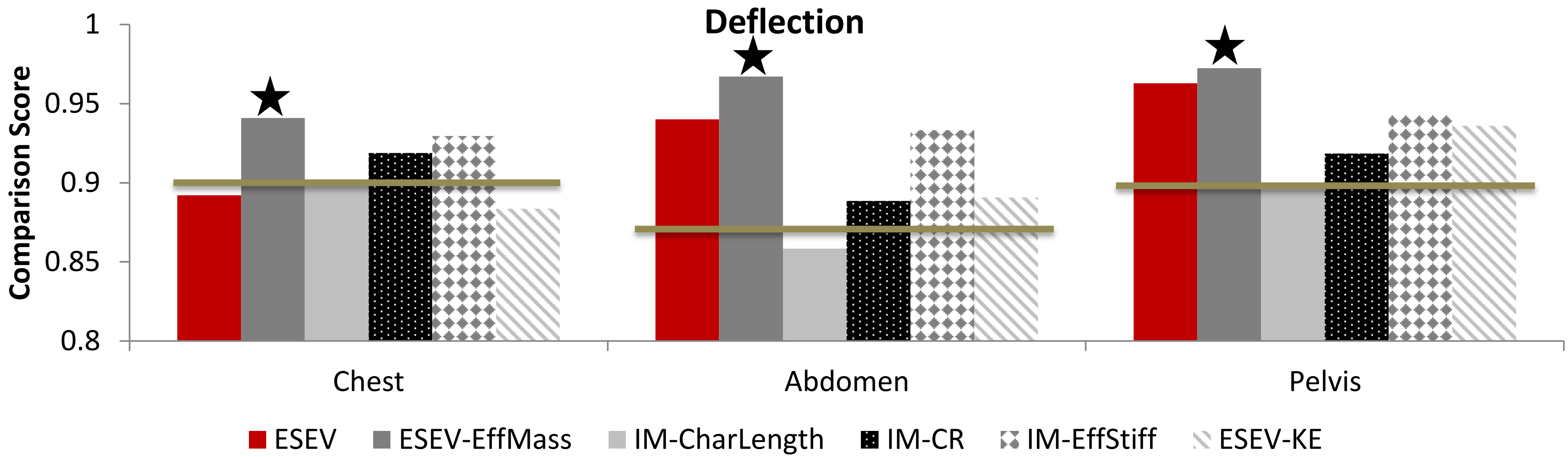

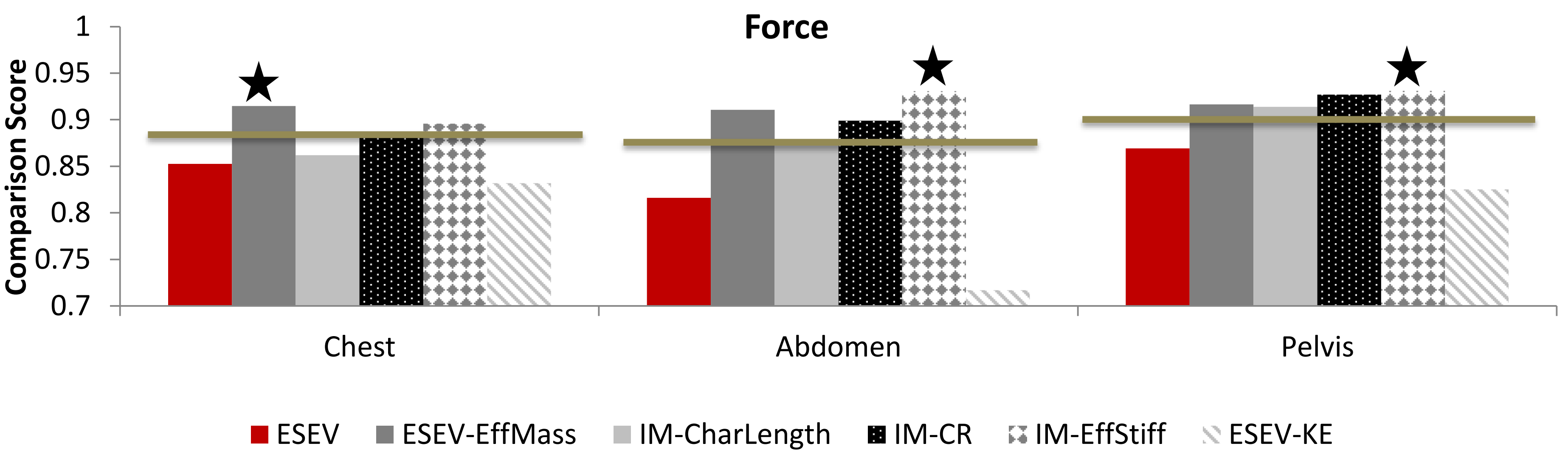

ISO-Results: Morphed Impactors

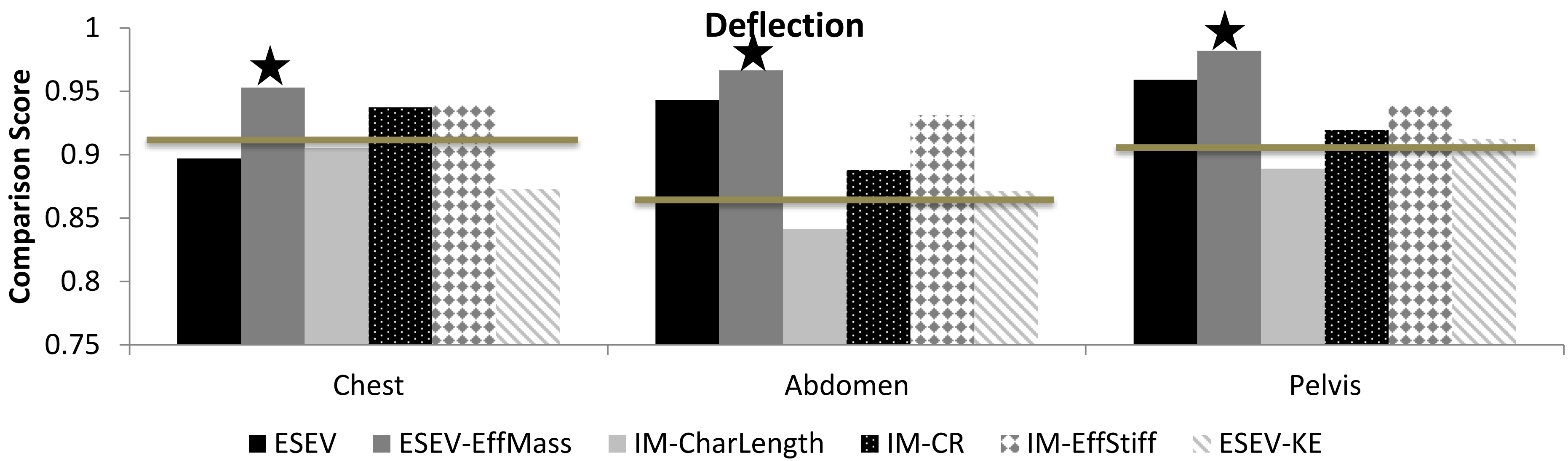

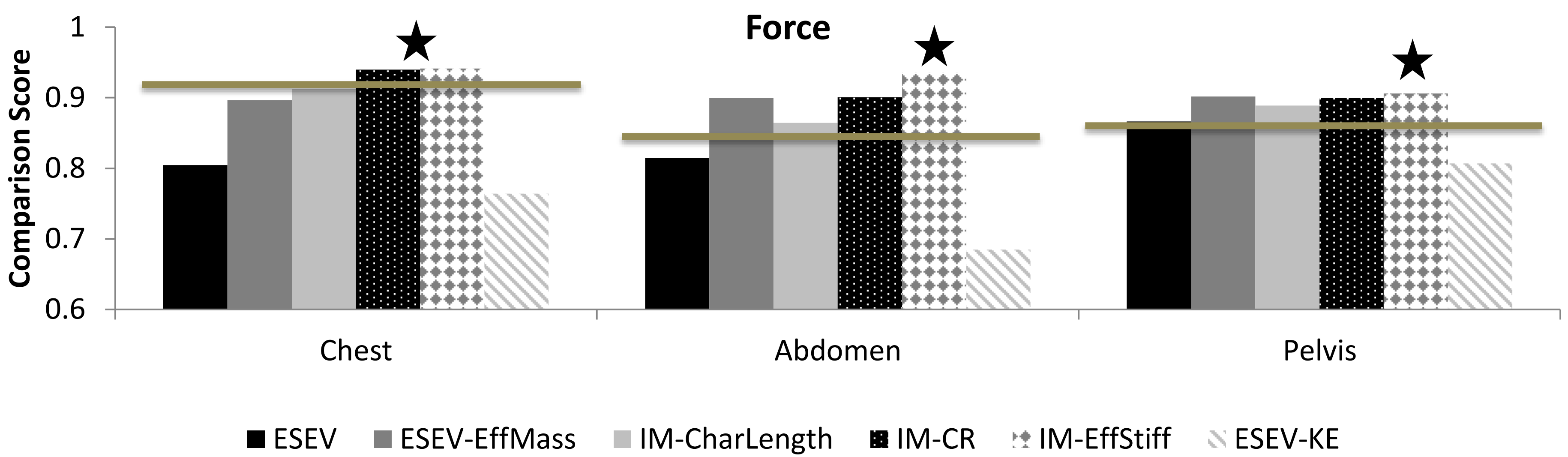

ISO-Results: Impacts with Infinite Mass

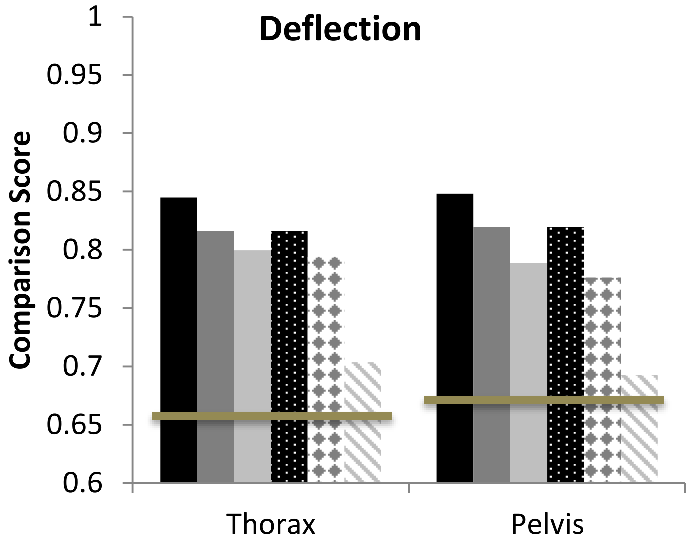

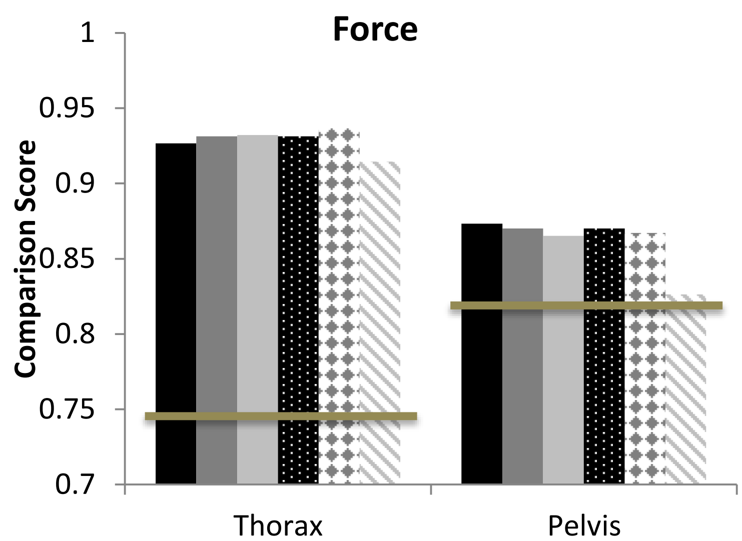

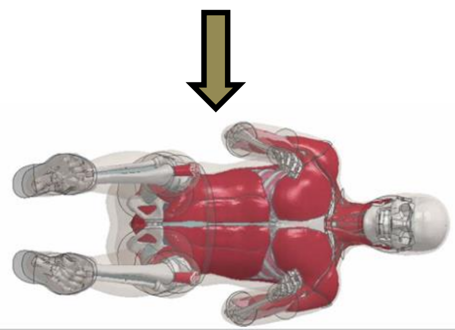

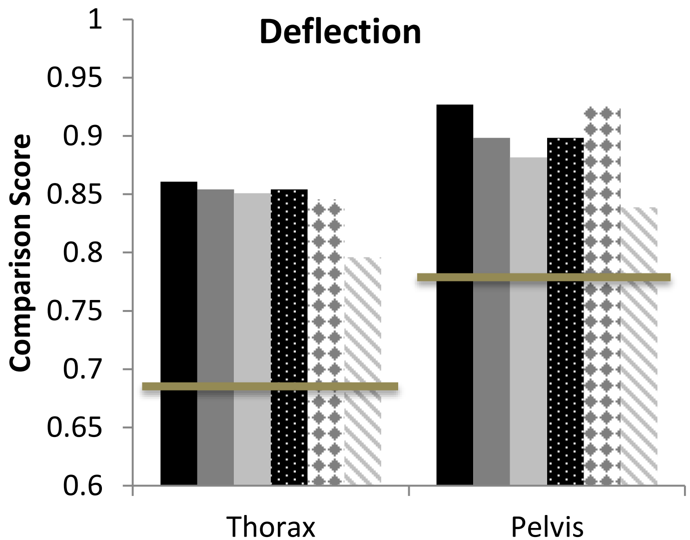

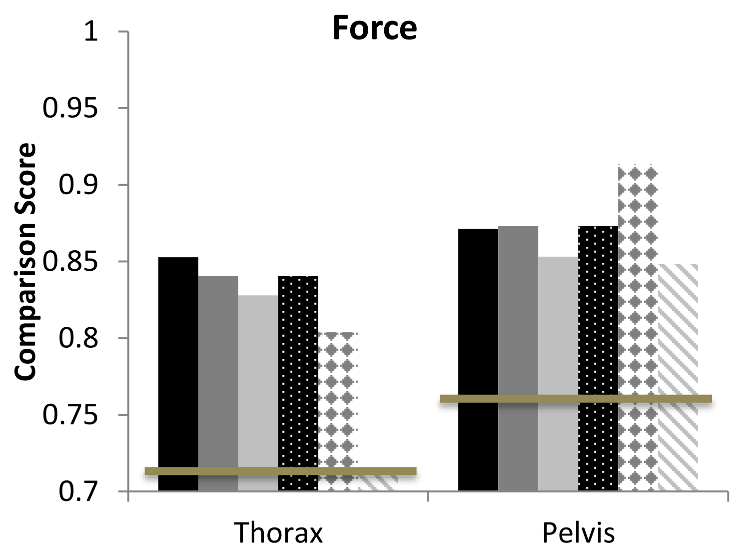

ESEV ESEV-EffMass IM-CharLength IM-CR IM-EffStiff ESEV-KE

Results: Impacts with Infinite Mass

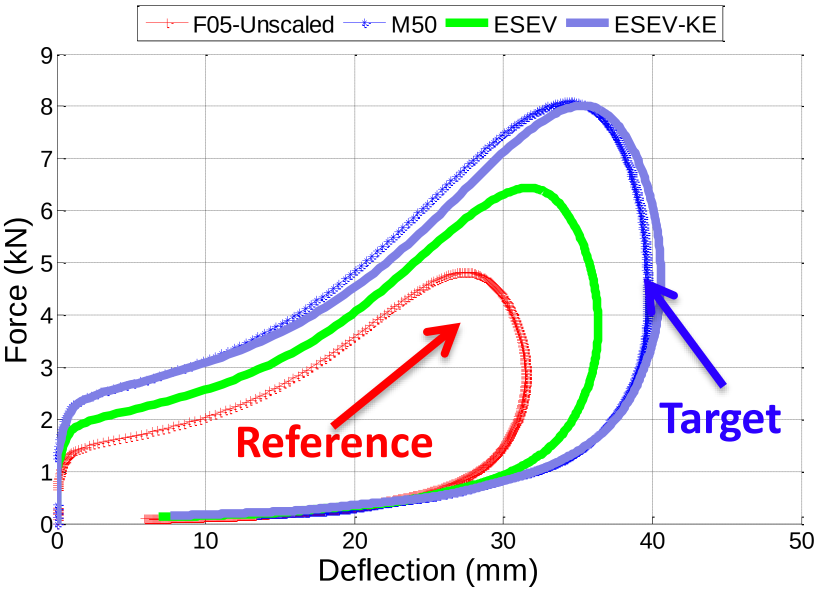

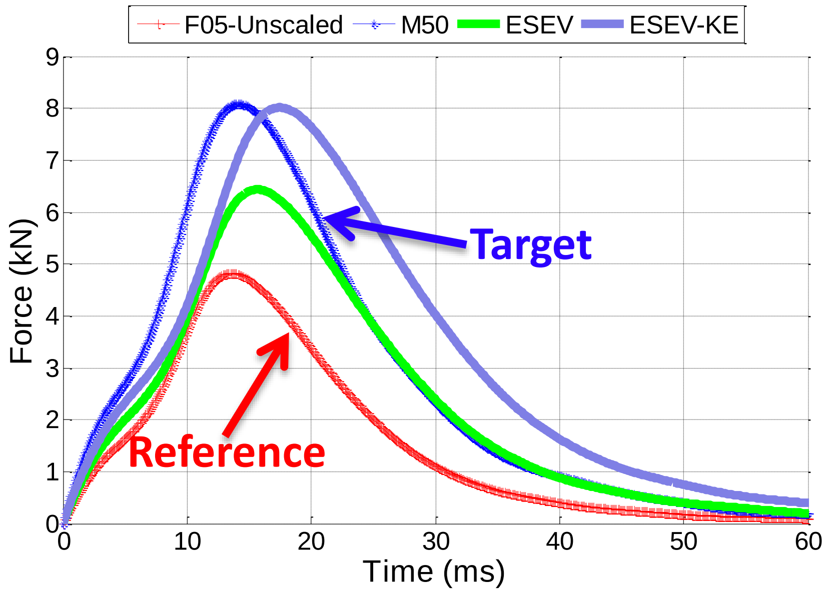

Force ISO Score				
Raw	Phase	Magnitude	Slope	Average
ESEV	0.87	0.89	0.87	0.88
ESEV-KE	0.73	0.97	0.89	0.86

Future Work

- Extend study with the existing GHBMC family of models
- More complex loading scenarios
- Study the effect on experimental corridor development

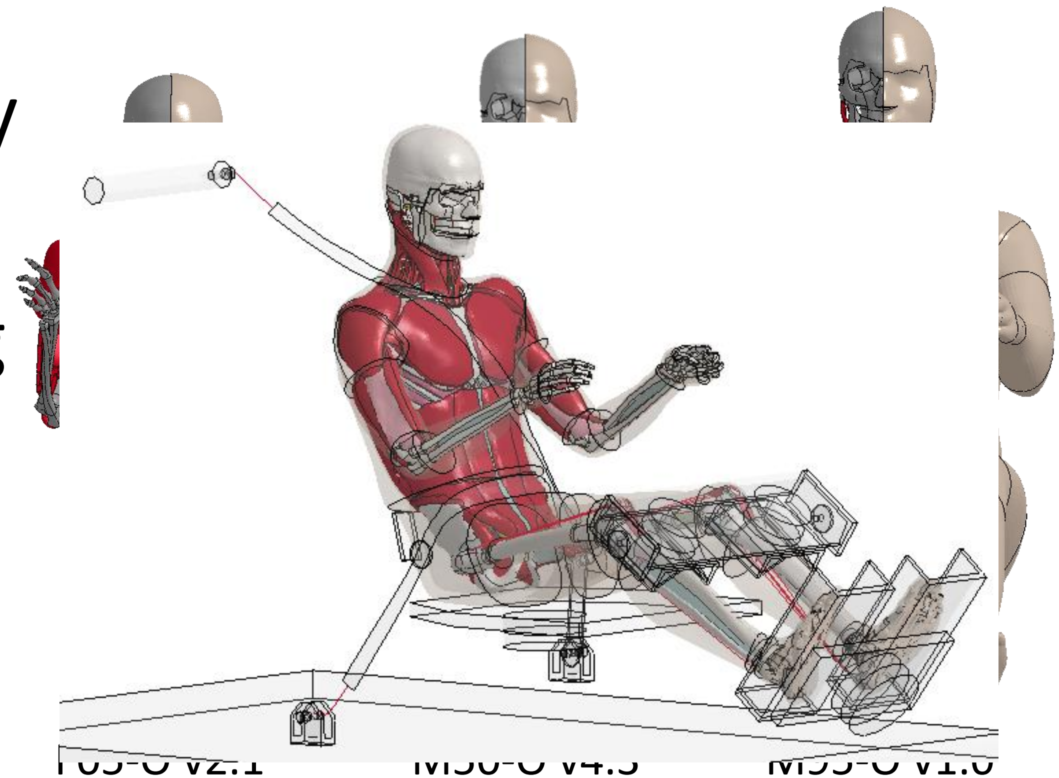

Summary

- Models are a useful tool for evaluating scaling techniques that can then be applied to experimental data
- Used a volumetrically scaled average male model to compare various scaling techniques
- Results indicate that one single method may not be appropriate for all situations
- Overall highest average ISO Score for **pendulum impacts**:
  - Equal Stress Equal Velocity with Effective Mass Ratio
- Overall highest average ISO Score for **infinite mass (whole body) impacts**:
  - Equal Stress Equal Velocity
  - Force deflection data shows that Equal Stress Equal Velocity w/ kinetic energy mass ratio does well when considering structural response only (no phasing)

Acknowledgements

Funding:

GHBMC
Global Human Body Models Consortium

NHTSA

FCA, LLC.
General Motors Corp.
Honda R&D Co.

Hyundai Motor Co.
Nissan Motor Corp. Ltd.
Ford Motor Co. *PDB*

Renault s.a.s.
Takata Corp.
PSA Peugeot-Citroën

GHBMC M50-O Developers:

Wayne State U. (Head), U. Waterloo (Neck), U. Virginia (Thorax), IFSTTAR & Virginia Tech (Abdomen), U. Virginia and U. Alabama-Birmingham (Plex), Wake Forest (Full Body)

Dr. Gayzik is a member of Elemance, LLC. which distributes academic and commercial license for GHBMC-owned Human Body Models. Data appearing in this document were prepared under the support of the Global Human Body Models Consortium by the FBM GHBMC Center of Expertise. Any opinions or recommendations expressed in this document are those of the authors and do not necessarily reflect the views of the Global Human Body Models Consortium.

An Objective Evaluation of Mass Scaling Techniques Utilizing Computational Human Body Models

Questions?

Center for Injury Biomechanics

Wake Forest School of Medicine

CIB

Virginia Tech
Wake Forest University
School of Biomedical Engineering and Sciences

Supplemental

Technique Overview

Equal Stress Equal Velocity	Impulse Momentum	Equal Stress Equal Velocity: Variations
Pros	**Pros**	**Pros**
• Simplicity • Versatility	• Body region specificity • Versatility	• Simplicity • Body region specificity • Versatility
Cons	**Cons**	**Cons**
• Differences in body morphology can be confounding	• May not be completely sensitive to body region characteristics in all loading conditions • Some variations require deflection data	• Effective mass may not be completely sensitive to body region characteristics in all loading conditions • Deflection data required for energy approach

U.S. ARMY RDECOM®

ARL

Framework for FEM Scaling and Posture

Dr. Adam Sokolow and Justin McKee

Framework Goal

Combine the strengths of a reduced-order model like ATB/MADYMO with those of a higher fidelity FEM

- "Simplicity" of posture specification
- Anthropometric data feeding into scaling
- Complex geometries, constitutive models, and "fracture"

Use the hybrid approach to:

- Target biological variability and its role in the uncertainty quantification for use with model validation
- Establish trends
- Assess a wider variety of threats with a single model

Framework

FE Model → Scaling Module → Posturing Module → Application

FE Model
- Mesh
- Constitutive models & parameters

Scaling Module
- ANSUR/GEBOD
- Mathematical description of scaling rules

Posturing Module
- Mathematically or empirically derived

Application
- Threat application
- Injury assessment

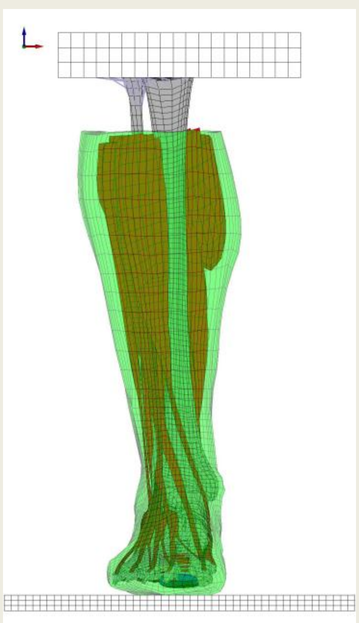

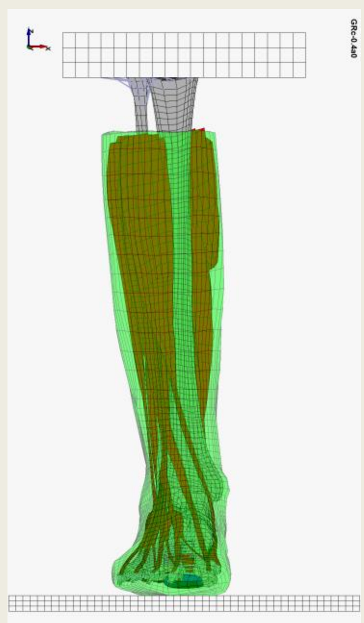

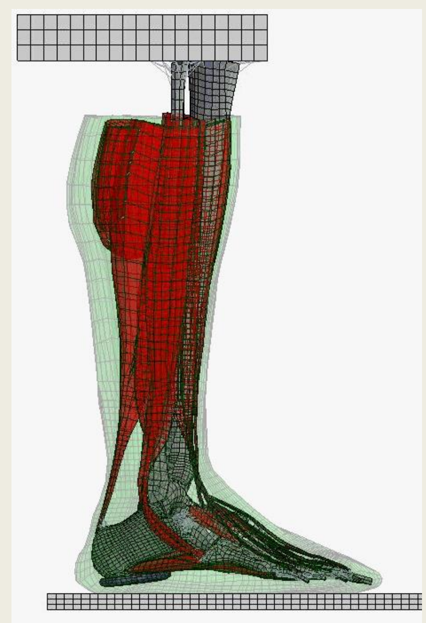

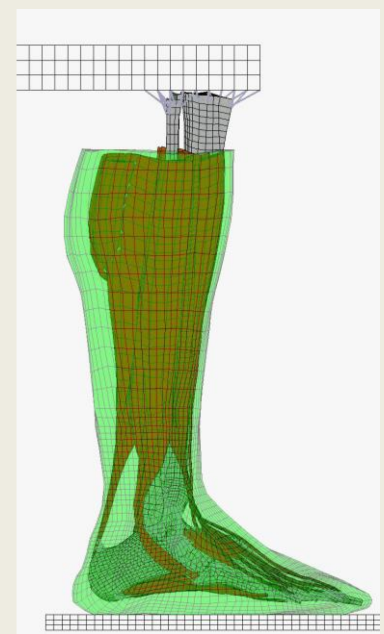

Scaling Methodology & Targeted Modes

Top down approach to scaling

- **Identify relevant subset of ANSUR-II results**
- **Mathematical functions convert scalar measurements to vector field approximations of a scaling mode**

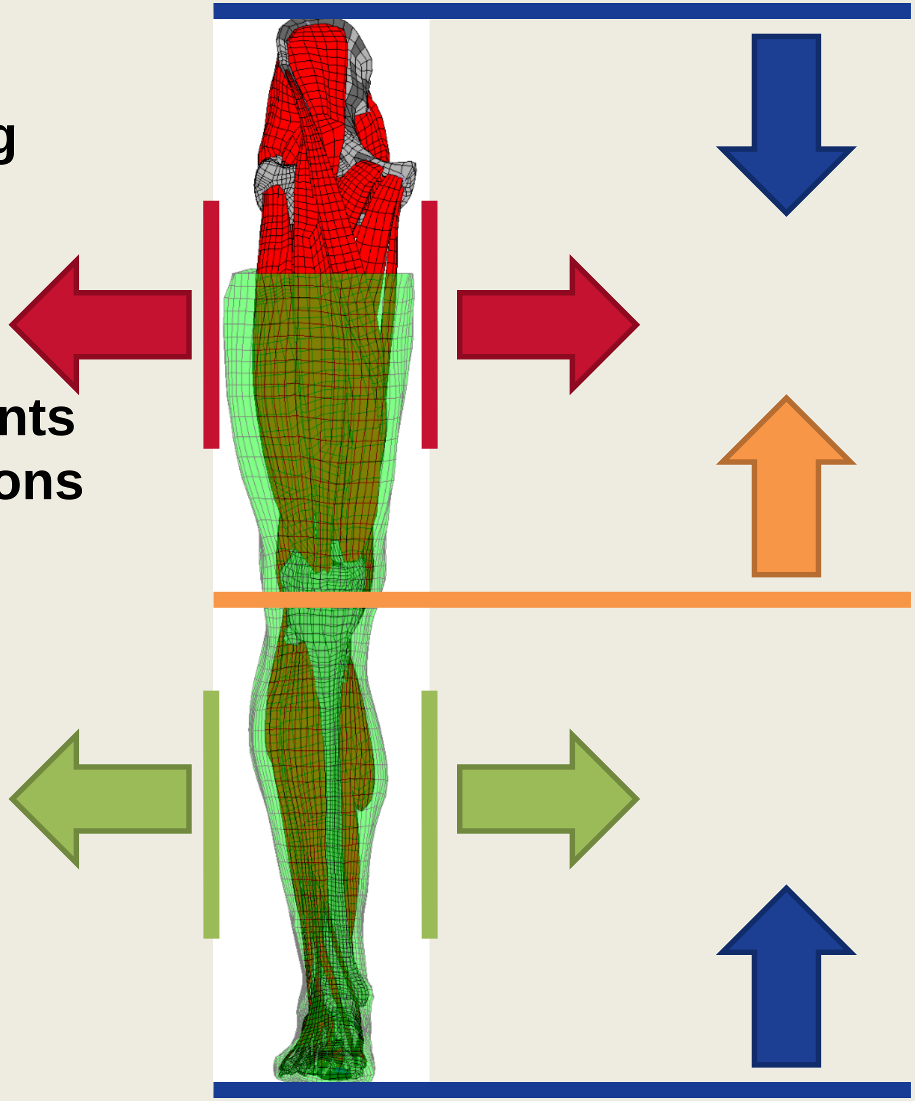

Scaling modes

1. Uniform Scaling
2. Relative Knee Location
3. Calf Circumference
4. Thigh Circumference
5. Foot Scaling (not shown)

Mode II

Total leg length unaffected by scaling mode II

Only relative location of the knee joint is shifted up or down

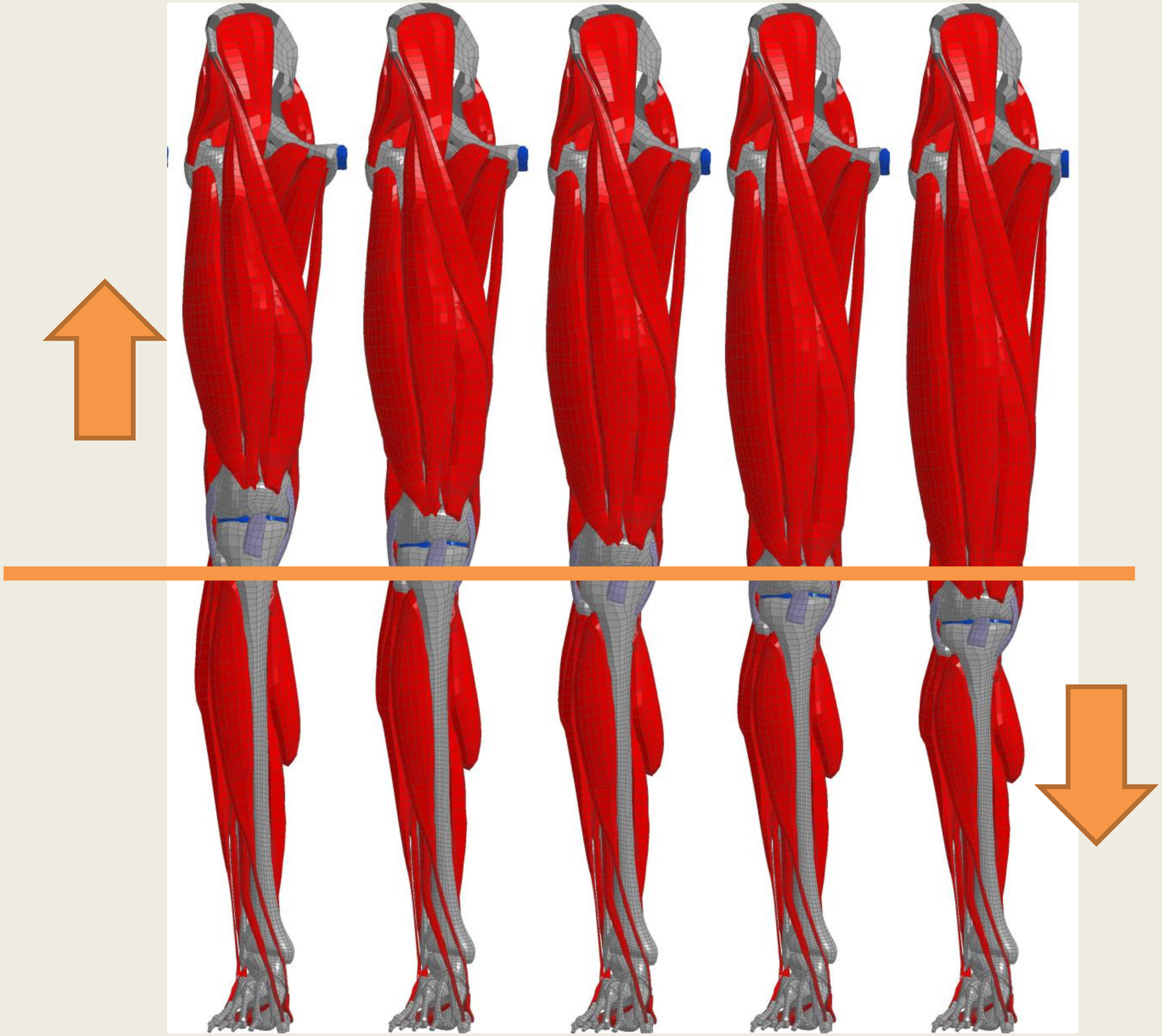

Modes III & IV

Modes III & IV target soft tissue only

Thigh expands radially around femur

Calf expands quasi-elliptically around both the tibia and fibula

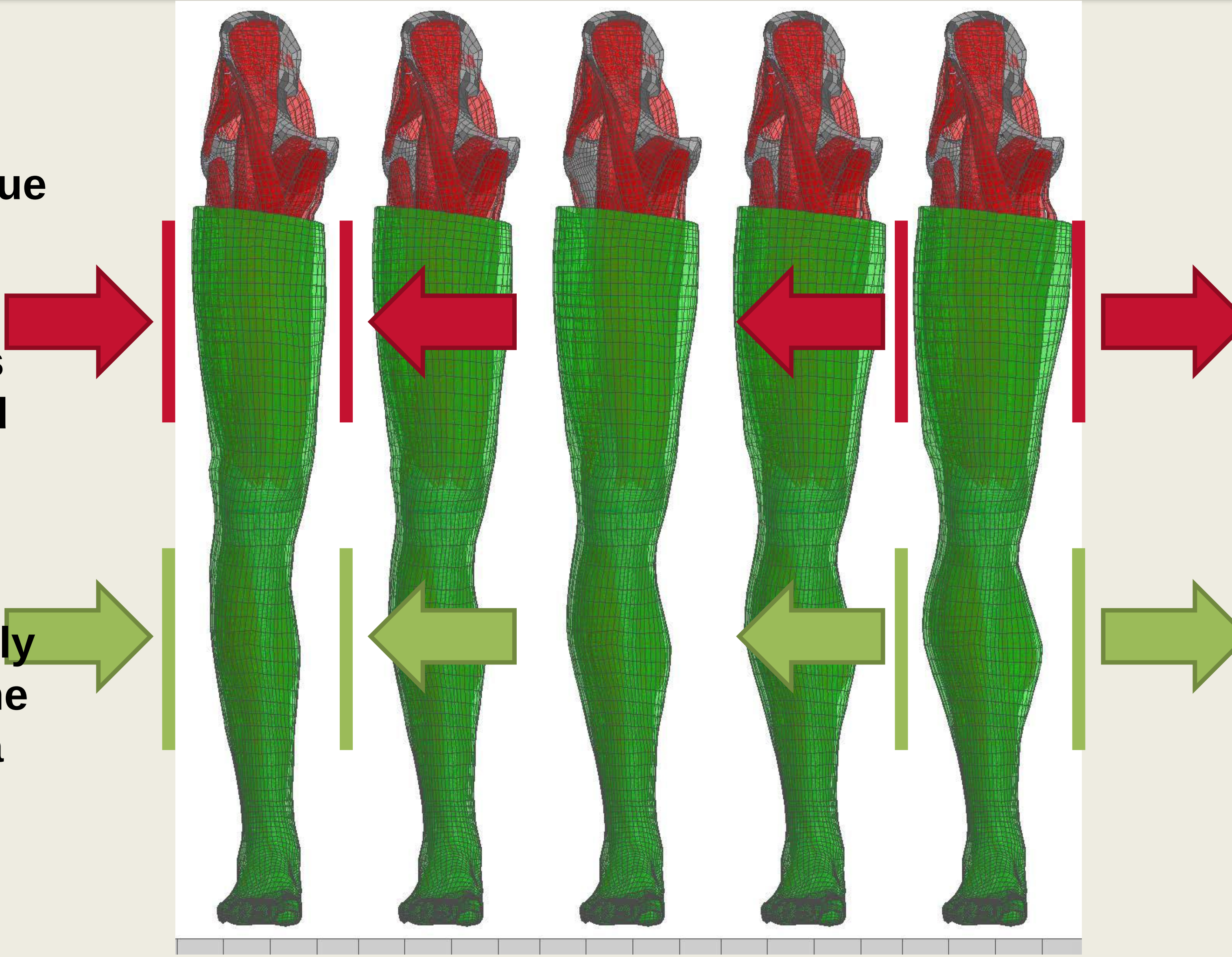

Posture Methodology

Quantify
- **Characterize posture with small number of angles, relative locations or other scalars**

Relate
- **Joint functions describe the relative motion of two rigid bodies parameterized by scalar values**

Impose
- **Compute system motion in global coordinate system and prescribed in time**

Simulate
- **Use FE simulation to determined the passive soft-tissue response**

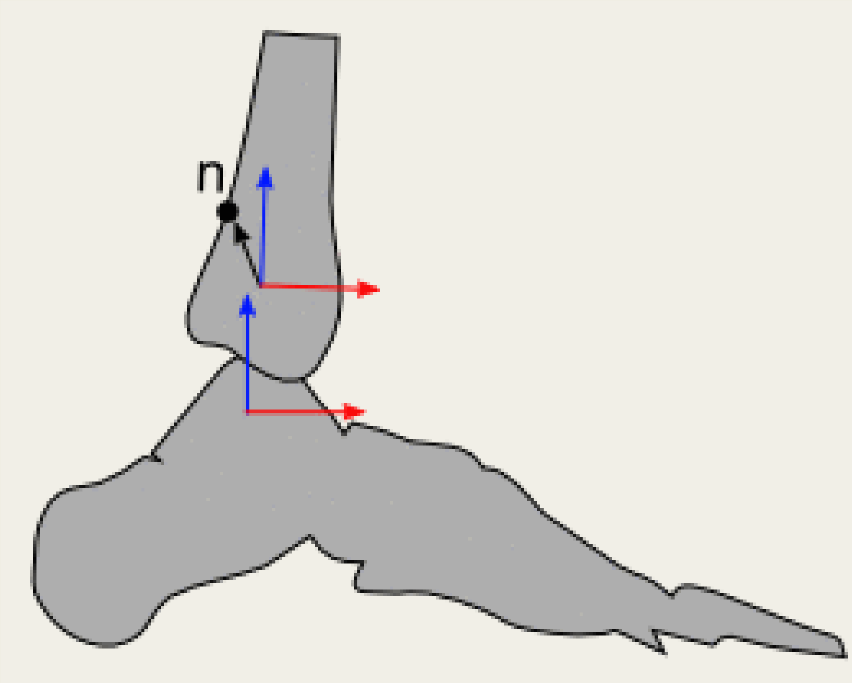

Posture: Leg

Hip: Flexion/extension, internal/external, abduction/adduction

Knee: Flexion (internal/external, varus/valgus, and translation are dependent on flexion)*

Ankle: Dorsiflexion/plantar flexion, inversion/eversion

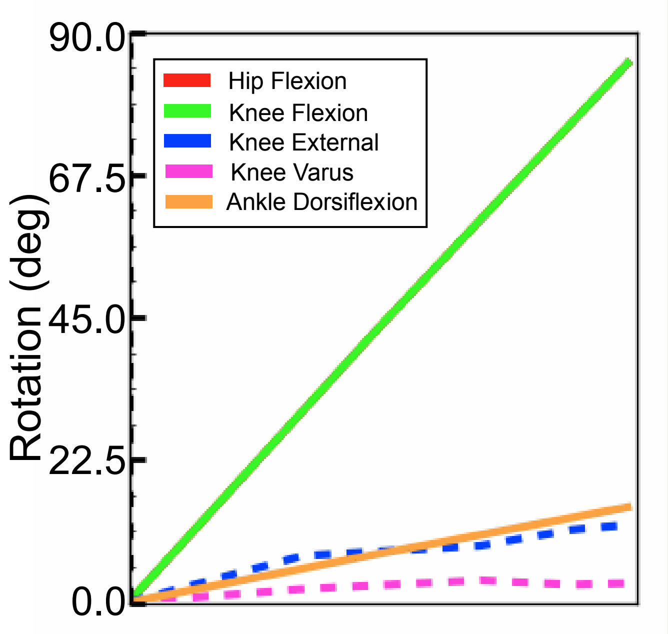

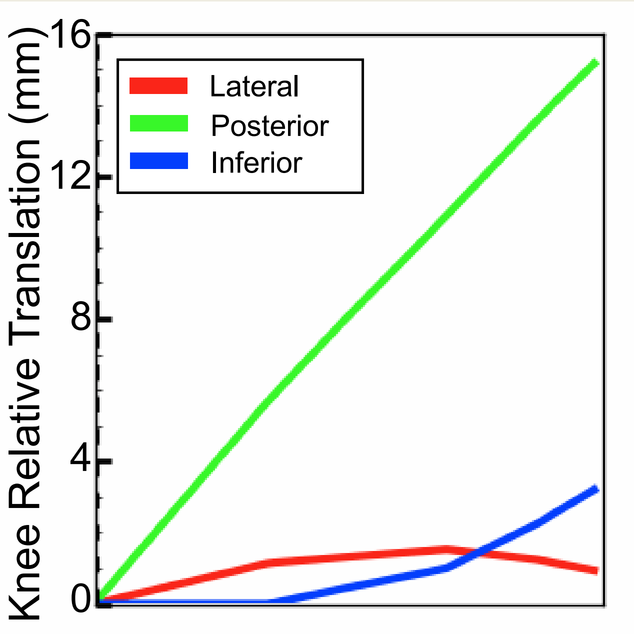

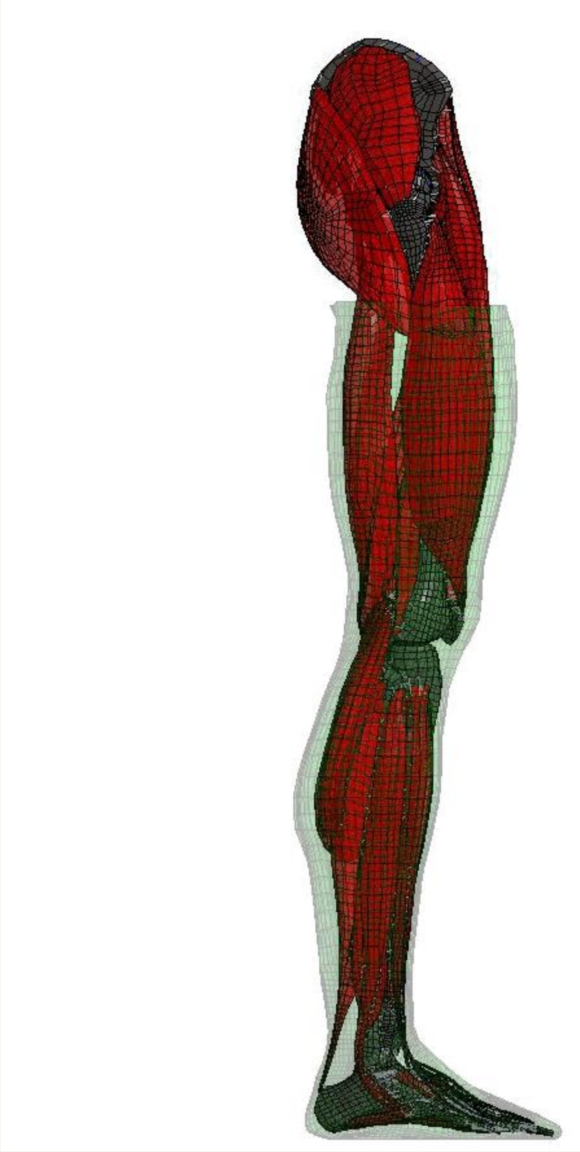

*Li, G., Papannagari, R., Nha, K. W., DeFrate, L. E., Gill, T. J., & Rubash, H. E. (2007). The coupled motion of the femur and patella during in vivo weight bearing knee flexion. Journal of biomechanical engineering, 129(6), 937-943.

Posture: Spine

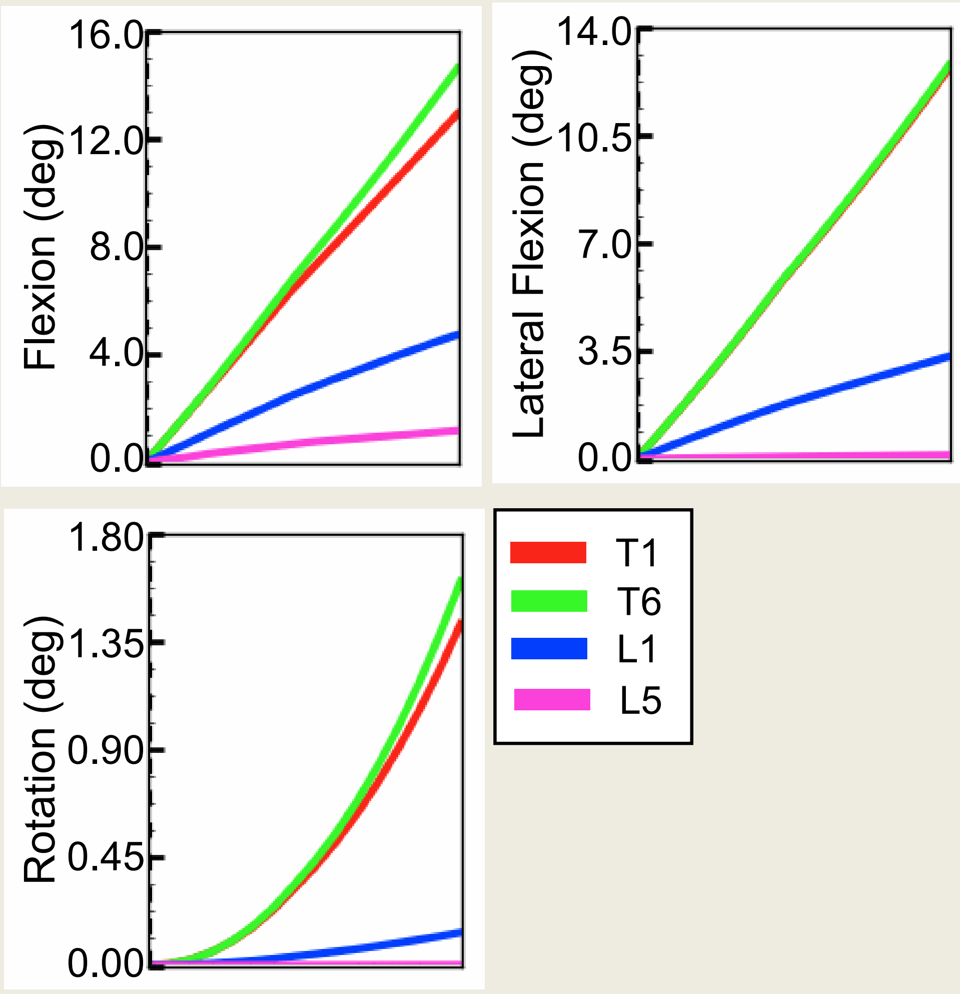

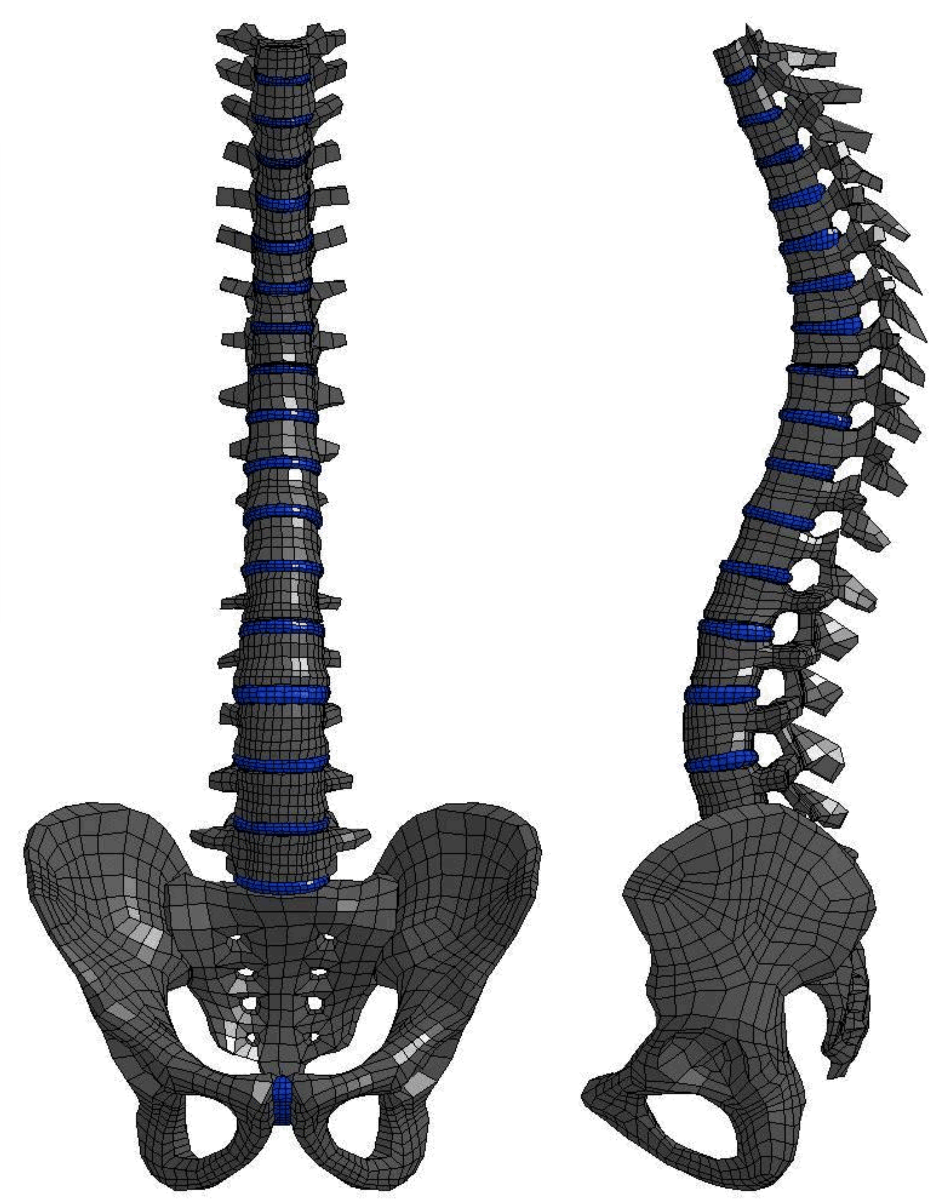

Application: Pendulum Impacts

Use scaling framework to investigate trends in the measured force with a set of scaled legs and re-balanced ballasts target scaling modes:

1. Uniform Scaling
2. Relative Knee Location (z-only scale)
3. Calf Circumference

Use posturing framework to investigate trends in dorsiflexed, neutral, and plantarflexed positions

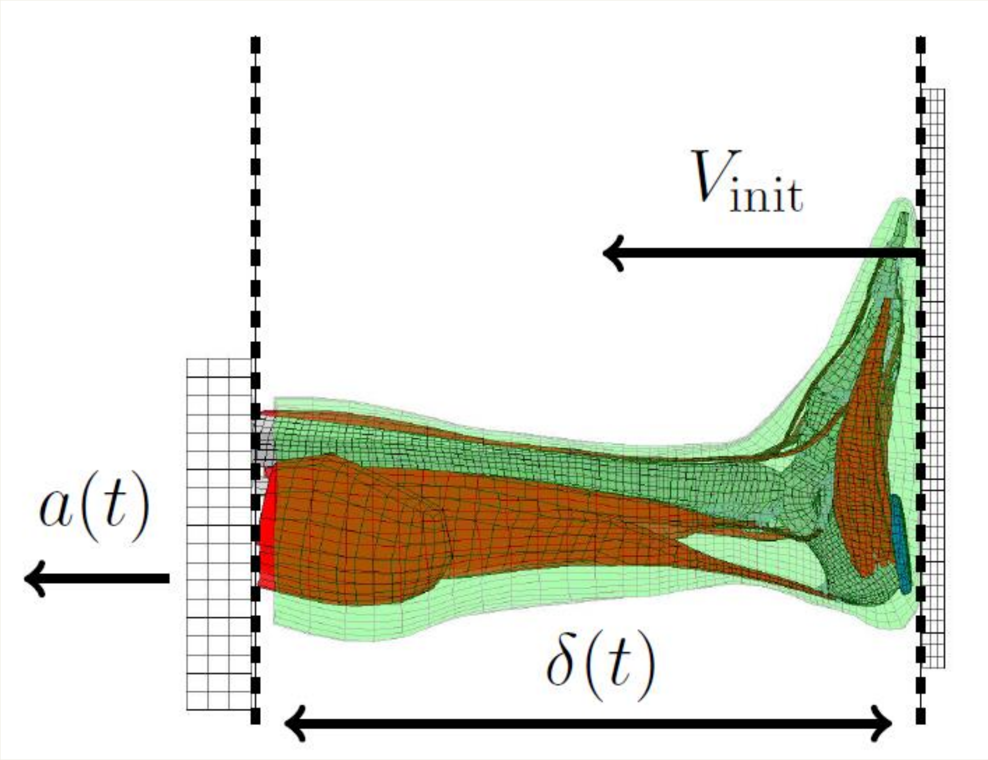

- Analyze simulation results in the context of pendulum impact tests: tibial force, lower-leg compression, etc.
- Extract trends, identify sensitivities, etc.

U.S. ARMY RDECOM

Calf Mode

ARL

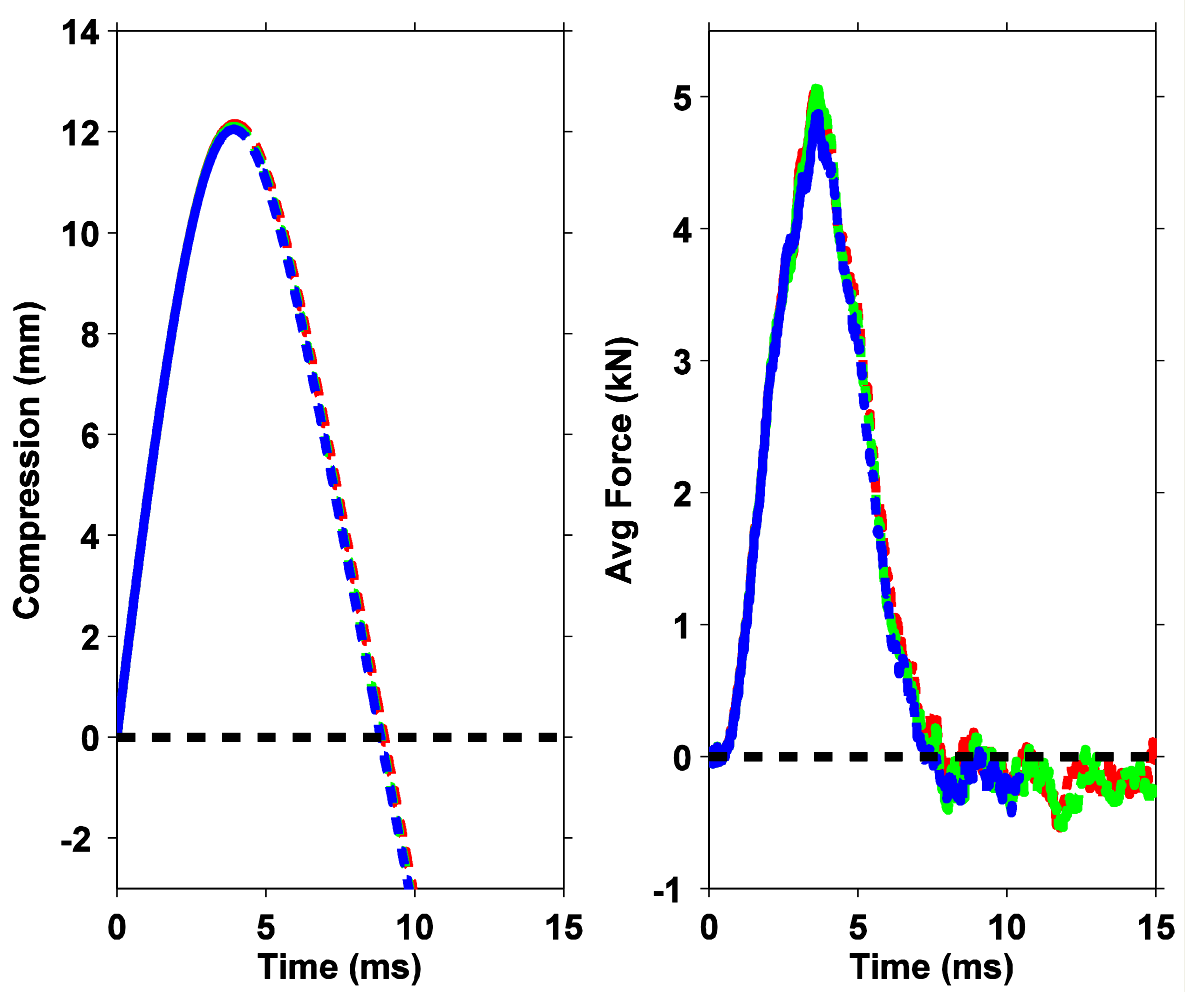

Introducing a 20% variability on the flesh mass has little-to-no effect

Z-Scale Only

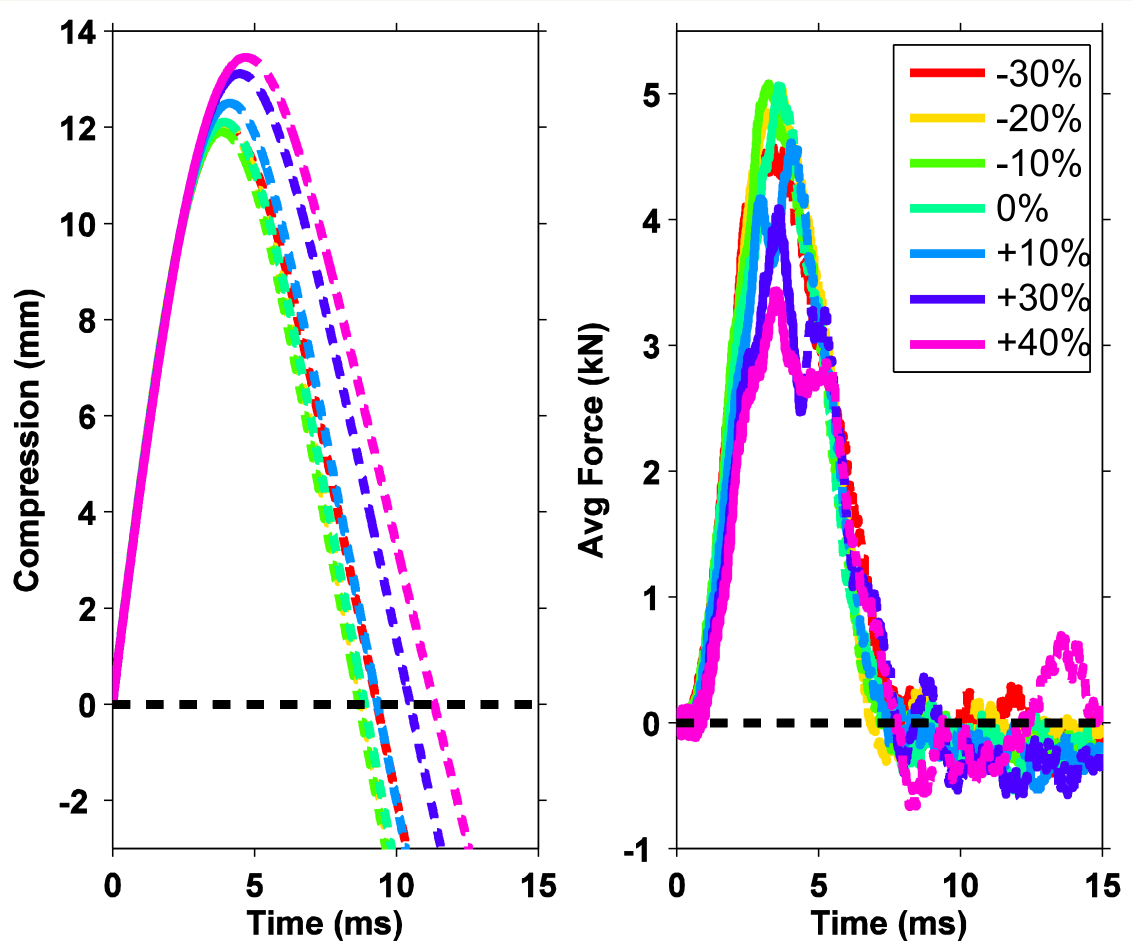

- Heaviest and longest leg has lowest forces, highest compressions
- Opposite extreme does not exhibit this trend
- Asymmetric response to z-scaling

Ankle Posturing & Pendulum Impacts

Six models produced by adjusting ankle rotation from 5 degrees plantar flexion to 20 degrees dorsiflexion

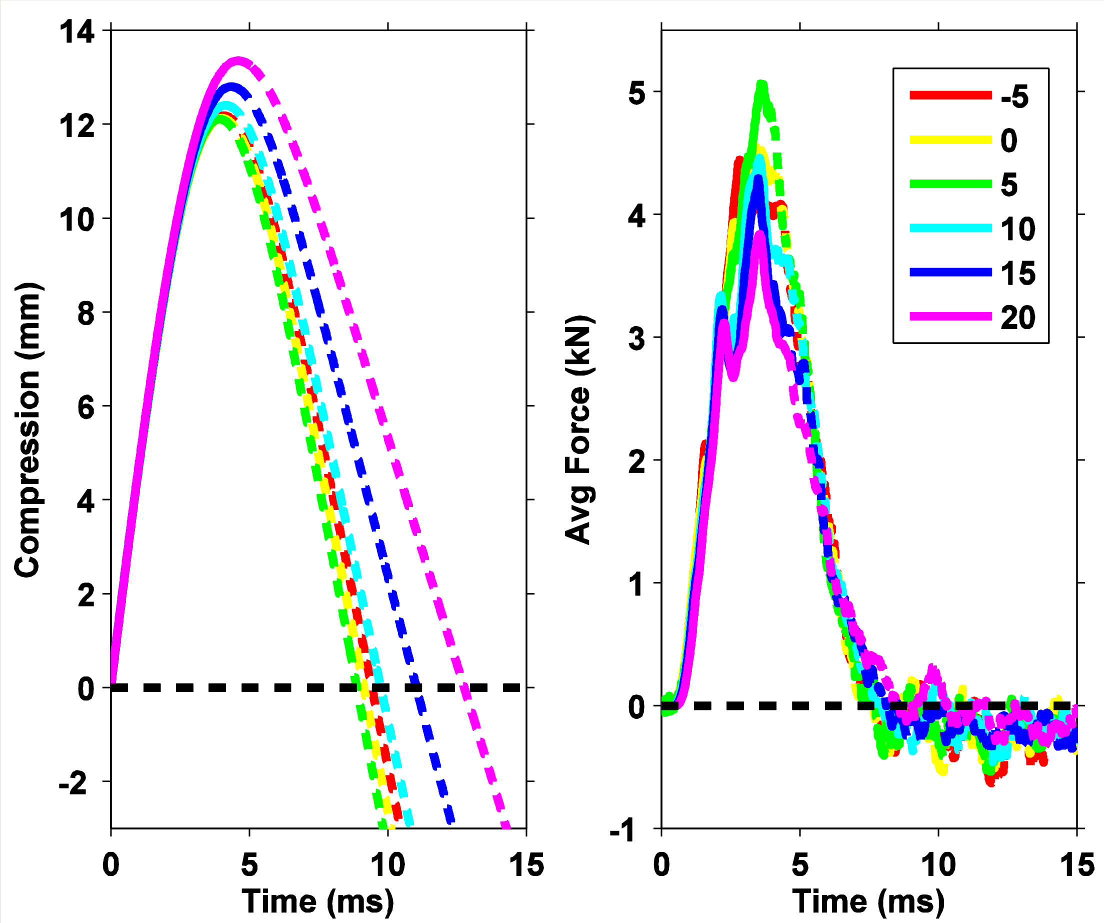

- **Peak compressions increase at extreme dorsiflexion**
- **Peak forces decrease at extreme dorsiflexion**

U.S. ARMY RDECOM

Summary & Future Work

ARL

- Preliminary simulations exhibit trends in force-compression data for a subset of the scaling modes and need to be explored further
- Connect to established anthropometric scaling laws
  - Current framework reduces scaling problem to ~4-5 scalar values.
  - Alternate scheme to find best-fit of 4-5 values to create a particular human test-subject
- Improve mathematical descriptions
  - scaling to minimize distortion
  - Make use of anthropometric and kinematic data to improve the motion at joints
  - Capture the detailed coupled motion of bones through simplified inputs (such as the subtalar joint as a function of plantar flexion)
- Empirically derive joint functions
- Address soft tissue posturing, simulation time, contact resolution

Questions?

Additional Slides

Future Posture

- Improve joint functions
- Empirically derived joint functions
- Soft tissue factors
- Simulation time boosts
- Contact resolution

Scaling Application: Pendulum Impacts

Typical pendulum impact test uses variable ballast mass to normalize some of the inertial properties from one leg to another

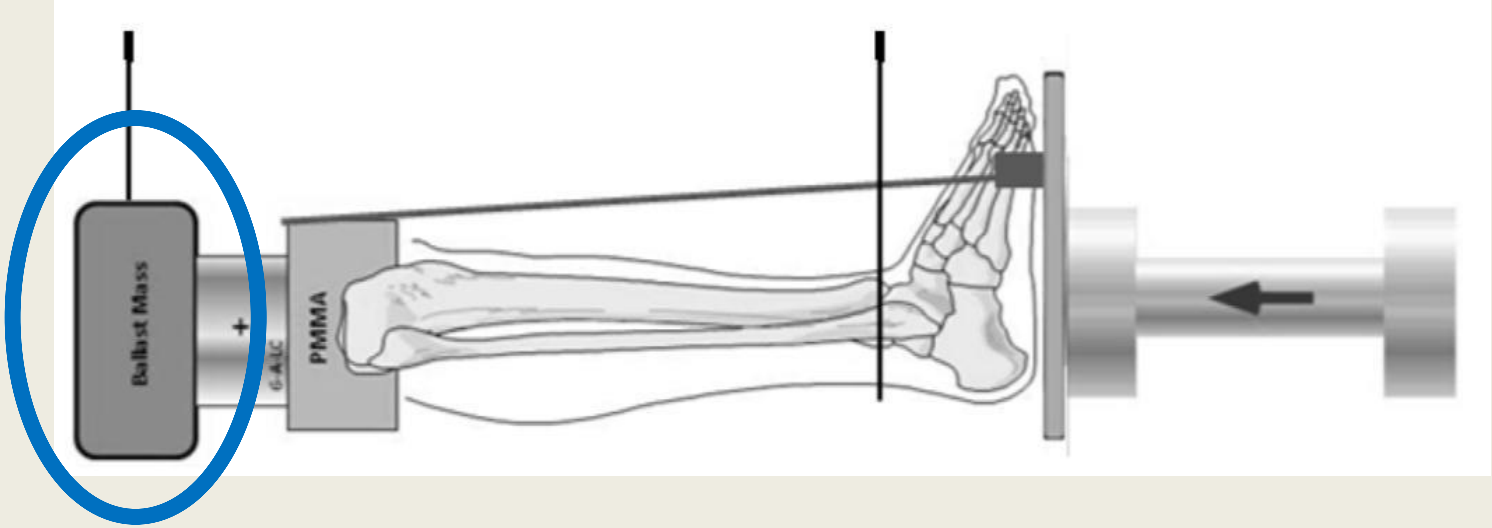

Use scaling framework to investigate any trends in the measured force with a set of scaled legs and re-balanced ballasts

Z-Scaling Corridors

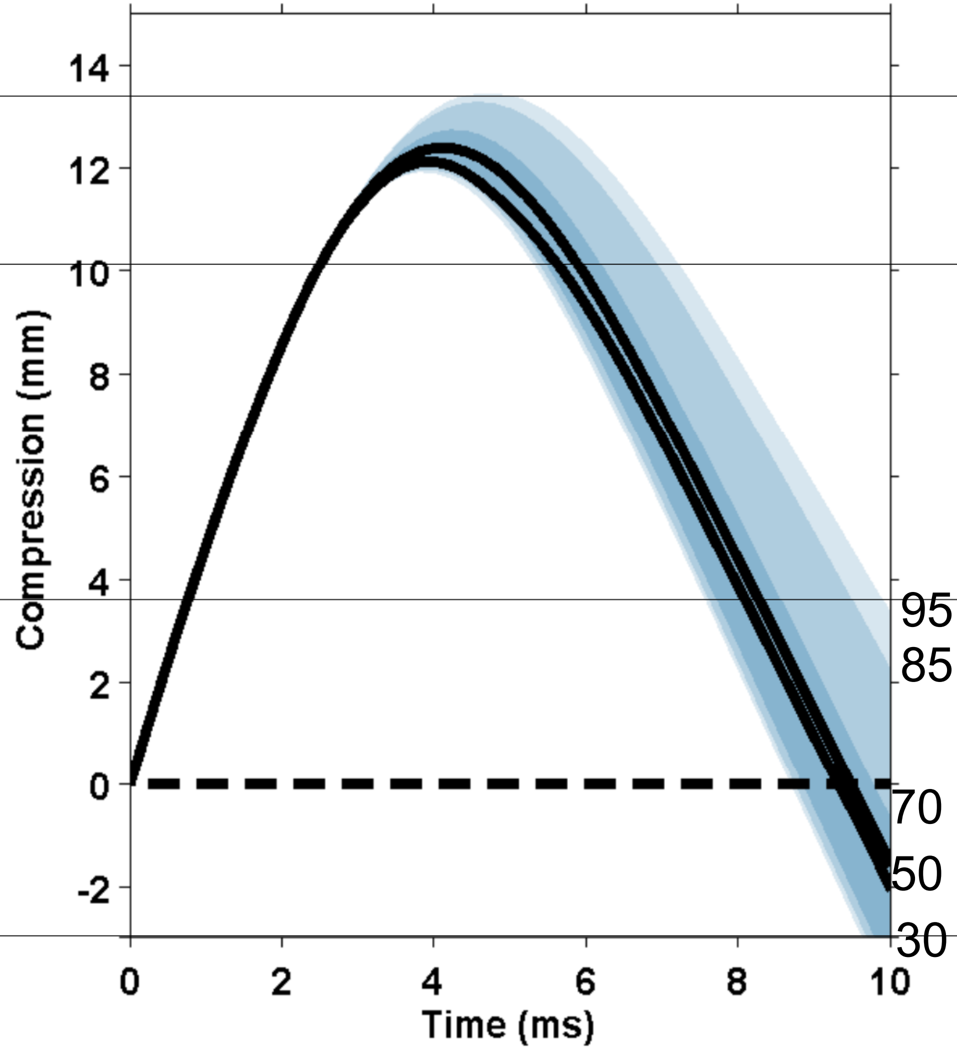

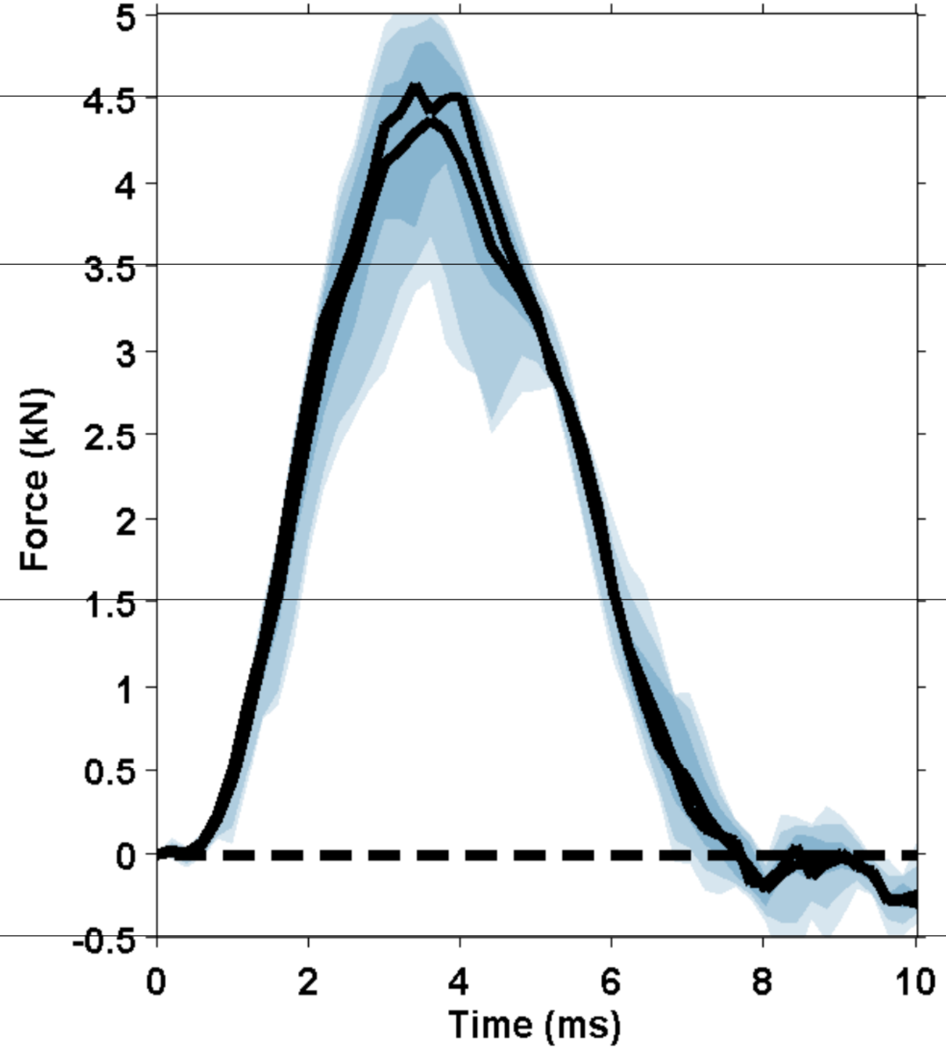

Uniform Scaling

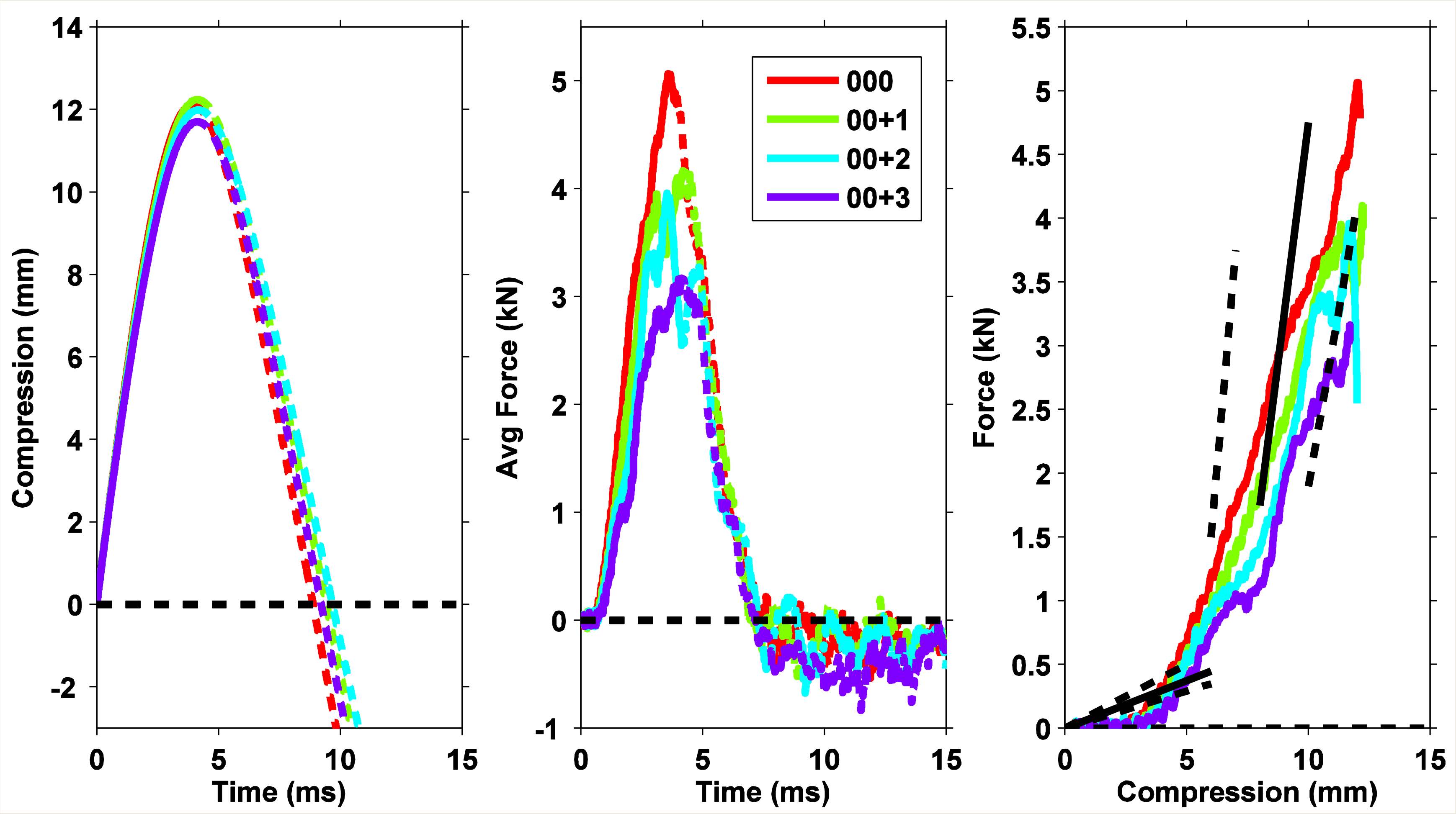

Larger legs experience lower peak forces

U.S. ARMY RDECOM

Uniform Scaling Corridors

ARL

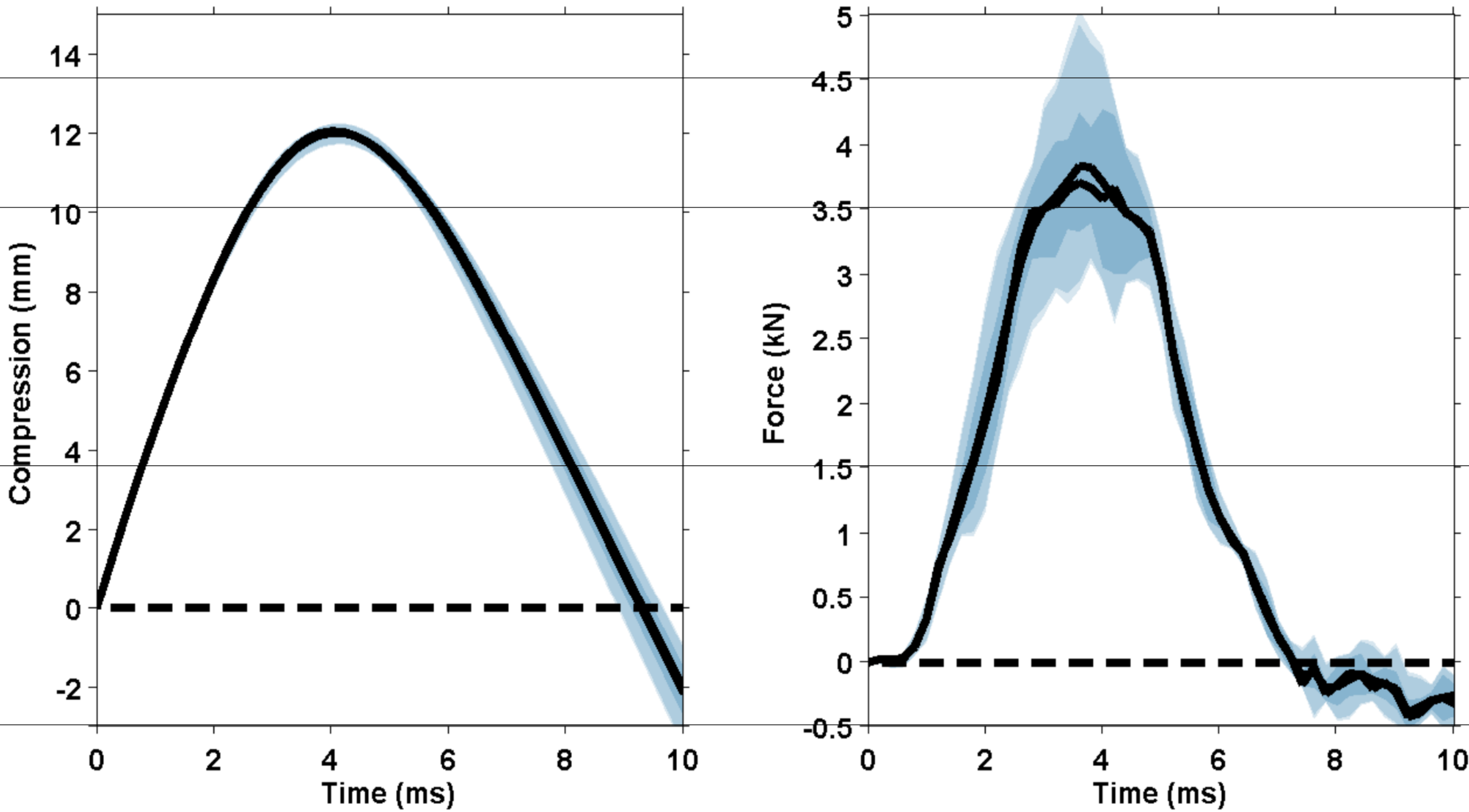

Ankle Flexion Corridors

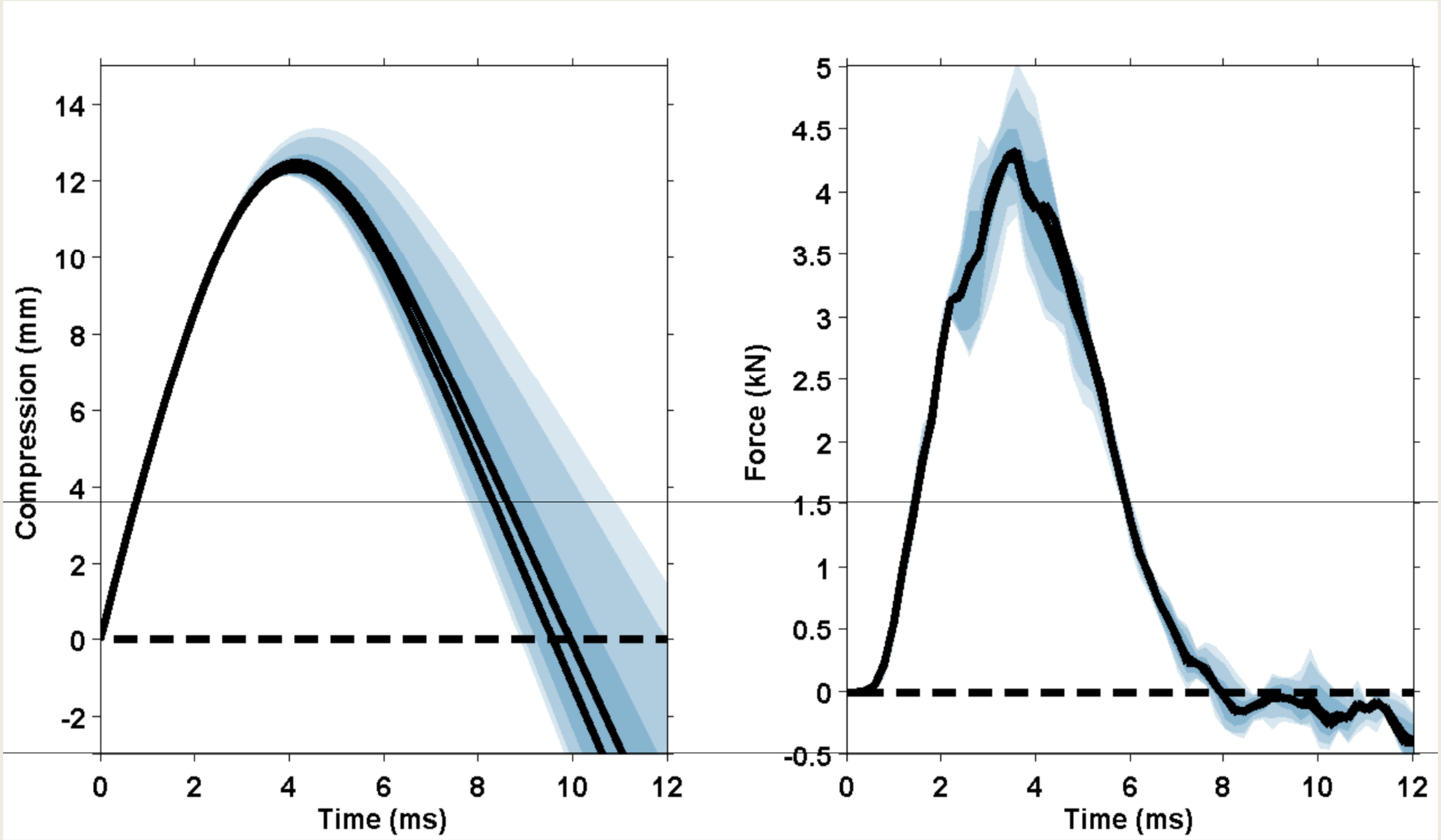

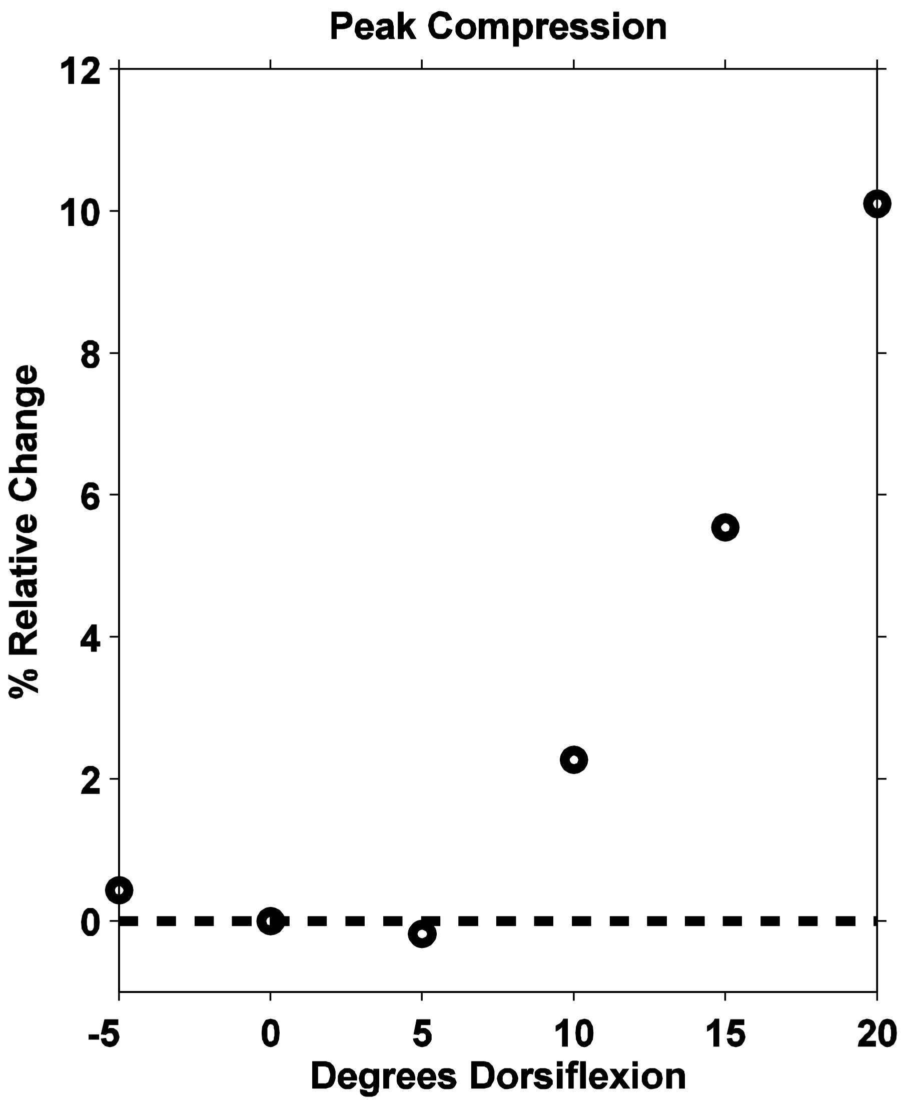
Peak Compression
% Relative Change
Degrees Dorsiflexion
12
10
8
6
4
2
0
-5
0
5
10
15
20

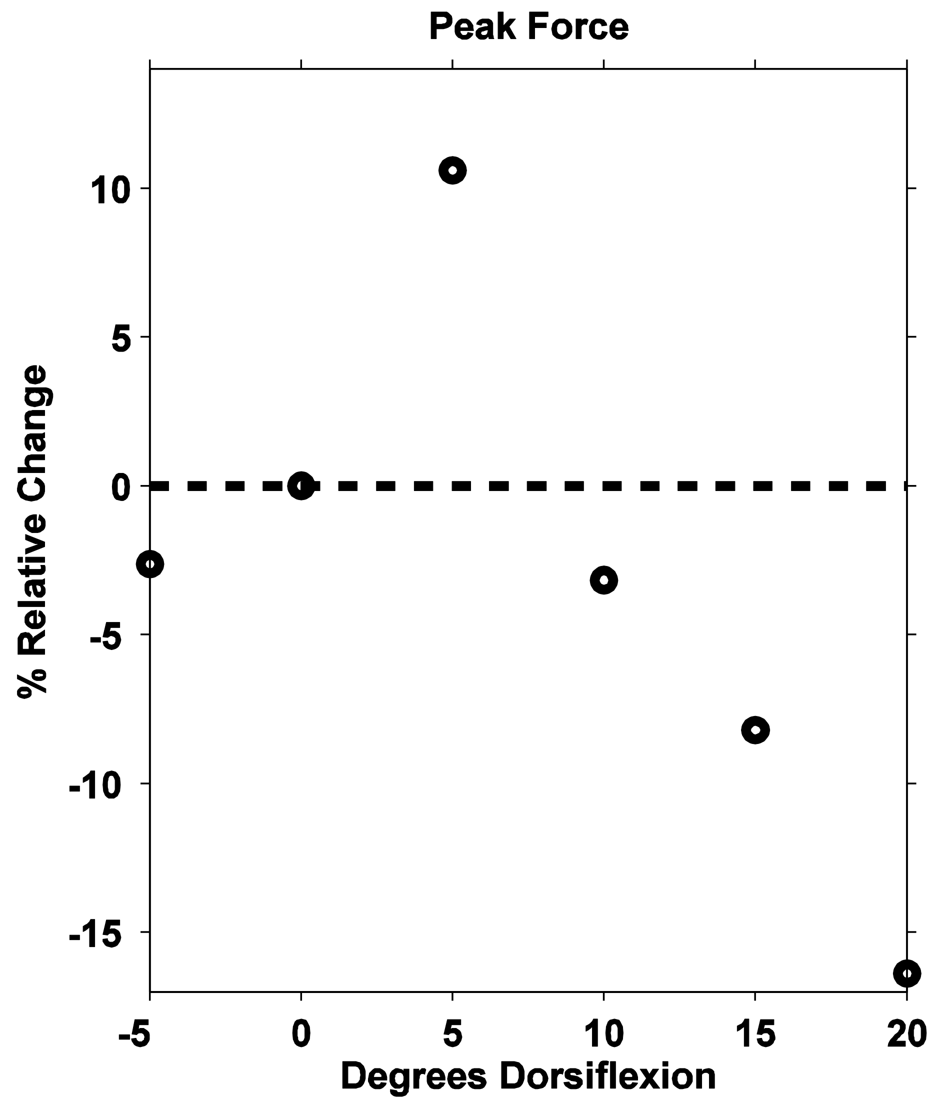
Peak Force
% Relative Change
Degrees Dorsiflexion
10
5
0
-5
-10
-15
-5
0
5
10
15
20

Scaling Methodology

- Use ANSUR-II dataset to identify a subset of relevant scaling rules to implement
  - Height
  - Weight
  - Relative Lengths
  - Circumferences
- Each of these can be thought of as an mode of scaling
- Develop ansatz mathematical functions to convert scalar ANSUR measurements to vector field approximations.

Study to determine the variation of vulnerable thoracic-abdominal structures using Computed Tomography

Numerical Analysis of Human and Surrogate Response to Accelerative Loading Workshop. ARL Aberdeen, January 2015.

Dr Rob Fryer – Dstl

Additional contributors:

Dr Johno Breeze – RCDM

Dr Eluned Lewis – DE&S

Page Intentionally Left Blank

Computational Pipeline Enabling the Generation of Multi-Organ Statistical Atlases for Improved Human Model Development

January 14, 2016

Project Team:

Nathan Drenkow[1], Jason Harper[1], Nathanael Kuo[1], Manuel Uy[1], Catherine Carneal[1], Andrew Merkle[1], Gaurav Thawait[2], Jan Fritz[2], Brian Corner[3], Michael Maffeo[3]

[1]JHU Applied Physics Laboratory
[2]JHU Medical Institute
[3]Army Soldier System Center (Natick)

US ARMY NATICK SOLDIER RD&E CENTER

APL JOHNS HOPKINS APPLIED PHYSICS LABORATORY

Motivation

- Build human models that accurately represent populations of interest
  - Single anatomies are insufficient

- Improve scaling of biomedical response and injury predictions
  - Often rely on height and weight
  - Limited data on how internal geometries scale

- Predict internal anatomy from anthropometric/demographic information

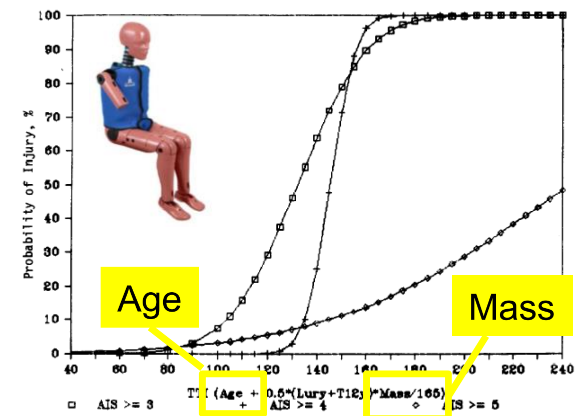

Abdominal injury risk for automotive side impacts scales with subject age and weight*

Understanding allometry (scaling law) critical for accurate human models

*Eppinger et al, “Development of Dummy and Injury Index for NHTSA’s Thoracic Side Impact Protection Research Program, 1994

Motivation

- **Statistical shape atlas provides a method to determine allometric relationships**

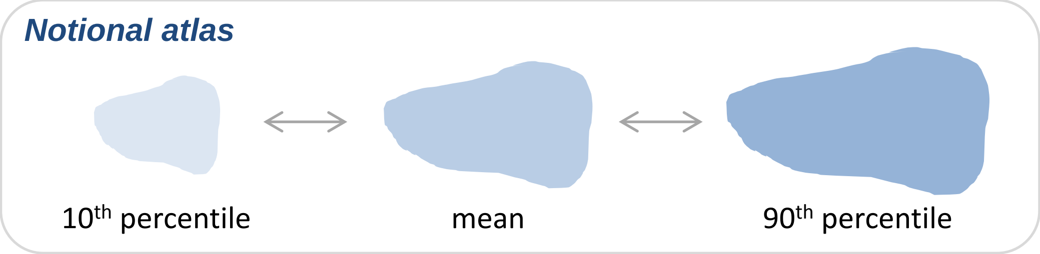

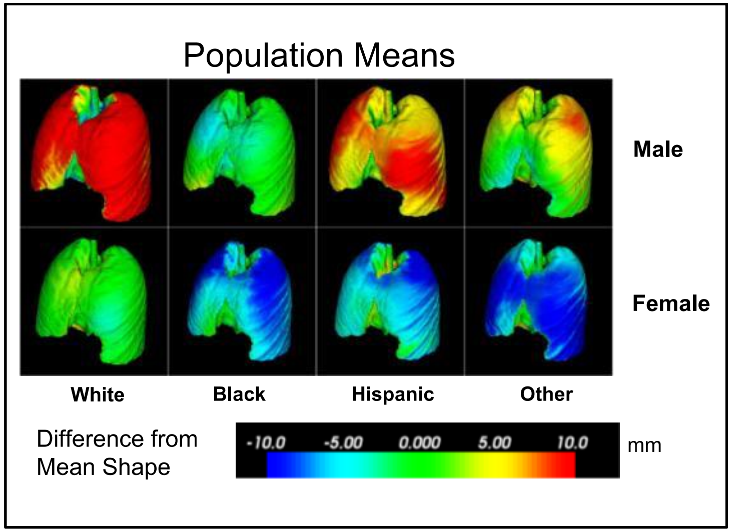

- **Previously developed a statistical lung atlas for a military-representative dataset***

Objective: Extend atlas to multiple organs

Focus on thorax (e.g., Lungs, liver, spleen, kidneys, bladder)

* Otake, Yoshito, et al. "Prediction of Organ Geometry from Demographic and Anthropometric Data Based on Supervised Learning Approach using Statistical Shape Atlas." ICPRAM. 2013.
* Presented at 2014 ARL workshop

Development of Statistical Multi-Organ Atlas
Overall Objectives

- ***Develop a modular, scalable, and automated computational pipeline to simultaneously segment organs (focus on thorax) from large set of medical CT scans and aggregate into a statistical shape atlas***
- ***Analyze variations of organ shape, size, and placement based on gender, race, anthropometrics, and age***

Key Technical Challenges

- Large variability in organ shape, size, and location
- Low image contrast between organs
- Complex multi-organ relationships

Pipeline Overview

Data Collection/ Preprocessing → **Automated Segmentation** → **Statistical Atlas Generation**

Collect and prepare a population-specific CT image dataset

Automatically label organs of interest for all CTs in the dataset

Use segmentations to learn major modes of organ shape variation

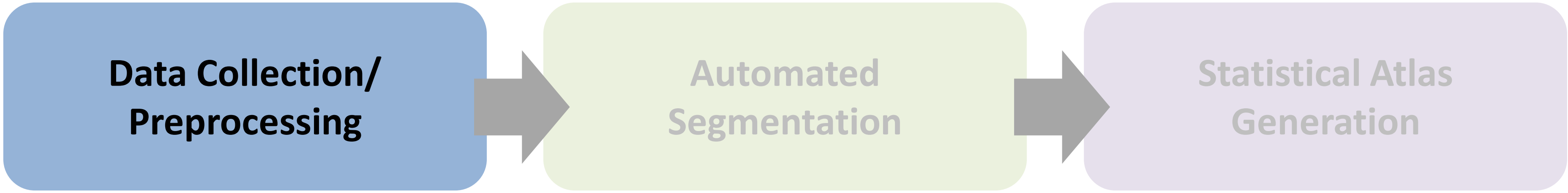
Data Collection/ Preprocessing
Automated Segmentation
Statistical Atlas Generation

Data Collection
Results

- **Goal: Collect military-representative image dataset for establishing allometric laws and organ models**
  - **Target: 200 images balanced across gender, ethnicity, & age**
- **CT images selected by expert radiologist at JHMI**
  - **13,000 CT images available**
  - **180 in final selection**
- **Demographic bins based on 2012 Army Anthropometric Survey (ANSUR2)**

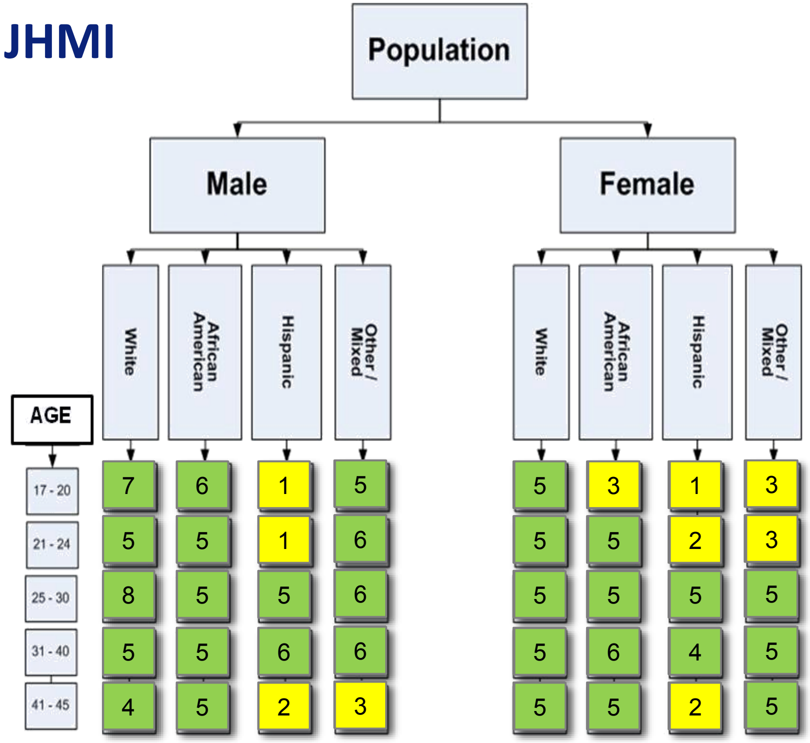

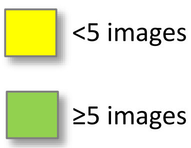

96 male, 84 female

Data source: Johns Hopkins Hospital Radiology Information Systems

Data Collection
External Measurements

- **Limited anthropometric data available for medical subjects**
- **Radiologists manually approximated external skin and skeletal based metrics from lung CT scans**

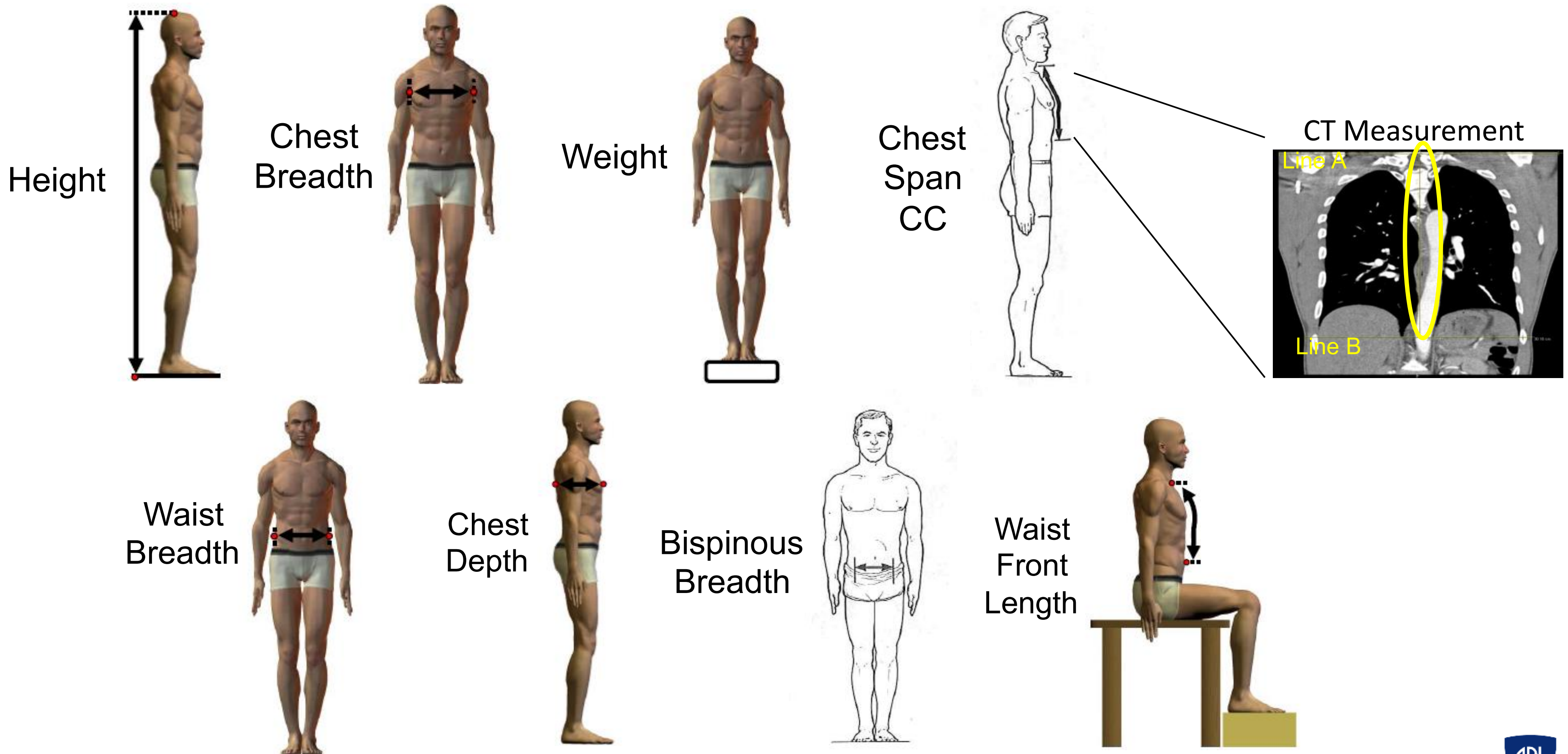

Pipeline Overview

Data Collection/ Preprocessing → **Automated Segmentation** → Statistical Atlas Generation

Automated Segmentation

Isomap, Manual segmentations

- **Select and manually segment images that span the population's variability**
  - Ground truth segmentations for evaluation
  - Create organ models to inform automated segmentation algorithms

- **Machine learning approaches required to identify major modes of variation across the entire image dataset**

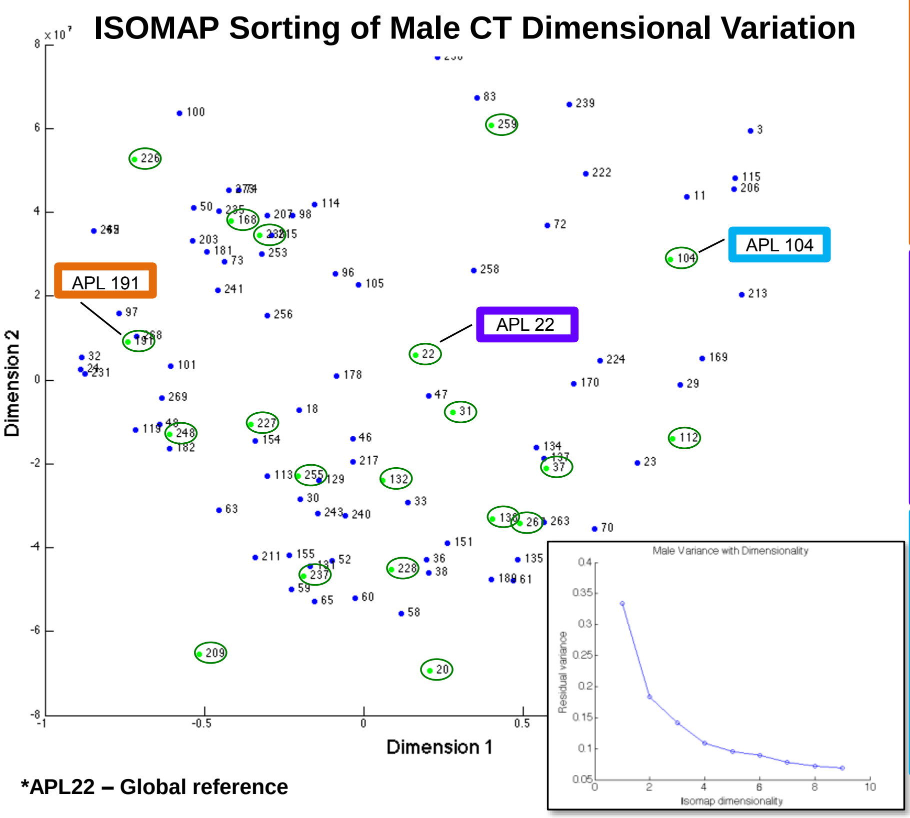

*APL22 – Global reference

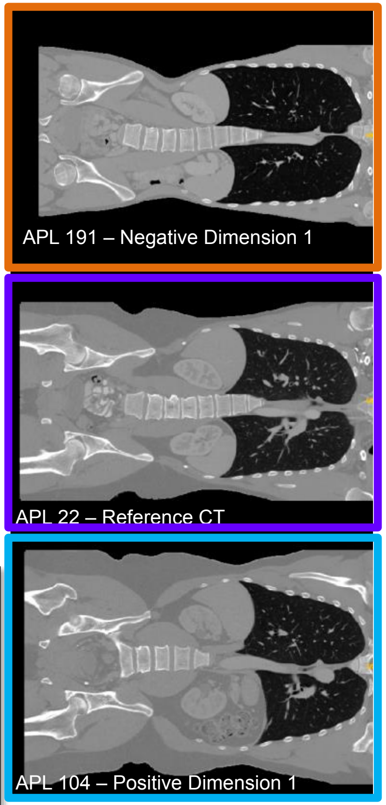

Selected images manually segmented by expert radiologist at JHMI

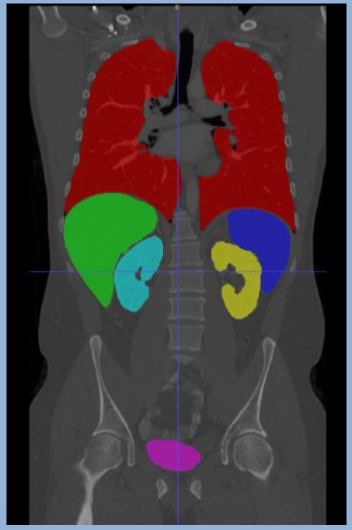

N=20

Organ Model Generation

Comprehensive organ model answers the question:
"Where *can* the organ exist?"

Approach:

- **Align manual segmentations in same physical space**
- **Manual segmentations 'vote' for organs at each voxel location**
- **Comprehensive model includes all voxels that receive at least one 'vote'**

Automated Segmentation Pipeline

Approach

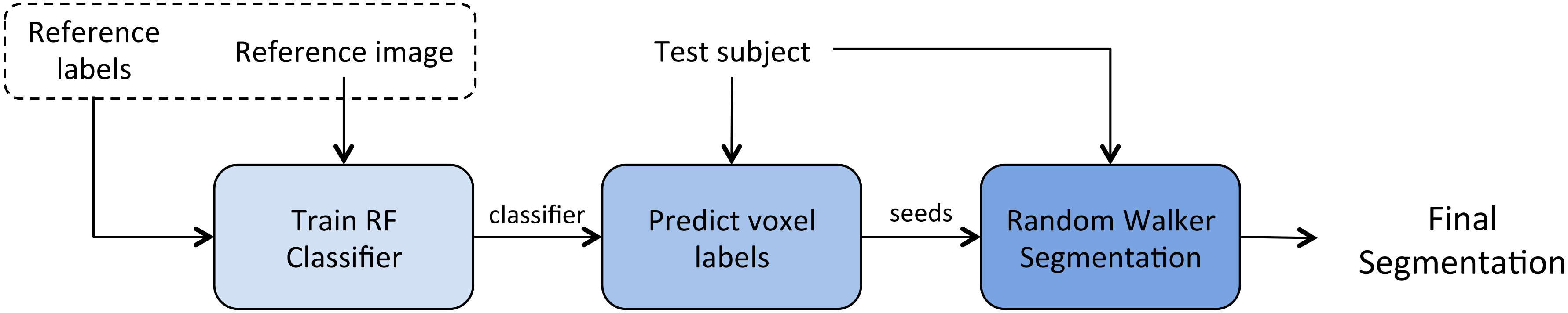

Random Forest (RF)

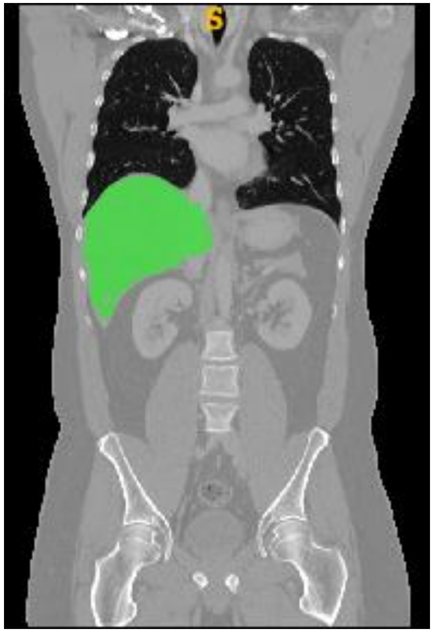

Process all organs in parallel

Random Walker

Automated Segmentation
Results

- **Pipeline enables automated segmentation of large datasets**
  - **Trivially scalable (more images and/or organs)**
  - **Faster images-to-atlas time**
  - **Lower labor cost**

Sample male segmentation results:

“GOOD”

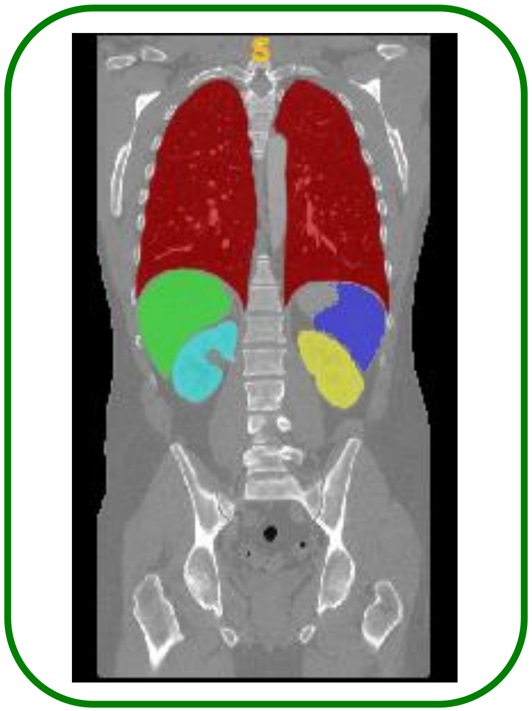

“OK”

“BAD”

Not included in the final atlas

Pipeline Overview

Data Collection/ Preprocessing → Automated Segmentation → **Statistical Atlas Generation**

Multi-Organ Atlas Pipeline

Statistical Atlas Generation Workflow

Mesh Generation | Mesh Alignment | Atlas Creation

Principal Component Analysis (PCA)

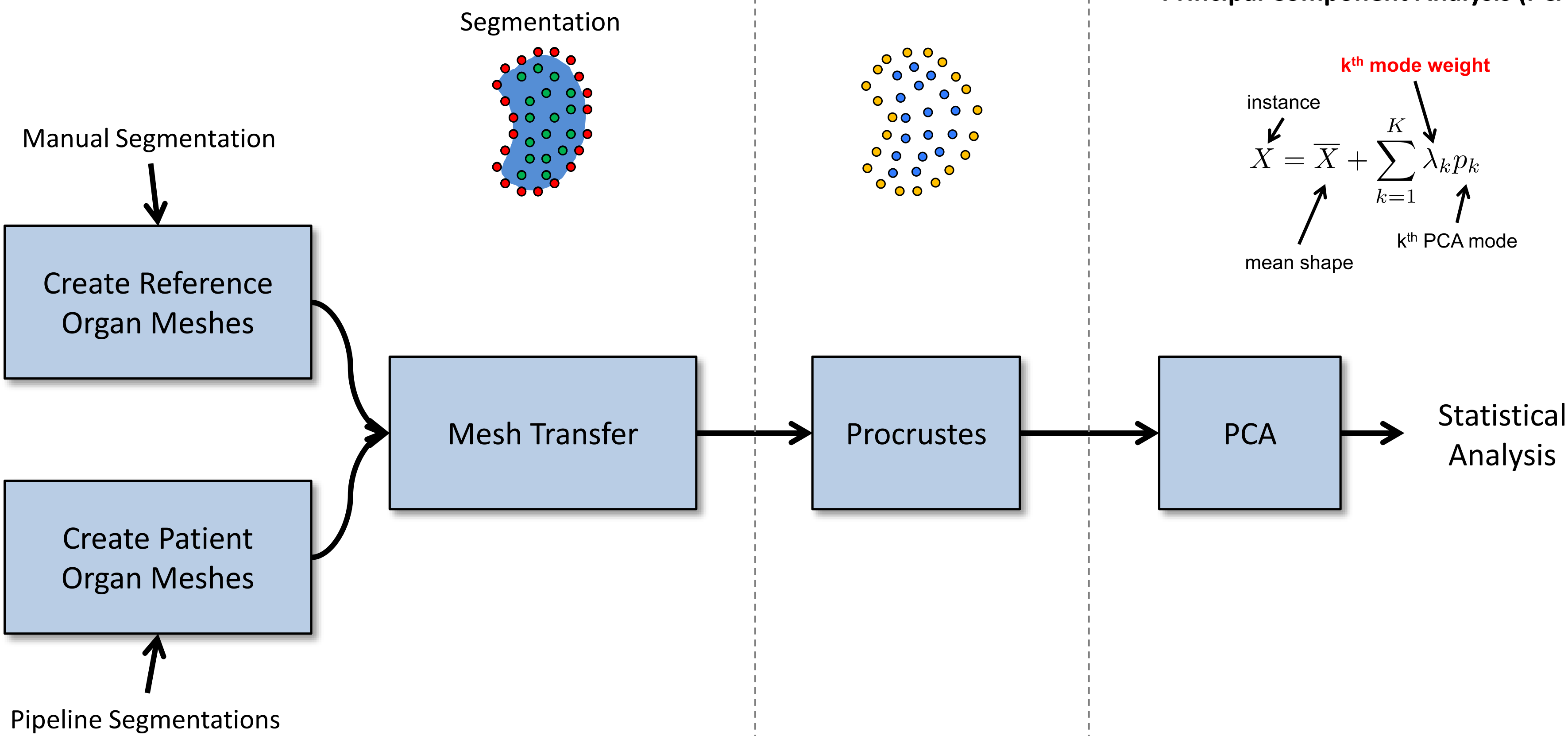

Identify corresponding points on organ segmentation surfaces

Align all point sets

Generate statistical atlas from aligned points

Atlas Generation
Average Geometries

Average Male

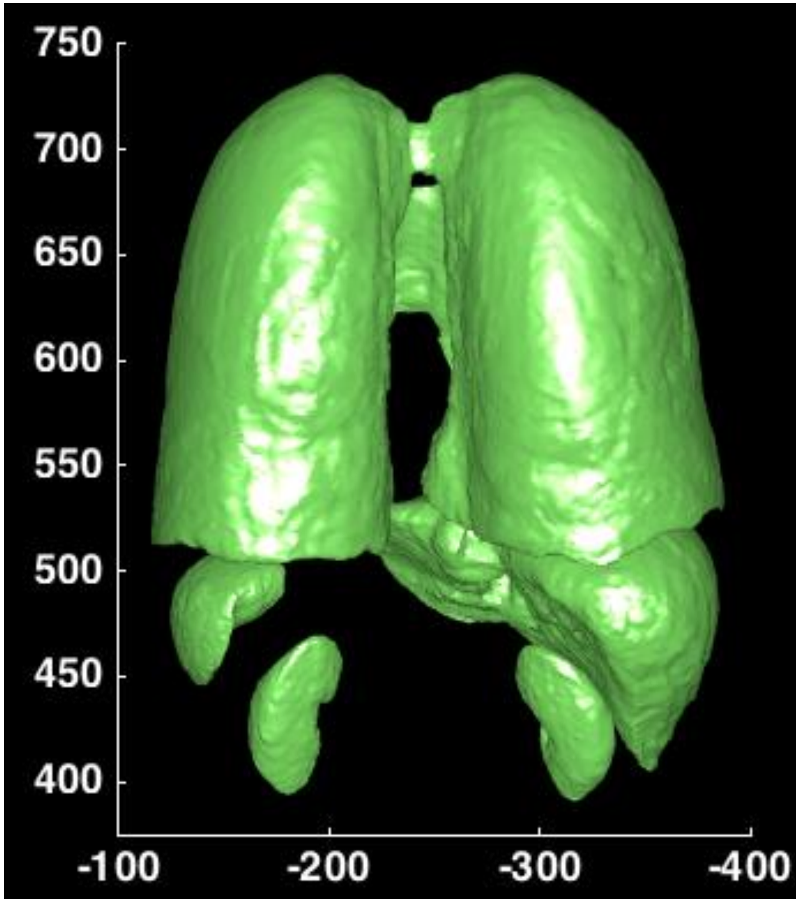

Average Female

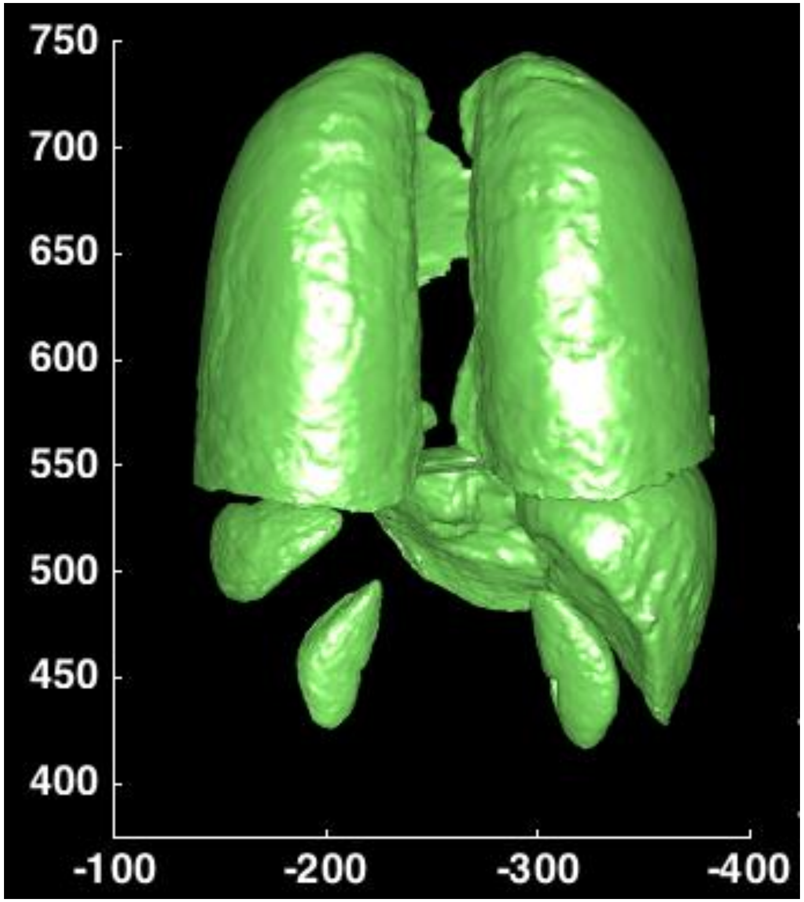

Statistical Atlas Creation
Results

- **PCA identifies major modes of variation**
  - Principal Components (PCs) ranked according to decreasing variance explained
  - Anatomies may be synthesized by computing a weighted sum of the PCs

- **Complex multi-organ geometries make direct interpretation of atlas modes intractable**
  - Deeper statistical analysis required

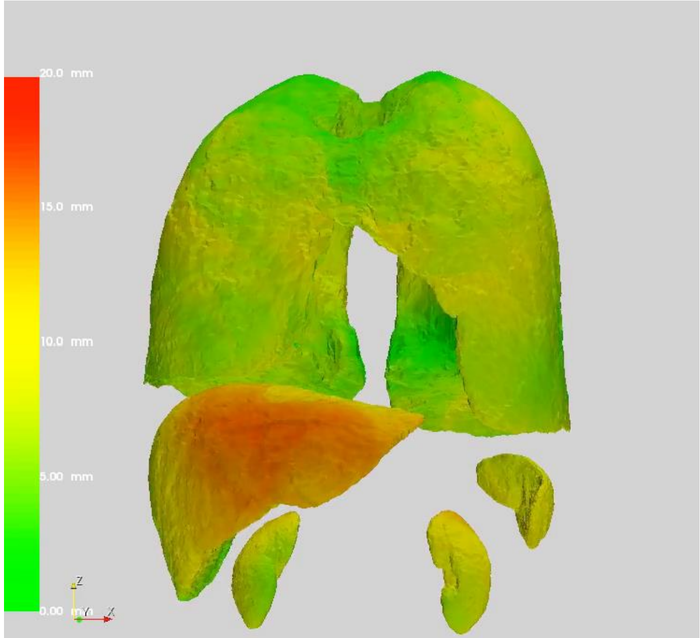

Effects of changing the 1st PC weight

Atlas Generation

Demographic Analysis

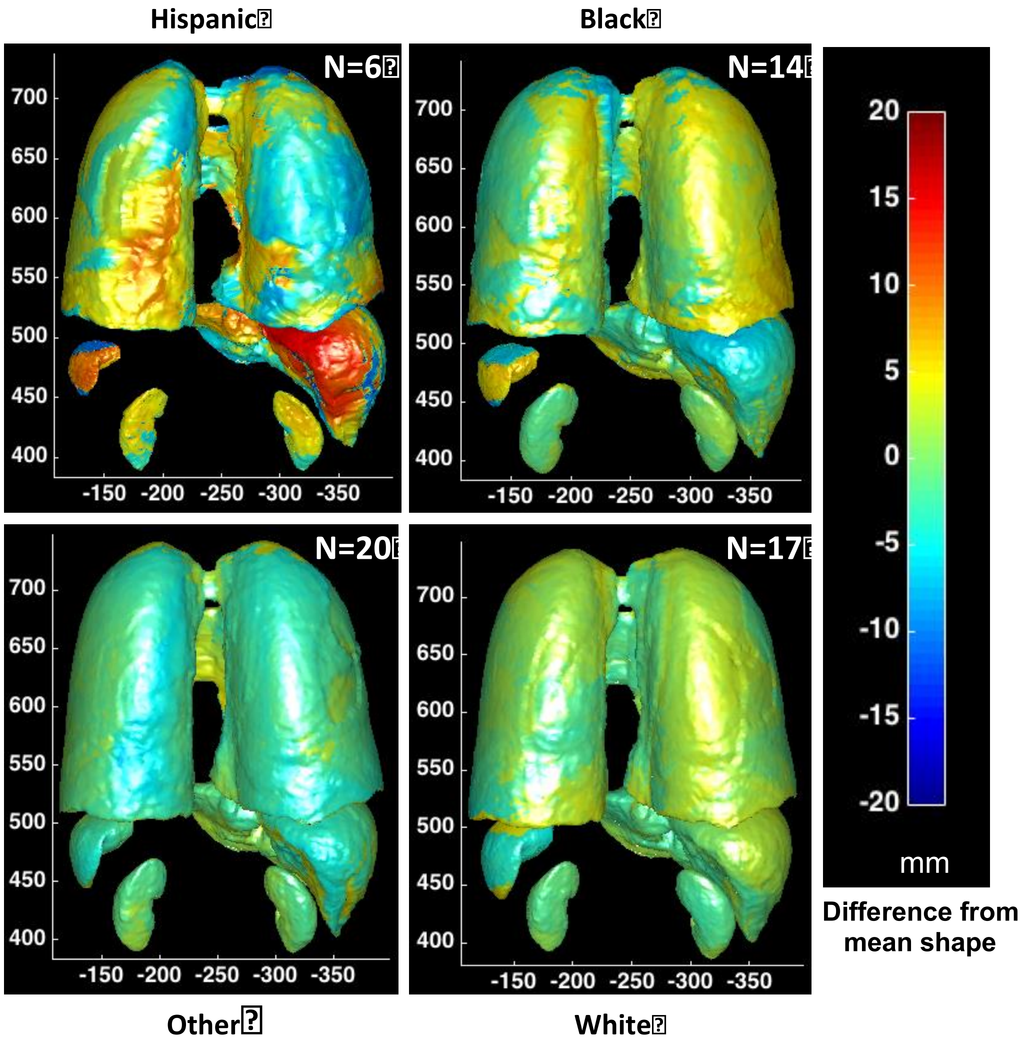

Atlas allows comparison of specific demographics to the average geometry

Statistical Analysis and Prediction

JOHNS HOPKINS
APPLIED PHYSICS LABORATORY

Statistical Analysis

Correlation Analysis

- **Goal: Investigate relationships between external and internal geometries**

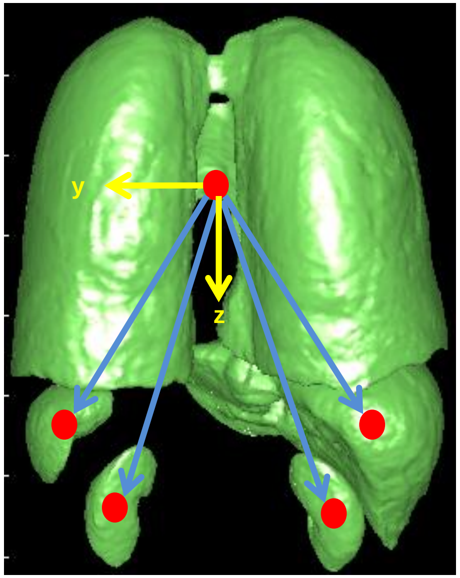

- **Internal metrics:**
  - ***Size –*** Organ volume
  - ***Position –*** Centroid (relative to lung centroid)
  - ***Shape –*** Eccentricities

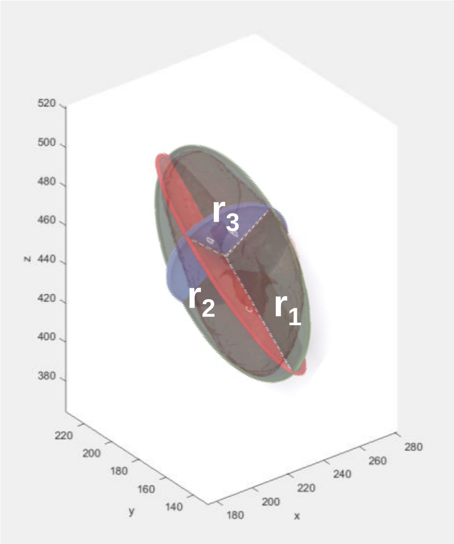

Anthropometric Measurement

Internal Metric

Pearson's Correlation Coefficient $r = \dfrac{\mathrm{cov}(X,Y)}{\sigma_X \sigma_Y} \longrightarrow t = \dfrac{r\sqrt{N-2}}{\sqrt{1-r^2}}$

Statistical significance if $p < 0.05$

Statistical Analysis
Strongest Correlations

Correlation pairs with magnitude >0.5

Lung

Internal	External
Volume	Chest Span CC
Volume	Waist Front Length
Volume	Chest Breadth

Spleen

Internal	External
Centroid z	Chest Span CC

Left Kidney

Internal	External
Volume	Chest Depth
Volume	Weight
Centroid z	Waist Front Length
Centroid y	Chest Depth

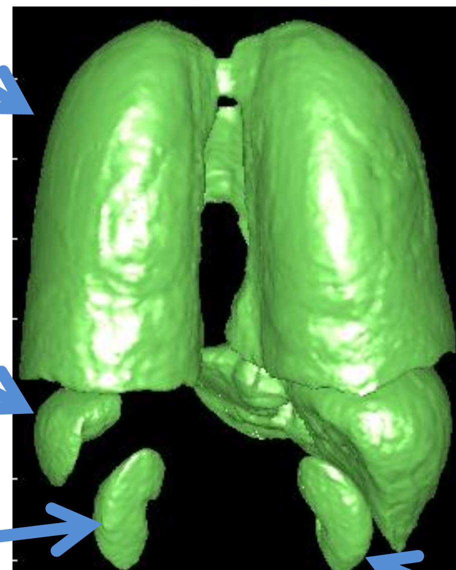

Liver

Internal	External
Volume	Chest Depth
Volume	Weight
Volume	Waist Breadth
Volume	Chest Breadth
Centroid y	Chest Breadth
Centroid y	Weight
Centroid y	Chest Depth
Centroid z	Chest Span CC

Right Kidney

Internal	External
Volume	Chest Depth
Volume	Weight

Organ volume and location show strongest correlation to external measurements

Statistical Analysis
Correlation Analysis

measurement	Percentage (%)
chest depth	23
weight	18
chest breadth	14
chest span cc	14
waist front length	9
waist breadth	5
height	0
bispinous breadth	0

metric	Percentage (%)	
volume	28	
centroid y	13	<--------- Left-Right
centroid z	9	<--------- Inferior-Superior
centroid x	0	<--------- Posterior-Anterior
norm ecc	0	

Percentage = # variable correlations with magnitude > 0.5 / # total variable correlations × 100

Measurements/metrics with higher percentages are better predictors than those with lower percentages.

Statistical Analysis

One-Way Analysis of Variance (ANOVA)

Goal: Examine relationship between measurements/metrics and categorical variables (e.g., ethnicity or sex)

First, use ANOVA to test *if* any group is significantly different from the others

Then, use Tukey's HSD test to find *which* groups are significantly different

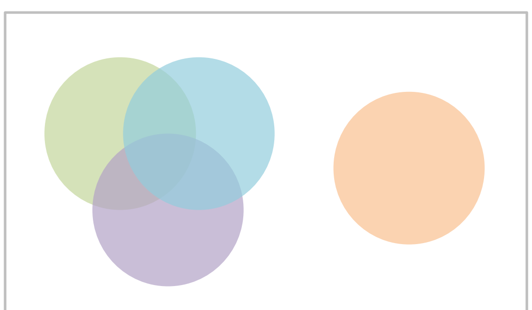

(ANOVA) Any different? ✓

(Tukey's HSD) Which group(s)?

Statistical Analysis
One-Way Analysis of Variance

	Metric	Organ	Sex	Ethnicity
Size	Volume	Lung		
		Liver		
		Spleen		
		Left Kidney		
		Right Kidney		
Position	X	Lung		
		Liver		
		Spleen		
		Left Kidney		
		Right Kidney		
	Y	Lung		
		Liver		
		Spleen		
		Left Kidney		
		Right Kidney		
	Z	Lung		
		Liver		
		Spleen		
		Left Kidney		
		Right Kidney		
Shape	Norm Ecc	Lung		
		Liver		
		Spleen		
		Left Kidney		
		Right Kidney		

Statistically significant difference ($p < 0.05$)

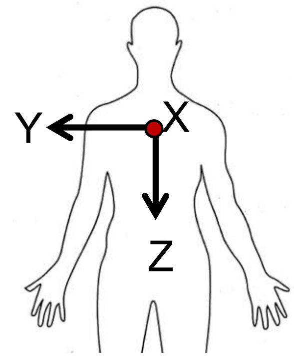

- Significant differences in organ size and Y-Z location across sex

Statistical Analysis
One-Way Analysis of Variance

	Metric	Organ	Sex	Ethnicity
Size	Volume	Lung		
		Liver		
		Spleen		
		Left Kidney		
		Right Kidney		
Position	X	Lung		
		Liver		
		Spleen		
		Left Kidney		
		Right Kidney		
	Y	Lung		
		Liver		
		Spleen		
		Left Kidney		
		Right Kidney		
	Z	Lung		
		Liver		
		Spleen		
		Left Kidney		
		Right Kidney		
Shape	Norm Ecc	Lung		
		Liver		
		Spleen		
		Left Kidney		
		Right Kidney		

Statistically significant difference ($p < 0.05$)

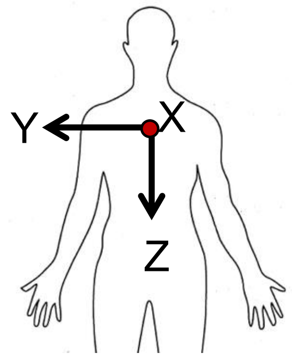

- Significant differences in organ size and Y-Z location across sex
- Vertical organ position, then size, varies most significantly across demographics

Statistical Analysis
One-Way Analysis of Variance

	Metric	Organ	Sex	Ethnicity
Size	Volume	Lung		
		Liver		
		Spleen		
		Left Kidney		
		Right Kidney		
Position	X	Lung		
		Liver		
		Spleen		
		Left Kidney		
		Right Kidney		
	Y	Lung		
		Liver		
		Spleen		
		Left Kidney		
		Right Kidney		
	Z	Lung		
		Liver		
		Spleen		
		Left Kidney		
		Right Kidney		
Shape	Norm Ecc	Lung		
		Liver		
		Spleen		
		Left Kidney		
		Right Kidney		

Statistically significant difference ($p < 0.05$)

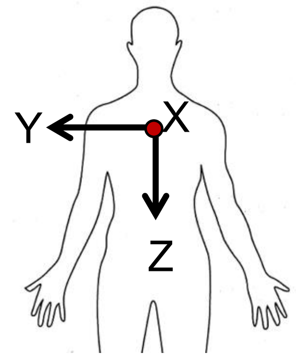

- Significant differences in organ size and Y-Z location across sex
- Vertical organ position, then size, varies most significantly across demographics
- Eccentricity and x-position metrics show least significant variance with demographics
  - Shape descriptor too broad for subtle variations?
  - Supine position influences x-direction results?

Summary & Limitations

- **Successfully developed a *modular*, *scalable*, *automated* segmentation and atlas generation pipeline**
  - **Enables large-scale batch processing for expanded statistical shape atlases**
  - **Computer vision algorithms developed to simultaneously segment multiple organ geometries**

- **Analyses identify statistically significant correlations and demographic differences**
  - **Chest depth most broadly correlated metric, followed by weight**
  - **Height was not significant for analyzed organ geometry metrics**
  - **Gender and ethnicity both important for organ volume and z-position**

- **Limitations**
  - **Small dataset limits ability to model complexity of human anatomy**
  - **Automated segmentation inaccuracies further reduce dataset size**
  - **Analysis does not control for multiple variables (e.g., variation in organ shape, size, or location for males and females of the same stature)**

Potential Applications & Next Steps

- **Use multi-organ atlas to predict an individual's internal anatomy based solely on external characteristics**
- **Develop Finite Element Models from atlas for modeling & simulation applications, enabled by rapid novel meshing approach**
- **Support design analysis tools for optimized armor coverage, placement, & sizing for range of demographics and anthropometries**

Subject Information

Measurement	*Units*	*Value*
Sex		Male
Age bin		21-24
Race		Other
Height	m	1.60
Weight	kg	73.0
Chest depth	cm	22.1
Chest breadth	cm	31.4
Chest span cc	cm	30.0
Waist front length	cm	36.5
Bispinous breadth	cm	26.7
Waist breadth	cm	32.6

Internal Organ Prediction

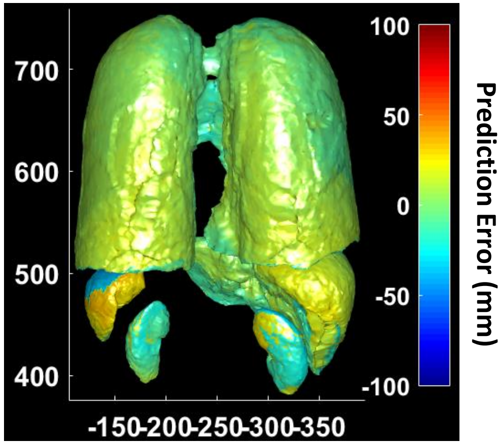

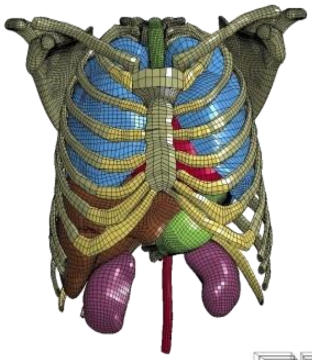

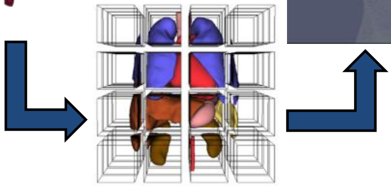

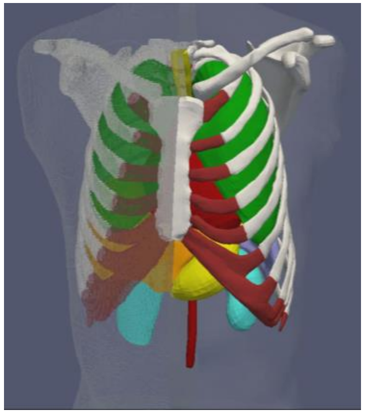

Computational Pipeline Enabling the Generation of Multi-Organ Statistical Atlases for Improved Human Model Development

January 14, 2016

Project Team:
Nathan Drenkow[1], Jason Harper[1], Nathanael Kuo[1], Manuel Uy[1], Catherine Carneal[1], Andrew Merkle[1], Gaurav Thawait[2], Jan Fritz[2], Brian Corner[3], Michael Maffeo[3]

[1]JHU Applied Physics Laboratory
[2]JHU Medical Institute
[3]Army Soldier System Center (Natick)

U.S. ARMY RDECOM

ARL

Mechanical Response of Human and Animal Bones: Overview of ARL Experimental Research

Tusit Weerasooriya, C. Allan Gunnarsson, and Stephen Alexander*
and Brett Sanborn (now at Sandia National Laboratory), Ann Mae DiLeonardi

US Army Research Laboratory
*** TKC Global Solutions, Herndon, VA 20171**

The research reported in this document was performed in connection with contract/instrument W911-QX-14-C0016 with the U.S. Army Research Laboratory. The views and conclusions contained in this document are those of TKC Global Inc. and the U.S. Army Research Laboratory. Citation of manufacturer's or trade names does not constitute an official endorsement or approval of the use thereof. The U.S. Government is authorized to reproduce and distribute reprints for Government purposes notwithstanding any copyright notation hereon

Summary of ARL experimental bone research

- Human femur - cortical
  - Fracture
  - Deformation
  - Microstructural quantification
- Minipig and Human Skull
  - Microstructural quantification
  - Deformation

Human Cortical Femur Bone Fracture

Fracture of Cortical Bone

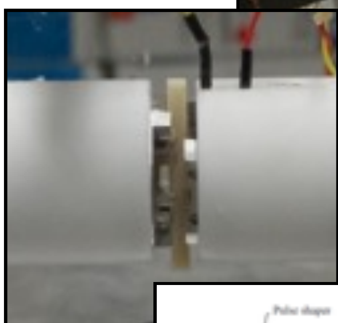

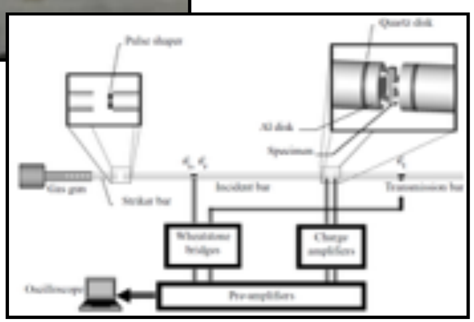

Fracture Experimentation

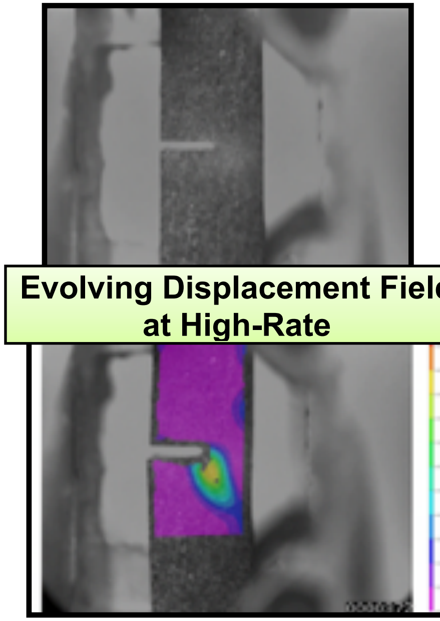

Evolving Displacement Field at High-Rate

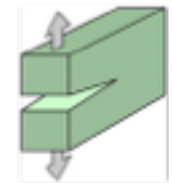

MODE I -Tensile

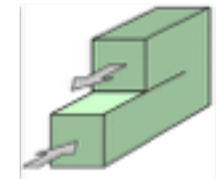

MODE II -Shear

Fracture Modes

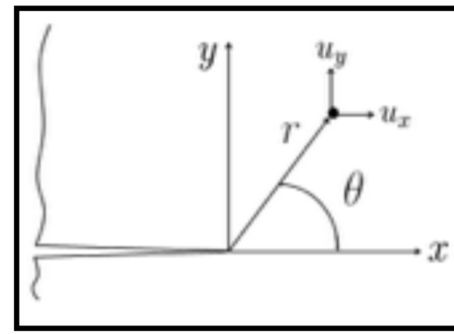

$$u_x = \sum_{n=1}^{N} \frac{(K_{\mathrm{I}})_n}{2\mu} \frac{r^{n/2}}{\sqrt{2\pi}} \left\{ \kappa \cos\frac{n}{2}\theta - \frac{n}{2}\cos\left(\frac{n}{2}-2\right)\theta + \left\{\frac{n}{2}+(-1)^n\right\}\cos\frac{n}{2}\theta \right\} + \sum_{n=1}^{N} \frac{(K_{\mathrm{II}})_n}{2\mu} \frac{r^{n/2}}{\sqrt{2\pi}} \left\{ \kappa \sin\frac{n}{2}\theta - \frac{n}{2}\sin\left(\frac{n}{2}-2\right)\theta + \left\{\frac{n}{2}-(-1)^n\right\}\sin\frac{n}{2}\theta \right\},$$

$$u_y = \sum_{n=1}^{N} \frac{(K_{\mathrm{I}})_n}{2\mu} \frac{r^{n/2}}{\sqrt{2\pi}} \left\{ \kappa \sin\frac{n}{2}\theta + \frac{n}{2}\sin\left(\frac{n}{2}-2\right)\theta - \left\{\frac{n}{2}+(-1)^n\right\}\sin\frac{n}{2}\theta \right\} + \sum_{n=1}^{N} \frac{(K_{\mathrm{II}})_n}{2\mu} \frac{r^{n/2}}{\sqrt{2\pi}} \left\{ -\kappa \cos\frac{n}{2}\theta - \frac{n}{2}\cos\left(\frac{n}{2}-2\right)\theta + \left\{\frac{n}{2}-(-1)^n\right\}\cos\frac{n}{2}\theta \right\},$$

Crack-tip Field for Stationary Crack

Different Fracture of Criteria (assuming isotropic)

Fracture Toughness vs K_dot

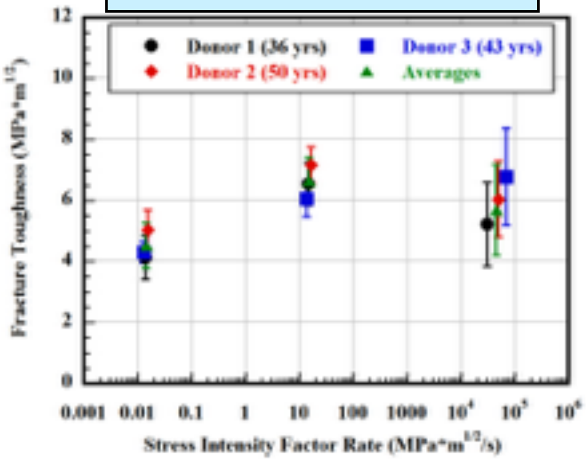

Critical max Strain for Crack Initiation

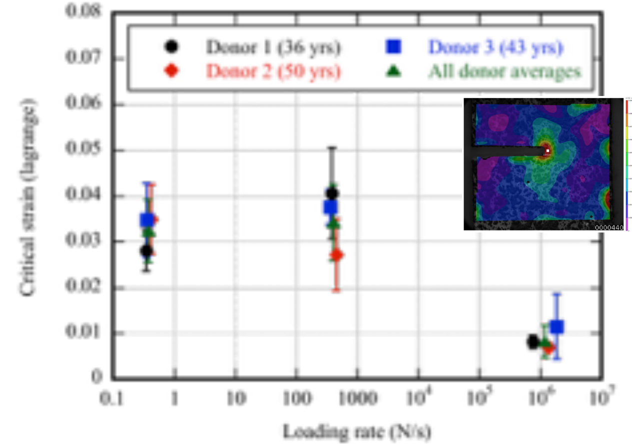

Fracture Toughness vs K_dot Comparison with Bovine and Equine

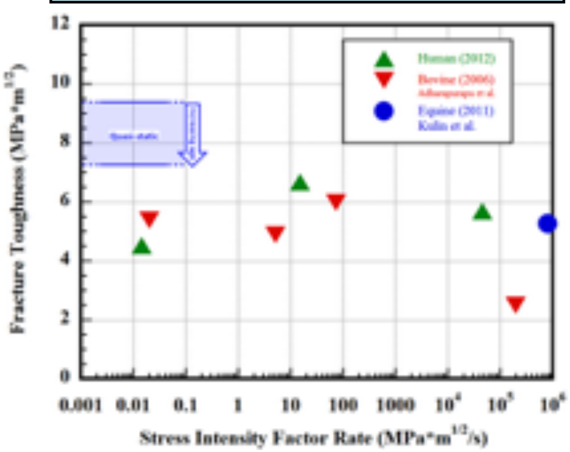

Critical Energy to Crack Propagation

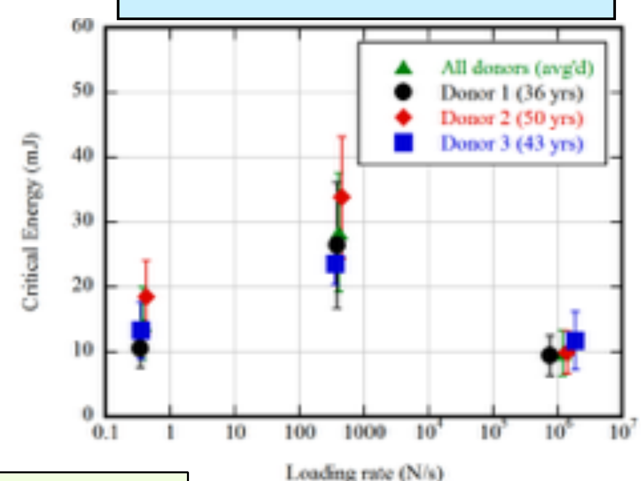

Fracture Criteria (assuming isotropic)

U.S. ARMY RDECOM

Mixed Mode Fracture of Cortical Bone (anisotropic)

ARL

Crack Initiation Mechanism Maps for Human Cortical Bone

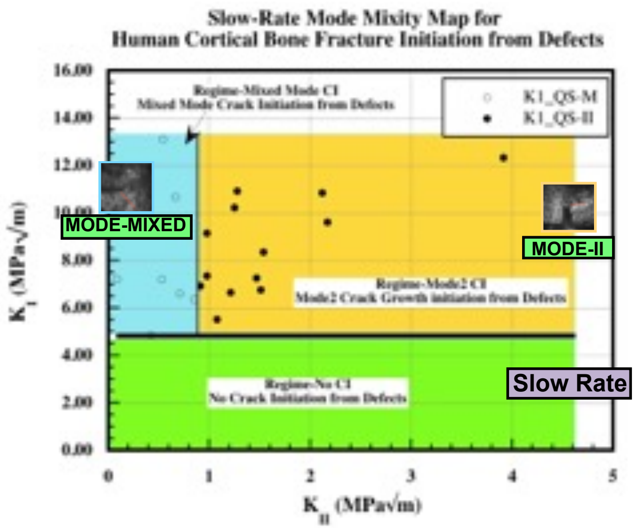

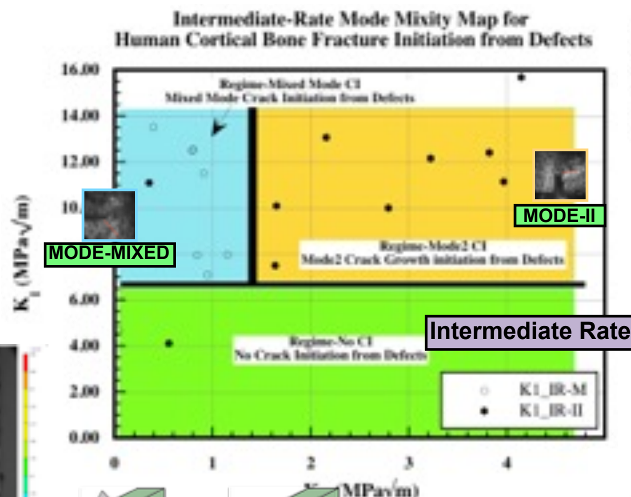

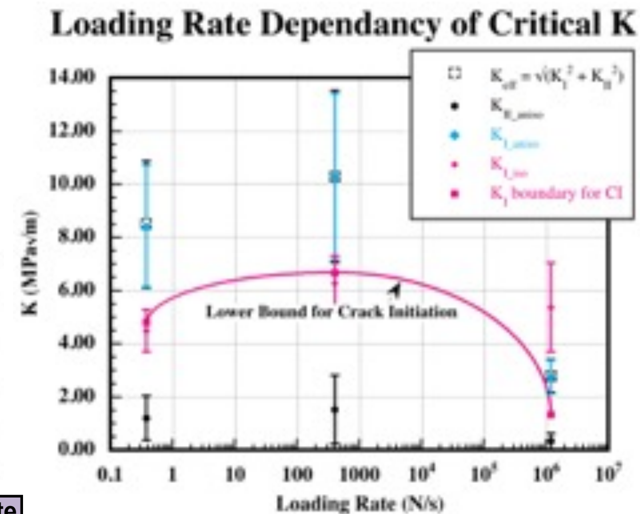

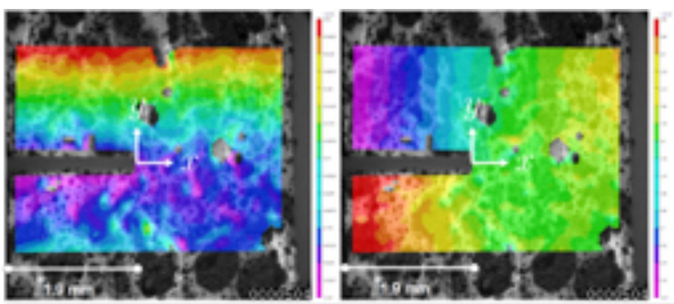

1L-A-4 u_x displacement field

1L-A-4 u_y displacement field

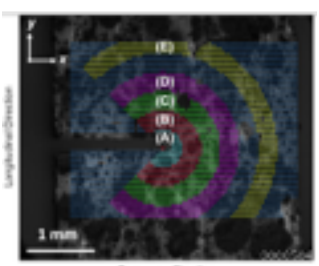

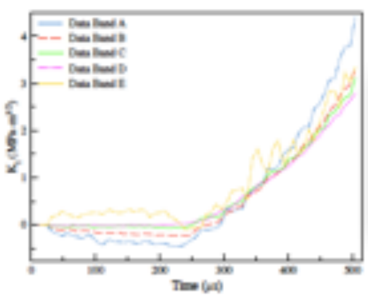

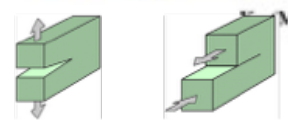

MODE I -Tensile

MODE II -Shear

Fracture Modes

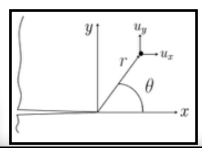

$$u_x = \sum_{n=1}^{N} \frac{(K_I)_n}{2\mu} \frac{r^{n/2}}{\sqrt{2\pi}} \left\{ \kappa \cos\frac{n}{2}\theta - \frac{n}{2}\cos\left(\frac{n}{2}-2\right)\theta + \left\{\frac{n}{2}+(-1)^n\right\}\cos\frac{n}{2}\theta \right\} + \sum_{n=1}^{N} \frac{(K_{II})_n}{2\mu} \frac{r^{n/2}}{\sqrt{2\pi}} \left\{ \kappa \sin\frac{n}{2}\theta - \frac{n}{2}\sin\left(\frac{n}{2}-2\right)\theta + \left\{\frac{n}{2}-(-1)^n\right\}\sin\frac{n}{2}\theta \right\},$$

$$u_y = \sum_{n=1}^{N} \frac{(K_I)_n}{2\mu} \frac{r^{n/2}}{\sqrt{2\pi}} \left\{ \kappa \sin\frac{n}{2}\theta + \frac{n}{2}\sin\left(\frac{n}{2}-2\right)\theta - \left\{\frac{n}{2}+(-1)^n\right\}\sin\frac{n}{2}\theta \right\} + \sum_{n=1}^{N} \frac{(K_{II})_n}{2\mu} \frac{r^{n/2}}{\sqrt{2\pi}} \left\{ -\kappa \cos\frac{n}{2}\theta - \frac{n}{2}\cos\left(\frac{n}{2}-2\right)\theta + \left\{\frac{n}{2}-(-1)^n\right\}\cos\frac{n}{2}\theta \right\},$$

Crack-tip Field for Stationary Crack

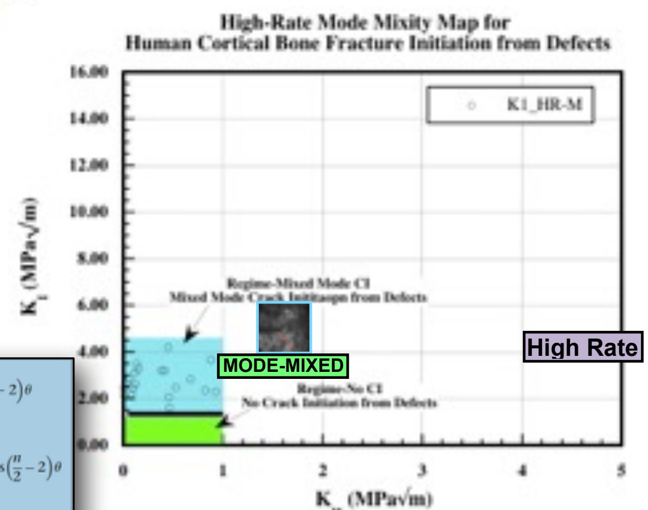

U.S. ARMY RDECOM

Deformation Response, Cracking Mechanisms, Microstructural Variability

ARL

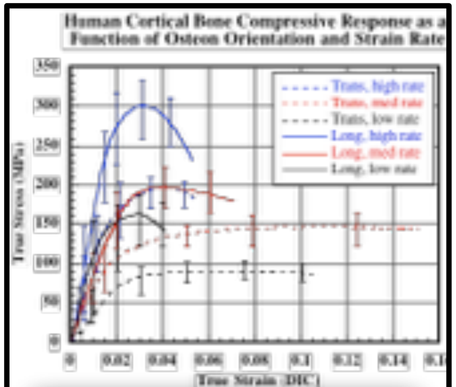

COMPRESSIVE RESPONSE (at different Loading

Compressive Response was Obtained as a Function Loading Rate and Direction

Crack Initiation and Growth Mechanisms

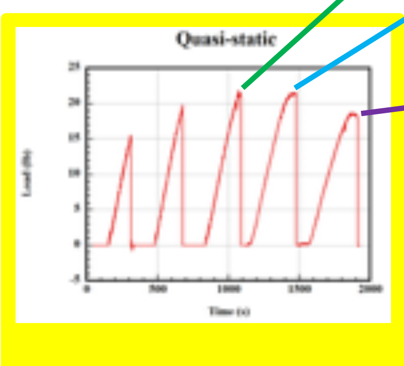

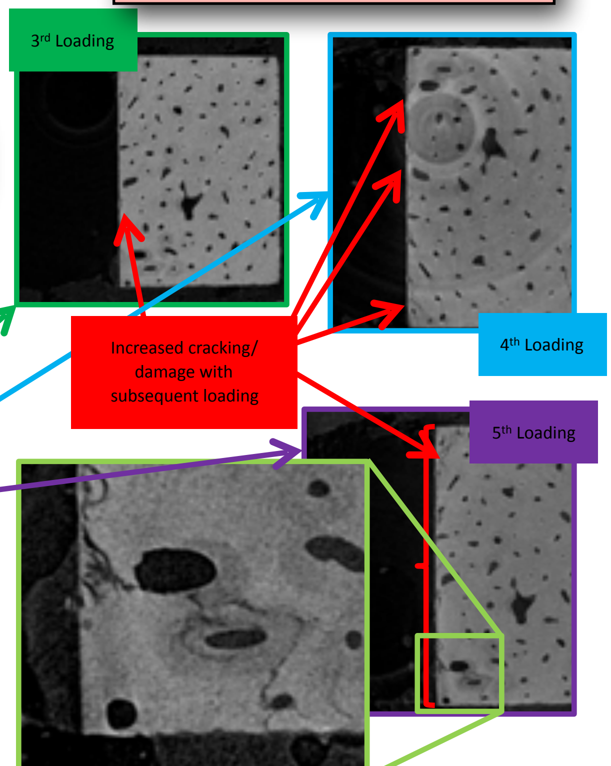

Quantification of Microstructural Variability

Donor	Age	Osteonal Areal Density		TMD		Cortical Bone Porosity	
		Average (#/mm^2)	Standard Deviation	Average (g/cm^3)	Standard Deviation	Average (%)	Standard Deviation
1	36	8.54	0.44	1.42	0.09	93.69	3.47
2	50	8.67	0.63	1.33	0.05	93.29	0.96
3	43	11.83	0.72	1.44	0.10	93.00	0.99

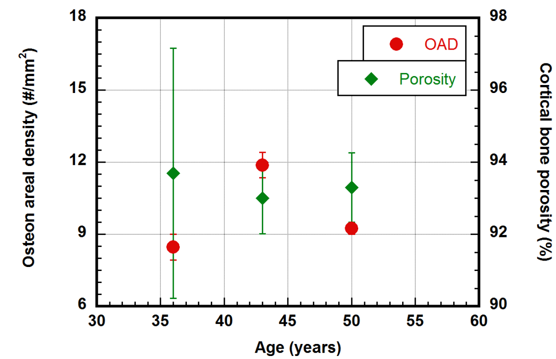

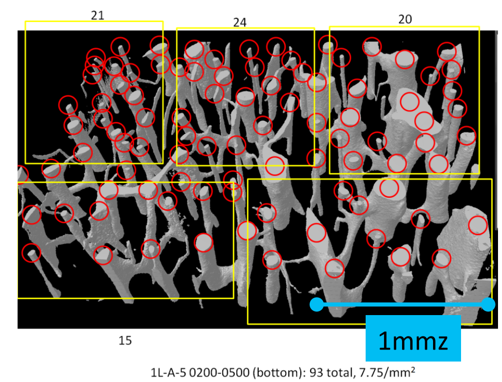

U.S. ARMY RDECOM

ARL

Minipig Skull Microstructural Quantification and Rate Dependent Deformation

U.S. ARMY RDECOM

Microstructural Quantification

ARL

SPECIMENS

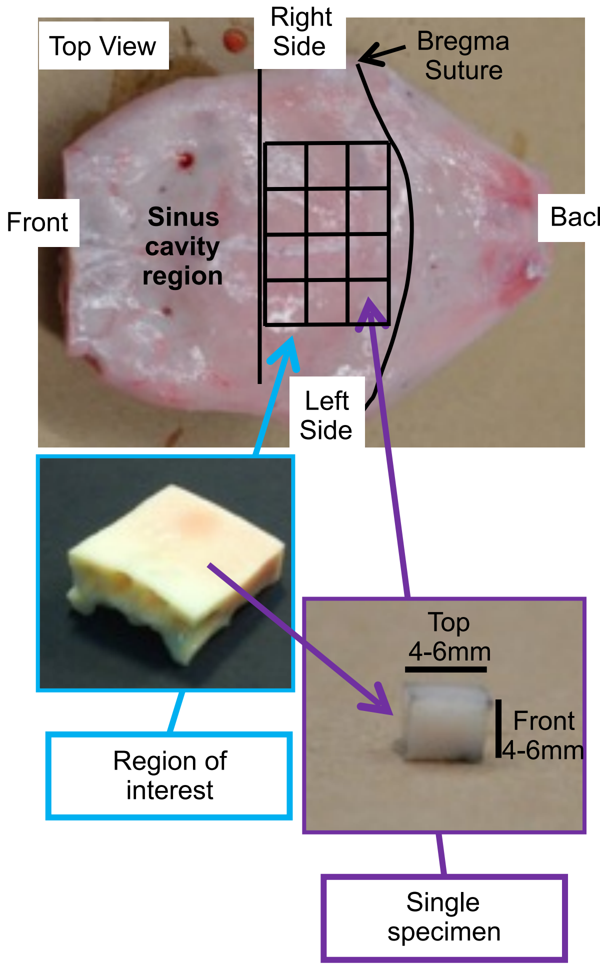

Porosity

Ratio of pores (voids) to total volume, expressed as a percentage

- Porosity = # of black pixels / total # of pixels within area of interest (red square)

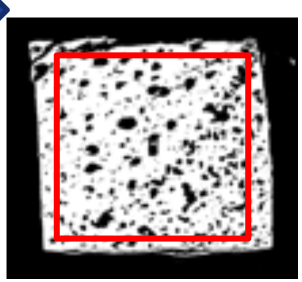

Structural Separation

A value for the distance separating the bone (aka a value for the thickness of the void), averaged over the entire 2D slice.

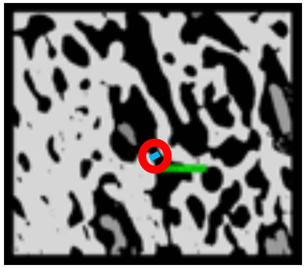

Structural Thickness

A value for the thickness of the bone averaged over the entire 2D slice.

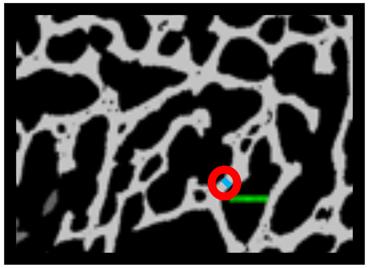

These three parameters were measured as a function of location (brain to skin) throughout the region of interest of the skull.

Structure Changes as a Function of Location within Thickness

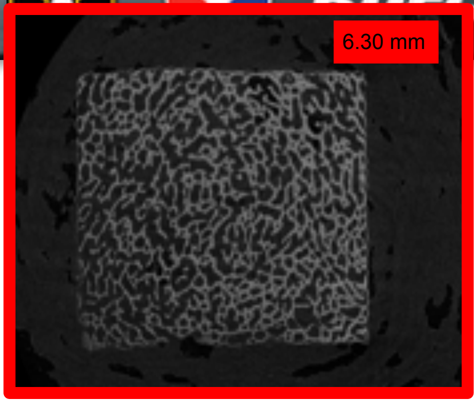

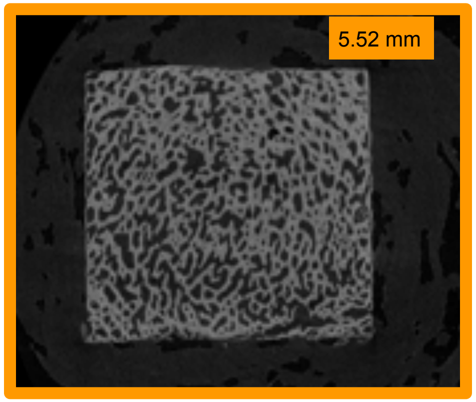

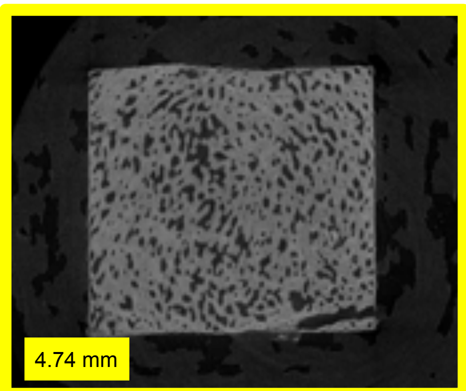

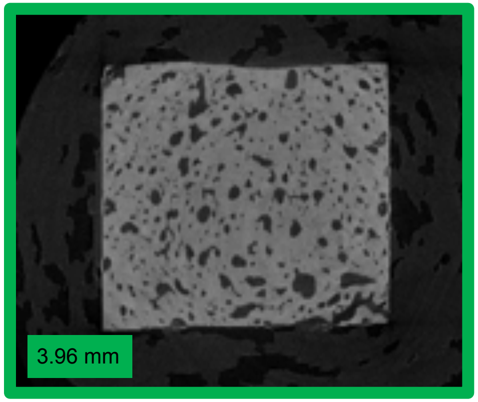

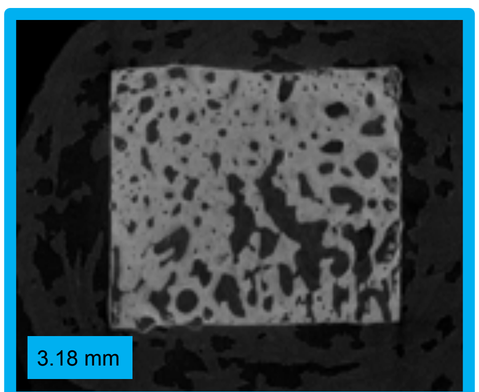

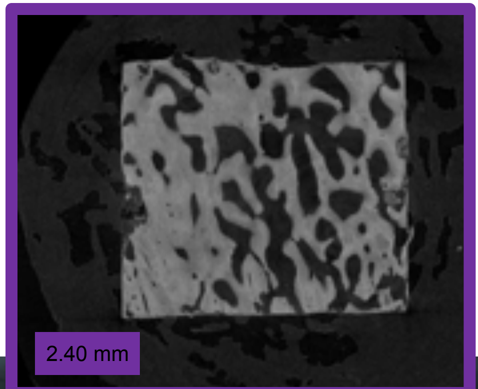

Top views (cross sections) at various heights

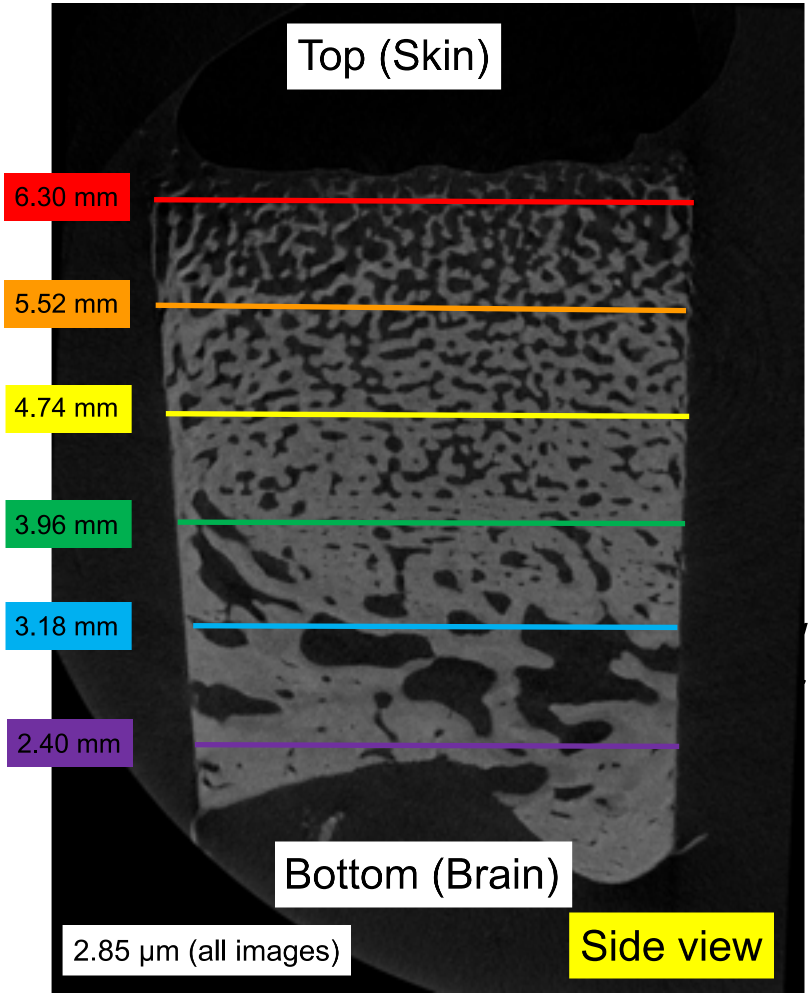

Side view

U.S. ARMY RDECOM

Structural Quantification Averaged Over the Thickness

ARL

Skull	Porosity	Structural Separation	Structural Thickness

MP14004

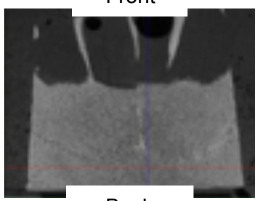

MP14005

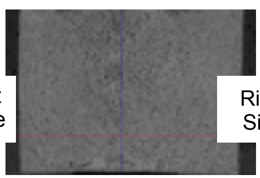

MP14006

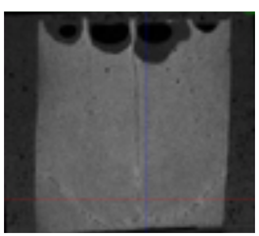

Front to Back

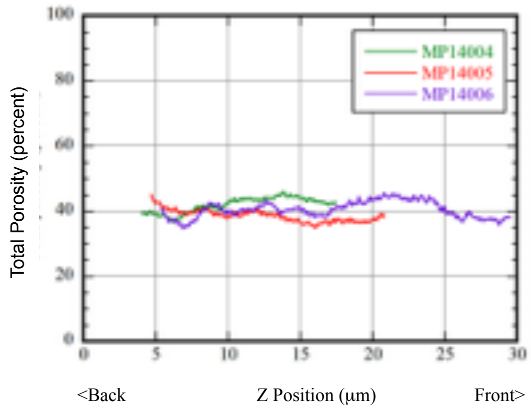

Front to Back

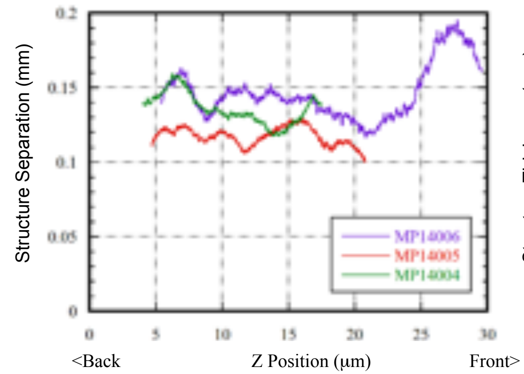

Front to Back

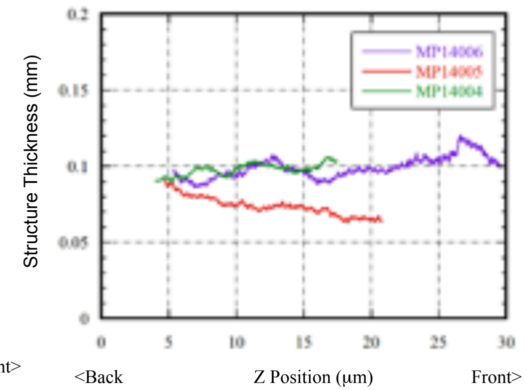

Left to Right

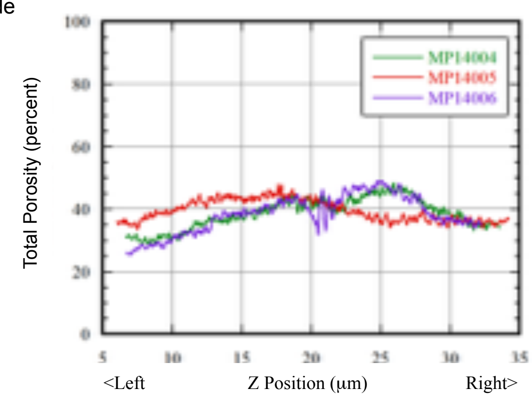

Left to Right

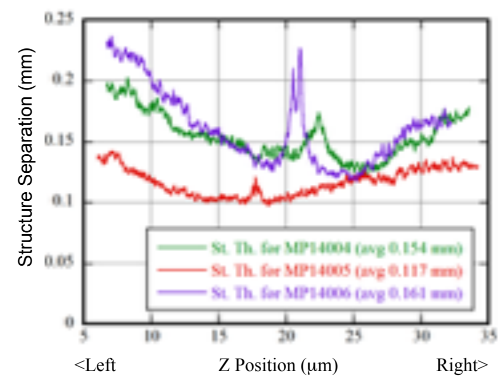

Left to Right

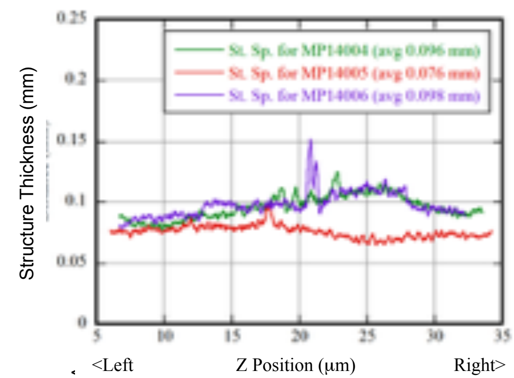

Porosity, structural separation and structural thickness were relatively similar from front to back, side to side and skull to skull across the regions of interest. Peaks indicate suture lines.

U.S. ARMY RDECOM

Structural Quantification for Individual Specimens

ARL

Porosity

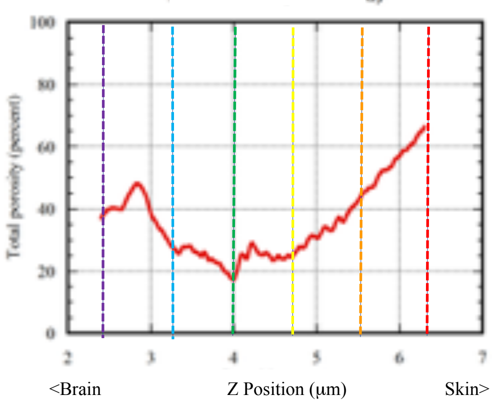

Structural Separation

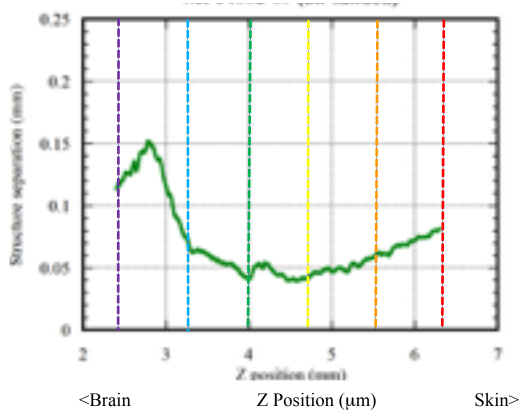

Structural Thickness

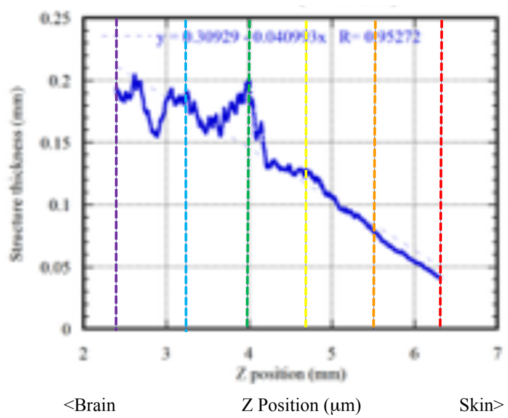

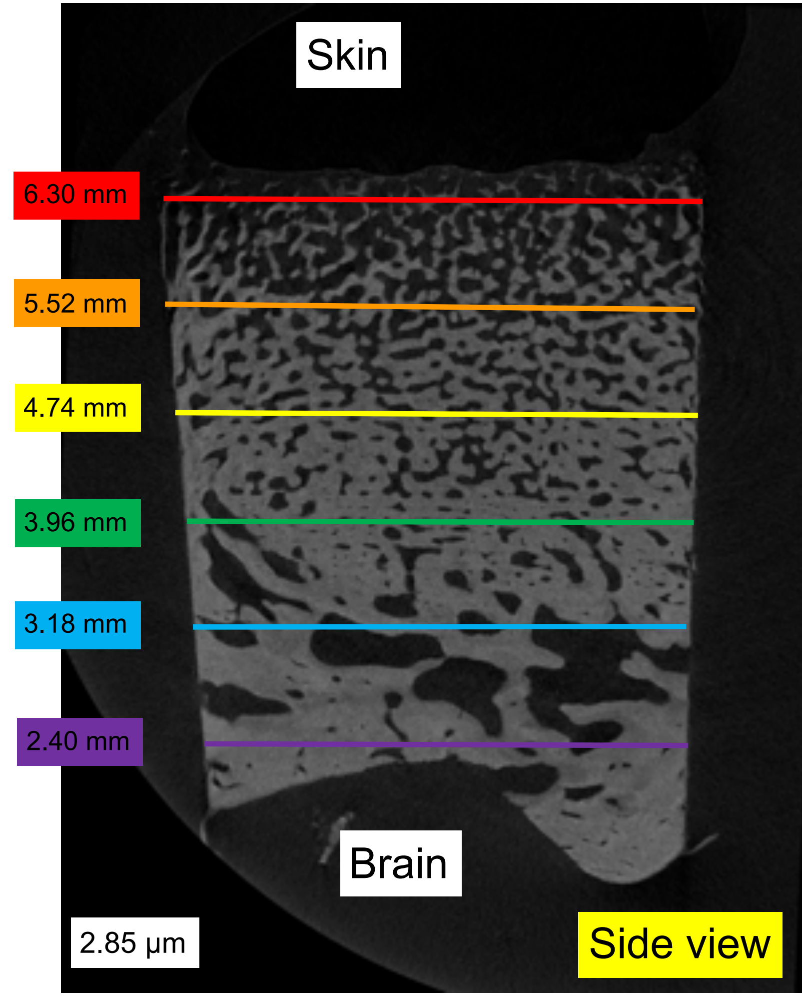

Microstructure changes as a function of depth through the skull and is more porous closer to skin of the skull

Compression Experiments

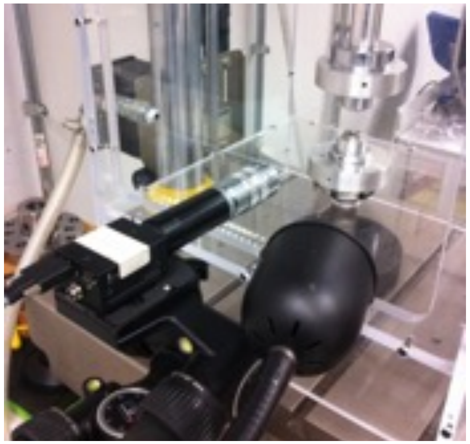

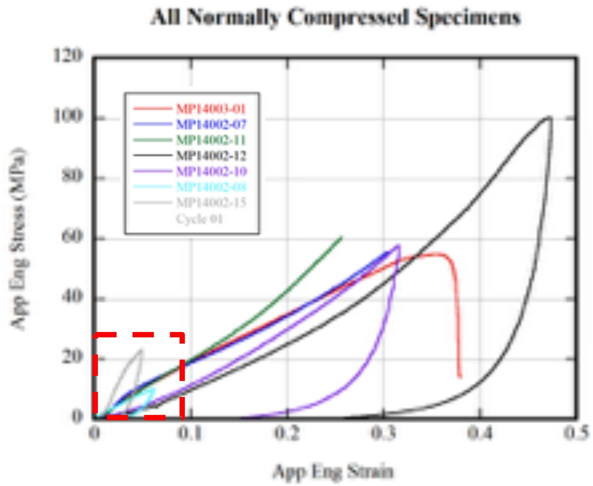

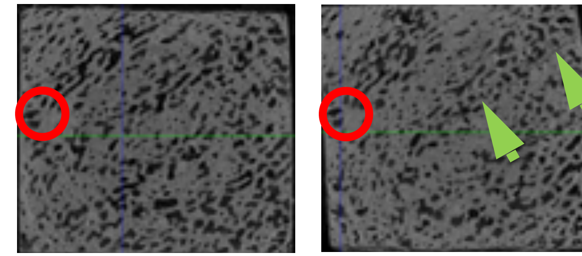

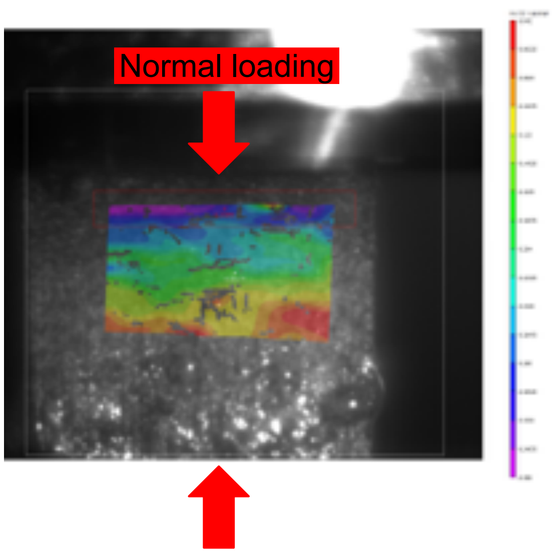

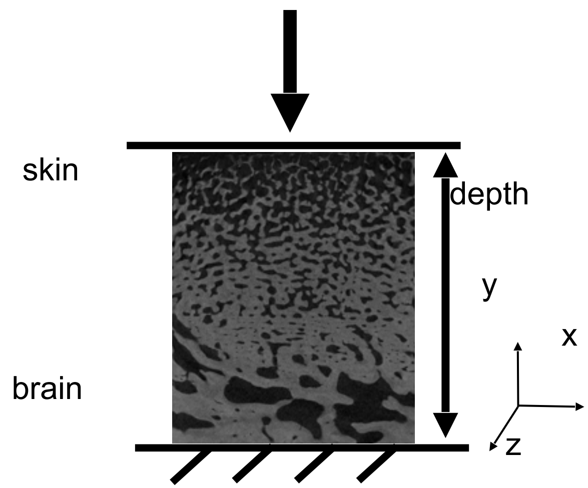

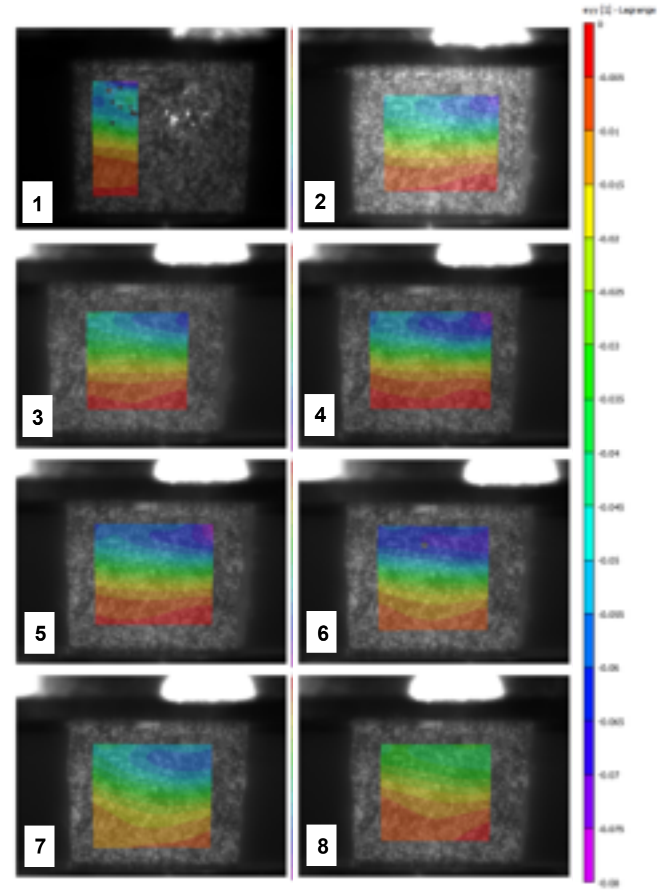

U.S. ARMY RDECOM

Relating microstructure and mechanical response

ARL

- Stress-strain response for each layer

4 specimens:
02-07
02-08
02-11
02-15

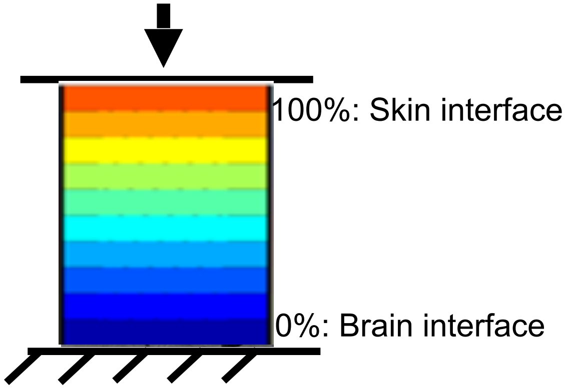

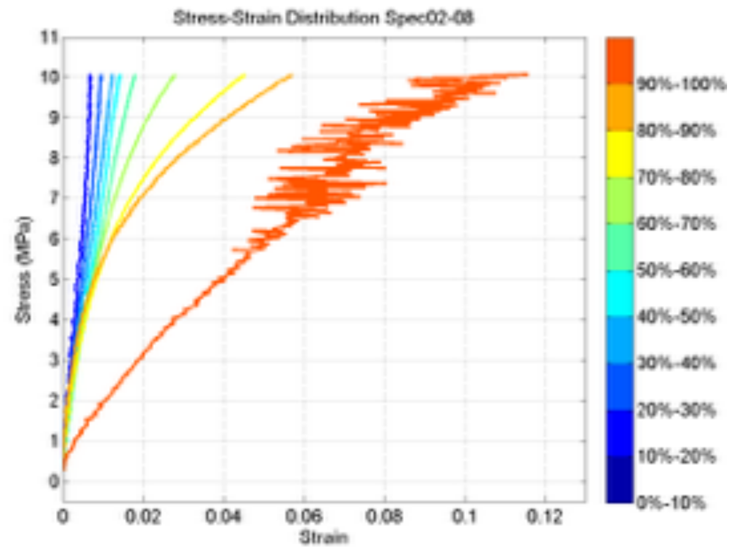

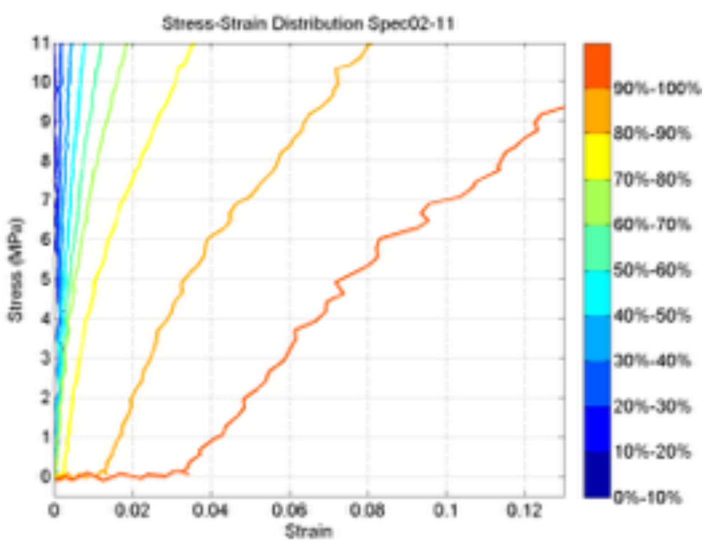

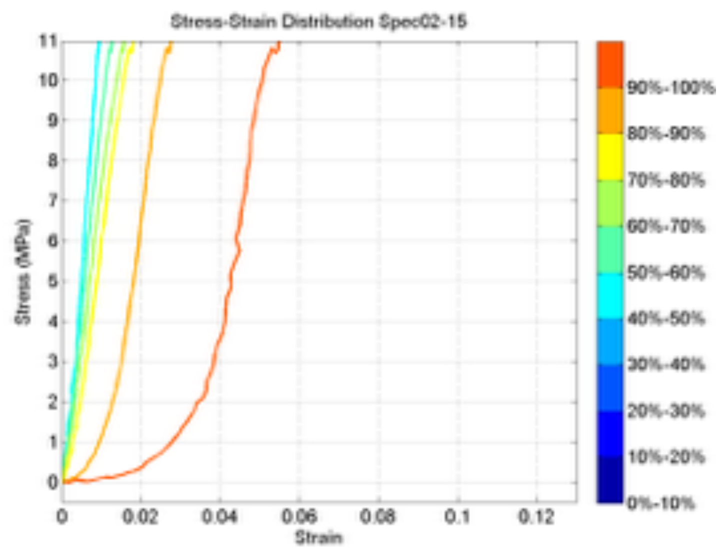

- **Fitting phenomenological model:** Predicting modulus from BV/TV and MIL data using model from lit[1]

Anisotropic within a layer:

$$E(f_{bv}, \boldsymbol{M}) = \frac{E_0 {f_{bv}}^k}{\sum_{i=1}^{3} \frac{{M_{33}^i}^2}{m_i^{2l}} + \zeta_0 \sum_{i<j=1}^{3} \frac{M_{33}^i M_{33}^j}{m_i^l m_j^l}}$$

BV/TV is depth-dependent. Used discrete values for each of the 10 layers

Isotropic within a layer:

$$E(f_{bv}, \boldsymbol{M}) = \frac{E_0 {f_{bv}}^k}{\sum_{i=1}^{3} \frac{{M_{33}^i}^2}{m_i^{2l}} + \zeta_0 \sum_{i<j=1}^{3} \frac{M_{33}^i M_{33}^j}{m_i^l m_j^l}}$$

~1

Orientation (MIL tensor) is not depth-dependent. Single value for the whole specimen

$$E = E_0 {f_{BV}}^k$$

$\mathbf{E_0}$ is the modulus of the bone material

1. Matsuura, Maiko, et al. "The role of fabric in the quasi-static compressive mechanical properties of human trabecular bone from various anatomical locations." *Biomechanics and modeling in mechanobiology* 7.1 (2008): 27-42.

Relating microstructure and mechanical response

- **Phenomenological modeling:** Results
  - Accounting for orientation (anisotropy) improves fit by only ~7%

	k	*L*	E0	Function Minimum
Anisotropic	3.097	0.015	3.031 GPa	3.90E+11 (7% lower than isotropic)
Isotropic	2.919	(none)	3.043 GPa	4.17E+11

$$E(f_{bv}, M) = \frac{E_0 f_{bv}{}^{k}}{\sum_{i=1}^{3} \frac{M_{33}^{i}{}^{2}}{m_i^{2l}} + \zeta_0 \sum_{i<j=1}^{3} \frac{M_{33}^{i} M_{33}^{j}}{m_i^{l} m_j^{l}}}$$

$$\boxed{E = 3043 f_{BV}{}^{2.919}}$$

Modulus as a function of bone volume fraction

Initial Modulus of Cortical Femur = 3.6±1.4 GPa

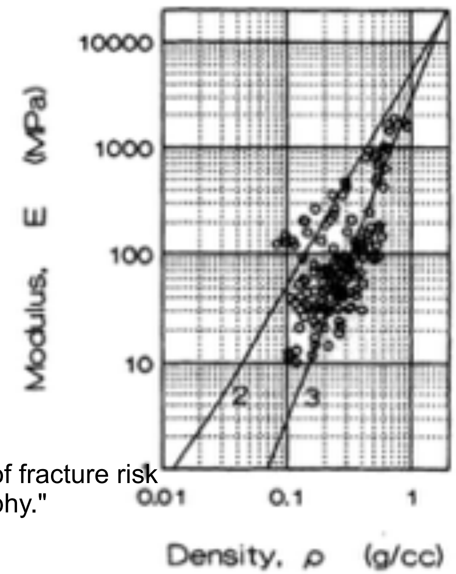

Hayes, Wilson C., S. J. Piazza, and P. K. Zysset. "Biomechanics of fracture risk prediction of the hip and spine by quantitative computed tomography." *Radiologic Clinics of North America* 29.1 (1991): 1-18.

Accounting for Anisotropy: Layer Anisotropy vs Isotropy compared to experimental data

Results:

4 specimens:
02-07
02-08
02-11
02-15

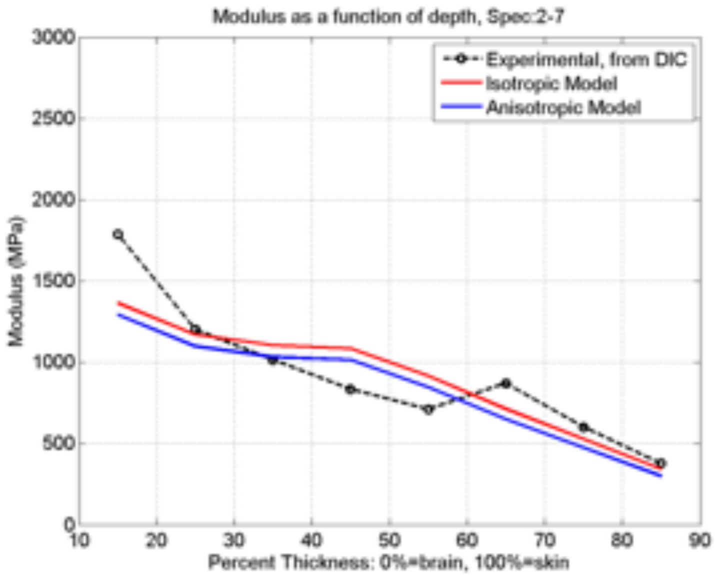

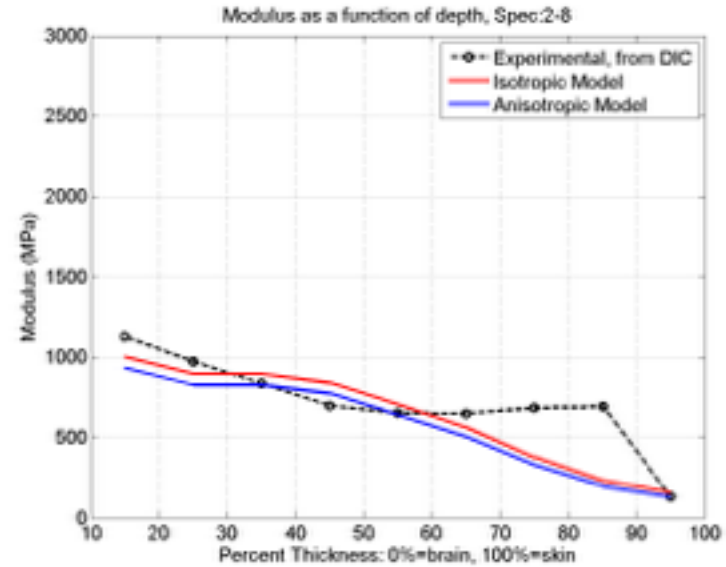

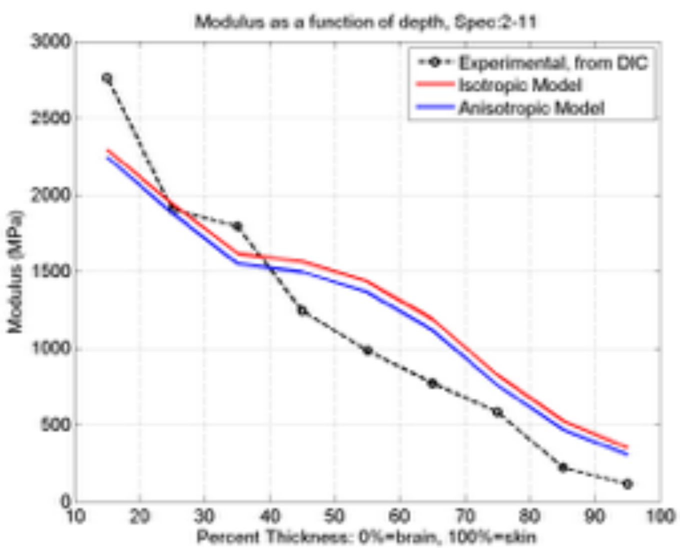

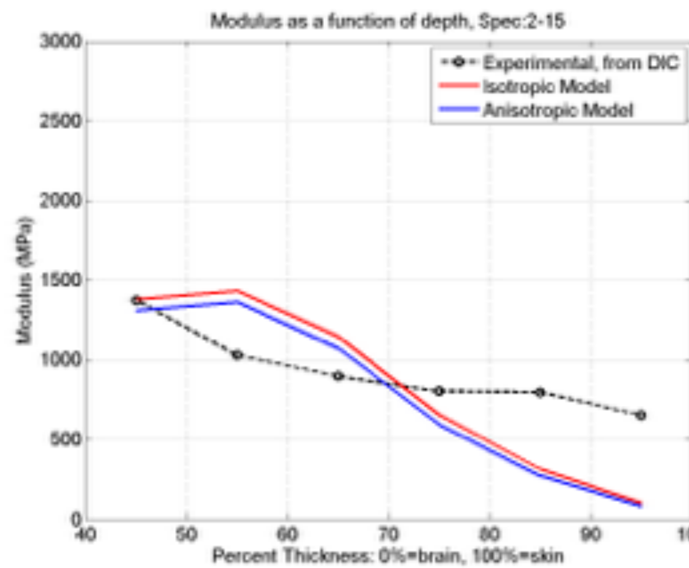

Relating microstructure and mechanical response

- Obtaining depth-dependent modulus for cohort
  - Applied isotropic results to BV/TV averages

porosity averages over all specimens:

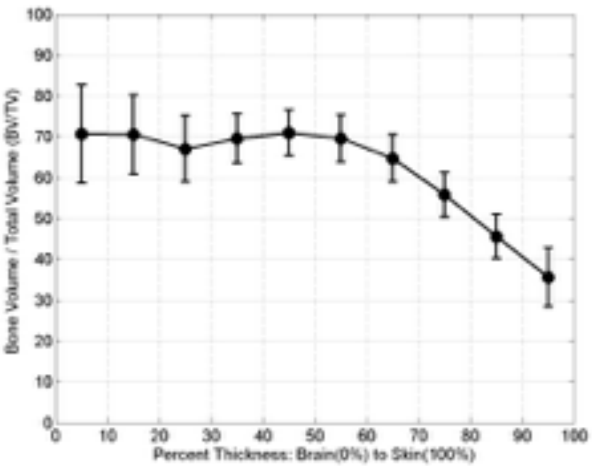

application of isotropic model

Modulus as function of depth from Model

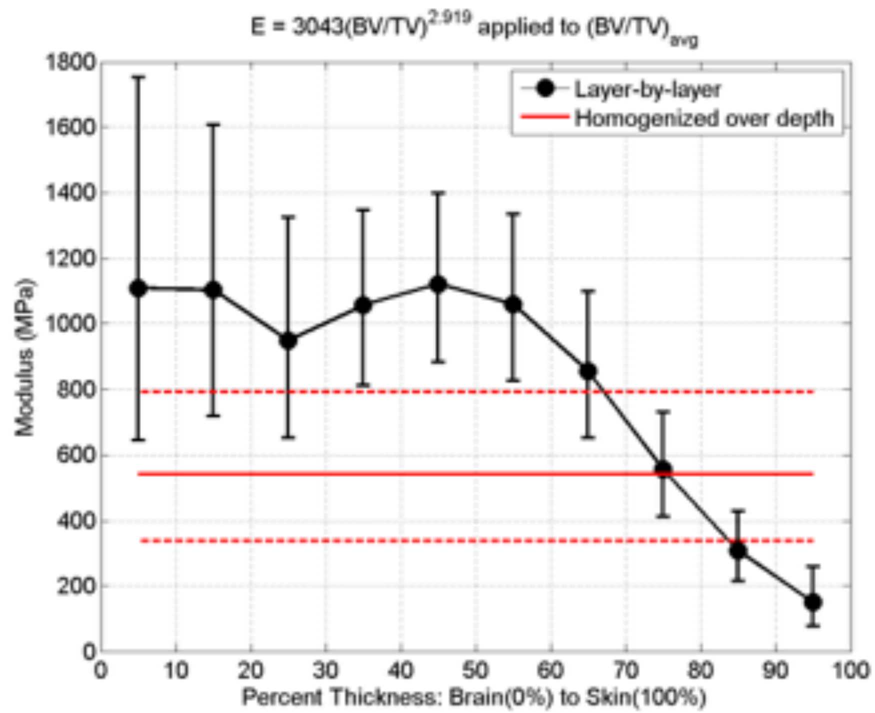

Relating microstructure and mechanical response

- Methodology: consider the specimen as a series of layers

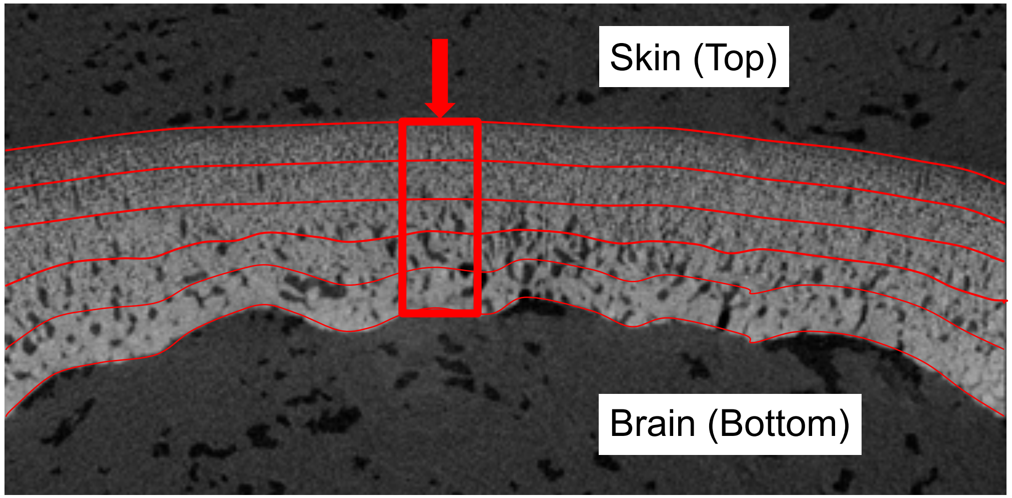

13 µm

Recall: relationship of porosity with depth

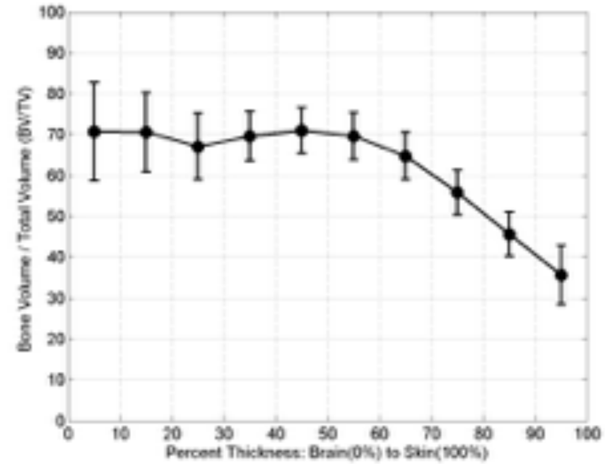

- NOTE: this methodology is directly applicable to human skull: a sandwich structure

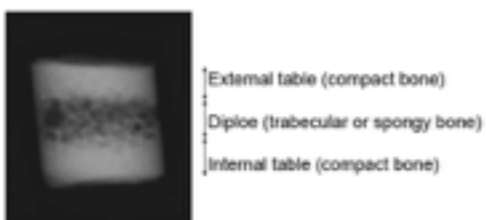

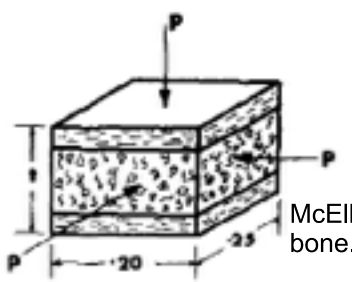

McElhaney, James H., et al. "Mechanical properties of cranial bone." *Journal of biomechanics* 3.5 (1970): 495-511.

Lynnerup, Niels, Jacob G. Astrup, and Birgitte Sejrsen. "Thickness of the human cranial diploe in relation to age, sex and general body build." *Head Face Med* 1.13 (2005): 1-7.

Human Skull Microstructural Quantification and Rate Dependent Deformation

- Ongoing work

Thank You!

Experimental Challenges in Determining Dynamic Response of Soft Tissues

Wayne Chen

Schools of Aeronautics/Astronautics and Materials Engr

Purdue University, West Lafayette, IN

Second Workshop on Numerical Analysis of Human and Surrogate Response to Accelerative Loadin

12-14 January 2016

PURDUE ENGINEERING

Outline

- Introduction
- A Brief Review of Kolsky Bars (SHPB)
    - Families of stress-strain curves at various strain rates
- Challenges in Soft Tissue Characterization
    - Low transmitted pulses, uniform loading, constant strain rates, intermediate strain rates, inertia effects, specimen gripping, and real-time damage visualization
- Experimental Solutions
    - Sensitive transmission bar, pulse shaping, long bar, washer-shape specimens, shear experiments, tissue-gripping methods, high-speed X-ray PCI and XRD
- Remaining Challenges
    - Hybrid experiments for extra soft tissues (brain, lung)
    - Optical measurements on polymer bars
    - Measurements through high-speed imaging (DIC, Virtual Field)
    - Improved gripping methods.

A Typical Kolsky Compression Bar

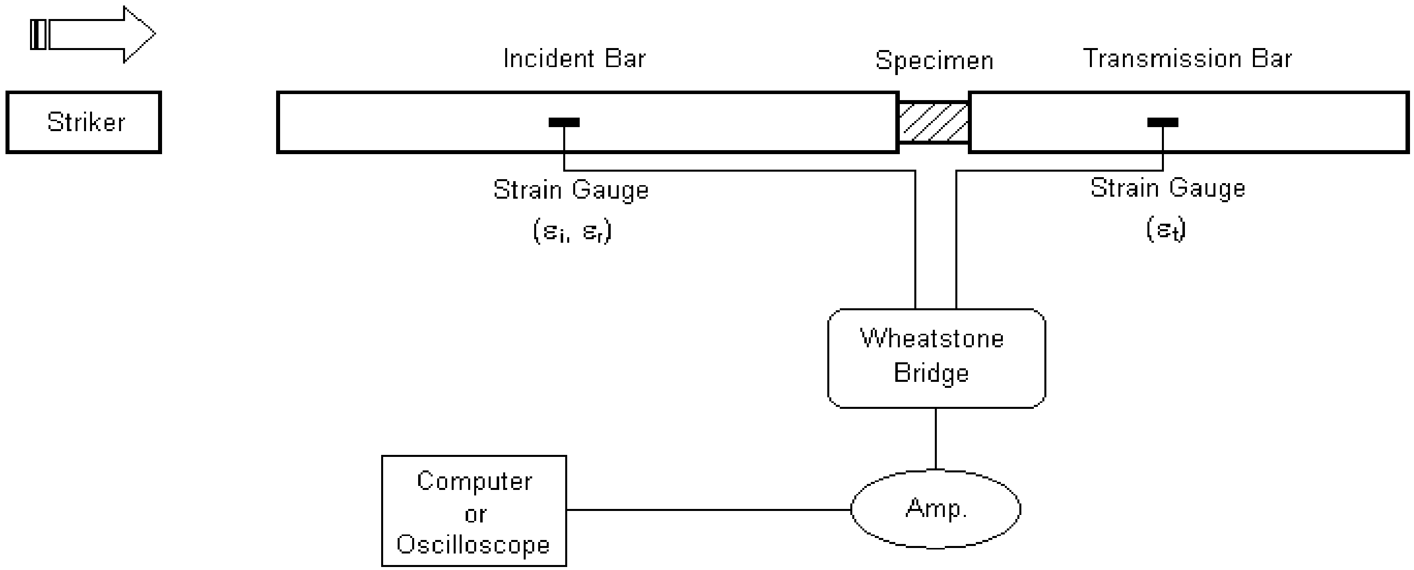

Lindholm, 1964

Principles of Kolsky Bar

- Bars remain elastic.
- 1-D planar waves in bars.
- Uniform uniaxial stress state in specimen.

$$u_1 = C_b\left(\varepsilon_i - \varepsilon_r\right)$$

$$u_2 = C_b \varepsilon_t$$

$$\dot{\varepsilon} = \frac{u_1 - u_2}{l_0} = \frac{C_b}{l_0}\left(\varepsilon_i - \varepsilon_r - \varepsilon_t\right)$$

$$\varepsilon = \int_0^t \dot{\varepsilon}\left(\tau\right) d\tau$$

$$F_1 = E_b A_b\left(\varepsilon_i + \varepsilon_r\right)$$

$$F_2 = E_b A_b \varepsilon_t$$

$$\sigma = \frac{F_1 + F_2}{2A_0} = \frac{E_b A_b}{2A_0}\left(\varepsilon_i + \varepsilon_r + \varepsilon_t\right)$$

$$\sigma \sim \varepsilon$$

Specimen Equilibrium not Automatic

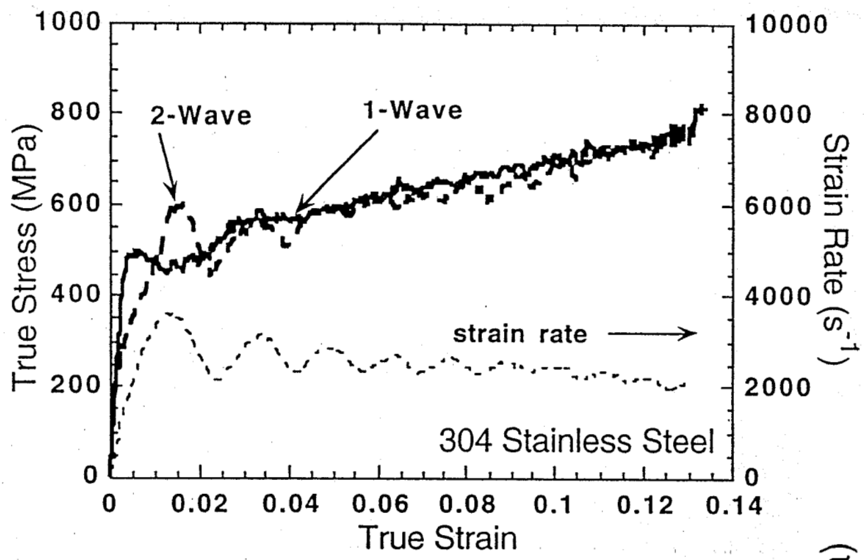

After Gray, 2000

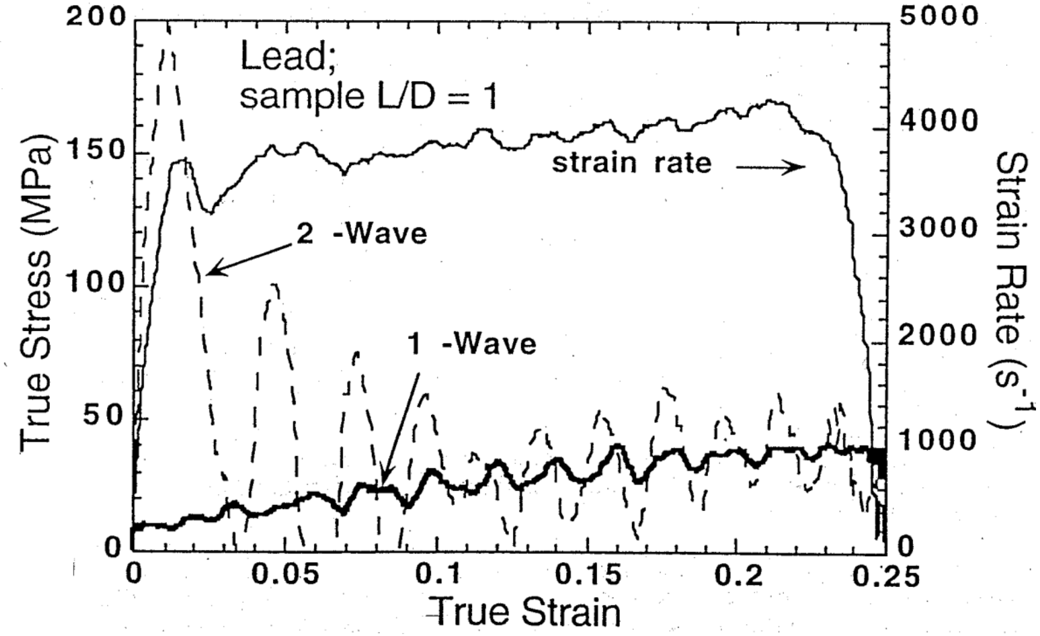

Low ε_t from a Silicone Rubber (RTV 630)

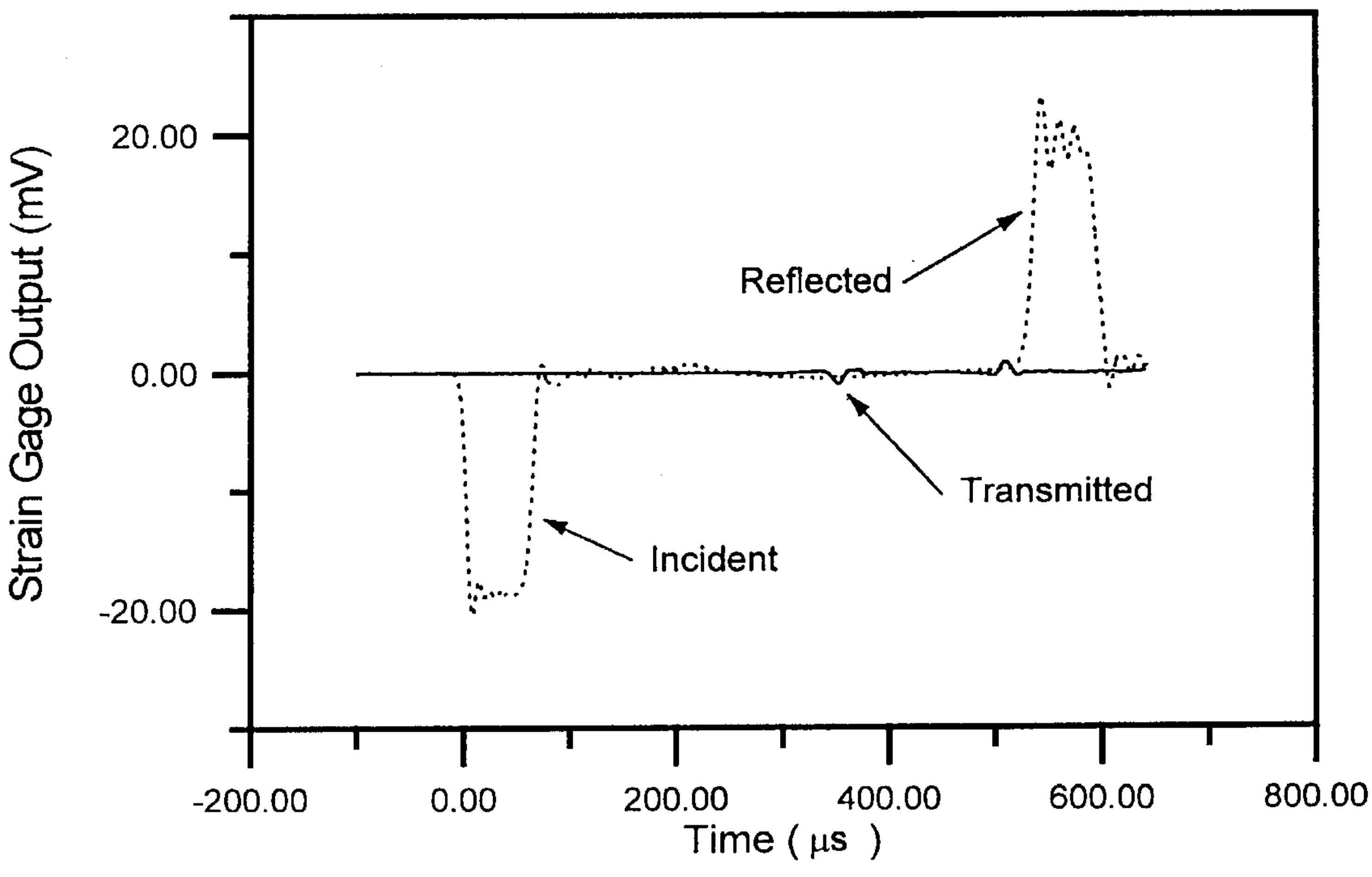

Methods for Enhanced ε_T

- Bars with Low *E*
  - Aluminum, Titanium, Beryllium, Magnesium, Polymers.
- Bars with Less *A*
  - Tubes.
- High-sensitivity Strain Gages
  - Semi-conductor gages, optical methods.
- Direct Force Measurements
  - Quartz crystal transducers.
  - Overcoming inertia effects from gages.
  - Load cells.

Dynamic Characterization of Soft Tissues

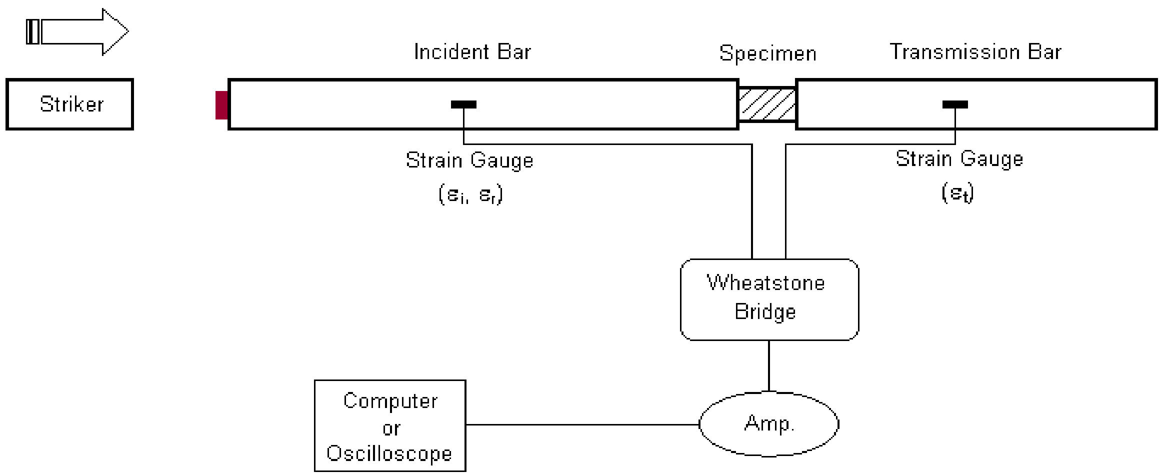

Casem, *et al.*

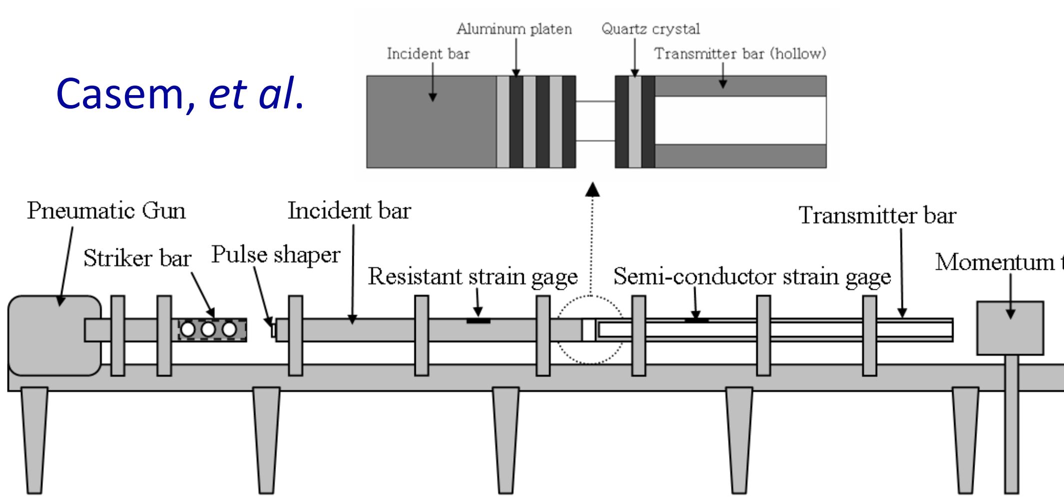

Non-Uniform Deformation

- Uniform deformation along specimen thickness
- Related to dynamic stress equilibrium in most cases

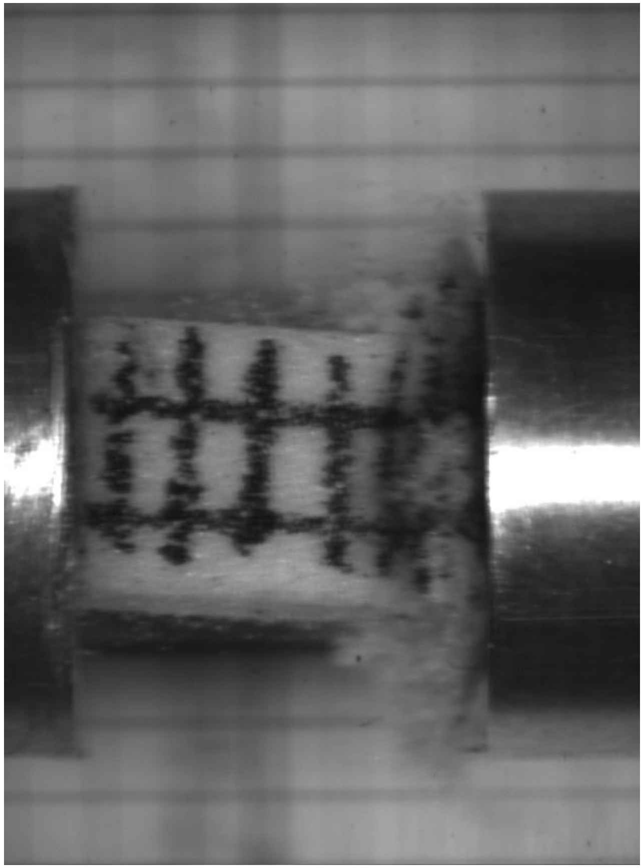
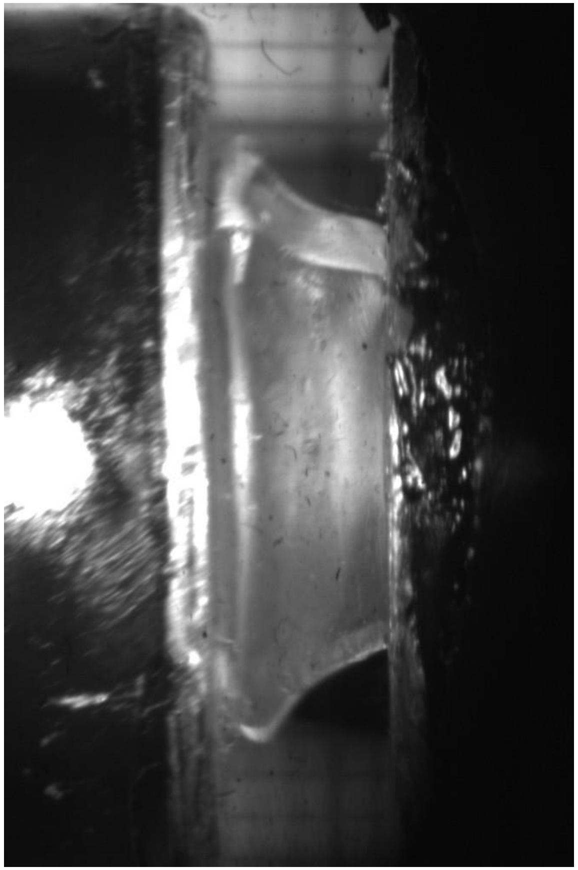
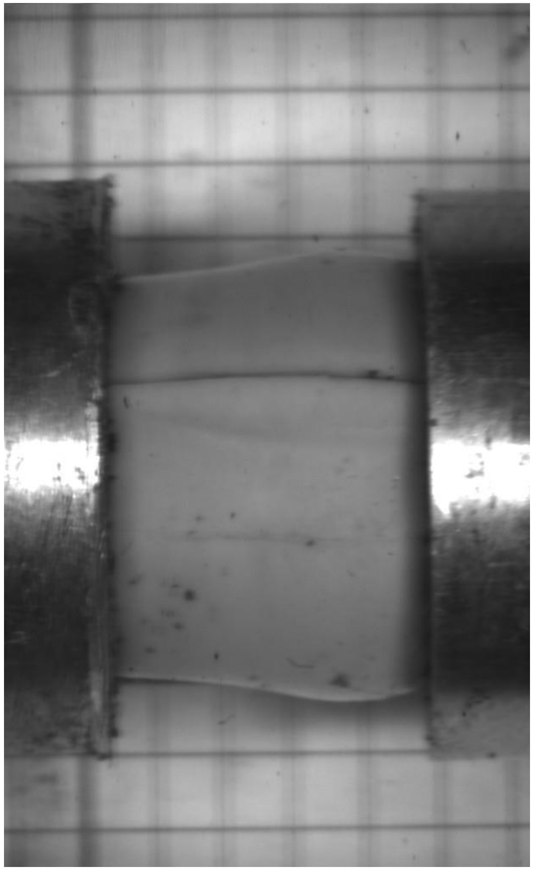

General Pulse Shaping Technique

- **Methods**
  - **Conical strikers**

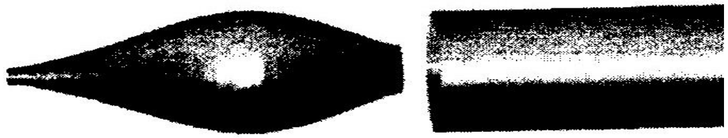

  - **Pre-loading bar (three-bar) technique**

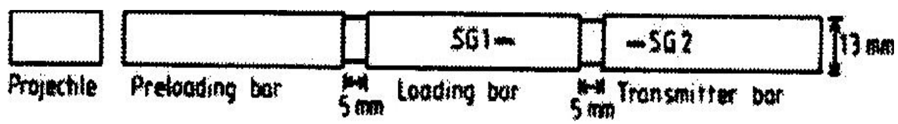

  - **Pulse shapers**

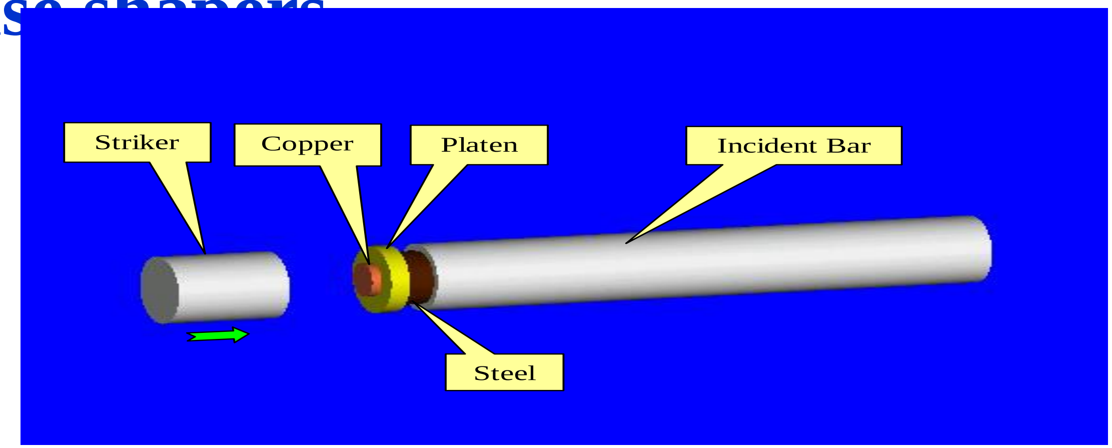

Constant True Strain Rate

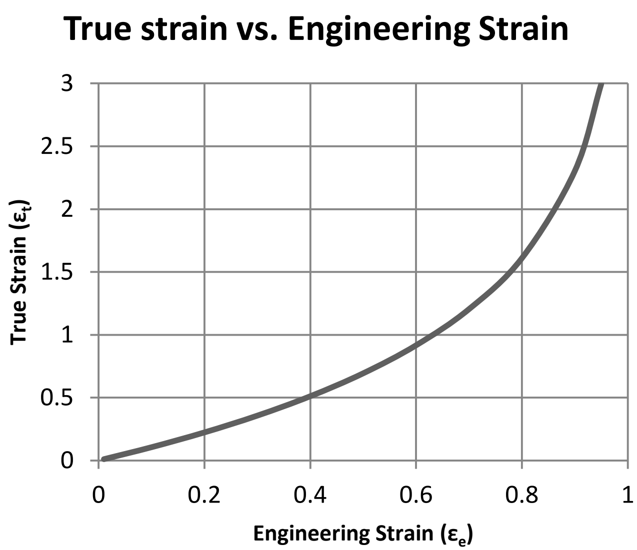

- Engineering strain rate must decrease in order to have constant true strain rate
- Shape the striker such that it will produce a desired stress wave
  - Mechanical Impedance (Z), area (A), density(ρ), and pulse speed (C)

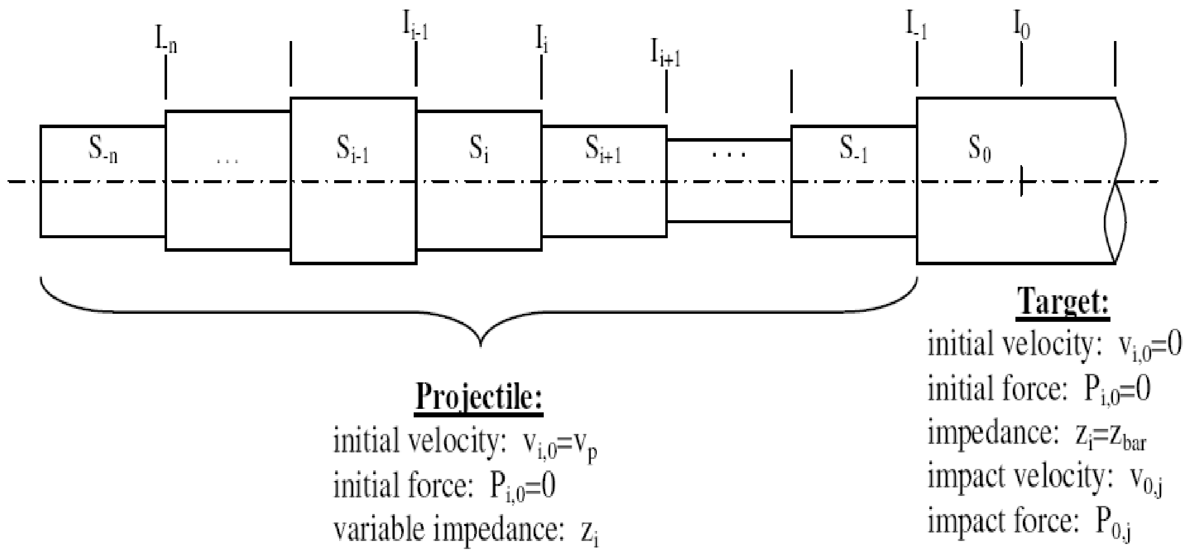

Force Histories on Specimen Faces

D = 13 mm, L = 1.5 mm, Al SHPB, No Pulse Shaper, $\dot{\varepsilon} = 2{,}900\,s^{-1}$

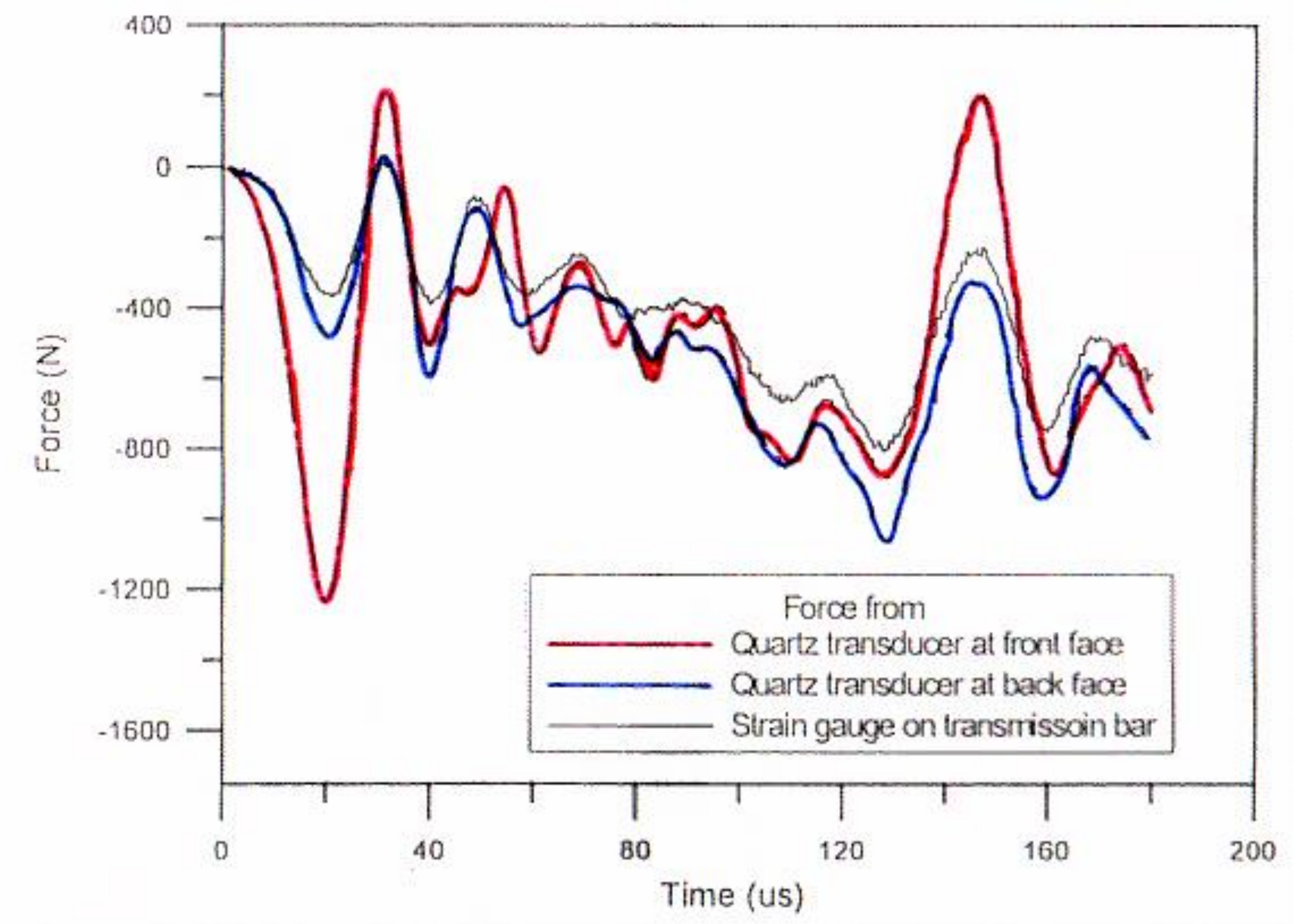

Force Histories on Specimen Faces

D = 13 mm, L = 1.56 mm, Al SHPB, Pulse Shaped, $\dot{\varepsilon} = 2{,}950 s^{-1}$

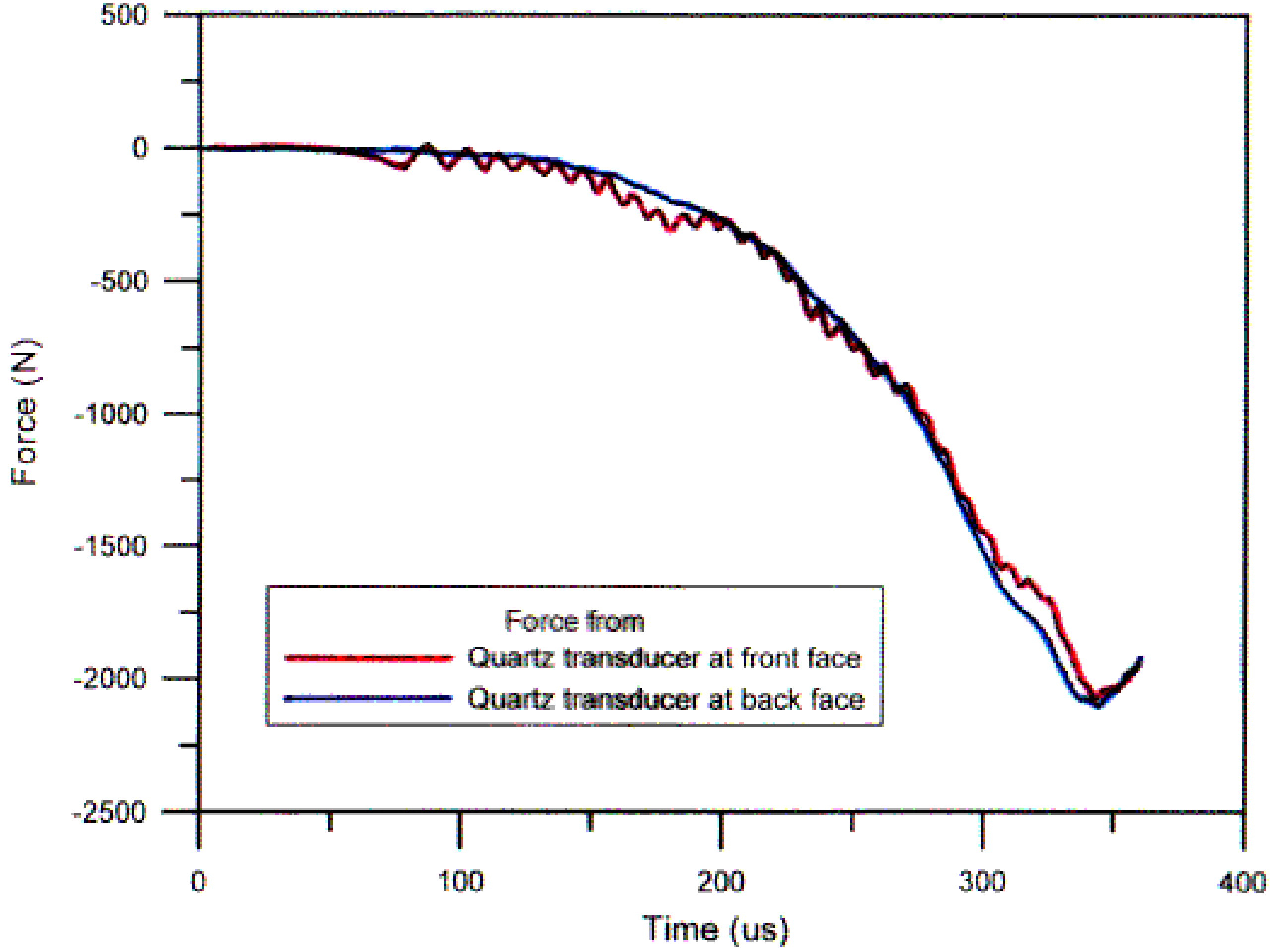

Needs for Intermediate Rates

- **Applications of Polymeric Foams**

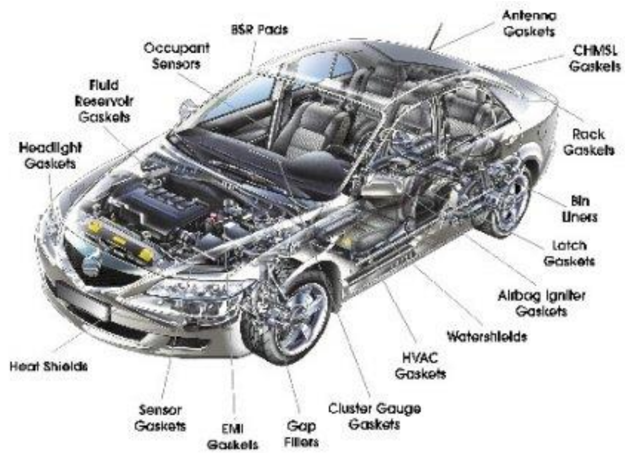

Besides static and high-speed impact loadings, tissues are often subjected to intermediate-speed impact.

For example, the strain rate in car collisions is in the range between 10^0 and 10^2 s^{-1}.

Missing Data Range

- **Mechanical Characterization of Polymeric Foams**

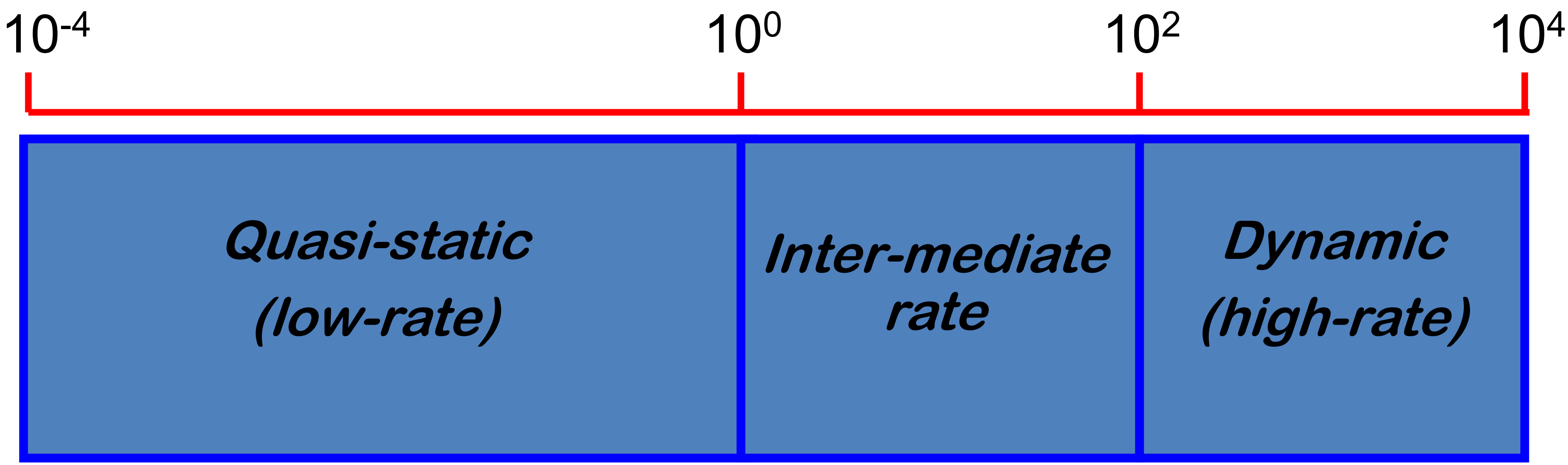

MTS; Instron, etc.

Kolsky Bar

A Long Kolsky Bar for Intermediate-rate Experiments

- Incident & transmission bars:
  - 36' long each
  - ¾'' diameter aluminum bars
- Strikers:
  - Up to 12' long
- Loading duration of pulses:
  - Up to 2 ms without waveform overlapping
  - Up to 3.5 ms (reflected pulse is overlapped)
- Strain rate:
  - Can be as low as 50 s^{-1}

Strain-rate Effects on Yield Strength

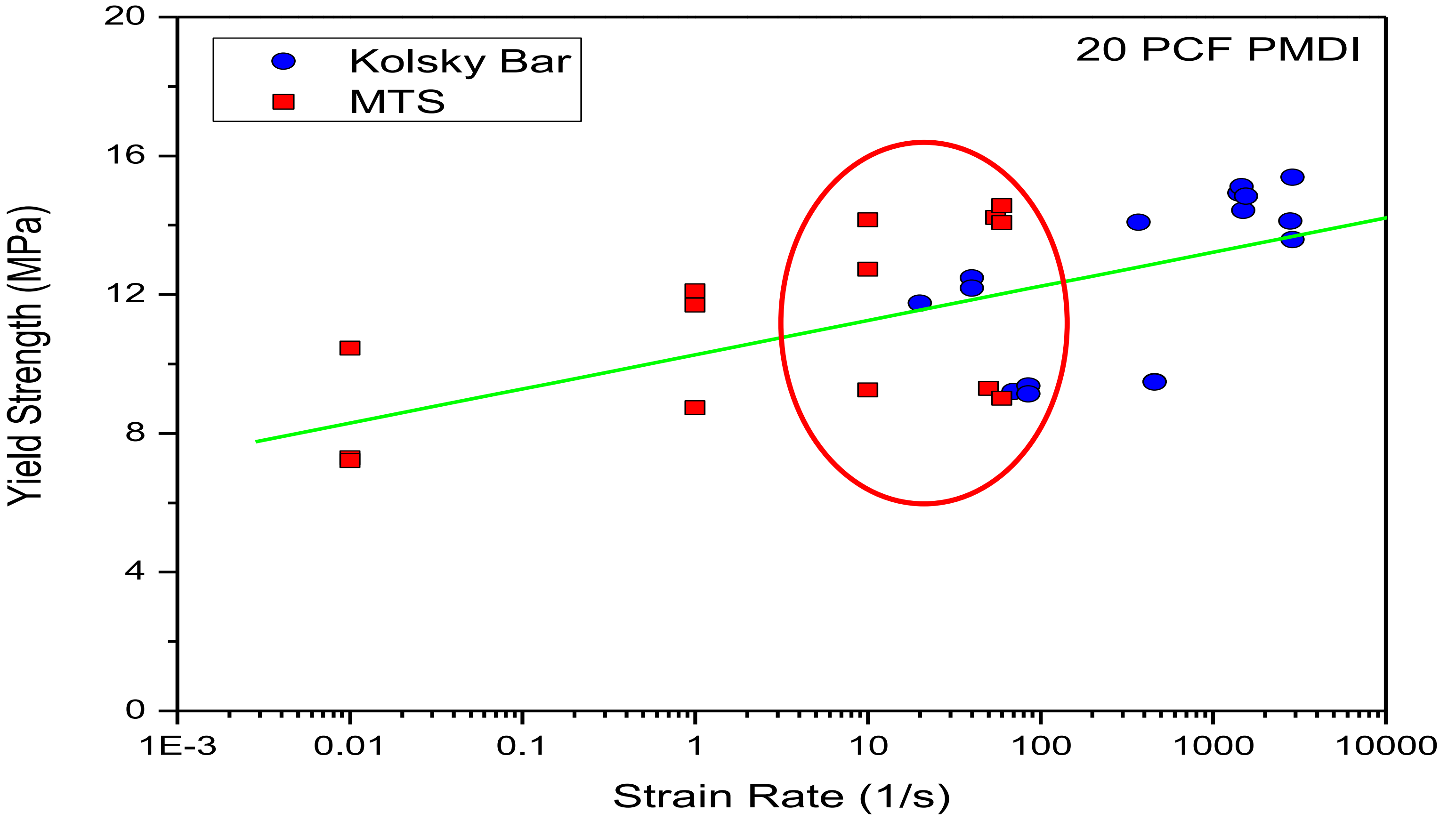

A Typical Conventional SHPB Experiment on A Gel Rubber Specimen

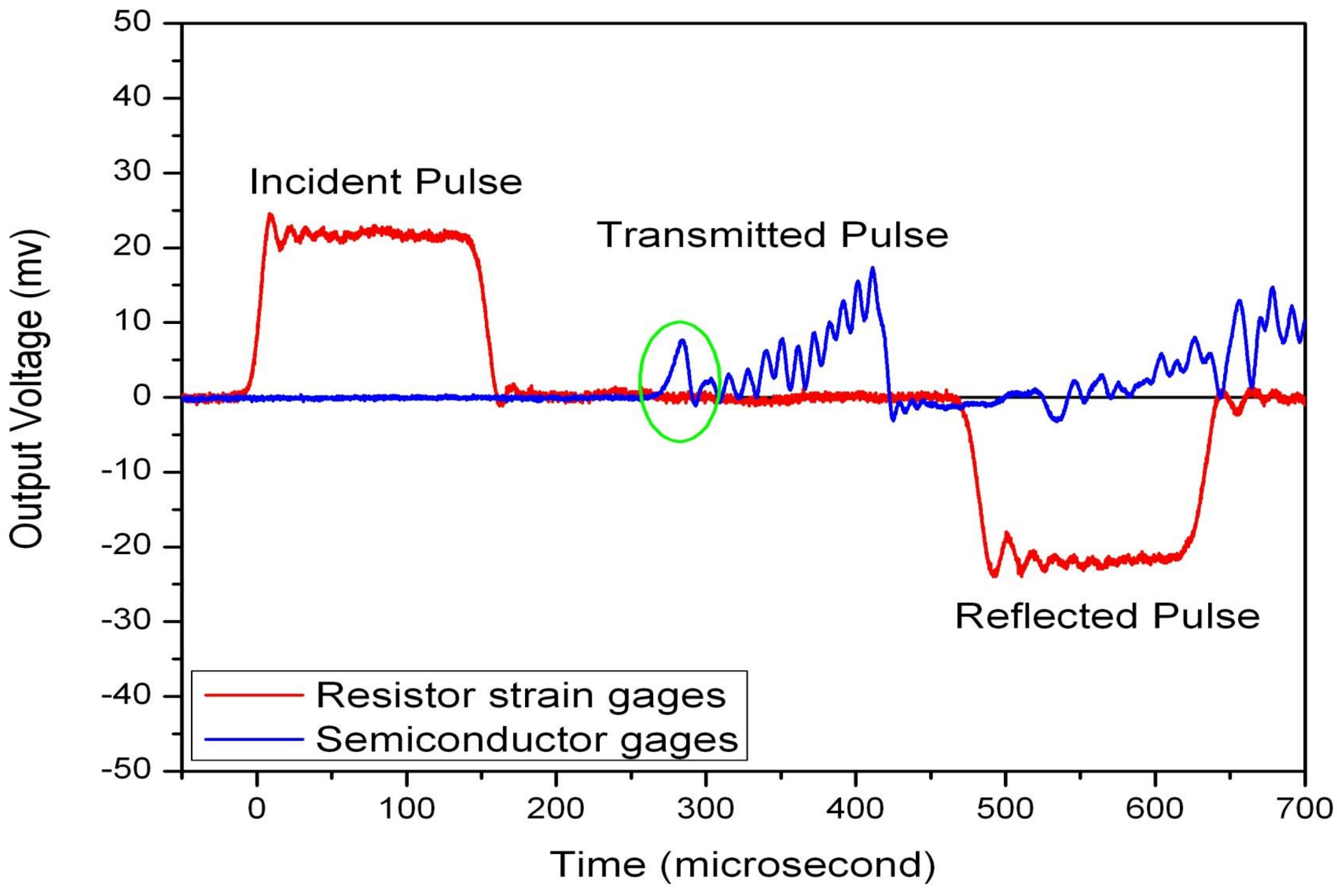

Spike and Radial Inertia

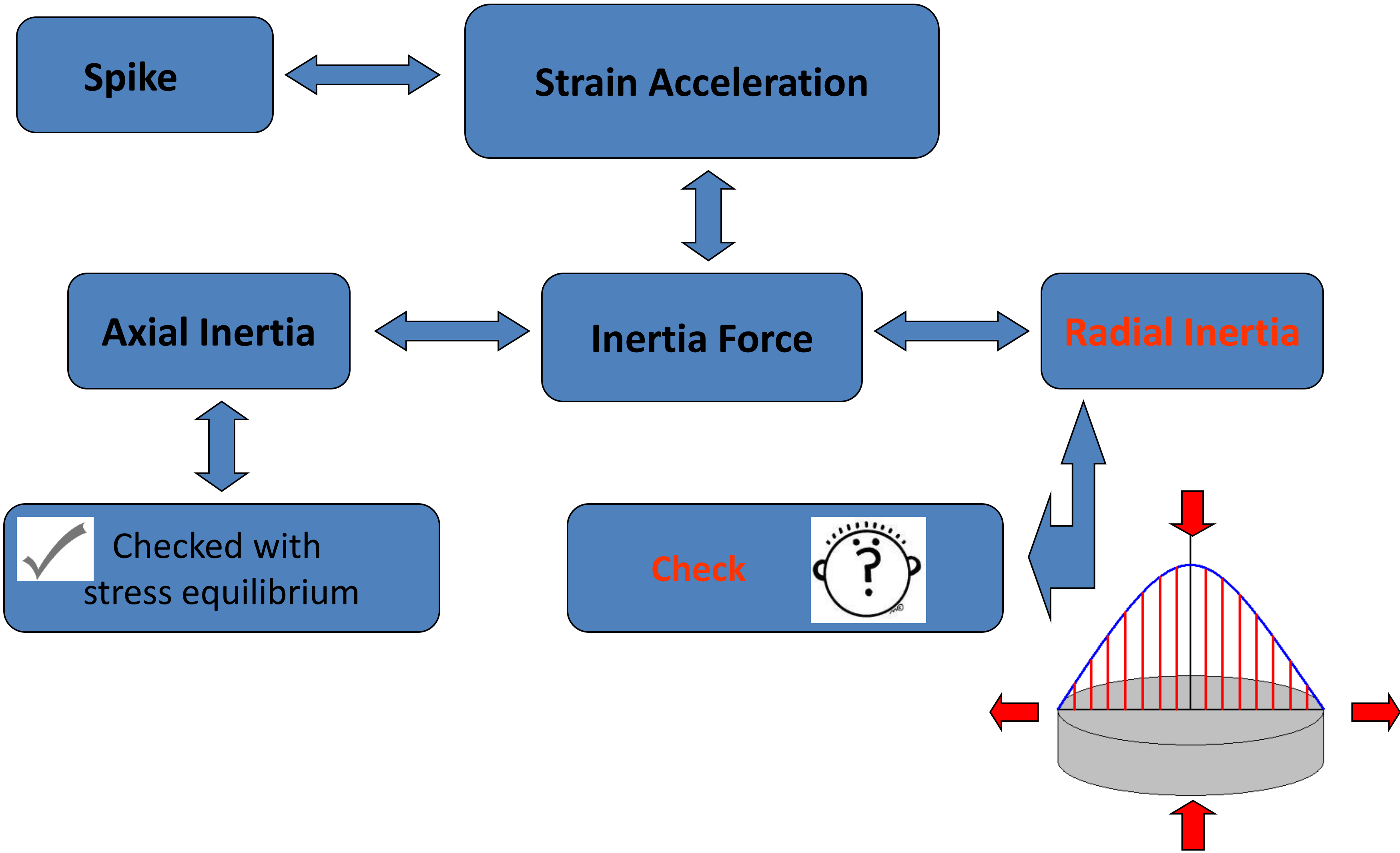

Specimen Geometry Change

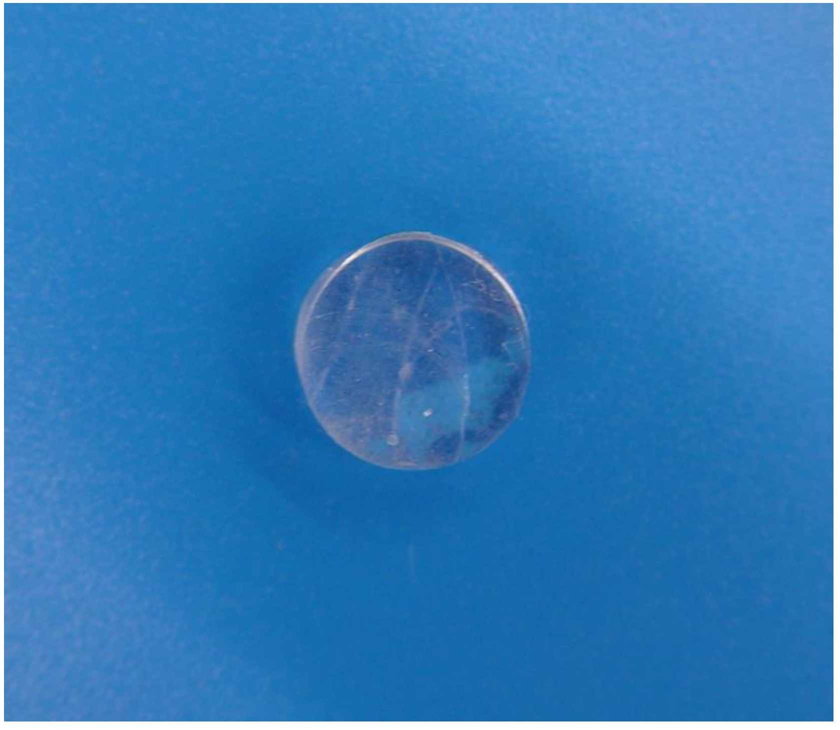

Solid Specimen

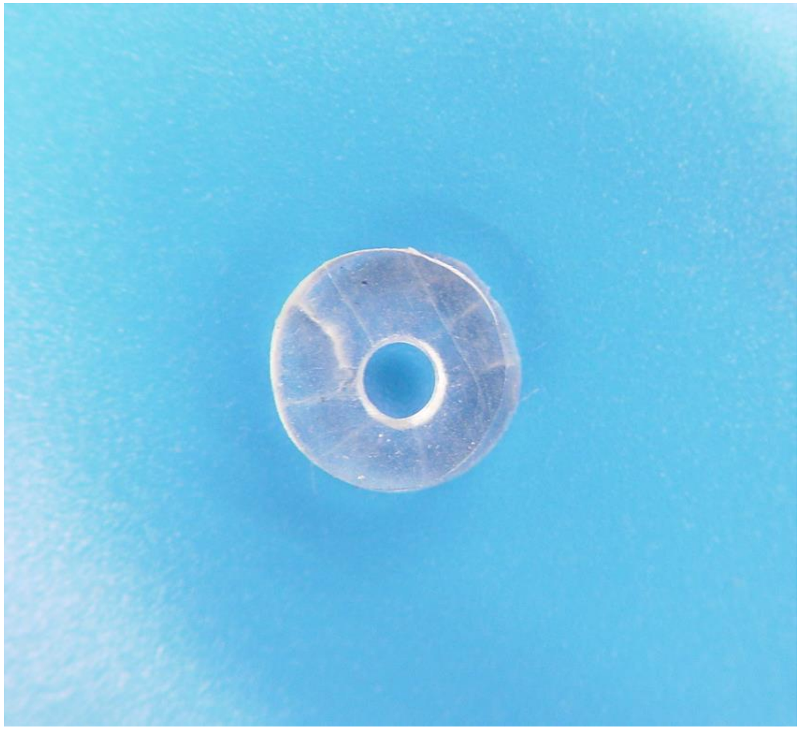

Annular Specimen

Spike Related to Specimen Geometry

The spike disappears when using an annular specimen.

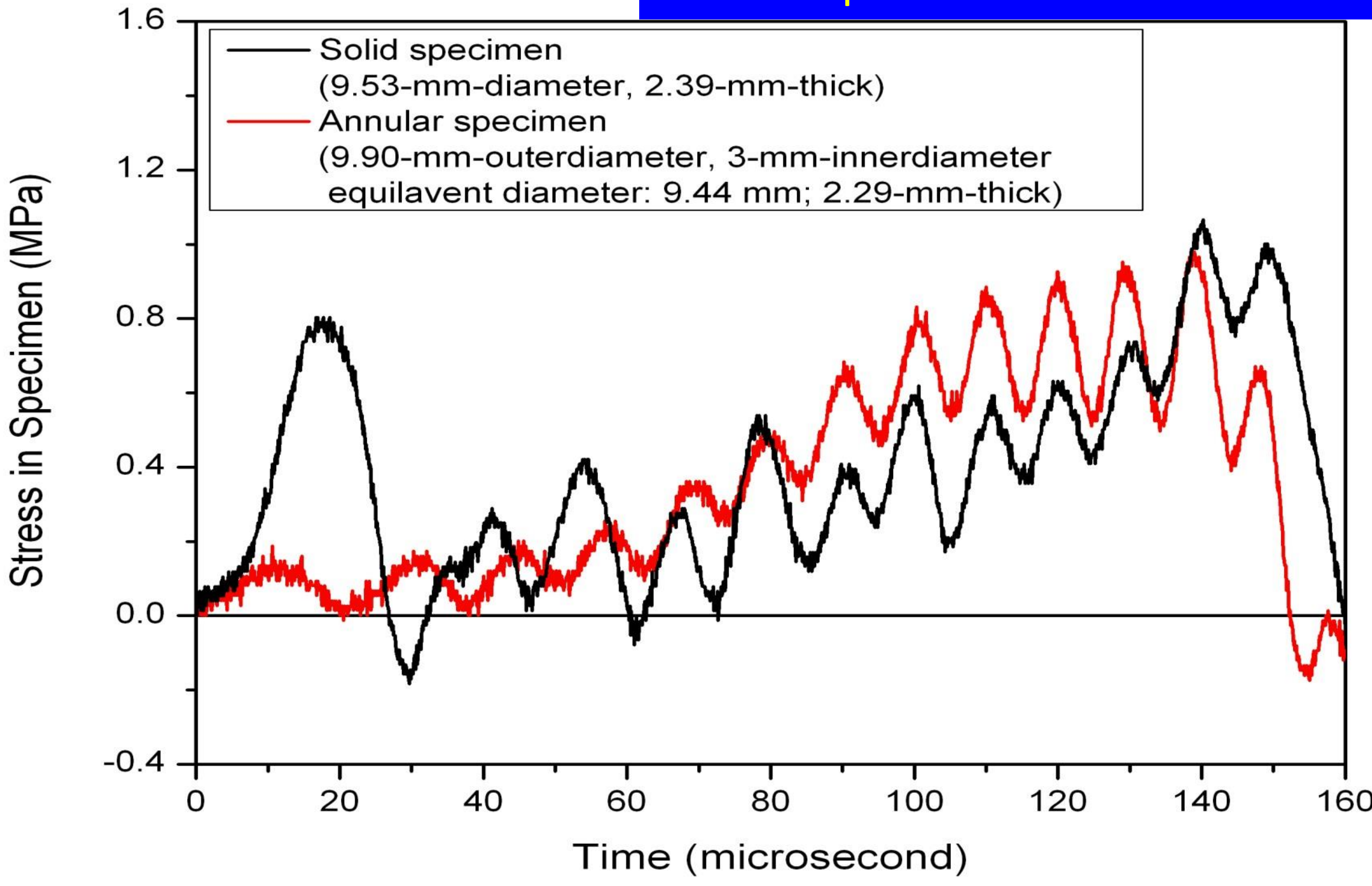

Dynamic Properties of Gray and White Matters

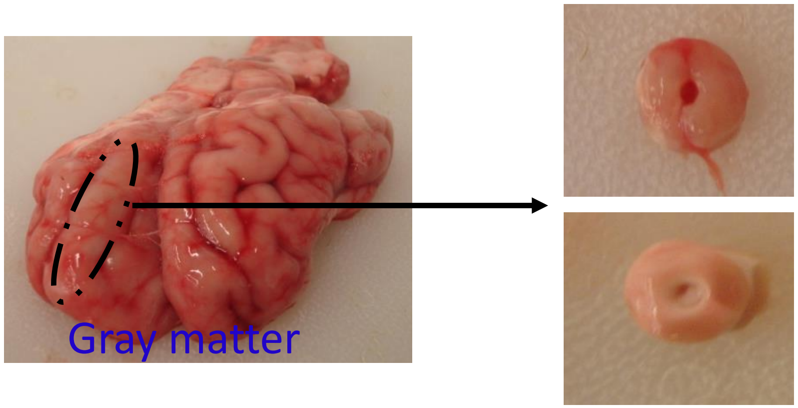

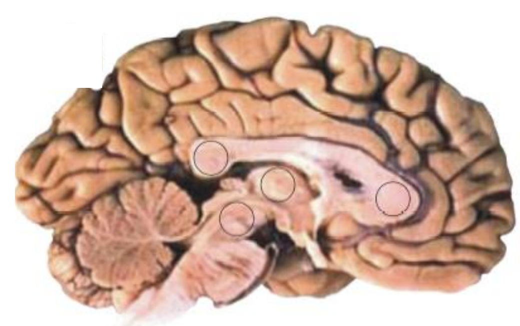

A Washer-shaped Gel Specimen under Compression

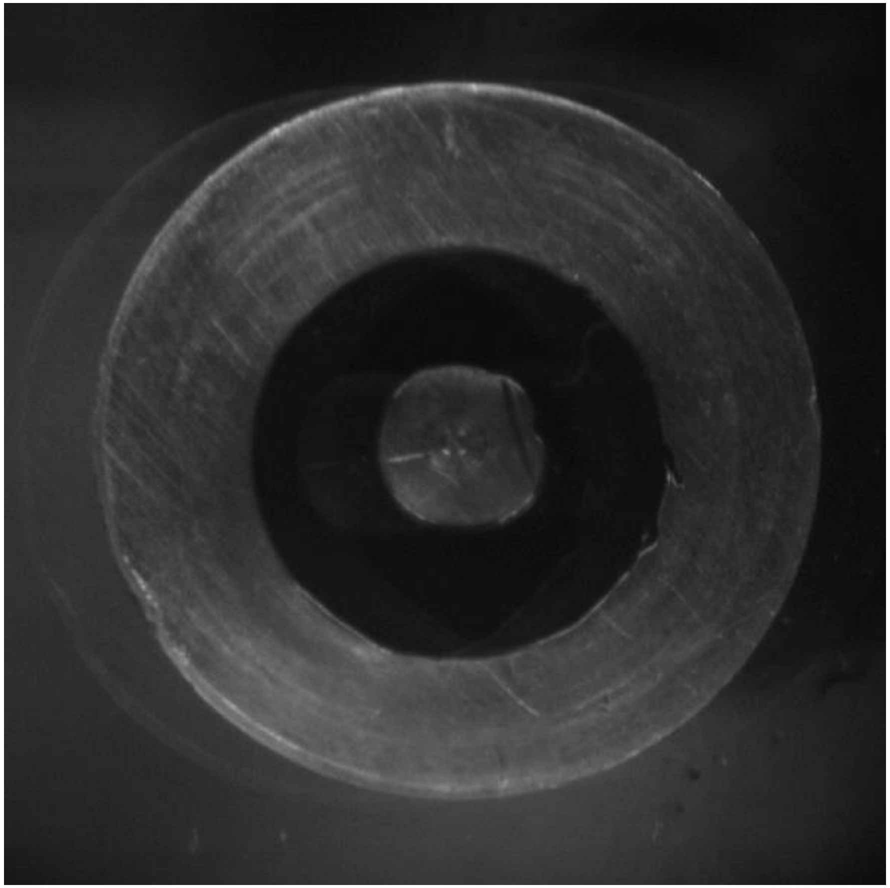

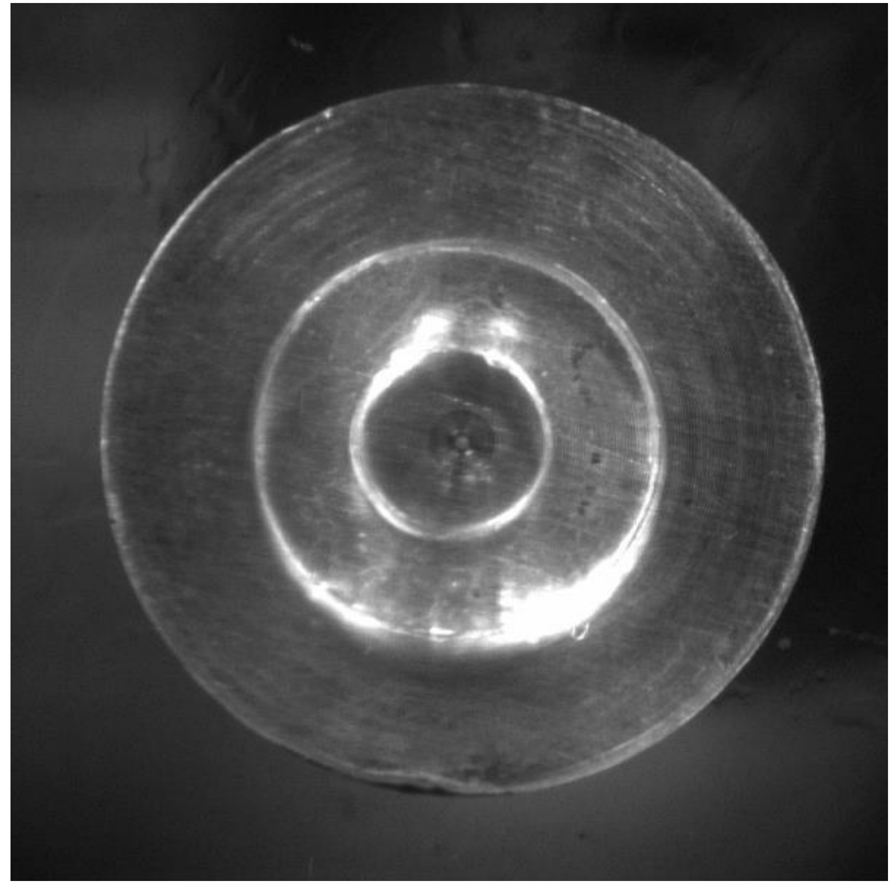

66% Peak Axial Strain

Strain Rate ~2,000/s
G ~ 5 MPa

Strain Rate ~2,000/s
G ~ 200 kPa

Kolsky Torsion Bar for Dynamic Shear Response

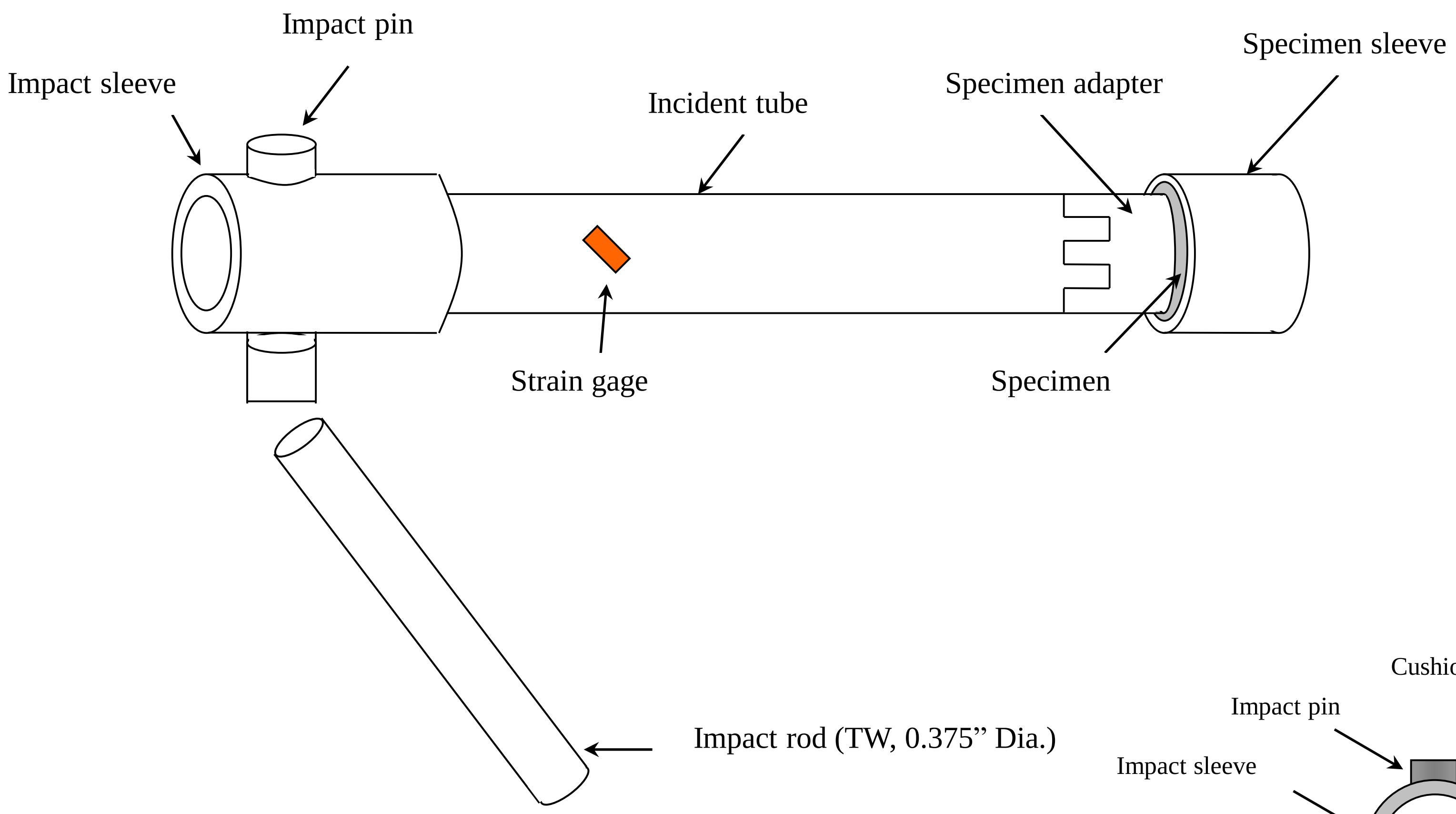

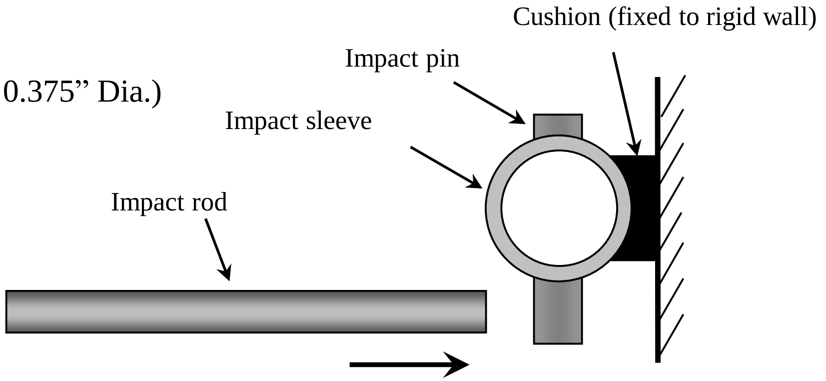

Kolsky Torsion Bar for Dynamic Shear Response

- **Dynamic shear response under torsional loading**
  - ✓ **No radial-inertia effect.**
  - ✓ **No stress concentrations at the edges.**
  - ✓ **Pure shear properties of the material at high rates.**

- **"Desk-top" Kolsky torsion bar setup**

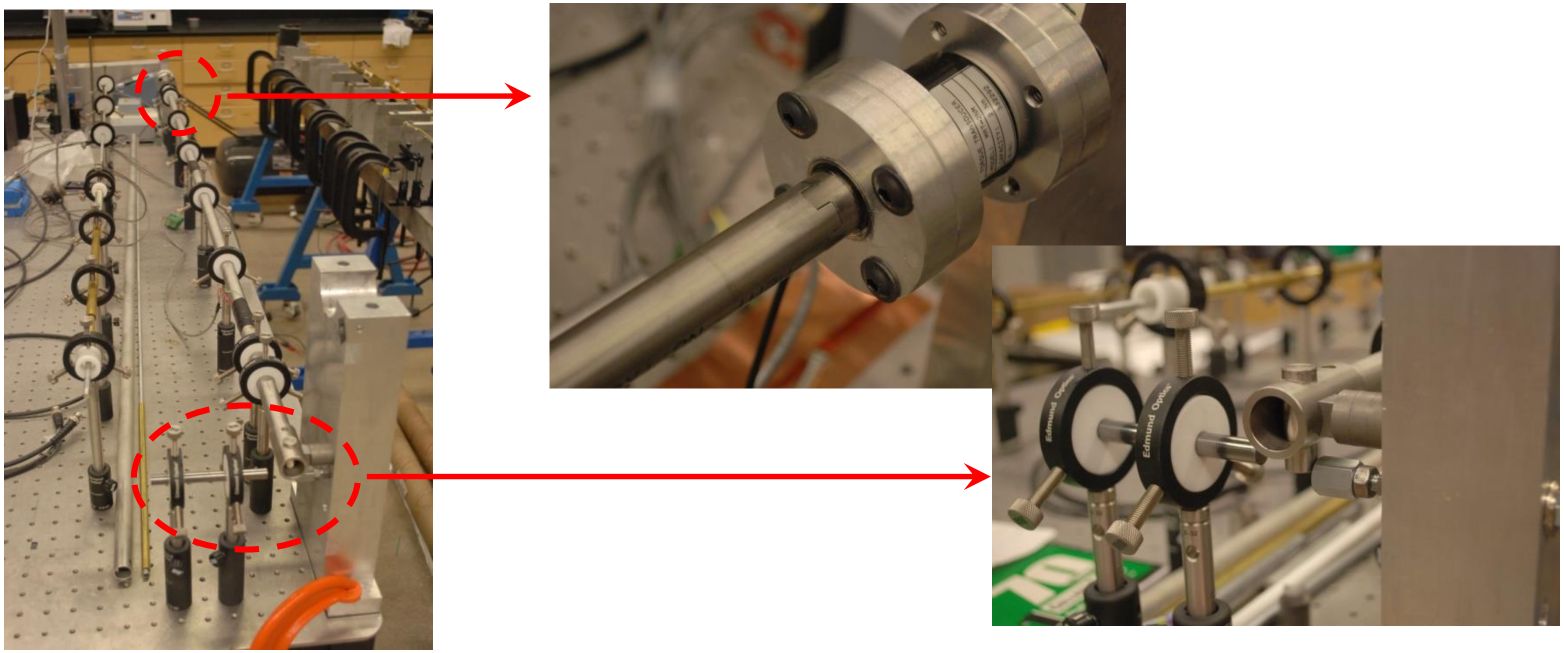

Ring-shaped Specimen

O.D. = 19 mm

I.D. = 14.3 mm

Thickness = 2 mm

A Comparison of Axial/Shear Responses

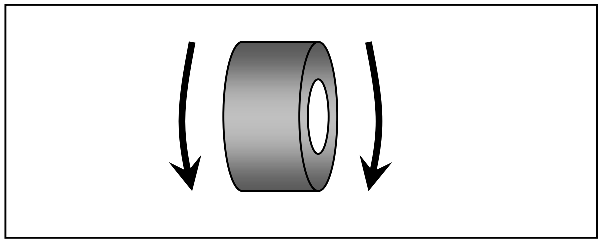

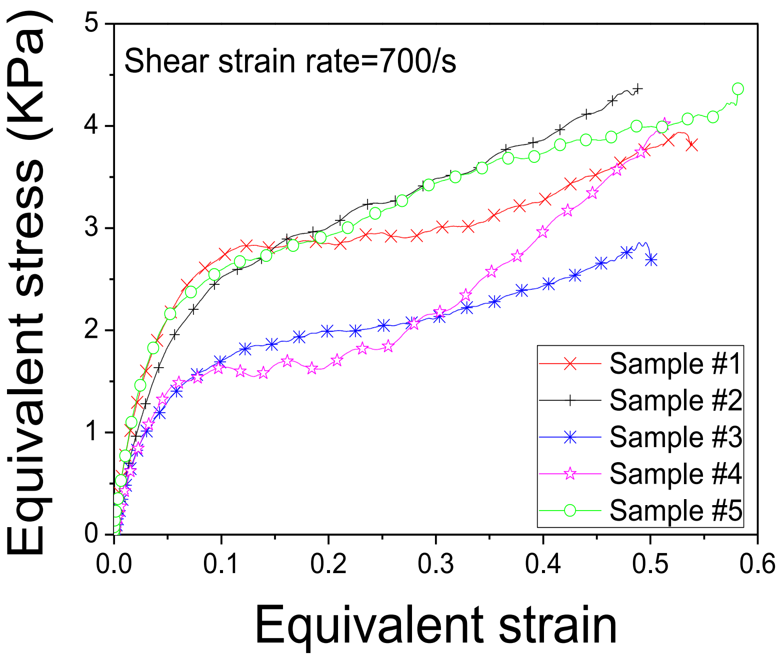

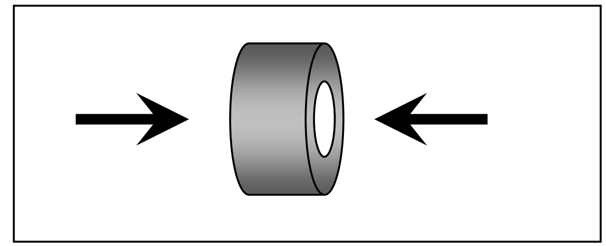

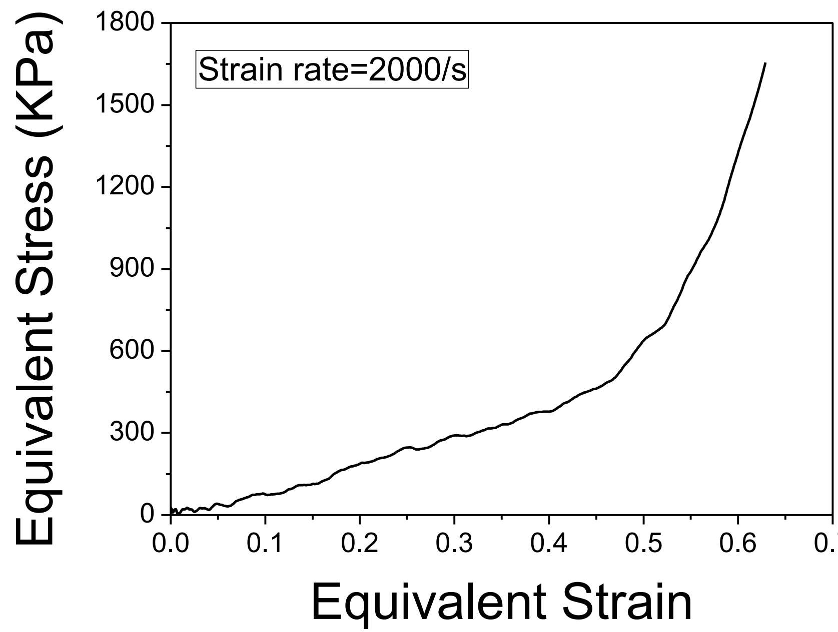

Gripping in Tension Experiments

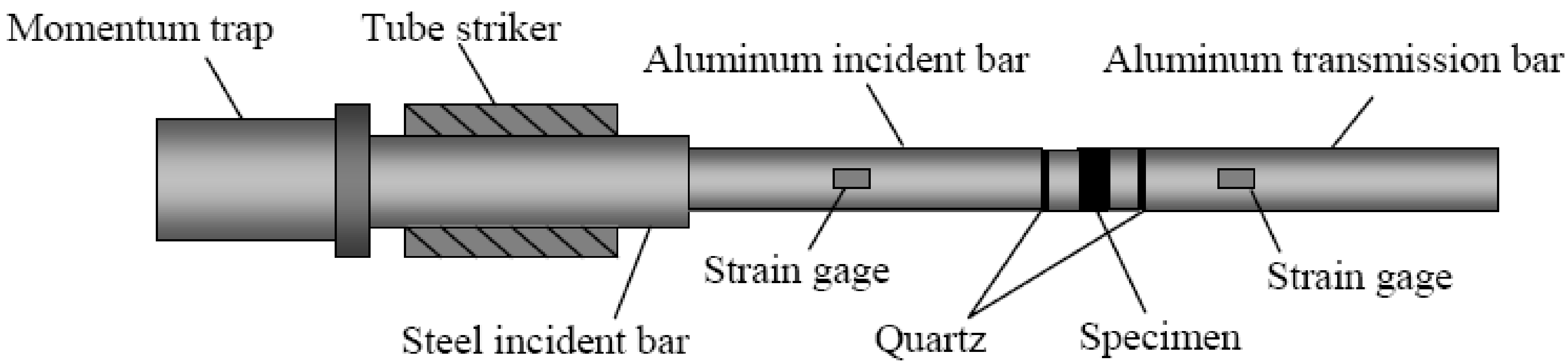

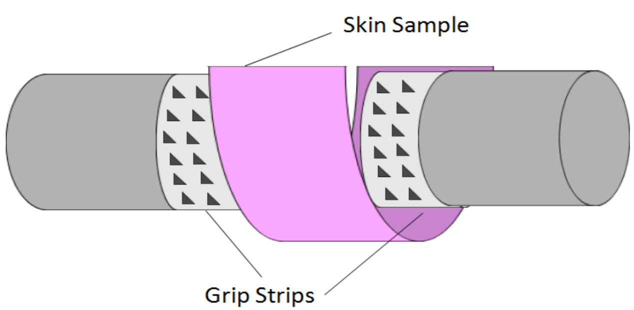

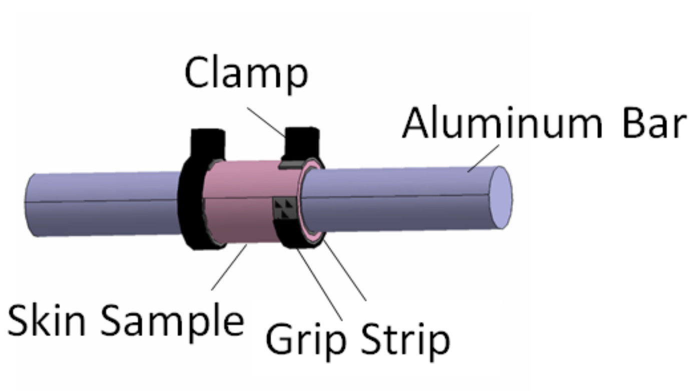

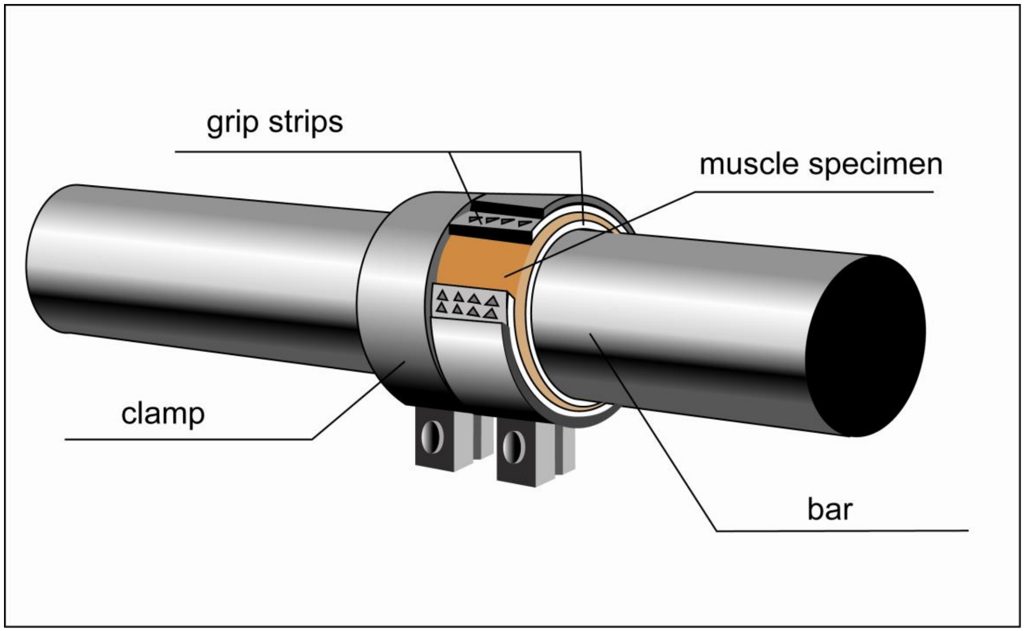

Dynamic Tension Experiments on Muscles

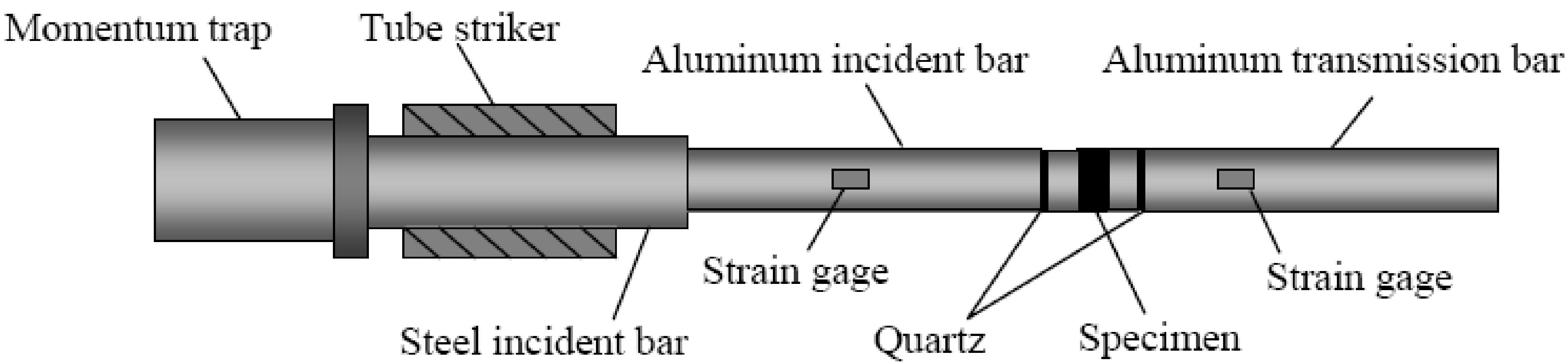

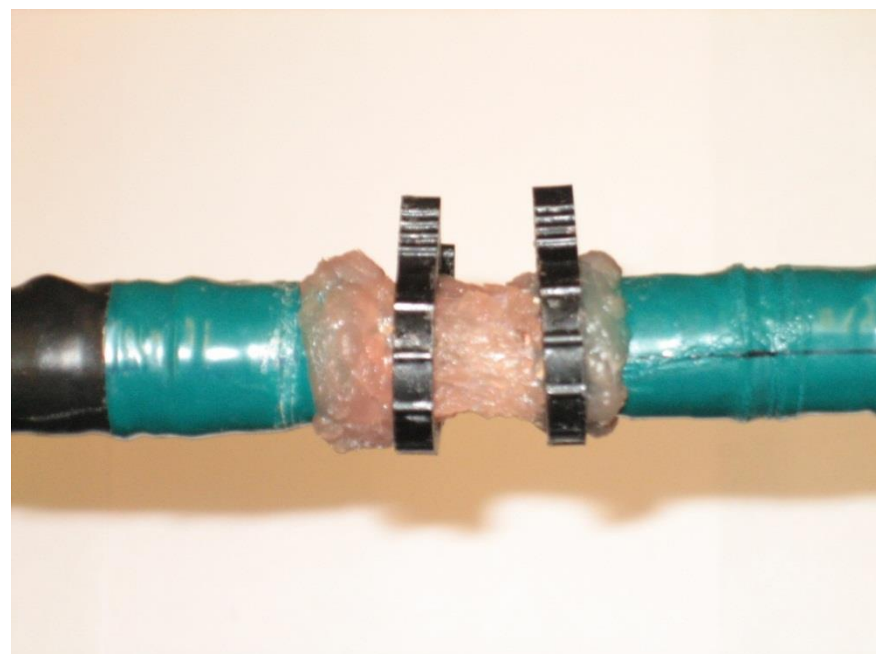

Bovine Tendon in Dynamic Tension

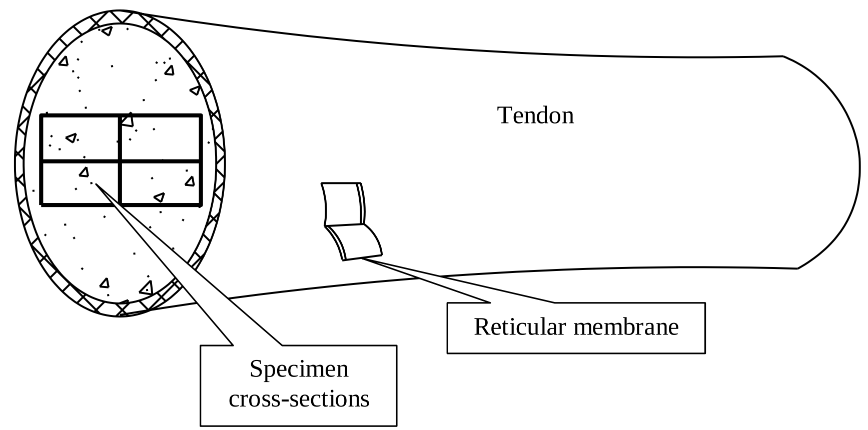

$$\sigma_E = \eta\mu \sum_{i=1}^{3} \mu_i \left(\lambda^{\alpha_i - 1} - \lambda^{-\frac{\alpha_i}{2} - 1} \right)$$

$$\eta(\lambda) = 1 - \frac{1}{r} erf\left[\frac{\mu}{m} \sum_{i=1}^{3} \frac{\mu_i}{\alpha_i} \left(\lambda_{\max}^{\alpha_i} - \lambda^{\alpha_i} + 2\lambda_{\max}^{-\frac{\alpha_i}{2}} - 2\lambda^{-\frac{\alpha_i}{2}} \right) \right]$$

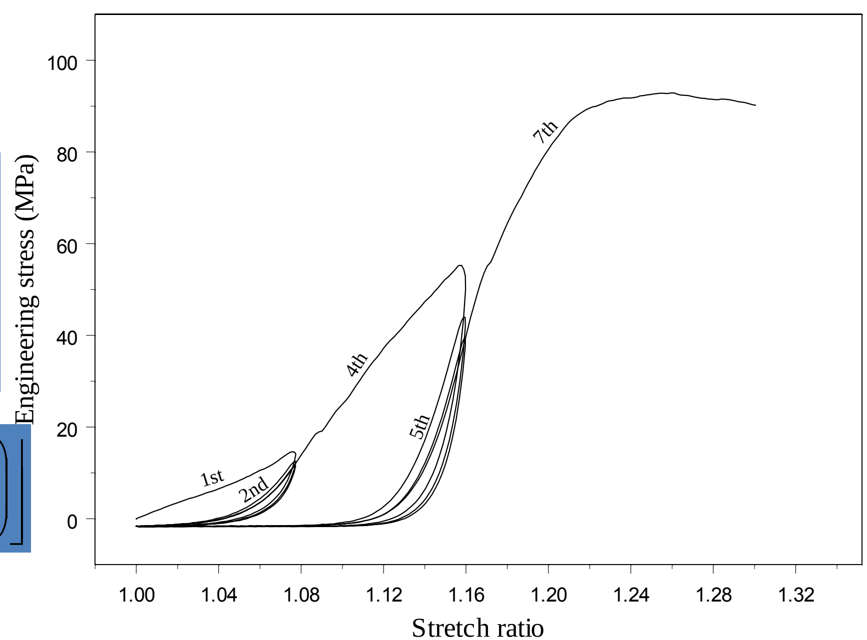

Dynamic Experiments

Stress-stretch behavior at 2500/s stretching rate

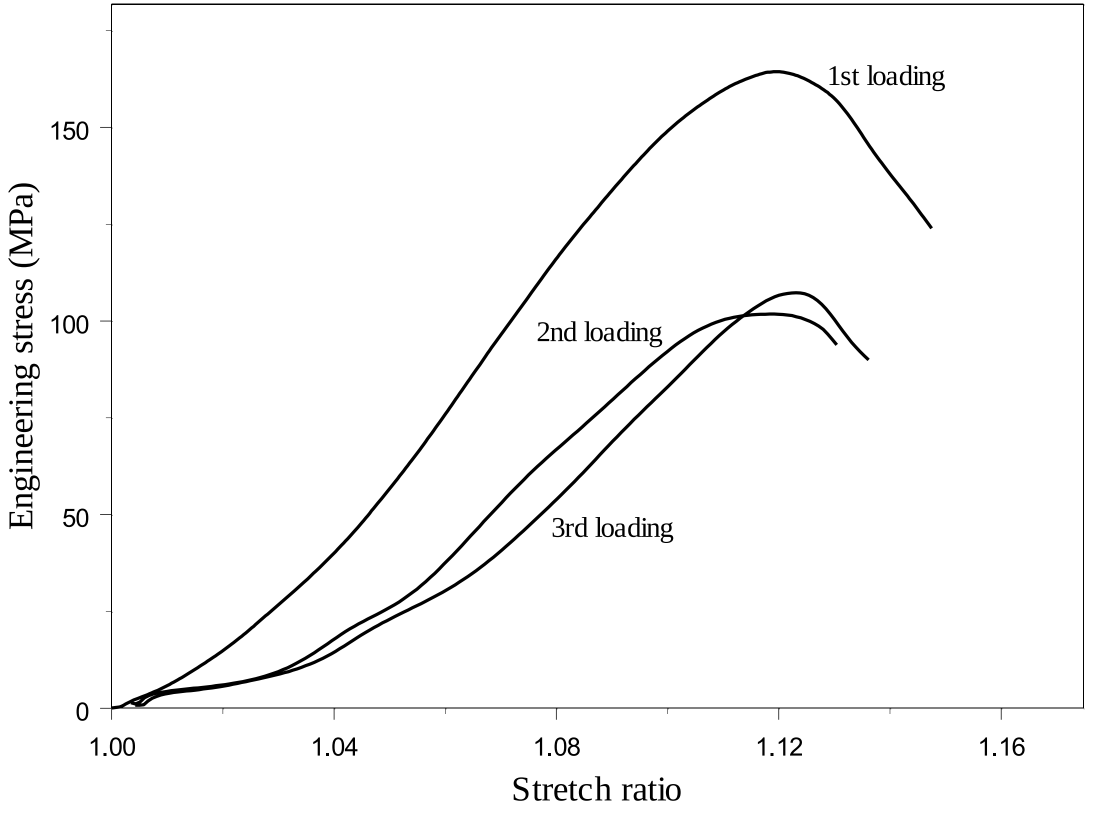

Dynamic Mulin's Effects

Kolsky Bar with Single Loading

- ✓ Pulse-shaper
- ✓ Quartz-crystal force transducers
- ✓ Semi-conductor strain gages
- ✓ Momentum trapping device

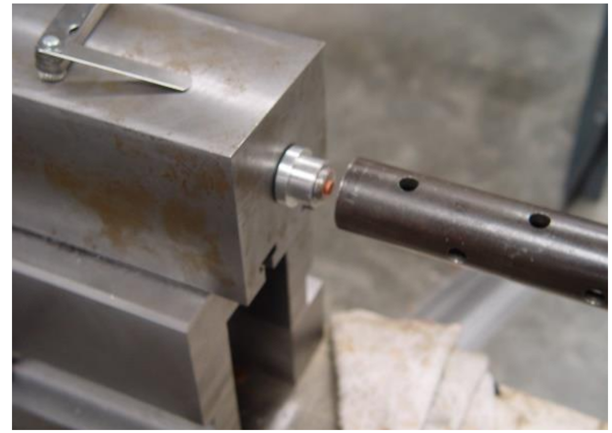

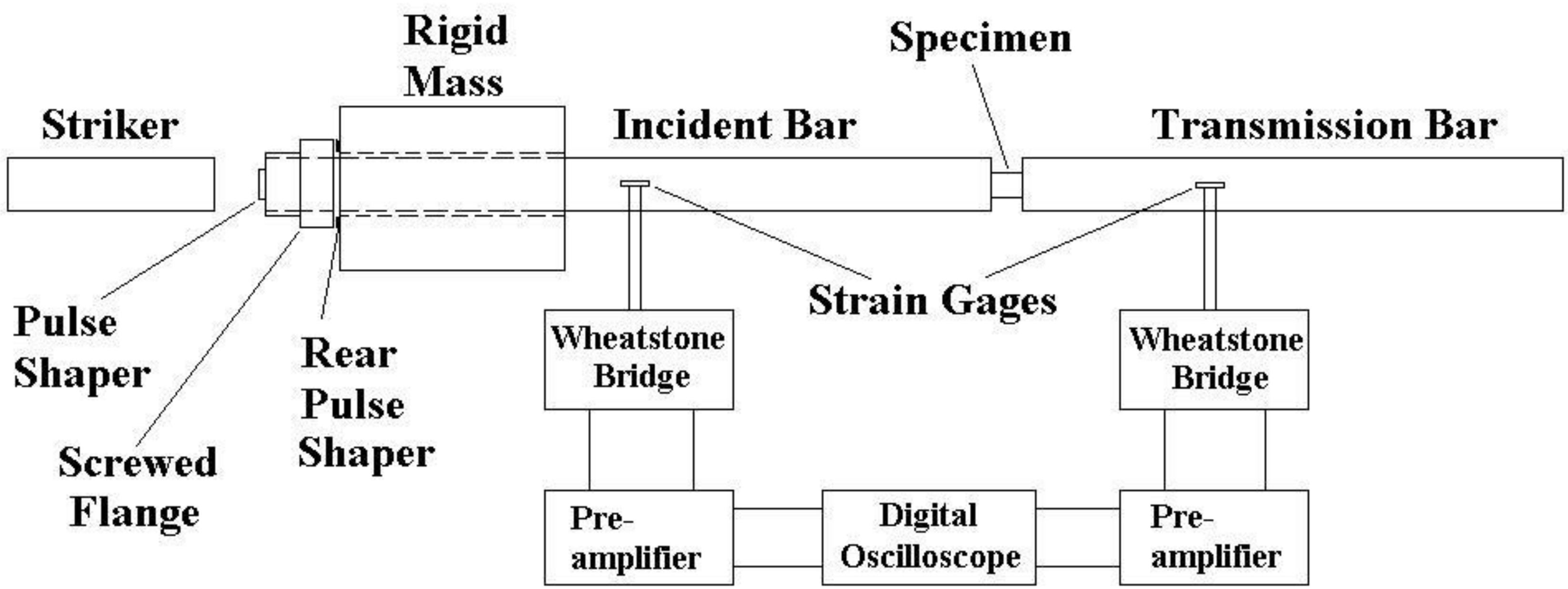

Kolsky Bar in Synchrotron X-ray

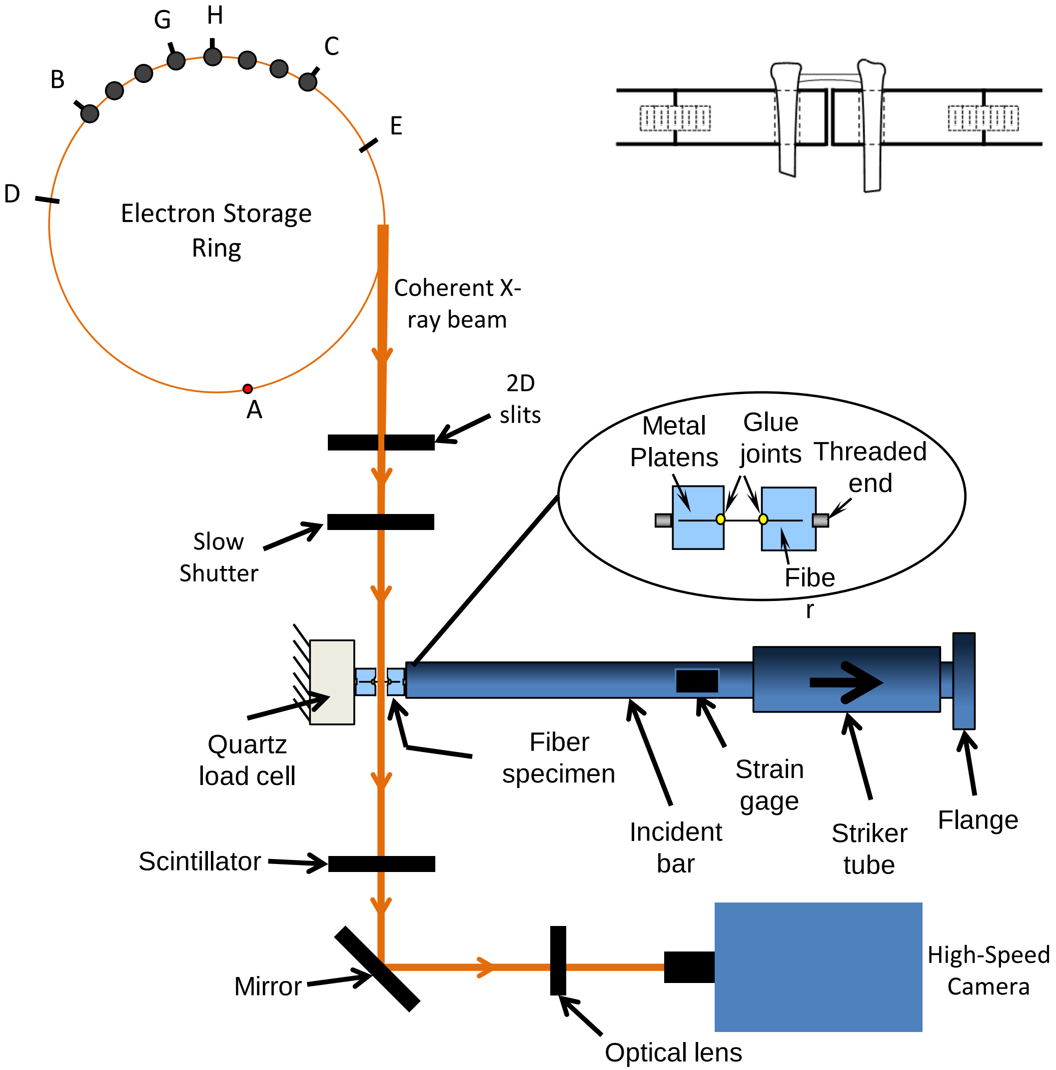

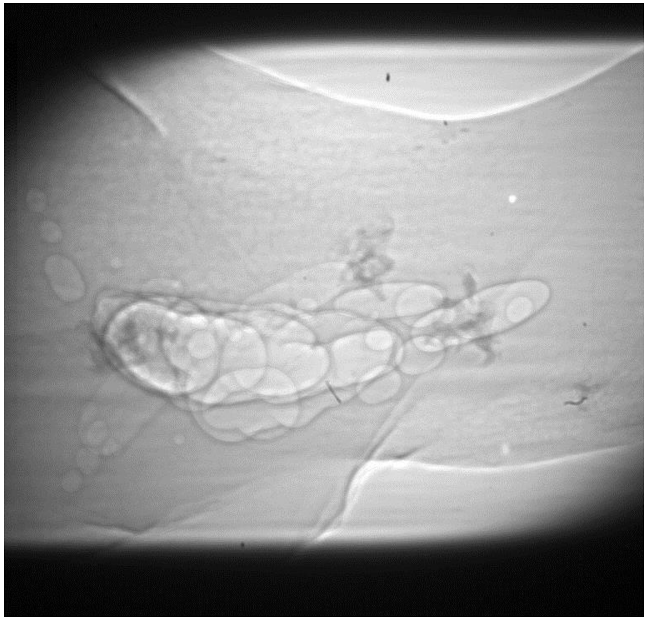

Tensile Damage of a Tendon/Bone Interface

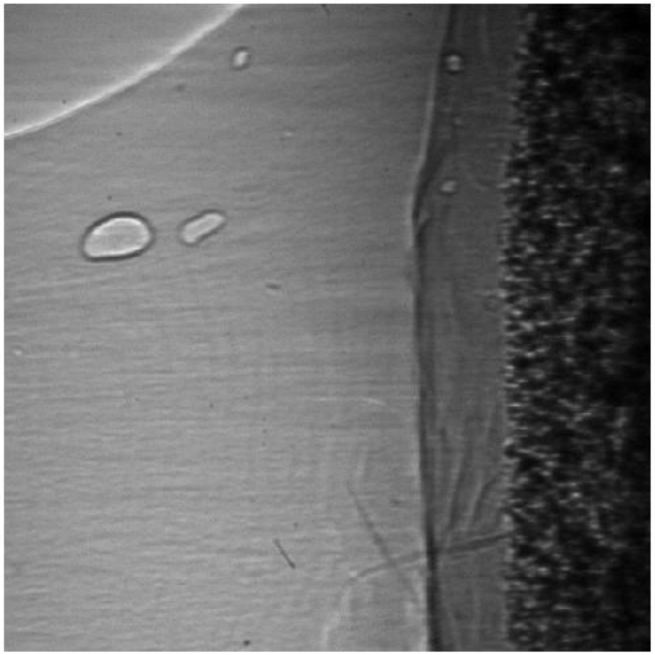

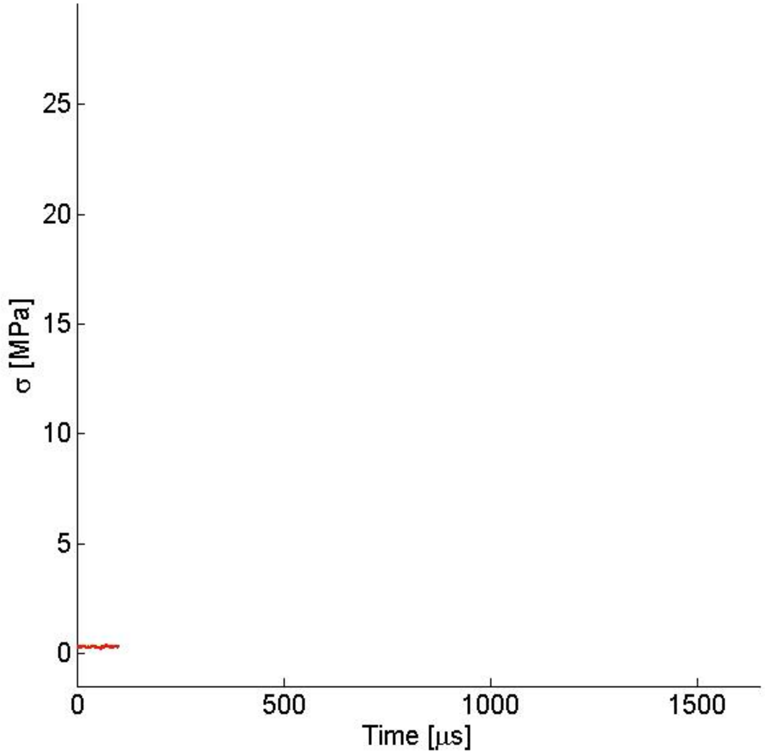

Bovine Cortical Bone Fracture

- Radial

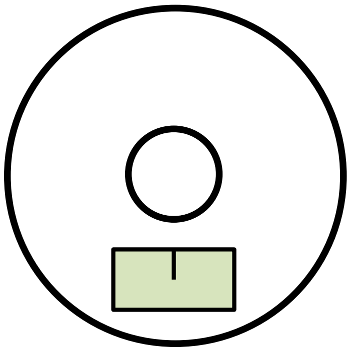

- Longitudinal

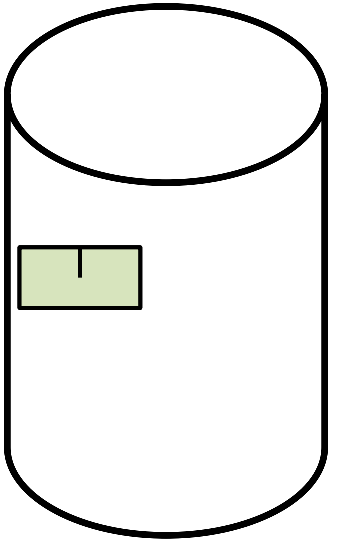

Bovine Bone Fracture

Sample 2 (radial)

- Static
  - thickness B = 2.69 mm
  - notch width a = 2.26 mm

- Dynamic (1 M fps)
  - Crack speed ~153 m/s

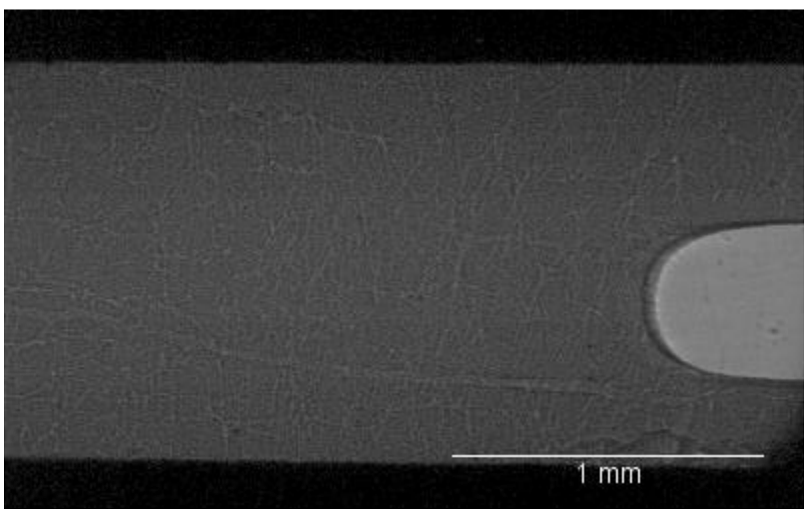

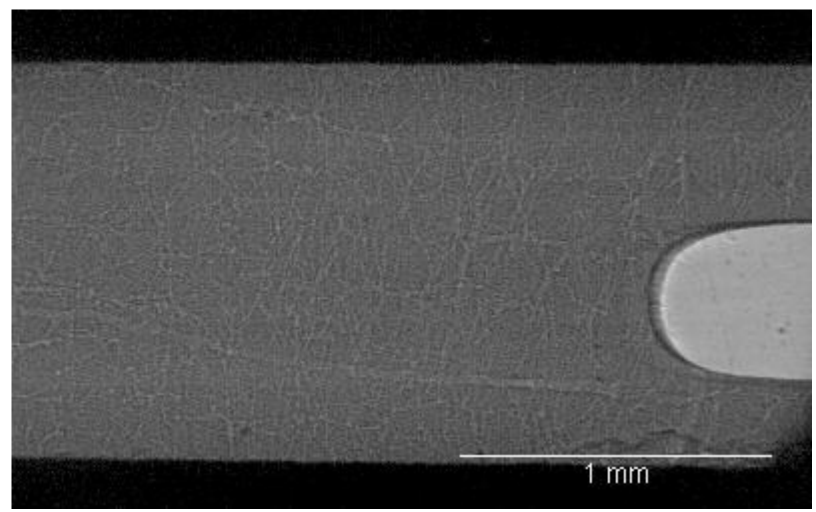

Bovine Bone Fracture

Sample 3 (radial)

- Static
  - thickness B = 0.97 mm
  - notch width a = 2.35 mm
- Dynamic (2 M fps)
  - Crack speed ~150 m/s

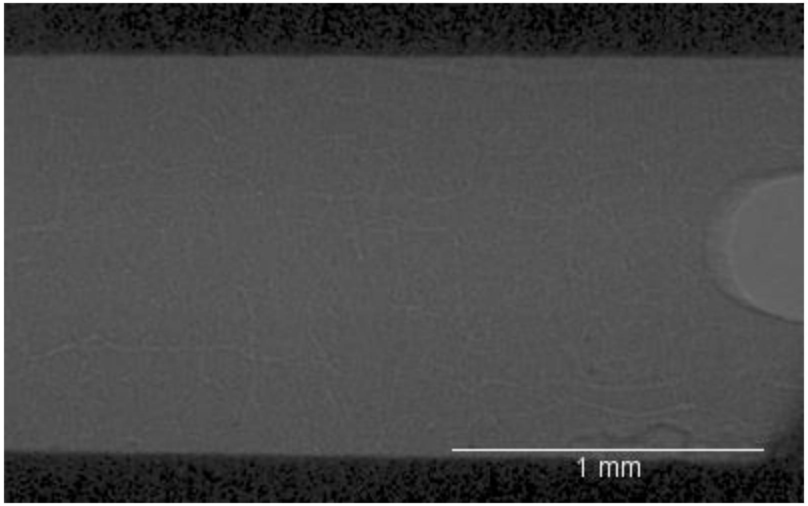

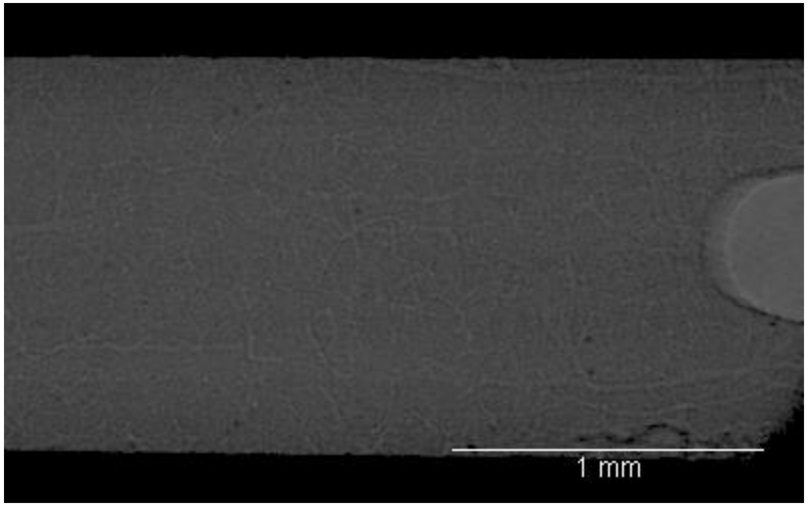

Future Improvements

- **Hybrid Experiments**
  - **Experimental/Modeling/Simulating.**
- **Full-field Measurements**
  - **DIC/VDIC/Virtual Field.**
- **Non-contact Strain Measurements**
  - **Interferometry on polymer bars.**
- **Improved Gripping Methods**
  - **Minimizing disturbance to gage section.**

1 (PDF) DEFENSE TECHNICAL INFORMATION CTR
DTIC OCA

2 (PDF) DIR ARL
IMAL HRA
RECORDS MGMT
RDRL DCL
TECH LIB

1 (PDF) GOVT PRINTG OFC
A MALHOTRA

12 (PDF) NATICK SOLDIER RSRCH DEV AND ENGRNG CTR
M G CARBONI
M CODEGA
D COLANTO
R DILALLA
J FONTECCHIO
B KIMBALL
J KIREJCZYK
M MAFFEO
M MARKEY
J PARKER
D PHELPS
J WARD

3 (PDF) PROG EXECUTIVE OFC SOLDIER
A FOURNIER
J MULLENIX
J ZHENG

2 (PDF) SOUTHWEST RSRCH INST
D NICOLELLA
T HOLMQUIST

1 (PDF) AUTO CELL PEO LAND SYS
A PURTELL

9 (PDF) INST FOR DEFNS ANLYS
Y MACHERET
M COUCH
J CZARNECKI
J HESTER
B TURNER
V VOLPE
J WALBERT
K WALZL
P WEBER

1 (PDF) US ARMED FORCES MEDICAL EXAMINER SYS
J GETZ

3 (PDF) MRMC DOD BLAST INJURY RSRCH PROG COORDINATING OFC
R GUPTA
M LEGGIERI
R SHOGE

5 (PDF) WIAMAN PMO
F HUGHES
R COATES
S MARSH
P RIIPPA
P FROUNFELKER

3 (PDF) MRMC JTAPIC PRGM OFC
F LEBEDA
W LEI
J USCILOWICZ

2 (PDF) US ARMY AEROMEDICAL RSRCH LAB
V CHANCEY
B MCENTIRE

5 (PDF) TARDEC
R SCHERER
C FOSTER
J KOSHKO
J RAMALINGAM
R THYAGARAJAN

2 (PDF) NATIONAL AERONAUTICS AND SPACE ADM
J SOMERS
T ROSS-SHEPARD

1 (PDF) PATUXENT RIVER NAS
B SHENDER

1 (PDF) RDECOM HQ
AMSRD PE
D RUSIN

41 (PDF) DIR USARL
RDRL DP
T BJERKE
RDRL SLB W
J GURGANUS
W MERMAGEN
RDRL WM
S SCHOENFELD
RDRL WMM
M VANLANDINGHAM
RDRL WMM A
T PLAISTED
E WETZEL

RDRL WMM D
  S WALSH
RDRL WMM E
  L VARGAS-GONZALEZ
RDRL WMP B
  A DAGRO
  A DILEONARDI
  A EIDSMORE
  A GUNNARSSON
  C HAMPTON
  C HOPPEL
  M KLEINBERGER
  J MCDONALD
  P MCKEE
  K RAFAELS
  K THOMPSON
  T WEERASOORIYA
  S WOZNIAK
  T ZHANG
RDRL WMP C
  R BECKER
  S SATAPATHY
  A SOKOLOW
RDRL WMP D
  R DONEY
  B SCOTT
RDRL WMP E
  P GILLICH
  M LOVE
  P SWOBODA
RDRL WMP F
  N GNIAZDOWSKI
  M TEGTMEYER
  R GUPTA
  M CHOWDHURY
  R KARGUS
  D KRAYTERMAN
  J NESTA
  J PRITCHETT
  D MALONE
  A GOERTZ